ACTA PATHOLOGICA ET MICROBIOLOGICA SCANDINAVICA

Founded 1924

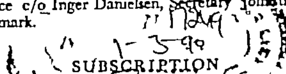
Acta Pathologica et Microbiologica Scandinavica is intended for the prompt publication of original research in the fields of pathology, microbiology, and immunology It is included in Current Contents, Excerpta Medica, and Medlars.

Acta Pathologica et Microbiologica Scandinavica is a nonprofit making scientific journal Since 1924 it has been published by the Scandinavian Societies for Medical Microbiology and Pathology It appears in three sections Section A Pathology Section B Microbiology and Section C Immunology

Acta Pathologica et Microbiologica Scandinavica has subscribers in more than seventy countries throughout the world with a wide readership in the major research institutes hospitals, laboratories, and specialist libraries.

EDITORIAL CORRESPONDENCE

All communications regarding manuscripts and editorial matters should be addressed to the Editorial Office c/o Inger Danielsen, Secretary Johnstrups Allé 6 DK 1923 Copenhagen V Denmark.



SUBSCRIPTION

At present one annual volume of Section A, one of Section B, and one of Section C (each section consisting of 6 issues appearing bimonthly) will contain a total of approximately 1600 pages. During the past few years approximately five free supplements have been issued annually These supplements will be delivered separately to the subscribers by surface mail at no extra charge. The subscription price is

Sect. A B and C	D.kr 770 – plus postage D.kr 40.–	($ 141 75 £ 86 70 DM 336.15)
Sect. A:	D.kr 462.– plus postage D.kr 15	($ 83.50 £ 51 05 DM 198.00)
Sect. B	D.kr 462.– plus postage D.kr 15 –	($ 83.50 £ 51 05 DM 198.00)
Sect. C	D.kr 308.– plus postage D.kr 10 –	($ 55 65 £ 34 10 DM 132.00)
Sect. A and C (combined)	D.kr 660.– plus postage D.kr 25 –	($ 119.90 £ 73 30 DM 284.30)
Sect. B and C (combined)	D.kr 660 – plus postage D.kr 25 –	($ 119 90 £ 73.30 DM 284.30)

Back numbers (whole volumes or single copies) are available.
NB. All prices are subject to exchange rate fluctuation.

All business communications regarding subscriptions, distribution, changes of address, advertisements, or orders of back numbers should be addressed to MUNKSGAARD International Publishers Ltd. 35 Nörre Sögade DK 1370 Copenhagen K Denmark.

Second class postage paid at New York, N Y., U.S.A. U.S mailing agent, Expediters of the Printed Word, Ltd. 527 Madison Avenue, New York, N Y 10022 Printed in Denmark.

Acta path. microbiol. scand. Sect. A 85: 1–18, 1977

THE EFFECTS OF CHOLESTEROL/FAT FEEDING ON LIPID LEVELS AND MORPHOLOGICAL STRUCTURES IN LIVER, KIDNEY AND SPLEEN IN GUINEA PIGS

CHRISTIAN A. DREVON and TORSTEIN HOVIG

Institute for Nutrition Research, School of Medicine, University of Oslo, Blindern, Oslo, and
Electron Microscopic Laboratory, Institute of Pathology, University of Oslo, National Hospital of Norway, Oslo, Norway

Drevon, C. A. & Hovig, T. The effects of cholesterol/fat feeding on lipid levels and morphological structures in liver, kidney and spleen in guinea pigs. Acta path. microbiol. scand. Sect. A, 85: 1–18, 1977.

Guinea pigs were fed a semisynthetic diet containing 10 per cent (by weight) cottonseed oil with or without 1 per cent cholesterol. In the animals fed fat, the lipid levels and the morphology remained normal in all tissues studied. Concomitantly with a marked accumulation of cholesteryl ester (CE) in the liver, however, many microscopical changes occurred in guinea pigs fed cholesterol/fat. A prominent deposition of lipid in vacuoles, mostly without delimiting membranes, where observed at centrilobular sites. Multivacuolated secondary lysosomes, membrane bound lipid vacuoles (lipolysosomes) and myelin figures were found both in hepatocytes and Kupffer cells. Myelin figures and crystalline clefts were observed more often in Kupffer cells than in hepatocytes. The granular endoplasmic reticulum in the Kupffer cells was grossly dilated and filled with an amorphous material. Both the biochemical and the morphological findings in hepatocytes and Kupffer cells are very similar to those observed in cholesteryl ester storage disease and in Wolman's disease. These two lipid storage diseases are both related to deficiency of an acid lipase in the liver. Measurement of the acid liver CE hydrolase in guinea pigs fed fat and in those fed cholesterol/fat showed similar activity. A relative deficiency of this enzyme activity could be the reason for the development of the enormous CE storage in guinea pig livers. These findings suggest that guinea pigs fed cholesterol/fat, in some respects, can be used as a model for Wolman's disease and cholesteryl ester storage disease. We did not find any microscopical changes in the kidneys from animals fed cholesterol/fat, thus indicating that the experimental condition is not useful as a model for studies of the kidney changes in lecithin cholesterol acyltransferase (LCAT) deficiency.

Key words: Cholesterol; hepatic cells; Kupffer cell; lysosomes; Wolman's disease; cholesterol ester storage disease; guinea pigs.

C. A. Drevon, Institute for Nutrition Research, School of Medicine, University of Oslo, Blindern, P. O. Box 1046, Oslo 3, Norway.

Received 25.vii.76   Accepted 1.ix.76

Guinea pigs are normally herbivorous. On a diet containing high amounts of fat and cholesterol these animals develop changes in different tissues, characterized by haemolytic anaemia, lipid depositions in liver, spleen, kidney and erythrocytes in addition to reduced gain in weight and increased death rate (21, 29). The plasma levels of lipids and lipoproteins in guinea pigs fed cholesterol/fat are grossly abnormal (25) and in many respects quite similar to the pathological lipoprotein pattern observed in cholestasis and familial lecithin cholesterol acyl transferase (LCAT) deficiency (11). It was therefore assumed that a closer understanding of the biochemical, physiological and morphological changes induced in guinea pigs by cholesterol/fat feeding might throw light on general aspects of the cholesterol metabolism. It seemed to be of special interest to evaluate whether guinea pigs fed cholesterol/fat could be used as model for LCAT deficiency. Accordingly studies of the cholesterol metabolism in guinea pigs receiving high cholesterol and fat diets were carried out (6). In the present paper a report on the morphological and biochemical changes in liver, kidney and spleen induced by cholesterol/fat feeding is submitted. The findings presented indicate that the animal model does not apply as much to LCAT deficiency as to Wolman's disease and cholesteryl ester storage disease.

MATERIALS AND METHODS

Chemicals

Cholesterol biochemical standard was purchased from British Drughouse Chemicals, Poole, England, stigmasterol from Koch-Light Lab. Colnbrooke and the glycerokinase and glycerol-3-phosphate-dehydrogenase from Boehringer, Mannheim, W. Germany. Phospholipid standards and bovine serum albumin were delivered by Sigma Chemical Co., St. Louis, Miss., USA. 1-amino-naftol-4-sulfonic acid, sodium bisulfite, sodium sulfite, perchloric acid, glycine and hydroxonium hydroxide were purchased from Merck, Darmstadt, W. Germany.

Animals and Diets

From birth until the age of 3 weeks, male, albino guinea pigs, from our own colony (Pir/Srr/c strain) were allowed to suckle their mothers and had free access to hay pellets, Swedish turnips, and water containing ascorbic acid (1 g/litre) as described (3).

From the age of three weeks, the animals received a diet containing 10 per cent (by weight) cottonseed oil with or without the addition of 1 per cent cholesterol. A detailed description of the semisynthetic diets is given elsewhere (6, 15, 22). The diet was mixed and pelleted by Astra Ewos AB, Södertälje, Sweden. Two animals from each group were examined after 2, 6 and 11 weeks of feeding. All animals had free access to food and water until samples were taken under diethyl ether anaesthesia. The liver was perfused with isotonic saline before specimens for morphological and biochemical studies were taken out.

Tissue samples for light and electron microscopy were taken while the animals were anaesthetized. These samples were immediately fixed in 2.5 per cent glutaraldehyde in 0.1 M phosphate buffer (pH 7.4) for 4 hours and postfixed in 1 per cent osmium tetroxide in Tyrode's solution (pH 7.4) for 2 hours. The specimens were dehydrated in graded ethanols, embedded in Epon 812 and sectioned by a LKB ultramicrotome. Semithin sections for light microscopy were stained with toluidine blue, and sections for electron microscopy were stained with uranyl acetate and lead citrate. The sections were examined in a Siemens Elmiskop I or a Jeol 100 B electron microscope.

Chemical Analysis

Determination of free (FC) and total cholesterol (TC) was carried out using gas liquid chromatography as described elsewhere (5). Cholesteryl ester (CE) was calculated as the difference between TC and FC. Triglyceride (TG) assays were carried out fluorometrically using a slightly modified version of *Wieland's* glyceridglycerol method (28). Protein was measured according to *Lowry* (17) using bovine serum albumin as standard. Phospholipids (PL) were extracted as described (4) and phosphate measured using a modified method of *Bartlett* (1).

Calculations

Wilcoxons test for paired comparison was used for the calculation of the significance of the differences in values in the individual groups of animals.

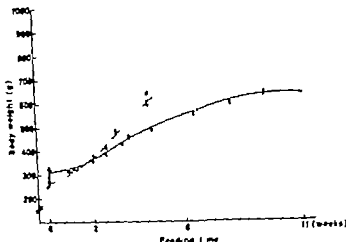


Fig. 1. Time course of body weight in guinea pigs fed fat ○---○ and in guinea pigs fed cholesterol/fat ●——●

RESULTS

I. *Macroscopic Observations*

The gain in body weight of the guinea pigs fed fat was twice that of animals fed cholesterol/fat (Fig. 1). The body weights of our guinea pigs fed for 11 weeks were about twice as high as those reported by *Ostwald et al.* (21). All guinea pigs in both groups appeared healthy during the observation period. No deaths occurred during the feeding period.

The weights of liver, kidneys, suprarenal glands, and the red blood cell counts were higher in the group of animals fed fat than in the group of animals fed cholesterol/fat, although the differences in liver and kidney weights in the two groups were not significant.

II. *Liver*

A. *Biochemical findings.* FC, TC, TG and PL in liver did not change significantly during the feeding period in animals fed fat. In the group of animals fed cholesterol/fat, however, FC increased by about three times, reaching a plateau after 6 weeks (Fig. 2). CE increased still more, and after 6 weeks, values in the animals fed cholesterol/fat were about 70 times higher than values in animals fed fat. From the 6th to the 11th weeks there

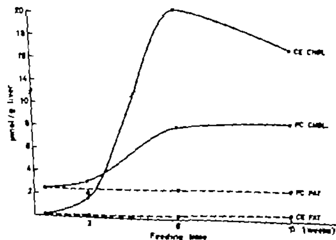


Fig. 2. Concentrations of free cholesterol (FC) and cholesteryl esters (CE) in livers in guinea pigs fed fat ○---○ and in guinea pigs fed cholesterol/fat ●——● related to feeding time.

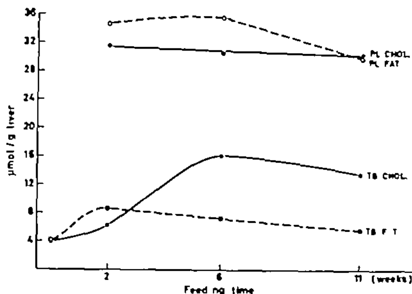


Fig 3 Concentrations of triglycerides (TG) and phospholipids (PL) in livers in guinea pigs fed fat O---O and in guinea pigs fed cholesterol/fat ●——● related to feeding time.

was a slight fall in the CE concentration after 11 weeks, the CE levels in the guinea pigs fed cholesterol/fat were about 30 times higher than those in the animals fed fat After 6 and 11 weeks of feeding the concentration of TG was 2–3 times higher in the animals exposed to cholesterol while the PL concentration remained identical in the two groups of animals (Fig 3)

B. *Light microscopy* Specimens from the animals fed fat revealed normal liver tissue architecture. The hepatocytes and the Kupffer cells appeared well preserved whether examined by light or electron microscopy



Fig 4 Light micrograph of semithin section from liver specimen, guinea pig fed fat for 2 week Central vein (CV) and portal region (PR) Practically no visible lipid. *Toluidine-blue staining*



Fig. 5a and b Light micrograph of centrilobular region (a) and periportal region (b) of liver specimen from an animal fed on cholesterol/fat diet for 6 weeks. Central vein (CV), portal region (PR). Note the numerous lipid vacuoles in the centrilobular region, but only little lipid in the periportal region. Toluidine blue stained semithin section

KC
CV
KC_2
KC_1
20μ
B

RBC
KC
RBC
MIT
SL
MIT
HC
HC
1 μ



Fig. 6. Light micrograph demonstrating large lipid vacuoles in the hepatic cells in a centrilobular region and vacuolated Kupffer cells (KC) after 6 weeks of cholesterol/fat feeding. Note the crystalline struc ture in KC, *Toluidin -blue* stained semithin section.

Fig. 7. Electron micrograph of liver specimen, after two weeks of cholesterol/fat feeding. Note the ac cumulation of small lipid droplets at the periphery of the hepatocytes. Hepatocytes (HC) Kupffer cell (KC) secondary lysosome (SL) mitochondria (MIT) red blood cells (RBC)

Fig. 8. Higher magnification of the framed part of Fig. 7. *Infolding* in the cytoplasm of a hepatocyte containing lipoprotein particles with a diameter about 400–500 Å. The particles are indicated by ar rows

KC
CV
KC2
KC1
20µ
6
RBC
KC
RBC
MIT
SL
HC
MIT
HC
1µ
7

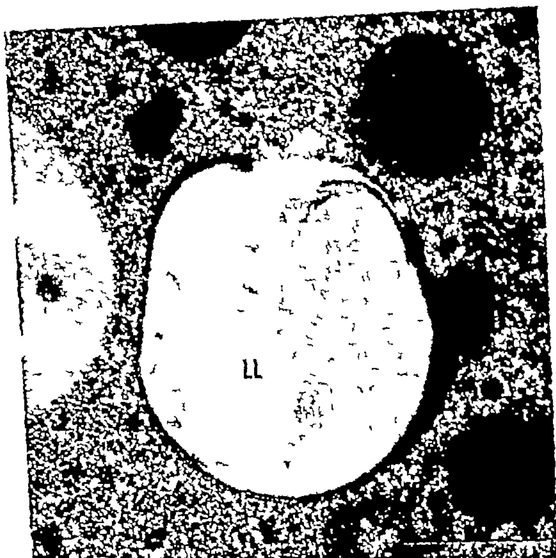


Fig. 10 Detail of a hepatocyte from a guinea pig fed cholesterol/fat for 6 weeks. Lipid droplet surrounded by layered membranes and an electron-dense protrusion. This secondary lysosomes is a typical lipolysome (LL). Lipid droplet without delimitating membranes (L)

that minor amounts of lipid droplets were present in the parenchymal cells (Fig. 4)

In liver from animals fed cholesterol/fat, the *accumulation of lipid droplets* increased with time. *After two* weeks, lipid deposits were usually detected *in the* central zones. During the feeding period, the distribution of lipid droplets became more widespread, but even after 11 weeks, the changes were consistently more prominent in the central *zones* of hepatic lobules than in the peripheral zones (Fig. 5 a and b)

After 2 weeks of feeding most of the lipid droplets were found in the hepatocytes. The size of the droplets varied, *but* after 6 weeks

Fig. 9 Detail of hepatocyte revealing primary lysosomes (LY) and multivacuolated secondary lysosomes (SLY). Note secondary lysosomes with lipid droplets (SL_1 and SL_2) and lipid droplet (L). Mitochondria (MIT) nucleus (N). Guinea pig fed cholesterol/fat for 11 weeks


L
SL_1
MT
SL_2
SLY
SLY

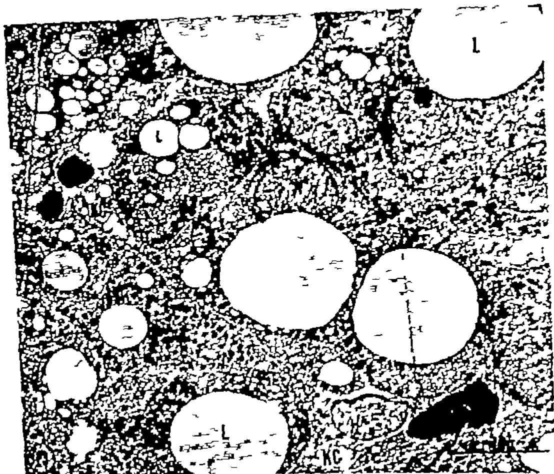


Fig 11 Low power electron micrograph of a section revealing hepatocytes where large lipid vacuoles are filling a great portion of the cytoplasm Note the well preserved cell borders of the hepatocytes. Vacuolated Kupffer cells (KC) lipid droplets (L) a peripherally located nucleus (*N*) *Cholesterol/*fat feeding for 11 weeks.

the size was considerably larger In the most affected cells, most of the cytoplasm was filled with one or a few large lipid droplets (Fig 6) The cell borders remained prominent and distinct. *After 11 weeks of feeding*, the lipid droplets tended to be fewer and smaller than after 6 weeks. Necrosis of hepatic cells was not observed. Mitoses were rarely seen there were no signs of erythropoiesis and only slight cell infiltration in the periportal regions.

Bile ducts, veins and *arteries* were *all* of normal appearance, without any signs of atheromatosis, in contrast to findings in rabbits fed cholesterol/fat (14)

After 2 weeks of feeding, the Kupffer cells appeared slightly vacuolated, especially in the central zone of the lobules. The difference between the central and peripheral regions, *however* was not as clear as that observed in the case of hepatic cells. During the feeding there was an increase both in number and size of the Kupffer cells they became vacuolated and occasionally they contained crystalline clefts (Fig 6) After 6 and 11 weeks, the Kupffer cells often clustered.

C. *Electron microscopy Hepatocytes* The presence of lipid vacuoles in the parenchymal cells *of guinea* pigs fed cholesterol/fat was confirmed. Clusters of small vacuoles were

Fig 11 An occasional hepatocyte with a secondary lysosome containing a crystalline cleft. Lipid droplet (L) mitochondria (MIT) Cholesterol/fat feeding for 6 weeks.

Fig 12 A hepatocyte containing a secondary lysosome with concentrically layered membranes. Cholesterol/fat feeding for 6 weeks.


L
L
ER
1 µ

often located peripherally in the cells (Fig 7) This was especially striking after 2 weeks of feeding when the numbers of large droplets were low The droplets were weakly stained or electron lucent with an osmiophilic peripheral zone usually without any lining bilayers. Occasionally uniform particles with a diameter of 400–500 A were found in the sinusoids and in the space of Disse as well as in infoldings of the plasma membrane (Fig 8) These particles probably represent lipoproteins After 2 and 6 weeks of feeding various types of secondary lysosomes (phagosomes) were found in the cytoplasm of the hepatocytes (Fig 9–13) Electron dense structures with several vacuoles (Fig 9) were often noted as well as lipid droplets within the limiting membrane of secondary lysosomes, lipopolysomes (Fig 9 and 10) An occasional crystalline cleft (Fig 11) and lamellated structures (Fig 12) were observed in secondary lysosomes. The mitochondria were usually well preserved Neither the smooth endoplasmic reticulum nor the Golgi apparatus were particularly prominent

The nucleus was often displaced to the periphery of the cell (Fig 13) Lipid vacuoles in parenchymal cells were found to be somewhat less numerous after 11 weeks of cholesterol/fat feeding than after 6 weeks. Otherwise the ultrastructural appearance was similar The enormous increase in the accumulation of lipid droplets in parenchymal cells (Fig 13) appeared concomitantly with the large increase in the CE concentration in liver (Fig 3) From 2 to 6 weeks there was a 2–3 fold increase in TG concentration in the liver but this increase was small as compared with the increase in concentration of CE It is therefore likely that the lipid vacuoles in the liver cells are composed mainly of CE *Forte et al* (8) and *Lee & Ho* (14) who treated livers from guinea pigs and rabbits fed cholesterol/fat with digitonine showed that some FC also is present inside the lipid vacuoles

Kupffer cells After 2 weeks of cholesterol/fat feeding the Kupffer cells often contained a dilated and well-developed granular endoplasmic reticulum with an amorphous material within the cisternae some lipid vacuoles were seen in the cytoplasma After 6 and 11 weeks, the Kupffer cells were much more prominent and were of a vacuolated, sometimes swollen appearance (Fig 14) The cells were almost filled with lipid vacuoles which sometimes might be lined with membranes as those in the hepatocytes The granular endoplasmic reticulum was pronounced and dilated and in some places there seemed to be direct communication between the endoplasmic reticulum and the lipid vacuoles. Furthermore, myelin figures were observed much more often in the Kupffer cells than in the hepatic cells (Fig 15) In addition, crystalline clefts were frequently observed (Fig 16) Such clefts were only occasionally seen in the hepatocytes. In some of the Kupffer cells, the mitochondria appeared slightly swollen with few cristae and an electron lucent matrix (Fig 14)

After feeding had continued for 6 weeks the endothelial cells would contain a few lipid vacuoles. Otherwise the cells were of normal appearance.

III *Spleen*

There was an enormous increase in CE concentration in the guinea pigs fed cholesterol/fat for 11 weeks (ca. 300 fold) while the value of PL was about half that in the animals fed fat. At 11 weeks, numerous lipid loaden cells were observed in guinea pigs fed cholesterol/fat, whereas no such cells were found in the control animals

IV *Kidney*

PL, FC and protein concentrations remained unaffected by cholesterol/fat feeding while CE increased significantly TG was

---

Fig 14 Part of a Kupffer cell containing lipid droplets (L) *Note the dilated endoplasmic reticulum* (ER) and mitochondria with loss of cristae and matrix (*MIT*) *Cholesterol/fat feeding for 11 weeks*


L
L
1 μ

often located peripherally in the cells (Fig 7) This was especially striking after 2 weeks of feeding when the numbers of large droplets were low The droplets were weakly stained or electron lucent with an osmiophilic pheripheral zone usually without any lining bilayers. Occasionally uniform particles with a diameter of 400-500 Å were found in the sinusoids and in the space of Disse as well as in infoldings of the plasma membrane (Fig 8) These particles probably represent lipoproteins After 2 and 6 weeks of feeding various types of secondary lysosomes (phagosomes) were found in the cytoplasm of the hepatocytes (Fig 9-13) Electron dense structures with several vacuoles (Fig 9) were often noted as well as lipid droplets within the limiting membrane of secondary lysosomes lipopolysomes (Fig 9 and 10) An occasional crystalline cleft (Fig 11) and lamellated structures (Fig 12) were observed in secondary lysosomes. The mitochondria were usually well preserved Neither the smooth endoplasmic reticulum nor the Golgi apparatus were particularly prominent

The nucleus was often displaced to the periphery of the cell (Fig 13) Lipid vacuoles in parenchymal cells were found to be somewhat less numerous after 11 weeks of cholesterol/fat feeding than after 6 weeks. Otherwise the ultrastructural appearance was similar The enormous increase in the accumulation of lipid droplets in parenchymal cells (Fig 13) appeared concomitantly with the large increase in the CE concentration in liver (Fig 3) From 2 to 6 weeks there was a 2-3 fold increase in TG concentration in the liver but this increase was small as compared with the increase in concentration of CE It is therefore likely that the lipid vacuoles in the liver cells are composed mainly of CE. *Forte et al* (8) and *Lee & Ho* (14) who treated livers from guinea pigs and rabbits fed cholesterol/fat with digitonine, showed that some FC also is present inside the lipid vacuoles

Kupffer cells After 2 weeks of cholesterol/fat feeding the Kupffer cells often contained a dilated and well-developed granular endoplasmic reticulum with an amorphous material within the cisternae some lipid vacuoles were seen in the cytoplasma After 6 and 11 weeks, the Kupffer cells were much more prominent and were of a vacuolated, sometimes swollen appearance (Fig 14) The cells were almost filled with lipid vacuoles which sometimes might be lined with membranes as those in the hepatocytes. The granular endoplasmic reticulum was pronounced and dilated and in some places there seemed to be direct communication between the endoplasmic reticulum and the lipid vacuoles. Furthermore myelin figures were observed much more often in the Kupffer cells than in the hepatic cells (Fig 15) In addition, crystalline clefts were frequently observed (Fig 16) Such clefts were only occasionally seen in the hepatocytes. In some of the Kupffer cells the mitochondria appeared slightly swollen with few cristae and an electron lucent matrix (Fig 14)

After feeding had continued for 6 weeks the endothelial cells would contain a few lipid vacuoles. Otherwise the cells were of normal appearance

III *Spleen*

There was an enormous increase in CE concentration in the guinea pigs fed cholesterol/fat for 11 weeks (ca. 300 fold) while the value of PL was about half that in the animals fed fat. At 11 weeks, numerous lipid loaden cells were observed in guinea pigs fed cholesterol/fat, whereas no such cells were found in the control animals

IV *Kidney*

PL, FC and protein concentrations remained unaffected by cholesterol/fat feeding while CE increased significantly TG was

---

Fig 14 Part of a Kupffer cell containing lipid droplets (L) Note the dilated endoplasmic reticulum (ER) and mitochondria with loss of cristae and matrix (MIT) Cholesterol/fat feeding for 11 weeks.



Fig. 16. Part of a Kupffer cell containing lipid vacuoles (L) and crystalline clefts. Cholesterol/fat feeding for 6 weeks.

DISCUSSION

LCAT-deficient patients develop renal failure, probably due to a disturbed lipoprotein metabolism. It has been proposed that the abnormal low-density lipoprotein (LDL) fraction in the LCAT-deficient patients could be responsible for the renal affection in these patients. Guinea pigs fed cholesterol/fat also get a LDL fraction of large molecular weight (25) and a renal damage described as glomerulosclerosis by light microscopy develop (9). Any pathological changes were not demonstrable in the kidneys of our guinea pigs. Especially there was no evidence of accumulation of lipid material in the glomeruli otherwise a striking finding in patients with LCAT-deficiency (15). Thus, the animal model did not appear to be useful in the study of the characteristics of renal changes in LCAT-deficiency.



Fig 15 Detail of Kupffer cell containing inclusions of the appearance of myelin figures. Nucleus (N) Cholesterol/fat feeding for 6 weeks.

significantly lower in the guinea pigs fed cholesterol/fat than in animals fed fat.

Any clear-cut differences between the renal glomeruli tubuli and vessels in the two animal groups could not be detected by light and electron microscopy

TABLE I. *Comparison of Liver Lipids in Patients with Wolman's Disease and in Patients with Cholesteryl Ester Storage Disease (CESD) with Upper Limits of Normal Individuals*

	Wolman	CESD	Guinea pigs fed cholesterol/fat
FC	0.5– 3	1 3	2 – 4
CE	7 –160	7 90	30–70
TG	3 – 10	3	2 – 3
PL	0.5– 4	0.5 4	0.8– 1

Data obtained from ref. (26). Guinea pigs fed cholesterol/fat (6–11 weeks) compared with guinea pigs fed fat. The figures indicate how many times larger the lipid concentrations are as compared with concentrations in controls.

Abbreviations:

FC = free cholesterol, CE = cholesteryl ester, TG = triglycerides, PL = phospholipids.

in lysosomes (16, 26). No lamellar membrane-like figures have been described but the endoplasmic reticulum is dilated and there is also a marked lipid accumulation in the Kupffer cells containing crystalline clefts. The pathogenesis of Wolman's disease and cholesteryl ester storage disease is related to a lack of an acid lipase which hydrolyses triglycerides and cholesteryl esters (2, 23). The acid cholesterol esterase has been measured in guinea pigs fed fat as well as in guinea pigs fed cholesterol/fat; any significant difference in the enzyme activity against exogenous added CE-labelled plasma lipoproteins in the two groups was not observed (6). This indicates that one reason why liver-changes similar to those observed in cholesteryl ester storage disease, develop in guinea pigs fed cholesterol/fat, could be a relative deficiency in cholesteryl ester hydrolase activity. Much CE accumulates in the smooth muscle cells of the arterial wall in rabbits fed cholesterol (7). One possible explanation of this accumulation is also a relative lack of the acid cholesteryl ester hydrolase activity.

The activity of the coenzyme A-dependent enzyme which esterifies cholesterol in the intestinal mucosa cells increases considerably in animals fed cholesterol/fat (19). This may be of importance for the increased absorption of cholesterol. Cholesterol esterification in the liver tissue (by acyl CoA:cholesterol acyltransferase) from guinea pigs fed cholesterol/fat is also increased 5–10 times as compared with findings in the controls, while cholesteryl ester hydrolysis is unchanged (6). These findings may explain the large accumulation of CE in their livers. The most harmful effect of cholesterol/fat feeding is probably the increased load of cholesterol. It seems to be important for the organism to regulate the amount of FC in all sorts of membranes, in order to prevent great alterations of the membrane functions (10). Thus, the great accumulation of CE in the guinea pig livers can be regarded as a reasonable way of handling the enormous amounts of cholesterol stored in the body.

The authors are indebted to Solveig Berg, Øystein Sødahl and Mai Britt Ringdal for skilled technical assistance. One of the authors (C.A.D.) is a fellow of the Norwegian Research Council for Science and the Humanities. This work has been supported by grants from Anders Jahre's Foundation, Hjelpestikkenes Af distrikts Forskningsfond and the Norwegian Research Council for Science and the Humanities.

REFERENCES

1. *Bartlett, G. R.*: Phosphorus assay in column chromatography. J. biol. Chem. *234*: 466–468, 1959.
2. *Burke, J. A. & Schubert, W. K.*: Deficient activity of hepatic acid lipase in cholesterol ester storage disease. Science *176*: 309–310, 1972.
3. *Drevon, C. A. & Norum, K. R.*: Cholesterol esterification and lipids in plasma and liver from newborn and young guinea pigs raised

1 Acta path. microbiol. scand. Sect. A, 83, 1

We have shown that there is a great accumulation of lipid in the guinea pig liver and that CE accounts for most of this increase. The most prominent changes appeared in the centrilobular areas. This was also found by *Lee & Ho* (14) in rabbits fed cholesterol, while hepatocytes in hamsters fed cholesterol/fat showed larger lipid inclusions in the periportal regions (20). The central localization of lipids in guinea pig liver may be related to the circulatory conditions in the liver and to the difference in functions of liver cells located in the peripheral and the central zones of liver lobules (20, 24). Any data are not available in the literature according to which the capability of clearing lipoproteins from blood plasma or synthesis of lipoproteins within the liver lobule might be different.

Hepatocytes seemed to accumulate visible amounts of lipids earlier than nonparenchymal cells. Lipoprotein particles were observed in the sinusoids and in infoldings of the hepatic cell cytoplasm and they are possibly picked up from plasma by endocytosis. We did not observe fusion of primary lysosomes and endocytosed lipoprotein particles.

Multivacuolated secondary lysosomes (Fig. 9), however, were found in some areas of the hepatocytes. *Nehemiah & Novikoff* (18) described an unusual type of lysosomes to be found only in hepatocytes of Syrian golden hamsters fed an ordinary or cholesterol/fat diet. Their residual bodies in hepatic cells were characterized by four features: 1) an outer tripartite membrane, often showing a "halo" beneath its innter leaflet, 2) the presence of electronopaque materials, including ferritine-like grains and membranous arrays, 3) electron lucent lipid inclusions and 4) cytochemically demonstrable acid hydrolase activity. In Fig. 10 a structure (LL) is shown comprising the first three features, and the fourth we have not tested.

The different types of secondary lysosomes and lipolysosomes resemble those observed in patients with Wolman's disease (16), cholesteryl ester storage disease (26), Wilson's disease (12) and in arterial smooth muscle cells in rabbits fed cholesterol (7). In our study, the lipopolysosomes were seen to develop as a consequence of dietary cholesterol and fat overload. The most probable fate of dietary lipids taken up by the hepatocytes is that endocytosed lipoproteins may fuse with lysosomes and form secondary lysosomes. We do not know why some of the lipid droplets are surrounded by membranes and most of them are not.

The presence of crystalline clefts in the Kupffer cells indicates cholesterol precipitation in these cells. Only occasionally such clefts were observed in hepatocytes. Furthermore, the Kupffer cells contained considerable amounts of myelin structures. Both of these findings, in addition to the dilatation of the endoplasmic reticulum in Kupffer cells, suggest that the lipid metabolism in Kupffer cells and hepatocytes is different. We have investigated the activity of acyl CoA: cholesterol acyltransfer in parenchymal and nonparenchymal cells from rats (5) and found that there was very low activity in nonparenchymal cells while the activity in parenchymal cells was very high. This enzymatic difference could possibly explain the different structural appearances observed.

The vacuolated and swollen Kupffer cells, filled with lipid droplets and with a distended granular endoplasmic reticulum, are very similar to the findings in mice intravenously injected with lipid emulsions (27) and to findings in cases of Wolman's disease (16).

If the biochemical data obtained by analysis of liver tissue in patients with Wolman's disease or cholesteryl ester storage disease are compared with those applying to guinea pigs fed cholesterol/fat, similarities of all the lipid classes is seen to be striking (Table 1). Accumulations of CE are large, 7–160 times the upper normal limit (26), and increases in FC, TG and phospholipids are only moderate in patients with Wolman's disease and cholesteryl ester storage disease.

The ultrastructural findings in hepatocytes and Kupffer cells are relatively similar in these two storage diseases. In the parenchymal cells there are big fat vacuoles in relation

Acta path. microbiol. scand. Sect. A, 85 19–24 1977

DEMONSTRATION OF HORMONAL SENSITIVITY IN GYNAECOMASTIC TISSUE BY THYMIDINE INCORPORATION *IN VITRO*

H. SKOVGAARD POULSEN

The Institute of Cancer Research Radiumstationen, and the Department of Surgery I
Aarhus County Hospital, Aarhus, Denmark

Skovgaard Poulsen, H. Demonstration of hormonal sensitivity in gynaecomastic tissue by thymidine incorporation *in vitro*. Acta path. microbiol. scand. Sect. A, 85 19–24 1977

Gynaecomastic tissue from six patients were tested for oestrogen and testosterone sensitivity as measured by thymidine incorporation in tissue fragments *in vitro*. The DNA synthesis of the cultures was increased in tissue from five out of the six patients under the influence of oestrogen, whereas it was increased in tissue from only one patient under the influence of testosterone. The results are discussed in relation to the medical histories of the patients and hormonal excretion studies done by others.

Key words: Gynaecomastic tissue; hormonal sensitivity

H. Skovgaard Poulsen, The Institute of Cancer Research, Radiumstationen, Nörrebrogade 44 DK-8000 Aarhus C, Denmark.

Received 28 . 76   Accepted 15 . i.76

Gynaecomastia is a benign enlargement of the breast. The hypertrophic tissue may be a centrally located tumour with the circumference concentric with the areolar border or an extensive enlargement of the breast. It may be unilateral or bilateral. Histologically the tumours are composed of dense fibrous connective tissue with proliferative epithelial ducts embedded. No cell atypia is found, and lobule formation is exceptional (9).

The aetiology is supposed to be a stimulation of the breast tissue referable to increased oestrogen levels in the body or an increased sensitivity to oestrogen in the target tissue (1, 9). It often occurs in puberty or in association with endocrine disorders. Furthermore, it is seen in patients with liver diseases and as a side effect of certain drugs (8, 25).

In recent years, *in vitro* techniques have been developed for the study of the influence of hormones on animal and human breast tissues, benign as well as malignant (4, 5, 7, 10, 13, 14, 15, 21, 22, 26, 27). These investigations have demonstrated that the *in-vitro* sensitivity may reflect the hormonal sensitivity in the tissue *in vivo*.

The present investigation was performed in an attempt to determine the oestrogen and androgen sensitivity of gynaecomastic tissue by measuring thymidine incorporation in tissue fragments from six patients who were admitted to Aarhus County Hospital in 1975.

PATIENTS

Patient A was a 33-year-old man with bilateral gynaecomastia. Fifteen years prior to admission he had suffered from bilateral mumps orchitis. He

Sponsored by the Danish Cancer Society

on milk and non milk diet. Nutr Metabol *18* 137–151 1975

4 *Drevon C A & Norum K R* Effect of lipid emulsions on the plasma lecithin: cholesterol acyltransfer in guinea pigs. *Nutr Metabol 19* 180–191 1975

5 *Drevon C A Berg T & Norum K R* Uptake and degradation of cholesterol ester labelled rat plasma lipoproteins in purified rat hepatocytes and nonparenchymal liver cells Biochim. biophys. Acta 1977 In press.

6 *Drevon C A* Cholesteryl ester metabolism in guinea pigs fed fat and cholesterol/fat containing diets. Nutr Metabol Submitted.

7 *de Duve C* The participation of lysosomes in the transformation of smooth muscle cells to foamy cells in the aorta of cholesterol fed rabbits. Acta cardiol *Suppl 20 9–25 1974*

8 *Forte T Nordhausen R & Ostwald R* Effects of chronic hypercholesteremia on guinea pig livers An electron microscopic study Circulation *52* Suppl II abstract no. *1048, 1975*

9 *French S W Yamanaka W & Ostwald R* Dietary induced glomerulosclerosis in the guinea pig Arch. Path *83* 204–210 1967

10 *de Gier J Haest G W M van der Neut Kok E C M Mandersloot J G & van Deenen L L M* Correlations between liposomes and biological membranes In van den Bergh S G Brost P., van Deenen, L. L. M., Riemersma, J C., Slater E. C & Tager J M (eds.) Mitochondria biogenesis and bioenergetics Biomembranes molecular arrangements and transport mechanisms. Eight FEBS Meeting N Holland/Am Publ Co *28* 263–*278 1972*

Glomset J A & Norum K R The metabolic role of lecithin cholesterol acyltransferase Perspectives from pathology Adv Lipid Res. *11* 1–65 1973

Hayashi H & Sternlieb I Lipolysosomes in human hepatocytes Ultrastructural and cytochemical studies of patients with Wilson's disease. Lab. Invest. *23* 1–7 1975

Hovig T & Gjone E Familial lecithin cholesterol acyltransferase deficiency Ultrastructural studies on lipid deposition and tissue reactions Scand. J clin Lab Invest. *33* Suppl *137* 135–146, 1974

Lee S-S & Ho K J Cholesterol fatty liver Morphological changes in the course of its development in rabbits Arch. Pathol. *99* 301–306 1975

Liu K C Typpo J T Lu J Y & Briggs G M Thiamine requirement of the guinea pig and the effect of salt mixtures in the diet on thiamine stability J Nutr *93* 480–482 1967

16 *Lough J Fawcett J & Wiegensberg, B.* Wolman's disease. An electronmicroscopic, histochemical and biochemical study Arch. Path. *89* 103–110 1970

17 *Lowry O H Rosebrough N J., Lewis Farr A & Randall R J* Protein measurement with the Folin phenol reagent. J biol. Chem *193* 265–275 1951

18 *Nehemiah J L & Novikoff A B* Unusual lysosomes in hamster hepatocytes. Exp. Mol Pathol *21 398–423 1974*

19 *Norum K R Lilljeqvist A C & Drevon, C A* CoenzymeA-dependent esterification of cholesterol in intestinal mucosa from guinea pig Influence of diet on the enzyme activity Scand J Gastroent. In press.

20 *Novikoff A B & Essner E.* The liver cell Some new approaches to its study Am. J Med. *29* 102–131 1960.

21 *Ostwald R & Shannon A* Composition of tissue lipids and anaemia of guinea pigs in response to dietary cholesterol. Biochem. J *91* 146–154 1964

22. *Ostwald R., Yamanaka W & Light M* The phospholipids of liver plasma, and red cells in normal and cholesterol-fed anemic guinea pigs. Proc Soc exp Biol. Med. *134* 814–820 1970

23 *Patrick A D & Lake B D* Deficiency of an acid lipase in Wolman's disease Nature *222* 1067–1068 1969

24 *Reith A & Schüler B.* Heterogeneity of rat liver cells—with special reference to mitochondria A quantitative stereological study Unpublished results

25 *Sardet C Hansma H & Ostwald R* Characterization of guinea pig plasma lipoproteins The appearance of new lipoproteins in response to dietary cholesterol J Lipid Res. *13* 624–639 1972

26 *Sloan H R & Frederickson D S* Rare familial diseases with neutral lipid storage Wolman's disease cholesteryl ester storage disease and cerebrotendinous xanthomatosis. In Stanbury J B., Wyngaarden, J B & Frederickson, D S (eds.) The metabolic basis of inherited disease, 3 ed. McGraw Hill Book Company New York 808–832, 1972

27 *Stuart A E & Smith I I* Histological effects of lipids on the liver and spleen of mice. J Pathol. *115* 63–71 1975

28. *Wieland O* Glycerol UV Method. In Bergmeyer H U (ed.) Methods of enzymatic analysis, 3 ed vol 3 Chemie Weinheim Academic Press, New York 1404–1409 1974

29 *Yamanaka W & Ostwald R* Lipid composition of heart, kidney and lung in guinea pigs made anemic by dietary cholesterol J Nutr *95* 381–387 1968

ta path microbiol. scand. Sect. A, 85 19–24 1977

DEMONSTRATION OF HORMONAL SENSITIVITY IN GYNAECOMASTIC TISSUE BY THYMIDINE INCORPORATION *IN VITRO*

H. Skovgaard Poulsen

The Institute of Cancer Research Radiumstationen, and the Department of Surgery I Aarhus County Hospital, Aarhus, Denmark

Skovgaard Poulsen, H. Demonstration of hormonal sensitivity in gynaecomastic tissue by thymidine incorporation *in vitro*. Acta path. microbiol. scand. Sect. A, 85 19–24 1977

Gynaecomastic tissue from six patients were tested for oestrogen and testosterone sensitivity as measured by thymidine incorporation in tissue fragments *in vitro*. The DNA synthesis of the cultures was increased in tissue from five out of the six patients under the influence of oestrogen, whereas it was increased in tissue from only one patient under the influence of testosterone. The results are discussed in relation to the medical histories of the patients and hormonal excretion studies done by others.

Key words. Gynaecomastic tissue hormonal sensitivity

H. Skovgaard Poulsen, The Institute of Cancer Research, Radiumstationen, Nörrebrogade 44 DK-8000 Aarhus C, Denmark.

Received 28.x.76 Accepted 15.xi.76

Gynaecomastia is a benign enlargement of the breast. The hypertrophic tissue may be a centrally located tumour with the circumference concentric with the areolar border or an extensive enlargement of the breast. It may be unilateral or bilateral. Histologically the tumours are composed of dense fibrous connective tissue with proliferative epithelial ducts embedded. No cell atypia is found, and lobule formation is exceptional (9).

The aetiology is supposed to be a stimulation of the breast tissue referable to increased oestrogen levels in the body or an increased sensitivity to oestrogen in the target tissue (1, 9). It often occurs in puberty or in association with endocrine disorders. Furthermore, it is seen in patients with liver diseases and as a side effect of certain drugs (8, 25).

In recent years, *in vitro* techniques have been developed for the study of the influence of hormones on animal and human breast tissues, benign as well as malignant (4, 5, 7, 10, 13, 14, 15, 21, 22, 26, 27). These investigations have demonstrated that the *in vitro* sensitivity may reflect the hormonal sensitivity in the tissue *in vivo*.

The present investigation was performed in an attempt to determine the oestrogen and androgen sensitivity of gynaecomastic tissue by measuring thymidine incorporation in tissue fragments from six patients who were admitted to Aarhus County Hospital in 1975.

PATIENTS

Patient A was a 33-year-old man with bilateral gynaecomastia. Fifteen years prior to admission he had suffered from bilateral mumps orchitis. He

Sponsored by the Danish Cancer Society

had atrophic testes, but his chromosomal picture was normal. Before admission he had been treated with gonadotrophin (Antex®) and Physex®) because of infertility. In relation to this treatment gynaecomastia developed.

Patient B was a 15-year-old boy with bilateral gynaecomastia. There was no secretion from the papillae and he had received no drugs.

Patient C was a 68-year-old man with left sided gynaecomastia. Five years before admission he underwent total gastrectomy because of cancer of the stomach. He had received no chemotherapy and on admission there were no signs of metastases or of impaired liver function.

Patient D was a 66-year-old man with right-sided gynaecomastia. Six months before admission he had started treatment with digitalis because of cardial incompensation. The liver function was normal and there was no sign of hepatic stasis.

Patient E was a 30-year-old man with left-sided gynaecomastia. Before admission he had repeatedly been admitted to hospital with nervous disorders. For several years he had been treated with a number of antipsychotic drugs, especially phenothiazine derivatives and benzodiazepine drugs. There were no signs of Klinefelter's syndrome. The liver function was normal.

Patient F was a 37 year-old man with left-sided gynaecomastia. Except for the development of gynaecomastia no other endocrine disorders were observed. Clinically the liver function was normal.

Liver Function

In patients A–E, the estimation of the liver function was based on the determination of the serum levels of bilirubin, GOT, GPT, alkaline phosphatase and prothrombin proconvertin.

In all the patients the results were within normal limits. Liver biopsy was not done in any of the patients. No liver investigation was performed in patient F but clinically no sign of impaired liver function was observed.

MATERIALS AND METHODS

Sterile biopsy specimens were placed in icecold Eagle's minimal essential medium (MEM) and prepared for cultivation within one hour after removal.

All damaged and fatty tissue was removed and the rest was minced to small fragments (approx. 0.5 mm³) with a pair of scissors, all done under aseptic conditions.

With a spatule 15–20 fragments were then randomly transferred to test tubes (of vol. 10 ml) containing 5.0 ml culture medium allowing them to float freely in the medium.

The medium was MEM with added antibiotics (100 IU/ml of penicillin and 100 μg/ml streptomycin). It was supplemented with foetal calf serum (Flow Laboratories) to a concentration of 5 per cent. Each tube contained 5.0 ml culture medium. Four cultures of 15–20 fragments each were set up for each hormone and control. All cultures were grown in an atmosphere of 95 per cent humidified air and 5 per cent CO_2 at 37 °C for 24 hours. The tissue fragments were cultivated under the following conditions: (1) controls, no hormone added; (2) 17-β-oestradiol 10^{-4} M; (3) testosterone 10^{-4} M.

The hormones were dissolved in ethanol. The final concentration of ethanol in each culture was 1 per cent of the total volume. The hormones were added to the medium when the cultures were set up. Twenty-four hours after explantation ³H-thymidine was added to the cultures for one hour (2.5 μCi/ml, 2.0 Ci/mmol) (The Radiochemical Centre, Amersham).

The incorporation was terminated by placing the cultures on ice. The supernatant was removed and 5 per cent trichloro-acetic acid was added for 45 minutes. After centrifugation (800 g) for 10 minutes the sediment was washed once with trichloro-acetic acid, centrifuged (800 g) for 10 minutes, and the final sediment was dissolved in 2.0 ml 0.5 M NaOH for two hours at 60 °C.

Each sample was divided into two. One portion, 200 μl was prepared for scintillation counting: 200 μl was mixed with 12 ml scintillation fluid (Insta-gel, Packard) and radioactivity was measured in a Packard TriCarb 3003 spectrofotometer. The efficiency was checked with channel-ratio correction. The other portion, 100 μl was prepared for protein measurement by the method described by *Lowry et al.* (16).

The results are expressed as CPM/mg protein. In each experiments the mean values of controls and hormone treated cultures were compared by means of the Mann-Whitney test.

Histological Procedure

In the initial histological examination performed when the cultures were set up, 15–20 fragments were studied and another 15–20 fragments were randomly selected for further study at the end of cultivation.

RESULTS

In Vitro

From Table 1 it appears that compared with the controls, cultures from five out of the six patients A, C, D, E and F showed a significantly higher thymidine uptake when cultivated with 10^{-4} M oestradiol ($p \leq 0.05$). In patient A the thymidine uptake was also stimulated by testosterone ($p \leq 0.05$). There

TABLE 1 *Effect of Hormones on the Incorporation of ³H Thymidine into Gynaecomastic Tissue from the Patients*

Patient		Control	Oestradiol 10^{-6} M	Testosterone 10^{-6} M
A	Right	538 ± 57	849 ± 83	834 ± 118
	Left	450 ± 37	831 ± 86	798 ± 39*
B		171 ± 28	160 ± 47	157 ± 32
C		743 ± 155	1094 ± 189*	714 ± 119
D		1594 ± 277	2001 ± 196	1890 ± 293
E		637 ± 83	809 ± 80*	595 ± 103
F		302 ± 90	486 ± 90*	350 ± 66

The results are expressed as *counts per min per mg protein* ± S.D. *(standard deviation)*
* $p \leq 0.05$.

was no effect of oestradiol or testosterone on the cultures from patient B. No inhibition of the thymidine uptake was seen in any of the cultures.

Histological Study

The biopsy specimens were of the appearance typical of gynaecomastia.

Histological examinations of the cultures showed that the tissue was in general well preserved after 24 hours. The cultivated fragments showed the same morphological type of cells reflecting those seen in the uncultivated histological preparation and if degenerative cytological abnormalities were observed, viz. pycnotic nuclei, necrosis and vacuolization of the cytoplasm, it was apparently not cell type specific. Furthermore, overgrowth of fibroblast-like cells was not observed.

DISCUSSION

Gynaecomastia is often seen in patients with endocrine disorders, e.g. tumours of the testis or adrenal cortex and in patients with liver diseases and Klinefelter's syndrome (9, 20). Gynaecomastia may be associated with physiological life epochs, e.g. puberty (8) and treatment with certain drugs (12, 17, 23, 25).

Oestrogen is supposed to be the most important factor in the development of gynaecomastia, but androgens and pituitary hormones (9, 11) have also been incriminated as promoting factors. Many hormone-excretion studies have been done in an attempt to elucidate the factors involved in gynaecomastia, and it has been shown that the excretion of oestrogens and 17 ketosteroids is elevated in some patients with gynaecomastia (9, 20). It has also been shown that puberty related gynaecomastia is not associated with elevated levels of steroids (11).

Various parameters have been used for assessing the effects of hormones *in vitro* (for review see 2). In this investigation the ³H TdR uptake into tissue fragments after 24 hours of cultivation was used to indicate the effects of hormones on the cell proliferation. Autoradiographic studies have shown that the incorporation of ³H TdR is restricted to nuclei of epithelial cells and not to the stroma cells (2, 3, 6, 24). It has, furthermore, been demonstrated that only the superficial cells in tissue fragments incorporate ³H TdR *in vitro* (2, 3, 6, 24) as also observed with this method (19). Obviously it is only the hormonal effect on the proliferating cells that is measured. When studies are based on scintillation counting different cellularity in the cultures can contribute to differences in the uptake of ³H TdR, but it has been shown in series of cultures each consisting of four replicates that the mean thymidine uptake did not differ significantly as measured by liquid scintillation counting (19). Different incorporation of ³H TdR in this investigation is therefore probably due to a hormonal effect on the tumour tissue.

The short term culture procedure used in this investigation has its advantages and disadvantages. The main advantages are that the risk of loosing hormone receptors during cultivation is reduced and that the selection of certain cell types is of minor importance. The main disadvantage is that the tissue may contain endogenous hormones which may reduce the effect of hormones added to the medium. The *in vitro* results presented here showed that tissue from five out of six patients was stimulated by oestrogen whereas androgen stimulation was observed in only one case. It is conceivable that various amounts of endogenous hormones in the explants may have influenced the results. This may explain the absence of *in vitro* hormonal stimulation in patient B. As far as the remaining five patients are concerned differences in endogenous tissue hormone concentrations have probably played no or a minor role, since statistically significant differences in thymidine uptake were observed in control and hormone treated cultures.

Tissue from both breasts in patient A was assayed and showed that the hormone sensitivity was identical. Here the gynaecomastia was probably induced by gonadotrophin. A direct action of gonadotrophin cannot be excluded but the results indicate that the growth of the breasts in this patient might be related to an oestrogen and androgen like action of gonadotrophin as growth stimulation of the tissue was obtained *in vitro* by these steroids. This action could be explained by an increased oestrogen and androgen production in the Leydig cells, which is known to occur in patients treated with gonadotrophin (17).

In patient D the symptom developed in relation to treatment with digitalis. The chemical similarity between cardiac glucosides and steroid hormones may be supposed to be of importance in this respect. Both steroids and glucosides contain the cyclopentanodihydrophenanthrene nucleus. It has therefore been proposed that during the metabolism of this substance changes occur in the structure imitating steroid hormones capable of stimulating the growth of the breast tissue (12). The *in vitro* results presented here showed that oestrogen was able to stimulate tissue growth whereas androgen was not. Accordingly, it seems reasonable to suggest that if some metabolic alteration of the glucoside had occurred in this patient, it was converted to an oestrogen like substance.

In patient B no effect was observed when the tissue was treated with oestrogen and androgen *in vitro*. This could be explained by a high level of endogenous hormone concentration in the tissue, but could also be consistent with the theory that puberty related gynaecomastia is not caused by steroid stimulation (11).

In patients C, E and F neither clinical nor laboratory data were obtained which allowed conclusions as to a possible causative relationship.

In patients C, D, E and F the gynaecomastia was unilateral. Clinically no abnormalities were observed in the other breast. This observation may lend support to the assumption that, in some patients, the development of gynaecomastia is not due simply to a generalized elevated hormone production. Local factors in the breast tissue resulting in a local elevation of the oestrogen level in the tissue could be involved (1).

This elevation could be produced in two ways. First, local factors in the breast capable of promoting a local elevation of the oestrogen concentration might result in increased oestrogen available for the cells. Secondly epithelial cells in the two breasts may differ as regards the concentration and utilization of oestrogen inside the cells. The *in vitro* results demonstrated that oestrogen induced a significant effect on the gynaecomastic tissue which indirectly indicates that the tissue contained oestrogen receptors, since it is now a well-documented fact that oestrogen action on target tissue is dependent on specific oestrogen receptor protein inside the epithelial cells (18).

On the basis of the *in vitro* studies reported above it seems reasonable to conclude (1) that the results support previous theories,

viz. that mainly oestrogen, but also androgen may be involved in the development of gynaecomastia (2) that drug-induced gynaecomastia is not only a direct effect of the drugs on the breast tissue but may also indirectly be due to the oestrogen action and (3) that tissue from patients with bilateral or unilateral gynaecomastia does not differ as regards oestrogen sensitivity

---

The author wishes to thank Dr *P Frederiksen* the University Institute of Pathology Aarhus Kommunehospital, for the histological examinations, Professor *S Kaae* the Radium Centre, Aarhus Kommunehospital, and Dr *P Lanart J pern* the Department of Surgery I Aarhus County Hospital, for helpful discussions in preparing the manuscript, and Mrs. *Mette Juhl* for skilful technical assistance.

REFERENCES

1 *Amtoft A* Gynækomasti. En oversigt og en kort gennemgang af 26 tilfælde. Ugeskr Læg 128 1359–1362, 1966.

2. *Aspegren K & Danielsson H* Growth quantitation of human mammary carcinoma in organ tissue culture Amer J Surg *128* 42–48, 1974

3. *Aspegren K & Håkansson L* Human mammary carcinoma studied for hormone responsiveness in short term incubations Acta chir scand *140* 95–99 1974

4 *Burstein N A., Kjellberg R N Raker J H & S hmid t H H* Human carcinoma of the breast, in vitro The effect of hormones. A preliminary report. Cancer *27* 1112–1116 1971

5 *De Souza, I Morgan L Lewis U J Raggatt P R Salih H & Hobbs J R.* Growth-hormone dependence among human breast cancers. Lancet ii. 182 184 1974

6 Finkelstein *M Geier A. Horn H Levij I S & Eser-Hadani, P* Effect of testosterone and estradiol-17β on synthesis of DNA, RNA and protein in human breast in organ culture. Int J Cancer *15* 78–90 1975

7 *Flax H Salih H Newton K A & Hobbs J R* Are some women's breast cancers androgen dependent? Lancet *i* 1204–1207 1973

8 *Haagensen C D* Diseases of the breast, 2 ed W B. Saunders Company Philadelphia, London, Toronto 1971 p 76–83

9 *Hall, P F* Gynaecomastia Australasian Medical Publishing Company Limited Glebe 1959

10 *Holmes H L & Little J M.* Tissue-culture microtest for predicting response of human cancer to chemotherapy Lancet ii 985 1974

11 *Jull J W & Dossett J A* Hormone excretion studies of gynaecomastia of puberty Brit. med. J 2 795–797 1964

12. *LeWinn E. B.:* Gynecomastia during digitalis therapy Report of eight additional cases with liver-function studies. New Engl. J Med. *248* 316–320 1953

13. *Lewis D & Hallowes R C:* Correlation between the effects of hormones on the synthesis of DNA in explants from induced rat mammary tumours and the growth of the tumours. J Endocr 62 225– 40 1974

14 *Lippman M E & Bolan G.* Oestrogen-responsive human breast cancer in long term tissue culture. Nature (Lond.) *56* 592 593, 1975

15. *Lippman M E., Bolan G & Huff K.* Human breast cancer responsive to androgen in long term tissue culture Nature (Lond.) *258* 339–341 1975

16. *Lowry O H., Rosebrough N J., Farr A L. & Randall R. J.* Protein measurement with the folin phenol reagent. J biol. Chem. *193* 265–275 1951

17 *Maddock W O & Nelson W O* The effects of chorionic gonadotropin in adult men: Increased estrogen and 17-ketosteroid excretion, gynecomastia, Leydig cell stimulation and seminiferous tubule damage. J clin. Endocr *12* 985–1014 1952.

18. *O'Malley B. W & Schrader W T.* The receptors of steroid hormones. Sci. American, Febr 1976, p 32–43

19 *Poulsen H* To be published.

20. *Rupp J Cantarow A. Rakoff A E. & Paschkis K. E.:* Hormone excretion in liver disease and in gynecomastia. J clin. Endocr *11* 688–699 1951

21 *Salih H Flax H & Hobbs J R.* In-vitro oestrogen sensitivity of breast-cancer tissue as a possible screening method for hormonal treatment. Lancet *i.* 1198–1202, 1972.

22. *Salih H Flax H Brander W & Hobbs J R.* Prolactin dependence in human breast cancers. Lancet *ii* 1103–1105 1972.

23 *Sotori C. & Veressi U.:* Gynecomastia. A review of 218 cases. Cancer *10* 645–654 1957

24 *Tchao R., Easty G C., Ambrose E J Raven R. W & Bloom H J G* Effect of chemotherapeutic agents and hormones on organ cultures of human tumours. Europ. J Cancer 4 39–44 1968.

25. *Treves N.* Gynecomastia. The origins of mammary swelling in the male An analysis of 406 patients with breast hypertrophy 525

with testicular tumors and 13 with adrenal neoplasms. Cancer *11* 1083–1107 1958.
26 *Turkington R H* Hormonal regulation of cell proliferation in breast cancer cells in vitro. N Y St J Med Oct. 15 2649–2655 1969
27 *Turkington R H* & *Hill R* Hormonal dependence of DNA synthesis in mammary carcinoma cells in vitro. Science *160* 1457–1459 1968.

Acta path. microbiol. scand. Sect. A, 85: 25–32, 1977

INTIMAL PITS OF AORTA IN RABBITS IMPRINTS OF VORTICES OF BLOOD FLOW?

Einar Svendsen and Leif Jørgensen

Institute of Medical Biology, Morphological Section, University of Tromsø, Tromsø, Norway

Svendsen, E. & Jørgensen, L. Intimal pits of aorta in rabbits. Imprints of vortices of blood flow? Acta path. microbiol. scand. Sect. A, 85: 25–32, 1977.

Scanning electron microscopy of rabbit aorta showed that the intimal folds had a regular linear pattern in areas of expected laminar flow. In areas of expected vortex formation, however, there was deviation of the fold pattern with the formation of rounded depressions or pits in the intimal surface. Platelet depositions were found in connection with some of the pits. In sections for light microscopy the pits corresponded to small areas of flattened folds of the innermost elastic membranes. It is concluded that the intimal pits probably reflect imprints of vortices of the whirling blood.

Key words: Aorta; intimal folds; electron microscopy; rabbit.

E. Svendsen, Institute of Medical Biology, University of Tromsø, Box 977, 9001 Tromsø, Norway.

Received 28.iii.76 Accepted 1.ii.76

It is well-known that the intimal folds created by the internal elastic membrane of arteries are parallel with the direction of blood flow. Furthermore the long axis of the endothelial cells are orientated in the same direction (4).

Flow-chamber models of arteries have shown fluid boundary layer separation with vortex formation at certain predilectional sites, i.e. at bifurcations, branches, and bends (1, 5, 7, 11).

The problem is whether such vortices occur in arteries *in vivo* and whether they are sufficiently enduring to create a different pattern in direction of folds. The present study was aimed at answering the latter question by means of scanning electron microscopy of rabbit aorta.

MATERIAL AND METHODS

Twenty rabbits of the white New Zealand and Dutch strain, weighing about 3.5 kg each, were used.

The animals were killed by an overdose of mebumal (Nembutal, Abbott) through an ear vein. The thorax and abdomen were rapidly opened, and the aorta dissected free and opened longitudinally along the ventral aspect. The aorta was rinsed in Tyrode solution and specimens for scanning electron microscopy and light microscopy were taken from the distal part of the lesser curvature of the aortic arch, from the area between neighbouring ostia of the intercostal arteries on the same side, and from the area at and lateral to these ostia, as shown in Fig. 1. The whole procedure was completed within 15 minutes.

The specimens for scanning electron microscopy were fixed in 2 per cent glutaraldehyde for 2 hours, dehydrated in increasing concentrations of alcohol and dried in a Hitachi critical point dryer. The specimens were glued on to metal stubs with conducting paint (Ladd Research Industries, Inc., Burlington, Vermont, USA) and covered by a thin layer of gold using a scanning electron microscopy sputtering coating unit (E 5000 Polaron Equip-

with testicular tumors and 13 with adrenal neoplasms. Cancer *11* 1085–1107 1958.

26 *Turkington R W* Hormonal regulation of cell proliferation in breast cancer cells in vitro. N Y St J Med., Oct. 15 2649 2655 1969

27 *Turkington R W & Hill R.* Hormonal dependence of DNA synthesis in mammary carcinoma cells in vitro. Science *160* 1457 1459 1968.

Acta path. microbiol. scand. Sect. A, 85 25–32, 1977

INTIMAL PITS OF AORTA IN RABBITS IMPRINTS OF VORTICES OF BLOOD FLOW?

EINAR SVENDSEN and LEIF JØRGENSEN

Institute of Medical Biology Morphological Section, University of Tromsø Tromsø, Norway

Svendsen, E. & Jørgensen, L. Intimal pits of aorta in rabbits Imprints of vortices of blood flow? Acta path. microbiol. scand. Sect. A, 85 25–32, 1977

Scanning electron microscopy of rabbit aorta showed that the intimal folds had a regular linear pattern in areas of expected laminar flow In areas of expected vortex formation, however there was deviation of the fold pattern with the formation of rounded depressions or pits in the intimal surface Platelet depositions were found in connection with some of the pits. In sections for light microscopy the pits corresponded to small areas of flattened folds of the innermost elastic membranes. It is concluded that the intimal pits probably reflect imprints of vortices of the whirling blood

Key words Aorta intimal folds electron microscopy rabbit.

E. Svendsen, Institute of Medical Biology University of Tromsø Box 977 9001 Tromsø, Norway

Received 28 m 76 Accepted 1 n.76

It is well-known that the intimal folds created by the internal elastic membrane of arteries are parallel with the direction of blood flow Furthermore, the long axis of the endothelial cells are orientated in the same direction (4)

Flow-chamber models of arteries have shown fluid boundary layer separation with vortex formation at certain predilectional sites, i.e. at bifurcations, branches, and bends (1 5 7 11)

The problem is whether such vortices occur in arteries *in vivo* and whether they are sufficiently enduring to create a different pattern in direction of folds. The present study was aimed at answering the latter question by means of scanning electron microscopy of rabbit aorta.

MATERIAL AND METHODS

Twenty rabbits of the white New Zealand and Dutch strain, weighing about 5.5 kg each, were used.

The animals were killed by an overdose of mebumal (Nembutal, Abbott®) through an ear vein. The thorax and abdomen were rapidly opened, and the aorta dissected free and opened longitudinally along the ventral aspect. The aorta was rinsed in Tyrode solution and specimens for scanning electron microscopy and light microscopy were taken from the distal part of the lesser curvature of the aortic arch, from the area between neighbouring ostia of the intercostal arteries on the same side, and from the area at and lateral to these ostia, shown in Fig. 1 The whole procedure was completed within 15 minutes.

The specimens for scanning electron microscopy were fixed in 2 per cent glutaraldehyde for 2 hours, dehydrated in increasing concentrations of alcohol and dried in a Hitachi critical point dryer. The specimens were glued on to metal stubs with conducting paint (Ladd Research Industries, Inc., Burlington, Vermont, USA) and covered by a thin layer of gold using a scanning electron microscopy sputtering coating unit (E 5000 Polaron Equip-

with testicular tumors, and 13 with adrenal neoplasms Cancer *11* 1083-1102, 1958

26 *Turkington R H* Hormonal regulation of cell proliferation in breast cancer cells in vitro. N Y St. J Med., Oct. 15 2649-2655 1969

27 *Turkington R H* & *Hilf R* Hormonal dependence of DNA synthesis in mammary carcinoma cells in vitro. Science *160* 1457 1459 1968.



Fig 6 An area of rabbit aorta lateral to the ostium of an intercostal artery with a pit (P) with a smooth bottom. At the edge a platelet thrombus (PLT) 450 ×

folds of the innermost elastic membrane, limited to both sides by somewhat elevated folds, often closely packed (Figs. 8 and 9) The elastic membrane just outside could show a similar but less pronounced pattern (Figs. 8 and 9) Between the two membranes there appeared to be an oedematous zone, the width of which varied with the fold patterns described (Figs. 9 and 10)

In some of the pits the elastic membranes appeared interrupted (Fig. 8) Endothelial cells could be lacking or partly detached from the surface corresponding to the pits and the adjacent folds (Fig. 10)

The depth of the pits corresponded to the maximum hight of the folds of the innermost elastic membrane or it might be a little deeper There was no obvious depression of the medial structures external to the second elastic membrane, and the muscle cells underneath appeared normal.

Fig 4 An area of the lesser curvature of the rabbit aortic arch showing two partly confluent pits (P) The height of the intimal folds (FL) becomes reduced as the folds extend into the bottom of the pits. Lateral to the pits (arrow) the endothelial folds seem packed together and are narrower 200 ×

Fig 5 An area of the lesser curvature of the rabbit aortic arch with two pits (P) separated by 8–9 compressed folds (FL) The endothelium on these folds appears to be lacking, but it remains at the bottom of the pits where it show a large number of bridge-like structures 450 ×

DISCUSSION

This study shows that in areas of rabbit aorta where linear flow was to be expected—between the ostia of the intercostal arteries (10 11)—the folds formed a more regular linear pattern, parallel with the long axis of the vessel. In areas where vortices were to be expected (5 7 10 11) the pattern of the intimal folds were altered. The height of the folds here was reduced and rounded, shallow depressions or pits were formed in the intimal surface

Peripheral to the pits, groups of folds which

P
P
F
A
P
F
P
5

were narrower curved and appeared compressed were seen. It is possible that the pits correspond to vortices of blood flow where centrifugal forces have acted on the intimal folds, with the result that some folds were deviated and the pits formed by a levelling of the height of the folds at the center of the vortex?

The presence of platelets and platelet aggregates at the edge of the pits supports this theory since platelets are known to be deposited as a result of this type of flow disturbance (6) Furthermore there were signs of endothelial damage in the form of endothelial cell loss and bridge like structures (14 15) Both platelet deposition and endothelial cell injury are thought to occur at the same predilectional sites as vortices (8, 9 10 12)

The pits described in this paper do not seem to have any relation to the depressions reported by *Duff et al.* (3) who depicted a depression of rabbit intimal surface said to be caused by medial degeneration. In our material there were no signs of medial alterations underneath the pits.

Weber & Ton (16) described depressions of the aortic intima of the guinea-pig and the rabbit equivalent to the pits reported in this paper They interpreted their findings as effects of cholesterol feeding, however and they did not mention how the lesions were distributed. In a series of experiments including short term cholesterol feeding of rabbits, scanning electron microscopy has so far revealed that occurrence and distribution of pits is the same as in rabbits fed regular low-fat diet (15) It is therefore questionable whether cholesterol feeding does influence the formation of pits.

Finally we conclude that, at certain predilectional sites, the intimal surface of rabbit aorta shows deviation of the fold pattern with formation of shallow pits. It is reasonable to consider these pits as imprints made by whirling blood.

Fig 7 Cross section of rabbit aorta from the area between two ostia of intercostal arteries on the same side. The intimal folds show only a moderate irregularity with no typical pits Victoria-blue stain 425 ×

Fig 8 Cross section from the distal part of the lesser curvature of the arch of rabbit aorta A pit is formed by the two innermost elastic membranes. At the bottom of the pit the elastic membranes are stretched and partly disrupted (arrow) The lateral crests consist of compressed intimal folds. Victoria-blue stain 1800 ×

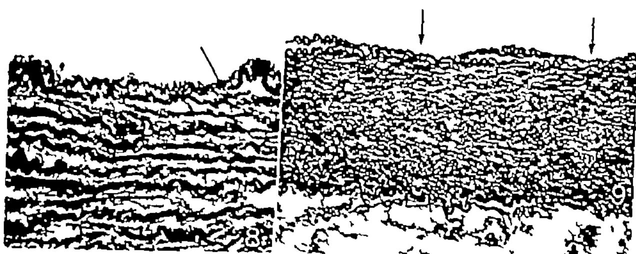
Fig 9 Cross section of rabbit aorta from area lateral to an intercostal artery Two pits (arrows) with smooth bottoms and typical edges consisting of compressed folds are seen The tissue between the two innermost elastic membranes is loose, probably indicating oedema Haematoxylin-eosin stain 720 ×

Fig 10 Cross section of rabbit aorta lateral to an intercostal artery A small pit with tall edges is shown There seems to be oedema between the two innermost elastic membranes In the lumen adjacent to the bottom of the pit apparently desquamated endothelial cells are seen Haematoxylin-eosin stain. 2000 ×

REFERENCES

1 *Aschoff L.* Thrombose und Sandbankbildung. Beitr Path. Anat. 52 203–212, 1912.
2. *Chisholm G M Gainer J L & Stoner G E.* SEM (Scanning electron microscope) studies of aortic structure Angiologica 10 10–14 1973
3 *Duff G Lyman, M Millan G C & Ritchie A C* The morphology of early atherosclerotic lesions of the aorta demonstrated by the surface technique in rabbits fed cholesterol. Amer J Path. 33 845–873 1957
4 *Flaherty J T Pierce J E, Ferrans V J, Patel, D J Tucker W K & Fry D L* Endothelial nuclear patterns in the canine arterial tree with particular reference to hemodynamic events Circ Res 30 23–33, 1972.
5 *Fox J A & Hugh A E* Localization of atheroma A theory based on boundary layer separation. Brit. Heart J 28 388–399 1966
6. *Goldsmith H L.* Motion of particles in a flowing system. Thrombos Diathes. Haemorrh. Suppl 40 91 109 1970
7 *Gutstein W H Farrel, G A & Armellini C.* Blood flow disturbance and endothelial cell injury in preatherosclerotic swine Lab. Invest. 29 134 149 1973
8 *Jorgensen L, Packham M A Rowsell H C & Mustard J F.* Deposition of formed elements of blood on the intima and signs of




8
9


10

CARDIAC HAEMANGIO-ENDOTHELIOSARCOMA

Review of the Literature and Report of a Case

OTTO GRØNTOFT and HENRIK HELLQUIST

Department of Pathology I, Linköping University, Sweden

Grøntoft, O. & Hellquist, H. Cardiac haemangio-endotheliosarcoma. Review of the literature and report of a case. Acta path. microbiol. scand. Sect. A, 85: 33–41, 1977.

A case of primary haemangio-endotheliosarcoma of the right atrium is reported. A review of the literature is given and in all but four of the 56 cases, the tumour originates in the right atrium projecting into the cavity. This explains why these tumours present a rather uniform clinical picture characterized by superior vena caval syndrome combined with pericardial effusion, cardiomegaly, dyspnoea and chest pain. A male dominant sex distribution of 3 to 1 is found. The tumour is highly malignant and has caused death within an average of six months. We emphasize the possibility of early diagnosis particularly since the clinical symptoms are rather typical and cases are reported where therapy apparently was successful.

Key words: Heart neoplasm; haemangio-endotheliosarcoma.

O. Grøntoft, Department of Pathology I, Linköping University, Linköping, Sweden.

Received 28.11.76 Accepted 10.ix.76

The primary cardiac tumour first to be reported in the literature was, according to *Fletcher* (16), described by *Columbus* in 1559 (11). In 1951 *Prichard* (45) reviewed 415 cases of cardiac neoplasm discovered at autopsy. Today more than 850 cases are published (1–60).

Generally about 50 per cent of all primary cardiac tumours are myxomas and about 20 per cent are sarcomas. The present study, which include a report of a new case of haemangioendotheliosarcoma, reveals that this tumour is located to the right atrium and combined with the superior vena caval syndrome. This tumour is, together with rhabdomyosarcoma, the most frequent malignant tumour of the heart (58).

CASE REPORT

A 68-year-old femal was admitted to the University Hospital, Linköping, in November 1974 with a seven-week history of cough, general weakness, fever and progressive dyspnoea. On examination she appeared ill, was pale and cyanotic and presented superior vena caval syndrome. The sedimentation rate was 40 to 80 millimeters per hour, serum lactic dehydrogenase was 600 and Haemoglobulin 9.3 to 10.9 gr per cent. Two chest X rays revealed gross cardiomegaly (890 ml/m² and 1090 ml/m²). Aortographs and cavographs showed massive pericardial effusion and an expansive process just above the right atrium. Two pericardiocenteses were performed and 1,200 ml of blood-tinged fluid was obtained. No malignant cells were found. The patient's condition deteriorated progressively and she died in January 1975.

Autopsy

The heart was enlarged and weighed 480 grams (0.7 per cent of the total weight). The pericardial

intimal injury in the aorta of rabbit, pig and man Lab Invest. *27* 341–350 1972
9 *Jørgensen L. Hærem J W & Moe N* Platelet thrombosis and non-traumatic intimal injury in mouse aorta Thromb. Diathes. Haemorrh *29* 470–489 1973
10 *Murphy E A Rowsell H C Downie H G Robinson G A & Mustard J F* Encrusta tion and atherosclerosis The analogy between early in vivo lesions and deposits which occur in extracorporeal circulations. Canad Med. Ass. J *87* 259–274 1962
11 *Mustard J F Rowsell H C Robinson G A Geissinger H D Downie H G & Murphy E A* Role of blood platelets in the etiology of myocardial infarction In *James T N & Keyes J W* (Ed.) The Etiology of Myocardial infarction. J & A Churchill Ltd., London 1963 p 624–644
12 *Packham M A Rowsell H C Jorgensen L. & Mustard J F* Localized protein accumulation in the wall of aorta. Exp Mol. Path. 7 214–232 1967
13 *Shimamoto T Yamashita Y Numano F & Sunaga T* Scanning and transmission electron microscopic observation of endothelial cells in normal condition and in initial stages of atherosclerosis. Acta Path. Jap *21* 93–119 1971
14 *Sunaga, T Shimamoto T & Nelson E* Correlated scanning and transmission electron microscopy of arterial endothelium. Pp 459–463 in Part III Scanning Electron Microscopy/1973 Proc Workshop Scan. Electr Micr in Path., ITT Research Inst., Chicago, Ill., 1973
15 *Svendsen E. & Jørgensen L.* Unpublished observations, 1976
16. *Weber G & Tosi P* Some observations with scanning electron microscope on the development of cholesterol aortic atherosclerosis in the rabbit Path Europ *6* 407–414 1971

Acta path. microbiol. scand. Sect. A, 85: 33–41, 1977

CARDIAC HAEMANGIO-ENDOTHELIOSARCOMA

Review of the Literature and Report of a Case

OTTO GRÖNTOFT and HENRIK HELLQUIST

Department of Pathology I, Linköping University, Sweden

Gröntoft, O. & Hellquist, H. Cardiac haemangio-endotheliosarcoma. Review of the literature and report of a case. Acta path. microbiol. scand. Sect. A, 85: 33–41, 1977.

A case of primary haemangio-endotheliosarcoma of the right atrium is reported. A review of the literature is given and in all but four of the 56 cases, the tumour originates in the right atrium projecting into the cavity. This explains why these tumours present a rather uniform clinical picture characterized by superior vena caval syndrome combined with pericardial effusion, cardiomegaly, dyspnoea and chest pain. A male dominant sex distribution of 3 to 1 is found. The tumour is highly malignant and has caused death within an average of six months. We emphasize the possibility of early diagnosis particularly since the clinical symptoms are rather typical and cases are reported where therapy apparently was successful.

Key words: Heart neoplasm; haemangio-endotheliosarcoma.

O. Gröntoft, Department of Pathology I, Linköping University, Linköping, Sweden.

Received 28.ii.76. Accepted 10.ix.76.

The primary cardiac tumour first to be reported in the literature was, according to *Fletcher* (16), described by *Columbus* in 1559 (11). In 1951 *Prichard* (45) reviewed 415 cases of cardiac neoplasm discovered at autopsy. Today more than 850 cases are published (1–60).

Generally about 50 per cent of all primary cardiac tumours are myxomas and about 20 per cent are sarcomas. The present study which include a report of a new case of haemangioendotheliosarcoma, reveals that this tumour is located to the right atrium and combined with the superior vena caval syndrome. This tumour is, together with rhabdomyosarcoma, the most frequent malignant tumour of the heart (58).

CASE REPORT

A 68-year-old femal was admitted to the University Hospital, Linköping, in November 1974 with a seven-week history of cough, general weakness, fever and progressive dyspnoea. On examination she appeared ill, was pale and cyanotic and presented superior vena caval syndrome. The sedimentation rate was 40 to 80 millimeters per hour, serum lactic dehydrogenase was 600 and Haemoglobulin 9.3 to 10.9 gr per cent. Two chest X-rays revealed gross cardiomegaly (890 ml/m² and 1090 ml/m²). Aortographs and cavographs showed massive pericardial effusion and an expansive process just above the right atrium. Two pericardiocenteses were performed and 1,200 ml of blood-tinged fluid was obtained. No malignant cells were found. The patient' condition deteriorated progressively and she died in January 1975.

Autopsy

The heart was enlarged and weighed 480 grams (0.7 per cent of the total weight). The pericardial



Fig 1 Haemangio-endotheliosarcoma in the right atrium with epicardial metastases.

cavity contained 1 400 ml haemorrhagic fluid A 9 by 6 by 4 cm large severely haemorrhagic, tumour was attached to the right atrial wall projecting into the atrial cavity The tumour was also infiltrating the upper parts of the right ventricle (Figure 1) About 30 per cent of the right atrial cavity was occupied by the tumour which also enclosed the right coronary artery though without constriction of the lumen of the vessel (Fig ?)

1) Numerous haemorrhagic tumour nodules were found in the subepicardial adipose tissue and the superior vena cava was surrounded by large matted nodules causing a slight narrowing of the vessel (Fig 1) A thrombus of three cm in length was also noticed at the orifice of the superior vena cava (Fig 2) Examinations revealed widespread dissemination of the tumour throughout the lungs, pleuras, liver kidneys, brain and bones, all of a strikingly haemorrhagic appearance

Histology

Sections from numerous blocks were stained with H & E, elastin van Gieson mixture PTAH PAS FE-stain, Laidlaw's reticulin and by Masson's trichrome method The tumour rich in vessels, infiltrated the atrial myocardium and showed areas with extensive haemorrhagic necroses. The tumour cells were small with round to spindleshaped hyperchromic nuclei and sparse cytoplasm (Fig 3) The cellular pleomorphism and mitotic activity were of moderate degree. The cells were fairly well arranged in numerous intercommunicating channels containing erythrocytes (Figs. 4 & 5) These anastomosing vascular channels were lined by one or more layers of swollen anaplastic endothelioblasts sometimes filling up the vascular lumen. The silver stained slides showed the vascular pattern to the best advantage the tumour cells being seen inside the delicate reticulin sheath. The tumour was rich in iron pigment. In PTAH-stained slides, no cross striations could be observed The nodules in all other organs were of a histological structure as those in the tumour in the heart. No epithelial malignant tumour was found any organ in the body



Fig 2 Haemangio-endotheliosarcoma involving the right atrium. A thrombus is seen above the intracavitary projecting part of the tumour

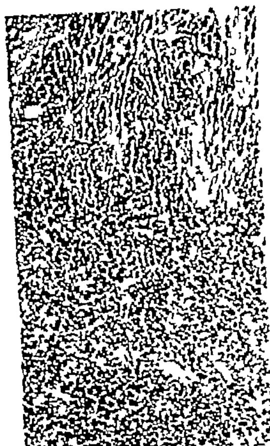


Fig. 3 Photomicrograph showing the aggressive nature of haemangio-endotheliosarcoma. The myocardium is widely invaded by the tumour (H & E, × 10)



Fig. 4 Photomicrograph showing the vascular structure of the tumour (H & E, × 40)

DISCUSSION

The diagnoses seriously considered included haemangioendotheliosarcoma the different types of rhabdomyosarcoma, malignant mesenchymoma, haemangiopericytoma, reticulum cell sarcoma, fibrosarcoma and metastatic carcinoma. On the basis of the morphology and the reticulin staining, the five last mentioned diagnoses can be excluded. To differentiate between haemangio-endotheliosarcoma and rhabdomyosarcoma, particularly that of the alveolar type, may be more difficult. Despite the fact that a rhabdomyosarcoma may be rich in vessels and do not always show cross striations in the tumour cells (53) the morphological picture was not identical with that of this tumour. The richness of irregular anastomosing vascular channels containing erythrocytes and lined by one or more layers of atypical endothelial cells often of immature appearance dominated the histological picture. This fact combined with the gross appearance and the similarity to cases published earlier support the diagnosis of haemangio-endotheliosarcoma. Table 1 gives a review of the patho-anatomical and clinical features in 55 previously reported cases (1–10, 12–26, 28–44 46–51 54 57 60) The site of primary involvement is almost exclusively the right atrium (Table 1) It is therefore not surprising that the clinical picture is rather uniform, including superior vena caval obstruction, pericardial effusion and cardiomegaly Cardiac sarcomas are more common on the right side of the heart, but no other type of sarcoma (58 59) is so strictly located to the right atrium as haemangio-endotheliosarcoma. Therefore, they generally give less characteristic clinical symptoms in the form of shortness of breath, chest pain, fever and cough (52) The 56 cases of haemangio-endotheliosarcoma (Table 1) represent patients of age averaging 41 years. Eight patients were less than 25 years old (2, 3 6 34 40 46, 57 60) and development of the tumour was three times as common in men as in women. This tum-

TABLE 1 *Main Symptoms and Findings*

Author	Ref	Primary site	Metastases
Aegerter E. & Peale A. R.	1	RA	+
Aikat, B & Nirodi N S	2	RA	+
Allaire, F J et al	3	RA	+
Amsterdam H J et al	4	RA	0
Berlov G A & Pigarev Yu. G	5	P	0
Blanchard A. J & Hetherington H	6	RA	+
Blanchard, A. J & Hetherington, H	6	RA	+
Brandenburg, R. O & Edwards J E.	7	RA	0
Bruzzone, P L. & Guglielmini, G	8	RA	0
Cheng T & Sutton D C.	9	RA	+
Choisser R M & Ramsey E. M	10	RA	+
Choisser R. M & Ramsey E M	10	RA	−
Contrearas, R.	12	RA (P)	+
Crenshaw J F et al	13	RA	+
Da Cunha Motta, L.	14	RA	+
Deloach, F J & Haynes, J W	15	RA	+
Florange, W	17	P	+
Freeland, J et al	18	RV	+
Freeland J et al	18	RA	+
Gelfand, M.	19	P	0
Glancy D L. et al	20	RA	+
Glassy F J & Massey F C.	21	RA	+
Greenberg M. & Angrist, A.	22	P	0
Gross, P & Englehart, C. E.	23	LA	0
Grosse-Brockhoff F & Schreiber H W	24	RA	0
Gröntoft, O & Hellquist, H *		RA	+
Gödel A.	25	RA	+
Hager W et al.§	26	LA	0
Harris, H. R.	28	RA	0
Hewer T F & Kemp R P	29	RA	+
Himmel A. et al	30	RV	+
Hollingsworth, J H. & Sturgill B C.†	31	P (RA)	0
Ito, Y	32	RA	0
Jucker P	33	RA	+
Kauder H et al.	34	RA	0
Kogan, R. P	35	RA	+
Kovalenko V L.	36	RA	+
Kurashova, M. V et Kogan, R P	37	RA	+
Lange H F et Christiansen, T	38	RV (RA, P)	+
Lukash, W M et al	39	RA	+
Lübschitz, K. et al.	40	RA	0
McNalley M C. et al	41	RA	+
Otsuki Y et al.	42	RA	−
Patt, Y et al.	43	RA	+
Penneman, G	44	LA	−
Redtenbacher L.	46	RA (P)	+
Reininger J A. et al.	47	RA	0
Robinson, D S & Machanic, P B	48	RA	+
Scheidegger S	49	P	+

Cases of Cardiac Haemangio-Endotheliosarcoma

t	Age	Sex	Obstruction of the venous inflow to the right heart	Cardiomegaly on X-ray	Haemopericardium	Duration of symptoms (months)
	60	M	+	−	+	−
	15	M	+	+	+	1
	24	M	+	+	+	8
	54	M	+	+	−	8
	33	M	+	−	+	5
	25	M	+	+	+	4
	33	M	+	+	Oblit. (+)	4
	35	M	+	+	+	24
	27	M	0	0	+	−
	45	M	+	+	−	1 2
	26	M	+	+	Oblit. (+)	2
	30	M	+	+	+	1 5
	43	M	+	+	+	−
	38	F	−	−	Oblit. (+)	6
	46	M	−	−	Oblit. (+)	−
	46	M	+	−	Oblit. (+)	8
	47	M	−	−	Oblit. (+)	5
	34	M	−	+	+	5
	76	M	+	+	+	5
	38	M	+	+	+	5
	35	F	0	0	Oblit. (+)	4
	26	M	+	+	Oblit. (+)	4
	27	M	+	+	Oblit. (+)	4
	45	F	0	−	Normal	−
	29	F	+	0	+	15
	68	F	+	+	+	4
	44	M	+	−	Oblit. (+)	1 5
	45	F	+	+	+	−
	52	F	+	−	+	0 5
	62	F	0	−	+	6
	46	M	+	+	+	−
	59	F	−	−	+	−
	41	M	−	−	−	1
	40	M	0	+	Oblit. (+)	9
	24	M	−	+	+	5
	39	F	+	−	Oblit. (+)	−
	32	M	−	−	−	4
	39	F	+	−	+	−
	47	M	0	+	+	2
	25	F	+	+	+	5
	23	F	+	+	+	21
	43	M	+	+	+	3
	69	F	−	−	−	1
	36	M	0	+	+	4 5
	70	F	−	−	−	−
	22	M	+	−	+	4
	45	M	+	+	+	1 2
	68	M	+	+	+	1
	44	M	+	+	+	6

Author	Ref	Primary site	Metastre
Schwartz, N H & Loder M	50	RA	+
Schwartzkopf H & Gais H	51	RA	0
Svedja J et al	54	RA	+
Tacket, H S	55	RA	+
Tatsumi T et al	56	RA (RV)	+
Tse R. & Frank M N	57	RA	+
Wight R P et al	60	RA	–

+ = present 0 = absent
– = insufficient information * = present case
§ = at the time of publication three years after the diagnosis had been confirmed the patient was still alive
† = at the time of publication ten months after the diagnosis had been confirmed the patient was still alive

our is highly malignant leading to death within six months on the average Despite the short interval of time between the first appearance of symptoms and death over 65 per cent oft the patients had extracardiac metastases. The metastases were most frequently localized to the lungs, liver thoracic lymphatic nodes bones and adrenals.

The diagnoses of primary haemangio-endotheliosarcoma of the heart were established ante mortem only on seven occasions (3 9 26 31 33 38 40) Two reports are available according to which treatment apparently had been successful (26 31) Haemangio-endotheliosarcoma of the heart should be kept in mind whenever a patient presents a



Fig 5 Photomicrograph showing numerous ascular structures lined by atypical endothelial cell In the vascular channel many erythrocytes are seen (H & E, × 100)

…ntinued)

Age	Sex	Obstruction of the enous inflow to the right heart	Cardiomegaly on X-ray	Haemopericardium	Duration of symptoms (months)
57	M	+	+	+	23
32	F	+	+	+	2
46	M	−	+	+	6
45	F	+	0	+	4
46	M	−	−	−	—
16	F	+	+	+	13
25	M	−	−	+	0.5

RV = right entricle LV = left entricle RA = right atrium LA = left atrium P = pericardium F = female M = male Oblit. = obliterated.

superior vena caval syndrome combined with haemopericardium, cardiomegaly dyspnoea and chest pain.

REFERENCES

1 *Aegerter E. & Peale A R.* Kaposi's sarcoma. A critical survey Arch Path. 34 413–422, 1942.

2 *Asbat B & Narula N S* Angiosarcoma of the heart. J Path *104* 73–75 1971

3 *Allaire F J Grimm, C A Taylor L M & Pfaff J P* Primary hemangioendothelioma of the heart Rocky Mtn. Med. J *61* 34–37 1964

4 *Amsterdam H J Grayzel, D M & Levine, A L* Hemangio-endothelioblastoma of the heart Am Heart J *37* 291–300 1949

5 *Berlin G A. & Pigarev Y G* A peculiar form of systemic tumour-like angiomatous (malignant hemangiothelioma of the pericardium, angiomatous polyp of the endocardium and progress. hemangiomatosis of the liver) Arkh. Pat 26 74 78 1964

6 *Blanchard A J & Hetherington H* Malignant hemangio-endothelioma of the heart. Canad. M A. J 66 147 150, 1952

7 *Brandenburg, R O & Edwards J E.* Cardiac sarcoma Report of a case and comparison with case of metastatic carcinoma of the pericardium Proc. Staff Meet. Mayo Clin 29 437 446 1954

8. *Bracesco P L & Guglielmini G* Immagini anatomoradiologiche cutanali del diaframma di destra dell' angolo cardio-frenico (Pseudoernia del diaframma angiosarcoma del cuore) Minerva Med. *1* 968–976, 1931

9 *Cheng T & Sutton D C* Primary hemangioendotheliosarcoma of the heart, diagnosed by angiocardiography Review of the literature and report of a case. Circulation *11* 456–461 1955.

10. *Cheater R M & Ramsey E. M* Angioreticuloendothelioma (Kaposi's disease) of the heart, Am. J Path. *15* 155–178, 1939

11 *Columbus M R.,* De Re Anatomica, Libri XV Venetiis. Ex typog. N Bevilacquae, p 268 1559

12. *Contreras R.,* Angiosarcoma de Kaposi primario del corazón revisión de la literatura y descripción del sexto caso Arch. Inst. Cardiol. México 27 465–479 1957

13 *Crenshaw J F., Dowling, E. A & Crowell W F Jr.,* Primary hemangio-endothelioma of the heart. Ann. Int. Med. 50 1289–1298, 1959

14 *De Cunha Motta, L.:* Hemangio reticulo-endothelioma. Ann. Fac. Med. Sao Paulo *17* 647–649 1941

15 *Deloach, F J & Haynes J W.,* Secondary tumours of the heart and the pericardium. Review of the subject and report of 137 cases. A.M.A. Arch Int. Med. *91* 224–249 1953

16. *Fletcher F H* Primary Cardiac Tumours. A review of cases at the State University of Iowa Hospitals since 1950 J of Iowa Med. Soc. *53* 545–550 1963

17 *Florange H.,* Über die Beobachtung eines angioplastischen Sarkoms des perikards zugleich ein Betrag zur Frage des ausgangsortes der Sarkome des Herzbeutels. Zentralbl. allg. Path. *91* 413–417 1954

18 *Freeland J P., Sy B. G., Ablaza, M S & Dumee G.:* Hemangiosarcoma of the heart. Chest *60* 222 224 1971

19. *Gelfand M.:* Kaposi's hemangiosarcoma of the heart. Brit. Heart. J *19* 290–292, 1957

20. *Glancy D L., Morale J B., J., & Roberts W C.,* Angiosarcoma of the heart. Am. J Cardiol. *21* 413–419 1968

Author	Ref	Primary site	Metastases
Schwartz, N H & Loder M	50	RA	+
Schwartzkopf H & Gais, H	51	RA	0
Svedja, J et al	54	RA	+
Tacket, H S	55	RA	+
Tatsumi T et al	56	RA (RV)	+
Tse R. & Frank, M. N	57	RA	+
Wight, R. P et al	60	RA	–

\+ = present. 0 = absent.
– = insufficient information. * = present case
§ = at the time of publication three years after the diagnosis had been confirmed the patient was still alive
† = at the time of publication ten months after the diagnosis had been confirmed the patient was still alive

our is highly malignant ledaing to death within six months, on the average Despite the short interval of time between the first appearance of symptoms and death over 65 per cent oft the patients had extracardiac metastases The metastases were most frequently localized to the lungs liver thoracic lymphatic nodes, bones and adrenals.

The diagnoses of primary haemangio-endotheliosarcoma of the heart were established ante mortem only on seven occasions (3 9 26 31 33 38, 40) Two reports are available according to which treatment apparently had been successful (26 31) Haemangio-endotheliosarcoma of the heart should be kept in mind whenever a patient presents a

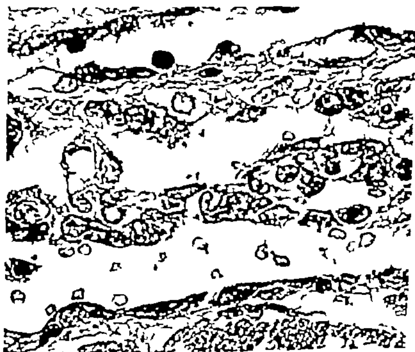


Fig 5 Photomicrograph showing numerous vascular structures lined by atypical endothelial cells In the vascular channel many erythrocytes are seen (H & E, × 100)

heart. First reported case in an adolescent. Angiology 22 147–152 1971
58. *Turiaf J., Battesti, J P Basset F & Iris, L.* Sarcome musculaire du coeur. Le Poumon et le Coeur T XXII 8 895–910 1966.
59. *Wharton, C M.*, Primary malignant tumour of the heart. Report of a case. Cancer 2 245 1949
60 *Wright R. P., McCall, M M & Wenger N K.* Primary atrial tumor Evaluation of clinical findings in ten cases and review of the literature. Am. J Cardiol. *11* 790–797 1963

Glassy F J & Massey F C Primary hemangioendothelial sarcoma of the heart. Am. J Med *8* 544–551 1950
Greenberg M & Angrist A Primary vascular tumours of the pericardium A report of two cases. Am Heart J *35* 623–634 1948
Gross P & Englehart C E. Primary hemangioendothelioma of the heart. Report of a case Am. J Cancer *30* 102–107 1937
Grosse Brockhoff F & Schreiber H H Angiosarkom des Herzbeutels. Zschr Kreislaufforsch. *44* 866–878, 1955
Gödel A Zur Kenntnis der primären Herzgeschwülste Zentrabl Herz & Gefässkr *14* 99–106 1922
Hager H Kremer K & Müller H Angiosarcoma of the heart. Deutsche Med. Wochenschrift *95* 680–684 1970
Hagström L. Malignant Mesenchymoma in pulmonary artery and right ventricle Acta Path et Microbiol Scandinav 51 87–94 1961
Harris H R Angiosarcoma of the heart J Clin Path *13* 205–209 1960
Hewer T F & Kemp R P Malignant hemangioendothelioma of the heart Report of a case. J Path. & Bact. 43 511–515 1936
Himmel A Gronowsky J Kuczyński F & Zgliczyński L Hemangio-endothelioma of the heart. Pol Arch Med *24* 795–806 1954
Hollingsworth J H & Sturgill B C Treatment of primary angiosarcoma of the heart Am. Heart J 78 254–258 1969
Ito Y Hemangioendothelioma of the heart. Report of a case and review of the literature. J Jap Soc Intern. Med 1235–1242 1964
Jucker P Die diagnose der primären Bösartigen Geschwulste der Perikards und der das Perikard infiltrierenden Herzwandtumoren. Zschr Klin. Med. *139* 208–225 1941
Kander H & Müller S Angioblastisches Sarkom des Herzens Thoraxchirurgie *16* 214–220 1968
Kogan R P (Tumors of the heart) Arkh Pat. *19* 66–70 1957
Kovalenko F L. Malignant hemangioendothelioma of the heart with lung metastases Voprosy Onkologii *11* 90–91 1965
Kurashova M I & Kogan R P (Angiosarcoma of the heart) Klin. Med *34* 77–79 1956
Lange H F & Christiansen T Hemopericardiumangiosarcom cordis. Acta med. Scand *127* 107–115 1947
Lukash H M Schneider P J & Sennett C O Angiosarcoma presenting as acute rheumatic pancarditis. J A M A. *193* 975–976, 1965
Lübschitz K Lundsteen E & Forchhammer E. Primary malignant heart tumor diagnosed in vivo with the aid of artificial pneumopericardium Radiology *52* 79–87 1949
41 *McNalley M C Kelble D., Pryer R. & Blount S G* Angiosarcoma of the heart. Report of a case and review of the literature. Am Heart J *65* 244–254 1963
42 *Ohtsuki Y., Kobayashi S., Hayashi T & Ohmori M* Angiosarcom of the heart. Report of a case and review of the literature. Acta Pathol Jap *23* 407–413 1973
43 *Pait Y Z Halkin H & Jaffe R* Primary cardiac angiosarcoma. Isr J Med. Sci. *10* 525–528, 1974
44 *Penneman G* Un cas d'hémangioendothéliome du coeur Ann Soc Méd. Grand. *88* 57–63 1908.
45 *Prichard R W* Tumors of the heart. Review of the subject and report of one hundred and fifty cases. Arch Path. *51* 98–129 1951
46 *Redtenbacher L.* Ein Fall von Angiosarcoma pericardii. Wien Klin Wschschr 2 214 216 1889
47 *Reisinger J A Pekin T J & Blumenthal, B* Primary tumor of the inferior vena cava and heart with hemopericardium and alternation of the ventricular complexes in the electrocardiogram Ann. Int Med. *17* 995–1004 1942.
48. *Robinson D S & Mackenzie P B* Hemangioendothelioma of the heart. J A M A. *189* 1026–1028 1964
49 *Scheidegger S* Malignes Hämangioblastom des Perikards Frankfurt Ztschr *51* 286–309 1937
50 *Schwarz N H & Loder M* Primary tumor of the heart New York J Med *52* 2658–2661 1952
51 *Schwarzkopf H & Gais H* Hamangiosarkom in Gebiet der rechten Kranzarterie Frankfurt Ztschr Path. *64* 483–490 1953
52 *Sochocky S* Rhabdomyosarcoma of the heart. Minnesota Medicine *54* 747–750 1971
53 *Stout A P* Tumors of the Soft Tissues Atlas of Tumor Pathology Sect. II Fasc 5 Washington D C Armed Forces Institute of Pathology 1953
54 *Stedja J Dvořak R Melichar F & Jedlicka F* Primary malignant hemangioma of the heart J Path. Bact *92* 564–567 1966.,
55 *Tacket H S Jones R S & Kyle J W* Primary angiosarcoma of the heart. Am Heart J *39* 912–917 1950
56 *Tatsumi T Nagatomo T & Kashiwai K* An autopsy case of primary heart tumor Gann. *40* 174–175 1949
57 *Tse R & Frank M N* Angiosarcoma of the







Fig 1 A. A low-magnification scanning electron micrograph (SEM) of the surface of the normal human gall bladder showing the mucosal folds. × 100

Fig 1 B. Light micrograph of material from the same normal gall bladder. Haematoxylin and eosin. × 96.

Fig 1 C. At higher SEM magnification, polygonal epithelial cells covered by microvilli are seen. × 1000

Acta path. microbiol scand. Sect. A 85 42–48 1977

OBSERVATIONS BY SCANNING ELECTRON MICROSCOPY OF NORMAL AND PATHOLOGICAL HUMAN GALL BLADDER EPITHELIUM

H Myllärniemi and J I Nickels

Second Department of Surgery Department of Electron Microscopy and Central Pathology Laboratory University of Helsinki, Helsinki Finland

Myllärniemi H & Nickels, J I Observations by scanning electron microscopy of normal and pathological human gall bladder epithelium Acta path. microbiol scand Sect. A, 85 42–48, 1977

Thirteen gall bladders presenting normal findings, cholesterolosis, chronic cholecystitis, mucosal hyperplasia and adenomyomatosis were studied by scanning and light microscopy In the bladder of patients with cholesterolosis the mucosal folds were clearly dilated but the individual epithelial cells had preserved their normal hexagonal structure. In the gall bladder of one patient with cholesterolosis, goblet like cells were seen in the epithelium. The greatest changes were seen in material from patients with chronic cholecystitis, in which the mucosal folds were clearly flattened and the cell boundaries indistinct and small polypoid structures were seen on the surface of the epithelium No special changes were seen in material obtained from patients with adenomyomatosis or mucosal hyperplasia.

Key words Gall bladder epithelium scanning electron microscopy

J I Nickels, Patologian keskuslaboratorio, Haartmaninkatu 3 00290 Helsinki 29 Finland

Received 31 v 76 Accepted 5 vii 76

The surface architecture of the gall bladder epithelium has been studied by dissecting microscopy using plastic models of histological sections (*Elfving et al* 1969 a) and by scanning electron microscopy (SEM) of normal adult and foetal preparations from man and animal (*Laitio & Nevalainen* 1972 a and b *Mueller et al* 1972) However SEM studies of pathological gall bladder epithelium are not available In many benign pathological conditions the mucosa is altered histopathologically and should be an interesting object for the high resolving power of the SEM

MATERIAL AND METHODS

The material consists of 13 human gall bladders obtained from patients operated on for cholecystolithiasis (5 cases) for cholesterolosis (6 cases) and from 2 patients with pancreatitis operated on for palliative purposes.

The gall bladders in relaxed state were fixed overnight in 3 per cent phosphate-buffered glutaraldehyde (pH 7 2) at 4 C. The specimens to be used for SEM were dehydrated in a graded series of ethanol solutions and dried in vacuum Critical point drying was not employed The surface of the dried tissue was coated with gold in vacuum evaporator SEM was accomplished by means of a Jeol U3 scanning electron microscope operating at 15 kV

Histological sections of adjacent tissue were

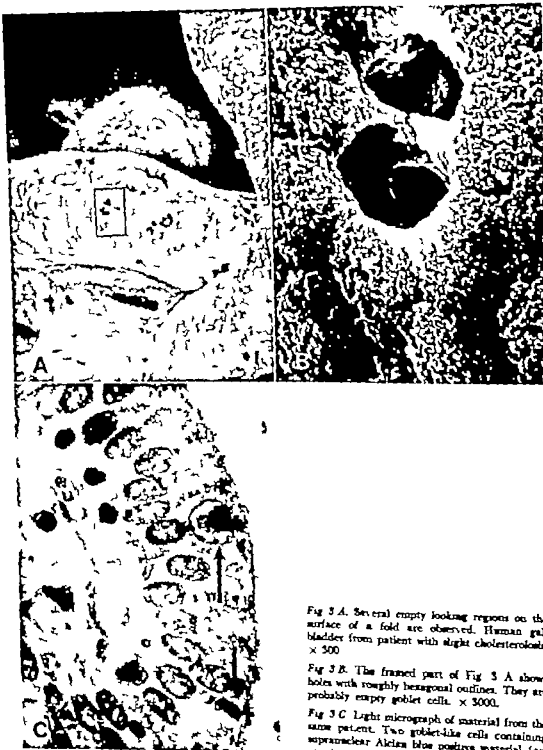


Fig 3 A. Several empty looking regions on the surface of a fold are observed. Human gall bladder from patient with slight cholesterolosis. × 300

Fig 3 B. The framed part of Fig 3 A shows holes with roughly hexagonal outlines. They are probably empty goblet cells. × 3000.

Fig 3 C. Light micrograph of material from the same patient. Two goblet-like cells containing supranuclear Alcian blue positive material (arrows) are shown. Alcian blue PAS × 960.





Fig 2 A A low power SEM of human gall bladder from a patient with cholesterolosis, showing a dilated mucosal fold covered by regular epithelium. × 100

Fig 2 B Light micrograph of material from the same patient. Foamy cells are present beneath the normal epithelium. Haematoxylin and eosin × 96

stained with haematoxylin eosin van Gieson Alcian blue and periodic acid Schiff (PAS) for acid and neutral mucosubstances after diastase treatment Nitrate silver (*Grimelius* 1968) and Fontana Masson (*Pearse* 1972) techniques were used to bring out possible argyrophilic and argentaffine reactions.

RESULTS

Histopathologically the following diagnoses could be established on the basis of the gall bladder specimens normal (2 cases) cholesterolosis (6 cases) chronic cholecystitis (5 cases) combined with adenomyomatosis in 2 cases. One case of cholesterolosis and two cases of chronic cholecystitis showed socalled mucosal hyperplasia (*Elfving et al* 1969 b) of different degrees.

At low magnification the high depth of focus of SEM clearly brought out the mucosal folds in normal gall bladder (Fig 1 A) corresponding to findings by light microscopy (Fig 1 B) At higher magnification the polygonal and roughly hexagonal boundaries of individual cells with slightly convex surfaces could be seen the microvilli on each cell giving the impression that the cell surface was of a feathery texture (Fig 1 C)

In cases of cholesterolosis the mucosal folds were dilated the degree of which depended on the accumulation of foam cells under the epithelium (Fig 2 A and B) The surface of the folds, however was regular as seen from the pictures obtained by SEM and ordinary light microscopy (Fig 2 A and B)

In one case of slight cholesterolosis, several empty-looking regions on the surface could be seen (Fig. 3 A). At higher magnification these regions appeared to be holes with hexagonal outlines (Fig 3 B). Histologically some acid mucosubstances containing goblet like cells were seen (Fig 3 C) but no enterochromaffine cells. Thus, the holes previously mentioned are probably goblet cell orifices measuring about 8–10 microns in diameter.

In cases of severe chronic cholecystitis, the folds were clearly flattened and broad (Fig 4 A and C). In many areas, the polygonal boundaries between the epithelial cells were indistinct and small polypoid structures were resolved at higher magnifications (Fig 4 B). Histologically the epithelium was multi layered with nuclei grouped in several layers (Fig. 4 C).

No abnormal epithelial structures could be seen in the material obtained from patients with mucosal hyperplasia and adenomyomatosis.

DISCUSSION

The hexagonal structure of the epithelial cells corresponds to the surface architecture of the epithelium of the stomach (*Pfeiffer* 1970) and the small intestine (*Marsh & Swift* 1969). The microvilli to be observed in the transmission microscope (*Laitio & Nevalainen* 1972 a and b, *Fox* 1972) as well as in the scanning electron microscope reflects the activity of absorption of the gall bladder epithelium. Principal cells, brush cells, migrating or granulated cells (*Luciano* 1972) could not be differentiated by way of SEM.

In cases of cholesterolosis, the epithelial cells preserved their polygonal structure and microvilli. This corresponds to the findings by transmission electron microscopy of gall bladders from patients with cholesterolosis (*Nevalainen & Laitio* 1972).

The goblet like cells seen in one case of slight cholesterolosis correspond probably to those observed in the socalled single cell metaplasia (*Järi & Meurman* 1964) to be seen in cases of cholecystolithiasis and cholecystitis. Considerable mucus secretion is known to occur in the human gall bladder in these conditions (*Fox* 1972). In the present investigation, the distended cells may have lost their surface during the process of preparation. Degenerative changes occur soon after the gall bladder has been excesed and are attributable to digestion caused by the bile (*Chapman et al* 1966).

In cases of chronic cholecystitis, the epithelial cells retain their hexagonal outline, but they may be multi layered (*Fox* 1972). The microvilli are partially absent and some cells show cytoplasmic protrusions from the surface (*Fox* 1972). The disappearance of the ridges and contours between the individual cells, as seen in the present SEM pictures, may be due to the presence of these cytoplasmic buds, of the multi-layered epithelium and to the highly columnar nature and thinness of the cells. There is a certain resemblance to colonic hyperplastic polyps the epithelium of which deviates from the regular polygonal shape in that the cellular diameter is increased and the microvilli are larger than normal (*Fenoglio et al* 1975).

In two cases of adenomyomatosis and in three cases of mucosal hyperplasia (*Elfving et al.* 1969 b) the mucosal folds and the epithelial cells did not differ from those of normal gall bladder. In cases of adenomyomatosis, the pathological process is intramural and hence, it cannot be studied by SEM. In cases of mucosal hyperplasia the folds are elongated being several millimeters thick for which reason they are difficult to study even by way of SEM.

REFERENCES

Chapman G., Chiaredo A J., Coffey R. J & Wieneke K.: The fine structure of mucosal epithelial cells of a pathological human gall bladder. Anat. Rec. 154 579–616, 1966.

Elfving, G., Teir H. Degerth H & Mäkelä V.: Mucosal hyperplasia in the gallbladder demonstrated by plastic models. Acta path. microbiol. scand. 77 384–388, 1969 a.

Elfving, G. Silvonen E. & Teir H.: Mucosal hyperplasia of the gallbladder in cases of chole







Fig 4 A A SEM picture of gall bladder from patient with chronic cholecystitis showing flattened and broad folds. × 100

Fig 4 B At higher magnification the boundaries between the epithelial cells are partly indistinct lending a polypoid appearance to the epithelium. × 1000

Fig 4 C Light micrograph of material from the same patient illustrates that the epithelium is multilayered with nuclei grouped in several layers. Haematoxylin and eosin × 96

In one case of slight cholesterolosis, several empty-looking regions on the surface could be seen (Fig. 3 A). At higher magnification these regions appeared to be holes with hexagonal outlines (Fig. 3 B). Histologically some acid mucosubstances containing goblet like cells were seen (Fig. 3 C) but no enterochromaffine cells. Thus, the holes previously mentioned are probably goblet cell orifices measuring about 8–10 microns in diameter.

In cases of severe chronic cholecystitis, the folds were clearly flattened and broad (Fig. 4 A and C). In many areas, the polygonal boundaries between the epithelial cells were indistinct and small polypoid structures were resolved at higher magnifications (Fig. 4 B). Histologically the epithelium was multi-layered with nuclei grouped in several layers (Fig. 4 C).

No abnormal epithelial structures could be seen in the material obtained from patients with mucosal hyperplasia and adenomyomatosis.

DISCUSSION

The hexagonal structure of the epithelial cells corresponds to the surface architecture of the epithelium of the stomach (*Pfeiffer* 1970) and the small intestine (*Marsh & Swift* 1969). The microvilli to be observed in the transmission microscope (*Laitio & Nevalainen* 1972 a and b, *Fox* 1972) as well as in the scanning electron microscope reflects the activity of absorption of the gall bladder epithelium. Principal cells, brush cells, migrating or granulated cells (*Luciano* 1972) could not be differentiated by way of SEM.

In cases of cholesterolosis, the epithelial cells preserved their polygonal structure and microvilli. This corresponds to the findings by transmission electron microscopy of gall bladders from patients with cholesterolosis (*Nevalainen & Laitio* 1972).

The goblet like cells seen in one case of slight cholesterolosis correspond probably to those observed in the socalled single cell metaplasia (*Jarvi & Meurman* 1964) to be seen in cases of cholecystolithiasis and cholecystitis. Considerable mucus secretion is known to occur in the human gall bladder in these conditions (*Fox* 1972). In the present investigation, the distended cells may have lost their surface during the process of preparation. Degenerative changes occur soon after the gall bladder has been excised and are attributable to digestion caused by the bile (*Chapman et al.* 1966).

In cases of chronic cholecystitis, the epithelial cells retain their hexagonal outline, but they may be multi-layered (*Fox 1972*). The microvilli are partially absent and some cells show cytoplasmic protrusions from the surface (*Fox* 1972). The disappearance of the ridges and contours between the individual cells, as seen in the present SEM pictures, may be due to the presence of these cytoplasmic buds, of the multi-layered epithelium and to the highly columnar nature and thinness of the cells. There is a certain resemblance to colonic hyperplastic polyps the epithelium of which deviates from the regular polygonal shape in that the cellular diameter is increased and the microvilli are larger than normal (*Fenoglio et al.* 1975).

In two cases of adenomyomatosis and in three cases of mucosal hyperplasia (*Elfving et al.* 1969 b) the mucosal folds and the epithelial cells did not differ from those of normal gall bladder. In cases of adenomyomatosis, the pathological process is intramural and hence it cannot be studied by SEM. In cases of mucosal hyperplasia the folds are elongated, being several millimeters thick for which reason they are difficult to study even by way of SEM.

REFERENCES

Chapman, G., Chiarodo, A. J., Coffey, R. J. & Wieneke, K.: The fine structure of mucosal epithelial cells of a pathological human gall bladder. Anat. Rec. *154*, 579–616, 1966.

Elfving, G., Teir, H., Degerth, H. & Mäkelä, V.: Mucosal hyperplasia in the gallbladder demonstrated by plastic models. Acta path. microbiol. scand. *77*, 381–388, 1969 a.

Elfving, G., Silvonen, E. & Teir, H.: Mucosal hyperplasia of the gallbladder in cases of chole-

cystolithiasis. Acta chir scand *135* 519–522 1969 b.

Fenoglio C M Richart R M & Kaye G I., Comparative electron-microscopic features of normal hyperplastic, and adenomatous human colonic epithelium. Gastroenterology *69* 100–109 1975

Fox H Ultrastructure of human gall bladder epithelium in cholelithiasis and chronic cholecystitis. J Path. *108* 157–164 1972.

Grimelius L Silver nitrate stain for α 2 cells in human pancreatic islets. Acta Soc. Med. upsalien. *73* 243–270 1968

Järvi O & Meurman L. Heterotopic gastric mucosa and pancreas in the gallbladder with reference to the question of heterotopias in general Ann. Acad. Sci fenn. A5 *106/22* 1–42 1964

Laitio M & Nevalainen T Scanning and transmission electron microscope observations on human gallbladder epithelium Adult structure. Z. Anat. Entwickl -Gesch *136* 319–325 1972 a.

Laitio M & Nevalainen T Scanning and transmission electron microscope observations on human gallbladder epithelium. Foetal development. Z. Anat. Entwickl.-Gesch *136* 326–335, 1972 b

Luciano L. Die Feinstruktur der Gallenblase und der Gallengänge. Z Zellforsch. *135* 87–102 1972

Marsh M N & Swift J A A study of the small intestinal mucosa using the scanning electron microscope. Gut *10* 940 949 1969

Mueller J C Jones A L & Long, J A Topographic and subcellular anatomy of the guinea pig gallbladder Gastroenterology *63* 856–868 1972

Nevalainen T & Laitio M Ultrastructure of gallbladder with cholesterolosis. Virchows Arch. path Anat. Abt. B Zellpath. *10* 237–242, 1972.

Pearse A G E Histochemistry theoretical and applied, 3 ed. Churchill Livingstone London 1972. p. 1379

Pfeiffer C J Surface topology of the stomach in man and the laboratory ferret. J Ultrastruct. Res. *33* 252 262 1970

Acta path. microbiol. scand. Sect. A, 85 49–56 1977

THE RELATIONSHIP BETWEEN EXPRESSION OF EPITHELIAL B-LIKE BLOOD GROUP ANTIGEN, CELL MOVEMENT AND CELL PROLIFERATION

I. C. Mackenzie, E. Dabelsteen and K. Zimmermann

The College of Dentistry The University of Iowa, Iowa City Iowa, USA, and
Department of Oral Pathology The Royal Dental College Copenhagen, Denmark

Mackenzie, I. C., Dabelsteen, E. & Zimmermann, K. The relationship between expression of epithelial B-like blood group antigen, cell movement and cell proliferation. Acta path. microbiol. scand. Sect. A, 85 49–56, 1977

Healing wounds in the oral mucosa of rhesus monkeys were examined by an immunofluorescence staining method to demonstrate the distribution of a blood group antigen cross reacting with human group B and by labelling with tritiated thymidine to localize areas of cell proliferation. Within hours, blood group antigen reactivity was lost from epithelial cells adjacent to the wound margin. Reactivity was absent from the epithelial outgrowth into the wound, but returned with restoration of epithelial continuity The zone of increased cell proliferation lay adjacent to, but outside of the area of antigen loss. Antigen loss appeared to be associated with an area of increased cell movement, a finding of interest in relation to reports of antigen loss from epithelial tumors.

Key words B-like blood group antigen cell movement cell proliferation.

E. Dabelsteen, Department of Oral Pathology The Royal Dental College, Copenhagen, Denmark

Received 20 II.76 Accepted 20 II.76

The blood group antigens A and B which are located on the outer surface of red blood cells are also found on other cell types widespread throughout the human body Partial or complete loss of blood group antigens A and B has been reported for both premalignant and malignant lesions which develop from epithelia in which such substances are normally present e.g. oral mucosa (13 14 29 30) cervical epithelium (16 17) gastrointestinal mucosa (7 27 33) and pancreas (18) However as not all cancer cells react negatively for blood group antigens (7 12, 15 16) and as loss of these antigens has been described in oral epithelia adjacent to wounds (11) altered blood group antigen activity in the above mentioned tissues may be considered a tumor associated rather than a tumor specific change.

Studies of blood group antigens in wound healing (11) and studies of the distribution of blood group antigens in normal stratified human oral epithelium (9 11) and in cultured cells (19 18) suggest that there may be some correlation between loss of detectable blood group antigens and certain cell processes such as mitosis and migration.

cystolithiasis. Acta chir scand *135* 519–522, 1969 b.

Fenoglio C M Richart R M & Kaye G I Comparative electron microscopic features of normal hyperplastic, and adenomatous human colonic epithelium Gastroenterology *69* 100–109 1975

Fox H Ultrastructure of human gall bladder epithelium in cholelithiasis and chronic cholecystitis. J Path. *108* 157–164 1972

Grimelius I *Silver nitrate stain for α 2 cells in human pancreatic islets.* Acta Soc Med upsalien. *73* 243–270 1968

Järvi O & Meurman L Heterotopic gastric mucosa and pancreas in the gallbladder with reference to the question of heterotopias in general Ann. Acad Sci. fenn A5 *106/2?* 1–42 1964

Laitio M & Nevalainen T Scanning and transmission electron microscope observations on human gallbladder epithelium Adult structure Z. Anat. Entwickl.-Gesch. *136* 319–325 1972 a

Laitio M & Nevalainen T Scanning and transmission electron microscope observations on human gallbladder epithelium. Foetal development. Z. Anat. Entwickl.-Gesch. *136* 326–335, 1972 b

Luciano L Die Feinstruktur der Gallenblase und der Gallengänge Z. Zellforsch. *135* 87–102, 1972

Marsh M N & Swift J A A study of the small intestinal mucosa using the scanning electron microscope. Gut *10* 940–949 1969

Mueller J C Jones A L & Long J A. Topographic and subcellular anatomy of the guinea pig gallbladder Gastroenterology *63* 856–868, 1972

Nevalainen T & Laitio M Ultrastructure of gallbladder with cholesterolosis. Virchows Arch path. Anat. Abt. B Zellpath. *10* 237–242, 1972

Pearse A G E Histochemistry theoretical and applied 3 ed., Churchill-Livingstone London 1972 p. 1379

Pfeiffer C J Surface topology of the stomach in man and the laboratory ferret. J Ultrastruct. Res. *33* 252–262 1970

THE RELATIONSHIP BETWEEN EXPRESSION OF EPITHELIAL B-LIKE BLOOD GROUP ANTIGEN CELL MOVEMENT AND CELL PROLIFERATION

I. C. Mackenzie, E. Dabelsteen and K. Zimmermann

The College of Dentistry The University of Iowa Iowa City Iowa, USA, and Department of Oral Pathology The Royal Dental College, Copenhagen, Denmark

Mackenzie, I. C., Dabelsteen, E. & Zimmermann, K. The relationship between expression of epithelial B-like blood group antigen, cell movement and cell proliferation. Acta path. microbiol. scand Sect. A, 85 49–56 1977

Healing wounds in the oral mucosa of rhesus monkeys were examined by an immunofluorescence staining method to demonstrate the distribution of blood group antigen cross reacting with human group B and by labelling with tritiated thymidine to localize areas of cell proliferation Within hours, blood group antigen reactivity was lost from epithelial cells adjacent to the wound margin. Reactivity was absent from the epithelial outgrowth into the wound, but returned with restoration of epithelial continuity The zone of increased cell proliferation lay adjacent to, but outside of, the area of antigen loss. Antigen loss appeared to be associated with an area of increased cell movement, a finding of interest in relation to reports of antigen loss from epithelial tumors.

Key words B-like blood group antigen cell movement cell proliferation.

E Dabelsteen, Department of Oral Pathology The Royal Dental College, Copenhagen, Denmark.

Received 20.vii.76 Accepted 20.vii.76

The blood group antigens A and B which are located on the outer surface of red blood cells are also found on other cell types wide spread throughout the human body Partial or complete loss of blood group antigens A and B has been reported for both premalignant and malignant lesions which develop from epithelia in which such substances are normally present e.g. oral mucosa (13 14 29 30) cervical epithelium (16, 17) gastrointestinal mucosa (7 27 33) and pancreas (18) However as not all cancer cells react negatively for blood group antigens (7 12, 15, 16) and as loss of these antigens has been described in oral epithelia adjacent to wounds (11) altered blood group antigen activity in the above mentioned tissues may be considered a tumor associated rather than a tumor specific change.

Studies of blood group antigens in wound healing (11) and studies of the distribution of blood group antigens in normal stratified human oral epithelium (9 11) and in cultured cells (19 18) suggest that there may be some correlation between loss of detectable blood group antigens and certain cell processes such as mitosis and migration.

cystolithiasis. Acta chir scand 135 519–522 1969 b.

Fenoglio C M Richart R M & Kaye G I Comparative electron-microscopic features of normal hyperplastic and adenomatous human colonic epithelium. Gastroenterology 69 100–109 1975

Fox H Ultrastructure of human gall bladder epithelium in cholelithiasis and chronic cholecystitis. J Path 108 157–164 1972

Grimelius L Silver nitrate stain for α 2 cells in human pancreatic islets. Acta Soc Med. upsalien. 73 243–270 1968

Järvi O & Meurman L. Heterotopic gastric mucosa and pancreas in the gallbladder with reference to the question of heterotopias in general Ann. Acad Sci fenn. A5 106/22 1–47 1964

Laitio M & Nevalainen T Scanning and transmission electron microscope observations on human gallbladder epithelium. Adult structure Z. Anat. Entwickl.-Gesch 136 319 325 1972 a

Laitio M & Nevalainen T Scanning and transmission electron microscope observations on human gallbladder epithelium. Foetal development Z. Anat Entwickl.-Gesch 136 326-335, 1972 b

Luciano L. Die Feinstruktur der Gallenblase und der Gallengange Z. Zellforsch. 135 87-102, 1972

Marsh M N & Swift J A A study of the small intestinal mucosa using the scanning electron microscope. Gut 10 940-949 1969

Mueller J C Jones A L & Long J A. Topographic and subcellular anatomy of the guinea pig gallbladder Gastroenterology 63 856–868, 1972

Nevalainen T & Laitio M Ultrastructure of gallbladder with cholesterolosis. Virchows Arch. path. Anat Abt. B Zellpath. 10 237-242, 1972

Pearse A G E. Histochemistry theoretical and applied, 3 ed., Churchill Livingstone London 1972 p 1379

Pfeiffer C J Surface topology of the stomach in man and the laboratory ferret. J Ultrastruct. Res. 33 252-262 1970

Acta path. microbiol. scand. Sect. A, 85 49–56, 1977

THE RELATIONSHIP BETWEEN EXPRESSION OF EPITHELIAL B-LIKE BLOOD GROUP ANTIGEN, CELL MOVEMENT AND CELL PROLIFERATION

I. C. Mackenzie, E. Dabelsteen and K. Zimmermann

The College of Dentistry The University of Iowa, Iowa City Iowa, USA, and
Department of Oral Pathology The Royal Dental College Copenhagen, Denmark

Mackenzie, I. C., Dabelsteen, E. & Zimmermann, K. The relationship between expression of epithelial B-like blood group antigen, cell movement and cell proliferation Acta path. microbiol. scand Sect. A, 85 49–56, 1977

Healing wounds in the oral mucosa of rhesus monkeys were examined by an immunofluorescence staining method to demonstrate the distribution of blood group antigen cross reacting with human group B, and by labelling with tritiated thymidine to localize areas of cell proliferation. Within hours, blood group antigen reactivity was lost from epithelial cells adjacent to the wound margin Reactivity was absent from the epithelial outgrowth into the wound, but returned with restoration of epithelial continuity The zone of increased cell proliferation lay adjacent to, but outside of, the area of antigen loss. Antigen loss appeared to be associated with an area of increased cell movement, a finding of interest in relation to reports of antigen loss from epithelial tumors.

Key words B-like blood group antigen cell movement cell proliferation.

E. Dabelsteen, Department of Oral Pathology The Royal Dental College, Copenhagen, Denmark.

Received 20. II.76 Accepted 20. II.76

The blood group antigens A and B which are located on the outer surface of red blood cells are also found on other cell types widespread throughout the human body Partial or complete loss of blood group antigens A and B has been reported for both premalignant and malignant lesions which develop from epithelia in which such substances are normally present e.g oral mucosa (13 14 29 30) cervical epithelium (16 17) gastrointestinal mucosa (7 27 33) and pancreas (18) However as not all cancer cells react negatively for blood group antigens (7 12, 15 16) and as loss of these antigens has been described in oral epithelia adjacent to wounds (11) altered blood group antigen activity in the above mentioned tissues may be considered a tumor associated rather than a tumor specific change.

Studies of blood group antigens in wound healing (11) and studies of the distribution of blood group antigens in normal stratified human oral epithelium (9 11) and in cultured cells (19 18) suggest that there may be some correlation between loss of detectable blood group antigens and certain cell processes such as mitosis and migration.

TABLE 1 *Controls for Establishing Specificity of Immunofluorescence Staining*

	Human blood group test serum	Conjugate	Results
Monkey oral epithelium and			
Human group B oral epithelium	Anti A	Anti-human IgG/FITC	—
Human group B oral epithelium	Phosphate buffered saline	Anti-human IgG/FITC	—
Human group B oral epithelium	Anti B absorbed with B-human erythrocytes	Anti human IgG/FITC	—
Human group B oral epithelium	Anti B	Labelled normal serum	—
Human group B oral epithelium	Anti B	Anti human IgG/FITC	+
Human group A oral epithelium	Anti-B	Anti human IgG/FITC	—

* Buccal mucosa for secretory (13)

The present study was designed to examine and correlate the epithelial blood group antigen changes which occur in the region of cell proliferation and movement adjacent to healing experimental wounds. Preliminary investigations showed that in normal and wounded oral epithelium of rhesus monkeys the distribution of an antigen *cross reacting with* human blood group antigen B is similar to that demonstrated in human oral mucosa (14 15) Rhesus oral mucosa was therefore used in the study to allow labelling of proliferating cells with tritiated thymidine

MATERIALS AND METHODS

Standardized wounds were made in a) the attached gingiva midway between the gingival margin and the mucogingival junction In b) the palate 5 mm lateral to the midline and c) in the buccal mucosa between the occlusal level and the mandibular sulcus. The linear wounds were approximately 3 cm long and were made using two blades held in a hemostat and spaced by a distance of 1 mm. Biopsies of the wounds were taken 3 and 6 hours and 1 2 4 and 6 days after wounding One hour prior to each biopsy 0 2 ml of an aqueous solution of tritiated thymidine (H^3Tdr) containing 0 5 mCi/mL (Sp activity 1 9 Ci/mM) was injected locally beneath the wound margins to label DNA synthesising cells.

The tissue was fixed in 10 per cent neutral formalin, dehydrated in graded alcohols, cleared in xylene embedded in paraffin wax, and cut as 5 μm sections for a) staining with haematoxylin and eosin to examine the histological appearance of the healing wounds, b) immunofluorescent staining to display blood group antigens c) *autoradiography for* counts of labelled cells.

Cross reacting blood group B-like antigens were detected in the epithelium by a double layer immunofluorescence (IF) staining method The first layer was a human blood group test serum (Hoechst Frankfurt, Germany) the second layer rabbit anti human IgG conjugated with fluorescein isothiocyanate (FITC) The blood group test serum has, in previous studies, proved useful for detection of human oral epithelial blood group antigens (9 14) The FITC conjugate was heavy chain-specific, had an antibody titer of 100 and a protein concentration of 2.5 mg/ml The optical density ratio at 495 nm/280 nm ranged from 0.95 to 0.30 with a mean of 0 66. By chessboard titration a working titre of 1 20 was found. The methods for the staining procedure and fluorescence microscopy have been described previously (15) The control reactions summarized in Table 1 were used to ensure the specificity of the IF stainings. The amount of antigen in the tissue was estimated by a two-fold serial dilution titration of the anti-B serum (9)

Sections for autoradiography were processed by standard methods (32) and were mounted on subbed slides, dipped in Kodak NTB-2 emulsion, dried and stored at 4 C in dessicated light-tight boxes for 5 weeks, developed for 2 minutes in Dektol fixed in 30 per cent sodium thiosulphate stained in Harris haematoxylin and mounted in balsam. The relative proliferative activity in the a) outgrowing epithelial projections into the wound b) epithelium adjacent to the wound and c) epithelium distant to the wound was assessed by estimating the number of labelled nuclei per unit length of epithelial surface

RESULTS

Examination of haematoxylin and eosin stained sections showed an essentially similar pattern of healing for the wounds of buccal

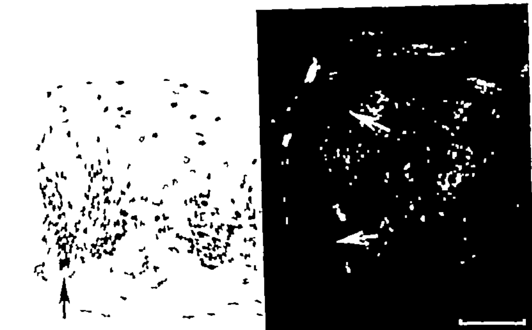


Fig. 1 Left Autoradiograph of palatal specimen taken 6 hours after wounding. Labelled cells are found close to the wound margin (arrow)
Right IF staining of section of the same specimen. A positive reaction is present at the membranes of the spinous cells in the epithelium way from the wound margin but antigen reactivity is absent from the cells in the region adjacent to the wound (arrows) Scale = 100 μm.

mucosa, gingiva and palate. Initially the gap between the epithelial margins was filled by a coagulum containing debris. Epithelial outgrowths from the margins grew down into, and then across, the wounded area to re-establish continuity by forming a epithelial bridge (Figs. 2, 3) This epithelium subsequently acquired the characteristics of a mature epithelium. The rate at which these processes occurred varied from site to site. Some epithelial outgrowth from the wound margins was seen in the six hour biopsy of buccal mucosa but the initial outgrowth was first seen in the one-day biopsy of the gingiva and palate. An epithelial bridge between the wound margins was established within one day in some regions of buccal wounds, but not until two to four days in the gingival and palatal wounds.

In the three-hour biopsy specimens some loss of antigen reactivity was seen in the epithelial cells adjacent to the cell-surface. In the six hour wound, blood group antigens were absent from the approximately 100 μm of epithelium adjacent to the wound margin (Fig. 1) The subsequent distribution of blood group antigens was essentially similar in the buccal mucosa, palate and gingiva except that some differences were seen which appeared to relate the varying rates of re-establishment of epithelial continuity In each case the antigen was not detectable in the epithelial projection into the wound (Fig 2) and remained absent from the newly formed epithelium until epithelial contact between the wound margins was re-established. Titration demonstrated that although the blood group antigen soon reappeared in the epithelial bridge when contact was re-established (Fig. 3) the reactivity did not reach normal levels until the epithelium presented histological evidence of maturation or reformation of a stratum corneum.

The pattern of cell labelling observed in

TABLE 1 *Controls for Establishing Specificity of Immunofluorescence Staining*

	Human blood group test serum	Conjugate	Results
Monkey oral epithelium and			
Human group B oral epithelium	Anti A	Anti human IgG/FITC	—
Human group B oral epithelium	Phosphate buffered saline	Anti human IgG/FITC	—
Human group B oral epithelium	Anti-B absorbed with B-human erythrocytes	Anti human IgG/FITC	—
Human group B oral epithelium	Anti B	Labelled normal serum	—
Human group B oral epithelium	Anti B	Anti-human IgG/FITC	+
Human group A oral epithelium	Anti B	Anti-human IgG/FITC	—

* Buccal mucosa for secretory (15)

The present study was designed to examine and correlate the epithelial blood group antigen changes which occur in the region of cell proliferation and movement adjacent to healing experimental wounds Preliminary investigations showed that in normal and wounded oral epithelium of rhesus monkeys the distribution of an antigen cross reacting with human blood group antigen B is similar to that demonstrated in human oral mucosa (14 15) Rhesus oral mucosa was therefore used in the study to allow labelling of proliferating cells with tritiated thymidine.

MATERIALS AND METHODS

Standardized wounds were made in a) the attached gingiva midway between the gingival margin and the mucogingival junction, in b) the palate 5 mm lateral to the midline and c) in the buccal mucosa between the occlusal level and the mandibular sulcus. The linear wounds were approximately 3 cm long and were made using two blades held in a hemostat and spaced by a distance of 1 mm Biopsies of the wounds were taken 3 and 6 hours and 1 2 4 and 6 days after wounding One hour prior to each biopsy 0.2 ml of an aqueous solution of tritiated thymidine (H^3Tdr) containing 0.5 mCi/mL (Sp activity 1 9 Ci/mM) was injected locally beneath the wound margins to label DNA synthesizing cells.

The tissue was fixed in 10 per cent neutral formalin, dehydrated in graded alcohols, cleared in xylene embedded in paraffin wax, and cut as 5 μm sections for a) staining with haematoxylin and eosin to examine the histological appearance of the healing wounds, b) immunofluorescent staining to display blood group antigens, c) autoradiography for counts of labelled cells.

Cross reacting blood group B-like antigens were detected in the epithelium by a double layer immunofluorescence (IF) staining method. The first layer was a human blood group test serum (Hoechst Frankfurt Germany) the second layer rabbit anti-human IgG conjugated with fluorescein isothiocyanate (FITC) The blood group test serum has, in previous studies, proved useful for detection of human oral epithelial blood group antigens (9 14) The FITC conjugate was heavy chain-specific, had an antibody titer of 100 and a protein concentration of 2.5 mg/ml. The optical density ratio at 495 nm/280 nm ranged from 0.95 to 0 30 with a mean of 0 66. By chessboard titration a working titre of 1 20 was found. The methods for the staining procedure and fluorescence microscopy have been described previously (15) The control reactions summarized in Table 1 were used to ensure the specificity of the IF stainings. The amount of antigen in the tissue was estimated by a two-fold serial dilution titration of the anti-B serum (9)

Sections for autoradiography were processed by standard methods (32) and were mounted on subbed slides, dipped in Kodak NTB-2 emulsion, dried and stored at 4 C in desiccated light tight boxes for 3 weeks, developed for 2 minutes in Dektol fixed in 30 per cent sodium thiosulphate stained in Harris haematoxylin and mounted in balsam The relative proliferative activity in the a) outgrowing epithelial projections into the wound, b) epithelium adjacent to the wound and c) epithelium distant to the wound, was assessed by estimating the number of labelled nuclei per unit length of epithelial surface.

RESULTS

Examination of haematoxylin and eosin stained sections showed an essentially similar pattern of healing for the wounds of buccal

Fig. 3 Upper: Autoradiography of a 4 day gingival wound. Labelled basal cells (arrows) are seen in the epithelium on either side of the epithelial bridge closing the wound but no labelling is seen in the bridge itself. Scale = 100 μm.

Lower: IF staining of a 4 day gingival wound showing strong reactivity of cells in the maturing epithelial bridge joining the wound margins (arrow).

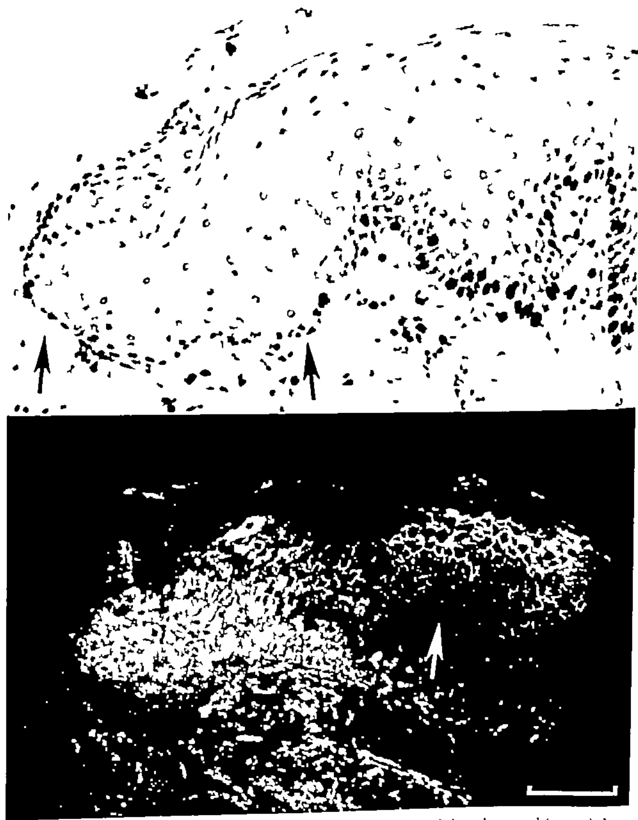


Fig 2 Upper Autoradiograph of 2 day gingival wound The outgrowth into the wound (arrows) shows no cell labelling but a large number of labelled basal cells are seen in the adjacent epithelium.
Lower I F staining of a section of the same specimen A positive reaction is present at the membranes of spinous cells of the epithelium adjacent to the outgrowth (arrow) but reactivity is absent from the membranes of cells in the outgrowth Nonspecific cytoplasmic staining is seen in the outgrowth. Scale = 100 μm.

Fig. 3 Upper. Autoradiography of a 4 day gingival wound. Labelled basal cells (arrow) are seen in the epithelium on either side of the epithelial bridge closing the wound but no labelling is seen in the bridge itself. Scale = 100 μm.

Lower. IF staining of 4 day gingival wound showing strong reactivity of cells in the epithelial bridge joining the wound margins (arrow).

healing wounds was also similar for the three locations examined In specimens taken up to six hours after wounding labelled basal cells were apparently uniformly scattered along the epithelium with some labelled nuclei being found close to the margin of the wounds in all specimens (Fig 1) In the specimens taken one day after wounding very few labelled cells were seen close to the original wound margin In the specimens taken on subsequent days very few labelled cells were seen in the epithelial outgrowth from the wound margin (Fig 2) Labelling in the new formed epithelium remained low even after re-establishment of epithelial continuity (Fig 3) Maximum cell labelling in the first few days after wounding was seen in the area of unwounded epithelium up to 0.5 mm from the original wound margin Here labelling reached several times the level found in the more distant normal epithelium.

DISCUSSION

The present study supports the results of previous studies of human oral epithelium (10) by demonstrating the absence of detectable blood group antigen on the surface of cells in the epithelial outgrowth from the margin of healing wounds The results also suggest that the region in which the major proliferative response occurs lies outside the region in which the changes in antigen activity are found

Abercrombie (1 2) has described two phenomena associated with the cell movement occurring during wounding healing He has described contact inhibition as the inhibition of locomotion of a cell in a direction taking it across another cell. It is apparently the release from contact inhibition of the cells of the wound margin which causes the movement of cells into the wound Another phenomenon "mobilization" is conceived as freedom from an influence which normally restrains cell movement even in the absence of contact inhibition Mobilization has been attributed to an altered adhesiveness of cells and the concept results from the observation that when previously wounded tissue is cultured the rate of outward cell migration occurs at a much higher rate from the wound margin than from the freshly cut tissue (1 2)

The pattern of antigen reactivity found in the healing wounds appears to indicate some general regional and temporal correspondence between the region of loss of antigen reactivity and the area which might correspond to release from contact inhibition and increased cell mobilization adjacent to healing wounds Antigen was lost from the edge prior to movement, remained absent from the outgrowing tissue, and was not regained until contact was re-established Discussing wound healing Abercrombie (1 2) has suggested an association between cell proliferation and cell migration with perhaps the increase in both processes resulting from a single stimulus. It is therefore of interest that proliferation appeared to be neither temporally nor spatially related to antigen loss. The major focus of cell proliferation occurred outside the area showing altered antigen reactivity and increased cell proliferation was not found until one or two days after antigen reactivity was lost from the adjacent tissue. Cell labelling was absent from the epithelial bridge even after antigen reactivity was re-established.

Recently there has been considerable interest in the investigation of differences between the cell surfaces of normal and transformed cells growing *in vitro* (8 20 23 25 31 35) and between normal and neoplastic cells growing *in vivo* (3 5 18, 24 27) These studies have shown a number of changes in cell surface glycolipid and glycoprotein components which are similar to these carrying blood group antigenicity *In vitro* studies of a cell surface galactoprotein have shown this protein to be present in confluent cell cultures but absent or reduced in nonconfluent cultures and in cultures of transformed cells (8 20 22 25) Other results indicate that this galacto-protein and various other cell membrane components are cell-cycle and cell-contact dependent and may play a role in cell adhesion (4 6 21 26 34) From the behavior of tumors growing *in vivo* it appears

that neoplastic cells show a reduced contact inhibition of movement and alteration of the control of cell proliferation (2). A number of differences in cell-surface glycoprotein and glycolipids have also been reported between human colonic adenocarcinomas and the normal mucosa from which they have arisen (24–27). Biochemical studies reporting loss in neoplasia of blood group antigens A and B and other cell-surface glycolipid and glycoprotein components are supported by histological immunofluorescent studies of biopsied tissues which show a loss of blood group antigens in premalignant and malignant epithelial lesions (12, 14–16). From the reports of these *in vitro* and *in vivo* studies it appears that there is, in general, a reduced level or some other alteration in various cell-surface carbohydrates, in a) nontransformed cultured cells in the noncontact inhibited, rapidly proliferating phase, in b) transformed cultured cells, which show an altered contact inhibition of movement and increased proliferation and in c) the cells of malignant and premalignant lesions.

The present finding of loss of surface antigen from the epithelial cells adjacent to and moving into, a wound appears to fit with this general pattern of a cell-surface alteration associated with movement. The lack of correlation between the region of antigen loss and the region of cell proliferation suggests that such cell-surface changes are related primarily to control of cell movement rather than to control of proliferation. *Hakomori* (23) has also suggested this relationship following the observation that "sparse quiescent cells" have the same glycolipid pattern as "sparse growing cells" but a different pattern to "confluent" cells. These findings support the concept that the altered blood group antigen reactivity previously demonstrated in some epithelial tumors is not a tumor-specific change and suggest that this change may reflect a common increased potential for cell mobility in both tumors and wounds. The present findings are of particular interest as a complete absence of blood group antigens has been found in metastatic gastric neoplasms, and it has been suggested that a relationship between altered blood group synthesis and the ability to form metastases exists (33).

This work was supported by the *Joh. A. Hartford Foundation Inc.* and the *Danish Medical Research Council* (Grant No. 512 5503).

REFERENCES

1. *Abercrombie M.*: Behaviour of cells toward one another. Ad. anc. Biol. Skin. 5: 95–112 1964.
2. *Abercrombie M. & Ambrose E. J.*: The surface properties of cancer cells: a review. Cancer Res. 22: 525–548, 1962.
3. *Alexander P.*: Escape from immunodestruction by the host through shedding of surface antigens. Is this a characteristic shared by malignant and embryonic cells. Cancer Res. 34: 2077–2082, 1974.
4. *Bertini M., Forni, A. & Cannofino P. M.*: A tumour-associated membrane antigen transient expressed by normal cells during mitosis. Clin. Exp. Immunol. 18: 101–108, 1974.
5. *Barton P., von Kleist S. & Sabine M. C.*: Loss of normal colonic membrane antigen in human cancers of the colon. Cancer Res. 31: 1038–1041, 1971.
6. *Gikas M.*: Express of membrane antigens on cultured tumour cells. Thesis. Stockholm, 1975.
7. *Cowan W. K.*: Blood group antigens on human gastrointestinal carcinoma cells. Br. J. Cancer 16: 535–540, 1962.
8. *Critchley D. R. & Macpherson I.*: Cell density dependent glycolipids in NIl 2 hamster cells, derived malignant and transformed cell lines. Biochem. Biophys. Acta 296: 145–159 1973.
9. *Dabelsteen, E.*: Quantitative determination of blood group substances A of oral epithelial cells by immunofluorescence and immunoperoxidase methods. Acta path. microbiol. scand. Sect. A, 80: 847–853, 1972.
10. *Dabelsteen E. & Fejerskov O.*: Loss of epithelial blood group antigen-A during wound healing in oral mucous membrane. Acta path. microbiol. scand. Sect. A, 82: 431–433, 1974.
11. *Dabelsteen E. & Fejerskov O.*: Distribution of blood group antigen A in human oral epithelium. Scand. J. Dent. Res. 82: 206–211 1974.
12. *Dabelsteen, E., Mygind N. & Henriksen B.*: Blood group substance A in carcinomas of the larynx. Acta Otolaryngol. 77: 360–367, 1974.
13. *Dabelsteen E. & Pindborg J. J.*: Loss of epithelial blood group substance A in oral carci-

nomas. Acta path. microbiol scand Sect A *81* 435–444 1973

14 *Dabelsteen E Roed Petersen B & Pindborg J J* Loss of blood group antigens A and B in oral premalignant lesions. Acta path. microbiol. scand. Sect. A, *83* 292–300 1975

15 *Dabelsteen E. & Rygaard J* A sensitive immunofluorescence technique for detecting blood group substances A and B Acta path. microbiol scand. Sect A, *80* 433–439 *1972*.

16 *Davidsohn I* Early immunologic diagnosis and prognosis of carcinoma. Am J Clin. Pathol. *57* 715–730 1972

17 *Davidsohn I Kovarik S & Ni L Y* Isoantigens A B and H in benign and malignant lesions of the cervix. Arch. Pathol *87* 306–314 1969

18. *Davidsohn I Ni L Y & Stejskal R.* Tissue isoantigens A B, and H in carcinoma of the pancreas. Cancer Res. *31* 1244–1250 1971

19 *Franks D & Dawson A* Variation in the expression of blood group antigen A in clonal cultures of rabbit cells. Exp. Cell Res. *42* 534–561 1966

20 *Gahmberg C G & Hakomori S* Altered growth behaviour of malignant cells associated with changes in externally labeled glycoprotein and glycolipid Proc. Nat. Acad Sci. USA *70* 3329–3333 1973

21 *Gahmberg C G & Hakomori S* Organization of glycolipids and glycoproteins in surface membranes Dependency of cell cycle and on transformation. Biochem. Biophys. Res. *59* 283–291 1974

22 *Gahmberg C G Kiehn D & Hakomori S* Changes in a surface-labelled galactoprotein and in glycolipid concentrations in cells transformed by a temperature-sensitive polyoma virus mutant. Nature *248* 413–415 1974

23 *Hakomori S* Glycolipids of tumour cell membrane In Advances in Cancer Research, No. 18 (Eds. *Klein G & Weinhouse S*) Academic Press, New York, 1973

24 *Hakomori S Koscielak J Bloch K J & Jeanloz R W* Immunologic relationship between blood group substances and a fucose-containing glycolipid of human adenocarcinoma. J Immunol *98* 31–38, 1967

25 *Hynes R O* Role of surface alterations in cells transformation the importance of proteases and surface proteins. Cell *1* 147–156, 1974

26 *Johnsen S., Stokke T & Prydz., H.* HeLa cell plasma membranes. Exp Cell Res. *93* 245–251 1975.

27 *Kim Y S & Isaacs R* Glycoprotein metabolism in inflammatory neoplastic diseases of human colon. Cancer Res. *35* 2092–2097 *1975*.

28. *Kuhns W J Pann C & Bramson S.* Differentiation of blood group H in a human transformed cell line. Am. J Pathol. *69* 389–402 *1972*.

29 *Liu P I McGregor D H., Liu J G., Dunlap D L. Jinks W L., Liu F Przybylski C. & Miller L A* Carcinoma of the oral cavity evaluated by specific red cell adherence test. Oral. Surg *38* 56–64 1974

30 *Prendergast R C Toto P D & Gargiulo A W* Reactivity of blood group substances of neoplastic oral epithelium. J Dent. Res. *47* 306–310 1968.

31 *Robbins P W & Macpherson I A* Glycolipid synthesis in normal and transformed animal cells. Proc. R. Soc. Lond. B. *177* 49–58, 1971

32 *Rogers A W* Techniques of autoradiography Elsevier New York, 1969

33 *Sheahan D G Horowitz S A & Zamcheck, N* Deletion of epithelial ABH isoantigens in primary gastric neoplasms and in metastatic cancer Dig. Dis. *16* 961–969 1971

34 *Thomas D B* Cyclic expression of blood group determinants in murine cells and their *relationship to growth control.* Nature *233* 317–321 1971

35 *Yamada K M & Weston J A* Isolation of a major cell surface glycoprotein from fibroblasts. Proc. Nat. Acad. Sci USA *71* 3492–3496, 1974

Acta path. microbiol. scand. Sect. A, 85 57–62, 1977

IN VITRO EFFECTS OF PROLACTIN AND HYDROCORTISONE ON 7,12 DMBA INDUCED MAMMARY TUMOUR AND VIRUS-INDUCED SARCOMA IN THE RAT

KNUT ASPEGREN and CLAES TROPÉ

The Tornblad Institute and the Department of Surgery University of Lund, Lund, Sweden

Aspegren, K. & Tropé, C. *In vitro* effects of prolactin and hydrocorthisone on 7 12-DMBA induced mammary tumour and virus-induced sarcoma in the rat. Acta path. microbiol. scand. Sect. A, 85 57–62, 1977

The *in vitro* effect of prolactin and hydrocortisone, singly or in combination, on the DMBA induced mammary tumour in the rat was investigated by organ cultures. Prolactin had a stimulating effect on the DNA synthesis in one out of five tumours. Hydrocortisone induced lobulo-alveolar differentiation but reduced the DNA synthesis or failed to affect it. The addition of prolactin to hydrocortisone did not alter this response. Virus induced rat sarcomas were studied as control tissue. Prolactin inhibited growth of one sarcoma. Hydrocortisone stimulated growth of sarcomas. The relevance of these findings in relation to similar *in vitro* experiments is discussed.

Key words Mammary tumours sarcomas, rat hormonal responsiveness prolactin organ cultures.

K. Aspegren, Department of Surgery University of Lund, S-221 85 Lund, Sweden.

Received 30. ii.76 Accepted 30. ii.76

The 7 12-dimethylbenz(a)anthracene (DMBA) induced mammary tumour in the rat is sensitive both to steroid and polypeptide hormones and is much used as experimental model for human mammary carcinoma. *Butler & Pearson* (4) have shown that prolactin is important for the *in vivo* growth of the tumour *Turkington* (7) showed that prolactin binds to the DMBA mammary tumour cell and *Kelly et al* (5) have demonstrated that prolactin binding *in vitro* is correlated to response of the tumour to prolactin treatment *in vivo*. *Leung & Sasaki* (6) have demonstrated that the probably effect of prolactin is to stimulate independently or cooperatively with oestrogen, the oestradiol binding capacity of the tumour cells.

In vitro culture techniques have the advantage over *in vivo* experiments that they measure directly the influences of added substances on tumour growth. Using an organ culture technique, *Welsh & Rivera* (8) observed that prolactin had a direct, stimulating effect on the DNA synthesis of the DMBA tumour in the rat. However these authors used corticosteroid as an adjuvant to the culture medium. On the basis of our earlier work of the same type (1) it was suspected that coritcosteroids can have toxic effects. Therefore the experiments carried out by *Welsh & Rivera* were repeated, using

prolactin and hydrocortisone singly or in combination

MATERIAL AND METHODS

Mammary tumours were induced in 50-day-old female Sprague Dawley rats (Anticimex, Stockholm) by intragastric instillation of 20 mg DMBA in oil suspension. The tumours were used about three months after the induction. Sarcomas were one rat tumour induced by polyoma virus and one induced by adeno virus. Both tumours were induced and propagated in female inbred Wistar rats and transplanted for 15 and 16 generations, respectively before use

The organ culture technique has been described in detail elsewhere (1) In brief twelve explants, approximately 1.5 square mm were placed on a milliporefilter on top of a thin piece of cellulose acetate and floated in Trowell's T 8 medium (Biocult, Glasgow) in a Carrel D5 glass culture flask. 50 IU/ml of benzyl penicillin and 50 μg/ml of streptomycin sulphate were added to the medium.

Bovine prolactin NIH P B4 was dissolved in 0.9 per cent saline. Hydrocortisone (Sigma St. Louis, Mo.) was dissolved in 96 per cent ethanol giving a final ethanol concentration of 1 per cent.

A tumour was cultured with the following hormones at the following concentrations

Prolactin 5 μg/ml

Hydrocortisone 1 μg/ml

Prolactin 5 μg/ml and hydrocortisone 1 μg/ml

Control flask had medium and solvents only

Three control flasks and three flasks for each hormone or hormone combination were cultured for three four and five days, respectively Thus, an entire series was composed of 36 flasks. Care was taken to randomize the explants from a tumour during the setting up of an experiment which was carried out at room temperature The cultures were incubated at 37 C without gassing Media were changed daily

Four hours before a culture was terminated the content of a flask was transferred into a glass tube containing one millilitre of its own medium upon which 2 μCi of H^3-TdR (methyl H^3-thymidine specific activity 1 9 Ci/mM Schwarz/Mann, Orangeburgh) was added. The culture was then continued at 37 C for a further four hours and terminated by centrifugation and washing the explants twice with cold (+4) trichloroacetic acid for half an hour The explants were finally dissolved in Soluene 350 (Packard Ltd) and the radioactivity of each flask was determined by liquid scintillation counting No correction of the counts was made for the DNA content in the tubes, as described previously (1)

Prior to statistical treatment a general (technical) error variance was determined on the basis of variances from the 84 available triple determinations. The uniformity of these variances was controlled by Bartlett's test.

"Hormone effect" was expressed as the difference between the mean $\log_{10}$ cpm of the three control flasks and three hormone treated flasks. The significance of a hormone effect was checked by F-tests between variances due to "hormone treatment" and "general error"

In the case of one tumour one additional flask was made for each hormone or hormone combination and control These explants were fixed after five days of culture they were sectioned at 5 μ, stained with haematoxylin and eosin and investigated by light microscopy

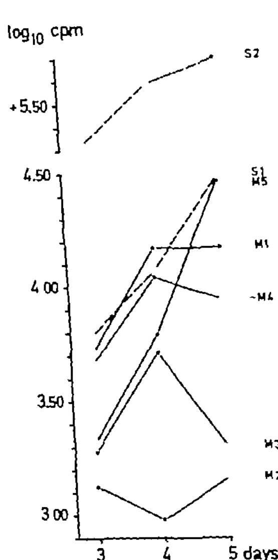
RESULTS

Five mammary tumours (M1 M5) and two sarcomas (S1-S2) were studied The results are given graphically in Figs. 1–5 The incorporation of H^3 TdR into DNA of controls is shown in Fig 1 Three mammary tumours (M1 M4 and M5) and the sarcomas (S1 and S2) were actively growing and increased their DNA synthesis from day 3 to 5 Mammary tumour M2 was fairly stationary while M3 increased from day 3 to day 4 though it decreased again to its original value on day 5 All tumours showed good incorporation, equivalent to that seen in previous experiments (1 2)

Fig 2 shows the effect of addition of prolactin to the cultures. One tumour M4 was significantly stimulated in its DNA synthesis at all culture times. M3 was stimulated on day 5 only The remaining mammary tumours remained unaffected. Sarcoma S1 was significantly inhibited on days 4 and 5 Sarcoma S2 was not affected by the treatment.

The effect of the addition of hydrocortisone is shown in Fig 3 Mammary tumours M1 M3 M4 and M5 were significantly inhibited on day 4 M1 and M4 also being inhibited on day 5 Sarcoma S1 was stimulated on days 3 and 4 but was not affected on day 5 Sarcoma S2 was stimulated on days 4 and 5

Fig 4 illustrates the effects of the combination of prolactin and hydrocortisone Mammary tumours M2 and M5 were not affected by the treatment M1 M3 and M4 were in



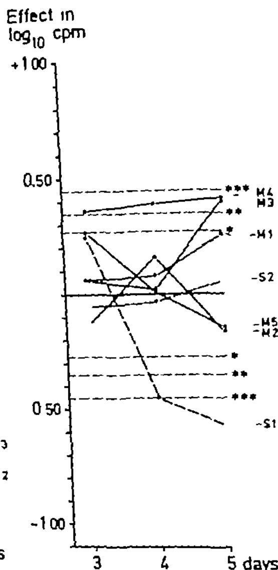


Fig. 1. Results of organ cultures of five mammary tumours (solid lines) and two sarcomas (dashed lines). Mean $\log_{10}$ cpm of H³-TdR incorporation into DNA of control flasks during 3, 4 and 5 days of culture is given for each tumour.

Fig. 2. Effects of prolactin on five mammary tumours (solid lines) and two sarcomas (dashed lines) during 3, 4 and 5 days of culture. Significance of F-test between "hormone effect" and general error" is given graphically. * $0.05 > p > 0.01$; ** $0.01 > p > 0.001$; *** $0.001 < p$.

hibited on day 4. M4 was also inhibited on day 5. Sarcoma S1 was stimulated at all culture times, S2 only on day 4.

In Fig. 3 hydrocortisone treated flasks are compared with hydrocortisone-prolactine treated ones. This combination corresponds to the experimental set up used by *Welsh & Rivera* (8). Tumour M1 is stimulated on days 4 and 5 and Tumour M5 is stimulated on day 4. All other tumours are not affected by the treatment.

Sections from mammary tumour M5 were studied. As appears from Fig. 1 this tumour was actively growing after five days. Control

prolactin and hydrocortisone singly or in combination.

MATERIAL AND METHODS

Mammary tumours were induced in 50-day-old female Sprague Dawley rats (Anticimex, Stockholm) by intragastric instillation of 20 mg DMBA in oil suspension. The tumours were used about three months after the induction. Sarcomas were one rat tumour induced by polyoma virus and one induced by adeno virus. Both tumours were induced and propagated in female inbred Wistar rats and transplanted for 13 and 16 generations, respectively before use.

The organ culture technique has been described in detail elsewhere (1). In brief, twelve explants, approximately 1.5 square mm were placed on a milliporefilter on top of a thin piece of cellulose acetate and floated in Trowell's T 8 medium (Biocult, Glasgow) in a Carrel D5 glass culture flask. 50 IU/ml of benzyl penicillin and 50 μg/ml of streptomycin sulphate were added to the medium.

Bovine prolactin, NIH P B4, was dissolved in 0.9 per cent saline. Hydrocortisone (Sigma, St. Louis, Mo.) was dissolved in 96 per cent ethanol giving a final ethanol concentration of 1 per cent.

A tumour was cultured with the following hormones at the following concentrations:

Prolactin 5 μg/ml

Hydrocortisone 1 μg/ml

Prolactin 5 μg/ml and hydrocortisone 1 μg/ml

Control flask had medium and solvents only.

Three control flasks and three flasks for each hormone or hormone combination were cultured for three, four and five days, respectively. Thus, an entire series was composed of 36 flasks. Care was taken to randomize the explants from a tumour during the setting up of an experiment which was carried out at room temperature. The cultures were incubated at 37° C without gassing. Media were changed daily.

Four hours before a culture was terminated, the content of a flask was transferred into a glass tube containing one millilitre of its own medium upon which 2 μCi of H^3 TdR (methyl H^3 thymidine, specific activity 1.9 Ci/mM, Schwarz/Mann, Orangeburgh) was added. The culture was then continued at 37° C for a further four hours and terminated by centrifugation and washing the explants twice with cold (+4) trichloroacetic acid for half an hour. The explants were finally dissolved in Soluene 350 (Packard Ltd) and the radioactivity of each flask was determined by liquid scintillation counting. No correction of the counts was made for the DNA content in the tubes, as described previously (1).

Prior to statistical treatment, a general (technical) error variance was determined on the basis of variances from the 84 available triple determinations. The uniformity of these variances was controlled by Bartlett's test.

"Hormone effect" was expressed as the difference between the mean $\log_{10}$ cpm of the three control flasks and three hormone treated flasks. The significance of a hormone effect was checked by F tests between variances due to "hormone treatment" and "general error".

In the case of one tumour one additional flask was made for each hormone or hormone combination and control. These explants were fixed after five days of culture, they were sectioned at 5 μ, stained with haematoxylin and eosin and investigated by light microscopy.

RESULTS

Five mammary tumours (M1–M5) and two sarcomas (S1-S2) were studied. The results are given graphically in Figs. 1–5. The incorporation of H^3 TdR into DNA of controls is shown in Fig. 1. Three mammary tumours (M1, M4 and M5) and the sarcomas (S1 and S2) were actively growing and increased their DNA synthesis from day 3 to 5. Mammary tumour M2 was fairly stationary while M3 increased from day 3 to day 4 though it decreased again to its original value on day 5. All tumours showed good incorporation equivalent to that seen in previous experiments (1, 2).

Fig. 2 shows the effect of addition of prolactin to the cultures. One tumour, M4, was significantly stimulated in its DNA synthesis at all culture times. M3 was stimulated on day 5 only. The remaining mammary tumours remained unaffected. Sarcoma S1 was significantly inhibited on days 4 and 5. Sarcoma S2 was not affected by the treatment.

The effect of the addition of hydrocortisone is shown in Fig. 3. Mammary tumours M1, M3, M4 and M5 were significantly inhibited on day 4, M1 and M4 also being inhibited on day 5. Sarcoma S1 was stimulated on days 3 and 4 but was not affected on day 5. Sarcoma S2 was stimulated on days 4 and 5.

Fig. 4 illustrates the effects of the combination of prolactin and hydrocortisone. Mammary tumours M2 and M5 were not affected by the treatment. M1, M3 and M4 were in

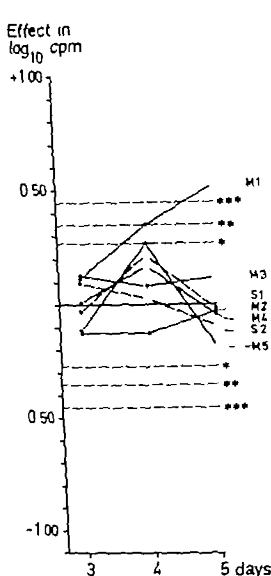


Fig. 5 Effects of prolactin on mammary tumours and sarcomas when the culture medium is "enriched" with hydrocortisone. For explanations, see text to Fig. 2.

used and thus the effects observed were due exclusively to the addition of hormones. Trowell's medium contains insulin at a concentration of 50 µg/ml. Thus, the present experimental set up was comparable to that used by *Welsh & Rivera* (8) who added insulin in doses of 5 µg/ml but differs from theirs that the effect of prolactin was investigated independently of hydrocortisone.

Prolactin effects were found in the present work. Two out of five mammary tumours were stimulated by the hormone. One of the two tumours, tumour M4 was actively growing and the observed stimulation was genuine. In the other M5 control flasks decrease their DNA synthesis after five days while prolactin treated flasks are maintained at the four-day-level. In Fig 2 the difference is given as a stimulatory effect of prolactin though it actually represents a maintenance effect of the hormone. A surprising finding was the effect of prolactin on sarcomas. One of these tumours remained completely unaffected while the DNA synthesis of sarcoma S1 a tumour induced by polyoma virus was significantly inhibited on days 4 and 5. As appears from Figs. 1 and 2, this effect is certainly not due to peculiarities of tumour growth *in vitro* and the statistical analysis shows that it is not due to technical errors. This finding raises the important question of specificity of *in vitro* hormone assays, a problem discussed elsewhere (1, 2). Some virus induced sarcomas in the rat are either prolactin sensitive, probably due to derepression of the tumour genome, or else, *in vitro* assays of the present type are not representative of *in vivo* hormone sensitivity.

Hydrocortisone has been used by many workers to enrich culture media. The reason why is apparently the extensive glandular differentiation induced by this hormone both *in vivo* and *in vitro*. This effect was confirmed in the present investigation. However hydrocortisone per se also exerted some effect. The DNA synthesis in sarcomas was stimulated while it was inhibited in mammary tumours. If hydrocortisone treated cultures were compared with hydrocortisone and prolactin treated cultures [cf. *Welsh & Rivera* (8)] the pattern of response was found to differ from that obtained by prolactin only. Tumours previously sensitive to prolactin become insensitive and other tumours are made sensitive to prolactin. An interesting observation is that after five days of hydrocortisone treatment the lobular alveolar differentiation was not followed by increase

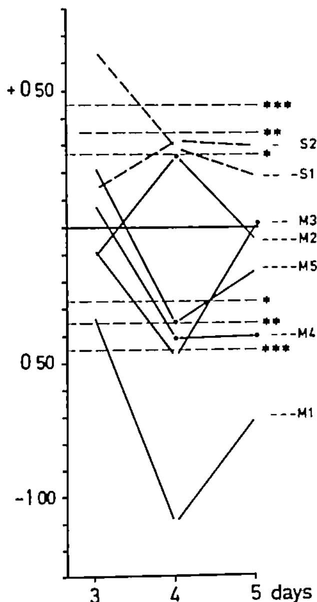


Fig 3 Effects of hydrocortisone on mammary tumours and sarcomas. For explanations, see text to Fig 2.

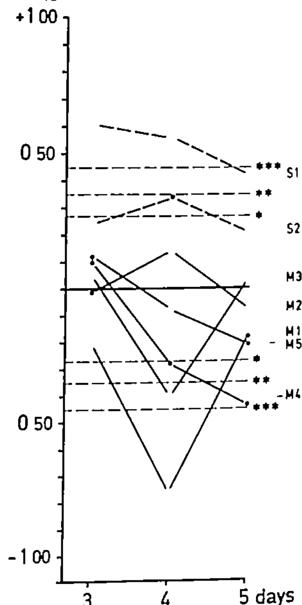


Fig 4 Effects of prolactin and hydrocortisone on mammary tumours and sarcomas. For explanations, see text to Fig 2.

flasks and prolactin treated flasks showed healthy cells but no glandular arrangement. There was a central necrosis, as previously recorded (1) Hydrocortisone treated flasks, however showed a very marked lobulo-alveolar differentiation and no central necrosis of the explant was visible. The addition of prolactin did not alter the histological picture in the two groups. Moreover there was no significant differences between DNA synthesis in the various groups, i.e the differentiation was not followed by an increase in DNA synthesis.

DISCUSSION

A defined medium was used in the present investigation i.e. protein additives were not

Acta path. microbiol. scand. Sect. A, 85 63 72, 1977

SECRETION OF CALCITONIN AND GASTRIN IN RATS WITH TRANSPLANTED MEDULLARY THYROID CARCINOMA

TRINE NORMANN, ELDAR NORMANN, ERIK SCHRUMPF and KAARE M. GAUTVIK

Department of Pathology and Norsk Hydro's Institute for Cancer Research, The Norwegian Radium Hospital, Oslo Research Laboratory of Gastroenterology Department IX, Ullevål Hospital, Oslo and Institute of Physiology University of Oslo, Oslo Norway

Normann, T Normann, E., Schrumpf E. & Gautvik, K. M. Secretion of calcitonin and gastrin in rats with transplanted medullary thyroid carcinoma. Acta path. microbiol. scand. Sect. A, 85 63–72, 1977

Rats transplanted with medullary thyroid carcinoma (MCT) were followed with radio-immuno assay of serum calcitonin (iCT) using antisera to human CT and I ¹²⁵ labelled calcitonin-M. From the 4th month after transplantation, serum from the tumour rats contained iCT in concentrations 6–10 fold higher than serum from the control rats. The tumour cells had retained their ability to react on pentagastrin and calcium injections with increased CT release. It was further shown that the tumour bearing rats had elevated basal gastrin concentrations in serum. While calcium injection lead to a rise in the serum gastrin concentration in the control group, the adverse effect was seen in the tumour bearing rats. The morphological features and the responsiveness of the rat tumour cells to physiological secretagogues make this tumour a suitable animal model for the study of interactions between CT and gastro-intestinal factors. It is suggested that the gastrin response to calcium might be of interest also in the diagnosis of human MCT

Key words Calcitonin gastrin medullary thyroid carcinoma transplanted.

T Normann, Department of Pathology The Norwegian Radium Hospital, Montebello, Oslo, Norway

Received 20 76 Accepted 3 m 76

Several experimental observations have suggested an interrelation between serum calcitonin (CT) serum gastrin, and gastric acid secretion (1 3 12) In patients with chronic hypercalcitoninaemia due to medullary thyroid carcinoma (MCT) peptic ulceration, gastric as well as duodenal, are frequent complaints (13 18 but the causal association, if any between MCT and peptic ulceration is obscure In healthy subjects CT has been shown to inhibit gastric acid secretion (12) and in patients with MCT serum gastrin levels are low (24) Furthermore, injection of CT to cats has been found to prevent ulcer formation (14) Conversely the stimulatory effect of gastrin and related gastro-intestinal hormones on CT secretion from normal mammals as well as from patients with MCT is well documented (8 9 11 17 25)

Since MCT is a rare tumour in man, the possibilities for studying the various biological aspects of the human disease are limited and there has been a need for an experimental

or decrease in DNA synthesis in tumour M5 Thus "enrichment" of culture media by hydrocortisone does not increase growth rate but often decreases DNA synthesis (Fig 3)

In accordance with findings in previous studies (1) the effects of hormone varied with culture time Thus, the inhibitory action of hydrocortisone had a tendency to be more marked on day four than on days 3 and 5 The effects of prolactin increased with culture time which may reflect clonal selection in the cultures.

Although the number of mammary tumours included in the present study is small, it confirms the findings in *in vivo* studies by *Leung & Sasaki* (6) and by *Bradley et al* (3) in so far as prolactin is shown to have a stimulatory effect on the DNA synthesis of the DMBA induced mammary tumour in the rat.

Bovine prolactin, NIH P B4 was generously donated by the *National Institute of Arthritis Metabolic and Digestive Diseases Md*

The work was supported by grants from the *Faculty of Medicine University of Lund Sweden*

REFERENCES

1 *Aspegren K.*, 7 12 DMBA induced rat mammary tumour studied for hormonal responsiveness *in vitro* 2 Organ cultures. Acta path. microbiol scand Sect. A 83 37–50 1975

2 *Aspegren K* Specificity of hormonal responsiveness *in vitro* Effect of sex steroids on nonmalignant rat cells compared with the effect on cells from rat tumours. Acta path. microbiol scand Sect. A, 84 198–200 1976.

3 *Bradley C J Kledzik G S & Meites J* Prolactin and estrogen dependency of rat mammary cancers at early and late stages of development. Cancer Res. 36 319–324 1976.

4 *Butler T P & Pearson O H* Regression of prolactin-dependent rat mammary carcinoma in response to antihormone treatment. Cancer Res. 31 817–820 1971

5 *Kelly P A Bradley C Shiu R P C Meites J & Friesen H G* Prolactin binding to rat mammary tumour tissue Proc. Soc. Exp. Biol Med. 146 816–819 1974

6. *Leung B. S & Sasaki G H* On the mechanism of prolactin and estrogen action in dimethylbenz(A)anthracene-induced mammary carcinoma in the rat. II *In vivo* tumor responses and estrogen receptor Endocrinology 97 564–572, 1975

7 *Turkington R W* Prolactin receptors in mammary carcinoma cells. Cancer Res. 34 758–763 1974

8 *Welsh C W & Rivera E. M* Differential effects of estrogen and prolactin on DNA synthesis in organ cultures of DMBA induced rat mammary carcinoma. Proc. Soc. Exp. Biol. Med. 139 623–626 1972.

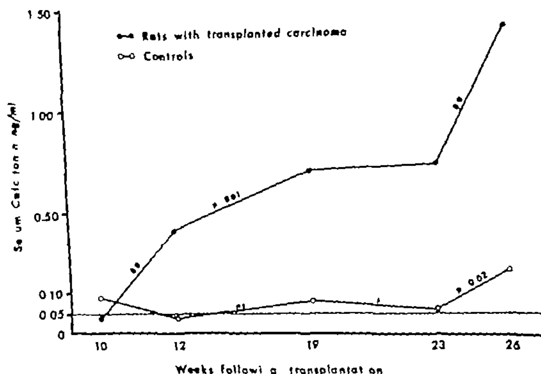


Fig 1 Median serum calcitonin levels in rats at different time intervals following transplantation of spontaneous rat thyroid C-cell carcinoma and in controls.

RESULTS

Basal concentration of calcitonin in serum Basal levels of serum rCT in the group of tumour bearing animals increased significantly from one observation to the next, except between the 19th and 23rd week (Fig 1) The individual results are presented in Table 1 From approximately the 4th month, the median values for the tumour group was above 0.50 ng/ml and 8–10 fold higher than in the control rats. Apart from a slight increase in rCT concentration from the 23rd to the 26th week, the observed variations between the values in the control group were within the variability of the method (10) The differences between the values for the tumour group and the control group were statistically significant ($p<0.01$) at every point of time, except for the first observation 10 weeks after the transplantation.

Basal concentration of gastrin in serum. The median concentration of immunoreactive gastrin in serum of the tumour rats approximately 4 months after transplantation was 410 (range *60–800) pg/ml, and in serum of the control rats 229 (range 110–340) pg/ml. The difference is statistically significant ($p<0.001$) The individual observations are depicted in Fig 2.

Effect of pentagastrin injection on serum calcitonin. Intravenous injection of 10 μg pentagastrin/rat lead to elevation of serum rCT in all the tumour rats and in 3 of the 4 controls (Fig 3) The maximal values in the tumour group ranged from 0.44 to 2.70 (median 0.97) ng/ml, and in the control group from 0.12 to 0.30 (median 0.29) ng/ml. The peak values for 5 of the tumour rats were attained between 1 and 5 minutes the sixth tumour bearing rat reacted with a slight increase 15 minutes after the injection.

Effect of calcium injection on serum calcitonin and gastrin Intraperitoneal injection of

model. Recently it has been shown that a thyroid tumour which occurs spontaneously in old rats is light and electron microscopically similar to MCT in man (5, 6, 15) and that the tumour cells secrete calcitonin (4, 26).

The present experiments were undertaken to study the secretion of calcitonin, gastrin and gastric acid in rats with transplanted medullary carcinoma.

MATERIALS AND METHODS

Experimental animals. The experiments were performed on 17 female Wlg/Rij rats transplanted with naturally occurring medullary thyroid carcinoma under the kidney capsule at 4 weeks of age. Ten control rats of the same strain, age and sex were included in the study. The tumour tissue was originally taken from the thyroid of two rats kept for a study of ageing processes. The transplantation procedure has been described previously in detail by *Boorman et al.* (5). If not otherwise specified the rats were fed an ordinary stock diet, receiving their usual food and water supply during the experiments.

Blood sampling and preparation of tissue. Serum for iCT determinations was obtained from tail blood from groups of animals counting 7–12 tumour rats and 7–10 controls and taken 5 times between 2 and 6 months following transplantation. Serum for basal gastrin measurements was taken from 12 tumour rats, approximately 4 months after the transplantation, and from 10 controls. All blood samples were allowed to clot, centrifuged and stored at −20 °C for radio-immuno assay.

Tissue samples for iCT assay from 8 transplanted tumours were weighed and stored at −20 °C. Tissue gastrin was determined on samples from 2 tumours. Antral an duodenal mucosa from the same animal served as reference organs. The samples were minced, mixed with 5 ml of distilled water and quickly immersed in a boiling water bath for 30 minutes. The supernatant was frozen to −20 °C for later analysis. The precipitate was homogenized in 2 ml of 0.2 M phosphate buffer and the protein was determined according to *Lowry et al.* (16) using bovine serum albumin as standard.

Determination of calcitonin. A heterologous radio-immuno assay employing I^{125} labelled human synthetic calcitonin-M (Ciba-Geigy Ltd.) and rabbit antiserum against the human hormone was used. Serum and homogenates of the transplanted tumours were analysed as described previously (10). Serial dilution of tumour homogenate gave a corresponding decrease in measured CT thereby suggesting an immunological relationship between human iCT and the material measured in the samples, designated rat iCT. The lowest detectable concentration was 0.05 ng/ml.

Determination of gastrin. Gastrin in serum and tissue homogenates was analysed radio-immunologically (22) using the Rehfeld & Stadil antibody 2604 measuring all major gastrin components. In preliminary experiments, no cross-reactivity between calcitonin and gastrin antiserum was found. All basal samples were analysed within one week using the same tracer.

Pentagastrin and calcium injections. Pentagastrin (10 µg/rat) was injected intravenously in six tumour rats and 4 controls (weight 180–200 g). Blood for iCT measurements was drawn from one femoral vein at 0, 1, 2, 5 and 15 minutes after the injection.

In 6 tumour rats and 4 controls, blood from one femoral vein was drawn at 0, 10, 20 and 45 minutes after intraperitoneal injection of $CaCl_2$ (2 mg Ca^{++}/rat). In these samples, both the concentration of gastrin and calcitonin were determined.

These experiments were performed approximately 5 months after transplantation.

Measurement of gastric acid secretion. The collection of gastric juice was carried out according to the technique described by *Shay et al.* (23) on 7 rats, 6 months after tumour transplantation, and on 5 control rats. The animals were starved for 48 hours but permitted water *ad libitum* until the morning of the experimental day. Pylorus ligation was performed under light ether anaesthesia and the stomach contents drained into tubes, and centrifuged. The supernatant was measured for volume and pH. The acidity was determined by titration against 0.05 N NaOH to pH 7.0. The results obtained from 3 of the tumour animals were discarded since the stomach contents were haemorrhagic at the second laparotomy.

Morphological studies. In all the animals, complete autopsy including microscopic examination was performed. The tumours were measured and inspected for necrosis as well as haemorrhages. For light microscopy slides were stained with Congo red in addition to H.E. Tumour tissue was also fixed in 2 per cent phosphate buffered glutaraldehyde, postfixed in osmium tetroxide and embedded in epon/araldite for electron microscopy.

The stomach, duodenum and proximal jejunum were opened and inspected for macroscopic ulcerations, fixed in formalin (4 per cent) and processed for routine histology.

Calculation analyses. The results of iCT and gastrin measurements are given at median and range values. The statistical significance of the differences was evaluated by the non parametric Wilcoxon rank test where p values less than 0.05 were considered significant. iCT values less than 0.05 ng/ml were given the same ranking number in the two groups under comparison.

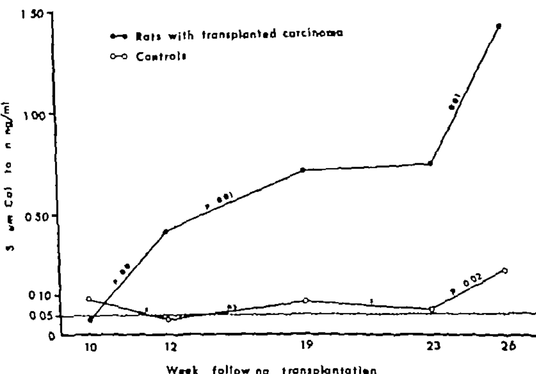


Fig 1 Median serum calcitonin levels in rats at different time intervals following transplantation of spontaneous rat thyroid C-cell carcinoma and in controls

RESULTS

Basal concentration of calcitonin in serum Basal levels of serum iCT in the group of tumour bearing animals increased significantly from one observation to the next, except between the 19th and 23rd week (Fig 1) The individual results are presented in Table 1 From approximately the 4th month, the median values for the tumour group was above 0.50 ng/ml and 8-10 fold higher than in the control rats. Apart from a slight increase in iCT concentration from the 23rd to the 26th week, the observed variations between the values in the control group were within the variability of the method (10) The differences between the values for the tumour group and the control group were statistically significant ($p<0.01$) at every point of time except for the first observation 10 weeks after the transplantation.

Basal concentration of gastrin in serum. The median concentration of immunoreactive gastrin in serum of the tumour rats approximately 4 months after transplantation was 410 (range 260-800) pg/ml, and in serum of the control rats 229 (range 110-340) pg/ml. The difference is statistically significant ($p<0.001$) The individual observations are depicted in Fig 2.

Effect of pentagastrin injection on serum calcitonin. Intravenous injection of 10 μg pentagastrin/rat lead to elevation of serum iCT in all the tumour rats and in 3 of the 4 controls (Fig 3) The maximal values in the tumour group ranged from 0 44 to 2.70 (median 0.97) ng/ml, and in the control group from 0.12 to 0.30 (median 0.29) ng/ml. The peak values for 5 of the tumour rats were attained between 1 and 5 minutes the sixth tumour bearing rat reacted with a slight increase 15 minutes after the injection.

Effect of calcium injection on serum calcitonin and gastrin Intraperitoneal injection of

TABLE 1 *Serum Calcitonin Concentration (ng/ml) in Rats with Transplanted Thyroid C cell Tumours and in Control Rats of the Same Age*

	Weeks after transplantation				
	10	12	19	23	26
Tumour rats					
1			0.81	0.82	1.66
2	<0.05	<0.05	0.34	0.33	1.17
3	<0.05	0.29	[illegible]	1.20	
4	<0.05	0.16	0.44	0.63	
5	<0.05	0.05	0.10	0.20	0.49
6	0.08	0.87	2.40	1.15	1.71
7	<0.05	<0.05	0.70	0.41	0.73
8	<0.05	0.76			2.92
9	<0.05	0.81	0.71		1.46
10	<0.05	0.46	0.66	0.97	
11	0.06	1.25	0.76		2.33
12	0.13	0.36	1.20		1.31
13	<0.05	0.59			1.30
Control rats					
14	0.17	<0.05	0.75		0.44
15	0.13	<0.05	0.32	0.06	0.31
16	0.13	<0.05	<0.05		0.22
17	<0.05	<0.05	0.07	0.07	0.21
18	0.07	<0.05	0.27	<0.05	
19	<0.05	0.17	<0.05	<0.05	<0.05
20	0.46	<0.05	0.08	<0.05	
21	0.10	<0.05	0.08	<0.05	0.12
22	<0.05	<0.05	0.41	0.10	0.20
23	<0.05	<0.05	<0.05	0.06	

2 mg Ca^{++}/rat was followed by an increase in serum iCT in 5 of the 6 tumour rats and in 3 of the 4 controls (Fig 4) The peak values, range 0.87 to 2.53 (median 2.19) ng/ml in the tumour group and 0.18 to 0.59 (median 0.36) ng/ml in the control group were seen at different intervals after calcium stimulation In only one animal the basal value was reached at the end of the 15 minutes observation period

Calcium injection lead to a fall in serum gastrin levels in all but one of the 6 tumour bearing rats whereas the reverse effect was observed in the control group (Fig 5) The gastrin response to calcium was significantly different ($p<0.025$) in the two groups at 20 minutes after the injection

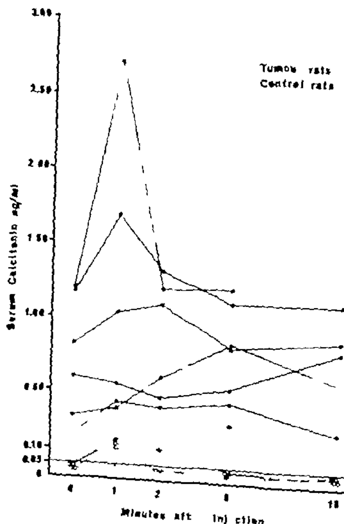
One tumour rat with basal hypercalcitonaemia (indicated by x in Figs. 4 and 5) reacted differently on Ca injection in this rat a slight decrease in iCT concentration was observed at 2 minutes whereas an increase in the gastrin level was seen at 45 minutes after Ca injection.

Gastric acid secretion It is evident from Table 2 that the median acid output/4 hours was 115 μEq in the tumour rats as compared with 170 μEq in the control group. This difference is not statistically significant The pH of the gastric secretion was significantly higher in the tumour rats than in the controls ($p<0.05$)

Calcitonin and gastrin content of tissue samples Tumour tissue from 8 different animals contained iCT in concentrations ranging from 334 to 1082 (median 708) ng/50 mg wet weight

Tumour samples from two animals with hypercalcitonaemia contained less than 10 pg gastrin/100 μg protein The gastrin contents

Fig. 3. Serum calcitonin concentration in response to iv injection of pentagastrin (10 µg/rat)



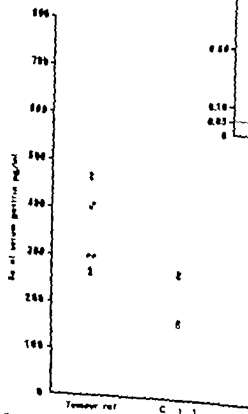


Fig. 2 Basal serum gastrin levels in 12 rats 4 months after tumour transplantation and in 10 controls.

of antral and duodenal mucosa from the two rats were 300 and 574 pg/100 µg protein and 24 and 38 pg/100 µg protein, respectively

Morphological findings The transplanted tumour occupied between 1/10 and 1/5 of the kidney In most cases there were multiple nodules and obvious infiltrating growth in the kidney parenchyma, but metastases (to the spleen) were seen in one animal only In the majority of tumours, the cells were well preserved but confluent necrosis was seen in the tumour from two of the animals. Microscopically the tumour cells appeared spindle shaped or polyhedrally arranged in solid nests (Fig. 6) In most tumours the cytological

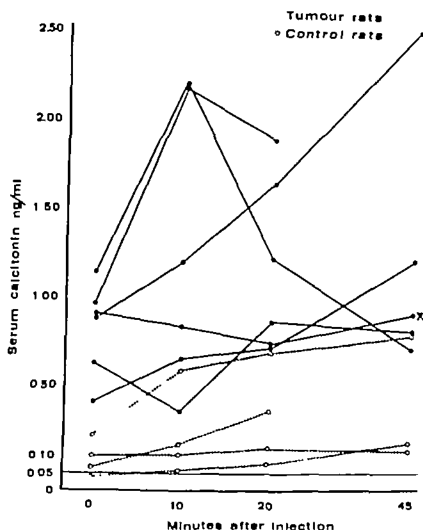


Fig 4 Serum calcitomn concentration in response to *intraperitoneal* injection of 2 mg Ca^{++}/rat

TABLE 2 *Gastric Acid in Pylorusligated Rats with Transplanted Medullary Thyroid Carcinoma (4 Rats) and in Controls (5 Rats) Values Are Given at Median and Range*

	Volumes (ml)	pH	Acid (mEq/ml/4 hours)
Tumour rats	3 2 (1 9–3 8)	4.5 (2 7–5 0)	115 (90–130)
Control rats	3 4 (1.5–5 0)	2 1 (1 2–2 7)	170 (110–430)

atypia was moderate Amyloid was not demonstrated in any of the tumours. Ultra structurally the tumour cells showed the same features *as those observed in human MCT* (19) with typical secretory granules (Fig 7)

Macroscopic, as well as microscop c ex amination of the stomach intestine and pancreas from the two groups failed to reveal pathological features.

DISCUSSION

The light and electron microscopic similarities between thyroid C-cell tumour of the rat *and human MCT* described by others (5 6, 15) were confirmed by this study *Burford et al* (7) demonstrated structural and immunological *similarities between rat and human* CT and we found that radio-immuno assay using antisera to human CT was a reliable method also for the detection of rat CT From the 12th week after transplanta

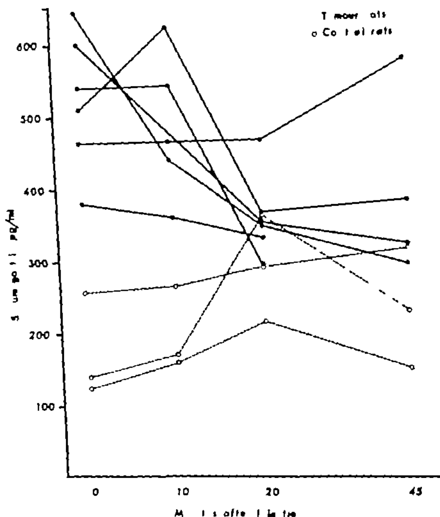


Fig 3 Serum gastrin concentration in response to intraperitoneal injection of 2 mg Ca^{++}/rat.

tion, serum from the tumour rats contained approximately 10 fold higher levels of iCT than serum from the control rats. The present study also reveals that the transplanted rat tumour responds to calcium and pentagastrin injection by an increase in serum iCT similar to the human medullary carcinoma (11 17 23)

No morphological changes were found in the gastro-intestinal mucosa of the tumour rats, but the difference in serum gastrin concentration in the two groups of animals clearly points to an interrelation between MCT and gastro-intestinal hormones. The basal serum gastrin levels in the tumour bearing animals with hypercalcitoninaemia were significantly higher than in the control group in which the hormone concentration was of the same magnitude as that found in normal Sprague Dawley rats (21) Since tumour tissue from two animals with hypercalcitoninaemia contained only minute amounts of gastrin, ectopic gastrin production by the tumour cells cannot explain the hypergastrinaemia.

The relation between serum calcitonin, serum gastrin and serum calcium is incom-

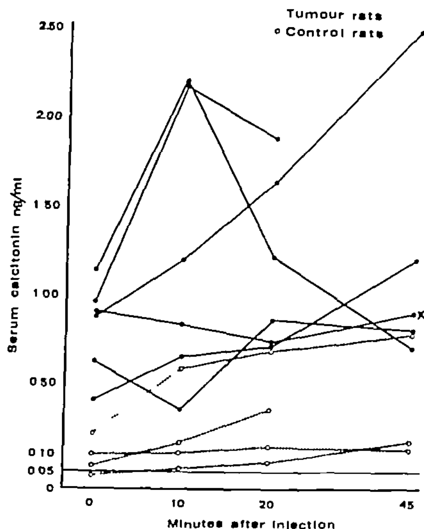


Fig 4 Serum calcitonin concentration in response to intraperitoneal injection of 2 mg Ca^{++}/rat.

TABLE 2. *Gastric Acid in Pylorusligated Rats with Transplanted Medullary Thyroid Carcinoma (4 Rats) and in Controls (5 Rats) Values Are Given at Median and Range*

	Volumes (ml)	pH	Acid (mEq/ml/4 hours)
Tumour rats	3 2 (1 9–3 8)	4.5 (2 7–5.0)	115 (90–130)
Control rats	3 4 (1.5–5 0)	2.1 (1 2–2 7)	170 (110–430)

atypia was moderate Amyloid was not demonstrated in any of the tumours. Ultrastructurally the tumour cells showed the same features as those observed in human MCT (19) with typical secretory granules (Fig 7)

Macroscopic, as well as microscopic examination of the stomach, intestine and pancreas from the two groups failed to reveal pathological features.

DISCUSSION

The light and electron microscopic similarities between thyroid C-cell tumour of the rat and human MCT described by others (5 6, 15) were confirmed by this study *Burford et al* (7) demonstrated structural and immunological similarities between rat and human CT and we found that radio-immuno assay using antisera to human CT was a reliable method also for the detection of rat CT From the 12th week after transplanta

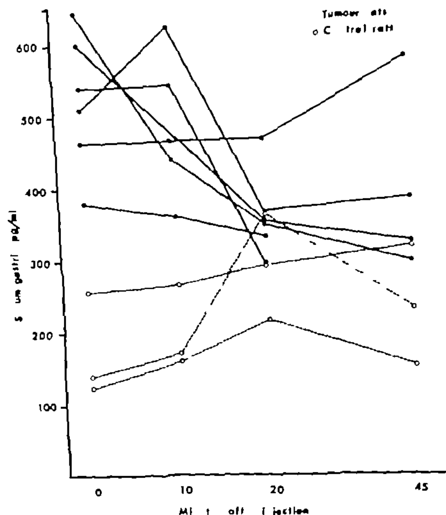


Fig 5 Serum gastrin concentration in response to intraperitoneal injection of 2 mg Ca^{++}/rat.

tion, serum from the tumour rats contained approximately 10 fold higher levels of rCT than serum from the control rats. The present study also reveals that the transplanted rat tumour responds to calcium and pentagastrin injection by an increase in serum rCT similar to the human medullary carcinoma (11 17 25)

No morphological changes were found in the gastro-intestinal mucosa of the tumour rats, but the difference in serum gastrin concentration in the two groups of animals clearly points to an interrelation between MCT and gastro-intestinal hormones. The basal serum gastrin levels in the tumour bearing animals with hypercalcitonaemia were significantly higher than in the control group in which the hormone concentration was of the same magnitude as that found in normal Sprague Dawley rats (21) Since tumour tissue from two animals with hypercalcitonaemia contained only minute amounts of gastrin, ectopic gastrin production by the tumour cells cannot explain the hypergastrinaemia.

The relation between serum calcitonin, serum gastrin and serum calcium is incom-

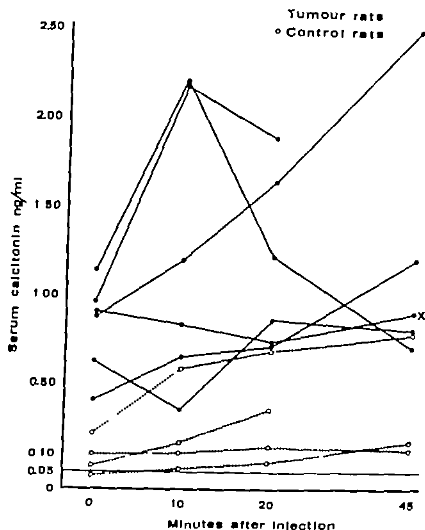


Fig 4 Serum calcitonin concentration in response to intraperitoneal injection of 2 mg Ca^{++}/rat.

TABLE 2 *Gastric Acid in Pylorusligated Rats with Transplanted Medullary Thyroid Carcinoma (4 Rats) and in Controls (5 Rats) Values Are Given at Median and Range*

	Volumes (ml)	pH	Acid (mEq/ml/4 hours)
Tumour rats	3 2 (1 9–3 8)	4 5 (2 7–5 0)	115 (90–130)
Control rats	5 4 (1.5–5 0)	2 1 (1 2–2 7)	170 (110–450)

atypia was moderate Amyloid was not demonstrated in any of the tumours. Ultrastructurally the tumour cells showed the same features as those observed in human MCT (19) with typical secretory granules (Fig 7)

Macroscopic, as well as microscopic examination of the stomach intestine and pancreas from the two groups failed to reveal pathological features.

DISCUSSION

The light and electron microscopic similarities between thyroid C-cell tumour of the rat and human MCT described by others (5 6 15) were confirmed by this study *Burford et al* (7) demonstrated structural and immunological similarities between rat and human CT and we found that radio-immuno assay using antisera to human CT was a reliable method also for the detection of rat CT From the 12th week after transplanta

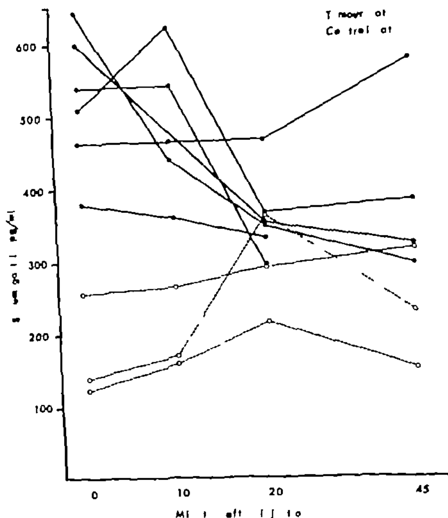


Fig 5 Serum gastrin concentration in response to intraperitoneal injection of 2 mg Ca^{++}/rat.

tion, serum from the tumour rats contained approximately 10 fold higher levels of iCT than serum from the control rats. The present study also reveals that the transplanted rat tumour responds to calcium and pentagastrin injection by an increase in serum iCT similar to the human medullary carcinoma (11 17 25)

No morphological changes were found in the gastro-intestinal mucosa of the tumour rats, but the difference in serum gastrin concentration in the two groups of animals clearly points to an interrelation between MCT and gastro-intestinal hormones. The basal serum gastrin levels in the tumour bearing animals with hypercalcitonaemia were significantly higher than in the control group in which the hormone concentration was of the same magnitude as that found in normal Sprague Dawley rats (21) Since tumour tissue from two animals with hypercalcitonaemia contained only minute amounts of gastrin, ectopic gastrin production by the tumour cells cannot explain the hypergastrinaemia.

The relation between serum calcitonin, serum gastrin and serum calcium is incom-

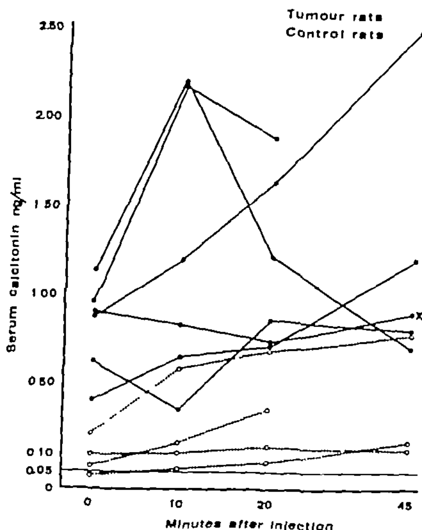


Fig 4 Serum calcitonin concentration in response to intraperitoneal injection of ? mg Ca⁺⁺/rat.

TABLE 2 *Gastric Acid in Pylorusligated Rats with Transplanted Medullary Thyroid Carcinoma (4 Rats) and in Controls (5 Rats) Values Are Given at Median and Range*

	Volumes (ml)	pH	Acid (mEq/ml/4 hours)
Tumour rats	3 2 (1.9–3 8)	4 5 (2 7–5 0)	115 (90–130)
Control rats	3 4 (1.5 5 0)	2 1 (1 2–? 7)	170 (110–430)

atypia was moderate Amyloid was not demonstrated in any of the tumours. Ultrastructurally the tumour cells showed the same features as those observed in human MCT (19) with typical secretory granules (Fig 7)

Macroscopic as well as microscopic examination of the stomach intestine and pancreas from the two groups failed to reveal pathological features.

DISCUSSION

The light and electron microscopic similarities between thyroid C-cell tumour of the rat and human MCT described by others (5 6, 15) were confirmed by this study *Burford et al* (7) demonstrated structural and immunological similarities between rat and human CT and we found that radio-immuno assay using antisera to human CT was a reliable method also for the detection of rat CT From the 12th week after transplanta

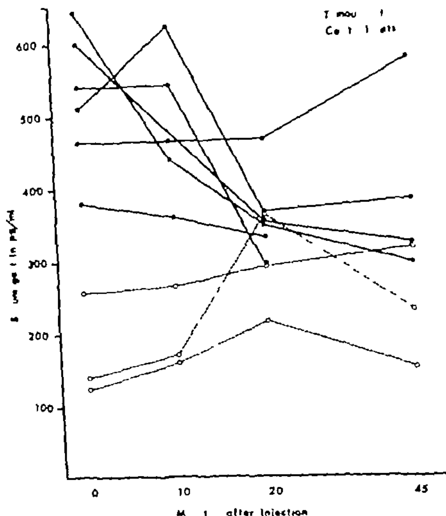


Fig. 5 Serum gastrin concentration in response to intraperitoneal injection of 2 mg Ca^{++}/rat.

tion, serum from the tumour rats contained approximately 10 fold higher levels of iCT than serum from the control rats. The present study also reveals that the transplanted rat tumour responds to calcium and pentagastrin injection by an increase in serum iCT similar to the human medullary carcinoma (11 17 25)

No morphological changes were found in the gastro-intestinal mucosa of the tumour rats, but the difference in serum gastrin concentration in the two groups of animals clearly points to an interrelation between MCT and gastro-intestinal hormones. The basal serum gastrin levels in the tumour bearing animals with hypercalcitonaemia were significantly higher than in the control group in which the hormone concentration was of the same magnitude as that found in normal Sprague Dawley rats (21) Since tumour tissue from two animals with hypercalcitonaemia contained only minute amounts of gastrin, ectopic gastrin production by the tumour cells cannot explain the hypergastrinaemia.

The relation between serum calcitonin, serum gastrin and serum calcium is incom-

pletely understood Since serum calcium in the animals was not measured a definite interpretation of the results cannot be made On the basis of the present and previous studies (2 3 20 24), however one apparently discrepant observation may be explained Patients with MCT and high serum iCT had low serum gastrin levels (24) and injection of large doses of CT to healthy subjects inhibited serum gastrin response to food (2) both studies suggest an inhibitory effect of high serum concentrations of CT on gastrin release Injection of smaller doses of CT had no effect on meal stimulated hypergastrinaemia (3) The tumour rats in the present study had significantly elevated serum iCT as compared with the control rats, but markedly lower values than the patients with MCT (24) It is therefore possible that the observed lack of inhibitory effect on gastrin in these animals is due to a sub-effective serum level of CT The increased serum gastrin concentration in the tumour rats may be explained as compensatory to decreased gastric acid secretion which in turn very probably is an effect of CT as CT repeatedly has been shown to be a potent inhibitor of gastric secretion (1 2 3 12 14) Serum calcium is probably involved in the secretion of these hormones and gastric juice in rats with MCT but the nature of this involvement is at present unknown

It is of special interest that it was demonstrated in this study that the gastrin response to calcium injection was different in tumour rats and controls While the control rats responded with an increase in serum gastrin similar to findings in the cat (1) in normal man in subjects with duodenal ulcer (20) as well as in patients with Zollinger Ellison disease (27) the hormone concentration in serum from tumour rats fell after calcium administration. The reason for this is not clear One possible explanation is that the CT concentration due to calcium stimulation in the tumour rats has reached a level which overrules the stimulatory effect of calcium on gastrin resulting in an inhibition of gastrin release If the same effect is present in patients with MCT this may be a useful test in the diagnosis of the disease

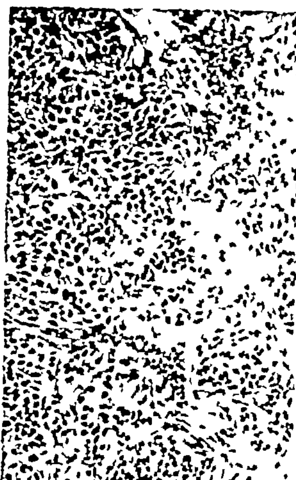


Fig 6 Light micrograph of rat thyroid C-cell tumour transplanted under the kidney capsule. Growth pattern and cell morphology not distinguishable from human MCT × 160 H E.

In conclusion rats bearing transplanted MCT develop hypercalcitonaemia, hypergastrinaemia and reduced gastric acid secretion The release of CT from the tumour is stimulated by calcium and pentagastrin The morphological similarities between the rat tumour and human MCT together with the changes in CT secretion in response to physiological secretagogues, make this a suitable animal model for the study of different pathophysiological aspects of MCT In addition the endocrine feed back mechanisms existing between gastro-intestinal hormones and CT can be elucidated in MCT bearing rats.



Fig 7 Electron micrograph showing three adjacent tumour cells with numerous intracytoplasmatic secretory granules. Uranyl acetate and lead citrate stain. × 1200.

W are greatly indepted to Dr *C F Hollander* and Mrs *Anita L. Noot boom* the Institute for Experimental Gerontology TNO Rijswijk, the Netherlands, who provided us with tumour-transplanted rats. W also want to thank Ciba-Geigy Ltd for the generous gift of human calcitonin-M

REFERENCES

1 *Be ker H D Konturek S J Reeder D D & Thompson, J C* Effect of calcium and calcitonin on gastrin and gastric secretion in cats. Am. J Phys. 225 277 280 1973

2 *Be ker H D R der D D Scurry M T & Thompson J C* Inhibition of gastrin release and gastric secretion by calcitonin in patients with peptic ulcer Am. J Surg 127 71 75 1974

3 *Becherdorf F A G ey T A Walsh, J H & Fordt en J S* Effect of calcitonin on meal-stimulated gastric acid secretion and serum gastrin concentration Gastroenterology 66 343–346 1974

4 *Bollman R. & P arse A G E.* Calcitonin secretion and APUD characteristics of naturally occurring medullary thyroid carcinomas in rats. Virchows Arch. Abt. B. Zellpath. 15 95–105 1974

5 *Boorman G A., Heersche J N M & Hollander C F* Transplantable calcitonin-secreting medullary carcinomas of the thyroid in the WAG/Rij rat J Nat. Cancer Inst. 53 1011–1015 1974

6 *Boorman G A., van Noord M J & Hollander C F* Naturally occurring medullary thyroid carcinoma in the rat. Arch. Path. 94 35–41 1972.

7 *Burford H J Ontjes D A., Cooper C W., Parlow A F & Hirsch P F* Purification, characterization and radioimmunoassay of thyrocalcitonin from rat thyroid glands. Endocrinology 96 340–348, 1975

8. *Care A D Bat R F L., Swaminathan, R. & Ganguli P C.* The role of gastrin as a calcitonin secretagogue. J Endocr 51 735–744 1971

9 *Cooper C. W., S hwesinger W H Mahgoub*

pletely understood Since serum calcium in the animals was not measured a definite interpretation of the results cannot be made On the basis of the present and previous studies (2 3 20 24), however one apparently discrepant observation may be explained Patients with MCT and high serum iCT had low serum gastrin levels (24) and injection of large doses of CT to healthy subjects inhibited serum gastrin response to food (2) both studies suggest an inhibitory effect of high serum concentrations of CT on gastrin release. Injection of smaller doses of CT had no effect on meal stimulated hypergastrinaemia (3) The tumour rats in the present study had significantly elevated serum iCT as compared with the control rats, but markedly lower values than the patients with MCT (24) It is therefore possible that the observed lack of inhibitory effect on gastrin in these animals is due to a sub-effective serum level of CT The increased serum gastrin concentration in the tumour rats may be explained as compensatory to decreased gastric acid secretion which in turn very probably is an effect of CT as CT repeatedly has been shown to be a potent inhibitor of gastric secretion (1 2 3 12 14) Serum calcium is probably involved in the secretion of these hormones and gastric juice in rats with MCT but the nature of this involvement is at present unknown

It is of special interest that it was demonstrated in this study that the gastrin response to calcium injection was different in tumour rats and controls While the control rats responded with an increase in serum gastrin similar to findings in the cat (1) in normal man in subjects with duodenal ulcer (20) as well as in patients with Zollinger Ellison disease (27) the hormone concentration in serum from tumour rats fell after calcium administration The reason for this is not clear One possible explanation is that the CT concentration due to calcium stimulation in the tumour rats has reached a level which overrules the stimulatory effect of calcium on gastrin resulting in an inhibition of gastrin release If the same effect is present in patients with MCT this may be a useful test in the diagnosis of the disease.

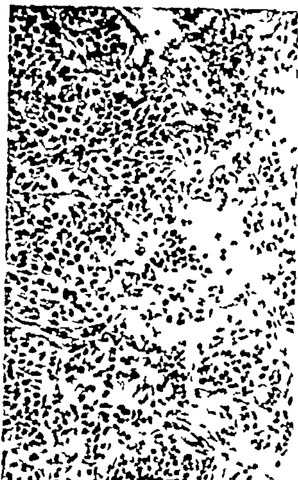


Fig 6 Light micrograph of rat thyroid C-cell tumour transplanted under the kidney capsule. Growth pattern and cell morphology not distinguishable from human MCT × *160* H.E.

In conclusion rats bearing transplanted MCT develop hypercalcitonaemia hypergastrinaemia and reduced gastric acid secretion The release of CT from the tumour is stimulated by calcium and pentagastrin. The morphological similarities between the rat tumour and human MCT together with the changes in CT secretion in response to physiological secretagogues, make this a suitable animal model for the study of different pathophysiological aspects of MCT In addition the endocrine feed back mechanisms existing between gastro-intestinal hormones and CT can be elucidated in MCT bearing rats.

Acta path. microbiol. scand. Sect. A, 85: 73–88, 1977

LIGHT MICROSCOPICAL AND ULTRASTRUCTURAL OBSERVATIONS ON THE EFFECT OF VINBLASTINE ON AMELOBLASTS OF RAT INCISORS *IN VIVO*

I. Short Term Effect on Secretory Ameloblasts

H. Moe and Hanne Mikkelsen

Anatomy Department C, University of Copenhagen, Denmark

Moe, H. & Mikkelsen, H. Light microscopical and ultrastructural observations on the effect of vinblastine on ameloblasts of rat incisors *in vivo*. I. Short-term effect on secretory ameloblasts. Acta path. microbiol. scand. Sect. A, 85: 73–88, 1977.

The highly polarized secretory ameloblasts in the incisors of rats fixed by perfusion with glutaraldehyde two or three hours after intravenous administration of vinblastine sulfate at a dosage of 5 mg per 100 g body weight were studied in the light microscope and the electron microscope. The following effects were observed: 1. All cytoplasmic microtubules in the ameloblasts had vanished. This was not accompanied by the appearance of paracrystals of microtubular protein or macrotubules. 2. The ameloblasts preserved their external features of polarized cells but lost their ability to maintain normal orderly segregation of the cell constituents, *i.e.* their normal internal compartmentalization and polarity had vanished. 3. The ameloblasts lost their capability of directional translocation of the secretory granules towards the cell apex. 4. Secretory granules already translocated to the cell apex regurgitated in the cell and a probably delayed discharge of secretory material had started in abnormal site at the surface. 5. The normal arrangement of ribosomes into polyribosomes on the membranes of the rough endoplasmic reticulum was no longer present; the ribosomes were apparently distributed at random. 6. New secretion was inhibited or brought to a standstill but secretory material already present in the Golgi complex appeared to be transported normally. 7. The centrioles had started to develop into cilia [illegible] in many of the cells. 8. The number of autophagic vacuoles had increased.

Key words: Ameloblasts; incisors, rat; vinblastine.

H. Moe, Anatomy Department C, Universitetsparken 1, DK-2100 Copenhagen Ø, Denmark.

Received 8 [illegible] 76. Accepted 10 [illegible] 76.

In vivo studies of the effect of the cancer chemotherapy agent vinblastine on normal secretory and absorptive cells and on normal differentiating cells are sparse. In tubule cells of the kidney (*Tyson & Bulger* 1973, 1974, *Silverblatt et al.* 1974), thyroid gland (*Ekholm et al.* 1974), B-cells of the pancreatic islets (*Ericson & Lundquist* 1975) and prolactin cells of the anterior pituitary gland (*Shiino & Rennels* 1975) administration of vinblastine causes disappearance of microtubules and often also formation of paracrystals of microtubular protein. In the endo-

A M & *Ontjes D A* Thyrocalcitonin Stimulation of secretion by pentagastrin Science *172* 1238–1240 1971

Gautvik K M Normann T Teig V Wille S O Brennhovd I O & Christensen L Radioimmunoassay of human calcitonin in serum and tissue from healthy individuals and patients with medullary carcinoma of the thyroid gland Scand J clin. Lab Invest. *36* 323–329 1976

Hennessy J F Gray T K Cooper C W & Ontjes D A Stimulation of thyrocalcitonin secretion by pentagastrin and calcium in two patients with medullary carcinoma of the thyroid Clin. Endocrinol. Metab *36* 200 203 1973

Hesch R D Hüfner M Schmidt H Winkler K Hasenjäger M Paschen K Becker H J Fuchs K & Creutzfeldt W Gastrointestinal effects of calcitonin in man In *Demling L* (ed) Gastrointestinal Hormones Stuttgart Thieme Verlag 1972 p 94–103

Hill C S Jr Ibanez M L Samaan N A Ahearn M J & Clark R L Medullary (solid) carcinoma of the thyroid gland An analysis of the M D Anderson Hospital experience with patients with the tumor its special features, and its histogenesis. Medicine *52* 141–171 1973

Konturek S J Radecki T Konturek D & Dimitrescu T Effect of calcitonin on gastric and pancreatic secretion and peptic ulcer formation in cats Am. J Dig Dis. *19* 235–241 1974

Lindsay S Nichols C W Jr & Chaikoff I L Naturally occurring thyroid carcinoma in the rat Arch. Path. *86* 353–364 1968.

Lowry O H Rosebrough N J Farr A L & Randall R J Protein measurement with the Folin phenol reagent *J biol Chem 193* 265–275 1951

Melvin K E W Tashjian A H Jr & Miller H H Studies in familial (medullary) thyroid carcinoma. Recent Progr Hormone Res. *28* 399–470 1972

18. *Normann T Gautvik K M Johannessen J V & Brennhovd I O* Medullary carcinoma of the thyroid in Norway Clinical course and endocrinological aspects. Acta endocrinol *83* 71–85 1976

19. *Normann T Johannessen J V Gautvik K M., Olsen B R. & Brennhovd I O* Medullary carcinoma of the thyroid. Diagnostic problems. Cancer *37* 366–377 1976.

20. *Reeder D D Jackson B M., Ban J Clendinnen B G Davidson W D & Thompson J C* Influence of hypercalcemia on gastric secretion and serum gastrin concentration in man. Ann. Surg *172* 540–546 1970

21. *Reeder D D Watayou T Booth R A D & Thompson J C* Depletion of antral gastrin after food in rats. Am. J Surg *129* 67–70, 1975

22. *Schrumpf E & Sand T.* Radioimmunoassay of gastrin with activated charcoal Scand. J Gastroent *7* 683–687 1972

23. *Shay H Sun D C H & Gruenstein M* A quantitative method for measuring spontaneous gastric secretion in the rat. Gastroenterology *26* 906–913 1954

24. *Sizemore G W Go V L W Kaplan E L Sanzenbacher L J Holtermuller K H & Arnaud C D* Relations of calcitonin and gastrin in the Zollinger Ellison syndrome and medullary carcinoma of the thyroid. New Engl J Med *288* 641–644 1973

25. *Tashjian A H Jr Howland B G Melvin K & Hill C S Jr* Immunoassay of human calcitonin. Clinical measurement relation to serum calcium and studies in patients with medullary carcinoma. New Engl J Med *283* 890–895 1970

26. *Triggs S M Hesch R D Woodhead J S & Williams E D* Calcitonin production by rat *thyroid tumours. J* Endocr *66* 37–43, 1975

27. *Trudeau W L & McGuigan J E.* Effects of calcium on serum gastrin levels in the Zollinger Ellison syndrome. New Engl J Med. *281* 862–866 1969



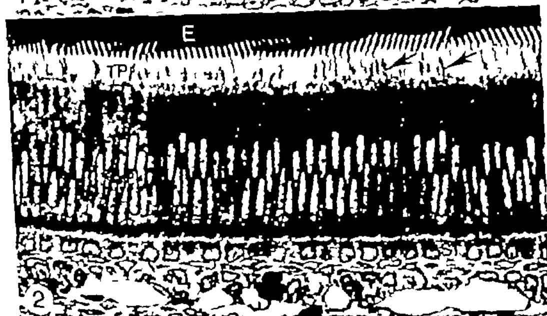


Fig. 1 Control rat. Light micrograph of secretory ameloblasts stained with toluidine blue. Note the zonation of the ameloblast layer. A light narrow zone (short arrow) basally abutting to the stratum intermedium cells (SI), a densely stained mitochondrial zone (M) in close relationship to the proximal end of the cell nuclei, nuclear zone, an extensive supranuclear cell region most intensely stained distally (long arrow) and a faintly stained zone of apical (Tomes') processes the distal part of which is embedded in enamel matrix (white arrow). D Dentin. PD Predentin. O Odontoblasts. × 600

Fig. 2 Vinblastine-treated rat. Light micrograph of secretory ameloblasts stained with toluidine blue. The mitochondria are still located proximally but the nuclei have moved in distal direction. The proximal part of the apical processes (TP) has increased considerably in length and is chromophob except for toluidine blue positive strands in some of the cells (arrows). SI Stratum intermedium. E Enamel matrix. × 600

crine glands vinblastine affects the secretion and in the liver (*Redman et al* 1975) it inhibits plasma protein secretion. In the proximal tubule cells of the kidney vinblastine alters the normal distribution of certain of the cell organelles and inhibits normal basal translocation of phagosomes (*Silver blatt et al* 1974)

The incisors of the rat are continuously growing organs which contain proliferating differentiating and mature secretory ameloblasts and transporting and degenerating ameloblasts in a regular successive arrangement This cell population appears well suited to studies of the short time and prolonged effects of vinblastine. The present paper deals with the short time effect of a large dose of vinblastine on mature secretory ameloblasts. A short description of the relevant normal structure of these cells is also given. For supplementary details the reader is referred to *Warshawsky* (1968) *Weinstock & Leblond* (1971) *Moe* (1971) *Katchburian & Holt* (1972) *Kallenbach* (1973) *Warshawsky & Smith* (1974) *Smith & Warshawsky* (1975)

MATERIALS AND METHODS

Seven young female Wistar rats weighing 95 to 125 g were used in this study Three of the animals served as controls. Four animals each received intravenously 5 mg vinblastine sulfate (Velbe) per 100 g body weight. The solution used was 10 mg vinblastine per ml in 0 9 per cent sodium chloride. In the controls vinblastine was omitted. The dose was divided equally between two injections and the second injection was given half an hour after the first one At sacrifice the animals were anaesthetized with Nembutal intraperitoneally The abdominal cavity was opened and the animals fixed by retrograde perfusion through the abdominal aorta. Before the perfusion the inferior vena cava was cut open and the blood washed out by infusion of 10 to 15 ml Tyrode solution containing 2 per cent polyvinylpyrrolidone. The fixative was 3 per cent glutaraldehyde in 0 08 M sodium cacodylate with 0 05 per cent calcium chloride pH 7 2 The perfusion started two or three hours after the first injection of vinblastine and lasted for 30 minutes.

Each half of the mandible and each maxillary incisor with surrounding bone intact were divided into smaller pieces by sawing through perpendicular to the long axis of the tooth with a 100 µ thick saw blade. The specimens were demineralized for 6 to 8 days at 4 C in 4 13 per cent EDTA containing 2 per cent glutaraldehyde, pH 7.2, rinsed in 0 15 M cacodylate buffer and postfixed in 2 per cent cacodylate-buffered osmium tetroxide for 2 hours. Dehydration was in alcohol and embedding in Epon.

The Epon blocks were sawn into 500 to 1,000 µ thick slices transversely to the tooth axis. Semithick sections for light microscopy were cut from the proximal end of each slice and stained with toluidine blue. Thin sections for electron microscopy were stained with uranyl acetate and lead citrate.

RESULTS

A Light Microscopy

a) Control tissue The secretory ameloblasts constitute a continuous and uniform epithelial layer covering the external convex aspect of the incisors in the region where enamel matrix is in process of formation The individual ameloblasts extend throughout the epithelial layer They are tall columnar cells with the long axis perpendicular to the tooth surface In the toluidine blue stained sections they exhibited a distinct zonation in accordance with the characteristic segregation of the cell organelles. From base to apex the following zones were seen in each cell (Fig 1) A light narrow zone facing the stratum intermedium cells, a densely stained mitochondrial zone, a zone comprising the elongated nucleus surrounded by a thin layer of cytoplasm, a long supranuclear cell region and a faintly stained Tomes process which consisted of a proximal part in contact with neighbouring cells and a distal part embedded in enamel matrix. The supranuclear cell region was relatively intensely stained by toluidine blue, especially in its distal part. In the middle two-thirds of the supranuclear region a more weakly stained core was often discernible. The supranuclear cell region and the distal part of the Tomes process contained a few intensely stained grains or small bodies.

b) Effect of vinblastine In the vinblastine-treated animals most of the zones described in the normal cell were changed (Fig 2)



4

The mitochondria were still seen close to the cell base but the nuclei had moved in a distal direction and were often situated in the middle of the cell Between the mitochondria and the nuclei a cytoplasmic area had appeared which stained with toluidine blue The distal part of the Tomes process had lost its stainab lity and also its granular material The proximal part of the Tomes process appeared considerably elongated. It had lost its stainability except for toluidine blue positive strands in some of the ameloblasts. The toluidine blue positive supranuclear cell region was intensely stained and appeared shortened in comparison with the control material

Changes in the ameloblasts following vinblastine treatment were present in all four incisors of each animal and in all the animals studied In the individual tooth the changes seemed to extend to the ent re area of matrix producing cells Certain differences in the degree of changes were apparent however Usually the least affected ameloblasts were those of the medial and lateral margins of the area Most affected were ameloblasts located in the transition between the mesial and middle thirds and the middle and lateral thirds of the ameloblasts area In these severely affected areas the apical cell parts were sometimes fragmented and disorganized.

B Electron Microscopy

1 Proximal Cell Portion

a) Control tissue Mitochondria were clustered beneath the nucleus and occupied the bulk of the infranuclear cytoplasm (Fig 3) They were intermingled with a few strands of rough endoplasmic reticulum, and the entire group of mitochondria were often incompletely surrounded by relatively large lamellar cisternae laterally and basally In addition to the mitochondria and the ER the cytoplasm contained a l mited number of free polyribosomes and a few smooth-surfaced and coated vesicles. A ring shaped cell web along the inner aspect of the lateral cell membrane was located a short distance above the cell base Lysosomes, multivesicular bodies, autophagic vacuoles and secretory granules were very rare.

b) Effect of vinblastine The mitochondria were retained in a cluster in the basal cell part but had lost their intimate relationship with the nucleus which had risen considerably in the cell (Fig 4) Some of the mitochondria were branched or circular Between the mitochondria and the nucleus organelles had appeared which in the normal cell were located supranuclearly They comprised arrays of lamellar endoplasmic cisternae accumulations of mature and immature secretory granules and structures resembling disorganized and dilated elements of Golgi complexes (Figs. 4 and 5) Secretory granules were also present basal to the mitochondria and in this area many cells also contained small early autophagic vacuoles (Fig 6) Such vacuoles also occurred in the remaining infranuclear cytoplasm.

2 Distal Cell Portion

a) Control tissue As mentioned this cell portion may be divided into a supranuclear part extending from the nucleus to the distal cell web and a distal part, the Tomes process. The supranuclear cell part was very long and contained an extensive rough endoplasmic reticulum and an elaborated Golgi system Endoplasmic cisternae occurred throughout the supranuclear cell part, and most of the cisternae were flattened and oriented

Fig 3 Control rat Electron micrograph of the basal part of secretory ameloblasts. Mitochondria (M) occupy the bulk of the infranuclear cytoplasm. N Nucleus. BW Basal web. ER Rough endoplasmic reticulum SI Stratum intermedium. × 11 700

Fig 4 Vinblastine-treated rat. Electron micrograph of the infranuclear part of four secretory ameloblasts. PM Cell membrane. The nuclei (N) have moved distally and arrays of endoplasmic reticulum (ER) and accumulations of secretory granules (SG) normally found in the supranuclear parts of the cells are seen between the mitochondria and the nuclei. × 10 500



4

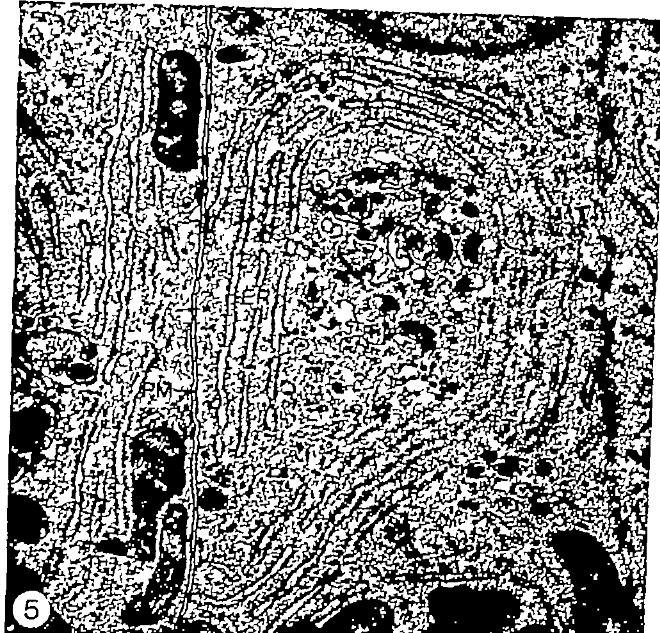


Fig 5 Vinblastine-treated rat. This micrograph shows details from the infranuclear part of two secretory ameloblasts. Flattened endoplasmic cisternae (ER) surround an area with immature secretory granules (SG) and elements from a distorted Golgi complex. N Lower nuclear pole. M Mitochondria. PM Cell membrane. AV Autophagic vacuole × 29 000

longitudinally in the cell in parallel array Distally the cisternae terminated abruptly close to the apical cell web (Fig 7) Cross sections of the cells showed that the lateral margins of many cisternae were agranular and formed subsurface cisternae. The reticulum was abundant in attached ribosomes arranged in spirals or rosettes (Fig 11)

The Golgi system was usually confined to the middle two-thirds of the supranuclear cell part. It consisted of numerous elongated complexes arranged longitudinally in the axial cell region and more or less in succession end to-end Each complex was made up of a stack of two to six flattened saccules. In cross-sections of the cells three or four complexes might be seen in a concentric arrangement with their concave maturing faces encircling axial cytoplasm. However in other cross-sections the complexes were less regu

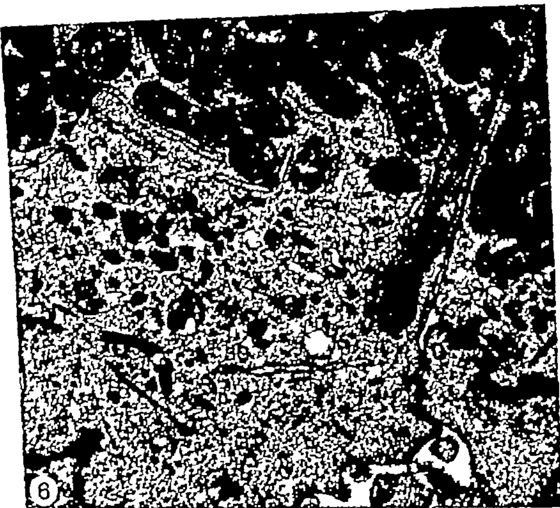


Fig 6 Vinblastine-treated rat Base of a secretory ameloblast containing various small bodies among which secretory granules (SG) and autophagic vacuoles (AV) may be recognized. F Filament bundles. A distinct basal web is not seen. × 19,000

larly arranged and might have more eccentric positions. The intermediate and inner saccules of a complex contained dense material, especially in dilated areas or in expanded extremities of the saccules. Smooth and coated vesicles, condensing vacuoles, mature secretory granules, a small centriole and a few endoplasmic cisternae were closely associated with the Golgi system. A few dense bodies and multivesicular bodies containing a varying number of small vesicles in a matrix of varying density were located among the endoplasmic cisternae outside the Golgi area. *Multivesicular bodies* apparently in the process of formation were seen now and then near the Golgi complex. Small autophagic vacuoles occurred sporadically

The apical (Tomes) process consisted of a proximal part, the lateral surface of which was in contact with other ameloblasts, and a distal part surrounded by enamel matrix (Fig 7) The distal cell web was located proximally in the apical process and occupied the peripheral cytoplasm. The remaining cytoplasm was abundant in small vesicular and irregular tubular elements with smooth

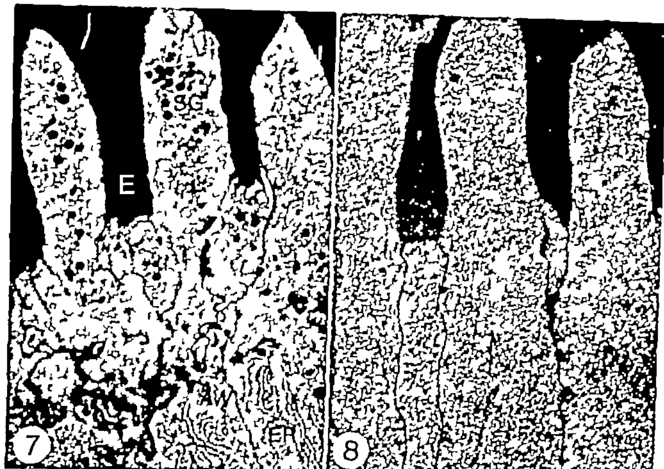


Fig 7 Control rat. Apical processes of secretory ameloblasts. The apical (Tomes) process is that portion of the secretory ameloblast which is distally to the apical web (AW) It consists of a proximal part which has irregular lateral surfaces in contact with other proximal parts of apical processes and a distal part embedded in enamel matrix (E) Secretory granules (SG) are abundant in the cytoplasmic core of the distal part of Tomes process and occur scattered in the proximal part of the processes. The endoplasmic cisternae (ER) of the supranuclear cell portion terminate abruptly proximally to the apical cell web × 10 000

Fig 8 Vinblastine-treated rat Apical processes of secretory ameloblasts. Each process consists of a cytoplasmic matrix surrounded by a smooth plasma membrane None of the structures normally present in the apical cytoplasm remain × 11 400

surfaces It also contained coated vesicles a few secretory granules and multivesicular bodies (Fig 16) Similar structures were present in the distal part of the Tomes process and gathered in the axial region In this cell part the secretory granules were often numerous.

b) Effect of vinblastine In severely affected ameloblasts the entire apical process had undergone profound changes (Fig 8) None of the structures normally present in this cell part remained except for a few uncharacteristic vesicles and an indistinct cell web The irregularities of the cell membrane normally seen in the distal cell portion were less pronounced or absent. The interior of the process was filled with cytoplasmic matrix. In some Tomes processes rough endoplasmic cisternae in parallel or concentric arrays also occurred (Fig 9) Such cisternae were not observed in the Tomes processes of the control material *In less severely affected ameloblasts* elements normally present in the proximal part of the Tomes process might be *retained in reduced amount in addition to* endoplasmic cisternae



Fig. 9 Vinblastine-treated rat. A region similar to Fig. 8. Rough surfaced endoplasmic cisternae (ER) has moved from the supranuclear cell region into the apical processes. × 10,000

The bulk of the supranuclear cell region was occupied by rough endoplasmic reticulum. There was a clear tendency towards increased orderly stacking of the cisternae in parallel array (Fig. 10). In most cells the normal arrangement of the attached ribosomes in loops, spirals or rosettes had disappeared completely and the ribosomes appeared randomly dispersed (Fig. 12). In some ameloblasts ribosome-free confronting cisternae had formed (Figs. 12 and 15).

Usually the Golgi system had lost its continuity of arrangement since many of its complexes were displaced laterally in the cell and were tilted in relation to the cell axis (Fig. 13). In general the saccules of the individual complex had *increased in extent* and number. Five to eight uniformly appearing saccules were found in many complexes. The lumen of the saccules was narrow and did not contain dense material (Figs. 12 and 13) as did intermediate and mature saccules in the controls. Large swarms of small vesicles occurred near many of the Golgi complexes. Only a few vesicles were coated. Condensing vacuoles did occur but in reduced number. Secretory granules were very conspicuous and numerous in the supranuclear cell region. Most of the granules were densely stained and accumulated into heaps close to the lateral cell membrane (Figs. 10 and 12). In these places coated vesicles containing material similar to that of the secretory granules were seen apparently in the process of discharge (Fig. 14). Their content was often connected with elongated masses of dense secretory material accumulated in widened areas of the intercellular space. The centriole normally situated in the axial cell part was often displaced laterally. In many cells it had started to develop into a cilium which protruded into the intercellular space with the tip pointing towards the cell base.

A considerable number of small and medium-sized early cytosegresomes had arisen in the supranuclear cell region (Fig. 15). They were most common near Golgi complexes and in the distal area of the region. The simplest ones contained a substance resem-

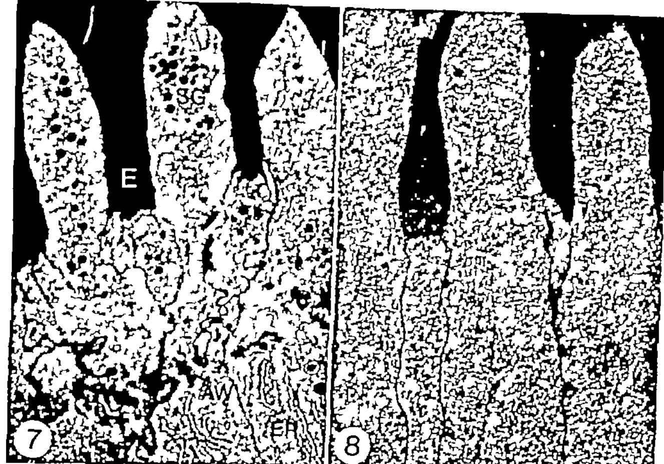


Fig 7 Control rat. Apical processes of secretory ameloblasts. The apical (Tomes) process is that portion of the secretory ameloblast which is distally to the apical web (AW) It consists of a proximal part which has irregular lateral surfaces in contact with other proximal parts of apical processes and a distal part embedded in enamel matrix (E) Secretory granules (SG) are abundant in the cytoplasmic core of the distal part of Tomes process and occur scattered in the proximal part of the processes. The endoplasmic cisternae (ER) of the supranuclear cell portion terminate abruptly proximally to the apical cell web × 10 000

Fig 8 Vinblastine-treated rat. Apical processes of secretory ameloblasts. Each process consists of a cytoplasmic matrix surrounded by a smooth plasma membrane. None of the structures normally present in the apical cytoplasm remain × 11 400

surfaces. It also contained coated vesicles, a few secretory granules and multivesicular bodies (Fig 16) Similar structures were present in the distal part of the Tomes process and gathered in the axial region In this cell part the secretory granules were often numerous.

b) Effect of vinblastine In severely affected ameloblasts the entire apical process had undergone profound changes (Fig 8) None of the structures normally present in this cell part remained except for a few uncharacteristic vesicles and an indistinct cell web. The irregularities of the cell membrane normally seen in the distal cell portion were less pronounced or absent. The interior of the process was filled with cytoplasmic matrix. In some Tomes processes rough endoplasmic cisternae in parallel or concentric arrays also occurred (Fig 9) Such cisternae were not observed in the Tomes processes of the control material. In less severely affected ameloblasts elements normally present in the proximal part of the Tomes process might be retained in reduced amount in addition to endoplasmic cisternae.

the mitochondrial zone distally to the basal cell web. On a level with the nucleus 20–30 microtubules were found scattered in the thin layer of perinuclear cytoplasm. In the supra nuclear cell part their number increased from about 25–30 close to the nucleus to 50–60 in sections proximally to the apical cell web. The highest number of microtubules was found in the proximal part of the apical processes (Fig 16) In this cell region the microtubules ran in different directions and their exact number was difficult to determine. Between 60 and 120 microtubules were counted in most cross-sections. In the distal part of the Tomes process the number of microtubules decreased rapidly towards the tip of the process.

The microtubules of the ameloblasts appeared singly in pairs, or in small bundles. Between the basal cell web and the apical web most of them were located closer to the lateral cell membrane than to the cell centre, whereas in the Tomes process they were mostly located in the core of the process.

b) Effect of vinblastine The microtubules had completely disappeared in all parts of the secretory ameloblasts in the vinblastine treated animals except for those of centrioles and cilia. Macrotubules were not seen in the cytoplasm and no remnants of microtubules were observed in the segresomes Paracrystalline inclusions of microtubular material were observed in the cytoplasm of the periodontal capillary endothelium and macrophages but not in the secretory ameloblasts.

DISCUSSION

The short time effects of a large dose of vinblastine on the secretory ameloblasts may be summarized as follows 1 All the cytoplasmic microtubules vanish. This is not accompanied by the appearance of paracrystals or macrotubules as described by *Bensch & Malawista* (1969) and *Krishan & Hsu* (1969) and seen in many cell types following vinblastine administration. 2. The ameloblasts preserve their external features of polarized cells but lose their ability to maintain normal orderly segregation of the cell constituents. Thus, their internal compartmentalization and polarity disappears. 3 The ameloblasts lose the capability of directional translocation of the secretory granules towards the cell apex. 4 The secretory processes normally taking place in the rough endoplasmic reticulum and in the Golgi system appears to be diminished or brought to a standstill, arrangement of the ribosomes of the reticulum into polyribosomes in most of the cell having ceased, no or only scanty secretory material being present in the Golgi saccules, and condensing vacuoles occurring in reduced number 5 The centriole starts to develop into a cilium in many of the ameloblasts.

Two activities clearly continue. One is isolation into segresomes of cell constituents or cell products which appear to be damaged, unused or useless to the cell. This occurs on a larger scale than in the normal cells. The other is discharge of the content of the secretory granules upon the cell surface. This activity appears delayed however and takes place at abnormal sites at the cell surface.

It is widely accepted that vinblastine causes disturbances within two major areas in mature cells, one involving the cytoplasmic microtubules, the other the biosynthesis of macromolecules. It is also suggested that disarrangement of the normal cytoplasmic organization and inhibition of directional translocation of particles or organelles are consecutive effects of the injury to the microtubuli. Changes induced by vinka-alkaloids on the distribution of the organelles are observed in cell cultures of leucocytes (*Bensch & Malawista* 1969) and macrophages (*Bhisey & Fried* 1971) *in vitro* in follicular cells of the thyroid gland (*Nève et al.* 1975) and chondrocytes (*Moskalewski et al.* 1975) and *in vivo* in proximal tubule cells of the kidney (*Silverblatt et al.* 1974) In the highly polarized secretory ameloblasts these changes are very obvious and the Golgi complexes, the endoplasmic reticulum, the centriole and even the nucleus change position. Much of this displacement appears to take place in bulk rather than by individual movement of



Fig 10 Vinblastine-treated rat Supranuclear cell region of longitudinally cut secretory ameloblasts showing stacks of endoplasmic cisternae (ER) accumulations of secretory granules (SG) close to the lateral cell membrane (PM) and extracellular secretory material in the intercellular spaces (arrows) × 10 400

bling condensed cytoplasmic matrix. Most of them however contained one or more structural elements such as small vesicles, membrane pieces, ribosomes, fragments of rough endoplasmic reticulum Golgi saccules or secretory granules. They were surrounded by one or two membranes which sometimes appeared incomplete Rounded dense bodies resembling lysosomes were often seen in areas with cytosegresomes (Fig 15)

3 The Microtubules

a) Control tissue With a few exceptions the microtubules were orientated lengthwise in the infra para and supranuclear parts of the ameloblasts. Counts of microtubular profiles in cross-sections of the cells showed that they were most numerous in the distal cell parts. In the most basal cell part no microtubules were seen They began to appear in

the mitochondrial zone distally to the basal cell web. On a level with the nucleus 20–30 microtubules were found scattered in the thin layer of perinuclear cytoplasm. In the supranuclear cell part their number increased from about 25–30 close to the nucleus to 50–60 in sections proximally to the apical cell web. The highest number of microtubules was found in the proximal part of the apical processes (Fig 16) In this cell region the microtubules ran in different directions and their exact number was difficult to determine Between 60 and 120 microtubules were counted in most cross-sections. In the distal part of the Tomes process the number of microtubules decreased rapidly towards the tip of the process.

The microtubules of the ameloblasts appeared singly in pairs, or in small bundles. Between the basal cell web and the apical web most of them were located closer to the lateral cell membrane than to the cell centre, whereas in the Tomes process they were mostly located in the core of the process.

b) Effect of vinblastine The microtubules had completely disappeared in all parts of the secretory ameloblasts in the vinblastine treated animals except for those of centrioles and cilia. Macrotubules were not seen in the cytoplasm and no remnants of microtubules were observed in the segresomes. Paracrystal line inclusions of microtubular material were observed in the cytoplasm of the periodontal capillary endothelium and macrophages but not in the secretory ameloblasts.

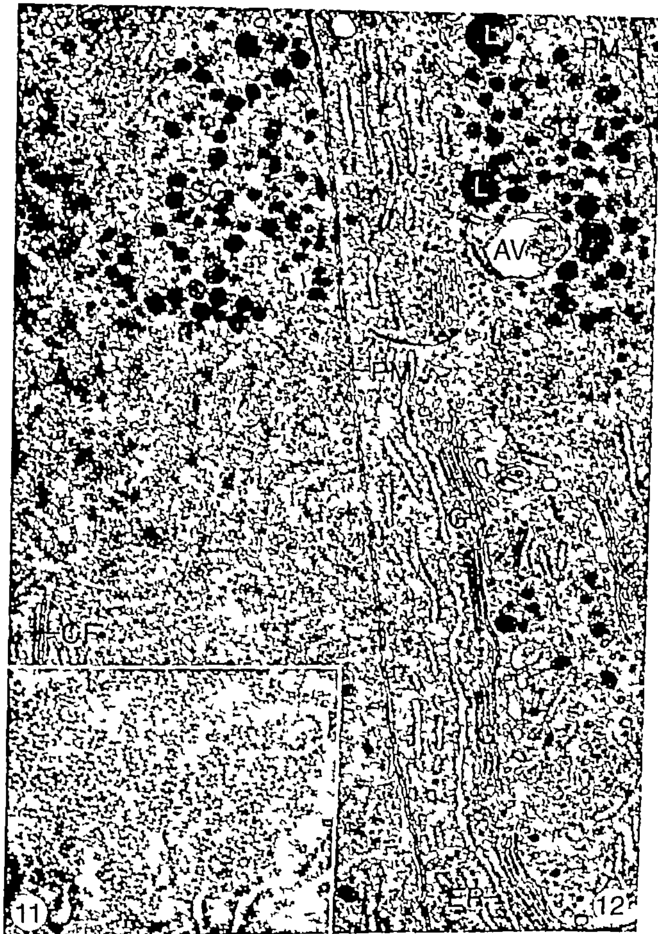
DISCUSSION

The short-time effects of a large dose of vinblastine on the secretory ameloblasts may be summarized as follows 1 All the cytoplasmic microtubules vanish. This is not accompanied by the appearance of paracrystals or macrotubules as described by *Bensch & Malawista* (1969) and *Krishan & Hsu* (1969) and seen in many cell types following vinblastine administration 2. The ameloblasts preserve their external features of polarized cells but lose their ability to maintain normal orderly segregation of the cell constituents. Thus, their internal compartmentalization and polarity disappears. 3 The ameloblasts lose the capability of directional translocation of the secretory granules towards the cell apex. 4 The secretory processes normally taking place in the rough endoplasmic reticulum and in the Golgi system appears to be diminished or brought to a standstill, arrangement of the ribosomes of the reticulum into polyribosomes in most of the cell having ceased, no or only scanty secretory material being present in the Golgi saccules, and condensing vacuoles occurring in reduced number 5 The centriole starts to develop into a cilium in many of the ameloblasts.

Two activities clearly continue. One is isolation into segresomes of cell constituents or cell products which appear to be damaged, unused or useless to the cell. This occurs on a larger scale than in the normal cells. The other is discharge of the content of the secretory granules upon the cell surface This activity appears delayed however and takes place at abnormal sites at the cell surface.

It is widely accepted that vinblastine causes disturbances within two major areas in mature cells, one involving the cytoplasmic microtubules, the other the biosynthesis of macromolecules. It is also suggested that disarrangement of the normal cytoplasmic organization and inhibition of directional translocation of particles or organelles are consecutive effects of the injury to the microtubuli. Changes induced by vinka alkaloids on the distribution of the organelles are observed in cell cultures of leucocytes (*Bensch & Malawista* 1969) and macrophages (*Bhisey & Freed* 1971) in vitro in follicular cells of the thyroid gland (*Nève et al* 1975) and chondrocytes (*Moskalewski et al* 1975) and in vivo in proximal tubule cells of the kidney (*Silverblatt et al.* 1974) In the highly polarized secretory ameloblasts these changes are very obvious and the Golgi complexes, the endoplasmic reticulum, the centriole and even the nucleus change position. Much of this displacement appears to take place in bulk rather than by individual movement of

6


L
PM
SG
L
AV
SG
PM
G
CF
SRE
11
12

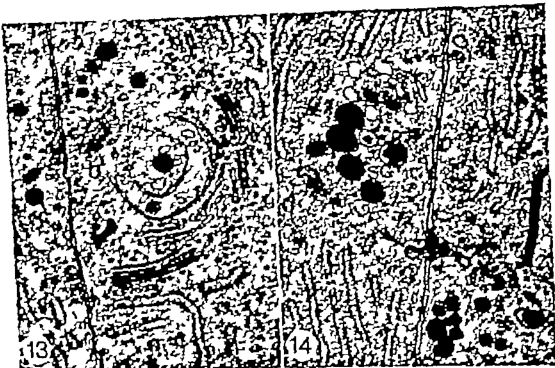


Fig. 13. Vinblastine-treated rat. This micrograph shows a laterally displaced and tilted Golgi complex from the supranuclear cell region. The lumen of the Golgi saccules is narrow and the inner saccules are curved and drifted away from the remaining part of the complex. × 33,000

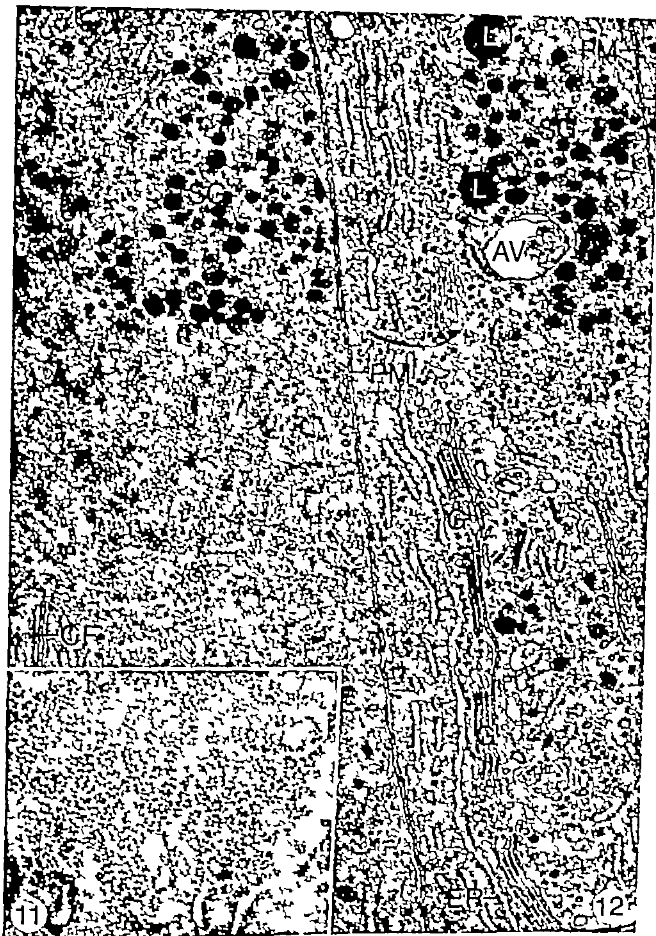
Fig. 14. Vinblastine-treated rat. Supranuclear cell region. Two coated vesicles (arrow) appear to be in the process of discharge into the intercellular space. SG Secretory granules. × 31,000

Fig. 11. Electron micrograph of a section passing tangential to a cisterna of the endoplasmic reticulum of a secretory ameloblast from a normal rat showing spiral and rosette configurations of polyribosomes. × 48,000

Fig. 12. Vinblastine treated rat. Supranuclear cell region of two longitudinally cut secretory ameloblasts. PM Plasma membrane. In the cell at right the Golgi complex (G) is oriented longitudinally as in a normal cell. Along the forming face of the complex extensive endoplasmic cisternae are seen (ER). The saccules of the complex appear empty and the innermost saccule is very extensive. In the cell at the left several tangentially cut endoplasmic cisternae are seen. Most of the ribosomes are distributed apparently at random. SG Secretory granules. CI Confronting cisternae. L Lysosome-like bodies. AV Autophagic vacuoles. × 29,000

the structural elements. This is obvious, for example from the displacement of Golgi complexes and their associated structures from the supranuclear cell region to the infranuclear cytoplasm (Fig. 4). It is remarkable that the mitochondria are not displaced in the ameloblasts but remain clustered near the cell base. So these organelles seem to be dependent on other factors than the presence of intact microtubules in their grouping and placing.

The involvement of microtubules in directional movements of particles and organelles in a variety of cells is discussed by *Rebhun* (1972). *In vivo* studies of this topic on secretory or absorptive cells are scarce. Recently *Silverblatt et al.* (1974) observed that vinblastine inhibits the translocation of phagosomes from cell apex to cell base in the prox


L
PM
SG
L
AV
SG
PM
G
CF
11
ER
12

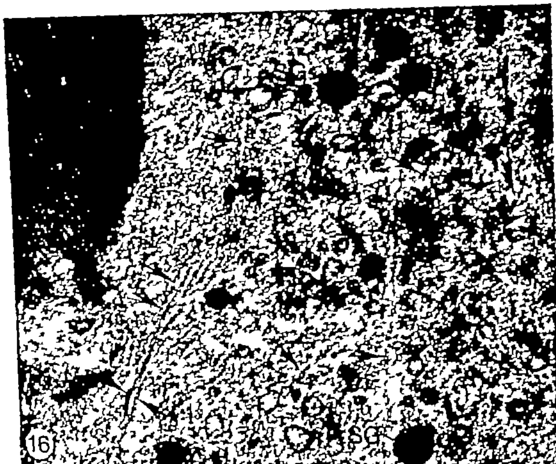


Fig 16 Control rat. Transition between proximal and distal part of a longitudinally cut Tomes process showing numerous microtubules (arrows) running in different directions, small vesicles, and secretory granules (SG) × 50,000

and decrease in collagen synthesis and secretion, but in these cells the Golgi complexes had diminished. *Redman et al* (1975) in their study of the effect *in vitro* and *in vivo* of colchicine and vinblastine on liver cells did not find inhibition of plasma protein synthesis and colchicine did not affect the movement of secretory proteins in the rough or smooth endoplasmic reticulum, nor did it affect the filling of Golgi vesicles however it impeded discharge and led to accumulation of secretory protein in all Golgi elements and in Golgi-derived secretory vacuoles. But with the amount of colchicine employed microtubules were still recognizable in the liver cells.

The authors are grateful to Miss *Kirsten Sjøberg* for her excellent technical assistance.

REFERENCES

1 *Bensch K. G & Malawista S E.* Microtubular crystals in mammalian cells. J Cell Biol. *40* 95–107 1969
2. *Bhisey A N & Freed J J* Ameboid movement induced in cultured macrophages by colchicine or vinblastine. Exp. Cell Res. *64* 419–429 1971
3. *Ehrlich H P., Ross, R. & Bornstein P.,* Effects of antimicrotubular agents on the secretion of collagen. A biochemical and morphological study J Cell Biol. *62* 390–403, 1974
4 *Ekholm R., Ericson L. E., Josefsson J.-O* &



Fig 15 Vinblastine treated rat Supranuclear cell region of secretory ameloblasts. Above a Golgi complex lysosome-like bodies (L) and autophagic vacuoles (arrows) are seen. CT Confronting cisternae × 29 000

imal tubule of the kidney suggesting that the presence of intact microtubules is essential for the normal basal translocation of phagosomes. In the secretory ameloblasts translocation of secretory granules from the Golgi system to the Tomes process was brought to a conclusion and many of the latest produced granules appeared to remain in the vicinity of the Golgi complexes and to accompany these in their displacement. Furthermore, the disappearance of secretory granules from the Tomes process coincident with the appearance of large accumulations of mature secretory granules along the lateral cell membrane in the supranuclear cell portion or even infranuclearly suggests a regurgitation of granules already translocated to the cell apex. Thus, the microtubules not only appear to determine the direction of the translocation of the granules but also to secure the accumulation of secretory granules in a proper place for release When the microtubules disrupt the granules regurgitate and normal exocytosis may stop

The mechanism of the inhibiting effect of vinblastine on the biosynthesis of secretory products has not been fully elucidated. It is not known whether the inhibition is an indirect effect of the disappearance of the microtubuli the disarrangement of the cell organelles, the stagnation in discharge of secretion, or the accumulation of the secretory products or whether the vinblastine interacts directly with steps in the complex processes of the biosynthesis.

At the large dose of vinblastine used in this study there is an indication of blocking of the secretory process at a relatively early stage, since polyribosomes to a large extent have disappeared However the transport of already produced secretory material through the Golgi complex and the formation of condensing vacuoles and maturation of secretory granules appear to continue since the Golgi saccules were empty and the number of condensing vacuoles sparse in the vinblastine treated animals. In fact the increase in number of saccules in individual Golgi complexes and the great extent of the saccules suggest formation in excess of Golgi membranes for secretory purposes in relation to the possibility of utilizing them. It cannot be excluded, however that parts of these membranes are destined for lysosome formation.

Ehrlich et al. (1974) also observed lack of stored material in the Golgi complex *in* cultured osteoblasts after vinblastine treatment

Acta path. microbiol. scand. Sect. A, 85 89–98 1977

ELECTRON MICROSCOPY OF LYMPH NODES OF HAMSTERS EXPERIMENTALLY INFECTED WITH *TREPONEMA PERTENUE*

J. BLOM, K. HOVIND-HOUGEN, H. J. SKOVGAARD JENSEN and A. BIRCH-ANDERSEN

Departments of Biophysics, Treponematoses and Laboratory Animals, Statens Seruminstitut, Copenhagen, Denmark

Blom, J., Hovind-Hougen, K., Jensen, H. J. Skovgaard & Birch-Andersen, A. Electron microscopy of lymph nodes of hamsters experimentally infected with *Treponema pertenue*. Acta path. microbiol. scand. Sect. A, 85 89–98 1977

The morphology of lymph node tissue from normal hamsters and from hamsters experimentally infected with *Treponema pertenue* Gauthier was compared by means of light and electron microscopy. The capsules of the lymph nodes from infected hamsters showed an increased thickness in comparison with those of the non-infected animals. The infected lymph nodes differed from normal lymph nodes by small accumulations of neutrophilic leucocytes in the cortical areas. In addition, the amount of intercellular collagenous matrix present between large elongated cells was greatly increased in lymph nodes from infected animals. Electron microscopy of thin sections of infected lymph nodes showed intercellularly located treponemes in the leucocyte infiltration areas. These regions also showed the increased amounts of the collagenous matrix. Treponemes were occasionally found intracellularly in macrophages. These treponemes did not show their typically helical shape but were present as spherical forms or cysts.

Key words: *Treponema pertenue*; ultrastructure; lymph nodes; hamsters; experimentally infected.

K. Hovind-Hougen, Department of Treponematoses, Statens Seruminstitut, Amager Boulevard 80, DK 2300 Copenhagen S, Denmark

Received 10.iii.76. Accepted 10.iii.76

Electron microscopy of the pathogenic treponemes, *T. pallidum* Nichols (5, 9), *T. cuniculi* (6) and *T. pertenue* Gauthier (8) has failed to demonstrate any ultrastructural differences of value for a differentiation between these treponemal species. It was also impossible to demonstrate characteristic differences in the ultrastructure of the host-parasite relationship in the treponematoses caused by the various species of the non-cultivable treponemes that we have studied. Electron microscopical studies of lesions in the mucous membranes and skin in primary and secondary human syphilis (7) and of skin lesions in rabbits naturally infected with *T. cuniculi* (6) did not reveal differences either between the localization of treponemes in the infected epithelia or in their effect on the host tissues. According to *Turner & Hollander* (16) the manifestations in hamsters of an infection caused by intradermal inocu-

Melander A In vivo action of vinblastine on thyroid ultrastructure and hormone secretion Endocrinol *94* 641–649 1974

Ericson L E & Lundquist I Effect of vinblastine in vivo on ultrastructure and insulin releasing capacity of the B-cell following sulphonylurea and isopropyl noradrenaline Diabetol *11* 467–473 1975

Kallenbach E The fine structure of Tomes process of rat incisor ameloblasts and its relationship to the elaboration of enamel Tissue & Cell *5* 501–524 1973

Katchburian F & Holt S J Studies on the development of ameloblasts I Fine structure J Cell Sci *11* 415–447 197?

Krishan A & Hsu D Observations on the association of helical polyribosomes and filaments with vincristine induced crystals in Earle s L-cell fibroblasts. J Cell Biol *43* 553–563 1969

Moe H Morphological changes in the infranuclear portion of the enamel producing cells during their life cycle. J Anat *108* 43–62 1971

Moskalewski S Thyberg J Lohmander S & Friberg U Influence of colchicine and vinblastine on the Golgi complex and matrix deposition in chondrocyte aggregates. Exp Cell Res. *95* 440–454 1975

Nève P Roemans P & Ketelbant Balasse P Microtubules and microtubule inhibitors and cytochalasin in the thyroid gland In Borgers, M & De Brabander M (Eds.) Microtubules and microtubule inhibitors, North Holland Publishing Company Amsterdam and Oxford 1975 p 177–185

Rebhun L I Polarized intracellular particle transport Saltatory movements and cytoplasmic streaming In Bourne G H & Danielli, J F (Eds.) International Review of Cytology vol 32. Academic Press, New York and London 1972 p 93–137

13 *Redman C M Banerjee D Howell, K & Palade G E* Colchicine inhibition of plasma protein release from rat hepatocytes. J Cell Biol. *66* 42–59 1975

14 *Shiino M & Rennels E G* Vinblastine-induced microtubular paracrystals in prolactin cells of anterior pituitary gland of lactating rats Am J Anat. *144* 399–405 1975

15 *Silverblatt F J Tyson G E & Bulger R E* Effects of vinblastine on the phagolysosome system of proximal tubule cells of rat kidney Administration of horseradish peroxidase Lab. Invest. *31* 170 180 1974

16 *Smith C E & Warshawsky H* Cellular renewal in the enamel organ and the odontoblast layer of the rat incisor as followed by radioautography using ³H thymidine Anat. Rec *183* 523–560 1975

17 *Tyson C E & Bulger R E* Vinblastine-induced paracrystals and unusually large microtubules (macrotubules) in rat renal cells. Z. Zellforsch. *141* 443–458, 1973

18. *Tyson G E & Bulger R. E.* Vinblastine-induced aggregates of smooth endoplasmic reticulum in proximal tubular cells of rat kidney Am. J Anat. *140* 201–?12, 1974

19 *Warshawsky H* The fine structure of secretory ameloblasts in rat incisors. Anat Rec. *161* 211–??9 1968.

20 *Warshawsky H & Smith C E* Morphological classification of rat incisor ameloblasts. Anat Rec *179* 4?3–446, 1974

21 *Weinstock A & Leblond C P* Elaboration of the matrix glycoprotein of enamel by the secretory ameloblasts of the rat incisor as revealed by radioautography after galactose-H injection. J Cell Biol. *51* 26–31 1971

Acta path. microbiol. scand. Sect. A, 85 89–98, 1977

ELECTRON MICROSCOPY OF LYMPH NODES OF HAMSTERS EXPERIMENTALLY INFECTED WITH *TREPONEMA PERTENUE*

J. Blom, K. Hovind-Hougen, H. J. Skovgaard Jensen
and A. Birch Andersen

Departments of Biophysics, Treponematoses and Laboratory Animals, Statens Seruminstitut, Copenhagen, Denmark

Blom, J., Hovind-Hougen, K., Jensen, H. J. Skovgaard & Birch-Andersen, A. Electron microscopy of lymph nodes of hamsters experimentally infected with *Treponema pertenue*. Acta path. microbiol. scand. Sect. A 85 89–98, 1977

The morphology of lymph node tissue from normal hamsters and from hamsters experimentally infected with *Treponema pertenue* Gauthier was compared by means of light and electron microscopy. The capsules of the lymph nodes from infected hamsters showed an increased thickness in comparison with those of the non-infected animals. The infected lymph nodes differed from normal lymph nodes by small accumulations of neutrophilic leucocytes in the cortical areas. In addition, the amount of intercellular collagenous matrix present between large elongated cells was greatly increased in lymph nodes from infected animals. Electron microscopy of thin sections of infected lymph nodes showed intercellularly located treponemes in the leucocyte infiltration areas. These regions also showed the increased amounts of the collagenous matrix. Treponemes were occasionally found intracellularly in macrophages. These treponemes did not show their typically helical shape, but were present as spherical forms or cysts.

Key words: *Treponema pertenue*; ultrastructure; lymph nodes; hamsters; experimentally infected.

K. Hovind-Hougen, Department of Treponematoses, Statens Seruminstitut, Amager Boulevard 80, DK 2300 Copenhagen S, Denmark

Received 10.viii.76 Accepted 10.ix.76

Electron microscopy of the pathogenic treponemes, *T. pallidum* Nichols (5, 9), *T. cuniculi* (6) and *T. pertenue* Gauthier (8) has failed to demonstrate any ultrastructural differences of value for a differentiation between these treponemal species. It was also impossible to demonstrate characteristic differences in the ultrastructure of the host parasite relationship in the treponematoses caused by the various species of the non-cultivable treponemes that we have studied. Electron microscopical studies of lesions in the mucous membranes and skin in primary and secondary human syphilis (7) and of skin lesions in rabbits naturally infected with *T. cuniculi* (6) did not reveal differences either between the localization of treponemes in the infected epithelia or in their effect on the host tissues. According to *Turner & Hollander* (16) the manifestations in hamsters of an infection caused by intradermal inocu-

Melander A In vivo action of vinblastine on thyroid ultrastructure and hormone secretion Endocrinol *94* 641–649 1974
Ericson L E & Lundquist I Effect of vinblastine in vivo on ultrastructure and insulin releasing capacity of the B-cell following sulphonylurea and isopropyl noradrenaline Diabetol. *11* 467–473 1975
Kallenbach E. The fine structure of Tomes process of rat incisor ameloblasts and its relationship to the elaboration of enamel. Tissue & Cell *5* 501–524 1973
Katchburian E & Holt S J Studies on the development of ameloblasts, I Fine structure J Cell Sci *11* 415–447 1972
Krishan A & Hsu D Observations on the association of helical polyribosomes and filaments with vincristine-induced crystals in Earle's L-cell fibroblasts. J Cell Biol. *43* 553–563 1969
Moe H Morphological changes in the infranuclear portion of the enamel producing cells during their life cycle. J Anat. *108* 43–62 1971
Moskalewski S Thyberg J Lokmander S & Friberg U Influence of colchicine and vinblastine on the Golgi complex and matrix deposition in chondrocyte aggregates. Exp Cell Res. *95* 440–454 1975
Nève P Rocmans P & Ketelbant Balasse P Microtubules and microtubule inhibitors and cytochalasin in the thyroid gland. In Borgers, M & De Brabander M (Eds.) Microtubules and microtubule inhibitors, North-Holland Publishing Company Amsterdam and Oxford 1975 p. 177–185
Rebhun L I Polarized intracellular particle transport Saltatory movements and cytoplasmic streaming In Bourne G H & Danielli, J F (Eds.) International Review of Cytology vol 32 Academic Press, New York and London 1972 p 93–137
13 *Redman C M Banerjee D Howell K & Palade G E* Colchicine inhibition of plasma protein release from rat hepatocytes J Cell Biol *66* 42–59 1975
14 *Shiino M & Rennels E G* Vinblastine-induced microtubular paracrystals in prolactin cells of anterior pituitary gland of lactating rats Am J Anat *144* 399–405 1975
15 *Silverblatt F J Tyson G E & Bulger R E* Effects of vinblastine on the phagolysosome system of proximal tubule cells of rat kidney Administration of horseradish peroxidase Lab. Invest. *31* 170–180 1974
16. *Smith C E & Warshawsky H* Cellular renewal in the enamel organ and the odontoblast layer of the rat incisor as followed by radioautography using ³H thymidine Anat. Rec *183* 523–560 1975
17 *Tyson C E & Bulger R E.* Vinblastine-induced paracrystals and unusually large microtubules (macrotubules) in rat renal cells. Z. Zellforsch. *141* 443–458 1973
18 *Tyson C E & Bulger R E* Vinblastine-induced aggregates of smooth endoplasmic reticulum in proximal tubular cells of rat kidney Am. J Anat. *140* 201–212, 1974
19 *Warshawsky H* The fine structure of secretory ameloblasts in rat incisors. Anat. Rec. *161* 211–229 1968.
20 *Warshawsky H & Smith C E.* Morphological classification of rat incisor ameloblasts. Anat Rec *179* 423–446 1974
21 *Weinstock A & Leblond C P* Elaboration of the matrix glycoprotein of enamel by the secretory ameloblasts of the rat incisor as revealed by radioautography after galactose-³H injection. J Cell Biol. *51* 26–51 1971

Acta path. microbiol. scand. Sect. A, 85 89-98, 1977

ELECTRON MICROSCOPY OF LYMPH NODES OF HAMSTERS EXPERIMENTALLY INFECTED WITH *TREPONEMA PERTENUE*

J. BLOM, K. HOVIND-HOUGEN, H. J. SKOVGAARD JENSEN
and A. BIRCH ANDERSEN

Departments of Biophysics, Treponematoses and Laboratory Animals, Statens Seruminstitut, Copenhagen, Denmark

Blom, J., Hovind-Hougen, K., Jensen, H. J. Skovgaard & Birch-Andersen, A. Electron microscopy of lymph nodes of hamsters experimentally infected with *Treponema pertenue*. Acta path. microbiol. scand. Sect. A, 85: 89-98, 1977.

The morphology of lymph node tissue from normal hamsters and from hamsters experimentally infected with *Treponema pertenue* Gauthier was compared by means of light and electron microscopy. The capsules of the lymph nodes from infected hamsters showed an increased thickness in comparison with those of the non-infected animals. The infected lymph nodes differed from normal lymph nodes by small accumulations of neutrophilic leucocytes in the cortical areas. In addition, the amount of intercellular collagenous matrix present between large elongated cells was greatly increased in lymph nodes from infected animals. Electron microscopy of thin sections of infected lymph nodes showed intercellularly located treponemes in the leucocyte infiltration areas. These regions also showed the increased amounts of the collagenous matrix. Treponemes were occasionally found intracellularly in macrophages. These treponemes did not show their typically helical shape but were present as spherical forms or cysts.

Key words: *Treponema pertenue*; ultrastructure; lymph nodes; hamsters; experimentally infected.

K. Hovind-Hougen, Department of Treponematoses, Statens Seruminstitut, Amager Boulevard 80, DK 2300 Copenhagen S, Denmark.

Received 10.iii.76 Accepted 10.iii.76

Electron microscopy of the pathogenic treponemes, *T. pallidum* Nichols (5, 9), *T. cuniculi* (6) and *T. pertenue* Gauthier (8) has failed to demonstrate any ultrastructural differences of value for a differentiation between these treponemal species. It was also impossible to demonstrate characteristic differences in the ultrastructure of the host parasite relationship in the treponematoses caused by the various species of the non-cultivable treponemes that we have studied. Electron microscopical studies of lesions in the mucous membranes and skin in primary and secondary human syphilis (7) and of skin lesions in rabbits naturally infected with *T. cuniculi* (6) did not reveal differences either between the localization of treponemes in the infected epithelia or in their effect on the host tissues. According to *Turner & Hollander* (16) the manifestations in hamsters of an infection caused by intradermal inocu-

lation in the groin region with *T pertenue* appear to be confined to the skin and the lymph nodes It therefore seemed reasonable to confine our study to the ultrastructure of skin biopsy specimens from regions with lesions and lymph node tissue from swollen lymph nodes of such infected hamsters. The results of our study of the skin lesions are reported in a previous paper (8) It was concluded that it was impossible to distinguish between these skin lesions and those studied after infection with other pathogenic treponemes if the following criteria were used the morphology of the infected epithelium the intercellular localization of the treponemes within the epidermis and the morphology of the treponemes themselves (8)

To the best of our knowledge no electron microscope studies on the morphology of lymph nodes from animals infected with treponemes have been published previously In this report however we present the results of studies on the ultrastructure of lymph nodes from hamsters infected with *T pertenue* Castellani by intradermal inoculation in the groin region

MATERIALS AND METHODS

The materials and methods used are described in a previously published paper (8) Briefly summarized the tissues were prefixed in Karnowsky's fixative or glutaraldehyde postfixed in osmium tetroxide and treated *en bloc* with uranyl acetate prior to dehydration with alcohol and embedding in Vestopal W Thin sections were counter-stained with magnesium uranyl acetate (4) and lead citrate (15) and examined in a Philips EM 300 electron microscope Photomicrographs of semithick sections stained with toluidine blue were taken with a Carl Zeiss photomicroscope II using Agfapan 25 professional film

RESULTS

Morphology of Lymph Nodes from Non Infected Hamsters

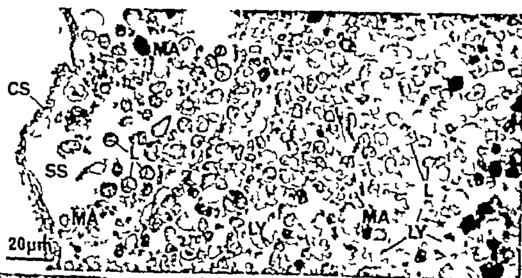
Light microscopy 2 µm thick sections from centrally sectioned inguinal lymph nodes from non infected hamsters were studied in the light microscope after staining of the Vestopal embedded tissue with toluidine blue. The nodes had a thin capsule consisting of two to three cell layers and subcapsular sinuses in which small lymphocytes and macrophages were predominant (Fig 1) In the cortical areas the lymphoid parenchyma adjacent to the subcapsular sinuses was dominated by small and medium sized lymphocytes (Fig 1) The germinal centres in the cortical areas consisted of large lymphoid cells and macrophages which often presented big cytoplasmic inclusions (Fig 1)

Other regions of the lymph nodes, e.g the paracortical areas and the medullary cords, are not included in Fig 1 but these regions were also studied in toluidine blue stained sections. The paracortical areas interdigitated with the cortical areas and were considered to be the loosely arranged lymphoid tissues present in close relation to the post-capillary venules. The medullary cords were seen centrally in the lymph nodes and generally con-

Figs 1–7 all show sections of inguinal lymph nodes from normal hamsters or from hamsters experimentally infected with *Treponema pertenue*

Fig 1 A 2 µm thick section from a non infected lymph node stained with toluidine blue Part of the cortical area and the subcapsular sinus (SS) is shown. Note the thin capsule (CS) Small and medium sized lymphocytes (L) are seen both in the sinus and in the lymphoid parenchyma. A few macrophages (MA) with large dense inclusions are also present in these two regions. Large lymphoid cells (LY) some with prominent nucleoli are seen in the inner part of the cortex. Light microscopy 650 ×

Fig 2 Part of the cortical area of a non-infected lymph node showing the capsule (CS) the subcapsular sinus (SS) and the lymphoid parenchyma. The sinus is lined by flattened endothelial cells (E) On the inner aspect of the sinus a gap (large arrow) is present between the endothelial cells. The sinus contains macrophages (MA) some of which are attached to endothelial cells (arrow heads) and lymphocytes (L) Cross sectioned trabeculae of collagen fibres (small arrows) are seen in contact with the endothelial cells. In the lymphoid parenchyma the dominating cell type is the small and the medium sized lymphocyte (L) A few big lymphoid cells (LY) with vesiculated nuclei are also present Electron microscopy 2450 ×


1
CS
MA
SS
MA
LY
MA
LY
L
20µm

2
MA
MA
CS
SS
LY
E
L
E
LY
E
5µm

tained large lymphoid cells as well as immature and mature plasma cells.

Electron microscopy. In thin sections the subcapsular lymphatic sinuses were readily identified in the electron microscope (Fig 2). A sinus was lined by flat and smooth surfaced lymphatic endothelial cells. The attenuated cytoplasm of the endothelial cells contained few organelles only. Adjoining endothelial cells of a sinus were found either to overlap or to interdigitate and small gaps were present between cells at the inner aspect of the sinus (Fig 2). Probably these gaps between cells were formed when migrating cells passed through the endothelium from or to the adjacent lymphoid parenchyma.

The endothelial cells were supported by a framework of lymphoid parenchyma which in addition to bundles of collagen fibres (trabeculae) (Fig 2) consisted of long slender cytoplasmic projections of fibroblasts.

In the lumen of the lymphatic sinus a population of circulating cells was found. Generally these cells consisted mainly of lymphocytes and macrophages, but occasionally a few neutrophilic leucocytes and erythrocytes were also present. Some of the macrophages within a sinus seemed to be anchored to the surface of the lymphatic endothelial cells by extensions of their cytoplasm (Fig 2). The nuclei of such macrophages were elongated and slightly folded with a peripheral condensation of the chromatin. This type of macrophage also contained lysosomes and inclusions of phagocytized material in the cytoplasm (Fig 2). The small lymphocytes were characterized by relatively large nuclei which frequently were deeply indented. The cytoplasm of these cells formed a small rim around the nucleus and contained only a few organelles.

The zone just below the subcapsular sinus, i.e. the cortical region, was dominated by small and medium sized lymphocytes (Fig 2). A few large lymphoid cells characterized by big ovoid or round nuclei were also present. The nuclei of these contained prominent nucleoli and presented a vesiculated appearance (Fig 2). These large lymphoid cells also had a moderate amount of cytoplasm with many polyribosomes and a few mitochondria. The germinal centres found in the cortical region of the lymph node were surrounded by a dense rim of cells mainly consisting of small lymphocytes. The germinal centre itself however contained mainly large lymphoid cells and macrophages. The macrophages had large amounts of cell debris and lysosomes in their cytoplasm. Very few plasma cells were seen in the germinal centres.

Intercellular collagen fibres traversed the lymphoid parenchyma. The collagen fibres were often found in bundles (trabeculae) and these constituted the basic framework of the lymph nodes. The bundles of intercellular collagen present in the parenchyma were found to be in intimate contact with cytoplasmic extensions of fibroblasts. The collagen bundles in the sinuses were seen to be in close association with cytoplasmic extensions of endothelial cells (Fig 2).

Fig 3. A 2 μm thick section from an infected lymph node stained with toluidine blue. Part of the cortex and the subcapsular sinus (SS) is shown together with the capsule (CS). Note the increase in thickness of the capsule (CS) compared with the capsule shown in Fig 1. Focal infiltrations of neutrophilic leucocytes (NL) are found in the lymphoid parenchyma. Macrophages (MA) with dense inclusions are also present in this region. The right half of the field is dominated by large elongated fibroblasts (FB) lying in a collagenous matrix. Light microscopy 650 ×

Fig 4. Part of the cortical area of an infected lymph node. The infiltrating treponemes (T) are easily identified. Note the intercellular location of the treponemes. Large lymphoid cells (LY) are present together with some plasma cells (PC). A few neutrophilic leucocytes (NL) are found. A macrophage (MA) with many lysosome-like bodies is present. This cell shows no sign of intracellularly located treponemes. A fibroblast (FB) with well developed granular endoplasmic reticulum is surrounded by treponemes. A small vessel (VE) is present. Note the absence of intraluminal treponemes in this vessel. Electron microscopy 2450 ×

3



tained large lymphoid cells as well as immature and mature plasma cells

Electron microscopy In thin sections the subcapsular lymphatic sinuses were readily identified in the electron microscope (Fig 2) A sinus was lined by flat and smooth surfaced lymphatic endothelial cells. The attenuated cytoplasm of the endothelial cells contained few organelles only *Adjoining endothelial cells of a sinus were found either to overlap or to interdigitate and small gaps were present between cells at the inner aspect of the sinus (Fig 2) Probably these gaps between cells were formed when migrating cells passed through the endothelium from or to the adjacent lymphoid parenchyma

The endothelial cells were supported by a framework of lymphoid parenchyma which in addition to bundles of collagen fibres (trabeculae) (Fig 2) consisted of long slender cytoplasmic projections of fibroblasts.

In the lumen of the lymphatic sinus a population of circulating cells was found Generally these cells consisted mainly of lymphocytes and macrophages, but occasionally a few neutrophilic leucocytes and erythrocytes were also present Some of the macrophages within a sinus seemed to be anchored to the surface of the lymphatic endothelial cells by extensions of their cytoplasm (Fig 2) The nuclei of such macrophages were elongated and slightly folded with a peripheral condensation of the chromatin This type of macrophage also contained lysosomes and inclusions of phagocytized material in the cytoplasm (Fig 2) The small lymphocytes were characterized by relatively large nuclei which frequently were deeply indented The cytoplasm of these cells formed a small rim around the nucleus and contained only a few organelles

The zone just below the subcapsular sinus i e the cortical region was dominated by small and medium sized lymphocytes (Fig 2) A few large lymphoid cells characterized by big ovoid or round nuclei were also present The nuclei of these contained prominent nucleoli and presented a vesiculated appearance (Fig 2) These large lymphoid cells also had a moderate amount of cytoplasm with many polyribosomes and a few mitochondria The germinal centres found in the cortical region of the lymph node were surrounded by a dense rim of cells mainly consisting of small lymphocytes. The germinal centre itself however contained mainly large lymphoid cells and macrophages. The macrophages had large amounts of cell debris and lysosomes in their cytoplasm. Very few plasma cells were seen in the germinal centres

Intercellular collagen fibres traversed the lymphoid parenchyma. The collagen fibres were often found in bundles (trabeculae) and these constituted the basic framework of the lymph nodes The bundles of intercellular collagen present in the parenchyma were found to be in intimate contact with cytoplasmic extensions of fibroblasts. The collagen bundles in the sinuses were seen to be in close association with cytoplasmic extensions of endothelial cells (Fig 2)

Fig 3 A 2 μm thick section from an infected lymph node stained with toluidine blue Part of the cortex and the subcapsular sinus (SS) is shown together with the capsule (CS) Note the increase in thickness of the capsule (CS) compared with the capsule shown in Fig 1 Focal infiltrations of neutrophilic leucocytes (NL) are found in the lymphoid parenchyma. Macrophages (MA) with dense inclusions are also present in this region. The right half of the field is dominated by large elongated fibroblasts (FB) lying in a collagenous matrix. *Light microscopy 630 ×*

Fig 4 Part of the cortical area of an infected lymph node The infiltrating treponemes (T) are easily identified Note the intercellular location of the treponemes Large lymphoid cells (LY) are present together with some plasma cells (PC) A few neutrophilic leucocytes (NL) are found. A macrophage (MA) with many lysosome-like bodies present. This cell shows no sign of intracellularly located treponemes. A fibroblast (FB) with well developed granular endoplasmic reticulum is surrounded by treponemes. A small vessel (VE) is present. Note the absence of intraluminal treponemes in this vessel. *Electron microscopy 2430 ×*

were found to be situated in the intercellular spaces and scattered between the various cell types in the cortical region of the gland (Fig 4) Few small lymphocytes were found, whereas many large lymphoid cells were present. The nuclei of the majority of these lymphoid cells were large and vesiculated, round or ovoid of shape (Fig 4) and they often contained a nucleolus. In some of the cells the chromatin was accumulated in clumps close to the nuclear membrane. The cytoplasm of the lymphoid cells contained many polyribosomes and small segments of granular endoplasmic reticulum.

Immature and mature plasma cells were found in the lymphoid parenchyma. The nuclear chromatin of these cells was clustered near the nuclear periphery and a nucleolus was often present. The cytoplasm of the plasma cells contained a substantial amount of granular endoplasmic reticulum which varied in arrangement from the sac like dilated type to the type with cisternae that are arranged in a more parallel manner (Fig. 4) Most of the plasma cells showed a well developed Golgi complex.

Neutrophilic leucocytes with hyperseg mented nuclei were scattered in the regions where the treponemes were located (Fig 4) At high magnifications the cytoplasmic granules of the neutrophils were seen to be rather poorly preserved. Although a very great number of treponemes was often seen surround ing the leucocytes, no treponemes were ever observed in the cytoplasm of these cells. Many macrophages were present in regions where the treponemes were abundant (Fig. 4) These macrophages varied considerably in shape and showed many pseudopodial processes of their cytoplasm. A few of these mac rophages contained a small number of intra cellularly located treponemes (Figs. 5 6, 7) The nuclei of the macrophages were round or ovoid with marginated chromatin (Fig 4) A nucleolus was often present (Fig 6) and the cytoplasm of the cells contained polyribosomes, mitochondria, and short segments of granular endoplasmic reticulum. A well developed Golgi complex was present in some



Fig 6 Part of a macrophage in which the treponemes (T) are found in the Golgi region (G) close to the nucleus of the cell. A nucleolus (NU) is seen in the nucleus. (M) denotes mitochondria. 15,000 ×

of the cells (Figs. 6 7) Membrane-bound lysosome-like bodies with a diameter of 0.5 µm were also present in some macrophages (Figs. 4 5)

The intracellularly located treponemes were observed to be coiled up in membrane-bound vacuoles (Figs. 5 6, 7) One or several dense lysosomal granules often seemed to be about to fuse with these vacuoles. A close relationship between treponemes and a Golgi complex was observed in several cells (Figs. 6, 7) This, we believe, shows some evidence for a true intracellular location of the treponemes in these cells.

On most of the intracytoplasmically situated treponemes the outer membrane was partly or completely lacking. The membrane appeared to have been torn off and was probably present as myelin-like figures in the in-



Fig 5 Detail from a macrophage which contains some intracellularly located treponemes (T) The treponemes are coiled up within a membrane bound vacuole The outer membrane (OM) of the treponemes appears to have been torn off A dense lysosomal granule (DL) containing a crystalline structure is seen close to the vacuole 95 000 ×

Morphology of Lymph Nodes from Infected Hamsters

Light microscopy Sections about 2 µm thick obtained from centrally sectioned inguinal lymph nodes from hamsters experimentally infected with *T pertenue* were studied after staining with toluidine blue The surrounding capsules were found to be thicker than those of the non infected lymph nodes (Fig 3 and cf Fig 1) The diameter of the subcapsular sinuses and their content of different cell types *i e* lymphocytes, macrophages and neutrophilic leucocytes, were seen to vary considerably in the infected nodes. In the cortical regions small accumulations of infiltrating neutrophilic leucocytes were observed (Fig 3) In addition an obvious increase, compared with the normal lymph nodes, was noted in the amount of intercellular collagenous matrix present between the large elongated cells of the lymphoid parenchyma (Fig 3) Macrophages with many dense inclusions in their cytoplasm were scattered among these large elongated cells (Fig 3) Plasma cells and large lymphoid cells were found but in moderate numbers, whereas small lymphocytes were only occasionally seen in the lymphoid parenchyma

In the paracortical and medullary areas no infiltration of neutrophilic leucocytes was found and no obvious morphological differences could be seen when comparing with the non infected lymph nodes.

Electron microscopy The infecting treponemes were easily identified even at low magnification when thin sections of lymph nodes from infected hamsters were studied in the electron microscope. The organisms

nodes are found to differ from those of the controls by a spot-wise localization of neutrophilic leucocytes, as well as by an increase in the amount of intercellular collagenous matrix in the cortical areas of the nodes. An increase in the thickness of the capsules of the infected lymph nodes was also found.

By electron microscopy an increased number of elongated fibroblasts with well developed granular endoplasmic reticulum was observed in the lymph nodes of the infected hamsters. These fibroblasts are probably responsible for the increased amounts of intercellular collagenous matrix present in these lymph nodes and thus reflect the chronical character of the infection.

Treponemes were revealed only in the leucocyte infiltrated area of the infected lymph nodes. A detailed examination of the cells showed that only in macrophages could treponemes be found intracellularly with some degree of certainty. The macrophages in which we found intracytoplasmic treponemes were characterized by a few dense cytoplasmic inclusions, whereas other macrophages with many big dense inclusions did not seem to have phagocytized any treponemes.

The treponemes that were engulfed by macrophages all seemed to have lost their helical shape and appeared in what has been termed "the spherical form" (see e.g. *Pillot* (13) for further details). Two reasons why only spherical forms were observed intracellularly in macrophages can be suggested: 1) macrophages are only capable of phagocytizing treponemes which have formed spheres or 2) the treponemes form spheres after having been phagocytized.

The first explanation seems the most plausible to us, since it is difficult to imagine how a cell can phagocytize a treponeme with a length of 10–15 μm which corresponds approximately to the diameter of an average sized macrophage.

Musher et al. (12) have studied the *in vitro* phagocytosis of cultivable treponemes by rabbit macrophages. Their electron micrographs illustrate intracellular localizations of spherical forms of treponemes in membrane bound vacuoles similar to what we observed. They concluded that macrophages actively phagocytized the treponemes, but they do not comment on the spherical form of the organisms.

Several other investigators have observed segments of treponemes within membrane bound vacuoles or interstices in the cytoplasm of macrophages (1, 10, 11, 14). These observations are corroborated by the present study. However, in the studies to date the vacuoles and interstices with segments of treponemes are always found near the cell border or in very indented cells. In addition, the vacuoles are often found in macrophages that are not too well preserved, and consequently it can not be excluded that these treponemes are sectioned within invaginations of the surface membrane and thus only seem to be intracellularly located.

According to *Cottier et al.* (3) the germinal centres in the cortical area of the lymph node elicit most of the humoral antibody response in immunization, whereas the paracortical area plays a major role in the cell-mediated immunity. In the present study the treponemes were located only in the cortical region of the lymph nodes. Plasma cells were found in close *proximity* to the treponemes in the cortical regions of the lymph nodes, and this raises the question whether these plasma cells are producing the humoral antibodies against the treponemes. If this is so, these humoral antibodies do not seem to have any effect either on the ultrastructure of the intercellular treponemes or on the degree of their phagocytosis by the neutrophilic leucocytes or macrophages often present in the vicinity of the plasma cells.

The authors wish to express their gratitude to Dr. *H. Aage Nielsen*, Department of Treponematoses, for his great interest in and support of our work. We also thank Mrs. *J. Berg*, Mrs. *H. Rasn* and Mr. *F. Laursen* for their excellent assistance in electron microscopy and Miss *A. G. Ostgaard* and Mr. *F. Laursen* for expert photographic work.

This study was supported by grants from the *Danish State Medical Research Council* (Nos. 512-2512 and 512-2980) and *WHO*, Geneva.



Fig 7 Detail from Fig 6 The outer membrane (OM) of the treponemes is partly torn off and has formed a myelin like figure The membrane-bound vacuole with the treponemes is surrounded by vesicles (V) and cisternae (C) of the Golgi complex. (N) denotes nucleus. 95 000 ×

terior of the phagocytic vacuoles of the macrophages (Fig 7)

Elongated cells with well developed granular *endoplasmic reticulum* were often seen in close association with the intercellular collagenous matrix which was present in increased amounts in the lymph nodes of the infected hamsters (Fig 4) No treponemes were ever observed in the lumina of the small vessels of the infected lymph nodes, not even in regions of the nodes in which treponemes were present intercellularly in great numbers (Fig 4)

DISCUSSION

Our observations on the general morphology of the hamster lymph node seen by light microscopy are in accordance with the results published by *Cottier et al* (3) In addition the results of the ultrastructural studies of the constituent cells in the lymph node are comparable to those published in a review by *Carr* (2)

We have chosen a time interval of 6 weeks between the intradermal inoculation of *T pertenue* Gauthier into the groin of hamsters and the removal of the inguinal lymph nodes. This was because we previously found that the number of treponemes in the lymph node tissues was then at a maximum (unpublished) a result which is also in accordance with the observations of *Turner & Hollander* (16) The morphological changes we found in the lymph nodes 6 weeks after the initiation of the infection seemed to be of a rather chronical character

When the morphology of the normal and the infected lymph nodes, as seen by light microscopy is compared, the infected lymph

Acta path. microbiol. scand. Sect. A, 85: 99–104, 1977

OSTEONECROSIS FOLLOWING RENAL ALLOTRANSPLANTATION

A Quantitative Histological Study of Iliac Bone

Flemming Melsen and Hans Egon Nielsen

University Institute of Pathology, Aarhus Amtssygehus, Aarhus, and Medical Department C, Aarhus Kommunehospital, Aarhus, Denmark

Melsen, F. & Nielsen, H. E. Osteonecrosis following renal allotransplantation. A quantitative histological study of iliac bone. Acta path. microbiol. scand. Sect. A, 85: 99–104, 1977.

Morphometric and dynamic studies of bone obtained by biopsy from a standard locality on the iliac crest were carried out in 10 patients with and 7 patients without radiological signs of osteonecrosis. All the patients had normally functioning kidney transplants. The results obtained in the two groups were compared and both groups were compared with a series of normal subjects where the age and sex distribution was the same. In the group of patients with osteonecrosis, the reduction in the amount of cancellous bone was found to be highly significant as compared with that in normal subjects and with that in the other group of patients. Apart from the reduction in bone, changes in all patients were characterized by an increased amount of osteoid and a low rate of mineralization, determined by double labelling with tetracycline. As there were no changes in the width of osteoid seams indicating osteomalacia, it is suggested that these patients suffered from a severe corticosteroid osteopenia.

Key words: Kidney transplantation; osteonecrosis; bone morphometry.

F. Melsen, University Institute of Pathology, Aarhus Amtssygehus, DK-8000 Aarhus C, Denmark.

Received 15.viii.76   Accepted 15.xii.76

Parallel with the increasing numbers of successful kidney transplants, the understanding of complications involved in post-transplantation including osteonecrosis, has become more important.

The sites of bone affection most often reported are weightbearing regions such as the femoral head, knee and shoulder and regions where the bone is mainly cancellous (Nielsen et al. 1976). Aseptic necrosis of bone has been attributed to various factors. Disturbances in vascularization as well as subchondral avascular necrosis as a consequence of vascular occlusion by fat embolism have been suggested (Evarts & Phalen 1971, Harrington et al. 1971, Pierides et al. 1975, Ølgård & Heerfordt 1975). Subchondral osteoporosis or osteopenia leading to fractures and necrosis (Frost 1965, Jaffe et al. 1972, Laurent et al. 1973) are in accordance with the known effect of long term corticosteroid therapy on bone (Jowsey & Riggs 1970, Gallagher et al. 1973, Laurent et al. 1973).

The purpose of the present study was to investigate whether the pathogenesis of osteonecrosis following renal allotransplantation could be elucidated through morphometric and dynamic studies of bone obtained by biopsy from a standard area of the iliac crest.

7*

REFERENCES

1 *Azar H A Pham T D & Kurban A K* An electron microscopic study of a syphilitic chancre Arch Path. *90* 143–150 1970

2 *Carr I* The fine structure of the mammalian lymphoreticular system. Int. Rev Cytol *27* 283–348 1970

3 *Cottier H Turk J & Sobin L.* A proposal for a standardized system of reporting human lymph node morphology in relation to immunological function Bull. Wld Hlth Org *47* 375–408, 1972

4 *Frasca J M & Parks V R* A routine technique for double-staining ultrathin sections using uranyl and lead salts. J Cell Biol *25* 157–161 1965

5 *Hovind Hougen K* Further observations on the ultrastructure of *Treponema pallidum* Nichols. Acta path. microbiol scand Sect B *80* 297–304 1972

6 *Hovind Hougen K Birch Andersen A & Jensen H J Skovgaard* Electron microscopy of *Treponema cuniculi* Acta path. microbiol scand. Sect. B *81* 15–26 1973

7 *Hovind Hougen K Birch Andersen A & Nielsen R* Electron microscopy of human syphilitic lesions. Paper given at the Meeting of Medical Society for the Study of Venereal Diseases, Brussels 1973

8 *Hovind Hougen K Birch Andersen A & Jensen H J Skovgaard* Ultrastructure of cells of *Treponema pertenue* obtained from experimentally infected hamsters. Acta path. microbiol scand. Sect. B, *84* 101–108, 1976.

9 *Jepsen O B Hovind Hougen K & Birch-Andersen A* Electron microscopy of *Treponema pallidum* Nichols. Acta path. microbiol. scand. *74* 241–258 1968.

10 *Lauderdale V & Goldman J N* Serial ultrathin sectioning demonstrating the intracellularity of *T pallidum* Brit. J vener Dis. *48* 87–96 1972

11 *Metz J & Metz G* Elektronenmikroskopischer Nachweiss von *Treponema pallidum* in Hauteffloreszenzen der unbehandelten Lues I und II Arch. Derm. Forsch. *243* 241–254 1972

12. *Musher D M Iesat N A Mrs A H & Györkey F* *In vitro* phagocytosis of avirulent *T pallidum* by rabbit macrophages. Acta derm.-venereol (Stockh.) *52* 349–352 1972.

13 *Pillot J* Contribution à l'étude du genre *Treponema. Structures anatomique et antigénique* Thèse, Univ Paris, 1965

14 *Ovčinnikov N M & Delektorskij V V* Electron microscopy of phagocytosis in syphilis and yaws. Brit. J vener Dis. *48* 227–248, 1972

15 *Reynolds E S* The use of lead citrate at high pH as an electron-opaque stain in electron microscopy J Cell Biol *17* 208–212, 1963

16 *Turner T B. & Hollander D H* Biology of the treponematoses. Wld Hlth Org Monogr Ser No. 35 Geneva 1957 p 57–64

Acta path. microbiol. scand. Sect. A, 85 99–104 1977

OSTEONECROSIS FOLLOWING RENAL ALLOTRANSPLANTATION

A Quantitative Histological Study of Iliac Bone

FLEMMING MELSEN and HANS EGON NIELSEN

University Institute of Pathology Aarhus Amtssygehus, Aarhus, and
Medical Department C, Aarhus Kommunehospital, Aarhus, Denmark

Melsen, F & Nielsen, H. E Osteonecrosis following renal allotransplantation. A quantitative histological study of iliac bone. Acta path. microbiol. scand. Sect. A, 85 99–104 1977

Morphometric and dynamic studies of bone obtained by biopsy from a standard locality on the iliac crest were carried out in 10 patients with and 7 patients without radiological signs of osteonecrosis. All the patients had normally functioning kidney transplants. The results obtained in the two groups were compared and both groups were compared with a series of normal subjects where the age and sex distribution was the same In the group of patients with osteonecrosis, the reduction in the amount of cancellous bone was found to be highly significant as compared with that in normal subjects and with that in the other group of patients. Apart from the reduction in bone changes in all patients were characterized by an increased amount of osteoid and low rate of mineralization, determined by double labelling with tetracycline. As there were no changes in the width of osteoid seams indicating osteomalacia, it is suggested that these patients suffered from a severe corticosteroid osteopenia.

Key words Kidney transplantation osteonecrosis bone morphometry

F Melsen, University Institute of Pathology Aarhus Amtssygehus, DK-8000 Aarhus C, Denmark.

Received 15 iii.76 Accepted 15 viii.76

Parallel with the increasing numbers of successful kidney transplants, the understanding of complications involved in post-transplantation including osteonecrosis, has become more important.

The sites of bone affection most often reported are weightbearing regions such as the femoral head, knee and shoulder and regions where the bone is mainly cancellous (*Nielsen et al.* 1976) Aseptic necrosis of bone has been attributed to various factors. Disturbances in vascularization as well as subchondral avascular necrosis as a consequence of vascular occlusion by fat embolism have been suggested (*Evarts & Phalen* 1971 *Harrington et al.* 1971 *Pierides et al* 1975 *Olgård & Heerfordt* 1975) Subchondral osteoporosis or osteopenia leading to fractures and necrosis (*Frost* 1965 *Jaffe et al.* 1972, *Laurent et al.* 1973) are in accordance with the known effect of long term corticosteroid therapy on bone (*Jowsey & Riggs* 1970 *Gallagher et al.* 1973 *Laurent et al.* 1973)

The purpose of the present study was to investigate whether the pathogenesis of osteonecrosis following renal allotransplantation could be elucidated through morphometric and dynamic studies of bone obtained by biopsy from a standard area of the iliac crest.

7*

PATIENTS AND METHODS

Seventeen patients of ages between 28 and 65 years in whom the kidney function was normal after successful kidney transplantation (C > 50 ml/min) were included in this study. Ten of these (group I) (mean 43.1 years of age) showed radiological signs of osteonecrosis at various sites, most frequently being localized to the femoral head. Seven patients (group II) (mean 42.6 years of age) showed no signs of bone affection.

At the time of study the patients in group I were receiving 3.1 mg prednisone and 125 mg azathioprine as mean daily dose. The patients in group II received 5.2 mg of prednisone and 89 mg of azathioprine respectively. As regards groups I and II the mean interval between kidney transplantation and study was 53.9 and 50.4 months, respectively.

The control material comprised bone specimens from 34 individuals of the same age (mean 41 years) and a distribution according to sex as that in the series of patients; the specimens were obtained by biopsy from volunteers or at necropsy of previously healthy individuals who had died suddenly from accident or coronary occlusion.

After double labelling with tetracycline (*Frost* 1969) biopsies were performed and two bone cylinders were obtained from the iliac crest (*Bordier et al.* 1964). The best specimen was embedded undecalcified in methyl metacrylate. 5–7 micron thick sections were produced and stained with toluidine, Masson Trichrome and Goldner Trichrome. The other specimens were decalcified in 15 per cent nitric acid and 4 micron thick conventional sections were stained with haematoxylin eosin and Van Gieson. In the section from the undecalcified material the following parameters were measured in the cancellous bone using point count principles and simple measurements (*Frost & Villanueva* 1962, *Frost* 1969, *Meunier et al.* 1971, *Melsen et al.* to be published).

Absolute volume of trabecular bone (AVTB). This parameter expresses the percentage of a given bone volume occupied by trabeculae of mineralized bone and osteoid.

Relative osteoid surfaces (OS). The percentage of the total trabecular surface covered by osteoid.

Relative osteoid volume (OV). The percentage of the total trabecular bone consisting of osteoid.

Mean width of osteoid seams (WOS). The mean of four extreme measurements of all the osteoid seams.

Trabecular osteoclastic resorption surfaces (RS). The percentage of total trabecular surface exhibiting "active" or "inactive" resorption, defined as scalloped interruption of the trabecular surface with or without osteoclasts.

Mean size of periosteocytic lacunae (POL). This parameter was measured on sections of the decalcified material as the mean product of length and width of 50 randomly selected lacunae using a conventional micrometric eyepiece.

In order to study bone dynamics, 20 micron thick unstained sections were produced from the undecalcified material and the following parameters were measured under the fluorescence microscope.

Calcification rate (CR in microns/day). The mean distance between the middle of the lines in all double labelled zones divided by the number of days between the given doses of tetracycline.

Active trabecular calcification surfaces (ATCS). The percentage of the total trabecular surface marked by tetracycline.

On the basis of the percentage of osteoid-covered surfaces (OS) and the percentage of active trabecular calcification surfaces (ATCS), the percentage of *active osteoid calcification surfaces* (AOCS) was calculated as $\frac{ATCS \times 100}{OS}$

The statistical significance of differences in group means was determined by the Wilcoxon test for two samples and correlation coefficients by *Spearman's* rank correlation (R).

RESULTS

The investigation included two groups: 10 patients with radiological signs of osteonecrosis and 7 without.

Group of Patients with Osteonecrosis

In this group the most striking feature is a highly significant reduction in the amount of trabecular bone (AVTB) (Table 1 and 2) as compared with the amount in normal subjects ($p < 0.01$) (Fig. 1) and in patients without osteonecrosis ($p < 0.01$). Furthermore an increase in the amount of osteoid, OS as well as OV, in relation to that in normal subjects ($p < 0.01$) is seen. Any changes in the resorptive activity were not observed. Studies of bone dynamics revealed that the extent of active surfaces in trabecular bone was normal. Thus the relationship between ATCS and OS (AOCS) was reduced as compared with that in normal subjects ($p < 0.01$). The CR was also reduced ($p < 0.01$), whereas the mean width of osteoid seams (WOS) was normal.

TABLE 1 *Morphometric and Dynamic Analysis of Trabecular Bone in Patients with and without Osteonecrosis as Compared with Findings in Normal Controls*

		AVTB	OS	OV	WOS	RS	POL	CR	ATCS	AOCS
+ Osteonecrosis	$\bar{x}$	11.2	32.0	4 8	8.2	4.2	51 4	0.53	12.5	39 4
	S.E.	1 1	3 7	1.0	0 7	0 5	1.3	0 03	3.2	7.5
	N	10	10	10	10	10	10	10	10	10
— Osteonecrosis	$\bar{x}$	19.1	24.5	2.3	7.9	4.5	52.3	0.50	9.8	40 1
	S.E.	1.0	3.2	0.7	0.8	0 8	1.3	0.03	2.1	7.0
	N	7	7	7	7	7	7	7	7	7
Normal	$\bar{x}$	21.8	15 7	2.0	9.0	3 9	51.2	0.63	13.5	86.6
	S.E.	1.2	1.6	0.3	0.5	0.2	0 4	0.03	1.5	5.7
	N	34	34	34	19	34	25	6	15	15

TABLE 2. *Morphometric and Dynamic Analysis of Trabecular Bone in Patients with and without Osteonecrosis as Compared with Findings in Normal Controls*

	+ Nec./ Nor	— Nec./ Nor.	+ Nec./ — Nec.
AVTB	$p<0.01$	N.S.	$p<0.01$
OS	$p<0.01$	$p<0.05$	N.S.
OV	$p<0.01$	N.S	N.S
RS	N.S	N.S	N.S.
CR	$p<0.01$	$p<0.01$	N.S.
POL	N.S	N.S	N.S.
ATCS	N.S.	N.S	N.S
AOCS	$p<0.01$	$p<0.01$	N.S.
WOS	N.S.	N.S	N.S.

Group of Patients without Osteonecrosis

The bone changes in patients in this group are similar to those in the other group of patients, but less pronounced. The only parameter by which the two groups of patients were separated was the significant difference in AVTB ($p<0.01$).

Morphometrically the bone in patients in this group could be distinguished from normal bone by an increased OS ($p<0.05$) a reduced CR ($p<0.01$) and a reduced AOCS ($p<0.01$). No significant changes in the amount of bone (AVTB) were found.

It applies to both groups of patients that the serumphosphorus level was found to be low ($p<0.001$) and that there was an inverse but insignificant correlation between serum phosphate and osteoid covered surfaces (OS) ($n = 17$, $R = -0.46$, $0.1>p>0.05$).

The morphometric analysis was followed by a descriptive morphological analysis. Signs of necrosis were not found and only a single microfracture was seen. Any striking changes in the vessels were not found either in the bone or in the surrounding soft tissues.

DISCUSSION

A quantitative histological analysis of iliac crest bone from 10 patients with osteonecrosis subjected to kidney transplantation and 7 transplant patients without osteonecrosis yielded morphometric data which were compared with data obtained in a series of normal controls. The most striking finding was that the volume of spongy bone in the transplanted patients with osteonecrosis was significantly reduced as compared with that in patients without osteonecrosis ($p<0.01$) and in normal individuals ($p<0.01$).

Apart from the reduction in volume of trabecular bone in patients with osteonecrosis, similar changes in bone remodelling in patients in both groups were found. The changes were characterized by an increased amount of unmineralized bone, a decreased rate of mineralization and normal widths of the osteoid seams. Any changes in the osteoclastic or osteocytic activity were not found.





Fig 1 A and B Bone biopsies from a normal individual (A) and from a patient with osteonecrosis (B) A reduced amount of trabecular bone is seen in B

As bone is known to rarefy parallel with age (*Courpron* 1972 *Delling et al* 1976 *Melsen et al* to be published) individuals of the same age were selected for this investigation thereby eliminating the explanation that senile involution of bone might be responsible for the loss of bone Furthermore the bone changes in patients in the two groups differed from senile involution with respect to the amount and rate of mineralization of osteoid (*Courpron* 1972 *Meunier et al* 1973) The observed changes also differ from osteoporotic bone disease in which the bone remodelling are within the normal range (*Meunier et al* 1973 *Minaire et al* 1974)

Although the amount of osteoid is increased the disease differs from true osteomalacia In the latter disease the volume of bone is normal or even increased (*Vignon & Meunier* 1973 *Rasmussen & Bordier* 1974 *Melsen & Mosekilde* 1975) The rate of calcification is seen to be reduced in cases of osteomalacia and to be followed by an in

crease in the amount of osteoid and in the width of osteoid seams (*Lignon & Meunier* 1973 *Rasmussen & Bordier* 1974 *Meunier et al.* 1975)

In the present study the width of the osteoid seams was not found to change this suggests that the rate of osteoid apposition is reduced corresponding to the reduced rate of calcification.

As regards the total group of transplanted patients the serum phosphorus was found to decrease ($p < 0.001$) as compared with that in normal subjects. The inverse correlation between serum phosphorus and osteoid covered surfaces ($R = -0.46$) suggests hypophosphataemic osteomalacia. This suggestion is to be discussed elsewhere (*Nielsen et al.* 1976)

Reduction in the amount of trabecular bone and increase in the amount of osteoid as well as reduction in the rate and activity of calcification of osteoid have been described previously by *Laurent et al.* (1973) in a report on patients in long term treatment with corticosteroids Similar depression of bone formation has been observed in hypercortisonism (*Jowsey & Riggs* 1970) and in kidney transplanted patients (*Bortolotti et al.* 1976) The findings in the present study are to a great extent similar to the findings of bone changes in patients treated with steroids.

Meunier et al (1973) have found a good correlation between the amount of trabecular bone in the iliac crest and in the lumbar vertebrae and a correlation between compressive strength of spongy bone in the iliac crest and 3th and 4th lumbar vertebrae was shown by *Nielsen et al* (1976) These relations and the results of the present investigations confirm the relationship between osteonecrosis and the amount of trabecular bone in biopsies, thus suggesting that osteonecrosis after renal transplantation is the consequence of osteopenia followed by microfractures and bone collapse.

In addition to findings in the patients in the present investigation, we have observed, that osteonecrosis might be manifest in kidneytransplanted patients in whom the renal function was reduced and in whom histological signs of renal osteodystrophy and osteopenia were present. Accordingly the pathogenesis of osteonecrosis may not be as simple as suggested above A combination of persistent pre-transplantation bone changes and steroid induced osteopenia is one possibility To further elucidate the pathogenesis, studies of bone-changes to arise if the immunosuppressive regime is altered combined with longitudinal studies of bone changes in transplant patients would be very helpful.

REFERENCES

Bordier P., Matrajt H., Miravet L. & Hioco D., Mésure histologique de la masse et de la resorption des travées osseuses. Path. et Biol. *12* 1238–1243 1964

Bortolotti, G. C Frizzi, C., Scolari M F & Benomini I., Sub-clinical Bone Pathology after Kidney transplantation in man. Poster presentation Calc. Tiss. symp., York, 1976, in press.

Courpron P., Données histologique quantitative sur le vieillissement osseux humain. These Médicine Lyon, 1972.

Delling G., Schulz A., Courpron P., Meunier P., Olah A & Schenk R., Normal cancellous bone mass. A comparative histomorphometric study of 3 European Centers. Proceed. Second International Workshop on Bone Histomorphometry Lyon, France 1976, in press.

Evarts C M & Phalen G S Osseous avascular necrosis associated with renal transplantation. Clin. Orthop.*78* 530, 1971

Frost H M & Villanueva A R. Human osteoclastic activity qualitative histological measurements. Henry Fords Hosp Med. Bul. *10* 229–236 1962.

Frost H M The etiodynamics of aseptic necrosis of the femoral head. Grant AM-0416 N.I.H. Bethesda Md. 393–409 1965.

Frost H M Tetracycline-based histological analysis of bone remodeling Calc. Tiss. res. *3* 211–237 1969

Gallagher J C., Aaron, J., Horsman A Wilkinson R. & Nordin B. E. C.: Corticosteroid osteoporosis. Clin. Endocrin. Metab. 2 355–368 1973

Harrington K D Murray W R Kountz, S L. & Belzer F O Avascular necrosis of bone after renal transplantation. J Bone Joint Surg *53*: 203 1971

Jaffe W L., Epstein M., Heyman N & Mankin H The effect of cortisone on femoral and humeral heads in rabbits. Clin. Orthop Rel. Res. *82* 221 226, 1972.

Jowsey J & *Riggs B L.* Bone formation in hypercortisonism. Acta Endocr 63 21–28 1970

Laurent J., Meunier P Courpron P Edouard C Bernard J & *Vignon C* Recherches sur la pathogénie des nécroses aseptiques de la tête femorale Nouv Pres. Med. 2 1755–1760 1973

Melsen F & *Mosekilde L.* A quantitative analysis of bone changes following anticonvulsant therapy Proceed. XIth European Symposium on Calcified Tissues, p 247 1975

Melsen F Viidik A Melsen B & *Mosekilde L.* Relation between ashweight compressive strength and quantitative histological analysis of trabecular bone Proceed Second International Workshop on Bone Histomorphometry Lyon France, 1976 in press.

Melsen F Mosekilde L. Melsen B & *Bergman S* Morphometric and dynamic studies of normal bone from the iliac crest To be published

Meunier P Bernard J & *Vignon G* The measurement of periosteocytic enlargement in primary and secondary hyperparathyroidism. Israel Journal of Medical Science 7 482–485 1971

Meunier P Courpron P Edouard C Bernard J Bringuier J & *Vignon G* Physiological senile involution and pathological rarefaction of bone Clin Endocrin. Metab 2 239–256 1973

Meunier P Edouard C Courpron P & *Toussaint F* Morphometric analysis of osteoid in the iliac trabecular bone. Methodology Dynamical significance of the osteoid parameters. Vitamin D and Problems related to Uremic Bone Disease *A W Norman et al.* (ed.) de Gruyter Berlin, 149–155 1975

Minaire P Meunier P Edouard C Bernard J Courpron P & *Bourret J* Quantitative histological data on disuse osteoporosis. Calc. Tiss. Res. 17 57 1974

Nielsen H E. Melsen F & *Christensen M S* Aseptic necrosis of bone following renal transplantation Clinical and biochemical aspects and bone morphometry Acta Med. Scand. In press 1976.

Olgaard K & *Heerfordt J.* Femoral head necrosis in renal transplanted patients. Evidence of a haemodynamic etiological factor Scand. J Urol Nephrol. 9 64 1975

Pierides A M Simpson W., Stainsby D Alvarez-Ude F & *Uldall P R.* Avascular necrosis of bone following renal transplantation. Quart. J Med. 44 459 1975

Rasmussen H & *Bordier P* The physiological and cellular basis of metabolic bone disease The Williams & Wilkins Company Baltimore, 1974

Vignon G & *Meunier P.* Les osteoses decalcifiantes diffuses de l'adulte Documenta Geigy Ciba-Geigy Ltd., Basle, 1973

Acta path. microbiol. scand. Sect. A, 85 105-112 1977

CHARACTERIZATION OF A SPLENIC FACTOR INHIBITING DNA-SYNTHESIS IN LYMPHOCYTES *IN VITRO*

ULF ERNSTRÖM and KLAS NORDLIND

Department of Histology Karolinska Institutet, Stockholm, Sweden

Ernström, U & Nordlind, K. Characterization of a splenic factor inhibiting DNA-synthesis in lymphocytes in vitro Acta path. microbiol. scand. Sect. A, 85 105-112, 1977

A factor inhibiting DNA synthesis in lymphocytes from lymph nodes and thymus of guinea pigs and rats has been isolated from the calf spleen. A crude extract was obtained by homogenization of the spleen in saline, centrifugation at 1,200 and 46,000 g, heat precipitation at 60° C, acetone precipitation, followed by lyophilization of the acetone precipitate. The active material was partly purified and characterized by gel chromatography ion exchange chromatography ultrafiltration and preparative electrofocusing The active factor was found to be acidic and heat stable (60° C, 10 min) with a molecular weight between 75,000 and 17,000 daltons. At preparative electrofocusing inhibiting material focused at pH 4.0 The splenic factor inhibited the DNA synthesis in lymphocytes from guinea pigs and rats, but not the DNA synthesis in HeLa cells. During the purification, material which enhanced the uptake of ^{3}H-thymidine in DNA of lymphocytes was separated from the inhibitor The stimulating factor had molecular weight below 10,000 daltons as judged by ultrafiltration and gel chromatography At preparative electrofocusing stimulating material focused around pH 8.5

Key words DNA-synthesis lymphocytes splenic factor

U Ernström, Department of Histology Karolinska Institutet, S-104 01 Stockholm 60 Sweden.

Received 24 vi.76 Accepted 27 viii.76

We have previously reported the existence of a soluble factor in calf spleen with inhibitory effect on the DNA synthesis in lymphocytes from lymph nodes and thymus (*Ernström & Nordlind* 1974) In the present paper this factor is further characterized. During the purification, a factor stimulating the uptake of ^{3}H-thymidine in DNA was separated from the inhibitory one.

MATERIAL AND METHODS

Chemicals. Hank solution and PBS (State Bact. Lab., Stockholm, Sweden) RPMI 1640 with glutamine, penicillin and streptomycin (Flow Labs.) The scintillation fluid used consisted of 5g PPO and 0.2 g POPOP in 1000 ml toluene (Nyakemi) Myoglobin, ovalbumin, bovine serum albumin and trypsin (Sigma) Sephadex was obtained from Pharmacia (Uppsala, Sweden) DEAE-cellulose from Serva (Heidelberg, Germany) and Ampholine® from LKB (Stockholm, Sweden)

Cell culture Suspensions of lymphocytes from lymph nodes and thymus of guinea pigs were prepared as described previously (*Ernström & Nordlind* 1974) The suspension with 5 × 10^{6} cells per ml was divided into 1 ml cultures which were incubated at 37 C in 10 per cent CO$_2$ in air The material to be tested (0.2 ml) was added to the cultures 30 min after start of incubation. The cultures were performed in duplicates or triplicates. Fractions inhibiting the uptake of ^{3}H-thymidine

Jowsey J & Riggs B L. Bone formation in hyper cortisonism. Acta Endocr 63 21–28 1970

Laurent J Meunier P Courpron P Edouard C Bernard J & Vignon G Recherches sur la pathogénie des nécroses aseptiques de la tête femorale Nouv Pres. Med 2 1755–1760 1973

Melsen F & Mosekilde L. A quantitative analysis of bone changes following anticonvulsant therapy Proceed. XIth European Symposium on Calcified Tissues, p. 247 1975

Melsen F Viidik A Melsen B & Mosekilde L. Relation between ashweight compressive strength and quantitative histological analysis of trabecular bone Proceed Second International Workshop on Bone Histomorphometry *Lyon, France 1976 In press.*

Melsen F Mosekilde L. Melsen B & Bergmann S Morphometric and dynamic studies of normal bone from the iliac crest To be published.

Meunier P Bernard J & Vignon G., The measurement of periosteocytic enlargement in primary and secondary hyperparathyroidism. Israel Journal of Medical Science 7 482–485 1971

Meunier P Courpron P Edouard C Bernard J Bringuier J & Vignon G Physiological senile involution and pathological rarefaction of bone Clin Endocrin. Metab 2 239–256 1973

Meunier P Edouard C Courpron P & Toussaint F Morphometric analysis of osteoid in the iliac trabecular bone Methodology Dynamical significance of the osteoid parameters. Vitamin D and Problems related to Uremic Bone Disease. *A W Norman et al.* (ed.) de Gruyter Berlin 149–155 1975

Minaire P Meunier P., Edouard C Bernard J., Courpron P & Bourret J Quantitative histological data on disuse osteoporosis. Calc. Tiss. Res. 17 57 1974

Nielsen H E. Melsen F & Christensen M S Aseptic necrosis of bone following renal transplantation. Clinical and biochemical aspects and bone morphometry Acta Med. Scand. In press 1976.

Olgaard K & Heerfordt J Femoral head necrosis in renal transplanted patients. Evidence of a haemodynamic etiological factor Scand J Urol. Nephrol 9 64 1975

Pierides A M Simpson W Stainsby D., Alvarez Ude F & Uldall P R., Avascular necrosis of bone following renal transplantation. Quart. J Med 44 459 1975

Rasmussen H & Bordier P., The physiological and cellular basis of metabolic bone disease The Williams & Wilkins Company, Baltimore, 1974

Vignon G & Meunier P Les osteoses decalcifiantes diffuses de l'adulte. Documenta Geigy Ciba-Geigy Ltd. Basle 1973

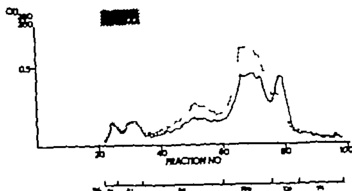


Fig. 2. Gel chromatography of splenic extract on Sephadex G-100. Column size 90 × 1.5 cm. Elution with 0.05 M phosphate buffer pH 7.2. Fraction volume 1.5 ml. Lymph node lymphocytes were used as test cells. Bovine serum albumin was added to control cultures. The deviations from the control cultures caused by different pooled fractions are given in per cent. Inhibition of the uptake of ^{3}H thymidine was obtained if material of a molecular weight higher than that of myoglobin was used, as indicated in the figure. Stimulation of the uptake of H-thymidine in lymphocytes was obtained with fractions 60–75.

In Figures 2, 3, 7, 10
—— 280 nm
260 nm.

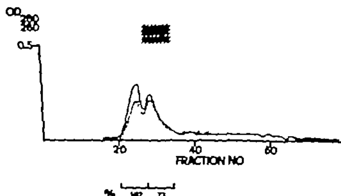


Fig. 3. Gel chromatography of a dialysed splenic extract on Sephadex G-75. Column size 90 × 1.5 cm. Elution with 0.05 M phosphate buffer pH 7.2. Fraction volume 1.5 ml. Lymph node lymphocytes were used as test cells. Elution buffer was added to control cultures. The deviations from the control cultures caused by pooled fractions from the two peaks are given in per cent. Inhibitory activity was found in the second peak, as indicated in the figure. No stimulatory activity was found.

measured by liquid scintillation. In most experiments, our control cultures resulted in 2000–4000 cpm in the case of lymph node cells and in 20,000–40,000 cpm in the case of thymocytes. As test cells, lymph node lymphocytes from guinea pigs were used. Selected preparations were tested also on thymocytes from guinea pigs and on lymphocytes and thymocytes from rats. The splenic extract was also tested on HeLa cells.

Splenic Extract

An extract of calf spleen prepared according to the schedule shown in Fig. 1 inhibited

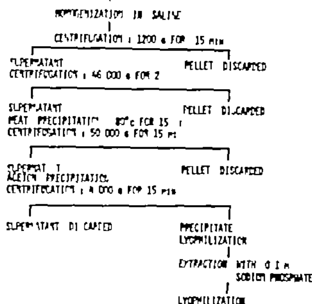


Fig 1 Schedule showing the preparation of an extract of calf spleen by homogenization in saline, centrifugation heat precipitation and acetone precipitation *The final extract was lyophilized and* stored in the freezer until it was used for further separation

with more than 20 per cent were considered as active.

Suspensions of HeLa cells were kindly supplied by Dr *Swanbeck* Dept. of Dermatology Karolinska Sjukhuset, Stockholm The HeLa cells were resuspended in RPMI to a concentration of 5×10^4 cells per ml and then treated as the lymphocytes.

Thymidine uptake ^{3}H thymidine 4 μCi (spec *act* 5 Ci/mM Radiochemical Centre Amersham) in 0 1 ml saline was added to each culture 1 h before harvest of the cultures. The incorporation of ^{3}H thymidine into DNA was measured by liquid scintillation of the acid insoluble material from the cultures (for details see *Ernström & Nordlind* 1974)

Viability test The viability of cultured cells was estimated by absolute cell counts and by trypan blue exclusion tests performed on cultures not given ^{3}H thymidine.

Preparative procedure An extract of calf spleen was prepared according to Fig 1 (see *Ernström & Nordlind* 1974)

Protein determination Protein estimates were based on UV absorption at 280 nm. Also absorption at 260 nm was measured

Dialysis The splenic extract prepared according to Fig 1 was dialysed against water or the appropriate buffer used at ion exchange chromatography (48 h, 2 changes)

Ultrafiltration An Amicon ultrafiltration cell with an ultramembrane cutting at 10,000 daltons was used (UM 10)

Trypsinization The splenic extract (Fig. 1) was dissolved in saline and exposed for 0 005 per cent trypsin at 37 C for 20 h. After 24 h at 30 C the sample was centrifugated at 1000 g for 5 min. The resulting supernatant was tested A splenic extract without trypsin and trypsin in saline without any extract were used as controls and treated in the same way

Gel chromatography Preparative gel chromatography was performed in columns of Sephadex G-75 G-100 G-150 (column 90×1.5 cm) and Sephadex G-25 (column $90 \times 0 9$ cm) The eluant was 0 05 M phosphate buffer pH 7.2.

Ionexchange chromatography Fibrous cellulose ion-exchanger (DEAE-cellulose) was used It was conditioned as prescribed by the manufacturer Different elution buffers were used. The best culturing conditions in the test system were obtained if phosphate buffers with pH 7 2 were used for fractionation Also buffers with tris-hydrochloride were used

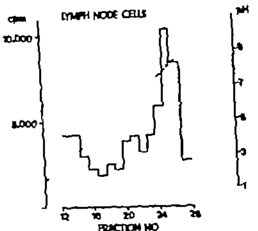
Iso-electric focusing Preparative iso-electric focusing was performed in a 110 ml electrofocusing column (LKB Stockholm Sweden) The material to be tested was dissolved in the heavy sucrose gradient solution. The experiments were performed in the broad pH range with Ampholines® 3.5–10 and with Ampholines® 2.5–5 After the column was filled with the electrode and gradient solutions the voltage was adjusted so as to give an effect of 5 W The voltage was adjusted after 2 h when the current had dropped. After about 20 h the current had stabilized. Then the focusing was allowed to continue for another 4 h. The column was emptied by the use of a peristaltic pump at a flow rate of 60 ml per h The fraction volume was 5 ml The pH of each fraction was determined. Electrofocusing with Ampholines® 3.5–10 and 2.5–5 without any sample was performed as a control In some experiments using Ampholines® 2.5–5 the pH of the fractions was adjusted to pH 7.5 ± 0.5 by sodium bicarbonate (Oroszlan et al. 1970) Both pH adjusted and not adjusted fractions were tested

For analytical electrofocusing, a Multiphor® (LKB Stockholm Sweden) with an Ampholine® polyacrylamide gel plate (LKB) was used

RESULTS

Test System

In guinea pigs and rats, the spontaneous uptake of ^{3}H thymidine in DNA of cultured thymocytes was about *10 times higher than* in DNA of cultured lymph node lymphocytes



THYMIC CELLS

cpm

pH

FRACTION NO

Fig. 5–6 Fractions obtained by preparative electrofocusing (Fig. 4) were tested on lymph node cells and on thymic cells of guinea pigs. An inhibition was obtained if material that focused around pH 4 was used and a stimulation if material that focused at an alkaline pH was used. Similar results were obtained when the fractions were tested on lymph node lymphocytes and thymocytes.

stimulating the incorporation of H thymidine into DNA was found in the dialysate. The dialysed inhibitory material was chromatographed on Sephadex G-75 (Fig. 3). Inhibitory activity was found in the second peak. The gel chromatography of dialysed material was repeated and gave identical results. Inhibitory activity in the second peak was found whether lymphocytes from guinea pigs or rats were used as test cells.

Ultrafiltration

The splenic extract was ultrafiltrated using Diaflo UM 10 ultramembranes. Inhibitory activity remained in the ultraconcentrate above the UM 10 membrane, while stimulating activity was found in the diafiltrate (Table 1).

Trypsinization

Lymph node lymphocytes from guinea pigs were used as test cells. After trypsinization of the splenic extract an inhibitory activity was not observed while a stimulating activity (153 per cent) was found. This stimulation was not due to the presence of trypsin as the

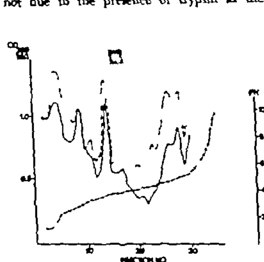


Fig. 7 Preparative iso-electric focusing in a 110 ml column with 2 per cent Ampholine® 2.5–5. The sample consisted of a dialysed splenic extract prepared according to the schedule in Fig. 1. Lymph node lymphocytes and thymocytes from guinea pigs and rats were used as test cells. Sterile water was added to control cultures. Inhibitory activity was found in material that focused at pH 3.8–4.0 indicated by the hatched area in the figure. The uptake of ^{3}H-thymidine was 39 per cent, 42 per cent and 59 per cent of the control values, when material focusing at pH 3.80, 3.95 and 4.00 was tested. At lower pH, higher uptake was obtained indicating that the inhibition was not due to the acid pH of the added fractions. This was further documented by adjustment of the pH of all fractions to 7 before they were tested. Even after this procedure, the material that focused around pH 4.0 retained its inhibitory activity. No stimulating activity was found.

TABLE 1 *Effect of Dialysed and Ultraconcentrated Splenic Extract on the Uptake of ^3H Tdr in DNA of Lymph Node Lymphocytes in vitro*

Material tested	Amount of protein added per ml	Uptake of ^3H Tdr in per cent of control
Dialysed SE	850 µg	20 %
Dialysed SE	213	17
Dialysed SE	53	65
Dialysed, ultraconcentrated SE	767	16
Dialysed, ultraconcentrated SE	192	13
Dialysed, ultraconcentrated SE	48	54
Dialysed, diafiltrated SE	<20	86
Ultraconcentrated SE	116	35
Diafiltrated SF	367	184
Diafiltrated SF	92	107

A splenic extract (SE) prepared according to Fig 1 was dialysed against water for 48 h and/or ultra concentrated *(UM 10)* Dialysed and/or ultraconcentrated material was found to inhibit the incorporation of ^3H Tdr in DNA while the diafiltrate was found to increase this incorporation.

the incorporation of ^3H thymidine into DNA of cultured lymphocytes and thymocytes (see *Ernstrom & Nordlind* 1974) When an amount of extract corresponding to 100 µg protein per ml was added to the cultures the inhibition varied between 20 and 80 per cent between different preparations HeLa cells incorporated more ^3H thymidine when a splenic extract or an identically prepared liver

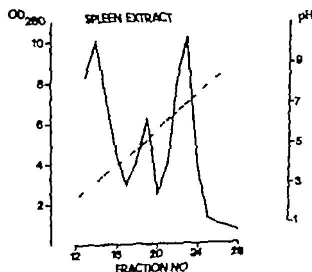


Fig 4 Preparative iso-electric focusing in a 110 ml column with 2 per cent Ampholine® 3.5–10 The sample consisted of a splenic extract prepared according to the schedule in Fig 1 A linear pH gradient between pH 3 and 9 was obtained.

extract was added to the RPMI in the cultures. Thus the splenic factor did not inhibit the growth of HeLa cells. With the aid of incorporation of ^3H thymidine in lymphocytes of guinea pigs as bioassay the splenic extract was further purified and analysed.

Gel Chromatography

Chromatography on Sephadex G 100 revealed that the inhibitory activity of the splenic extract was due to material of higher molecular weight than myoglobin. A fraction with low molecular weight was found to stimulate the incorporation of ^3H thymidine into DNA of lymph node lymphocytes and thymocytes of guinea pigs (Fig 2) The gel chromatography on Sephadex G-100 was repeated twice with almost identical results Inhibition with the high molecular peak (67 per cent) and stimulation with the large low molecular peak (151 per cent)

Dialysis

The splenic extract was dialysed against water Both the material remaining in the dialysis bag and the dialysate were lyophilized and redissolved in water The bio-assay showed that the inhibitory activity had remained in the dialysis bag while material

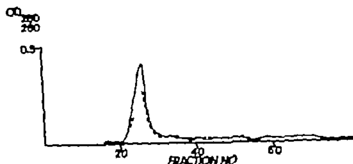


Fig. 10. Gel filtration of the inhibitory material from DEAE-cellulose, Fig. 9, on Sephadex G-75. One peak was obtained.

The results from electrofocusing of Ampholines® without any extract showed that the most acid Ampholines® depressed the incorporation of ^{3}H-thymidine into DNA of lymphocytes. After adjustment of pH to about 7 this inhibition due to the low pH disappeared. When the splenic material was electrofocused and the pH of the fractions was adjusted to 7 an inhibition was still obtained at pH 4.0. Seven fractionations of the splenic material with Ampholines® 2.5–5 were performed. Maximal inhibition was obtained at pH 4.05, 3.80, 3.95, 3.70, 3.75, 3.95, 4.0. The two last determinations were obtained after adjustment of the pH to 7.0.

Ion Exchange Chromatography

A splenic acetone precipitate (see Fig. 1) was dissolved in tris-buffer and fractionated on DEAE-cellulose. The result showed that the inhibitory factor could be eluted as an acid material (Fig. 8). When a splenic extract prepared according to Fig. 1 was dialysed against phosphate buffer and then used for fractionation on DEAE-cellulose a sharp peak containing the active factor was obtained (Fig. 9). The material from this peak caused an inhibition of the uptake of ^{3}H-thymidine in lymph node lymphocytes from guinea pigs and rats to 40 and 43 per cent of control values and in thymocytes from guinea pigs and rats to 79 and 84 per cent of control values. When the active material was chromatographed on Sephadex G-75 one peak was obtained (Fig. 10). Electrophoresis of the active material in an agarose gel resulted in a single band, migrating as a pre albumin. When the active material was analysed by analytical electrofocusing a major component appeared around pH 4 but several minor acid components were also seen. Determination of the molecular weight of the major component by SDS-electrophoresis in polyacrylamide gel showed a molecular weight between that of ovalbumin (45,000) and bovine serum albumin (67,000).

DISCUSSION

The knowledge of the control of growth in different tissues is incomplete. One hypothesis postulates the existence of tissue-specific growth-regulating inhibitors acting either on cells in G1 or on cells in G2 blocking the initiation of DNA synthesis or the initiation of mitosis. Such substances are believed to remain essentially unchanged during evolution and to be species non-specific (*Bullough* 1962). Such hypothesis can only be tested if the postulated inhibitory factors are purified and tested on different cell types. The first studied tissue-specific growth regulating substance was an epidermal growth inhibitor. Inhibitory factors from the spleen have been described by several authors, i.e. *Garcia-Giralt et al.* (1970) and *Houck et al.* (1971). The present paper confirms that the spleen contains a factor which inhibits the uptake of ^{3}H-thymidine in DNA of lymphocytes from lymph nodes and thymus from guinea pigs and rats. This factor migrated electrophoretically as a

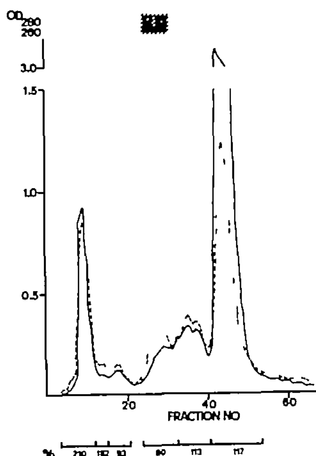


Fig 8 Ionexchange chromatography on DEAE-cellulose of a splenic acetone precipitate dissolved in 0.01 M tris buffer. Column size 20 × 1.5 cm. Eluted by a linear gradient of tris buffer (0.01 M to 0.4 M). Lymph node lymphocytes from guinea pigs were used as test cells. Tris buffer was added to control cultures. The deviations from the control cultures caused by pooled fractions are given in per cent. Stimulating activity was found in the first peak. Inhibitory activity is indicated by the hatched area in the figure.

identically treated mixture of saline and trypsin was totally inactive.

Preparative Iso-electric Focusing

The splenic extract was fractionated by iso-electric focusing. When Ampholines® 3.5–10 was used the inhibitory activity was found in fractions corresponding to an iso-electric point around 4 whether the fractions were tested on lymph node lymphocytes or on thymic lymphocytes from guinea pigs (Figs. 4–6). As seen in the figures stimulating material focused at an alkaline pH. Several electrofocusing experiments using Ampholines® 3.5–10 were performed with non-dialysed and dialysed splenic extracts. Inhibitory activity was repeatedly found at pH 3.6 to pH 4.3 when the fractions were tested on lymph node lymphocytes and thymocytes of guinea pigs.

The inhibitory material was further characterized by electrofocusing with Ampholines® 2.5–5. A splenic extract dialysed against water was used. The inhibitory activity was found in fractions corresponding to an isoelectric point of 3.8 to 4.0 (Fig. 7).

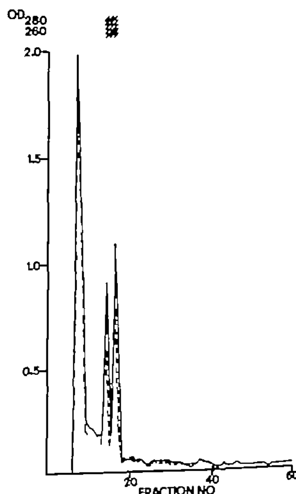


Fig 9 Ionexchange chromatography on DEAE cellulose of a splenic extract dialysed against 0.02 M phosphate buffer pH 7.2. Column size 20 × 1.5 cm. Eluted by a linear gradient of phosphate buffer pH 7.2 (0.02 M to 0.2 M). Lymph node lymphocytes and thymocytes from guinea pigs and rats were used as test cells. The inhibitory material was eluted by the gradient as indicated by the hatched area in the figure. No stimulating material was found.

Acta path. microbiol. scand. Sect. A, 85: 113–121, 1977

FOCAL NODULAR HYPERPLASIA OF THE LIVER

Possible Influence of Female Reproductive Steroids on the Histological Picture

JØRGEN MOESNER, PHILIP BAUMGAARD, HENRIK STARKLINT and NIELS THOMMESEN

The Departments of Pathology at Randers Hospital, Odense Hospital, Holbæk Hospital, Århus County Hospital and Copenhagen Municipal Hospital, Hvidovre, Denmark

Moesner, J., Baumgaard, P., Starklint, H. & Thommesen, N. Focal nodular hyperplasia of the liver. Possible influence of female reproductive steroids on the histological picture. Acta path. microbiol. scand. Sect. A, 85: 113–121, 1977.

In a series of 18 patients with focal nodular hyperplasia of the liver characteristic histological changes were found in the lesions of 5 patients receiving female reproductive steroids, e.g. four women taking oral contraceptives for several years, and one man treated with synthetic estrogenic compound for carcinoma of the prostate. These lesions contained young, connective tissue septa with abundant proliferation of bile ducts, piecemeal necroses and lymphocytic infiltration. Much less or no activity was found in the lesions of 11 women and 2 men without hormone treatment. Possible mechanisms for this activity are discussed, and it is proposed that focal nodular hyperplasia represents a congenital malformation, possibly a hamartoma, the liver cells of which may suffer from enzymatic defects, which may render them especially vulnerable to female sex hormones.

Key words: Liver hyperplasia, focal, nodular; steroids; histology.

Moesner, J., Patologisk Institut, Amtssygehuset, DK-8000 Århus, Denmark.

Received 9.ix.76. Accepted 9.ix.76.

Focal nodular hyperplasia of the liver (f.n.h.) is an uncommon, benign, localized lesion of the non-cirrhotic liver. The term f.n.h. was introduced by *Edmondson* (1956) who described the lesion as consisting of normal-appearing liver cells, subdivided into pseudolobules by connective tissue strands containing bile ducts. The condition was first described in 1884 by *Simmonds* and cases have later been published under several different headings, reflecting the authors' different opinions concerning the etiology, such as benign hepatoma (*Hoffman* 1942), hepatic adenoma (*Gerencsi et al.*, 1969), adenoma—mixed type (*Kay & Talbert* 1950), hamartomatous cholangiohepatoma (*Gerding et al.* 1951), hepatic hamartoma (*Phillips et al.* 1973), parenchymal hamartoma (*Tate et al.*, 1972), solitary hyperplastic nodule (*McBurney* 1950) and focal cirrhosis (*Benz & Baggenstoss* 1953). The lesion is to be separated from liver cell adenoma which does not contain bile ducts (*Edmondson* 1958).

Several reports of increased incidence and clinical significance of f.n.h. (*Grabowski et al.* 1975, *Mays et al.* 1974) as well as of adenomas (*Baum et al.* 1973, *Edmondson et al.*, 1976) have appeared in recent litera-

pre albumin and was eluted as an acid material if chromatographed on DEAE-cellulose The results of ultrafiltration and gel chromatography indicated a molecular weight above 17,000 daltons and below 75 000 daltons. The specificity of this factor can now be tested Any inhibition of the uptake of ^{3}H thymidine in DNA of HeLa cells was not found. If the splenic factor was tested on suspensions of normal liver cells from guinea pigs an inhibition of the uptake of ^{3}H thymidine would be obtained (*unpubl. results*) The implication is that the splenic inhibitory material does not affect the growth of a tumour cell line while it affects the growth of normal lymphocytes and liver cells.

The splenic inhibitory factor may be of functional importance in the regulation of growth of lymphocytes. Our factor may be identical with the suppressor factor believed to regulate the proliferation of lymphocytes in an immune response (*Thomas et al* 1975) and with the postulated factor responsible for antigenic competition (see *Sjöberg* 1972) The relation to the proliferation inhibiting factor from PHA-stimulated human blood lymphocytes remains to be elucidated (*Green et al* 1970) Our splenic inhibitory factor cannot be identical with the immunosuppressive α_2-glycoprotein from bovine serum (*Mowbray* 1963) or with the immunosuppressive α-globulin from bovine thymus (*Carpenter et al* 1971)

This investigation was supported by grants from the *Swedish Medical Research Council* (project No B75-12X-4206-02) and from the funds of *Karolinska Institutet*

REFERENCES

Bullough W S The control of mitotic activity in adult mammalian tissues. Biol. Rev 37 307-342 1962

Carpenter C B Boyldon A W & Merrill J P Immunosuppressive alpha globulin from bovine thymus 1 Preparation and assay Cell Immunol. 2 425-434 1971

Ernström U Splenic inhibition of thymic release of lymphocytes. Acta path. microbiol scand. Sect. A, 80 427-428 1972

Ernström U & Nordlind K Inhibition of lymphocyte proliferation in vitro by a splenic factor Acta path. microbiol scand. 82 445-449 1974

Garcia-Giralt E LaSalvia E. Florentin I & Mathé G Evidence for a lymphocytic chalone. Europ. J clin. biol. Res. 15 1012-1015 1970.

Green J A Cooperband S R., Rutstein J A & Kibrick S Inhibition of target cell proliferation by supernatants from cultures of human peripheral lymphocytes. J Immunol 105 48-54 1970

Houck J C Irausquin H & Leikin S Lymphocyte DNA synthesis inhibition. Science 173 1139-1141 1971

LaSalvia E Garcia-Giralt E & Macieira-Coelho A Extraction of an inhibitor of DNA synthesis from human peripheral blood lymphocytes and bovine spleen. Europ J clin. biol. Res. 15 789 792 1970

Mowbray J F Ability of large doses of an alpha$_2$ plasma protein fraction to inhibit antibody production. Immunology 6 217-225 1963

Oroszlan S Fisher C L., Stanley T B & Gilden R V Proteins of the murine C-type RNA tumour viruses Isolation of a group-specific antigen by isoelectric focusing. J gen. Virol 8 1-10 1970

Sjöberg O Studies on antigenic competition and tolerance Two immunological phenomena characterized by decreased immunological responsiveness. Thesis, Basel and Stockholm 1972.

Thomas D W., Roberts W K & Talmage D W Regulation of the immune response Production of a soluble suppressor by immune spleen cells in vitro J Immunol 114 1616-1622 1975

TABLE 1 *Focal Nodular Hyperplasia. Clinical Summary*

Case no.	Age at diagnosis (yrs)	Sex	Diameter of lesion (mm)	Presenting symptoms *Year of diagnosis*	Concurrent disease Drugs
I	69	F	3	Accidental finding at autopsy 1976	Heart insufficiency, left ventricular hypertrophia. Digoxin, spironolactone
II	62	F	4	Accidental finding at autopsy 1972.	Diabetes since 1951, carcinoma of breast 1952 and of endometrium 1967, cerebral haemorrhage. Insulin.
III	64	F	3	*Accidental finding at* cholecystectomy 1975	*Cholelithiasis.* No drugs known.
IV	82	F	3	Accidental finding at autopsy 1974	Diabetes, *cerebral infarction*, bronchopneumonia. No drugs known.
V	65	F	7	Accidental finding at autopsy 1975.	Rheumatoid arthritis, parkinsonism, bronchopneumonia. Sodium aurothiomalphate, levodopa, salicylates.
VI	79	F	7	Accidental finding at autopsy 1975	Pulmonary embolism. No drugs known.
VII	43	F	8	Accidental finding at autopsy 1965	Carcinoma of cervix uteri 1964 with infiltration and stenosis of ureters, uremia. Local radium, prednisone, 6 mths.
VIII	78	M	9	Accidental finding at autopsy 1974	Carcinoma of prostate, sepsis, heart insufficiency Diethylstilboestrol 30 mg per day 2 yrs.
IX	61	F	10	Accidental finding at autopsy 1970	Myocardial infarction. No drugs known.
X	66	F	12	Accidental finding at autopsy (2 nodes) 1975	Shock from bleeding gastric ulcer No drugs known.
XI	71	M	12	Accidental finding at autopsy 1971	Arterial hypertension, myocardial infarction, bronchopneumonia. Spironolactone, frusemide 6 yrs.
XII	51	M	13	Accidental finding at autopsy 1972.	Left ventricular aneurysm, pulmonary edema. No drugs known.
XIII	52	F	20	Accidental finding at autopsy 1975	Arterial hypertension. Bendroflumethiazide, 6 mths.
XIV	61	F	22	Accidental finding at autopsy 1976.	Myocardial infarction. Barbiturate and unknown *psychosedative*, about 20 yrs.
XV	26	F	40	Intermittent pain and *palpable* mass in right hypochondrium. 1973.	Oral anticonception (preparation unknown) for about 5 yrs.
XVI	28	F	45	Accidental *finding at* Caesarean section 1974	*Mestranol* 0.1 mg, ethynodiol acetate 1 mg (Ovulen®) and norethisterone acetate 3 mg, *ethinyloestradiol* 50 μg (*Anovlar*®) 7 yrs before pregnancy
XVII	52	F	50	Accidental finding at cholecystectomy (3 nodes) 1971	Cholelithiasis. Mestranol 75 μg, lynestrenol 2.5 mg (Noracyclin®) 4 yrs.
XVIII	34	F	105	Uncharacteristic dyspepsia. Accidental finding at cholecystectomy 1975	Cholelithiasis. Norgestrel 0.5 mg, ethinyloestradiol 50 μg (Eugynon®) 3 yrs, and d-norgestrel 0.25 mg, ethinyloestradiol 50 μg (Neogynon®) 3 yrs

ture. The purpose of the present study is to evaluate possible histological differences between f.n.h. in patients receiving female sex hormones and patients without hormone treatment.

MATERIAL AND METHODS

In the files of the five participating departments of pathology 19 lesions from 18 patients fulfilled the above-mentioned criteria of f.n.h. Case XV has previously been published as case I of *Sorensen & Almersjö* (1976). Information about accompanying diseases, pregnancies and drug intake was obtained from the patients' clinical records.

The material included 15 women and 3 men. In 13 patients the lesion was an accidental finding at autopsy. In 4 cases the lesion was accidentally found at laparotomy while one patient (case XV) was operated because of a palpable mass. Sixteen patients had a solitary node while two patients had 2 and 3 lesions, respectively. In the last mentioned patient (case XVII) only one node was biopsied. Four women were using oral contraception for four to seven years, one of them (case XVI) became pregnant following withdrawal. The lesion was found accidentally during Caesarean section, performed because of fetal bradycardia during labour. One male patient (case VIII) was treated with dietylstilboestrol 30 mg per day for prostatic carcinoma for two years until death occurred.

Paraffin sections from the available blocks were stained with hematoxylin-eosin, PAS, van Gieson and stains for reticulin and elastin elements. The histological characteristics were independently graded by the authors, scoring the individual components O to + + + relative to one another, O representing none or very slight occurrence, and + + + the maximal occurrence of an individual component in the material.

RESULTS

The clinical conditions are summarized in Table 1, in which the patients are arranged in order of increasing size of f.n.h. The lesion was most often located in the right lobe of the liver and most often immediately beneath the fibrous capsule. The tumour in case XVIII was attached to the anterior margin of the liver through a broad stalk containing large blood vessels. The four women using oral anticonception had the largest lesions, 4.0 to 10.5 cm maximum diameter. Smaller nodes, 0.3 to 2.2 cm were found in 11 women of postmenopausal age and in three men.

The histological investigation showed all the lesions circumscribed, but not encapsulated. The surrounding liver tissue showed no evidence of hepatitis or cirrhosis, but in three cases (VIII, XV and XVII) moderate dilatation of sinusoids in the periportal zones occurred. The periphery of the lesions was made up by flattened concentrically arranged liver cell plates of the adjacent tissue, with hyperemic and dilated sinusoids. Flattened portal structures, often containing rather large sized blood vessels, took part in the pseudo-capsule formation. In 8 cases we saw prominent hepatic veins in the surroundings.

In the center of the lesions a scar like area of varying size was formed by dense collagen tissue. From this area branching connective tissue strands went out, containing groups of small bile ducts and a few collections of inflammatory cells, predominantly lymphocytes. Bile ducts of interlobular size were rarely encountered.

The blood vessels of the fibrous tissue component (Table 2) showed hyperplastic changes in ten lesions. Five of these showed intimal fibrosis, in two a narrowing of the lumen was caused by hyperplasia of smooth muscle cells. One of these (case XVI) had complete obliteration of the lumen (Fig. 1). In three cases a combination of fibrosis and hyperplasia was seen, one (case XV) possessing a few vessels with mucoid degeneration of the wall and a single vessel with recent thrombosis. As judged from the elastic tissue stains both arteries and veins were affected. There were no infarctions. Dilated thin walled veins occurred in the fibrous tissue in two cases (VIII and XVII) (Fig. 2).

The parenchyma of the lesions was made up by rather uniform plates, though irregularly arranged and with a thickness of one to two liver cells. Efferent veins were randomly dispersed without any constant relationship to the connective tissue elements. There were no normal portal tracts inside

Histological Changes

VIII	IX	X	XI	XII	XIII	XIV	XV	XVI	XVII	XVIII
+ + +	+	+	+	+	+	+	+ +	+ +	+ + +	+ + +
+ + +	+	+	+	+	+	+	+ + +	+ +	+ +	+ +
+ +	+	O	O	+ +	+	+	+ +	+ + +	+ + +	+ + +
+	+ +	O	+	O	O	+	O	O	O	+
O	O	O	O	O	O	O	O	+	O	O
+ +	+ +	O	+ +	+ +	+ + +	+ +	+	+	+ +	+
+ +	+	O	O	+ + +	+ + +	O	+ +	+ + +	+ +	+ + +
+	O	+ + +	O	+	O	O	+ + +	+ +	+ +	+

duct proliferation was, on the contrary, very distinct. Presumably similar although less pronounced alterations, the "foci of cellular growth" (*Edmondson* 1958) have been described in large lesions, also in children and men, but liver cell necrosis is rarely reported.

The basic nature of f.n.h. is not known. Some authors have considered it an adenoma (*Key & Talbert* 1950, *Gerancis et al.* 1969). In recent years several reports of liver cell adenomas in women using oral contraceptives have accumulated, beginning with that of *Baum et al.* (1973). The characteristic septal structure and bile ducts of f.n.h., however, are not found in these cases (*Edmondson et al.* 1976). The microscopic picture of f.n.h. is, in most cases, more compatible with a regenerative process (*Benz & Baggenstoss* 1953, *Edmondson* 1956). An adequate traumatic or infectious noxe, however, has not been consistently reported.

There is ample evidence that the lesion may be a congenital one, as judged from its existence in childhood. The small nodes found accidentally in old patients are not necessarily early lesions. Some authors have proposed a parenchymal hamartoma as a primary condition (*Tate et al.* 1972, *Phillips et al.* 1973, *Mangold et al.* 1975), others an aberrant blood supply or bile duct malformation (*Benz & Baggenstoss* 1953).

Whatever the etiology, if the afore-mentioned alterations confined to the lesions, are caused by the action of female reproductive steroids, the primary lesion must represent a *locus resistentiae minoris* in the liver as to the damaging effect of hormones. Oral contraceptives, as well as stilboestrol, may in some subjects cause cholestasis and necrosis of liver cells (*Adlercreutz & Tenhunen* 1970). Cholestasis is not a prominent feature of our material, and liver cell necrosis progressing to a picture of hepatitis is rarely seen in drug injury due to female sex hormones (*Bianchi et al.* 1975), unless heavy doses are applied (*Stoll et al.* 1966).

A hamartoma, possibly represented by our case I and II, may theoretically possess a congenital defect of the drug metabolizing enzyme system of the liver cells. Such a defect is known from recurrent jaundice of pregnancy in which many drugs, especially oral contraceptives, may affect the liver function (*Adlercreutz & Tenhunen* 1970). A great number of drugs, including synthetic hormonal compounds, barbiturates, hydantoins and diazepam, causes hyperplasia of the endoplasmatic reticulum of liver cells (*Conney* 1967, *Sherlock* 1975). Prolonged, heavy enzyme induction may result in exhaustion and cell death (*Adlercreutz & Tenhunen* 1970). The multiplicity of such drugs may offer an explanation why similar but less pronounced changes were found in cases not treated by hormones. Some cases in women of post-menopausal age may also represent

Case no.	I	II	III	IV	V	VI	VII
Parenchymal changes							
Inflammation	O	O	O	+	+	+	O
Piecemeal necrosis	O	O	+	+	+	+	+
Bile duct proliferation	O	O	+	+	+	+	+
Steatosis	O	+	O	+ +	+	+ + +	O
Cholestasis	O	O	O	O	O	+ + +	+
Fibrosis	O	O	+	+ +	+	+ +	+ +
Changes of blood vessels							
Hyperplastic vessel walls	O	O	O	O	O	O	+
Sinusoidal dilatation	O	O	+	O	O	O	O

the lesions. Pseudolobules of varying sizes were *separated by connective tissue strands.* Steatosis was found in nine cases within the lesion in only one case also in the adjacent liver tissue although to a minor degree. In three cases bile thrombi were found in canaliculi, but *in only one to a marked degree.* The Kupffer cells appeared normal and *evenly distributed Focal areas of sinusoidal* dilatation and hyperemia were, however seen *in eight cases most often located near the* center of the pseudolobules, in 4 cases to a *degree of peliosis (case X XV XVI and* XVIII) (Fig 3)

The amount of piecemeal necroses and focal necroses varied in different lesions. In one case (XV) a few confluent necroses occurred. Mallory bodies acidophilic bodies or ground glass appearance of the cytoplasm of the liver cells were not demonstrated.

The lesions in patients treated with female sex hormones exhibited a highly characteristic picture. At the peripheral branchings of the fibrous septa incomplete or unlinked septa were seen showing a marked proliferation of small bile ducts placed partly in apposition to liver cells as nude bile ducts partly in loose connective tissue with capillaries and inflammatory cells mainly lymphocytes In *relation to these* septa the amount of piecemeal necroses was considerable (Fig 4) The neighbouring liver cells showed increased size and were often binuclear

DISCUSSION

In this material, comprising 18 patients with f.n.h. the largest lesions were found in four *young women using oral contraceptives,* the smallest in two elderly women representing *the only nulliparae in this series.* The preponderance of women of fertile age in *clinical series (Sorensen & Baden* 1975) the apparently increased incidence of f.n.h. after *the introduction of* "the pill" (*Grabowski et al* 1975) and the reported growth of a large node during pregnancy (*Whelan et al.* 1973) further indicate that f.n.h. may grow under the influence of female sex hormones. The lesser sex difference in necropsy series however makes it unlikely that hormonal factors initiate the lesions (*Sorensen & Baden* 1975)

Histologically 15 out of the 19 lesions showed a cirrhosis-like picture with pseudolobules of liver cells departed by fibrous strands. In the lesions of the oral contraceptive group and in one male patient, treated with synthetic estrogen because of a prostatic carcinoma, *however* characteristic histological changes were found comprising young connective tissue septa with a pronounced proliferation of bile ducts piecemeal necrosis and lymphocytic infiltration, resembling the active septa found in chronic aggressive hepatitis (*De Groote et al* 1968) The parenchymal destruction was, however slight compared to *that condition* The bile

…istological Changes

VIII	IX	X	XI	XII	XIII	XIV	XV	XVI	XVII	XVIII
+ + +	+	+	+	+	+	+	+ +	+ +	+ + +	+ + +
+ + +	+	+	+	+	+	+	+ + +	+ +	+ +	+ +
+ +	+	○	○	+ +	+	+	+ +	+ + +	+ + +	+ + +
	+ +	○	+	○	○	+	○	○	○	+
○	○	○	○	○	○	○	○	+	○	○
+ +	+ +	○	+ +	+ +	+ + +	+ +	+	+	+ +	+
+ +	+	○	○	+ + +	+ + +	○	+ +	+ + +	+ +	+ + +
+	○	+ + +	○	+	○	○	+ + +	+ +	+ +	+

duct proliferation was, on the contrary very distinct. Presumably similar although less pronounced alterations, the "foci of cellular growth" (*Edmondson* 1958) have been described in large lesions, also in children and men, but liver cell necrosis is rarely reported.

The basic nature of f.n.h. is not known. Some authors have considered it an adenoma (*Kay & Talbert* 1950 *Garancis et al.* 1969). In recent years several reports of liver cell adenomas in women using oral contraceptives have accumulated, beginning with that of *Baum et al.* (1973). The characteristic septal structure and bile ducts of f.n.h., however are not found in these cases (*Edmondson et al.* 1976). The microscopic picture of f.n.h. is, in most cases, more compatible with a regenerative process (*Benz & Baggenstoss* 1953 *Edmondson* 1958). An adequate traumatic or infectious noxe, however has not been consistently reported.

There is ample evidence that the lesion may be a congenital one, as judged from its existence in childhood. The small nodes found accidentally in old patients are not necessarily early lesions. Some authors have proposed a parenchymal hamartoma as a primary condition (*Tate et al.* 1972 *Phillips et al.* 1973 *Mangold et al.* 1975), others an aberrant blood supply or bile duct malformation (*Benz & Baggenstoss* 1953).

Whatever the etiology if the afore mentioned alterations confined to the lesions are caused by the action of female reproductive steroids, the primary lesion must represent a *locus resistentiae minoris* in the liver as to the damaging effect of hormones. Oral contraceptives, as well as stilboestrol, may in some subjects cause cholestasis and necrosis of liver cells (*Adlercreutz & Tenhunen* 1970). Cholestasis is not a prominent feature of our material, and liver cell necrosis progressing to a picture of hepatitis is rarely seen in drug injury due to female sex hormones (*Bianchi et al.* 1973) unless heavy doses are applied (*Stoll et al.* 1966).

A hamartoma, possibly represented by our case I and II may theoretically possess a congenital defect of the drug-metabolizing enzyme system of the liver cells. Such a defect is known from recurrent jaundice of pregnancy in which many drugs, especially oral contraceptives, may affect the liver function (*Adlercreutz & Tenhunen* 1970). A great number of drugs, including synthetic hormonal compounds, barbiturates, hydantoins and diazepam, causes hyperplasia of the endoplasmatic reticulum of liver cells (*Conney* 1967 *Sherlock* 1975). Prolonged, heavy enzyme induction may result in exhaustion and cell death (*Adlercreutz & Tenhunen* 1970). The multiplicity of such drugs may offer an explanation why similar but less pronounced changes were found in cases not treated by hormones. Some cases in women of post menopausal age may also represent

TABLE 2 *Focal Nodular Hyperpl*

Case no	I	II	III	IV	V	VI	VII
Parenchymal changes							
Inflammation	O	O	O	+	+	+	O
Piecemeal necrosis	O	O	+	+	+	+	+
Bile duct proliferation	O	O	+	+	+	+	+
Steatosis	O	+	O	+ +	+	+ + +	O
Cholestasis	O	O	O	O	O	+ + +	+
Fibrosis	O	O	+	+ +	+	+ +	+ +
Changes of blood vessels							
Hyperplastic vessel walls	O	O	O	O	O	O	+
Sinusoidal dilatation	O	O	+	O	O	O	O

the lesions. Pseudolobules of varying sizes were separated by connective tissue strands. Steatosis was found in nine cases within the lesion in only one case also in the adjacent liver tissue, although to a minor degree In three cases bile thrombi were found in cana liculi, but in only one to a marked degree. The Kupffer cells appeared normal and evenly distributed Focal areas of sinusoidal dilatation and hyperemia were however seen in eight cases, most often located near the center of the pseudolobules in 4 cases to a degree of peliosis (case X, XV XVI and XVIII) (Fig 3)

The amount of piecemeal necroses and focal necroses varied in different lesions. In one case (XV) a few confluent necroses oc curred Mallory bodies, acidophilic bodies or ground glass appearance of the cytoplasm of the liver cells were not demonstrated

The lesions in patients treated with female sex hormones exhibited a highly characteri stic picture At the peripheral branchings of the fibrous septa incomplete or unlinked septa were seen showing a marked proli feration of small bile ducts placed partly in apposition to liver cells as "nude bile ducts" partly in loose connective tissue with capil laries and inflammatory cells, mainly lymphocytes. In relation to these septa the amount of piecemeal necroses was considerable (Fig 4) The neighbouring liver cells showed in creased size and were often binuclear

DISCUSSION

In this material, comprising 18 patients with f n h the largest lesions were found in four young women using oral contraceptives, the smallest in two elderly women representing the only nulliparae in this series. The preponderance of women of fertile age in clinical series (*Sorensen & Baden* 1975) the apparently increased incidence of f.n.h. after the introduction of "the pill" (*Grabowski et al* 1975) and the reported growth of a large node during pregnancy (*Whelan et al.* 1973) further indicate that f n.h may grow under the influence of female sex hormones. The lesser sex difference in necropsy series, however makes it unlikely that hormonal factors initiate the lesions (*Sorensen & Baden* 1975)

Histologically 15 out of the 19 lesions showed a cirrhosis-like picture with pseudolobules of liver cells departed by fibrous strands. In the lesions of the oral contraceptive group and in one male patient, treated with synthetic estrogen because of a prostatic carcinoma, however characteristic histological changes were found, comprising young connective tissue septa with a pronounced proliferation of bile ducts, piecemeal necrosis and lymphocytic infiltration resembling the active septa found in chronic aggressive hepatitis (*De Groote et al.* 1968) The parenchymal destruction was, however slight compared to that condition The bile

Fig. 3 Peliosis-like area of sinusoidal dilatation. Case XVI HE × 70

Fig. 4 Peripheral septum with bile duct proliferation, piecemeal necroses and inflammation. Case XVIII HE × 175

Fig 1 Blood vessels with obliterating hyperplasia of smooth muscle cells. Case XVI HE × 175

Fig 2 Part of central scar containing dilated thin-walled ...ins. Case VIII HE × 70

Gerards J C., Teng, T., Pauwels R. & Jurevics, J Hepatic adenoma. Biochemical and electron microscopic study Cancer *24* 560–568, 1969

Gerding W J., P pp M F & Martineau P C. Hamartomatous cholangiohepatoma. Report of case. J Amer med. Ass. *145* 821–822, 1951

Grabowski M Stenram U & Bergqvist A Focal nodular hyperplasia of the liver benign hepatomas, oral contraceptives and other drugs affecting the liver Acta path. microbiol. scand. Sect. A, *83* 615–622, 1975

Hoffman, H T.: Benign hepatoma review of the literature and report of a case Ann. Intern Med. *17* 130–139 1942.

I ey N S & Norris, H J Intimal vascular lesions associated with female reproducth steroids. Arch. Path. *96* 227 234 1973

Ishak K. G & Rabin L. Benign tumors of the liver Med. Clin. N Amer *59* 995–1013 1975.

Kay S & Talbert P C Adenoma of the liver mixed type (hamartoma) Report of two cases. Cancer *3* 307–315 1950.

Mangold, G Kirchner P., Wagner R. & Hahn P Zur Differentialdiagnose benigner Lebertumoren. Zwei Fälle von fokaler nodulärer Hyperplasie. Dtsch med. Wschr *100* 241 245 1975.

Mays E T Christopherson W M & Barrows G H Focal nodular hyperplasia of the liver Possible relationship to oral contraceptives. Amer J Clin. Path. *61* 735–746, 1974

McBurney R. P. Solitary hyperplastic nodule of the liver simulating a neoplasm report of a case. Proc. Mayo Clin. *25* 606–611 1950.

Phillips M J., Langer B., Stone R., Fisher M M & Ritchie S. Benign liver cell tumors. Classification and ultrastructural pathology Cancer *32* 463–470, 1973

Sherlock S Diseases of the liver and biliary system. 5. ed. Blackwell Scientific Publication, London, Oxford, Edinburgh, Melbourne 1975 p p. 343–345 and 350–351

Simmonds M. Die knotige Hyperplasie und das Adenom der Leber Dtsch. Arch. klin. Med. *34* 388–408, 1884

Stell, B. A. Andrews, J T & Mottram R. Liver damage from oral contraceptives. Brit. med. J *1:* 960–961 1966

Sorensen T I A & Baden H. Benign hepatocell lar tumours. Scand. J Gastroent. *10* 133–119 1975

Sorensen T I A & Almersjö O. Focal nodular hyperplasia of the liver Fn cases. Scand. J Gastroent. *11:* 97–101 1976.

Tat R. C., Chacko M V Singh S & Ogden L. Parenchymal hamartoma of the liver in infants and children. Amer J Surg. *123* 346–350 1972.

Whelan T J Baugh J H & Chandor S. Focal nodular hyperplasia of the liver Ann. Surg. *177* 150–158, 1973

Winkler K. & Poulsen, H Liver disease with periportal sinoidal dilatation. A possible complication to contracepth steroids. Scand. J Gastroent. *10* 699–704 1975

partly burnt out lesions activated in previous pregnancies.

An element of biliary obstruction in f n.h. may be suggested by the rarity of large bile ducts and the vigorous bile duct proliferation, seen in the hormonal treated group A few cases of recurrent juandice of pregnancy developing into the picture of primary biliary cirrhosis after several pregnancies are on record (*Albot et al* 1972) The mechanism is unknown.

Some investigators have stressed the abnormal vessels of f n h (*Whelan et al* 1973) An arteriovenous shunt was demonstrated in the case of *Aronsen et al* (1968) and portal hypertension has been present in a few multiple cases (*Ishak & Rabin* 1975) It is however difficult to accept an abnormal vascularisation as a primary lesion in f n h., as no alterations of vessels were apparent in the smallest nodes. Intimal thickening of blood vessels very much like those found in some of our cases of f n h has been described in connection with estrogenic therapy and pregnancy (*Irey & Norris* 1973) but is not limited to hormonal treated cases of f n.h The dilated thin walled veins encountered in the lesions of young women taking oral anticonceptives, presenting with intraperitoneal bleeding from f n h. (*Mays & al* 1974) were only seen twice in our material in which no dramatic symptoms occurred Peliosis-like areas of sinusoidal dilatation have been described in liver biopsies of patients receiving oral contraceptives (*Winkler & Poulsen* 1975)

The size and composition of this material does not allow conclusions about the specificity of the changes found in the lesions of patients treated with female reproductive steroids. In relation to the literature referred to however we find it justified to propose that f n h is a congenital lesion possibly a parenchymal hamartoma the liver cells of which may suffer from defects of the drug metabolizing enzyme system This may render them especially vulnerable to the noxious effect of female sex hormones, resulting in secondary changes of the liver parenchyma, blood vessels and bile ducts of the lesion.

The authors are indebted to professor *Henning Poulsen* department of pathology Hvidovre Hospital for fruitful discussion and helpful correction of the manuscript.

REFERENCES

Adlercreutz H & Tenhunen R Some aspects of the interaction between natural and synthetic female sex hormones and the liver Amer J Med *49* 630–648 1970

Albot G Zerolo J Camilleri J P Kapandji, I A & Lafon J Ictère récidivant de la grossesse et cholangiolite chronique isolée ou maladie de Hanot et Mac Mahon. Sem Hôp. Paris *48* 3425 3441 1972.

Aronsen K F Ericsson B Lunderquist A Malmborg O & Nordén J G A case of operated focal nodular cirrhosis of the liver Scand J Gastroent *3* 58–64 1968.

Baum J K Holtz F Bookstein J J & Klein E W Possible association between benign hepatomas and oral contraceptives. Lancet II 926–929 1973

Benz E J & Baggenstoss A H Focal cirrhosis of the liver its relation to the so-called hamartoma (adenoma, benign hepatoma) Cancer *6* 743–755 1953

Bianchi L. De Groote J Desmet V Gedigk P Korb G Popper H Poulsen H Scheuer P J Schmied M Thaler H & Wepler W Richtlinien für die histologische Beurteilung arzneimittelbidingter (medikamentöser) Leberschäden Dtsch. med Wschr *100* 1746–1750, *1975*

Conney A H Pharmacological implications of microsomal enzyme induction Pharmacol Rev *19* 317–366 1967

De Groote J Desmet V J Gedigk P Korb G Popper H Poulsen H Scheuer P J Schmid M Thaler H Uehlinger E. & Wepler W A classification of chronic hepatitis. Lancet II 626–628 1968

Edmondsson H A Differential diagnosis of tumors and tumor like lesions of the liver in infancy and childhood J Dis. Child. *91* 168–186 1956

Edmondson H A Atlas of tumor pathology Fascicle 25 Armed Forces Institute of Pathology Washington D C 1958 p. 193

Edmondsson H A Henderson B & Benton B Liver-cell adenomas associated with use of oral contraceptives. New Engl. J Med *294* 470–472 1976.



Fig 1 Dorsal aspect of the heart showing the transected hibernoma situated posteriorly in the inter atrial septum (A, × 0.5) The cut surface is mottled, brown-yellow and yellow the tumour margins are poorly defined (B, × 1.5)

Significant findings at autopsy included moderate atherosclerotic changes in most of the large arteries, pulmonary congestion and oedema, acute tracheobronchitis and a moderately congested spleen (weight 270 g) The common and hepatic bile ducts were thick-walled and enlarged, up to 1 cm in diameter No intraductal gallstones were found. The liver 1060 g, was of a light grey brown colour and of a texture as fine sandpaper it was firm, fairly dry the cut surfaces being without prominent nodularity The microscopic picture of the liver was consistent with secondary biliary cirrhosis. The most distinctive histological features were the regularly arranged periportal scars which extended to adjacent portal triads, some inspissated bile within canaliculi and ductules, bile duct proliferation and heavy leucocytic infiltration within the scars The gross appearance of the urinary bladder was consistent with chronic haemorrhagic cystitis The autopsy findings concerning the heart are described below

PATHOLOGY

Gross Appearance

The somewhat dilated heart weighed 550 g Within the wall of the right atrium there were two tumours, one measuring 4 × 4 × 3 cm and the other 2 × 2 × 1.5 cm. The larger tumour was located within the inter atrial septum protruding into the right atrium while the smaller was situated close to the entrance of the inferior vena cava. The overlying endocardial and pericardial surfaces were unaffected. The cut-surfaces of the tumours were mottled yellow-brown and yellow and the margins were poorly defined (Fig. 1 A and B) The myocardium of the right ventricle showed marked disseminated fibrosis.

Microscopic Appearance

The two intramyocardial tumours (Fig 2) were composed of a mixture of multi vacuolated and univacuolated fat cells, the former predominating in most areas (Fig. 3 and 4) The multivacuolated cells showed a variable, but usually large number of small vacuoles within one and the same cells of fairly equal size (Fig 5) The nucleus of this cell type was rather small, centrally or eccentrically placed it was vesicular and chromatin-rich. Frozen sections stained for

Acta path microbiol. scand Sect. A, 85 122–126 1977

MULTIPLE HIBERNOMAS OF THE HEART

A Case Report

LARS-GUNNAR KINDBLOM and ULF SVENSSON

Department of Pathology II Sahlgren's Hospital Göteborg, Sweden

Kindblom, L.-G & Svensson U Multiple hibernomas of the heart A case report. Acta path. microbiol scand. Sect. A 85 122–126 1977

The autopsy findings of two intramyocardial infiltrating hibernomas situated in the right atrium of a 84-year-old woman are presented The tumours might have contributed to the clinically observed sinus arrythmia prolonged PQ interval and bundle branch block.

Key words Hibernomas heart.

L.-G Kindblom Department of Pathology Vasa Hospital, S-411 33 Göteborg Sweden.

Received 8.ix.76   Accepted 8.ix 76

Primary cardiac and pericardial tumours are rare the incidence has been estimated to be less than 0 03 per cent (*Fine* 1968) Most reported primary cardiac tumours have been endocardial myxomas (*Newman et al* 1966) Malignant tumours such as rhabdomyosarcoma (*Porter et al* 1961) angiosarcoma (*Fine* 1968) and fibrosarcoma (*Johnson & Stokes 1964*) as well as benign intramyocardial tumours such as lipoma, myolipoma, fibroma and haemangioma (*Fine* 1968) have been described.

Hibernomas have occurred in many parts of the body predominantly in the neck axilla mediastinum and perirenal areas, where brown adipose tissue persists in adults (*Seemayer et al* 1975) Several hibernomas in areas not known to contain brown adipose tissue have been reported e g the thigh (*Angervall et al* 1964 *Kindblom et al* 1975) and intracranially (*Vagn Hansen & Osgdrd* 1972) To our knowledge no unequivocal case of hibernoma arising in the heart has been reported.

The case report of an 84-year-old woman in whom autopsy disclosed multiple infiltrating hibernomas in the right atrial wall is presented.

CASE REPORT

In 1958 a 66-year-old woman who had previously enjoyed good health developed acute cholecystitis. Cholecystectomy was performed some months later when the hyperbilirubinaemia had diminished. Thirteen years later she had a bout of fever with hyperbilirubinaemia presumed to be caused by cholangitis Coeliaco-angiographic findings showed straightened intrahepatic vessels suggestive of an incipient cirrhosis. During the following 5 years she experienced five more attacks of cholangitis combined with suspected extrahepatic cholestasis due to gallstones in the biliary tree. The patient refused surgical exploration. Clinical and laboratory findings indicated a secondary biliary cirrhosis. In 1974 she had a transitory episode of prominent oedema of the legs. In January 1976, at the age of 84 she was admitted to hospital with a fracture of the right femur which was treated conservatively During the following months, while immobilized, her condition deteriorated with the development of pulmonary congestion and oedema. ECG examination revealed episodes of fibrillation sinus arrythmia, increased PQ-time up to 0 26 s, left bundle branch block and ST elevation in V_1 and V_2. The patient died in July 1976 presenting the clinical picture of cardiac failure.

fat (Oil Red O) revealed that the vacuoles were composed of homogeneous lipid material. Some cells of this type contained pleomorphic PAS-positive cytoplasmic granules, staining as lipofuschin. The univacuolated cells were usually larger than the multivacuolated cells and were similar to ordinary fat cells (Fig 5). No significant nuclear polymorphism was found and no mitotic figures were seen. The areas where the multivacuolated cells predominated were very rich in fine vessels which mostly were capillaries measuring less than 15 μ in diameter (Fig 5). Individual multivacuolated cells were often surrounded by fine capillaries. Occasional wide vessels lined by endothelium and enclosed by fibrous tissue were found. Areas where univacuolated fat cells predominated were fairly poor in vessels. The tumours were unencapsulated. The muscle fibres at the periphery of both tumours were split up by the infiltrating hibernoma tissue (Fig 2); most muscle fibres were atrophic and showed proliferation of the sarcolemma (Fig 3). In addition, the central parts of the tumours contained single or small bundles of atrophic muscle fibres (Fig 4).

DISCUSSION

Lipomatous tumours involving the heart are rare. On reviewing the literature *Fine* (1968) found 45 lipomas of the heart, 3/4 of these being subendocardial and subpericardial. Occasional cases of intramyocardial infiltrating lipomas, most of which were situated in the right atrium, have been reported (*Hull et al.* 1955, *Esteves et al.* 1964, *Fine* 1968). Five cases of lipomatous hypertrophy of the interatrial septum have been reported, 2 of which histologically disclosed areas composed of multivacuolated fat cells microscopically similar to hibernoma tissue (*Prior* 1964). Furthermore, judging from the microscopic illustrations, one case described as an interatrial lipoma may have been of hibernoma type (*Klein & Schaefer* 1973). Most hibernomas described in the literature were situated in parts of the body where brown adipose tissue may persist. Considering our unique case report of multiple hibernomas of the heart it is interesting to note that the presence of small numbers of brown fat cells in the interatrial septum is not abnormal (*Prior* 1964).

In most cases of cardiac lipomatous tumour the clinical manifestations have been insignificant (*Fine* 1968). It is known that cardiac lipoma occasionally may cause compression of the tricuspidal valve, cardiac enlargement, bundle branch block and even sudden death (*Esteves et al.* 1964, *Fine* 1968). ECG-changes supposed to be due to an interatrial lipoma have been reported (*Klein & Schaefer* 1973). In the present case the episodes of fibrillation, sinus arrythmia, prolonged PQ-interval and the bundle branch block might have been caused by the two infiltrating hibernomas located close to the sinus node and the A-V node.

Hibernomas are highly vascular and angiographically they have been found to have a rapid circulation with arteriovenous shunting (*Angervall et al.* 1964, *Arndblom et al.* 1974). Thus, in the present case a significant part of the arterial coronary blood flow may have supplied the two fairly large hibernomas and thereby caused a considerable myocardial ischaemia. This might also have contributed to the disturbances of the conducting system as well as to the myocardial fibrosis of the right ventricle.

REFERENCES

Angervall L., Nilsson L. & Stener B. Microangiographic and histological studies in 2 cases of hibernoma. Cancer 17: 685–692, 1964.

Esteves J. M., Thompson, D. S. & Lichtman J. P. Lipoma of the heart. Review of the literature and report of two autopsied cases. Arch. Path. (Chicago) 77: 638–642, 1964.

Fine G. Neoplasms of the pericardium and heart. In *Gould S. E.* (Ed.) Pathology of the heart and blood vessels. Charles C Thomas Publisher, Springfield 1968, p. 851–883.

Hull H., Kusano R. H. & Fidler R. A. Myolipoma of the heart. A case report. Exp. Med. Surg. 13: 300–304, 1955.

Johnson A. G. & Stokes, J. F. Fibrosarcoma of the heart diagnosed during life. Brit. Med. J. 1: 480–481, 1964.

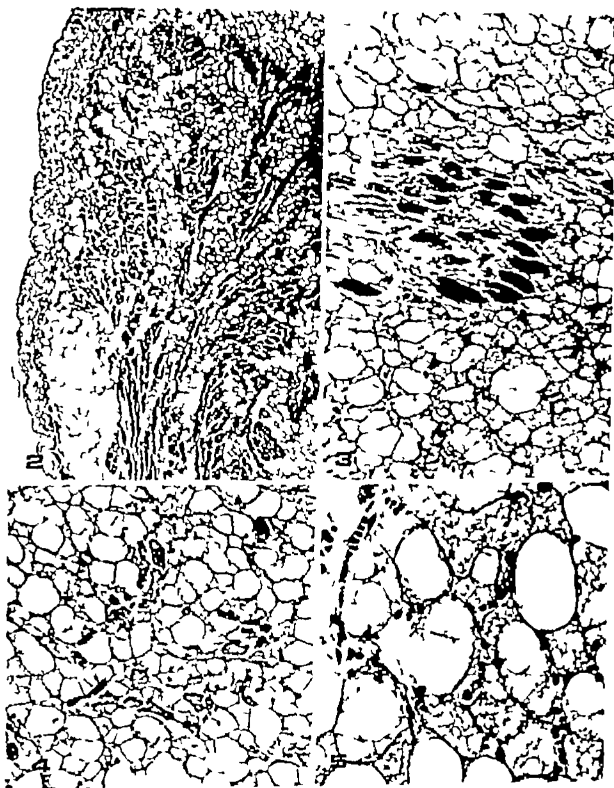


Fig 2 Intramyocardial hibernoma covered by the pericardium (left) and diffusely infiltrating the muscle tissue (H & E × 30)

Figs. 3 and 4 Atrophic muscle fibres enclosed by multivacuolated and univacuolated fat cell The multivacuolated fat cells predominate in Fig 3 while the larger univacuolated fat cells predominate in Fig 4 (H & E, × 120)

Fig 5 Hibernoma composed of a mixture of multi and uni acuolated fat cells Several of the multi vacuolated cells are surrounded by fine blood filled capillaries, less than 10 μ in diameter (H & E, × 225)

Acta path. microbiol. scand. Sect. A, 85: 127–140, 1977

MYXOFIBROSARCOMA

A Study of 30 Cases

Lennart Angervall, Lars-Gunnar Kindblom and Christer Merck

The Department of Pathology II, University of Göteborg, Sweden

Angervall, L., Kindblom, L.-G. & Merck, C. Myxofibrosarcoma. A study of 30 cases. Acta path. microbiol. scand. Sect. A, 85: 127–140, 1977.

A series of 30 myxofibrosarcomas is described. These malignant soft tissue tumours are characterized by a mucoid and nodular appearance, a coarse plexiform capillary pattern, and they are mostly seen subcutaneously (26 out of 30) in the extremities (24 out of 30) and trunk (4 out of 30) of elderly people. Histochemical studies, comprising staining with Alcian blue and toluidine blue at different pH, with and without preceding digestion with testicular hyaluronidase and with the Scott technique, indicated the presence of hyaluronic acid but not sulphated glycosaminoglycans as chondroitinsulphates. Myxofibrosarcoma is believed to belong to the general category of fibroblastic and histiocytic malignant soft tissue tumours. The median diameter of the tumours was 7 cm. They were divided into 4 grades according to cellularity, cell atypia and mitotic activity. The grade III and IV tumours showed pronounced atypia, often with bi- and multinucleated giant tumour cells and occasionally with giant cells of Touton's type, suggesting a relationship to malignant fibroxanthoma. All of the patients were treated surgically and one received also pre- and post-operative irradiation. None of the 2 grade I myxofibrosarcomas recurred, while 2 out of 7 grade II tumours, 6 out of 10 grade III tumours, and 7 out of 11 grade IV tumours recurred once and up to 9 times. Metastasis appeared in 7 out of 30 patients; grade I tumours were not seen in any of these cases. By the time of follow-up after intervals ranging from 1 month up to 27 years, 14 patients had died; 6 of these had died post-operatively or of intercurrent disease. The differential diagnosis between myxofibrosarcoma and other myxoid soft tissue tumours is discussed.

Key words: Myxofibrosarcoma; sarcoma; soft tissues.

L. Angervall, Department of Pathology, Vasa Hospital, S-411 33 Göteborg, Sweden.

Received 1.x.76 Accepted 1.x.76

Several types of malignant soft tissue tumours may be partly myxoid in character. Myxoid areas are characteristic of some of these tumours. Myxoid liposarcoma (*Enzinger & Winslow* 1962, *Kindblom et al.* 1975) and extraskeletal myxoid chondrosarcoma (*Enzinger & Shiraki* 1972) can be entirely myxoid. The distinguishing features of myxoma and so-called myxosarcoma have not always been clearly defined and it is widely believed that the former tumour recurs frequently (*Stout* 1948 a). However, the intramuscular myxoma has been shown to be a perfectly benign tumour (*Enzinger* 1965, *Ireland et al.* 1973, *Kindblom et al.* 1974).

Myxofibrosarcoma is sometimes used in the literature as a descriptive term applied to tumours which have not been defined as a specific entity. For many years we have ap-

Kindblom L-G Angervall L Stener B & Wickbom I Intermuscular and intramuscular lipomas and hibernomas. A clinical, roentgenologic, histologic and prognostic study of 46 cases. Cancer *33* 754–762 1974

Kindblom L-G Angervall L & Svendsen P Liposarcoma. A clinicopathologic radiographic and prognostic study Acta path. microbiol scand. Sect A Suppl 253 1975

Klein P J & Schaefer H E Das interatriale Lipom des Herzens Z. Krebsforsch. *79* 11–18 1973

Newman H A Cordell A R & Prichard R W Intracardiac myxomas Literature review and report of six cases one successfully treated. Amer Surg *32* 219 1966

Porter G A Berroth M & Brostow J D. Primary rhabdomyosarcoma of the heart and complete atrioventricular block. A case report and review of literature Amer J Med. *31* 820–827 1961

Prior J T Lipomatous hypertrophy of cardiac interatrial septum. A lesion resembling hibernoma lipoblastomatosis and infiltrating lipoma Arch Path. *78* 11–15 1964

Seemayer T A Knaack J Wang N S & Ahmed M N On the ultrastructure of hibernoma. Cancer *36* 1785–1793 1975

Lagu Hansen P L & Osgård O Intracranial hibernoma. Acta path. microbiol scand. Sect. A *80* 145–149 1972

mours appeared 2 months later and 1 year later respectively was reported. The only case of a retroperitoneal tumour in the present series presented with pain and abdominal swelling followed later by vomiting and diarrhoea. In one patient, scleroderma was diagnosed 9 years before the tumour was excised. One year later this woman was operated on for a cystadenocarcinoma of the ovary. An unaccountable polyglobulinaemia and thrombocytopenia developed gradually over a period of 3 years in one patient who in that period had several tumour recurrences.

The interval between onset of symptoms and operation varied from 1 month to 2 years. 15 patients were operated on within 6 months. Only 3 patients had been aware of the tumour for more than 2 years.

Anatomical Location (Fig. 2)

Twenty four of the 30 tumours occurred in the extremities, 19 involved the lower extremities (including the buttock and groin) and 5 involved the upper extremities. Four tumours were located in the back, 3 of the latter involved the scapular region. One patient had a tumour in the subcutaneous tissue on the left side of the forehead. One large lobulated tumour was located in the lower retroperitoneal space. The tumour extended into the mesenteries of the small and large intestines and partly enclosed the inferior vena cava and the ureters.

Twenty-six of the 30 tumours were located in the subcutaneous tissue, 4 of these involving the superficial muscle fascia. Three tumours were deep seated, inter- or intramuscular. One of the latter was situated in the iliac muscle while the others involved the gastrocnemius and soleus muscles.

PATHOLOGY

Gross findings. The tumours were oval or spherical, the largest diameter ranging between 1.5 and 15 cm. The median diameter was 7 cm. The cut surfaces were characteristically nodular showing distinct nodules of varying sizes, ranging from a few mm up to 1–2 cm. Most tumours were fairly soft to palpation and were of a grey-white or yellow-grey glistening mucoid appearance. Necroses and haemorrhages were found predominantly in the central part or in solid tumour areas. Grossly most tumours appeared well-delineated from the subcutaneous and muscle tissues.

Microscopic appearance. Histologically all tumours, being partly or completely myxoid in character were of a more or less distinct nodular appearance (Figs. 3 & 4). There was a large variation in cellularity, polymorphism and mitotic activity.

At one end of the spectrum (grade I, 2 cases and grade II, 7 cases) the tumours showed a relative paucity of cells or were moderately cellular (Figs. 5, 6, 7, 8 & 9). In these tumours, a conspicuous mucoid matrix was seen to enclose fairly uniform, stellate oval-shaped or fusiform, fibroblast like cells with an abundant, bipolar slightly eosinophilic cytoplasm (Figs. 6 & 9). Occasional tumour cells contained small cytoplasmic vacuoles, but no multivacuolated lipoblasts were encountered. The nuclei revealed a granular or coarse chromatin structure and one or two eosinophilic nucleoli. In the 2 grade I tumours, the number of mitotic figures per 10 HPF ranged between zero and 2, ranging between 2 and 10 in the 7 grade II tumours.

At the other end of the spectrum (grade III, 10 cases and grade IV, 10 cases) the tumours were more cellular. However all tumours were nodular and showed prominent myxoid areas (Figs. 10 & 11), some tumours were partly solid.

The tumour cells in grade III and grade IV tumours were larger and more polymorphic, some were slender, others more plump or rounded with an abundant eosinophilic, well-delineated cytoplasm (Fig. 12 & 13). The nuclei were frequently of irregular shape with coarse chromatin and prominent nucleoli (Fig. 14). The mitotic activity in the grade III tumours varied from 5 to 30

plied this term to malignant soft tissue tumours characterized by their mucoid and nodular appearance with no evidence of lipoblastic myoblastic or chondroblastic differentiation and believed to belong to the category of fibroblastic and histiocytic soft tissue tumours. They are mostly seen subcutaneously, in the extremities and trunk of elderly people

This paper draws attention to this tumour and the findings in 30 cases are presented

MATERIAL AND METHODS

The material was obtained by reviewing the files at the Department of Pathology Sahlgren Hospital Göteborg Sweden from 1947 to 1975 The original diagnoses are listed in Table 1

TABLE 1 *Original Diagnosis of 30 Myxofibrosarcomas*

No of cases	Original diagnosis
9	Myxofibrosarcoma
4	Myxosarcoma
2	Malignant fibromyxoma
3	Fibrosarcoma
2	Liposarcoma
1	Rhabdomyosarcoma
1	Haemangioendotheliosarcoma
1	Myxochondrosarcoma
2	Sarcoma unspecified
1	Myxoma
1	Neurofibroma
1	Lipomyxoma
1	Myxofibromatous tumour
1	Mycosis fungoides

Tumour tissue blocks were available in each case From the blocks, new 5 µ sections were made and stained with haematoxylin-eosin and according to Weigert-van Gieson Gordon's silver impregnation was used for the demonstration of reticulin fibres and Weigert's elastin method for the study of elastic tissue in the tumour vessels Some tumours were stained according to the PAS-method (McManus) with and without preceding digestion with diastase In order to demonstrate fat in paraffin sections, Sudan black B method (Merck, 0 1 per cent solution) was used In each case Alcian blue (Chroma-Gesellschaft) and toluidine blue stains (E. Merck Darmstandt) were applied at different pH's, namely pH's 2.5 and 0.5 and 4 0 and 0.5 respectively for the detection of glycoseaminoglycans as described previously (*Angervall et al* 1975) these stains were performed with and without preceding treatment of the sections with testicular hyaluronidase (hyaluronidase from bovine testes, type IV Sigma) All tumours were stained according to *Scott & Dorling* (1965) at pH 5 6 with 0 05 per cent Alcian blue in 0.025 M acetate buffer with the addition of increasing concentrations of $MgCl_2$ in order to determine the "*critical electrolyte concentration*" (*CEC*) of the dye-polymer binding in the mucoid material of the tumour stroma. The following series of $MgCl_2$ concentrations was used 0 0 M, 0 025 M, 0 05 M, 0 1 M 0 25 M 0 35 M 0 45 M 0.55 M, 0 65 M, 0 75 M 0 85 M 1 0 M The staining time was 16 hours.

Histologically the tumours in the present series were divided into 4 grades according to the degree of tumour cellularity cell atypia and prevalence of mitotic figures.

RESULTS

Clinical Data

The clinical information is summarized in Table 2

Age and Sex (Fig 1)

In the present series, most patients were elderly the median age being 65 The youngest patient was a 24-year-old man with a small tumour in the left calf and the oldest, a 91 year-old woman with a large subcutaneous ulcerated mass on the left knee Twelve of the 30 patients were female.

Signs and Symptoms

The presenting symptom was a painless palpable mass in 24 of the 30 patients. Pain and tenderness was reported only in 6 cases. Two patients sought medical advice because of an ulcerated and bleeding tumour One tumour which was located in the ulnar part of the elbow caused pain which radiated into the 2 ulnar fingers. Signs of deep venous thrombosis in the leg was demonstrated in one patient some time before the tumour in the popliteal fossa was discovered. In 2 cases, previous trauma to the areas where the tu-

Cases of Myxofibrosarcoma

Histological grade	Follow-up period (yrs)	Results
3	–	–
3	2 2/12	Recurrences after 9 13 and 14 months. Died with metastasis to pleura, no autopsy
4	4 1/12	Recurrence after 48 months Accidental death.
2	10	Alive and well.
4	3 6/12	Recurrences after 5 and 10 months Died of cerebral haemorrhage no autopsy
4	3 3/12	Recurrences after 10 15 20, 25, 26 27 31 34 and 36 months. Metastasis to bone (femur) and lung. Died with tumour
2	6 3/12	New tumours after 36 and 51 months in the left vastus lateralis muscle and the left biceps muscle respectively Died with metastasis to lung, mesentery and pancreas.
3	11	Recurrences after 81 and 132 months. Alive and well.
1	5	Alive and well.
4	10/12	Recurrence after 4 month Died with tumour and metastasis to inguinal lymph nodes.
4	1 3/12	Recurrence after 7 months. Metastasis to the upper lip after 7 months and multiple subcutaneous tumours after 10 months. Died with multiple metastases (pancreas, lung and kidney)
3	3	Alive and well.
4	4/12	Alive and well.
2	2	Alive and well.
3	4/12	Alive and well
2	10 8/12	Recurrences after 48, 57 64 70 85, 89 ad 100 months. Died with tumour no autopsy
4	5	Recurrences after 13, 16, 17 and 30 months. Died free from tumour of chronic pyelonephritis.
2	12	Recurrences after 42 and 57 months. Alive and well.
1	4/12	Alive and well
3	3 2/12	Recurrences after 6 months. Died, no autopsy
2	27	Alive and well.
3	4/12	Recurrences after 3 months. Died postoperatively of myocardial infarction, no autopsy
3	2	Recurrences after 2, 5 and 12 months. Metastasis to inguinal lymph nodes after 12 and 17 months. Died with tumour no autopsy
4		
4	1/12	Died postoperatively of pulmonary emboli.
	3 6/1	Died with metastasis to paravertebral tissue and bronchopneumonia.
3	1	Alive and well.
3	6/12	Recurrence after 2 months. Alive and well.
4	3	Recurrences after 12 and 26 months. Alive and well
4	2/12	Alive and well.

formed a branching network without distinct cytoplasmatic boundaries, i.e. a syncytium-like pattern (Figs. 12 & 13). Two of the tumours, both of grade IV also contained areas with an alveolar arrangement of the cells. In 5 of the grade III and IV tumours, the tumour cells formed whorls and curves, thus producing a feather-like pattern.

In tumours with solid areas, the cells occasionally showed a tendency to form intertwining bundles giving these parts a fibrosarcoma-like pattern (Fig. 15). A storiform or

Case no	Age (yrs)	Sex	Anatomical location	Size (cm
1	71	M	Popliteal fossa, R	7 × 4
2	65	M	Lower arm, R	8 × 5
3	55	M	Calf L	2 × 2
4	72	M	Thigh, R	5 × 5
5	73	M	Calf L	–
6	74	M	Scapular area, R	8 × 5
7	76	F	Buttock R	5 × 5
8	65	M	Anterior surface of lower leg L	6 × 6
9	24	M	Calf L	3 × 3
10	72	F	Popliteal fossa R	6 × 5
11	87	M	Ankle I	9 × 5
12	69	F	Knee L	? × 2
13	63	M	Upper arm L	12 × 12
14	59	F	Thigh, R	8 × 6
15	51	F	Elbow R	9 × 5
16	75	M	Flank R	5 × 5
17	70	M	Lower back, R	7 × 5
18	69	M	Scapular area R	Four tumours ea 5 × 3
19	46	F	Forehead, L	2 × 1
20	78	F	Knee, R	7 × 5
21	49	F	Groin, L	6 × 4
22	80	F	Elbow I	7 × 4
23	76	F	Knee R	7 × 7
24	64	M	Upper arm R	15 × 15
25	60	M	Retroperitoneum	12 × 12
26	69	M	Thigh, R	8 × 6
27	40	F	Thigh L	10 × 6
28	91	F	Knee L	15 × 15
29	63	F	Iliac fossa, R	15 × 12.5
30	73	F	Thigh, L	4 × 4

mitoses per HPF and in grade IV from 15 to 30 mitoses per HPF Pathological mitotic figures were frequent in some of the latter Occasional, or small groups of grotesque uni or multinucleated tumour giant cells were found in 13 of these tumours (Fig 14) Five of these revealed occasional cells with multiple nuclei peripherally arranged as seen in giant cells of Touton's type. In 2 tumours, small clusters of foam cells were observed.

In the myxoid areas, the tumour cells often

Fig. 3 & 4 Two myxofibrosarcomas growing subcutaneously (skin, top Fig. 3; subcutaneous adipose tissue left Fig. 4). Both tumours are characterized by a multinodular growth pattern, showing myxoid nodules separated by fibrous septa. H & E, × 5.





surgical treatment. In 7 of the patients, amputation was performed after 1 to 3 recurrences.

One patient had pre- and post-operative irradiation of the primary tumour which was located in the right scapular region. The tumour was not radically removed; several recurrences followed which were treated by excision and irradiation. The patient died of metastatic spread 4 years after the primary operation. Irradiation of the tumour recurrence in the back of a 75-year-old man resulted in apparently complete regression of the tumour. Later on, however, new recurrence appeared and the patient died from tumour.

Follow-up

Recurrence and metastases (see Table 2)
None of the grade I tumours and only 2 of

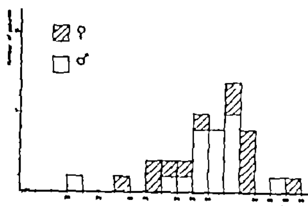


Fig 1 Age and sex distribution of 30 patients with myxofibrosarcoma

cart wheel appearance was found in small predominantly solid areas in 7 tumours. However this pattern was not a prominent feature in any of the tumours. An abundant collagen matrix was prominent in 14 tumours.

The nodules within the tumours were separated by fibrous connective tissue often infiltrated with inflammatory cells occasionally showing thrombosed vessels Necrotic areas and haemorrhages were frequently encountered especially in the central parts of the largest tumours.

A characteristic feature was a plexiform pattern of capillary like vessels, 5 to 15 μ in diameter which were prominent in myxoid areas (Figs 5 7 & 8) However the solid areas were also highly vascular showing a similar plexiform capillary pattern with prominent perivascular fibrosis, although the rich vascular pattern was partly obscured by the highly cellular tumour tissue In solid areas, much wider vessels were also seen up to 2 mm in diameter they were enclosed by fibrous tissue and lined by a single layer of endothelial cells

At pH 2.5 the mucoid tumour matrix stained with Alcian blue and it stained metachromatically with toluidine blue at pH 4 0 Neither the Alcian blue nor the toluidine blue staining was positive at pH 0 5 The positive stainings at the higher pHs were abolished by predigestion of the sections with testicular hyaluronidase The mucoid tumour matrix stained with Alcian blue up to 0.1 M $MgCl_2$ The results of these stainings indicated the presence of hyaluronic acid but not sulphated glucosaminoglycans (cf *Angerwall & Angervall* 1975)

Treatment

All of the 30 patients were treated surgically As the tumours were subcutaneously located they were often mistaken for benign lesions (i e. lipoma) pre-operatively and therefore treated by "enucleation" As a result of this, tumours in 20 of the 30 patients were not radically removed. However 5 of these 20 patients were operated on shortly after the primary excision At that time the pathologist did not observe any tumour tissue in the margins of the surgical specimen. According to the description of the operation and examination of the tissue specimens, the tumours in 8 of the 30 patients were radically removed at the primary operation One myxofibrosarcoma was explored and a biopsy was taken for histological examination. This biopsy was followed by a second radical operation 14 days later The retroperitoneal tumour was explored and found to be irremovable and only a biopsy was taken. Amputation was in no instance the primary

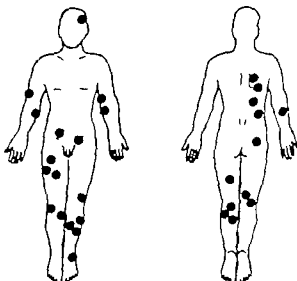


Fig 2 Localization of 29 myxofibrosarcomas.

the 7 grade II tumours recurred. One of these recurred 7 times over a period of 10 years. Six of the 10 grade III tumours and 7 out of the 11 grade IV tumours recurred. One patient with a grade IV tumour had 9 recurrences within a period of 3 years.

The location of metastases, to appear in 7 patients, is recorded according to grade in Table 3. Multicentric tumours were suspected in one patient with a large, subcutaneous, grade II myxofibrosarcoma in the right buttock, in whom deep-seated tumours developed in the left thigh (vastus lateralis muscle) and in the left upper arm (biceps muscle) 36 and 52 months after the primary operation all tumours were principally of the same appearance.

Prognosis

The patients were under observation for 1 month to 27 years. Follow-up results were obtained in all but 2 cases. At follow-up after 4 months and 5 years, the 2 patients with grade I tumour were still alive. Three of the patients with grade II tumours died with recurrences and/or metastases within 3 years and 6 months, 6 years and 6 months and 10 years and 8 months. The other 4 patients with grade II tumours were well and free from tumour 2 to 27 years after the primary excision. Two of the 10 patients with grade III tumours died with recurrence and/or metastases within 2 years and 2 years and 2 months. Two patients died of intercurrent diseases. The other 5 patients observed for from 4 months up to 11 years post-operatively were alive and free from tumour Three of the 11 patients with grade IV tumours died with recurrences and/or metastases within 10 months to 3 years and 5 months. One patient died post-operatively and 3 others of intercurrent diseases, but they had been free from tumour for 3 years, 3 years and 6 months and 4 years and 1 month after the primary operation. The remaining 3 were alive and well after intervals of time from 2 months to 3 years.

Fig 5. Grade I. Paucity of cells within a myxoid matrix The capillaries are arranged in a characteristic plexiform pattern. H & E, × 120.

Fig 6 Grade I The spindle-shaped tumour cells show elongated dark staining nuclei with moderate polymorphism. H & E, × 225

Fig 7 Grade II Prominent plexiform capillary pattern within moderately cellular tumour tissue. H & E, × 120

Fig 8. Grade II. Prominent plexiform capillary pattern and perivascular fibrosis. H & E, × 90



Fig 9 Grade II. The spindle-shaped tumour cells show an oval or elongated slightly polymorphous nucleus and a fusiform cytoplasm. There is an abundant acuolated mucoid matrix. H & E, × 225

DISCUSSION

The tumours in patients in the present series were characterized by histiocyte and/or fibroblast-like cells, a nodular and myxoid


5
6
8

cervical region, most chordomas are situated in the soft tissue of the presacral region, a site at which myxofibrosarcoma has not been found to develop in patients in the present series.

The myxoid form of nodular fasciitis should be considered when myxofibrosarcoma is to be diagnosed. It may cause certain difficulties to recognize a myxofibrosarcoma of low grade as they occasionally may be present in the form of a small tumour not unlike nodular fasciitis. A radiating vascular pattern instead of the plexiform capillary pattern the presence of inflammatory cells and lack of encapsulation and of anaplasia of the proliferating fibroblasts may serve to distinguish nodular fasciitis from myxofibrosarcoma (*Allen* 1972, *Dahl et al* 1972)

One tumour in the present series was originally diagnosed as myxoma and we realize that it occasionally may be difficult to distinguish clearly between myxofibrosarcoma grade I and myxoma. The latter appears predominantly in the skin or it is deep-seated, but it is rarely located subcutaneously (cf *Stout* 1948 a, *Enzinger* 1965 *Ireland et al* 1973 *Kindblom et al*. 1974) Myxoma is less cellular anaplasia is absent and it lacks the prominent plexiform vascular pattern of myxofibrosarcoma.

Embryonal rhabdomyosarcoma is often myxoid and the lobulated form of sarcoma botryoides may be completely myxoid (*Albores-Saavedra et al* 1963 *Stout & Lattes* 1967 *Davis et al*. 1969) The histological picture of primitive-looking cells mingling with characteristic round cell rhabdomyoblasts and/or strap- and ribbon-shaped rhabdomyoblasts with or without definite cross striation leave no doubt about the classification of this tumour The typical location in the midline and the incidence according to age as well as the polypoid growth and the subepithelial cambium layer of the sarcoma botryoides confirm the diagnosis in most cases.

Spindle cell lipoma is a recently recognized benign tumour entity predominantly seen subcutaneously in the shoulder and neck area in elderly people (*Enzinger & Harvey* 1975 *Angervall et al* 1976) The spindle cell lipoma with a prominent myxoid character may be difficult to differentiate from myxofibrosarcoma The presence of fat cells, the abundant haphazardly arranged collagen and the absence of mitotic activity distinguish this tumour from myxofibrosarcoma.

Dermatofibrosarcoma protuberans may be partly myxoid. A characteristic feature of this tumour supposed to be fibroblastic in origin, is the constant storiform or cartwheel cellular arrangement (*Taylor & Helwig* 1962, *Butler* 1963) This, together with its almost always cutaneous location, distinguishes it from myxofibrosarcoma.

Pleomorphic liposarcoma may reveal only relatively few scattered multivacuolated lipoblasts and shows numerous grotesque pleomorphic cells with abundant eosinophilic granular cytoplasm (*Kindblom et al* 1975) The solid pattern, the presence of multivacuolated lipoblasts and the almost invariably deep location of pleomorphic liposarcoma help in the differential diagnosis.

Soft tissue tumours composed of cells of an appearance resembling both fibroblasts and histiocytes have been designated fibrous histiocytomas (*Stout & Lattes* 1967) By now data are obtained by tissue cultures and ultrastructural studies suggesting a histogenesis common to these cells. It has been suggested that both cell types may be derived from an undifferentiated stem cell (*Fu et al* 1975) Another theory is that the basic tumour cells of the malignant fibrous histiocytoma is a histiocyte which can act as a facultative fibroblast (*Ozello et al* 1963 *Merkow et al*. 1971) This may explain the variation in the histological appearance of myxofibrosarcomas in the present series both within the individual tumour but above all between these. Although many myxofibrosarcomas, especially those of low grade, showed *only* fibroblast like and stellate-shaped cells they are different from those which have been described as fibrosarcomas of low grade (*Stout* 1948 b *Butler* 1963, *Pritchard et al*. 1974)



Figs 10 & 11 Grade III A partly solid nodular myxofibrosarcoma surrounded by condensed collagen bundles. Fibrous septa show a tendency to separate the tumour in lobules. H & E, × 30

appearance a plexiform capillary vascular pattern and the tumours were usually superficially located. It was possible to divide them into four grades (grades I to IV) according to the degree of cellularity and cellular atypia as well as to prevalence of mitotic figures. Thus, tumours of grade IV showed pronounced atypia often presenting bi and multinucleated giant tumour cells and occasionally giant cells of Touton's type thus suggesting a relationship to malignant fibroxanthoma (*O'Brien & Stout* 1964 *Kempson & Kyriakos* 1972 *Soule & Enriquez* 1972)

It is well known that malignant soft tissue tumours often contain myxoid areas. Tumours such as myxoid liposarcoma extraskeletal chodrosarcoma and chordoma may be purely myxoid Myxoid (embryonal) liposarcoma and myxofibrosarcomas of low grade both have conspicuous myxoid appearance and show a plexiform capillary pattern which is coarser in myxofibrosarcoma In contrast to myxofibrosarcoma myxoid liposarcoma contains multivacuolated lipoblasts and show the so-called pooling phenomenon, and is almost always deep-seated (*Kindblom et al.* 1975) The tumour cells in extraskeletal chondrosarcoma as well as in chordoma are arranged in lobules and often form syncytial strands in a mass of mucus (*Dahlin* 1970, *Enzinger & Shiraki* 1972) i.e features that can also be found in myxofibrosarcomas. However the absence of a coarse plexiform capillary pattern together with the histochemical demonstration of sulphated glucosaminoglycans (*Kindblom & Angervall* 1975) distinguish these tumours from myxofibrosarcomas. Furthermore disregarding the

clivus region, most chordomas are situated in the soft tissue of the presacral region, a site at which myxofibrosarcoma has not been found to develop in patients in the present series.

The myxoid form of nodular fasciitis should be considered when myxofibrosarcoma is to be diagnosed. It may cause certain difficulties to recognize a myxofibrosarcoma of low grade as they occasionally may be present in the form of a small tumour not unlike nodular fasciitis. A radiating vascular pattern instead of the plexiform capillary pattern, the presence of inflammatory cells and lack of encapsulation and of anaplasia of the proliferating fibroblasts may serve to distinguish nodular fasciitis from myxofibrosarcoma (*Allen* 1972, *Dahl et al* 1972)

One tumour in the present series was originally diagnosed as myxoma and we realize that it occasionally may be difficult to distinguish clearly between myxofibrosarcoma grade I and myxoma. The latter appears predominantly in the skin or it is deep-seated, but it is rarely located subcutaneously (cf *Stout* 1948 a, *Enzinger* 1965 *Ireland et al.* 1973 *Kindblom et al.* 1974) Myxoma is less cellular anaplasia is absent and it lacks the prominent plexiform vascular pattern of myxofibrosarcoma.

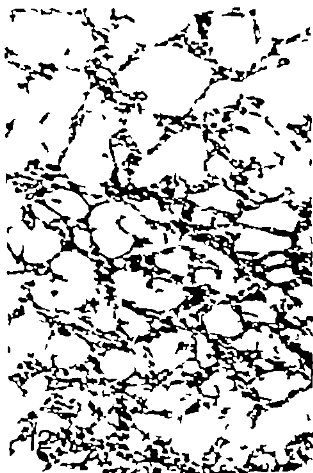
Embryonal rhabdomyosarcoma is often myxoid and the lobulated form of sarcoma botryoides may be completely myxoid (*Albores-Saavedra et al.* 1963 *Stout & Lattes* 1967 *Davis et al* 1969) The histological picture of primitive looking cells mingling with characteristic round cell rhabdomyoblasts and/or strap- and ribbon-shaped rhabdomyoblasts with or without definite cross striation leave no doubt about the classification of this tumour The typical location in the midline and the incidence according to age as well as the polypoid growth and the subepithelial cambium layer of the sarcoma botryoides confirm the diagnosis in most cases

Spindle cell lipoma is a recently recognized benign tumour entity predominantly seen subcutaneously in the shoulder and neck area in elderly people (*Enzinger & Harvey* 1975 *Angervall et al.* 1976) The spindle cell lipoma with a prominent myxoid character may be difficult to differentiate from myxofibrosarcoma The presence of fat cells, the abundant haphazardly arranged collagen and the absence of mitotic activity distinguish this tumour from myxofibrosarcoma.

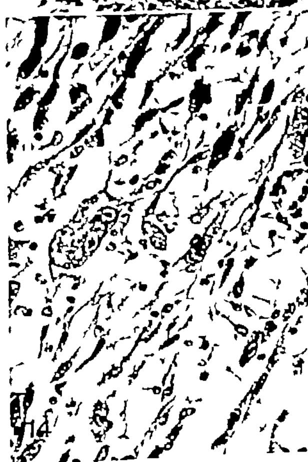
Dermatofibrosarcoma protuberans may be partly myxoid. A characteristic feature of this tumour supposed to be fibroblastic in origin, is the constant storiform or cartwheel cellular arrangement (*Taylor & Helwig* 1962, *Butler* 1963) Thus, together with its almost always cutaneous location, distinguishes it from myxofibrosarcoma

Pleomorphic liposarcoma may reveal only relatively few scattered multivacuolated lipoblasts and shows numerous grotesque pleomorphic cells with abundant eosinophilic granular cytoplasm (*Kindblom et al* 1975) The solid pattern, the presence of multivacuolated lipoblasts and the almost invariably deep location of pleomorphic liposarcoma help in the differential diagnosis.

Soft tissue tumours composed of cells of an appearance resembling both fibroblasts and histiocytes have been designated fibrous histiocytomas (*Stout & Lattes* 1967) By now data are obtained by tissue cultures and ultrastructural studies suggesting a histogenesis common to these cells. It has been suggested that both cell types may be derived from an undifferentiated stem cell (*Fu et al.* 1975) Another theory is that the basic tumour cells of the malignant fibrous histiocytoma is a histiocyte which can act as a facultative fibroblast (*Ozello et al.* 1963 *Merkow et al.* 1971) This may explain the variation in the histological appearance of myxofibrosarcomas in the present series, both within the individual tumour but above all between these. Although many myxofibrosarcomas, especially those of low grade showed only fibroblast like and stellate-shaped cells they are different from those which have been described as fibrosarcomas of low grade (*Stout* 1948 b, *Butler* 1963 *Pritchard et al.* 1974)


12


13


14

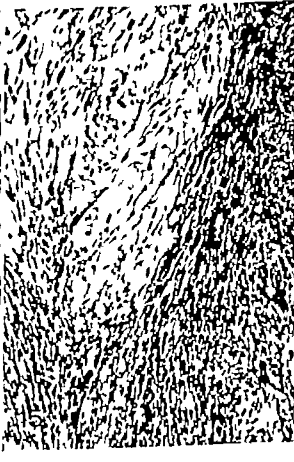


TABLE 3 *Location of Metastases According to Grade*

	Grade			
No. of patients with metastases	I	II	III	IV
	0/2	2/7	2/10	3/11
Location				
Lung, pleura		1	1	2
Lymph node			1	1
Skeleton		1		1
Pancreas		1		1
Mesentery		1		1
Subcutaneous tissue				1
Kidney				1

Malignant soft tissue tumours of probable histiocytic origin vary considerably in histological appearance. Malignant fibroxanthoma (malignant fibrous xanthoma, malignant fibrous histiocytoma, malignant histiocytoma), malignant giant cell tumour of soft tissue (*Guccion & Enzinger* 1972) and epitheloid sarcoma (*Enzinger* 1970) have been considered as separate entities because of their different histological and clinical characteristics but all are supposed to be of histiocytic origin (*Soule & Enriquez* 1972, *Guccion & Enzinger* 1972). The pleomorphic myxofibrosarcomas (grades III and IV) may possess features which histologically are similar to those of malignant fibroxanthoma. However, features typical of malignant fibroxanthoma such as foam cells, giant cells of Touton's type and foci of inflammatory cells (*O'Brien & Stout* 1964, *Kempson & Kyriakos* 1972, *Soule & Enriquez* 1972) are lacking in myxofibrosarcoma of grade I and II and only occasionally found in tumours of grade III and IV. According to our opinion the prominent myxoid character, the plexiform capillary-like vascular pattern, the nodular appearance and superficial location of myxofibrosarcomas justify their classification as a separate group within the general category of fibroblastic and histiocytic malignant soft tissue tumours.

The follow-up study of tumours of grades II, III and IV showed a high frequency of recurrence and metastases. The present series is too small to allow any definite prognostic conclusions to be drawn. However, the results obtained suggest that a grading as that used in the present series can be of prognostic significance. Further studies of larger series are necessary if the influence of different clinical and morphological factors is to be evaluated. The high frequency of recurrences indicates that simple enucleation should be avoided and that the treatment of choice is wide local excision.

Fig. 12. Grade III. Tumour cells forming anastomosing strands giving a syncytium-like appearance. H & E, × 90.

Fig. 13. Grade III. Polymorphous tumour cells growing in syncytium-like strands. Scattered mitotic figures are indicated by arrows. H & E, × 300.

Fig. 14. Grade IV. Polymorphous spindle-shaped tumour cells and bizarre multinucleated giant cells with large nucleoli. H & E, × 300.

Fig. 15. Grade IV. Partly solid area with tumour cells parallelly arranged forming fascicles giving fibrosarcoma-like appearance. H & E, × 120.

Supported by a research grant from the Swedish Cancer Society 530-K73-02X.

REFERENCES

Albores-Saavedra, J., Butler, J. J. & Martin, R. G.: Rhabdomyosarcoma: clinicopathologic considerations and report of 85 cases. In Tumors of bone and soft tissue. Year Book Medical Publ., Chicago 1965, p. 349–366.

Allen, P. W.: Nodular fasciitis. Pathology 4: 9–26, 1972.

Angervall, L., Enerbäck, L. & Knutson, H.: Chondrosarcoma of soft tissue origin. Cancer 32: 507–513, 1973.

Angervall, L., Dahl, I., Kindblom, L. G. & Säve-Söderbergh, J.: Spindle cell lipoma. Acta Path. Microbiol. scand. Sect. A, 84: 477–487, 1976.

Butler, J. J.: Fibrous tissue tumours: nodular fasciitis, dermatofibrosarcoma protuberans and fibrosarcoma, grade I desmoid type. In Tumors or bone and soft tissue. Year Book Medical Publ., Chicago 1965, p. 402–407.

Dahl, I., Angervall, L., Magnusson, S. & Stener, B.: Classical and cystic nodular fasciitis. Path. Europ. 7: 211–221, 1972.

Dahlin D C Chordoma. In Bone tumors. General aspects and data on 3,987 cases 2nd ed., Charles C Thomas Springfield 1970 p 222–233

Davis G L Kissane J M & Ishak K G Embryonal rhabdomyosarcoma (sarcoma botryoides) of the biliary tree report of five cases and review of the literature Cancer *24* 333–342 1969

Enzinger F M Intramuscular myxoma. A review and follow up study of 34 cases. Am J Clin Path *43* 104–113 1965

Enzinger F M Epitheloid sarcoma A sarcoma simulating a granuloma or a carcinoma. Cancer *26* 1029–1041 1973

Enzinger F M & Harvey D A Spindle cell lipoma. Cancer *36* 1852–1859 1975

Enzinger F M & Shiraki M Extraskeletal myxoid chondrosarcoma. An analysis of 34 cases. Human Pathology *3* 421–435 1972

Enzinger F M & Winslow D J Liposarcoma. A study of 103 cases. Virchows Arch Path. Anat. *335* 367–388 1962

Fu Y S Gabbiani G Kaye G I & Lattes R Malignant soft tissue tumors of probable histiocytic origin (malignant fibrous histiocytomas) general considerations and electron microscopic and tissue culture studies Cancer *35* 176–198 1975

Guccion J G & Enzinger F M Malignant giant cell tumor of soft parts An analysis of 32 cases. Cancer *29* 1518–1528 1972.

Ireland D C R Soule F H & Ivins J C Myxoma of somatic soft tissues. A report of 58 patients, 3 with multiple tumors and fibrous dysplasia of bone Mayo Clin. Proc *48* 401 410 1973

Kempson R L & Kyriakos M Fibroxanthosarcoma of the soft tissues. A type of malignant fibrous histiocytoma Cancer *29* 961–976 1972

Kindblom L G & Angervall L Histochemical characterization of mucosubstances in bone and soft tissue tumors. Cancer *36* 985 994 1975

Kindblom L G Stener B & Angervall L Intramuscular myxoma. Cancer *34* 1737–1744, 1974

Kindblom L G Angervall L & Svendsen P Liposarcoma A clinicopathologic, radiographic and prognostic study Acta path. microbiol. scand. suppl. 253 1975

Merkow L P Frick J C., Slifkin M Kyreages, C G & Pardo M Ultrastructure of a fibroxanthosarcoma (malignant fibroxanthoma) Cancer *28* 372–383 1971

O'Brien J E & Stout A P Malignant fibrous xanthomas. Cancer *17* 1445–1455 1964

Ozello L Stout A P & Murray M R Cultural characteristics of malignant histiocytomas and fibrous xanthomas. Cancer *16* 331–344 1963.

Pritchard D J Soule E H., Taylor W F & Ivins J C Fibrosarcoma—a clinicopathologic and statistical study of 199 tumors of the soft tissues of the extremities and trunk. Cancer *33* 888–897 1974

Scott J E & Dorling J Differential staining of acid glucosaminoglycans (mucopolysaccharides) by Alcian blue in salt solutions. Histochemie *5* 221–233 1965

Soule E H & Enriquez P Atypical fibrous histiocytoma malignant fibrous histiocytoma, malignant histiocytoma and epithelioid sarcoma. A comparative study of 65 tumors. Cancer *30* 128–143 1972

Stout A P Myxoma the tumor of primitive mesenchyme Ann. Surg *127* 706–719 1948 a

Stout A P Fibrosarcoma, the malignant tumor of fibroblasts. Cancer *1* 30–63 1948 b.

Stout A P & Lattes R Rhabdomyosarcoma. In Tumors of the soft tissues. Atlas of tumor pathology Second series. Fascicle 1 Armed Forces Institute of Pathology Washington 1967 p. 134–144

Taylor H B & Helwig E B Dermatofibrosarcoma protuberans. A study of 115 cases. Cancer *15* 717–725 1962.

Acta path. microbiol. scand. Sect. A, 85: 141-150, 1977

MORPHOMETRIC AND DYNAMIC STUDIES OF BONE CHANGES IN HYPERTHYROIDISM

FERNANDO MELSEN and LEIF MOSEKILDE

University Institute of Pathology and Medical Department III, Aarhus Amtssygehus, Aarhus, Denmark

Melsen, F. & Mosekilde, L. Morphometric and dynamic studies of bone changes in hyperthyroidism. Acta path. microbiol. scand. Sect. A, 85: 141-150, 1977.

Bone biopsies were performed after tetracycline double-labelling by transfixing the right iliac crest in forty hyperthyroid patients. The bone changes in cortical and trabecular bone were determined by simple measurement and point counting on decalcified and undecalcified stained sections. A slight decrease in the amount of cancellous bone was found. The mean cortical width was normal. The amount of osteoid and the length of the osteoid seams were increased, whereas the mean width of osteoid seams was decreased. The cortical osteoclastic activity and porosity were markedly increased. The trabecular osteoclastic activity was moderately increased and the mean size of periosteocytic lacunae was slightly increased. The calcification rate in cancellous bone was increased as were the active calcification surfaces (tetracycline-labelled). The osteoclastic activity in cortical bone was positively correlated to the free thyroxine index and to the urinary calcium and phosphorus excretion. The findings indicate that the bone changes in hyperthyroidism are specific and that thyroid hormone( ) stimulates both bone formation and resorption followed by increased porosity in cortical bone and by mobilization of bone mineral.

Key words: Hyperthyroidism; bone changes; morphometric and dynamic studies.

F. Melsen, University Institute of Pathology, Aarhus Amtssygehus, DK-8000 Aarhus, Denmark.

Received 19 76. Accepted 16.ix.76

Radiological signs of bone changes in hyperthyroid patients are relatively rare when conventional techniques are used (*Williams & Morgan* 1940, *Meunier et al.* 1972), but using a special technique *Meema & Meema* (1972) found a very high frequency (75 per cent) of bone changes characterized by intracortical striation.

The histological changes in hyperthyroid bone disease have been described as similar to ostitis fibrosa (*Hunter* 1930, *Follis* 1953, *Askanazy & Rutishauser* 1933), osteoporosis and osteomalacia (*Follis* 1953). *Meunier et al.* (1972) described the bone changes as specific with increased remodelling activity and porosity in cortical bone. Microradiographic studies in man (*Adams et al.* 1967) and in thyroxine fed dogs (*Adams & Jowsey* 1967) have demonstrated increased resorption and increased cortical porosity.

The aim of the present study was to describe the bone morphology in hyperthyroidism in detail using undecalcified bone sections and the point count principle, and to study bone dynamics using tetracycline

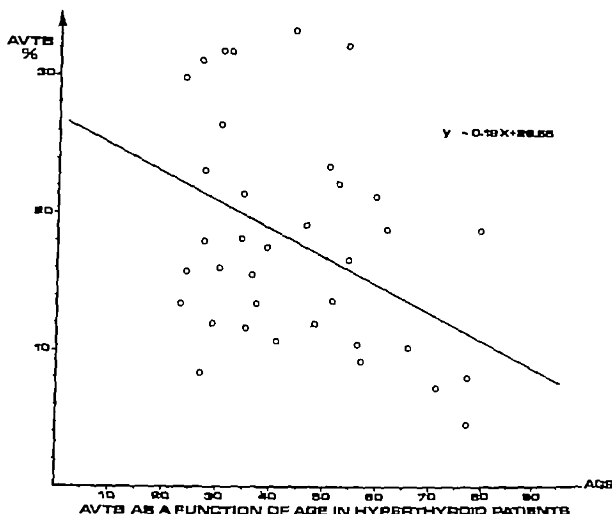


Fig 1 a b Correlations between absolute volume of trabecular bone (AVTB) and age in hyperthyroid patients (a) and in normal controls (b) The interrupted line in (b) indicates the regression line in the hyperthyroid patients.

double labelling Furthermore some preliminary findings of interrelationships between bone morphometry and biochemical parameters with respect to thyroid function tests and chemical quantities of calciumphosphorus are given

PATIENTS AND METHODS

The investigation comprised 40 patients with hyperthyroidism 33 women aged 16–79 years (mean 44) and 7 men aged 29–57 years (mean 48) The diagnosis was based upon clinical symptoms and signs, determination of serum thyroxine serum tri-iodo-thyronine uptake and absolute [131]I iodine uptake. All patients had normal serum creatinine values.

The control groups comprised 30 persons presenting the same age and sex distribution and selected from our series of normal subjects (*Melsen et al.*, to be published)

Double-labelling with tetracycline (*Frost* 1969) was performed in all patients and volunteers (n = 11) Biopsies were obtained from the right iliac crest (*Bordier et al* 1964) Morphometric analysis was performed on decalcified and undecalcified stained sections. The following parameters were measured

A In Cortical Bone

Thickness and width of external and internal cortex As the mean of 10 measurements using a conventional micrometric eyepice.

Total number of Haversian canals by counting.

Total number of canals with active osteoclastic resorption by counting. The osteoclastic resorption was defined as a scalloped interruption of the surrounding lamellar system with or without osteoclasts.

P[illegible] ority of external and internal cortical bone

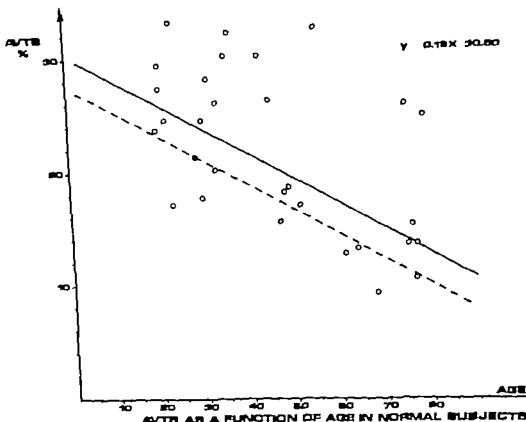


Fig. 1 b

by pointcount principles using 100 point Zeiss integrating filter. The filter was projected over 20 fields in each cortex, and the porosity was calculated as the percentage of the total number of points projected into canals.

Mean no. of periosteocytic lacunae (POL)

The following parameters were calculated from the measurements:

Number of canals per mm² of bone

Per cent of canals occupied by active osteoclastic resorption (CAR)

B. 1. Trabecular Bone

Absolute volume of trabecular bone (AVTB)

Per cent of osteoid covered surface (OS)

Relative osteoid volume (OV)

Mean width of osteoid seams (WOS)

Trabecular osteoclastic resorption surfaces (RS)

Active trabecular calcification surfaces (ATCS)

Per cent active osteoid calcification surfaces (AOCS) (= calcification fronts)

In the present investigation, the measurements in cortical bone are of special interest and are therefore described in detail. The measurements in trabecular bone (AVTB, OS, OV and RS) and the dynamic parameters (CR, ATCS and AOCS) measured on unstained undecalcified sections have been previously described (*Bordier et al.* 1964, *Courpron* 1972, *Meunier et al.* 1969, *Meunier et al.* 1971, *Melsen et al.*, to be published). The statistical significance of differences in group means was determined by Wilcoxon test for two samples and correlation coefficients by Spearman's rank correlation (R).

RESULTS

The morphometric analysis of cancellous and cortical bone in hyperthyroid patients compared with normal controls is given in Table 1.

Amount and structure of bone. In cancellous bone the AVTB was significantly decreased in hyperthyroid patients. This parameter was inversely correlated to age both in

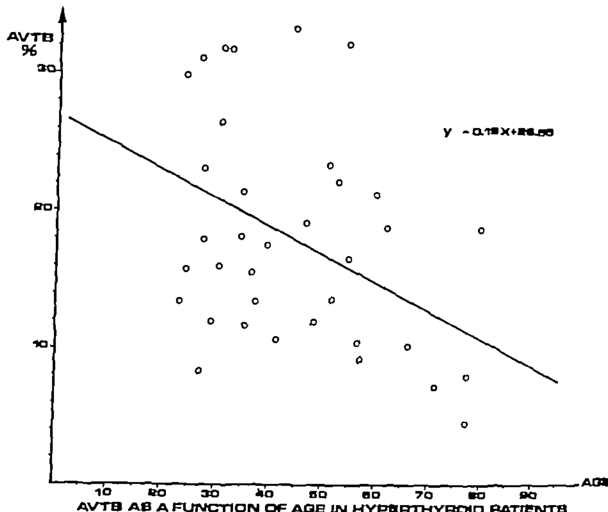


Fig 1 a b Correlations between absolute volume of trabecular bone (AVTB) and age in hyperthyroid patients (a) and in normal controls (b) The interrupted line in (b) indicates the regression line in the hyperthyroid patients

double labelling Furthermore some preliminary findings of interrelationships between bone morphometry and biochemical parameters with respect to thyroid function tests and chemical quantities of calciumphosphorus are given.

PATIENTS AND METHODS

The investigation comprised 40 patients with hyperthyroidism 33 women aged 16 79 years (mean 44) and 7 men aged 29–57 years (mean 48) The diagnosis was based upon clinical symptoms and signs determination of serum thyroxine serum tri iodo-thyronine uptake and absolute 131I iodine uptake All patients had normal serum creatinine values.

The control groups comprised 30 persons presenting the same age and sex distribution and selected from our series of normal subjects (*Melsen et al. to be published*)

Double-labelling with tetracycline (*Frost* 1969) was performed in all patients and volunteers (n = 11) Biopsies were obtained from the right iliac crest (*Bordier et al* 1964) Morphometric analysis was performed on decalcified and undecalcified stained section The following parameters were measured

A In Cortical Bone

Thickness and width of external and internal cortex As the mean of 10 measurements using a conventional micrometric eyepice

Total number of Haversian canals by counting

Total number of canals with active osteoclastic resorption by counting The osteoclastic resorption was defined as a scalloped interruption of the surrounding lamellar system with or without osteoclasts.

Porosity of external and internal cortical bone

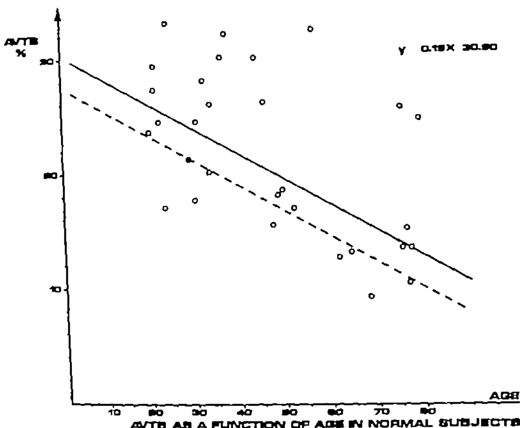


Fig 1 b

by pointcount principles using a 100 point Zeiss integrating filter The filter was projected over 20 fields in each cortex, and the porosity was calculated as the percentage of the total number of points projected into canals

Mean size of periosteocytic lacunae (POL)

The following parameters were calculated from the measurements

Number of canals per mm² of bone

Per cent of canals occupied by active osteoclastic resorption (CAR)

B In Trabecular Bone

Absolute volume of trabecular bone (AVTB)

Per cent of osteoid covered surface (OS)

Relative osteoid volume (OV)

Mean width of osteoid seams (WOS)

Trabecular osteoclastic resorption surfaces (RS)

Active trabecular calcification surface (ATCS)

Per cent active osteoid calcification surfaces (AOCS) (= calcification fronts)

In the present investigation, the measurements in cortical bone are of special interest and are therefore described in detail. The measurements in trabecular bone (AVTB, OS, OV and RS) and the dynamic parameters (CR, ATCS and AOCS) measured on unstained undecalcified sections have been previously described (*Bordier et al.* 1964 *Courpron* 1972, *Meunier et al* 1969 *Meunier et al.* 1971 *Melsen et al.*, to be published) The statistical significance of differences in group means was determined by Wilcoxon test for two samples and correlation coefficients by Spearman rank correlation (R)

RESULTS

The morphometric analysis of cancellous and cortical bone in hyperthyroid patients compared with normal controls is given in Table 1

Amount and structure of bone In cancellous bone the AVTB was significantly decreased in hyperthyroid patients. This parameter was inversely correlated to age both in

TABLE 1 *Morphometric and Dynamic Analyses of Trabecular Bone and Cortical Bone in Hyperthyroid Patients as Compared with Normal Controls*

Trabecular bone

	AVTB %	OS %	OV %	WOS µm	CR µm/day	RS %	ATCS %	AOCS %
Norm								
x̄	21.6	14.0	1.9	9.0	0.70	3.8	13.5	86.6
SE (N)	1.3 (30)	1.2 (30)	0.2 (30)	0.3 (19)	0.03 (11)	0.2 (30)	1.3 (10)	5.7 (10)
Thyr								
x̄	18.0	19.8	2.2	7.2	0.92	6.6	18.9	85.6
SE (N)	1.3 (36)	1.7 (37)	0.3 (37)	0.4 (31)	0.05 (29)	0.6 (37)	1.9 (19)	5.1 (19)
p	<0.05	<0.002	N.S.	<0.01	<0.01	<0.001	<0.05	N.S.

Cortical bone

	Mean (µm) cortical thickness	Canals per mm²	Porosity %	CAR %	POL µm²
Norm.					
x̄	1176	7.3	5.0	7.0	51.2
SE (N)	93 (29)	0.5 (28)	0.4 (29)	0.3 (29)	0.4 (25)
Thyr					
x̄	1367	6.1	12.3	12.2	35.4
SE (N)	80 (41)	0.3 (43)	1.1 (41)	1.6 (41)	1.6 (26)
p	N.S.	<0.05	<0.001	<0.001	<0.10





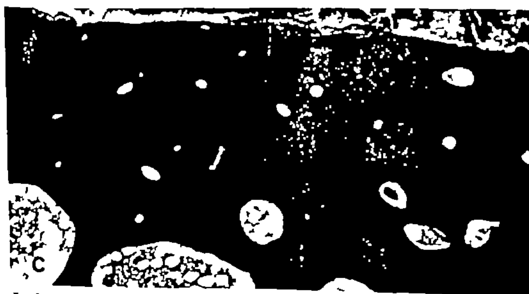


Fig. 2 a, b ( ) Remodelling unit in cortical bone with osteoclastic resorption (left) and osteoid covered surface (right). (b) Cortical bone in a hyperthyroid patient with increased porosity and dilated canals with active resorption. ( ) Normal cortical bone.

hyperthyroid patients ($R = -0.35$, $p < 0.05$) and in normal controls ($R = -0.50$, $p < 0.01$) (Fig. 1). In cortical bone no difference in the mean thickness of internal and external lamella was found, but the porosity was significantly increased in the hyperthyroid patients, the mean value being 2.7 times higher than that in normal controls. The mean number of canals per square mm was reduced.

Amount and shape of osteoid seams. In the hyperthyroid patients OS but not OV was significantly increased and WOS was decreased.

Bone resorption activity In cancellous bone RS was increased ($p<0.01$) the mean value being 1.9 times higher in hyperthyroid patients than in normal controls. In cortical bone POL was slightly but insignificantly increased ($p<0.10$) The relative number of canals in cortical bone with active resorption (CAR) was markedly increased (Fig 2) the mean value in hyperthyroid patients being 5 9 times that in normal controls. Fibrosis was not remarkable in cancellous bone In cortical bone fibrosis was found in the canals with active resorption

Dynamic parameters (tetracycline labelling) The calcification rate (CR) measured in cancellous bone was significantly increased in the hyperthyroid patients, as was the ATCS No significant difference was found in AOCS

The prevalence of abnormal morphometric bone parameters is given in Table 2 within 95 per cent confidence limits. It is seen that an elevated number of canals in cortical bone with active resorption and an increase in the cortical porosity are the most prominent features in hyperthyroid bone disease

TABLE 2 *Prevalence of Abnormal Morphometric Bone Parameters (Exceeding 2SD from Normal Means) in Hyperthyroid Patients*

	%	95 % confidence limits
Cancellous bone		
Decreased AVTB	5 6	0 7–18 7
Increased OS	21 6	9 8–38.2
Decreased WOS	32 3	16 7–51 4
Increased CR	42 1	20 3–66 3
Increased RS	46.0	29.5–63 1
Increased ATCS	26 7	7 8–55 1
Cortical bone		
Increased porosity	70 2	57 1–85 8
Increased CAR	80.5	65 1–91 2
Increased POL	38.5	20 2–59 4

Interrelationships between morphometric bone parameters Correlation between OS and OV ($R = 0.79$ $p<0.001$) and between OS and ATCS ($R = 0.85$ $p<0.001$) was found to be highly significant (Fig 3) The cortical porosity was positively correlated to the number of canals in cortical bone with active resorption ($R = 0.78$ $p<0.001$) (Fig 4) No other significant correlations were found

Interrelationship between morphometric bone parameters and biochemistry Correlation between the free thyroxine index (se-thyroxine × se-tri iodo-thyronine) the number of canals with active resorption in cortical bone ($R = 0.34$ $p<0.05$) cortical porosity ($R = 0.32$ $p<0.05$) and the trabecular osteoclastic resorption surfaces was found to be positive ($R = 0.40$ $p<0.01$) Furthermore, CAR was positively correlated to the urinary excretion of calcium ($R = 0.50$ $p<0.01$) and phosphorus ($R = 0.35$, $p<0.05$)

DISCUSSION

The present study has demonstrated that changes in bone structure and bone dynamic are a very frequent finding in hyperthyroid patients. The changes are most prominent in cortical bone where increased porosity was found in 70 per cent of the patients and an increased percentage of canals with active resorption in 81 per cent This is in accordance with *Meema & Meema* (1972) who by means of a special X ray technique found that the intracortical striation had increased in 73 per cent of their patients with hyperthyroidism. The prevalence of abnormal morphological parameters is even higher than the prevalence of abnormal biochemical parameters of calciumphosphorus metabolism (*Baxter & Bondy* 1966 *Mosekilde & Christensen* in press)

The bone changes, in the present study differ from bone changes induced by parathyroid hormone (*Meunier et al* 1969) Fibrosis in the marrow along the trabeculae is a dominating factor in ostitis fibrosa, but not in hyperthyroid bone disease whereas fibrosis in the cortical canals is a frequent finding in this disease The mean size of the periosteocytic lacunae in the hyperthyroid patients

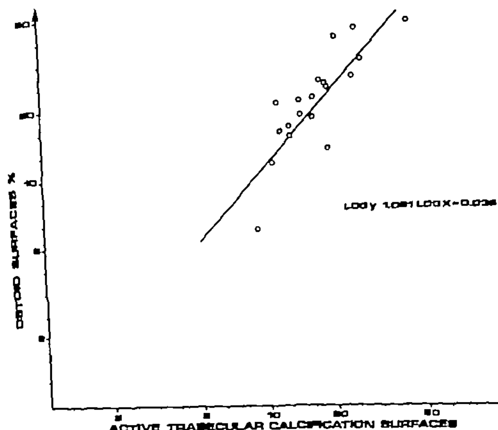


Fig 3 Correlation between osteoid covered surfaces (OS) and active (tetracycline-labelled) calcification surfaces in trabecular bone in hyperthyroid patients

was only insignificantly increased and the osteoclastic activity was increased, being most pronounced in the cortical bone. In primary and secondary hyperparathyroidism there is a considerable increase in the osteocytic osteolysis and in the trabecular osteoclastic resorption surfaces (*Meunier* 1969)

The morphometric bone changes in hyperthyroidism are quite different from those seen in osteoporosis, in which the trabecular surfaces are inactive though the amount of osteoid and osteoclastic activity may vary within normal range (*Meunier et al.* 1975 *Croux et al* 1975) the rate of calcification being either normal or slightly reduced (personal observation to be published) The bone changes in hyperthyroidism differ from those seen in osteomalacia in which an increase in the mean width of osteoid seams and a decrease in the calcification rate and in the active calcification surfaces are prominent features (*Vignon & Meunier* 1975 *Rasmussen & Bordier* 1974 *Delling* 1975)

The differences in the distribution of the resorption activity in hyperthyroidism and hyperparathyroidism raise the question whether there are two types of osteoclasts, one situated on the surfaces of trabecular bone which is sensitive to parathyroid hormone and to a lesser degree to thyroid hormone(s) and another located in the cortical bone which is highly sensitive to thyroid hormone(s) The increase in resorptive activity in hyperthyroidism is a direct effect of thyroid hormone(s) on bone and not an effect of parathyroid activation in hyperthyroidism. This

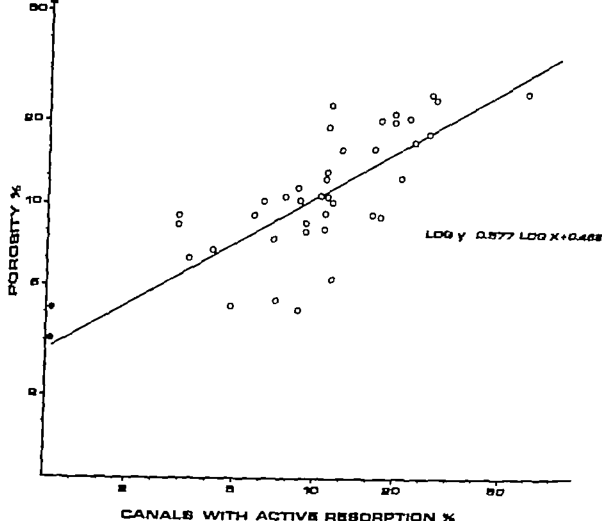


Fig 4 Correlation between porosity and relative number of canals with active resorption in hyper thyroid patients.

is documented by the finding of low serum concentrations of immunoreactive parathyroid hormone in hyperthyroid patients, inversely correlated to the degree of hyper thyroidism and hypercalcaemia (*Mosekilde & Christensen* in press) and by the finding that both normal and parathyreoidectomized dogs show increased levels of bone resorption after thyroxine feeding (*Adams & Jowsey* 1967)

The increase in bone resorption in hyper thyroidism leads to a decreased amount of bone in spite of a stimulated bone formation Both resorption and formation are increased but the former more than the latter leading to a mobilization of bone mineral. This is demonstrated by the significant correlation between the cortical osteoclastic activity and the urinary excretion of calcium and phosphorus which are increased in hyperthyroidism and positively correlated to the degree of thyroid function (*Mosekilde & Christensen* in press) The decrease in the amount of bone is accompanied by a decrease in the content of bone mineral and of bone ash (*Smith et al* 1973) and spontaneous fractures may be the consequence (*Ryckewaert et al* 1968, *Meunier et al* 1972)

A thorough explanation of the hyperthyroid bone lesions have previously been forwarded by *Meunier et al.* (1972) Applying a morphometric bone analysis identical to the present they found a high incidence of bone changes Apart from the findings of cortical porosity and of the number of Haversian canals with active resorption, the

present findings corroborates those of Meunier and collaborators. With reference to cortical porosity the inconsistency might be explained by differences in methods. *Meunier et al.* (1972) correct for oblique cutting of the canals. In the present investigation we have not corrected the measurement of porosity since variation in the diameter of canals due to variation in the plane of sectioning is identical to that of the interjacent bone. The porosity (area of canals/area of bone) is therefore independent of the variations of the plane of sectioning.

Meunier et al. (1972) did not measure the osteoclastic activity in cortical bone, a parameter which is probably the most important in hyperthyroid bone disease since it is positively correlated to chemical indices of bone mineral mobilization (urinary calcium and phosphorus excretion) and gives a reasonable explanation of the increase in the cortical porosity.

Due to difficulties in obtaining controls in the form of tetracycline labelled material in biopsies from normal subjects, only few authors have been able to describe the changes in bone dynamics in patients with hyperthyroidism (*Adams et al.* 1967, *Meunier et al.* 1972). The present investigation shows a high activity in the extent as well as in the linear mineralization rate as compared with the values obtained in a normal, sex and age matched series, and thus confirms earlier results and assumptions.

The present study of 40 hyperthyroid patients further substantiates and supports the now well-accepted concept that the bone change in hyperthyroidism is a specific disease. The bone lesions are characterized by increased bone turn-over with a preponderance of osteoclastic activity in cortical bone, which is correlated to the thyroid function and leads to mobilization and increased urinary excretion of bone mineral.

REFERENCES

Adams P., Jowsey J., Kelly P. J., Riggs B. L., Kinney V. R. & Jones J. D.: Effects of hyperthyroidism on bone and mineral metabolism in man. Quart. J. Med. *36*: 141, 1–15, 1967.

Adams P. & Jowsey J.: Bone and mineral metabolism in hyperthyroidism. An experimental study. Endocrinology *81*: 735–740, 1967.

Askanazy M. & Rutishauser E.: Die Knochen der Basedow-Kranken. Virchows Arch. Path. Anat. *291*: 653–681, 1933.

Baxter J. D. & Bondy P. K.: Hypercalcemia of thyrotoxicosis. Ann. Intern. Med. *65*: 429–442, 1966.

Bordier P., Matrajt H., Miravet L. & Hioco D.: Mesure histologique de la masse et de la résorption des travées osseuses. Path. Biol. *12*: 23–24, 1238–1243, 1964.

Cirona J. M., Courpron P. & Meunier P.: Histomorphometrie de l'osteopenie physiologique senile. Thèse Lyon, 1973.

Courpron P.: Données histologiques quantitatives sur le vieillissement osseux humain. Thèse Lyon, 1972.

Delling, G.: Endokrine Osteopathien. Gustav Fischer Verlag, Stuttgart, 1975.

Follis R. H.: Skeletal changes associated with hyperthyroidism. Bull. Johns Hopkins Hosp. *92*: 405–421, 1953.

Frost H. M.: Tetracycline-bases histological analysis of bone remodelling. Calc. Tiss. Res. *3*: 211–237, 1969.

Hunter D.: The significance to clinical medicine of studies in calcium and phosphorus metabolism. Lancet *i*: 947–957, 1930.

Meema, H. E. & Meema S.: Comparison of microradioscopic and morphometric findings in the hand bones with densitometric findings in the proximal radius in thyrotoxicosis and in renal osteodystrophia. Investigative Radiology 88–96, 1972.

Melsen F., Mosekilde L., Melsen, B. & Bergmann S.: Morphometry and dynamics in normal bone from the iliac crest (to be published).

Meunier P., Bernard J. & Vignon G.: Measuring and periosteocytic enlargement in primary and secondary hyperparathyroidism. Israël J. Med. Sci. *7*: 482–485, 1971.

Meunier P., Vignon, G., Vauzelle J. L. & Zech P.: Etude histologique quantitative de la resorption ostéoclastique dans les hyperparathyroidies primitives et secondaires. Path. Biol. *1*: 21–22, 927–938, 1969.

Meunier P., Courpron P., Edouard C., Bernard J. Bringuir J. & Vignon G.: Physiological senile involution and pathological rarefaction of bone. Clin. Endocr. Metab. *2*: 239–256, 1973.

Meunier P., Bianchi G. G. S., Edouard C. M. Bernard J. C. Courpron P. & Vignon G. E.: Bone manifestations of thyrotoxicosis. Orthoped. Clin. of North America *3*: 745–774, 1972.

Mosekilde L. & Christensen, M. S.: Decreased

parathyroid function in hyperthyroidism. Interrelationships between serum PTH, calcium phosphorus metabolism and thyroid function. Acta Endocr. in press.

Rasmussen H. & Bordier P. The physiological and cellular basis of metabolic bone disease. The Williams & Wilkins Company, p. 64, 1974.

Ryckewaert A., Bordier P., Miravet L. & Antonini A. L'ostéose thyroïdienne. Sem. Hop. Paris 4: 222–229, 1968.

Smith D. A., Fraser S. A. & Wilson G. M. Hyperthyroidism and Calcium Metabolism. Clin. Endocr. Metab. 2: 333–354, 1973.

Vignon G. & Meunier P. Les ostéoses décalcifiantes diffuses de l'adulte. Documenta Geigy. Ciba-Geigy Ltd. 1973.

Williams R. H. & Morgan H. J. Thyrotoxic osteoporosis. Internat. Clin. 2: 48, 1940.

Acta path. microbiol. scand. Sect. A, 85: 151–156, 1977

DEMONSTRATION OF OCHRATOXIN A IN KIDNEYS OF PIGS AND RATS BY IMMUNOFLUORESCENCE MICROSCOPY

FOLMER ELLING

Renal Laboratory Department of Pathology Rigshospitalet, Copenhagen, Denmark

Elling, F Demonstration of ochratoxin A in kidneys of pigs and rats by immunofluorescence microscopy Acta path. microbiol. scand. Sect. A, 85 151–156, 1977

Ochratoxin A was localized in the kidneys of pigs and rats by means of immunofluorescence microscopy after short-time exposure Antibody against ochratoxin A was obtained from rabbits after repeated injections of bovine serum albumin-ochratoxin A conjugate. Ochratoxin A was localized exclusively in the proximal tubule. Light microscopically necrosis and desquamation of epithelial cells in the pig kidneys were restricted to the proximal tubule where the toxin was found. The investigation has demonstrated conclusively that the proximal tubule is the target part of the nephron in ochratoxin A-induced acute mycotoxic nephropathy

Key words Ochratoxin A nephropathy mycotoxic immunofluorescence pig rat.

Folmer Elling, Department of Pathology Rigshospitalet, DK 2100 Copenhagen Ø Denmark.

Received 30.ix.76 Accepted 30.ix.76

Ochratoxin A is a mycotoxin produced by several fungal species included in the genera *Aspergillus* and *Penicillium* (Review Chu 1974) This mycotoxin has been associated with spontaneously occurring toxic nephropathy in pigs and poultry in Denmark (*Krogh et al.* 1973 *Elling et al.* 1975) and its nephrotoxic effect was demonstrated experimentally using crystalline ochratoxin A (*Krogh et al.* (1976)) The renal changes in mycotoxic nephropathy in pigs are characterized by tubular degeneration and atrophy accompanied by interstitial fibrosis, and histological and clinical observations suggest that the proximal tubule is the target segment of the nephron (*Elling & Møller* 1973 *Szczech et al* 1973 *Krogh et al.* 1974) Ochratoxin A is chemically a dihydro-isocoumarin derivative linked by its 7-carboxyl group to L-beta-phenylalanine. Due to its low molecular weight (M.W 403) ochratoxin A does not demonstrate antigenic properties. However a recent investigation has shown that ochratoxin A, when coupled to bovine IgG acts as a hapten, and as such can be used for antibody production in rabbits. This was employed in a radioimmunoassay for ochratoxin A (*Aalund et al.* 1975 *Chu et al.* 1976)

However attempts to demonstrate the localization of ochratoxin A after peroral administration have not yet been made.

The present paper describes the microscopical localization in the kidney of pigs and rats by an indirect immunofluorescence technique

parathyroid function in hyperthyroidism Inter relationships between serum PTH calcium phosphorus metabolism and thyroid function. Acta Endocr in press.
Rasmussen H & Bordier P The physiological and cellular basis of metabolic bone disease The Williams & Wilkins Company p. 64 1974
Ryckewaert A Bordier P Miravet L. & Antonini A L'ostéose thyroïdienne. Sem. Hop. Paris 4 22?–229 1968.
Smith D A Fraser S A & Wilson G. M. Hyperthyroidism and Calcium Metabolism Clin Endocr Metab 2 333–354 1973
Vignon G & Meunier P. Les ostéoses décalcifiantes diffuses de l'adulte. Documenta Geigy, Ciba-Geigy Ltd. 1973
Williams R. H & Morgan H J. Thyrotoxic osteoporosis. Internat. Clin. 2 48, 1940.

TABLE 1 *Controls for Establishing Specificity of the Indirect Immunofluorescence Staining*

	Antigen	Antiserum	Conjugate	Results of staining reaction
1	Kidney with ochratoxin A	Rabbit anti-ochratoxin A BSA + anti-BSA	Labelled anti-rabbit immunoglobulin	Positive
2	Kidney with ochratoxin A	—	—	Negative
3	Kidney without ochratoxin A	Rabbit anti-ochratoxin A BSA + anti-BSA	Labelled anti-rabbit immunoglobulin	Negative
4	Kidney with ochratoxin A	Rabbit anti-ochratoxin A	Unlabelled anti-rabbit immunoglobulin followed by labelled anti-rabbit immunoglobulin	Negative
5	Kidney with ochratoxin A	Saline	Labelled anti-rabbit immunoglobulin	Negative
6	Kidney with ochratoxin A	Non-immune rabbit serum	Labelled anti-rabbit immunoglobulin	Negative
7	Kidney with ochratoxin A	Rabbit anti-ochratoxin A BSA	Labelled anti-rabbit immunoglobulin	Positive
8	Kidney with ochratoxin A	Rabbit anti-ochratoxin A-BSA precipitated with ochratoxin A BSA	Labelled anti-rabbit immunoglobulin	Negative

tion as in 4. The supernatants of 3, 4 and 5 were therefore pooled and used partly for incubation on slides and partly for precipitation with ochratoxin A-BSA.

When the specific anti-ochratoxin A antibodies are eliminated from the antiserum, the staining reaction should be negative. Precipitation of anti-ochratoxin A antibodies in the antiserum (control 8, Table 1) was made as follows. O-BSA in borate buffer at pH 8.0 was used for precipitation of anti-ochratoxin antisera that had been absorbed with BSA. To 150 μl aliquots of antiserum was added 150 μl from solutions containing the following concentrations of O-BSA:

1 2.5 mg/ml	2 1.0 mg/ml	3 0.5 mg/ml
4 0.1 mg/ml	5 0.05 mg/ml	6 0.01 mg/ml

RESULTS

Pigs. In two pigs given 400 μg ochratoxin A per kg b.w. daily for 5 days the ochratoxin A residue in the kidneys was 250 μg/kg. Light microscopical examination revealed desquamation and focal necrosis of epithelial cells in the proximal tubules (Fig. 1). By means of the indirect immunofluorescence technique ochratoxin A was demonstrated in the proximal tubules. The tubules exhibiting ochratoxin A deposits were identified by histological examination of the adjacent sections stained PAS. The deposits were seen as granules of varying size in the cytoplasm. The granules frequently coalesced giving the cells a bright, diffuse fluorescence but leaving the nuclei unstained (Fig. 2). Frequently detritus of necrotic proximal tubular cells and desquamated cells located in the distal tubules showed a positive reaction. Approximately one third of the epithelial cells of the proximal tubules in a section showed a positive reaction while glomeruli, the loops of Henle, the distal tubules, the collecting tubules, the vascular system, the interstitial tissue, and the pelvis always displayed negative staining.

Rats. Two groups of rats (Group 1 & 2) were given 250 μg and 1000 μg ochratoxin A per kg b.w. respectively and the residues in the kidneys were 100 and 600 μg/kg for group 1 and group 2 respectively. Neither of the two groups showed microscopical renal lesions. The immunofluorescence examination of the kidney sections revealed the same

MATERIAL AND METHODS

Animals

Pigs Two female pigs weighing approximately 10 kg were daily given 400 µg/kg b.w of ochratoxin A in gelatine capsules orally for 5 days. The dose level was identical to the high levels found in feed associated with spontaneous toxic nephropathy in bacon pigs (10) On the fifth day the pigs were anaesthetized as previously described (6) After laparotomy the left kidney was rapidly removed and snapfrozen in liquid nitrogen. The kidney was stored at −80 C Material from the right kidney was fixed in 10 per cent buffered formalin and processed for histology Two pigs, that had been on a diet free from ochratoxin A served as controls.

Rats Nine conventional albino female rats from the same litter weighing approximately 40 g were divided into 3 groups.

Group 1 was given 250 µg of ochratoxin A/kg b.w daily for 5 days via a stomach tube Group 2 received 1000 µg/kg b.w., while group 3 served as controls The two doses were approximately 1/80 and 1/20 of the LD_{50} values for female rats (14) Ochratoxin A was dissolved in 0 01 N sodium bicarbonate On the fifth day all rats were anaesthetized by intraperitoneal injections of sodium pentobarbital, 100 mg/kg b.w and the kidneys were removed and processed as described for the pigs.

Antigen Preparation and Immunization

Crystalline ochratoxin A recovered from *Aspergillus ochraceus* (*Krogh et al* 1976) was conjugated to bovine serum albumin BSA (Behringwerke) by use of the mixed anhydride method (*Erlanger et al* 1957 Worsaae personal communication) The number of ochratoxin A molecules per mole BSA, determined by ultraviolet spectroscopy was 20

Six rabbits were immunized with 0.5 ml ochratoxin A BSA (O-BSA) in trisbuffer pH 8.5 (1 mg O-BSA/ml) emulsified in 0.5 ml Freund's complete adjuvant and administered intradermally at 10 sites on the back. The rabbits were reimmunized after 2 4 6 and 8 weeks and then every 4 weeks They were bled 10 days after each inoculation The serum was stored at −30 C.

Staining Procedure

Cryostat sections (4 µm) of the snap-frozen kidneys were washed for 5 min in phosphate buffered saline (PBS pH 7 2) and incubated with undiluted anti-ochratoxin A antiserum (AO antiserum) for 24 h at 4 C (Albrechtsen personal communication) After 2 × 5 min washings in PBS the sections were incubated with fluorescein isothiocyanate conjugated goat anti rabbit serum IgG (FITC-GAR, Behringwerke) for 30 min. at room temperature followed by 2 washings in PBS and one washing in distilled water The sections were air-dried and mounted in Eukitt® and the microscopical examination was made with a Reichert Zetopan® equipped with an Osram HBO 200 lamp In addition to the interference filters (*Rygaard & Olsen* 1969) a suppression filter (λ>480 Leitz) was used as a primary filter in order to reduce fading

Fixation of Tissue Sections

Frozen sections are most suitable for demonstration of insoluble antigens that do not become dislocated during staining and washing Although ochratoxin A has got its optimal aqueous solubility at pH 8.5–9.5 and the saline used for washing of the sections prior to incubation is adjusted to pH 7 2, it should be anticipated however that parts of the minute amounts of ochratoxin A on a 4 µm thick section may diffuse or disappear during the washing procedure.

In order to elucidate this, attempts were made to conjugate ochratoxin A to the proteins in the sections by preincubating with 50 mg carbodiimide/ml 0 05 phosphate buffer pH 7 4 for 30 min. at room temperature (1 ethyl 3 (3-dimethyl-aminopropyl) carbodiimide HCl Sigma)

Controls

The specificity of the staining reaction in the indirect immunofluorescence technique was investigated as shown in Table 1

When rabbits are immunized with ochratoxin A conjugated to bovine serum albumin (BSA) it should be anticipated that anti BSA antibodies as well as anti-ochratoxin A antibodies are formed. The specificity of the antiserum is confined to the anti-ochratoxin A antibodies. In order to demonstrate that anti BSA antibodies do not produce a false positive reaction, these antibodies should be eliminated from the antiserum, which still should produce a positive staining The precipitation procedure of anti-BSA antibodies (control 7 Table 1) was as follows

Bovine serum albumin in borate buffer at pH 8.0 was used for precipitation of anti-O-BSA antisera. To 200 µl aliquots of antiserum was added 200 µl from solutions containing the following concentrations of BSA

1 10 mg/ml	*2* 2 mg/ml.	*3* 1 mg/ml.
4 0 2 mg/ml	*5* 0 1 mg/ml	*6* 0 02 mg/ml.

The mixtures were incubated at 37 C for one h. at 4 C for 48 h and then centrifuged for 30 min. at 2 × 10^3G No precipitate was formed in 1 and 6 and the largest amount was found in 4 In 3 and 5 the precipitate was of about the same vol

TABLE 1 *Controls for Establishing Specificity of the Indirect Immunofluorescence Staining*

Antigen	Antiserum	Conjugate	Results of staining reaction
1 Kidney with ochratoxin A	Rabbit anti-ochratoxin A-BSA + anti-BSA	Labelled anti-rabbit immunoglobulin	Positive
2 Kidney with ochratoxin A	—	—	Negative
3 Kidney without ochratoxin A	Rabbit anti-ochratoxin A-BSA + anti-BSA	Labelled anti-rabbit immunoglobulin	Negative
4 Kidney with ochratoxin A	Rabbit anti-ochratoxin A	Unlabelled anti-rabbit immunoglobulin followed by labelled anti-rabbit immunoglobulin	Negative
5 Kidney with ochratoxin A	Saline	Labelled anti-rabbit immunoglobulin	Negative
6 Kidney with ochratoxin A	Non-immune rabbit serum	Labelled anti-rabbit immunoglobulin	Negative
7 Kidney with ochratoxin A	Rabbit anti-ochratoxin A BSA	Labelled anti-rabbit immunoglobulin	Positive
8 Kidney with ochratoxin A	Rabbit anti-ochratoxin A BSA precipitated with ochratoxin) A BSA	Labelled anti-rabbit immunoglobulin	Negative

same as in 4 The supernatants of 3 4 and 5 were therefore pooled and used partly for incubation on slides and partly for precipitation with ochratoxin A-BSA.

When the specific anti-ochratoxin A antibodies re eliminated from the antiserum, the staining reaction should be negative. Precipitation of anti ochratoxin A antibodies in the antiserum (control Table 1) was made as follows O-BSA in borate uffer at pH 8.0 was used for precipitation of anti-ochratoxin antisera that had been absorbed with BSA. To 150 µl aliquots of antiserum was dded 1.0 µl from solutions containing the following oncentrations of O-BSA

2.5 mg/ml	2 1.0 mg/ml	3 0.5 mg/ml
1 0.1 mg/ml	5 0.05 mg/ml.	6 0.01 mg/ml.

RESULTS

Pigs In two pigs given 400 µg ochratoxin A per kg b w daily for 5 days the ochratoxin A residue in the kidneys was 250 µg/kg Light microscopical examination revealed desquamation and focal necrosis of epithelial cells in the proximal tubules (Fig. 1) By means of the indirect immunofluorescence technique ochratoxin A was demonstrated in the proximal tubules. The tubules exhibiting ochratoxin A deposits were identified by histological examination of the adjacent sections stained PAS The deposits were seen as granules of varying size in the cytoplasm. The granules frequently coalesced giving the cells a bright, diffuse fluorescence but leaving the nuclei unstained (Fig 2) *Frequently detritus* of necrotic proximal tubular cells and desquamated cells located in the distal tubules showed a positive reaction. Approximately one third of the epithelial cells of the proximal tubules in a section showed a positive reaction while glomeruli, the loops of Henle, the distal tubules, the collecting tubules, the vascular system, the interstitial tissue, and the pelvis always displayed negative staining.

Rats Two groups of rats (Group 1 & 2) were given 250 µg and 1000 µg ochratoxin A per kg b w respectively and the residues in the kidneys were 100 and 600 *µg/kg for* group 1 and group 2 respectively Neither of the two groups showed microscopical renal lesions. The immunofluorescence examination of the kidney sections revealed the same

MATERIAL AND METHODS

Animals

Pigs Two female pigs weighing approximately 10 kg were daily given 400 μg/kg b w of ochratoxin A in gelatine capsules orally for 5 days The dose level was identical to the high levels found in feed associated with spontaneous toxic nephropathy in bacon pigs (10) On the fifth day the pigs were anaesthetized as previously described (6) After laparotomy the left kidney was rapidly removed and snapfrozen in liquid nitrogen. The kidney was stored at −80 C Material from the right kidney was fixed in 10 per cent buffered formalin and processed for histology Two pigs, that had been on a diet free from ochratoxin A served as controls

Rats Nine conventional albino female rats from the same litter weighing approximately 40 g were divided into 3 groups

Group 1 was given 250 μg of ochratoxin A/kg b w daily for 5 days via a stomach tube Group received 1000 μg/kg b w., while group 3 served as controls The two doses were approximately 1/80 and 1/20 of the LD_{50} values for female rats (14) Ochratoxin A was dissolved in 0 01 N sodium dicarbonate. On the fifth day all rats were anaesthetized by intraperitoneal injections of sodium pentobarbital 100 mg/kg b w and the kidneys were removed and processed as described for the pigs

Antigen Preparation and Immunization

Crystalline ochratoxin A recovered from *Aspergillus ochraceus* (*Krogh et al* 1976) was conjugated to bovine serum albumin BSA (Behringwerke) by use of the mixed anhydride method (*Erlanger et al* 1957 Wormae personal communication) The number of ochratoxin A molecules per mole BSA determined by ultraviolet spectroscopy was 20

Six rabbits were immunized with 0 5 ml ochratoxin A BSA (O-BSA) in trisbuffer pH 8.5 (1 mg O-BSA/ml) emulsified in 0.5 ml Freund s complete adjuvant and administered intradermally at 10 sites on the back The rabbits were reimmunized after 2 4 6 and 8 weeks and then every 4 weeks They were bled 10 days after each inoculation The serum was stored at 30 C

Staining Proced e

Cryostat section (4 μm) of the snap-frozen kidneys were washed for 5 min in phosphate buffered saline (PBS pH 7.2) and incubated with undiluted anti-ochratoxin A antiserum (AO antiserum) for 24 h at 4 C (Albrechtsen personal communication) After 2 × 5 min washings in PBS the sections were incubated with fluorescein isothiocyanate conjugated goat anti-rabbit serum IgG (FITC-GAR Behringwerke) for 30 min. at room temperature followed by 2 washings in PBS and one washing in distilled water The sections were air-dried and mounted in Eukitt® and the microscopical examination was made with a Reichert Zetopan® equipped with an Osram HBO 200 lamp In addition to the interference filters (*Rygaard & Olsen 1969*) a suppression filter (λ>480, Leitz) was used as a primary filter in order to reduce fading

Fixation of Tissue Sections

Frozen sections are most suitable for demonstration of insoluble antigens that do not become dislocated during staining and washing Although ochratoxin A has got its optimal aqueous solubility at pH 8.5–9 5 and the saline used for washing of the sections prior to incubation is adjusted to pH 7 2 it should be anticipated, however that parts of the minute amounts of ochratoxin A on a 4 μm thick section may diffuse or disappear during the washing procedure

In order to elucidate this, attempts were made to conjugate ochratoxin A to the proteins in the sections by preincubating with 50 mg carbodiimide/ml 0 05 phosphate buffer pH 7 4 for 30 min. at room temperatore (1 ethyl 3 (3-dimethyl-aminopropyl) carbodiimide HCl Sigma)

Controls

The specificity of the staining reaction in the indirect immunofluorescence technique was investigated as shown in Table 1

When rabbits are immunized with ochratoxin A conjugated to bovine serum albumin (BSA) it should be anticipated that anti BSA antibodies as well as anti-ochratoxin A antibodies are formed. The specificity of the antiserum is confined to the anti-ochratoxin A antibodies. In order to demonstrate that anti BSA antibodies do not produce a false positive reaction, these antibodies should be eliminated from the antiserum, which still should produce a positive staining The precipitation procedure of anti-BSA antibodies (control 7 Table 1) was as follows

Bovine serum albumin in borate buffer at pH 8 0 was used for precipitation of anti-O-BSA antisera To 200 μl aliquots of antiserum was added 200 μl from solutions containing the following concentrations of BSA

1 10 mg/ml	*2* 2 mg/ml	*3* 1 mg/ml
4 0 2 mg/ml	*5* 0 1 mg/ml	*6* 0 02 mg/ml.

The mixtures were ncubated at 37 C for one h at 4 C for 48 h., and then centrifuged for 30 min at 2 × 10^3G No precipitate was formed in 1 and 6 and the largest amount was found in 4 In 3 and 5 the precipitate was of about the same vol





Fig. 2 Indirect immunofluorescence staining of ochratoxin A deposits in the same kidney as Fig. 1. The fluorescing granules in the cytoplasm of the epithelial cells of the proximal tubule frequently coalesce leaving only the nucleus unstained (arrow) × 380.

Fig. 3 Indirect immunofluorescence ochratoxin A staining of a kidney from a rat receiving 250 μg of ochratoxin A/kg b.w. daily for 5 days. The ochratoxin A deposits are seen as granules in the basal part of the epithelial cells of the proximal tubule × 380.

ly observed focal necrosis of the proximal tubules in the pig kidneys.

Carbodiimides are known to couple compounds containing many types of functional groups e.g. carboxylic acids (8). In this case preincubation with carbodiimide should couple ochratoxin A via its carboxylic acid group to lysin of the proteins in the tissue sections and thus prevent ochratoxin from disappearing during the washing procedure. In fact preincubation with carbodiimide contributed significantly to the intensity of the fluorescence in the rats but not in the pigs.

The present experiment has demonstrated that the proximal tubule is the target part of the nephron in ochratoxin A-induced mycotoxic nephropathy. This is in accordance with the data concerning the kidney function obtained in a previous study which revealed impairment of the transtubular transport illustrated by decrease of Tm_{PAH}, the Tm_{PAH}/C_{In} ratio and glucose reabsorption (10).

The author thanks *B. Hald* for carrying out the ochratoxin A analyses and is indepted to *O. Aalund, H. Worsaae* and *K. Poulsen*, Royal Veterinary and Agricultural University and *E. B. Lillehøj*, NRRL, Peoria, Ill. and *A. Paulsen*, Institute of Exp. Med., University of Copenhagen for advice and technical assistance.

Supported by the *Danish Agricultural and Veterinary Research Council* (Grant no. 513-6554).

REFERENCES

1. *Aalund O., Brunfeldt K., Hald B., Krogh P. & Poulsen K.*: A radioimmunoassay for ochratoxin A. A preliminary investigation. Acta path. microbiol. scand. Sect. C 83: 390–392, 1975.
2. Chu F. S.: Studies on ochratoxins. CRC Critical review in Toxicology 2: 499–524, 1974.

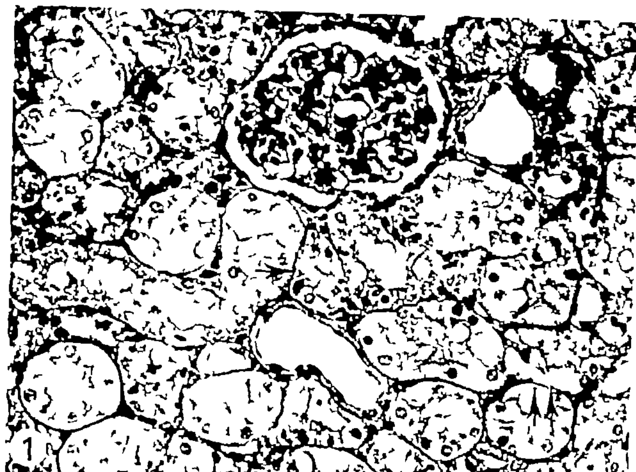


Fig 1 Kidney from a pig given 400 μg of ochratoxin A/kg b w daily for 5 days. The damage of the epithelial cells of the proximal tubules ranges from vacuolization of the cytoplasm (arrow) to necrosis of the epithelial cells leaving a naked basement membrane (double arrow) The glomerulus and the distal tubules appear morphologically normal. PAS × 350

localization of the toxin in the two groups and there was no difference in the intensity of the staining reaction A positive reaction was seen as a granular staining in the basal part of the proximal tubular cells (Fig 3) *As in the pigs negative reactions were seen* in all other elements of the cortex and the medulla

Controls In pigs and rats fed an ochratoxin A free diet a negative reaction was constantly observed.

The preincubation with carbodiimide prior to the specific staining contributed significantly to the preservation of the microscopic structure In the rats the fluorescence intensity was higher in the fixed than in the unfixed sections *while in the pigs the fluorescence* intensity appeared the same in fixed and unfixed sections.

DISCUSSION

By means of the indirect immunofluorescence technique the low molecular mycotoxin ochratoxin A (M W 403) was localized in the proximal tubules of the nephron in pigs *and rats. In the pigs the* dose level corresponded to the high levels found in feed for bacon pigs with spontaneous mytotoxic nephropathy (10) In the rats the dose level in Group 1 corresponded to that of the pigs while Group 2 received a 4 times higher amount.

The localization was confined to the proximal tubule in both pigs and rats and in the rats the intensity of the fluorescence was independent of the amount of toxin employed. Ochratoxin A *was not observed in all* proximal tubules This focal localization of the toxin was in accordance with the histological

Acta path. microbiol. scand. Sect. A, 85 157-168 1977

A COMPARISON OF THE EFFECTS OF THREE WIDELY USED GLUTARALDEHYDE FIXATIVES ON CELLULAR VOLUME AND STRUCTURE

A TEM SEM Volumetric and Cytochemical Study

V P Collins, B. Arborgh and U Brunk

Department of Tumor Pathology Karolinska Institutet, Stockholm, and
Department of Pathology Sabbatsberg Hospital, Karolinska Institutet, Stockholm, and
Institute of Pathology University of Uppsala, Uppsala, Sweden

Collins, V P Arborgh, B. & Brunk, U A comparison of the effects of three widely used glutaraldehyde fixatives on cellular volume and structure. A TEM, SEM volumetric and cytochemical study Acta path. microbiol. scand. Sect. A, 85 157-168 1977

The effects of three widely used glutaraldehyde-based fixatives on cellular volume and structure have been studied utilizing TEM, SEM, time-lapse micrography during the fixation procedure, volumetry and demonstration of the lysosomal enzyme acid phosphatase The cells used were in vitro cultivated human glia and glioma cells and suspensions of isolated rat liver parenchymal cells. The fixatives compared were the following 2 per cent glutaraldehyde (GA) in 0.1 M Na-cacodylate-HCL buffer (cac) with 0.1 M sucrose (pH 7.2); total osmolality (T) 510 mOsmol vehicle osmolality (V) 300 mOsmol, 2 per cent GA in 0.1 M cac (pH 7.2 T = 410 mOsmol V = 200 mOsmol) and 1.5 per cent GA in 0.067 M cac with 0.033 M sucrose (pH 7.2 T = 320 mOsmol V = 170 mOsmol) It was found that the fixative with a vehicle osmolality of 300 mOsmol gave results which were interpreted as ideal while the two fixatives with hypotonic vehicles resulted in changes which were easily demonstrated using volumetry time-lapse micrography SEM and cytochemistry However the differences observed in the TEM were less obvious and difficult to interpret, the major alterations being changes in the configuration of the ER in the liver cells. In conclusion, our findings show that even small variations in the composition of a glutaraldehyde fixative can result in structural changes which do not correspond to the functional morphology of a living cell Such changes make correct interpretation of micrographs difficult

Key words Glutaraldehyde fixatives cellular volume and structure.

V P Collins, Department of Tumor Pathology Karolinska Institutet, Fack, S-104 01 Stockholm 60, Sweden.

Received 16.xi.76 Accepted 4.x.76

The quality of information obtainable from material studied in the electron microscope is determined first of all by the preparative techniques used. One of the first steps in the preparation of biological material is fixation which naturally should be carried out in as perfect a manner as possible This

3 *Chu F S Chang F C C & Hindskill R D* Production of antibody against ochratoxin A. Appl. & Environmental Microbiol. *31* 831–835 1976

4 *Elling F & Møller T* Mycotoxic nephropathy in pigs. Bull Wld Hlth Org *49* 411–418, 1973

5 *Elling F Hald B Jacobsen Chr & Krogh P* Spontaneous cases of toxic nephropathy in poultry associated with ochratoxin A. Acta path. microbiol. scand. Sect A, *83* 739–741 1975

6 *Elling F Hasselager E. & Friis C* Perfusion fixation of kidneys in adult pigs for electron microscopy Acta anatomica in press.

7 *Erlanger B F Borek F Beiser S M & Lieberman S* Steroid protein conjugates. I Preparation and characterization of conjugates of bovine serum albumin with testosterone and cortisone J biol Chem *228* 713–727 1957

8 *Goodfriend T L., Levine L. & Fasman G D.*, Antibodies to bradykinin and angiotensin A use of carbodiimides in immunology Science *144* 1344–1346 1964

9 *Krogh P Hald B & Pedersen E. J* Occurrence of ochratoxin A and citrinin in cereals associated with mycotoxic porcine nephropathy Acta path. microbiol. scand. Sect. B *81* 689–695 1973

10 *Krogh P Axelsen N H Elling F Gyrd Hansen N Hald B Hyldgaard Jensen J Larsen A E. Madsen A Mortensen H P Møller T Petersen O K Ravnskov U Rostgaard M & Aalund O* Experimental porcine nephropathy Changes of renal function and structure induced by ochratoxin A contaminated feed Acta path. microbiol. scand. Sect. A. suppl. no. 246, 21 p.p., 1974.

11 *Krogh P Elling F Hald B., Jylling, B Petersen V E. Skadhauge E. & Svendsen, C K* Experimental avian nephropathy Changes of renal function and structure induced by ochratoxin A-contaminated feed. Acta path. microbiol. scand. Sect. A, *84* 215–?21 1976

12 *Krogh P Elling, F Gyrd Hansen N., Hald B Larsen A E. Lillehøj E. B Madsen A Mortensen H P & Ravnskov U.* Experimental porcine nephropathy Changes of renal function and structure perorally induced by crystalline ochratoxin A. Acta path. microbiol. scand. Sect. A *84* 429–434 1976.

13 *Krogh P* Mycotoxic porcine nephropathy A possible model for Balkan endemic nephropathy Proc. 2 nd Int. Symp. on endemic nephropathy (Sofia) 266–270 1972.

14 *Purchase I F H & Theron J J* The acute toxicity of ochratoxin A to rats. Food Cosmet. Toxicol *6* 479–483 1968.

15 *Rygaard J & Olsen W* Interference filters for improved immunofluorescence microscopy Acta path. microbiol. scand. *76* 146–148, 1969

16 *Szczech G M Carlton W W., Tuite J & Caldwell R* Ochratoxin A toxicosis in swine. Vet. Path. *10* 347–364 1973

Acta path. microbiol. scand. Sect. A, 85: 157-168, 1977

A COMPARISON OF THE EFFECTS OF THREE WIDELY USED GLUTARALDEHYDE FIXATIVES ON CELLULAR VOLUME AND STRUCTURE

A TEM, SEM, Volumetric and Cytochemical Study

V. P. Collins, B. Arborgh and U. Brunk

Department of Tumor Pathology, Karolinska Institutet, Stockholm, and
Department of Pathology, Sabbatsberg's Hospital, Karolinska Institutet, Stockholm, and
Institute of Pathology, University of Uppsala, Uppsala, Sweden

Collins, V. P., Arborgh, B. & Brunk, U. A comparison of the effects of three widely used glutaraldehyde fixatives on cellular volume and structure. A TEM, SEM, volumetric and cytochemical study. Acta path. microbiol. scand. Sect. A, 85: 157-168, 1977.

The effects of three widely used glutaraldehyde-based fixatives on cellular volume and structure have been studied utilizing TEM, SEM, time-lapse micrography during the fixation procedure, volumetry and demonstration of the lysosomal enzyme acid phosphatase. The cells used were *in vitro* cultivated human glia and glioma cells and suspensions of isolated rat liver parenchymal cells. The fixatives compared were the following: 2 per cent glutaraldehyde (GA) in 0.1 M Na-cacodylate-HCl buffer (cac) with 0.1 M sucrose (pH 7.2) total osmolality (T) 510 mOsmol, vehicle osmolality (V) 300 mOsmol; 2 per cent GA in 0.1 M cac (pH 7.2, T = 410 mOsmol, V = 200 mOsmol) and 1.5 per cent GA in 0.067 M cac with 0.033 M sucrose (pH 7.2, T = 320 mOsmol, V = 170 mOsmol). It was found that the fixative with vehicle osmolality of 300 mOsmol gave results which were interpreted as ideal while the two fixatives with hypotonic vehicles resulted in changes which were easily demonstrated using volumetry, time-lapse micrography, SEM and cytochemistry. However, the differences observed in the TEM were less obvious and difficult to interpret, the major alterations being changes in the configuration of the ER in the liver cells. In conclusion, our findings show that even small variations in the composition of a glutaraldehyde fixative can result in structural changes which do not correspond to the functional morphology of a living cell. Such changes make correct interpretation of micrographs difficult.

Key words: Glutaraldehyde fixatives; cellular volume and structure.

V. P. Collins, Department of Tumor Pathology, Karolinska sjukhuset, Fack, S-104 01 Stockholm 60, Sweden.

Received 16.ix.76. Accepted 4.x.76

The quality of information obtainable from material studied in the electron microscope is determined first of all by the preparative techniques used. One of the first steps in the preparation of biological material is fixation which naturally should be carried out in as perfect a manner as possible. This

3 *Chu F S Chang F C C & Hindskill R D* Production of antibody against ochratoxin A. Appl & Environmental Microbiol *31* 831–835 1976.

4 *Elling F & Møller T* Mycotoxic nephropathy in pigs. Bull. Wld. Hlth. Org *49* 411–418 1973

5 *Elling F Hald B Jacobsen Chr & Krogh P* Spontaneous cases of toxic nephropathy in poultry associated with ochratoxin A Acta path. microbiol. scand Sect A *83* 739–741 1975

6 *Elling F Hasselager E. & Friis C* Perfusion fixation of kidneys in adult pigs for electron microscopy Acta anatomica in press

7 *Erlanger B. F Borek F Beiser S M & Lieberman S* Steroid protein conjugates. I Preparation and characterization of conjugates of bovine serum albumin with testosterone and cortisone J biol Chem. *228* 713–727 1957

8. *Goodfriend T L. Levine L. & Fasman G D* Antibodies to bradykinin and angiotensin A use of carbodiimides in immunology Science *144* 1344–1346 1964

9 *Krogh P Hald B & Pedersen E. J* Occurrence of ochratoxin A and citrinin in cereals associated with mycotoxic porcine nephropathy Acta path microbiol scand Sect. B *81* 689–695 1973

10 *Krogh P., Axelsen N H Elling F Gyrd Hansen N Hald B Hyldgaard Jensen J Larsen A E., Madsen A Mortensen H P Møller T Petersen O K Ravnskov U Rostgaard M & Aalund O* Experimental porcine nephropathy Changes of renal function and structure induced by ochratoxin A contaminated feed. Acta path. microbiol scand. Sect. A. suppl. no. 246, 21 p p., 1974.

11 *Krogh P., Elling F., Hald B Jylling, B, Petersen I E. Skadhauge E. & Stendsen, C K* Experimental avian nephropathy Changes of renal function and structure induced by ochratoxin A-contaminated feed. Acta path. microbiol scand. Sect. A, *84* 215–221 1976

12 *Krogh P Elling F Gyrd-Hansen N Hald, B Larsen A E., Lillehøj E. B., Madsen A., Mortensen H P & Ravnskov U* Experimental porcine nephropathy Changes of renal function and structure perorally induced by crystalline ochratoxin A. Acta path. microbiol scand. Sect. A *84* 429–434 1976.

13 *Krogh P* Mycotoxic porcine nephropathy A possible model for Balkan endemic nephropathy Proc. 2'nd Int. Symp. on endemic nephropathy (Sofia) 266–270 1972.

14 *Purchase I F H & Theron J J.* The acute toxicity of ochratoxin A to rats. Food Cosmet. Toxicol. *6* 479–483 1968.

15 *Rygaard J & Olsen H* Interference filters for improved immunofluorescence microscopy Acta path. microbiol. scand *76* 146–148, 1969

16 *Szczech G M Carlton W W Tuite J & Caldwell R* Ochratoxin A toxicosis in swine Vet. Path *10* 347–364 1973

tures were washed for 60 minutes at 0 C in three different changes of 0.2 M sucrose in 0.05 M cacodylate buffer (pH 7.2 T = 300 mOsmol). Acid phosphatase was demonstrated in situ in the plastic dishes with Gomori-type medium (3) containing 0.22 M sucrose and 10 per cent dimethylsulphoxide (DMSO) (14). The reaction was run at +37° C in a N milieu with continuous agitation of the solution for 45 minutes (pH 5.0 about 1800 mOsmol, DMSO contributing 1500 mOsmol). The reaction product, lead phosphate was converted to lead sulphide by treatment of the cultures for 60 sec. with 1 per cent ammonium sulphide.

Transmission Electron Microscopy (TEM)

Subsequent to fixation in fixatives I III for 1 hour at +4 C the cells were postfixed in 2 per cent OsO in s-collidine buffer (pH 7.2) for 1 hour at room temperature. The cells were dehydrated and embedded in Epon 812 as previously described (1). Ultrathin sections were cut on an LKB Ultrotome stained with lead citrate (25) and examined in Jeol—100 C electron microscope.

Scanning Electron Microscopy (SEM)

Cells were cultured on coverslips (diameter 12 mm) or on specially cut glass pieces, 12 × 6 × 1 mm, placed in plastic Petri dishes. The cells were then fixed in one of the fixatives I III by changing the medium for the warm fixative (+37 C). Great care was taken t every step to avoid air drying of the cells during the solution changes. The cells ere postfixed in OsO in the same way as the cultures intended for TEM. The cells were dehydrated and critical point dried, as previously described (1).

The specimens were acuum coated with gold in an Edward E12 E 2 E aporation unit and were studied in Jeol JSM-S1 microscope t 10 KV or in a Jeol-100C electron microscope equipped with side entrance goniometer and a scanning attachment at 40 KV.

Liver Cells

Liver cell preparation. Rat liver parenchymal cells were prepared as described previously (5 6) by perfusion of the liver via the portal vein with a 0.05 per cent collagenase solution containing 4 mM Ca. After 6–8 minutes of perfusion, the liver cells were dissociated in Hank's balanced salt solution, buffered with HEPES and containing 2 per cent albumin. A purified parenchymal cell fraction was obtained after repeated sedimentation at low centrifugation speed. Before fixation, the cells were resuspended in Hank's HEPES solution without albumin and cell iability was checked by the trypan blue exclusion test. Only 1 3 per cent of the cells stained.

Fixation of the liver cells. 0.2 ml of the cell suspension was mixed with 9.8 ml of the fixative solutions (I III). Fixation was carried out for 12 hours at +4 C. For TEM, the cell were post fixed for 1 hour in 2 per cent OsO_4, buffered with s-collidine t room temperature.

Vol metric analysis of the liver lls. Samples of the liver cells, fixed and suspended in fixati es I III were studied as regards size distribution in a model 6300 cytograph with a model 2100 multichannel distribution analyzer (Bio Physics System Inc., Baldwin Place Road, Mahopac New York 10541 U.S.A.)

These instruments generate a size histogram and cytogram based on the light emission from single cells as they pass through a laser beam, measured within two angula ranges. The cell suspensions can thus be examined directly in their respectiv fixatives.

To ensure that the different fixati solutions did not influence the light emission, a control of previously fixed mouse thymocytes suspended in the various fixatives was run.

T ansmission electron microscopy (TEM). After fixation of the cells in glutaraldehyde (fixatives I III) and post-fixation in OsO dehydration and embedding in Epon 812 was performed as earlier reported. Thin sections, cut with an LKB Ultrotome, were stained with lead citrate (25) and examined in Jeol 100 C electron microscope.

RESULTS

In Vitro Cultivated Cells

Time-lapse micrography of glia and glioma cells in vitro. Addition of fixative I resulted in the almost immediate "freezing" of ruffling membranes and the cessation of all organell movements within 90 sec. No further morphological changes could be detected.

Fixative II and III resulted in cellular changes which were more or less identical. Time-lapse photography of these cells showed that movement of cellular organelles ceased within 10–20 sec. and was followed by the formation of bubbles, which mainly formed along the ruffling portions and the cell margin (Figs. 2 and 3). Bubbles began to form within 30 sec. of the onset of fixation and they enlarged rapidly often reaching their maximum size within 5 minutes of their appearance (Figs. 2 c and 3 c arrows). Approximately 5 minutes after the initiation of the fixation this was followed by a decrease

implies a minimum of distortion and no artifact production However should artifacts be unavoidable they must be recognized for what they are

At present the most widely accepted fixation procedure for the ultrastructural study of mammalian cells and tissues is primary fixation in buffered glutaraldehyde followed by post fixation in osmium tetroxide Glutaraldehyde fixation as opposed to osmium tetroxide fixation does not result in an immediate or total loss of the cell membranes semipermeable properties (9 10, 18 20 22, 28 29) Thus the cell is osmotically active both during and following glutaraldehyde fixation The osmotic properties of a glutaraldehyde fixative must accordingly be such that artifacts resulting from swelling or shrinking are avoided

Over the last few years evidence has accumulated showing that the total osmotic pressure of a fixative is of less importance than that of the fixative vehicle (1 2 4 12 14 15 21 23 27) The question thus arises as to what extent glutaraldehyde exerts an effective osmotic pressure in such systems. Effective osmotic pressure being the osmotic pressure produced by those molecules and ions which do not freely pass the semipermeable membrane concerned and is to be distinguished from for example the total osmotic pressure as measured by freeze point depression

In recent communications we have shown that glutaraldehyde in the case of *in vitro* cultivated glia cells and isolated mammalian liver cells appears to have no effective osmotic pressure (1 2 4)

A look at the last few years publications on the applications of electron microscopy in biology shows that many continue to use glutaraldehyde fixatives with hypotonic vehicles for the fixation of mammalian cells and tissues. We have thus studied the effects of two fixatives of this kind which are in much use and compared them to a glutaraldehyde fixative with a vehicle osmotic pressure of 300 mOsmol using cytochemistry transmission electron microscopy (TEM) scanning electron microscopy (SEM) and volumetric methods on *in vitro* cultivated cells and suspensions of liver cells. The use of cell suspensions and cell monolayers avoids all penetration problems which limit the use of tissues in such a study

MATERIAL AND METHODS

Composition of the Glutaraldehyde Fixatives Used

I 2 per cent glutaraldehyde (GA) in 0 1 M Na cacodylate HCl buffer (cac) with 0 1 M sucrose (pH 7 2 total osmolality (T) = 510 mOsmol vehicle osmolality (V) = 300 mOsmol)

II 2 per cent GA in 0 1 M cac (pH 7.2 T = 410 mOsmol V = 200 mOsmol)

III 1.5 per cent GA in 0 067 M cac with 0.033 M sucrose (pH 7 2 T = 320 mOsmol V = 170 mOsmol)

All fixatives were freshly prepared from vacuum-distilled glutaraldehyde and stock buffer and sucrose solutions. The glutaraldehyde was examined by scanning spectrophotometry between 210 and 350 nm. The absence of a peak at 235 nm was considered a criteria for purity

In Vitro Cultivated Cells

Cell lines and culture conditions. Experiments were performed on *in vitro* cultivated diploid human glia cells in phase II (17) and on an established line U-251 MG of glioma cells. The cells were derived and maintained in culture as described by *Pontén et al* (24) They were grown in Eagle's minimal essential medium (EMEM) supplemented with 10 per cent calf serum The cells were harvested for the experiments 3 days after subcultivation when they were actively dividing but still did not form a confluent layer

Time lapse micrography of cells undergoing fixation The glia and glioma cells were cultivated in 60 mm Falcon® plastic Petri dishes. Sparse cultures were studied in a Leitz inverted phase contrast microscope with a camera attachment. Cells with active ruffling membranes were selected and photographed prior to during and following the replacement of the culture medium for the different fixatives. This examination was carried out at +37 C The cell to be studied was photographed each 5 sec for the first minute and then every minute for 20 minutes following the initiation of fixation

Enzyme Cytochemistry

The cell cultures were fixed at 0 C for 60 minutes in fixatives I III After fixation the cul

in bubble size and after 10 minutes they had diminished considerably (Figs. 2 d and 3 d). From then on there were no further changes in the cellular morphology detectable with the light microscope with either of the fixatives.

Enzyme cytochemistry. At the light microscopic level, a discrete granular deposition of the final reaction product was observed in in vitro cultivated glia and glioma cells following fixation with fixative I (Fig. 4). When fixatives II and III were employed, a slight diffuse cytoplasmic and nuclear "staining" was noted (Figs. 5 and 6). The differences between the three groups were easily evaluated at light microscopy but considerably more difficult to clearly demonstrate in black and white micrographs.

Scanning electron microscopy (SEM). The interphase glia cells were flat and thinly spread with ruffling lamellae and thread like extrusions from the periphery. On the upper surface could be found occasional microvilli. The gracile ruffling membranes were often studded with slender microvilli and occasional longer microspikes (Figs. 7 and 8). The glia upper cell surfaces were smooth except for a variable number of delicate microvilli and haphazardly distributed small caveolae and pits, probably representing endocytotic invaginations. The interphase glioma cells were similar to the glia except for varying amounts of ruffling which morphologically differed from glia somewhat and an increased numbers of surface microvilli. Following fixation in fixatives II and III changes in both the glia and glioma cell surfaces morphology mainly concerned the microvilli and the ruffling membranes. These changes, interpreted as artifacts due to swelling consisted of swollen and thick ruffles which were studded with small drop-like protrusions often along the cell edges and distal swelling of the microvilli resulting in club-like structures (Figs. 9–12).

When using the low resolution scanning electron microscope JSM-S1 operating at 10 KV and using magnification ranges below 6 000, the above changes were difficult to detect. However when the scanning attachment to the Jeol-100 C which gives a maximum resolution of approximately 50 Å, was used at magnifications above 10,000, these changes were easily recognizable on most cells (c.f. inset Fig. 11).

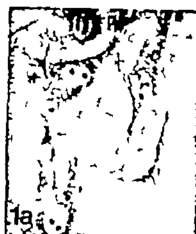
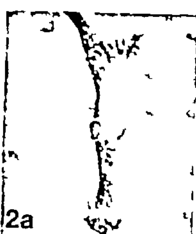
Transmission electron microscopy (TEM). Fixation of human in vitro cultivated glia and glioma cells in fixative I resulted in an apparently well preserved cellular structure. No regularly anomalous structural changes were noted following fixation in fixative II and III.

Liver Cells

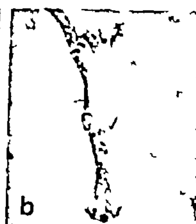
Volumetric analysis of liver Cells. In each fixative group a minimum of 8,000 liver cells were analyzed and classified according to size using 70 of the available 100 channels. The analysis of variance one way classification gave a highly significant result ($F = 253$, $p < 0.005$). The size of the liver cells in the three different groups differed significantly as compared by the *t*-test. The results are shown in Table 1.

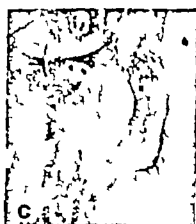
The results of the morphometric analysis of the cells following fixation in fixatives I–III are presented in histogram-form in Fig. 13 which demonstrates a shift to the right of the histograms for fixative groups II and III as compared to fixative group I. This indicates an increase in cell size. The various fixative solutions did not effect the light

Figs. 1–3 show the appearance of in vitro cultivated glia cells during fixation in various fixatives. Figs. 1 a–d, 2 per cent glutaraldehyde in 0.1 M cac and 0.1 M sucrose. Figs. 2 a–d, 2 per cent glutaraldehyde in 0.1 M cac. Figs. 3 a–d, 1.5 per cent glutaraldehyde in 0.067 M cac and 0.033 M sucrose. a, b, c and d represent 3 seconds, 30 seconds, 4 minutes and 10 minutes respectively after the start of fixation. Maximum size of the bubbles produced (swelling artifacts) are noted in Figs. and 3 (arrows). After 10 minutes fixation these bubbles have diminished considerably (Figs. 2 d and 3 d). During fixation in the fixative having a ... osmolality of 300 mOsm there is no change in morphology (Figs. 1 ... d). – × 190.


1a

2a

3a

b

b

b

c

c

c

d

d

d

in bubble size and after 10 minutes they had diminished considerably (Figs. 2 d and 3 d). From then on there were no further changes in the cellular morphology detectable with the light microscope with either of the fixatives.

Enzyme cytochemistry. At the light microscopic level, a discrete, granular deposition of the final reaction product was observed in *in vitro* cultivated glia and glioma cells following fixation with fixative I (Fig. 4). When fixatives II and III were employed a slight diffuse cytoplasmic and nuclear "staining" was noted (Figs. 5 and 6). The differences between the three groups were easily evaluated at light microscopy but considerably more difficult to clearly demonstrate in black and white micrographs.

Scanning electron microscopy (SEM). The interphase glia cells were flat and thinly spread with ruffling lamellae and thread like extrusions from the periphery. On the upper surface could be found occasional microvilli. The gracile ruffling membranes were often studded with slender microvilli and occasional longer microspikes (Figs. 7 and 8). The glia upper cell surfaces were smooth except for a variable number of delicate microvilli and haphazardly distributed small caveolae and pits, probably representing endocytotic invaginations. The interphase glioma cells were similar to the glia except for varying amounts of ruffling which morphologically differed from glia somewhat and an increased numbers of surface microvilli. Following fixation in fixatives II and III changes in both the glia and glioma cell surfaces' morphology mainly concerned the microvilli and the ruffling membranes. These changes, interpreted as artifacts due to swelling consisted of swollen and thick ruffles which were studded with small drop-like protrusions often along the cell edges and distal swelling of the microvilli resulting in club-like structures (Figs. 9–12).

When using the low resolution scanning electron microscope JSM-S1 operating at 10 KV and using magnification ranges below 6,000 the above changes were difficult to detect. However when the scanning attachment to the Jeol 100 C, which gives a maximum resolution of approximately 50 Å, was used at magnifications above 10,000, these changes were easily recognizable on most cells (c.f. inset Fig. 11).

Transmission electron microscopy (TEM). Fixation of human *in vitro* cultivated glia and glioma cells in fixative I resulted in an apparently well preserved cellular structure. No regularly anomalous structural changes were noted following fixation in fixative II and III.

Liver Cells

Volumetric analysis of liver Cells. In each fixative group a minimum of 8,000 liver cells were analyzed and classified according to size using 70 of the available 100 channels. The analysis of variance one way classification gave a highly significant result ($F = 253$ $p < 0.005$). The size of the liver cells in the three different groups differed significantly as compared by the *t*-test. The results are shown in Table 1.

The results of the morphometric analysis of the cells following fixation in fixatives I–III are presented in histogram form in Fig. 13 which demonstrates a shift to the right of the histograms for fixative groups II and III as compared to fixative group I. This indicates an increase in cell size. The various fixative solutions did not effect the light

Figs. 1–3 show the appearance of *in vitro* cultivated glia cells during fixation in various fixatives. Figs. 1 a–d, 2 per cent glutaraldehyde in 0.1 M cac and 0.1 M sucrose. Figs. 2 a–d, 2 per cent glutaraldehyde in 0.1 M cac; Figs. 3 a–d, 1.5 per cent glutaraldehyde in 0.067 M cac and 0.033 M sucrose, a, b, c and d represent 3 seconds, 30 seconds, 4 minutes and 10 minutes respectively after the start of fixation. Maximum size of the bubbles produced (swelling artifacts) are noted in Figs. 2 and 3 c (arrow). After 10 minutes fixation these bubbles have diminished considerably (Figs. 2 d and 3 d). During fixation in the fixative having vehicle osmolality of 300 mOsm there is no change in morphology (Figs. 1 a–d). × 190.

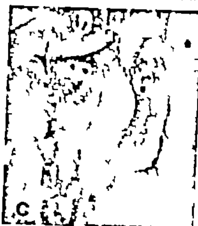
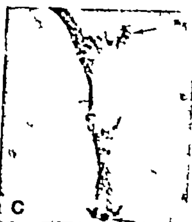

1a

2a

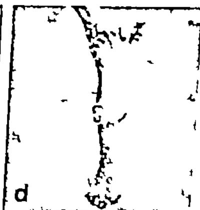
3a

b

b

b

c

c

c

d

d

d

in bubble size and after 10 minutes they had diminished considerably (Figs. 2 d and 3 d). From then on there were no further changes in the cellular morphology detectable with the light microscope with either of the fixatives.

Enzyme cytochemistry. At the light microscopic level, a discrete, granular deposition of the final reaction product was observed in *in vitro* cultivated glia and glioma cells following fixation with fixative I (Fig. 4). When fixatives II and III were employed a slight diffuse cytoplasmic and nuclear "staining" was noted (Figs. 5 and 6). The differences between the three groups were easily evaluated at light microscopy but considerably more difficult to clearly demonstrate in black and white micrographs.

Scanning electron microscopy (SEM). The interphase glia cells were flat and thinly spread with ruffling lamellae and thread like extrusions from the periphery. On the upper surface could be found occasional microvilli. The gracile ruffling membranes were often studded with slender microvilli and occasional longer microspikes (Figs. 7 and 8). The glia upper cell surfaces were smooth except for a variable number of delicate microvilli and haphazardly distributed small caveolae and pits, probably representing endocytotic invaginations. The interphase glioma cells were similar to the glia except for varying amounts of ruffling which morphologically differed from glia somewhat and an increased numbers of surface microvilli. Following fixation in fixatives II and III changes in both the glia and glioma cell surfaces morphology mainly concerned the microvilli and the ruffling membranes. These changes, interpreted as artifacts due to swelling consisted of swollen and thick ruffles which were studded with small drop-like protrusions often along the cell edges and distal swelling of the microvilli resulting in club-like structures (Figs. 9–12).

When using the low resolution scanning electron microscope JSM-S1 operating at 10 KV and using magnification ranges below 6,000 the above changes were difficult to detect. However when the scanning attachment to the Jeol 100 C, which gives a maximum resolution of approximately 50 Å, was used at magnifications above 10,000, these changes were easily recognizable on most cells (c.f. inset Fig. 11).

Transmission electron microscopy (TEM). Fixation of human *in vitro* cultivated glia and glioma cells in fixative I resulted in an apparently well preserved cellular structure. No regularly anomalous structural changes were noted following fixation in fixative II and III.

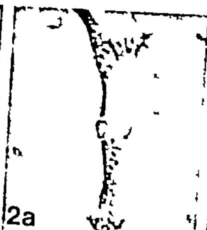
Liver Cells

Volumetric analysis of liver Cells. In each fixative group a minimum of 8,000 liver cells were analyzed and classified according to size using 70 of the available 100 channels. The analysis of variance one way classification gave a highly significant result ($F = 253$ $p < 0.005$). The size of the liver cells in the three different groups differed significantly as compared by the t-test. The results are shown in Table I.

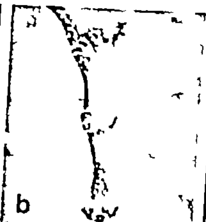
The results of the morphometric analysis of the cells following fixation in fixatives I–III are presented in histogram-form in Fig. 13 which demonstrates a shift to the right of the histograms for fixative groups II and III as compared to fixative group I. This indicates an increase in cell size. The various fixative solutions did not effect the light

---

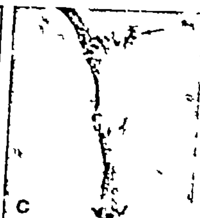
Figs. 1–3 show the appearance of *in vitro* cultivated glia cells during fixation in various fixatives. Figs. 1 a–d, 2 per cent glutaraldehyde in 0.1 M cac and 0.1 M sucrose. Figs. 2 a–d, 2 per cent glutaraldehyde in 0.1 M cac. Figs. 3 a–d, 1.5 per cent glutaraldehyde in 0.067 M cac and 0.035 M sucrose. a, b, c and d represent 3 seconds, 30 seconds, 4 minutes and 10 minutes respectively after the start of fixation. Maximum size of the bubbles produced (swelling artifacts) are noted in Figs. 2 and 3 c (arrows). After 10 minutes fixation these bubbles have diminished considerably (Figs. 2 d and 3 d). During fixation in the fixative having vehicle osmolality of 300 mOsm there is no change in morphology (Figs. 1 a–d). × 190.


1a

2a

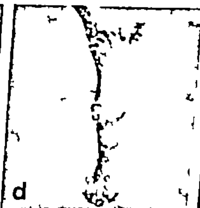
3a

b

b

b

c

c

c

d

d

d


4
5
6

TABLE 1 *Comparison between the 3 Fixatives using paired t-tests*

FIX I			FIX II			FIX III				
n	$\bar{x}$	SD	n	$\bar{x}$	SD	n	$\bar{x}$	SD	t	p
8261	37 6	15 4	8985	40 4	15 8				12.0	0.001
8261	37 6	15 4				9168	42.8	14.6	23 0	0.001
			8985	40 4	15.8	9168	42.8	14 6	10 6	0 001

emission as judged by the measurements of thymocyte size

Transmission electron microscopy (TEM) After primary fixation of the isolated liver parenchymal cells in fixative I the cell sap had a homogenous dense appearance The endoplasmic reticulum was regular with thin cisternal lumina (Fig 14) Both fixatives II and III resulted in a somewhat different cellular structure, the cisternae of the endoplasmic reticulum being generally irregularly dilated (Figs. 15–16) No obvious differences could be observed in the structure of mitochondria lysosomes and Golgi apparatus when comparing the results obtained with the three fixatives.

DISCUSSION

Since the introduction of glutaraldehyde as a fixative agent by Sabatini Bensch and Barrnett (26) this aldehyde has been extensively used. It is now recognized as the most suitable of the aldehydes for the routine fixation of biological material for ultrastructural examination (16 18 19) Usually aldehyde fixation is followed by postfixation in osmium tetroxide before further processing With both glutaraldehyde and osmium tetroxide a great number of different vehicles have been used, including various buffers and electrolytes, also non-electrolytes such as sucrose glucose or macromolecules such as dextran (8 16)

The results have been generally empirically evaluated following the study of sections of biological materials in the transmission electron microscope *without* the use of quantifiable parameters. In the last few years, other methods have been utilized such as physical measurements of swelling or shrinking, (1 23) redistribution of intracellular enzymes (2 14) evaluation with the scanning electron microscope (1 4 11 12) and time-lapse filming studies during fixation (1, 4)

As a result of such investigations, glutaraldehyde fixatives nowadays usually contain vehicles based on phosphate or cacodylate buffers with or without sucrose as a non-electrolyte additive.

It has become increasingly accepted that the total osmotic pressure of the fixative solution is of minor importance as compared to the osmotic pressure of the vehicle. It has been found that the vehicle should be more or less isotonic with the solution surrounding the cells in their lifetime (1 4 9 10 12, 14 21 27) This means that the total osmotic pressure of the fixative solution is distinguished from the solutions effective osmotic pressure. It has recently been demonstrated that glutaraldehyde apparently does not add to the effective osmotic pressure, while sucrose and cacodylate ions do so (1 4)

Even if it seems to be generally accepted

Figs 4 6 depict the result of the cytochemical demonstration of acid phosphatase on in vitro cultivated glia cells. Fig 4 shows a distinct granularity following fixation in fixative I (2 per cent glutaraldehyde 0 1 M cac 0 1 M sucrose while *Figs. 5 and 6 demonstrate diffusion* artifacts following fixation in fixative II (2 per cent glutaraldehyde, 0 1 M cac) and III (1 5 per cent glutaraldehyde 0 067 M cac 0 033 M sucrose) respectively × 780

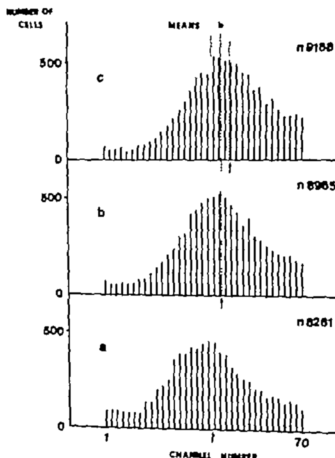


Fig. 13 Size distribution histograms of isolated liver cells fixed in fixatives I, II and III (a, b and c respectively). Each bar represents the number of cells in two channels. n = number of cells analyzed. Means are indicated by dotted lines.

that the vehicle osmolality is of great importance and should be iso-osmotic to the fluid normally surrounding the cells being studied, it is still rather common to find in the literature expressions like "the tissues were fixed in buffered 3 per cent glutaraldehyde" or that vehicles such as 0.1 M cacodylate or phosphate buffers without further additives have been used. In the first case, it is obviously not at all possible to judge whether or not the fixation might have resulted in a change of the initial volume of the tissue. In the latter case, present knowledge indicates that the material really has changed its volume and has become somewhat swollen.

The aim of this paper has been to investigate in some detail, using various methods, the result of fixation in three *different* fixatives which are frequently used today. All fixatives are based on glutaraldehyde and sodium cacodylate HCl buffer. Two of them also contain sucrose. One of the fixatives (fixative I) has been used by us for a number of years for different cytochemical and morphological investigations. The two others

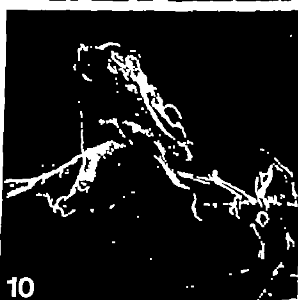
---

Figs 7–12 show the SEM appearance of the cells following fixation in fixative I (Figs 7 and 8), fixative II (Figs 9 and 10) and fixative III (Figs 11 and 12). Note gracile ruffling membranes in Figs 7 and 8 and distorted, clumsy ruffling membranes and microvilli with swollen tips in Figs 9–12. Note in Fig 11 that in low magnification the elements of the ruffling membrane is difficult to evaluate while it is evident at higher magnification (inset). Fig 7 × 12,000, Fig 8 × 15,000, Fig 9 × 12,000, Fig 10 × 15,000, Fig 11 × 4,500, inset 15,000, Fig 12 × 30,000

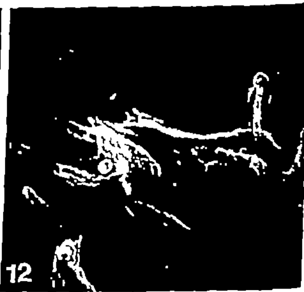

7


8


9


10


11


12

(fixative II and III) are commonly reported in the current literature.

It became obvious from the analysis of the mean volumes of fixed populations of suspended liver cells that both fixatives II and III gave rise to significant swelling. Using time-lapse micrography of glia cells during fixation followed by scanning electron microscopy it was evident that this swelling was more pronounced in certain areas. It appeared that structures like ruffling membranes and microvilli are especially fragile. It is not clear why hypotonic swelling tends to especially affect ruffles and microvilli, although it is possible that these structures, due to their low radii of curvature, are more permeable than other parts of the cell surface (22).

The shrinking of the bubbles from their maximum size during further fixation is a phenomenon not understood. It is possible that this shrinking may be due to a lowering of the intracellular osmotic pressure by the loss of diffusible substances (23) and or by molecular cross-linking during the fixation process.

The cytochemical demonstration of acid phosphatase following fixation in fixative I showed a distinct granular "staining". A rather indistinct picture with a diffusely distributed reaction product in the cytoplasm, and also nuclear staining, followed fixation in fixatives II and III. This observation shows the possibility of demonstrating minor deviations in the effective osmotic pressure of a fixative with rather simple methods. This method for detecting intracellular redistribution of cytoplasmic proteins (in this case the lysosomal enzyme acid phosphatase) has been used by us previously in studies on fixation (14). It is thus possible obviously to obtain a diffuse reaction product only by the use of incorrect fixation.

It was found that transmission electron microscopy probably was the least sensitive method for the detection of artifactual swelling possibly because the inevitable shrinking during embedding in plastic can diminish the effects of the previous swelling. The fact that an electron micrograph is a two-dimensional projection of the original three-dimensional object adds to the difficulty. We found the regular ER of the liver cells constantly changed due to hypotonic fixation. Glia and especially glioma cells lack this uniformity of ER cisternae, and possible changes could thus not be easily evaluated. Changes in the configuration of the mitochondria—generally accepted as being the "osmometers" of the cell—were not observed with any consistency in the cells following fixation in fixative II and III.

Even if changes following fixation in the hypotonic fixatives may be small and difficult to detect with some methods, we consider them important when interpreting the results from scanning and transmission electron microscopy, cytochemistry and stereology. The evaluation and interpretation of pathological processes at the cellular level will not be simplified if fixation artifacts are superimposed on the sometimes subtile structural changes.

Figs. 14–16 show the appearance in TEM of hepatocytes following fixation in fixative I (Fig. 14), fixative II (Fig. 15) and fixative III (Fig. 16). Observe the dilatation of the rough endoplasmic reticulum cisternae after fixation in fixatives II and III. Fig. 14 × 36,000. Fig. 15 × 36,000. Fig. 16 × 30,000.

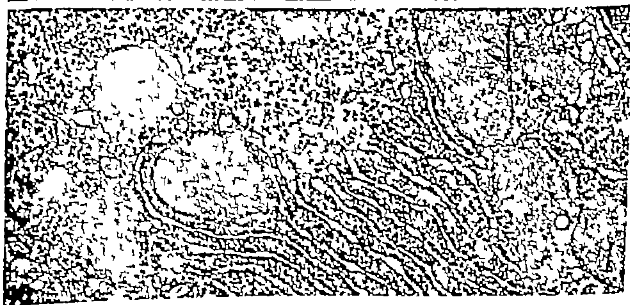
This investigation was supported by grants from the *Swedish Medical Research Council* and *Stockholms Cancer Society*.

REFERENCES

1. *Arborgh, B., Bell, P., Brunk, U. & Collins, V. P.:* The osmotic effect of glutaraldehyde. J Ultrastruct. Res. 56, 339–350, 1976.
2. *Arborgh, B., Brunk, U. & Ericsson, J. L. E.:* Osmotic pressure and other factors influencing the fine structure and localization of acid phosphatase in glutaraldehyde-fixed cells and tissues. 8th Int. Congr. on Electron Microscopy, Canberra, Vol. II, pp. 146–147.
3. *Barka, T. & Anderson, P. J.:* Histochemical methods for acid phosphatase using hexa-







Acta path. microbiol. scand. Sect. A, 85 169–173 1977

IMMUNOHISTOCHEMICAL DEMONSTRATION OF LYSOZYME IN THE LYMPH NODES AND KVEIM REACTION PAPULES IN SARCOIDOSIS

MATTI KLOCKARS and OLOF SELROOS

IV Department of Medicine, Helsinki University Central Hospital Helsinki, Finland

Klockars, M. & Selroos, O Immunohistochemical demonstration of lysozyme in the lymph nodes and Kveim reaction papules in sarcoidosis. Acta path. microbiol. scand. Sect. A, 85 169–173, 1977

Lysozyme (LZM) was demonstrated by an immunoperoxidase method in some but not all epithelioid-cell granulomas, free macrophages and giant cells in the lymph nodes and Kveim reaction papules of patients with sarcoidosis. I nactive disease, LZM staining was weak or absent in fibrotic lymph nodes The pattern of LZM staining in K eim reaction papules was similar to that seen in the "active" sarcoid lymph nodes. The presence of LZM in sarcoid tissue explains the high concentration of serum LZM in patients with activ sarcoidosis and the extent of LZM distribution in tissues is probably an index of disease activity

Key words Sarcoidosis lysozyme immunohistochemistry

Matti Klockars, IV Department of Medicine, Unionsgatan 38, SF-00170 Helsinki 17 Finland.

Received 24.ix.76 Accepted 5.x.76

Lysozyme (LZM) is present in high concentrations in certain inflammatory cells, such as neutrophilic granulocytes and mononuclear phagocytes (3 11 13) Raised concentrations of LZM in serum in a variety of granulomatous inflammatory diseases includ ing tuberculosis (16) sarcoidosis (14 15) and Chron s disease (5) have been reported. Moreover the concentration of serum LZM has been correlated with clinical disease acti ity (6 15) There is now evidence that LZM originates in part in the mononuclear phagocytes that participate in the granulomatous inflammation (13)

To learn more about the distribution of LZM in sarcoid tissue we studied the pat tern of LZM staining in lymph nodes and Kveim positive papules of patients with sar coidosis.

PATIENTS AND METHODS

W examined biopsy specimens from the lymph nodes of four patients with sarcoidosis and the K eim positive papules from three others. All patients fulfilled the criteria for sarcoidosis defined by the Second International Conference on Sar coidosis, Washington DC 1960. All had marked supraclavicular mediastinal or bilateral lymphadenopathy and/or pulmonary infiltrates. The Kveim reactivity was tested as described elsewhere (17)

LZM was demonstrated by an immunoperoxidase method (11) Briefly the tissue LZM of glutaraldehyde fixed, paraffin-embedded and conventionally processed tissue sections was visualized by an immunoglobulin-enzyme bridge method involving the separate application of three antisera, i.e. rab-

xonium pararosanilin as coupler J Histochem Cytochem. *10* 741–753 1962.
4 *Bell P B Brunk U Collins P Forsby A & Fredriksson B A* SEM of cells in culture Osmotic effects during fixation *in* Scanning Electron Microscopy O Johari and I Corvin, eds. ITT Research Institute Chicago, Illinois p. 380–386 1975
5 *Berg T Boman D & Seglen P O* Induction of tryptophan oxygenase in primary rat liver cell suspensions by glucocorticoid hormone Exptl Cell Research *72* 571–574 1972.
6 *Berry A M & Friend D S* High-yield preparation of isolated rat liver parenchymal cells a biochemical and fine structural study J Cell Biol *43* 506–520 1969
7 *Biberfeld P* A method for the study of monolayer cultures with preserved cell orientation and interrelationship. J Ultrastruct. Res. *25* 158–159 1968.
8. *Bohman S-O & Maunsbach A* Additions of dextran to glutaraldehyde fixatives effects on tissue fine structure J Ultrastruct. Res. *25* 171 1968.
9 *Bone Q & Denton E J* The osmotic effects of electron microscope fixatives. J Cell Biol. *49* 571–581 1971
10 *Bone Q & Ryan K P* Osmolarity of osmium tetroxide and glutaraldehyde fixatives. Histochem. J *4* 331–347 1972.
11 *Boyde A* Biological specimen preparation for the scanning electron microscope—an overview *in* Scanning Electron Microscopy O Johari and I Corvin eds. ITT Research Institute Chicago Illinois, p. 265–272 1972.
12 *Boyde A & Vesely P* Comparison of fixation and drying procedure for preparation of some cultured cell lines for examination in the SEM *in* Scanning Electron Microscopy O Johari and I Corvin, eds. ITT Research Institute, Chicago, Illinois p 265–272 1972
13 *Brunk U Ericsson J L E Pontén J & Westermark B* Specialization of cell surfaces in contact inhibited human glia like cells in vitro Exptl Cell Res. *67* 407–415 1971
14 *Brunk U & Ericsson J L E* The demonstration of acid phosphatase in vitro cultured tissue cells. Studies on the significance of fixation, tonicity and permeability Histochem J *4* 349–363 1972
15 *Fahimi H D & Drochmans P* Essais de standardisation de la fixation au glutaraldéhyde. II Influence des concentrations en aldéhyde et de l'osmolalité J Microscopie *4* 737–748 1965
16 *Hayat M A* *in* Principles and Techniques of Electron Microscopy Vol 1 p. 5 Van Nostrand Reinhold Company New York, 1970
17 *Hayflick L.* Senescence and cultured cells. Persp. Exptl. Gerontol *14* 195–211 1966.
18 *Hopwood D* Fixatives and fixation—a review Histochem. J *1* 323–360 1969
19 *Hopwood D* Theoretical and practical aspects of glutaraldehyde fixation Histochem J *4* 267–303 1972
20 *Jard S Bourguet J Carasso N & Favard, P* Action de divers fixateurs sur la perméabilité et l ultrastructe de la vessie de grenouille J Microscopie *5* 31–50 1966.
21 *Maunsbach A B* The influence of different fixatives and fixation methods on the ultrastructure of rat kidney proximal tubule cells J Ultrastruct. Res. *15* 283–309 1966
22 *Oschman J L. Wall B J & Gupta, B. L.* Cellular basis of water transport. Symp. Soc. Exptl Biol. *28* 305–350 1974
23 *Penttila A Kalimo H & Trump B F* Influence of glutaraldehyde and/or osmium tetroxide on cell volume ion content, mechanical stability and membrane permeability of Ehrlich ascites tumor cells. J Cell Biol. *63* 197–214 1974
24 *Pontén J Westermark B & Hugosson P* Regulation of proliferation and movement of human glia like cells in culture. Exptl. Cell Res. *58* 393–400 1969
25 *Reynolds E S* The use of lead citrate at high pH as an electronopaque stain in electron microscopy J Cell Biol *17* 208–212 1963
26 *Sabatini D D Bensch K & Barrnett R. J* Cytochemistry and electron microscopy J Cell Biol. *17* 19–58 1963
27 *Schultz R L & Karlsson U* Fixation of the central nervous system for electron microscopy by aldehyde perfusion. II Effect of osmolality pH of perfusate, and fixative concentration J Ultrastruct. Res. *12* 187–206, 1965
28. *Tooze J* Measurement of some cellular changes during fixation of amphibian erythrocytes with osmium tetroxide solutions. J Cell Biol *22* 551–563 1964
29 *Tormey J McD* Artifactual localization of ferritin in the ciliary epithelium in vitro. J Cell Biol *25* 1–7 1965



Fig. 4 LZM-positive macrophages, giant cells and the formation of epitheloid cell granulomas in a Kveim reaction papule. Magnification 100 ×

Fig. 5 Higher magnification of LZM-positive cells in an epitheloid cell granuloma in a Kveim reaction papule. Epidermis did not stain for LZM. Magnification 240 ×

RESULTS

The presence of epitheloid cell granulomas, giant cells and fibrosis in the lymph nodes was histopathologically typical of sarcoidosis. Most epitheloid cell granulomas contained intense LZM activity (Fig. 1). These LZM positive granulomas were usually fresh, whereas epitheloid cells within fibrotic areas did not stain for LZM. Within the granulomas, various numbers of epitheloid cells exhibited a granular cytoplasmic LZM staining (Fig. 2). In giant cells, the staining was homogenous and gauze-like but less intense than that of epitheloid cells (Fig. 3).

The Kveim reaction papules contained numerous LZM positive cells and cell clusters including free macrophages, giant cells and epitheloid-cell granulomas (Fig. 4, 5). The cytoplasmic LZM staining of these cells was similar to that of the corresponding cell types in the sarcoid lymph nodes. The epidermis, dermal collagen and invading lymphocytes of the papules contained no LZM.

DISCUSSION

The development of granulomas in sarcoidosis and Kveim reactions involves a generalized activation of monocytes and macrophages and a transformation of these cells into epitheloid cells and giant cells. Our results support the observation of *Mason & Taylor* (13) that these cells are involved in the secretion of LZM. One of the morphological and biochemical changes that accompany the transformation of monocytes into macrophages and epitheloid cells is the increased synthesis of lysosomal enzymes including LZM in these cells (5, 18). Consistent with previous reports on the distribution of other lysosomal enzymes was the variability with which epitheloid cells in granulomas stained for



Fig 1 LZM positive free macrophages and epitheloid cell granulomas of a sarcoid lymph node. Note that some granulomas do not contain LZM (left) Lymphocytes did not stain for LZM Counterstained with cresyl echt violet Magnification 100 ×

Fig 2 Higher magnification of an epitheloid cell granuloma Magnification 240 ×

Fig 3 A LZM positive giant cell with homogenous and gauze-like cytoplasmic LZM staining. Magnification 400 ×

bit anti human LZM (dilution 1 200) sheep anti-rabbit globulin antiserum (Sycco Sylvana, N J USA) (dilution 1 20) and rabbit anti-horseradish peroxidase (dilution 1 150) After it had reacted with its antiserum horseradish peroxidase (Type VI Sigma Chemical Co) was stained by the method of *Graham & Karnovsky* (9) To test the immunospecificity of the "bridge" control sections were stained in a similar manner except that the primary antiserum was rabbit anti hen egg white LZM known to be immunologically different from its human counterpart. All sections were counter stained with cresyl echt violet (Chroma Stuttgart Untertürkheim Germany)

14 *Osserman E. F. & Lawlor D. P.* Serum and urinary lysozyme (muramidase) in monocytic and monomyelocytic leukemia. J. exp. Med. *124* 921–952, 1966.

15. *Pasqual R. S., Gee J. B. L. & Finch S. C.* Usefulness of serum lysozyme measurement in diagnosis and evaluation of sarcoidosis. New Engl. J. Med. *289* 1074–1076, 1973.

16. *Perillie P. E., Khan K. & Finch S. C.* Serum lysozyme in pulmonary tuberculosis. Amer. J. Med. Sci. *265* 297–302, 1973.

17 *Selroos O.*, The frequency, clinical picture and prognosis of pulmonary sarcoidosis in Finland. Acta med. scand. Suppl. *503* 1–73 1969

18. *Sutton J. S. & Weiss L.*, Transformation of monocytes in tissue culture into macrophages, epitheloid cells and multinucleated giant cells. J. cell. Biol. *28* 303–332, 1966.

19 *Tsuda T., Dannenberg, A. M. Jr., Ando M., Rojas-Espinosa O. & Shima, K.*, Enzymes in tuberculous lesions hydrolyzing protein, hyaluronic acid and chondroitin sulfate. A study of isolated macrophages and developing and healing rabbit BCG lesions with substrate film techniques: the shift of enzyme pH optima towards neutrality in "intact" cells and tissues. J. Reticuloendothel. Soc. *16* 220–231 1974

LZM some cells staining intensely and others not at all staining. Such variability has been reported to apply also to the proteinases and enzymes that hydrolyse hyaluronic acid and chondroitin sulphate in dermal BCG lesions (19) and to the acid phosphatase in sarcoid granulomas (7). This variability in LZM activity among epitheloid cells both in sarcoidosis and Kveim reaction papules is most likely related to the various stages of their development, each stages being marked by changes in their cytoplasmic constituents (8-10).

It is not known whether LZM during the events of granuloma formation as outlined by *Chapman* (2) non-specifically accompanies the macrophage responses or whether it also participates in the intra- or extracellular processing of an undefined antigen. The cellular distribution of certain other lysosomal enzymes, e.g. β-galactosidase, β-glucuronidase and acid phosphatase has been shown to be associated with the local presence of bacilli of tuberculous granulation tissue (4). The discharge of lysosomal enzymes into the extracellular environment during late stages of epitheloid and giant cell development might cause an extracellular milieu in which LZM enhances the local immunoglobulin induced bacteriolysis (1) and phagocytic activity (12).

Our results might also explain why the acute stages of sarcoidosis, when many active macrophages infiltrate the tissues, are accompanied by raised concentrations of plasma LZM whereas in burnt-out sarcoidosis the considerable disappearance of LZM from fibrous tissue lesions might cause the reversal to normal concentrations of plasma LZM. We believe that the immunohistochemical demonstration of LZM in sarcoid tissue gives additional information about the activity of disease over and above the determinations of LZM activity in plasma.

This study was supported by grants from the *Finnish Antituberculosis Association* and the *S. and Jusélius Foundation*, Finland.

REFERENCES

1. *Adinolfi M., Glynn A. A., Lindsay M. & Milne C.* Serological properties of γA antibodies to Escherichia coli present in human colostrum. Immunology *10*: 517–526, 1966.
2. *Chapman J. S.* The pathogenesis of granuloma formation. Proceedings of the Fifth International Conference on Sarcoidosis, Prague, University of Karlova Press, 1971, pp. 105–109.
3. *Cohn Z. A. & Benson B.* The differentiation of mononuclear phagocytes. Morphology, cytochemistry and biochemistry. J. exp. Med. *121*: 152–169, 1965.
4. *Dannenberg A. M. Jr., Meyer O. T., Esterly J. R. & Kambara T.* The local nature of immunity in tuberculosis, illustrated histochemically in dermal BCG lesions. J. Immunol. *100*: 931–941, 1968.
5. *Falchuk K. R., Perrotto J. L. & Isselbacher K. J.* Serum lysozyme in Crohn's disease and ulcerative colitis. New Engl. J. Med. *292*: 395–397, 1975.
6. *Falchuk K. R., Perrotto J. L. & Isselbacher K. J.* Serum lysozyme in Crohn's disease. A useful index of disease activity. Gastroenterology *69*: 893–896, 1975.
7. *Fukushiro R., Hirone T. & Eryo I.* Ultrastructural and cytochemical observations on sarcoid granulomas. Proceedings of the Sixth International Conference on Sarcoidosis, Tokyo, University of Tokyo Press, 1973, pp. 276–279.
8. *Fuse Y. & Hiraga Y.* The fine structure of sarcoidal and Kveim granulomas. Proceedings of the Sixth International Conference on Sarcoidosis, Tokyo, University of Tokyo Press, 1973, pp. 269–275.
9. *Graham R. C. & Karnovsky M. J.* The early stages of absorption of injected horseradish peroxidase in the proximal tubules of mouse kidney. Ultrastructural cytochemistry by a new technique. J. Histochem. Cytochem. *14*: 291–302, 1966.
10. *Gusek W. & Behrend H.* The Kveim granuloma. A comparative study on formal genesis and electron microscopical structure. Proceedings of the Fifth International Conference on Sarcoidosis, Prague. University of Karlova Press, 1971, pp. 124–126.
11. *Klockars M. & Reitamo S.* Tissue distribution of lysozyme in man. J. Histochem. Cytochem. 29: 932–940, 1975.
12. *Klockars M. & Roberts P.* Stimulation of phagocytosis by human lysozyme. Acta Haemat. *55*: 289–295, 1976.
13. *Mason D. Y. & Taylor C. R.* The distribution of muramidase (lysozyme) in human tissues. J. clin. Path. *28*: 124–132, 1975.

Care Unit, Department II Copenhagen Municipal Hospital, on account of disturbed a.-v. conduction and who died after a course including different dysrhythmias.

PATIENTS AND TECHNIQUE

The Coronary Care Unit of the Copenhagen Municipal Hospital has earlier been described (*Christiansen et al. 1971*). Throughout a two-year-period we have selected the patients who died during their stay in the Unit because of clinical coronary occlusion and who, during the monitoring, showed serious dysrhythmias: their hearts were thoroughly studied, particularly with regard to the conduction system.

The rhythm of each patient was stored during the entire period of hospitalization and was daily read from tape-recorder by one of us (E.S.). The autopsies were performed at the Department of Pathology Copenhagen Municipal Hospital, whereas the heart examinations were made at the University Institute of Forensic Medicine Copenhagen, one of us (J. V.).

The autopsy technique was as follow. After the heart had been measured the coronary arteries were cut open as far as possible using a pair of scissors and the changes were evaluated. Then the heart was cut into slices, approximately 3/4 cm in thickness, from the apex to the atrioventricular valves perpendicularly to the axis, and finally the rest was cut open in the traditional way. All the pieces were weighed after removal of blood clots. The thickness of the ventricular walls was measured and the extent and localization of the pathological changes in the myocardium were evaluated, which was quite easy by the autopsy technique used. It was decided whether the circumflex branch of the left coronary artery or the continuation of the right coronary artery was the dominant branch, i.e. which of these arteries was passing the crux cordis on the inferior face of the heart and giving off the branch to the a.-v. node.

The histological technique was almost in accordance with H dson method (1965). The sinus node was found in one or more blocks from the right superior [illegible] junction (Hudson [illegible]) and the a.-v. system was found in a block comprising the adjacent parts of the atrial and ventricular septum from the ostium sinus coronarii to [illegible] well in front of the membraneous septum. This block was divided into two through the posterior part of the membraneous septum, and each half was cut in serial sections, 5 microns thick, from the dividing plane and forwards and backwards, respectively. Every 20th section was stained, and this procedure was continued until the whole system had been investigated in this way. The stains used have been Sirius Red/Celestin Blue and Goldner trichrome staining: the latter will only exceptionally give information of any value. We find that this method is fairly good, sufficient and practicable in investigations of the relevant changes in the sinus node and conduction system. It is hardly probable that significant changes could have been present only in the discarded sections.

The histopathological evaluation has been "blind" i.e. the investigator had not in advance been informed about the clinical findings, incl. the findings by electrocardiography (e.c.g.).

Good correlation between the e.c.g. findings and the histopathology of the conduction system means that we have found atrio-ventricular or intraventricular conduction disturbances and significant changes at relevant localizations in the conduction system. Relatively good correlation means conduction disturbances combined with slight changes at relevant localization. The correlation is dubious if conduction disturbances and only very slight changes were found in the expected parts of the conduction system.

Definition of Intraventricular and Atrioventricular Blocks

Right bundle branch block (RBBB): QRS-duration ≥ 0.12 sec. M-configuration in V_{1-2}, broad S-waves in I and V_{5-6}.

Left bundle branch (LBBB): QRS-duration ≥ 0.12 sec. M-configuration in V_{5-6} and broad S-waves in V_{1}.

Incomplete intraventricular blocks were of the same form, but QRS-duration < 0.12 sec. *As regards atrio-ventricular A.V. blocks* we have listed A-V blocks of second degree (2°) when 2:1 block, Mobitz type I or II were present. Total A-V block is listed as 3° A-V block.

Permanent intraventricular and atrioventricular blocks were present in patients throughout their stay in hospital, whereas the transient blocks appeared and disappeared during the hospitalization.

RESULTS

The series comprises 9 patients, 2 females and 7 males of ages ranging from 54 to 84 years, on the average 70 years.

The case histories appear from *Table I*. Three patients had previously experienced acute myocardial infarction (AMI). Patient no. 9 is exceptional in that he did not present any cardiac symptoms: this patient was admitted on account of a varicose ulcer; pneumonia developed and he was transferred to

Acta path microbiol scand Sect. A 85 174-182 1977

HISTOPATHOLOGY OF THE CONDUCTION SYSTEM IN PATIENTS WITH ATRIO-VENTRICULAR OR INTRAVENTRICULAR CONDUCTION DISTURBANCES

J Voigt and E. Steinmetz

University Institute of Forensic Medicine Copenhagen and Copenhagen Municipal Hospital, Department II Copenhagen, Denmark

Voigt J & Steinmetz, E. Histopathology of the conduction system in patients with atrioventricular or intraventricular conduction disturbances. Acta path microbiol scand. Sect. A, 85 174-182 1977

In 9 lethal cases where clinical signs gave rise to the suspicion of acute myocardial infarct (AMI) where well-characterized e.c.g.-changes, permanent or intermittent, were found by monitoring, a very careful autopsy of the heart was carried out, combined with a meticulous histological investigation of the conduction system. Acute changes of mild degree in the conduction system were found only in one case possibly explaining the left bundle branch block found in this case In the remaining cases nothing but chronic changes were found and they did not exceed significantly the changes otherwise to be found in the agegroups concerned in a "control series" of violent deaths not preceded by symptoms of heart disease According to an estimate there was good correlation between the conduction disturbances demonstrated and the localization of histopathological changes in seven of nine patients in one of the latter correlation was relatively good correlation was dubious only in one case. On this basis the authors conclude that present changes in the conduction system which are assumed mainly to be age related are the factors to determine the type of conduction disturbances from which the patient will suffer if acute heart ischaemia sets in for instance due to an AMI in fact, changes by which he will be predisposed to such disturbances.

Key words Conduction system atrioventricular and intraventricular disturbances histopathology

J Voigt, University Institute of Forensic Medicine Frederik den Femtesvej 11 DK 2100 Copenhagen Denmark.

Received 20 vii.76 Accepted 8.x.76

The introduction of continuous electrocardiographic monitoring in coronary care units has made it possible to show that temporary and/or more permanent conduction disturbances are complications that are much more frequent than previously realized and – in fatal cases – to correlate the dysrhythmias, especially the atrio-ventricular (a. v.) conduction disturbances to the histology of the conduction system

In order to study this relationship we have examined in detail the hearts from nine patients who were admitted to the Coronary

Care Unit, Department II Copenhagen Municipal Hospital, on account of disturbed a-v conduction and who died after a course including different dysrhythmias.

PATIENTS AND TECHNIQUE

The Coronary Care Unit of the Copenhagen Municipal Hospital has earlier been described (Christiansen *et al.* 1971) Throughout a two-year-period we have selected the patients who died during their stay in the Unit because of clinical coronary occlusion and who, during the monitoring, showed serious dysrhythmias their hearts were thoroughly studied, particularly with regard to the conduction system.

The rhythm of each patient was stored during the entire period of hospitalization and was daily read from tape-recorder by one of us (E.S.). The autopsies were performed at the Department of Pathology Copenhagen Municipal Hospital whereas the heart examinations were made at the University Institute of Forensic Medicine Copenhagen, by one of us (J. V.)

The autopsy technique was as follow After the heart had been measured the coronary arteries were cut open as far as possible using pair of scissors and the changes were evaluated Then the heart was cut into slices, approximately 3/4 cm in thickness from the apex to the atrioventricular plane perpendicularly to the axis, and finally the rest was cut open in the traditional way All the pieces were weighed after removal of blood clots. The thickness of the ventricular walls was measured and the extent and localization of the pathological changes in the myocardium were evaluated, which is quite easy by the autopsy technique used. It was decided whether the circumflex branch of the left coronary artery or the continuation of the right coronary artery was the dominant branch, which of these arteries was passing the crux cordis on the inferior face of the heart and giving off the branch to the a-v node

The histological technique was almost in accordance with *Hudson's* method (1965) The sinus node was found in one or more blocks from the right superior atriocaval junction (*Hudson* ...) and the a-v system was found in a block comprising the adjacent parts of the atrial and ventricular septum from the ostium sinus coronarii to ... well in front of the membraneous septum. This block was divided into two through the posterior part of the membraneous septum, and each half was cut serial sections, 5 microns thick, from the dividing plane and forwards and backwards, respectively. Every 20th section was stained, and this procedure was continued until the whole system had been investigated in this way. The stains used have been Sirius Red/Celestin Blue and Goldner trichrome staining the latter will only exceptionally give information of any value. We find that this method is fairly good, sufficient and practicable in investigations of the relevant changes in the sinus node and conduction system. It is hardly probable that significant changes could have been present only in the discarded sections.

The histopathological evaluation has been "blind" i.e. the investigator had not in advance been informed about the clinical findings, incl. the findings by electrocardiography (e.c.g.)

Good correlation between the e.c.g. findings and the histopathology of the conduction system means that we have found atrio-ventricular or intraventricular conduction disturbances and significant changes at relevant localizations in the conduction system. Relatively good correlation means conduction disturbances combined with slight changes at relevant localization. The correlation is dubious if conduction disturbances and only very slight changes were found in the expected parts of the conduction system

Definition of Intraventricular and Atrioventricular Blocks

Right bundle branch block (RBBB) QRS-duration ≥ 0.12 sec. M-configuration in V_{1-2}, broad S-waves in I and V_{5-6}.

Left bundle branch (LBBB) QRS-duration ≥ 0.12 sec M-configuration in V_{5-6} and broad S-waves in V_{1-2}.

Incomplete intraventricular blocks were of the same form, but QRS-duration < 0.12 sec. As regards *atrio-ventricular A.V. blocks* we have listed A-V blocks of second degree (2°) when 2:1 block, Mobitz type *I* or *II* were present Total A V block is listed as 3° A V block.

Permanent intraventricular and atrioventricular blocks were present in patients throughout their stay in hospital, whereas the transient blocks appeared and disappeared during the hospitalization.

RESULTS

The series comprises 9 patients, 2 females and 7 males of ages ranging from 54 to 84 years, on the average 70 years.

The case histories appear from *Table 1*. Three patients had previously experienced acute myocardial infarction (AMI) Patient no. 9 is exceptional in that he did not present any cardiac symptoms this patient was admitted on account a varicose ulcer pneumonia developed and he was transferred to

TABLE 1 *Clinical Features*

Age	Clinical history	Interval between onset of symptoms and death	Clinical course	Cause of dea
4	No past history of heart disease only some dyspnoea on exertion. Admitted after precordial pain had persisted for 7 days.	9 days	1 day after admission, therapy resistant cardiogenic shock occurred.	Cardiogenic
3	During 6 years hypertension. 1970 myocardial infarction Precordial pain for 5 days before admission re-infarction 1 week later in hospital died 9 days after this.	23 days	After re-infarction, increasing heart failure died 18 days after admission.	Pulmonary e bolism.
	No information available possibly precordial pain before admission	?	Admitted with therapy-resistant cardiogenic shock died after a few hours in hospital.	Cardiogenic shock —
	Angina pectoris for some months Admitted with severe precordial pain of 1 day's duration	5 days	4 days after admission sudden deterioration and death in cardiogenic shock.	Rupture of the anterior wall of the heart.
	Slight precordial pain for 10 days, severe for a few hours. Rheum. fever of 17 years standing.	10 days, only severe pain for a few hours	Transvenous pacemaker because of 3 A V block Died in cardiogenic shock	Cardiogenic shock
	Acute myocardial infarction occurred in 1970 since then precordial pain 1 day before admission, the sensations aggravated	2 days	Only 1 day in hospital.	Cardiogenic shock
	Asthma and chronic bronchitis for 25 years. During the last 3 years treated with steroids Precordial pain for 12 hours before admission	16 days	5 days after admission a holosystolic murmur was heard. Heart insufficiency 16 days after admission.	Cardiogenic shock
	L.E.D developed in 1959 since 1969 treated with steroids and cytostatics. In 1970 acute myocardial infarction with 3 block and Adams-Stokes occurred. Since then sinus rhythm and LBBB Admitted after precordial pain had persisted for 3 hours.	Few hours.	A few hours after admission, acute severe therapy-resistant cardiogenic shock occurred.	Rupture of the anterior wall of the heart.
	No cardiac symptoms. Admitted because of varicose ulcer fever and acute 3 block developed transferred because acute myocardial infarction was suspected.	1 day	Treated with transvenous pace-maker Died in cardiogenic shock 1 day after transfer	Pulmonary embolism and cardiogenic shock, complicated with hyperosmolar non-ketotic diabetic coma.

TABLE 1. *Pathological Anatomy*

No.	Heart & body weight & height	Coronary arteriosclerosis	Coronary occlusion	Myocardium	Hypertrophy of the heart	Dominant circumflex branch
1	490 g 65 kg 162 cm	Medium to severe degree	Thrombus of few days standing in the left circumflex branch Earlier occlusion the right coronary artery	Recent af retion (2–4 days) in inferior wall.	Slight	Left
2	390 g 78 kg/164 cm	Medium to severe degree	Recent thrombus (10–12 days) in the left circumflex branch. Haemorrhage in the wall of the ant. descendent branch with earlier occlusion	Recent infarction (approximately 4 weeks and quite recent) in nferior wall and papillary muscle. Earlier anterior infarction.	Slight	Right
3.	330 g 53 kg/155 cm	Severe degree	Stenosis of left anterior desc & circumflex arteries no total occlusion	Mass fibrosis in anterior wall and septum	Moderate	Left
4	400 g 51 kg/160 cm	Slight to medium	Recent thrombosis (less than 4 days) in the left anterior descendent artery	Recent infarction (3–4 days) n anterior wall with rupture.	Moderate	Left
5	635 g 82 kg/175 cm	Severe degree	Thrombosis in the right coronary artery (2 3 months + approximately 1 day)	Recent infarction (8 hours—approximately 24 hours) dispersed fibrosis (6–8 weeks) in inferior wall and sept m. N sequelae of endocarditis.	Severe	Right
6.	400 g 60 kg/173 cm	Medium degree	Recent thrombosis (pproximately 1 day) in the left anterior descendent branch. Earlier occlusion in circumflex artery	Recent (less than 2 3 days) infarction in anterior wall imminent rupture. Earlier infarct in inferior wall.	Slight	Right
7	620 g 80 kg/181 cm	Medium degree	0.	Recent antero-septal infarction (2 3 weeks) rupture of the septum.	Severe	Equal
8.	425 g 74 kg/179 cm	Medium degree	Recent thrombosis (1 2 days) in left descendi g artery	Recent infarction (approximately 1 day) in anterior wall. No earlier infarction.	Slight	Right
9	430 g 81 kg/178 cm	Slight degree	0	Slight fibrosis.	No.	Left

the unit because his condition deteriorated severely, probably on account of a myocardial infarction A total a v block was found and, in addition the blood sugar level was severely elevated (1200 mg/100 ml) The actual cause of death was a pulmonary embolus from a deep thrombosis in the left lower extremity

The duration of symptoms ranged from a few hours up to 21 days, in one case the duration was not ascertained

Five patients died in cardiogenic shock two died of heart rupture and the remaining two of pulmonary embolism

The macroscopical pathological anatomy is shown in *Table 2* When the heart weight is related to the body weight as well as to the body length 8 out of 9 hearts could be evaluated as, at least slightly hypertropic. The dominant of the two arterial branches in the coronary sulcus is indicated

Six cases showed a thrombotic occlusion of one of the major coronary artery branches and, as a consequence to this recent infarction in the areas expected was found The age of the thrombi and the corresponding myomalacias were estimated and showed very good accordance (methods, see *Irniger* 1963 *Mallory et al* 1939 and *Lodge Patch* 1951) On the other hand there was only poor correlation between the duration of symptoms, on the one side, and the age of the thrombi and the changes in the myocardium on the other In one case (no. 7) we found a subrecent infarction but no coronary occlusion at all Case no. 3 showed an earlier occlusion and a corresponding scar and finally case no 9 showed no significant coronary changes and only slight myocardial fibrosis acute changes which could not explain the clinical picture which must have been caused by the pulmonary embolus

In *Table 3* the e c.g -changes are matched with the histopathological changes in the sinus node and the a. v system In the two first columns the predominant change (most often signs of acute infarction) and the possible permanent block are listed – one case of an a. v block one RBBB and 5 LBBBs No hemiblocks were observed The next column shows the intermittent e.c.g -changes observed during the monitoring

The histopathological changes are shown in the succeeding columns. It is remarkable that no acute necroses were found. It was only in one case that the infarcted area reached close to the conduction system, i e the left bundle branch, which in this case was slightly infiltrated with lymphocytes. On the other hand, all cases showed chronic changes of varying degree.

DISCUSSION

When histopathological changes in the conduction system are to be evaluated it is necessary to consider the more or less physiological changes to develop with age, and it is very difficult to distinguish these changes from slight pathological changes. Age-related changes in the conduction system, have been described for instance by *Erickson & Lev* (1952) *Davies* (1967) and *Rossi* (1969) and one of the authors of the present paper has personally investigated a normal series composed of persons who died a violent death and who in vivo had not presented symptoms of heart disease (*Voigt* 1975) It was shown that even before the age of 50 a considerable number of persons had changes in the conduction system such as varying degree of fibrosis in the sinus node and/or the atrioventricular system

Many attempts have been made to find a correlation between conduction disturbances and histopathological changes in the conduction system (e g *Davies* 1967 *Davies & Harris* 1969 *Harper et al* 1969 *Rossi* 1969 *Davies* 1971 *Demoulin et al* 1972 *Rosen et al* 1973) and on the whole only a partial accordance between e.c.g -changes and the histological findings has been found

The changes in the conduction system in cases of AMI have also been investigated and been described by several authors (*Blondeau et al* 1961 and 1967 *Davies* 1967 *Fluck et al* 1967 *James* 1968, *Sutton & Davies* 1968 *Rossi* 1969 *Davies* 1971 *Hackel et al* 1971 *Ekelund et al.* 1972 *Hackel et al* 1972

No.	[illegible] change	Permanent block	Transient dysrhythmias	S-A node	A V node	His bundle and branches	Correlation
1	Inferior infarction	Incomplete RBBB	Nodal tachycardia and sinus bradycardia. Nodal escape rhythm	Thickened wall of sinus node artery	Slight fibrosis	Presumably slight fibrosis in both branches.	Relatively good
2.	No definite	Incomplete LBBB	Nodal escape beats, trial fibrill tion. Just before death, sinus bradycardia and entricular tachycardia.	Normal	Fibrosis	Fibrosis in the His bundle and extreme fibrosis in the left bundle branch.	Good
3.	Anterior nfarction	2 and 3 A-V block	Ventricular fibrillation.	Normal	Slight fibrosis	Severe fibrosis in the right bundle branch.	Dubious
4	Anterior inf rction	0.	Ventricular ectopic beats Alternating sinus rhythm and nodal rhythm. LBBB.	Normal	Vacuolization of muscle fibres.	Vacuolization of fibres in the His bundle; left bundle branch close to the infarct slight lymphocytic infiltration.	Good
5	Old anterior infarction (deep Q_{V1-4})	Incomplete LBBB	3 A V block with idioentricular rhythm.	Normal	Fibrosis	Fibrosis in the His bundle, normal bundle branches.	Good
6.	Anterior infarction	Incomplet LBBB	Ventricular ectopic beats 1 A-V block. 2 A V block. 3 A V block with nodal rhythm.	Normal	Normal	Fibrosis in the His bundle.	Good
7	Antero-septal infarction	0.	Sinustachycardia. Atrial fibrillation. RBBB.	Normal	Slight fibrosis	Slight fibrosis in the His bundle and moderat fibrosis in the right bundle branch.	Good
8.		Incomplete LBBB	3 A V block and sinoatrial block. Wandering pace-maker	Normal	Severe f brosis, arteriolosclerosis.	Severe fibrosis in the bundle moderate fibrosis in the right bundle branch, arteriolosclerosis.	Good
9	Old anterior infarction Q_{V4-6}	Incomplete LBBB	3 A-V block. Just before death: sinus tachycardia.	Slight fibrosis. Moderate arteriolosclerosis in the sinus node artery	Severe fibrosis: arteriolosclerosis.	Sev ere fibrosis in the left bundle branch.	Good

the unit because his condition deteriorated severely probably on account of a myocardial infarction. A total a. v block was found and, in addition, the blood sugar level was severely elevated (1200 mg/100 ml) The actual cause of death was a pulmonary embolus from a deep *thrombosis in the left lower extremity*

The duration of symptoms ranged from a *few hours up to 21 days* in one case, the duration was not ascertained.

Five patients died in cardiogenic shock two died of heart rupture and the remaining two of pulmonary embolism

The macroscopical pathological anatomy is shown in *Table 2* When the heart weight is *related to the body weight as well as to the* body length, 8 out of 9 hearts could be evaluated as, at least slightly hypertropic. The dominant of the two arterial branches in the coronary sulcus is indicated.

Six cases showed a thrombotic occlusion of one of the major coronary artery branches and as a consequence to this, recent infarction in the areas expected was found The *age of the thrombi and the corresponding* myomalacias were estimated and showed very good accordance (methods, see *Irniger* 1963 *Mallory et al* 1939 and *Lodge Patch* 1951) On the other hand there was only poor correlation between the duration of symptoms on the one side, and the age of the thrombi and the changes in the myocardium on the other In one case (no 7) we found a subrecent infarction but no coronary occlusion at all Case no 3 showed an earlier occlusion *and a corresponding scar and finally case* no 9 showed no significant coronary changes *and only slight myocardial fibrosis, acute* changes which could not explain the clinical picture which must have been caused by the pulmonary embolus.

In *Table 3* the e c g -changes are matched with the histopathological changes in the sinus node and the a v system In the two first columns the predominant change (most often signs of acute infarction) and the possible permanent block are listed – one case of an a. v block, one RBBB and 5 LBBBs. No hemiblocks were observed. The next column shows the intermittent e c.g -changes observed during the monitoring

The histopathological changes are shown in the succeeding columns. It is re*markable that no acute necroses were found.* It was only in one case that the infarcted area reached close to the conduction system, i e the left bundle branch, which in this case was slightly infiltrated with lymphocytes. On the other hand, all cases showed chronic changes of varying degree.

DISCUSSION

When histopathological changes in the conduction system are to be evaluated it is necessary to consider the more or less physiological changes to develop with age and it is very difficult to distinguish these changes from slight pathological changes. Age related changes in the conduction system, have been described for instance by *Ericksson & Leo* (1952) *Davies* (1967) and *Rossi* (1969) and one of the authors of the present paper *has personally investigated a "normal series* composed of persons who died a violent death and who *in vivo had not presented symptoms* of heart disease (*Voigt* 1975) It was shown that even before the age of 50 a considerable number of persons had changes in the conduction system such as varying degree of fibrosis in the sinus node and/or the atrioventricular system.

Many attempts have been made to find a correlation between conduction disturbances and histopathological changes in the conduction system (e.g *Davies* 1967 *Davies & Harris* 1969 *Harper et al.* 1969 *Rossi* 1969 *Davies* 1971 *Demoulin et al.* 1972 *Rosen et al* 1973) and on *the whole only* a partial accordance between e.c.g -changes and the *histological findings has been found*

The changes in the conduction system in cases of AMI have also been *investigated* and been described by several authors (*Blondeau et al* 1961 and 1967 *Davies* 1967 *Fluck et al* 1967 *James* 1968, *Sutton & Davies* 1968 *Rossi* 1969 *Davies* 1971 *Hackel et al.* 1971 *Ekelund et al* 1972 *Hackel et al.* 1972,

mal node was combined with a bundle showing fibrosis. This is in accordance with Voigt (1975) who in the age groups concerned found a.-v. changes to varying degrees, but only exceptionally in all the segments at the same time. The changes demonstrated in our 9 cases only slightly exceeded those found in Voigt's control series.

Among the patients with a.-v. block (nos. 3, 5, 6, 8, and 9), 3 presented considerable fibrosis in the a.-v. node (nos. 5, 8, and 9); no. 3 showed *only slight fibrosis* in the node and severe fibrosis in the right bundle branch whereas the last case (no. 6) had significant fibrosis *in the bundle* which *in cases* nos. 5 and 8 also was found together with the node changes. On the other hand, in case no. 2, fibrosis was considerable *both* in the node and the bundle and, even so, it showed only nodal escape beats and terminal ventricular tachycardia. The vacuolization of the fibres in the node and bundle in case no. 4 has *apparently* not caused any severe functional disturbance, and the slight fibrosis at both sites in case no. 7 did not provoke e.c.g. changes.

Among the patients with bundle branch block, corresponding histopathological changes in the bundle branches were observed in 5 cases. In the remaining 3 cases the branches did not show the changes otherwise to be expected but presented significant fibrosis in the bundle; thus, the explanation of a bundle branch block may in some cases be found in the a.-v. bundle itself and not in the branch in question. In the analysis, distinction between complete and incomplete blocks has not been made.

The correlation between the e.c.g.-changes and the histological changes has been evaluated as *shown in Table 3*, *looking for* morphological changes corresponding with demonstrated functional changes. The correlation was good *in 7 of our 9 cases*, relatively good in 1 case and dubious in 1.

REFERENCES

1. *Blondeau M., Rivet P. & Lenègre J.*: Les troubles de la conduction auriculo-ventriculaire dans l'infarctus myocardique récent. II. Etude anatomique. Arch. Mal. Coeur *54*: 1104–1117, 1961.
2. *Blondeau M., Maurice P., Reverdy V. & Lenègre J.*: Troubles du rhythme et de la conduction auriculo-ventriculaire dans l'infarctus myocardique récent. Considérations anatomiques. Arch. Mal. Coeur *60*: 1733–1751, 1967.
3. *Christensen I., Iversen K. & Skouby A. P.*: Benefits obtained by the introduction of a coronary-care unit. Acta med. scand. *189*: 285–291, 1971.
4. *Davies M.*: Histological study of the conduction system in complete heart block. J. Path. Bact. *94*: 351–358, 1967.
5. *Davies, M. J.*: Pathology of conducting tissue of the heart. Butterworths, London, 1971, p. 48–61.
6. *Davies, M. & Harris A.*: Pathological basis of primary heart block. Brit. Heart J. *31*: 219–226, 1969.
7. *Demoulin J. C. & Kulbertus H. E.*: Histopathological examination of concept of left hemiblock. Brit. Heart J. *34*: 807–814, 1972.
8. *Editorial*: Coronary thrombosis and fatal myocardial ischemia. Circulation *49*: 1–3, 1974.
9. *Eklund L. G., Moberg, A., Olsson A. G. & Orö L.*: Recent myocardial infarction and the conduction system, a clinico-pathological correlation. Brit. Heart J. *34*: 774–780, 1972.
10. *Eliot R. S., Baroldi G. & Leone A.*: Necropsy studies in myocardial infarction with minimal or no coronary luminal reduction due to atherosclerosis. Circulation *49*: 1127–1131, 1974.
11. *Erickson, E. E. & Lev M.*: Ageing changes in the human atrioventricular node, bundle and bundle branches. J. Gerontol. *7*: 1–12, 1952.
12. *Fluck D. C., Olsen E., Pentecost B. L., Thomas M., Fillmore S. J., Shillingford J. P. & Mounsey J. P. D.*: Natural history and clinical significance of arrhythmias after acute cardiac infarction. Brit. Heart J. *29*: 170, 1967.
13. *Hackel, D. B. & Estes J. E. H.*: Pathologic features of atrioventricular and intraventricular conduction disturbances in acute myocardial infarction. Circulation *43*: 977–979, 1971.
14. *Hackel, D. B., Wagner G., Ratliff N. B., Cies A. & Estes E. H.*: Anatomic studies of the cardiac conducting system in acute myocardial infarction. Am. Heart J. *83*: 77–81, 1972.
15. *Harper J. R., Harley A., Hackel, D. B. & Estes, E. H.*: Coronary artery disease and major conduction disturbances. Am. Heart J. *77*: 411–422, 1969.
16. *Hudson R. E. B.*: Cardiovascular pathology

Hunt et al 1973 *Lie* 1975) It appears in general from these *investigations that acute* changes in the specific conduction tissue which might explain the *conduction disturbances* are only seldom found. Thus *Lie* (1975) found acute *changes only in 2 out of* 39 well investigated patients who died of AMI, but it is *mentioned that chronic* changes (vacuolization, fibrosis) were observed in an insignificant number of the cases and that the localizations might vary besides it was not always that they *exceeded the* changes otherwise found in the normal series mentioned above. Histopathological changes but absence of the e.c.g.-changes to be expected were seen

The degree of accordance between disturbances in the heart rhythm and the pathoanatomical alterations varies very much from one investigation to another According to *Sutton & Davies* (1968) *Ekelund et al* (1972) and *Hunt et al* (1973) correlation seemed to be good. It seems to be established that infarction of the inferior wall of the heart most often is combined with atrioventricular blocks, whereas infarctions in the anterior wall chiefly provoke blocks at more peripheral sites (BBB) This is confirmed by *Paulsen & Vetner* (1973) by means of post mortem coronary angiography

The e.c.g.-changes, but absence of a pathoanatomical explanation are interpreted in different ways, for instance as local temporary disturbances of the blood circulation (*Fluck et al* 1967 *Harper et al* 1969) liberation of potassium ions or of adenosine or normal intracellular enzymes such as lysosomal enzymes, because of ischaemia, or neuroreflexes (*James 1968 Hackel et al.* 1971) *Lie* (1975) mentions only electrical instability The resistance against reduced blood circulation which seems to be a characteristic of the conduction *tissues but not* of the other myocardium is explained by a lower need for oxygen combined with the possibility of oxygen diffusion directly from the interior of the heart through the endocardium (*Hackel et al* 1971) the particular vascularization should also be remembered

In *our series* we found one case (no. 3) where the e.c.g pointed to an AMI though it could not be confirmed at autopsy This patient died however a few hours after the onset of symptoms. The HBFP stain (*Lie et al 1971*) gave *dubious results in this case*, but in accordance with *Lichtig et al.* (1975) one *of the authors (J V* unpublished) *found* this method unreliable and unable to disclose *with certainty a quite recent infarction.*

In case no. 7 a recent anteroseptal infarct *was found but no intravascular occlusion.* Such "infarctus sine thrombosi" are wellknown *Eliot et al (1974) stated that 7 per* cent of the patients who die of a typical AMI have only *minimal or no coronary affection*—the explanation of this phenomenon is not known.

In 3 cases (nos. 2 5 and 8) the e.c.g did not show the recent infarct which was found at autopsy (2 inferior infarctions, 1 anterior)

In 2 cases (nos. 1 and 9) a significant arteriosclerosis with resulting narrowing of the sinus node artery was found, and in case no. 9 some fibrosis of the sinus node was also observed. In the other cases, the sinus node and the corresponding artery were normal. In case no. 1 sinus bradycardia was seen and, in the last case, only terminal sinus tachycardia Atrial dysrhythmias were also seen in cases 2 4 7 and 8 but absence of pathological changes of the sinus node or its artery in these cases, however there was a varying degree of fibrosis and fatty infiltration in the surrounding atrial wall *and in* case no. 7 chronic pericarditis and changes in close relation to the sinus node were also observed. The role of these changes is uncertain.

Changes in the a v node and His bundle were *more common.* There was a varying degree of changes in the node in all cases but *one (no. 6)* mostly in the form of fibrosis in one case, however vacuolization of fibres was seen (no. 4) Two cases (nos. 8 and 9) showed also arteriolar changes. The bundle was normal in 3 cases (nos. 1 3 and 9) but in these cases the node showed changes, at least to a slight degree and in case no. 6 the nor

nal node was combined with a bundle showing fibrosis. This is in accordance with Vogt (1975) who in the age groups concerned found a-v changes to varying degrees, but only exceptionally in all the segments at the same time. The changes demonstrated in our 9 cases only slightly exceeded those found in Vogt's control series.

Among the patients with a-v block (nos. 3 5 6, 8 and 9) 3 presented considerable fibrosis in the a-v node (nos. 5 8, and 9) no. 3 showed only slight fibrosis in the node and severe fibrosis in the right bundle branch whereas the last case (no. 6) had significant fibrosis in the bundle which in cases nos. 5 and 8 also was found together with the node changes. On the other hand, in case no. 2, fibrosis was considerable both in the node and the bundle and, even so, it showed only nodal escape beats and terminal ventricular tachycardia. The vacuolization of the fibres in the node and bundle in case no. 4 has apparently not caused any severe functional disturbance, and the slight fibrosis at both sites in case no. 7 did not provoke e.c.g changes.

Among the patients with bundle branch block, corresponding histopathological changes in the bundle branches were observed in 5 cases. In the remaining 3 cases the branches did not show the changes otherwise to be expected but presented significant fibrosis in the bundle thus, the explanation of a bundle branch block may in some cases be found in the a.-v. bundle itself and not in the branch in question. In the analysis, distinction between complete and incomplete blocks has not been made.

The correlation between the e.c.g.-changes and the histological changes has been evaluated as shown in Table 3, looking for morphological changes corresponding with demonstrated functional changes. The correlation was good in 7 of our 9 cases, relatively good in 1 case and dubious in 1

REFERENCES

1 *Blondeau M. Rivon P & Lenègre J.*. Les troubles de la conduction auriculo-ventriculaire dans l'infarctus myocardique récent: II. Etude anatomique. Arch. Mal. Coeur 54 1104–1117 1961

2. *Blondeau M., Maurice P., Reverdy V & Lenègre J.*: Troubles du rhytme et de la conduction auriculo-ventriculaire dans l'infarctus myocardique récent. Considérations anatomiques. Arch. Mal. Coeur 60 1733–1751 1967

3. *Christiansen I., Iversen K. & Skouby A P.*. Benefits obtained by the introduction of a coronary-care unit. Acta med. scand. 189 285–291 1971

4 *Davies M.*. Histological study of the conduction system in complete heart block. J Path. Bact. 94 351–358, 1967

5 *Davies M J.*. Pathology of conducting tissue of the heart. Butterworths, London, 1971 p. 48–61

6 *Davies M & Harris A.*. Pathological basis of primary heart block. Brit. Heart J 31: 219–226, 1969

7 *Demoulin, J C & Kulbertus H E.*. Histopathological examination of concept of left hemiblock. Brit. Heart J 34 807–814 1972.

8. *Editorial.* Coronary thrombosis and fatal myocardial ischemia. Circulation 49 1 3 1974

9 *Ekelund L. G., Moberg A., Olsson A G & Orö L.*. Recent myocardial infarction and the conduction system, a clinico-pathological correlation. Brit. Heart J 34 774–780, 1972.

10 *Elliot R. S., Baroldi G & Leone A* Necropsy studies in myocardial infarction with minimal or no coronary luminal reduction due to atherosclerosis. Circulation 49 1127–1131 1974

11 *Erickson E. E. & Lev M.*: Ageing changes in the human atrioventricular node, bundle and bundle branches. J Gerontol. 7 1 12, 1952.

12. *Fluck D C., Olsen E., Pentecost B. L., Thomas M., Fillmore S J., Shillingford J P & Mounsey J P D* Natural history and clinical significance of arrhytmias after acute cardiac infarction. Brit. Heart J 29 170 1967

13 *Hackel, D B. & Estes J E. H* Pathologic features of atrioventricular and intraventricular conduction disturbances in acute myocardial infarction. Circulation 43 977–979 1971

14 *Hackel, D B Wagner G Ratliff N B., Cies A. & Estes E H.*. Anatomic studies of the cardiac conducting system in acute myocardial infarction Am. Heart. J 83 77–81 1972.

15. *Harper J R., Hartley A., Hackel, D B. & Estes, E H* Coronary artery disease and major conduction disturbances Am. Heart J 77 411-422, 1969

16. *Hudson, R E B.* Cardiovascular pathology

Hunt et al 1973, *Lie* 1975) It appears in general from these investigations that acute changes in the specific conduction tissue which might explain the conduction disturbances are only seldom found. Thus *Lie* (1975) found acute changes only in 2 out of 39 well investigated patients who died of AMI but it is mentioned that chronic changes (vacuolization fibrosis) were observed in an insignificant number of the cases and that the localizations might vary besides it was not always that they *exceeded the* changes otherwise found in the normal *series mentioned above Histopathological* changes but absence of the e.c.g.-changes to be expected were seen

The degree of accordance between disturbances in the heart rhythm and the pathoanatomical alterations varies very much from one investigation to another According to *Sutton & Davies* (1968) *Ekelund et al* (1972) and *Hunt et al* (1973) correlation seemed to be good It seems to be established that infarction of the inferior wall of the heart most often is combined with atrioventricular blocks, whereas infarctions in the anterior wall chiefly provoke blocks at more peripheral sites (BBB) This is confirmed by *Paulsen & Vetner* (1973) by means of post mortem coronary angiography

The e.c.g.-changes, but absence of a pathoanatomical explanation are interpreted in different ways, for instance as local, temporary disturbances of the blood circulation (*Fluck et al.* 1967 *Harper et al* 1969) liberation of potassium ions or of adenosine or *normal intracellular enzymes such as* lysosomal enzymes, because of ischaemia or *neuroreflexes* (*James* 1968 *Hackel et al* 1971) *Lie* (1975) mentions only electrical *instability The resistance against reduced* blood circulation which seems to be a characteristic *of the conduction* tissues but not of the other myocardium is explained by a *lower need for oxygen* combined with the possibility of oxygen diffusion directly from the interior *of the heart through* the endocardium (*Hackel et al* 1971) the particular *vascularization should also* be remembered

In *our series* we found one case (no. 3) where the e.c.g pointed to an AMI, though it could not be confirmed at autopsy This patient died however a few hours after the onset of symptoms. The HBFP stain (*Lie et al.* 1971) gave dubious results in this case, but in accordance with *Lichtig et al.* (1975) one of the authors (*J. V., unpublished*) *found* this method unreliable and unable to disclose *with certainty a quite recent infarction*

In case no. 7 a recent anteroseptal infarct was *found but no* intravascular occlusion. Such "infarctus sine thrombosi" are well-known *Eliot et al.* (*1974*) stated that 7 per cent of the patients who die of a typical AMI have only minimal or no coronary affection—the explanation of this phenomenon is not known.

In 3 cases (nos. 2 5 and 8) the e.c.g did not show the recent infarct which was found at autopsy (2 inferior infarctions, 1 anterior)

In 2 cases (nos. 1 and 9) a significant arteriosclerosis with resulting narrowing of the sinus node artery was found, and in case no 9 some fibrosis of the sinus node was also observed In the other cases, the sinus node and the corresponding artery were normal. In case no 1 sinus bradycardia was seen and, in the last case only terminal sinus tachycardia Atrial dysrhythmias were also seen in cases 2 4 7 and 8 but absence of pathological changes of the sinus node or its artery in these cases, however there was a varying degree of fibrosis and fatty infiltration in the surrounding atrial wall and in case no. 7 chronic pericarditis and changes in close relation to the sinus node were also observed. The role of these changes is uncertain.

Changes in the a v node and His bundle were more common. There was a varying degree of changes in the node in all cases but one (no. 6) mostly in the form of fibrosis in one case, however vacuolization of fibres was seen (no 4) Two cases (nos. 8 and 9) showed also arteriolar changes The bundle was normal in 3 cases (nos. 1 3 and 9) but in these cases the node showed changes, at least to a slight degree and in case no 6 the nor

Acta path. microbiol. scand. Sect. A, 85 183-192, 1977

THE FINE STRUCTURE OF THREE DIMENSIONAL COLONIES OF HUMAN GLIOMA CELLS IN AGAROSE CULTURE

J Carlsson and U Brunk

Department of Physical Biology The Gustaf Werner Institute, University of Uppsala, and Institute of Pathology and the Wallenberg Laboratory University of Uppsala, Uppsala, Sweden

Carlsson, J & Brunk, U The fine structure of three-dimensional colonies of human glioma cells in agarose culture. Acta path. microbiol. scand. Sect. A, 85 183-192, 1977

The fine structure of human glioma cells cultivated as three-dimensional colonies in agarose was investigated during exponential growth. The colonies did not show central degeneration, although they reached diameters of up to 600 μm. Large extra-cellular spaces extended throughout the colonies. The mean volumetric fraction of the spaces increased from about 20 per cent at the periphery up to nearly 40 per cent in the central regions. The quotient between nuclei and cytoplasm showed a slight decrease with depth. A proliferative gradient existed in the colonies, i e the mitotic index decreased almost exponentially with the distance from the surface. The distance at which the mitotic index changed by factor of 2 was about 90 μm, corresponding to nearly five cell diameters. Cytoplasmic extensions, with a ruffling-like appearance, occurred both at the periphery and in the centre of the colonies but were larger and more frequent at the periphery The fractions of mitochondria and vacuoles in the cytoplasm showed rather large local variations. However the mean number of mitochondria decreased somewhat towards the centre and the number of vacuoles containing highly electron-absorbing substance increased in the most central regions.

Key words Glioma cells, human sub-cellular structures agarose culture.

J Carlsson, Department of Physical Biology The Gustaf Werner Institute, University of Uppsala, Box 531 S-751 21 Uppsala, Sweden.

Received 23 iii 76 Accepted 8.x.76

In many tumour studies, there is a requirement for an experimental system of neoplastic cells arranged in a reproducible and geometrically simple growth pattern. This is, for example, the case in studies of radiation-induced disturbances in solid tumours, where the radiation-resistant cells are often situated in irregular patterns, due to irregular vascularization

High requirement as regards reproducibility of shape and growth rate can probably be met only with special types of cell cultures. Three-dimensional, proliferative growth in *vitro* starting from single cells, has been demonstrated by for example, hamster-lung cells in suspension culture or by some tumour cells in a semi-solid medium (agar agarose and methyl cellulose) In such cultures, growth is restricted by insufficient diffusion of oxygen and nutrients and by the accumulation of catabolic products (cf *Folkman et al.* 1974) Such growth-limiting factors are of course, important also for solid tumours in

vol. I Edward Arnold (Publishers) Ltd., London 1965 p 59–90
17 *Hunt D Lie J T Vohra J & Sloman G* Histopathology of heart block complicating acute myocardial infarction correlation with the His bundle electrogram. Circulation *48* 1252–1261 1973
18. *Irniger W* Histologische Altersbestimmung von Thrombosen und Embolien. Virchows Arch. Path. Anat. *336* 220–237 1963
19 *James T N* The coronary circulation and conduction system in acute myocardial infarction Progr cardiovasc. Dis. *10* 410–449 1968
20 *Lichtig, C Brooks H., Chassagne G., Glagow S & Wissler R W.* Basic fuchsin picric acid method to detect acute myocardial ischemia. An experimental study in swine Arch Pathol 99 158–161 1975
21 *Lie J T Holley K E Vampa W R & Titus J L* New histochemical method for morphologic diagnosis of early stages of myocardial ischemia. Mayo Clin. Proc. *46* 319–327 1971
22. *Lodge-Patch I.* The ageing of cardiac infarcts and its influence on cardiac rupture. Brit. Heart J *13* 37–42 1951
23 *Mallory G K White P D & Salcedo-Salgar J.* The speed of healing of myocardial infarction Am Heart J *18* 647–671 1939
24 *Paulsen S & Vetner M.* Atrioventriculære og intraventriculære ledningsforstyrrelser ved akut myocardieinfarct. Ugeskr Læg *135* 522–526 1973
25 *Rosen K M Loeb H G Chaqimia R Sinno M Z Rahimtoola, S H & Gunnar R M* Site of heart block in acute myocardial infarction. Circulation *42* 925–933 1970.
26 *Rosen K M Rahimtoola S H Bharati, S. & Lev M* Bundle branch block with intact atrioventricular conduction. Am J Cardiol. *32* 783–793 1973
27 *Rossi L.* Histopathologic features of cardiac arrhytmias, Casa Editrice Ambrosiana, Milano 1969 p.p. 297
28. *Sutton R & Davies M* The conduction system in acute myocardial infarction complicated by heart block. Circulation *38* 987–992 1968
29 *Voigt J* Investigations of the cardiac conduction system in sudden and unexpected deaths, II 7th International Meeting of Forensic Sciences, Zürich, 1975

THE FINE STRUCTURE OF THREE-DIMENSIONAL COLONIES OF HUMAN GLIOMA CELLS IN AGAROSE CULTURE

J Carlsson and U Brunk

Department of Physical Biology The Gustaf Werner Institute, University of Uppsala, and Institute of Pathology and the Wallenberg Laboratory University of Uppsala, Uppsala, Sweden

Carlsson, J & Brunk, U The fine structure of three-dimensional colonies of human glioma cells in agarose culture. Acta path. microbiol. scand. Sect. A, 85 183–192, 1977

The fine structure of human glioma cells cultivated as three-dimensional colonies in agarose was investigated during exponential growth. The colonies did not show central degeneration, although they reached diameters of up to 600 µm. Large extra-cellular spaces extended throughout the colonies. The mean volumetric fraction of the spaces increased from about 20 per cent at the periphery up to nearly 40 per cent in the central regions. The quotient between nuclei and cytoplasm showed a slight decrease with depth. A proliferative gradient existed in the colonies, i.e. the mitotic index decreased almost exponentially with the distance from the surface The distance at which the mitotic index changed by a factor of 2 was about 90 µm, corresponding to nearly five cell diameters. Cytoplasmic extensions, with a ruffling-like appearance, occurred both at the periphery and in the centre of the colonies but were larger and more frequent at the periphery The fractions of mitochondria and vacuoles in the cytoplasm showed rather large local variations However the mean number of mitochondria decreased somewhat towards the centre and the number of vacuoles containing highly electron-absorbing substance increased in the most central regions.

Key words Glioma cells, human sub-cellular structures agarose culture.

J Carlsson, Department of Physical Biology The Gustaf Werner Institute, University of Uppsala, Box 531 S-751 21 Uppsala, Sweden.

Received 25.viii 76 Accepted 8.x.76

In many tumour studies, there is a requirement for an experimental system of neoplastic cells arranged in a reproducible and geometrically simple growth pattern. This is, for example, the case in studies of radiation-induced disturbances in solid tumours, where the radiation-resistant cells are often situated in irregular patterns, due to irregular vascularization.

High requirement as regards reproducibility of shape and growth rate can probably be met only with special types of cell cultures. Three-dimensional, proliferative growth *in vitro* starting from single cells, has been demonstrated by for example, hamster-lung cells in suspension culture or by some tumour cells in a semi-solid medium (agar agarose and methyl cellulose) In such cultures, growth is restricted by insufficient diffusion of oxygen and nutrients and by the accumulation of catabolic products (cf. *Folkman et al.* 1974) Such growth-limiting factors are of course, important also for solid tumours *in*

vivo, where regions with poor vascularization and cell necrosis are regularly seen especially in malignant neoplasias.

Sutherland et al (1969) showed that the V79 strain of Chinese-hamster lung cells formed multicellular spheroids in suspension culture and that these spheroids resembled nodular carcinomas. It has also been shown that the spheroids contained radiation resistant hypoxic cells (*Sutherland & Durand* 1973). In agar and agarose gel (*Macpherson* 1973) many cell lines also grow as spherical colonies reminiscent of tissue. For example McAllister et al. (1967) showed that cells from virus-induced hamster tumours grew as colonies in agar and that such colonies morphologically resembled the original tumours.

No detailed studies of the fine structure in cultured spherical colonies are known to the present authors. Studies of the amount of extra-cellular space and the numbers of mitochondria and vacuoles in the cytoplasm as a function of the distance from the surface must be of importance for example, for a better understanding of the proliferative and metabolic alterations due to insufficient nutrition and accumulation of acid and other catabolic products.

We have studied an established line of human glioma cells that easily grow as spherical colonies in agarose gel. Sections of the colonies were studied in the light microscope for quantification of the mitotic activity. They were also studied in the transmission electron microscope namely for quantification of the intercellular space, the cytoplasm nucleus relation and the volumetric fraction of vacuoles and mitochondria in the cytoplasm. All the variables were measured as a function of depth in the colonies.

MATERIAL AND METHODS

Cell Culture

The establishment of the permanent cell line studied (118 MG) from a human malignant glioma has been described by *Westermark et al.* (1973). The cells are normally grown in Eagle's minimal essential medium (MEM) supplemented with 10 per cent calf serum and antibiotics (100 IU/ml penicillin, 50 µg/ml streptomycin and 125 µg/ml amphotericin B).

The cells were cultivated in the semi-solid medium as described by *Macpherson* (1973) except that agarose was employed instead of agar. Five millilitres of 0.5 per cent agarose medium, containing 10 per cent calf serum and 10 per cent tryptose-phosphate broth in Eagle's MEM, were poured into a 5-cm plastic dish and allowed to solidify at room temperature. On top of this layer 1.5 ml of 0.33 per cent agarose medium containing 10^5 cells were added. The dishes were incubated at 37 °C in a humid atmosphere containing 5 per cent CO_2. During the experiments, 0.2 ml of fresh medium (Eagle's MEM + 10 per cent calf serum) was added to the cultures three times a week.

Choice of Colony Size and Age

Colonies of different initial sizes could be studied due to cell aggregations before and during the plating of the dishes. In fact it was possible to choose the mean initial size of the colonies if the cells were left to aggregate a suitable time in suspension before plating.

In spite of the aggregations all the colonies were nearly spherical within 1 day after plating which could be checked if the colonies were picked out of the dishes by a Pasteur pipette and allowed to rotate in a thin liquid layer under the microscope. A few colonies, however, grew out between the agarose layers and formed a nearly two-dimensional colony. These colonies were immediately discovered because they were very transparent as compared with the three-dimensional colonies. All such two-dimensional colonies were rejected. The increasing volume of the colonies after plating was due to proliferation.

All colonies prepared for stereological studies were fixed 4–5 days after plating (in the exponential growth phase see Fig 2). Only colonies which, at that time, had diameters in the range 400–600 µm were analysed.

Light Microscopy

The cells were fixed in methanol-acetic acid (3:1) for 2 hours and kept in 70 per cent alcohol in the plastic dish while the cell colonies remained in the agarose. Using an inverted microscope representative colonies were selected and an area of about 0.5 × 1.0 cm was cut by a knife to permit the agarose piece to be transferred to a dehydration bath (100 percent alcohol) for about 20 minutes. It was found that xylene made the agarose matrix shrink and become extremely hard and brittle and thus, it was difficult to obtain good histological preparations, using paraffin, if the cell colonies re-

mained in the agarose. Instead we used glycol methacrylate (Sorvall JB-4 embedding kit) a water and alcohol soluble plastic. Infiltration and moulding were performed as described in *Sorvall's* manual (1971)

Sections of 2 μm were cut by glass knif they were stained with haemotoxylin (10 min) washed in running water (15 min) stained with eosin (30 sec) and finally rinsed in 90 per cent alcohol.

Transmission Electron Microscopy

For electron-microscope studies, colonies remaining in small pieces of agarose (3 mm × 3 mm) were fixed for 6 hours in 2 per cent glutaraldehyde in 0 1 *M* Na-cacodylate HCl buffer with 0.1 *M* sucrose (pH 7 2, about 540 mOsm) at 0–4 C (*Bru k & Ericsson* 1972) They were then post-fixed in 2 per cent osmium tetroxide in *s*-collidine buffer (pH 7 2) for 90 minutes, dehydrated in a graded series of alcohols, stained *en bloc* with uranyl acetate in 100 per cent ethanol for 10 minutes, and embedded in Epon Thin sections were stained with lead citrate and examined and photographed in JEOL 100C electron microscope at 60 kV

Q antification of Mitotic Activity

Sections, stained with haemotoxylin and eosin, from 27 colonies were analysed in Leitz Ortho-plan microscope. The distance from the centre of each mitotic figure to the nearest surface point in the sections was measured by means of a lattice mounted in the eyepiece. Some mitotic figures possibly had their nearest surface points out of the plane of the sections studied. This error however was minimized because only sections from the central area of the colonies (sections with maximal diameter) were analysed.

Quantification of Cytoplasm nuclei and Extra-Cellular Spac

About ten, low-magnification (1100 ×) elec tron-microscope photographs, size 17 × 23 cm (corresponding to 154 × 209 μm) per colony were pasted on cardboard to allow reconstruction of the colonies Subsequently the area fractions of cytoplasm, nuclei and extra-cellular space were evaluated by counting the number of test point, in a regular point lattice (containing 6 × 6 points) that lay on transsections of the structures in the pictures The distance between the points in the lattice was 1 cm

The olumetric fractions were immediately obtained by the Delesse principle (*Weibel & Elias* 1968) according to which the volume fraction of component the tissue is equal to the area fraction of that component provided that the analysed sections are randomly selected

The counting was carried out in sections chosen from four parallel colonies.

Quantification of Vacuoles and Mitochondria

High-magnification (27,500 ×) electron-microscope photographs, size 17 × 23 cm (corresponding to 6.2 × 8.4 μm) taken along many diameters of three parallel colonies, were analysed. The photographs were divided into four groups according to their positions relative to the surface of the colonies (0–55 55–110 110–165 and 165–200 μm) A point lattice consisting of 15 × 15 points was used in the quantification of vacuoles and mitochondria (the distance between the points was 1 cm) For each photograph, the number of points lying on acuoles or mitochondria was divided by the total number of points lying on cytoplasm. Thus, the results obtained were the volumetric fractions of vacuoles or mitochondria in the cytoplasm. Three types of vacuoles were distinguished—vacuoles with nearly electron-transparent contents (probably endocytotic vacuoles) vacuoles filled with highly electron-absorbing, amorphous material (probably secondary lysosomes of residual-body type) and third group containing both electron-transparent and highly electron-absorbing material (probably lysosomes engaged in lytic activity)

Growth Curves

Growth curves applying to individual colonies in the agarose could easily be constructed by means of a reticle, manipulated by a micrometer screw in the eyepiece of an inverted microscope. The volume of each colony was calculated from the relation $V = 4/3 \pi (ab)^{3/2}$ where *a* and *b* were the minimum and maximum radii measured at right angles.

The individual colonies were identified in a coordinate system on the bottom of the dishes.

RESULTS

Cellular Arrangement

The exponentially growing colonies of the 118 MG glioma cells were morphologically tissue-like (Fig 1) The cells seemed to have a fairly high degree of mutual adhesion because the colonies were always round with rather smooth boundaries. The cells were concentrically lined up in some regions, as if they had been pressed outwards by ex panding central cell masses. No massive de generation in the centres of the exponentially growing colonies was seen.

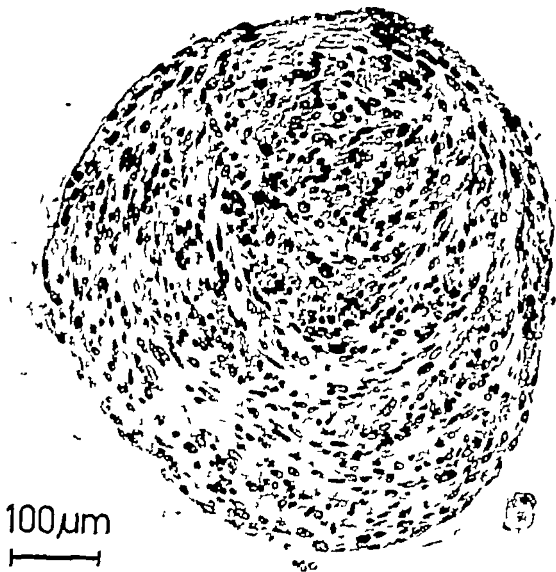


Fig 1 A 2 µm thin section of a plastic-embedded glioma spheroid (fixed 12 days after plating) stained with haemotoxylin and eosin Note the absence of massive degenerative changes.

Growth Curves

The growth curves of the 118 MG colonies showed an exponential growth phase which was suddenly changed into a plateau (Fig 2) It applies to nearly all the colonies that the change occurred about 10 days after plating independent of their size The occurrence of the plateau phase was probably due to an increasing ion strength in the dishes due to evaporation of water and accumulation of catabolic products. In preliminary experiments in which excessive amounts of nutrition were added, it was shown that medium depletion was not the critical factor The pH remained normal up to 20 days after plating

The lowest growth curve in Fig 2 shows the growth of a colony that started from only one cell while the other curves show the growth of colonies that due to aggregations started with several cells. The volume-doubling time for the colonies was nearly independent of colony size

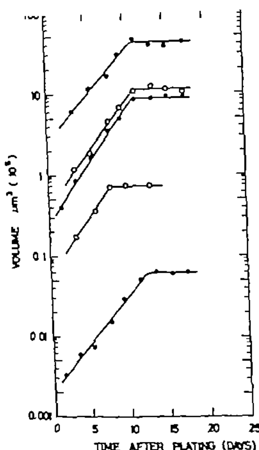


Fig 2. Growth curves for colonies of different sizes.

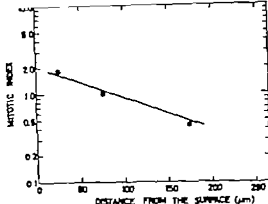


Fig 3. The mitotic index in different regions of the colonies.

Mitotic Figures

The number of mitotic figures as a function of depth in the colonies was evaluated. Taking into account the total number of cells seen in each region the mitotic index was calculated and an exponential curve was fitted to the data by the technique of least squares (Fig. 3). The adaption was reasonably good and the existence of a proliferative gradient is evident. The radial distance at which the mitotic index changed by a factor of 2 was about 90 μm (corresponding to nearly five cell diameters).

The goodness of fit for the mitotic index curve was tested by the chi-square test, which in the case of the exponential curve gave a chi-square value of about 0.6 (cf. *Spiegel* 1961). A chi-square value of 1.2 was obtained when the data were adapted to a straight line. Thus, although both curves yielded a fairly good fit, the exponential was preferable.

Cytoplasm and Nuclei

The mean fractions of cytoplasm and nuclei decreased somewhat with depth in the colonies, as seen in Fig. 4 *a* and *b*. The data were adapted to straight lines (by the technique of least squares). The quotient between nuclei and cytoplasm was also calculated and showed a slight decrease with depth.

Extra-cellular Spaces

It appears from the low-power electron-microscope picture in Fig. 5 *a*, that fairly large extra-cellular spaces existed inside the colonies. These spaces were situated all over the colonies. Fig. 5 *b* shows the volumetric fraction of extra-cellular space as a function of depth in the colonies. The data were adapted to a straight line (by the technique of least squares). The mean volume of the extra-cellular spaces increased from about 20 per cent in the periphery up to nearly 40 per cent in the central region.

Cell-to-cell Contacts

The cell-to-cell interrelationships in the colonies was most typical if cell membranes

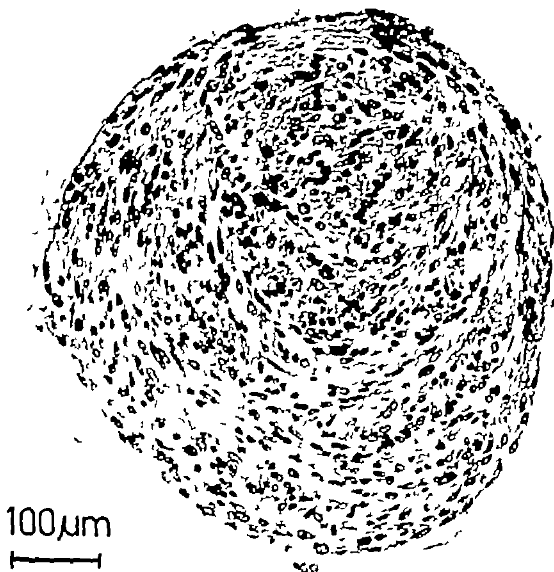


Fig. 1 A 2 µm thin section of a plastic-embedded glioma spheroid (fixed 12 days after plating) stained with haemotoxylin and eosin. Note the absence of massive degenerative changes.

Growth Curves

The growth curves of the 118 MG colonies showed an exponential growth phase which was suddenly changed into a plateau (Fig. 2). It applies to nearly all the colonies that the change occurred about 10 days after plating independent of their size. The occurrence of the plateau phase was probably due to an increasing ion strength in the dishes due to evaporation of water and accumulation of catabolic products. In preliminary experiments in which excessive amounts of nutrition were added, it was shown that medium depletion was not the critical factor. The pH remained normal up to 20 days after plating.

The lowest growth curve in Fig. 2 shows the growth of a colony that started from only one cell, while the other curves show the growth of colonies that due to aggregations started with several cells. The volume-doubling time for the colonies was nearly independent of colony size.

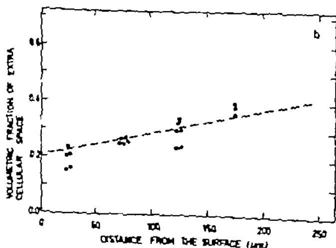


Fig. 5 (*a*) Low-power electron microscope picture, showing the presence of large extra-cellular space. (*b*) Volumetric fraction of the spaces as a function of depth in the colonies. Each point corresponds to the mean value from five independent evaluations in one section. The standard errors of these mean values varied between 10–15 per cent. The sites chosen for evaluation in each section were from five regions, determined by the distance from the surface.

No extensive degenerative changes in the central regions of exponentially growing colonies were seen, which is rather surprising. Central necrosis, however, could sometimes be seen by light microscopy of older colonies that had reached the plateau phase of growth. The fine structure of these old colonies has not been investigated.

McAllister et al. (1967) found that hamster tumour cells cultivated in agar showed massive necrosis inside a 100–150-µm-thick layer of viable cells. In the case of spheroids

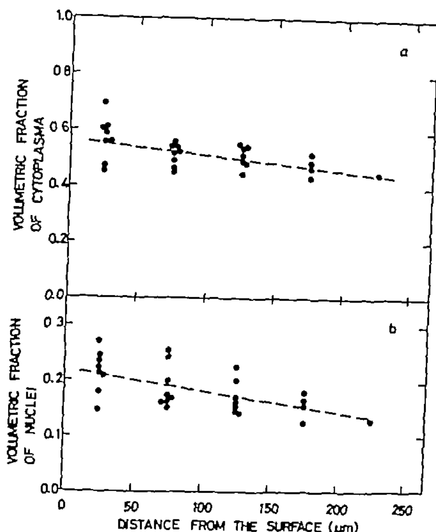


Fig 4 Volumetric fraction of cytoplasm (*a*) and nuclei (*b*) as a function of depth in the colonies. Each point corresponds to the mean value from five independent evaluations in one section. The standard errors of these mean values for the cytoplasm values varied between 5–10 per cent and between 15–20 per cent for the nuclei values. The sites chosen for evaluation in each section were from five regions, determined by the distance from the surface.

lay rather close to each other with no junctions or desmosomes. Only one junction was found among the several hundred cells studied in 25 sections from five colonies.

Ruffling

Proliferative cells *in vitro* usually show ruffling although the size and the frequency may vary between cell types. Cytoplasmic extensions of a ruffling-like appearance occurred both at the surface of the glioma colonies and in the central regions. The centrally situated extensions were, however, smaller and less frequent. In the colony shown in Fig 5 *a* one large ruffle-like structure and several smaller cytoplasmic extensions can be seen.

Mitochondria and Vacuoles

The volumetric fractions of mitochondria and vacuoles in the cytoplasm are shown in Fig 6. The dashed lines in Fig 6 a and *b* were adapted by the technique of least squares. The dashed curves in Fig 6 *c* and *d* were adapted by hand because they did not seem to follow any simple relation (linear or exponential). The variations within the regions were rather large.

DISCUSSION

The colonies showed geometrically simply arranged variations in morphology and proliferation. The reproducibility of growth seemed as good as that in conventional monolayer cultures.

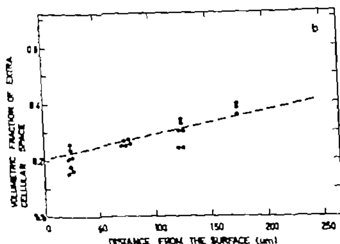


Fig. 5 ( ) Low-power electron-microscope picture, showing the presence of large extra-cellular space. (*b*) Volumetric fraction of the spaces as a function of depth in the colonies. Each point corresponds to the mean value from fiv independent evaluations in one section. The standard errors of these mean values varied between 10–15 per cent. The sites chosen for evaluation in each section were from five regions, determined by the distance from the surface

No extensive degenerative changes in the central regions of exponentially growing colonies were seen, which is rather surprising. Central necrosis, however, could sometimes be seen by light microscopy of older colonies that had reached the plateau phase of growth. The fine structure of these old colonies has not been investigated.

McAllister et al. (1967) found that hamster tumour cells cultivated in agar showed massive necrosis inside a 100–150-µm-thick layer of viable cells. In the case of spheroids

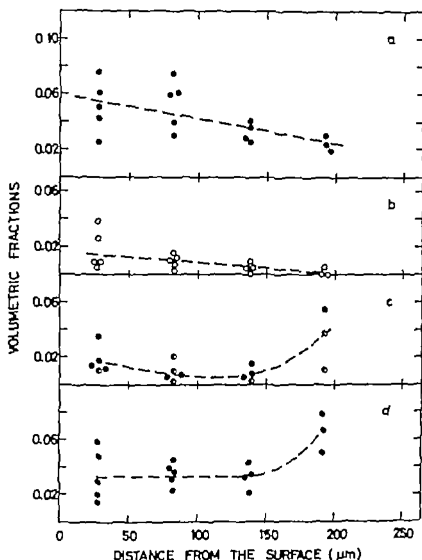


Fig 6 Volumetric fractions of mitochondria (*a*) vacuoles with electron-transparent content (*b*) vacuoles with both electron-transparent and highly electron-absorbing contents (*c*) and vacuoles with only highly electron-absorbing contents (*d*)
Each point corresponds to the mean value from 10 to 15 independent evaluations in one section. The standard errors of the mean values varied between 20–40 40–60 40–60 and 20 30 per cent for the case in (*a*) (*b*) (*c*) and (*d*) respectively The sites chosen for evaluation in each section were from four regions, determined by the distance from the surface.

of V79 Chinese-hamster cells *Sutherland et al* (1971) showed that proliferation only occurred in an outer layer about 75 µm thick and that massive necrosis occurred inside a 120-µm thick cell layer Similar results have recently been reported by *Folkman et al* (1974) The absence of central degeneration is surprising also if compared with the morphology of solid tumours *in vivo* which often shows areas of necrosis inside 50–200-µm thick, viable cell layers (see for example *Thomlinson* & *Gray* 1955 *Tannock* 1968)

Calculations by *Thomlinson* & *Gray* (1955) and *Tannock* (1968) show that the diffusion length (the distance from the source of supply at which the concentration of a substance falls to zero) of oxygen in tumour tissue is probably shorter than 200 µm while the diffusion length of glucose is probably in the range of 200–400 µm Thus, it cannot be excluded that the glioma cells, in the centre of the colonies manage to be viable and also enter mitosis only through anaerobically obtained energy This explanation implies that glioma cells would be better fitted for an anaerobical life than many other mammalian-cell types.

Another factor that may contribute to viability is suggested by the inspection of the low power electron microscope picture in Fig 5 *a* which shows that rather large extracellular spaces existed inside the colonies It is likely that these inter-cellular channels" contain medium. The cells may continuously change their sizes and positions, which implies changes in the sizes and positions of the

spaces, thus enabling nutrients and catabolic products to be more efficiently transported through the cell colonies.

The mitotic index decreased almost exponentially with the distance from the surface of the colonies (see Fig 5) The shape of the proliferative gradient is unusually well-defined, due to the high viability which allowed of radial analysis in many regions. The exponential shape of the curve does not contradict either the diffusion of nutrients or random transport in extra-cellular spaces as the limiting process for proliferation.

Not only proliferation but also ruffling-like activity was much more intense at the periphery of the colonies than in the central regions. This is in accordance with recent results obtained from glia cells where a correlation *between ruffling activity and cell proliferation* was found (*Schellens et al* 1976 *Brunk et al.* 1976)

The sum of the volumetric fractions of cytoplasm and nuclei decreased with the distance from the surface. A slight decrease in the quotient between nuclei and cytoplasm towards the central regions was observed, which was possibly due to the lowered proliferative activity

The occurrence of mitochondria seemed to decrease somewhat towards the central regions, possibly reflecting a lowered metabolic activity (Fig 6 *a*) The amount of vacuoles was fairly constant with depth. However the vacuoles containing highly electron-absorbing material seemed to increase to a certain degree in the central regions (Fig. 6 *c* and *d*) an observation that may reflect an increased autophagocytosis and formation of secondary lysosomes of the residual-body type The variations within each region were at least of the same size as the depth-dependent variations, however.

The absence of junctions and desmosomes in the spheroids is in accordance with the observation (*Loewenstein* 1968) that neoplastic cells develop fewer junctions than non-neoplastic cells. According to *Sutherland et al.* (1971) the non neoplastic, hamster lung V79 cells, grown as spheroids, had tight, intermediate and desmosome junctions.

The studies presented here show that is is possible to investigate the growth pattern of tumour cells, cultivated as three-dimensional spheroids, in detail and that the amount of cytoplasm, nuclei, extra-cellular space subcellular structures and proliferation can be quantified as a function of the distance from the surface. The system seems to be suitable not only for studies of growth and cellular organization conditioned by insufficient diffusion of nutrients and accumulation of catabolic products but also for studies of the interplay between proliferation, nutritive state (for example oxygen tension) and radiation sensitivity Such studies of suspension-cultured, hamster lung cells have already been started by *Sutherland & Durand* (1976) In comparison with three-dimensional suspension culture, the agarose technique has the advantage that the growth of individual colonies can be easily followed.

The authors are indebted t Prof *Börje Lar son* and Prof. *Jan Pontén* for their continuous encouragement.

The assistance of Mrs *U J hansson* (stereologic evaluations) Miss *M Halvarsson* (EM preparations) Mrs *L Nål nd* and Mr *O Lindroth* (LM preparations) Miss *M Lindström* (cell culture) Miss *C Henriksson* and Miss *I Sjö* (typing the manuscript) and Mrs *A Ast öm* (figure drawings) is greatly ppreciated

The work has financially been supported by the *Swedish Can er Society* and the *Swedish Nat al Scie Resear h Council*

REFERENCES

Brunk U & Ericsson, J The demonstration of acid phosphatase in *in vit o* cultured tissue cells. Studies on the significance of fixation, tonicity and permeabil ty Histochemical J 4 349–363 1972.

Brunk U Schellens J & West rmark B. Influence of epidermal growth factor (EGF) on ruffling activity pinocytosis and proliferation of cultivated human glia cells. Exptl. Cell Res. 1976 In press

Folkman J Hochberg M & Knighton, D. Self regulation of growth in three dimensions The

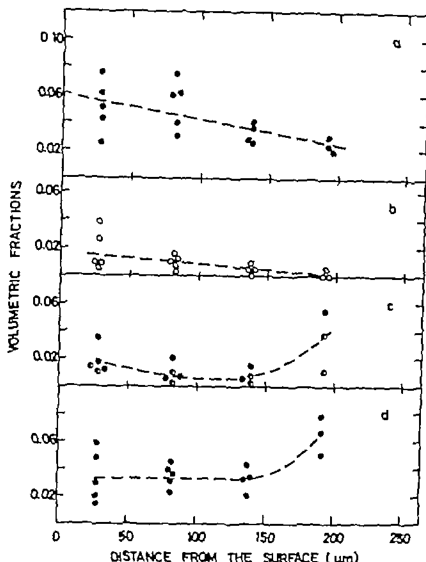


Fig 6 Volumetric fractions of mitochondria (*a*) vacuoles with electron-transparent content (*b*) vacuoles with both electron-transparent and highly electron-absorbing contents (*c*) and vacuoles with only highly electron-absorbing contents (d)
Each point corresponds to the mean value from 10 to 15 independent evaluations in one section The standard errors of the mean values varied between 20-40 40-60 40-60 and 20-30 per cent for the case in (*a*) (*b*) (*c*) and (*d*) respectively The sites chosen for evaluation in each section were from four regions, determined by the distance from the surface.

of V79 Chinese hamster cells *Sutherland et al* (1971) showed that proliferation only occurred in an outer layer about 75 µm thick and that massive necrosis occurred inside a 120-µm thick cell layer Similar results have recently been reported by *Folkman et al* (1974) The absence of central degeneration is surprising also if compared with the morphology of solid tumours *in vivo* which often shows areas of necrosis inside 50–200-µm thick, viable cell layers (see for example *Thomlinson & Gray* 1955 *Tannock* 1968)

Calculations by *Thomlinson & Gray* (1955) and *Tannock* (1968) show that the diffusion length (the distance from the source of supply at which the concentration of a substance falls to zero) of oxygen in tumour tissue is probably shorter than 200 µm while the diffusion length of glucose is probably in the range of 200–400 µm. Thus, it cannot be excluded that the glioma cells, in the centre of the colonies, manage to be viable and also enter mitosis only through anaerobically obtained energy This explanation implies that glioma cells would be better fitted for an anaerobical life than many other mammalian-cell types.

Another factor that may contribute to viability is suggested by the inspection of the low power electron microscope picture in Fig 5 *a* which shows that rather large extracellular spaces existed inside the colonies. It is likely that these inter-cellular "channels" contain medium. The cells may continuously change their sizes and positions, which implies changes in the sizes and positions of the

spaces, thus enabling nutrients and catabolic products to be more efficiently transported through the cell colonies.

The mitotic index decreased almost exponentially with the distance from the surface of the colonies (see Fig 3) The shape of the proliferative gradient is unusually well-defined, due to the high viability which allowed of radial analysis in many regions. The exponential shape of the curve does not contradict either the diffusion of nutrients or random transport in extra-cellular spaces as the limiting process for proliferation.

Not only proliferation but also ruffling like activity was much more intense at the periphery of the colonies than in the central regions. This is in accordance with recent results obtained from glia cells where a correlation between ruffling activity and cell proliferation was found (*Schellens et al.* 1976, *Brunk et al.* 1976)

The sum of the volumetric fractions of cytoplasm and nuclei decreased with the distance from the surface. A slight decrease in the quotient between nuclei and cytoplasm towards the central regions was observed, which was possibly due to the lowered proliferative activity

The occurrence of mitochondria seemed to decrease somewhat towards the central regions, possibly reflecting a lowered metabolic activity (Fig. 6 *a*) The amount of vacuoles was fairly constant with depth. However the vacuoles containing highly electron-absorbing material seemed to increase to a certain degree in the central regions (Fig 6 *c* and *d*) an observation that may reflect an increased autophagocytosis and formation of secondary lysosomes of the residual-body type The variations within each region were at least of the same size as the depth-dependent variations, however

The absence of junctions and desmosomes in the spheroids is in accordance with the observation (*Loewenstein* 1968) that neoplastic cells develop fewer junctions than non-neoplastic cells. According to *Sutherland et al.* (1971) the non-neoplastic, hamster lung V79 cells, grown as spheroids, had tight, intermediate and desmosome junctions.

The studies presented here show that is is possible to investigate the growth pattern of tumour cells, cultivated as three-dimensional spheroids, in detail and that the amount of cytoplasm, nuclei, extra-cellular space sub-cellular structures and proliferation can be quantified as a function of the distance from the surface. The system seems to be suitable not only for studies of growth and cellular organisation conditioned by insufficient diffusion of nutrients and accumulation of catabolic products but also for studies of the interplay between proliferation nutritive state (for example oxygen tension) and radiation sensitivity Such studies of suspension-cultured, hamster lung cells have already been started by *Sutherland & Durand* (1976) In comparison with three-dimensional suspension culture the agarose technique has the advantage that the growth of individual colonies can be easily followed.

The authors are indebted to Prof *Börje Larsson* and Prof. *Jan Pontén* for thei continuous encouragement.

The assistance of Mrs *U J hansson* (stereologic evaluations) Miss *M Halter sen* (EM preparations) Mrs *L. Näslund* and Mr *O Lindroth* (LM preparations) Miss *M Lindström* (cell culture) Miss *C Henriksson* and Mrs *I Sjö* (typing the ma uscript) and Mrs *A Ali öm* (figure drawings) is greatly appreciated.

The work has financially been supported by the *Sw dish Cancer Society* and the *Swedish Nat ral Science Research Council*

REFERENCES

Brunk U & Ericsson J: The demonstration of acid phosphatase in *in vi ro* cultured tissue cells. Studies on the significance of fixation, tonicity and permeability Histochemical J 4 349-363 1972.

Brunk, U S hellens J & Westermark B. Influence of epidermal growth factor (EGF) on ruffling activity pinocytosis and proliferation of cultivated human glia cells. Exptl. Cell Res. 1976 I press.

Folkman J Hochberg M & Knighton D. Self regulation of growth in three dimensions The

role of surface area limitation In *Clarkson B & Baserga R* (Ed) Control of Proliferation in Animal Cells, vol 1 section V Cold Spring Harbor 1974 p 833 842

Loewenstein W R Communication through cell junctions. Implications in growth control and differentiation In *Locke M* (Ed.) The Emergence of Order in Developing Systems. Academic Press 1968. p 151

Macpherson I *Soft agar techniques. In Kruse P F & Patterson M K* (Ed.) Tissue Culture Methods and Applications section V chapter 7 Academic Press 1973 p 276–280

McAllister R M Reed G & Huebner R J. Colonial growth in agar cells derived from adenovirus induced hamster tumours J Nat. Cancer Inst *39* 43–53 1967

Schellens J Brunk U & Lindgren A Influence of serum on ruffling activity pinocytosis and proliferation of *in vitro* cultivated human glia cells *Cytobiologie 1976 In press.*

Sorvall I Instructions for using JB-4 plastic embedding kit Sorvall Inc., Newton, Connecticut 06470 USA Bulletin 33–71

Spiegel M R Statistics. Schaum's Outline Series. Chapter 12 McGraw Hill 1961 p 209

Sutherland R M., McCredie J A & Inch, W R. Growth of multicell spheroids in tissue culture as a model of nodular carcinomas. J Nat. Cancer Inst. *46* 113–120 1971

Sutherland R M & Durand R E. Hypoxic cells *in an in vitro tumour model* Int. J Radiat. Biol *23* 235–246 1973

Sutherland R M & Durand R E. Radiation response of multicell spheroids. An *in vitro* tumour model. *Current Topics in Radiation Research* Quarterly Vol. II No. 1 p. 87–139 1976

Tannock I. The relation between cell proliferation and the vascular system in a transplanted mouse mammary tumour Brit. J Cancer *22* 258–273, 1968

Thomlinson R H & Gray L. H. The histologic structure of some human lung cancers and the possible implications for radiotherapy Brit. J Cancer *9* 539–549 1955

Weibel E R & Elias H *Quantitative* Methods in Morphology Springer Verlag 1967 p 91 93

Westermark B Pontén J & Hugosson R Determinants for the establishment of permanent tissue culture lines from human gliomas. Acta path. microbiol scand. *81* 791–805 1973

THE INCIDENCE OF THE SO-CALLED ACUTE SELECTIVE NECROSIS OF THE GRANULAR LAYER OF CEREBELLUM IN 1000 AUTOPSIED PATIENTS

REIDAR ALBRECHTSEN

The Department of Pathology, Rigshospitalet and the Institute of Neuropathology, University of Copenhagen, Copenhagen, Denmark

Albrechtsen, R. The incidence of the so-called acute selective necrosis of the granular layer of cerebellum in 1000 autopsied patients. Acta path. microbiol. scand. Sect. A, 85: 193–202, 1977.

Acute selective necrosis of the granular layer of the cerebellum (NGL) was demonstrated in 264 patients out of a total of 1000 autopsies.
The relatively high incidence of NGL was distributed evenly over the main groups of causes of death, and over all age groups, with the exception of children under the age of 10 years, in whom the incidence was lower.
The lack of correlation between NGL and any particular disease makes it difficult to put forward a plausible explanation of the necrosis. In view of recent studies it is concluded that NGL develops after death.

Key words: Cerebellum; granular layer; necrosis; autolysis.

R. Albrechtsen, Department of Pathology, Rigshospitalet, Frederik den V's Vej, DK-2100 Copenhagen, Denmark.

Received 16. 78   Accepted 16. 78

Microscopic examination of autopsy material may disclose a condition with acute severe degeneration of the internal granular layer of cerebellum. The granule cells may be almost completely destroyed, with pronounced fall in nuclear density while both the Bergmann glial cells and the Purkinje cells are unaffected. A review the literature reveals that various names have been attached to this condition: "clumping of the granular cells" (*Ferraro and Morrison* 1928), "conglutination" (*Williams* 1934), "état glacé" (*Bertrand and Godet-Guillain* 1942), "selective degeneration and necrosis of the granular layer of the cerebellum" (*Hirn kelman* 1945), "status bulbosus" (*Schrappe* 1955) and "acute selective necrosis of the granular layer of the cerebellar cortex" (*Olsen* 1959 a, b).

The two first names indicate a condition with clumping of numerous granule cells, which form irregular and solid masses, and not a true cell destruction.

The so-called acute selective necrosis of the granular layer (NGL) is found in various conditions to be common in patients both dying of neurological and other disorders, even though there would seem to be some clues as to etiology (*Olsen* 1961).

role of surface area limitation. In *Clarkson B & Baserga R* (Ed.) Control of Proliferation in Animal Cells, vol. 1 section V Cold Spring Harbor 1974 p. 833–842.

Loewenstein W R Communication through cell junctions. Implications in growth control and differentiation. In *Locke M* (Ed) The Emergence of Order in Developing Systems. Academic Press 1968. p. 151

Macpherson I Soft agar techniques. In *Kruse P F & Patterson M K* (Ed.) Tissue Culture Methods and Applications, section V chapter 7 Academic Press 1973 p 276–280

McAllister R M Reed G & Huebner R J Colonial growth in agar cells derived from adenovirus-induced hamster tumours. J Nat. Cancer Inst 39 43–53 1967

Schellens J Brunk U & Lindgren A Influence of serum on ruffling activity pinocytosis and proliferation of *in vitro* cultivated human glia cells Cytobiologie 1976 In press.

Sorvall I Instructions for using JB-4 plastic embedding kit Sorvall Inc., Newton, Connecticut 06470 USA Bulletin 33-71

Spiegel M R Statistics. Schaum's Outline Series. Chapter 12 McGraw Hill, 1961 p 209

Sutherland R M McCredie J A & Inch W R Growth of multicell spheroids in tissue culture as a model of nodular carcinomas. J Nat. Cancer Inst. 46 113–120 1971

Sutherland R M & Durand R E Hypoxic cells in an *in vitro* tumour model Int. J Radiat Biol 23 235–246 1973

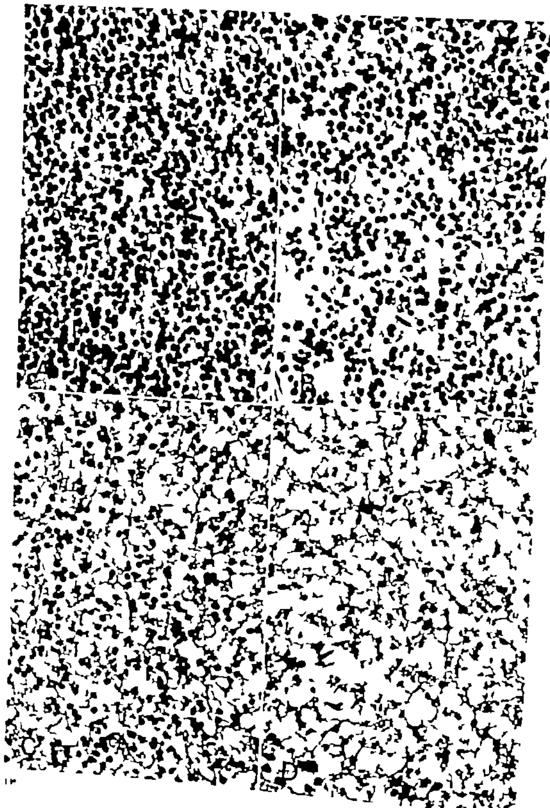
Sutherland R M & Durand R E Radiation response of multicell spheroids. An *in vitro* tumour model Current Topics in Radiation Research Quarterly Vol II No 1 p. 87 134 1976.

Tannock I The relation between cell proliferation and the vascular system in a transplanted mouse mammary tumour Brit. J Cancer 22 258-273, 1968

Thomlinson R H & Gray L H The histologic structure of some human lung cancers and the possible implications for radiotherapy Brit. J. Cancer 9 539–549 1955

Weibel E R & Elias H Quantitative Methods in Morphology Springer Verlag 1967 p. 91 93.

Westermark B Pontén J & Hugosson R Determinants for the establishment of permanent tissue culture lines from human gliomas. Acta path. microbiol scand 81 791–805 1973



Most authors consider NGL to be a vital phenomenon, arising before agony presumably during the last few days (*Olsen* 1961) or hours (*Hojgaard* 1965) of the patient's life in the terminal phase of the illness.

A few others, however regard the development of NGL as postmortem and feel that it should be considered as an autolytic process. This has been established by the fact that identical histologic changes could be obtained after incubating human cerebellar tissue taken at autopsy in a suitable medium at optimum temperature for 24–48 hours (*Ikuta et al* 1963) Furthermore morphometric studies using an electronic image analysing system have revealed that during conventional immersion fixation of human cerebella in formalin there is a marked fall in the number of granule cell nuclei in the deeper portion of cerebellum These changes were indistinguishable from NGL, but could however be prevented or considerably reduced by cutting the cerebellar cortex in an appropriate manner before fixation (*Albrechtsen* 1975)

Regardless of whether or not "NGL" is a postmortem phenomenon, it is still remarkable that in certain disease states there is an almost total destruction of the granule cells, and that this is so selective. The present study was instituted to determine whether there were any statistically valid associations between the frequency of the "NGL" and disease states or physiochemical circumstances in a large number of patients.

MATERIAL AND METHODS

Cerebellar sections from 1000 consecutive brain sections carried out in the Institute of Pathology Rigshospitalet and the Forensic Institute University of Copenhagen during the years 1966–1970 were reviewed to determine the incidence of NGL

The brains were treated according the routine procedure in these Institutes, i.e. at least 15 days of fixation at room temperature in 10 per cent solution of formalin in water with added glycerine, rinsing in cold water for several hours, and division by the routine cuts. Perfusion fixation was not employed. During the sectioning of the brain the cerebellum was cut in the horizontal plane.

From every cerebellum an approx. 4×3×0.4 cm slice was removed from the right hemisphere, and occasionally from both hemispheres. Apart from this standard slice tissue was removed from any pathological process visible on gross examination. The slices were post-fixed in 10 per cent formalin solution if necessary otherwise they were dehydrated (manually) through increasing alcohol concentrations, in 70 per cent alcohol for 12 hours, 96 per cent for 48 hours, 99 per cent for 24 hours, and then transferred to a xylol bath fo 7 hours. The tissue was placed in a paraffin oven at 60 C for 24 hours, and moulded onto wooden blocks.

The tissue was cut at 6 µ and stained with haematoxylin-eosin, and by van Gieson Hansen's Einarson's gallocyanin and Weil's method. In a few cases special stains (Bodian Klüver Mallory) were also employed (*Romeis* 1968)

The following histological criteria were used in the classification of the degree of necrosis in the granular cell layer:

Grade 1 About 25 per cent of the granule cell nuclei showed variable pyknosis and hypochromasia with early dissolution of the nuclei. The remaining nuclei were either normal or showed only slight changes. Further a few intranuclear vacuoles could be seen (Fig 1B)

Grade 2 About 50 per cent of the granule cell nuclei either showed severe changes or were totally destroyed, and early pyknosis or hypochromasia were seen in an increasing number of the remaining nuclei. There were very few normal nuclei left. There was an increasing number of vacuoles, many of them intranuclear leading to navicular like nuclear shape (Fig 1C)

Grade 3 Over 75 per cent of the nuclei had disappeared and the remainder showed severe changes. Further there were large numbers of vacuoles (Fig 1D)

The areas with necrosis, together with the neighbouring areas, were investigated for vascular changes (capillary proliferation and thrombosis) non-specific inflammatory reactions (granulocytes, lymphocytes, plasma cells or Hortega cells) and gliosis. The tissue stained by Weil's method were examined to see whether there was reduction or absence of stainability of the myelin fibres in the areas of necrosis. No attempt was made to determine whether the number of Purkinje cells was

---

Fig 1 Necrosis of the granular layer (NGL) with increasing severity in Fig B, C and D corresponding to the histological criteria grades 1–3 defined in text. Normal number of granule cells at upper left (A) Haematoxylin-eosin ×465

TABLE 2. *Incidence of Necrosis of the Granular Layer in Different Diseases and Medicolegal Cases*

Diagnosis		Total		Necrosis number		Necrosis percentage	
1 Malformation		36		2		6	
2 Neoplasm	cranial primary	28	136	7	25	25	18
	cranial secondary	19		1		5	
	extracranial	89		17		19	
3 Specific brain diseases and collagenoses		52		10		19	
4 Operation and post-operation complications	cranial	38	115	9	26	24	23
	extracranial	77		17		22	
5 Hepatic coma		39		9		23	
6 Severe infection and sepsis		63		15		24	
7 Uraemia		46		13		28	
8 Arteriosclerotic diseases of heart and brain		268		81		30	
9 Medicolegal cases violent accident, suicide and homicide		158		49		31	
10 Blood diseases		72		27		38	
11 Diabetic coma		15		7		47	
Total		1000		264		26.4	

lower than the average *for the whole material* ($p<0.05$ $\chi^2 = 4.741$ d.f. = 1)

NGL was found with equal frequency in groups 4, 5 and 6, and groups 7, 8 and 9, the frequencies being 23–24 per cent and 28–31 per cent, respectively. There was a significantly more marked tendency to NGL in group 10, which comprised mainly patients with leucaemia, and 7 patients with myelofibrosis ($p<0.05$ $\chi^2 = 4.23$ d.f. = 1)

Group 11 comprised the patients with diabetes mellitus with coma, almost half of whom had necroses. There were too few in this last group to determine whether there was a significantly increased incidence of NGL.

Table 3 shows the incidence of NGL according to the time of the year at which death occurred. There was a marked increased in the incidence of necrosis in April, May, June, July and August, with a maximum in June, when 43 per cent of cases examined showed necrosis. There is a statistically significant increase in the average incidence in these months compared with the remainder of the year ($p<0.005$ $\chi^2 =$ *26.961 df = 1). It must be emphasized that there was the same distribution of age and cause of death in the warmer months as compared with the rest of the year, i.e. the increase in the incidence of NGL cannot be due to an increase in deaths from disorders with a higher tendency to necrosis.*

Table 4 shows the incidence of necrosis according to severity related to the interval between death and autopsy. There would seem to be a tendency for increased number of necroses with increasing interval, but the difference is not statistically significant.

In none of the correlations was it possible to demonstrate any marked changes in the composition of the various degrees of NGL.

Of the 49 cases with necrosis investigated in the Institute of Forensic Medicine it was

TABLE 1 *Incidence of Necrosis of the Granular Layer According to Age and Sex in 1000 Patients*

Age in years	Total		Number with necrosis		Percentage	
	Female	Male	Female	Male	Female	Male
0– 1	15	23	–	1	–	4
2– 9	21	22	5	3	24	14
10–19	18	29	7	8	39	28
20–29	24	35	8	12	33	34
30–39	27	30	6	7	22	23
40–49	46	81	10	19	22	24
50–59	81	125	23	37	28	30
60–69	79	143	30	34	38	24
70–	88	113	27	27	31	24
Total	399	601	116	148	29 1	24.6

reduced. In most cases the evaluation of the histological changes was made on the original routine sections, and only occasionally was it necessary to make supplementary sections from the paraffin blocks.

The histological findings were recorded on punch cards (Selector 102) which were already marked with the number of the section. Not until all histological specimens had been examined and the results coded were further data recorded on the punch cards, viz. age sex and primary cause of death. The following diagnostic groups were employed congenital malformations, malignant disease (*both intra and extra-cranial* and both of epithelial and mesothelial origin) a group comprising collagenosis lipoidosis and demyelinising disorders, deaths within one month of an operation (postoperative deaths) coma hepaticum sepsis or severe bronchopneumonia, uraemia arteriosclerosis diabetes mellitus with coma and cases from the Institute of Forensic Medicine comprising mainly traffic accidents, with a few suicides and homicides.

This diagnostic grouping (Table 2) has been based on both clinical observation and the findings at autopsy The punch cards also contained the time of death and the time of autopsy n hour month and year

The results were processed on an Olivetti Computer using a dated χ^2 test.

RESULTS

Review of the cerebellar sections from 1000 autopsies revealed the presence of NGL in 264 cases (26 4 per cent) Grade 3 changes were found in 112 cases.

Table 1 shows the incidence of NGL in the various age groups and the two sexes. The incidence in women was 29 1 per cent, and in men 24.6 per cent. This difference is not statistically significant. In children under the age af 10 years however there is a highly significantly lower incidence of necroses with $p<0\,00005$ ($\chi^2 = 12.969$(df. = 1) Apart from this there were no significant differences between the various age-groups or sexes in the adults, although in the women aged 10–19 years and 60-69 years there was a tendency *towards* an increased incidence of necrosis. Comparison of the incidence of NGL, as an average, in the men and women revealed no significant difference between the age-groups in the adult patients, and there was no evidence of increasing incidence with age.

Table 2 shows the incidence of NGL according to the various categories of cause of death shown in order of increasing incidence of NGL. The lower incidence in group 1 is possibly due to the fact that this group comprised mainly children. The two cases with necrosis were both adults with severe congenital heart disease The incidence *in this group is* significantly lower than that in the remaining groups ($p<0\,0'$ $\chi^2 = 7.27$ df $= 1$)

Group 2 comprised both intra and extra cranial tumours.

The incidence in this group and in group 3 (collagenosis, lipoidosis) was significantly

TABLE 2 *Incidence of Necrosis of the Granular Layer in Different Diseases and Medicolegal Cases*

Diagnosis		Total		Necrosis number		Necrosis percentage	
1 Malformation		36		2		6	
2. Neoplasm	cranial primary	28	136	7	25	25	18
	cranial secondary	19		1		5	
	extracranial	89		17		19	
3. Specific brain diseases and collagenoses		52		10		19	
4 Operative and post-operative complications	cranial	38	115	9	26	24	23
	extracranial	77		17		22	
5. Hepatic coma		39		9		23	
6 Severe infection and sepsis		63		15		24	
7 Uraemia		46		13		28	
8 Arteriosclerotic diseases of heart and brain		268		81		30	
9 Medicolegal cases violent accident, suicide and homicide		138		43		31	
10 Blood diseases		72		27		38	
11 Diabetic coma		15		7		47	
Total		1000		264		26.4	

lower than the average for the whole material ($p<0.05$ $\chi^2 = 4.741$ df. = 1)

NGL was found with equal frequency in groups 4, 5 and 6, and groups 7 8 and 9 the frequencies being 23–24 per cent and 28–31 per cent, respectively. There was a significantly more marked tendency to NGL in group 10 which comprised mainly patients with leucaemia, and 7 patients with myelofibrosis ($p<0.05$ $\chi^2 = 4.23$ df = 1)

Group 11 comprised the patients with diabetes mellitus with coma, almost half of whom had necroses. There were too few in this last group to determine whether there was a significantly increased incidence of NGL.

Table 3 shows the incidence of NGL according to the time of the year at which death occurred. There was a marked increase in the incidence of necrosis in April, May, June, July and August, with a maximum in June, when 43 per cent of cases examined showed necrosis. There is a statistically significant increase in the average incidence in these months compared with the remainder of the year ($p<0.005$ $\chi^2 = 26.961$ df = 1). It must be emphasized that there was the same distribution of age and cause of death in the warmer months as compared with the rest of the year i.e. the increase in the incidence of NGL cannot be due to an increase in deaths from disorders with a higher tendency to necrosis.

Table 4 shows the incidence of necrosis according to severity related to the interval between death and autopsy. There would seem to be a tendency for increased number of necroses with increasing interval, but the difference is not statistically significant.

In none of the correlations was it possible to demonstrate any marked changes in the composition of the various degrees of NGL.

Of the 49 cases with necrosis investigated in the Institute of Forensic Medicine it was

TABLE 3 *Incidence of Necrosis of the Granular Layer According to the Month of the Year*

Months	Number of necroses	percentage	total no. investigated
January	19	22	86
February	20	21	96
March	16	16	98
April	22	29	77
May	33	38	88
June	33	43	77
July	23	32	71
August	24	29	83
September	17	20	87
October	18	26	69
November	19	26	74
December	20	21	94
Total	264	26.4	1000

TABLE 4 *Incidence and Severity of Necrosis of the Granular Layer Correlated to the Time-Interval between Death and Autopsy*

Interval between death and autopsy	Necrosis grade 1	2	3	percentage	total investigated
6 – 11 hours	3	5	3	18	63
12 – 17	14	11	16	25	167
Over 18	49	70	93	28	770
Total	66	86	112	26 4	1000

TABLE 5 *Review of Medicolegal Cases with Necrosis of the Granular Layer where Death Occurred Shortly after a Trauma*

Age/sex	Time interval between accident and death	Time interval between death and autopsy	Severity of NGL (grade)
10/male	1 hour and 40 min	38 hours	3
20/male	2 „ 45	75	2
59/male	4 „ 0	34	[illegible]
75/female	4 25	32	2
62/male	4 40	83	3

found that 5 had died shortly after a trauma Table 5 gives a review of the ages and duration of survival after trauma, correlated to the degree of necrosis In these 5 cases autopsy did not revealed any other severe disorder which might be responsible for the pathology finding

In no case was it possible to demonstrate any definite reactive changes in the cerebellum in the form of inflammatory reaction vascular changes or loss of myelin that is, no vital reaction

In no case was it possible to demonstrate group dying with arteriosclerosis it was pos-

sible to see small, healed encephalomalacias in the cerebellum. These always involved parts of the molecular layer as well as the granule cell layer and there was widespread gliosis.

In some of the cases with malignant disease there was invasion of tumour in the cerebellar gyri, which was not associated with necrosis.

DISCUSSION

The results presented here demonstrate that NGL is a frequent finding, being present in 26.4 per cent of the 1000 cases studied.

The incidence of NGL in larger unselected autopsy materials has been very varied 8 per cent in 65 internal medical and surgical patients (*Olsen* 1959) 13 per cent in 100 cases (*Schmid* 1957) 18 per cent in 162 cases (*Ikuta et al.* 1963) and 33.6 per cent in 1000 consecutive autopsies (*Okazaki et al.* 1961)

This variation in the incidence of NGL is probably not solely due to true differences, but must depend on the composition of the different materials, as some of the authors have presumably only included severe necroses in their figures. For example *Okazaki et al.* (1961) found a total incidence of 33.6 per cent, but only 12.7 per cent could be characterised as severe. There were 11.2 per cent severe necroses in the present material.

In the present material we have found no correlation between definite clinical disorders and NGL except in patients dying from diabetes mellitus with coma (Table 2, group 11) where there was an increase which was not statistically significant (as there were too few patients in the group) There have been reports of a high incidence of NGL in patients with diabetes mellitus both with (*Bertrand & Tiffeneau* 1942, *Schmid* 1957) and without coma (*Okazaki et a.* 1961) the latter found NGL in 66 per cent of 97 patients with diabetes mellitus. In contrast *Ikuta et al* (1963) could not demonstrate any similar tendency as they found only 20 per cent of 12 cases of diabetes mellitus with necrosis.

The increased high incidence of NGL in blood diseases (Table 2, group 10) which has been demonstrated in the present material, may be due to a reduction in resistance following cytostatic therapy with subsequent sepsis, a factor which *Ikuta et al* (1963) consider to be associated with an increased incidence of NGL. As shown in table 5 there were 5 patients among the group examined in the Institute of Forensic Medicine in whom no disorder which might be associated with the occurrence of NGL could be demonstrated. In these cases the necroses must be regarded as due either to the trauma, or to post mortem changes.

A further possible explanation of the occurrence of NGL is circulatory disturbances (Table 2, group 8) The localization of the NGL is usually symmetrical, and unrelated to the areas supplied by the various arteries, (*Olsen* 1961) On demonstration of the capillary system of the human cerebellar cortex using the McHoney technique it was not possible to correlate NGL to any significant reduction in the capillary density (*Courville* 1964) It has likewise not been possible to demonstrate reactive changes in or around the areas of NGL, apart from in a few cases of long-lasting uraemia, in which there was capillary proliferation (*Olsen* 1961) The presence of NGL could not be correlated to thrombosis in the vessels in the area involved, inflammatory cells, Hortega cells or neuronophagy (*Olsen* 1959 *Okazaki et al.* 1961 *Ikuta et al.* 1963)

Olsen (1961) and *Courville* (1964) found no relation between loss of Purkinje cells and NGL by contrast *Olsen* (1961) demonstrated a definite loss of Purkinje cells in patients who died of severe circulatory changes and cerebral ischaemia. *Okazaki et al* (1961) found no relation to arteriosclerosis of mainly cardiac or cerebral localisation. The present material, in accordance with these findings, revealed no increased incidence in NGL in patients with arteriosclerotic changes. In earlier reports NGL has in particular been considered to be related to liver failure (*Okazaki et al.* 1961) malignant neoplasms

TABLE 3 *Incidence of Necrosis of the Granular Layer According to the Month of the Year*

Months	Number of necroses	percentage	total no. investigated
January	19	22	86
February	20	21	96
March	16	16	98
April	22	29	77
May	33	38	88
June	33	43	77
July	23	32	71
August	24	29	83
September	17	20	87
October	18	26	69
November	19	26	74
December	20	21	94
Total	264	26 4	1000

TABLE 4 *Incidence and Severity of Necrosis of the Granular Layer Correlated to the Time Interval between Death and Autopsy*

Interval between death and autopsy	Necrosis grade 1	2	3	percentage	total investigated
6 – 11 hours	3	5	3	18	63
12 – 17 "	14	11	16	25	167
Over 18 "	49	70	93	28	770
Total	66	86	112	26 4	1000

TABLE 5 *Review of Medicolegal Cases with Necrosis of the Granular Layer where Death Occurred Shortly after a Trauma*

Age/sex	Time-interval between accident and death	Time-interval between death and autopsy	Severity of NGL (grade)
10/male	1 hour and 40 min	38 hours	3
20/male	2 45	75	2
59/male	4 0	34	2
75/female	4 25	32 "	2
62/male	4 40 "	83	3

found that 5 had died shortly after a trauma Table 5 gives a review of the ages and duration of survival after trauma correlated to the degree of necrosis. In these 5 cases autopsy did not revealed any other severe disorder which might be responsible for the pathology finding

In no case was it possible to demonstrate any definite reactive changes in the cerebellum in the form of inflammatory reaction vascular changes or loss of myelin that is, no vital reaction.

In no case was it posible to demonstrate group dying with arteriosclerosis, it was pos-

According to *Bradley* (1937) an increased acidity possibly due to release of proteolytic enzymes from lysosomes, is an important factor in the development of post mortem autolysis. In this connection it may be mentioned that pH-measurements, post-mortem, have revealed a significantly greater acidity in human cerebella which develop NGL (*Albrechtsen* 1976) as compared with normal brains. Furthermore naphthylamidase, which is used as a lysosome marker (*Sylven* 1968) has been demonstrated selectively in the granule cell layer in the rat, among other animals (*Albrechtsen* & *Jensen* 1975)

CONCLUSION

A relatively high incidence of acute selective necrosis in the granular layer of the cerebellum (26.4 per cent) was found in an autopsy material of 1000 consecutive routine autopsies. There was equal distribution among all categories of disease.

The lack of correlation to any given disorder and the increased incidence of NGL demonstrated during the warmer months of the year together with recent investigations by the author (*Albrechtsen* 1975) lend support to the hypothesis that NGL develops after death.

The author wishes to thank *L. Klinken*, Director of the Institute of Neuropathology for his help in the planning of the histological evaluations

REFERENCES

Albrechtsen R. Loss of nuclear density of the granule cell of cerebellum during conventional immersion fixation simulating acute selective necrosis of the granular layer. Proc. VIIth Intern. Congr. Neuropath. Budapest 1974. Excerpta medica Amsterdam *II* pp. 269–272, 1975

Albrechtsen R. The pathogenesis of acute selective necrosis of the granular layer of the human cerebellar cortex. Acta Neuropath. (Berl.) In press

Albrechtsen R. & *Jensen H.* Histochemical demonstration of an LNA-splitting enzyme in the cerebellum of the rat. Acta path. microbiol. scand. Sect. A. *83* 503–510, 1975

Bert and J. & *Godet-Guillain J.:* Dégénérescences cérébelleuses latentes chez les cancéreux. C. r. Séanc. Soc. Biol. *136* 664–665, 1942.

Bertrand I. & *Tiffeneau R.*, Les dégénérescences systématisées centrales dans le coma diabétique. C. r. Séanc. Soc. Biol. *136* 300–501 1942.

Courville C. B.: Cerebellar degeneration as a consequence of chronic alcoholism (with particular reference to the granular layer) Bull. Los Ang. neurol. Soc. *29–30* 198–207 1964

Ferraro A. & *Morrison R. L.* Illuminating gas poisoning Psychiat. Q. *2* 506–541 1978

Hjgaard K. The granular layer of the cerebellar cortex. I anoxia. Proceeding of the Fifth International Congress of Neuropathology. September 1965, Zürich.

Ikuta F., Hirano A. & *Zimmerman H. M.* A experimental study of post-mortem alterations in the granular layer of the cerebellar cortex. J. Neuropath. exp. Neurol. *22* 581 594 1963

Leigh A. D. & *Meyer A.* Degeneration of the granular layer of the cerebellum. J. Neurol. Neurosurg. Psychiat. *12* 287 296, 1949

Neuburger K. T. The hanging neuropathologic picture of chronic alcoholism. Archs. Path. *63* 1–6, 1931

Okazaki H., Aronk I. & *Aronson S. M.*, Acute selective necrosis of the cerebellar internal granular layer. Trans. Am. neurol. Ass. *86* 181–183 1961

Olsen S. Acute selective necrosis of the granular layer of the cerebellar cortex. J. Neuropath. exp. Neurol. *18* 609–619 1959 (a)

Olsen S. Über die akute Nekrose der Körnerschicht des Kleinhirns. Eine echte, akute holotopistische Gewebsnekrose Arch. Psychiat. NervKrankh. *199* 1–13 1959 (b)

Olsen S. The brain in uremia. diss. Munksgaard Copenhagen 1961 pp 56–67

Romeis B., Mikroskopische Technik. R. Oldenbourg Verlag München Wien 1968, p. 419 495.

Schmid A. H. & *Riede U. N.* A morphometric study of the cerebellar cortex from patients with carcinoma. Acta neuropath. (Berl.) *28* 343–352, 1974

Schmidt H. Die Bedeutung der Körnerschichtnekrose für die histologische Diagnose der Hirnschwellung Zbl. allg. Path. Anat. *97* 194 1957

Schreppe O. Frühschäden des Kleinhirns. Arch. Psychiat. NervKrankh. *193* 229–242, 1955

Sylvén B. Studies on the histochemical "leucine aminopeptidase" reaction. VI. The selective demonstration of cathepsin B activity by means of the naphthylamide reaction. Histochemie. *15* 150–159 1968.

(*Bertrand & Godet-Guillain* 1912 *Leigh & Meyer* 1949 *Ule* 1969 *Schmid & Riede* 1974) chronic alcoholism (*Neubuerger* 1951 *Okazaki et al* 1961 *Courville* 1964) and uraemia (*Olsen* 1959 1961)

In uraemia the incidence of NGL is over 60 per cent (35 out of 59 cases) according to *Olsen* (1959 1961) and *Okazaki et al* (1961) found the incidence in this condition twice as high as the average for their entire material (67 per cent) In contrast, *Ikuta et al* (1963) did not find an increased incidence when they correlated incidence to the blood urea nitrogen In the present material NGL was found in 28 per cent of the patients who died in uraemia. It is unlikely that these differences are merely coincidental and it is necessary to consider whether there are differences in the histological evaluation of the tissues in the various studies. Furthermore, one must evaluate the various theories about which factors are responsible for the development of NGL. The parameters employed in the histological assessment on this study would appear to correspond to those used in the previous reports. The incidence of NGL in the present material, as measured by the total number is comparable with that given in other reports. It would therefore not appear that there are errors of diagnosis In *Olsen*'s material (1959 1961) there were a number of patient who had developed uraemia following shock or acute poisoning A high incidence of NGL has also been found by among others, *Høygard* (1965) who reported its presence in 28 per cent of 215 patients. In the present material there are very few patients who died of poisoning

A number of workers have investigated whether NGL might occur in relation to various severe metabolic or endogenous toxic disturbances *Schmid* (1957) mentions in this connection that it is probably not the causative illness, but more the circumstances around the time of death (the image course of death) which are of primary importance for the development of NGL.

The seasonal variation in NGL, with the higher frequency during the warmer months, has not previously been mentioned in the literature as an important factor Even though this relation might merely be due to a coincidental accumulation of NGL during these months, other investigations have supported the theory that there is a certain temperature correlation to the incidence of NGL. Thus *Ikuta et al* (1963) found NGL in 23 per cent of 99 patients with an agonal temperature of over 37°C, but in only 6 per cent of 63 patients with an agonal temperature under 37°C. This observation, in association with the complete absence of reactive changes in NGL, has led to the condition being considered to be of postmortem origin.

Ikuta et al (1963) demonstrated that the incidence of NGL increased as the interval from death to autopsy was prolonged they found necrosis in only 6 per cent of cases in which autopsy was performed 3 hours after death compared with 43 per cent of those in which autopsy was performed 18 hours after death In the present material it has been possible to demonstrate a slight increase in incidence with interval from death to autopsy but this was not statistically significant. It is possible that this is due to the fact that due to Danish law it was not possible to carry out autopsy 3 hours after death, the earliest possible time being 6 hours after death

Ikuta et al (1963) considered NGL to be post mortem changes. This conclusion was, among other things, based on the observation that NGL-like changes could be produced by incubating human cerebellar tissue at 37–45 C for 24–48 hours.

The development of NGL would also seem to continue during fixation of the brain, as witnessed by the fact that these changes are more often found in the deeper parts of the cerebellar sulci, while the more superficial areas are usually well preserved (*Olsen* 1961 *Ikuta et al* 1963 Albrechtsen 1975) A significant reduction in the incidence of NGL could thus be achieved by the simple measure of cutting through the cerebellum before conventional fixation (*Albrechtsen* 1975)

Acta path. microbiol. scand. Sect. A, 85: 203–218, 1977

ULTRASTRUCTURAL CHANGES IN THE PARATHYROIDS OF MONGOLIAN GERBILS INDUCED EXPERIMENTALLY *IN VITRO*

Effects of Variations in Ca^{2+} and Mg^{2+} Concentrations

LENNART BOQUIST

The Department of Pathology, University of Umeå, Umeå, Sweden

Boquist, L. Ultrastructural changes in the parathyroids of Mongolian gerbils induced experimentally in vitro. Effects of Variations in Ca^{2+} and Mg^{2+} Concentrations. Acta path. microbiol. scand. Sect. A, 85: 203–218, 1977.

Isolated parathyroid glands from normal adult Mongolian gerbils were incubated for 15 minutes to 3½ hours either at high or low concentrations of Ca^{2+} and Mg^{2+} after which they were studied ultrastructurally using the pyroantimonate technique and x-ray analysis for identification and structural localization of cations. Glands maintained at high cation concentrations were mainly composed of suppressed chief cells with moderate or high cytoplasmic density, sparsely developed endoplasmic reticulum, often large Golgi complex, occasional cytoplasmic accumulations of secretory granules, lipoid bodies, glycogen-like particles, and numerous often large mitochondria. Ca^{2+}-containing precipitates were found mainly in mitochondria. Autophagic vacuoles contained Ca^{2+}-loaded degenerating mitochondria. Glands exposed to low concentrations of Ca^{2+} and Mg^{2+} were mainly composed of stimulated and active chief cells, characteristic features were a moderate or low cytoplasmic density, prominent endoplasmic reticulum, small Golgi complex, medium-sized or small mitochondria, and smooth electron lucent vacuoles with or without an association to mitochondria. Ca^{2+}-containing precipitates were found mainly in smooth vacuoles and cytosol, but also in mitochondria and rough vacuoles. Myelin-like figures and crystalloid bodies occurred in some mitochondria, and normal or degenerating mitochondria without Ca^{2+} loading were seen in autophagic vacuoles. In addition, some stimulated chief cells exhibited double membrane bounded sequestered areas of cytoplasm with a rich content of free ribosomes and glycogen-like particles. The chief cell mitochondria seem to possess capacity for rapid accumulation of Ca^{2+} associated with an increase in volume at functional suppression. At stimulation of parathyroid function the endoplasmic reticulum is prominent in the active cells, and there seems to be a decrease in the volume and Ca^{2+}-content of the mitochondria occasionally associated with degenerative changes, and a decrease also in the number of free ribosomes and glycogen-like particles in the stimulated cells.

Key words: Parathyroids; mongolian gerbils; ultrastructure; Ca^{2+} and Mg^{2+}.

L. Boquist, Department of Pathology, University of Umeå, 901 87 Umeå, Sweden

Ule G Klinisch bisher unbekannte Kleinhirnveränderungen bei Carcinomen Klin. Wschr *37* 1204 1959

Ule G & Rossner J A Elektronmikroskopische Studien zur akuten Körnerzellnekrose im Kleinhirn, Verh dt. path Ges. *44* 210–215 1960

Williams E Y Structural changes in the granular layer of the cerebellum. Archs. Path. *17* 206–217 1934

Winkelmann N W Selective degeneration and necrosis of the granular layer of the cerebellum. J Neuropath. exp. Neurol. *2* 413-414 1943


2

Received 13.x.76 Accepted 1.xi.76

In a preceding study of gerbilline parathyroid glands cultured for 2 to 6 days, structural differences were found between glands maintained at a high and those maintained at a low concentration of Ca^{2+} (*Boquist & Lundgren* 1975). The former glands were mainly composed of suppressed chief cells whereas the latter glands mainly consisted of stimulated and active chief cells. Differences were recorded in the content and distribution of Ca^{2+}-containing precipitation in the suppressed, stimulated and active cells.

Since functional changes in response to adequate stimuli occur rapidly in endocrine glands, the present study was undertaken with the aim to get information about the structural appearance and the structurally detectable cation distribution in parathyroid glands subjected to different cation concentrations for shorter periods of time than those used in the preceding investigation in which tissue culture technique was used. The study was carried out on isolated gerbilline parathyroid glands which were incubated at different concentrations of Ca^{2+} and Mg^{2+}, since both these cations are well known to affect the synthesis and secretion of parathyroid hormone (PTH) both *in vivo* and *in vitro* (*Copp & Davidson* 1961, *Raisz* 1963, *Raisz et al.* 1965, *Sherwood et al.* 1966, 1970, *Hamilton & Cohn* 1969, *Care & Bates* 1970, 1972).

MATERIAL AND METHODS

Animals and Operative Procedure

The animals used were 22 healthy adult Mongolian gerbils of both sexes, aged 9 to 20 months, which had been kept under standard laboratory conditions with free access to drinking water and a standard laboratory diet (*Boquist* 1975 a).

Parathyroidectomy was carried out under ether anaesthesia through a midline incision with the aid of an operation microscope. In all animals two parathyroid glands could be identified, freed from adherent tissues and removed, after which they immediately were used for incubation. Then the animals were killed.

Incubation Technique

The glands were placed on small pieces of Millipore filters (0.45 μ) in plastic cups. Pre-incubation was carried out in basal medium for 10 minutes at 37 C under 95 per cent O_2 and 5 per cent CO_2. The basal medium was a modified Krebs-Ringer bicarbonate buffer with the following composition: NaCl 115 mM/l, KCl 4.7 mM/l, KH_2PO_4 1.2 mM/l, $MgSO_4 \cdot 7H_2O$ 0.3 mM/l, $NaHCO_3$ 24 mM/l, glucose 3 mM/l, bovine albumin 1 g/l and distilled water.

Then the glands were incubated on similar filters in other plastic cups for 15 minutes to 3½ hours at 37 C under 95 per cent O_2 and 5 per cent CO_2, either in plain basal medium without added Ca^{2+} ("stimulatory medium") or in basal medium with added $CaCl_2$ (3.0 mM/l) and $MgCl_2$ (1.5 mM/l) giving a total magnesium concentration of 1.8 mM/l) ("inhibitory medium"). The magnesium concentration of the stimulatory medium was kept at 0.3 mM/l since it has been reported that low concentrations of magnesium inhibit PTH secretion (*Anast et al.* 1972, *Breitenbach et al.* 1973, *Suh et al.* 1973); at Mg^{2+} concentration less than 0.5 mM the secretion decreases markedly (*Sherwood et al.* 1972).

Electron Microscopic Technique

After the incubation the glands were fixed by immersion as in preceding studies (*Boquist & Fahraeus* 1975, *Boquist & Lundgren* 1975) for 2 hours in 3 per cent glutaraldehyde and 2 per cent potassium pyroantimonate adjusted to pH 7.4 with 0.01 M acetic acid followed by fixation for 1 hour in 1 per cent osmium tetroxide and 2 per cent potassium pyroantimonate. The sections were either unstained or stained with uranyl acetate and lead citrate after which they were viewed in a Siemens-Elmiskop 101.

The specificity of the pyroantimonate precipitates was investigated by X-ray analysis using an energy dispersive system (Kevex X-ray energy spectrometer subsystem 5000 A) combined with a JEOL JSEM 200 scanning-transmission-microscope operated in the transmission microscope mode at 80 kV accelerating voltage and a counting time of 180 seconds at each point of analysis.

Fig. 1. Portion of suppressed chief cells showing cytoplasmic accumulations of vesicular structures interpreted as secretory granules, and coated vesicles. A rich intercellular pyroantimonate precipitation is also seen. × 20 000.

Fig. 2. Cytoplasm of a suppressed chief cell showing rather large mitochondria and a prominent Golgi complex. × 19 000.

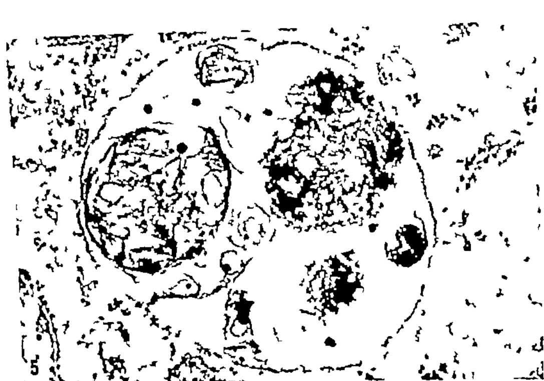


Fig. 5. Autophagic vacuole in suppressed chief cell containing degenerating mitochondria with pyroantimonate precipitates. ×28,000

RESULTS

Suppressed Glands

At 15 minutes there was a rich pyroantimonate precipitation in most intercellular spaces, whereas some spaces showed a moderate, or seldom a sparse precipitation. Most chief cells exhibited a moderate cytoplasmic electron density and occasional accumulations of secretory granules (Fig 1) often with an admixture of coated vesicles. Free ribosomes and glycogen-like particles were seen in the cytoplasm. The Golgi complex was often expanded (Fig 2) whereas the endoplasmic reticulum was sparsely or moderately developed. Most mitochondria were slightly or moderately enlarged.

At the following observation times essentially similar findings were made. Most chief cells were of suppressed type, only an occasional active or so-called stimulated cell (*Boquist & Fåhraeus* 1975 *Boquist & Lundgren* 1975) was recorded. The suppressed chief cells showed rounded, oval or irregular nuclei with moderate chromatin density and medium-sized nucleoli. The cytoplasm exhibited a moderate or rather high density and contained free ribosomes and glycogen particles. The endoplasmic reticulum was inconspicuous, whereas the Golgi complex was occasionally enlarged. Accumulations of structures interpreted as secretory granules, as well as some coated vesicles, could be seen in some cells and a few so-called storage granules were also found. Most mitochondria were enlarged and contained pyroantimonate precipitates, sometimes surrounded by (artifactual?) electron lucent areas (Fig 3). A few giant mito-

---

Fig 3 Portion of suppressed chief cell showing numerous large mitochondria with pyroantimonate precipitates and more or less distinct cristae 17,000

Fig 4 Portion of suppressed chief cells showing mitochondrion close to a large lipoid body 19,000


3
4


8
t
Li
9



Fig 6 Stimulated chief cell showing smooth vacuoles with pyroantimonate precipitates, some of them in direct contact with mitochondria. Pyroantimonate precipitates are also seen in the mitochondrial matrix. Glycogen-like particles (gl) and lysosomal bodies (L) are also present. × 19 000

Fig 7 Portion of suppressed chief cells believed to be a transition to stimulated cells showing smooth vacuoles with a rich content of pyroantimonate precipitates localized close to the plasma membranes. × 22 000

Fig 8 Portion of suppressed chief cell in a stimulated parathyroid gland showing crystalloid inclusions in mitochondria. Pyroantimonate precipitates are seen in the mitochondria and in a perivascular space. × 28,000

Fig 9 Two autophagic vacuoles in a stimulated chief cell containing mitochondria (M), a lipoid body (Li), accumulations of glycogen-like particle (gl) and membranous structures. × 24 000



Fig 10 Portion of two stimulated chief cells showing low cytoplasmic density pyroantimonate precipitates in cytosol (p) smooth vacuoles ( ) and moderately large mitochondria (M) Sequestered areas of cytoplasm containing rich amount of glycogen-like particles and free ribosomes (S) and an autophagic vacuole (A) containing two smooth vacuoles with pyroantimonate precipitates are also seen Differences in density are demonstrated between the sequestered areas and the surrounding cytoplasm 12,000

chondria were recorded. Mitochondria were seen close to, or in contact with small or large lipoid bodies (Fig 4) and plasma membranes. Some mitochondria showed heavy pyroantimonate precipitation. Autophagic vacuoles were observed containing degenerating mitochondria with pyroantimonate precipitates (Fig 5). The cell membranes were usually straight.

Stimulated Glands

At 15 minutes the glands were composed of active stimulated and some suppressed cells. The mitochondria of stimulated and suppressed cells exhibited electron lucent areas in the inner compartment, unfolding or cristae, separation of the membranes occasionally with the appearance of bulbous projections, and formation of smooth vacuoles with pyroantimonate precipitates (Fig 6). Similar vacuoles were also seen in the cytoplasm without any association to mitochondria, occasionally close to or in contact with the plasma membranes (Fig 7). In the stimulated cells pyroantimonate precipitates were also seen seemingly lying free in the cytosol. In suppressed and stimulated cells there were also mitochondria with crystalloid inclusions (Fig 8).

Similar findings were also made at the following observation times, at which stimulated and active cells predominated. In the stimulated cells there were autophagic vacuoles containing normal or degenerating mitochondria without pyroantimonate precipitates, lipoid bodies, accumulations of glycogen like particles, membranous structures (Fig 9) and smooth vacuoles with pyroantimonate precipitates. There were also sequestered areas of cytoplasm containing a rich amount of glycogen like particles and free ribosomes (Fig 10) surrounded by double smooth membranes (Fig 11). The smooth membranes limiting these sequestered areas were occasionally separated forming electron lucent spaces which could contain some pyroantimonate precipitates (Fig 12). The smooth membranes of sequestered areas were occasionally seen in direct contact with the plasma membranes. Myelin like figures were also observed in mitochondria of suppressed and stimulated cells.

The intercellular spaces of stimulated glands usually possessed a sparse or more seldom a moderate pyroantimonate precipitation (Fig 13). The active cells exhibited a moderate or low cytoplasmic density, small or medium-sized mitochondria without electron dense precipitation, a well-developed rough lamellar endoplasmic reticulum and usually small Golgi complexes (Fig 14). Whorls of rough lamellar endoplasmic reticulum were often encountered (Fig 15). These cells contained no or only few secretory granules. The cell membranes were often interdigitating (Fig 14).

X Ray Analysis

Pyroantimonate precipitates which were large enough for analysis showed significant peaks for calcium, but not for other cations, apart from those associated with the ultrastructural techniques used.

DISCUSSION

The present morphological data show that clear differences exist in distribution of pyroantimonate precipitates and morphological appearance of the chief cells, between gerbilline parathyroid glands incubated at high concentrations of Ca^{2+} and Mg^{2+} and those incubated at low concentrations of these cations. Structural differences were recorded already at the first observation time after 15 minutes of incubation indicating that structural alterations, apparently based upon changes in functional activity occur rapidly in the parathyroid parenchymal cells.

Conforming to the findings made in parathyroid glands of Mongolian gerbils subjected to functional suppression *in vivo* (*Boquist* 1975 a, *Boquist & Fåhraeus* 1975) and *in vitro* using tissue culture technique for 2 to 6 days (*Boquist & Lundgren* 1975) the suppressed parathyroid glands were characterized


11
V
12

by a predominance of chief cells with moderate or high cytoplasmic density, sparsely developed endoplasmic reticulum, numerous, often large mitochondria, and occasional cytoplasmic accumulations of secretory granules. However, quantitative differences were recorded between the preceding and the present experiments. Thus, there were generally a higher cytoplasmic density and more numerous and larger mitochondria in the previously investigated glands. Moreover, in contrast to the findings in the preceding studies, the Golgi complexes were often enlarged in the presently studied glands, which may denote that the capacity for hormone storage is retained and possibly characteristic for the chief cells during the first few hours of functional suppression. In this context it is of interest that the parathyroid glands of many species under "normal conditions" possess rather few secretory granules, reflecting a limited capacity for hormone storage (*Roth & Raisz* 1964, *Hamilton et al* 1971), contrasting to the case in other endocrine glands. A continued hormone storage during the early stage of functional suppression may be one cause of the presence of accumulations of secretory granules in the cytoplasm of some suppressed chief cells. Another cause is probably inhibition of the secretion of hormone. Since the endoplasmic reticulum was sparsely developed, it seems that the synthesis of hormone on the other hand was rapidly reduced although not completely inhibited, conforming to what is known from functional studies of suppressed parathyroid glands (*Oldham et al* 1971). The possibility also remains that at least some of the cytoplasmic accumulations are of non hormonal (*e.g.* lysosomal) nature and are involved in a degradation of PTH (*Chu et al* 1973, *Habener et al* 1975) and that the enlargement of the Golgi complexes is associated with a formation of such substances.

Consistent with the findings in the preceding studies of gerbilline parathyroid glands, the stimulated glands were characterized by a predominance of active and so-called stimulated chief cells (*Boquist* 1975 a, *Boquist & Fåhraeus* 1975, *Boquist & Lundgren* 1975). The former showed a low or moderate cytoplasmic density and a prominent lamellar rough endoplasmic reticulum, occasionally arranged in whorls. However, the Golgi complexes were rather small, which with regard to the sparse occurrence or absence of secretory granules denotes that newly formed hormone may be directly released from the chief cells without any intermediate storage stage.

The intercellular calcium-containing precipitation was more marked in the suppressed glands subjected to high cation concentrations than in the stimulated glands exposed to low cation concentrations, which suggests an effective equilibration between the experimental media and the parathyroid tissue. A rich Ca-containing precipitation was found mainly in mithochondria in the suppressed cells, and mainly in smooth vacuoles and cytosol of the stimulated cells, whereas the intracellular precipitation was sparse or absent in the active chief cells. This conforms to the findings in the preceding studies of gerbilline parathyroid glands.

The finding in the suppressed glands of enlarged mitochondria often with rich Ca^{2+} containing precipitation is, as far as can be learnt on purely morphological and histochemical grounds, consistent with the previously presented idea of a role of the mitochondria in parathyroid cells as sites for accumulation and storage of intracellular calcium (*Boquist* 1975 b, *Boquist & Lundgren* 1975). It is known that changes in mitochondrial volume are closely related to active

Fig 11 Portion of stimulated chief cell showing a sequestered area with closely packed glycogen-like particles and free ribosomes and occasional pyroantimonate precipitates, limited by double smooth membranes. × 26 000

Fig 12 Cytoplasm of stimulated chief cell showing sequestered cytoplasmic areas limited by double membranes which in some places are separated forming electron lucent spaces with pyroantimonate precipitates (v). Pyroantimonate precipitates are also seen in the cytosol. × 24,000


11
V
P
12

13

14

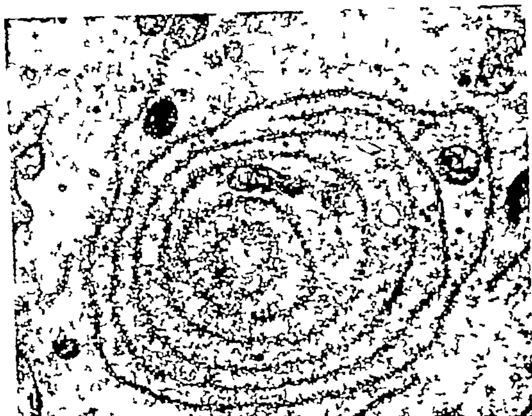


Fig 15. Whorl of rough endoplasmic reticulum in an activ chief cell. The mitochondria are rather small. A few pyroantimonate precipitates are seen intracisternally in a dilated portion of the endoplasmic reticulum × 16,000

ion accumulation (*Lerity et al.* 1974) and that this volume is increased in association with the accumulation of calcium (*Hackenbrock & Caplan* 1969 *Rungrok & Elbers* 1972) Moreover mitochondria also n other tissues have been suggested to serve as a store or buffer for calcium, regulating the intra cellular calcium levels (*Rasmussen et al* 1963 *Borle* 1972 *Matthews et al.* 1971 *Rasmussen et al* 1972, *Bonucci & Sadun* 1973) and studies of isolated mitochondria have disclosed that of all the common uni and bivalent cations present in cells it is only Ca^{2+} which is rapidly accumulated by mitochondria (*Lehninger* 1970) In addition to enlargement and Ca^{2+}-containing precipitates some mitochondria of the suppressed chief cells showed structural alterations the cristae were unfolded and the membranes were separated. Such alterations may be associated with a massive loading of mitochondria with Ca^{2+} (*Lehninger et al* 1967)

Myelin-like figures were observed in some chief cell mitochondria of stimulated glands. Such figures have repeatedly been reported in different tissues and have usually been thought to be the result of non-specific reac

Fig 13 Portion of tw activ chief cells showing interdigitating membranes and rather sparse intercellular pyroantimonate precipitation × 13,000

Fig 14 Active chief cells showing rather low cytoplasmic density small mitochondria without precipitates, rough lamellar endoplasmic reticulum, and interdigitating membranes × 8,000



13
14



Fig 15 Whorl of rough endoplasmic reticulum in an active chief cell. The mitochondria are rather small. A few pyroantimonate precipitates are seen intracisternally in a dilated portion of the endoplasmic reticulum. ×16,000

ion accumulation (*Verity et al.* 1974) and that this volume is increased in association with the accumulation of calcium (*Hackenbrock & Caplan* 1969 *Ruigrok & Elbers* 1977) Moreover mitochondria also in other tissues have been suggested to serve as a store or buffer for calcium, regulating the intra cellular calcium levels (*Rasmussen et al* 1963 *Borle* 1972, *Matthews et al* 1971 *Rasmussen et al.* 1972, *Bonucci & Sadun* 1973) and studies of isolated mitochondria have disclosed that of all the common uni- and bivalent cations present in cells it is only Ca which is rapidly accumulated by mitochondria (*Lehninger* 1970) In addition to enlargement and Ca^{2+}-containing precipitates some mitochondria of the suppressed chief cells showed structural alterations the cristae were unfolded and the membranes were separated. Such alterations may be associated with a massive loading of mitochondria with Ca^{2+} (*Lehninger et al.* 1967)

Myelin-like figures were observed in some chief cell mitochondria of stimulated glands. Such figures have repeatedly been reported in different tissues and have usually been thought to be the result of non-specific reac

Fig 13 Portion of two active chief cells showing interdigitating membranes and a rather sparse intercellular pyroantimonate precipitation ×15 000

Fig 14 Active chief cells showing rather low cytoplasmic density small mitochondria without precipitates, rough lamellar endoplasmic reticulum, and interdigitating membranes ×8,000

tive processes and to represent a form of focal mitochondrial phospholipid membrane degeneration under various stimuli (*LeBeux et al* 1969) An absence or strong inhibition of the mitchondrial respiratory enzyme synthesis has been suggested a role in the formation of these figures (*LeBeux et al* 1969) In regard of the supposed role of parathyroid mitochondria in the intracellular accumulation of Ca^{2} the need for such organelles may be reduced or absent in stimulated glands which are exposed to low ambient concentrations of Ca and exhibit less Ca^{2} containing precipitation than the suppressed glands and which as far as can be learnt on these grounds, are believed to possess a lower intracellular concentration of Ca than the suppressed glands Therefore the presence of myelin like figures in mitochondria of stimulated glands may represent a stage in or one form of degeneration of "un needed storage organelles" associated with a reduction of the available mitochondrial population to the volume needed in parathyroid cells subjected to functional stimulation.

The significance of the crystalloid mitochondrial inclusions occasionally found in suppressed chief cells is not clearly known Also such mitochondrial changes have frequently been reported in other tissues without any clarified significance Among possible interpretations can be mentioned that such inclusions have been suggested to represent a non specific reaction to previous mitochondrial swelling (*Sun et al* 1972) a possibility which in the present case might be consistent with a transformation of large Ca^{2} rich mitochondria into small Ca^{2} poor ones.

The possibility that the mitochondrial alterations described above represent degenerative phenomena is supported by the finding of autophagic vacuoles containing more or less well preserved mitochondria without Ca^{2} containing precipitation in the stimulated glands. This may also be consistent with a reduction of the mitochondrial volume Autophagic vacuoles containing mitochondria were also found in suppressed glands However although also these mitochondria showed degenerative changes, they differed from those observed in the autophagic vacuoles of the stimulated glands in the possession of Ca^{2}-containing percipitates. Therefore mitochondrial autophagy in suppressed cells may rather represent a disposal of mitochondria damaged by excessive Ca^{2+} loading

A close association was often observed between mitochondria and lipoid bodies in suppressed cells there was occasionally a direct contact between these organelles. The cause of this association is not clearly known, but it may be related to the supposed mitochondrial accumulation of Ca since in other tissues swelling and formation of endogenous free fatty acids have been disclosed in mitochondria exposed to high (2 to 4 mM) concentrations of Ca^{2+} (*Wojtczak & Lehninger 1961*)

The double membrane limited sequestered areas of cytoplasm seen in some stimulated chief cells are believed to be involved in autophagy Some of them made contact with the plasma membranes which might denote a derivation of autophagic vacuoles from the plasma membranes, or be associated with an extracellular discharge of its contents. Autophagy of free ribosomes and glycogen-like particles is believed to play a role in the transformation of suppressed cells with a rich content of these organelles into stimulated cells which are poor in these organelles. The sequestered areas were clearly more electron dense than the other portions of the cytoplasm indicating that the difference in cytoplasmic density between suppressed and stimulated chief cells is due at least in part to differences in the content of ribosomes and glycogen like particles. The somewhat higher density observed in the active chief cells compared with the stimulated chief cells may also be due to a more rich content of ribosomes and also of other organelles in the active cells.

Like in the preceding studies of gerbilline parathyroid glands the stimulated chief cells were found to possess smooth vacuoles containing pyroantimonate precipitates. Some of

these vacuoles were directly associated with mitochondria and it seems that they were derived from mitochondria, probably by a process of separation of the external mitochondrial membranes, a subsequent development of bulbous processes, and a final formation of a vacuole. The vacuoles might be involved in a transport of cations. Some of them were in direct contact with the plasma membranes, possibly representing a discharge of their contents into the intercellular spaces.

REFERENCES

Anast C S, Mohs J M, Kaplan S L, & Burns T W. Evidence for parathyroid failure in magnesium deficiency. Science 177 606–608 1972.

Bencosme, E & Sadan, R. Experimental calcification of the myocardium. Ultrastructural and histochemical investigations. Am. J Path. 71 167 192, 1973

Boquist, L. Parathyroid morphology in gerbils after calcium and parathormone administration. Horm Metab Res 7 261 266, 1975 a

Boquist L. Occurrence of oxyphil cells in suppressed parathyroid glands. Cell. Tiss. Res. 163 465–470, 1975 b

Boquist L & Fahraeus B. Parathyroid morphology in gerbils after thyroidectomy and calcium administration. Acta path. microbiol. scand Sect. A, 83 539–549 1975

Boquist L & Lundgren E. Effects of variations in calcium concentration on parathyroid morphology in vitro. Lab Invest. 33 638–647 1975

Borle A B. Parathyroid hormone and cell calcium. In Calcium, parathyroid hormone and the calcitonins. R V Talmage and P L Munson, eds. Proc. IV Parathyroid Conference Exc Med Amsterdam, pp. 484 491 1972

Breitenbach R P, Gonnerman W A, Erfling W L & Anast C S. Dietary magnesium, calcium homeostasis, and parathyroid gland activity of chickens. Am. J Physiol. 225 12 17 1973

Care A D & Bates R F L. The secretion of parathyroid hormone and calcitonin. Hormones 1 364 378, 1970

Care A D & Bates R F L. Control of secretion of parathyroid hormone and calcitonin in mammals and birds. Gen Comp Endocr Suppl. 3 44 458, 1972.

Copp D H & Davidson A G F. Direct humoral control of parathyroid function in the dog. Proc Soc Exp Biol Med 107 342 344 1961

Habener J F, Kemper B & Potts J T J. Calcium-dependent intracellular degradation of parathyroid hormone a possible mechanism for the regulation of hormone stores. Endocrinology 97 431–441 1975.

Hackenbrock C R & Caplan A I. Ion-induced ultrastructural transformations in isolated mitochondria. The energized uptake of calcium. J Cell Biol. 42 221–234 1969

Hamilton J W & Cohn D V. Studies on the biosynthesis in vitro of parathyroid hormone. I Synthesis of parathyroid hormone by bovine parathyroid gland slices and its control by calcium. J Biol. Chem. 244 5421–5429 1969

Hamilton J W, Spierto F W, MacGregor R R & Cohn D V. Studies on the biosynthesis in vitro of parathyroid hormone J Biol. Chem. 246 3224–3233 1971

Le Beux, Y, Hetenyi, G., J & Phillips M J. Mitochondrial myelin-like figures. A nonspecific reactive process of mitochondrial phospholipid membranes to several stimuli. Z. Zellforsch. 99 491 506, 1969

Lehninger A L. Mitochondria and calcium ion transport Biochem. J 119 129 138, 1970

Lehninger A L, Carafoli E & Rossi C S. Energy-linked ion movements in mitochondrial systems. Adv Enzymology 29 259–320, 1967

Matthews J L, Martin J H, Arsenis C, Eisenstein R & Kuettner K. The role of mitochondria in intracellular calcium regulation. In Cellular mechanism for calcium transfer and homeostasis. G Nichols Jr., and R. H. Wasserman, eds. Academic Press, New York and London, pp. 239–255 1971

Oldham S B, Fischer J A, Capen C C, Sizemore G W & Arnaud C D. Dynamics of parathyroid hormone secretion in vitro. Am. J Med. 50 650–657 1971

Raisz, L G. Regulation by calcium of parathyroid growth and secretion in vitro Nature (London) 197 1115–1116 1963

Raisz L G, Au W Y W & Stern P H. Regulation of parathyroid activity. In The parathyroid glands, ultrastructure, secretion and function. P J Gaillard et al., University of Chicago Press, Chicago, pp. 37 52, 1965

Rasmussen H, DeLuca H., Arnaud C, Hawker C & von Stedingk M. The relationship between vitamin D and parathyroid hormone. J Clin. Invest. 42 1940–1946, 1963

Rasmussen H, Kurokawa, K, Mason J & Goodman D B P. Cyclic AMP calcium and cell activation. In Calcium, parathyroid hormone and the calcitonins. R. V Talmage and P L. Munson, eds. Proc. IV Parathyroid Conference Exc. Med., Amsterdam, pp. 492 501 1972.

Roth S I & Raisz, L, G. The course and reversibility of the calcium effect on the ultrastructure of the rat parathyroid gland in organ culture. Lab. Invest. 15 331 343, 1966

tive processes and to represent a form of focal mitochondrial phospholipid membrane degeneration under various stimuli (*LeBeux et al* 1969) An absence or strong inhibition of the mitochondrial respiratory enzyme synthesis has been suggested a role in the formation of these figures (*LeBeux et al* 1969) In regard of the supposed role of parathyroid mitochondria in the intracellular accumulation of Ca^{2} the need for such organelles may be reduced or absent in stimulated glands which are exposed to low ambient concentrations of Ca and exhibit less Ca^{2}-containing precipitation than the suppressed glands and which as far as can be learnt on these grounds, are believed to possess a lower intracellular concentration of Ca^{2} than the suppressed glands. Therefore the presence of myelin like figures in mitochondria of stimulated glands may represent a stage in or one form of degeneration of "un needed storage organelles" associated with a reduction of the available mitochondrial population to the volume needed in parathyroid cells subjected to functional stimulation.

The significance of the crystalloid mitochondrial inclusions occasionally found in suppressed chief cells is not clearly known Also such mitochondrial changes have frequently been reported in other tissues without any clarified significance Among possible interpretations can be mentioned that such inclusions have been suggested to represent a non specific reaction to previous mitochondrial swelling (*Sun et al* 1972) a possibility which in the present case might be consistent with a transformation of large Ca^{2} rich mitochondria into small Ca^{2} poor ones

The possibility that the mitochondrial alterations described above represent degenerative phenomena is supported by the finding of autophagic vacuoles containing more or less well preserved mitochondria without Ca^{++}-containing precipitation in the stimulated glands. This may also be consistent with a reduction of the mitochondrial volume Autophagic vacuoles containing mitochondria were also found in suppressed glands. However although also these mitochondria showed degenerative changes, they differed from those observed in the autophagic vacuoles of the stimulated glands in the possession of Ca^{2}-containing percipitates. Therefore, mitochondrial autophagy in suppressed cells may rather represent a disposal of mitochondria damaged by excessive Ca^{2+} loading

A close association was often observed between mitochondria and lipo d bodies in suppressed cells there was occasionally a direct contact between these organelles. The cause of this association is not clearly known, but it may be related to the supposed mitochondrial accumulation of Ca^{2} since in other tissues swelling and formation of endogenous free fatty acids have been disclosed in mitochondria exposed to high (2 to 4 mM) concentrat ons of Ca^{2} (*Wojtczak & Lehninger* 1961)

The double membrane limited sequestered areas of cytoplasm seen in some stimulated chief cells are believed to be involved in autophagy Some of them made contact with the plasma membranes, which might denote a derivation of autophagic vacuoles from the plasma membranes or be associated with an extracellular discharge of its contents. Autophagy of free ribosomes and glycogen-like particles is believed to play a role in the transformation of suppressed cells with a rich content of these organelles into stimulated cells which are poor in these organelles. The sequestered areas were clearly more electron dense than the other portions of the cytoplasm, indicating that the difference in cytoplasmic density between suppressed and stimulated chief cells is due, at least in part, to differences in the content of ribosomes and glycogen like particles. The somewhat higher density observed in the active chief cells compared with the stimulated chief cells may also be due to a more rich content of ribosomes and also of other organelles in the active cells.

Like in the preceding studies of gerbilline parathyroid glands the stimulated chief cells were found to possess smooth vacuoles containing pyroantimonate precipitates. Some of

Acta path. microbiol. scand. Sect. A, 85: 219–229, 1977

THE ENDOCRINE PANCREAS IN EARLY ALLOXAN DIABETES

Including Study of the Alloxan Inhibitory Effect of Feeding and Some Hexoses

LENNART BOQUIST

Department of Pathology, University of Umeå, Umeå, Sweden

Boquist, L. The Endocrine Pancreas in Early Alloxan Diabetes. Including Study of the Alloxan Inhibitory Effect of Feeding and Some Hexoses. Acta path. microbiol. scand. Sect. A, 85: 219–229, 1977.

Starved animals were sensitive to alloxan, whereas a more or less inhibitory effect towards alloxan was observed in fed animals, and in starved animals pretreated with glucose, mannose or fructose, but not in those pretreated with galactose. The islets of starved controls possessed larger B-cell mitochondria than those of fed ones. The earliest B-cell changes in the alloxan-treated animals were localized to the mitochondria which showed swelling, and disruption of inner and occasionally outer membranes. Later many mitochondria were disintegrated, and the endoplasmic reticulum and Golgi complex disorganized. The secretory granules were preserved, although sometimes with atypical configuration, in degenerating but non-necrotic B-cells, suggesting that insulin stored in granules is not released until the cells are necrotic. Finally frank necrosis was seen in some B-cells, whereas others were unaffected. The Ca^{++} precipitation studied by pyroantimonate technique and x-ray analysis differed in the B-cells of the alloxan-treated animals from that in the controls: the former animals exhibited no or only sparse precipitation in mitochondria and secretory granules, but a rich precipitation in the cytoplasmic ground substance, whereas the precipitation in the controls mainly was localized to mitochondria and secretory granules. The primary site of alloxan action in the B-cells is believed to be localized to the mitochondria.

Key words: B-cell morphology; alloxan; experimental diabetes; Ca^{++}-precipitation.

L. Boquist, Department of Pathology, University of Umeå, S-901 87 Umeå, Sweden.

Received 18.76. Accepted 1.xi.76

The pathogenesis of alloxan diabetes is still unknown, in spite of intense research during the last three decades. In preceding morphological and functional studies of rodent species carried out in this laboratory comparison was made between alloxan diabetes (*Boquist* 1968 a and b) and spontaneous diabetes (*Boquist* 1969 a) in Chinese hamsters: the two variants of diabetes were found to differ from each other mainly with respect to the capacity for B-cell regeneration, which was retained in the animals with experimental diabetes but absent from those with the spontaneous disease (*Boquist* 1969 b and 1976 a). In recent years, the interest has mainly been directed to mice with "mutation" diabetes because excellent controls are available (*Boquist et al.* 1974 a and b), and to Mongolian gerbils (*Boquist* 1972). There is no previous report on the effect of alloxan in these kinds of animals, nor any report on the cation precipitation in the endocrine pancreas of alloxan-treated animals of any species.

Ruigrok J C & Elbers P F The effects of calcium acetate on mitochondria in the perfused rat liver I Accumulation of Ca and concomitant swelling Cytobiol. 5 51–64 1972.

Sherwood L M Potts J T Jr Care A D Mayer G P & Aurbach G D Evaluation by radioimmunoassay of factors controlling the secretion of parathyroid hormone intravenous infusions of calcium and ethylene-diamine tetra acetic acid in the cow and goat. Nature (London) 209 52–55 1966

Sherwood L M Herrmann I & Bassett C A Parathyroid hormone secretion *in vitro* regulation by calcium and magnesium ions Nature (London) 225 1056–1057 1970

Sherwood L M Lundberg W B Jr Targovnik J H, Rodman J S & Seyfer A Synthesis and secretion of parathyroid hormone *in vitro* Am J Med 50 658–669 1971

Sherwood L M Abe M Rodman J S Lundberg W B Jr & Targovnik J H Parathyroid hormone synthesis, storage and secretion. *In* Calcium, parathyroid hormone and the calcitonins. R. V Talmage and P L Munson, eds, Proc. IV Parathyroid Conference. Exc. Med., Amsterdam pp. 183–196 1972

Suh S M Tashjian A H Jr., Matsuo N Parkinson D K & Fraser D Pathogenesis of hypocalcemia in primary hypomagnesemia normal end-organ responsiveness to parathyroid hormone, impaired parathyroid gland function. J Clin. Invest. 52 153–160 1973

Sun C N White H J & Towbin E J Crystalloid inclusions in mitochondria of renal tubules. Exp Path 7 166–171 1972

Vesity M A Brown W J & Cheng M Mitochondrial conformation and swelling-contraction reactivity during early liver regeneration. Am. J Path. 74 241–262, 1974

Wojtczak L & Lehninger A L Formation and disappearance of an endogenous uncoupling factor during swelling and contraction of mitochondria. Biochim Biophys. Acta 51 442–456, 1961

TABLE 1 Blood Glucose Concentration (mg/100 ml) in Groups of Differently Fed and Pretreated Mice before (0 Minutes) and at Different Intervals after Intraperitoneal Injection of 200 mg/kg Body Weight of Alloxan or Saline (Controls) The Values Represent the Concentration in Each of the Two Mice Comprised in the Groups

Animal group	Starvation	Pretreatment	Treatment	Blood glucose concentration					
				Minutes		Hours			
				0	10	1	4	24	48
I	Yes	No	Alloxan	51	128	230	266	145	–
				62	141	274	266	88	235
II		Glucose		89	99	133	129	92	122
				84	98	124	158	73	128
III		Mannose		91	90	127	131	90	112
				88	94	140	137	89	120
IV		Fructose		80	94	124	153	91	128
				99	92	115	124	83	143
V		Galactose		87	145	265	–	–	–
				75	124	241	238	72	238
VI	No	No		95	99	156	114	98	125
				79	93	167	159	77	131
VII			Saline	91	93	84	72	68	61
				84	73	62	55	42	45
VIII	Yes			54	62	73	61	58	51
				64	73	58	49	51	48

RESULTS

Blood Glucose

The blood glucose determinations were carried out as a complement to the morphological studies to see whether the treatments were effective and whether the morphological changes were associated with alterations in the blood glucose concentration. The results obtained in mice are given in Table 1 and those obtained in gerbils are given in Table 2. Essentially similar alterations in blood glucose concentration in the two species in response to alloxan and saline were recorded. A typical triphasic blood glucose curve was found in most animals treated with alloxan (group I to VI) whereas the controls (group VII and VIII) remained normoglycaemic. The hyperglycaemic responses were more marked in groups I and V than in groups II, III, IV and VI, suggesting a partial inhibition of alloxan toxicity by feeding, or by injection of glucose, mannose and, fructose, but not by injection of galactose.

One mouse in group I died about 40 hours after alloxan injection and one mouse in group V died 3 hours after the administration of alloxan. A strong positive reaction for glucosuria was obtained in both these animals. Thus, the only spontaneous deaths (apparently in association with hyperglycaemia) were found in those groups in which there seemed to be no protective influences (feeding or pretreatment with glucose, mannose or fructose) against alloxan toxicity.

Light Microscopy

Essentially similar findings were made in mice and gerbils both in the light microscopic and electron microscopic studies, including the investigation of the pyro-antimonate precipitation. Therefore no differentiation will be made in the following text between findings made in mice and gerbils.

The islets and exocrine parenchyma of the controls (group VII and VIII) were normal at each observation time.

At 24 and 48 hours, inflammatory cell infiltration was found in the exocrine parenchyma around some of the islets which exhibited degenerative B-cell changes in groups

Pilot studies disclosed that Mongolian gerbils and non-diabetic mice (KsJ +/+) with the same genetic background as the mice with "mutation" diabetes (KsJ-*db/db*) were sensitive to alloxan. Therefore the present study was carried out with the aim to get information about the effect of alloxan on the structural appearance and cation precipitation in the endocrine pancreas of these animals. The main interest was directed to the earliest changes since it is well known that alloxan is active only for a few minutes after its administration into the organism. Blood glucose determinations were also carried out mainly as a complement to the structural studies. Furthermore the inhibitory effect towards alloxan of some hexoses, known from studies of other species (*Sen & Bhattacharya* 1952, *Bhattacharya* 1954, *Villar Palasi et al* 1957, *Kaneko & Logothetopoulos* 1963, *Scheynius & Taljedal* 1971, *Zawalich & Beidler* 1973, *Rossini et al* 1974) and of feeding was investigated.

MATERIAL AND METHODS

Animals, Pretreatment and Alloxan Administration

The animals used were non-diabetic adult C57BL-KsJ +/+ mice and Mongolian gerbils of both sexes from local stocks, kept under standard laboratory conditions with free access to drinking water and standard laboratory diet.

The following animal groups consisting of both mice and gerbils were used: I. Starved 24 hours. II. Starved 24 hours, pretreated with glucose 100 mg/kg body weight. III. Starved 24 hours, pretreated with mannose 100 mg/kg body weight. IV. Starved 24 hours, pretreated with fructose 100 mg/kg body weight. V. Starved 24 hours, pretreated with galactose 100 mg/kg body weight. VI. Fed *ad libitum*. VII. Fed *ad libitum* (controls). VIII. Starved 24 hours (controls).

The sugars used for pretreatment were dissolved in saline and injected intraperitoneally 20 minutes before alloxan injection. All injections were carried out on animals anaesthetized with ether.

Groups I to VI were injected intraperitoneally with alloxan (Alloxan monohydrate, Eastman Kodak Co., Rochester, N.Y.) dissolved in a citrate-phosphate buffer pH 4.2 in a dose of 200 mg/kg body weight, whereas groups VII and VIII received intraperitoneal injections of saline in volumes corresponding to those used for alloxan injection.

Tissue Preparation and Blood Glucose Determination

Two mice (in groups in which no spontaneous deaths had occurred) and two gerbils were killed at each of the following time intervals following alloxan or saline injection: 10 minutes, 1 hour, 4 hours, 24 hours and 48 hours. The pancreas was removed immediately after killing of the animals and small pieces from the head, body and tail were taken for electron microscopic study whereas the rest of the organ was used for light microscopic investigation. The pancreas was also taken for light microscopic examination from the two mice which died spontaneously (see Results).

Blood glucose was assayed by the glucose oxidase method using Glox® (AB Kabi, Stockholm, Sweden) before the injections on blood obtained by cutting the tip of the tail, and after killing of the animals on blood obtained from the heart. In two mice which died spontaneously paper strip tests (Clinistix, Ames Co., London, England) for glucosuria were carried out.

Light Microscopy

After fixation in Bouin's fluid the following stains were applied: haematoxylin-eosin, van Gieson's stain, aldehyde fuchsin, and the silver impregnations according to Hellerström and Hellman (1960) and Grimelius (1968).

Transmission Electron Microscopy, Pyro-antimonate Technique and X-Ray Analysis

Some specimens were fixed in 2.5 per cent glutaraldehyde in 0.34 M Veronal acetate buffer adjusted to pH 7.4 followed by postfixation in osmium tetroxide in the same buffer. Embedding was carried out in Epon 812 and thick sections stained with toluidine blue were used for identification of the islets. The thin sections were stained with uranyl acetate and lead citrate and were then examined in a Siemens Elmiskop 101.

Other specimens were fixed for 2 hours in 3 per cent glutaraldehyde and 2 per cent potassium pyro-antimonate adjusted to pH 7.4 with 0.01 M acetic acid followed by fixation for 1 hour in 1 per cent osmium tetroxide and 2 per cent potassium pyro-antimonate. The sections were either unstained or stained with uranyl acetate and lead citrate after which they were viewed in a Siemens Elmiskop 101.

The specificity of the pyro-antimonate precipitates was investigated by x-ray analysis using an energy dispersive system (Kevex X-ray energy spectrometer subsystem 5000 A) combined with a JEOL JSEM 200 scanning transmission-microscope, operated in the transmission microscope mode at 80 kV accelerating voltage and a counting time of 180 seconds at each point of analysis.

TABLE 2. Blood Glucose Concentration (mg/100 ml) in Groups of Differently Fed and Pretreate Gerbils, before (0 Minutes) and at Different Intervals after Intraperitoneal Injection of 200 mg/kg Body Weight of Alloxan or Saline (Controls) The Values Represent the Concentration in Each of the Two Gerbils Comprised in the Groups

Animal group	Starvation	Pretreatment	Treatment	Blood glucose concentration					
				Minutes		Hours			
				0	10	1	4	24	48
I	Yes	No	Alloxan	57	90	225	201	69	253
				54	109	207	211	93	271
II		Gucose		84	93	121	127	80	105
				85	91	138	141	101	128
III		Mannose		69	78	103	129	87	121
				89	99	113	134	71	129
IV		Fructose		90	101	110	118	98	120
				63	74	98	97	67	109
V		Galactose		50	104	180	259	73	266
				64	94	167	195	85	249
VI	No	N		94	99	105	126	83	129
				80	89	129	138	90	118
VII			Saline	83	95	99	83	74	70
				91	92	98	79	81	72
VIII	Yes			49	51	53	50	46	45
				59	69	60	65	57	49

I III, V and VI Apart from this, the exocrine parenchyma was normal at each obser vation time in all the alloxan-treated animals.

The islets of all the alloxan-treated animals were normal at 10 minutes. At 1 hour an oc casional B-cell in group I was swollen. Four hours after alloxan injection, some B-cells in groups I and V and a few B-cells in groups II III, IV and VI showed cytoplasmic vacuolation. The B-cell granulation remained un affected during the first 4 hours after alloxan administration.

At 24 hours some B-cells in groups I and V were necrotic, whereas others showed de generative changes of varying severity in nu

Fig 1 B-cell from mouse 1 hour after alloxan injection showing swollen mitochondria with partly disrupted inner membranes and preserved secretory granules × 19,000

Fig 2 B-cells from gerbil 4 hours after alloxan injection showing vesicular endoplasmic reticulum ER an expanded Golgi complex (G) and partly irregular nuclei 8,000

clei and cytoplasm, including vacuolation, swelling and disintegration of the cytoplasm B-cells with preserved cytoplasm exhibited unaffected β-granulation whereas no, or only very sparse, granulation was observed in association with necrotic B-cells. Other B-cells in groups I and V were normal. Scattered B-cells with degenerative or necrotic changes were observed also in groups II III, IV and VI

At 48 hours, more B-cells in groups I and V were necrotic than at 24 hours. The other B-cells were either normal or possessed degenerative alterations of varying severity Non-necrotic B-cells exhibited a normal β-granulation. In groups II, III IV and VI most B-cells were normal, whereas others either exhibited cytoplasmic and nuclear changes of a type similar to the above mentioned, or they were necrotic.

Extensive B-cell necrosis was seen in the mouse from group I which died spontane ously 40 hours after alloxan administration. The B-cells of the mouse from group V which died spontaneously after 3 hours showed

1

2

G

ER

marked degenerative changes in the B-cells, but no obvious necroses.

The A- and D-cells were normal at all observation times in the alloxan-treated groups.

Transmission Electron Microscopy

The ultrastructural studies were only aimed at endocrine parenchyma. No degenerative changes in the controls were recorded at any observation time (group VII). However although no quantitative determination was carried out it appeared from the qualitative study that many mitochondria were larger in the B-cells from the starved controls (group VIII), than in those from the fed ones (group VII). The A- and D-cells were normal at all observation times in the alloxan-treated groups. No alterations in the blood vessels or connective tissue components of the islets were recorded.

At 10 minutes, the mitochondria of some B-cells in groups I and V were more or less swollen and, in a few of these organelles, the inner membranes were partly disrupted. All other organelles, as well as the nucleus, plasma membrane and cytoplasmic ground substance were unaffected. Similar mitochondrial changes, although less conspicuous, in a few B-cell mitochondria from group VI were recorded. No obvious changes of similar kind were found in the B-cells from groups II, III and IV.

At 1 hour, the mitochondria of many B-cells in groups I and V were swollen and the inner and occasionally the outer membranes were disrupted (Fig. 1). The swollen mitochondria possessed low matriceal density. A few mitochondria were disintegrated. Distended Golgi complex was seen in a few B-cells. In most B-cells, however, the Golgi complex remained unaffected. The other organelles, and the nucleus, plasma membrane and cytoplasmic ground substance were normal. At 1 hour also a few B-cells in groups II, III, IV and VI contained some swollen mitochondria with occasional disruptions of the inner membranes. No other alterations in these groups were noted.

At 4 hours, still more B-cells in groups I and V showed marked mitochondrial degeneration and disintegration. The Golgi complex was occasionally expanded or disorganized. The endoplasmic reticulum was often vesicular (Fig 2) and in some cells there was loss of ribosomes and disorganization of the endoplasmic reticulum. The perinuclear spaces were irregularly dilated. The secretory granules were preserved (Fig. 3) although the cores often showed atypical configuration (Fig. 4). Occasional, completely unaffected B-cells were also encountered. Mitochondrial degeneration was found in a few B-cells of groups II, III, IV and VI and in an occasional B-cell in group VI there was degeneration of the Golgi complex and endoplasmic reticulum.

At 24 hours, many B-cells in groups I and V and a few B-cells in groups II, III, IV and VI were necrotic, leaving debris with some seemingly preserved secretory granules; most secretory granules, however, had disappeared. A few B-cells in groups I and V and most B-cells in groups II, III, IV and VI were unaffected. Other B-cells in all groups showed degenerative changes af varying severity in mitochondria, Golgi complex and endoplasmic reticulum, and pyknotic nuclei.

At 48 hours, still more B-cells in groups I and V were necrotic; some islets were composed mainly of necrotic B-cells. B-cells without degenerative changes often possessed a prominent endoplasmic reticulum and Golgi complex. Other B-cells exhibited pyknosis and degenerative changes in mitochondria, Golgi complex and endoplasmic reticulum, but preserved secretory granules. A few necrotic B-cells and some B-cells with degenerative changes were seen also in groups II, III, IV and VI.

Pyro-antimonate Technique

In the B-cells of the controls, pyro-antimonate precipitates were found at each observation time, mainly in mitochondria, secretory granules and nuclei. Scattered precipitates could be seen also in the endoplasmic



Fig 3 Portion of mouse islet 4 hours after alloxan injection showing unaffected A-cells (to the left) and degenerating B-cells (to the right) with preserved secretory granules. ×11 000

Fig 4 Portion of B-cell cytoplasm from gerbil 4 hours after alloxan injection showing swollen secretory granules with electron lucent halos and atypical configuration of the cores ×25 000

reticulum and *Golgi complex*. The Mitochondrial precipitates were localized to the inner compartment. The precipitates in the secretory granules were mainly localized to the halo. In addition, a few granules exhibited precipitates over the granule cores.

The amount of the precipitation varied considerably in different cells and in different organelles. Some mitochondria and secretory granules possessed a rich, fine or coarse, precipitation whereas others showed a sparse precipitation and still others were free from precipitates. In most B-cells, precipitates were found only in rather few of the secretory granules whereas most granules were devoid of precipitation. Secretory granules with precipitates were observed in any portion of the cytoplasm, but were somewhat more frequent at the periphery.

The A- and D-cells of the controls also possessed precipitates the distribution of which was similar to that observed in the B-cells. However, the overall frequency of precipitates was lower in the A- and D-cells than in the B-cells. In all alloxan-treated groups, the A- and D-cells possessed a precipitation similar to that in the controls.

Most B-cells in the alloxan-treated animals showed a distribution of precipitates different from that in the controls. Thus, already at 10 minutes, only few precipitates were observed in mitochondria and secretory granules of many B-cells from groups I and V whereas a rather rich fine precipitation was seen diffusely in the cytoplasmic ground substance (Fig 5). Precipitates were occasionally seen on the outside of the secretory granule membranes (Fig 6). Other B-cells from these groups, as well as the B-cells from groups II, III, IV and VI, showed a distribution of precipitates similar to that in the controls.

At the following observation times, the distribution of precipitates in many of the non-necrotic B-cells of groups I and V resembled that seen in these groups at 10 minutes. The degenerating mitochondria were most often free from precipitates. However, a few mitochondria with marked degenerative changes possessed a rich, coarse precipitation.

At the observation times from 1 hour and onwards also some of the B-cells from groups II, III, IV and VI exhibited a distribution of precipitates similar to that observed in the case of B-cells from groups I and V, whereas most B-cells possessed a precipitation resembling that of the controls.

X-Ray Analysis

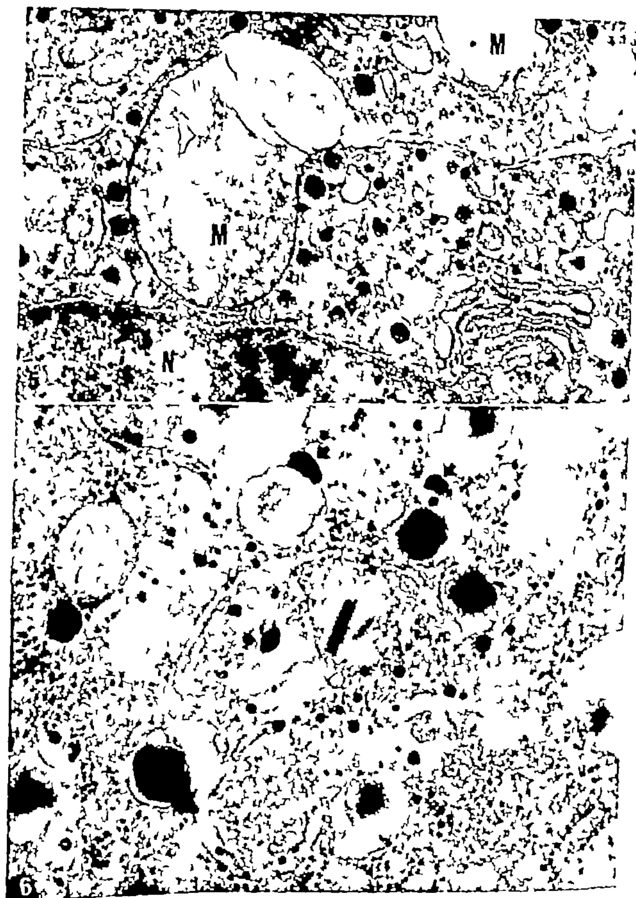
Pyro-antimonate precipitates which were large enough for analysis showed significant peaks for calcium, but not for other cations, apart from those associated with the ultrastructural techniques.

DISCUSSION

Although no quantitative determination was carried out, it appeared from the ultrastructural study of the controls that the mitochondria in the B-cells from the starved animals were larger than those in B-cells from the fed ones. This agrees with the finding that the mitochondrial volume in the B-cells from islets cultured in a low glucose medium for 6 days is increased as compared with that in islets cultured in the presence of a high glucose concentration (*Boquist* 1976 b) and may indicate an effect of starvation upon mitochondrial volume. Since the starved animals were more sensitive to alloxan than the fed ones and since the earliest changes in the alloxan-treated animals were localized to the

Fig 5. B-cells from mouse 10 minutes after alloxan injection showing swollen, partly electron lucent mitochondria (M) with disrupted inner membranes and rather few fine precipitates. A rather rich, coarse precipitation is seen in the cytoplasmic ground substance. Precipitates are also seen in the nucleus (N). Pyro-antimonate-technique. ×18,000

Fig 6. Portion of B-cell from group I 10 minutes after alloxan injection showing rich fine or coarse precipitation in the cytoplasmic ground substance and sparse precipitation in the secretory granules. Occasional precipitates are seen on the outside of the secretory granule membranes (arrow). Pyro-antimonate-technique. ×28,000


M
M
N
A
Б

Logothetopoulos 1963 *Scheynius & Täljedal* 1971 *Zawalich & Beidler* 1973 *Rossini et al.* 1974) The cause of the protective effect of feeding and administration of some hexoses is not known but it is interesting to note that the mitochondrial enlargement which might be associated with the sensitivity to alloxan seemed to be absent in the fed animals which showed decreased sensitivity to alloxan.

Finally it should be emphasized that the sensitivity to alloxan in the species investigated was relative in the sense that some of the B-cells remained unaffected after alloxan-treatment. The cause of this is so far unknown.

Supported by Grants from the *Swedish Medical Research Council* (Project No B76-12X-00718-11B)

REFERENCES

- *Bhattacharya D* On the protection against alloxan diabetes by hexoses. Science *120* 841–843 1954
- *Boquist L.* Alloxan administration in the Chinese hamster I Blood glucose variations, glucose tolerance and light microscopical changes in pancreatic islets and other tissues. Virch Arch. Abt B Zellpath *1* 157–168, 1968 a.
- *Boquist L* Alloxan administration in the Chinese hamster II Ultrastructural study of degeneration and subsequent regeneration of the pancreatic islet tissue. Virch. Arch. Abt. B Zellpath. *1* 169–181 1968 b
- *Boquist L* Pancreatic islet morphology in diabetic Chinese hamsters A light and electron microscopic study Acta path. microbiol. scand. *75* 399–414 1969 a.
- *Boquist L* The endocrine pancreas in the Chinese hamster Studies on non-diabetic, alloxan-treated, zinc-deficient, and spontaneously diabetic animals Thesis, Tryckeriaktiebolaget City Umeå, 1969 b
- *Boquist L* Obesity and pancreatic islet hyperplasia in the Mongolian gerbil. Diabetologia *8* 274 282, 1972
- *Boquist L Hellman B Lernmark A & Täljedal, I B* Influence of the mutation "diabetes" on insulin release and islet morphology in mice of different genetic backgrounds J Cell. Biol. 62 77–89 1974
- *Boquist L Hellman B., Lernmark A & Täljedal I B* Content of adenosine 3',5'-cyclic monophosphate in the pancreatic islets of mice with a hereditary defect of insulin secretion. Biochem. Biophys. Res. Commun. *60*: 1391 1396 1974 b
- *Boquist L.:* Differences in the expression of spontaneous and induced diabetes in Chinese hamsters, Mongolian gerbils and C57BL-KsJ and C57BL-6J mice In Diabetes, Proc. XIth Congr Internat. Diab. Fed., ed. *J S Bajaj*, Exc. Med., Amsterdam, in press, 1976 a
- *Boquist L.* Pancreatic islets subjected to different concentrations of glucose *in vitro* A study with special regard to mitochondrial changes. Virch. Arch. B Cell Path., in press, 1976 b
- *Grimelius, L.* A silver nitrate stain for A_2 cells in human pancreatic islets. Acta Soc. Med. Upsal. *73* 243–270, 1968
- *Hellerström C & Hellman B.:* Some aspects of silver impregnation of the islets of Langerhans in the rat. Acta Endocr *35*: 518–532, 1960.
- *Herman L., Sato T., & Hales C. N.:* The electron microscopic localization of cations to pancreatic islets of Langerhans and the possible role in the insulin secretion. J Ultrastruct. Res. *72* 298–311 1973
- *Howell, S L. Montague W & Tyhurst M.:* Calcium distribution in islets of Langerhans. A study of calcium concentrations and of calcium accumulation in B cell organelles. J Cell Sci. *19* 395–409 1975
- *Kuzuya M & Logothetopoulos J* Sensitivity of beta cells to alloxan after inhibition by insulin or stimulation by glucose Diabetes *12* 435–436, 1963
- *Lehninger A L.* Mitochondria and calcium ion transport. Biochem. J *119* 433–436, 1970
- *Pearse A G E:* Histochemistry Theoretical and applied., Vol. 2, 3rd ed., Churchill Livingstone Edinburgh and London, 1972, pp 1342–1343
- *Rossini A A., Berger M., Shadden J & Cahill, G F Jr.:* Beta cell protection to alloxan necrosis by anomers of D-Glucose. Science *183* 424 1974
- *Schäfer H J & Klöppel, G* The significance of calcium in insulin secretion. Ultrastructural studies and identification and localization of calcium in activated and inactivated B cells of mice. Virch. Arch. A. Path. Anat. *362* 231–245 1974
- *Scheynius A & Täljedal, I.-B.* On the mechanism of glucose protection against alloxan toxicity Diabetologia *7* 252 255 1971
- *Sen P B, & Bhattacharya, G* Protection against alloxan diabetes by glucose. Ind. J Physiol. All. Sci. *6* 112 114 1952.
- *Villar-Palasi, C., Carballido A Sols A & Arteta J L.* Sensitivity of pancreas hexokinase towards alloxan and its modification by glucose. Nature *180* 387–388 1957
- *Zawalich W S & Beidler L. M.:* Glucose and alloxan interactions in the pancreatic islets. Am. J Physiol. *224* 963–966, 1973

B-cell mitochondria, it is possible that swollen mitochondria are more vulnerable than those of smaller size

The earliest structural alterations observed in the B-cells of the alloxan treated animals were mitochondrial swelling and disruption of inner and, occasionally, of outer membranes Later many mitochondria were disintegrated These changes may be deleterious to the B-cells the result is a deranged energy production which secondarily may lead to B-cell necrosis Structural changes in endoplasmic reticulum and Golgi complex of the B-cells were recorded after the mitochondrial lesions were manifest. It is well known that mitochondria in different kinds of cells undergo structural changes in response to various noxious stimuli and therefore, it was also considered whether the mitochondrial lesions in the B-cells could represent unspecific changes not directly associated with alloxan toxicity However since no similar alterations were observed in the A D- and exocrine cells or in the controls this possibility is not plausible Therefore the mitochondrial alterations are believed to represent the primary and most essential structural lesion to be induced by alloxan selectively in the B-cells.

The cation precipitation in many B-cells of the alloxan treated animals was different from that in the controls. The most conspicuous feature in the alloxan treated animals was a sparse occurrence or absence of pyro-antimonate precipitates in the preserved and damaged mitochondria and the secretory granules, and a rich precipitation in the cytoplasmic ground substance Although it is by no means clarified that a rich Ca^{2+} precipitation revealed by the potassium pyro-antimonate technique and X ray analysis is equivalent to a rich Ca^{2+} concentration and although the precipitation may not be representative of the localization of Ca *in vivo* before the fixation of the tissue, clear difference in Ca^{2+} precipitation between organelles or cells probably indicate the existence of differences in Ca^{2+} binding and/or content.

Applying the potassium pyro-antimonate technique to the endocrine pancreas Ca^{2+} precipitation has, according to previous reports, mainly ocurred in the secretory granules, Golgi complex and mitochondria of the B-cells (*Herman et al.* 1973 *Howell et al* 1975 *Schafer and Kloppel* 1974 *Boquist* 1976 b)

Supposing that there is at least a rough parallelism between Ca^{2+} precipitation and Ca^{2+}-concentration the finding in the present study of a decreased mitochondrial Ca^{2+}-precipitation in the alloxan treated animals may be the result either of a decreased uptake of Ca^{2+} into these organelles, or a loss of cations from swollen or damaged mitochondria, or a combination of the two the underlying cause of each of these possibilities may be an alloxan induced mitochondrial functional and/or structural alteration.

It is well known from studies of other tissues that there is a correlation between structural changes and alterations in Ca^{2+}-accumulation in mitochondria. Under some conditions, swollen isolated liver mitochondria accumulate less Ca^{2+} than non swollen ones (*Lehninger* 1970) On the other hand, release of intramitochondrial Ca^{2+} from damaged mitochondria has been reported, to impair the process of oxidative phosphorylation and thus resulting in a failure to synthesize ATP (*Pearse* 1972)

The fact that the secretory granules were preserved in structurally altered B-cells, even in those with marked degenerative changes, suggests that insulin stored in granules is not released in the alloxan treated animals until the cells are necrotic Since Ca^{2+} is well-known to play an important role in insulin secretion the Ca^{2+} precipitation observed in the B-cells of the alloxan treated animals may in some way be associated with the insulin secretory defect believed to exist in early alloxan-diabetes.

The finding of a decreased sensitivity to alloxan in fed animals and in animals pretreated with glucose, mannose or fructose but not in those pretreated with galactose is consistent with observations in other species (*Sen & Bhattacharya* 1952 *Bhattacharya* 1954 *Villar Palasi et al* 1957 *Kaneko &*

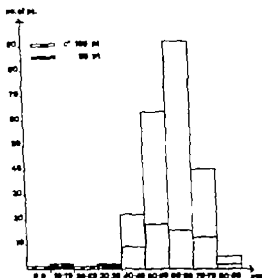


Fig 1 Sex and age distribution of the 225 patients in the material

one case the reason for rejection was a suspected, later verified, ecchinococcus cyst, in another the patient was physically and in a third mentally disabled

The age of the patient, the size or the location of the lung lesion never prevented biopsy attempt.

METHODS

Sixteen biopsies (7 per cent) were performed by the clinicians and 211 biopsies (93 per cent) by the pathologists.

Guided by television fluoroscopy and assisted by a radiologist the lung infiltrate was localized in two planes. In local anaesthesia a 1 mm guide needle was placed in the thoracic wall. The aspiration biopsy was performed using the *Franzén* (4, 12) equipment and technique. Needles of 0.6 mm external diameter 18 cm length were used. The thin needle was inserted through the guide needle, and on contact with the lesion aspiration was started, moving the needle to and fro a couple of times. Before withdrawing the thin needle from the lesion, the pressure was equalized in order to avoid spreading of tumour cells into the needle track. Three hours and twenty-four hours after the biopsy procedure, a chest X-ray was taken, the patients being kept in bed during that time.

Cytological investigation The aspirated material was smeared on at least two dry glass slides. In most cases one of these was immediately fixed in methanol to be stained according to Papanicolaou's method. The rest of the slides were airdried and stained according to the May-Grünwald-Giemsa method. In a few cases, depending on the cytological findings, smears were restained for identification of microorganisms or abnormal pigments.

The diagnoses used for the single biopsies were grouped as follows

a) malignant cells biopsies containing a large number of cells of cancer like appearance different from inflammatory and epitheloid cells.
b) malignancy suspected biopsies containing a few or badly preserved cells which when present in larger numbers would have resulted in group a-diagnosis.
c) benign tumour cells biopsies containing a large number of well preserved and rather monomorphous tumour cell not showing nuclear atypism or abnormal mitotic activity
d) no tumour cells biopsies without findings as in a, b or c.
   Included in this group were biopsies dominated by inflammatory cells and biopsies without diagnostic cellular material.

Histological investigation Histological verification was in most cases attained from lung resections (56 per cent) or autopsy specimens (40 per cent)

TABLE 1 *Cytological Findings in 227 Transthoracic Fine-needle-aspiration Biopsies Compared with Histological Diagnoses*

Cytological findings	Histological diagnoses			Total
	Cancer	Benign tumour	Benign lesion	
Malignant cells	139	–	1	140
Malignancy suspected	13	–	6	19
Benign tumour cells	2	9	1	12
No tumour cells	26	2	28	56
Total	180	11	36	227

TRANSTHORACIC FINE-NEEDLE ASPIRATION BIOPSY

A Histologically Verified Material

DORTHE FRANCIS

Institute of Pathological Anatomy Bispebjerg Hospital Copenhagen Denmark

Francis, D Transthoracic fine-needle aspiration biopsy A histologically verified material. Acta path. microbiol. scand Sect. A 85 230–234 1977

A material consisting of 227 histologically verified transthoracic fine-needle aspiration biopsies is presented The result of the first biopsy attempt gave a diagnostic sensitivity with regards to malignancy of 77 per cent and a diagnostic specificity of 98 per cent. The method is recommended in cases where conventional preoperative diagnostic procedures fail to reveal the nature of lung lesions.

Key words Fine-needle aspiration biopsy transthoracic.

Dorthe Francis, Snebærvænget 13 DK 2850 Virum, Denmark

Received 4.ix.76 Accepted 5.xi 76

Transthoracic needle biopsies have been performed during the last fifty years, but have only become part of the daily routine in a few centers, though several authors have claimed the diagnostic accuracy (2 5 6 8)

The aim of the present work is to present the result of the fine needle aspiration biopsy method used as a diagnostic procedure in a large hospital of a Scandinavian metropolis.

MATERIAL

In the period 1 Feb. 1972 – 31 Jan. 1975 a total of 435 transthoracic aspiration biopsies were performed, and the present material consists of those 227 which at the end of the period were histologically verified either by surgical biopsy or by autopsy The 227 biopsies were performed on 225 patients, as two patients had biopsies taken from infiltrates in both lungs In six cases the biopsy was repeated after two to twelve weeks, but only the material from the first biopsy attempt has been included in this investigation.

Of the patients 59 were women (26.2 per cent) and 166 were men. The mean age was 61.3 years, the oldest being 86 years old and the youngest only five months (Fig 1)

In 146 cases (64 per cent) the aspiration biopsies were performed after the conventional preoperative diagnostic methods (sputum cytology bronchoscopy and mediastinoscopy) had proved negative or failed to identify the nature of the process. In 33 cases (15 per cent) the aspiration biopsy method was chosen as the first diagnostic procedure for patients in whom the lung lesions were mainly small or peripherally located. In the last 48 cases (21 per cent) the aspiration biopsy was performed in order to obtain guidance as to the choice of treatment of clinically inoperable patients or to get a tissue sample for microbiological evaluation.

In only a few instances was the performance of a transthoracic biopsy rejected following a clinical conference. This happened in cases of severe anaemia, altered coagulation status, lung function impaired to the extent that a temporary pneumothorax was expected to be hazardous to life In

of benign tumours, and one case of post pneumonia fibrosis.

Finally no tumour cells were found in 56 cases, of which the histological diagnoses stated malignant tumour in 26, hamartoma in 2, and no neoplasm in 28 cases.

Based on these data relevant probabilities can be calculated as shown in Table 2.

In 28 cases of malignant tumours the aspiration biopsy method failed to give the right diagnosis. An analysis of the circumstances which might have influenced this negative result is given in Table 3.

Complications. Noticeable pneumothorax developed in one third of the cases, but only in nine patients (4 per cent) drainage of the thoracic cavity was necessary. During the biopsy procedure two patients had a minor haemoptysis, and two other patients were treated for cardiac arrest ten minutes after the biopsy performance. One patient is alive and well, the other died six days later and the autopsy revealed an inoperable lung cancer and massive embolism of the pulmonary arteries.

DISCUSSION

The sensitivity of the biopsy method was 77.2 per cent, illustrated by the number of positive cytological diagnoses among all the cases having a histologically malignant tumour. This result obtained with our biopsy method should be compared with the number of positive biopsies from the first biopsy attempt using the *Nordenström* method reported by *Dahlgren & Lind* (1) (68.5 per cent) and *Sinner* (7) (51.2 per cent). The same authors diagnosed 87.7 per cent and 96.2 per cent, respectively, of all malignant tumours by repeating the biopsy up to five times. Our experience concerning the repetition of the aspiration biopsy until now is hardly sufficient for a comparison.

The number of biopsies given the diagnosis malignancy suspected seems rather high and they must be accepted in the beginning of a newly introduced diagnostic method. It is the author's personal experience that the number diminished considerable from the first year to the third year in the period of investigation.

The cytologic diagnosis *malignant tumour cells* was correct in 99.28 per cent (PV-positive). One false positive cytological diagnosis was made in a patient having radiation pneumonitis, an error which has also been experienced by other authors (2).

An analysis of the circumstances concerning the false negative biopsies showed that in four cases the cytological pictures were misinterpretated, as in two cases the abnormal cells were overlooked and in another two the tumour cells present were believed to represent a benign tumour. In the last mentioned two cases the autopsies showed highly differentiated sarcomas, and only distant metastases proved the true biological behavior of the neoplasms. In two cases the aspirated material was totally necrotic without preserved cells. In three cases of rather small well defined lung lesions (1.5, 2.5 and 3 cm in diameter respectively) there was visible and palpable contact with the lesion but the surface could not be penetrated. A possible explanation might be the size of the lesion in an otherwise healthy and elastic lung tissue. Difficulties in penetrating such small freely movable infiltrates were serious. Two of the three cases mentioned were small cell anaplastic carcinomas. It might be possible to fix the infiltrate with one thin needle and then penetrate with another needle from a different angle. In one case the infiltrate was surrounded by several air-filled cysts. In spite of visible contact, aspiration of air was unavoidable and possible tumour cells were lost in the syringe.

The location of the malignant lung lesion seems to have been the reason for insufficiently aspirated material in the rest of the cases. In two of these cases the lesion was situated just behind a rib or beneath the scapular bone. In such cases of small infiltrates, immovable by respiration, and hidden behind a bone, the intercostal space and the thickness of the thoracic wall were the limit

TABLE 2 *Relevant Probabilities Concerning the Accuracy of Diagnosing Malignant Tumours in a Transthoracic Aspiration Biopsy Material of 227 Histologically Verified Cases*

Criteria for a positive biopsy	Malignant cells	Malignant cells and suspected malignancy
True Positive (TP)	139	152
False Positive (FP)	1	7
True Negative (TN)	46	40
False Negative (FN)	41	28
Sensitivity $\frac{TP}{TP + FN}$ %	77.22 (70.38–83 11)	84 44 (78.29–89.39)
Specificity $\frac{TN}{TN + FP}$ %	97 76 (88 71–99 95)	85 10 (71.69–93.80)
PV positive $\frac{TP}{TP + FP}$ %	99.28 (96 08–99.98)	95.59 (91 10–98.15)
PV negative $\frac{TN}{TN + FN}$ %	52.87 (41.87–63 67)	58.82 (46.23–70 63)

Figures in brackets being the 95 per cent confidence limits.
PV positive being the predictive value of a positive result.
PV negative being the predictive value of a negative result.

TABLE 3 *Evaluation of 28 False Negative Aspiration Biopsies from Histologically Malignant Lung Lesions*

False negative biopsies (n = 28)	Lesion seemingly hit (n = 10)	Cytological misinterpretation	4
		Material totally necrotic	2
		Lesion can not be penetrated	3
		Cystic lung formations	1
	Lesion hit? (n = 7)	Inexperience in biopsy procedure	7
	Lesion not hit (n = 11)	Location of lesion	2
		Indefinite lesion radiologically	3
		Lesion more centrally located	6

in a few cases from surgical biopsies taken during thoracoscopy ([illegible] per cent) or explorative thoracotomy (2 per cent) The histological specimens were stained with hematoxyline-eosin and by *Kreyberg's* method (10)

The significance of the results will be expressed in the terms of *Vecchio* (3 9 11)

RESULTS

Table 1 shows a comparison between the original cytological findings and the histological diagnoses. In 140 cases malignant tumour cells were found This was correct in 139 cases while histological examination revealed that one case presented changes after radiation of a mammary carcinoma but no tumour

In 19 cases the cytological diagnosis was suspected malignancy Of these 13 had a malignant tumour while in six cases granulomatous lesions or inflammatory changes in metaplastic epithelium were found

In 12 cases benign tumour cells were found. There were two cases of sarcoma, nine cases

Acta path. microbiol. scand. Sect. A, 85: 235–239, 1977

ASPIRATION BIOPSIES FROM DIAGNOSTICALLY DIFFICULT PULMONARY LESIONS

A Consecutive Case Material

DORTHE FRANCIS

Department of Pathology, Bispebjerg Hospital, Copenhagen, Denmark

Francis, D. Aspiration biopsies from diagnostically difficult pulmonary lesions. A consecutive case material. Acta path. microbiol. scand. Sect. A, 85: 235–239, 1977.

A consecutive material of 244 cases of transthoracic aspiration biopsies collected in a two year period is presented. The biopsy method, the indications, and the contraindications are described. The sensitivity of the biopsy method concerning malignant tumour cells and suspected malignant tumour cells was 82.8 per cent, the specificity was 94.9 per cent. It is suggested that the biopsy method might be applied earlier in the sequence of preoperative diagnostic procedures.

Key words: Aspiration biopsy; pulmonary lesions.

Dorthe Francis, Soabærvænget 13, DK 2830 Virum, Denmark.

Received 24.ix.76 Accepted 5.xi.76

In a previous report (4) covering 227 histologically verified transthoracic aspiration biopsies from our first three year period we found a method sensitivity of 77.2 per cent. A positive result was defined as a primary cytological diagnosis of malignant tumour cells. If biopsies containing suspected malignant cells were included, the sensitivity increased to 84.4 per cent.

In the following investigation the results from the first two year period are given for transthoracic aspiration biopsies in a consecutive case material, the follow-up time being 2 to 4 years in non-histologically verified cases.

MATERIAL AND METHODS

From February 1st, 1972 to January 31st, 1974 transthoracic aspiration biopsies were performed on 244 patients. The patients were referred to the pulmonary surgical or medical departments at Bispebjerg Hospital because of lung lesions. Conventional preoperative diagnostic procedures had in no case revealed the nature of the lesion. The present investigation comprises the original cytological diagnoses based on the first aspiration biopsies, i.e. 244 biopsies.

The deadline for the investigation was February 1st, 1976.

Indication for Transthoracic Aspiration Biopsy

In biopsies performed by the pathologists the decision to undertake a transthoracic aspiration biopsy was taken solely by the senior staff members of the pulmonary surgical and/or medical departments. In each routine case we required a chest X-ray and if necessary tomograms less than one week old, a blood count, and a coagulation status within normal limits (i.e. haemoglobin above 8.0 m mol/l for men and 7.0 m mol/l for women, capillary bleeding time and coagulation time < 5 minutes) and lung function that on clinical assessment would be able to tolerate a

ing factors. In future similar cases a curved guide cannula will be tried. In three cases of multiple loose and ill-defined infiltrates the autopsies revealed pleural carcinosis and no intrapulmonary deposits. Finally in six cases —two patients with a middle lobe atelectasis and four with an upper lobe atelectasis—the biopsies were negative even though the chosen location for the aspiration biopsy was the most central or proximal part of the infiltrate. The surgical or autopsy reports showed that the malignant lesions in these cases were located much more proximally in the bronchial system than illustrated by the X ray

As the sensitivity is shown to be high the method is highly recommended in cases of obscure intrathoracic lesions. The biopsy procedure demands some experience It is well accepted by the patients and the complication rate is low It can be carried out in any hospital equipped with a proper X ray service and with a surgeon in charge being able to drain a tension pneumothorax.

The cytological interpretation too, demands some experience but a pathologist with interest in this special field and with experience in diagnostic cytology will be able to obtain results in diagnosing malignant lung lesions as here illustrated.

REFERENCES

1 *Dahlgren S* & *Lind B* Comparison between diagnostic results obtained by transthoracic needle biopsy and sputum cytology Acta Cytologica *16* 53–58 1972.

2 *Dahlgren S* & *Nordenström B* Transthoracic needle biopsy Almqvist & Wiksell, Stockholm 1966 p 31–39 59–62, 114–126

3 Documenta Geigy Scientific table 7 ed. Basel 1968.

4 *Franzén S* Personal communication. 1971

5 *Hajdu S I* & *Melamed M R*. The diagnostic value of aspiration smears. J Clin. Path. *59* 350–356 1973

6 *Hayata Y Oho K Ishiba M*, *Goya Y* & *Hayashi T* Percutaneous pulmonary puncture for cytologic diagnosis. Its value for small peripheral pulmonary carcinoma. Acta Cytologica *17* 469–475 1973

7 *Sinner W N*. Transthoracic needle biopsy of small peripheral malignant lung lesions. Investigative Radiology *8* 305–314 1973.

8 *Struve Christensen E.* Perkutan transtorakal lungebiopsi DADL s forlag, København 1976. p. 20–22 58–82.

9 *Vecchio T J* Predictive value of a single diagnostic test in unselected populations. New Engl. J Med. *274* 1171–1173 1966.

10 WHO Kreyberg L. Liebow A. A. & Uehlinger E. A. International histological classification of tumours no 1 Histological typing of lung tumours. Geneva 1967 p. 27–28.

11 *Wulff H R* Rational diagnosis and treatment. Blackwell Oxford 1976 p. 95

12 *Zajicek J* Aspiration Biopsy Cytology I. Karger Basel 1974 p 2.

TABLE 1 *Cytological Findings in 244 Consecutive Cases of Aspiration Biopsies Compared to Histological and Clinical Diagnoses*

Cytological findings		Histological diagnosis			Clinical diagnosis	
		Malignant tumour	Benign tumour	No tumour	Malignant tumour	Benign lesion
Malignant cells	122	109			13	
Malignancy suspected	17	13		4		
Benign tumour cells	12		8	1		3
No tumour cells	93	29	2	23	1	38
Total	244	151	10	28	14	41

TABLE 2 *Relevant Probabilities Concerning the Accuracy of Diagnosing Malignant Tumours in a Transthoracic Aspiration Biopsy Material of 244 Cases*

Criteria for a positive biopsy	Malignant cells	Malignant cells and suspected malignancy
True Positive (TP)	122	135
False Positive (FP)	0	4
True Negative (TN)	79	75
False Negative (FN)	43	30
Sensitivity $\frac{TP}{TP + FN}$ %	73.94 (66.30–80.40)	82.82 (76.10–88.23)
Specificity $\frac{TN}{TN + FP}$ %	100.00 (93.44–100.00)	94.94 (87.54–98.60)
PV positive $\frac{TP}{TP + FP}$ %	100.00 (97.70–100.00)	97.12 (96.80–99.21)
PV negative $\frac{TN}{TN + FN}$ %	64.75 (54.84–73.17)	71.42 (61.76–79.76)

Figures in brackets being the 95 per cent confidence limits.
PV positive being the predictive value of a positive result.
PV negative being the predictive value of a negative result.

Biopsy Findings

189 biopsies were histologically verified, and 55 cases were clinically investigated.

Table 1 shows the cytological findings compared to the histological and clinical diagnoses. Malignant tumour cells were found in 122 biopsies, out of which 109 have been histologically verified. Of the remaining 13 patients, six died without an autopsy being performed, the death certificates stating carcinoma of the lung. Seven patients were reported still alive, but all were showing clinical signs of a malignant lung lesion.

Suspected malignancy was found in 17 biopsies. The histological diagnoses were in 13 of these cases carcinoma, in two a granulomatous lesion and in the last two abscess cavities partly covered by metaplastic epithelium.

possible temporary pneumothorax. Conventional diagnostic procedures such as *sputum cytology* bronchoscopy and mediastinoscopy had proven negative On these premises the punctures were performed by the pathologists with assistance from the radiological department and a technician to run the fluoroscope.

In a number of cases however the demand for a diagnosis of the lung lesion led to a puncture *even though some of the above requirements were* not met In such cases the clinician in charge was consulted—and if necessary—asked to be present during the biopsy performance In five instances this consultation led to a rejection of a biopsy attempt. In additional cases the reason for rejection was in one instance a suspect and later verified ecchinococcus cyst in another it was the patient having contractures to an extent that made proper positioning impossible and in a third case the patient was unable for mental reasons to co-operate properly These eight patients were not included in the case material

The author has been informed that similar precautions were taken as to indications and contraindications regarding the biopsies performed by the senior staff members of the pulmonary medical department.

Biopsy Procedures

Guided by television fluoroscopy the lung infiltrate was localized in two planes, the patient being either in supine or in prone position. Only in three cases where small infiltrates were hidden behind a bone was the route chosen for the puncture not in the sagittal plane

In local anaesthesia a 1 mm guide needle was placed in the thoracic wall Two or three aspirations were performed employing a *Franzén* (11) syringe and needles of 0 6 mm external diameter 18 cm length The thin needle was inserted through the guide needle and on contact with the lesion aspiration was started moving the needle to and fro a couple of times. Before withdrawing the aspiration needle the pressure was equalized in order to avoid spreading of tumour cells into the needle canal.

In the cytological report of each case a drawing was made of the radiological findings including the chosen route of puncture This drawing was often useful in the diagnostic work and later served as a guidance in the search for possible tumour spread to the puncture track

Chest X rays were taken three and twentyfour hours after the puncture the patients being kept in bed during that time.

Size of Lung Lesions

The lung infiltrates were measured on the basis of the X rays and the fluoroscopical findings For rounded lesions the diameter was measured, and for *well-defined* but unevenly shaped infiltrates the largest extension was used in order to avoid underestimation.

Cytological Histological and Clinical Diagnoses

The aspirated material was smeared on several dry glass-slides, one of which often was immediately fixed in methanol to be stained according to Papanicolaou s method. The rest of the slides were air dried and stained according to the May-Grünwald-Giemsa method. For each case a cytological diagnosis was made as to contents of malignant tumour cells, suspected malignant cells, benign tumour cells or no tumour cells.

In biopsies containing no tumour cells a specific non neoplastic diagnosis was sought for Restaining was carried out in one or several smears using the PAS Gram and/or Ziehl-Neelsen staining methods. Included in this group were biopsies containing unsuitable or inconclusive material.

Histological verification was achieved from available autopsy and surgical specimens. In non-histologically verified cases the clinical diagnoses were based on death certificates, clinical reports from various hospital departments, and on information from the general practitioners.

Statistics

By the aid of *Bayes Theorem* (5 10) relevant probabilities have been calculated. 95 per cent confidence limits were achieved from the tables of *Geigy* (3)

RESULTS

Clinical Data

The study included 77 women (32 per cent) mean age 60 6 years, and 167 men, mean age 62.2 years, the oldest patient being 85 the youngest 18 years of age

212 biopsies were performed by the pathologists (87 per cent) and 32 by the senior staff members of the pulmonary medical department.

Radiologically the sizes of the lung lesions punctured varied from 0.5 to 15 cm. A comparison between the sizes of the radiological findings and the surgically removed tumours was possible in 92 cases. This showed agreement in 42 instances (46 per cent) 33 tumours (36 per cent) were one to three cm larger and 17 tumours (18 per cent) were one to four cm smaller

TABLE 1 *Cytological Findings in 244 Consecutive Cases of Aspiration Biopsies Compared to Histological and Clinical Diagnoses*

Cytological findings		Histological diagnosis			Clinical diagnosis	
		Malignant tumour	Benign tumour	No tumour	Malignant tumour	Benign lesion
Malignant cells	122	109			13	
Malignancy suspected	17	13		4		
Benign tumour cells	12		8	1		3
N tumour cells	93	29	2	23	1	38
Total	244	151	10	28	14	41

TABLE 2. *Relevant Probabilities Concerning th Accuracy of Diagnosing Malignant Tumours in a Transthoracic Aspiration Biopsy Material of 244 Cases*

Criteria for positive biopsy	Malignant cells	Malignant cells and suspected malignancy
True Positive (TP)	122	135
False Positive (FP)	0	4
True Negatn (TN)	79	75
False Negatn (FN)	43	30
Sensitivity $\frac{TP}{TP + FN}$ %	73.94 (66.50–80 40)	82.82 (76 10–88.23)
Specificity $\frac{TN}{TN + FP}$ %	100.00 (93 44–100.00)	94 94 (87.54–98.60)
PV positn $\frac{TP}{TP + FP}$ %	100 00 (97 70–100 00)	97 12 (98 80–99.21)
PV negatn $\frac{TN}{TN + FN}$ %	64 75 (54 84–73 17)	71 42 (61 76–79.76)

Figures in brackets being the 95 per cent confidence limits.
PV positn being the predictive value of a positi result.
PV negatn being the predictive alue of a negative result

Biopsy Findings

189 biopsies were histologically verified, and 33 cases were clinically investigated.

Table 1 shows the cytological findings compared to the histological and clinical diagnoses. Malignant tumour cells were found in 122 biopsies, out of which 109 have been histologically verified. Of the remaining 13 patients, six died without an autopsy being performed the death certificates stating carcinoma of the lung. Seven patients were reported still alive, but all were showing clinical signs of a malignant lung lesion.

Suspected malignancy was found in 17 biopsies. The histological diagnoses were in 13 of these cases carcinoma, in two a granulomatous lesion and in the last two abscess cavities partly covered by metaplastic epithelium.

Benign tumour cells were found in 12 biopsies. Nine patients have been operated on and the histological diagnoses were *carcinoid tumour thymoma haemangioma, histiocytoma* benign epidermoid papillary tumour pseudolymphomatous hyperplasia, two *hamartomas and one case of post pneumonia* fibrosis. Three cases of hamartoma have not been operated on the X ray findings being stationary during the control period.

Finally no tumour cells were found in 93 biopsies Among the 54 cases histologically verified 29 were found to represent malignant tumours, two chondromatous hamartomas, and in 23 cases no neoplasms were diagnosed Among the 39 patients whose biopsies were not histologically verified one patient had developed radiological signs of a costal metastasis, while the clinical reports in the rest of the cases until now have been in accordance with non neoplastic lung lesions.

Based on these data relevant probabilities can be calculated as shown in Table 2

An attempt to investigate the reasons for a false negative biopsy result was given in a previous report (4)

Complications

Two patients were treated for cardiac arrest ten minutes after the biopsy procedure. One is alive and well the other a 67 year old woman died one week later of inoperable lung cancer and massive pulmonary embolism. Haemoptysis during the biopsy procedure occurred in four patients, but no treatment was required

One patient had to be placed in *Trendelenburg's position for ten* minutes because of what appeared to be a minor attack of a vasovagal shock. No abnormal neurological findings or sequelae were noted

Noticeable pneumothorax appeared in about one third of the cases, ten of which required drainage of the pleural cavity Special attention in each case was paid to signs of air embolism and tumour implantation into the thoracic wall. No such complications were registered

DISCUSSION

Our case material did not differ essentially from that reported by other authors (1 8) with respect to age, incidence of specific disease or to the size of the punctured lesions.

We find that the diagnostic value of a biopsy method should be expressed by the sensitivity and the specificity in diagnosing a specific lesion. In this investigation the specific lesion was a malignant tumour

Very few authors have given detailed information about a positive diagnosis of the first biopsy attempt. *Thommesen* found 72.2 per cent (9) *Dahlgren & Lind* 68.3 per cent (2) and *Sinner* 51.9 per cent (6), as compared *to our results 82 8 per cent.*

Comparing our results with those of other authors (1 6 8) it is noted that the clinical observation period of two to four years was rather short, as a lung infiltrate disappearing after antibiotic treatment in fact might represent a tumour-caused obstruction atelectasis (7) Three such cases were observed among our false negative biopsies.

Our biopsy method sensitivity is therefore regarded as a maximum value

The present consecutive case material was investigated in order to confirm the previ*ously reported results of a histologically* verified material of 227 biopsies (4) The differences in biopsy method sensitivities and specificities are minimal and insignificant.

The sensitivity of the biopsy method is high. The biopsy procedure is well accepted by the patients, and the complication rate is low It would seem reasonable to suggest placing the transthoracic aspiration biopsy earlier in the sequence of diagnostic procedures in almost any case of *lung lesion.*

REFERENCES

1 *Dahlgren S & Nordenström B* Transthoracic needle biopsy Almqvist & Wiksell Stockholm, 1966 p. 31 59 124
2 *Dahlgren S & Lind B* Comparison between diagnostic results obtained by transthoracic needle biopsy and by sputum cytologi. Acta Cytologica *16* 53–58 1972

3 Documenta Geigy Scientific tables, 7 ed. Basel 1968.
4 Francis, D Transthoracic fine-needle aspiration biopsy A histologically verified material. Acta path. microbiol. scand. Sect. A, 85 230–234 1977
5 Lusted L. B. Introduction to medical decision making. Charles C. Thomas, Springfield, Illinois, USA, p. 24
6 Sinner W N Transthoracic needle biopsy of small peripheral malignant lung lesions. Investigatn radiolog. 8 305–314 1973.
7 Sinner W N The diagnosis of pulmonary lesions by percutaneous transthoracic needle aspiration biopsy Thesis, Stockholm I I 2, 1976.
8. Struve-Christensen E.: Perkutan transtorakal lungebiopsi. DADL s forlag, København, 1976, p. 20, 58.
9 Thommesen P Finnålspunktur af lungetumorer Ugeskrift for læger 133: 1925–1927 1971
10. Wulff H R. Rational diagnosis and treatment. Blackwell, Oxford, 1976, p. 95
11 Zajicek, J.: Aspiration biopsy cytology I S. Karger Basel, 1974 p. 2.

Benign tumour cells were found in 12 biopsies. Nine patients have been operated on, and the histological diagnoses were carcinoid tumour thymoma, haemangioma histiocytoma, benign epidermoid papillary tumour, pseudolymphomatous hyperplasia, two hamartomas and one case of post pneumonia fibrosis. Three cases of hamartoma have not been operated on the X ray findings being stationary during the control period

Finally no tumour cells were found in 93 biopsies. Among the 54 cases histologically verified 29 were found to represent malignant tumours, two chondromatous hamartomas, and in 23 cases no neoplasms were diagnosed Among the 39 patients whose biopsies were not histologically verified one patient had developed radiological signs of a costal metastasis, while the clinical reports in the rest of the cases until now have been in accordance with non neoplastic lung lesions.

Based on these data relevant probabilities can be calculated as shown in Table 2

An attempt to investigate the reasons for a false negative biopsy result was given in a previous report (4)

Complications

Two patients were treated for cardiac arrest ten minutes after the biopsy procedure. One is alive and well the other a 67 year old woman died one week later of inoperable lung cancer and massive pulmonary embolism Haemoptysis during the biopsy procedure occurred in four patients, but no treatment was required.

One patient had to be placed in *Trendelenburg's* position for ten minutes because of what appeared to be a minor attack of a vasovagal shock No abnormal neurological findings or sequelae were noted

Noticeable pneumothorax appeared in about one third of the cases ten of which required drainage of the pleural cavity Special attention in each case was paid to signs of air embolism and tumour implantation into the thoracic wall. No such complications were registered.

DISCUSSION

Our case material did not differ essentially from that reported by other authors (1 8) with respect to age, incidence of specific disease or to the size of the punctured lesions

We find that the diagnostic value of a biopsy method should be expressed by the sensitivity and the specificity in diagnosing a specific lesion In this investigation the specific lesion was a malignant tumour

Very few authors have given detailed information about a positive diagnosis of the first biopsy attempt. *Thommesen* found 72.2 per cent (9) *Dahlgren & Lind* 68.5 per cent (2), and *Sinner* 51 9 per cent (6), as compared to our results 82.8 per cent.

Comparing our results with those of other authors (1, 6 8) it is noted that the clinical observation period of two to four years was rather short, as a lung infiltrate disappearing after antibiotic treatment in fact might represent a tumour-caused obstruction atelectasis (7) Three such cases were observed among our false negative biopsies.

Our biopsy method sensitivity is therefore regarded as a maximum value.

The present consecutive case material was investigated in order to confirm the previously reported results of a histologically verified material of 227 biopsies (4) The differences in biopsy method sensitivities and specificities are minimal and insignificant.

The sensitivity of the biopsy method is high The biopsy procedure is well accepted by the patients, and the complication rate is low It would seem reasonable to suggest placing the transthoracic aspiration biopsy earlier in the sequence of diagnostic procedures in almost any case of lung lesion.

REFERENCES

1 *Dahlgren S & Nordenström B* Transthoracic needle biopsy Almqvist & Wiksell, Stockholm, 1966 p. 31 59 1 4
2 *Dahlgren S & Lind B* Comparison between diagnostic results obtained by transthoracic needle biopsy and by sputum cytology Acta Cytologica *16* 53–58 1972.

3. Documenta Geigy Scientific tables, 7 ed. Basel 1968.
4 *Francis, D.:* Transthoracic fine-needle aspiration biopsy A histologically verified material. Acta path microbiol. scand. Sect. A, *85* 230–234 1977
5 *Lusted L. B.* Introduction to medical decision making. Charles C. Thomas, Springfield, Illinois, USA, p. 24
6 *Sinner W N* Transthoracic needle biopsy of small peripheral malignant lung lesions. Investigative radiolog. *8* 305–314 1973.
7 *Sinner W N* The diagnosis of pulmonary lesions by percutaneous transthoracic needle aspiration biopsy Thesis, Stockholm *11:* 2, 1976.
8. *Struve-Christensen E.*, Perkutan transtorakal lungebiopsi. DADL's forlag, København, 1976, p. 20 58.
9 *Thommesen P.*, Finnålspunktur af lungetumorer. Ugeskrift for læger *133* 1925–1927 1971
10 *Wulff H R.*, Rational diagnosis and treatment. Blackwell, Oxford, 1976, p. 95
11 *Zajicek J.:* Aspiration biopsy cytology I 8. Karger Basel, 1974 p. 2.

THE DIAGNOSTIC SIGNIFICANCE OF INTESTINAL METAPLASIA IN ENDOSCOPIC GASTRIC BIOPSIES

AAGE JOHANSEN and BENTE SIKJÄR

Institute of Pathology Bispebjerg Hospital, Copenhagen, Denmark

Johansen, Aa. & Sikjär B The diagnostic significance of intestinal metaplasia in endoscopic gastric biopsies. Acta path microbiol scand. Sect. A, 85 240-244 1977

The incidences of intestinal metaplasia in two groups of benign endoscopic biopsies taken from stomachs with malignant and benign lesions respectively were compared. 315 single biopsies were taken from stomachs with proven carcinoma, but outside the carcinomatous area. They were compared to 786 single biopsies taken from stomachs with proven benign lesions. Each single biopsy was placed in one of three groups intestinal metaplasia absent, or making up less or more than 50 per cent of the epithelium in the biopsy The results showed that single *biopsies with intestinal metaplasia regardless of the extension of the metaplasia in the biopsy* were found more often in stomachs with carcinoma than in stomachs with benign lesions but without any significant difference If more than half of the benign biopsies taken during an examination demonstrated extensive grades of intestinal metaplasia a slightly significant difference in favour of carcinomas was found

Key words Intestinal metaplasia gastric biopsies diagnostic significance.

Aa. Johansen, Institute of Pathology Bispebjerg Hospital, DK 2400 Copenhagen NV Denmark.

Received 10.ix.76 Accepted 18.x.76

Intestinal metaplasia is generally looked upon as an important change in the gastric mucosa regarding the development of cancer A group of carcinomas designated "intestinal type carcinoma was considered by *Laurén* (1965) to take origin from areas of metaplastic epithelium. *Morson* (1955 a) found that intestinal metaplasia was most common in stomachs with carcinoma and demonstrated (*Morson* 1955 b) transitions from intestinal metaplastic areas to carcinomas. He considered this epithelial change as a precancerous lesion in the broad sense of the word (*Morson* 1962)

Modern fibrogastroscopy with biopsies has made it possible to estimate whether intestinal metaplasia is present or not in all parts of the stomach prior to operation.

Now and then pathologists are asked whether the presence of intestinal metaplastic epithelium in one or several biopsies from a stomach is of any importance in the differential diagnosis between malignant and benign gastric lesions The question is naturally only well founded in such cases where carcinoma is suspected on account of other examinations and all the biopsies taken failed to reveal malignancy The purpose of this paper is to contribute to the answer of this question by investigating the frequency of intestinal metaplasia in a material of benign endoscopic biopsies from patients with proven malignant or benign lesions.

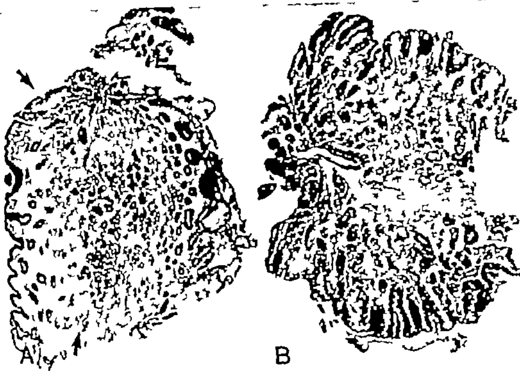


Fig. 1. Biopsies where A less than half and B more than half of the epithelium demonstrate intestinal metaplasia. (PAS and H.E., × 25)

MATERIAL AND METHODS

I the years 1970 to 1972 practically all patients in this hospital suffering upper abdominal symptoms ere endoscopically examined. In 886 patients localized lesion was revealed and biopsy was performed. The diagnostic accuracy of the biopsy examination has been published elsewhere (*Johansen & Sikjær* 1975).

The endoscopic biopsies were in most patients the only histological verification of the lesion, but in 336 patients (38 per cent) the lesion was also proven through operation or autopsy. 142 of these had carcinomas and 194 benign lesions, mainly ulcers. These patients make p the material.

The investigation was carried out in such a way hat each single biopsy alw y was kept separated from the others both regarding fixation and further preparation. Its position the stomach was indicated on sketch. About 20 sections were made from each biopsy and the sections were stained by haematoxylin-eosin and double mucin staining namely the *Mork & Drysdale* (1957) modification of the Zimmermann method with added colloidal iron procedure which makes intestinal metaplastic epithelium ery distinct. A diagnosis as applied to each single biopsy. The biopsies were strictly consecutively collected and the investigation was prospective.

From the 142 carcinomas a total of 662 single biopsies were taken. The average number of biopsies per endoscopic procedure was 4.3. A few patients underwent two endoscopic procedures which here were put together making one biopsy examination. I this way the average number of biopsies per examination for the 142 patients was 4.7. Forty-one examinations showed exclusively single biopsies demonstrating carcinomas. 18 examinations disclosed exclusively benign biopsies and the remaining 83 examinations showed single biopsies of which some revealed carcinoma, some benign conditions. All single biopsies demonstrating carcinoma were rejected. The total number of completely benign biopsies was 315. They were considered as representativ for the mucosa in stomachs with carcinoma. All were serial sectioned but no carcinoma appeared in any of them.

From the 194 benign lesions—mainly ulcers—a total of 786 biopsies were taken. The average number of biopsies per endoscopic procedure was 3.9 and per examination 4.1.

These 1101 *benign* biopsies, the 315 from stomachs with proven carcinomas and the

786 from stomachs with proven benign lesions were each examined and graded according to their contents of metaplastic epithelium. Three groups were made: 1. Intestinal epithelium absent. 2. Intestinal epithelium moderate present (Fig. 1 A) meaning that less than half of the epithelium was of metaplastic type and 3. intestinal metaplasia extensively present (Fig. 1 B) meaning that half or more than half of the epithelium was metaplastic. If the sections made from one single biopsy were different the one which demonstrated most intestinal metaplasia was chosen for the grading. Biopsies composed solely of granulation tissue were rejected. At last the incidence of the graded biopsies in each examination was registered.

RESULTS

In Table 1 is given a survey of all the benign, graded biopsies *without considering their distribution in the examinations*. It is shown that biopsies with intestinal metaplasia are most common in the groups which were taken from stomachs with carcinoma but the difference is insignificant. This involves that if biopsy examinations only contain one benign biopsy with intestinal metaplasia irrespective the degree such examinations will be of no diagnostic importance. This is—a little redundant—demonstrated in Table 2.

However, often more than one of the benign biopsies taken during an examination demonstrate intestinal metaplasia—moderate-

TABLE 1. *Distribution of Biopsies with Different Degrees of Intestinal Metaplasia (IM) in Relation to Two Groups of Benign Biopsies Taken from Stomachs with Carcinoma and Benign Lesions Respectively*

		Benign single biopsies	Benign biopsies evaluable for IM*	Degree of intestinalization in the biopsies: IM totally absent	IM moderately present	IM extensively present
	336	1101	889	608	215	66
Stomachs with carcinoma	142	315	251 (80%)	163 (65%)	63 (25%)	25 (10%)
Stomachs with benign lesions	194	786	638 (81%)	445 (70%)	152 (24%)	41 (6%)
			Chi^2	1.710 N.S	0.098 N.S	3.006 N.S

* 212 biopsies demonstrating granulation tissue with epithelium was rejected.

TABLE 2. *Distribution of Examinations Where at Least One Single Biopsy Showed Either 1) Moderately IM or 2) Extensively IM in Relation to Stomachs with Carcinoma or Benign Lesions*

		Examinations with benign biopsies evaluable for IM	Examinations where only one single biopsy showed: extensively IM	moderately IM
	336	271	104	45
Stomachs with carcinoma	142	82	23 (28%)	17 (21%)
Stomachs with benign lesions	194	189	81 (43%)	28 (15%)
		Chi^2	3.215 N.S	1.051 N.S

* 65 examinations contained exclusively biopsies demonstrating carcinoma or carcinoma and granulation tissue.

TABLE 3 *Distribution of Examinations Where Half or More Than Half of the Number of Single Biopsies Showed 1) Moderately IM or 2) Extensively in Relation to Stomachs with Carcinoma and Benign Lesions*

		Examinations with benign biopsies evaluable for IM	Examinations where half or more than half of the number of biopsies showed	
			moderately IM	extensively IM
	336	271	84	28
Stomachs with carcinoma	142	82	19 (23%)	14 (17%)
Stomachs with benign lesions	194	189	65 (42%)	14 (7%)
		Chi²	3.203 N.S.	4.774 p<0.05

65 examinations contained exclusively biopsies demonstrating carcinoma or carcinoma and granulation tissue

ly or extensively. After having compared a large number of examinations of different compositions it was calculated that significant differences between examinations from stomachs with carcinoma and benign lesions were first achieved when (Table 3) half or more than half of the benign biopsies in the examinations demonstrated extensively intestinal metaplasia and the level of significance was even low (5 per cent). The level was only inconsiderable raised if examinations where all benign biopsies demonstrated extensively intestinal metaplasia were compared (chi² = 3.228) and no significant difference was found in any case for examinations containing biopsies with moderately intestinal metaplasia irrespective the number of biopsies.

DISCUSSION

Although some of the single biopsies which demonstrated *malignant* changes in fact could have been evaluated for intestinal metaplasia because some parts of the biopsies were left uninvolved by the carcinoma, the investigation was limited to those which were completely benign. It is the occurrence of intestinal metaplasia in such biopsies which is of interest.

Since all biopsies showing malignant changes were rejected the number of benign biopsies in the examinations from carcinomas was naturally very limited and "half or more than half" in such examinations often means only 2 biopsies. Yet it has to be remembered that 18 examinations from carcinomas exclusively showed benign biopsies.

It is well known from other investigations (*Debray et al.* 1974, *Myren & Serck Hanssen* 1974, *Miller & Kaufmann* 1975) that a large percentage of biopsies and, as it was the case here, some total examinations, from a diagnostic point of view are false negative because the endoscopist does not reach the carcinoma but takes the biopsies outside the carcinomatous area.

Since intestinal metaplasia by nearly all authors is considered to be most marked in stomachs with carcinoma (*Magnus* 1937, *Gutts & Stewart* 1943, *Järvi & Laurén* 1951, *Morson* 1955 a, 1955 b, *Elster et al.* 1960, *Heinkel et al.* 1960, *Nagayo et al.* 1965, *Ming et al.* 1967, *Correa et al.* 1970) it seemed worth investigating whether this fact could be used diagnostically in the biopsy examination, but the results show that the phenomenon probably is too insignificant.

It has to be remembered that all the biopsies in this study were intended to diagnose a localized lesion and therefore reflect the condition of the mucosa in close proximity to

carcinomas and ulcers This might have disturbed the results because it has been shown that not only carcinomas but also ulcers often are surrounded by areas of intestinal metaplasia (*Blomquist* 1956 *Heinkel et al* 1956, *Graham & Schade* 1965 *Gear et al* 1971) In this study 48 single biopsies, not tabulated were according to the sketches, taken far from the localized lesion for evaluating the degree of gastritis. Inclusion of these biopsies in the study did not cause any change

The study must conclude that although biopsies showing intestinal metaplasia are found most often in stomachs with cancer and although the difference is slightly significant if more than half of the taken biopsies in a false negative examination shows extensive metaplasia the difference can hardly be used for diagnostic purposes

REFFRENCES

1 *Blomquist H E* Incidence of metaplasia around and at varying distance from chronic duodenal and gastric ulcers. Acta chir Scand *111* 465–474 1956

2 *Correa P Cuello C & Duque E* Carcinoma and intestinal metaplasia of the stomach in Columbian migrants J Nat Cancer Inst. *44* 297–306 1970

3 *Debray C Housset P Marche C de Parco J C & Verdier A* Diagnosis of stomach cancer today In Grundmann, E. Grunze H & Witte S (Eds.) Early Gastric Cancer Current status of diagnosis. Springer Berlin-Heidelberg New York 1974 p 120–126

4 *Elster K Reiss S & Heinkel K* Histotopographische Untersuchungen uber die intestinale Metaplasia in Karzinom- und Ulkusmagen. Z. inn Med *15* 1053–1058 1960

5 *Gear M W L Truelove S C & Whitehead R* Gastric ulcer and gastritis Gut *12* 639–645 1971

6 *Graham R I & Schade R O K* The distribution of intestinal metaplasia in macrospecimen, demonstrated by a histochemical method. Acta path microbiol scand *65* 53 59 1965

7 *Guiss L & Stewart F W* Chronic atrophic gastritis and cancer of the stomach. Arch. Surg *46* 823–843 1943

8 *Heinkel K Elster K & Henning, N* Untersuchungen über die Fundusschleimhaut bei ulcus ventriculi. Dtsch. Arch. klin. Med. *202* 675–691 1956

9 *Heinkel K Henning, N & Conrad G* Häufigkeit und Bedeutung von Becherzellen in der menschlichen Magenschleimhaut. Gastroenterologia *93* 269–278 1960

10 *Johansen Aa. & Sikjaer B* Gastroscopic biopsy Reliability of histological diagnosis with special reference to the single biopsy Scand. J Gastroent. *10* 453–458, 1975.

11 *Järvi O & Laurén P* On the role of heterotopias of the intestinal epithelium in the pathogenesis of gastric cancer Acta path. microbiol. scand *29* 26–43 1951

12. *Laurén P* The two histological main types of gastric carcinoma Diffuse and so-called intestinal type carcinoma. Acta path. microbiol. scand. *64* 31–49 1965

13 *Magnus H A* Observations on the presence of intestinal epithelium in the gastric mucosa J Path. Bact. *44*: 389–397 1937

14 *Marks J N & Drysdale K M.* A modification of Zimmermann's method for differential staining of gastric mucosa. Stain Technol. *32* 48–50 1957

15 *Miller G & Kaufmann M.* Das Magenfrühkarzinom in Europa. Dtsch. med. Wschr *100* 1946–1949 1975

16 *Ming S-C Goldman H & Freiman, D G* Intestinal metaplasia and histogenesis of carcinoma in human stomach Cancer *20* 1418–1429 1967

17 *Morson B C* Intestinal metaplasia of the gastric mucosa. Brit. J Cancer *9* 365–376, 1955 a.

18 *Morson B C* Carcinoma arising from areas of intestinal metaplasia in the gastric mucosa. Brit. J Cancer *9* 377–385 1955 b.

19 *Morson B C* Precancerous lesions of upper gastrointestinal tract. J amer med. Ass. *179* 311–315 1962.

20 *Myren J & Serck Hanssen A* Gastroscopic biopsies in gastric disease. Acta path. microbiol scand Sect A, Suppl *248* 137 144 1974

21 *Nagayo T Ito M Yokoyama H & Komagoe T* Early phases of human gastric cancer Morphological study Gann *56* 101–120, 1965

Acta path. microbiol. scand. Sect. A, 85: 245–250, 1977

THE DIAGNOSTIC SIGNIFICANCE OF RUSSELL BODIES IN ENDOSCOPIC GASTRIC BIOPSIES

AAGE JOHANSEN and BENTE SIKJÆR

Institute of Pathology, Bispebjerg Hospital, Copenhagen, Denmark

Johansen, Aa. & Sikjær, B. The diagnostic significance of Russell bodies in endoscopic gastric biopsies. Acta path. microbiol. scand. Sect. A, 85: 245–250, 1977.

The incidence of cells containing so-called Russell bodies in 315 benign single gastric biopsies taken from stomachs with proven carcinoma, but outside the carcinomatous area and 786 biopsies taken from stomachs without carcinoma were compared. The Russell body containing cells were counted in a fixed area and on the basis of the counting each biopsy was classified in one of four groups: Russell body containing cells absent or present in a number of 1–5, 6–10 or more than 10 in the area. The results showed that endoscopic biopsy examinations containing one single benign biopsy with more than 5 Russell body containing cells in the counted area were significantly most common among examinations taken from stomachs with carcinoma. If half or more than half of the biopsies in an examination contained 1–5 Russell body containing cells significant differences were also found. The sensitivity of such examinations was low but their predictive values (PV_{pos}) varied from 46 per cent to 95 per cent, meaning that such examinations may be of importance for the diagnosis of gastric cancer.

Key words: Russell bodies; gastric biopsies; diagnostic significance.

Aa. Johansen, Institute of Pathology, Bispebjerg Hospital, DK 2400 Copenhagen NV, Denmark.

Received 10.ix.76. Accepted 18.x.76

It is of common occurrence that endoscopic biopsies performed for diagnosing gastric cancer sometimes demonstrate benign conditions because the endoscopist does not reach the carcinoma but takes the biopsies from the adjacent non-malignant mucosa. If this is the case for all biopsies taken during an endoscopic procedure the examination is false negative.

It is of diagnostic interest to investigate whether any pathological change in such benign, false negative biopsies is found with significant difference from what is found in benign biopsies taken from stomachs without carcinomas.

Atrophic gastritis is known to accompany gastric cancer frequently (*Guiss & Stewart* 1943, *Järvi & Lauren* 1951, *Morson* 1955, *Siurala et al.* 1966). Nevertheless, it has been shown that the presence of the most conspicuous finding of atrophic gastritis, the intestinal metaplasia, in endoscopic gastric biopsies is of hardly any importance for the differential diagnosis between malignant and benign lesions (*Johansen & Sikjær* 1976). It is the purpose of this paper to investigate whether another marked change of atrophic gastritis, the so-called Russell bodies, may be of any importance for this differential diagnosis. It will especially be evaluated whether biopsies with a conspicuous number of Russell

carcinomas and ulcers. This might have disturbed the results because it has been shown that not only carcinomas but also ulcers often are surrounded by areas of intestinal metaplasia (*Blomquist* 1956 *Heinkel et al* 1956 *Graham* & *Schade* 1965 *Gear et al* 1971) In this study 48 single biopsies not tabulated were, according to the sketches, taken far from the localized lesion for evaluating the degree of gastritis. Inclusion of these biopsies in the study did not cause any change

The study must conclude that although biopsies showing intestinal metaplasia are found most often in stomachs with cancer and although the difference is slightly significant if more than half of the taken biopsies in a false negative examination shows extensive metaplasia the difference can hardly be used for diagnostic purposes

REFERENCES

1 *Blomquist H E.* Incidence of metaplasia around and at varying distance from chronic duodenal and gastric ulcers. Acta chir Scand *111* 465–474 1956

2. *Correa P Cuello C & Duque E.* Carcinoma and intestinal metaplasia of the stomach in Columbian migrants J Nat Cancer Inst. *44* 297–306 1970

3 *Debray C Houssel P Marche C de Parco J C & Verdier A* Diagnosis of stomach cancer today In Grundmann, E., Grunze, H. & Witte S (Eds.) Early Gastric Cancer Current status of diagnosis. Springer Berlin-Heidelberg New York 1974 p 120–126

4 *Elster K Reiss S & Heinkel K* Histotopographische Untersuchungen über die intestinale Metaplasia in Karzinom- und Ulkusmägen. Z inn Med *15* 1053–1058 1960

5 *Gear M W L Truelove S C & Whitehead R* Gastric ulcer and gastritis. Gut *12* 639–645 1971

6 *Graham R I & Schade R O K* The distribution of intestinal metaplasia in macroscopic specimen, demonstrated by a histochemical method. Acta path. microbiol. scand *65* 53 59 1965

7 *Gulss L. & Stewart F W.* Chronic atrophic gastritis and cancer of the stomach. Arch. Surg. *46* 823–843 1943

8 *Heinkel K Elster K & Henning N* Untersuchungen über die Fundusschleimhaut bei ulcus ventriculi Dtsch. Arch. klin. Med. *202* 675–691 1956

9 *Heinkel K Henning N & Conrar G* Häufigkeit und Bedeutung von Becherzellen in der menschlichen Magenschleimhaut. Gastroenterologia *93* 269–278, 1960

10 *Johansen Aa. & Sikjaer B* Gastroscopic biopsy Reliability of histological diagnosis with special reference to the single biopsy Scand J Gastroent. *10* 453–458, 1975

11 *Järvi O & Laurén P* On the role of heterotopias of the intestinal epithelium in the pathogenesis of gastric cancer Acta path. microbiol. scand *29* 26–43 1951

12 *Laurén P* The two histological main types of gastric carcinoma Diffuse and so-called intestinal-type carcinoma. Acta path. microbiol. scand. *64* 31–49 1965

13 *Magnus H A* Observations on the presence of intestinal epithelium in the gastric mucosa J Path. Bact *44* 389–397 1937

14 *Marks J N & Drysdale K M.* A modification of Zimmermann's method for differential staining of gastric mucosa. Stain Technol. *32* 48–50 1957

15 *Müller G & Kaufmann M* Das Magenfrühkarzinom in Europa. Dtsch. med. Wschr *100* 1946–1949 1975

16 *Ming S-C Goldman H & Freiman D G* Intestinal metaplasia and histogenesis of carcinoma in human stomach. Cancer *20* 1418–1429 1967

17 *Morson B C* Intestinal metaplasia of the gastric mucosa. Brit. J Cancer *9* 365–376, 1955 a

18. *Morson B C* Carcinoma arising from areas of intestinal metaplasia in the gastric mucosa. Brit. J Cancer *9* 377–385 1955 b.

19 *Morson B C* Precancerous lesions of upper gastrointestinal tract. J amer med Ass. *179* 311–315 1962

20 *Myren J & Serck Hanssen A* Gastroscopic biopsies in gastric disease Acta path. microbiol scand Sect. A Suppl. *248* 137–144 1974

21 *Nagayo T Ito M Yokoyama H & Komagoe T* Early phases of human gastric cancer' Morphological study Gann *56* 101–120, 1965

Acta path. microbiol. scand. Sect. A, 85: 245–250, 1977

THE DIAGNOSTIC SIGNIFICANCE OF RUSSELL BODIES IN ENDOSCOPIC GASTRIC BIOPSIES

AAGE JOHANSEN and BENTE SIKJÄR

Institute of Pathology, Bispebjerg Hospital, Copenhagen, Denmark

Johansen, Aa. & Sikjär, B. The diagnostic significance of Russell bodies in endoscopic gastric biopsies. Acta path. microbiol. scand. Sect. A, 85: 245–250, 1977.

The incidence of cells containing so-called Russell bodies in 315 benign single gastric biopsies taken from stomachs with proven carcinoma, but outside the carcinomatous area and 786 biopsies taken from stomachs without carcinoma were compared. The Russell body containing cells were counted in a fixed area and on the basis of the counting each biopsy was classified in one of four groups: Russell body containing cells absent or present in a number of 1–5, 6–10 or more than 10 in the area. The results showed that endoscopic biopsy examinations containing one single benign biopsy with more than 5 Russell body containing cells in the counted area were significantly most common among examinations taken from stomachs with carcinoma. If half or more than half of the biopsies in an examination contained 1–5 Russell body containing cells significant differences were also found. The sensitivity of such examinations was low but their predictive values (PV_{pos}) varied from 46 per cent to 95 per cent, meaning that such examinations may be of importance for the diagnosis of gastric cancer.

Key words: Russell bodies; gastric biopsies; diagnostic significance.

Aa. Johansen, Institute of Pathology, Bispebjerg Hospital, DK-2400 Copenhagen NV, Denmark.

Received 10.ix.76   Accepted 18.x.76

It is of common occurrence that endoscopic biopsies performed for diagnosing gastric cancer sometimes demonstrate benign conditions because the endoscopist does not reach the carcinoma but takes the biopsies from the adjacent non-malignant mucosa. If this is the case for all biopsies taken during an endoscopic procedure the examination is false negative.

It is of diagnostic interest to investigate whether any pathological change in such benign, false negative biopsies is found with significant difference from what is found in benign biopsies taken from stomachs *without* carcinoma.

Atrophic gastritis is known to accompany gastric cancer frequently (*Guiss & Stewart* 1943, *Järvi & Laurén* 1951, *Morson* 1955, *Siurala et al.* 1966). Nevertheless, it has been shown that the presence of the most conspicuous finding of atrophic gastritis, the intestinal metaplasia, in endoscopic gastric biopsies is of hardly any importance for the differential diagnosis between malignant and benign lesions (*Johansen & Sikjär* 1976). It is the purpose of this paper to investigate whether another marked change of atrophic gastritis, the so-called Russell bodies, may be of any importance for this differential diagnosis. It will especially be evaluated whether biopsies with a conspicuous number of Russell

bodies are of importance for the diagnosis of cancer

MATERIAL AND METHODS

Russell bodies are small round bodies which according to *Hanaoka* (1953) develop in plasma cells whose mitochondrias transform to a homogeneous light microscopically visible matrix. They are of different size often faceted and gradually fill up the entire cytoplasm of the plasma cells displacing the nucleus and at last cause cell rupture. They are then found in the connective tissue forming small morula like masses. In this study it is the collection of Russell bodies in a plasma cell or a morula like formation, and not the single Russell body which is counted. These collections will be abbreviated RB.

The material was collected as previously mentioned (*Johansen & Sikjær* 1976). Among the biopsies taken from 142 stomachs with carcinomas 315 showed completely benign conditions. They were compared to 786 benign biopsies taken from 194 stomachs with benign lesions. Each single biopsy was stained with haematoxylin-eosin and a double mucin staining namely the *Marks & Drysdale's* modification (1957) of the Zimmermann's reaction with added colloidal iron. This staining makes the Russell bodies very distinct because they are stained by both the PAS-reaction and on account of their acidophilia also by the Aurantia. They demonstrate an orange-red colour contrasting against the magenta colour of the surface and pit epithelium.

Since the size of the biopsies varied considerably the following technique was used for counting (Fig. 1). Each biopsy was examined with a Leitz Orthoplan microscope. Using a moderate magnification the area where Russell bodies were most densely distributed in the biopsy was selected. At a magnification of 400 the specimen were moved and the rectangle of the photo-ocular (magnification 10 ×) was rotated until the greatest possible number of Russell bodies were enclosed by the frame. This area corresponds to 0.042 mm². On the basis of the counting the biopsies were placed in one of three groups 1–5, 6–10 or more than 10 RB per counted area. The counting was carried out by both authors independently and only very few divergences came up. Such biopsies were reexamined and agreement was reached. It should be stressed that the only purpose of the counting was to place the biopsies in one of the three groups. No exact number of Russell bodies was intended and therefore the thickness of the sections was not considered. Only Russell bodies localized inside the frame and not on the frame itself were counted.

After classifying the single biopsies, an examination (the group of biopsies from one patient) was classified according to its composition of RB-containing biopsies. Examinations of equal compositions which were found with significant different frequencies in the group from carcinoma and from benign lesions were estimated for their diagnostic accuracy. Three expressions, defined by *Leckie* (1966) were used. 1. sensitivity: percentage of patients with cancer demonstrating a positive examination. 2, predictive value of a positive examination (PV_{pos}): percentage of patients demonstrating a positive examination having cancer and 3. predictive value of a negative examination (PV_{neg}): percentage of patients with a negative examination not demonstrating cancer.

RESULTS

All mentioned biopsies were evaluated for the presence of RB. They were found in 30.4 per cent of all single biopsies. From Table 1 is seen that RB were most often found in biopsies from stomachs with carcinomas. The difference was insignificant if only a small number was present. On the other hand a high level of significance was reached if more than 5 RB per counted area were present in a biopsy. The table do not consider the distribution of the single biopsies with RB in the examinations, but in Table 2 or 3 this distribution is given for four examinations. Table 2 demonstrates that if only one benign biopsy with 5 or more RB per counted area is present significant difference between the number of examinations from stomachs with carcinoma and benign lesions is achieved. In Table 3 is shown that significant difference also is found for examinations with biopsies containing one to five RB per counted area if such biopsies make up half or more than half of the number of benign biopsies in an examination.

In Table 4 is given the diagnostic accuracy for examinations which were found with significant difference from stomachs with carcinoma and benign lesions. The sensitivity is very low but it is noteworthy that the PV_{pos} extends from 46 per cent to 95 per cent while the PB_{neg} is nearly constant

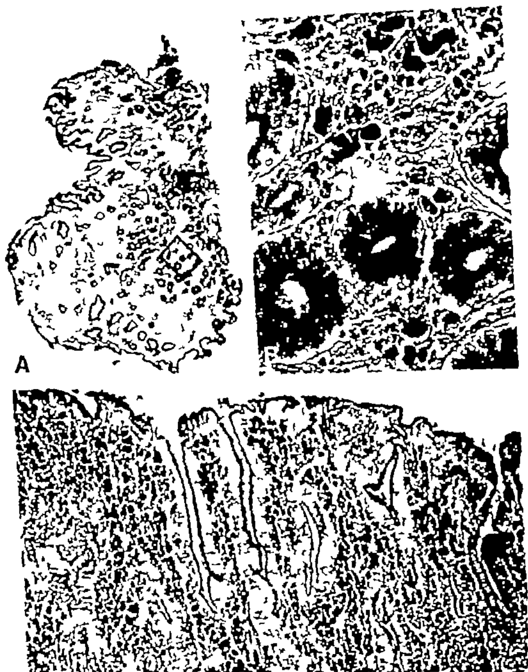


Fig. 1 RB present in conspicuous high number. A. The whole biopsy (× 25). B. Exactly the counted area indicated in A (× 400). C. Detail of the resection specimen from which the biopsy was taken × 100. PAS

TABLE 1 *Distribution of Biopsies with Different Contents of Russell Bodies (RB) in Relation to Two Groups of Benign Biopsies Taken from Stomachs with Carcinoma and Benign Lesions Respectively*

		Benign single biopsies	Number of Russell bodies per counted area			
			0	1–5	6–10	>10
	336	1101	766	240	65	30
Stomachs with carcinoma	142	315	194 (62 %)	70 (22 %)	32 (10 %)	19 (6 %)
Stomachs with benign lesions	194	786	572 (73 %)	170 (22 %)	33 (4 %)	11 (1 %)
		Chi²	1 277 N S	0 018 N.S	13.328 p<0 0005	17.679 p<0 0005

TABLE 2 *Distribution of Examinations Where Only One Single Biopsy Showed either 1) 1 to 5 RB or 2) More than 5 RB per Counted Area in Relation to Stomachs with Carcinoma and Benign Lesions Respectively*

		Examinations containing benign biopsies*	Examinations where only one single biopsy per counted area showed	
			1–5 RB	more than 5 RB
	336	295	126	32
Stomachs with carcinoma	142	101	50 (50 %)	25 (25 %)
Stomachs with benign lesions	194	194	76 (39 %)	7 (4 %)
		Chi²	2.844 N.S	31 496 p<0 0005

* 41 examinations contained solely biopsies demonstrating carcinoma

irrespective the composition of the examinations.

DISCUSSION

It is beyond the scope of this paper to discuss the basic biology of RB. They were already related to carcinoma by *Russell* (1890) who considered them a sort of cancer parasites. They have for years been described in association with gastritis (*Versé* 1908, *Konjetzny* 1928, *Lintrup* 1929, *Joske et al* 1955). *Yoshida et al* (1964) found RB in 26 per cent of 3006 biopsies from normal and pathological stomachs, a result very close to the present. Furthermore they found a good correlation between their incidence and the severity of gastritis. RB in exceptional numbers have been described in relation to superficial spreading carcinoma by *Johansen* (1967).

The applied technique of counting would probably have been inadequate if it was aspired to obtain a very precise number for RB but the method was considered sufficient for the purpose to reveal biopsies with a conspicuous number of RB.

Evaluating the results it has to be remembered that all the biopsies were taken for diagnosing localized lesions in the stomach and therefore reflect the condition of the mucosa in close proximity to such lesions.

Since all biopsies showing malignant changes were rejected from the study the number of benign biopsies in the examinations from carcinomas was naturally very

TABLE 3 *Distribution of Examinations Where Half or More than Half of the Number of Single Biopsies Showed 1) 1 to 5 RB or 2) More than 5 RB per Counted Area in Relation to Stomachs with Carcinoma and Benign Lesions Respectively*

		Examinations containing benign biopsies	Examinations where half or more than half of the number of biopsies per counted area showed 1–5 RB	more than 5 RB
	336	295	87	21
Stomachs with carcinoma	142	101	40 (40 %)	20 (20 %)
Stomachs with benign lesions	194	194	47 (24 %)	1 (1 %)
		Chi²	6 829 p<0.001	34 497 p<0.0005

41 examinations contained solely biopsies demonstrating carcinoma.

TABLE 4 *Sensitivity, PV pos and PV neg Values of Different Sorts of Examinations Found with Significant Different Frequency from Stomachs with Cancer and Benign Lesions*

Examinations	Chi²	Sensitivity $\frac{TP}{TP+FN}$ %	PV pos $\frac{TP}{TP+FP}$ %	PV neg $\frac{NT}{TN+FN}$ %
Half or more of the number of single benign biopsies showed 1–5 RB	6.829	39.6 %	46.0 %	70.6 %
One single benign biopsy showed more than 5 RB	31 496	24 7 %	78.1 %	71.8 %
Half or more of the number of single benign biopsies showed more than 5 RB	34 497	19.8 %	95.2 %	70.4 %

T True F False P Positive N Negative.

limited and "half or more than half" often means only one or two biopsies.

The study shows clearly that RB more often are present in the gastric mucosa from patients with cancer than with benign lesions, but it is noteworthy that the difference is by far most expressed when the RB are very numerous. When it was possible to include more than five RB in the small area counted the whole biopsy usually was stuffed with them and they were the most conspicuous feature of the biopsy impossible to overlook if the mentioned staining or even a pure PAS-reaction was used.

The presence of RB naturally implies the presence of plasma cells There is little doubt that the incidence of RB to some degree parallels the severity of the gastritis. On the other hand the reverse is not the case. Severe degrees of gastritis with heavy plasma cell infiltration were met in many biopsies without a single RB. This led to the conclusion that their incidence is influenced by some other at the moment, unknown factors. The study pays evidence for relating such factors to the development or presence of carcinoma.

Concerning the diagnostic importance of RB the constantly low sensitivity makes them quite unsuitable for screening purposes—they were completely absent in more than 50 per cent of the single biopsies. When they

were met in great numbers in examinations the relative high PV_{pos} values justify a well founded suspicion of the patient having carcinoma

The diagnostic value of RB in the given sense has to our knowledge never been reported for the stomach

Using discriminant analysis for examining the histological features of oral leucoplakias developing to carcinoma *Kramer et al* (*1970*) found high values for the presence of RB in the same way as in this study

Conclusively it can be said that the presence of RB in a conspicuous number in *biopsies from stomachs with localized lesions* is helpful in the diagnosis of gastric cancer

REFERENCES

1 *Cmss L. H & Stewart F H* Chronic atrophic gastritis and cancer of the stomach. Arch Surg *46* 823–843 1943

2 *Hanaoka M* Studies on the ability of biosynthesis of protein by mitochondria in plasma cells. *Acta path. jap 3 53 63 1953*

3 *Johansen Aa* Russell bodies in the gastric mucosa with special reference to the superficial spreading type of carcinoma. Acta path. microbiol scand, *suppl. 187* 49 50 1967

4 *Johansen Aa & Sikjär B* The diagnostic significance of intestinal metaplasia in endoscopic gastric biopsies. Acta path microbiol scand Sect. A *85* 240 244 1977

5 *Joske R A Finckh E S & Wood I J* Gastric biopsy A study of 1000 consecutive successful gastric biopsies Quart J Med *24* 269 291 1955

6 *Järvi O & Lauren P* On the role of heterotopias of the intestinal epithelium in the pathogenesis of gastric cancer Acta path. microbiol. scand *29* 26–43 1951

7 *Konjetzny G E* Die Entzündungen des Magens. In Henke-Lubarsch (Ed.) Handbuch der speziellen pathologischen Anatomie und Histologie *Bd 4 II* Teil, Berlin 1928.

8 *Kramer I R H Lucas R B El Labban N & Lister L* The use of discriminant analysis for examining the histological features of oral keratoses and lichen planus Brit. J Cancer *24* 673–686 1970

9 *Marks J S & Drysdale K M* A modification of Zimmermann's method for differential staining of gastric mucosa Stain Technol. *32* 48 50 1957

10 *Morson B C* Intestinal metaplasia of the gastric mucosa, Brit. J Cancer *9* 365 376, 1955

11 *Russell W* An address on a characteristic organism of cancer Brit. med J *II* 1356-1360 1890

12 *Siurala M Lamas K & Varis K & Wiljasalo M* Studies of patients with atrophic gastritis *A 10 15 year follow up* Scand. J Gastroent *1* 40–48 1966

13 *Vecchio T J* Predictive value of a single diagnostic test in unselected populations New Engl. J med *274* 1171–1173 1966

14 *Versé M* Über die Entstehung den Baues und das Wachstum der Polypen, Adenome und Karzinome des Magen Darmkanals. In Marchand F (Ed.) Arbeiten aus dem pathologischen Institute zu Leipzig Vol. I Hef 5 Hirzel Leipzig 1908 p. 1–168

15 *Vimtrup B* To forelæsninger over gastritis Levin & Munksgaard København 1929

16 *Yoshida T., Landgraf J Heinkel K Henning N & Elster K* Die sogenannte Russellschen Körperchen in der Magenschleimhaut Münch med Wschr *106* 1350–1353, 1964

Acta path. microbiol. scand. Sect. A, 85: 251-262, 1977

ULTRASTRUCTURAL AND FUNCTIONAL ASPECTS OF FROG HEART LESIONS AFTER ISOPROTERENOL

A. Carlsten, R. Ekholm, L. E. Ericson and O. Poupa

Departments of Clinical Physiology and Anatomy, University of Göteborg, Sweden

Carlsten, A., Ekholm, R., Ericson, L. E. & Poupa, O. Ultrastructural and functional aspects of frog heart lesions after isoproterenol. Acta path. microbiol. scand. Sect. A, 85: 251-262, 1977.

The purpose of the present study was to explore the possible correlation between the ultrastructural changes and the functional changes induced by isoproterenol (IPR) in the myocardium of the frog. The study was performed on winter frogs (R. pipiens). The experimental animals were moved from +8° C to +25° C, kept there for 3 days and then given 2 daily doses of IPR (200 mg/kg b.w.). Twenty-four hours after the second IPR dose, specimens were taken from the heart ventricle and subjected to electron microscopical examination and to analysis of the isometric force decay in response to anoxia produced by sodium cyanide. Specimens were taken from macroscopically non-damaged portions of the ventricle as well as from aneurysms. Control animals were kept at +8° C and +25° C and injected with saline. In all IPR-injected animals the specimens from macroscopically non-damaged parts of the myocardium showed ultrastructural changes characterized by a relative increase in mitochondrial mass and a pronounced reduction of glycogen. Specimens from aneurysms showed similar changes but in some fibres signs of more severe injury were observed such as fragmentation of the cristae of the mitochondria and disintegration of myofibrils. The functional analyses showed that the isometric force decay of the heart muscle strips induced by the respiratory block by cyanide was much greater in specimens from IPR-treated animals than in those from control frogs. The augmented force decay was found both in strips from macroscopically normal parts of the myocardium and in those from aneurysms although it was somewhat greater and more rapid in the latter. The observed, minor functional difference between macroscopically non-damaged portions of the myocardium and aneurysms is remarkable with respect to the different preservation of myofilaments in these regions. This similarity in functional decline could possibly be due to the observed homogeneous reduction of glycogen in the IPR-exposed myocardium, since glycogen was the only source of ATP under the experimental conditions of current interest.

Key words: Heart lesions; frog; isoproterenol; ultrastructure.

A. Carlsten, Department of Clinical Physiology, University of Göteborg, Sweden.

Received 2.x.76. Accepted 1.xi.76.

Since the discovery of the cardiotoxic effects of isoproterenol (IPR) some comprehensive studies of the ultrastructural changes induced by IPR in the myocardium of homoiotherm animals have been published (*Ferrans et al.* 1969, *Moravec & Hatt* 1969). In contrast, very little information about the influence of IPR on the ultrastructure of the heart of poikilotherms is available.

Among poikilotherms, the frog was found to have a myocardium resistant to cardio-

were met in great numbers in examinations the relative high PV_{pos} values justify a well founded suspicion of the patient having carcinoma

The diagnostic value of RB in the given sense has to our knowledge never been reported for the stomach

Using discriminant analysis for examining the histological features of oral leucoplakias developing to carcinoma *Kramer et al (1970) found high values for the presence* of RB in the same way as in this study

Conclusively it can be said that the presence of RB in a conspicuous number in biopsies from stomachs with localized lesions is helpful in the diagnosis of gastric cancer

REFERENCES

1 *Cain L. H & Stewart F H* Chronic atrophic gastritis and cancer of the stomach. Arch Surg *46* 823–843 1943

2 *Hanaoka M* Studies on the ability of biosynthesis of protein by mitochondria in plasma cells. Acta path. jap. *3* 53–63 1953

3 *Johansen Aa.* Russell bodies in the gastric mucosa with *special reference to the superficial spreading type of carcinoma* Acta path. microbiol. scand *suppl 187* 49–50 1967

4 *Johansen Aa & Sikjær B.* The diagnostic significance of intestinal metaplasia in endoscopic gastric biopsies Acta path. microbiol scand. Sect. A *85* 240–244 1977

5 *Joske R A Finckh F S & Wood I J* Gastric biopsy A study of 1000 consecutive successful gastric biopsies. Quart J Med. *24* 269–294 1955

6 *Järvi O & Laurén P* On the role of heterotopias of the intestinal epithelium in the pathogenesis of gastric cancer Acta path. microbiol scand. 29 26–43 1951

7 *Konjetzny G E.* Die Entzündungen des Magens. In Henke-Lubarsch (Ed.) Handbuch der speziellen pathologischen Anatomie und Histologie Bd 4 II Teil Berlin 1928.

8 *Kramer I R H Lucas R B El Labban A & Lister L* The use of discriminant analysis for examining the histological features of oral keratoses and lichen planus. Brit. J Cancer 24 673–686, 1970

9 *Marks J S & Drysdale A M* A modification of Zimmermann's method for differential staining of gastric mucosa. Stain Technol 32 48 50 1957

10 *Morson B C* Intestinal metaplasia of the gastric mucosa. Brit J Cancer 9 365 376, 1955

11 *Russell W* An address on a characteristic organism of cancer Brit med *J II* 1356–*1360 1890*

12 *Siurala M Isaris A & Wiljasalo M* Studies of patients with atrophic gastritis A 10 15 year follow-up. Scand. J Gastroent. *1* 40–48 1966.

13 *Vecchio T J* Predictive value of a single diagnostic test in unselected populations. New Engl J med 274 1171–1173 1966

14 *Versé M* Über die Entstehung den Bau und das Wachstum der Polypen, Adenome *und Karzinome des Magen Darmkanals* In Marchand, F (Ed.) Arbeiten aus dem pathologischen Institute zu Leipzig, Vol I Heft 5 Hirzel, Leipzig 1908 p 1–168.

15 *Faintrup B* To forelæsninger over gastritis Levin & Munksgaard København 1929

16. *Yoshida T Landgraf J Heinkel K Henning N & Elster K* Die sogenannte Russellschen Körperchen in der Magenschleimhaut. Münch. med. Wschr *106* 1350–1353 *1964*

Acta path. microbiol. scand. Sect. A, 85: 251–262, 1977

ULTRASTRUCTURAL AND FUNCTIONAL ASPECTS OF FROG HEART LESIONS AFTER ISOPROTERENOL

A. Carlsten, R. Ekholm, L. E. Ericson and O. Poupa

Departments of Clinical Physiology and Anatomy, University of Göteborg, Sweden

Carlsten, A., Ekholm, R., Ericson, L. E. & Poupa, O. Ultrastructural and functional aspects of frog heart lesions after isoproterenol. Acta path. microbiol. scand. Sect. A, 85: 251–262, 1977.

The purpose of the present study was to explore the possible correlation between the ultrastructural changes and the functional changes induced by isoproterenol (IPR) in the myocardium of the frog. The study was performed on winter frogs (R. pipiens). The experimental animals were moved from +8° C to +25° C, kept there for 5 days and then given 2 daily doses of IPR (200 mg/kg b.w.). Twenty four hours after the second IPR dose specimens were taken from the heart ventricle and subjected to electron microscopical examination and to analysis of the isometric force decay in response to anoxia produced by sodium cyanide. Specimens were taken from macroscopically non-damaged portions of the ventricle as well as from aneurysms. Control animals were kept at +8° C and +25° C and injected with saline. In all IPR-injected animals the specimens from macroscopically non-damaged parts of the myocardium showed ultrastructural changes characterized by a relative increase in mitochondrial mass and a pronounced reduction of glycogen. Specimens from aneurysms showed similar changes but in some fibres signs of more severe injury were observed such as fragmentation of the cristae of the mitochondria and disintegration of myofibrils. The functional analyses showed that the isometric force decay of the heart muscle strips induced by the respiratory block by cyanide was much greater in specimens from IPR-treated animals than in those from control frogs. The augmented force decay was found both in strips from macroscopically normal parts of the myocardium and in those from aneurysms although it was somewhat greater and more rapid in the latter. The observed, minor functional difference between macroscopically non-damaged portions of the myocardium and aneurysms is remarkable with respect to the different preservation of myofilaments in these regions. This similarity in functional decline could possibly be due to the observed homogeneous reduction of glycogen in the IPR-exposed myocardium since glycogen is the only source of ATP under the experimental conditions of current interest.

Key words: Heart lesions; frog; isoproterenol; ultrastructure.

A. Carlsten, Department of Clinical Physiology, University of Göteborg, Sweden.

Received 2.ix.76 Accepted 1.xi.76

Since the discovery of the cardiotoxic effects of isoproterenol (IPR) some comprehensive studies of the ultrastructural changes induced by IPR in the myocardium of homoiotherm animals have been published (Ferrans et al. 1969, Moravec & Hatt 1969). In contrast, very little information about the influence of IPR on the ultrastructure of the heart of poikilotherms is available.

Among poikilotherms, the frog was found to have a myocardium resistant to cardio-

toxic IPR-effects even at high doses. However frogs (R pipiens) could be sensitized to the cardiotoxic effect of IPR by increased (+25° C) environmental temperature in such animals, IPR caused single or multiple acute aneurysms of the ventricular wall (*Poupa & Carlsten* 1969 and 1970) In contrast to IPR induced lesions in homoiotherms and in turtles (*Ostadal et al* 1968) these heart lesions in the frog showed a complete lack of secondary tissue reaction even within those areas of the aneurysms which displayed the most pronounced cellular lesions (*Korb et al* 1973) In an isometric procedure ventricular strips from frogs treated with IPR at +25 C showed an abnormal response towards histotoxic anoxia this occurred after IPR in hearts with and without aneurysms (*Carlsten & Poupa* 1975)

The aim of the present study was to compare the ultrastructure of the cardiac muscle in IPR treated frogs with and without macroscopic lesions and to study the possible correlation between ultrastructure and *in vitro* function of macroscopically damaged and undamaged portions of the same ventricle.

MATERIALS AND METHODS

Production of IPR-lesions Winter frogs (R pipiens, northern type Mogul Wisc n = 63) of both sexes were moved from +8 C and kept for 3 days at +25 C and then injected twice with IPR into the dorsal lymphatic sac (200 mg/kg b.w) within the following 48 hours. Twenty four hours after the last injection the frogs were decerebrated and the chest was opened. The beating heart *in situ* was inspected under magnification (6–40 ×) In 30 per cent (n = 19) of the survivors (88 per cent) macroscopically visible cardiac lesions (acute aneurysms) were observed i.e. bulging areas of the ventricular wall with paradoxical movements during the heart cycle The sites of predilection were the left and right basal corners and the apical region (Fig 10) (For further details of the procedure, see *Poupa & Carlsten* 1970) Control animals were kept at +25 C and +8 C and injected with saline.

Electron microscopy Glutaraldehyde fixative (2.5 per cent glutaraldehyde in 0 05 per cent sodium cacodylate) was dripped onto the heart In cases where one and the same heart was subject to both structural and functional analyses (Fig. 10) the part of the ventricular wall used as a ventricular strip for the isometric contraction procedure was excised prior to fixation. Samples for electron microscopy were taken from both the left and the right upper corner and from the apex of the ventricle. In the presence of aneurysm the sample was taken from the middle of the bulging area. After excision, the specimens were immersed in the same glutaraldehyde solution for 2 hours and then post fixed in 1 per cent osmium tetroxide in cacodylate buffer for 2 hours. Specimens were embedded in Epon and sections, cut on an LKB Ultrotome, were contrasted with uranyl acetate and lead citrate and examined in a Philips 300 electron microscope.

Morphometric analyses were performed on randomly selected longitudinal sections of muscle fibres from 4 normal ventricles (controls kept at 25 C) and from 4 IPR-exposed, macroscopically normal ventricles. The fibres were photographed at a magnification of 3 200 and the measurements were performed on photocopies enlarged 3 times in printing. The relative volumes (volume densities) of myofibrils mitochondria and glycogen-containing species were determined by pointcounting (*Weibel* 1969) and the number of sarcoplasmic reticulum-related dense granules was counted and related to section area.

Examination of the function of ventricular strips in a Cortland Ringer solution (pH 7.8–8 0) was performed using an isometric procedure with a view to having the response of the heart to anoxia produced by sodium cyanide defined. The cellular respiratory failure thus induced was indicated by the force decay curves of the slowly paced heart specimens of IPR treated frogs and controls. After the addition of NaCN to the bath, the depression of the contraction amplitude under the anoxia was continuously followed over 60 min and expressed as per cent of the pre-anoxic amplitude (*Carlsten & Poupa* 1975)

In the present paper only strips of the ventricle from hearts also examined by electron microscopy were tested before and during cyanide anoxia.

RESULTS

Electron Microscopical Observations

Results are based on the examination of 5 control animals (kept at +8 C or +25 C)

Fig 1 Survey electron micrograph of a heart muscle fibre of a frog kept at +25 C. A Golgi area is located close to the nuclear pole. Numerous spherical dense granules are present. Typical mitochondria are embedded in glycogen. × 20 000

Fig 2 Mitochondria present in a heart of a frog kept at +25 C Several vesicles with a content of very high density are present. × 36 000



and 22 IPR treated animals, 8 of which had no macroscopic ventricular lesions and 14 with acute aneurysms.

Control frogs The structure of the ventricular muscle of frogs kept at +8° C or +25° C as observed in the present study is in most respects in fair agreement with earlier descriptions (*Staley & Benson 1968, Sommer & Johnson 1969 Page & Niedergerke 1972*)

The cardiac muscle of the frog has no blood vessels. It consists of a spongy three-dimensional meshwork of muscle trabeculae covered by an unfenestrated endothelium. The lacunae in between the trabeculae are in wide communication with the ventricular cavity The trabeculae contain a varying number of muscle fibres with a diameter of 2–4 μm.

Each muscle fibre contains 1–5 myofibrils which is of the well known composition of thick and thin filaments. The A band I band and Z line are easily distinguished in longitudinal sections The myofibrils are separated by nuclei and by accumulations of cytoplasmic matrix in which glycogen and mitochondria are the predominant components (Fig 1)

In longitudinal sections, the glycogen particles are found in dense aggregates at both poles of the nuclei and as fusiform or strand shaped aggregates between the myofibrils or beneath the cell membrane (Figs. 1 2)

All mitochondria are found within the interfibrillar glycogen aggregates. Most mitochondria are ovoid but elongated straight or curved specimens, the longest achieving a length of 3–4 μm, are common The orientation of the mitochondria seems to be random (Fig 1) The most characteristic feature of the mitochondrial structure is the high density of the matrix, markedly contrasting with the low density of the interior of the cristae The closely spaced cristae are most often transversely disposed, but longitudinally and obliquely oriented cristae are common. The cristae are deep and if transversely arranged, they generally almost bridge the whole width of the mitochondrion they are straight or curved and vary in width along their course (Fig 2)

A Golgi complex is present near one pole of the nucleus (Fig 1) In all sections through the Golgi area, but also in other areas containing glycogen a varying number of spherical, dense granules, with a mean diameter of about 150 nm is present (Fig 1) In previous descriptions of the ultrastructure of the frog heart, the identity of these granules with the specific atrial granules generally occurring in heart muscle cells of vertebrate, has been suggested (*Sommer & Johnson* 1969) The nature of these granules seems to be unknown.

A second type of membrane-limited structures with a dense content is also observed (Fig 2) These structures appear as spherical, oval or elongated vesicles which contain one or several nuclei of very high electron density (Fig 2) Such vesicles are most often found in glycogen areas.

The very dense content of the vesicles probably represents material precipitated in the sarcoplasmic reticulum as the limiting membrane of the vesicles not unfrequently is observed in continuity with tubules of the sarcoplasmic reticulum.

The sarcoplasmic reticulum, consisting of

TABLE 1 *Relative Volumes of Cytoplasmic Components in Muscle Fibres from Control Animals (kept at 25 °C) and in Macroscopically Normal Specimens from IPR Injected Frogs (mean ± SEM)*

	Myofibrils	Mitochondria	Glycogen-containing spaces	Remaining components
Controls	56 7 ± 1 42	21.5 ± 1 15	15.2 ± 1 45	6 6 ± 2.04
IPR injected	58 6 ± 2 48	28.4 ± 2 07	1.3 ± 0 54	11 7 ± 1 14
	n.s.	<0 05	<0 01	<0 05

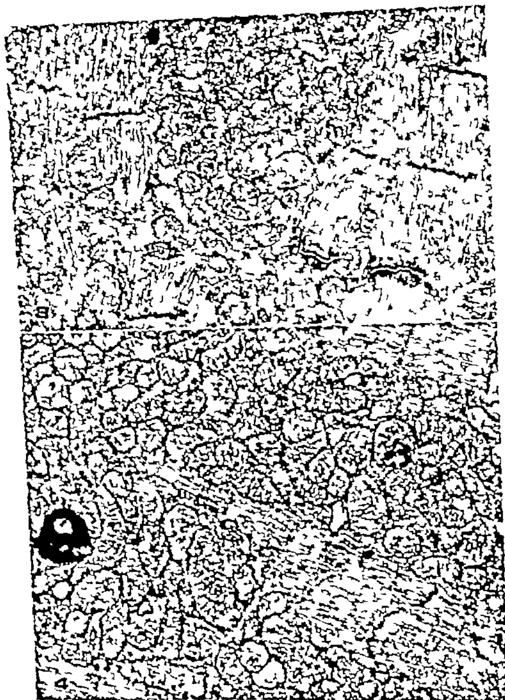


Fig. 3 From frog injected with IPR. Glycogen particles are reduced in number. In this particular area the mitochondria display rather normal appearance. × 18,000

Fig. 4 From frog injected with IPR. Glycogen particles are almost absent. A large number of mitochondria is densely packed in an interfibrillary area. × 18,000

and 22 IPR treated animals, 8 of which had no macroscopic ventricular lesions and 14 with acute aneurysms.

Control frogs The structure of the ventricular muscle of frogs kept at +8° C or +25° C, as observed in the present study is in most respects in fair agreement with earlier descriptions (*Staley & Benson* 1968 *Sommer & Johnson* 1969 *Page & Niedergerke* 1972)

The cardiac muscle of the frog has no blood vessels. It consists of a spongy three-dimensional meshwork of muscle trabeculae, covered by an unfenestrated endothelium. The lacunae in between the trabeculae are in wide communication with the ventricular cavity The trabeculae contain a varying number of muscle fibres with a diameter of 2–4 μm.

Each muscle fibre contains 1–5 myofibrils which is of the well known composition of thick and thin filaments. The A band, I band and Z line are easily distinguished in longitudinal sections The myofibrils are separated by nuclei and by accumulations of cytoplasmic matrix in which glycogen and mitochondria are the predominant components (Fig 1)

In longitudinal sections the glycogen particles are found in dense aggregates at both poles of the nuclei and as fusiform or strand shaped aggregates between the myofibrils or beneath the cell membrane (Figs. 1 2)

All mitochondria are found within the interfibrillar glycogen aggregates. Most mitochondria are ovoid but elongated, straight or curved specimens, the longest achieving a length of 3–4 μm are common The orientation of the mitochondria seems to be random (Fig 1) The most characteristic feature of the mitochondrial structure is the high density of the matrix, markedly contrasting with the low density of the interior of the cristae. The closely spaced cristae are most often transversely disposed but longitudinally and obliquely oriented cristae are common. The cristae are deep and if transversely arranged, they generally almost bridge the whole width of the mitochondrion they are straight or curved and vary in width along their course (Fig 2)

A Golgi complex is present near one pole of the nucleus (Fig 1) In all sections through the Golgi area, but also in other areas containing glycogen a varying number of spherical dense granules, with a mean diameter of about 150 nm is present (Fig 1) In previous descriptions of the ultrastructure of the frog heart the identity of these granules with the specific "atrial granules" generally occurring in heart muscle cells of vertebrate, has been suggested (*Sommer & Johnson* 1969) The nature of these granules seems to be unknown

A second type of membrane-limited structures with a dense content is also observed (Fig 2) These structures appear as spherical oval or elongated vesicles which contain one or several nuclei of very high electron density (Fig 2) Such vesicles are most often found in glycogen areas.

The very dense content of the vesicles probably represents material precipitated in the sarcoplasmic reticulum as the limiting membrane of the vesicles not unfrequently is observed in continuity with tubules of the sarcoplasmic reticulum.

The sarcoplasmic reticulum, consisting of

TABLE I *Relative Volumes of Cytoplasmic Components in Muscle Fibres from Control Animals (kept at 25 C) and in Macroscopically Normal Specimens from IPR Injected Frogs (mean ± SEM)*

	Myofibrils	Mitochondria	Glycogen-containing spaces	Remaining components
Controls	56.7 ± 1.42	21.3 ± 1.13	15.2 ± 1.45	6.6 ± 2.04
IPR injected	58.6 ± 2.48	28.4 ± 2.07	1.3 ± 0.54	11.7 ± 1.14
	n.s.	<0.05	<0.01	<0.05

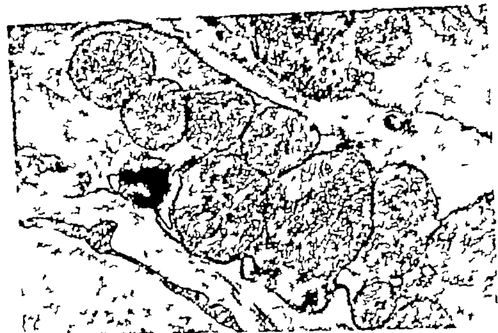


Fig. 7. From the wall of an aneurysm. Swollen mitochondria with broken and vesiculated inner membranes are seen in seriously damaged cell. × 22,000.

vesicles and tubules, is rather sparse but easily recognized in all parts of the muscle fibre. No consistent relation to the sarcomere can be observed.

Any conspicuous and general structural differences between the cardiac muscle of control frogs kept at 25° C and that of animals kept at +8° C could not be observed. However, in some muscle fibres in hearts from frogs in the group kept at 25° C, two types of changes are indicated. One is a slight decrease in the amount of glycogen, apparent as a less dense packing of the glycogen particles in some cells. The other change concerns the mitochondria which in some cells show a decreased density of their matrix resulting in the disappearance of the characteristic marked contrast between the matrix and the interior of the cristae.

IPR-injected frogs. Specimens from hearts which did not develop aneurysms and specimens taken from *macroscopically normal parts* of the ventricle between aneurysms show similar changes.

As shown in Table 1, the relative mitochondrial volume is significantly increased and many interfibrillar spaces are completely filled with densely packed mitochondria (Fig. 4). In some of these spaces, the size and shape of the mitochondria seem similar to those seen in the controls (Fig. 3) while in other areas the mitochondria appear enlarged (Fig. 4). In both normal-sized and enlarged mitochondria the matrix density is reduced. The large mitochondria are further characterized by an increased number of cristae. In all muscle cells the amount of glycogen is decreased. The relative volume of the glycogen-containing spaces is significantly reduced (Table 1) and in many interfibrillar areas, normally filled with a mixture of glycogen and mitochondria, practically no glycogen particles are seen (Figs. 3, 4).

The number of dense vesicles related to the sarcoplasmic reticulum is significantly increased. The number of vesicles per 100 μm^2 section area was 7.0 ± 0.98 (mean ± SEM) in the specimens from controls kept at 25° C and 20.4 ± 3.46 in the specimens from IPR-exposed, macroscopically normal myo-



Fig 5 From the wall of an aneurysm. Enlarged mitochondria are aggregated in interfibrillar areas of two neighbouring cells. Lipid droplets are present × 18 000

Fig 6 From the wall of an aneurysm. Mitochondria are densely packed and appear to be increased in number and size. Several small vesicles with a very dense content are present. The fibrils are disorganized with prominent Z bands. × 16,000

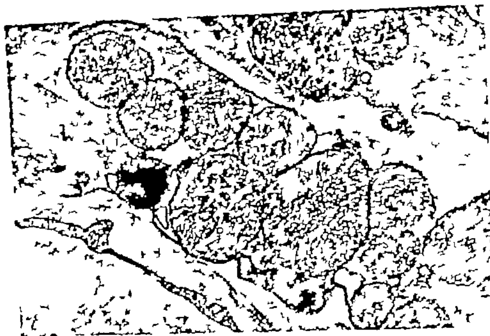


Fig. 7. From the wall of an aneurysm. Swollen mitochondria with broken and vesiculated inner membranes are seen in a seriously damaged cell. × 22,000

vesicles and tubules, is rather sparse but easily recognized in all parts of the muscle fibre. No consistent relation to the sarcomere can be observed.

Any conspicuous and general structural differences between the cardiac muscle of control frogs kept at 25 C and that of animals kept at +8 C could not be observed. However in some muscle fibres in hearts from frogs in the group kept at 25 C, two types of changes are indicated. One is a slight decrease in the amount of glycogen, apparent as a less dense packing of the glycogen particles in some cells. The other change concerns the mitochondria which in some cells show a decreased density of their matrix resulting in the disappearance of the characteristic marked contrast between the matrix and the interior of the cristae.

IPR-injected frogs. Specimens from hearts which did not develop aneurysms and specimens taken from *macroscopically normal part* of the ventricle between aneurysms show similar changes.

As shown in Table 1 the relative mitochondrial volume is significantly increased and many interfibrillar spaces are completely filled with densely packed mitochondria (Fig. 4). In some of these spaces, the size and shape of the mitochondria seem similar to those seen in the controls (Fig. 3) while in other areas the mitochondria appear enlarged (Fig. 4). In both normal-sized and enlarged mitochondria the matrix density is reduced. The large mitochondria are further characterized by an increased number of cristae. In all muscle cells the amount of glycogen is decreased. The relative volume of the glycogen-containing spaces is significantly reduced (Table 1) and in many interfibrillar areas, normally filled with a mixture of glycogen and mitochondria, practically no glycogen particles are seen (Figs. 3, 4).

The number of dense vesicles related to the sarcoplasmic reticulum is significantly increased. The number of vesicles per 100 μm^2 section area was 7.0 ± 0.98 (mean ± SEM) in the specimens from controls kept at 25 C and 20.4 ± 3.46 in the specimens from IPR-exposed, macroscopically normal myo-



Fig 5 From the wall of an aneurysm. Enlarged mitochondria are aggregated in interfibrillar areas of two neighbouring cells. Lipid droplets are present × 18 000

Fig 6 From the wall of an aneurysm. Mitochondria are densely packed and appear to be increased in number and size. Several small vesicles with a ery dense content are present The fibrils are disorganized with prominent Z bands. × 16 000

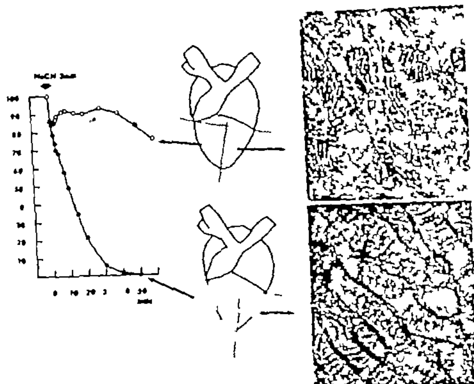


Fig. 10 To the left: force decay curves of ventricular strips during 1 hour after cyanide, plotted as per cent of the pre-anoxic amplitude from one control frog above (o–o–o) and one frog after IPR below (●–●–●). To the right: representativ electron micrographs of the same hearts showing the difference in structure of mitochondria. × 24,000

In the present experiments the previous observation was confirmed, namely that this abnormal force decay in anoxia also occurred in hearts with IPR provoked aneurysms, although to a somewhat smaller extent, in parts of the same ventricular wall where no aneurysmatic lesions were observed. This is illustrated in Fig. 9 where the isometric contraction amplitude at certain intervals after NaCN is expressed in per cent of the pre-anoxic value (F per cent) obtained by simultaneous registration of two strips from one and the same heart, one from an aneurysmatic part of the ventricle, the other from a macroscopically intact part. The force decay after NaCN is abnormal in both parts though more marked and more rapid in the strip including the aneurysm, as shown by the distribution of the plots from the simultaneously obtained values of F per cent after cyanide. This result indicates that such parts of the ventricular wall which include aneurysms may be more seriously damaged than parts without such macrofindings.

Fig. 10 illustrates the relationship between structure and function of the ventricular myocardium from two frogs kept at +25° C. The ventricular strip from the control frog without IPR showed only a slight depression of the contraction amplitude after cyanide, whereas the part of the ventricle from the IPR injected frog including two aneurysms stopped beating 50 min after cyanide. One part of each heart ventricle from these two frogs was subjected to examination at the structure; representative electron micrographs are presented in the figure. The localization of the IPR-provoked aneurysms is typical; the part of the heart used for the study of force decay after cyanide as well as the part

17*

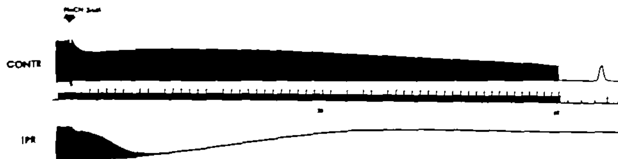


Fig 8 Simultaneous force decay curves after cyanide (NaCN) of ventricular strips from two frogs at 25 C *Contr* = without and *IPR* after isoproterenol (aneurysm)

cardium In order to arrive at a meaningful functional interpretation of this observation further information about the nature of the very dense material in these vesicles seems necessary

An increased number of lipid droplets is present in areas containing mitochondria

In samples of *aneurysms* many fibres are essentially of the same appearance as those in macroscopically unaffected parts of the ventricular wall between the aneurysms (Figs. 5 6) Other fibres display signs of more severe injury (Figs 6 7) A characteristic feature of such fibres is the very large, rounded mitochondria with fragmented or vesiculated cristae (Fig 7) In these fibres, many myofibrils are also deranged and disintegrated.

Functional Changes

The isometric force decay of the heart muscle strips induced by the respiratory block by cyanide is considerably more pronounced in strips from animals treated by IPR at +25° C than in those from control frogs (Fig 8) This finding is in agreement with previous results (*Carlsten & Poupa* 1975)

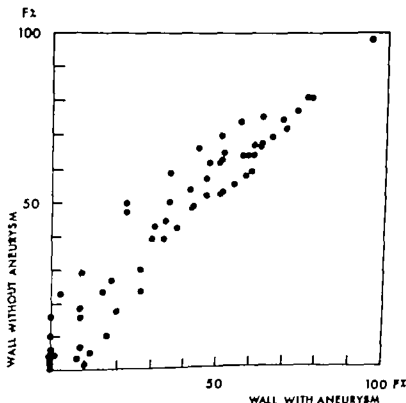


Fig 9 Values of force decay after cyanide, obtained from two strips of the same heart from a frog injected with IPR on the horizontal axis a strip including an aneurysm and on the vertical axis a macroscopically intact part of the heart. The plots represent values obtained simultaneously from the two parts of the heart of the contraction amplitude in per cent of the pre-anoxic value (F per cent) at certain intervals within one hour after cyanide

In macroscopically non-damaged segments of the ventricle of IPR-injected frogs, the mitochondrial mass showed a relative increase. The mitochondria were often densely packed and sometimes enlarged but without obvious signs of distinction of the inner membrane. The latter findings are similar to those reported to occur in homoiotherms as early as 30 min after IPR (*Korb* 1965 *Ferrans et al.* 1969) Furthermore, the glycogen granules were scarce or almost absent. In contrast to observations in homoiotherms, the myofilaments were of normal appearance. The observed changes in the mitochondria and the reduced amount of glycogen after IPR in hearts without macrolesions indicate cellular effects of this catecholamine which were not evident in light microscopy (*Korb et al.* 1973) In some way these effects may be responsible for the lowered resistance to anoxia previously observed by *Carlsten & Poupa* (1975) and confirmed in the present paper Another pattern of ultrastructural changes was found in the areas of the ventricle with macroscopically apparent aneurysms. These changes included signs of more profound derangement in the form of destruction of the mitochondrial cristae and also fragmentation of myofilaments similar to the described changes observed in the hearts of IPR-treated homoiotherms.

Two conclusions may be drawn from the present observations First, that the development of ultrastructural lesions in the poikilotherm heart is slower than that in the heart of homoiotherms and, secondly that the "homoiotherm type" of lesions is present only in bulging segments of the poikilotherm ventricle These differences between poikilotherms and homoiotherms could be due to several factors. One such factor is that the work of the cardiac muscle is less intense in poikilotherms than in homoiotherms (lower temperature lower frequency lesser contraction velocity etc) which means lower load on the heart muscle cell working also under unfavourable conditions such as those presumably created by IPR Taking this fact into consideration, it is understandable also why severe ultrastructural changes, leading to the formation of aneurysm, mainly occur in the upper corners.

As the contractile elements are preserved in macroscopically non-damaged areas of the ventricle, in contrast to those in areas with bulging aneurysms, the functional performance in strips from aneurysms might be expected to be inferior to the former As shown in Fig 2, however in this respect, the macroscopically damaged and non-damaged segments subjected to the mitochondrial respiratory failure by a submaximal dose of cyanide were found to differ slightly (*Carlsten & Poupa* 1975) This phenomenon could possibly be explained by the fact that the production of ATP under these conditions is extramitochondrial (glycolysis) and, as glucose free Ringer was used, the only source of ATP was glycogen, the amount of which was markedly decreased both in macroscopically damaged and non-damaged myocardium in all IPR-treated animals. Analogous results have been obtained in homoiotherms (dogs) and reported by *Gudbjarnason* (1972) who after coronary ligation observed biochemical derangement (ATP and creatine phosphate reduction and release of catecholamines) not only in infarcted areas but also within non-infarcted segments of the same ventricle.

This work was supported by the *Swedish Medical Research Council* (projects Nos B75-14X 2729 and B75-14P 3025)

REFERENCES

Carlsten A. & Poupa, O. Force development of IPR-damaged frog heart muscle in cyanide anoxia. I *Roy P-E. & Harris P* (Eds.) Recent Advances in Studies on Cardiac Structure and Metabolism. Vol. 8. The Cardiac Sarcoplasm. University Park Press, Baltimore, 1975

Carlsten A. & Poupa O. Effect of time on the response to cyanide anoxia of IPR-damaged frog heart. To be published 1976.

Ferrans V J., Hibbs R. G Walsh, J J & Burch, G. E. Histochemical and electron microscopical studies on the cardiac necroses produced by sympathicomimetic agents. Ann. N.Y Acad. Sci. *156* 309–332, 1969

used for the study of structure include aneurysms.

DISCUSSION

Myocardial contractility is enhanced by catecholamines through the production of cyclic AMP they accelerate the relaxation in the heart thus permitting diastolic filling at the increased heart rate. Isoproterenol (IPR) is a synthetic catecholamine exclusively stimulating β receptors and like the natural catecholamines adrenaline and noradrenaline, it can cause myocardial lesions. However, in contrast to the two other agents, IPR does not induce appreciable pulmonary oedema and even after high doses, the mortality is low This makes IPR very suitable for the production and study of myocardial necrosis of uniform severity (*Kahn et al* 1969) Myocardial lesions can be observed also after IPR doses corresponding to those used for therapeutic purposes (*Moravec & Hatt* 1969)

In homoiotherms (rats) the IPR induced cardiac cell necrosis starts very rapidly Characteristic electron microscopical changes, described by several authors, include fading striation fragmentation and melting of myofibrils, destruction of mitochondrial cristae dilatation of the sarcoplasmic reticulum, reduction in the number of glycogen granules, and increased number of lipid droplets. The earliest changes concern mainly the contractile elements and are described as thickening and increased density of the Z lines (*Ferrans et al* 1969) which resemble contraction bands (*Korb* 1965) these changes are observed within 30 min after IPR injection. Later on mitochondria become swollen and the inner membrane starts to break (*Ferrans et al* 1969) The length of some mitochondria surpasses that of many sarcomeres (*Korb* 1965) The peak of the final regressive alterations and the beginning of the fibroplasia (*Rona et al* 1961) as well as the mesenchymal reaction (*Korb* 1965) are observed two days after administration of IPR.

In previous papers we have demonstrated that the frog heart is insensitive to high doses of IPR when the animals are kept at +4 to +12 C, in animals kept at +25 C, however much lower doses of IPR provoke lesions in the ventricular wall, single or multiple aneurysms being the dominant finding (*Poupa & Carlsten* 1969 1970) in addition, the resistance to histotoxic anoxia is decreased (*Carlsten & Poupa* 1975) In the light microscope we observed (*Korb et al.* 1973) cavities or local rarefaction of the spongy structure of the ventricular wall where an aneurysm was identified *in vivo*, these cavities were partly filled by broken trabeculae, isolated cardiac cells and nucleated erythrocytes. The outer wall of the cavities was formed by a thin layer of remnants of myocardial cells, sometimes in combination with single or multiple subepicardial blisters the outer wall of which was built up by a single layer of serosal lining cells with basal membrane. Cells in the affected areas were oedematous with fragmented fibrils and contraction bands but without coagulation necrosis or mesenchymal reaction. It should be emphasized, however that histological changes were never found in IPR treated frogs without macroscopic heart lesions a phenomenon which is in contrast to the finding in a later investigation (*Carlsten & Poupa* 1975) namely that IPR decreased the resistance to anoxia also in hearts without any visible heart lesions. We also found (*Carlsten & Poupa* 1976) that the macroscopically verified lesions never occur after a single injection of IPR but start to appear a few hours after the second injection of IPR. Aneurysms of the ventricular wall usually occur at their maximal rate during the first two days after the second IPR injection.

In the present study the samples to be used for the electron microscopic examination were taken 24 hours after the second IPR injection at +25 C. This time schedule is the same as that used for the previous light microscopical examination (*Korb et al.* 1973) As judged from the studies of homoiotherms, this schedule should provide sufficient time for the IPR induced ultrastructural alterations to develop.

Acta path. microbiol. scand. Sect. A, 85 263–266 1977

OCCURRENCE OF AMYLOIDOSIS SECONDARY TO THE INDUCTION OF EXPERIMENTAL HYPERTENSION IN MICE

ULRIK GEORG SVENDSEN

The University Institute for Experimental Medicine, Copenhagen, Denmark

Svendsen, U. G. Occurrence of amyloidosis secondary to the induction of experimental hypertension in mice. Acta path. microbiol. scand. Sect. A, 85: 263–266, 1977.

Following the induction of three different forms of experimental hypertension, deposits of amyloid were found in the spleens of 5–20 per cent of the mice late in the course of the hypertension. Amyloidosis was found in nude (with genetical aplasia of the thymus) as well as in haired (normal) mice. The highest frequency of amyloidosis was observed in mice with hypertension due to partial infarction of one kidney and contralateral nephrectomy. The hypertensive vascular disease, involving lesion of the vessels and of the organs supplied by the affected vessels, is believed to represent a stimulus for the reticulo-endothelial system (RES) with development of amyloidosis as a secondary event.

Key words: Amyloidosis; experimental hypertension; mice.

U. G. Svendsen, The University Institute for Experimental Medicine, Nørre Allé 71, 2100 Copenhagen Ø, Denmark.

Received 8. 76   Accepted 1.xi.76

Recent discussions concerned with the pathogenesis of amyloid have dealt primarily with immunological mechanisms and have implicated the reticulo-endothelial system (RES) as the responsible organ system (16, 17). The association of amyloid in man with a variety of chronic infectious diseases together with chemical and immunological studies in which the relation of amyloid to immunoglobulin light chains has been demonstrated, are in support of these concepts (3, 4).

Studies of rats (8, 10) and mice with experimental hypertension have suggested that immune reactions are involved in the pathogenesis of hypertensive vascular disease. It was previously reported that, following the induction of Goldblatt one-kidney hypertension, a similar and severe hypertension developed in nude and haired mice. Contrary to the thymus independence of this early phase of the hypertension, perivascular round cell infiltrations around damaged heart arteries were found to be thymus-dependent (15). A similar initial, thymus independent phase of hypertension has been demonstrated in mice with either Loomis (14) or DOCA/salt (15) hypertension. The chronic phase of the hypertension in the latter two models seemed to be dependent on the presence of thymus, since it could not be maintained in athymic mice. The occurrence in the same groups of mice of amyloidosis secondary to the induction of the three different forms of experimental hypertension is reported in the present paper.

Gudbjarnason S Acute alterations in energetics of ischemic heart muscle. Cardiology *56* 232–244 1971/72.

Gudbjarnason S Reparative processes following acute coronary artery occlusion. In *Oliver Julian Donald* (Ed.) Effect of acute ischemia on myocardial function. Churchill Livingstone 1972.

Korb G Elektronenmikroskopische Untersuchungen zur Isoproterenolschädungen des Herzmuskels. Virchows Arch. Pathol Anat. *339* 136–150 1965

Korb G Poupa O & Carlsten A. Isoproterenol induced lesions in sensitized frog heart. J Molec. Cell Cardiol *5* 313–317 1973

Moravec J & Hatt P Y Effects of isuprel on the myocardium Electron microscopic analysis. In *Lamarche M & Royer R* (Eds.) Drugs and Metabolism of Myocardium and Striated Muscle International symposium (Nancy) p 85–92 1969

Page S G & Niedergerke R Structures of physiological interest in the frog heart ventricle J Cell Sci. *11* 179–203 1972

Poupa O & Carlsten A. Experimental aneurysms of frog heart observed in vivo. In *Lamarche M & Royer R (Eds)* Drugs and Metabolism of Myocardium and Striated Muscle. International symposium, (Nancy) p. 93–98, 1969.

Poupa O & Carlsten A Isoproterenol-induced cardiac lesions in frog observed in vivo. Canad J Physiol Pharmacol. *48* 306–311 1970

Rona G Kahn D S & Chappel, G I. Study on the healing of cardiac necrosis in the rat. Amer J Pathol. *39* 473–489 1961

Sommer J R & Johnson E. A Cardiac muscle. A comparative ultrastructural study with special reference to frog and chicken hearts. Z. Zellforsch. mikr Anat *98* 437–468, 1969

Staley N A & Benson E. S The ultrastructure of frog ventricular cardiac muscle and its relationship to mechanism of excitation-contraction coupling J Cell Biol *38* 99–115 1968.

Weibel E. R Stereological principles for morphometry in electron microscopic cytology Int. Rev Cytol *26* 235–302, 1969



Fig. 1 shows deposits of amyloid in the spleen from a nude mouse with Loomis hypertension for 120 days (grade 4). 56 × VGH staining.

DISCUSSION

Amyloidosis may develop in mice with experimental hypertension and vascular disease as shown in the present study. Deposits of amyloid, if any, were found in the spleen and only once in the liver. This is in accordance with observations by others concerning the sequence of organs in mice in which amyloidosis occur (1). The development of amyloidosis in experimental hypertension combined with vascular disease and ischaemic tissue lesions is consistent with the concept advanced by *Teilum* (16, 17) concerning the "two-phase theory". According to this theory an antigenic stimulus may cause proliferation of reticulo-endothelial cells which in the first phase exhibit a strong pyroninophilia. After exhaustion (presumably a loss of their normal protein-synthesizing capacity) these cells loose their pyroninophilia and give a positive periodic acid Schiff reaction, indicating that the cells in this second stage synthesize a glycoprotein that eventually becomes amyloid. An increment of large pyroninophilic cells in the regional lymph node (9) following acute angiotensin II induced hypertension in rats strongly suggest that the vascular disease resulting from high intravascular pressure involves the reticuloendothelial system. Experimental hypertension due to infarction of the kidney ("Loomis hypertension") was found to cause amyloidosis more frequently than the two other forms of experimental hypertension. The great amount of infarcted kidney tissue might well be an extra stimulus for the RES which could explain this difference. Furthermore, only 3 out of 31 nude mice, in contrast to 11 out of 36 haired mice with "Loomis" hypertension developed amyloidosis. The observed scarcity of hypertensive vascular disease involving tissue destruction in the nude mice, in contrast to the pronounced lesions in the haired mice, might explain this difference. Thus, the possibility that thymus-derived lymphocytes might play a role in the pathogenesis of amyloidosis by secreting an "amyloid inducing factor" (16) which might seem to fit with findings in Loomis hypertensive mice is less likely however in view of the observation that amyloidosis apparently developed equally well in nude and haired mice with Goldblatt one kidney hypertension and DOCA/salt hypertension.

The author is grateful to Miss *Lisbeth Olsen* for her valuable technical assistance. The Percorten® was kindly supplied by Ciba-Geigy, Copenhagen. This work was supported by grants from the *Danish Medical Research Council* and *Ingenio Søren Alfred Andersens Foundation*, Frederikssund.

REFERENCES

1. *Christensen, H. E.:* Amyloidosestudier. En oversigt på grundlag af experimentelle undersøgelser. Copenhagen 1963.
2. *Christensen, H. E. & Hjort, G. H.:* X-irradiation as accelerating factor in caseinate induced amyloidosis in mice. Acta path. microbiol. scand. *47*, 140–152, 1959.

MATERIAL AND METHODS

Animals Outbred NMRI mice (SPF Gl Bomholtgård Ltd., Ry Denmark) 20-25 g 6-7 weeks of age received tetracycline (Tetracyclin Novo Vet. 100 mg/l) in the drinking water Nude mice carrying the mutant allele (nu/nu) and with congenital aplasia of the thymus and no or almost no thymus-derived lymphocytes, as estimated according to functional as well as histological criteria (for literature see 11 12) and their haired litter mates (Nu/+) were used Almost equal amounts of males and females were used the sex being of no importance for the results.

The animals were divided into 4 groups.

Group I (Controls) 20 nude and 20 haired untouched mice 3-6 months of age

Group II (Goldblatt one kidney hypertensive) 31 haired and 30 nude unilaterally nephrectomized mice with 0 10 mm (internal diameter) clips on their remaining renal artery The kidney was placed subcutaneously (5) Most animals were investigated around day 10-15 or at signs of sickness (thin apathetic hunchbacked and with forced respiration)

Group III (Loomis hypertensive) 36 haired and 31 nude unilaterally nephrectomized mice in which the left kidney was partly infarcted by ligation of the anterior branch of the renal artery and placed subcutaneously (7) Randomly selected groups of mice were investigated after 5 15 30 60 90 and 120 days.

Group IV (DOCA and salt hypertensive) 41 haired and 41 nude unilaterally nephrectomized mice received 1 per cent saline as drinking water and 6 mg DOCA (desoxycorticosterone acetate Percorten® microcrystalline Ciba-Geigy) was applied subcutaneously once a week. Randomly selected mice were investigated after 21 57 and 78 days of treatment The further treatment was the same in all groups Prior to sacrifice systemic arterial pressures in the conscious mice were recorded through a polyethylene catheter inserted in the left carotid artery during a light ether anaesthesia prior to the recording as previously described (14) Amyloid was identified by its morphology and by its birefringence with Congo red under crossed polars. It was stained orange with Congo red red with periodic Schiff (PAS) while it remained unstained with the Van Gieson Hansen (VGH) stain. The degree was evaluated in sections of the spleen using a scale ranging from 0 to 6 according to the semiquantitative method described by *Christensen & Hjort* (2)

RESULTS

Group I (control mice) The mean blood pressure was 114 ± 2 (SEM) mm Hg (range 90-140) similar in nude and haired mice. The spleen weight ranged between 60 and 200 mg *Microscopic investigation the heart, kidney pancreas liver and spleen* no vascular disease no amyloidosis.

Among the animals in groups II III and IV in which amyloidosis was found, 15 were hypertensive, i.e. blood pressure above 140 mm Hg 9 were normotensive and 3 died before the blood pressure could be recorded. The spleen had increased in size (i.e. more than 200 mg) in many mice. Any relation between the spleen weight and deposits of amyloidosis was not observed.

Group II (Goldblatt one kidney hypertensive mice) Microscopic investigation the heart kidney and pancreas no amyloidosis. Vascular disease as previously reported *The liver* in one nude mouse amyloidosis was found around a central vein. *The spleen* Two out of 31 haired mice and 4 out of 30 nude mice had amyloidosis. One haired mouse had a grade 3 and one a grade 2 amyloidosis Three nude mice had amyloidosis of grade 3 and one of grade 1

Group III (Loomis hypertensive mice) Microscopic investigation the heart kidney pancreas and liver vascular disease as previously described. No amyloidosis. *The spleen* Eleven out of 36 haired mice and 3 out of 31 nude mice had amyloidosis (Fig 1) In the group of haired mice, amyloidosis of grade 1 was found in 2 mice of grade 2 in 5 and of grade 3 in 4 mice Among the nude mice, grade 1 was found in one mouse grade 2 in one and grade 4 in one.

Group IV (DOCA and salt hypertensive mice) Microscopic investigation the heart kidney pancreas and liver vascular disease as previously described No amyloidosis. *The spleen* amyloidosis was found in 3 out of 41 haired mice and in 2 out of 41 nude mice Two haired mice had amyloidosis of grade 2 and 1 of grade 3 In the group of nude mice amyloidosis of grade 2 was found in one animal and of grade 3 in one.

Acta path. microbiol. scand. Sect. A, 85 267-269 1977

BRIEF REPORTS

PROLONGATION OF SURVIVAL OF RENAL XENOGRAFTS BY INFUSION OF DONOR BLOOD

Ejvind Kemp, Grethe Kemp, Ib Abildgaard Jacobsen and Carl Johan Lundborg

Department of Nephrology, Laboratory of Nephropathology and Institute of Pathology, Odense University Hospital

Kemp, E., Kemp, G., Abildgaard Jacobsen, I. and Lundborg, C. J. Prolongation of survival of renal xenografts by infusion of donor blood. Acta path. microbiol. scand. Sect. A, 85: 267-269, 1977.

Renal xenotransplantation between cat (donor) and rabbit (recipient) leads to hyperacute rejection and destruction of the graft in a few hours. Infusion of donor blood to the recipient prolongs the graft survival considerably.

Key words: Xenotransplantation; renal transplantation; transplant rejection.

Ejvind Kemp, Department of Nephrology, Odense University Hospital, DK 5000 Odense, Denmark.

Received 18.iii.76 Accepted 9.xii.76

Xenograft survival has been prolonged by infusion of donor blood from a rabbit to a dog in a liver transplantation system (*Olszewski* 1973).

We have examined this phenomenon in renal xenografts between the species rabbit and cat with similar results.

Material and Methods

25 renal xenotransplantations were performed. Kidneys from cats were transplanted to rabbits. The donor cat was pre-treated with chlorpromazine, heparin and furosemide before nephrectomy.

The left kidney from the donor cat was flushed with a slightly modified Collins solution immediately after removal. The kidney was then stored in a refrigerator at 4 C until implanted.

Technique of operation. Brown lop-eared rabbits of either sex weighing 2-4 kg were used as recipients.

Bilateral nephrectomy was performed through an abdominal transperitoneal midline incision from the xiphoid process to the symphysis.

The aorta and inferior vena cava were dissected between two lumbar arteries and veins, respectively, distal to the original renal vessels.

The inferior vena cava was clamped above and below between two lumbar veins with one pair of curved forceps. A 5 mm incision was made on the front side of the vein and the graft vein was anastomosed end to side with continuous 8-0 nylon. The aorta was then clamped in the same manner as the vein and opened by removing an ellipsoid patch (2×1 mm) immediately distal to the venous anastomosis. End to side anastomosis of the graft artery was subsequently performed with continuous 8-0 nylon.

The ureter was left free in the abdominal cavity and the abdominal wall was stitched in layers with continuous 3-0 silk.

Group I (18 experiments) served as a control group. In group II (7 experiments) injections of donor whole-blood were given intravenously in quantities of 10 ml at a time immediately before and after transplantation, corresponding to a total of 30-40 ml.

After 8 or 24 hours the animals were killed and autopsy was performed, including removal of graft tissue for histology.

Pathological Findings

Microscopy was performed without prior knowledge of the treatment of the animals.

3 *Franklin E. C & Zucker Franklin D* Current concepts of Amyloid Advances in Immunology *15* 249–304 1972
4 *Glenner G G & Page D L* Amyloid amyloidosis, and Amyloidogenesis. In *Richter G H & Epstein M* (eds.) International Review of Experimental Pathology Vol. 15 Academic Press New York 1976 p 1–92
5 *Goldblatt H Lynch J Hanzal R F & Summerville H H* Studies on experimental hypertension. I The production of persistent elevation of systolic blood pressure by means of renal ischaemia J Exp Med. *59* 347–379 1934
6 *Hardt F & Ranlov P* Transfer Amyloidosis. Israel J Med Sci. *9* 862–867 1973
7 *Loomis D* Hypertension and necrotizing arteritis in the rat following renal infarction Arch Path *41* 231–268 1946
8 *Okuda T & Grollman A* Passive transfer of autoimmune induced hypertension in the rat by lymph node cells Texas Rep Biol Med. *25* 257–264 1967
9 *Olsen F* Lysosomes and pyroninophilia in mononuclear cells in hypertensive arterioles. Acta path microbiol. scand Sect A *78* 443–450 1970
10 *Olsen F* Inflammatory cellular reaction in hypertensive vascular disease. *Munksgaard*, Copenhagen 1971
11 *Raff M C* 0-bearing lymphocytes in nude mice Nature *246* 350–351 1973
12. *Rygaard J & Poulsen C O (eds.)* Proceedings of the First International Workshop in Nude Mice Gustav Fisher Verlag Stuttgart 1974
13 *Svendsen U G* Studies elucidating the importance of thymus on the degree of increased blood pressure and vascular disease in renal hypertensive mice. Acta path. microbiol. scand. Sect. A *83* 568–572, 1975
14 *Svendsen U G* The role of thymus for the development and prognosis of hypertension and hypertensive vascular disease in mice following renal infarction. Acta path. microbiol. scand. Sect. A, *84* 235–243 1976.
15 *Svendsen U G* Evidence for an initial, thymus independent and a chronic, thymus dependent phase of DOCA and salt hypertension in mice. Acta path. microbiol. scand. Sect A, *84* 523–528, 1976
16 *Teilum G* Pathogenesis of amyloidosis. The two-phase cellular theory of local secretion. Acta path. microbiol scand. *61* 21–45 1964a.
17 *Teilum G* Origin of amyloidosis from PAS-positive reticuloendothelial cells in situ and basic factors in pathogenesis. In *Mandema E. Ruinen L. Scholten J H & Cohen A S* (eds.) Proceedings of the symposium of amyloidosis. Groningen, September 1967 Excerpta *Medica Amsterdam.*

Acta path. microbiol. scand. Sect. A, 85: 267–269, 1977

BRIEF REPORTS

PROLONGATION OF SURVIVAL OF RENAL XENOGRAFTS BY INFUSION OF DONOR BLOOD

Ejvind Kemp, Grethe Kemp, Ib Abildgaard Jacobsen and Carl Johan Lundborg

Department of Nephrology, Laboratory of Nephropathology and Institute of Pathology, Odense University Hospital

Kemp, E., Kemp, G., Abildgaard Jacobsen, I. and Lundborg, C. J. Prolongation of survival of renal xenografts by infusion of donor blood. Acta path. microbiol. scand. Sect. A, 85: 267–269, 1977.

Renal xenotransplantation between cat (donor) and rabbit (recipient) leads to hyperacute rejection and destruction of the graft in a few hours. Infusion of donor blood to the recipient prolongs the graft survival considerably.

Key words: Xenotransplantation; renal transplantation; transplant rejection.

Ejvind Kemp, Department of Nephrology, Odense University Hospital, DK-5000 Odense, Denmark.

Received 16.xi.76. Accepted 9.xii.76.

Xenograft survival has been prolonged by infusion of donor blood from rabbit to a dog in a liver transplantation system (Olszewski 1973).

We have examined this phenomenon in renal xenografts between the species rabbit and cat with similar result.

Material and Methods

25 renal xenotransplantations were performed. Kidneys from cats were transplanted to rabbits. The donor cat was pre-treated with chlorpromazine, heparin and furosemide before nephrectomy.

The left kidney from the donor cat was flushed with slightly modified Collins solution immediately after removal. The kidney was then stored in refrigerator at 4 C until implanted.

Technique of operation. Brown lop-eared rabbits of either sex weighing 2–4 kg were used as recipients.

Bilateral nephrectomy was performed through an abdominal transperitoneal midline incision from the xiphoid process to the symphysis.

The aorta and inferior vena cava were dissected between two lumbar arteries and veins, respectively distal to the original renal vessels.

The inferior vena cava was clamped above and below between two lumbar veins with one pair of curved forceps. A 5 mm incision was made on the front side of the vein and the graft vein was anastomosed end to side with continuous 8-0 nylon. The aorta was then clamped in the same manner as the vein and opened by removing an elipsoid patch (2×1 mm) immediately distal to the venous anastomosis. End to side anastomosis of the graft artery was subsequently performed with continuous 8-0 nylon.

The ureter was left free in the abdominal cavity and the abdominal wall was sutched in layers with continuous 3-0 silk.

Group I (18 experiments) served as a control group. In group II (7 experiments) injections of donor whole-blood were given intravenously in quantities of 10 ml at time immediately before and after transplantation, corresponding to a total of 30–40 ml.

After 8 or 24 hours the animals were killed and autopsy was performed, including removal of graft tissue for histology.

Pathological Findings

Microscopy was performed without prior knowledge of the treatment of the animals.

3 *Franklin F C & Zucker-Franklin D* Current concepts of Amyloid Advances in Immunology *15* 249–304 1972.

4 *Glenner G G & Page D L* Amyloid *amyloidosis, and Amyloidogenesis In Richter G W & Epstein M* (eds.) International Review of Experimental Pathology Vol. 15 Academic Press, New York 1976 p 1–92

5 *Goldblatt H Lynch J Hanzal R F & Summerville W W* Studies on experimental hypertension. I The production of persistent elevation of systolic blood pressure by means of renal ischaemia. J Exp Med. *59* 347–379 1934

6 *Hardt F & Ranløv P* Transfer Amyloidosis. Israel J Med Sci *9* 862–867 1973

7 *Loomis D* Hypertension and necrotizing arteritis in the rat following renal infarction Arch Path *41* 231–268, 1946

8 *Okuda T & Grollman A* Passive transfer of autoimmune induced hypertension in the rat by lymph node cells Texas Rep Biol Med. *25* 257–264 1967

9 *Olsen F* Lysosomes and pyroninophilia in mononuclear cells in hypertensive arterioles. Acta path microbiol. scand Sect A *78* 445–450 1970

10 *Olsen F* Inflammatory cellular reaction in hypertensive vascular disease Munksgaard Copenhagen 1971

11 *Raff M C* θ-bearing lymphocytes in nude mice. Nature *246* 350 351 1973

12 *Rygaard J & Poulsen C O (eds.)* Proceedings of the First International Workshop in Nude Mice. Gustav Fisher Verlag, Stuttgart 1974

13 *Svendsen U G* Studies elucidating the importance of thymus on the degree of increased blood pressure and vascular disease in renal hypertensive mice Acta path. microbiol. scand. Sect. A *83* 568–572 1975

14 *Svendsen U G*. The role of thymus for the development and prognosis of hypertension and hypertensive vascular disease in mice following renal infarction. Acta path. microbiol scand Sect. A, *84* 235–243 1976.

15 *Svendsen U G* Evidence for an initial, thymus independent and a chronic, thymus dependent phase of DOCA and salt hypertension in mice. Acta path. microbiol. scand. Sect. A, *84* 523–528, 1976

16 *Teilum G* Pathogenesis of amyloidosis The two-phase cellular theory of local secretion. Acta path. microbiol. scand. *61* 21–45, 1964a.

17 *Teilum G* Origin of amyloidosis from PAS-positive reticuloendothelial cells in situ and basic factors in pathogenesis. In *Mandema E. Ruinen L. Scholten J H & Cohen A S (eds.)* *Proceedings of the symposium of amyloidosis* Groningen, September 1967 Excerpta Medica Amsterdam.

interstitium, glomeruli and blood vessels was present.
Fig. 2 shows a picture from this group.

Comments

We are unaware of previous reports of renal xenotransplantation between the species cat and rabbit, but the model described here is suitable for the study of xenotransplantation in smaller animals.

Disseminated microthrombosis could not be demonstrated, but otherwise we consider the reaction to correspond to the descriptions of hyperacute allograft rejection phenomena (*Kissmeyer-Nielsen* et al. 1966, *Starzl et al.* 1974). The disseminated microthrombosis has been described in other xenograft models, and we were also able to demonstrate this phenomenon in other xenograft experiments made by our group. In the present series both species differences and differences in fibrinolytic activity in various xenografts may explain the discrepancy.

A delay observed in the onset of the xenograft rejection after infusion of a rather large quantity of blood from donor to recipient was found in experiments with erythrocyte stroma used for "trapping" the antibodies in the serum of the recipient (*Lien et al.* 1968). That infusion of donor blood has a similar effect is demonstrated from our experiments and those of *Olszewski and Lukasiewicz* (1973). The explanation might probably be that antigens on erythrocytes bind a great number of the recipient, naturally occurring, preformed serum antibodies against foreign tissue.

Renal xenotransplantation with a donor rabbit kidney to a recipient cat leads usually to rejection of the former in 5–15 minutes. The rejection seen in this situation can be prevented or delayed for hours by infusion of anti-cat-serum produced by immunization of ducks with serum from cat (*Kemp et al.* 1976). The delay is probably due also in these experiments to removal of preformed antibodies from the serum of the recipient.

Conclusions

A renal xenograft model with cat as donor and rabbit as recipient was carried out and found suitable for the study of xenograft rejection. Usually rejection starts shortly after transplantation and the organ is almost totally destroyed within a few hours. However, in the present paper it has been demonstrated that the rejection can be delayed by infusion of donor blood to the recipient.

References: Kemp E., Kemp G., Scendien P., Nielsen E., Buhl M R., Jacobsen I A & Lundborg C J., Acta path. microbiol. scand. Sect. C, *84* 342-344 1976.—*Kissmeyer-Nielsen F., Olsen S., Petersen V P & Fjeldborg, O.* The Lancet Sept. 24 662–665, 1966.—*Lien, B. S., Jensen J A., Portal P & Snyder G B.*, Journal of Surgical Research *8* 211-215 1968.—*Olszewski, W & Lukasiewicz, H.*, Acta Med. Pol. *14* 131–138 1973.—*Starzl, T E., Porter K. A., Husberg B S., Ishikawa, M & Putnam, C W.*, Current Problems in Surgery. Renal Homotransplantation, part II p. 28–30 1974



Fig 1 Kidney from group I with necrosis of tubuli and the glomerulus. Severe oedema and haemorrhage Sirius red stain. ×128.



Fig 2 Kidney from group II Necrosis of the tubular epithelium. The glomerulus and interstitium are essential normal. Sirius red stain. ×128

Group I (18 grafts)

Renal tissue with recognisable cortex and medulla were fixed in 10 per cent buffered formalin Sections were stained with Hæmatoxylin-eosin, PAS and Sirius, PTAH and Lendrum for fibrin For plasma cells the Unna Pappenheim method was used

Macroscopically we found that two kidneys were pale while the others were red in colour The consistency was soft some almost liquefying However the cortex and medulla could be distinguished.

Clots or thrombi were seen in the extrarenal vessels, generally in the veins.

Microscopy revealed total necrosis of both cortex and medulla Leucocytes or thrombi were not seen in the glomeruli In the arcuate and in some of the interlobular arteries thrombi could be seen In all the grafts severe oedema and haemorrhage were found In the grafts small foci of lymfocytes could be demonstrated Neutrophilic cells were seen in three grafts and pyrinophilic cells in two grafts.

In several of the grafts, the structure was severely disturbed Basement membranes of the tubuli, the walls of the arterioles and arteries and the tuft were ruptured.

Fig 1 shows a picture from group I

Group II (7 grafts)

A) In four grafts the same morphological changes as described in group I were seen.

B) The remaining three grafts were essentially normal macroscopically In two, the extrarenal vessels were patent. However one graft showed thrombosis in the renal vein and artery

Microscopy showed nearly normal glomeruli. The tubuli revealed some cytoplasmic degenerative vacuolisation and necrosis of the epithelial lining cells. Besides slight interstitial oedema perivascular and focal infiltration of small lymfocytes and some pyroninophylic cells were present. There was no vasculitis or thrombosis.

Infiltration of eosinophilic granulocytes in the

TABLE 1 *Labelling Indices in Human Psoriatic Epidermal Cells Cultured in Diffusion Chambers in Diffusion Chambers in Control and Interferon-Treated Mice (N = Number of Cultures)*

Exp.	*Group*	*N*	Dose in units	Amount of protein injected (mg)	Human psoriatic skin Labelling index (mean ± SD)
A	Control	9	–	–	7.8 ± 2.5
	Interferon	10	10^4	1.0	12.7 ± 6.4
B	Control	8	–	–	9.6 ± 6.0
	Interferon	9	10^4	2.4	13.3 ± 2.2
C	Control	4	–	–	10.6 ± 2.2
	Interferon	5	3×10^4	3.0	10.0 ± 2.7
	Mock-interferon	4	3×10^4	3.0	10.3 ± 2.5

of partially purified human leucocyte interferon (P.IF) kindly supplied by Prof. K. Cantell (prepared as described by Cantell et al. (4)) with a specific activity of 10^4 units/mg protein, dissolved in 1.0 ml of phosphate buffered saline were injected intraperitoneally into the experimental mice. In experiment B 10^4 units of P.IF with a specific activity of 0.42×10^4 units/mg protein, dissolved in 0.5 ml of phosphate buffered saline were used. The control animal received the corresponding amount of phosphate buffered saline. In experiment C, the animals were divided into three groups. A part of the experimental mice received 3×10^4 units of P.IF (spec. act. 10^4 units/mg protein) dissolved in 0.5 ml of phosphate buffered saline. The other group of animals were given the same amount of mock interferon which was prepared like P.IF but without the induction by the Sendai virus (1). The control animals were treated as in experiments A and B. The injections were started on the operation day and continued daily for a period of five days.

One hour before killing, 20 μCi of ^{3}H-thymidine (methyl-^{3}H, spec. act. > 10 Ci/mmol, The Radiochemical Centre, Amersham, England) was injected into each animal intraperitoneally. The animals were killed on the fifth day after the operation and the chambers were recovered. The samples of psoriatic skin were fixed in 10 per cent neutral formalin, processed by the usual techniques, sectioned at 4 μ, and covered by stripping film (Kodak AR 10). The exposure time was five days. The samples were stained with Harris hematoxylin.

Labelling indices for the epidermal cells were determined from the autoradiograms (identity sealed) by counting 100 epidermal cells in the three lowest layers of the epidermis at the cut edges of each explant: a total of 1000 epidermal cells was scored from each piece of skin. Cells with five or more grains were recorded as positive; the background was usually less than one grain per cell and the average grain count was about 30.

RESULTS

The labelling indices for the psoriatic skin cultured in the control and interferon-treated animals are given in Table 1. Human leucocyte interferon did not suppress DNA synthesis in human epidermal cells derived from psoriatic skin in any of these experiments; on the contrary, in experiments A and B DNA synthesis appeared to be stimulated (63 per cent and 38 per cent, P<0.05 and P<0.1 respectively). In experiment C where mock interferon was used as an additional control, no differences were seen between the groups.

DISCUSSION

The nature of the modest stimulatory effect of human leucocyte interferon on human epidermal cells seen in two of the three experiments remains obscure. It is clearly not associated with the amount of interferon injected or with the protein content of the preparations. The amount of injected protein was greater in experiment B than in experiment A (2.4 mg and 1.0 mg protein per injection, respectively) but the stimulation was smaller. In experiment C the amount of both interferon and injected protein were greater than in the other experiments, but neither stimulatory nor inhibitory effects were seen. In any case, it is clear that human leucocyte interferon does not inhibit DNA synthesis in human epidermal cells cultured for five days in diffusion chambers.

The interferon concentration and the rate of cell growth in the culture seem to be important in demonstrating the inhibitory effect of interferon (13). A single intramuscular or subcutaneous injection of 2.3×10^4 units of interferon per kg of body weight into a mouse maintains a fairly constant level of 100 units per ml of serum for about 12 hrs (4). Accordingly the 100–300 times greater interferon amount used in the present study (10

Acta path microbiol scand. Sect. A, 85 270-272 1977

EFFECT OF HUMAN LEUCOCYTE INTERFERON ON DNA SYNTHESIS IN HUHAN PSORIATIC SKIN CULTURED IN DIFFUSION CHAMBERS

Arja Leena Karniemi

Second Department of Pathology University of Helsinki and Department of Dermatology University Central Hospital Helsinki Finland

Karniemi, Arja Leena Effect of human leucocyte interferon on DNA synthesis in human psoriatic skin cultured in diffusion chambers. Acta path microbiol. scand. Sect. A, 85 270-272 1977

Pieces of human psoriatic skin were cultured for five days in diffusion chambers implanted intraperitoneally in mice Partially purified human leucocyte interferon was injected into the experimental animals daily during the culture period Phosphate buffered saline and, in one experiment, also mock interferon were used as control materials. On the fifth day incorporation of ^3H thymidine into the epidermal cells was studied autoradiographically The results showed that human leucocyte interferon does not depress DNA synthesis in human psoriatic epidermal cells cultured by this method. In fact DNA synthesis seemed to be stimulated in two of the three experiments but the effect was not statistically significant.

Key words Interferon human epidermal cells psoriasis diffusion chamber culture.

Arja-Leena Karniemi Second Department of Pathology University of Helsinki, Haartmaninkatu 3 SF-00290 Helsinki 29 Finland.

Received 1.xii.76 Accepted 30.xii.76

Interferons are glycoproteins which are produced by vertebrate cells in response to virus infection and many other stimuli. They inhibit the multiplication of all known animal viruses and exert a number of the other biological effects (9) For example they inhibit the growth of homologous "normal" and tumour cells in culture and tumour growth *in vivo* (7 8) The antiviral activity cannot be separated from the growth inhibitory effect (11) the mechanism of this effect is unknown.

The cell growth inhibitory effect of interferon has led to attempts to use interferon preparations in the treatment of human malignancies (15) Theoretically interferon could also be effective in other hyperproliferative diseases, such as psoriasis. Following this assumption, the aim of the present study was to investigate whether or not human leucocyte interferon depresses DNA synthesis in human epidermal cells.

Human epidermal cells, both uninvolved and psoriatic, can be cultured in diffusion chambers carried by mice in these conditions there is no significant difference between the labelling indices in normal and psoriatic skin (10) Proliferating basal cells derived from psoriatic skin were used in this study as a target tissue to study the effects of interferon on human epidermal cells.

MATERIAL AND METHODS

Punch biopsies 2 mm in diameter were taken from five patients with histologically verified psoriasis and stored at 4 C in Hanks' solution with 100 µl/ml of penicillin and streptomycin. The diffusion chambers were made from acryl rings and Millipore filters and sterilized as described earlier (10) The skin pieces were halved. Two halves were placed in each chamber which were then implanted in the peritoneal cavity of WHt/Ht albino mice.

Three experiments (19 17 and 11 cultures, respectively) were made. In experiment A and B the animals were divided into two groups experimental and control ones. In experiment A, 10^4 units

Acta path. microbiol. scand. Sect. A, 85: 273–285, 1977

PATHOLOGY OF THE ANAL GLANDS WITH SPECIAL REFERENCE TO THEIR MUCIN HISTOCHEMISTRY

C. Fenger and M. I. Filipe

Research Department, St. Mark's Hospital, London EC1 and the Department of Histopathology Udall Street Laboratories, Westminster Medical School, London

Fenger C. & Filipe, M. I. Pathology of the anal glands with special reference to their mucin histochemistry. Acta path. microbiol. scand. Sect. A, 85: 273–285, 1977.

The anal gland pathology comprises cystic anal glands (so-called anal gland cyst hamartomas), anal gland carcinomas, and anal fistulas with or without carcinoma. The differential diagnosis of these conditions from other cysts and carcinomas of the anal region can be difficult. The authors have therefore compared conventional histology with mucin histochemistry in normal and pathological anal glands. In contrast to normal rectal mucosa the mucus of anal glands was characterized by strong PAS-reactivity that was completely abolished after periodate borohydride saponification indicating scarcity or absence of O-acylated sialic acids in the anal gland mucus. A pattern similar to this was found in one of two tumours classified histologically as anal gland carcinomas, in four of eight colloid carcinomas arising in preexisting fistulas, and in two cases of mucoepidermoid carcinoma of the anal region. The results indicate that the method in some cases may be of value in differentiating between carcinomas arising in anal gland epithelium and in rectal mucosa. The cystic anal glands showed decreased secretion but no qualitative histochemical differences from anal glands. On the basis of the patients' histories it is suggested that the so-called anal gland cyst hamartomas at least in some cases could be an inclusion cyst of anal glands on an inflammatory basis.

Key words: Anal glands; mucin; histochemistry.

C. Fenger, Patologisk afdeling 134, Hvidovre Hospital, DK 2650 Hvidovre, Denmark.

Received 20.ix.76. Accepted 18.xi.76.

ANATOMY AND HISTOLOGY

The anal intramuscular glands were first described by Gay in 1871 (15). A recent study by McColl in 1967 (17) has contributed essentially to the knowledge of the comparative anatomy and the pathology of these structures. The anal glands seem to be present in most, if not all, human beings in a number of six to twelve. They arise from the anal crypts that are lying in the transitional zone between the rectal mucosa and the anal mucosa. They extend from the crypts into the submucosa and about two thirds of them penetrate the internal sphincter to end between this and the external sphincter. The course is most often caudal, and the glands only ramify sparsely. The epithelial lining varies, often being squamous at the openings, transitional with or without cylindrical cells at the surface in the middle part and simple columnar in the deepest part. The mucous secretion is normally sparse (16, 17, 21).

times greater than the effective dose in most *in vitro* studies) should have been sufficient to induce growth inhibition

However the effect of interferon is not immediate. Although the inhibitory effect has usually been observed after 4–6 days of culture (1 13) *Cantell* (5) showed that interferon does not affect human RPMI 1196 cells derived from human leucocytes until after 10 days of culture It is possible therefore, that the culture period of five days used in the present study was not long enough to show the inhibitory effect

The cell growth inhibitory effect of interferon has mostly been demonstrated in cultures of established cell lines, malignant cells and virus transformed cells (7 8) but interferon can also affect the growth of "normal" cells (5) It appears however that "normal" cells may be less sensitive to interferon than tumour cells or established cell lines (2 6 12) *Borecky et al.* (2) found that mouse embryo cells showed enhanced sensitivity to interferon action after prolonged passage *in vitro* These authors suggested that the interferon sensitivity of the cells may reflect the "degree of transformation and thus signal surface alterations of the cells.

Electron microscopical studies show surface alterations in psoriatic epidermal cells *in vivo* (14) However it is not certain that the target cells derived from psoriatic skin remain "psoriatic" in the diffusion chamber cultures. Therefore, although human leucocyte interferon in the present study did not inhibit DNA synthesis in cultured psoriatic cells definite conclusions regarding the responsiveness of true, rapidly proliferating psoriatic cells *in vivo* are not warranted

References *Adams A Strander H & Cantell, K* J gen. Virol *28* 207–217 1975 —*Borecky L Fuchsberger N & Hajnicka V* Intervirology *3* 369–377 1974 —*Cantell K* Ann. N Y Acad. Sci. *173* 160–168 1970 —*Cantell K Hirvonen S Mogensen K E. & Pyhälä L.* In Vitro Monogr *3* 35–38 1974 —*Dahl H & Degré M.* Acta path. microbiol. scand. Sect. B, *84* 285–292, 1976 —*Gaffney E. V., Picciano P T & Grant C A.* J nat. Cancer Inst *50* 871–878, 1973 —*Gresser I* Advanc. Cancer Res. *16* 97–140 1972.—*Gresser I* Cancer in press, 1976 —*Ho M & Armstrong J A.* Ann. Rev Microbiol. 29 131 161 1975 —*Karvaniemi A L.* J invest. Derm. *63* 388–391 1974 —*Knight E.* Nature (Lond.) *262* 302 303 1976.—*Lee S H S O'Shaughnessy M V & Rozee K R* Proc. Soc. Exp Biol. Med. *139* 1438–1440 1972.—*Lindahl-Magnusson P., Leary P & Gresser I* Proc. Soc. Exp. Biol. Med. *138* 1044–1050 1971 —*Orfanos C E., Schaumburg-Lever G Mahrle G & Lever W F* Arch. Derm. *107* 38–46 1973 —*Strander H., Cantell K Ingimarsson S., Jakobsson P A Nilsonne U & Söderberg, G* J nat. Cancer Inst. in press.

TABLE 1 *Histochemical Methods to Visualise Epithelial Mucus in the Gastrointestinal Tract*

Method	Interpretation
PAS-methods Diastase-Periodic acid-Schiff (D-PAS) (Ref. nr 22)	Magenta a) all MS containing hexoses and deoxyhexoses with vicinal glycol groups b) neutral MS c) some non-sulphated acid MS (sialomucins)
Periodate-borohydride/saponification/PAS (PB/KOH/PAS) (Ref no. 7 24)	*PB* abolishes PAS reactivity of the periodateengendered aldehydes in the tissues. *KOH* removes a) 0-acyl esters from a potential vicinal glycol or b) a sialic acid residue linked glycosidically to a potential vicinal glycol group *PAS* activity after PB/KOH may indicate presence of 0-acylated sialic acids.
PB/KOH/Neuraminidase/PAS (Ref. no. 7)	Removal of most sialic acids, 0-acyl derivatives in C are resistant but become labile after KOH.
AB-methods Alcian blue pH 2.5 (AB 2.5) (Ref. no. 22)	Basophilia a) weakly sulphated MS b) carboxyl groups of sialomucins
KOH/Neuraminidase/AB pH 2.5 (Ref. no. 7)	As for KOH/Neuraminidase/PAS.
High iron-diamine-Alcian blue pH 2.5 (HID-AB) (Ref no. 29)	Brown-black sulphated MS. Basophilia non-sulphated acid MS (sialomucins)

Key MS Mucosubstances

no cyst formation or *neoplasia*. The sections of the anal glands all showed the same picture. Near the openings the gland was lined by a squamous epithelium that almost immediately was replaced by transitional epithelium. The latter showed a characteristic tendency to differentiate into cylindrical cells at the surface (Fig 1) None of the sections showed a definite muscular coat. In some of the cases the surrounding tissue presented signs of non-specific inflammation in addition to small aggregates of well-differentiated lymphocytes.

The mucus in the transitional epithelium was scanty and located at the luminal border while in the cylindrical cells it was more abundant in the supranuclear cytoplasm. In both, the secretory product showed similar histochemical characteristics (Table 2) The strong PAS-reactivity was completely abolished after PB/KOH treatment (Fig. 2 B+C) but only a slight decrease in the Alcian blue basophilia was obtained after neuraminidase digestion. The HID-AB technique revealed the presence of both sialomucins and sulphated material with predominance of the former

B Cystic Anal Glands

Six patients had cystic anal glands. Two females, aged 50 and 47 had had operations for anal fissures 4 and 1½ years earlier and at these operations posterior lumps were felt. In one of these cases the lump was excised, and the histology showed a dermoid cyst. Two males aged 37 and 41 had had operations for anal fistulas 7 and 16 years ago. No lumps were felt. One male, aged 22, had had a history of unclassified colitis, and a 51 year

PATHOLOGY

The essential pathology of the anal glands comprises anal fistulas cystic anal gland hamartomas and anal gland carcinomas. Although *anal fistulas* have been mentioned in the medical literature from ancient times – among others by *John of Arderne* about 1376 (15) – their relationship to the anal glands was first pointed out by *Chiari* in 1878 (4) In a later study by *Parks* (20) it was found that 21 of 30 consecutive cases of fistulas were manifestly caused by infected anal glands.

Cyst of various types in the tissues surrounding the anal canal have often been described. Most cysts are lined by epithelium of columnar squamous or transitional type (3 11) occasionally by a ciliated epithelium resembling the respiratory type (2 31) *Dukes* (9) in 1929 described two cases of retrorectal cyst developing after rectal surgery and regarded these as *implantation cysts Clarke* (5) in 1940 and *Pouget* (23) in 1961 advocated the term *myoepithelial hamartomas* and *Edwards* (11) in 1961 the term *cyst hamartomas*

Sixty years after the detection of the anal glands the first case of carcinoma together with an anal fistula was reported by *Rosser* (25) and three years later in 1934 he suggested the possibility of origin from an anal gland (26) Since then numerous cases of submucously located carcinomas of the anal region have been reported and their possible origin from anal glands discussed (14 19 30 32) Most of the cases have been described as carcinomas located beneath an apparently normal or slightly ulcerated mucosa

Since the anal glands are lined by epithelium of different types it is to be expected that the tumours could show varying histological appearances (6 14) A tendency towards mucinous types, nevertheless, seems to be typical for carcinomas in combination with fistulas (10 19 27) Mucoepidermoid carcinomas with possible anal gland origin have been described by *Berg* (1) and *Seidenverg & Kleinhans* (28)

Evidence of origin from anal glands by the demonstration of transition between normal anal gland epithelium and the tumour has, however, only been possible in a few cases such as the adenocarcinoma with ductlike structures presented by *Wellmann* in 1962 (30) and the colloid carcinoma presented by *Winkelmann* in 1964 (32) This is probably due to the fact that these tumours are often misdiagnosed as inflammatory lesions and not biopsied before they have reached a considerable size. During this process they will often have destroyed the gland from which they may have arisen.

In order to establish a better basis for the diagnosis of anal gland tumours (cysts, carcinomas) the authors have found it of interest to investigate the histology and the mucin pattern of the epithelium of the anal glands and neighbouring structures in normal and pathological conditions.

MATERIAL AND METHODS

The authors have investigated, both histologically and histochemically cases from the Pathology department records of St. Mark's Hospital. These include normal or slightly inflamed anal glands (four cases) cystic anal glands (six cases) possible anal gland carcinomas (two cases) carcinoma in anal fistulas (eight cases) and mucoepidermoid carcinomas (two cases) As controls for rectal mucosa and anal glands we used three surgical specimens of rectum and anal region obtained by abdomino-perineal resection for carcinoma. The tumours were located at 5 cm, 6 cm and 11 cm respectively from the anal margin The ano-rectal region of each specimen was cut into nine or ten blocks of tissue, each being 1 by 4 cm. From each tissue block 5 µ serial sections were cut from three different levels

All tissues were fixed in 10 per cent formal saline and routinely embedded in paraffin. Sections were stained by H & E and van Gieson and by various histochemical techniques to characterise epithelial mucosubstances, details of which are given in Table 1

RESULTS

A Normal Anal Glands

These include the three controls and four patients, two males and two females, aged 27–53 who had a histological diagnosis of normal or slightly inflamed anal glands with

TABLE 2. *Histochemical Characteristics of Epithelial M cins Rectal M sa and Anal Glands Normal and Disease*

Histology	D-PAS	PAS-methods PB/KOH/PAS	PB/KOH/Neur./PAS	AB 2.5	AB-methods KOH/Neur AB 2.5	HID-AB
A. *Normal A al Glands*	+ + +	0	0	+ + +	+/+ +	B + + + D +
B. *Cystic Anal Glands*	+ +/+ + +	0	0	+ +	+	B + D +
C. *P sable A al Gland Carcin mas*						
Case 1	+ +	0	0	+ +	+/+ +	D + + +
Case 2	+ +	?	?	+ +	0	B +/+ +
D. *C cinom i l al Fist as*						
Group A (4 cases)	+ + +	+ +	+ +	+ + +	+ +	B + + + D +
Group B (4 cases)	+ + +	0	0	+ + +/+ +	+ +/+	D + + + or B + + + D +
E. *M epidermoid Carci mas*	+ +	0	0	+ +	+	D + + + B +
F. *Normal Rectal M cosa and Rectal Carci om*						
Normal	+ + +	+ + +	+ +	+ + +	+ + +	B +
Adjacent to carcinoma	+ + +	+ + +	+	+ + +	+	D + + +
Adenocarcinoma	+ + +	+ +	0	+ + +	0	B + + + B + + +

Key Histochemical reactions see Table 1
D = brown colour (sulphated mucins)
B = blue colour (sialomucins)
0 to + + + = grades of staining i tensity
? = not done



Fig 1 Normal anal gland Transitional epithelium with scattered secretory cells at the surface. HE ×450.
Fig 2A Normal rectal glands showing PAS-positi e reaction after PB/KOH treatment. ×300

3

4

Fig. 3 Cystic anal gland. Transitional epithelium with secretory cells and intraepithelial microcysts. HE × 450

Fig. 4 Tumour histologically and histochemically classified as carcinoma of anal glands (case 1). Irregular tubules and disperse microcyst formation. HE × 450.

Fig 2B Normal anal glands showing a strong PAS-reaction × 300

Fig 2C Normal anal glands, PAS-reaction totally abolished after PB/KOH treatment. × 300.



Fig. 5A. Carcinoma in anal fistula, mucinous area. Group A. Strong PAS-reaction. ×180

Fig. 5B. Same carcinoma after PB/KOH treatment. PAS-reaction persists, though less intense. ×180.

old female had years ago had an anal trauma when she had fallen down from a horse

The sections of the cystic anal glands showed comparatively more glandular tissue per square unit than normal and the glands were lined by transitional epithelium of the same type as the normal glands, but typically with intraepithelial microcysts (Fig 3) Besides the cystic glands that were lined with flattened epithelium, there were normal glands lined by tall epithelium None of the sections showed evidence of recent or old bleeding and there were no signs of inflammation In none of the cases was a definite muscular coat demonstrable but some of the cystic glands were surrounded by a rather concentric condensation of fibrous tissue just beneath the epithelium

Mucous secretion was much decreased or even absent in both the transitional epithelium and the cylindrical cells in the glands as compared with the normal but no qualitative histochemical changes were noticed (Table 2)

C Possible Anal Gland Carcinomas

Two patients had a histological diagnosis of anal gland carcinoma The first patient was a 76 year old female with a history of ischio-rectal abscess 38 years ago. She presented with a moderate anal stenosis. Local excision of an indurated area between four and twelve o clock was performed. Six years after the patient is still alive, buth with signs of local recurrence.

The second patient was a 52 year old male with a history of hemorrhoids for the greater part of his life He presented with a shallow chronic ulcer of the rectum and a hard mass proximal to the ulceration covered with apparently normal mucoa. Abdomino-perineal excision with resection of hemorrhoidal and inguinal glands was performed. The patient died 3½ months later and autopsy showed metastatic deposits in the liver lungs and preaortic glands.

The histology of these two cases was rather similar Both tumours were located beneath normal rectal and anal mucosa They showed small irregular tubules lined by cuboidal to high columnar epithelium with dispersed microcyst formation (Fig. 4) The rapidly progressing tumour was the more undifferentiated. Particularly in the deeper part faintly staining cells with pleomorphic nuclei infiltrated as solid strands or diffusely In neither case a transition between normal anal glands and the tumour could be demonstrated.

Histochemically the type of mucus produced by the two tumours showed different staining properties (Table 2) In case one the mucous secretion showed characteristics similar to those observed in the normal anal glands though less intense, the PAS-activity was totally abolished by PB/KOH treatment. Neuraminidase digestion had no effect or only slightly reduced the Alcian blue basophilia However in contrast to the normal, the HID-AB technique revealed a predominance of sulphated material

The second case showed no basophilia when sections were treated with neuraminidase followed by AB pH 2.5 staining There was a predominance of sialomucins as shown by the HID AB staining

D Carcinoma in Anal Fistulas

Eight patients five males and three females, aged 45–69 years, were operated upon for a carcinoma developing in an anal fistula. All cases showed a predominantly mucinous adenocarcinoma infiltrating the smooth muscle and covered by an apparently normal mucosa with a fistulous tract. Otherwise the histology did not differ from that of a mucinous carcinoma of the rectum.

From the histochemical point of view these eight cases were divided into two groups, A and B according to the staining characteristics of their mucous secretion (Table 2)

In both groups, all cases showed intense PAS-reactivity In group A this activity was slightly reduced after PH/KOH treatment (Fig 5 A+B) and further digestion of the sections with neuraminidase did not show any effect. In group B, however saponification removed all the PAS-positive material from

the tissues (Fig. 6 A+B). While a strong basophilia with AB pH 2.5 was seen in all cases in both groups, the response to neuraminidase digestion differed. The enzymatic action was mild in group A cases and variable in group B cases where a more marked decrease in basophilia could be found. The HID-AB staining revealed mainly sialomucins mixed occasionally with sulphated material in group A sections and in three of group B cases. In the latter group, however one case contained apparently only sulphated mucins which correlated well with the greater proportion of neuraminidaseresistant basophilia observed in this case.

Generally the mucus secreted by the tumour cells had similar staining properties to the extracellular mucus. However in one of the B-cases the HID-AB technique showed tumour cells producing mainly sialomucins, while sulphated material was predominant in the extracellular mucus.

E. Mucoepidermoid Carcinomas

The mucoepidermoid carcinomas showed neoplastic squamous epithelium with formation of rather big cysts, of which many were filled with desquamated material. Other rather small, essentially intraepithelial cysts were filled with mucin-like material. This latter feature was similar to that seen in the possible anal gland carcinomas.

Histochemically the tumours showed a weak PAS-reactivity that was totally removed by saponification in combination with a moderate decrease in basophilia after neuraminidase incubation. Sulphated material was predominant as shown by HID-AB.

F. Normal Rectal Mucosa and Rectal Carcinomas

For comparison, as it may be useful for differential diagnosis, we included in *Table 2* results we obtained (to be published) using the same histochemical techniques on large intestinal mucosa from specimens resected for carcinoma. Mucins secreted by the normal rectal mucosa, the apparently normal mucosa adjacent to carcinoma and the tumour itself, despite showing similar reactions with PAS and AB pH 2.5 differed according to their staining properties after saponification and neuraminidase digestion (Fig. 2A). In the normal mucosa, neuraminidase incubation had only a slight effect on PAS-activity none on the basophilia, and the HID-AB revealed the presence of mainly sulphated mucins. In contrast, in the mucosa adjacent to carcinoma a marked decrease in PAS-activity and basophilia was induced by neuraminidase digestion which correlated well with predominance of sialomucins as shown by the HID-AB. This neuraminidase effect was even more marked in the adenocarcinoma with the total supression on PAS and AB pH 2.5 staining by saponification and enzymatic digestion.

DISCUSSION

The histological identification of normal anal glands is not difficult, and the type of mucin secreted by the glands differs, histochemically from that produced by the goblet cells in the rectal mucosa. A strong PAS-positive material is shown in both types of epithelium, but in the anal glands in contrast to the rectal mucosa the reaction is totally abolished after borohydride KOH treatment.

In paraffin-embedded material, the PAS-reaction after diastase digestion and controlled periodate oxidation, demonstrates vicinal glycols which are present only in neutral and some acid mucosubstances (containing N-acetyl and some O-acetyl derivatives of sialic acid). The reaction can be made more specific for sialic acid derivatives if the sections are treated with borohydride followed by saponification prior to PAS-staining (24). A positive PAS-reaction would then reveal the presence of O-acylated sialic acids, probably substituents at C_7 and C_8. A negative result would indicate either the presence of neutral mucins only or/and other sialic acid derivatives such as N-acetyl or O-acetyl substituents at C or C_9 (7). However to us such a fine discrimination between sialic acids is difficult

6A

6B

Fig 6A Carcinoma in anal fistula. Glandular area. Group B Strong PAS-reaction. ×180

Fig 6B Same carcinoma after PB/KOH treatment. PAS-reaction totally abolished. ×180.

the tissues (Fig 6 A+B) While a strong basophilia with AB pH 2.5 was seen in all cases in both groups, the response to neuraminidase digestion differed. The enzymatic action was mild in group A cases and variable in group B cases where a more marked decrease in basophilia could be found. The HID-AB staining revealed mainly sialomucins mixed occasionally with sulphated material in group A sections and in three of group B cases. In the latter group, however one case contained apparently only sulphated mucins which correlated well with the greater proportion of neuraminidaseresistant basophilia observed in this case

Generally the mucus secreted by the tumour cells had similar staining properties to the extracellular mucus. However in one of the B-cases the HID-AB technique showed tumour cells producing mainly sialomucins, while sulphated material was predominant in the extracellular mucus.

E. Mucoepidermoid Carcinomas

The mucoepidermoid carcinomas showed neoplastic squamous epithelium with formation of rather big cysts, of which many were filled with desquamated material. Other rather small, essentially intraepithelial cysts were filled with mucin-like material. This latter feature was similar to that seen in the possible anal gland carcinomas.

Histochemically the tumours showed a weak PAS-reactivity that was totally removed by saponification in combination with a moderate decrease in basophilia after neuraminidase incubation. Sulphated material was predominant as shown by HID-AB.

F Normal Rectal Mucosa and Rectal Carcinomas

For comparison, as it may be useful for differential diagnosis, we included in *Table 2* results we obtained (to be published) using the same histochemical techniques on large intestinal mucosa from specimens resected for carcinoma. Mucins secreted by the normal rectal mucosa, the apparently normal mucosa adjacent to carcinoma and the tumour itself despite showing similar reactions with PAS and AB pH 2.5 differed according to their staining properties after saponification and neuraminidase digestion (Fig 2A) In the normal mucosa, neuraminidase incubation had only a slight effect on PAS-activity none on the basophilia, and the HID-AB revealed the presence of mainly sulphated mucins. In contrast, in the mucosa adjacent to carcinoma, a marked decrease in PAS-activity and basophilia was induced by neuraminidase digestion which correlated well with predominance of sialomucins as shown by the HID-AB This neuraminidase effect was even more marked in the adenocarcinoma with the total supression on PAS and AB pH 2.5 staining by saponification and enzmatic digestion.

DISCUSSION

The histological identification of normal anal glands is not difficult, and the type of mucin secreted by the glands differs, histochemically from that produced by the goblet cells in the rectal mucosa. A strong PAS-positive material is shown in both types of epithelium, but in the anal glands in contrast to the rectal mucosa the reaction is totally abolished after borohydride-KOH treatment.

In paraffin-embedded material, the PAS-reaction after diastase digestion and controlled periodate oxidation, demonstrates vicinal glycols which are present only in neutral and some acid mucosubstances (containing N acetyl and some O-acetyl derivatives of sialic acid) The reaction can be made more specific for sialic acid derivatives if the sections are treated with borohydride followed by saponification prior to PAS-staining (24) A positive PAS-reaction would then reveal the precense of O-acylated sialic acids, probably substituents at C_7 and C_8. A negative result would indicate either the presence of neutral mucins only or/and other sialic acid derivatives such as N-acetyl or O-acetyl substituents at C or C_9 (7) However to us such a fine discrimination between sialic acids is difficult

6A

6B

Fig 6A Carcinoma in anal fistula. Glandular area. Group B. Strong PAS-reaction. × 180

Fig 6B Same carcinoma after PB/KOH treatment PAS-reaction totally abolished. × 180

REFERENCES

1. Berg, J W Lone F & Stearns J M W., Mucoepidermoid anal cancer Cancer 13 914–916, 1960
2. Bonser G M., Raper F P & Schucksmith H S Epidermoid cysts in the region of the rectum and anus. Brit. J Surg. 37 303–306, 1950
3. Campbell, W L. & Wolff Marianne Retrorectal cysts of developmental origin. Am. J Roentgenol. Radium Ther Nucl. Med. 117 307–313 1973
4. Chiari, H Über die Analen Divertikel der Rectumschleimhaut und ihre Bedeutung Med. Jahrb Wien 419 1878.
5. Clarke B. E., Myoepithelial hamartoma of the gastrointestinal tract. Report of eight cases with comment concerning genesis and nomenclature. Arch. Pathol. 30 143–152, 1940.
6. Close A S & Schwab R L., History of the anal ducts and anal-duct carcinoma Report of a case Cancer 8 979–983 1955.
7. Culling C F A., Reid P E Clay M G & Dunn W L. The histochemical demonstration of 0-acylated sialic acid in gastrointestinal mucins. Their association with the potassium hydroxide-periodic acid-Schiff effect. J Histochem. Cytochem. 22 826–831 1974
8. Culling, C F A Reid P E., Burton J D & Dunn, W L., A histochemical method of differentiating lower gastrointestinal tract mucin from the mucins in primary and metastatic tumours. J Clin. Pathol. 28 656–658, 1975
9. Dukes C E., Submucous implantation cysts of the rectum. Proc. R. Soc. Med. 22 715–718, 1929
10. Dukes C. E. & Galton C., Colloid carcinoma arising within fistulae in the ano-rectal region. Ann. R. Coll Surg. Engl. 18 246–261 1956
11. Edwards, M Multilocular retrorectal cystic disease – cyst-hamartoma Report of twelve cases. Dis Colon Rectum 4 103–110, 1961
12. Filipe M I & Branfoot A C Mucin histochemistry of the colon. I Current Topics in Pathology Vol. 63 Pathology of the Gastrointestinal Tract. Ed. B. C. Morson. Springer Verlag, Berlin, Heidelberg & New York, 1976
13. Gay A. Die Circumanaldrüsen des Menschen. A B-Akad Wiss Wien Math-nat. Kl. 63 329 1871
14. Grinvalsky H T & Helwig, E B. Carcinoma of the perianal ducts Abstract. Am. J Pathol. 29 610, 1953.
15. John of Arderne (c. 1376) Treatises of fistula in ano, haemorrhoids and clysters. Ed. by sir D'Arcy Power Kegan Paul, London, 1910
16. Kratzer G L & Dockerty M B., Histopathology of the anal ducts. Surg. Gynecol. Obstet. 84 333–338, 1947
17. McColl, I., The comparative anatomy and pathology of anal glands. Ann. R. Coll. Surg. Engl. 40 36–67 1967
18. Morson B. C & Volkstädt H., Muco-epidermoid tumours of the anal canal. J Clin. Pathol. 16 200–205 1963
19. Nielsen O V & Koch F., Carcinomas of the anorectal region of extramucosal origin with special references to the anal ducts. Acta Chir Scand. 139 299–303, 1973
20. Parks A. G., Pathogenesis and treatment of fistula-in-ano. Br Med. J 1 463–469 1961
21. Parks A G Modern concepts of the anatomy of the anorectal region. Postgrad. Med. J 34 360–366 1958.
22. Pearse A G E., In "Histochemistry – theoretical and applied" 3. ed., vol. 1 J A. Churchill Ltd., London, 1968.
23. Pesget R R & Bacon, H E Myoepithelial hamartoma of the rectum. Dis. Colon Rectum 4 409–412, 1961
24. Reid P E., Culling, C F A & Dunn, W L., Saponification-induced increase in the periodic acid-Schiff reaction in the gastrointestinal tract. Mechanism and distribution of the reactive substance. J Histochem. Cytochem. 21 473–482, 1973
25. Rosser C., The etiology of anal cancer Am. J Surg. 11 328–333 1931
26. Rosser C., The relation of fistula in ano to cancer of the anal canal. Tr Am. Proct. Soc. 35: 65–71 1934
27. Rundle F F & Hales I B.: Mucoid carcinoma supervening on fistula-in-ano. Ann. Surg. 137: 215–219 1953
28. Seldenrijk, V & Kleinkens, R. J.: Mucoepidermoid carcinoma of the anus. Am. J Surg. 117: 413–415 1969
29. Spicer S S Diamine methods for differentiating mucosubstances histochemically J Histochem. Cytochem. 13 211–234 1965
30. Wellman K F., Adenocarcinoma of anal duct origin. Can. J Surg. 5 311–318 1962.
31. Wilson, E., Rectal Cyst. Aust. NZ. J Surg. 34 32–35 1964
32. Winkelman J., Grosfeld J & Bigelow B Colloid carcinoma of anal-gland origin Report of a case and review of the literature. Am. J Clin. Pathol. 42 395–401 1964
33. Wood W S & Culling C F A Perianal Paget disease. Histochemical differentiation utilizing the borohydride-KOH PAS reaction. Arch. Pathol. 99 442–445 1975

to assess, as we know that the epithelial mucins are complex glycoproteins containing a mixture of N acetyl and O acetyl sialic acids and ester sulphates in variable proportions (12)

The fact remains, however that the goblet cell mucin in the normal rectal mucosa and in carcinoma show the KOH/PAS effect in contrast to the anal glands which are negative thus establishing a basis for the identification of the origin of neoplastic tumours of the anal region. Similar results have been reported by *Wood & Culling* (33) in a study of perianal Paget disease. On the other hand the basophilia shown by Alcian blue pH 2.5 staining is often decreased but never abolished by neuraminidase digestion thus confirming the presence of sialomucins as well as sulphated material in the anal glands which is further confirmed by the HID AB technique.

The histological picture was rather similar in the two possible cases of anal gland carcinoma The histochemical investigation however showed different characteristics which raises the possibility of their arising from different sources. The first tumour had staining properties similar to those of the anal glands, particularly the negative PAS-reactions after saponification In the second, less differentiated tumour the material was insufficient to carry out the PB/KOH/PAS reactions. However the effect of the neuraminidase on the basophilia with the AB 2 5 and the HID-AB revealed the presence mainly of neuraminidase-sensitive sialic acids, suggesting an origin from the rectal mucosa rather than from the anal glands.

Similarly two histochemically distinct types were apparent in the group of carcinomas associated with fistulas although the histology showed colloid carcinomas in all cases. Group B tumours showed staining reactions like those of the anal glands and are therefore likely to have arisen in that type of epithelium while group A tumours showed the KOH/PAS effect which only occurs in the colonic and rectal mucins (8) Since these patients all had a diagnosis of anal fistulas previous to the development of carcinoma, it seems possible that the fistulas could be of different origin (i e. from anal glands and from rectal mucosa)

The two cases of mucoepidermoid carcinomas showed the histological picture described by *Morson* and *Volkstadt* (18) The histochemical reactions were like those of the anal glands, the first case of anal gland carcinoma and group B of the carcinomas in fistulas, thus suggesting an origin from anal glands.

Our data reveal differences in the composition of mucins secreted by the anal glands and the rectal mucosa. These are essentially a predominance of O-acylated sialic acids in the rectal mucosa as compared to scarcity or absence in the anal glands. These variations in carbohydrate content can be readily demonstrated by the borohydride-saponification-PAS sequence which seems a useful technique to assist in the differential diagnoses of some pathological conditions of the anal region. On the other hand the Alcian blue pH 2.5 with and without neuraminidase digestion and the HID-AB methods have apparently very little or no diagnostic value in the material examined

In addition the technique confirms that the so-called cystic anal gland hamartoma is of anal gland origin. The histories of our patients showed anal operations, inflammations and trauma features often reported in the literature. Thus, *Duke's* two cases (9) three out of *Campbell's* four cases (3) seven out of *Edward's* ten cases (11) and *Wilson's* case (31) have all been found in patients who had had previous treatment, – often surgical – for anal fistulas, fissures, abscesses or hemorrhoids. This makes us suggest that these cysts – at least in some cases – should be considered as inclusion cysts rather than hamartomas.

Our thanks are due to Dr *B C Morson* for his inspiring interest and to Mr *J Patel* for his excellent technical assistance. This work was supported in part by a grant from the *cancer research campaign* (United Kingdom) to one of us (MIF) and carried out during a fellowship from the *European Council* for the other (CF)

REFERENCES

1 *Berg J W., Lone F & Stearns J., M W* Mucoepidermoid anal cancer Cancer *13* 914 916, 1960

2 *Bauer G M Raper F P & S huckwith, H S.*, Epidermoid cysts in the region of the rectum and anus. Brit. J Surg *37* 303–306, 1950.

3 *Campbell, W L. & Wolff Marianne* Retrorectal cysts of developmental origin. Am. J Roentgenol. Radium Ther Nucl. Med. *117* 307–313, 1973.

4 *Chiari H.:* Über die Analen Divertikel der Rectumschleimhaut und ihre Bedeutung Med. Jahrb. Wien 419 1878.

5 Clarke B. E.. Myoepithelial hamartoma of the gastrointestinal tract Report of eight cases with comment concerning genesis and nomenclature Arch. Pathol. *30* 143–152, 1940

6 *Close A. S & Schwab R. L.* History of the anal ducts and anal-duct carcinoma Report of a case. Cancer *8* 979–983 1955.

7 *Culling, C F A Reid P E Clay M G & Dunn W L.* The histochemical demonstration of 0-acylated sialic acid in gastrointestinal mucins. Their association with the potassium hydroxide-periodic acid-Schiff effect. J Histochem Cytochem. *22* 826–831 1974

8. *C lling, C F A Reid P E., Burton J D & Dunn, W L..* A histochemical method of differentiating lower gastrointestinal tract mucin from the mucins in primary and metastatic tumours. J Clin. Pathol. *28* 656–658, 1975

9 D k r C E.. Submucous implantation cysts of the rectum. Proc R. Soc. Med. *22* 715–718, 1929

10. *Dukes C E. & Galvin C* Colloid carcinoma arising w thin fistulae in the ano-rectal region. Ann. R. Coll Surg. Engl. *18* 246–261 1956

11 *Edwards, M* Multilocular retrorectal cystic disease – cyst-hamartoma Report of twelve cases. Dis Colon Rectum *4* 103–110, 1961

12 *Filipe M I & B anfoot A. C* Mucin histochemistry of the colon. I Current Topics in Pathology Vol 63 Pathology of the Gastrointestinal Tract. Ed. B. C. Morson. Springer Verlag, Berlin, Heidelberg & New York, 1976.

13 *Gay A* Die Circumanaldrusen des Menschen. A B -Akad Wiss Wien. Math-nat. Kl. *63* 329 1871

14 *Gnaccisky H T & Helwig, E B.* Carcinoma of the perianal ducts Abstract. Am. J Pathol. *29* 610, 1953

15 *John of Arderne* (c. 1376) Treatises of fistula in ano haemorrhoids and clysters. Ed. by sir D'Arcy Power Kegan Paul, London, 1910.

16. *Kratzer G L. & Dockerty M B..* Histopathology of the anal ducts. Surg. Gynecol. Obstet. *84* 333–338, 1947

17 *McColl I* The comparative anatomy and pathology of anal glands. Ann. R. Coll. Surg Engl. *40* 36–67 1967

18 *Morson, B. C & Volkstädt H..* Muco-epidermoid tumours of the anal canal. J Clin. Pathol. *16* 200–205 1963

19 *Nielsen O V & Koch F..* Carcinomas of the anorectal region of extramucosal origin with speciel references to the anal ducts. Acta Chir Scand. *139* 299–305 1973

20. *Parks A G..* Pathogenesis and treatment of fistula-in-ano. Br Med. J *1* 463–469 1961

21 *Parks A G* Modern concepts of the anatomy of the anorectal region. Postgrad. Med. J *34* 360–366, 1958.

22. *Pearse A G E..* In "Histochemistry – theoretical and applied" 3 ed., ol. 1 J A. Churchill Ltd., London, 1968.

23. *Pouget R R. & Bacon H E..* Myoephtelial hamartoma of the rectum. Dis. Colon Rectum *4* 409–412 1961

24 *Reid P E.*, Culling, C. F A & Dunn *W L..* Saponificationinduced increase in the periodic acid-Schiff reaction in the gastrointestinal tract. Mechanism and distribution of the reactive substance. J Histochem. Cytochem. *21* 473–482, 1973

25. *Rosser C* The etiology of anal cancer Am. J Surg. *11* 328–333 1931

26. *R sser C* The relation of fistula in ano to cancer of the anal canal. T Am. Proct. Soc. *35* 65–71 1934

27 *Rundle F F & Hales I B..* Mucoid carcinoma supervening on fistula-in-ano. Ann. Surg *137* 215–219 1953

28. *Saldanberg, N & Kleinhaus, R. J* Mucoepidermoid carcinoma of the anus. Am. J Surg. 117 413–415 1969

29 *Spicer S S* Diamine methods for differentiating mucosubstances histochemically J Histochem Cytochem. *13* 211–234 1965.

30. *Wellman K F.:* Adenocarcinoma of anal duct origin. Can. J Surg. *5* 311 318, 1962.

31 Wilson E.. Rectal Cyst. Aust. NZ. J Surg. *34* 32–35 1964

32. *Winkelman J Grosfeld J & Bigelow B* Colloid carcinoma of anal-gland origin Report of a case and review of the literature. Am. J Clin. Pathol. *42* 395–401 1964

33 *Wood W S & Culling, C F A..* Perianal Paget disease. Histochemical differentiation utilizing the borohydride-KOH PAS reaction. Arch. Pathol. *99* 442–445, 1975.

Acta path. microbiol scand. Sect. A 85 286–296 1977

CORONARY ARTERY CHANGES IN NEWBORN BABIES

A Histological and Electron Microscopical Study

JUHANI RAPOLA and ERKKI PESONEN

Children's Hospital University of Helsinki Helsinki Finland

Rapola J & Pesonen, E. Coronary artery changes in newborn babies. A histological and electron microscopical study Acta path microbiol scand Sect. A, 85 286 296 1977

The main branch of the left coronary artery of 14 autopsied newborn babies was studied both in light and electron microscopy Intimal and medial changes of varying severity were found in most cases The lesions show edema and suggest insudation of the blood solutes into the vessel wall The edematic phase is followed by proliferation of smooth-muscle and undifferentiated cells, leading to a thickening of the arterial wall. The structure of the lesions resembles the so-called preatherosclerotic changes found frequently in adults The relationship of the neonatal coronary changes to arteriosclerosis is discussed

Key words Neonatal infant coronary arteries atherosclerosis pathology electron microscopy

Juhani Rapola, Children's Hospital University of Helsinki Stenbäckinkatu 11 SF-00290 Helsinki 29 Finland

Received 9 viii 76 Accepted 19.xi 76

Significant stenosing lesions in the coronary arteries appear in newborn babies and in children (2 4 10 15 18 19 20 23 29 30) These may cause almost total obstruction of the lumen (13) The prevalence of stenoses in the coronary arteries of newborn babies is high In an autopsy series of 87 children under one week of age over twenty per-cent narrowing was found in over one fifth of the cases (13) Whether these lesions are connected with the atherosclerosis which becomes clinically manifest several decades later is not known The more frequent presence of intimal thickenings in boys as compared to girls (2 4 15 18 29) and in children belonging to an ethnic group with a high prevalence of coronary heart disease as compared to children from another group with a low prevalence of the disease, indicated that the pathological foundations of atherosclerosis are visible already in early childhood (20, 29) In a previous study (19) it was found that the intimal thickenings were usually located at the sites where atherosclerotic plaques appear later The thickenings show splitting of the internal elastic lamina (IEL), short and thin elastic fibers in several layers, and an increase of cells in the intimal tissue with an edematic appearance (10 15 18)

In order to obtain a better insight into the cellular changes and the pathogenesis of the arterial lesions in newborn children, we have studied their coronary arteries with the aid of an electron microscope. We have also attempted to correlate our observations with the early changes of atherogenesis as revealed in human and experimental studies.

TABLE 1 *Material and the Light Microscopical Grade of the Vascular Change*

Case no	Birth weight	Age at death		Main cause of death	Light microscopic grade of change
		Days	Hours		
1	1270	1	12	PA	2
2	2700	0	23	Pneumonia	3
3	1590	8	00	Single ventricle of heart	1
4	2600	10	04	HLH	2
5	3220	2	19	HLH	0
6	3630	0	16	Pneumonia, HMD	0
7	2300	15	00	Comm. trunc. arteriosus	2
8	3820	4	04	Pneumonia, HMD	3
9	2370	1	13	HMD	2
10	3400	0	06	Intrauter. asphyxia	2
11	3000	7	11	Subdural haemorrhage	2
12	2740	13	00	Bilocular heart	3
13	1140	0	22	HMD IVH	2
14	1650	0	14	IVH, HMD	1

Pulmonary atelectasis, ²Hypoplastic left heart syndrome, ³Hyaline membrane disease, Intraventricular haemorrhage of brain.

MATERIAL AND METHODS

14 newborn babies from the age of a few hours to 15 days were autopsied within six hours after death (Table 1).

The cases were consecutive and unselected provided that the autopsy could be performed shortly after death. After exposing the heart, a 2–4 mm piece was dissected from proximal left coronary artery before the branching of the main left descending and circumflex tributaries. The piece was immersed immediately in *Karnovsky's* fixative (12) at room temperature. After primary fixation for 30 to 60 min., all surrounding tissue was removed and the vessel was cut under a dissecting microscope into about 0.5 mm thick rings perpendicular to the long axis. The circular slices were studied under the dissecting microscope, and pieces of the artery showing intimal thickenings bulging to the lumen were selected and processed further. In several cases no such thickenings were visible and an occasional section was selected. The adjacent section was transferred to formalin for conventional histology. The tissue pieces selected for electron microscopy consisted of the entire thickness of the artery and the entire circumference of the smallest arteries. They were kept in the same fresh fixative for 6–12 hours at 4 C, transferred to 0.2 M cacodylate buffer pH 7.2 at 4 C and after 1–2 days in this buffer postfixed in phosphate buffered OsO for 90 min. After dehydration in increasing concentrations of acetone the embedding and polymerization took place in *Spurr* (26) resin.

Sections of 1–2 µm in thickness were stained with toluidine-blue. They were used for the selection of the final thin sections with most severe changes for electron microscopy. The thin sections were stained with uranyl-acetate and lead-citrate and studied in an electron microscope (Zeiss EM 9A).

RESULTS

Light Microscopy

The observations were made from the toluidine-blue stained semithin sections and supplemented by the Weigert's elastin stained paraffin sections.

In 2 cases no changes of the arterial wall were present, and the layers appeared normal in every respect. There was a single layer of attenuated endothelial cells on the smooth IEL. The latter is either straight or wavy. The media consist of about four to six layers of smooth-muscle cells (SMC). Most of the SMC are circularly oriented, but those closest to the IEL show partially radial orientation (Fig 1). This basic structure was also seen in many arteries showing alterations at different locations.

Deviation from normal was present in different grades of severity. Three arbitrary







Fig 1 Light microscopic picture of the normal coronary arterial wall. There is a single layer of endothelial cells on the continuous internal elastic lamina (IEL). Tol. blue × 1400

Fig 2 Grade 1 lesion The endothelial layer is detached from the IEL, which displays fragmentation. The arrow shows an area where a cell seems to traverse the disrupted IEL. Tol. blue × 1400

Fig 3 Grade 3 lesion The organization of the endothelium and the intima is damaged No IEL is visible Severe edema and disorganization of the media is also present Tol blue × 1400

grades can be distinguished. Overlapping of the grades is common even in the same section.

Grade 1 represents the least change from normal. The endothelium appears almost unchanged but some cells display cytoplasmic

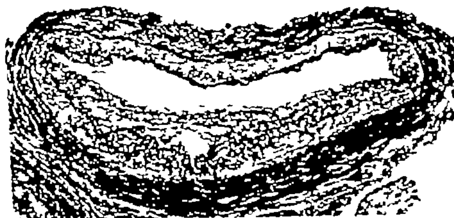


Fig. 4. Paraffin section of a coronary artery showing disruption of the IEL and thickening of the medial and intimal layers in the lower part of the picture. Verhoeff – Van Gieson × 60.

vacuolization. The IEL has also maintained its continuous structure but some loosening and fragmentation, especially on its luminal border is seen. The most significant change is the separation of the endothelium from the IEL, causing a widening of the subendothelial space. This space appears mainly empty with some fibrillar amorphous structures. Sometimes short breaks in the IEL are visible. In such places it seems that the cells are traversing from the media to the subendothelial space (Fig. 2). The cellular layers and the total thickeness of the arterial wall are not appreciably increased in this type of change.

Grade 2 was the most common finding. The endothelium is present but has some tendency to shed single cells. Cytoplasmic vacuolization of the endothelium is also evident. The subendothelial space is markedly increased. The essential feature is the fragmentation of the IEL. Fragments of elastic tissue are visible, though with difficulty in the resin-embedded sections, but are better seen in the paraffin section stained for elastin. Elastic fibres of varying lengths and thinner than the original IEL are seen in several layers. Also several layers of mainly smooth-muscle cells appear between the elastic fragments. They are oriented in cross section of the artery towards the vascular lumen. The cells are loosely arranged, giving an appearance of interstitial edema. The circular medial cell layer also often appears edematic. This grade is associated with a moderate thickening of the vessel wall.

In the most severe, grade 3 lesions, the intimal part of the arterial wall was greatly thickened, causing stenosis of the lumen (Fig. 4). Most of the endothelial cells had disappeared. The innermost layer consists of loose reticular matrix with scattered and haphazardly oriented cells. Some of these are typical SMC, but many cannot be identified. Slightly deeper in the vessel wall there are more cells, also in an unorderly fashion. Many cells in the intima and media have small cytoplasmic vacuoles. The edematic appearance extends deep into the media, and sometimes large empty looking spaces, several tenths of microns in diameter are present in the vessel wall (Fig. 3).

Electron Microscopy

Despite the relatively long period of time between dead and the fixation, satisfactory cellular preservation was maintained in the



6

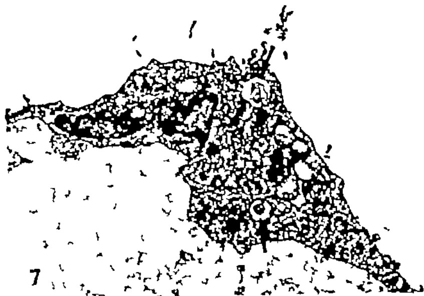


Fig 7 An endothelial cell from a similar lesion as in Fig. 6. The mitochondria appear swollen with disrupted cristae, and there are two vacuoles containing myelin-like figures (shown by arrows) × 12,000

samples. Some minor organelle changes may be caused by autolysis, however and this has to be taken into account in the interpretation of the electron micrographs.

The different grades of arterial wall changes observed in light microscopy were also evident in electron microscopy The cells of the normal endothelium are flat, interdigitating and show junctional complexes. The space between the endothelium and the IEL is narrow and consists of finely granular material. At places it resembles basal membrane The luminal aspect of the IEL is rough-surfaced, but the medial aspect is smooth (Fig. 5) Practically all the medial cells are SMC, displaying numerous myofilaments, dense attachments at the plasma membrane and sparsity of other organelles. The SMC are surrounded by a well-developed basal membrane. There is very little other intercellular material except occasional bundles of collagen fibers.

The widening of the subendothelial space is the least pronounced lesion seen in electron microscopy (Fig 6) The space contains finely granular material resembling blood plasma. Some cytoplasmic fragments can also be seen scattered in the space. Some of the endothelial cells are now roundish, and their cytoplasm is less electron-dense than before. Mitochondrial swelling, with disruption of the cristae, is common. Single detached endothelial cells are also seen.

Together with the subendothelial edema, disintegration of the IEL takes place. Although broken, disrupted, the IEL still permits a demarcation between the subendothelial space and media. In slightly more advanced lesions the course of the original IEL cannot be distinguished, owing to the presence of cells between the pieces of elastic lamina.

Fig 5 Electron micrograph of the endothelial layer of a normal artery. There are attenuated endothelial cells on the continuous IEL indicated by arrows. × 5100.

Fig 6 Endothelial cells are detached from the IEL and show vacuolization. There is layer of scanty amorphous material between the endothelial cells and the IEL (shown by arrows) The IEL still forms boundary between the intima and media. × 5100



Fig 8 The Intimal layer from a grade 3 lesion. Endothelial cells have disappeared. The rare cells showing severe degenerative changes are enmeshed in an edematic matrix showing amorphous substance and fragments of elastic material (shown by arrows) × 5100

In grade 2 and 3 lesions as revealed by light microscopy profound cellular and intercellular alterations have taken place Endothelium if present appears edematic and looser than earlier Cells are roundish less interdigitating and vacuolated Some of the vacuoles are degenerated mitochondria but residual body like vacuoles with electron-dense fibrillar or myelin like configurations are also seen (Fig 7) In many grade 3 lesions the endothelium has been destroyed. The wide subendothelial area contains loose granulofibrillar material This material is sometimes condensed in electron-dense clumps suggesting fibrinogen although typical fibrin was not found Fragments of elastic material and occasional collagen fibers are also present. The cells in the innermost layer are



Fig. 9. A smooth-muscle cell of the medial layer showing abundant rough-surfaced endoplasmic reticulum. The rare dense bodies are located close to the cell membrane. × 20,000.

scanty and degenerated (Fig. 8). Most of them are SMC, but the origin of several cells cannot be identified. Loose cellular fragments with a ghost like appearance are also present. In the deeper layer the cell density is higher. Part of the smooth muscle cells give indications of increased metabolic activity. The basal membrane is less developed than before. The number of myofibrils has decreased, and there is abundant rough-surfaced endoplasmic reticulum with a greater number of free ribosomes (Fig. 9). Undifferentiated *mesenchymal cells* are present. Also in the medial layer the intercellular space is increased and contains elastic fibers and collagen.

No intracellular or intercellular lipid in any appreciable amount was found, and no platelet aggregations or microthrombi were present in this material.

From the light and electron microscopic observations the following dynamic sequence of events is suggested. The initial change from normal is the intimal edema. This is followed by a disintegration of IEL and a spreading of the edema to the deeper layers. Edematic transformation is accompanied by cellular degeneration and proliferation. New elastic fibers and collagen are laid down in the regenerative tissue: this causes the thickening of the arterial wall.

DISCUSSION

Present results confirm these earlier studies (2, 4, 10, 13, 15, 18, 19, 20, 23, 29, 30), i.e. that the arterial wall of newborn babies already shows myointimal thickenings. These changes have not been studied before by electron microscopy. The present findings are essentially similar to those described by *Geer* (7) as simple thickenings in adult human arteries. The "gray gelatinous elevations" described by *Haust* (8) are also of similar structure.

Experimental studies have provided an insight into the possible pathogenesis of the lesions found in the present study. Intimal

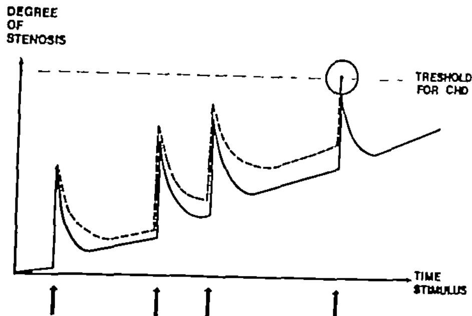


Fig 10 Diagrammatic presentation of the hypothetical model of the development of coronary arteriosclerosis. Every stimulus causes partially reversible thickening of the vessel wall until the stenosis becomes so severe that it causes clinical coronary heart disease (CHD) The continuous line shows the situation without predisposing risk factors the broken line with risk factors

injury mechanical (11 27) hypoxic (3) infective (1) and endotoxin caused (28) lead within a few hours or days to degeneration of the innermost layers of the artery accompanied by edema. Evidence has been presented that the edema is due to the influx of plasma constituents through injured endothelium (3 11) Within 1–2 weeks cellular proliferation with thickening of the intima takes place (5 6 16 27) The proliferating cells are mainly SMC with some undifferentiated cells. Cellular degeneration, edema and proliferation have also been caused by an atherogenic diet (24 25) and hypertension (9) Evidence of the importance of the initial endothelial injury in the genesis of lipid-containing plaques is provided by the enhancement of their formation if the arterial wall has been affected by mechanical (17) or immunological (14) means together with an atherogenous diet.

By comparison with previously published experimental results we assume that lesions in the coronaries of the newborn babies are a result of short term noxious factors. Children dying during the neonatal period can hardly have suffered for more than a few days from conditions injuring the arteries. Hypoxaemia, metabolic acidosis, and various aspects of infection may very well be the causes of the injuries. In a previous study (19) it was shown that the coronary thickening of infants correlated well with the presence of infection The essential question concerns the further development of these thickenings and their possible relationship with the development of atherosclerosis. Some features of the pathological reaction suggest healing and regression of the lesions. The severe lesions usually do not heal to quite the same state as before and some minor defects remain permanently (5 22)

There is some circumstantial evidence that the changes represent the earliest signs of future atherogenesis. The structure of the most pronounced lesions is in several respects similar to those thought to represent early atherosclerosis, both in man and in experimental animals (7 22 31) *Haust* (8) has presented a theory about the development of three preatherosclerotic lesions, viz fatty streaks, gelatinous elevations and microthrombi into an atherosclerotic plaque. If this theory holds true, the lesions found in

this material being similar with the gelatinous elevations, might be preatherosclerotic. We have previously shown (19) that similar lesions as in the present study are located mainly in the typical predilection sites of coronary atherosclerotic plaques left coronary close to the branching point of the main tributaries of the artery

These considerations led us to formulate the following hypothesis about the role of neonatal changes observed earlier and in this study in atherogenesis. The arterial wall reacts at any time of life to the various injurious agents in a similar fashion. The first event is the influx of the blood fluids and solutes through the endothelium. This is followed by the disruption of the IEL and spreading of the exudate to the deeper layers of the vessel wall. The cells react by degeneration and by proliferation at the site of the injury. Evidence has been presented that the SMC of the arterial wall produce intercellular matrix material such as collagen, glycosaminoglycans and elastin (21). The edematic proliferative change will partially regress, but it renders the wall more susceptible to future injuries. The healing process after every new reaction is less complete until the scarring and lipid accumulation of a true atherosclerotic plaque takes place (Fig 10). This hypothesis does not exclude the role of known atherogenetic risk factors such as hypertension and hypercholesterolemia, which will contribute to and enhance the development of lesions present since infancy

---

This work was supported by *The Paavo Nurmi Foundation*

REFERENCES

1. *Burch G E, Tsui, C Y & Harb J M* Pathologic changes of aorta and coronary arteries of mice infected with Coxsackie B virus Proc Soc exp Biol Med. *137* 657–661 1971
2. *Dock W* The predilection of atherosclerosis for the coronary arteries J Amer Med. Ass. *131* 875–878, 1946
3. *Elemer G, Kerenyi T & Jellinek H* Effect of temporary hypoxia on the permeability of the rat aorta. Path. Europ. *10* 123–128, 1975.
4. *Fangman R. C & H Hellwig, C A.:* Histology of coronary arteries in newborn infants. Amer J Path. *23* 901 902, 1947
5. *Fishman J A, Graeme B. R & Karnovsky M J.:* Endothelial regeneration in the rat carotid artery and the significance of endothelial denudation *in the pathogenesis of* myointimal thickening. Lab. Invest. *32* 339–351 1975
6. *Friedman R. J, Moore S & Singal, D P.:* Repeated endothelial injury and induction of atherosclerosis in normolipemic rabbits by human serum. *Lab Invest. 30 404–415 1975.*
7. *Geer J C.* Fine structure of human aortic intimal thickening and fatty streaks. Lab Invest. *14* 1764–1783 1965.
8. *Haust M D.* The morphogenesis and fate of potential and early atherosclerotic lesions in man. Human Path. *2* 1 29 1971
9. *Hüttner I., Moore R H & Rona G.: Fine* structural evidence of specific mechanism for increased endothelial permeability in experimental hypertension Amer J Path *61* 395–412, 1970.
10. *Jaff D., Hartroft S Manning M & Elstein, G.* Coronary arteries in newborn children. Intimal variations in longitudinal sections and their relationship to clinical and experimental data. Acta ped. scand. suppl. 219, 1971
11. *Jorgensen L., Packam M A., Rowsell H C., Buchanan M R. & Mustard J F.* Focal aortic injury caused by cannulation. Increased plasma protein accumulation and thrombosis. Acta path. microbiol. scand. Sect. A, *82* 637–647 1974
12. *Karnovsky M J* A formaldehyde-glutaraldehyde fixative of high osmolarity for use in electron microscopy J Cell Biol. *27*: 137A, 1965
13. *MacMahon, H E. & Dickinson P C T.* Occlusive fibro elastosis of coronary arteries in the newborn Circulation *35* 3–9 1967
14. *Minick C R Murphy G E & Campbell, W G J.* Experimental induction of athero-arteriosclerosis by the synergy of allergic injury to arteries and lipid-rich diet. J *Effect of* repeated injections of horse serum in rabbits fed a dietary cholesterol supplement. J exp. Path. *124* 635–651 1966.
15. *Moon H D* Coronary arteries in fetuses, infants and juveniles. Circulation *16* 263–267 1957
16. *Moore* Thromboatherosclerosis in normolipemic rabbits. A result of continued endothelial damage. Lab Invest. *29* 478–487 1973.
17. *Nam, S C., Lee W M Jarmolych, J., Lee K T & Thomas W A* Rapid production of

advanced atherosclerosis in swine by a combination of endothelial injury and cholesterol feeding Exp mol Path. *18* 369–379 1973
18. *Neufeld H N Wagenvoort C A & Edwards J E.* Coronary arteries in fetuses, infants, juveniles and young adults. Lab. Invest. *11* 837–844 1962
19 *Pesonen E* Coronary wall thickening in children An analysis of the factors associated with the growth of arterial layers. Atherosclerosis *20* 173–187 1974
20 *Pesonen E Norio R & Sarna S* Thickenings in the coronary arteries in infancy as an indication of genetic factors in coronary heart disease Circulation *51* 218–225 1975
21 *Ross R* The arterial smooth muscle cell In *The Pathogenesis of Atherosclerosis, edited by* Wissler R W., Geer J C. Baltimore Williams and Wilkins, 1971 p 147–162.
22. *Ross R. & Glomset J A* Atherosclerosis and the arterial smooth muscle cell Science *180* 1332–1339 1973
23 *Schornagel H E.* Intimal thickening in the coronary arteries in infants. Arch. Path *62* 427–432 1956
24 *Scott R F Daoud A S & Florentin R A* Animal models in atherosclerosis. In The Pathogeneus of Atherosclerosis, edited by Wissler R. W., Geer J C. Baltimore, Williams and Wilkins, 1971 p. 120–146
25 *Shimamoto T., Yamashita Y., Numano F & Sunaga T* The endothelial cell damages of pre-atheromatous and atheromatous lesions observed by scanning electron microscope Proc. Jap Acad. *45* 761–766, 1969
26 *Spurr A R* A low viscosity epoxy resin embedding medium for electron microscopy J. Ultrastruct. Res. *26* 31–43 1969.
27 *Stemerman M B & Ross R.* Experimental arteriosclerosis. Fibrous plaque formation in primates, an electron microscope study J exp. Med *136* 769–789 1972.
28 *Stewart G J & Anderson M J* An ultrastructural study of endotoxin induced damage in rabbit mesenteric arteries. Brit. J exp. Path *52* 75–79 1971
29 *Vlodaver Z. Kahn H A & Neufeld H N* The coronary arteries in early life in three different ethnic groups. Circulation 39 541 550 1969
30 *Vlodaver Z & Neufeld H N* The musculo-elastic layer in the coronary arteries. Vasc. Dis *4* 136–145 1967
31 *Wilens S L.* The nature of diffuse intimal thickening of arteries J Path. 27 825–839, 1951

REPAIR IN ARTERIAL TISSUE

The Role of Endothelium in the Permeability of a Healing Intimal Surface. Vital Staining with Evans Blue and Silver-staining of the Aortic Intima After a Single Dilatation Trauma

B. Collatz Christensen, J. Chemnitz, L. Tkocz and O. Blaabjerg

Winslow Institute of Human Anatomy, University of Odense, and
Department of Clinical Chemistry, Odense University Hospital, Odense, Denmark

Christensen, B. C., Chemnitz, J., Tkocz, I. & Blaabjerg, O. Repair in arterial tissue. The role of endothelium in the permeability of a healing intimal surface. Vital staining with Evans blue and silver-staining of the aortic intima after a single dilatation trauma. Acta path. microbiol. scand. Sect. A, 85 297–310 1977

The role of the endothelium as factor determining the permeability of a healing aortic intima after a severe mechanical lesion in the rabbit was studied by vital staining with Evans blue by surface light microscopy after silver-staining, fluorescence microscopy and by other methods. Endothelium to develop from pre-existing endothelium in the mouths of intercostal arteries and at the borders of the lesion, remained unstained by vital staining, whereas denuded surfaces as well as pseudo-endothelium, probably derived from smooth muscle cells in the neo-intima, were intensely coloured. There was general tendency towards a decreasing permeability of the aortic wall throughout an experimental period of 6 months. The determinant factor in the decreasing permeability was the presence of genuine endothelium, but changes in the endothelium, probably in the form of differentiation of intercellular junctions and changes in the connective tissue in the deeper layers, seemed to be additional factors which influenced the permeability.

Key words: Experimental arteriosclerosis; endothelium; embolectomy catheter lesion; Evans blue; vital staining; permeability; silver-staining.

B. Collatz Christensen, Winslow Institute of Human Anatomy, University of Odense, DK 5000 Odense, Denmark.

Received 14.vii.76. Accepted 15.xi.76

In the present study the importance of the endothelium for the permeability of a healing aortic intima after a severe mechanical lesion is tested. The uptake of dye by vital staining with Evans blue was correlated with the patterns of surface cells in the silver-stained intima after re-endothelialization. The albumin-dye complex was traced in the arterial wall by fluorescence microscopy of macroscopically stained and unstained intimal areas at various time intervals after a lesion caused by an embolectomy catheter.

Vital staining with Evans blue has been shown to be based on the staining of tissue with a protein-dye complex (*McGill et al.* 1957, *Packham et al.* 1967, *Heck et al.* 1976). Apart from some small foci situated in particular around the intercostal arteries, Evans blue does not stain the normal thoracic aorta

advanced atherosclerosis in swine by a combination of endothelial injury and cholesterol feeding. Exp mol Path. *18* 369–379 1973

18. *Neufeld H N Wagenvoort C A & Edwards J E* Coronary arteries in fetuses, infants, juveniles and young adults. Lab. Invest. *11* 837–844 1962.

19 *Pesonen E* Coronary wall thickening in children. An analysis of the factors associated with the growth of arterial layers. Atherosclerosis *20* 173–187 1974

20 *Pesonen E Norio R & Sarna S* Thickenings in the coronary arteries in infancy as an indication of genetic factors in coronary heart disease Circulation *51* 218–225 1975

21 *Ross R* The arterial smooth muscle cell In The Pathogenesis of Atherosclerosis edited by Wissler R. W., Geer J C. Baltimore Williams and Wilkins 1971 p 147–162.

22 *Ross R & Glomset J A.* Atherosclerosis and the arterial smooth muscle cell. Science *180* 1332–1339 1973

23 *Schornagel H E.* Intimal thickening in the coronary arteries in infants. Arch Path. *62* 427–432 1956

24 *Scott R F Daoud A S & Florentin R. A* Animal models in atherosclerosis. In The Pathogenesis of Atherosclerosis, edited by Wissler R. W., Geer J C. Baltimore, Williams and Wilkins, 1971 p. 120–146.

25 *Shimamato T Yamashita, Y., Numano F & Sunaga T* The endothelial cell damages of pre-atheromatous and atheromatous lesions observed by scanning electron microscope, Proc. Jap Acad. *45* 761–766 1969

26 *Spurr A R* A low viscosity epoxy resin embedding medium for electron microscopy J Ultrastruct. Res. *26* 31–43 1969

27 *Stemerman M B & Ross R.* Experimental arteriosclerosis. Fibrous plaque formation in primates an electron microscope study J exp. Med *136* 769–789 1972.

28 *Stewart G J & Anderson M J* An ultrastructural study of endotoxin induced damage in rabbit mesenteric arteries. Brit. J exp. Path. *52* 75–79 1971

29 *Vlodaver Z. Kahn H A & Neufeld H N* The coronary arteries in early life in three different ethnic groups. Circulation *39* 541 550 1969

30 *Vlodaver Z & Neufeld H N* The musculoelastic layer in the coronary arteries. Vasc. Dis *4* 136–145 1967

31 *Wilens S L* The nature of diffuse intimal thickening of arteries. J Path. 27 825–839, 1951

Acta path. microbiol. scand. Sect. A, 85 297–310, 1977

REPAIR IN ARTERIAL TISSUE

The Role of Endothelium in the Permeability of a Healing Intimal Surface. Vital Staining with Evans Blue and Silver-staining of the Aortic Intima After a Single Dilatation Trauma

B. Collatz Christensen, J. Chemnitz, I. Tkocz and O. Blaabjerg

Winslow Institute of Human Anatomy, University of Odense, and
Department of Clinical Chemistry, Odense University Hospital, Odense, Denmark

Christensen, B. C., Chemnitz, J., Tkocz, I. & Blaabjerg, O. Repair in arterial tissue. The role of endothelium in the permeability of a healing intimal surface. Vital staining with Evans blue and silver-staining of the aortic intima after a single dilatation trauma. Acta path. microbiol. scand. Sect. A, 85: 297–310, 1977.

The role of the endothelium as a factor determining the permeability of a healing aortic intima after a severe mechanical lesion in the rabbit was studied by vital staining with Evans blue, by surface light microscopy after silver-staining, fluorescence microscopy and by other methods. Endothelium *to develop from pre-existing endothelium* in the mouths of intercostal arteries and at the borders of the lesion, remained unstained by vital staining, whereas denuded surfaces as well as *pseudo-endothelium, probably derived from smooth muscle cells in the neo-intima, were intensely coloured. There was a general tendency towards decreasing permeability of the aortic wall throughout an experimental period of 6 months. The determinant* factor in the decreasing permeability was the presence of genuine endothelium, but changes in the endothelium, probably in the *form of differentiation of intercellular junctions* and changes in the connective tissue in the deeper layers, seemed to be additional factors which influenced the permeability.

Key words: Experimental arteriosclerosis; endothelium; embolectomy catheter lesion; Evans blue; vital staining; permeability; silver-staining.

B. Collatz Christensen, Winslow Institute of Human Anatomy, University of Odense, DK 5000 Odense, Denmark.

Received 14.vii.76. Accepted 13.xi.76.

In the present study the importance of the endothelium for the permeability of a healing aortic intima after a severe mechanical lesion is tested. The uptake of dye by vital staining with Evans blue was correlated with the patterns of surface cells in the silver-stained intima after re-endothelialization. The albumin-dye complex was traced in the arterial wall by fluorescence microscopy of macroscopically stained and unstained intimal areas *at various time intervals after a* lesion caused by an embolectomy catheter.

Vital staining with Evans blue has been shown to be based on the staining of tissue with a protein-dye complex (*McGill et al.* 1957, *Packham et al.* 1967, *Heck et al.* 1976). Apart from some small foci situated in particular *around the intercostal arteries*, Evans blue does not stain the normal thoracic aorta

advanced atherosclerosis in swine by a combination of endothelial injury and cholesterol feeding Exp. mol Path *18* 369–379 1973

18 *Neufeld H N Wagenvoort C A & Edwards J E.* Coronary arteries in fetuses, infants, juveniles and young adults. Lab. Invest *11* 837–844 1962

19 *Pesonen E* Coronary wall thickening in children An analysis of the factors associated with the growth of arterial layers. Atherosclerosis *20* 173–187 1974

20 *Pesonen E Norio R & Sarna S* Thickenings in the coronary arteries in infancy as an indication of genetic factors in coronary heart disease Circulation *51* 218–225 1975

21 *Ross R* The arterial smooth muscle cell In The Pathogenesis of Atherosclerous, edited by Wissler R. W Geer J C. Baltimore Williams and Wilkins, 1971 p 147–162

22 *Ross R & Glomset J A* Atherosclerosis and the arterial smooth muscle cell Science *180* 1332–1339 1973

23 *Schornagel H E* Intimal thickening in the coronary arteries in infants. Arch. Path. *62* 427–432 1956.

24 *Scott R F Daoud A S & Florentin R A* Animal models in atherosclerosis. In The Pathogenesis of Atherosclerosis, edited by Wissler R. W., Geer J C. Baltimore, Williams and Wilkins, 1971 p. 120–146.

25 *Shimamato T., Yamashita Y Numano, F & Sunaga T* The endothelial cell damages of pre atheromatous and atheromatous lesions observed by scanning electron microscope Proc Jap Acad. *45* 761–766 1969

26 *Spurr A R* A low viscosity epoxy resin embedding medium for electron microscopy J Ultrastruct. Res. *26* 31–43 1969

27 *Stemerman M B & Ross R.* Experimental arteriosclerosis. Fibrous plaque formation in primates an electron microscope study J exp Med *136* 769–789 1972

28 *Stewart G J & Anderson M J* An ultrastructural study of endotoxin induced damage in rabbit mesenteric arteries. Brit. J exp Path *52* 75–79 1971

29 *Vlodaver Z Kahn H A & Neufeld H N* The coronary arteries in early life in three different ethnic groups. Circulation 39 541–550 1969

30 *Vlodaver Z & Neufeld H N.* The musculo elastic layer in the coronary arteries. Vasc Dis *4* 136–145 1967

31 *Wilens S L.* The nature of diffuse intimal thickening of arteries. J Path. 97 825–839 1951

ere stained as follows Haematoxylin and eosin (*McManus & Mowry* 1964) v Gieson Hansen (*Romeis* 1948) PA-Schiff and Orcein (*McManus & Mowry* 1964) toluidine blue with varied pH (*Pearse* 1968) and von Kossa staining for calcifications (*Pearse* 1972) The sites of necrobiopsies were marked on a photograph of the vessel.

RESULTS

Control animals The four sham operated animals, of which two had been silver stained, had macroscopically normal aortae. There was no staining of the thoracic aorta (Fig 3 a) apart from some small discrete longitudinal stripes on the dorsal wall of the cephalic part of the thoracic aorta.

Experimental Animals

Gross changes. All the vessels were dilated, the degree of dilatation increasing with the time of survival after the lesion. Round indentations, transverse folds and whitish plaques, as previously described by *Helin et al.* 1971 occurred to a varying degree in 12 of the 19 experimental animals observed from the 8th day and up to six months after the lesion.

Vital Staining with Evans Blue

A Methodological Studies

1 Rates of disappearance from the blood of Evans blue Provided that all the Evans blue is bound to albumin, the slope of the curve in Fig 1 represents the rate constant for the transfer of albumin from the circulation to the interstitial tissue the transcapillary escape rate (TER) (*Rossing* 1971) The plasma volume was calculated from the extrapolated concentration of Evans blue to time 0 (linear regression) In the two control rabbits, the values of TER were 18.3 and 20.3 per cent per hour being 21.6 and 23 0 per cent per hour in the experimental animals. These values are not significantly different from the values in the control animals. The

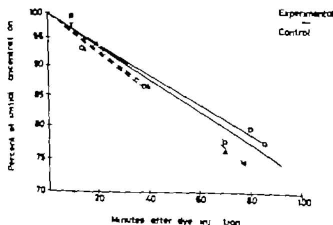


Fig 1 Rates of disappearance from the blood of Evans blue. Ordinate the scale is logarithmic, showing concentration of Evans blue in serum in percentage of extrapolated initial concentration. Abscissa Minutes after dye injection.

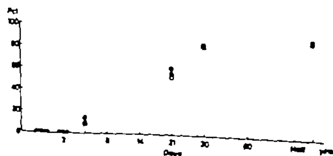


Fig 2 Planimetry Vital staining of the rabbit thoracic aorta using Evans blue. Abscissa Time of survival after lesion produced by an embolectomy catheter Ordinate unstained white areas in percentage of total area between the second and ninth intercostal artery

(*McGill et al* 1957 *Friedman & Byers* 1963 *Bell et al* 1972 *Somer et al* 1972 *Caplan et al* 1974)

The genuine endothelium remained macroscopically unstained while denuded surfaces and surfaces covered with pseudo-endothelium had an intense blue colour The expansion of genuine endothelium brought about a time dependent decrease in the total permeability of the arterial wall throughout the experimental period.

MATERIALS AND METHODS

Male albino rabbits of the Danish country race were employed. They were about 5 months old and weighed approximately 3 kg Twenty-nine animals were subjected to lesion of the thoracic aorta by means of an embolectomy catheter 4 were subjected to a sham operation with ligature of the femoral artery the latter were used as controls a further 4 animals were used only for biochemical analysis of the Evans blue in the blood 2 on which sham operation had been performed and 2 presenting a one week old lesion produced by an embolectomy catheter

Lesion produced by an *embolectomy catheter* A single short lasting dilatation of the thoracic aorta was induced by a Fogarthy embolectomy catheter (12-080-5F) (*Collatz Christensen & Garbarsch* 1973)

Vital staining Evans blue (Merck art 3169) 0 5 per cent dissolved in physiological saline, was injected slowly into an ear vein 3½ to 4 hours prior to autopsy in a dosage of 3 ml/kg body weight, through a 0 22 µm filter (Millipore GSWPO 2500) Extinction measurement of the dye solution before and after passage through the filter ensured that no adsorption to the filter had taken place

Biochemical analyses 1 Evans blue elimination curve The serum was diluted 100 times before reading the extinction at 620 nm (Zeiss PMQ II) Owing to the strong dilution of the serum, correction for lipaemia and haemolysis was not necessary inasmuch a the extinction at 740 nm is 0 (*Nielsen & Nielsen* 1962) Depiction was on semilogarithmic paper *2 The degree of protein binding of Evans blue* 2000 µl of the sample material was ultrafiltered (Amicon, Centriflo CF 50) at 800 g until approximately one half of the fluid had been filtered In order to reduce the unspecific binding of Evans blue to the filter the binding sites of the filter were previously saturated by filtration of 2000 µl of 50 µg/ml of an aqueous Evans blue solution. The extinction of the filtrate of the sample was read at 620 nm and conversion to concentrations took place by means of a series of aqueous standard solutions which were filtered under the same conditions.

Autopsy Silver-staining and perfusion fixation were carried out according to a method previously used (*Collatz Christensen & Garbarsch* 1973) twenty animals were silver-stained whereas thirteen remained unstained The autopsies were performed 1-2-4-8-14-21-30-60 days and six months after the lesion had been inflicted to the experimental animals the control animals were autopsied 21 days and six months after the sham operation. Each of these experimental groups comprised animals stained with silver

Planimetry The aorta was removed atraumatically It was cleaned of peri-adventitial tissue cut open on the ventral side, pinned on a teflon mat, examined for macroscopical changes, and finally photographed Planimetry was carried out by weighing It was registered as unstained white area after vital staining with Evans blue in percentage of the total surface area from the origin of the intercostal arteries No. 2 to No. 9

Whole-mount specimens for surface light microscopy (surface LM) In total, 4–6 whole-mount specimens per animal were studied. With the exception of one centimeter long segments used for Häutchen preparation and strips cut to be used for light microscopy (LM) the whole intimal surface was studied by surface LM (*Collatz Christensen & Garbarsch* 1973)

Häutchen. A monolayer of the surface of the tunica intima from 27 animals was produced by incubation of the endothelial surface in celloidin, according to a method described by *Poole et al.* 1958. Staining Harris HE and Feulgen (*McManus & Mowry* 1964) Various blue and white areas from the middle part of the thoracic aorta were selected for study

Fluorescent microscopy of frozen sections to be used for the demonstration of Evans blue was carried out on all the animals. Around the levels of intercostal arteries from number four to eight strips of tissue were excised transversely and longitudinally to the long axis of the vessel from blue and white areas of the immersion-fixed pinned aorta the sites of necrobiopsies were marked on a photograph of the vessel Frozen sections of 10 µm thickness were cut on the cryostat (R Jung Heidelberg) and mounted in aqueous glycerine The sections were examined in a Leitz Orthoplan fluorescence microscope with oblique light, ultraviolet light source Osram HB 0200 exitor filter BG 12/2 secondary filter K 510 Photomicrographs were taken, using a *Leitz Orthomat* camera on Agfachrome 50 S film.

Transmission LM Sections from paraffin embedded specimens, selected at random from the cephalic and the caudal third of the thoracic aorta

were stained as follow Haematoxylin and eosin (*McManus & Mowry* 1964) v Gieson Hansen (*Romeis* 1948) PA-Schiff and Orcein (*McManus & Mowry* 1964) toluidine blue with aried pH (Pearse 1968) and on Kossa staining for calcifications (*Pearse* 1972) The sites of necrobiopsies were marked on a photograph of the vessel

RESULTS

Control animals. The four sham operated animals, of which two had been silver-stained, had macroscopically normal aortae. There was no staining of the thoracic aorta (Fig. 5 a) apart from some small discrete longitudinal stripes on the dorsal wall of the cephalic part of the thoracic aorta.

Experimental Animals

Gross changes. All the vessels were dilated, the degree of dilatation increasing with the time of survival after the lesion Round indentations, transverse folds and whitish plaques, as previously described by *Helin et al.* 1971 occurred to a varying degree in 12 of the 19 experimental animals observed from the 8th day and up to six months after the lesion.

Vital Staining with Evans Blue

A Methodological Studies

1 Rates of disappearance from the blood of Evans blue Provided that all the Evans blue is bound to albumin, the slope of the curve in Fig 1 represents the rate constant for the transfer of albumin from the circulation to the interstitial tissue the transcapillary escape rate (TER) (*Rossing* 1971) The plasma volume was calculated from the extrapolated concentration of Evans blue to time 0 (linear regression) In the two control rabbits, the values of TER were 18.3 and 20.3 per cent per hour being 21.6 and 23 0 per cent per hour in the experimental animals. These values are not significantly different from the values in the control animals. The

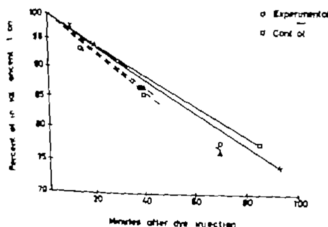


Fig 1 Rates of disappearance from the blood of Evans blue. Ordinate the scale is logarithmic showing concentration of Evans blue in serum in percentage of extrapolated initial concentration. Abscissa Minutes after dye injection

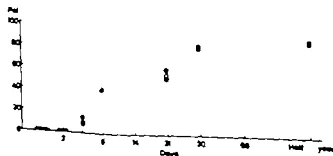


Fig 2 Planimetry Vital staining of the rabbit thoracic aorta using Evans blue. Abscissa Time of survival after lesion produced by an embolectomy catheter Ordinate unstained white areas in percentage of total area between the second and ninth intercostal artery



Fig 3 Rabbit thoracic aorta vital stained with Evans blue. a) Sham operated control, 21 days after ligature of the left femoral artery b) 4 days, c) 8 days and d) 6 months after the lesion inflicted by embolectomy catheter
Arrows Genuine endothelium, white expanding from intercostal arteries.
Arrowheads Sites of selective excision of tissue by a stamp.

plasma volume of the two experimental animals was found to be 46 2 and 48.2 ml/kg which is in agreement with *Tornberg* 1958 52 4 ± 8.6 ml/kg ($\bar{x}$ ± 2 SD)

2 Protein binding of Evans blue has been estimated by means of ultrafiltration According to *McCall* 1957 an almost complete binding of the dye to the plasma proteins was observed. In our experiments, the degree of protein binding 180 minutes after injection exceeded 98 per cent in the two experimental animals. The degree of binding was found to exceed 96 per cent after the addition of Evans blue, to normal rabbit serum *in vitro* The added quantity was equivalent to the amount occurring *in vivo* following immediate admixture directly after injection

B Staining of the Thoracic Aorta

1 Vital staining and planimetry Vital staining of 29 experimental animals showed totally blue intima the first and second day From the 4th day (Fig 3 b and c) small isolated islands of white occurred around the intercostal arteries. Later on these areas coalesced firstly in the cephalic half of the thoracic aorta, and after 6 months the majority of the intima was white (Fig 3d) Planimetry (Fig 2) showed increasing dissemination of the white during the observation period though the spread of observations was considerable

2 Surface LM of silver stained aortae from 18 animals In white areas, normal and hexagonal endothelium interspersed with giant cells spread out from the mouths of intercostal arteries (Fig 3 a and b) Giant endo-

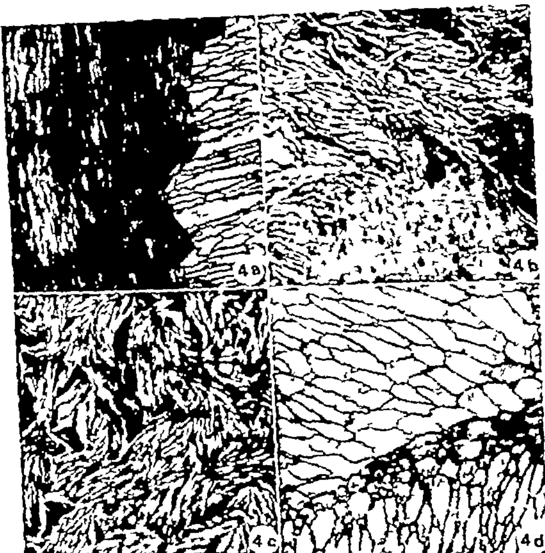


Fig 4 Surface light microscopy of tal stained abbit thoracic aorta.) and b) 2 days after lesion. a) T the right intact endothelium around an intercostal artery To the left continuous layer of smooth muscle cells × 160 Original magnification × 40. b) Penetrated elastic membrane nd spindle shaped cells, probably smooth muscle cells × 160 Original magnification × 40 c) and d) Reparatory changes 8 and 21 days after infliction of the lesion. c) Rosettes of partly separated spindle shaped cells, probably smooth muscle cells, blue areas × 160 Original magnification × 40 d) Boundary between genuine endothelium (top) white area, and *pseudo-endothelium* (bottom) blue area., × 400. Original magnification × 100

thelial cells occurred n and around the edges of white areas (Fig 5 a and b, Fig 7 a) and a small corona of endothelium near the edge was blue coloured (Fig. 4 a and Fig 6 c) After 6 months, large areas were covered by normal looking endothelium (Fig 5 d)

In blue areas, a mixed pattern of denuded surfaces (Fig. 4 a and b) spindle shaped cells resembling smooth muscle cells (Fig. 4 c) and pleomorphic patterns of typical pseudo-endothelium (Fig. 6 a and b) was observed. The border zones between *endo-*



Fig 3 Rabbit thoracic aorta vital stained with Evans blue. a) Sham operated control, 21 days after ligature of the left femoral artery b) 4 days, c) 8 days and d) 6 months after the lesion inflicted by embolectomy catheter
Arrows Genuine endothelium, white expanding from intercostal arteries.
Arrowheads Sites of selective excision of tissue by a stamp.

plasma volume of the two experimental animals was found to be 46 2 and 48 2 ml/kg which is in agreement with *Tornberg* 1958 52 4 ± 8 8 ml/kg ($\bar{x}$ ± 2 SD)

2 *Protein binding of Evans blue* has been estimated by means of ultrafiltration According to *McCall* 1957 an almost complete binding of the dye to the plasma proteins was observed In our experiments the degree of protein binding 180 minutes after injection exceeded 98 per cent in the two experimental animals. The degree of binding was found to exceed 96 per cent after the addition of Evans blue to normal rabbit serum *in vitro* The added quantity was equivalent to the amount occurring *in vivo* following immediate admixture directly after injection

B Staining of the Thoracic Aorta

1 *Vital staining and planimetry* Vital staining of 29 experimental animals showed totally blue intima the first and second day From the 4th day (Fig 3 b and c) small isolated islands of white occurred around the intercostal arteries. Later on these areas coalesced firstly in the cephalic half of the thoracic aorta and after 6 months the majority of the intima was white (Fig 3d) Planimetry (Fig 2) showed increasing dissemination of the white during the observation period though the spread of observations was considerable

2 *Surface EM of silver stained aortae from 18 animals* In white areas, normal and hexagonal endothelium interspersed with giant cells spread out from the mouths of intercostal arteries (Fig 5 a and b) Giant endo-

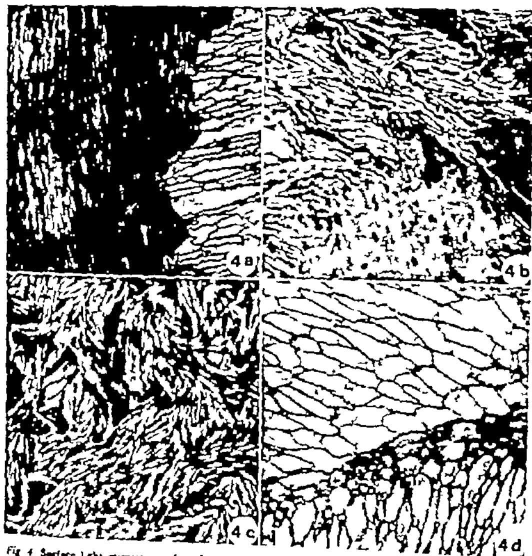


Fig. 4 Surface light microscopy of ital stained rabbit thoracic aorta) and b) 2 days after lesion.) To the right intact *endothelium* around an intercostal artery. To the left continuous layer of smooth muscle cells × 160. *Original magnification* × 40. b) Fenestrated elastic membrane and spindle shaped cells, probably smooth muscle cells × 160. Original magnification × 40) and d) Reparatory changes 8 and 21 day *after infliction of the lesion.*) "Rosettes" of partly separated spindle shaped cells, probably smooth muscle cells, blue areas, × 160. Original magnification × 40. d) Boundary between genuine *endothelium* (top) white area, and pseudo-endothelium (bottom) blue area, × 400. Original magnification 100

thelial cells occurred in and around the edges of white areas (Fig. 5 a and b, Fig. 7 a) and a small orona of endothelium near the edge was blue coloured (Fig. 4 a and Fig. 6 c). After 6 months, large areas were covered by normal looking endothelium (Fig. 5 d).

In blue areas, a mixed pattern of denuded surfaces (Fig. 4 a and b), spindle shaped cells resembling smooth muscle cells (Fig. 4 c) and pleomorphic patterns of typical pseudo-endothelium (Fig. 6 a and b) was observed. The border zones between endo-

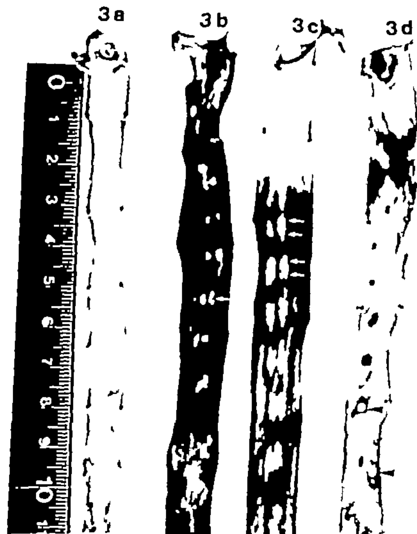


Fig 3 Rabbit thoracic aorta vital stained with Evans blue. a) Sham operated control 21 days after ligature of the left femoral artery b) 4 days, c) 8 days and d) 6 months after the lesion inflicted by embolectomy catheter
Arrows Genuine endothelium, white expanding from intercostal arteries.
Arrowheads Sites of selective excision of tissue by a stamp.

plasma volume of the two experimental animals was found to be 46 2 and 48 2 ml/kg which is in agreement with *Tornberg* 1958 52 4 ± 8 8 ml/kg (X ± 2 SD)

2 *Protein binding of Evans blue* has been estimated by means of ultrafiltration According to *McGill* 1957 an almost complete binding of the dye to the plasma proteins was observed In our experiments the degree of protein binding 180 minutes after injection exceeded 98 per cent in the two experimental animals. The degree of binding was found to exceed 96 per cent after the addition of Evans blue to normal rabbit serum *in vitro* The added quantity was equivalent to the amount occurring *in vivo* following immediate admixture directly after injection

B Staining of the Thoracic Aorta

1 *Vital staining and planimetry* Vital staining of 29 experimental animals showed totally blue intima the first and second day From the 4th day (Fig 3 b and c) small isolated islands of white occurred around the intercostal arteries. Later on these areas coalesced firstly in the cephalic half of the thoracic aorta and after 6 months the majority of the intima was white (Fig 3d) Planimetry (Fig 2) showed increasing dissemination of the white during the observation period though the spread of observations was considerable

2 *Surface I M of silver stained aortae from 18 animals* In white areas, normal and hexagonal endothelium interspersed with giant cells spread out from the mouths of intercostal arteries (Fig 5 a and b) Giant endo-

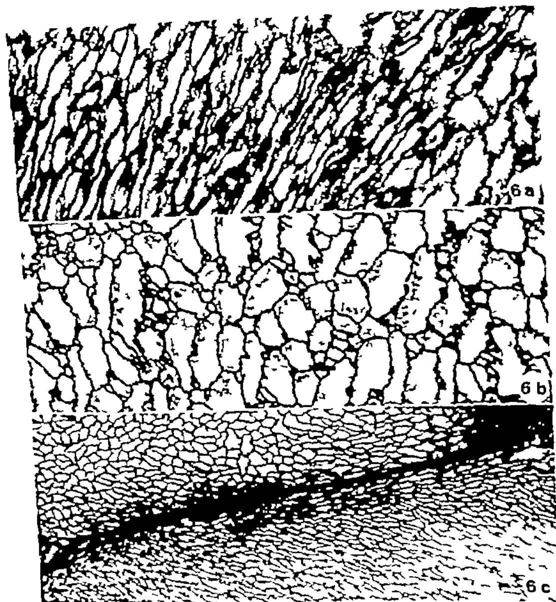


Fig. 6 Surface light microscopy of ital stained rabbit thoracic aorta. Various types of pseudo-endothelium) 8 days b) 60 days, and c) 21 days after infliction of the lesion. a) Gradual transition between elongated cells (centrally in the picture) and pseudo-endothelium to both sides, blue area. × 400 Original magnification × 100 b) Pseudo-endothelium with "foam-like" patterns of silver-lines between the cells, blue area 400 Original magnification × 100) Tapering areas of pseudo-endothelium, blue connected by an isthmus across large field of genuine endothelium, white. At the boundary zone the genuine endothelium is shaded blue probably representing a zone of expanding endothelium and regressing pseudo-endothelium × 160 Original magnification × 40.

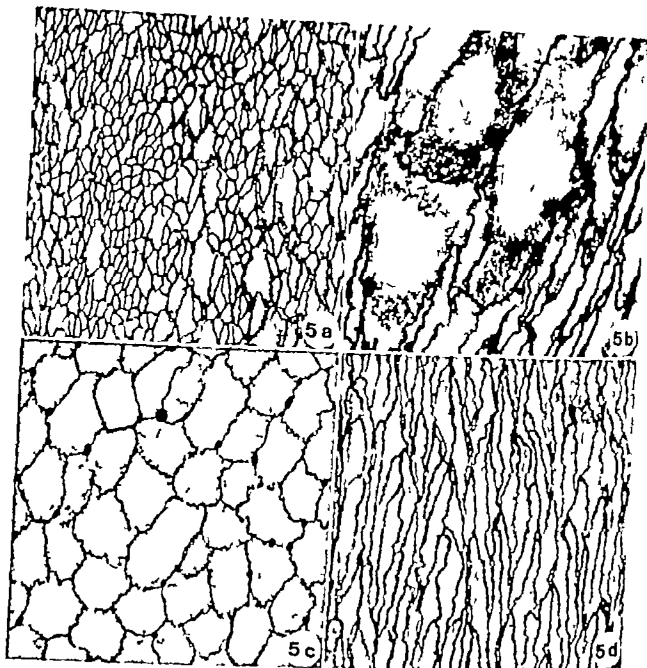


Fig 5 Surface light microscopy of vital stained rabbit thoracic aorta. Various types of genuine endothelium a) 8 days, b) 4 days, c) 21 days and d) 6 months after infliction of the lesion. a) Hexagonal endothelium with endothelial giant cells white area. × 160 Original magnification × 40 b) Normal endothelium with endothelial giant cells, white area. × 400 Original magnification × 100 c) Hexagonal endothelium with stomata faintly blue × 640 Original magnification × 160 d) Normal endothelium, white area dominates the intimal surface 6 months after lesion complete restitution of endothelial surface ×400 Original magnification × 100

thelium and pseudo-endothelium (Fig 4 d and Fig 6 c) were extremely sharp (*Collatz Christensen & Garbarsch* 1973) After three weeks typical pseudo-endothelium presenting "foam like" patterns dominated blue areas (Fig 6 b)

Exception to the rule that genuine endothelium was macroscopically white border zones of white areas covered with endothelium (Fig 6 c) and sporadically hexagonal endothelium with stomata (Fig 5 c)

From and including the 8th day round indentations and plaques were recognizable as deep-lying amorphic and granular fields

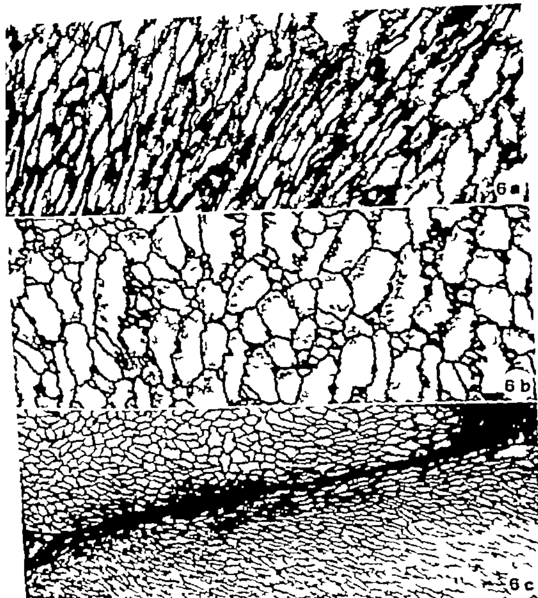


Fig. 6 Surface light microscopy of ral stained rabbit thoracic aorta. Various types of pseudo-endothelium a) 8 days b) 60 days and c) 21 days after infliction of the lesion. a) Gradual transition between elongated cells (centrally in the picture) and pseudo-endothelium to both sides, blue area. × 400 Original magnification × 100 b) Pseudo-endothelium with "foam-like" patterns of silver-lines between the cells, blue area × 400 Original magnification × 100. c) Tapering areas of pseudo-endothelium, blue connected by an isthmus across a large field of genuine endothelium, white At the boundary zone the genuine endothelium is shaded blue, probably representing a zone of expanding endothelium and retreating pseudo-endothelium × 160 Original magnification × 40



Fig 7 Häutchen stained by the Feulgen reaction a) Endothelial giant cells with several centrally localized nuclei and a solitary mitotic figure 4 days after lesion × 640 Original magnification × 160. b) Hexagonal endothelium several cells are binucleate and multinucleate 14 days after lesion. × 640. Original magnification × 160

under white areas covered mainly by hexagonal endothelium, as well as under blue coloured areas covered by pseudo-endothelium.

3 Surface LM of aortae unstained of silver from 11 animals rendered no information on the patterns of surface cells as the cell boundaries were hardly visible

4 Hautchen from 25 animals (Fig 7 a and b) White areas Normal and hexagonal endothelium showed cells with double nuclei and giant endothelial cells containing more than 5 centrally situated nuclei. Blue areas Smooth muscle with typical spindle formed cells together with pseudo-endothelium with oval nuclei often as double nuclei, presented even transition. Non-uniform staining and size of the nuclei were prominent particularly in the white area, but unmistakeable mitotic figures were very rare

5 Fluorescence microscopy of 33 animals (Fig 9) Fluorescence microscopy provides the possibility of locating Evans blue albumin colour complex by the prominent orange red fluorescence of this stain (*Steinwall & Klatzo* 1966 *Heck et al.* 1976)

Control animals Yellow and/or green fluorescence of the elastic lamellae was prominent (Fig 9 a) Opposite the discrete blue stripes on the dorsal wall of the normal thoracic aorta there was a weak reddish fluorescence of the internal elastic membrane and a suggestion of reddish fluorescence in the nearest elastic lamellae (Fig 9 b)

Experimental animals Without regard to the stain binding the following changes were recognized Neo-intima increased in thickness until the 30th day The thickness decreased after 2 and 6 months. Cushion shaped thickenings of the neo-intima (Fig 9 e) were prominent between the 14th day and 2 months after 6 months the neo-intima was uniformly thickened Necrosis occurred in the media from and including the 8th day with increasing dissemination in the later experiments. After 6 months, the elastic lamellae were indistinct, with irregularly arranged lamellae (Fig 9 g)

Sections from macroscopically white areas Until the 30th day the neo-intimal thickening presented a diffuse reddish fluorescence including the neo-intima and the adjacent

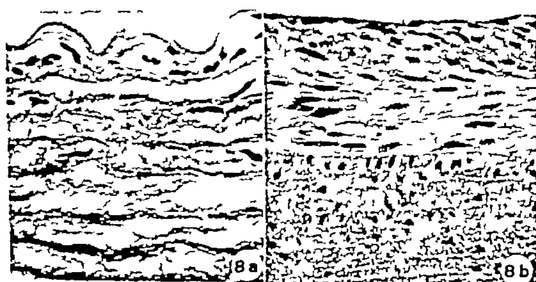


Fig 8 Conventional light microscopy) Toluidine blue, pH 3, 1 day b) V Gieson Hansen, 30 days after lesion.) Intima is totally removed, round cell infiltration and oedema in the luminal zone of media × 640 Original magnification × 160 b) Neo-intima with spindle shaped cells, probably smooth muscle cells. × 400 Original magnification × 100

elastic membranes. This diminished within the observation period (Fig 9 f) After 60 days, the reddish fluorescence was rare in the neo-intima and after 6 months, it was completely absent from the luminal zone of the vessel (Fig. 9 g)

Sections from macroscopically blue areas During the first 14 days of the experiment, the walls of the vessel were strongly reddish in their fluorescence in all of the layers (Fig. 9 c) In the majority of sections, at intervals of from 21 and 30 days after the lesion, a narrow green-red fluorescent zone occurred on the adventitial side of the media. After 6 months, approximately half of the luminal zone of the media was uniformly orange-red, whereas the neo-intima presented a yellow fluorescence (Fig 9 h) A common feature in the experimental animals was a decreasing reddish fluorescence in the wall of the aorta throughout the whole of the experimental period. This was most obvious in the macroscopically white areas which, 6 months after the lesion, appeared to have no albumin-bound Evans blue in the luminal zone of the aortic wall.

Zones of transition between the macroscopically white and blue intima The border between the greenish and reddish fluorescent media was relatively sharp and, after 14 days (Fig 9 d) a massive cushion-formed intimal thickening (Fig 9 e) was often seen luminally to the transitional zone. The cushion-shaped neo-intimal thickening presented intense orange red fluorescence.

6 Transmission LM Conventional connective tissue staining of sections from 19 experimental animals from various blue white and mixed blue and white areas showed the same time dependent changes as those earlier described (*Helin et al.* 1971) (Fig. 8 a and b) A coarse correlation of LM with the sites of necrobiopsies indicated on the photograph revealed no qualitatively different structure of neo-intima and media in sections from blue and white areas.

DISCUSSION

The method of vital staining used in our investigation is analogous with the method used by *McGill et al* 1957 *Packham et al.* 1967

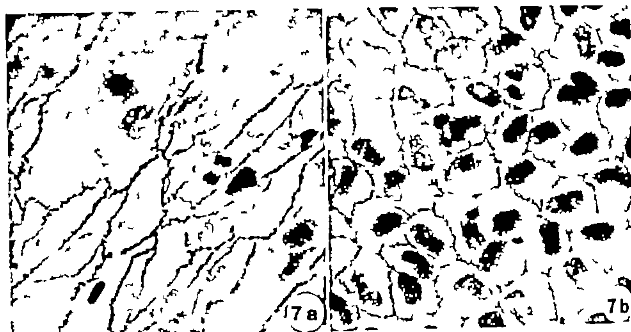


Fig 7 Häutchen stained by the Feulgen reaction a) Endothelial giant cells with several centrally localized nuclei, and a solitary mitotic figure 4 days after lesion × 640 Original magnification × 160. b) Hexagonal endothelium several cells are binucleate and multinucleate 14 days after lesion. × 640. Original magnification × 160

under white areas covered mainly by hexagonal endothelium as well as under blue coloured areas, covered by pseudo-endothelium.

3 Surface LM of aortae unstained of silver from 11 animals rendered no information on the patterns of surface cells, as the cell boundaries were hardly visible.

4 Hautchen from 25 animals (Fig 7 a and b) White areas Normal and hexagonal endothelium showed cells with double nuclei and giant endothelial cells containing more than 5 centrally situated nuclei. Blue areas Smooth muscle with typical spindle formed cells together with pseudo-endothelium with oval nuclei often as double nuclei presented even transition. Non uniform staining and size of the nuclei were prominent particularly in the white area but unmistakeable mitotic figures were very rare

5 Fluorescence microscopy of 33 animals (Fig 9) Fluorescence microscopy provides the possibility of locating Evans blue albumin colour complex by the prominent orange-red fluorescence of this stain (*Steinwall & Klatzo* 1966 *Heck et al.* 1976)

Control animals Yellow and/or green fluorescence of the elastic lamellae was prominent (Fig 9 a) Opposite the discrete blue stripes on the dorsal wall of the normal thoracic aorta there was a weak reddish fluorescence of the internal elastic membrane, and a suggestion of reddish fluorescence in the nearest elastic lamellae (Fig 9 b)

Experimental animals Without regard to the stain binding the following changes were recognized Neo-intima increased in thickness until the 30th day The thickness decreased after 2 and 6 months. Cushion shaped thickenings of the neo-intima (Fig 9 e) were prominent between the 14th day and 2 months after 6 months, the neo-intima was uniformly thickened. Necrosis occurred in the media from and including the 8th day with increasing dissemination in the later experiments. After 6 months, the elastic lamellae were indistinct, with irregularly arranged lamellae (Fig 9 g)

Sections from macroscopically white areas Until the 30th day the neo-intimal thickening presented a diffuse reddish fluorescence, including the neo-intima and the adjacent

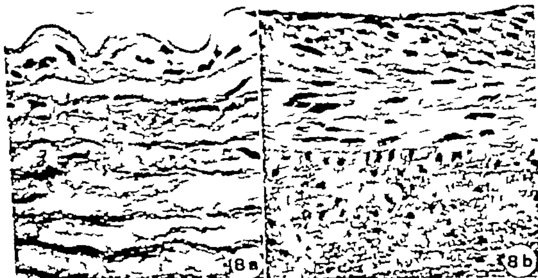


Fig 8 Conventional light microscopy) Toluidine blue, pH 3 1 day b) V. Gieson Hansen, 30 days after lesion. a) Intima is totally removed, round cell infiltration and oedema in the luminal zone of media. × 640. Original magnification × 160 b) Neo-intima with spindle shaped cells, probably smooth muscle cells. × 400. Original magnification × 100

elastic membranes. This diminished within the observation period (Fig 9 f) After 60 days, the reddish fluorescence was rare in the neo-intima and after 6 months, it was completely absent from the luminal zone of the vessel (Fig 9 g)

Sections from macroscopically blue areas During the first 14 days of the experiment, the walls of the vessel were strongly reddish in their fluorescence in all of the layers (Fig 9 c) In the majority of sections, at intervals of from 21 and 30 days after the lesion, a narrow green-red fluorescent zone occurred on the adventitial side of the media. After 6 months, approximately half of the luminal zone of the media was uniformly orange-red, whereas the neo-intima presented a yellow fluorescence (Fig. 9 h) A common feature in the experimental animals was a decreasing reddish fluorescence in the wall of the aorta throughout the whole of the experimental period. This was most obvious in the macroscopically white areas which, 6 months after the lesion, appeared to have no albumin-bound Evans blue in the luminal zone of the aortic wall.

Zones of transition between the macroscopically white and blue intima The border between the greenish and reddish fluorescent media was relatively sharp and, after 14 days (Fig 9 d) a massive cushion-formed intimal thickening (Fig 9 e) was often seen luminally to the transitional zone. The cushion-shaped neo-intimal thickening presented in tense orange red fluorescence.

6 Transmission LM Conventional connective tissue staining of sections from 19 experimental animals from various blue, white and mixed blue and white areas showed the same time dependent changes as those earlier described (*Helin et al.* 1971) (Fig 8 a and b) A course correlation of LM with the sites of necrobiopsies indicated on the photograph revealed no qualitatively different structure of neo-intima and media in sections from blue and white areas.

DISCUSSION

The method of vital staining used in our investigation is analogous with the method used by *McGill et al* 1957 *Packham et al.* 1967

Bjorkerud & Bondjers 1971 *Somer et al.* 1972, *Bell et al* 1972 *Caplan & Schwartz* 1973 *Caplan et al* 1974

According to *Zi...a*, 1958 there was a considerable difference in the measurements of the plasma volume determined by Evans blue and by I^{131} labelled rabbit albumin, inasmuch as the following values of TER_{EB} = 27 4 per cent per hour and $TER_{I^{131}\,Alb}$ = 15.5 per cent per hour were found In our investigation, the amounts of dye given are 50 times greater than those used in the above mentioned investigation even so it does not bring about an increase in the percentage of free Evans blue, whether estimated *in vivo* on the basis of the value found to apply to TER of 20 8 ± 4 0 per cent per hour ($\bar{x}$ ± 2 SD) or on the basis of *in vitro* measurement where ultrafiltration shows a degree of protein binding exceeding 96 per cent. These results indicate that the staining agent in our experiments is protein bound Evans blue cf *Packham et al* 1967 who ascribed macroscopical blue staining to local accumulation both of albumin and Evans blue in the aortic wall.

Two routes may be considered in the staining of the aortic wall The intimal zone is exposed to the dye via the blood in the lumen of the vessel whereas the adventitial zone probably receives the dye via vasa vasorum (*Heck et al* 1976) The presence or absence of the orange red fluorescence characteristic of protein bound Evans blue (*Steinwall et al.* 1966) was used to examine the penetration of dye from the lumen into the vascular wall.

Vital staining with Evans blue revealed a decreasing permeability of the aortic wall associated with expansion of macroscopically unstained white areas A common feature to be observed by LM of white areas were continuous and unbroken silver lines of the patterns of normal and hexagonal endothelium A preliminary study using EM (*Collatz Christensen et al* 1976) seems to suggest that the cell junctions in the white areas of experimental animals were extensive with well-differentiated, flaplike junctions between cells which were of an appearance as modified endothelial cells. Our investigation using fluorescence microscopy showed that the normal aortic wall was totally impermeable to Evans blue apart from the discrete longitudinal blue stripes on the dorsal aortic wall, which probably are the sites of a haemodynamic strain and increased endothelial

---

Fig 9 Fluorescence photomicrographs of the rabbit thoracic aorta after vital staining with Evans blue. Brilliant orange-red fluorescence Evans blue, probably coupled with plasma albumin. Green and yellow fluorescence autofluorescence of elastic tissue and unspecific fluorochromes, Original magnification of all photomicrographs × 40

a) Sham operated control, 21 days after ligature of the left femoral artery *Intima* hardly visible. *Media* Internal and external elastic membranes are yellow The bulk of elastic membranes are green with dispersed yellow shading. Adventitia almost completely removed.

b) Sham operated control 21 days after operation Section from a longitudinal blue stripe. Orange-red fluorescence of the luminal sector of media. Yellow fluorescence of adventitia and approximate zone of media.

c) One day after lesion caused by embolectomy catheter: intense orange-red fluorescence of the entire wall.

d) Transitional zone between macroscopical blue and white area 14 days after lesion inflicted by embolectomy catheter To the left Section from blue area shows brilliant orange-red media and a narrow peripheral unstained green sector To the right Section from a white area presents unstained green media except for a narrow orange-red luminal zone. The intima, partly lost by section, appears almost unstained.

e) Transitional zone 30 days after lesion, covered by a cushion-like neo-intimal thickening The cushion is intensely orange-red. The media immediately below the cushion and a yellow intimal elastic membrane seemed to remain unstained, whereas the neighbouring media not covered by the cushion is intensely orange-red throughout all layers.

f) Macroscopical white area 30 days after lesion. The neo-intimal thickening appears unstained the luminal part of the media is faintly stained, yellow with traces of orange.

g) Macroscopical white area, 6 months after lesion, The aortic wall is unstained green the contours of elastic lamellae are distinct and blurred.

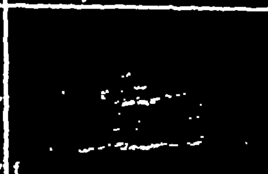
h) Macroscopical blue area, 6 months after lesion. The neo-intimal thickening is yellow and, approximately half of the media is uniformly orange-red. The adventitia is almost missing and the adjacent part of the media is unstained.


a

b

c

d

e

f

g

h

turnover (*Schwartz* & *Bendit* 1972 *Wright et al* 1975 *Ross* & *Glomset* 1976) It remained an unanswered question why macroscopically white endothelial areas in the experimental animals were partially permeable during the first weeks and later on after 60 days and half a year, resisted penetration of the dye. The problem of endothelial permeability is complex and besides differentiation of intercellular junctions (*Schwartz et al* 1975) multiple factors may play a role under pathophysiological conditions (*Hüttner et al* 1970 *Schwartz* & *Bendit* 1972) with regard to the passage of macromolecules through the aortic endothelium.

The blue areas of the vital stained intimal surface were generally denuded surfaces and surfaces covered with pseudo-endothelium. It cannot be precluded that Evans blue protein complex may have penetrated between discontinuous cell junctions, a feature which was suggested by surface LM of the prominence of serrated and foam-like patterns of silver lines in the pseudo-endothelium. In a previous study based on EM (*Collat Christensen et al* 1976) discontinuous cell junctions between surface cells resembling modified smooth muscle cells were evident in sections from blue areas covered by pseudo-endothelium. The importance of discontinuous cell junctions in the vascular permeability of Evans blue may find some further support in the fact that hexagonal endothelium with stomata in the silver lines also presented a certain degree of macroscopical blue staining However the possible role of stomata in the complex of problems concerning the permeability of the endothelium is still under debate (*Bjorkerud* & *Bondjers* 1972 *Bjorkerud et al* 1972 *Caplan et al* 1974)

The boundary zones between white and blue stained intima presented a blue stained brim on the endothelial side of the linear boundary between endothelium and pseudo-endothelium. Proliferative processes in these zones were presently suggested from the prominence of endothelial giant cells (*Poole et al* 1958 *Poole et al.* 1959 *Cotton et al.* 1961) and of hexagonal endothelium the increased permeability was probably caused by t local dominance of newformed "unripe" cells (*Gottlob* & *Zinner* 1962) By fluorescence microscopy the border zones of white and blue intimal areas were represented by elastin rich cushion-shaped neo-intimal thickenings which were intensely stained by Evans blue not withstanding its function as a barrier against staining of the media. The boundary zones between endothelium and pseudo-endothelium may represent a zone of interaction between growth of endothelium and of smooth muscle cells or cells derived from smooth muscle cells pseudo-endothelium on the intimal surface and myo-elastic tissue in the thickened neo-intima. According to *Schwartz et al* 1975 *Spaet et al* 1975 *Fishman et al* 1975 the endothelium inhibits proliferation of smooth muscle cells in the neo-intima The replacement by genuine endotheilum of the pseudoendothelium which most probably is derived from smooth muscle cells, could possibly be attributed to analogous factors governing this interplay

Generally the permeablity of the aortic wall decreased throughout the experimental period, the phenomenon was most distinct in areas covered by endothelium which was rendered impermeable within 2-6 months Denuded areas and areas covered by pseudo-endothelium remained permeable. On the consideration that transmission LM and fluorescence microscopy did not reveal qualitative differences in the morphology of the neo-intima and media from white and blue areas it was concluded that genuine endothelium played the decisive role in the re-establishment of an efficient barrier against penetration of macromolecules from the blood into the deeper layers. However biochemical and structural changes in these layers which may affect their dye-binding capacity may also be involved. Macroscopically blue areas presented decreased reddish fluorescence after intervals of 60 days up to six months and on the assumption that the penetrability of pseudo-endothelium does not decrease with time, a decreased dye-binding capacity of the neointima and media must be suggested Ac

cording to *Helin et al.* 1971 the increased permeability to I[125]-albumin following the lesion caused by an embolectomy catheter normalized after 60 days. Time dependent changes in the vascular connective tissue including an increased content of hyaluronic acid in conjunction with an expansion of the endothelium on the intimal surface, may have been co-factors in processes leading to a decreased permeability of the healing aortic wall.

The lesion caused by an embolectomy catheter is induced via an unphysiological trauma. However pathophysiological processes relevant to human pathology may be submitted to research by the study of injury and repair processes following the lesion. In a previous work mentioned above, *Helin et al.* 1971 observed time dependent alterations in glycosaminoglycans and in collagen, alterations which were related to those in unspecific granulation tissue and resembling biochemical changes in human arteriosclerosis (*Lo cuzen* 1975). In a survey on the pathogenesis of atherosclerosis *Ross & Glomset* 1976, have recently emphasized the importance of disruption of the endothelial barrier, platelets and smooth muscle cell proliferation.

In the present study the permeability of a healing intimal surface seemed primarily to depend on the luminal penetrability of the neo-intima. The factor of primary importance was the presence of a genuine endothelium, the expansion of a genuine endothelium brought about a decrease in the total permeability of the aortic wall. Changes in the new-formed endothelium, probably in the form of differentiation of intercellular junctions, and connective tissue changes in the neo-intima and media seemed to be additional factors which influenced the uptake and binding of Evans blue protein-complex in the arterial wall.

The hypothesis according to which reestablishment of normal permeability of a damaged intimal surface depends on growth and expansion of endothelial cells and on differentiation of intercellular contacts between endothelial cells found support in the outstanding ultrastructural research by *Schwartz et al.* 1975 who studied the healing of lesions caused by an embolectomy catheter.

REFERENCES

Bell, F. P., Somer J. B., Craig I. H. & Schwartz, C. J. Patterns of aortic Evans blue uptake in vivo and in vitro. Atherosclerosis *16* 369–375 1972.

Björkerud, S. & Bondjers G. Arterial repair and atherosclerosis after mechanical injury. Part 1. Permeability and light microscopic characteristics of endothelium in non-atherosclerotic and atherosclerotic lesions. Atherosclerosis *13* 355–363 1971.

Björkerud S. & Bondjers G. Endothelial integrity and viability in the aorta of the normal rabbit and rat as evaluated with dye exclusion tests and interference contrast microscopy. Atherosclerosis *15* 285–300 1972.

Björkerud S., Hansson, H.-A. & Bondjers, G. Subcellular valves and canaliculi in arterial endothelium and their equivalence to so-called stigmata. Virchows Arch. Abt. B *11* 19–23 1972.

Caplan B. A., Gerrity R. G. & Schwartz C. J. Endothelial cell morphology in focal areas of in vivo Evans blue uptake in the young pig aorta. I. Quantitative light microscopic findings. Exp. molec. Path. *21* 102–117 1974.

Caplan B. A. & Schwartz, C. J. Increased endothelial cell turnover in areas of in vivo Evans blue uptake in the pig aorta. Atherosclerosis *17* 401–417 1973.

Collatz Christensen B., Chemnitz J. & Thoee, L. Repair in arterial tissue. Electron microscopy of Evans blue vital stained embolectomy catheter lesion of the rabbit thoracic aorta. Acta path. microbiol. scand. Sect. A, *84* 355–357 1976.

Collatz Christensen B. & Garbarsch C. Repair in arterial tissue. A scanning electron microscopic (SEM) and light microscopic study on the endothelium of rabbit thoracic aorta following a single dilatation injury. Virchow Arch. Abt. A *360* 93–106 1973.

Cotton R. E., Harwood T. R. & Wartman, W. B. Regeneration of aortic endothelium. J. Path. Bact. *81* 175–180, 1961.

Fishman J. A., Ryan G. B. & Karnovsky M. J. Endothelial regeneration in the rat carotid artery and the significance of endothelial denudation in the pathogenesis of myointimal thickening. Lab. Invest. *32* 339–351 1975.

Friedman M. & Byers S. O. Endothelial permeability in atherosclerosis. Arch. Path. *76* 99–105 1963.

Cattlob R & Zinner C Über die Regeneration geschädigter Endothelien nach hartem und weichem Trauma. Virchows Arch. path Anat. *336* 16 52 1962

Heck A F Hasuo M Furuse M Brock M & Dietz H Distribution of serum protein labelled with Evans blue in the walls of extra and intracranial blood vessels of the cat. *Atherosclerosis 23* 227-238 1976

Helin P Lorenzen I Garbarsch C & Matthiessen M E Repair in arterial tissue Morphological and biochemical changes in rabbit aorta after a single dilatation injury Circulat Res. *29* 542-554 1971

Hüttner I More R H & Rona G Fine structural evidence of specific mechanism for increased endothelial permeability in experimental hypertension. Amer J Path. *61* 395-412 1970

Lorenzen I Injury and repair in vascular connective tissue In Biology of Fibroblast. Ed F Kulonen & J Pikkarainen Acad. Press. London New York 1973 p 601-614

McGill H Geer J G & Holman R L Sites of vascular vulnerability in dogs demonstrated by Evans blue Arch Path. *64* 303 311 1957

McManus J F A & Mowry R H Staining Methods. Histologic and Histochemical Harper & Row New York 1964

Nielsen M H & Nielsen N C Spectrophotometric determination of Evans blue dye in plasma with individual correction for blank density by a modified Gaeblers method. Scand. J clin Lab. Invest. *14* 605-617 1962

Packham M A Rowsell H C Jorgensen L & Mustard J F Localized protein accumulation in the wall of the aorta. Exp molec Path. *7* 214-232 1967

Pearse A C E Histochemistry Theoretical and Applied 3 ed vol I and II Churchill London 1968 1972

Poole J C F Sanders A G & Florey H W The regeneration of aortic endothelium. J Path Bact. *75* 133 145 1958

Poole J C F, Sanders A G & Florey H W Further observations on the regeneration of aortic endothelium in the rabbit. J Path. Bact *77* 637 1959

Romeis B Mikroskopische Technik. Leibniz, München 1948

Ross R & Glomset J A The pathogenesis of atherosclerosis. The New England Journ. Med *295* 369-377 1976

Rossing N Human Albumin Metabolism Determined with Radioiodinated Albumin. Munksgaard Copenhagen 1971 p 16

Schwartz S M & Benditt E P Studies on the aortic intima. I Structure and permeability of rat thoracic aortic intima Amer J Path *66* 241-264 1972

Schwartz S M Stemerman M B & Benditt E P The aortic intima. II Repair of the aortic lining after mechanical denudation. Amer. J Path *81* 15-42 1975

Somer J B Evans G & Schwartz C J Influence of experimental aortic coarctation on the pattern of aortic Evans blue uptake in vivo Atherosclerosis *16* 127-133 1972.

Spaet T H Stemerman M B Veith F J & Lejnieks I Intimal injury and regrowth in the rabbit aorta. Medial smooth muscle cells as a source of neointima Circulat. Res. *36* 58-70 1975

Steinwall O & Klatzo I Selective vulnerability of the bloodbrain barrier to chemically induced lesions. J Neuropath. exp. Neurol. *25* 542-559 1966

Tornberg A Determination of T 1824 (Evans blue dye) in lipemia and hemolysis with a modified extraction method. Acta med scand. *161* 69-77 1958

Wright H P Evans M & Green R P Aortic endothelial mitosis and Evans blue uptake in cholesterol fed subscorbutic guinea pigs. Atherosclerosis *21* 105-113 1975

Zizza F & Reeve E B Erroneous measurement of plasma volume in the rabbit by T *1824* Amer J Physiol *194* 522-526 1958

Acta path. microbiol. scand. Sect. A, 85 311-318, 1977

SPONTANEOUS MAMMARY CARCINOMA IN C57BL AND C3H MICE

A Histochemical Study

A. Gad C. Rowlatt and M U Sheriff

The Department of Histopathology Royal Postgraduate Medical School, Du Cane Road, London W12 OHS and The Department of Cellular Pathology Imperial Cancer Research Fund, Lincoln Inn Fields, London WC2

Gad, A Rowlatt, C. & Sheriff, M. U Spontaneous mammary carcinoma in C57BL and C3H Mice: A histochemical study Acta path. microbiol. scand. Sect. A, 85 311 318, 1977

The mucosubstances in series of 12 mammary carcinomas arising in C57BL mice were compared with those in tumours in some C3H mice and with normal resting" and lactating glands. A strain difference rather than a difference according to tumour type was found. The epithelial elements in the C57BL tumours contained mainly sialomucin with a little neutral mucosubstance and sulphomucin was present in some. Sulphated mucopolysaccharide was prominent in the stroma of these tumours. The C3H mice tumours contained no sulphomucin, less sialomucin but more neutral mucosubstance. The mucosubstances were studied in serial transplants of four tumours. An acid to neutral mucosubstance change with dedifferentiation of the tumour has been observed and found to be similar to series of changes previously observed in a group of human gastrointestinal tumours.

Key words Mammary carcinoma, spontaneous C57BL and C3H mice histochemistry

A Gad, Department of Histopathology and Cytology Falu Hospital, Falun, Sweden.

Received 25 viii.76 Accepted 9.xi.76

Whereas C3H and other mouse strains carrying mammary tumour virus (MTV) are known to have a high incidence of spontaneous breast cancer the incidence of epithelial tumours of the mammary gland in C57BL mice is low (*Murphy* 1966)

Dunn (1959) stated that mammary tumours in mice are the tumours most completely studied However we have found no studies of the mucosubstances of these tumours comparable to that on human breast cancer (*Gad & Azzopardi* 1975) Such investigation of mouse mammary carcinoma might indicate the extent to which this tumour in mice can be compared with the human disease. Furthermore differences in the histochemical behaviour of tumours in strains with high and low tumour incidence might be of interest. Similar comparative studies of the alimentary tract in man and mouse were undertaken (*Gad* 1967 *Rowlatt et al.* 1969)

The mucosubstances of mammary carcinomas from inbred strains of mice with high and low incidence of these tumours are described in this paper Spontaneous tumours as well as transplants from them were studied.

MATERIALS AND METHODS

The tumours arose in mice from a colony maintained at The Imperial Cancer Research Fund,

London (ICRF) primarily to provide adult and aged mice for tissue culture and other experiments. The management has been described (*Rowlatt et al* 1969) The mammary tumours from C57BL mice (12) were collected from 1488 autopsies carried out between 1964 and 1970. Nine mammary tumours from C3H/He C3H/Bi or C3H/A vy (Table 3) were taken for comparison The tumours were grouped using *Dunn's* classification adenocarcinomas type A B and C adenoacanthoma and anaplastic carcinoma (Tables 3 & 4) "Resting" and lactating mammary tissue from normal C57Bl and C3H mice were included in the study Small pieces from four tumours were transplanted subcutaneously into young syngeneic mice using a Bashford needle

This histochemical study was performed on tissues satisfactorily fixed in 4 per cent formaldehyde to which 1 per cent $CaCl_2$ was added they were paraffin embedded and sectioned at 5 μm. In addition to routine haemalum (Erlich's) and eosin staining of all samples, histochemical mucosubstance techniques similar to those used by *Gad* (1969) were employed Staining included Periodic acid-Schiff both with and without diastase pre treatment, D/PAS and PAS (*Lillie* 1954 *McManus* 1946) Alcian blue "pH 2.5"/Periodic acid-Schiff AB/PAS (*Mowry & Winkler* 1956) High iron diamine/Alcian blue HID/AB (*Spicer* 1965) sialidase and hyaluronidase digestion followed by AB/PAS Sial and Hyal. AB/PAS (*Spicer & Warren* 1960 *Curran & Kennedy* 1955) Scott's critical electrolyte concentration technique (CEC) (*Scott & Dorling* 1965 *Scott* 1972) was also used in all cases for further characterization of stromal mucopolysaccharides

RESULTS

Results were interpreted according to usual estimation of the intensity of colour reactions of the histochemical methods listed in Table 1 Table 2 summarizes the results of staining of most of the tissues studied

Normal 'Resting' and Lactating Mammary Glands

A thin layer of sialidase-susceptible sialomucin was found to line the luminal surface of the ducts and the lobular terminal units in the "resting" mammary gland. The lumina contained a predominantly neutral mucosubstance with a minimal amount of sialomucin mainly located at the margins. In the lactating gland, sialomucin was located on the luminal surface of ducts as well as of acini Acini are present only in lactating tissue Sialomucin formed the bulk of the luminal secretion in the acini together with a little neutral mucosubstance (Fig 1) Globules of sialomucin were also present in the acinar cells. The very small amount of blue staining acid mucosubstance in AB/PAS preparations was masked by the red neutral mucosubstance in the "resting" gland. In the lactating gland there was more alcianophilic acid mucosubstance (Fig 2) Mast cells were distributed around gland lobules, between the acini and along the basement membranes of ducts and ductules.

TABLE 1 *Results and Significance of the Histochemical Methods*

Method	Result	Conclusion
PAS	Red or magenta	Glycogen neutral or acid mucosubstances
D/PAS	Disappearance of red colour	Glycogen
AB/PAS	Blue Red or magenta Purple	Acid mucosubstances Neutral mucosubstances A mixture of both
HID/AB	Grey to black Blue	Sulphomucins Acid non-sulphated mucosubstances
Sial AB/PAS	Loss of blue	Sialic acid
Hyal AB/PAS	Loss of blue	Hyaluronic acid and chondroitin sulphate A & C

TABLE 2. *Histochemical Reactions of the Epithelial Elements of "Resting" and Lactating Breast and Mammary Tumours from C57BL and C3H Mice*

Tissue		PAS	D/PAS	AB/PAS	HID/AB	Sial. AB/PAS	Hyal. AB/PAS
Normal "resting"	luminal secretion	+ + + M	+ + + M	+ + M + BP	+ B	+ + MR	+ + M + BP
	cell surface	+ + M	+ + M	+ + BP	+ + B	+ + MR	+ + BP
Lactating glands	acinar lumina	+ + + M	+ + + M	+ + P + B	+ + B	+ + M	+ + P + B
	cells	+ M	+ M	+ B	+ B	+ M	+ B
C57BL tumour epithelium		+ + + M	+ + + M	+ + B + P + MR	+ + B ± G to Br	+ + M ± B	+ + B + P + MR
C3H tumour epithelium		+ + + M	+ + + M	+ + M + BP	+ + B	+ + M	+ + M + BP

Abbreviations and designations used in the table B = blue Br = brown, G = grey M = magenta, P = purple and R = red. A strongly positive reaction is designated (+ + +) a moderately positive reaction (+ +) a weak positive reaction (+) and a trace reaction (±)

Mammary Tumours

Typing of the tumours strictly according to Dunn's criteria proved to be difficult. Type C tumours could be characterized by a continuous layer of myo-epithelial cells and prominent stroma. Most A and B types proved to be mixed with areas of either type within a single section. The tumour was labelled A or B if either of these types formed more than 60 per cent of the section area. Tumours with almost equal parts of the two were classified as "Mixed A & B" (Table 3). In this paper the term anaplastic carcinoma was used to describe all poorly differentiated adenocarcinomas and not exclusively to describe "Carcinosarcoma" as in *Dunn's* classification.

In this small series, the C3H tumours were more uniform in type (mostly B or mixed A & B with a single type A tumour) than the C57BL tumours. The whole range of possible tumour types were found in C57BL mice and, not infrequently more than one type was seen in the same tumour The tumours in C57BL mice occurred in older animals.

Histochemical studies of the spontaneous tumours showed that the relative distribution of the mucosubstances in the tumours appeared to depend on the strain of mouse rather than on the histological type of tumour The

TABLE 3 *Tumour Types in Strains of Mice*

Tumour type	Mouse strain			
	C57BL	C3H He	C3H Bi	C3H Avy
Type A		1	–	–
Type B	2		5	2
Mixed A & B		2		1
Type C	5		–	–
Adenoacanthoma	2	–		–
Anaplastic carcinoma	3	–		–

TABLE 4 *Age Distribution and Types of Mammary Tumours in C57BL and C3H Mice*

Age (months)	C57BL No	C57BL Tumour types	C3H No.	C3H Tumour types
4–6	–		3	B B B + A
7–9	–		–	
10–12	–		2	B, B + A
13–15	–		–	
16–18	1	anapl carc.	2	B B + A
19–21	1	adenoacanthoma anapl carc. ×?	1	B
22–24	5	adenoacanthoma C, C	1	A
25–27	2	B C	–	
28–30	1	C	–	
31–33	2	B C	–	

N B anapl carc. anaplastic carcinoma

secretions from the tumour cells in C57BL mice contained predominantly sialomucins with a little neutral mucosubstance (Fig 3–7) Sulphomucins were seen in the epithelial secretions (Fig 8) in three out of twelve C57BL tumours. Sialomucins were found on the surface of the epithelial cells as well as in the luminal secretion (Fig 7) while sulphomucins were found only in the secretion (Fig 8) The epithelial tumour cell secretion in C3H mice contained more neutral mucosubstance than the C57BL mouse tumours and relatively less acid mucosubstances. No luminal sulphomucins were seen in the secretion from these tumours.

In the stroma of the C57BL mouse tumours sulphated mucopolysaccharides were prominent (Fig 3–6) although they were absent in the stroma of normal glands (Fig 1 & 2) Very small quantities of this material were found in the stroma of a few C3H tumours This stromal mucopolysaccharide was hyaluronidase susceptible and stained with Alcian blue up to 0.5 M $MgCl_2$ with *Scott's* method This indicated that the stromal mycopolysaccharide contained chondroitin sulphate A and/or C

Different types of mammary tumours (Tables 3 & 4) were observed in these mice However we were unable to associate any particular mucosubstance with any of these tumour types. But as the histological structure of the tumour altered to a less differ

Fig 1 Lactating C57BL mammary gland with purple mucosubstances in the lumina and blue mast cells along the basement membranes of ducts and acini. Alcian blue/Periodic acid-Schiff. × 100.

Fig 2 Lactating C57BL mammary gland showing Alcian blue positive mucosubstances in the lumina of ducts and acini and brown, high iron diamine positive mast cells. High iron diamine/Alcian blue × 100

Fig 3 C57BL mammary tumour showing Alcian blue positive stromal mucopolysaccharides and purplish glandular mucosubstances. AB/PAS. × 200.

Fig 4 The same tumour after digestion with hyaluronidase and subsequent staining with AB/PAS Disappearance of the blue colour from the stroma indicates digestion of the stromal mucopolysaccharides. Hyal AB/PAS × 250

Fig 5 The same tumour after digestion with sialidase showing persistence of the Alcian blue staining of the stromal mucopolysaccharides. Sial. AB/PAS × 250

Fig 6 C57BL mammary tumour showing dark brown stromal mucopolysaccharides and blue glandular mucosubstances. HID/AB. × 250.

Fig 7 A larger magnification of the same tissue as that seen in figure 6. HID/AB. × 400

Fig 8 C57BL mammary tumour with HID-positive intraluminal glandular sulphomucin. HID/AB. × 400



entiated form as in anaplastic carcinoma and as seen during serial transplantation described below there was a change in the proportions from mainly acid to neutral mucosubstances. *In anaplastic tumours*, the secretion was mainly a neutral mucosubstance with minimal amounts of sialomucins. Sulphomucins in the secretion and mucopolysaccharides in the stroma were absent in these cases.

Mammary Tumour Transplants

Serial transplant generations of three C57BL and one C3H/He tumour were included in the study. C57BL tumours did not have a well-defined pattern. One poorly differentiated tumour with some tubular areas produced a rather well-differentiated tubular tumour in the two transplant generations studied. Another well-differentiated tumour was similar to the original tumour in the first passage though it became less well-differentiated during subsequent passages: by the ninth passage it was a carcinosarcoma. In passages 10 to 18 "sarcomatoid" elements were present. The third transplanted tumour was originally anaplastic: it persisted in this form for seven passages. The C3H tumour changed from a moderately differentiated carcinoma to a "carcinosarcoma" over eight passages.

The staining pattern of the transplanted C57BL tumours varied with the degree of differentiation of the tumour. The stable tumour types retained a correspondingly stable pattern of mucosubstances whether differentiated or anaplastic. The transition from carcinoma to carcinosarcoma was marked by a loss of sulphated mucosubstances both in stromal and glandular elements during the initial dedifferentiation. "Carcinosarcoma" had only a minor amount of neutral mucosubstance as related to the epithelial tissue. No stromal mucopolysaccharides were found in the sarcomatous passages. In the C3H tumour, the carcinoma "carcinosarcoma" transition was marked by the disappearance of the small amounts of neutral and weakly acid mucosubstances.

DISCUSSION

In the present paper a retrospective study of the histochemistry of the mucosubstances of mammary tumours which arise very rarely in a long lived strain of mice C57BL is described. Mammary tumours are rare in C57BL mice and in this colony the incidence was 0.34 per cent (*Rowlatt et al.* 1976). These tumours were compared with a small group of the common mammary tumours to arise in C3H mice. The age distribution of mammary tumours fitted the range accepted for C3H mice while they occurred in an older age category in the C57BL mice between 16 and 33 months (Table 4).

The mucosubstances produced by the mammary tumours did not show a difference consistent with their histological types, but depended rather on a strain difference. Stromal sulphated mucopolysaccharides containing chondroitin sulphate A and/or C were prominent in tumours from C57BL mice but rare or absent in tumours from C3H mice. Epithelial sulphomucins were found only in the tumours from C57BL mice, not even in all of these. As regards this strain difference it is of interest that the type of mucin found in a variety of human mammary tumours is similar to that found in the C3H mice. No mucin secreting human mammary carcinoma was found to produce significant amounts of stromal sulphated mucopolysaccharides (*Spicer et al.* 1962, *Cooper* 1974, *Gad & Azzopardi* 1975).

The development of mammary tumours in mice is known to be influenced by a variety of factors including genotype, viral agents, chemical carcinogens, endocrine status and obesity (*Nandi & McGrath* 1973). Our results are in agreement with the conclusions drawn by *Murphy* (1966), namely that mammary tumours in high incidence strains (such as C3H) tend to occur during the latter half of the first year of life and in the early part of the second year (Table 4). In the C3H strain, two mammary tumour viruses have been recognized: the mammary tumour virus (MTV, Bittner's milk agent) of high and

early oncogenic activity and the transplacentally transmitted nodule-inducing-virus (NIV) of high, but late oncogenic activity (*Medina et al.* 1973). Our C3H/A^{vy} mice have been found to carry both MTV and NIV (*Heston & Vlahakis* 1968). In addition we used two substrains, C3H/Bi and C3H/He, reputedly carrying the agent or agents which have been maintained at ICRF since 1941 and 1958, respectively. The C3H type of mucosubstance staining was maintained in these substrains.

Sarcomatoid changes in transplanted mammary carcinomas are generally known to occur *in vivo* (Snell 1958. Toolan & Kidd 1950) and *in vitro* (*Ludford & Barlow* 1945). Four explanations have been advanced with a view to defining this phenomenon in pulmonary tumours (*Stewart et al.* 1947): overgrowth by a sarcomatous element in the original tumour; transformation by mutation of carcinoma cells into sarcomatoid cells; neoplastic transformation of normal stromal cells to be carried over from the original animal or alternatively to be derived from recipient animals. When sarcomatoid change takes place stainable mucosubstances disappear from the neoplastic tissues. As the epithelial elements of the transplanted tumours dedifferentiate on repeated passage, we have found that they lose their acidic mucins prior to this stage and that only small amounts of a neutral mucosubstance are to be found. The postulated change of type of mucosubstance accordingly as the tumours become less differentiated is consistent with the finding of a similar series of changes in a group of human gastrointestinal tumours previously reported (*Gad* 1969).

Epithelial stromal interaction is known to be important in the differentiation of tissues. It is therefore interesting to find a situation in which differences in stromal secretions are present in tumours in strains with high and low tumour incidence.

We thank Professor *J. G. Azzopardi*, Dr. *I. M. F. Hicks* and Dr. *St. Clair Young* for their valuable advice and criticism. We are indebted to Mr. *W. F. Hicks* for photography, Miss *Ulla Backlund* and Mrs. *Kristina Lärka* for secretarial help. The support of the *Imperial Cancer Research Fund* for publishing the coloured plate is appreciated.

REFERENCES

1. *Cooper, D. J.*: Mucin histochemistry of mucous carcinomas of breast and colon and non-neoplastic breast epithelium. J. Clin. Path. 27: 311-314, 1974.
2. *Curran, R. C. & Kennedy, J. S.*: The distribution of the sulphated mucopolysaccarides in the mouse. J. Path. Bact. 70: 449-457, 1955.
3. *Dunn, T. B.*: Morphology of mammary tumours in mice. In The physiopathology of cancer. 2nd ed., edited by F. Homburger. New York, p. 38, 1959.
4. *Gad, A.*: A histochemical study of alimentary tract mucins in health and disease with special reference to the stomach. Ph. D. Thesis, London University, 1967.
5. *Gad, A.*: A histochemical study of human alimentary tract mucosubstances in health and disease. I. Normal and tumours. Brit. J. Cancer 23: 52-63, 1969.
6. *Gad, A. & Azzopardi, J. C.*: Lobular carcinoma of the breast: a special variant of mucin-secreting carcinoma. J. Clin. Path. 28: 711-716, 1975.
7. *Heston, W. E. & Vlahakis, G.*: C3H-A^{vy}—a high hepatoma and high mammary tumour strain of mice. J. Natl. Cancer Inst. 40: 1161-1166, 1968.
8. *Lillie, R. D.*: Histopathologic technic and practical histochemistry. 2nd ed. The Blakiston Co., New York, 1954.
9. *Ludford, R. J. & Barlow, H.*: Sarcomatous transformation of the stroma of mammary carcinomas that stimulated fibroblastic growth in vitro. Cancer Research 5: 257-264, 1945.
10. *McManus, J. F. A.*: The histological demonstration of mucin after periodic acid. Nature (London) 158: 202, 1946.
11. *Medina, D., Lange, J. & Sedlacek, R.*: Mammary nodulogenesis and tumourigenesis in pathogen-free C3Hf mice. J. N. C. Cancer Inst. 151: 961-964, 1973.
12. *Mowry, R. W. & Winkler, C. H.*: The coloration of acidic carbohydrates of bacteria and fungi in tissue sections with special reference to capsules of cryptococcus neoformans, pneumococci, and staphylococci. Amer. J. Path. 32: 628-629, 1956.
13. *Murphy, E. D.*: Characteristic tumours. In Biology of the laboratory mouse, 2nd ed., edited by E. L. Green, New York, p. 521, 1966.

14 *Nandi S & McGrath C M* Mammary neoplasia in mice Advan. Cancer Res. *17* 353–414 1973
15 *Rowlatt C., Chesterman F C & Sheriff M U* Lifespan, age changes and tumour incidence in an ageing C57BL mouse colony Laboratory animals *10* 419-442 1976
16 *Rowlatt C Franks L M Sheriff M U & Chesterman F C* Naturally occurring tumours and other lesions of the digestive tract in the treated C57BL mice J Nat. Cancer Inst. *43* 1353–1364 1969
17 *Scott J E.* Histochemistry of Alcian blue. III The molecular biological basis of staining by Alcian blue 8GX and analogous phthalocyanins Histochemie *32* 191–212 1972
18 *Scott J E & Dorling J.* Differential staining of acid glycosaminoglycans (mucopolysaccharides) by Alcian blue in salt solutions. Histochemie 5 221–233 1965
19 *Snell G D* Transplantable tumours. In *The physiopathology of cancer* 2nd ed., edited by F Homburger New York, p 293 1958.
20 *Spicer S S* Diamine methods for differentiating mucosubstances histochemically J Histochem. Cytochem. *13* 211–234 1965
21 *Spicer S S Neubecker R. D., Warren L & Henson J G* Epithelial mucins in lesions of the human breast. J Nat Cancer Inst. *29* 963–975 1962.
22 *Spicer S S & Warren L.* Histochemical demonstration of rodent sialomucins. J Histochem. Cytochem. *8* 324–325 1960
23 *Stewart H L Grady M D & Andervont H B* Development of sarcoma at site of transplantation of pulmonary in inbred mice J Nat. Cancer Inst. 7 207–225 1947
24 *Toolan H W & Kidd J G* Sarcomatoid growths resulting from mammary carcinoma cells that had sojourned in immune mice. "abstracted in" Amer J Path. *26* 753–754, 1950

Acta path. microbiol. scand. Sect. A, 85 319–329 1977

ON THE EFFECT OF VINBLASTINE ON AMELOBLASTS OF RAT INCISORS *IN VIVO*

2. Protracted Effect on Secretory Ameloblasts. A Light Microscopical Study

H. Moe and Haroe Mikkelsen

Anatomy Department C, University of Copenhagen, Denmark

Moe, H. & Mikkelsen, H. On the effect of vinblastine on ameloblasts of rat incisors in vivo. 2. Protracted effect on secretory ameloblasts. A light microscopical study. Acta path. microbiol. scand. Sect. A, 85: 319–329, 1977.

The effects of vinblastine sulphate at a dosage of 0.2 mg per 100 g body weight on the secretory ameloblasts of rat incisors were studied 3, 6 and 24 hours and 3 and 7 days after administration of the drug. The vinblastine affected the secretion profoundly, caused a reduction in size of the cells and death of many ameloblasts. Most of the surviving ameloblasts restored initially-induced loss of polarity. Many also resumed secretion and deposition of enamel matrix. The Tomes processes were extremely sensitive to vinblastine and all matrix deposited after administration of the drug appeared abnormal in structure. Ameloblasts not resuming secretory activity were less than half the size (height) of normal cells. In some areas all the ameloblasts were destroyed with the exception of a varying number of surviving ameloblast parts consisting only of a nucleus and a small amount of cytoplasm. The ameloblasts which had re-established secretory activity and most of the ameloblasts which had not, retained their ability to transform into transporting ameloblasts. Large amounts of ameloblast debris present 3 and 6 hours after administration of the vinblastine were effectively engulfed and digested by the cells of the stratum intermedium within 24 hours.

Key words: Ameloblasts; vinblastine; rat.

H. Moe, Anatomy Department C, Universitetsparken 1, 2100 Copenhagen Ø, Denmark.

Received 10.xi.76. Accepted 17.xi.76

It is well known that the cancer chemotherapy agent vinblastine sulphate not only has a cytostatic effect but also causes morphological alterations and functional disturbances in several mature cell types. Thus, in secretory cells vinblastine rapidly affects secretion, disrupts microtubules, disturbs normal cytoplasmic organization and inhibits directional translocation of secretory granules. These short-term effects of vinblastine on secretion have been observed in several secretory cell types and are pronounced in the highly polarized secretory ameloblasts (*Moe & Mikkelsen* 1977). The long-range effect of vinblastine on normal secretory cells *in vivo* is sparsely clarified, however. The present work deals with the protracted effect of vinblastine on the secretory ameloblasts of the incisors of the rat.

Secretory ameloblasts were chosen in this study for the following reasons: 1) Their secretory character is well documented (see *Weinstock & Leblond* 1971). 2) They are highly polarized with a regular uniform internal organization. 3) Their secretory pro-

duct, the enamel matrix, is apposed *in loco* upon the tooth surface, permitting evaluation of the activity of the individual cells for a considerable period 4) They make up a well defined stage in a "cell cycle" comprising proliferating and differentiating ameloblasts and mature secretory and transporting ameloblasts all arranged in an orderly way allowing comparison with the various stages of the cycle and allowing study of the transition of one stage into the next.

The extent of the zone of secretory ameloblasts in proximo-distal direction is about 5 1 mm in the mandibular incisors and 3 8 mm in the maxillar incisors (*Warshawsky & Smith* 1974) The ameloblasts migrate with the continuously growing tooth and the individual cells secrete enamel matrix for about 8 (mandibular incisors) or 7 (maxillar incisors) days (*Smith & Warshawsky* 1975) The effect of vinblastine on ameloblasts, which were secretory when exposed to the drug was studied from 3 hours to 7 days after administration of the drug

MATERIALS AND METHODS

17 young female Wistar SPF rats weighing 90 to 120 g were used 7 animals served as controls and 10 animals each received intravenously 0 2 mg vinblastine sulphate (Velbe) per 100 g body weight. The solution used was 1 mg vinblastine per ml in 0 9 per cent sodium chloride The vinblastine-treated animals were sacrificed 3 hours (one animal) 6 hours (two animals) 24 hours (two animals) 3 days (three animals) and 7 days (two animals) after administration of the drug. In the controls vinblastine was omitted. One µm thick sections cut at short intervals perpendicular to the long axis of the teeth which were embedded in Epon were stained with toluidine blue The details of the preparative procedure was as earlier published (*Moe & Mikkelsen* 1977)

RESULTS

The controls The control tissue was as earlier described (*Moe & Mikkelsen* 1977)

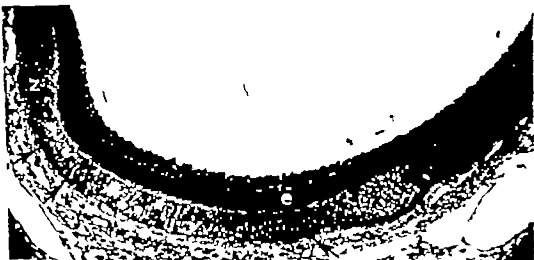
3 hours after administration of vinblastine The alterations consisted essentially of displacement of many nuclei to the middle or distal cell portion and of reduced stainability of the Tomes processes and the apical cytoplasm.

6 hours after administration of vinblastine Alterations had occurred in the entire ameloblast layer (Fig 1) In areas with slight alterations the findings were similar to those described above In addition many ameloblasts contained dense globules and toluidine blue positive strands in the Tomes processes. Secretory material had appeared in the intercellular spaces. This material was seen at all levels in the ameloblast layer

In more severely affected areas the number of dense globules had increased considerably and dense bodies were also present between the ameloblast layer and the stratum intermedium and in the cytoplasm facing the ameloblasts of the stratum intermedium cells. In highly damaged areas degenerating ameloblasts were very common (Figs. 4 and 5)

Figs 1–3 Labial part of cross sections of three mandibular incisors in the zone of enamel matrix formation. The pulp was removed prior to decalcification and postfixation. Most of the layer of secretory ameloblasts (a) is shown. e enamel matrix. d dentin × 50

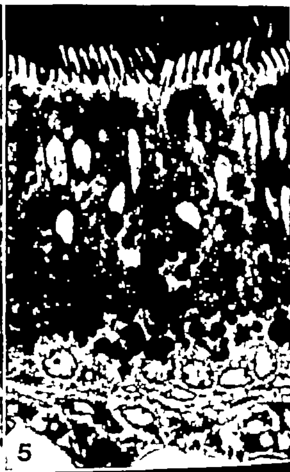
Fig 1 6 hours after vinblastine administration Profound damages in the areas marked x and z At x disintegrated ameloblasts cause a bulging of the enamel organ. At z numerous dense globules and degenerated ameloblasts. In some areas only a few dense globules are seen but many ameloblast nuclei are dislocated to the middle or distal (apical) part of the cells At several places large amounts of dense ameloblast debris are seen in the stratum intermedium (arrows) *Fig 2* 24 hours after vinblastine administration. Note the varying thickness of the ameloblast layer Most dense globules and ameloblast debris have disappeared from the ameloblast layer and from the stratum intermedium even in areas where great reduction in thickness of the ameloblast layer indicates that large amounts of debris must have been present (arrows) In the most heavily damaged areas (x and z) debris is still present. *Fig 3* Three days after vinblastine administration. Enamel matrix deposited prior to administration of the drug is marked with white bars. In most of this section no matrix has been formed after administration of the vinblastine. In less damaged areas the ameloblasts (a) have resumed secretion and a layer of atypical matrix has been deposited (arrows)


Z
e


Z
e


e


4


5


d
e


d
e
7

They were easily distinguishable from vital cells by their dense cytoplasm and by the aggregation of chromatin in the extremities of the nuclei (Fig 4) Degenerating ameloblasts often seem to fragmentize, and such fragments were extruded from the ameloblast layer and engulfed by the cells of the stratum intermedium (Figs. 4 and 5) Fragmentation of the ameloblasts were most obvious in areas where all or nearly all the ameloblasts were degenerating. In such areas cellular fragments and debris caused the entire enamel organ to bulge (Fig 1) Small vital looking cells of varying shape lined the inner aspect of the stratum intermedium (Fig 6) These cells were apparently ameloblasts which had freed themselves of large amounts of degenerating cytoplasm.

In most areas the ameloblast layer was 70 to 80 μm thick as in the controls. In areas abundant in dense globules and degenerating ameloblasts the thickness was about 60 μm. Many ameloblasts appeared not to stretch through the entire thickness of the epithelium. Ameloblasts with a well defined base abutting on the stratum intermedium contained a cluster of mitochondria located basally as in normal cells.

24 hours after administration of vinblastine In these animals the ameloblast layer varied in thickness from about 70 to about 20 μm (Figs. 2 and 8–12) Degenerating ameloblasts or degenerating parts of ameloblasts were now rare. The ameloblasts still contained many dense globules, of which relatively few were large, however Dense globules and cellular debris commonly present in the stratum intermedium 6 hours after vinblastine administration were only occasionally seen in this layer (Figs. ? 8, 9 and 10) Extracellular secretory material was abundant and typically localized between the basal (proximal) parts of the ameloblasts (Figs. 8–11) It also occurred intercellularly in the stratum intermedium.

In many areas the ameloblast epithelium appeared stratified (Fig. 10) Most of the cells were elongated with the long axis perpendicular to the tooth surface. Ameloblasts abutting on the stratum intermedium contained mitochondrial clusters in the basal cell portion. Tomes processes were often irregular Small rounded cells with relatively small nuclei and with basophilic cytoplasm were seen scattered in the epithelium. They were usually localized between the distal parts of elongated ameloblasts (Fig 10) or in the border area between the ameloblasts and the stratum intermedium (Fig 8) and were probably partly degenerated ameloblasts. *In areas* with very short ameloblasts lining the tooth surface (Figs. 11 and 12) and in areas where the enamel organ was bulging due to accumulation of debris, the remaining ameloblasts contained abundant dense globules.

3 days after administration of vinblastine When three days had elapsed after vinblastine administration the ameloblast layer was clear of degenerating cells and cellular debris and the surviving ameloblasts were rearranged into a simple columnar epithelium (Figs. 13–16) The thickness of this epithelium varied from about 60 μm to about 20 μm. This epithelium undoubtedly represented areas

Figs 4–6 These figures show varying degrees of injury to secretory ameloblasts 6 hours after vinblastine administration × 1,000

Fig 4 Several degenerating ameloblasts or parts of ameloblasts are seen (da) dn marks degenerating ameloblast nuclei with condensed chromatin at the nuclear poles. Several Tomes' processes are also degenerating (arrows) The cells of the stratum intermedium (si) are seen in the process of engulfing and digesting ameloblast debris. *Fig 5* Heavily injured and disorganized ameloblasts with numerous dense globules. Phagocytosis of ameloblast debris by stratum intermedium cells. *Fig 6* A sector of the most damaged area of the ameloblast layer similar to that marked x in Fig 1 Only a few ameloblast nuclei and small amount of cytoplasm (arrows) appear to have survived the injury from the drug. e enamel matrix, deb ameloblast debris. si stratum intermedium.

Fig 7 An area similar to that shown in Fig 6 3 days after administration of vinblastine In the area shown many small ameloblast remnants have survived (arrows) The stratum intermedium is not well defined d dentin enamel matrix formed prior to vinblastine administration × 400

p

where the destruction and elimination of ameloblast organelles had been extensive. Thick epithelium represented areas injured to a smaller degree (Fig 13) In the latter areas the ameloblasts differed from normal ones in presenting a reduced or lost inclination of the distal part of the Tomes process with respect to the ameloblast axis, and in the occurrence of secretory material between the basal parts of the ameloblasts and in the stratum intermedium region These characteristics were also present in areas with shorter ameloblasts in which the Tomes processes were usually long and slender or short and irregular or split (Figs. 14 and 15) The short ameloblasts contained dense globules, were broader than normal ameloblasts had oval nuclei and contained a reduced amount of mitochondria A distinct axial fibre was often seen in the supranuclear cell region

In heavily injured areas the tooth surface was lined by a layer of rounded or irregular cells resembling the small rounded surviving ameloblasts described above Similar cells were also present along the inner aspect of the stratum intermedium in areas where the enamel organ was bulging In the bulges most of the ameloblast debris had disappeared (Fig 7)

In the animals sacrificed 3 or 7 days after vinblastine administration the enamel layer yields valuable information on the secretory activity of the ameloblasts in the period following the application of the drug (Fig 3) In no part of the matrix formation zone were the secretory ameloblasts unaffected This was evident from disturbances in the structure of the enamel (Figs. 3 13, 14 and 16) In the inner and middle layers of the enamel crossing of enamel rods, alternating from layer to layer normally forms a typical herring bone pattern (Figs. 7 and 16) This pattern was not seen in enamel formed after vinblastine was administered (Figs. 13 14 16 and 18) In the hours following the application of the drug the deposition of enamel matrix appeared to be reduced or brought to a standstill In some areas matrix formation was not resumed at all (Figs. 3 15 and 16) In most areas matrix deposition was resumed but nowhere did the matrix have the structure which it had before the drug was administered The herring bone pattern of the rods was replaced by a layer of enamel crossed by slits or channels perpendicular to the tooth surface (Figs. 14 and 16) The maximal thickness of the matrix layer formed during the 3 days after the vinblastine injection was about 20 to 25 µm.

In areas where no matrix was deposited the height of the ameloblasts was 35 µm or less. In other areas where 30-35 µm high ameloblasts were present a 15 to 20 µm thick layer of matrix had been formed. Morphological differences between the active and the nonactive 30 to 35 µm high ameloblasts were not revealed under the light microscope

7 days afted administration of vinblastine In these animals most of the zone which contained secretory ameloblasts at the time of vinblastine treatment had passed into the zone of so-called transporting ameloblasts. In the normal teeth transporting ameloblasts originate from secretory ameloblasts by complicated changes consisting primarily of the disappearance of organelles engaged in secretion migration of mitochondria from the

---

Figs. 8–12 Secretory ameloblasts 24 hours after vinblastine administration. × 1 000
The thickness of the ameloblast epithelium in Figs. 9 10 and 11 is about 55 µm, 53 µm and 30 µm, respectively The thickness of the corresponding epithelium in areas in the controls was 75 to 80 µm. The great reduction in thickness of the ameloblast layer in the vinblastine-treated animals is due to formation of large amounts of ameloblast debris which have been removed by the stratum intermedium cells (si) Only a few remnants of debris are still visible in these cells. The small rounded cells marked with short arrows in Figs. 8 and 10 are thought to be surviving ameloblasts which have lost most of their cytoplasm. The area shown in Fig 8 is but slightly injured and shows displaced nuclei. In the heavily injured area shown in Fig. 12 the number of surviving ameloblasts are few and the cells are small and irregular In Figs. 8 to 11 relatively large amounts of secretory material are seen in the basal part of the intercellular spaces (long arrows)







ea

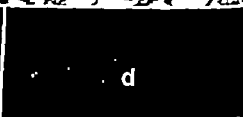
ep

ea

d

ep









Figs 13–15 Secretory ameloblasts 3 days after vinblastine administration. × 1,000.
The ameloblasts shown in Figs. 13 and 14 have resumed secretion after the vinblastine injury those in *Fig. 15* have not. Enamel matrix formed prior to administration of the vinblastine is marked ep. Matrix formed after administration of the drug differ in appearance from normal matrix and is marked ea. d in Fig. 15 is dentin. The thickness of the epithelium in Figs. 13, 14 and 15 is about 55 µm, 40 µm and 55 µm, respectively. The surviving ameloblasts are rearranged into a regular columnar epithelium. With a few exceptions the nuclei are localized in the basal half of the cells and the stratum intermedium cells have cleansed themselves of cellular debris. Small amounts of intercellular secretory material still remain in the slightly injured ameloblast area shown in Fig. 13 (arrow). I this area the Tomes processes are relatively ample but their inclination with respect to the cell axis is lost. In the shorter cells show in Fig. 14 the Tomes processes also lack inclination and are slender.

Fig. 16 Part of a cross section of the zone of enamel matrix formation of a mandibular incisor 3 days after vinblastine administration. A 50 µm thick layer of matrix has been deposited prior to the vinblastine treatment (ep) note its herringbone pattern. To the right a 25 µm thick layer of matrix (ea) has been deposited after the treatment with vinblastine it does not show herringbone pattern. T the left no matrix has been formed after the vinblastine treatment. a secretory ameloblasts. d dentin. × 375

Fig. 17 Part of a cross section of the zone of enamel maturation of a mandibular incisor 7 days after vinblastine administration. To the right a 50 µm thick layer of enamel matrix (ep) has been formed before and a 15 µm thick layer (ea) after the treatment with vinblastine. To the left practically no matrix has been formed after vinblastine treatment. In both areas the secretory ameloblasts have transformed int transporting ameloblasts ( ). The low density of the enamel layer (compare with Fig. 16) indicates that the enamel maturation was progress d dentin. Note that the areas shown in Figs. 16 and 17 were approximately in the same position with respect to the bl c) le of the ameloblast at the time of vinblastine administration. × 375

Fig. 18 Part of enamel maturation zone of mandibular incisor 7 days after vinblastine administration. The transporting ameloblasts are furnished with brush border like structure facing the enamel. The dark area below this structure contains mitochondria (arrow). The stars mark the border between enamel formed before and after vinblastine administration. d dentin. × 450

proximal to the distal (apical) end of the cell and development of an apical structure which under the light microscope resembles a striated border.

The transition of secretory ameloblasts into transporting ameloblasts was not affected perceptibly by the vinblastine. The structure and varying thickness of the enamel deposited indicated that ameloblasts which were secretory at the time of vinblastine administration had suffered just as described above in the experiments of shorter duration (Figs. 17 and 18). However in all areas where enamel matrix had been formed, transporting ameloblasts had developed from the more or less affected secretory ameloblasts and at about the expected time. Even in areas where matrix formation had stopped, cells with features like those of transporting ameloblasts had developed (Fig. 17). Judged by the decreasing stainability of the enamel towards the incisal end of the teeth the maturation of the enamel seems to take place as in the normal animals.

DISCUSSION

The results reported indicate that probably all ameloblasts in the secretory stage were damaged following administration of 0.2 mg vinblastine sulphate per 100 g body weight. Disarrangement of the normal cytoplasmic organization and cessation of translocation of secretory material to Tomes' processes were early disturbances, as in experiments with colchicine (*Kudo* 1975) or with a much larger dosage of vinblastine (*Moe & Mikkelsen* 1977). These early disturbances were probably due to loss of cytoplasmic microtubules, which at the large dosage (5 mg vinblastine sulphate per 100 g body weight) was complete. Instead of discharging their secretion from the cell apex, the ameloblasts emptied secretory material onto their lateral surfaces. Concomitantly formation of new secretion appeared to be inhibited.

Slightly damaged ameloblasts recovered relatively rapidly. However normal deposition of the enamel matrix was not re-estab-

lished, apparently due to loss of the normal inclinations of the Tomes processes with respect to the ameloblast axis. The Tomes processes contain numerous microtubules (*Moe & Mikkelsen 1977*). The findings suggest that these microtubules are extremely sensitive to vinblastine.

Some of the more profoundly damaged areas of the ameloblast layer contained abundant dense globules which undoubtedly represent cytosegresomes and autodigestive vacuoles similar to those described in the transitional zone of the normal enamel organ (*Reith 1970, Moe & Jessen* 1972) and in liver cells of vinblastine treated rats (*Arstila et al 1974*). In other areas disintegration and death of ameloblasts were extensive. In most of the profoundly damaged areas these two types of degenerative changes were intermingled. The cellular debris derived from the degenerated cells moved towards the stratum intermedium and was rapidly engulfed and digested by the cells that constitute this layer. These events in the secretory zone following vinblastine administration resemble closely the processes which take place in the transitional zone of the enamel organ in the normal rat incisor (*Moe & Jessen* 1972) and demonstrate an important function of the stratum intermedium.

The vinblastine induced lesions caused a reduction in height of the surviving secretory ameloblasts which often was considerable. Most of the cells were able to re-establish secretory activity. However the Tomes processes had extensively changed and all the matrix was abnormal. The large depositions of secretory material in the intercellular spaces of the ameloblast layer 24 hours after administration of vinblastine suggest that the ability to translocate secretory granules towards the cell apex was regained after the recovery of secretion.

The critical size (height) of the ameloblasts with respect to re-establishment of secretion was 30 to 35 μm. In some areas cells of this size appeared nearly as active as cells in areas much less damaged. In other areas cells of this size did not demonstrate secretory activity at all but were apparently vegetating. Under the light microscope no conclusive differences were observed between secreting and non-secreting cells of similar size. In no case had areas with cells less than 30 μm in height re-established matrix formation.

Secretory ameloblasts which had resumed secretion were able to transform into transporting ameloblasts. Severely damaged ameloblasts which had not resumed secretory activity were also converted into transporting ameloblasts. They were reduced in size but developed morphological features like normal transporting ameloblasts and the maturation of the enamel appeared to proceed as in the normal teeth.

In short, the present experiments have shown that vinblastine affected the secretory ameloblasts profoundly and caused reduction in size or death of many of the cells. The surviving cells may restore lost polarity and orderly arrangement; most of the ameloblasts in addition resumed secretory activity. The delicate manner of deposition of matrix depending on intact Tomes processes was extremely sensitive to vinblastine. In some areas of surviving non-secreting ameloblasts and in all areas with ameloblasts which had re-established secretion the cells retained their ability to transform into transporting ameloblasts. The ability of the stratum intermedium cells to engulf and digest ameloblast debris appeared unaffected.

The authors wish to thank Miss *Bodil Iversen* and Mr *K. Stub Christensen* for excellent technical assistance and Mrs *Lis Skarteany* for typing the manuscript.

REFERENCES

1. *Arstila A U, Nuuja I J M & Trump B F.* Studies on cellular autophagocytosis. Vinblastine-induced autophagy in the rat liver. Exp Cell Res. *87*: 249–252, 1974.
2. *Kudo N.* Effect of colchicine on the secretion of matrices of dentine and enamel in the rat incisor: an autoradiographic study using (³H) proline. Calcif Tiss. Res. *18*: 37–46, 1975.

3. *Moe H & Jessen H* Phagocytosis and elimination of amelocyte debris by stratum intermedium cells in the transitional zone of the enamel organ of the rat incisor. Z. Zellforsch. *131* 63–75 1972.
4. *Moe H & Mikkelsen H* Light microscopical and ultrastructural observations on the effect of vinblastine on ameloblasts of rat incisors in vivo. I Short-term effect on secretory ameloblasts. Acta path. microbiol., scand. Sect. A, *85* 73–88, 1977
5. *Reith E. J* The stages of amelogenesis as observed in molar teeth of young rats. J Ultrastruct. Res. *30* 111 151 1970
6. *Smith, C E. & Warshawsky H.,* Cellular renewal in the enamel organ and the odontoblast layer of the rat incisor as followed by radioautography using ³H thymidine. Anat. Rec. *183* 523–561 1975
7. *Warshawsky H & Smith C E.:* Morphological classification of rat incisor ameloblasts. Anat. Rec. *179* 423–445 1974
8. *Weinstock A & Leblond C P* Elaboration of the matrix glycoprotein of enamel by the secretory ameloblasts of the rat incisor as revealed by radioautography after galactose-H injection. J Cell Biol. *51* 26–51 1971

Acta path. microbiol. scand Sect. A 85 330 334 1977

ON THE EFFECT OF VINBLASTINE ON AMELOBLASTS OF RAT INCISORS *IN VIVO*

3 Acute and Protracted Effect on Differentiating Ameloblasts A Light Microscopical Study

H Moe

Anatomy Department C, University of Copenhagen, Denmark

Moe H. On the effect of vinblastine on ameloblasts of rat incisors *in vivo* 3 Acute and protracted effect on differentiating ameloblasts. A light microscopical study Acta path. microbiol scand Sect. A 85 330-334 1977

The acute effect of vinblastine sulphate at a dosage of 0.2 mg per 100 g body weight on ameloblasts in the progress of differentiation in rat incisors and the ability of these cells to develop into secretory ameloblasts after exposure to the drug were studied under the light microscope In the early stages of differentiation (exclusively dividing cells) no changes were seen In more advanced stages of differentiation the cell apices were altered and the nuclei normally placed near the cell base were located at all levels in the ameloblast layer These changes were reversible and the cells developed into secretory ameloblasts of normal appearance and function. Ameloblasts in the most advanced stage of differentiation in which secretion had begun were severely damaged and the mature secretory ameloblast population derived from these cells was decimated and produced enamel matrix with abnormal structure It is concluded that differentiating ameloblasts are relatively invulnerable to vinblastine, whereas in secretory ameloblasts the organelles directly engaged in the secretory processes are particularly exposed to damage from the drug

Key words Ameloblasts vinblastine rat.

H Moe Anatomy Department C Universitetsparken 1 DK 2100 Copenhagen Ø Denmark.

Received 25.xi 76 Accepted 5.xi 76

Recently it was shown that vinblastine has a profound effect on mature secretory ameloblasts in rat incisors (*Moe & Mikkelsen* 1977a, 1977b) The present work reals with the precursors to these cells, the differentiating ameloblasts. The differentiating ameloblasts migrate anteriorly from a continuously proliferating pool of stem cells at the posterior end of the tooth, and the cytodifferentiation takes about 1.5 days in the normal rat (*Smith & Warshawsky* 1975) The acute effect of vinblastine and the ability of the differentiating ameloblasts to develop into mature secretory ameloblasts after exposure to the drug were studied.

MATERIALS AND METHODS

The same animals (rats weighing 90 to 120 g) and methods were used as in the previous paper (*Moe & Mikkelsen* 1977b) The rats each received intravenously 0.2 mg vinblastine sulphate (Velbe) per 100 g body weight.

RESULTS

The controls. The zone examined, in the following called the differentiation zone, began posteriorly where the pulp cells adjacent to the ameloblasts were organized into a layer of cuboidal or low columnar odontoblasts and ended anteriorly where the development of the Tomes processes was complete. The posterior part of the zone overlapped the anterior portion of the proliferative compartment and its anterior extremity coincided with the beginning of the matrix secretion zone. Posteriorly in the differentiation zone the ameloblasts were organized into a stratified columnar epithelium with three or four staggered levels of oval nuclei. In the long middle region the ameloblasts faced predentin and thereafter dentin and developed gradually all the structural features of secretory ameloblasts except for Tomes' processes. The length of this region is 1,381 ± 90 µm in the mandibular incisor and 1,210 ± 81 µm in the maxillar incisor (*Warshawsky & Smith* 1974). About half-way along the region the cells began to elongate and nuclei began to move towards the basal (abdentinal) cell ends. Anteriorly in the region the ameloblasts had developed into tall columnar cells arranged in a single layer. Their nuclei now lay at two staggered levels in the basal portion of the epithelium and the mitochondria had gathered between the nucleus and the cell base. In the anterior extremity of the differentiation zone the Tomes processes developed coincidentally with the secretion of the first layers of enamel matrix.

Mitotic figures were relatively frequent posteriorly in the differentiation zone and disappeared gradually in the area where ameloblasts faced predentin. According to *Smith & Warshawsky* (1975) the most advanced mitotic figures are most frequently situated between 50 and 200 µm anterior to the start of predentin secretion.

6 hours after administration of vinblastine. In the posterior part of the differentiation zone numerous arrested mitoses were seen, but under the light microscope no differences were observed in non-dividing ameloblasts between the vinblastine treated animals and the controls. In the entire middle region nuclei were situated at all levels in the ameloblast layer whereas the mitochondria were gathered at the base of the cells as in the controls. The cell apices stained but faintly with toluidine blue and an apical web or terminal bar system which was distinct in the controls was seldom seen. A degenerating cell or a few dense cytoplasmic globules were seen occasionally.

In the anterior extremity of the zone where the secretion had begun, striking changes had occurred. In extensive areas the ameloblast layer contained degenerating nuclei, many dense globules, and depositions of secretory material in the intercellular spaces. In the stratum intermedium area only sparse dense globules and cellular debris were seen, contrary to the situation further anterior in the matrix secretion zone.

24 hours after administration of vinblastine. In the posterior and middle part of the differentiation zone the findings were similar to those 6 hours after administration of the drug (Fig. 1). In the anterior extremity large areas of the epithelium were stratified and highly disorganized and contained large dense globules and abundant secretory material in the intercellular spaces (Figs. 2 and 3). Degenerating ameloblasts or parts of ameloblasts were seen in the ameloblast layer but only small amounts of ameloblast debris were present in the stratum intermedium area.

3 and 7 days after administration of vinblastine. The ameloblasts which at the time of vinblastine administration were situated in the differentiation zone had now migrated to the zone of matrix formation. Three days after vinblastine they had reached the posterior part of the zone (Fig. 4) and on the seventh day they were in its anterior half (Fig. 5). The position was easily determined since the ameloblasts ahead of (Fig. 7) and behind (Fig. 6) the cell cohort from the large middle region of the differentiation zone were decimated and changed, whereas the cell cohort from this region had developed into

Acta path microbiol scand Sect. A, 85 330-334 1977

ON THE EFFECT OF VINBLASTINE ON AMELOBLASTS OF RAT INCISORS *IN VIVO*

3 *Acute and Protracted Effect on Differentiating Ameloblasts A Light Microscopical Study*

H Moe

Anatomy Department C, University of Copenhagen, Denmark

Moe H. On the effect of vinblastine on ameloblasts of rat incisors *in vivo* 3 Acute and protracted effect on differentiating ameloblasts. A light microscopical study Acta path. microbiol. scand Sect A, 85 330 334 1977

The acute effect of vinblastine sulphate at a dosage of 0.2 mg per 100 g body weight on ameloblasts in the progress of differentiation in rat incisors, and the ability of these cells to develop into secretory ameloblasts after exposure to the drug, were studied under the light microscope. In the early stages of differentiation (exclusively dividing cells) no changes were seen. In more advanced stages of differentiation the cell apices were altered and the nuclei normally placed near the cell base were located at all levels in the ameloblast layer These changes were reversible and the cells developed into secretory ameloblasts of normal appearance and function. Ameloblasts in the most advanced stage of differentiation in which secretion had begun were severely damaged, and the mature secretory ameloblast population derived from these cells was decimated and produced enamel matrix with abnormal structure It is concluded that differentiating ameloblasts are relatively invulnerable to vinblastine, whereas in secretory ameloblasts the organelles directly engaged in the secretory processes are particularly exposed to damage from the drug.

Key words Ameloblasts vinblastine rat.

H Moe, Anatomy Department C, Universitetsparken 1 DK 2100 Copenhagen Ø Denmark.

Received 25.xi 76   Accepted 25 xi 76

Recently it was shown that vinblastine has a profound effect on mature secretory ameloblasts in rat incisors (*Moe & Mikkelsen* 1977a 1977b) The present work reals with the precursors to these cells, the differentiating ameloblasts The differentiating ameloblasts migrate anteriorly from a continuously proliferating pool of stem cells at the posterior end of the tooth and the cytodifferentiation takes about 1 5 days in the normal rat (*Smith & Warshawsky* 1975) The acute effect of vinblastine and the ability of the differentiating ameloblasts to develop into mature secretory ameloblasts after exposure to the drug were studied

MATERIALS AND METHODS

The same animals (rats weighing 90 to 120 g) and methods were used as in the previous paper (*Moe & Mikkelsen* 1977b) The rats each received intravenously 0 2 mg vinblastine sulphate (Velbe) per 100 g body weight.

RESULTS

The controls. The zone examined, in the following called the differentiation zone began posteriorly where the pulp cells adjacent to the ameloblasts were organized into a layer of cuboidal or low columnar odontoblasts and ended anteriorly where the development of the Tomes processes was complete. The posterior part of the zone overlapped the anterior portion of the proliferative compartment and its anterior extremity coincided with the beginning of the matrix secretion zone. Posteriorly in the differentiation zone the ameloblasts were organized into a stratified columnar epithelium with three or four staggered levels of oval nuclei. In the long middle region the ameloblasts faced predentin and thereafter dentin and developed gradually all the structural features of secretory ameloblasts except for Tomes processes. The length of this region is 1,381 ± 90 μm in the mandibular incisor and 1,210 ± 81 μm in the maxillar incisor (*Warshawsky & Smith 1974*) About half-way along the region the cells began to elongate and nuclei began to move towards the basal (abdentinal) cell ends Anteriorly in the region the ameloblasts had developed into tall columnar cells arranged in a single layer Their nuclei now lay at two staggered levels in the basal portion of the epithelium and the mitochondria had gathered between the nucleus and the cell base In the anterior extremity of the differentiation zone the Tomes processes developed coincidentally with the secretion of the first layers of enamel matrix.

Mitotic figures were relatively frequent posteriorly in the differentiation zone and disappeared gradually in the area where ameloblasts faced predentin. According to *Smith & Warshawsky* (1975) the most advanced mitotic figures are most frequently situated between 50 and 200 μm anterior to the start of predentin secretion.

6 hours after administration of vinblastine In the posterior part of the differentiation zone numerous arrested mitoses were seen, but under the light microscope no differences were observed in non-dividing ameloblasts between the vinblastine treated animals and the controls. In the entire middle region nuclei were situated at all levels in the ameloblast layer whereas the mitochondria were gathered at the base of the cells as in the controls. The cell apices stained but faintly with toluidine blue and an apical web or terminal bar system which was distinct in the controls was seldom seen. A degenerating cell or a few dense cytoplasmic globules were seen occasionally

In the anterior extremity of the zone, where the secretion had begun striking changes had occurred. In extensive areas the ameloblast layer contained degenerating nuclei, many dense globules, and depositions of secretory material in the intercellular spaces. In the stratum intermedium area only sparse dense globules and cellular debris were seen, contrary to the situation further anterior in the matrix secretion zone.

24 hours after administration of vinblastine In the posterior and middle part of the differentiation zone the findings were similar to those 6 hours after administration of the drug (Fig 1) In the anterior extremity large areas of the epithelium were stratified and highly disorganized and contained large dense globules and abundant secretory material in the intercellular spaces (Figs. 2 and 3) Degenerating ameloblasts or parts of ameloblasts were seen in the ameloblast layer but only small amounts of ameloblast debris were present in the stratum intermedium area.

3 and 7 days after administration of vinblastine The ameloblasts which at the time of vinblastine administration were situated in the differentiation zone had now migrated to the zone of matrix formation. Three days after vinblastine they had reached the posterior part of the zone (Fig 4) and on the seventh day they were in its anterior half (Fig 5) The position was easily determined since the ameloblasts ahead of (Fig. 7) and behind (Fig 6) the cell cohort from the large middle region of the differentiation zone were decimated and changed, whereas the cell cohort from this region had developed into

Acta path. microbiol scand Sect. A, 85 330–334 1977

ON THE EFFECT OF VINBLASTINE ON AMELOBLASTS OF RAT INCISORS *IN VIVO*

3 Acute and Protracted Effect on Differentiating Ameloblasts A Light Microscopical Study

H Moe

Anatomy Department C University of Copenhagen, Denmark

Moe H On the effect of vinblastine on ameloblasts of rat incisors *in vivo* 3 Acute and protracted effect on differentiating ameloblasts. A light microscopical study Acta path. microbiol scand Sect A, 85 330 334 1977

The acute effect of vinblastine sulphate at a dosage of 0 2 mg per 100 g body weight on ameloblasts in the progress of differentiation in rat incisors, and the ability of these cells to develop into secretory ameloblasts after exposure to the drug were studied under the light microscope. In the early stages of differentiation (exclusively dividing cells) no changes were seen In more advanced stages of differentiation the cell apices were altered and the nuclei normally placed near the cell base were located at all levels in the ameloblast layer These changes were reversible and the cells developed into secretory ameloblasts of normal appearance and function. Ameloblasts in the most advanced stage of differentiation in which secretion had begun were severely damaged, and the mature secretory ameloblast population derived from these cells was decimated and produced enamel matrix with abnormal structure. It is concluded that differentiating ameloblasts are relatively invulnerable to vinblastine whereas in secretory ameloblasts the organelles directly engaged in the secretory processes are particularly exposed to damage from the drug.

Key words Ameloblasts vinblastine rat.

H Moe, Anatomy Department C, Universitetsparken 1 DK 2100 Copenhagen Ø Denmark

Received 25.xi 76 Accepted 25.xi 76

Recently it was shown that vinblastine has a profound effect on mature secretory ameloblasts in rat incisors (*Moe & Mikkelsen* 1977a 1977b) The present work reals with the precursors to these cells, the differentiating ameloblasts. The differentiating ameloblasts migrate anteriorly from a continuously proliferating pool of stem cells at the posterior end of the tooth and the cytodifferentiation takes about 1 5 days in the normal rat (*Smith & Warshawsky* 1975) The acute effect of vinblastine and the ability of the differentiating ameloblasts to develop into mature secretory ameloblasts after exposure to the drug were studied.

MATERIALS AND METHODS

The same animals (rats weighing 90 to 120 g) and methods were used as in the previous paper (*Moe & Mikkelsen* 1977b) The rats each received intravenously 0.2 mg vinblastine sulphate (Velbe) per 100 g body weight.

RESULTS

The controls. The zone examined in the following called the differentiation zone, began posteriorly where the pulp cells adjacent to the ameloblasts were organized into a layer of cuboidal or low columnar odontoblasts and ended anteriorly where the development of the Tomes processes was complete. The posterior part of the zone overlapped the anterior portion of the proliferative compartment and its anterior extremity coincided with the beginning of the matrix secretion zone. Posteriorly in the differentiation zone the ameloblasts were organized into a stratified columnar epithelium with three or four staggered levels of oval nuclei. In the long middle region the ameloblasts faced predentin and thereafter dentin and developed gradually all the structural features of secretory ameloblasts except for Tomes processes. The length of this region is 1,381 ± 90 µm in the mandibular incisor and 1,210 ± 81 µm in the maxillar incisor (*Warshawsky & Smith* 1974). About half-way along the region the cells began to elongate and nuclei began to move towards the basal (abdentinal) cell ends. Anteriorly in the region the ameloblasts had developed into tall columnar cells arranged in a single layer. Their nuclei now lay at two staggered levels in the basal portion of the epithelium and the mitochondria had gathered between the nucleus and the cell base. In the anterior extremity of the differentiation zone the Tomes processes developed coincidentally with the secretion of the first layers of enamel matrix.

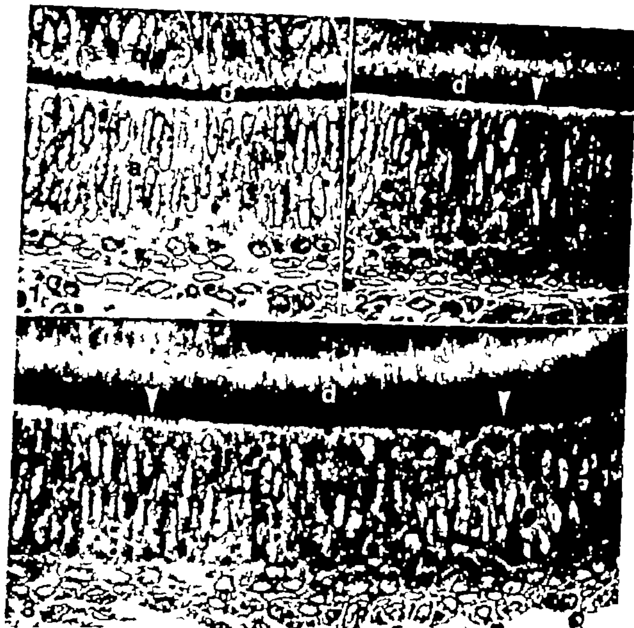
Mitotic figures were relatively frequent posteriorly in the differentiation zone and disappeared gradually in the area where ameloblasts faced predentin. According to *Smith & Warshawsky* (1975) the most advanced mitotic figures are most frequently situated between 50 and 200 µm anterior to the start of predentin secretion.

6 hours after administration of vinblastine. In the posterior part of the differentiation zone numerous arrested mitoses were seen, but under the light microscope no differences were observed in non-dividing ameloblasts between the vinblastine treated animals and the controls. In the entire middle region nuclei were situated at all levels in the ameloblast layer whereas the mitochondria were gathered at the base of the cells as in the controls. The cell apices stained but faintly with toluidine blue and an apical web or terminal bar system which was distinct in the controls was seldom seen. A degenerating cell or a few dense cytoplasmic globules were seen occasionally.

In the anterior extremity of the zone, where the secretion had begun, striking changes had occurred. In extensive areas the ameloblast layer contained degenerating nuclei many dense globules, and depositions of secretory material in the intercellular spaces. In the stratum intermedium area only sparse dense globules and cellular debris were seen, contrary to the situation further anterior in the matrix secretion zone.

24 hours after administration of vinblastine. In the posterior and middle part of the differentiation zone the findings were similar to those 6 hours after administration of the drug (Fig. 1). In the anterior extremity large areas of the epithelium were stratified and highly disorganized and contained large dense globules and abundant secretory material in the intercellular spaces (Figs. 2 and 3). Degenerating ameloblasts or parts of ameloblasts were seen in the ameloblast layer but only small amounts of ameloblast debris were present in the stratum intermedium area.

3 and 7 days after administration of vinblastine. The ameloblasts which at the time of vinblastine administration were situated in the differentiation zone had now migrated to the zone of matrix formation. Three days after vinblastine they had reached the posterior part of the zone (Fig. 4) and on the seventh day they were in its anterior half (Fig. 5). The position was easily determined since the ameloblasts ahead of (Fig. 7) and behind (Fig. 6) the cell cohort from the large middle region of the differentiation zone were decimated and changed, whereas the cell cohort from this region had developed into

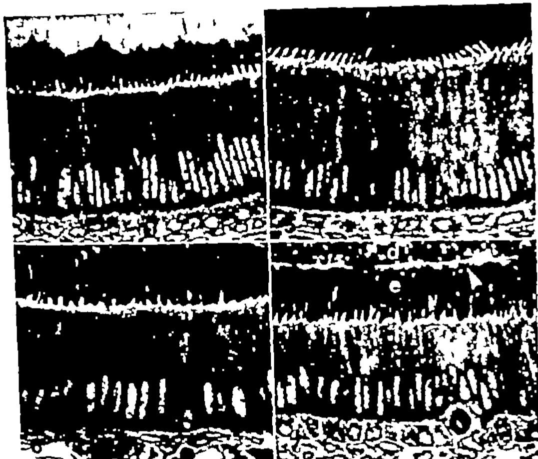


Figs 1 to 3 24 hours after vinblastine administration. a ameloblasts. o odontoblasts. d predentin or dentin. si stratum intermedium. × 600

Fig 1 is from the middle part of the differentiation zone. Ameloblast nuclei are seen at all levels in the ameloblast layer.

Fig 2 The anterior part of the differentiation zone. An initial, very thin layer of enamel matrix has been formed (white arrow head). The ameloblast layer appears stratified and several nuclei are irregular with indented nuclear membranes. Dense globules (thick arrows) and intercellular secretory material (thin arrow) are seen.

Fig 3 This micrograph shows that the degenerative changes rapidly aggravate in the area where the Tomes processes develop and the ameloblasts become fully differentiated. To the left the cells are in a slightly more advanced stage than those in Fig 2. To the right the distal parts of the Tomes processes are fully developed. It is believed that most of or all the enamel matrix (white arrow heads) was deposited prior to the administration of vinblastine and that secretory material delivered from the cells after the injury from the drug was secreted into the lateral intercellular spaces (arrows).



Figs. 4 and 5 3 and 7 days after administration of vinblastine respectively × 600
Ameloblasts which at the time of vinblastine administration were in the middle region of the differentiation zone. The cells have developed into secretory ameloblasts and resemble closely normal secretory ameloblasts with Tomes processes

Fig. 6 7 days after administration of vinblastine Ameloblasts which at the time of vinblastine administration were in the anterior part of the proliferation zone. Cell loss due to arrested mitoses has resulted in thinning out of the epithelium. The remaining ameloblasts are shorter than normal and the Tomes processes and the structure of the enamel are abnormal. × 600.

Fig. 7 3 days after administration of vinblastine Ameloblasts which at the time of administration of the drug were just fully differentiated into secretory cells. The ameloblasts are shorter than normal, has abnormal Tomes processes, and are thinned out owing to death and disappearance of cells. A degeneration body consisting of flattened cells encapsulating a densely stained substance with a light core is seen between the ameloblasts and the stratum intermedium. Intercellular secretory material is still present between the basal parts of the ameloblasts (arrow) d dentin, e enamel matrix. White arrow-head marks matrix formed prior to administration of vinblastine × 600

typical, tall secretory ameloblasts with segregation of the cell constituents as in normal cells and with regular Tomes processes with distinct inclinations of their distal parts with respect to the cell axes (Figs. 4 and 5) In addition, the enamel matrix produced by the ameloblasts from the middle region of the differentiation zone showed a distinct herring bone pattern as in normal teeth wheras the enamel ahead of and behind the region was abnormal

In the area derived from the anterior ex

tremity of the differentiation zone where the ameloblasts had started secretion when exposed to the vinblastine, and in the area of secretory ameloblasts immediately ahead of this site peculiar large degeneration bodies had arisen between the ameloblast layer and the stratum intermedium (Fig 7) The bodies had a strongly stained core with a light central area and a shell of flattened faintly stained cells. These bodies migrated anteriorly with the cells of the enamel organ and were still present when these had arrived in the maturation zone (unpublished observation)

DISCUSSION

After the same dosage of vinblastine the alterations in differentiating ameloblasts which had not yet begun secretion were very slight compared to the changes in secretory ameloblasts (*Moe & Mikkelsen* 1977 b and this paper) In secretory ameloblasts vinblastine caused disturbance in the normal orderly segregation of the cell constituents and subsequent degeneration of organelles and death of many cells. In differentiating ameloblasts vinblastine caused displacement of the nuclei and alterations in the cell apices, but only exceptionally degenerative changes visible under the light microscope. The changes were reversible and the cells continued differentiation into secretory ameloblasts of normal appearance and function though probably delayed Only ameloblasts which at the time of drug administration were at the conclusion of differentiation, but not yet secreting showed a tendency to lack inclination of the Tomes processes.

Secretory ameloblasts which had migrated from areas which included the anterior part of the proliferative compartment were reduced in number and changed probably as a consequence of death of cells arrested in mitosis or of injuries to the proliferating mesenchymal odontogenic cells, which are supposed to have an inductive influence upon the amelogenic epithelium, and which are severely damaged by cyclophosphamide (*Adatia* 1975) Whether vinblastine has a similar effect is not known.

The severe damage to the cells in the anterior extremity of the differentiation zone indicates that the secretory apparatus in the ameloblasts is particularly susceptible to damage from vinblastine This vulnerability first appears when the cells are actively secreting. Our previous observations cited above substantiate the presumption that the organelles directly engaged in the secretory processes are the ones which suffer primarily and are eliminated by segregation into dense globules or cytosegresomes. The provoking factor may be the effect of the drug on the microtubular system and the ensuing cessation of normal intracellular transport of secretory material.

It is concluded that the ameloblast differentiation is only slightly and reversibly affected by vinblastine at a dosage which seriously affects the proliferating stem cells and the mature secretory ameloblasts.

REFERENCES

1 *Adatia A* A Cytotoxicity of cyclophosphamide in the rat incisor Br J Cancer 32 208-218, 1975.

2 *Moe H & Mikkelsen H* Light microscopical and ultrastructural observations on the effect of vinblastine on ameloblasts of rat incisors in vivo I Short term effect on secretory ameloblasts. Acta path. microbiol. scand. Sect. A, *85* 73–88, 1977a.

3 *Moe H & Mikkelsen H* On the effect of vinblastine on ameloblasts of rat incisors in vivo 2 Protracted effect on secretory ameloblasts A light microscopical study In press: Acta path. microbiol scand Sect. A 319-328, 1977 b.

4 *Smith C E & Warshawsky H*. Cellular renewal in the enamel organ and the odontoblast layer of the rat incisor as followed by radioautography using ³H-thymidine. Anat. Rec *183* 523–562 1975

5 *Warshawsky H & Smith C E*. Morphological classification of rat incisor ameloblasts Anat. Rec. *179* 423–446 1974

Acta path. microbiol. scand. Sect. A, 85 335–344 1977

THE ULTRASTRUCTURE OF MACROPHAGES FOUND IN CONTACT WITH PLASMA CELLS IN THE BONE MARROW OF PATIENTS WITH MULTIPLE MYELOMA*

JENS BLOM

Department of Biophysics, Statens Seruminstitut, Copenhagen, Denmark

Blom, J The ultrastructure of macrophages found in contact with plasma cells in the bone marrow of patients with multiple myeloma. Acta path. microbiol. scand Sect. A, 85 335–344 1977

The ultrastructure of macrophage found in the bone marrow of 15 patients with multiple myeloma is described The macrophage is designated the dendritic bone marrow macrophage, due to the various branching cell forms in which it can be found. It is further distinguished by having contact with plasma cells. At the contact zones a thickening of the inner leaflet of the cytoplasmic membrane of the plasma cells is observed, whereas no morphological changes are present in the adjoining membranes of the macrophage. These macrophages show a great variation in their phagocytic capacity and only few show morphological evidence of being actively phagocytic. A few dendritic bone marrow macrophages show a localized thickening of the inner leaflet of their cytoplasmic membrane but this thickening is never found in the regions of contact with plasma cells.

Key words Contact zones dendritic bone marrow macrophages electron microscopy; multiple myeloma; plasma cells.

Jens Blom, Department of Biophysics, Statens Seruminstitut, Amager Boulevard 80 DK-2300 Copenhagen S, Denmark.

Received 18.xi.76 Accepted 18.xi.76

A previous study (9) showed that a small number of plasma cells in bone marrow aspirations from patients with IgG multiple myeloma were in direct contact with cytoplasmic processes of some large stellated cells. These stellated cells have now for reasons given in this paper been designated dendritic bone marrow macrophages (DBMM)

A characteristic thickening of the inner leaflet of the cytoplasmic membrane of the plasma cells was observed in the contact zones with the DBMM whereas no morphological changes could be seen in the adjoining membranes of the macrophages. This type of cellular contact has now been observed in bone marrow samples from 15 patients with multiple myeloma. The ultrastructure of the DBMM will be described based on observations from this material. In addition the se

* This work is part of a project on study of multiple myeloma, which is carried out as a co-operation between Department of Biophysics, Statens Seruminstitut, and Division of Haematology Department of Medicine, University Hospital, Hvidovre Hospital, Copenhagen.

rum M-components were classified in serum from peripheral blood drawn from each patient and it was found that contact zones between plasma cells and DBMM occurred independent of the immunoglobulin type secreted by the plasma cells of the patient in question

MATERIAL AND METHODS

Patients

The blood of each of the 15 patients studied contained a serum M-component. Blood from five of the patients contained an M-component of the IgG type kappa from six patients an IgG type lambda, from two patients an IgA type kappa, and from two Bence-Jones proteins of the type kappa. The number of plasma cells in relation to the total number of the nucleated cells in the bone marrow of the patients was in all cases abnormally high ranging from 5–80 per cent. Most of the patients were followed regularly over a period of several years and a total of 70 bone marrow aspirations were examined The first bone marrow sample from a patient was always taken prior to the initiation of treatment with cytostatics (melphalan or cyclophosphamide)

Electron Microscopy

Bone marrow aspirations were immediately injected into a solution containing 3 per cent glutaraldehyde (TAAB Laboratories Emmer Green Reading England) in 0 1 M sodium cacodylate buffer pH 7.2 (16) with 0 01 M $CaCl_2$. The material was kept in this solution for 1 hour at room temperature (20–23 C) Clumps of clotted cells and marrow fragments were then cut into 1 mm^3 cubes and fixation was continued in fresh fixative of the same composition for a further 4 hours at room temperature After transfer to 0 2 M sucrose in 0 1 M cacodylate buffer pH 7 2 with 0 01 M $CaCl_2$, the specimens were stored overnight at 4 C They were then postfixed for 1 hour at room temperature in 1 per cent osmium tetroxide in 0 1 M barbiturate buffer pH 7 3 with 4 5 per cent sucrose added (b)

After fixation the specimens were treated en bloc for 1 hour with 2 per cent uranyl acetate in barbiturate buffer without sucrose and dehydrated in alcohol followed by propylene oxide (11) prior to the final embedding in Vestopal-W (15) In a few experiments the en bloc treatment with uranyl acetate was omitted

Sections were prepared and counter-stained with uranyl and lead salts according to the general routine of the laboratory and electron microscopy of the sectioned material was also performed as previously described (4) For the present study approximately 3000 electron micrographs were studied

RESULTS

A dendritic bone marrow macrophage (DBMM) was occasionally situated centrally in a cluster of plasma cells. Each macrophage could be in contact with one or several plasma cells. In this study contacts from one DBMM to as many as four different plasma cells were noted (Figs. 1 2) More frequently only a single extension of the cytoplasm from a DBMM could be seen parallel and in close proximity to the surface of a plasma cell (Figs. 6 7 8 9) Contact zones were never seen between any other cells than plasma cells and DBMM This type of zone was found in the bone marrow aspirates from all patients studied and the presence of these zones bears no relation to the immunoglobulin type present in the blood of the patient For this reason the material has been treated as a whole and the results given are valid for marrow cells from all patients

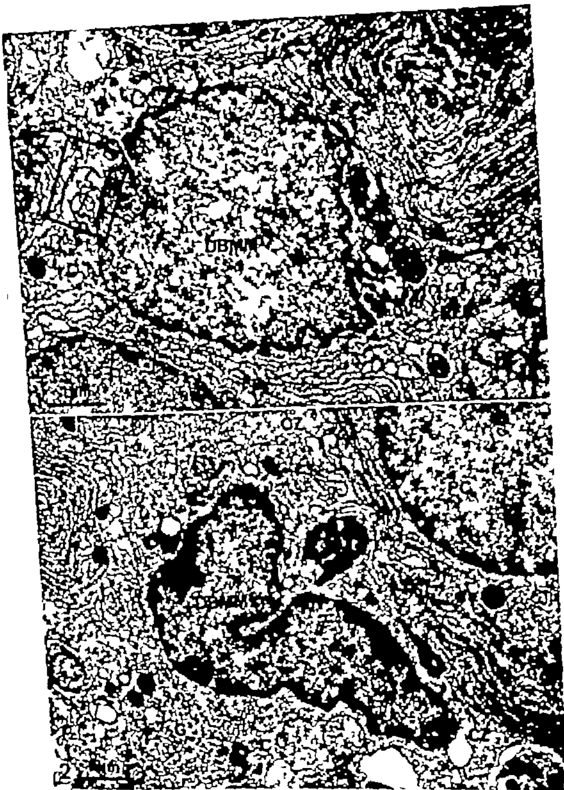
Thirty different DBMM were found in which the plane of sectioning has passed through the central region of the nucleus

---

Figs. 1–11 all show electron micrographs of sections obtained from bone marrow specimens from patients with multiple myeloma. The bar on each micrograph represents 100 nm unless otherwise stated

Fig 1 A survey with a dendritic bone marrow macrophage (DBMM) in the centre of the field Three contact zones (CZ) with surrounding plasma cells (PC) can be seen. A few strands of rough endoplasmic reticulum (RER) and some dense bodies (DB) are present in the macrophage 16 000 ×

Fig 2 A DBMM which shows two contact zones (CZ) with a plasma cell (PC) The outline of the macrophage nucleus is irregular with the chromatin condensed at the nuclear membrane. Phagocytized material (P) is present in the cytoplasm. Note the centriole (C) and the prominent Golgi complex (G) 16 000 ×




M
M
PO
PO
FE
L
CM
CZ
PC
CZ
F
RER
F
RER
PNS
N

(Figs. 1 2) In survey micrographs of these DBMM no specific relationship to blood vessels or vascular sinuses was found, except in a very few instances in which the macrophage seemed to be in close contact with the wall of the vessel. The length and width of the DBMM ranged from 20 to 5 μm and from 5 to 2 μm, respectively. The DBMM thus, appeared in survey electron micrographs as elongated cells in which the cytoplasm often was drawn out into very thin and delicate processes (Figs. 6, 7 8). As a consequence the cell shape of the sectioned DBMM varied from bipolar to more stellated or dendritic forms. The cytoplasmic matrix of the cell was generally electron lucent compared to other nucleated cells of the bone marrow and often only a small rim of cytoplasm surrounded the nucleus (Fig 1). Most of the DBMM possessed a single centrally located, indented nucleus which frequently contained some chromatin condensed close to the nuclear envelope (Figs. 1 2). A nucleolus was present in one third of the cells studied. The length and width of the nucleus ranged from 2 to 8 μm and 1 to 4 μm, respectively. In addition to the cells, the nuclei of which were included in the sections available for study 380 different cytoplasmic processes of DBMM which possessed contact zones with plasma cells have been studied in detail (Figs. 6, 7 8, 10). The width of the cytoplasmic extensions could vary from 0.1 μm to 2 μm.

Many membrane bound vesicles were found in the cytoplasm of about half of the DBMM studied (Figs. 6, 7). Some of these vesicles were located in close proximity to or directly adhering to the cell membrane, whereas others were distributed in the cytoplasm. The diameter of the vesicles measured approximately 70 to 80 nm, and many were coated vesicles. Their contents varied from electron lucent to more electron dense material in which ferritin was often found.

Short segments of the rough endoplasmic reticulum with parallel cisternal membranes were found in the cytoplasm of each DBMM and the cisternae were only occasionally dilated (Fig 4). The number of free cytoplasmic ribosomes was small and most of them were present as polyribosomes consisting of 4 to 8 single ribosomes (Figs. 3 7). Filaments about 6 to 8 nm in diameter were frequently observed in the cytoplasm (Fig. 4). Mitochondria about 0.6 μm long and 0.3 μm wide with well-developed cristae were found in all macrophages in which the nuclei were included in the sections (Fig 3) whereas a Golgi complex was only seen in 20 per cent of these cells (Fig 2).

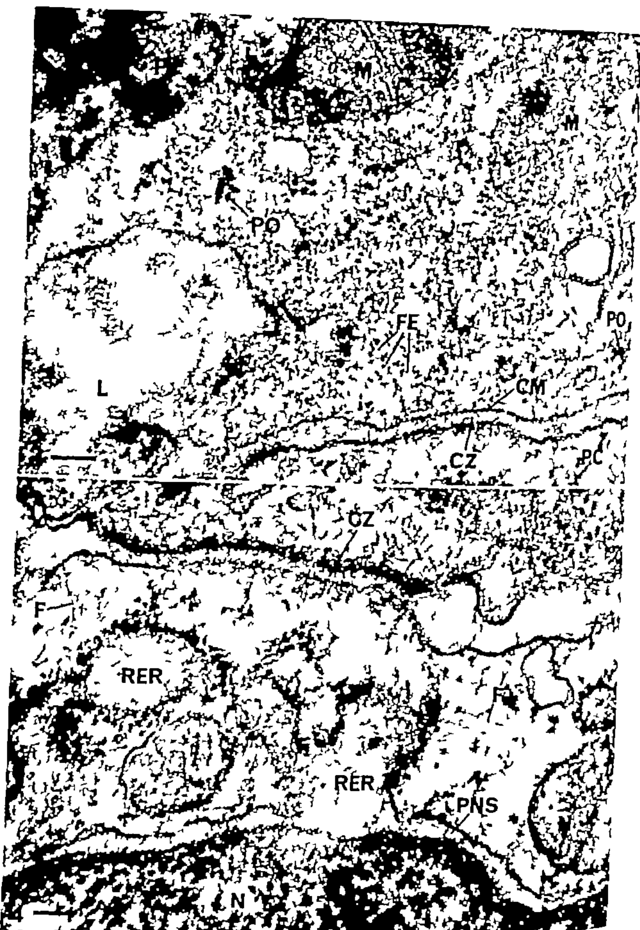
Lysosome like dense bodies bound by a unit membrane were found in 60 per cent of the cells which were cut more or less centrally (Figs. 1 2, 7). Other membrane bound cytoplasmic inclusions were found to contain lipid-like material (Fig. 3). In four of the 30 cells in which the nuclei were included in the section, morphological evidence of phagocytosis of erythrocytes was found and residues of other cell types were also observed (Figs. 2, 3). Such inclusions of phagocytized material were always surrounded by unit membranes. The characteristic electron dense molecules of ferritin were found in the cytoplasm of 40 per cent of the total of 410 different DBMM studied. The amount of ferri-

---

Fig 3 Part of DBMM showing a contact zone (CZ) with plasma cell (PC). Ferritin molecules (FE) are dispersed in the cytoplasm of the macrophage and well preserved mitochondria (M) are also present. In the upper left corner part of a phagocytized cell (P) is seen and below that membrane bound inclusion with lipid-like material (L). The cytoplasmic membrane (CM) of the macrophage show no changes in the region corresponding to the contact zone with the plasma cell (PO) denotes polyribosomes. This bone marrow specimen was not treated *en bloc* with uranyl acetate prior to dehydration. 93,000 ×

Fig 4 High-power view of the framed part of Fig. 1. Part of the nucleus (N) and cytoplasm of the DBMM is shown. The contact zone (CZ) is well illustrated even though the cell membranes are obliquely sectioned. The rough endoplasmic reticulum (RER) of the macrophage is slightly dilated and connected with the perinuclear space (PNS). Note few filaments (F) in the electron lucent cytoplasm of the macrophage 93,000 ×

22*


M
M
PO
PO
FE
L
CM
CZ
PC
CZ
F
RER
RER
PNS
N

(Figs. 1 2) In survey micrographs of these DBMM no specific relationship to blood vessels or vascular sinuses was found, except in a very few instances in which the macrophage seemed to be in close contact with the wall of the vessel. The length and width of the DBMM ranged from 20 to 5 μm and from 5 to 2 μm, respectively The DBMM thus, appeared in survey electron micrographs as elongated cells in which the cytoplasm often was drawn out into very thin and delicate processes (Figs. 6, 7 8) As a consequence the cell shape of the sectioned DBMM varied from bipolar to more stellated or dendritic forms. The cytoplasmic matrix of the cell was generally electron lucent compared to other nucleated cells of the bone marrow and often only a small rim of cytoplasm surrounded the nucleus (Fig. 1) Most of the DBMM possessed a single centrally located, indented nucleus which frequently contained some chromatin condensed close to the nuclear envelope (Figs. 1 2) A nucleolus was present in one third of the cells studied. The length and width of the nucleus ranged from 2 to 8 μm and 1 to 4 μm, respectively In addition to the cells, the nuclei of which were included in the sections available for study 380 different cytoplasmic processes of DBMM which possessed contact zones with plasma cells have been studied in detail (Figs. 6, 7 8 10) The width of the cytoplasmic extensions could vary from 0.1 μm to 2 μm.

Many membrane bound vesicles were found in the cytoplasm of about half of the DBMM studied (Figs. 6, 7) Some of these vesicles were located in close proximity to or directly adhering to the cell membrane, whereas others were distributed in the cytoplasm The diameter of the vesicles measured approximately 70 to 80 nm, and many were coated vesicles. Their contents varied from electron lucent to more electron dense material in which ferritin was often found.

Short segments of the rough endoplasmic reticulum with parallel cisternal membranes were found in the cytoplasm of each DBMM and the cisternae were only occasionally dilated (Fig 4) The number of free cytoplasmic ribosomes was small and most of them were present as polyribosomes consisting of 4 to 8 single ribosomes (Figs. 3, 7) Filaments about 6 to 8 nm in diameter were frequently observed in the cytoplasm (Fig 4) Mitochondria about 0.6 μm long and 0.3 μm wide with well-developed cristae were found in all macrophages in which the nuclei were included in the sections (Fig 3) whereas a Golgi complex was only seen in 20 per cent of these cells (Fig 2)

Lysosome like dense bodies bound by a unit membrane were found in 60 per cent of the cells which were cut more or less centrally (Figs. 1 2 7) Other membrane bound cytoplasmic inclusions were found to contain lipid-like material (Fig 3) In four of the 90 cells in which the nuclei were included in the section, morphological evidence of phagocytosis of erythrocytes was found and residues of other cell types were also observed (Figs. 2 3) Such inclusions of phagocytized material were always surrounded by unit membranes. The characteristic electron dense molecules of ferritin were found in the cytoplasm of 40 per cent of the total of 410 different DBMM studied. The amount of ferri-

---

Fig 3 Part of DBMM showing a contact zone (CZ) with a plasma cell (PC) Ferritin molecules (FE) are dispersed in the cytoplasm of the macrophage and a ll preserved mitochondria (M) are also present. I the upper left corner part of a phagocytized cell (P) is seen and below that a membrane bound inclusion with lipid-like material (L) The cytoplasmic membrane (CM) of the macrophage show no changes in the region corresponding to the contact zone with the plasma cell (PO) denotes polyribosomes. This bone marrow specimen was not treated *en bloc* with uranyl acetate prior to dehydration. 93,000 ×

Fig 4 High-power view of the framed part of Fig. 1 Part of the nucleus (N) and cytoplasm of the DBMM is shown. The contact zone (CZ) is well illustrated even though the cell membranes are obliquely sectioned The rough endoplasmic reticulum (RER) of the macrophage is slightly dilated and connected with the perinuclear space (PNS) Note few filaments (F) in the electron lucent cytoplasm of the macrophage. 93,000 ×


M
M
PO
PO
FE
L
CM
CZ
PC
CZ
F
RER
F
RER
PNS
N

(Figs. 1 2) In survey micrographs of these DBMM no specific relationship to blood vessels or vascular sinuses was found, except in a very few instances in which the macrophage seemed to be in close contact with the wall of the vessel. The length and width of the DBMM ranged from 20 to 5 μm and from 5 to 2 μm, respectively The DBMM thus, appeared in survey electron micrographs as elongated cells in which the cytoplasm often was drawn out into very thin and delicate processes (Figs. 6, 7 8) As a consequence the cell shape of the sectioned DBMM varied from bipolar to more stellated or dendritic forms. The cytoplasmic matrix of the cell was generally electron lucent compared to other nucleated cells of the bone marrow and often only a small rim of cytoplasm surrounded the nucleus (Fig 1) Most of the DBMM possessed a single centrally located, indented nucleus which frequently contained some chromatin condensed close to the nuclear envelope (Figs. 1 2) A nucleolus was present in one third of the cells studied. The length and width of the nucleus ranged from 2 to 8 μm and 1 to 4 μm, respectively In addition to the cells, the nuclei of which were included in the sections available for study 380 different cytoplasmic processes of DBMM which possessed contact zones with plasma cells have been studied in detail (Figs. 6, 7 8, 10) The width of the cytoplasmic extensions could vary from 0 1 μm to 2 μm.

Many membrane bound vesicles were found in the cytoplasm of about half of the DBMM studied (Figs. 6, 7) Some of these vesicles were located in close proximity to or directly adhering to the cell membrane, whereas others were distributed in the cytoplasm. The diameter of the vesicles measured approximately 70 to 80 nm, and many were coated vesicles. Their contents varied from electron lucent to more electron dense material in which ferritin was often found.

Short segments of the rough endoplasmic reticulum with parallel cisternal membranes were found in the cytoplasm of each DBMM and the cisternae were only occasionally dilated (Fig 4) The number of free cytoplasmic ribosomes was small and most of them were present as polyribosomes consisting of 4 to 8 single ribosomes (Figs. 3 7) Filaments about 6 to 8 nm in diameter were frequently observed in the cytoplasm (Fig 4) Mitochondria about 0.6 μm long and 0.3 μm wide with well-developed cristae were found in all macrophages in which the nuclei were included in the sections (Fig 3) whereas a Golgi complex was only seen in 20 per cent of these cells (Fig. 2)

Lysosome-like dense bodies bound by a unit membrane were found in 60 per cent of the cells which were cut more or less centrally (Figs. 1 2 7) Other membrane bound cytoplasmic inclusions were found to contain lipid-like material (Fig 3) In four of the 30 cells in which the nuclei were included in the section, morphological evidence of phagocytosis of erythrocytes was found and residues of other cell types were also observed (Figs. 2, 3) Such inclusions of phagocytized material were always surrounded by unit membranes. The characteristic electron dense molecules of ferritin were found in the cytoplasm of 40 per cent of the total of 410 different DBMM studied. The amount of ferri-

Fig. 3 Part of DBMM showing contact zone (CZ) with plasma cell (PC) Ferritin molecules (FE) are dispersed in the cytoplasm of the macrophage and well preserved mitochondria (M) are also present. In the upper left corner part of a phagocytized cell (P) is seen and below that membrane bound inclusion with lipid-like material (L) The cytoplasmic membrane (CM) of the macrophage shows no changes in the region corresponding to the contact zone with the plasma cell (PO) denotes polyribosomes. This bone marrow specimen was not treated *en bloc* with uranyl acetate prior to dehydration. 93,000 ×

Fig 4 High-power view of the framed part of Fig 1 Part of the nucleus (N) and cytoplasm of the DBMM is shown The contact zone (CZ) is well illustrated even though the cell membranes are obliquely sectioned. The rough endoplasmic reticulum (RER) of the macrophage is slightly dilated and connected with the perinuclear space (PNS) Note few filaments (F) in the electron lucent cytoplasm of the macrophage. 93,000 ×

22*

tin varied considerably from cell to cell, but the ferritin was found both evenly dispersed in the cytoplasm and in aggregates surrounded by unit membranes (Fig 3) Such aggregates of ferritin were occasionally packed very densely together and could be seen in a crystalloid arrangement (Fig 5)

More than 400 DBMM were studied and all have shown one or more contacts with one or several different plasma cells (Figs. 1, 2) However, no characteristic alterations were observed in the morphology of the cytoplasm or of the cell membrane of the DBMM in the regions of contacts with plasma cells. This was irrespective of whether the zones were formed between thin cytoplasmic processes and plasma cells or formed in the vicinity of the nucleus of the DBMM (Figs. 3 4, 6 7 10) Some of the thin cytoplasmic processes from the DBMM were found to be electron dense and these could also make contact with plasma cells (Fig 8)

A small number of DBMM were found which in addition to contact zones with plasma cells, contained short segments of electron dense material (25–30 nm in thickness) adhering to the inner leaflet of the cell membrane (Figs. 9 10 11) Filaments with a diameter of 6–8 nm were found to radiate from these dense regions into the cytoplasm of the macrophage Some fuzzy material was found outside the plasma membrane in these regions, but no contact zones with other cells were ever seen (Fig 11) These DBMM were further characterized by an abundance of cytoplasmic filaments (6–8 nm in diameter) which were present in large bundles. No obvious sign of phagocytosis was observed nor was ferritin demonstrated in the few cells of this type studied

DISCUSSION

The ultrastructure of the dendritic bone marrow macrophage (DBMM) found in the bone marrow of patients with multiple myeloma is described in this report. The cell has been identified solely on ultrastructural criteria the formation of the contact zones with plasma cells being considered of main importance The DBMM appear to have an influence on the ultrastructure of the plasma cells which show a thickening of the inner leaflet of the cytoplasmic membrane in the regions of contact (Figs. 1 2)

According to the literature three types of cells in the bone marrow show some structural resemblance to the DBMM 1) the reticulum cells which constitute the sponge-like framework of the bone marrow 2) the endothelial cells which line the sinuses of the bone marrow and 3) the promonocytes with their descendants, the monocytes and the macrophages Of these the reticulum cell and the sinus endothelial cell are derived from the mesenchymal cells (12) and are considered to belong to the Reticulo-Endothelial System (1), whereas the promonocyte and its descendants are derived from the haemopoietic stem cell (13) and thus belong to the Mononuclear Phagocyte System (9 10)

The small number of DBMM with electron dense regions and filaments attached to the inner aspect of the plasma membrane at these regions had ultrastructural details very similar to those of the sinus endothelial cells from human bone marrow described recently by *Chen* & *Weiss* (8) These authors described how endothelial cells extended processes into the haematopoietic compartment and how

---

Fig 5 A detail from the cytoplasm of a DBMM showing a membrane bound inclusion with ferritin molecules (FE) packed in a crystalloid arrangement. 93 000 ×

Fig 6 A thin cytoplasmic projection of a DBMM extending in the interspace between two plasma cells (PC) In each plasma cell a contact zone (CZ) is seen. A coated vesicle (CV) is present in the cytoplasm of the macrophage 93,000 ×

Fig 7 Two cytoplasmic extensions of DBMM can be seen parallel to two plasma cells (PC) Note a contact zone (CZ) in each plasma cell. Many vesicles (V) a vacuole (VA) and a few dense bodies (DB) are present in one of the macrophage extensions. (PO) denotes a polyribosomal cluster 93 000 ×


5
FE
6
CZ
CZ
BBM
CZ
PC
VA
CZ
PC

tin varied considerably from cell to cell but the ferritin was found both evenly dispersed in the cytoplasm and in aggregates surrounded by unit membranes (Fig 3) Such aggregates of ferritin were occasionally packed very densely together and could be seen in a crystalloid arrangement (Fig. 5)

More than 400 DBMM were studied and all have shown one or more contacts with one or several different plasma cells (Figs. 1, 2) However, no characteristic alterations were observed in the morphology of the cytoplasm or of the cell membrane of the DBMM in the regions of contacts with plasma cells. This was irrespective of whether the zones were formed between thin cytoplasmic processes and plasma cells or formed in the vicinity of the nucleus of the DBMM (Figs. 3 4 6 7, 10) Some of the thin cytoplasmic processes from the DBMM were found to be electron dense and these could also make contact with plasma cells (Fig 8)

A small number of DBMM were found which in addition to contact zones with plasma cells, contained short segments of electron dense material (25–30 nm in thickness) adhering to the inner leaflet of the cell membrane (Figs. 9 10 11) Filaments with a diameter of 6–8 nm were found to radiate from these dense regions into the cytoplasm of the macrophage Some fuzzy material was found outside the plasma membrane in these regions, but no contact zones with other cells were ever seen (Fig 11) These DBMM were further characterized by an abundance of cytoplasmic filaments (6–8 nm in diameter) which were present in large bundles. No obvious sign of phagocytosis was observed nor was ferritin demonstrated in the few cells of this type studied

DISCUSSION

The ultrastructure of the dendritic bone marrow macrophage (DBMM) found in the bone marrow of patients with multiple myeloma is described in this report. The cell has been identified solely on ultrastructural criteria, the formation of the contact zones with plasma cells being considered of main importance The DBMM appear to have an influence on the ultrastructure of the plasma cells which show a thickening of the inner leaflet of the cytoplasmic membrane in the regions of contact (Figs. 1 2)

According to the literature three types of cells in the bone marrow show some structural resemblance to the DBMM 1) the reticulum cells which constitute the sponge-like framework of the bone marrow 2) the endothelial cells which line the sinuses of the bone marrow and 3) the promonocytes with their descendants, the monocytes and the macrophages Of these the reticulum cell and the sinus endothelial cell are derived from the mesenchymal cells (12) and are considered to belong to the Reticulo-Endothelial System (1) whereas the promonocyte and its descendants are derived from the haemopoietic stem cell (13) and thus belong to the Mononuclear Phagocyte System (9 10)

The small number of DBMM with electron dense regions and filaments attached to the inner aspect of the plasma membrane at these regions had ultrastructural details very similar to those of the sinus endothelial cells from human bone marrow described recently by *Chen & Weiss* (8) These authors described how endothelial cells extended processes into the haematopoietic compartment and how

---

Fig 5 A detail from the cytoplasm of a DBMM showing a membrane bound inclusion with ferritin molecules (FE) packed in a crystalloid arrangement. *93 000* ×

Fig 6 A thin cytoplasmic projection of a DBMM extending in the interspace between two plasma cells (PC) In each plasma cell a contact zone (CZ) is seen. A coated vesicle (CV) is present in the cytoplasm of the macrophage 93 000 ×

Fig 7 Two cytoplasmic extensions of DBMM can be seen parallel to two plasma cells (PC) *Note* a contact zone (CZ) in each plasma cell. *Many* vesicles *(V)* a vacuole (VA) and a few dense bodies (DB) are present in one of the macrophage extensions. (PO) denotes a polyribosomal cluster 93 000 ×

Macrophages (or phagocytic reticulum cells) are usually found in the interstitial space of the bone marrow where they are frequently situated in the centre of a group of erythroblasts or plasma cells (2, 5, 7, 19). According to these authors the macrophages are elongated cells with the cytoplasm often extended into very thin processes which intertwine with other cells. The macrophage nucleus is often irregular in outline with the chromatin condensed near the nuclear membrane and one or two nucleoli are generally present. Ribosomes, polyribosomes, a moderately developed Golgi complex and short segments of rough endoplasmic reticulum are found in the cytoplasm. Large phagolysosomes can be seen in the cytoplasm. Degenerated red blood cells, endocytic vesicles and other membrane bound inclusions often containing ferritin can be distinguished in the phagolysosomes.

I consider the DBMM cells to belong to the macrophage or the phagocytic reticulum cell line for the following reasons: 1) the ultrastructure of the cells corresponds very well to the ultrastructural details given by others for bone marrow macrophages, as stated in the preceding paragraph, 2) about 40 per cent of the cells, in which the nuclei were included in the sections, showed morphological evidence of endocytosis (17) and the phagocytized material generally consisted of debris of erythrocytes and/or leucocytes. However, the remaining DBMM in which the nuclei were included in the section did not show any sign of phagocytic activity. This could be due to the fact that only 1 per cent of the total cell volume is included in each cell section studied, or it could indicate that these macrophages do not possess a high phagocytic activity. Finally, I chose the designation "dendritic bone marrow macrophage" because the cells showed characteristic branching forms which ended in fine cytoplasmic processes, and with this term some reference to the type of tissue in which the cells are found is also given.

Canley & Haykov (7) studied the ultrastructure of haemic cells and described a characteristic association between plasma cells and phagocytic reticulum cells. The connections between the two cell types were found both in specimens from normal human bone marrow and from patients with multiple myeloma. The ultrastructure of the phagocytic reticulum cells they describe is comparable to that of the present DBMM, both with respect to nuclear morphology and to cytoplasmic organelles and inclusions. These authors did not describe any membrane thickenings in the plasma cells at the contact regions, but occasionally they found small cytoplasmic bridges connecting the cell membranes of the two cell types. Such cytoplasmic bridges have never been found in this study.

Dendritic cell types have been described in other tissues than the bone marrow. These cell types will be discussed briefly because they show some similarity in morphology with the DBMM of this study. Dendritic reticular (follicular) cells have been described by several authors (14, 21) and were found in lymphoid organs of various laboratory animals. These cells were shown to retain in vivo injected antigens on their surfaces as shown by immunofluorescence and electron microscopical autoradiography, but they showed only rare signs of phagocytic capacity. Recently Steinman & Cohn (18) described a dendritic cell which was found in the spleen of mice, but never in the bone marrow. The nuclear ultrastructure of this cell resembles that described for the present DBMM, but very little evidence for endocytosis was seen in this mouse spleen cell and its function is still unknown.

In conclusion, I find that my morphological studies on the DBMM from patients with multiple myeloma have provided evidence that the majority of these cells belong to the Mononuclear Phagocyte System (9) of the bone marrow. However, the finding of macrophages with low phagocytic activity is in agreement with the view that populations of macrophages from a single tissue source can be functional heterogeneous (20).

The physiological significance of the contact zones between the DBMM and the

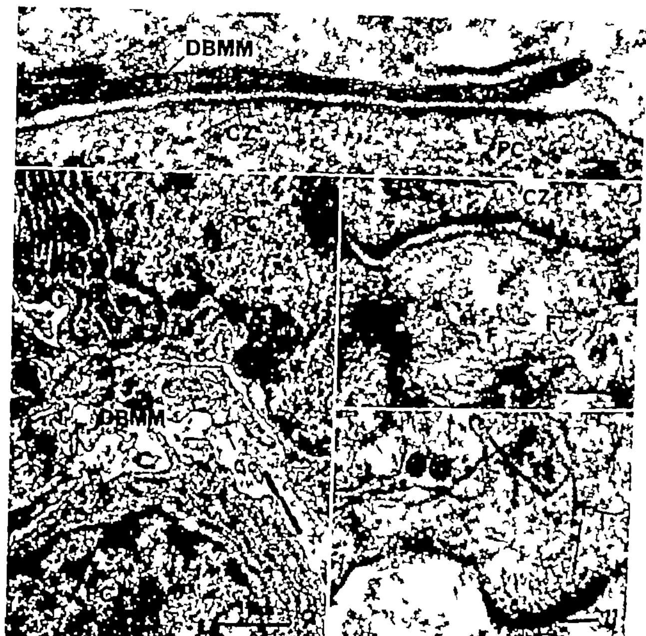


Fig 8 A high-power view of a dense cytoplasmic extension of a DBMM in close association with a plasma cell (PC) Note the constant distance between the cell membranes of the macrophage and the plasma cell in the contact zone region (CZ) 93 000 ×

Fig 9 A survey field showing parts of two plasma cells (PC) between which a cytoplasmic extension of a DBMM is seen. A contact zone (CZ) is present in the upper plasma cell. Note a dense zone (arrow) in the cell membrane of the macrophage. 16 000 ×

Fig 10 High-power view of part of Fig 9 showing the contact zone (CZ) Note the high content of cytoplasmic filaments (F) in the macrophage. 93 000 ×

Fig 11 High power view of part of the DBMM of Fig. 9 A dense zone is present at the cell membrane No contact with any other cell is seen at this zone Many cytoplasmic filaments (F) are present. 93 000 ×

the cells frequently surrounded developing blood cells. The sinus endothelial cells were also found to be attached to each other by junctional complexes of various kinds. It is tempting to speculate whether the dense regions I have observed on a limited number of DBMM membranes could be remnants of such junctions and whether this type of DBMM belongs to the sinus endothelial cell line

Macrophages (or phagocytic reticulum cells) are usually found in the interstitial space of the bone marrow where they are frequently situated in the centre of a group of erythroblasts or plasma cells (2 5 7 19). According to these authors the macrophages are elongated cells with the cytoplasm often extended into very thin processes which intertwine with other cells. The macrophage nucleus is often irregular in outline, with the chromatin condensed near the nuclear membrane and one or two nucleoli are generally present. Ribosomes, polyribosomes, a moderately developed Golgi complex and short segments of rough endoplasmic reticulum are found in the cytoplasm. Large phagolysosomes can be seen in the cytoplasm. Degenerated red blood cells, endocytic vesicles and other membrane bound inclusions often containing ferritin can be distinguished in the phagolysosomes.

I consider the DBMM cells to belong to the macrophage or the phagocytic reticulum cell line for the following reasons 1) the ultrastructure of the cells corresponds very well to the ultrastructural details given by others for bone marrow macrophages, as stated in the preceding paragraph, 2) about 40 per cent of the cells, in which the nuclei were included in the sections, showed morphological evidence of endocytosis (17) and the phagocytized material generally consisted of debris of erythrocytes and/or leucocytes. However the remaining DBMM in which the nuclei were included in the section did not show any sign of phagocytic activity. This could be due to the fact that only 1 per cent of the total cell volume is included in each cell section studied, or it could indicate that these macrophages do not possess a high phagocytic activity. Finally I chose the designation dendritic bone marrow macrophage because the cells showed characteristic branching forms which ended in fine cytoplasmic processes and with this term some reference to the type of tissue in which the cells are found is also given.

Cawley & Hayhoe (7) studied the ultrastructure of haemic cells and described a characteristic association between plasma cells and phagocytic reticulum cells. The connections between the two cell types were found both in specimens from normal human bone marrow and from patients with multiple myeloma. The ultrastructure of the phagocytic reticulum cells they describe is comparable to that of the present DBMM both with respect to nuclear morphology and to cytoplasmic organelles and inclusions. These authors did not describe any membrane thickenings in the plasma cells at the contact regions, but occasionally they found small cytoplasmic bridges connecting the cell membranes of the two cell types. Such cytoplasmic bridges have never been found in this study.

Dendritic cell types have been described in other tissues than the bone marrow. These cell types will be discussed briefly because they show some similarity in morphology with the DBMM of this study. Dendritic reticular (follicular) cells have been described by several authors (14 21) and were found in lymphoid organs of various laboratory animals. These cells were shown to retain *in vivo* injected antigens on their surfaces as shown by immunofluorescence and electron microscopical autoradiography but they showed only rare signs of phagocytic capacity. Recently *Steinman & Cohn* (18) described a dendritic cell which was found in the spleen of mice, but never in the bone marrow. The nuclear ultrastructure of this cell resembles that described for the present DBMM but very little evidence for endocytosis was seen in this mouse spleen cell and its function is still unknown.

In conclusion, I find that my morphological studies on the DBMM from patients with multiple myeloma have provided evidence that the majority of these cells belong to the Mononuclear Phagocyte System (9) of the bone marrow. However the finding of macrophages with low phagocytic activity is in agreement with the view that populations of macrophages from a single tissue source can be functional heterogeneous (20).

The physiological significance of the contact zones between the DBMM and the

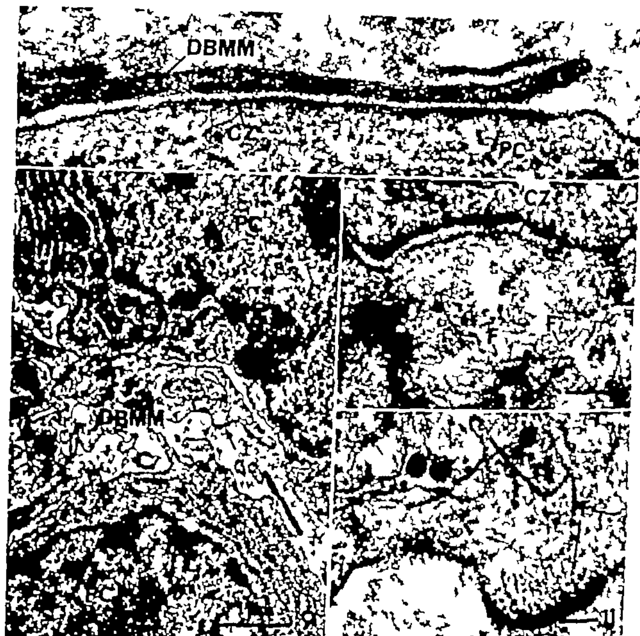


Fig 8 A high-power view of a dense cytoplasmic extension of a DBMM in close association with a plasma cell (PC) Note the constant distance between the cell membranes of the macrophage and the plasma cell in the contact zone region (CZ) 93 000 ×

Fig 9 A survey field showing parts of two plasma cells (PC) between which a cytoplasmic extension of a DBMM is seen. *A contact zone (CZ) is present in the upper plasma cell. Note* a dense zone (arrow) in the cell membrane of the macrophage. 16 000 ×

Fig 10 High power view of part of Fig 9 showing the contact zone (CZ) Note the high content of cytoplasmic filaments (F) in the macrophage 93 000 ×

Fig 11 High power view of part of the DBMM of Fig 9 A dense zone is present at the cell membrane. No contact with any other cell is seen at this zone. Many cytoplasmic filaments (F) are present. 93 000 ×

the cells frequently surrounded developing blood cells. The sinus endothelial cells were also found to be attached to each other by junctional complexes of *various kinds. It is* tempting to speculate whether the dense *regions I have observed on a* limited number of DBMM membranes could be remnants of such junctions and whether this type of *DBMM belongs to the sinus endothelial* cell line.

Acta path. microbiol. scand. Sect. A, 85 345-355, 1977

THE ULTRASTRUCTURE OF CONTACT ZONES BETWEEN PLASMA CELLS AND MACROPHAGES IN THE BONE MARROW OF PATIENTS WITH MULTIPLE MYELOMA*

JENS BLOM

Department of Biophysics, Statens Seruminstitut, Copenhagen, Denmark

Blom, J. The ultrastructure of contact zones between plasma cells and macrophages in the bone marrow of patients with multiple myeloma. Acta path. microbiol. scand. Sect. A, 85 345-355, 1977

The ultrastructure of intercellular connections between plasma cells and dendritic bone marrow macrophages found in bone marrow aspirations from 15 patients with multiple myeloma is described. Two types of cell-to-cell contact were observed 1) a juxtaposed type and 2) a mortise-joint type. In both types the zones are characterized by an amorphous electron dense layer adherent to the inner leaflet of the cytoplasmic membrane of the plasma cell, whereas no morphological changes are present in the macrophage. The thickness of the electron dense layer in the plasma cell was found to range from 11 to 33 nm and its extension along the membrane from 0.2 µm to 2-3 µm. The distance from plasma cell surface to the surface of the macrophage was found to range from 11 to 27 nm, but the two cell membranes were always parallel at the contact zone region. At the contact zones small amounts of electron dense material were generally present in the interspace between the cells, and sometimes fine bridges of this material were seen to connect the two cells. The cytoplasm of the plasma cell was sparse in organelles at the contact zone region except for cytoplasmic filaments (7-8 nm in diameter). However more than 30 per cent of the plasma cells did show a few electron dense, membrane bound granules close to the contact zones. In some plasma cells few coated vesicles were also found adjacent to the dense layers of the contact zones.

Key words: Contact zones; dendritic bone marrow macrophages; electron microscopy; multiple myeloma; plasma cells.

Jens Blom, Department of Biophysics, Statens Seruminstitut, Amager Boulevard 80, DK 2300 Copenhagen S, Denmark

Received 18.xi.76 Accepted 18.xi.76

This work is part of a project on a study of multiple myeloma, which is carried out as a co-operation between Department of Biophysics, Statens Seruminstitut, and Division of Haematology, Department of Medicine, University Hospital, Hvidovre Hospital, Copenhagen.

A previous paper briefly described cell-to-cell contacts between plasma cells and macrophages present in bone marrow specimens from patients with multiple myeloma (1). This cell-to-cell contact is characterized by an accumulation of amorphous, electron dense material at the inner leaflet of the cytoplas-

plasma cells is at present unknown. The ultrastructure of the contact zones will be described in a subsequent paper

The author thanks *Aage Drivsholm* M.D., Chief of the Division of Haematology Department of Medicine University Hospital Hvidovre Hospital, Copenhagen for the initiation and the valuable help during the study. I am indebted to *Joan Rhodes* Ph. D., Collaborative Centre for Reference and Research on Escherichia (WHO) Statens Seruminstitut, for her valuable and constructive criticism of the manuscript. The excellent and patient technical assistance of Mrs. *Jytte Berg* is gratefully acknowledged. Mr *Finn Lauritsen* and Miss *Anne Grethe Overgaard* are thanked for their expert photographic work.

I wish to thank the chiefs of the Medical Department of Finsen Hospital Copenhagen and the Medical Department B of Hillerød County Hospital respectively for providing me bone marrow aspirations from some of the patients.

REFERENCES

1 *Aschoff L.* Das reticulo-endotheliale System. Ergebn. inn. Med Kinderheilk *26* 1–119 1924
2. *Bessis M* Living blood cells and their ultrastructure Springer Berlin 1973 p. 486
3 *Blom J* The ultrastructure of contact zones between plasma cells and dendritic macrophages from patients with multiple myeloma. Acta path. microbiol. scand Sect. A *81* 7 4–736, 1973
4 *Blom J Mansa B & Wiik A* A study of Russell bodies in human monoclonal plasma cells by means of immunofluorescence and electron microscopy Acta path. microbiol scand Sect. A, *84* 335–349 1976
5 *Carr I* The macrophages A review of ultrastructure and function. Academic Press London and New York 1973 p. 29
6 *Caulfield J B* Effect of varying the vehicle for osmic acid in tissue fixation. J biophys. biochem. Cytol *3* 827 830 1957
7 *Cawley J C & Hayhoe F G J* Ultrastructure of haemic cells. W B Saunders Company London 1973 p 132 and 248
8. *Chen Li Tsun & Weiss L.* The development of vertebral bone marrow of human fetuses Blood *46* 389–408, 1975
9 *Furth R van Langevoort H L. & Schaberg A* Mononuclear phagocytes in human pathology—Proposal for an approach to improved classification *In* van Furth, R. (Ed.) Mononuclear Phagocytes in Immunity Infection and Pathology Blackwell Scientific Publ. Oxford 1975 p. 1–15
10 *Langevoort H L, Cohn Z. A. Hirsch J G Humphrey J H Spector W G & van Furth, R* The nomenclature of mononuclear phagocyte cells a proposal for a new classification. *In* van Furth, R. (Ed.) Mononuclear Phagocytes. Blackwell Scientific Publ., Oxford 1970, p 1
11 *Luft J H* Improvements in epoxy resin embedding methods. J biophys. biochem. Cytol *9* 409–414 1961
12 *Maximow A A* Handbuch der mikroscopischen Anatomie des Menschen. Part I Bindgewebe und blutbildende Gewebe, vol. 2. Springer Berlin 1927
13 *Metcalf D & Moore M A S* Haemopoietic cells. North Holland Amsterdam. Monographs Frontiers of Biology vol 24 1971 p. 295
14 *Nossal G J V & Ada G L.* Antigens, lymphoid cells and the immune response Academic Press, New York and London 1971 p 125
15 *Ryter A & Kellenberger E* L inclusion au polyester pour l ultramicrotomie. J Ultrastruct. Res. *2* 200–214 1958.
16 *Sabatini D D., Bensch K & Barrnett R J* Cytochemistry and electron microscopy The preservation of cellular structure and enzymatic activity by aldehyde fixation. J Cell. Biol *17* 19–58, 1963
17 *Simson J V & Spicer S S* Activities of specific cell constituents in phagocytosis (endocytosis) Int. Rev exp Path. *12* 79–118, 1973
18. *Steinman R M & Cohn Z A* Identification of a novel cell type in peripheral lymphoid organs of mice. I Morphology quantitation tissue distribution. J exp Med. *137* 1142–1162 1973
19 *Tanaka Y & Goodman J R* Electronmicroscopy of human blood cells Harper & Row (Publ) New York and London, 1972 p. 374
20 *Walker W S* Functional heterogeneity of macrophages in the induction and expression of acquired immunity J reticuloendothel. Soc. *20* 57-65 1976
21 *White R G French V J & Stark J M* A study of the localisation of a protein antigen in the chicken spleen and its relation to the formation of germinal centres J med. Microbiol. *3* 65–83 1970

mic membrane of the plasma cell whereas there were no morphological changes in the cell membranes of the macrophage The study has since been extended to bone marrow aspirations from 15 patients with multiple myeloma. For reasons given in another paper in which the ultrastructure of the macrophages that show contacts with plasma cells was studied this type of macrophage was termed a dendritic bone marrow macrophage (DBMM) (3)

The purpose of the present report is to describe the ultrastructure of the contact zones between the plasma cells and the DBMM and to describe in detail the contents of the plasma cell cytoplasm at the regions of contact

MATERIAL AND METHODS

Patients

The blood of each of the 15 patients studied contained a serum M-component. Blood from five of the patients contained an M-component of the IgG type kappa from six patients an IgG type lambda from two patients an IgA type kappa, and from two Bence Jones proteins of the type kappa The number of plasma cells in relation to the total number of the nucleated cells in the bone marrow of the patients was in all cases abnormally high ranging from 5–80 per cent Most of the patients were followed regularly over a period of several years and a total of 70 bone marrow aspirations were examined The first bone marrow sample from a patient was always taken prior to the initiation of treatment with cytostatics (melphalan or cyclophosphamide)

Methods for Electron Microscopy

The methods used are described in detail in previously published papers (2 3) Briefly summarized the bone marrow specimens were prefixed in glutaraldehyde postfixed in osmium tetroxide treated *en bloc* with uranyl acetate prior to dehydration with alcohol and propyleneoxide and finally embedded in Vestopal W Thin sections were counter stained with magnesium uranyl acetate (8) and lead citrate (13) and examined in a Philips 300 electron microscope For this study approximately 5000 electron micrographs were studied

RESULTS

Over 2500 different plasma cells from the bone marrow of 15 patients with multiple myeloma were studied Among these cells about 500 which showed contact zones with DBMM were found and studied in detail Most of the plasma cells whether in contact with DBMM or not, exhibited structural features which showed a disparity between the degree of maturity of the nucleus and that of the cytoplasm. This asynchrony was manifested by a mature well-organized cytoplasm with numerous stacks of flattened cisternae of the rough endoplasmic reticulum (Fig 4) and a nucleus with dispersed small aggregates of chromatin In the nucleus a large and prominent nucleolus was often present (Fig. 2) These nuclear characteristics are in contrast to those of the typically mature plasma

---

Figs 1 to 15 all show electron micrographs of sections obtained from bone marrow specimens from *patients with multiple myeloma. The bar* on each micrograph represents 100 nm unless otherwise stated.

Fig 1 Detail from a plasma cell (PC) which shows a contact zone (CZ) with a dense cytoplasmic extension (DCE) of a dendritic bone marrow macrophage (DBMM) Note the dense layer attached to the inner leaflet of the cell membrane of the plasma cell in the contact region. Delicate electron opaque bridges are present between the cells at the contact zone The dilated cisternae of the rough endoplasmic reticulum (RER) of the plasma cell show few ribosomes (R) attached to the parts of the membranes which are closest to the contact zone. 93 000 ×

Fig 2 A survey of a part of a plasma cell (PC) in which the immature appearing nucleus (N) with a large nucleolus (NU) is illustrated together with the mature well differentiated cytoplasm. A large Golgi complex (G) with a pair of centrioles (C) is present. Several dense bodies (DB) are found in the vicinity of the contact zone (CZ) with a macrophage. 16 000 ×

Fig 3 High-power view of the framed part of Fig 2 In this particular contact zone (CZ) the apposed cell membranes are obliquely sectioned and not very well resolved. In the plasma cell (PC) the cytoplasm adjacent to the contact zone is rich in cytoplasmic filaments, some of which are cross cut (FC) and some (F) which radiate from the dense layer (DL) of the contact zone. A dense body (DB) and mitochondria (M) are also present. Some ferritin (FE) is found in the DBMM 93 000 ×

DCE
CZ
RER
FE
FC
PC
M
PC
DL
RER
CZ
N
PC
DB
DB

mic membrane of the plasma cell whereas there were no morphological changes in the cell membranes of the macrophage. The study has since been extended to bone marrow aspirations from 15 patients with multiple myeloma For reasons given in another paper in which the ultrastructure of the macrophages that show contacts with plasma cells was studied this type of macrophage was termed a dendritic bone marrow macrophage (DBMM) (3)

The purpose of the present report is to describe the ultrastructure of the contact zones between the plasma cells and the DBMM and to describe in detail the contents of the plasma cell cytoplasm at the regions of contact

MATERIAL AND METHODS

Patients

The blood of each of the 15 patients studied contained a serum M-component Blood from five of the patients contained an M-component of the IgG type kappa from six patients an IgG type lambda, from two patients an IgA type kappa and from two Bence-Jones proteins of the type kappa The number of plasma cells in relation to the total number of the nucleated cells in the bone marrow of the patients was in all cases abnormally high ranging from 5 80 per cent Most of the patients were followed regularly over a period of several years and a total of 70 bone marrow aspirations were examined. The first bone marrow sample from a patient was always taken prior to the initiation of treatment with cytostatics (melphalan or cyclophosphamide)

Methods for Electron Microscopy

The methods used are described in detail in previously published papers (2 3) Briefly summarized the bone marrow specimens were prefixed in glutaraldehyde, postfixed in osmium tetroxide treated *en bloc* with uranyl acetate prior to dehydration with alcohol and propyleneoxide and finally embedded in Vestopal-W Thin sections were counter stained with magnesium uranyl acetate (8) and lead citrate (13) and examined in a Philips 400 electron microscope For this study approximately 5000 electron micrographs were studied

RESULTS

Over 2500 different plasma cells from the bone marrow of 15 patients with multiple myeloma were studied Among these cells about 500 which showed contact zones with DBMM were found and studied in detail. Most of the plasma cells, whether in contact with DBMM or not, exhibited structural features which showed a disparity between the degree of maturity of the nucleus and that of the cytoplasm. This asynchrony was manifested by a mature well-organized cytoplasm with numerous stacks of flattened cisternae of the rough endoplasmic reticulum (Fig 4) and a nucleus with dispersed small aggregates of chromatin. In the nucleus a large and prominent nucleolus was often present (Fig. 2) These nuclear characteristics are in contrast to those of the typically mature plasma

---

Figs 1 to 15 all show electron micrographs of sections obtained from bone marrow specimens from patients with multiple myeloma. The bar on each micrograph represents 100 nm unless otherwise stated.

Fig 1 Detail from a plasma cell (PC) which shows a contact zone (CZ) with a dense cytoplasmic extension (DCE) of a dendritic bone marrow macrophage (DBMM) Note the dense layer attached to the inner leaflet of the cell membrane of the plasma cell in the contact region. Delicate electron opaque bridges are present between the cells at the contact zone The dilated cisternae of the rough endoplasmic reticulum (RER) of the plasma cell show few ribosomes (R) attached to the parts of the membranes which are closest to the contact zone 93 000 ×

Fig 2 A survey of a part of a plasma cell (PC) in which the immature appearing nucleus (*N*) with a large nucleolus (NU) is illustrated together with the mature well differentiated cytoplasm. A large Golgi complex (G) with a pair of centrioles (C) is present Several dense bodies (DB) are found in the vicinity of the contact zone (CZ) with a macrophage 16 000 ×

Fig 3 High-power view of the framed part of Fig 2 In this particular contact zone (CZ) the apposed cell membranes are obliquely sectioned and not very well resolved. In the plasma cell (PC) the cytoplasm adjacent to the contact zone is rich in cytoplasmic filaments, some of which are cross cut (FC) and some (F) which radiate from the dense layer (DL) of the contact zone. A dense body (DB) and mitochondria (M) are also present Some ferritin (FE) is found in the DBMM 93,000 ×

cell in which the chromatin is present mainly as large peripheral aggregates. However the degree of asynchrony varied from patient to patient.

The percentage which plasma cells with contact zones constitute of the total number of plasma cells in the bone marrow has been estimated for one patient only. The reason for this is that micrographs of 456 different plasma cells were obtained from this patient, whilst we were unaware of the existence of the contact zones with the DBMM. Afterwards a careful examination of these cells showed that 41 possessed contact zones, corresponding to 9 per cent. However it is a general impression in our laboratory that plasma cells with contact zones were more numerous in samples from patients at the terminal stage of the disease than in samples from patients in a steady state of the disease. On the other hand, the contact zones were observed in plasma cells from specimens taken before as well as after treatment of the patients with melphalan or cyclophosphamide.

Two types of cell-to-cell connections were observed in the contact zones between plasma cells and the DBMM 1) a juxtaposed type and 2) a mortise joint type. Of these the juxtaposed type is by far the most common and examples are shown in Figs. 1 3 6 8, 9 11 12, 13 and 15. The mortise joint type has only been observed in a few cases, some in which the cytoplasmic extensions were longitudinally sectioned (Fig. 5) and others where they were transversally cut (Fig. 6).

The distance between the apposing cell membranes of the DBMM and the plasma cells is constant through the length of each contact zone, but can vary between individual zones. Values ranging from 11 to 27 nm with a mean of 18 nm were obtained from measurements of 130 zones. Some electron opaque material was always present in the interspace between cells at the contact zones, but sometimes fine bridges of this material was seen to connect the two cell surfaces (Figs. 1 5). An accumulation of some electron dense amorphous material was found on the inner aspect of the cell membrane of the plasma cell at each contact zone. The exact thickness of this dense layer could not be determined because the demarcation between this and the interior part of the cytoplasm was always diffuse (Figs. 1 5) but values from 11 to 33 nm with a mean of 25 nm were obtained from measurements at 130 contact zones. The length of the zone ranged from 0.2 to 2.5 µm. Serial sections of a few zones were prepared in order to determine the depth of the contact zones. Calculations from serial sections of the juxtaposed type showed that the zones were at least 400 to 700 nm deep. Up to three different contact zones have been found on a single plasma cell. Such contact zones were often situated diagonally with respect to each other on the cell surface. However the two different types of contact zones with the DBMM have been encountered on one and the same plasma cell (Fig. 6).

About 10 per cent of the plasma cells which showed a dense layer at the inner aspect of their cell membranes did not appear

---

Fig. 4 Survey of a part of a plasma cell (PC) in which an immature nucleus and a mature well differentiated cytoplasm are illustrated. An abundance of rough endoplasmic reticulum (RER) with cisternae parallel to each other is present in the plasma cell together with large mitochondria (M) and dense bodies (DB). In the upper right corner a DBMM extension has formed contact zone (CZ) of the mortise-joint type with the plasma cell. 16,000 ×

Fig. 5 High-power view of the framed part of Fig. 4. The mortise-joint type of contact zone (CZ) between a plasma cell (PC) and a dense cytoplasmic extension (DCE) from a DBMM is shown. Note the uniform thickness of the dense layer (DL) and the constant distance between the two apposing cell membranes (CM). 93,000 ×

Fig. 6 A detail which shows that the two types of contact zones (see text) can occur in different regions of a plasma cell (PC). The juxtaposed type is marked (JP) and the mortise-joint type (MJ). The mortise-joint type is seen in cross section with cytoplasmic extension of the plasma cell (PC) surrounded by the DBMM. Note the dense layers on the plasma cell membrane, but no morphological changes at the cell membrane of the DBMM in the contact zone regions. 93,000 ×

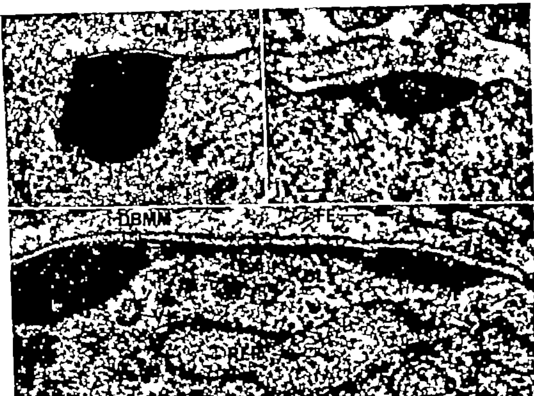


Fig 10 Part of plasma cell in which an extremely thick dense layer (DL) is present at the inner aspect of the cell membrane. This type of dense layer was found in the plasma cells of one particular patient. Fluffy material is seen exterior to the cell membrane (CM) at the dense layer region. 93,000 ×

Fig 11 Part of another plasma cell from the same patient as the cell shown in Fig. 10 A contact zone (CZ) is seen in which the thick dense layer (DL) is lens-shaped, Ribosomes (R) are present in the plasma cell cytoplasm close to the dense layer 93,000 ×

Fig 12 A long contact zone between a plasma cell (PC) and a DBMM of the same patient, as the cells show in Figs 10 and 11 The lenticular dense layers (DL_1) and (DL_3) are connected with dense layer (DL_2) of uniform thickness. Small vesicles (V) some of which contain electron dense material are seen in the adjacent plasma cell cytoplasm. RER denotes rough endoplasmic reticulum of the plasma cell Ferritin (FE) is present in the DBMM extension. 93,000 ×

seem to have any definite connection with the dense layer of the zone, although in some instances (Fig 3) they appeared to be radiating from the dense layer Apart from these filaments the cytoplasm in the immediate vicinity of the contact zone was very sparse in organelles. Dense, membrane-bound granules were, however found in the cytoplasm close to the contact zones in more than 50 per cent of the plasma cells (Figs. 3 9) The rough endoplasmic reticulum has not been observed in direct contact with the dense layers of the contact zones and only few ribosomes were found on the parts of the reticulum membranes which were present in the adjacent cytoplasm (Fig 1) Free ribosomes of the cytoplasm were rarely present in the contact zone region (Fig 11) Coated vesicles, often with direct connection to the cell membrane, were present in a few per cent of the plasma cells studied. These coated vesicles were sometimes seen in close contact with the dense layer of a contact zone on the cell (Figs. 13 14 15)

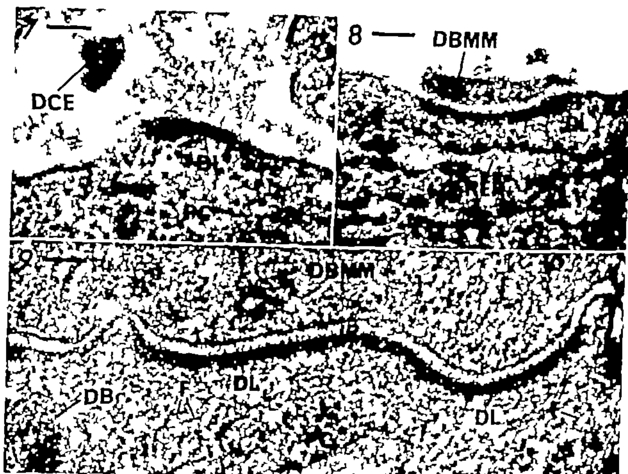


Fig 7 Part of a plasma cell (PC) in which a dense layer (DL) is adhering to the cell membrane. Corresponding to this layer some fluffy material is present on the exterior of the cell membrane. At some distance a cross sectioned dense cytoplasmic extension (DCE) probably from a DBMM is seen. 93 000 ×

Fig 8 A short contact zone with the rough endoplasmic reticulum (RER) close to the dense layer (DL) in the *cytoplasm of the plasma cell (PC) The dense layer is only present in a region* which corresponds exactly to the length of the cytoplasmic extension of the DBMM 93 000 ×

Fig 9 A long and well-developed contact zone of the juxtaposed type (JP) between a plasma cell (PC) and a DBMM Note the dense body (DB) and the many filaments (F) present in the plasma cell cytoplasm adjacent to the dense layer (DL) 93 000 ×

to be in close contact with a DBMM (Figs. 7 10 14) Instead patches of fluffy material were adhering to the outer aspect of the cell membrane at regions where the dense layer was present.

Contact zones with an extraordinarily thick dense layer were observed to constitute up to 30 per cent of the zones present on the plasma cells of one particular patient (Figs. 11 12) This patient a 68-year-old woman suffered from multiple myeloma with a serum M-component of the IgG type lambda, and despite treatment with cytostatics immediately after diagnosis she died after three months. The dense layer at the contact zones of the plasma cells of this patient was often lens-shaped and did not show any structural organization Layers as thick as 300 nm were observed (Figs. 10 11 12) This type of dense layer was seen to fuse with the normal type of dense layer in some of the plasma cells of this patient (Fig 12)

Cytoplasmic filaments (7–9 nm in diameter) were present in the cytoplasm of the plasma cells at the contact zones with the DBMM (F



Fig. 10 Part of plasma cell in which an extremely thick dense layer (DL) is present at the inner aspect of the cell membrane. This type of dense layer was found in the plasma cells of one particular patient. Fluffy material is seen exterior to the cell membrane (CM) at the dense layer region. 93,000 ×

Fig. 11 Part of another plasma cell from the same patient as the cell shown in Fig. 10. A contact zone (CZ) is seen in which the thick dense layer (DL) is lens-shaped. Ribosomes (R) are present in the plasma cell cytoplasm close to the dense layer. 93 000 ×

Fig. 12 A long contact zone between a plasma cell (PC) and a DBMM of the same patient, as the cells shown in Figs. 10 and 11. The lenticular dense layers (DL_1) and (DL_2) are connected with a dense layer (DL_3) of uniform thickness. Small vesicles (V), some of which contain electron dense material are seen in the adjacent plasma cell cytoplasm. RER denotes rough endoplasmic reticulum of the plasma cell. Ferritin (FE) is present in the DBMM extension. 93,000 ×

seem to have any definite connection with the dense layer of the zone, although in some instances (Fig. 5) they appeared to be radiating from the dense layer. Apart from these filaments the cytoplasm in the immediate vicinity of the contact zone was very sparse in organelles. Dense, membrane bound granules were, however, found in the cytoplasm close to the contact zones in more than 50 per cent of the plasma cells (Figs. 5–9). The rough endoplasmic reticulum has not been observed in direct contact with the dense layers of the contact zones and only few ribosomes were found on the parts of the reticulum membranes which were present in the adjacent cytoplasm (Fig. 1). Free ribosomes of the cytoplasm were rarely present in the contact zone region (Fig. 11). Coated vesicles, often with direct connection to the cell membrane, were present in a few per cent of the plasma cells studied. These coated vesicles were sometimes seen in close contact with the dense layer of a contact zone on the cell (Figs. 13, 14, 15).

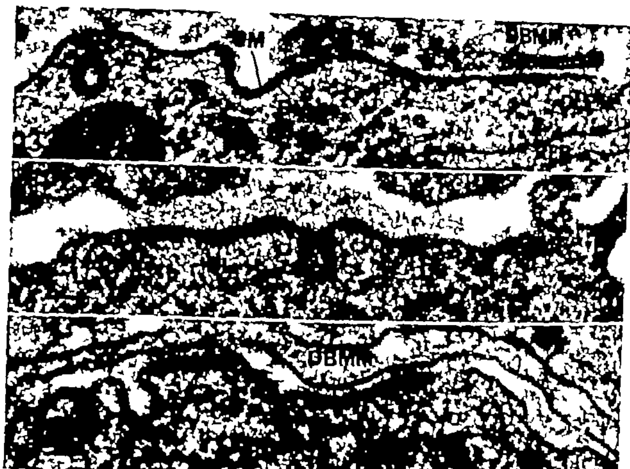


Fig 13 Part of a plasma cell which has a very thin dense layer (DL_1) at the zone of contact with a DBMM extension. The contact zone ends at an indentation of the cell membrane (CM) where another thin dense layer (DL_2) is seen. A coated vesicle (CV) which appears to show a thin connection to the cell membrane is present in the nearby cytoplasm. Part of a mitochondrion (M) and some of the rough endoplasmic reticulum (RER) are also seen. 93 000 ×

Fig 14 Part of a plasma cell with a dense layer (DL) at the cell membrane, but without contact with a DBMM Some fluffy material is present on the outer leaflet of the cell membrane at the region of the dense layer A coated vesicle (CV) is seen in contact with the cell membrane in the middle of the dense layer region. The vesicle seems to be in direct communication with the extracellular space 93 000 ×

Fig 15 Part of a plasma cell showing two contact zones (CZ) with a DBMM extension. The dense layer of one of the contact zones is confluent with a coated vesicle (CV) 93 000 ×

Apart from the zones of contact with the DBMM the morphology of the plasma cells which showed these zones did not differ from the other malignant plasma cells present in the bone marrow samples of these patients.

DISCUSSION

This paper has described the ultrastructure of contact zones between plasma cells and DBMM in bone marrow specimens from patients with multiple myeloma At present plasma cells with these characteristic contact zones with DBMM have only been found in the marrow of patients with multiple myeloma. However so far only a limited number of marrow specimens from patients lacking a serum M-component, have been studied in our laboratory Consequently it is uncertain whether or not bone marrow plasma cells with contact zones are confined exclusively to patients with multiple myeloma.

The specimen preparation technique used throughout has included *en bloc* treatment

with uranyl acetate prior to dehydration. This treatment should ensure optimal preservation of cell membranes and cellular junctions (9, 17). The presence of a dense layer in the plasma cells at the contact regions is, however, independent of whether this treatment is included or not (see Fig. 3 in ref. 3). Furthermore, the contact zones are not produced as a result of treatment of the patients with cytostatics, because the zones were present in plasma cells obtained from patients prior to treatment with melphalan or cyclophosphamide. There is thus no reason to believe that the contact zones are artifacts produced during specimen preparation or as a result of metabolic alterations after therapeutical treatment of the patients.

The ultrastructure of the association between plasma cells and macrophages or phagocytic reticulum cells has been studied by only a few investigators. *Thiéry* (18) described plasmocytic islets, with a central macrophage surrounded by a group of plasma cells, in spleen and lymph nodes from normal and hyperimmunized mice and rats. Results from bone marrow specimens were not reported. *Thiéry* also described a close contact between the macrophage and the plasma cells, and on the micrographs published in that paper a distance of 25 nm can be measured between the apposing cell membranes. Furthermore, micropinocytotic vesicles or coated vesicles—some of which contain ferritin—are seen to be present in the plasma cells corresponding to the "contact zones". No dense layer seems to be present, and *Thiéry* does not refer to such a layer in the paper. I have been unable to confirm *Thiéry's* observations of ferritin in coated vesicles of the plasma cells. Ferritin has never been observed in plasma cells in contact with DBMM, although ferritin was present in 40 per cent of the corresponding DBMM (3).

Cawley & Hayhoe (4) describe the finding of plasma cells grouped around a phagocytic reticulum cell both in normal human bone marrow and in bone marrow from patients with multiple myeloma. In their micrographs the distance between the apposing cell membranes far exceeds the distance observed in the present study. However, these authors show a high magnification of a narrow cytoplasmic bridge connecting a phagocytic reticulum cell and a plasma cell in a specimen from a normal human bone marrow. They have used the same methods for fixation and dehydration as I have, except for the *en bloc* treatment with uranyl acetate, but they have not observed any dense layers in the plasma cells at the regions of contact with the reticulum cells.

The physiological significance of the described contact zones is at present completely unknown, but some tentative speculations in this respect will be given briefly.

The contact zone shows some resemblance to the hemi-desmosome found in the basal cells of the stratified squamous epithelium (6). However, cytoplasmic filaments are very seldom seen to converge upon the dense layer in the plasma cells, as they generally do on the dense plaque of the hemi-desmosome. If, nevertheless, the contact zones are some sort of hemi-desmosomes, it could mean that they have a possible role in the maintenance of the position of the plasma cell within the structural configuration of the bone marrow. Of the two types of contact zones described, the juxtaposed type and the mortise-joint type, the last mentioned in particular must be able to link the cells firmly together. About 10 per cent of the plasma cells in the material studied possessed a dense layer adjacent to the cell membrane, but lacked the cell-to-cell contact with a DBMM. Very often, however, small cytoplasmic extensions which could be from DBMM were found at some distance from the plasma cell (cf. Fig. 7). This may indicate that the cells were torn apart when the marrow was aspirated or later during specimen preparation.

Bone marrow plasma cells from patients with multiple myeloma can be grown in short term tissue cultures (15, 16). Under such conditions these cells are able to produce a bone-resorbing factor which resembles an osteoclast activating factor and which causes local bone destruction (12). It has



Fig 13 Part of a plasma cell which has a very thin dense layer (DL_1) at the zone of contact with a DBMM extension. The contact zone ends at an indentation of the cell membrane (CM) where another thin dense layer (DL_2) is seen. A coated vesicle (CV) which appears to show a thin connection to the cell membrane is present in the nearby cytoplasm. Part of a mitochondrion (M) and some of the rough endoplasmic reticulum (RER) are also seen. 93 000 ×

Fig 14 Part of a plasma cell with a dense layer (DL) at the cell membrane but without contact with a DBMM. Some fluffy material is present on the outer leaflet of the cell membrane at the region of the dense layer. A coated vesicle (CV) is seen in contact with the cell membrane in the middle of the dense layer region. The vesicle seems to be in direct communication with the extracellular space. 93 000 ×

Fig 15 Part of a plasma cell showing two contact zones (CZ) with a DBMM extension. The dense layer of one of the contact zones is confluent with a coated vesicle (CV) 93 000 ×

Apart from the zones of contact with the DBMM the morphology of the plasma cells which showed these zones did not differ from the other malignant plasma cells present in the bone marrow samples of these patients.

DISCUSSION

This paper has described the ultrastructure of contact zones between plasma cells and DBMM in bone marrow specimens from patients with multiple myeloma. At present plasma cells with these characteristic contact zones with DBMM have only been found in the marrow of patients with multiple myeloma. However so far only a limited number of marrow specimens from patients lacking a serum M-component, have been studied in our laboratory Consequently it is uncertain whether or not bone marrow plasma cells with contact zones are confined exclusively to patients with multiple myeloma.

The specimen preparation technique used throughout has included *en bloc* treatment

tions between T cells, B cells and macrophages. Transplant. Rev *13* 3–34 1972.

8. *Franca, J M & Parks V R.* A routine technique for double-staining ultrathin sections using uranyl and lead salts. J Cell Biol. *25* 157–161 1965.

9. *Ghadially F N* Ultrastructural pathology of the cell. Butterworths, London and Boston 1975 p 472.

10. *Lachmann P J.* Lymphocyte cooperation. Proc. roy Soc B *176* 425–426 1971

11. *Mc kleen N A.* The immunogenic capacity of antigen taken up by peritoneal exudate cells. Immunology *16* 1–14 1969

12. *Mundy G R Raisz, L. G., Cooper R. A., Schechter G P & Salmon, S E.* Evidence for the secretion of an osteoclast stimulating factor in myeloma. New Engl J Med. *291* 1041–1046 1974

13. *Reynolds, E. S* The use of lead citrate at high pH as an electron-opaque stain in electron microscopy J Cell Biol. *17* 208–212, 1963.

14. *Roth, T F & Porter K. R.:* Yolk protein uptake in the oocyte of the mosquito *Aedes aegypti* L. J Cell Biol. *20* 313–332, 1964

15. *Salmon S E & Smith B. A.:* Sandwich solid phase radioimmunoassays for the characterization of human immunoglobulins synthesized in *vitro* J Immunol. *104* 665–672, 1970.

16. *Salmon S E & Smith B. A.* Immunoglobulin synthesis and total body tumor cell number in IgG multiple myeloma. J clin. Invest. *49* 1114–1121 1970.

17. *Terzakis, J A.* Uranyl acetate a stain and a fixative. J Ultrastruct. Res. *22* 168–184 1968.

18. *Thiéry J P* Étude au microscope électronique de l'ilot plasmocytaire. J Microscopie *1* 275–286 1962.

19. *Unanue E. R. & Calderon J.* E aluation of the role of macrophages in immune induction. Fed. Proc. *34* 1737–1742, 1975

20. *Waldenström J* Diagnosis and treatment of multiple myeloma. Grune and Stratton, New York 1970 p. 15

also been found that bone marrow cultures of malignant plasma cells from patients with multiple myeloma released interferon into the growth medium (5) However, none of these studies describe the ultrastructure of the cultured plasma cells. It is tempting to speculate, nevertheless, whether the plasma cells with contact zones described here could produce any such biologically active compounds. Morphologically these cells show well-developed cytoplasmic organelles and should be at a high level of maturity with regard to cellular synthesis and secretion.

Thiéry (18) as well as *Cawley* & *Hayhoe* (4) discuss the role of the close association between the macrophages or the phagocytic reticulum cells and the plasma cells. They suggest that this type of connection could provide a means of transferring immunological information from the phagocytic cells to the plasma cells. I have found coated vesicles very close to the dense layer of the contact zone of the plasma cells and such vesicles are believed to be formed by cells concerned with protein uptake (14) There may thus, be some morphological evidence for the immunological information hypothesis, but we still do not know whether the coated vesicles of these plasma cells take part in endo- or exocytotic processes.

Several studies have shown that a collaboration between thymus-dependant (T) and bone marrow derived (B) lymphocytes is necessary and also that the participation of macrophages seems to be of importance for the elicitation of a primary antibody response to many antigens (7 10 11) The function of these macrophages involved in the immune induction is related directly or indirectly to the uptake and handling of the antigen (19) It is possible that the contact zones described here represent areas in which antigen is retained on the surface of the macrophages as an immunogen in concentrations which could be sufficient to stimulate lymphocytes.

Finally it should be borne in mind that the histopathological feature of the disease multiple myeloma is a malignant proliferation of plasma cells (20) which are the endproduct of stimulated B-lymphocytes. The observed contact zones between the plasma cells and the DBMM in the bone marrow of patients with multiple myeloma might thus simply be manifestations, at the ultrastructural level, of this abnormal plasma cell proliferation.

The author thanks *Aage Drivsholm* MD Chief of the Division of Haematology Department of Medicine, University Hospital, Hvidovre Hospital, Copenhagen, for the initiation and the valuable help during the study I am indebted to *Jean Rhodes* Ph. D Collaborative Centre for Reference and Research on Escherichia (WHO) Statens Seruminstitut, for her valuable and constructive criticism of the manuscript. The excellent and patient technical assistance of Mrs. *Jytte Berg* is gratefully acknowledged. Mr *Finn Laursen* and Miss *Anne Grethe Overgaard* are thanked for their expert photographic work.

I wish to thank the chiefs of the Medical Department of Finsen Hospital Copenhagen, and the Medical Department B of Hillerød County Hospital respectively for providing me bone marrow aspirations from some of the patients.

REFERENCES

1 *Blom J.* The ultrastructure of contact zones between plasma cells and dendritic macrophages from patients with multiple myeloma. Acta path. microbiol. scand. Sect. A, *81* 734–736 1973

2 *Blom J Mansa B & Wiik A* A study of Russell bodies in human monoclonal plasma cells by means of immunofluorescence and electron microscopy Acta path. microbiol. scand. Sect. A *84* 335–349 1976

3 *Blom J* The ultrastructure of macrophages found in contact with plasma cells in the bone marrow of patients with multiple myeloma. Acta path. microbiol. scand. Sect. A, *85* 335–344 1977

4 *Cawley J C & Hayhoe F G J* Ultrastructure of haemic cells. W B Saunders, London and Philadelphia 1973 p 132 and 248.

5 *Epstein L. B & Salmon S E.* The production of interferon by malignant plasma cells from patients with multiple myeloma. J Immunol. *112* 1131–1138 1974

6 *Fawcett D W* An atlas of fine structure. The cell its organelles and inclusions. W B Saunders, London and Philadelphia 1966, p *370*

7 *Feldmann M & Nossal G J V* Tolerance enhancement and the regulation of interac-

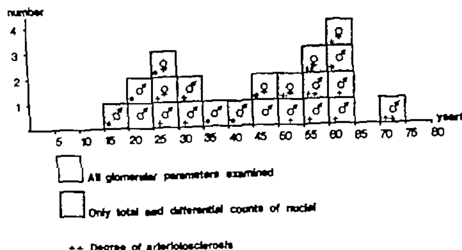


Fig. 1. Sex and age distribution and degree of arteriolosclerosis.

meters seems to be most essential. An attempt was therefore made to investigate the possible relationship between age and the numerical values of glomerular parameters, and to estimate the possible influence of physiological degrees of arteriolosclerosis on the quantitative parameters.

As it is not uncommon for diagnostic renal biopsies to contain changes which are difficult to evaluate on light microscopy quantitative glomerular examination might be a valuable diagnostic procedure for selected cases. A group of normal kidneys was therefore studied in order to collect data that could be used for comparison with individual renal biopsies.

Finally the present study attempted to give information as to what extent, in a normal material, the total variation of glomerular parameters is due to interrenal, interfocal or interglomerular variation.

MATERIAL AND METHODS

Acting on the results of a previous study (*Hamberg Sørensen* 1975) it was decided to use normal renal tissue specimens taken and applied to the fixation medium within 12 hours post mortem.

The total series included 22 kidneys from 21 persons. The sex and age distribution and the degree of arteriolosclerosis appear from Fig. 1. In a 60-year-old male kidney-donor tissue specimens were available from both kidneys as the warm ischemic period after bilateral nephrectomy precluded renal transplantation.

12 of the 22 kidneys were contralateral donor kidneys fixed by immersion in Carnoy's fluid 1 to 36 hours after removal; 4 contralateral donor kidneys were fixed in 4 per cent aqueous formaldehyde; 5 kidneys originated from a legal autopsy material of sudden death where autopsy was performed within 12 hours post mortem. The fixation medium was formalin. The last specimen was obtained at liver biopsy from a 28-year-old female. The patient had no chronic liver disease and the biopsy consisted of normal renal tissue. This biopsy was fixed in formalin. All tissue specimens except the last were taken as wedges, approximately 2 mm thick. Paraffin sections were cut on a microtome adjusted to 2 mμ and stained with periodic-acid-Schiff-hematoxylin.

None of the persons from whom renal tissue originated were known to have had previous or actual renal disease, and in all cases where laboratory tests had been taken before death serum kreatinin was found to be within normal range. The causes of death of the 20 persons from whom tissue samples had been taken post mortem were as follows:

	no.
Cerebral lesions	12
Coronary occlusion	3
Stab wounds	2
Hanging	1
Multiple traumatic lesions	1
Burns	1

QUANTITATIVE STUDIES OF THE RENAL CORPUSCLES IV

Determination of Normal Values in Various Age Categories and an Analysis of the Possible Influence of Physiological Degrees of Arteriolosclerosis

F Hanberg Sorensen

University Institute of Pathology Kommunehospitalet, Arhus, Denmark

Sorensen, F H Quantitative studies of the renal corpuscles IV Determination of normal values in various age categories, and an analysis of the possible influence of physiological degree of arteriolosclerosis. Acta path. microbiol. scand Sect. A 85 356–366 1977

A quantitative study including total and differential counts of nuclei and determination of mesangial and total glomerular area was carried out on kidney tissue from 21 persons without renal disease in order to determine the normal values of glomerular parameters and to estimate the possible influence of age and physiological degrees of arteriolosclerosis. No age dependency was found to exist for the glomerular parameters within the age category of 17 to 45 years. Above the age of forty -five a rise in mesangial area per cent of total area and mesangial nuclei per cent of total nuclei was found on increasing age, while a decline on increasing age was demontsrated for epithelial nuclei per cent of total nuclei The mean value of mesangial nuclei per 1000 $m\mu^2$ of mesangial area was found to be significantly higher in the older age category than in the younger Arteriolosclerosis did not appear to influence the parameters. The study also attempted to describe the three variance components interrenal, interfocal and interglomerular variation. Interfocal variation was the smallest part of the total variation, and interrenal plus interfocal variation was at most of the same size as interglomerular variation

Key words Renal corpuscles age arteriolosclerosis

F Hanberg Sorensen, The University Institute of Pathology Arhus Kommunehospital 8000 Arhus C Denmark.

Received 1.iii 76 Accepted 2.xi.76

In previous studies of the renal corpuscles by light microscopy (*Hanberg Sorensen* 1972 *Hanberg Sorensen & Ledet* 1972 *Hanberg Sorensen* 1975) a description was given of 1) the available methods 2) the variation in glomerular parameters in the normal kidney 3) the influence of the duration of tissue fixation on glomerular parameters, and 4) the effect of progressive post mortem delay before taking renal tissue samples.

Since 1968 investigations comprising nuclear counting and mesangial area determination have been carried out in order to give a quantitative morphological description of the glomerular lesions in different renal diseases (*Fukuhara* 1968 *Iidaka et al.* 1968, *Kawano et al.* 1971 *Hara* 1972, *Torhorst* 1974 *Wehner* 1974) When comparing biopsies with significant or suspected glomerular lesions with normal material, a knowledge of the influence of age on glomerular para

TABLE 2. *Total and Differential Count of N clei, A Blind Study / Ten Glomeruli, Two Examiners*

Glomerulus no.	Total nuclei Examinator A	Total nuclei Examinator B	Total nuclei Difference A B	Mesangial nuclei Examinator A	Mesangial nuclei Examinator B	Mesangial nuclei Difference A–B	Endothelial nuclei Examinator A	Endothelial nuclei Examinator B	Endothelial nuclei Difference A–B	Epithelial nuclei Examinator A	Epithelial nuclei Examinator B	Epithelial nuclei Difference A–B
1	89	86	+3	27	25	+2	37	35	+2	25	26	—1
2	105	105	0	30	29	+1	32	35	—3	43	41	+2
3	116	117	—1	32	33	—1	51	49	+2	33	35	—2
4	112	102	+10	26	19	+7	53	51	+2	33	32	+1
5	77	73	+4	23	20	+3	27	27	0	27	26	+1
6	100	91	+9	23	25	—2	50	39	+11	27	27	0
7	84	85	—1	16	19	—3	42	37	+5	26	29	—3
8	83	87	—4	20	22	—2	36	37	—1	27	28	—1
9	88	92	—4	27	7	0	36	35	+1	25	30	—5
10	94	97	—3	22	22	0	36	37	—1	36	38	—2
Total	948	935	+13	246	241	+5	400	382	+18	302	312	—10
IEM %			3.8			8.3			7.5			3.2

A = first examinator
B = second examinator

IEM % = index of error of measurements per cent = $\frac{\text{SD difference}}{\bar{x}} \times 100.$

SD difference = standard deviation of differences (A–B) $\bar{x}$ = mean.

TABLE 1 *Age and Degree of Arteriolosclerosis of Specimens*

Category		Parameter number 1–4		Parameter number 5–8	
Age (Yr)	Degree of arteriolosclerosis	Age interval (Yr)	Kidneys/ Glomeruli	Age interval (Yr)	Kidneys/ Glomeruli
<45	0 and +	17–43	10/220	22–35	6/180
≥45	0 + and + +	47–73	12/240	47–60	6/180
<45	0	17–43	6/120	22–35	3/90
≥45	0 and +	47–61	7/150	47–60	4/120
<45	+	27–34	4/100	27–34	3/90
≥45	+ +	54–73	5/90	54–60	2/60

Parameter number see text.
Kidneys/Glomeruli represents the number of kidneys and glomeruli examined.

Before the quantitative examination was carried out all tissue specimens were histologically examined by an experienced renal pathologist and found to be normal renal tissue minor or medium degrees or arteriolosclerosis being considered as a normal process of age (*Heptinstall* 1974) A semiquantitative evaluation of arteriolosclerosis using 0 + + + and + + + was included in the histological examination. The degrees 0 and + were accepted as normal for persons below the age of 45 years, while the degrees 0 + and + + were considered to be within normal limits for persons above the age of 45 years. The results of the semiquantitative examinations were concealed from the quantitative examinator until all quantitative examinations had been carried out.

The quantitative examination included the following glomerular parameters

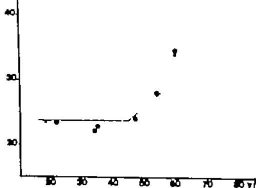
1 Mesangial nuclei per cent of total nuclei.
2. Endothelial nuclei per cent of total nuclei.
3 Epithelial (visceral) nuclei per cent of total nuclei.
4 Total nuclei (mesangial endothelial and visceral epithelial nuclei)
5 Total glomerular area.
6 Mesangial area per cent of total area.
7 Total nuclei per 1 000 $m\mu^2$ of total area.
8. Mesangial nuclei per 1 000 $m\mu^2$ of mesangial area.

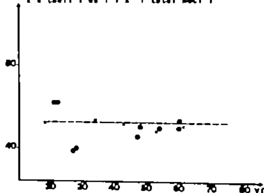
Of the 12 kidneys fixed in Carnoy's fluid 3 specimens were examined. In each a quantitative examination was made on central sections (*Hanberg Sørensen* 1972) of 10 glomeruli equal distribution of subcapsular intermediate and juxtaglomerular glomeruli being attempted The quantitative examination of these 12 kidneys included all the above-mentioned glomerular parameters. As to the remaining 10 kidneys the quantitative examination was made on 1 tissue specimen from each kidney Central sections of 10 glomeruli were studied with regard to the above-mentioned parameters 1–4 The reason for not doing area measurements in this part of the material was that the fixation medium was formalin the results of the area measurements would not, therefore, be comparable to the results of the measurements obtained from the material fixed in Carnoy's fluid

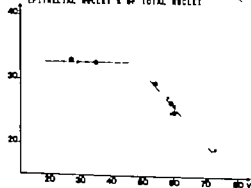
An outline of the number of kidneys, glomeruli and glomerular parameters examined in the various age categories and degrees of arteriolosclerosis appears from Table 1

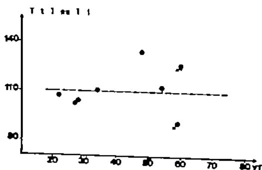
The quantitative methods have previously been described in detail (*Hanberg Sørensen & Leidt* 1972) Point counting was used for determination of total glomerular and mesangial areas, the point spacing being 17 mμ. Previously the total and differential counts of nuclei were carried out directly in the microscope The technique, however was changed so that the nuclei were counted on a projected glomerulus. For each nucleus a mark was put on the paper onto which the glomerulus was projected. The nuclei were counted with a laboratory counter The reason for using a projected glomerulus instead of counting directly in the microscope was that counting a projected glomerulus seemed less of a strain, and that it was easier to keep track of the nuclei counted. The time used for counting nuclei was found to be almost the same with the two techniques. A Leitz Ortholux microscope was used with a mirror for projection. The objective was a Leitz PLApo 40/075 Total magnification of the projected glomeruli was × 920

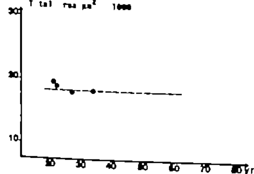
All area determinations in this study were carried out by the author while the total and differential counts of nuclei were done partly by the author and partly by a technical assistant. The technical assistant had received 8 weeks of training The count reproducibility of the two examinators was tested blindly using 10 glomeruli from the same

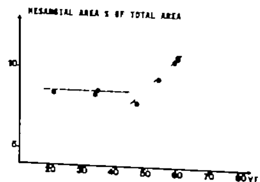

MESANGIAL NUCLEI % OF TOTAL NUCLEI
40
30
20
20 30 40 50 60 70 80 yr

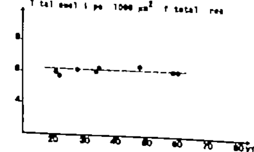

80
40
20 30 40 50 60 70 80 yr

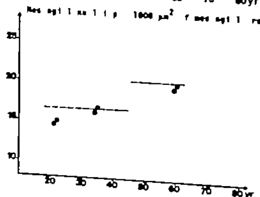

EPITHELIAL NUCLEI % OF TOTAL NUCLEI
40
30
20
20 30 40 50 60 70 80 y


140
110
80
20 30 40 50 60 70 80 yr


30
20
10
20 30 40 50 60 70 80 yr


MESANGIAL AREA % OF TOTAL AREA
10
5
20 30 40 50 60 70 80 yr


8
6
4
20 30 40 50 60 70 80 yr


25
20
15
10
20 30 40 50 60 70 80 yr

tissue specimen as test material The results of the study appear from Table 2. With regard to a previous reproducibility test (*Hanberg Sorensen & Ledet* 1972) *reproducibility was found to be al*most the same between two observers and between one observer and himself The technical assistant also tried doing part of the area measurements. This was given up however partly because of rather *varying test results and partly because the* assistant herself felt uncertain as to what was the mesangial borderline

Statistical methods In case of no age dependence the comparison of younger and older persons and the comparison *of different degrees of* arteriolosclerosis were done by the three level nested analysis of variance (F test) Estimation of natural heterogeneity (variance components) of the glomerular parameters was done by the two level nested analysis of variance (*Sokal & Rohlf* 1969)

In case of age dependence a nested variance component model was used the mean being a linear function of age Similar methods to those above were used for the comparison of different degrees of arteriolosclerosis and for the estimation of the natural heterogeneity of the glomerular parameters.

The prediction limits were calculated in the following way For a given glomerular parameter the difference between the mean of 10 glomeruli and the predicted mean was considered (in case of *no age dependence the predicted mean is the mean* of the observed values, and in case of age dependence the value of the estimated regression for the given age) The variance of this difference was estimated. The prediction limits were calculated by using the fact that this difference divided by the square root of the estimated variance has approximately a t-distribution with *f* degrees of freedom, where *f* depends on the precision of the estimate of the variance

A detailed description of the statistical methods could be ordered from the author

RESULTS

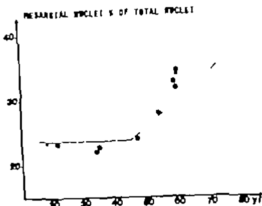
The means of the glomerular parameters for each kidney are given in Fig 2.

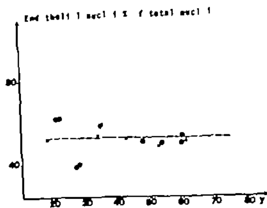
Age dependence Looking at Fig 2 there seems to exist an age dependence only for the following four parameters mesangial nuclei per cent of total nuclei epithelial nuclei per cent of total nuclei mesangial area per cent of total area and mesangial nuclei per 1 000 $m\mu^2$ of mesangial area the age dependence being only after the age of *45* years. Concerning mesangial nuclei per cent of total nuclei epithelial nuclei *per cent of total* nuclei and mesangial area per cent of total area, the age dependence after the age of 45 years seems to be linear while for mesangial nuclei per 1 000 $m\mu^2$ of mesangial area there seems only to be a higher level of the older age category For the three parameters with a linear age dependence after the age of 45 years no significant difference ($p>0.05$) was found in the two regression lines comparing arteriolosclerosis degree 0 + and ++ The significant level of the three common regression lines (arteriolosclerosis 0 + ++) was found to be as follows mesangial nuclei per cent of total nuclei b = .39 ($p<0.05$), epithelial nuclei per cent of total nuclei b = -.55 ($p<0.01$) and mesangial area per cent of total area b = *.19* ($p<0.01$)

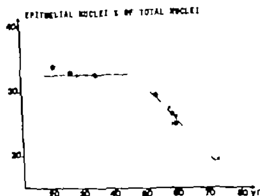
Comparison of different degrees of arteriolosclerosis within the same age category For glomerular parameters where no linear age dependence was postulated a comparison of the means was carried out regarding arteriolosclerosis degree 0 and + within age category <45 years and comparing arteriolosclerosis 0 + and ++ within age category ≥45 years. The parameter means of the different degrees of arteriolosclerosis within the two age categories appear from Table 3 The comparison demonstrated no significant differences.

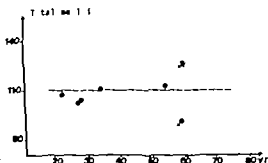
Comparison between age category <45 years and age category ≥45 years For glomerular parameters where no linear age dependence was postulated, a comparison of the means was carried out between age category <45 years and age category ≥45 years. The parameter means of the two age categories were compared regardless of the degree of arteriolosclerosis. With reference to age, the mean values of the glomerular parameters appear from Table 3 A significant difference ($p<0.05$) was demonstrated for only one parameter namely mesangial nuclei per *1 000*

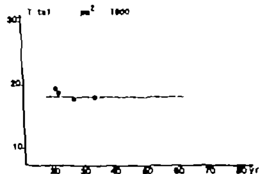
Fig 2 Mean values of glomerular parameters from 22 kidneys each. × *1* specimen examined, • mean value of 3 specimens.

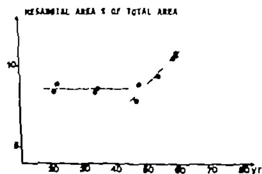

MESANGIAL NUCLEI % OF TOTAL NUCLEI
40
30
20
70
80 yr

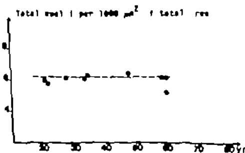

40
70
80 y


EPITHELIAL NUCLEI % OF TOTAL NUCLEI
40
30
20
40
70
80 yr


140
110
80
40
70
80 yr


30
20
10
40
70
80 yr


MESANGIAL AREA % OF TOTAL AREA
10
5
40
70
80 yr


8
6
4
40
70
80 yr

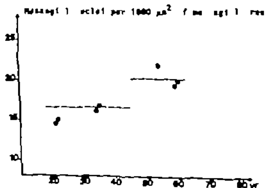

25
20
15
10
40
70
80 yr

TABLE 3 *Mean Values of Glomerular Parameters in Relation to Age and the Degree of Arteriolosclerosis*

Glomerular parameters	Age <45 years Arteriolosclerosis degree			Age ≥45 years Arteriolosclerosis degree		
	0 +	0	+	0 + ++	0 +	++
Mesangial nuclei per cent of total nuclei	23 73	22.58	25 10		Age dependent	
Endothelial nuclei per cent of total nuclei	43 64	44 85	42.18	42 82	41 81	44.52
Epithelial nuclei per cent of total nuclei	32 62	32.55	32.70		Age dependent	
Total nuclei	105 1	105 0	105 1	114.5	112.9	117 1
Total area $m\mu^2 \times 1\,000$	17 76	17 74	17 78	18.89	18.17	20.34
Mesangial area per cent of total area	8.60	8 69	8.52		Age dependent	
Total nuclei per 1 000 $m\mu^2$ of total area	6.04	6.06	6.03	6.50	6 62	6.27
Mesangial nuclei per 1 000 $m\mu^2$ of mesangial area	16 61*	15 49	17 72	20.20*	20.97	18.65

* Significant difference $p < 0\ 05$

TABLE 4 *The Variance Components Epressed as Percentage of the Overall Variance*

	Parameter number Age	1 <45	1 ≥45	2 all	3 <45	3 ≥45	4 all	5 all	6 <45	6 ≥45	7 all	8 <45	8 ≥45
Variance components	Interrenal	26	30	19	2	20	45	42	0	0	22	24	36
	Interfocal	0	7	2	0	3	3	15	19	26	21	8	17
	Interglomerular	74	62	79	98	77	52	43	81	74	57	68	47

Parameter number see text.

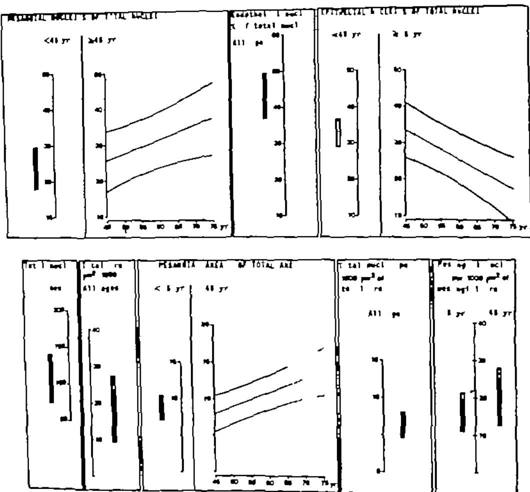


Fig. 3. 95 per cent prediction limits for normal renal biopsies. The prediction limits are calculated for mean values of central sections from 10 different glomeruli.

ing of mesangial area, the mean of the older age category being higher than that of the younger.

Interrenal, interfocal and interglomerular variation. The total variation of the glomerular parameters is composed of the variation between kidneys, the variation between different macrolocalizations within the same kidney and the variation between glomeruli at the same macrolocalization. To illustrate the composition of the total variation the percentual part of the three estimated variance components is given in Table 4. It can be seen from the Table that interfocal variation is generally the smallest part of the total variation, the percentual part, however, differing somewhat from one parameter to another. Concerning mesangial area per cent of total area the estimated interrenal variation was found to be 0. This could be explained by the rather small number of kidneys used for examination of this parameter. The Table also demonstrates that interrenal plus interfocal variation, in the long run, is of at most the same size as interglomerular variation.

95 per cent prediction limits for normal renal biopsies. Utilizing the information above

on glomerular parameters, normal prediction limits were calculated for use in evaluation of individual renal biopsies. The prediction limits were calculated for mean values of central sections from 10 different *glomeruli*. The prediction limits of the different parameters are given in the following form

a) endothelial nuclei per cent of total nuclei total nuclei total area and total nuclei per 1 000 $m\mu^2$ of total area by establishing prediction limits independent of age and the degree of *arteriolosclerosis*.
b) mesangial nuclei per 1 000 $m\mu^2$ of mesangial area by establishing prediction limits for age category <45 years respectively age category ≥45 years, in both cases independently of the degree of arteriolosclerosis.
c) mesangial nuclei per cent of total nuclei epithelial nuclei per cent of total nuclei and mesangial area *per cent of* total area by establishing prediction limits for age category <45 *years* and prediction limits for age category ≥45 years, *in* both cases independently of the degree of arteriolosclerosis.

A graphical representation of the 95 per cent prediction limits is given in Fig 3

DISCUSSION

The present study comprising total and differential counts of nuclei and determination of mesangial and total glomerular area, indicates that no age dependency exists for glomerular parameters within the age category 17 to 45 years. Above the age of 45 a rise in mesangial area per cent of total area and mesangial nuclei per cent of total nuclei was found on increasing age A decline on increasing age was demonstrated for epithelial nuclei per cent of total nuclei. As regards physiological degrees of arteriolosclerosis, no effect on the glomerular parameters was seen. A comparison of age category <45 years and age category ≥45 years revealed a significant *difference* between the means of mesangial nuclei per 1 000 $m\mu^2$ of mesangial area, the *mean of the* older age category being higher than that of the younger This finding might indicate that mesangial nuclear proliferation is to some extent more distinct in the age category above 45 years than the increase of the mesangial matrix.

The size of glomeruli seems to alter during life, increasing especially during the first years of life (*Elias & Hennig* 1967) *Zolan & Pallowitz* (1965) have observed that maximum glomerular size is attained during the fourth decennium whereupon the glomeruli become smaller again. In the present study and that of *Torhorst* (1974) no significant difference in glomerular size was found between kidneys from younger adults and kidneys from older adults, suggesting that the change in glomerular size during adult life is not very distinct.

A significant increase in mesangium from the new born to old age was demonstrated by *Wehner* in 1968 The present study indicates a mesangial increase after the age of forty five. Comparing the results of these two studies and the study of *Hara* (1972) the possibility exists that the increase in the mesangium mostly takes place during childhood and the second half of adult life In contrast to the present study and the study of *Wehner* *Torhorst* found no difference in mesangial volume on comparing kidneys from young adults with kidneys from old adults. The discrepancy in the studies is not immediately apparent.

Comparing kidneys from young and old adults *Torhorst* found no difference in total number of nuclei a finding that is in agreement with the results of the present study In *Torhorst's* study however differential counts of nuclei were not carried out. The results of the present study indicate that a proliferation of mesangial nuclei and a decline in epithelial nuclei take place after the age of forty five. No explanation of this finding can be given but the same trend is seen in diabetic glomerulosclerosis, where a reduction in the number of epithelial nuclei seems

to take place simultaneously with a prolifera tion of mesangial nuclei and an increase in the mesangium (*Idaka et al.* 1968, *Kawano et al.* 1969 *Wehner* & *Anders* 1968, *Wehner* & *Anders* 1970)

Without specifying the degree of arteriolosclerosis, *Torhorst* compared kidneys with arteriolosclerosis to control kidneys. He found no significant differences with regard to glomerular diameter mesangial volume and the number of nuclei. This agrees with the result of the present study i.e. that physiological degrees of arteriolosclerosis do not af fect the glomerular parameters. In contrast to the finding in arteriolosclerosis, however *Torhorst* demonstrated a nuclear proliferation in kidneys with stenosis of the main renal artery

In a previous study (*Hanberg Sørensen* 1972) statistically significant differences were found between different macrolocalizations within the same kidney (interfocal variation) The present study demonstrated that inter focal variation generally comprises the smallest part of the total variation, however dif fering somewhat from one parameter to another

Normal series from the *Kimmelstiel* group (*Idaka et al.* 1968) as well as those from *Wehner* (1974) and *Torhorst* (1974) have only been used for comparison of normal glomeruli to glomerular lesions in specific renal diseases under study Possibly the quantitative method can be used in future as a diagnostic procedure in selected renal biopsies and to assess the results of theraphy using biopsies taken at intervals during the course of a disease. The present study provides a diagram which can be used for comparison with individual diagnostic renal biopsies if these contain sufficient glomeruli to permit the examination of central sections from 10 different glomeruli.

The present study does not include the period from newborn to adult. In a future study therefore, an estimation of the possible glomerular changes during childhood should be carried out, especially since the studies of *Kawano et al.* (1971) and *Rudon* (1974) might indicate that glomerular differences exist between children and adults.

The present study has estimated the influence of age and arteriolosclerosis on glomeruli and illustrated the total variation of glomerular parameters. A normal reference base has been prepared for use with individual biopsies, the sample are being 10 central glomerular sections. Future studies must define the indication for using the quantitative methods.

My thanks are due to Assistant Professor *A. Holst Andersen* and Assistant Professor *S. Terp* for doing the statistical calculation. I am also very much indebted to Professor *Aa. Juhl Therkelsen* for statistical advice.

The present study was supported by a grant from the *Danish Medical R search Council*.

REFERENCES

1 *Elias H* & *Hennig, A* Stereology of the human renal corpuscles. In: Weibel, E. R. & Elias, H. (Ed.) Quantitative Methods in Morphology 1 ed., Springer Verlag. Berlin, Heidelberg, New York 1967 p 130–166.

2. *Fukuhara, N* Histometrical studies on the kidneys in diabetes mellitus Tohoku J exp Med. 95 15–33 1968.

3 *Hanberg Sorensen F.,* Quantitative studies of the renal corpuscles intraglomerular inter glomerular and interfocal variation in the normal kidney Acta path. microbiol. scand. Sect. A, 80 115–124 1972.

4 *Hanberg Sorensen F* & *Ladet T.,* Quantitative studies of the renal corpuscles II methodological study Acta path. microbiol. scand. Sect. A, 80 721–728, 1972.

5 *Hanberg Sorensen F* Quantitative studies of the renal corpuscles III the importance of post mortem delay before taking renal tissue samples, and of the duration of tissue fixation Acta path. microbiol. scand. Sect. A, 83 251–258, 1975.

6. *Hara, M.:* Persistent glomerular changes after glomerulonephritis. A histometrical study of 34 autopsy cases. Beitr Path. *147* 133–144 1972.

7 *H pinstall, R H* Pathology of the Kidney Little, Brown and Company Boston. 2. ed. 1974

8 *Idaka, K McCoy J* & *Kimmelstiel P.,* The glomerular mesangium. A quantitative analysis. Lab. Invest. *19* 573–579 1968.

9 *Kawano K., A shama, K., McCoy J., Porch J* & *Kimmelstiel, P.,* Quantitative study of

glomeruli. Focal glomerulonephritis and diabetic glomerulosclerosis Lab Invest. *21* 269–275 1969

0 *Kawano K Wenzl J McCoy J Porch J & Kimmelstiel P* Lipoid nephrosis. A multipoid study including quantitation. Lab. Invest. *24* 499–503 1971

1 *Risdon R A* Quantiation of histological changes in the glomeruli in renal biopsy specimens from children total and differential glomerular cell counts. J Path. *114* 185–197 1974

2 *Sokal R R & Rohlf F J* Biometry Freeman & Company San Francisco 1969 p 274–287

3 *Torhorst J* Studies on the pathogenesis and morphogenesis of glomerulonephrosis (application of a newly developed morphometric method) Current Topics in Pathology *59* 1–68 1974

14 *Wehner H* Stereologische Untersuchungen am Mesangium normaler menschlicher Nieren Virchows Arch. Abt. A Path. Anat. *344* 286-294 1968.

15 *Wehner H & Anders E* Quantitativ-morphologische Befunde an den Glomerula in Nieren von Diabetikern. Verh. Dtsch. Ges. Path. *53* 380–383 1969

16 *Wehner H & Anders E* Quantitativ morphologische Analyse glomerulärer Veränderungen bei Diabetikern. Diabetologia 6 505-511 1970

17 *Wehner H* Quantitative Pathomorphologie des Glomerulum der menschlichen Niere. Veröffentlichungen aus der Pathologie. 95 1–67 1974

18. *Zolnai B & Palkovits M* Glomerulometrische Untersuchungen der Niere während des Lebens. Verh. Anat. Ges. 60 Verlg. Wien, Erg H *115* 389–400 1965

Acta path. microbiol. scand. Sect. A, 85 367-372 1977

A QUANTITATIVE STUDY OF THE RENAL CORPUSCLES IN ACUTE RENAL ALLOGRAFT REJECTION

F Hamberg Sorensen

University Institute of Pathology Kommunehospitalet, Arhus, Denmark

Sørensen, F H. A quantitative study of the renal corpuscles in acute renal allograft rejection. Acta path. microbiol. scand. Sect. A, 85 367-372, 1977

A quantitative examination including total and differential counts of nuclei and determination of total glomerular and mesangial areas was carried out in a consecutive series of biopsies from 14 patients with acute renal allograft rejection. The biopsies included in the study were taken within 4-30 days after transplantation because of suspected acute rejection, and histological examination revealed interstitial and vascular signs of rejection without the presence of cortical infarcts. Mesangial area per cent of total area was found to be significantly higher in allografts than in control kidneys, just as a statistically significant increase in the number of mesangial nuclei was demonstrated. Three of the 14 allografts had to be removed 7 22 and 25 days after the biopsy because of irreversible rejection. The quantitative changes in these 3 biopsies were more pronounced than those in the remaining biopsies. It is suggested that quantitative glomerular studies might yield data of significance for prediction of the ultimate fate of the graft.

Key words Renal corpuscles renal allograft rejection, acute.

F Hamberg Sørensen, The University Institute of Pathology Arhus Kommunehospital, 8000 Arhus C, Denmark.

Received 1.III.76 Accepted 2.III.76

The most important components of the histopathologic picture in acute renal allograft rejection are arterial intimal hyperplasia and interstitial infiltration with mononuclear cells. Glomerular lesions are sparse in rejection of minor and medium degree, but have been reported to be conspicuous in clinically severe cases (*Busch et al.* 1971, *Kincaid Smith* 1967 *Porter et al.* 1965 *Porter* 1967) Thickening of the glomerular capillary walls, infiltration with leucocytes and capillary microthrombi have been reported in such cases. Precise quantitative studies of the glomeruli in acute rejection have not been performed earlier

In later years it has been demonstrated that reliable methods exist by which it is possible to perform a quantitation of glomerular parameters, including total and differential counts of nuclei and determination of total glomerular and mesangial areas (*Kawano et al.* 1971 *Hamberg Sørensen & Ladet* 1972) The purpose of the present report is to present a description of the quantitative glomerular parameters in a series of biopsies from patients with acute rejection, and to investigate whether these parameters have a

predictive value for the ultimate fate of the graft.

MATERIAL AND METHODS

The present consecutive study of quantitative glomerular parameters in acute renal allograft rejection included one biopsy from each of 14 grafts. The criteria for inclusion in the material were 1) The biopsy was taken within 4–30 days after transplantation because of clinically suspected acute rejection. 2) The histological examination revealed interstitial and vascular signs of rejection without the presence of cortical infarcts. 3) The biopsy contained a number of glomeruli that permitted a quantitative examination of central sections (*Hanberg Sorensen* 1972) from 10 different glomeruli.

The donor group included 14 persons 11 males and 3 females with a mean age of 33 years (11–53). All allografts were necro-kidneys and in no case was knowledge obtained of previous or present renal disease among the donors. The cause of death in 12 donors was various types of cerebral lesions, in 1 a gunshot wound and the other barbiturate poisoning. Of the 14 recipients 8 were males and 6 females, the mean age being 26 years (9–61). Two male recipients aged 36 and 39 years, had diabetes mellitus the remaining recipients had no complicating diseases other than those caused by uremia. The warm and cold ischemia times before transplantation averaged 18 minutes (4–34) and 7 hours (3–16) respectively. Compatibility tests between donors and recipients demonstrated one A, three B-(C) five C, one C-(D) and four D matches.

In three patients one B-(C) one C and one C-(D) match) a graftectomy was performed 16, 30 and 43 days after transplantation because of massive irreversible rejection. The histological changes seen by conventional microscopy at the time of biopsy (9, 8 and 18 days after transplantation) however did not differ significantly from the findings in the remaining biopsies performed an average of 15 days after transplantation (4–23). A graftectomy was furthermore performed in one patient 34 days after transplantation because of venous thrombosis. The histological examination showed no signs of severe rejection in this case. The two patients with diabetes mellitus died from septicemia 4 and 6 weeks after transplantation. In one patient post mortem examination revealed a slight degree of allograft rejection in the other the renal allograft was found to be almost normal. The remaining 8 allografts were functioning 2 months to 4 years after transplantation.

Before transplantation all recipients had a loading dosis of azathioprine 5 mg per kilogram body weight. Postoperatively the immunosuppressive treatment included prednison 150 mg daily decreasing to 30 mg 5 weeks after operation, and azathioprine 25–150 mg daily depending on renal function. Before the renal biopsies were taken the standard immunosuppressive treatment was supplemented with methyl prednisolon in 3 patients, the total dosis being 10.5 mg, 2.0 mg and 0.5 mg. None of these 3 patients belonged to the group in which graftectomy was later performed because of massive rejection.

The ordinary histological examination on the biopsies used in this study was done by an experienced renal pathologist, and findings, together with clinical data, were concealed from the quantitative examinator (the author) until all quantitative examinations had been carried out. Results were compared to the values obtained from a group of 22 normal kidneys from 21 persons (*Hanberg Sorensen* 1977).

All grafts biopsies were fixed in Carnoy's fluid, and paraffin sections were cut on a microtome adjusted to 2 mµ, the staining method being periodic acid Schiff-hematoxylin. In each biopsy a quantitative examination was carried out on central sections of 10 different glomeruli. If more than 10 glomeruli were available, the three glomeruli situated most subcapsularly and most juxtamedullary were examined together with the four glomeruli most centrally placed in the intermediate layer.

The quantitative methods used in this study have previously been described in detail (*Hanberg Sorensen & Ledet* 1972, *Hanberg Sorensen* 1977). Point counting was used for determination of total glomerular and mesangial areas, the point spacing being 17 mµ. The total and differential counts of nuclei were carried out on the projected glomerulus putting a mark for each nucleus counted. A Leitz Ortolux microscope was used with a mirror for projection. The objective was a Leitz PL Apo 40/0.75. Total magnification of the projected glomeruli was × 920.

Statistical methods. Estimation of the means and the variances of the means were done in the way described in a previous paper (*Hanberg Sorensen* 1977). Comparisons of the parameter means of kidneys with acute allograft rejection and normals were done by a modified t-test (*Hald* 1952).

RESULTS

Table 1 gives the results of total and differential counts of nuclei and determination of total glomerular and mesangial areas in allograft biopsies and biopsies from normal kidneys. For the glomerular parameters related to age (*Hanberg Sorensen* 1977) only 12 of

TABLE 1 *Quantitative Glomerular Findings in Acute Renal Allograft R jection*

Parameters	No. kidneys		Mean alues and ariances of means		Level of significance of difference
	Acute rejection	Normals	Acute rejection	Normals	
Number of mesangial nuclei. Age<45 years	12	10	37.9 (10 641)	25 0 (0.767)	**
Number of endothelial nuclei. All ages	14	22	45.4 (4 126)	47 7 (2 838)	
Number of epithelial uclei. Age<45 years	12	10	31 8 (0 983)	34 1 (1 447)	
Mesangial uclei % of total uclei Age<45 years.	12	10	32.3 (1.541)	23 7 (0 659)	***
Endothelial uclei % of total uclei All ges.	14	22	39 4 (0 206)	43 2 (0.364)	***
Epithelial uclei % of total uclei. Age<45 years.	1	10	28 4 (1.333)	32.6 (0.180)	**
Total glomerular nuclei. All ages.	14	22	116.0 (24 978)	110.0 (14.699)	
Total glomerular area mμ × 1 000. All ages.	14	12	19.3 (1 086)	18.3 (1 041)	
Mesangial area % of total area. Age<45 years	12	6	12.1 (0 403)	8 6 (0.033)	***
Total uclei per 1 000 mμ of total are All ages	14	12	6.2 (0.103)	6.3 (0 033)	
Mesangial uclei per 1 000 mμ of mesangial area Age<45 years.	12	6	17 1 (0 963)	16.6 (0.313)	

Variances of means are in parenthesis ** $p<0.01$ ** $p<0.001$

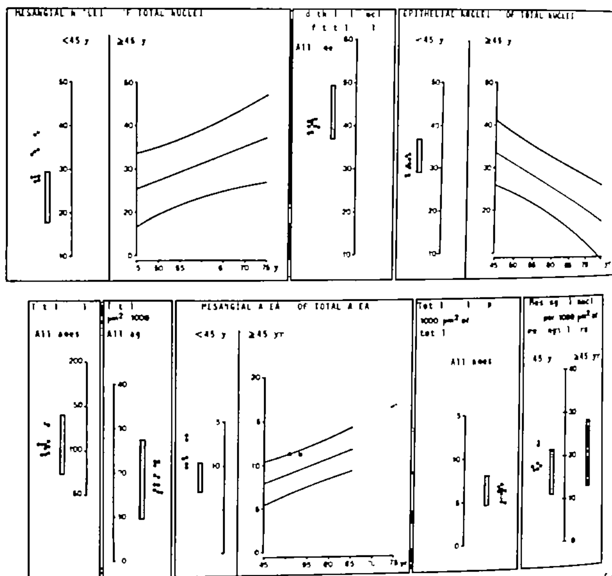


Fig. 1. Mean values of biopsies from renal allografts in relationship to 95 per cent prediction limits for normal renal biopsies.
The prediction limits are calculated for mean values of central sections from 10 different glomeruli.
O represents mean values of rejected allografts while ● represents mean values of remaining allografts.

the allografts were used for comparison as the age of two donors was above 45 years. Comparing mean values of allografts and normal biopsies, mesangial area per cent of total area was found to be significantly higher in allografts than in control kidneys. As regards total and differential counts of nuclei, the numbers of mesangial nuclei was found to be significantly higher in allografts than in control kidneys. Total nuclei was also greater in allografts, but this finding was not statistically significant. The procentual distribution of mesangial, endothelial and epithelial nuclei demonstrated a significant increase of mesangial nuclei per cent of total nuclei and a significant decrease of endothelial and epithelial nuclei per cent of total nuclei. As the number of endothelial and epithelial nuclei did not differ significantly from controls, the decrease of endothelial and epithelial nuclei in percentage of total nuclei should only be taken as a result of the increase in mesangial nuclei.

To illustrate the quantitative glomerular changes in the 3 biopsies from kidneys later removed because of rejection, in contrast to

the remaining allograft biopsies, mean values of each biopsy were marked in a diagram designed for individual renal biopsies (*Hansberg Sørensen* 1977). It can be seen from Fig. 1 that the 3 rejected allografts had the highest number of glomerular nuclei and the most pronounced changes in differential counts of nuclei. The mesangial area per cent of total area was also on an average higher than in the remaining allografts. Note should be made 1) that none of the recipients of these 3 allografts had an age above 45 years, 2) that only standard immunosuppressive treatment was given, 3) that no significant difference in warm and cold ischemic periods existed between the 3 mentioned and the remaining allografts, just as 4) there was no difference as to the match degree.

Leucocytes were also counted in the glomeruli. In only one biopsy was the mean number of leucocytes more than two per glomerulus, the number counted being 4. This biopsy did not originate from any of the 3 rejected allografts.

3 patients had been treated with methylprednisolone before the renal biopsies were taken. Mesangial area per cent of total area in these 3 patients averaged 11 per cent and did not differ significantly from the mean value in the remaining allografts.

As regard compatibility between donors and recipients, no correlation was found in this study between different match types and the degree of changes in glomerular parameters.

DISCUSSION

In the present study a comparison of renal allografts with normal non-transplanted kidneys revealed an increase in mesangial area per cent of total area and an increase in the number of mesangial nuclei; the increase of mesangial nuclei, however, was not so great that a statistically significant increase of total nuclei was demonstrable.

Several factors may produce changes in the graft; some are associated with the rejection process, while others reflect non-immunological influences (ischemia, mechanical damage, interruption of the lymphatic drainage, immunosuppressive treatment, compensatory hypertrophy). The present data do not permit any conclusions concerning pathogenesis. Ideally it would be preferable to compare the graft biopsies with a control series of human autografts, which is obviously impossible. Another alternative would be to use well-functioning allografts as controls. This was, however, not possible because of a reluctance to submit such patients to the potential danger of a graft biopsy. Because of the tendency towards more conspicuous quantitative changes in cases of severe irreversible rejection, however, it seems reasonable to assume that immunological damage is of importance. Changes could also, at least partly, be caused by the immunosuppressive treatment. No data are available concerning the action of azathioprine on the glomerular parameters. Changes in the mesangium as a result of corticosteroid treatment have previously been reported, but the data are conflicting. Some authors (*Bourgoin et al.* 1966, *Wehner* 1971, *Wehner* 1974) report a mesangiolytic action of cortisone, while others (*McCluskey & Vassali* 1969, *Torhorst* 1974) have found that a broadening of the mesangium could be elicited by cortisone.

3 allografts in this study were removed because of massive rejection. The quantitative changes in these 3 biopsies were more prominent than in the remaining biopsies. As the present study includes only a rather small number of biopsies, it is not possible to conclude that the most pronounced changes are always seen in allografts with a poor prognosis. Continued investigation is necessary in order to clarify whether quantitative changes of a certain size can be of prognostic significance for the ultimate fate of the graft.

My thanks are due to Assistant Professor [illegible] for doing the statistical calculations. [illegible] very much indebted to Assistant Professor [illegible] Andersen for statistical advice.

The present study was supported by [illegible] the Danish Medical Research Council.

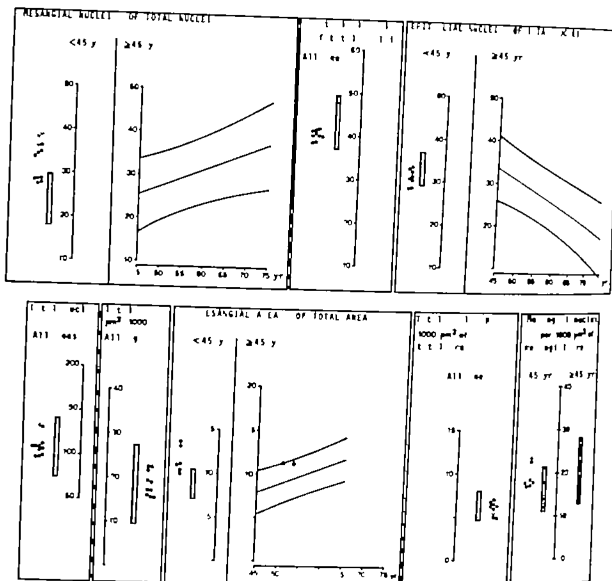


Fig. 1. Mean values of biopsies from renal allografts in relationship to 95 per cent prediction limits for normal renal biopsies.
The prediction limits are calculated for mean values of central sections from 10 different glomeruli.
O represents mean values of rejected allografts while ● represents mean values of remaining allografts.

the allografts were used for comparison, as the age of two donors was above 45 years. Comparing mean values of allografts and normal biopsies, mesangial area per cent of total area was found to be significantly higher in allografts than in control kidneys. As regards total and differential counts of nuclei, the numbers of mesangial nuclei was found to be significantly higher in allografts than in control kidneys. Total nuclei was also greater in allografts, but this finding was not statistically significant. The procentual distribution of mesangial, endothelial and epithelial nuclei demonstrated a significant increase of mesangial nuclei per cent of total nuclei and a significant decrease of endothelial and epithelial nuclei per cent of total nuclei. As the number of endothelial and epithelial nuclei did not differ significantly from controls, the decrease of endothelial and epithelial nuclei in percentage of total nuclei should only be taken as a result of the increase in mesangial nuclei.

To illustrate the quantitative glomerular changes in the 3 biopsies from kidneys later removed because of rejection, in contrast to

Acta path. microbiol. scand. Sect. A, 85 373–383 1977

GLUTARALDEHYDE FIXATION FOR ELECTRON MICROSCOPY OF NEEDLE BIOPSIES FROM HUMAN LIVERS

PALLE PETERSEN

Medical department A, division of hepatology Rigshospitalet, Copenhagen, Denmark

Petersen, P Glutaraldehyde fixation for electron microscopy of needle biopsies from human livers. Acta path. microbiol. scand Sect. A, 85 373–383 1977

A study including light and electron microscopy of needle biopsies from normal and fatty human livers fixed by immersion into glutaraldehyde is presented. Four zones which can be detected by light microscopy of toluidine blue stained sections are found: zone 1, the outer one is presumably mechanically damaged. Zone 2 is usually considered to be the most well-preserved region, whereas zones 3 and 4 present increasing swelling of mitochondria, progressive condensation of microbodies and an increasingly pronounced vesiculation of the smooth endoplasmic reticulum (SER). The alterations observed in zone 3 and 4 are of types which might simulate pathological changes. An increasing irregularity of the outline of the nuclei and a greater accumulation of chromatin along the nuclear membrane is also observed in these two zones. The perimembraneous cytoplasmic ground substance appears to be more dense and the intercellular spaces to be less distinct in the deeper zones in which the path of diffusion of the fixative is long. As regards the penetration into the tissue of glutaraldehyde, normal and steatotic livers were not found to differ. Fixation at 0°C was found to be less effective than fixation at 22°C.

Key words: Liver; ultrastructure.

P. Petersen, Medical department A, division of hepatology Rigshospitalet, Blegdamsvej 9, DK 2100, Copenhagen, Denmark.

Received 3. 76 Accepted 19.xi.76

During recent years, fixation for electron microscopic studies of the liver tissue obtained by needle biopsy has most commonly been done by immersion of the tissue into glutaraldehyde (2, 3, 4, 7, 8). Using this method it is of importance to safeguard that the thickness of the tissue block does not exceed 0.5 mm in order that the glutaraldehyde may be allowed to penetrate the tissue within an interval of time sufficiently short (2) to achieve good preservation. But even if this point is observed, parts of the tissue may be poorly preserved and artefacts which could be mistaken for an in vivo occurrence of pathological alterations may appear (5).

Various pathological conditions of the liver parenchyma, e.g. severe fatty metamorphosis, might inhibit the penetration of glutaraldehyde, and thus result in a fixation less optimal than that obtained if normal tissue was used.

This study was performed in order to evaluate the width of the optimal fixation zone in human needle biopsies when glutaraldehyde was used as the first fixation medium. The width of the fixation zones obtained in tissue of steatotic and non steatotic liver was compared and the alterations presented by

REFERENCES

1 *Bouissou H Durroux R Rakotondrainibe A Familiades J & Julian M* Le glomérule rénal cortisonique en microscopie optique et électronique Etude expérimentale Path. Biol. *14* 189–204 1966.

2. *Busch G J Reynolds E S Galvanek E. G., Braun H E. & Dammin G J* Human renal allografts. Medicine *50* 29–83 1971

3 *Hald A* Statistical theory with engineering applications. John Wiley & Sons. London-New York Tokyo. 1952 p 397–398.

4 *Hanberg Sorensen F* Quantitative studies of the renal corpuscles I intraglomerular inter glomerular and interfocal variation in the normal kidney Acta path. microbiol scand. Sect. A *80* 115–124 1972.

5 *Hanberg Sorensen F* Quantitative studies of the renal corpuscles IV determination of normal values in various age categories, and an analysis of the possible influence of phy siological degrees of arteriosclerosis. Acta path. microbiol scand Sect A *85* 356–366 1977

6 *Hanberg Sorensen F & Ledet T* Quantitative studies of the renal corpuscles II a methodological study Acta path. microbiol scand. Sect A, *80* 721–728 1972

7 *Kawano K McCoy J Wenzl J Porch J., Howard C Goddard M & Kimmelstiel P* Quantitation of glomerular structure. A study of methodology Lab. Invest. *25* 343-348, 1971

8 *Kincaid-Smith P.* Histological diagnosis of rejection of renal homografts in man. Lancet, 849–852, 1967 ii.

9 *McCluskey R T & Vassali, P.* Experimental glomerular diseases. In The kidney morphology biochemistry physiology (Rouiller C Muller A. F., eds.) vol. 2 Acad Press. New York, London 1969 p. 84–198.

10 *Porter K A* Rejection in treated renal allografts. J clin. Path. suppl. *20* 518-534 1967

11 *Porter K A., Marchioro T L. & Starzl, T E.* Pathological changes in 37 human renal homotransplants with immunosuppressive drugs. Brit. J Urol. *37* 250-273 1965.

12. *Torhorst J* Studies on the pathogenesis and morphogenesis of glomerulonephritis (application of a newly developed morphometric method) Current Topics in Pathology *59* 44-51 1974

13 *Wehner H* Quantitative Pathomorphologie des Glomerulum der menschlichen Niere Veröffentlichungen aus der Pathologie 95 41 43 1974

14 *Wehner H Feurer F & Wehner I* Histometrical glomerular studies on the kidneys in multiple myeloma and in acute membranous glomerulonefritis (lipoid nephrosis) Path. europ. *6* 422–432, 1971

Acta path. microbiol. scand. Sect. A, 85: 373-383, 1977

GLUTARALDEHYDE FIXATION FOR ELECTRON MICROSCOPY OF NEEDLE BIOPSIES FROM HUMAN LIVERS

PALLE PETERSEN

Medical department A, division of hepatology, Rigshospitalet, Copenhagen, Denmark

Petersen, P. Glutaraldehyde fixation for electron microscopy of needle biopsies from human livers. Acta path. microbiol. scand. Sect. A, 85: 373-383, 1977.

A study including light- and electron microscopy of needle biopsies from normal and fatty human livers fixed by immersion into glutaraldehyde is presented. Four zones which can be detected by light microscopy of toluidine blue stained sections are found: zone 1, the outer one, is presumably mechanically damaged. Zone 2 is usually considered to be the most well-preserved region, whereas zones 3 and 4 present increasing swelling of mitochondria, a progressive condensation of microbodies and an increasingly pronounced vesiculation of the smooth endoplasmic reticulum (SER). The alterations observed in zone 3 and 4 are of types which might simulate pathological changes. An increasing irregularity of the outline of the nuclei and greater accumulation of chromatin along the nuclear membrane is also observed in these two zones. The perimembraneous cytoplasmic ground substance appears to be more dense and the intercellular spaces to be less distinct in the deeper zones in which the path of diffusion of the fixative is long. As regards the penetration into the tissue of glutaraldehyde, normal and steatotic livers were not found to differ. Fixation at 0°C was found to be less effective than fixation at 22°C.

Key words: Liver; ultrastructure.

P. Petersen, Medical department A, division of hepatology, Rigshospitalet, Blegdamsvej 9, DK-2100, Copenhagen, Denmark.

Received 3.v.76. Accepted 19.xi.76

During recent years, fixation for electron microscopic studies of the liver tissue obtained by needle biopsy has most commonly been done by immersion of the tissue into glutaraldehyde (2, 3, 4, 7, 8). Using this method it is of importance to safeguard that the thickness of the tissue block does not exceed 0.5 mm in order that the glutaraldehyde may be allowed to penetrate the tissue within an interval of time sufficiently short (2) to achieve good preservation. But even if this point is observed, parts of the tissue may be poorly preserved and artefacts which could be mistaken for an in vivo occurrence of pathological alterations may appear (5).

Various pathological conditions of the liver parenchyma, e.g. severe fatty metamorphosis, might inhibit the penetration of glutaraldehyde, and thus result in a fixation less optimal than that obtained if normal tissue was used.

This study was performed in order to evaluate the width of the optimal fixation zone in human needle biopsies when glutaraldehyde was used as the first fixation medium. The width of the fixation zones obtained in tissue of steatotic and non steatotic liver was compared and the alterations presented by





1 2

Figs. 1 and 2. 1 µm sections of liver tissue cylinders. The glutaraldehyde fixation zones are marked. Fig. 1 shows normal liver tissue. Fig. 2 shows fatty liver. The fatty vacuoles are stained black during osmium fixation. EPON embedding. ×60. Toluidine blue staining.

the cellular organelles in different fixation zones were also compared.

MATERIAL AND METHODS

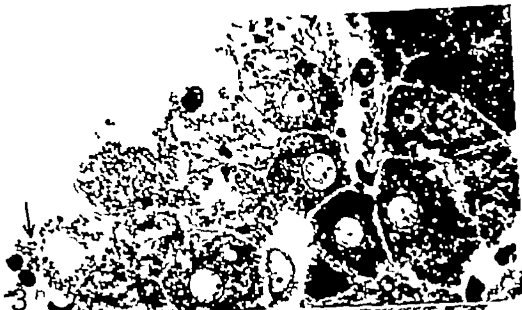
Liver biopsies were obtained from 17 patients. Ten of the patients had various degrees of steatosis while conditions were found to be normal in seven. Liver biopsies were performed by a Menghini needle with an internal diameter of 1.9 mm. A tissue cylinder measuring 3 mm was fixed in toto in 0 C or ? C 0.1 M cacodylate-buffered 2.5 per cent glutaraldehyde for 2 h. After washing overnight in 0.1 M sodium cacodylate, a disk was cut from the middle part of the tissue cylinder. The disk was fixed in 0.1 M cacodylate-buffered 1 per cent osmium tetroxide, dehydrated in graded ethanol and embedded in EPON in order that transverse sections of the cylinder could be cut.

A survey section of the disk was cut and stained with toluidine blue. A wedge from which ultrathin sections were made was trimmed out, thus allowing that the ultrastructure of the cylindrical block could be followed from the surface to the centre. The ultrathin sections were counter stained with uranyl acetate and lead citrate prior to examination in a Zeiss EM 9 a electron microscope.

RESULTS

Light Microscopy

In toluidine blue stained survey sections studied by light microscopy mitochondria, nuclei, cytoplasmic ground substance and plasma membranes showed more or less continuous changes from the surface to the



RER

SER

4

Fig. 3. 1 μm section showing the light cells of zone 1. Plasma membrane broken (arrow). ×1,260. Toluidine blue staining.

Fig. 4. Hepatocyte from zone 1. Mitochondria (m) are dark with dilated intercristal spaces. Microbodies (mb) are bigger than mitochondria and their matrix is inhomogeneous. Cisternae of the rough endoplasmic reticulum (RER) and the smooth endoplasmic reticulum (SER) are markedly dilated. The plasma membrane is distinct and the perimembraneous cytoplasmic ground substance is electron lucid. Electron micrograph. ×29,500.





Figs 1 and 2 1 µm sections of liver tissue cylinders. The glutaraldehyde fixation zones are marked. Fig 1 shows normal liver tissue Fig 2 shows fatty liver The fatty vacuoles are stained black during osmium fixation. EPON embedding ×60 Toluidine blue staining

the cellular organelles in different fixation zones were also compared

MATERIAL AND METHODS

Liver biopsies were obtained from 17 patients Ten of the patients had various degrees of steatosis while condition were found to be normal in seven Liver biopsies were performed by a Menghini needle with an internal diameter of 1 9 mm. A tissue cylinder measuring 3 mm was fixed in toto in 0 C or 2 C 0 1 M cacodylate-buffered 2 5 per cent glutaraldehyde for h. After washing overnight in 0 1 M sodium dacodylate a disk was cut from the middle part of the tissue cylinder This disk was fixed in 0 1 M cacodylate-buffered 1 per cent osmium tetroxide dehydrated in graded ethanol and embedded in EPON in order that transverse section of the cylinder could be cut

A survey section of the disk was cut and stained with toluidine blue. A wedge from which ultrathin sections were made was trimmed out, thus allowing that the ultrastructure of the cylindrical block could be followed from the surface to the centre The ultrathin sections were counter stained with uranyl acetate and lead citrate prior to examination in a Zeiss EM 9 a electron microscope

RESULTS

Light Microscopy

In toluidine blue stained survey sections studied by light microscopy mitochondria, nuclei cytoplasmic ground substance and plasma membranes showed more or less continuous changes from the surface to the

Fig. 7 1 μm section showing hepatocytes of fixation zone 3. Mitochondria are faintly visible. The intercellular spaces are narrow, sometimes invisible. × 1 260. Toluidine blue staining.

Fig. 8 Hepatocytes from zone 3. Mitochondria (m) are swollen with partial loss of matrical granules and cristae. The cisternae of the SER are of rather vesiculated appearance. Microbodies (mb) are more compact than mitochondria. Much chromatin is accumulated along the nuclear membranes. Electron micrograph. × 29 500.

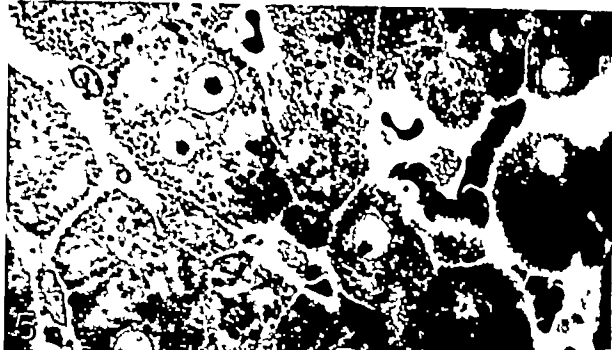


Fig 5 1 μm section showing hepatocytes of fixation zone 2 The mitochondria are distinct. The intercellular spaces are narrow and distinct. ×1 260 Toluidine blue staining

Fig 6 Hepatocyte from zone 2 Mitochondria (m) contain normal cristae and granules The nuclear chromatin is moderately accumulated at the nuclear membrane The microbodies (mb) are small and as compact as the mitochondria. Cisternae of the RER and the SER are narrow The plasma membrane is distinct the perimembraneous hyaloplasm is moderrately electron dense and the intercellular space is electron lucid Electron micrograph × 29 500

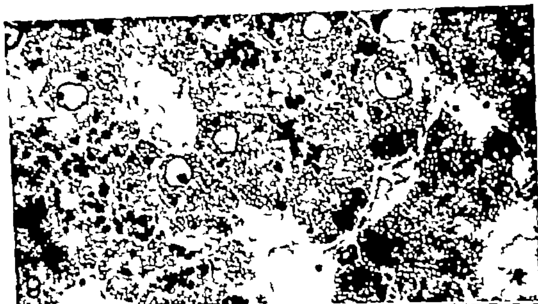


Fig. 9 1 μm section showing hepatocytes of fixation zone 4. The mitochondria are vacuolated. The intercellular spaces also appear to be stained to some extent. ×1,260. Toluidine blue staining.

Fig. 10 Hepatocytes from zone 4. The matrix of the mitochondria (m) is extracted and their cristae and matrical granules are lost. Mitochondrial membranes are broken in places (arrow). Microbodies (mb) are dark. Cisternae of the SER are vesiculated, but the cisternae of the RER are narrow. The nuclear chromatin is aggregated into dense patches. Electron micrograph. × 29,500

centre of the tissue block. Four different zones could be identified. (Figs 1 and 2)

Zone 1 was next to the surface of the tissue block at which site the cells were partly torn the cytoplasmic ground substance being very pale. The mitochondria stained very strongly. This zone consisted only of 1 or 2 cell layers and measured about 30 μm (Fig 3)

Zone 2 showed light or moderately stained cytoplasmic ground substance regular round nuclei with moderately stained nuclear membrane and only slightly condensed chromatin at the periphery of the nucleus. The mitochondria were a little larger than those in zone 1 and moderately but distinctly, stained with toluidine blue. The intercellular spaces were narrow and distinct and the plasma membrane was thin (Fig 5)

In zone 3 the cytoplasm was darker the mitochondria were bigger more faintly stained and rather difficult to distinguish from the cytoplasmic ground substance. The nuclei and the plasma membranes did not show any alterations (Fig 7) as compared with those in zone 2

In zone 4, the nuclei showed slightly irregular outlines and accumulations of the chromatin were present along the nuclear membrane. The intercellular spaces were less distinct than those in zone 2 and the plasma membranes were darker. In the biopsies fixed at 0°C the cytoplasm of the hepatocytes appeared vacuolated. Such vacuolation was not observed in the biopsies fixed at 22°C in which the cytoplasmic ground substance was homogeneous, resembling that of the cells of zone 3 where mitochondria were unrecognizible (Fig 9)

In zone 4 usually present around the centre of the tissue block cells with dark cytoplasm concave outlines, and thick plasma membranes were found. Vacuoles occupied the cytoplasm of these cells whether tissue was fixed at 0°C or 22°C. The nuclei were shrunken they were very dark and contained coarse accumulation of chromatin (Fig 11)

The width of each of the four different zones in biopsies from steatotic and non steatotic livers fixed at 0°C is recorded in Table 1 while Table 2 records findings in specimens fixed at 22°C. The penetration of the fixative through normal and steatotic hepatic parenchyme was not found to differ significantly and the same applies to fixations carried out at 0°C and 22°C, respectively.

Electron Microscopy

The hepatocytes of zone 1 contained cytoplasm in which the cisternae of the smooth endoplasmic reticulum (SER) and the rough endoplasmic reticulum (RER) were dilated. The mitochondria had a dark matrix which contained some dense granules and the cristae of the mitochondria showed dilated intercristal spaces. The matrix of the microbodies was rather inhomogeneous, and the microbodies tended to be as big as, or even bigger than the mitochondria. The nuclei were round containing evenly dispersed chromatin and accumulation of chromatin along the nuclear envelopes was only slight. If intact the plasma membranes were distinct and the perimembraneous part of the cell cytoplasm was electron lucid. (Fig 4)

In zone 2, the mitochondria were larger than those in zone 1 their matrix being lighter and only moderately electron dense. The cristae were abundant distinct and without widening of the intercristal space. The granules in the matrix of the mitochondria were dark and distinct. The microbodies were smaller than the mitochondria and the matrix was homogeneous. The cisternae of the RER appeared narrow or only slightly dilated, and the cisternae of the SER were somewhat irregular. The nuclei were round, and some accumulation of chromatin along the nuclear envelopes was demonstrable. The plasma membrane of each cell was distinct, the intercellular spaces were electron lucid and the perimembraneous hyaloplasm in each cell was moderately electron dense (Fig 6)

The mitochondria of zone 3 were even larger than those in zone 2 their matrix was less electron dense, and cristae were less numerous. Granules were present in the matrix of the mitochondria though they were less

TABLE 1 *Needle Biopsies from Human Livers with and without Steatosis Fixed in Glutaraldehyde at 0° for 2 h.*

Fatty liver	zone 1	zone 2	zone 3	zone 4 center
P 90	38 µm	212 µm	275 µm	750 µm
	50	225	288	813
P 78	38	188	500	838
	25	375	750	750
P 209	38	300	563	750
	38	300	450	763
P 73	25	150	300	750
	25	150	275	750
P 211	25	125	275	713
	38	225	325	725
mean value	34 µm	225 µm	400 µm	760 µm
Normal liver	**zone 1**	**zone 2**	**zone 3**	**zone 4 center**
P 105	25 µm	125 µm	250 µm	663 µm
	25	113	375	750
P 207	63	225	413	750
	38	238	538	663
P 210	25	100	350	713
	25	150	375	713
P 228	13	175	275	713
	25	125	400	675
mean value	30 µm	156 µm	344 µm	705 µm

The limits of the different fixation zones are given in µm, measured from the surface of the tissue block. For each biopsy 2 measurements of the zones are made at intervals of 90°

electron dense than those of the mitochondria in zone 2, especially in the central regions of the granules. The cisternae of the RER were narrow while those of the SER tended to be dilated. The nuclear membranes were slightly irregular and peripherical accumulations of chromatin were more marked than accumulations observed in zone 2. The plasma membranes and the perimembraneous cytoplasmic ground substance of the cells did not differ from those in zone 2 (Fig. 8).

Zone 4 was characteristic in that the electron density of the matrices in the mitochondria was less marked than that in the other zones. After fixation at 0 C, the matrix of the mitochondria showed considerable loss of the substance, thus accounting for the vesiculated appearance of the cytoplasm noticed by light microscopy. After fixation at 22 C, the matrix of the mitochondria was only slightly more electron lucid than that in zone 3. In the mitochondriae of zone 4, however, no cristae could be observed and only few matrical granules were present. If present, they would be less electron dense in the central region. The double membranes of the mitochondria were broken in several places. The microbodies were of the same size as those in zones 2 and 3, while the mitochondria were larger. The cisternae of the RER were dilated, but ribosomes were still attached to the reticular membranes. The vesiculated appearance of the SER was similar to that observed in zone 3. The nuclei were of irregular shape and accumulation of chromatin was marked both in the form of dense patches along the



Fig 11 1 µm section showing "dark" hepatocytes in fixation zone 4. The cell borders of these cells are curved outwards. The mitochondria appear as vacuoles. The nuclei of the cells are dark. ×1,260. Toluidine blue staining

Fig 12 "Dark" hepatocytes from zone 4. The mitochondria (m) are almost completely empty. Microbodies (mb) are small and dense. The cisternae of the SER are vesiculated. The cisternae of the RER are narrow. The perimembraneous hyaloplasm is dark and the plasma membrane indistinct. Electron micrograph. × 29 500

etrates about 300 μm within one hour Rat livers had been used in both studies.

Owing to the good preservation of this zone, it is also easily detected by light microscopy of toluidine blue stained 1 μm thick sections where well-stained mitochondria are distinct, in contrast to the less intensively stained cytoplasm of the cells. At the ultra structural level it is also the well-preserved appearance of the mitochondria which most distinctly characterises this zone. Microbodies are well-preserved in this zone 2, but seem to shrink while the density of their matrix increase in the deeper zones, i.e. with increasing path of diffusion of the fixative. These alterations are almost probably a result of anoxia. Similar alterations are found in a liver tissue from rat fixed by immersion into osmium in which case the livers in vivo were exposed to ischaemia (1 9) Comparison of the size and the density of the matrices of the mitochondria and microbodies facilitates determination of the most suitable zones, in the present study zone 2, for an electron microscopic examination.

Zone 1 is probably a mechanically damaged region. Light microscopic alterations within the surface zone which could be resolved by light microscopy are described by *Lyon et al.* (6) who found an artefactual staining of nuclei and cytoplasm.

The changes in the cells of zone 3 and 4 similar to those found in the present study were described by *Fahimi* in a study of rat liver immersed into glutaraldehyde (3)

The vesiculated appearance of the SER as a result of insufficient fixation in a particular region of the tissue block is a very important feature as mentioned by *Jacobson et al.* (5) Numerous papers have been concerned with a proliferation of the SER which, as judged from the illustrations, equally well might be vesiculations of the SER to be found in insufficiently fixed zones The changes in the distribution of the nuclear chromatin in poorly fixed zones correspond to those observed in liver necrosis in the mouse studied in vivo

It has not been possible to demonstrate any difference between steatotic and normal livers as regards the quality of the fixation using glutaraldehyde. Either the glutaraldehyde penetrates the fatty droplets as easily as the normal cytoplasmic ground substance of the hepatocytes, or the fixative follows other routes of penetration, e.g via the sinusoids.

This study was supported by a grant from *Danish Stat Medical Research Council* (512 3719)

REFERENCES

1 *Bassi M & Bernelli-Zazzera, A.*, Ultrastructural cytoplasmic changes of liver cells after reversible and irreversible ischemia. Experimental and Molecular Path. *3* 332–350 1964
2. *Ericsson J L E, & Biberfeld P.*, Studies on aldehyde fixation. Lab. Invest. *17* 281–298 1967
3. *Fahimi H D.*, Perfusion and immersion fixation of rat liver with glutaraldehyde. Lab. Invest. *16* 736–750 1967
4 *Hopwood D* Some aspects of fixation with glutaraldehyde. J Anat. *101* 83–92, 1967
5 *Jacobson, S., Ericsson J L E & Obel, A.-L.*, Histopathological and ultrastructural changes in the human liver during complete intravenous nutrition for seven months. Acta Chir. Scand. *137* 335–349 1971
6. *Lyon, H & Prento P.*, Artefactual staining of the peripheral zone of needle biopsies. Acta path. microbiol. scand. *81* 9–15 1973
Sabatini D D Bensch K & Barrnett R. J., Cytochemistry and electron microscopy The preservation of cellular ultrastructure and enzymatic activity by aldehyde fixation. J Cell. Biol *17* 19–57 1963
8. *Trump B. F & Bulger R. E.*, New ultrastructural characteristics of cells fixed in glutaraldehyde-osmium tetroxide mixture. Lab. Invest. *15* 368–379 1966.
9. *Trump B. F., Goldblatt P J & Stowell, R. E.*, Studies on necrosis of mouse liver in vitro. Ultrastructural alterations in the mitochondria of hepatic parenchymal cells. Lab. Invest. *14* 343–371 1965
10. *Trump B. F., Goldblatt P J & Stowell, R. E.*, Studies of mouse liver necrosis in vitro. Ultrastructural and cytochemical alterations in hepatic parenchymal cell nuclei. Lab. Invest. *14* 1969 1965

TABLE 2 *Needle Biopsies from Human Livers with and without Steatosis Fixed in Glutaraldehyde at 22 for 2 h*

Fatty liver	zone 1	zone 2	zone 3	zone 4 center
P 159	25 μm	225 μm	300 μm	588 μm
	38	250	300	713
P 161	13	175	375	800
	0	225	300	775
P 178	25	200	250	563
	25	175	268	563
P 166	0	225	325	663
	0	200	325	750
P 179	25	188	375	688
	25	250	500	625
mean value	18 μm	211 μm	332 μm	673 μm
Normal liver	**zone 1**	**zone 2**	**zone 3**	**zone 4 center**
P 120	13 μm	225 μm	313 μm	688 μm
	25	125	375	625
P 167	25	150	225	775
	25	175	263	750
P 185	50	175	350	688
	38	250	350	750
mean value	30 μm	183 μm	313 μm	713 μm

The limits of the different fixation zones are given in μm, measured from the surface of the tissue block. For each biopsy 2 measurements of the zones are made at intervals of 90

nuclear envelope and diffusely dispersed in the nucleoplasm (Fig 10)

The cells from zone 4 which by light microscopy were found to be intensively stained showed mitochondria which by electron microscopy were found to be severely damaged The matrix of these mitochondria was almost completely extracted and only few granules and cristae were left. The double membranes of these mitochondria were broken in several places. The microbodies of these cells were smaller than those of the cells in zones 2 3 and 4 and their matrix was darker A considerable vesiculation of the SER was found while the RER only showed minor dilations The nuclei were shrunken and large, dense agglomerations of chromatin and dark nucleoplasm were demonstrable The cytoplasmic ground substance of these cells was electron dense and the intercellular spaces were darker and less distinct than those observed between cells of the other zones. The plasma membranes of these dense cells showed a pronounced tendency to be outward curved. (Fig 12)

DISCUSSION

Four zones showing different degrees of preservation of cellular details were obtained if needle biopsies 1 9 mm thick were fixed by immersion in glutaraldehyde. Of these zones, zone 2 which extends from a site about 30 μm to less than 200 μm from the surface of the tissue block is considered to represent the most genuine picture of the ultrastructure of the hepatic cells. Correspondingly *Ericsson et al* (2) found that immersion in 3 per cent glutaraldehyde for one hour could yield good fixation in a zone from 0.2 mm, and *Hopwood* (4) has shown that glutaraldehyde pen-

TABLE 1 *Clinical, Light Microscopical and Laboratory Data of 6 Patients with Alcoholic Hepatitis*

...and sex		27 ♂	47 ♂	54 ♂	43 ♂	61 ♀	44 ♂
...mated daily alcohol intake		150 g	200 g	150 g	150 g	75 g	75 g
...ration of alcohol intake		10 y	2 y	10 y	10 y	3–4 y	2 y
...ne from cessation of alcohol ...ake to biopsy		1 day	4 days	3 days	4 days	7 days	4 days
Microscopical findings	degree of steatosis	+ + +	+ + +	+ + +	+ + +	+ +	+ + +
	cirrhosis	+	+	+	0	0	+
	necrosis of liver cells	+	+	+	+	+	+
	Mallory bodies	many	many	many	few	few	few
...rum alanin aminotransferase (normal value <40 U/l)		36	20	18	101	54	28
...rum bilirubin (normal value <17 mmol/l)		30	24	53	11	14	49
...rum alkaline phosphatases (normal value <275 µmol/l)		680	784	304	440	248	1074
...sma albumin (normal value >532 µmol/l)		341	477	478	385	630	–
...sma prothrombin-proconvertin (normal value 70–110 per cent)		90	88	49	109	85	44

ments (6). As microfilaments and microtubules often appear at one and the same localization, the object of the present study was to examine the morphological relationship of alcoholic hyalin fibrils to microfilaments and microtubules in parenchymal cells of liver tissue in biopsies obtained from patients with alcoholic hepatitis.

METHODS AND MATERIAL

Preparations to be studied by electron microscopy six blocks of liver tissue not exceeding 0.5 mm in diameter were obtained from each patient. the blocks were fixed at room temperature in 2.5 per cent glutaraldehyde buffered with 0.1 M sodium cacodylate, followed by short-term washing in 0.1 M sodium cacodylate, fixation in 1 per cent osmium tetroxide buffered with 0.1 M sodium cacodylate dehydration, and embedding in EPON. Ultrathin sections were stained with uranyl acetate and lead citrate and studied in a Zeiss electron microscope 9 a. Adjacent sections of thickness of 1 µm were stained with toluidine blue and used for light microscopic examinations.

The study includes 6 patients in whom histological diagnosis of alcoholic hepatitis could be established on the basis of biopsies showing necrosis of the liver parenchymal cells, severe steatosis, and Mallory bodies. The clinical data together with light microscopic and laboratory findings are specified in Table 1. The biopsy specimens showed numerous Mallory bodies in 3 patients, and few Mallory bodies in the remaining 3. Approximately one hundred Mallory bodies were studied in the electron microscope.

RESULTS

Electron microscopy showed that alcoholic hyalin consisted partly of light filaments with diameters of about 20 nm (Fig. 1), partly of darker and swollen filaments (Fig. 2) which sometimes formed an amorphous, electron-dense core. In some places the light filaments revealed a double contour but they were never of a tubular appearance in cross sections.

In 1 µm thick toluidine blue stained sections, the alcoholic hyalin consisting only of light filaments was difficult to see light microscopically, their refraction being the same as that of hyaloplasm. Alcoholic hyalin containing dark filaments could be seen as irreg

Acta path. microbiol scand. Sect. A 85 384-394 1977

ALCOHOLIC HYALIN, MICROFILAMENTS AND MICROTUBULES IN ALCOHOLIC HEPATITIS

PALLE PETERSEN

Medical Department A, Division of Hepatology Rigshospitalet, Copenhagen Denmark

Petersen P Alcoholic hyalin, microfilaments and microtubules in alcoholic hepatitis. Acta path. microbiol scand. Sect. A 85 384-394 1977

The alcoholic hyalin which is composed of light and dark occasionally swollen and conglomerating filaments, is found to be surrounded by proliferated RER, hypertrophied Golgi apparatus and mitochondria containing enlarged matrical granules. Besides, microfilaments and some microtubules are seen in relation to the hyaline bodies. In biopsies where hyaline bodies are scarce, hepatocytes without alcoholic hyalin present similar changes and the Golgi apparatus is seen to contain very low density lipoprotein like particles. These ultrastructural changes are suggested to be related to an early stage in the development of alcoholic hyalin. The *abundance of microfilaments indicates an increased motility of the hepatocytes, possibly as a part* of the regenerative processes. It can hardly be precluded that microfilaments disintegrate and accumulate in the alcoholic hyaline mass

Key words Liver ultrastructure alcoholism.

Palle Petersen, Medical Department A Division of Hepatology Rigshospitalet, 2100 Copenhagen, Denmark.

Received 17.v.76 Accepted 24.xi.76

Previous electron microscopic studies (1 2 3 4 13, 17 18) have shown that Mallory's alcoholic hyalin consists of filaments with diameters ranging between 5.5 and 20 nm The electron microscopic appearance of the alcoholic hyalin filaments is varying Some alcoholic hyalin consists of light filaments of slightly irregular contours, others of swelled dark filaments and in the centre of some alcoholic hyalin, a condensed electron opaque mass of fused filaments is seen (2 3) Sometimes the filaments are of a tubular appearance both in isolated hyaline material and in situ (17)

Reports are available according to which bundles of fine parallel filaments of much smaller diameter may be associated with alcoholic hyalin such bundles are often found along its entire circumference. In the same biopsies the amount of similar filaments is found to be excessive in liver cells not containing alcoholic hyalin (18)

It has been demonstrated by immunofluorescence technique that alcoholic hyalin binds immune sera containing anti-actin antibodies (12) Actin filaments of the normal hepatocyte bind heavy meromyosin, while filaments of alcoholic hyalin do not. This suggests a *functional impairment* of the fila-

TABLE 1 *Clinical, Light Microscopical and Laboratory Data of 6 Patients with Alcoholic Hepatitis*

	27 ♂	47 ♂	54 ♂	43 ♂	61 ♀	44 ♂
…and sex						
…mated daily alcohol intake	150 g	200 g	150 g	150 g	75 g	75 g
…ation of alcohol intake	10 y	2 y	10 y	10 y	3–4 y	2 y
…e from cessation of alcohol …ake to biopsy	1 day	4 days	3 days	4 days	7 days	4 days
Microscopical findings: degree of steatosis	+ + +	+ + +	+ + +	+ + +	+ +	+ + +
cirrhosis	+	+	+	0	0	+
necrosis of liver cells	+	+	+	+	+	+
Mallory bodies	many	many	many	few	few	few
…um alanine aminotransferase (normal value <40 U/l)	36	20	28	101	54	28
…um bilirubin (normal value <17 µmol/l)	30	24	53	11	14	49
…um alkaline phosphatases (normal value <275 µmol/l)	680	784	304	440	248	1074
…um albumin (normal value >532 µmol/l)	541	477	478	385	630	–
…sma prothrombin-proconvertin (normal value 70–110 per cent)	90	88	49	109	85	44

ments (6). As microfilaments and microtubules often appear at one and the same localization, the object of the present study was to examine the morphological relationship of alcoholic hyalin fibrils to microfilaments and microtubules in parenchymal cells of liver tissue in biopsies obtained from patients with alcoholic hepatitis.

METHODS AND MATERIAL

Preparations to be studied by electron microscopy are blocks of liver tissue not exceeding 0.5 mm in diameter were obtained from each patient. The blocks were fixed at room temperature in 2.5 per cent glutaraldehyde buffered with 0.1 M sodium cacodylate, followed by short term washing in 0.1 M sodium cacodylate, fixation in 1 per cent osmium tetroxide buffered with 0.1 M sodium cacodylate, dehydration, and embedding in EPON. Ultrathin sections were stained with uranyl acetate and lead citrate and studied in a Zeiss electron microscope 9 A. Adjacent sections of a thickness of 1 µm were stained with toluidine blue and used for light microscopic examinations.

The study includes 6 patients in whom a histological diagnosis of alcoholic hepatitis could be established on the basis of biopsies showing necrosis of the liver parenchymal cells, severe steatosis, and Mallory bodies. The clinical data together with light microscopic and laboratory findings are specified in Table 1. The biopsy specimens showed numerous Mallory bodies in 3 patients, and few Mallory bodies in the remaining 3. Approximately one hundred Mallory bodies were studied in the electron microscope.

RESULTS

Electron microscopy showed that alcoholic hyalin consisted partly of light filaments with diameters of about 20 nm (Fig. 1), partly of darker and swollen filaments (Fig. 2) which sometimes formed an amorphous, electron-dense core. In some places the light filaments revealed a double contour but they were never of a tubular appearance in cross sections.

In 1 µm thick toluidine blue stained sections, the alcoholic hyalin consisting only of light filaments was difficult to see light microscopically, their refraction being the same as that of hyaloplasm. Alcoholic hyalin containing dark filaments could be seen as irreg-



Fig 1 Part of a liver parenchymal cell with an accumulation of alcoholic hyalin consisting of light filaments (lf) and darker filaments (df) Mitochondrial material granules are enlarged (mg) × 13,500 Inset light microscopic appearance of the same alcoholic hyaline mass, toluidine blue stained, × 1,600

ular accumulation of a tint darker than that in the surrounding hyaloplasm in cases where the filaments conglomerated centrally to a dense core, this core could be seen in the light microscope as an irregular contoured body of a strongly blue colour



Fig 2 I this cell the lcoholic hyalin shows darker and more swollen filaments (df) The rough endoplasmic reticulum is dilated and invaginated (RER) Enlarged mitochondrial matrical granules (mg) and fatty acuoles ( ) are seen. × 28,500.

The ultrastructure of the hepatocytes containing this alcoholic hyalin was consistently abnormal. A highly proliferated rough endoplasmic reticulum (RER) with dilated and frequently invaginated cisternae was seen to surround the alcoholic hyalin (Figs. 1 and 2)



Fig 1 Part of a liver parenchymal cell with an accumulation of alcoholic hyalin consisting of light filaments (lf) and darker filaments (df) Mitochondr al material granules are enlarged (mg) × 13,500. Inset light microscopic appearance of the same alcoholic hyaline mass, toluidine blue stained, × 1 600.

ular accumulation of a tint darker than that in the surrounding hyaloplasm in cases where the filaments conglomerated centrally to a dense core this core could be seen in the light microscope as an irregular contoured body of a strongly blue colour



Fig. 4. In this cell a microtubule (mt) is seen within the alcoholic hyaline mass. × 45,000.

between the proliferated RER and a hypertrophied Golgi complex containing very low density lipoprotein (VLDL) like particles (Figs. 7 and 8). Not infrequently centrioles could be found in these cells. The mitochondria were of various forms and sizes and contained enlarged material granules. Cells presenting the same ultrastructural pattern could be found in the liver biopsies containing much alcoholic hyalin, but not as frequently as in those with little alcoholic hyalin.

DISCUSSION

The well-known appearance of alcoholic hyaline filaments (1 2 3 4 13 17 18) is confirmed in this study. The light, rather sharply contoured, filaments are considered to be "young" filaments and they are often arranged at the peripheral part of the alcoholic hyalin. The darker swollen filaments are presumed to be older while the condensed, fused filaments in the centre are considered to be the oldest (2, 3).

In hepatocytes from the same biopsies, some with alcoholic hyalin, and some without alcoholic hyalin the ultrastructural pattern is seen to be the same, i.e. numerous microfilaments, proliferated, dilated and invaginated RER, hypertrophied Golgi complex, and large mitochondral matrical granules. Similar changes were more frequent in the the 3 patients in whom the liver biopsy contained little alcoholic hyalin except that the RER consisted of slender cisternae. The ultrastructural alterations were especially concentrated in the region of Golgi. It is conceivable that some of the changes may be related to the fully developed alcoholic hyalin.

In the present study microfilaments are found in direct continuity of the alcoholic hyaline filaments. In accordance with find-

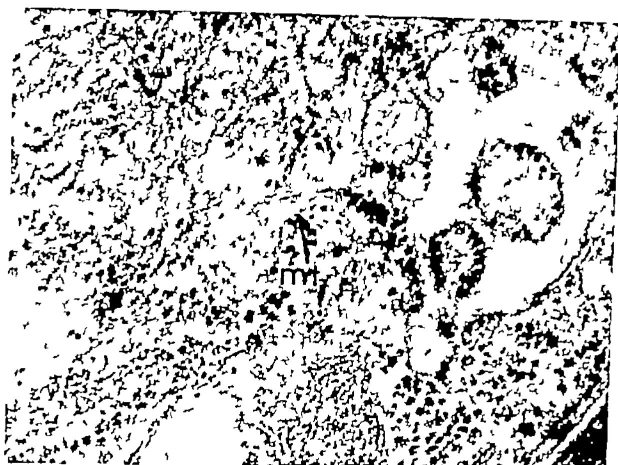


Fig 3 In this cell some microtubules (mt) are present adjacent to the mass of alcoholic hyalin. × 84 000

The Golgi apparatus was hypertrophied to a high degree. The mitochondria were polymorphous and contained enlarged, dark granules in the matrix (Fig 1) Some microtubules were found adjacent to the alcoholic hyalin (Fig 3) occasionally they might penetrate the hyaline mass (Fig 4) As the dimension of the microtubules and alcoholic hyaline filaments was nearly identical 24 and 20 nm respectively a search was made for a direct continuity between the two structures, but such continuity could not be demonstrated

In a few places, microfilaments were seen to be in close connection with the light filaments of alcoholic hyalin. There seemed to be direct transition between the two types of filaments (Fig 5) These microfilaments were arranged in bundles which in longitudinal sections showed parallel filamentous structures. In cross sections, a paired arrangement of the filaments in the bundles appeared (Fig 5) The interval between the filaments of one pair was 20–25 nm, equalling the diameter of the double contoured light filaments of alcoholic hyalin

As a rule, the cells containing alcoholic hyalin contained few microfilaments, while other cells contained excessive amounts stretching in bundles through the cell In these cells the microfilaments were often in direct contact with the desmosomes between cells, particularly cells which showed pseudopodia like protrusions and invaginations of the plasma membrane (Fig 6) Centrioles were often found in such cells.

The ultrastructural pattern of the liver cells of liver biopsies in which light microscopy showed only minor content of alcoholic hyalin was often characteristic. The cells contained large amount of microfilaments in close relationship to or intermingled with microtubules (Fig 7) especially in the region



Fig 4 In this cell microtubule (mt is seen within the alcoholic hyaline mass × 45,000

between the proliferated RER and a hypertrophied Golgi complex containing very low density lipoprotein (VLDL) like particles (Figs. 7 and 8) Not infrequently centrioles could be found in these cells. The mitochondria were of various forms and sizes and contained enlarged material granules. Cells presenting the same ultrastructural pattern could be found in the liver biopsies containing much alcoholic hyalin, but not as frequently as in those with little alcoholic hyalin.

DISCUSSION

The well-known appearance of alcoholic hyaline filaments (1 2 3 4 13 17 18) is confirmed in this study The light, rather sharply contoured, filaments are considered to be "young" filaments and they are often arranged at the peripheral part of the alcoholic hyalin. The darker swollen filaments are presumed to be older while the condensed, fused filaments in the centre are considered to be the oldest (2, 3)

In hepatocytes from the same biopsies, some with alcoholic hyalin, and some without alcoholic hyalin the ultrastructural pattern is seen to be the same, i.e. numerous microfilaments, proliferated, dilated and invaginated RER, hypertrophied Golgi complex, and large mitochondrial matrical granules. Similar changes were more frequent in the the 3 patients in whom the liver biopsy contained little alcoholic hyalin except that the RER consisted of slender cisternae The ultrastructural alterations were especially concentrated in the region of Golgi. It is conceivable that some of the changes may be related to the fully developed alcoholic hyalin.

In the present study microfilaments are found in direct continuity of the alcoholic hyaline filaments. In accordance with find



Fig 5 Part of a liver parenchymal cell in which bundles of microfilaments (mf) continue in between the alcoholic hyaline filaments (hf) Arrows show cross sectioned microfilaments and their paired arrangement in the bundles. × 84 000

ings by other investigators (18) bundles of microfilaments in hepatocytes without alcoholic hyalin are found in biopsies from patients suffering from alcoholic hepatitis. Such actin like filaments are identifiable in the normal hepatocyte (6 7 15) but are far



Fig. 4 Parts of two liver parenchymal cells with bundles of microfilaments (mf). Some of the filaments appear to be in direct contact with the desmosomes between the cells. A protrusion of the cell surface (p) is indicated. × 28,500

more abundant after partial hepatectomy (7, 9, 15). As actin-like microfilaments are involved in cell motility and division (16), the great amount of microfilaments found in hepatocytes from patients suffering from alcoholic hepatitis suggests an increased cell moti-



Fig 7 Part of a liver parenchymal cells in a biopsy from a patient with alcoholic hepatitis with only sparse alcoholic hyalin. The rough endoplasmatic reticulum shows elongated parallel cisternae The Golgi apparatus contains VLDL particles (VLDL) Bundles of microfilaments (mf) and some microtubules (mt) are seen. × 5 400

lity possibly as part of regenerative processes The contact of the microfilaments with the desmosomes as well as the irregular cell borders with invaginations and protrusions of the plasma membrane may indicate amoeboid movements of the liver cells.

So far the occurrence of microtubules has not been considered in pathological conditions of the human liver Microtubules and microfilaments constitute one part of the fibres of the mitotic spindle which is composed of chromosomes, centrioles and spindle fibres. The microtubules are presumed to be a cytoskeleton on which the microfilaments are anchored in order that the microfilaments may draw the chromosomes to the poles during cell division In the present work some observations are indicative of cellular division Firstly centrioles are observed in the region of the Golgi apparatus in many hepatocytes and in the same region, microtubules together with many microfilaments are observed. Secondly the matrical granules of the mitochondria are enlarged and more electron dense than normal (10) a phenomenon seen at onset of the cell division (16) On the assumption that alcoholic hyaline filaments are disintegrated microfilaments, it might be imagined that alcohol may influence the process of division possibly through an interference with the mitotic spindle

Another aspect is the influence of alcohol on the secretory role of the microtubular system this aspect has been studied in experiments with colchicine Colchicine binds strongly to tubulin, the precursor protein of



Fig. 8. A higher magnification showing part of a liver parenchymal cell. This field shows particles of size of 50–80 nm and with only slight osmiophilia. These particles resemble the VLDL particles of dog liver (see text). Microfilaments (mf) are also present. × 84,000

microtubules, and causes a breakdown of microtubules, destruction of spindles and a concomitant block of chromosome movement (5). On the basis of a study including perfusions of mouse livers, colchicine being added to the perfusate, *Le Marchand et al.*

(11) concluded that the microtubular system was of importance for the intracellular movement and the possible release of VLDL particles. They also observed that the overall protein secretion by the liver was inhibited by the drug. In agreement with this, *Stein & Stein* (14) found serum triglyceride levels to be 50–80 per cent lower in colchicine treated rats than in controls. Moreover they found an accumulation of Golgi-derived secretory vesicles containing VLDL particles. They concluded that colchicine blocks the final step of the lipoprotein release from the liver by interfering with the integrity of the microtubular system. In the present study VLDL particles of human liver are presented for the first time (Figs. 8 and 9). They are of a size from 50 to 80 nm and slightly to moderately osmiophilic like the triglyceride containing fatty vacuoles (Fig. 2). They are of identical appearance to VLDL particles of dog liver (8) but do not resemble the strongly osmiophilic VLDL particles of rat liver, the rat being the commonly used animal for lipoprotein research of the liver.

The presence of many microtubules in liver cells from patients with alcoholic hepatitis as found in the present work may be explained as an attempt by those cells to facilitate the lipoprotein release in order to eliminate the accumulated triglyceride.

This study was supported by a grant from *Danish State Medical Council* (512 3719)

REFERENCES

1. *Albukerk J. & Duffy J. L.* Origin of alcoholic hyaline. Arch. Path. *93* 510–517 1972
2. *Biava C.* Mallory alcoholic hyaline: a heretofore unique lesion of hepatocellular ergastoplasm. Lab. Invest. *13* 301–320 1964
3. *Feldmann G. Oudea P. Molas G. Lomart Oudea M.-C. & Fauvert R.* L'ultrastructure des hépatocytes au cours des cirrhoses alcooliques. La Presse Med. 78 409–414 1970
4. *Flax M. H. & Tisdale W. A.* An electron microscopic study of alcoholic hyaline. Amer. J. Path. *44* 441–453 1964
5. *Forer A.* Possible roles of microtubules and actin like filaments during cell-division. 319–336 in "Cell Cycle Controls" edited by Padilla G. M. Cameron, I. L. & Zimmer A. Acad. Pr. 1974
6. *French S. W. Davies P. I. & Carr B. N.* The nature of Mallory body filaments. Lab. Invest. *30* 374 a, 1974
7. *Gabbiani F. Ryan, G. B. Lamelin J.-P., Vassalli P. Majno G. Bouvier C. A., Cruchaud A. & Lüscher E. F.* Human smooth muscle autoantibody. Its identification as antiactin antibody and a study of its binding to "nonmuscular" cells. Am. J. Path. 72 473 1973
8. *Hamilton R. L.* Ultrastructural aspects of hepatic lipoprotein synthesis and secretion. Proc. of the 1968 Deuel conference on lipids, on The Turnover of Lipid and Lipoproteins. Febr. 21–24 1968 Carmel, California, Pag. 3–31
9. *Lampert I. A. Trenchev P. & Holborrow E. J.* Contractile protein changes in the regenerating rat liver. Virchows Arch. (Zellpathol.) *15* 351 1974
10. *Ma M. H. & Biempica L.* The normal human liver cell. Cytochemical and ultrastructural studies. Am. J. Path. *62* 353–391 1971
11. *Le Marchand Y. Singh M. Assimacopoulos-Jeannet F. Orci L. Rouiller C. & Jeanrenaud B.* A role for the microtubular system in the release of very low density lipoproteins by perfused mouse livers. J. of Biol. ch. *248* 6862–6870 1973
12. *Nenci I.* Identification of Actin-Like Proteins in Alcoholic Hyaline by Immunofluorescence. Lab. Invest. *32* 257–260 1975
13. *Smuckler E. A.* The ultrastructure of human alcoholic hyaline. The Am. J. of Cl. Path. *49* 790–797 1968.
14. *Stein O. & Stein Y.* Colchicine induced inhibition of very low density lipoprotein release by rat liver in vivo. Biochem. et Biophys. Acta *306* 142–147 1973
15. *Trump E. F. Dees J. H. & Shelburne J. D.* The ultrastructure of the human liver cell and its common pattern of reaction to injury. In The Liver, edited by Gall, E. A. & Mostofi, F. K. P. 80 Baltimore, Williams & Wilkins Co. 1973
16. *Wessells N. K. Spooner B. S., Ash J. F. Bradley M. O., Luduena M. A. Taylor E. L. Wrenn J. T. & Yamada K. M.* Microfilaments in cellular and developmental processes. Sc. *171* 135–145 1971
17. *Wiggers K. D. French S. W., French B. A. & Carr B. N.* The ultrastructure of Mallory body filaments. Lab. Invest. *29* 652–658, 1973
18. *Yokoo H. Minick O. T., Batti F. & Kent G.* Morphologic variants of alcoholic hyaline. Am. J. of Path. *69* 25–40 1972.

Acta path. microbiol. scand. Sect. A, 85 595–598, 1977

PRIMARY MALIGNANT MELANOMA OF THE OESOPHAGUS

TRYGGVE MÅNSSON and THORBJÖRN BERGE

Department of Pathology Kärnsjukhuset, Skövde, Sweden

Månsson, T & Berge, T Primary malignant melanoma of the oesophagus. Acta path. microbiol. scand. Sect. A, 85 595–598, 1977

A case of a primary malignant melanoma of the oesophagus is described and the criteria for diagnosis are discussed.

Key words Melanoma, primary malignant oesophagus

T Berge, Department of Pathology Kärnsjukhuset, Skövde, Sweden.

Received 18.xi.76 Accepted 26.xi.76

Primary malignant melanoma of the oesophagus is rare. It was first described by *Bauer* in 1906, since then, a further 30 cases have been reported, but none from Scandinavia. It was therefore thought of relevance to publish the following case.

CASE REPORT

A B a 74-year-old woman, who for 10 years had been suffering from diabetes mellitus, was admitted to hospital on the 14th December 1973 She complained of pain in the lumbosacral region physical examination did not reveal anything remarkable except pain on rotation of the right hip Laboratory tests Haemoglobin 9 4 g/100 ml, leucocytes 5300, E S R 50 mm/1hr bilirubin 0.3 mg/100 ml, alkaline phosphatase 490 units (upper normal limit <250 units) GPT 25 units (normal) total protein 6.3 g/100 ml. The serum electrophoretic pattern showed activity and normal immune proteins. X-ray examination of the pelvis, hips and spine revealed osteoporosis and compression of several vertebrae

Because of the high alkaline phosphatase activity and activity of the electrophoretic pattern, malignancy was suspected and the gastro-intestinal tract was therefore roentgenographically examined. The roentgenograms showed a 7 cm long, polypoid tumour with stenosis of the middle of the oesophagus. The patient declared that swallowing did no cause any difficulties. Oesophagoscopy revealed polypoid partly necrotic, tumour Histological examination of several biopsy specimens showed malignant melanoma. As primary malignant melanoma of the oesophagus is a rare phenomenon, we thought it might be an extension via a contiguition of an affected mediastinal lymph node.

Careful examination of the skin failed to reveal any signs of naevi, tumours or scars. Examination on two occasions by an ophthalamologist showed only diabetic retinopathy and no tumour Careful inspection of the mouth, nose, epipharynx, rectum and external genitals revealed nothing remarkable. A scintiscan of the skeleton suggested the presence of three lesions in the sciality of costae IV V on the right side. Chest X-ray showed pleural metastases on the right side and, in the upper half of the mediastinum, a protuberance containing air and fluid. Owing to the metastases and the patient's age, operation was not suggested. The patient became weak and anaemic she died on July 16, 1974

Necropsy (339/74)

Gross examination revealed no signs of a cutaneous tumour In the middle of the oesophagus, polypoid, partly necrotic, dark, pigmented, oval tumour measuring 12.5 × 6 × 3.5 cm was seen (Fig. 1) On the right pleura, very close to the oesophageal tumour three spheroidal black-brown metastases, 3 cm in diameter were present. Prod-

(11) concluded that the microtubular system was of importance for the intracellular movement and the possible release of VLDL particles. They also observed that the overall protein secretion by the liver was inhibited by the drug In agreement with this, *Stein & Stein* (14) found serum triglyceride levels to be 50–80 per cent lower in colchicine treated rats than in controls. Moreover they found an accumulation of Golgi-derived secretory vesicles containing VLDL particles. They concluded that colchicine blocks the final step of the lipoprotein release from the liver by interfering with the integrity of the microtubular system In the present study VLDL particles of human liver are presented for the first time (Figs. 8 and 9) They are of a size from 50 to 80 nm and slightly to moderately osmiophilic like the triglyceride containing fatty vacuoles (Fig 2) They are of identical appearance to VLDL particles of dog liver (8), but do not resemble the strongly osmiophilic VLDL particles of rat liver the rat being the commonly used animal for lipoprotein research of the liver

The presence of many microtubules in liver cells from patients with alcoholic hepatitis, as found in the present work may be explained as an attempt by those cells to facilitate the lipoprotein release in order to eliminate the accumulated triglyceride.

This study was supported by a grant from *Danish State Medical Council* (512 3719)

REFERENCES

1 *Albukerk J & Duffy J L* Origin of alcoholic hyaline Arch. Path. *93* 510–517 1972

2 *Biava C* Mallory alcoholic hyaline a heretofore unique lesion of hepatocellular ergastoplasm. Lab. Invest. *13* 301–320 1964

3 *Feldmann G Oudea P Molas G Lomart Oudea M -C & Fauvert R* L ultrastructure des hépatocytes au cours des cirrhosisalcoholiques. La Presse Med. *78* 409–414 1970

4 *Flax M H & Tisdale W A* An electron microscopic study of alcoholic hyaline Amer J Path. *44* 441–453 1964

5 *Forer A* Possible roles of microtubules and actin-like filaments during cell-division 319-336 in "Cell Cycle Controls" edited by Padilla G M., Cameron, I L. & Zimmer A. Acad. Pr 1974

6 *French S W Davies P I & Carr B N* The nature of Mallory body filaments. Lab. Invest. *30* 374 a, 1974

7 *Gabbiani F Ryan G B Lamelin, J-P Vassalli P Majno G Bouvier C A Cruchaud A & Lüscher E. F* Human smooth muscle autoantibody its identification as antiactin antibody and a study of its binding to "nonmuscular" cells. Am. J Path. *72* 473, 1973

8. *Hamilton R L* Ultrastructural aspects of hepatic lipoprotein synthesis and secretion. Proc. of the 1968 Deuel conference on lipids, on The Turnover of Lipid and Lipoproteins Febr 21–24 1968 Carmel California, Pag. 5–31

9 *Lampert I A Trencker P & Holborrow E J* Contractile protein changes in the regenerating rat liver Virchows Arch. (Zellpathol.) *15* 351 1974

10 *Ma M H & Biempica L* The normal human liver cell Cytochemical and ultrastructural studies. Am. J Path. 62 353–391 1971

11 *Le Marchand Y Singh M., Assimacopoulos-Jeannet F Orci L. Rouiller C & Jeanrenaud B* A role for the microtubular system in the release of very low density lipoproteins by perfused mouse livers. J of Biol. ch. *248* 6862–6870 1973

12 *Nenci I* Identification of Actin-Like Proteins in Alcoholic Hyaline by Immunofluorescence. Lab. Invest. *32* 257–260 1975

13 *Smuckler E. A* The ultrastructure of human alcoholic hyaline. The Am. J of Cl. Path. *49* 790–797 1968.

14 *Stein O & Stein Y* Colchicine-induced inhibition of very low density lipoprotein release by rat liver in vivo. Biochem. et Biophys. Acta *306* 142–147 1973

15 *Trump E. F Dees J H & Shelburne J D* The ultrastructure of the human liver cell and its common pattern of reaction to injury In The Liver edited by Gall E. A. & Mostofi, F K. P 80 Baltimore Williams & Wilkins Co 1973

16. *Wessells N K Spooner B S Ash J F Bradley M O Luduena M A Taylor E. L. Wrenn J T & Yamada K M* Microfilaments in cellular and developmental processes. Sc *171* 135–143 1971

17 *Wiggers K D French S W French B. A & Carr B N* The ultrastructure of Mallory body filaments. Lab. Invest. *29* 652–658, 1973

18. *Yokoo H Minick O T Batti F & Kent G* Morphologic variants of alcoholic hyaline Am. J of Path. *69* 25–40 1972.

Acta path. microbiol. scand. Sect. A, 85 395–398, 1977

PRIMARY MALIGNANT MELANOMA OF THE OESOPHAGUS

TRYGGVE MÅNSSON and THORBJÖRN BERGE

Department of Pathology Kärnsjukhuset, Skövde, Sweden

Månsson, T & Berge, T Primary malignant melanoma of the oesophagus. Acta path. microbiol. scand. Sect. A, 85 395–398, 1977

A case of a primary malignant melanoma of the oesophagus is described and the criteria for diagnosis are discussed.

Key words Melanoma, primary malignant oesophagus

T Berge, Department of Pathology Kärnsjukhuset, Skövde, Sweden.

Received 18.xi.76 Accepted 26.xi.76

Primary malignant melanoma of the oesophagus is rare. It was first described by *Bauer* in 1906, since then, a further 50 cases have been reported, but none from Scandinavia. It was therefore thought of relevance to publish the following case.

CASE REPORT

A.B. 74-year-old woman, who for 10 years had been suffering from diabetes mellitus, was admitted to hospital on the 14th December 1973 She complained of pain in the lumbosacral region physical examination did not reveal anything remarkable except pain on rotation of the right hip. Laboratory tests. Haemoglobin 9.4 g/100 ml, leucocytes 5300, E.S.R. 50 mm/1hr bilirubin 0.3 mg/100 ml, alkaline phosphatase 490 units (upper normal limit <250 units) GPT 23 units (normal) total protein 6.3 g/100 ml. The serum lectrophoretic pattern showed activity and normal immune proteins. X-ray examination of the pelvis, hips and spine revealed osteoporosis and compression of several vertebrae

Because of the high alkaline phosphatase activity and activity of the electrophoretic pattern, malignancy was suspected and the gastro-intestinal tract was therefore roentgenographically examined. The roentgenograms showed a 7 cm long polypoid tumour with stenosis of the middle of the oesophagus. The patient declared that swallowing did no cause any difficulties. Oesophagoscopy revealed a polypoid, partly necrotic, tumour Histological examination of several biopsy specimens showed a malignant melanoma. As primary malignant melanoma of the oesophagus is a rare phenomenon, we thought it might be an extension via a continuation of an affected mediastinal lymph node.

Careful examination of the skin failed to reveal any signs of naevi, tumours or scars. Examination on two occasions by an ophthalmologist showed only diabetic retinopathy and no tumour. Careful inspection of the mouth, nose, epipharynx, rectum and external genitals revealed nothing remarkable. A scintiscan of the skeleton suggested the presence of three lesions in the vicinity of costae IV V on the right side. Chest X ray showed pleural metastases on the right side and, in the upper half of the mediastinum, a protuberance containing air and fluid. Owing to the metastases and the patient's age, operation was not suggested. The patient became weak and anaemic she died on July 16, 1974

Necropsy (339/74)

Gross examination revealed no signs of a cutaneous tumour In the middle of the oesophagus, a polypoid, partly necrotic, dark, pigmented, oval tumour measuring 12.5 × 6 × 3.5 cm was seen (Fig. 1) On the right pleura, very close to the oesophageal tumour three spheroidal black-brown metastases, 5 cm in diameter, were present. Prom-



Fig 1 Polypoid, pigmented tumour in the oesophagus. In the upper part, one of the pigmented pleural metastases



Fig 2 Periphery of the tumour growing in the submucosa under the surface epithelium. H & E × 30

mal to the tumour the oesophagus was dilated containing grey semifluid material. Via a narrow fistula immediately above the tumour the oesophagus was in open communication with an irregularly outlined abscess, the size of a fist, in the mediastinum, involving adjacent parts of the right lung. This process corresponded to the mediastinal protuberance seen on the chest X ray. The cut surface of the lesion was grey and fleshy with dark, pigmented areas it extended downwards to the muscularis propria in the upper half of the oesophagus. At the level of the cardia a tumourous, pigmented lymph node was observed, measuring 4 × 3.5 × 3 cm. Otherwise there were no relevant findings. The whole oesophagus was fixed in formaldehyde and several blocks were excised from macroscopically unaffected parts of the oesophagus as well as from the tumour

Microscopically the tumour was confined to the mucosa and submucosa except in the upper half where it extended through the whole thickeness of the muscularis propria (Fig 2). The tumour was a malignant melanoma in some areas containing melanin (Fig 3). The histological picture of the three pleural tumours and the mediastinal lymph node was one and the same. In several sections of the oesophagus, areas with melanocytes in the



Fig 3 Periphery of the tumour with pigment loaded cells. A few melanocytes in the epithelium Masson × 125

basal layer of the epithelium were seen (Fig. 4). These areas were found close to, as well as at a distance from the tumour but not in the upper third of the oesophagus.

DISCUSSION

The occurrence of a primary malignant melanoma is related to the presence of melanocytes (*Allen* 1949). *De la Pava et al.* (1963) found typical melanin-containing melanocytes in 4 out of 100 randomly selected oesophagi. The pigmented area, however, could not be seen with the naked eye. *Tateishi et al.* (1974) demonstrated melanocytes in normal oesophageal mucosa in 4 out of 50 consecutive necropsies. They suggested that the incidence of oesophageal melanocytes might vary with race, and that the incidence of melanocytes in the oesophagus probably is higher among coloured people than among white subjects. The literature contains 4 reports on malignant melanoma combined with gross melanosis of the oesophagus (*Raven* 1941, *Fowler & Sutherland* 1952, *Fleming & van der Merwe* 1958, *Piccone et al.* 1970). Microscopically pigmented cells were seen in the basal layer of the epithelium.

In 1953 *Allen & Spitz* described the histological and diagnostic criteria set up for primary malignant melanoma and emphasized the presence of junctional changes in the adjacent epithelium. Still, *Robertsson* (1954) contended that such changes easily may be destroyed by a rapidly growing tumour. Any junctional changes were not demonstrable in our case.

Dysphagia is the most common clinical feature of an obstructing oesophageal tumour though our patient had no such symptoms at the time of diagnosis. Barium X-ray examination usually reveals a malignant melanoma as a polypoid lesion (*Raven & Dawson* 1964, *Bingham et al.* 1971). A differential diagnosis requires biopsy. Malignant melanoma may appear in any segment of the oesophagus, but is most common in the middle third (*Raven & Dawson* 1964). A firm diagnosis requires a thorough search by which a primary tumour



Fig. 4. Melanocytes in the epithelium in the vicinity of the tumour. Masson × 500.

elsewhere in the body can be ruled out; the diagnosis of primary malignant melanoma should be based on the following criteria: (1) The tumour should have the characteristic structure of a melanoma and must contain melanin. (2) The tumour should be polypoid. (3) The adjacent epithelium should contain melanocytes. (4) The tumour should preferably though not necessarily arise in an area of junctional changes in the squamous epithelium.

We believe that the tumour in our case was a primary malignant melanoma of the oesophagus. The structure of the polypoid tumour was like that of a melanoma. The oesophageal mucous membrane contained melanocytes. The tumour had spread only to a regional lymph node, and local pleural metastases owing to penetration of the tumour into the mediastinum were in evidence.



Fig 1 Polypoid pigmented tumour in the oesophagus. In the upper part, one of the pigmented pleural metastases.

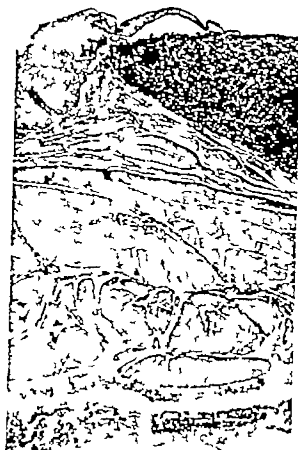


Fig 2 Periphery of the tumour growing in the submucosa under the surface epithelium, H & E × 30

mal to the tumour the oesophagus was dilated containing grey semifluid material Via a narrow fistula immediately above the tumour the oesophagus was in open communication with an irregularly outlined abscess, the size of a fist, in the mediastinum, involving adjacent parts of the right lung This process corresponded to the mediastinal protuberance seen on the chest X ray The cut surface of the lesion was grey and fleshy with dark pigmented areas it extended downwards to the muscularis propria in the upper half of the oesophagus At the level of the cardia, a tumourous, pigmented lymph node was observed, measuring 4 × 3.5 × 3 cm Otherwise these were no relevant findings. The whole oesophagus was fixed in formaldehyde and several blocks were excised from macroscopically unaffected parts of the oesophagus as well as from the tumour

Microscopically the tumour was confined to the mucosa and submucosa except in the upper half where it extended through the whole thickeness of the muscularis propria (Fig 2) The tumour was a malignant melanoma In some areas containing melanin (Fig 3) The histological picture of the three pleural tumours and the mediastinal lymph node was one and the same. In several sections of the oesophagus, areas with melanocytes in the



Fig 3 Periphery of the tumour with pigment loaded cells. A few melanocytes in the epithelium Masson × 125

PERIPHERAL IMMUNOFLUORESCENCE OF HEPATOCYTES

Relation to Smooth Muscle Antibodies and Bile Canaliculi

HANS DIEDERICHSEN KIRSTEN RIISOM and INGER ANDERSEN

The Blood Bank and Medical Department M,
Odense University Hospital, Odense, Denmark

Diederichsen, H., Riisom, K. & Andersen, I. Peripheral immunofluorescence of hepatocytes. Acta path. microbiol. scand. Sect. A, 85 399–404 1977

By means of indirect immunofluorescence microscopy a peripheral fluorescence reaction with hepatocytes was found, surrounding the entire cell, with sera from patients with cancer and acute hepatitis and from normal blood donors. It was proved that this reaction was not related to bile canaliculi, contrary to bile canaliculi antibody demonstrated previously from patients with cronic active liver disease. By using fluorescein-conjugated anti-human IgG the reaction with the periphery of the hepatocytes was produced to a more or less pronounced degree with almost all sera studied. The reaction seems not to be directed against contractile proteins on the liver cell membrane as only minor part of these sera had also IgG smooth-muscle antibody and anti actomyosin antibody obtained by affinity chromatografy did not react with the hepatocyte. When applying fluorescein-conjugated anti-human IgM the reaction with the periphery of the hepatocytes was observed in one fourth of the patients with acute hepatitis and only sera which contained also IgM smooth-muscle antibody.

Key words: Hepatocytes; immunofluorescence; smooth-muscle antibodies; bile canaliculi.

H. Diederichsen, Medical Department M Odense University Hospital, Odense, Denmark.

Received 1.iii.76 Accepted 1.xii.76

In serum from patients with chronic active hepatitis, cancer and acute viral hepatitis an immunofluorescence pattern outlining the hepatocytes in a polygonal pattern has been described (9 10). The antibody producing the polygonal pattern was considered to be directed against a component resembling smooth muscle actomyosin present in liver cells. (7) In previous studies we have found that serum from patients with chronic active liver disease produced a staining pattern partly encircling the bovine hepatocytes by the immunofluorescence method (2, 3). This fluorescence staining later could be shown to be cofined to the bile canaliculi (13).

In the present study we have investigated the relationship between the content of smooth muscle antibody (SMA) in sera from patients with acute hepatitis and cancer and normal donors and the capability of the sera to produce immunofluorescence staining of the periphery of bovine hepatocytes (polygonal pattern) and tried to delimit the immunofluorescence staining of the periphery of the hepatocytes from that of bile canaliculi.

REFERENCES

Allen A C A reorientation on the histogenesis and clinical significance of cutaneous nevi and melanomas. Cancer *2* 28–56 1949

Allen A C & Spitz S Malignant melanoma. Cancer *6* 1–45 1953

Bingham D L. C Chadsey L. C Ramchand S & Dorts P J Primary melanocarcinoma of the esophagus. Can. Med Ass. J *105* 607–610 1971

De la Pava S Nigogosyan G Pickren J W & Cabrera A Melanosis of the esophagus. Cancer *16* 48–50 1963

Fleming P C & van der Merwe S B A case of primary malignant melanoma of the esophagus. Br J Surg *46* 121–123 1958.

Fowler M & Sutherland H D Malignant melanoma of the oesophagus. J Path. Bact. *64* 473–477 1952

7 *Piccone V A Kopstock R., le Veen, H H & Sika J* Primary malignant melanoma of the esophagus associated with melanosis of the entire esophagus. J Thorac. Cardiovasc. Surg *59* 864–870 1970

8. *Raven R W & Dawson I* Malignant melanoma of oesophagus. Br J *Surg. 51* 551–555 1964

9 *Ranieri M* quoted by *Bingham et al.*, 1971

10 *Robertson J W* Malignant melanoma of the esophagus as one of multiple malignant tumours. Gastroenterology *27* 121–126, 1954

11 *Tateishi R. Taniguchi H., Wada A Horai, T & Taniguchi K* Argyrophil cells and melanocytes in esophageal mucosa. Arch. Pathol. *98* 87–89 1974

Acta path. microbiol. scand. Sect. A, 85 399–404 1977

PERIPHERAL IMMUNOFLUORESCENCE OF HEPATOCYTES

Relation to Smooth Muscle Antibodies and Bile Canaliculi

HANS DIEDERICHSEN KIRSTEN RISOM AND INGER ANDERSEN

The Blood Bank and Medical Department M,
Odense University Hospital, Odense, Denmark

Diederichsen, H Risom, K. & Andersen, I. Peripheral immunofluorescence of hepatocytes. Acta path microbiol. scand. Sect. A, 85 399–404 1977

By means of indirect immunofluorescence microscopy a peripheral fluorescence reaction with hepatocytes was found, surrounding the entire cell, with sera from patients with cancer and acute hepatitis and from normal blood donors. It was proved that this reaction was not related to bile canaliculi, contrary to bile canaliculi antibody demonstrated previously from patients with cronic active liver disease. By using fluorescein-conjugated anti-human IgG the reaction with the periphery of the hepatocytes was produced to a more or less pronounced degree with almost all sera studied. The reaction seems not to be directed against contractile proteins on the liver cell membrane as only a minor part of these sera had also IgG smooth-muscle antibody and anti actomyosin antibody obtained by affinity chromatografy did not react with the hepatocyte When applying fluorescein-conjugated anti-human IgM the reaction with the periphery of the hepatocytes was observed in one fourth of the patients with acute hepatitis and only sera which contained also IgM smooth-muscle antibody

Key words Hepatocytes immunofluorescence smooth-muscle antibodies bile canaliculi.

H Diederichsen, Medical Department M, Odense University Hospital, Odense, Denmark.

Received 1.xii.76 Accepted 1.xii.76

In serum from patients with chronic active hepatitis, cancer and acute viral hepatitis an immunofluorescence pattern outlining the hepatocytes in a polygonal pattern has been described (9 10) The antibody producing the polygonal pattern was considered to be directed against a component resembling smooth muscle actomyosin present in liver cells. (7) In previous studies we have found that serum from patients with chronic active liver disease produced a staining pattern partly encircling the bovine hepatocytes by the immunofluorescence method (2, 3) This fluorescence staining later could be shown to be cofined to the bile canaliculi (13)

In the present study we have investigated the relationship between the content of smooth muscle antibody (SMA) in sera from patients with acute hepatitis and cancer and normal donors and the capability of the sera to produce immunofluorescence staining of the periphery of bovine hepatocytes (polygonal pattern) and tried to delimit the immunofluorescence staining of the periphery of the hepatocytes from that of bile canaliculi.

MATERIAL

Sera were studied from 52 patients with various types of malignant neoplasm 21 patients with acute viral HB_sAg positive hepatitis and 73 blood donors of identical age and sex

METHODS

The immunofluorescence method The sera were stored at −20 C until use They were inactivated by heating to 56 C for 30 minutes and diluted to 1/10 before testing As antigen for the examination of peripheral fluorescence of the hepatocytes, fresh bovine liver frozen in liquid nitrogen was used We decided to use bovine liver for this study because this tissue has previously been found to be best suited for demonstration of bile canaliculi antibody (BCA) (5) Rat liver was also used for comparison of the fluorescence patterns. As antigen for the examination of SMA we used fresh frozen rat stomach which is generally used when testing for SMA (18 6) The tissue was sectioned at 6 µ in a cryostat microtome and used the same day The sections were first incubated with serum for 30 minutes at room temperature then for a further 30 minutes with *fluorescein iso-thiocyanat-conjugated* (FITC) anti human IgG or IgM Following each *incubation period the sections were washed three* times, for five minutes each time with phospate-*buffered saline pH 7 2 (PBS) At last equal volu*mes of glycerin and PBS were added The preparations were then covered with glass. The FITC conjugates were supplied by Behringwerke The FITC anti IgG had a molar F/P ratio of 2,3 The plateau end point titre was 1/80 The dilution applied was 1/20 The conjugate was absorbed once with freeze-dried bovine liver powder When testing for SMA the conjugate was furthermore absorbed twice with freeze-dried rat uterus. The FITC anti IgM had a molar F/P ratio of 1 9 The plateau end point titre was 1/80 The delution applied was 1/20 The conjugate was absorbed once with homogenized freeze-dried bovine liver powder None of the absorbed conjugates reacted with liver or stomach when applied direct.

Microscopic study was made with a Zeiss dark field microscope with an HBO 200 W mercury lamp as the light source exciter filter BG 12/3 and a barrier filter 50 The photographs of the immunofluorescence reactions were taken with Kodak high speed Ektachrome tungsten EHB 135 film 22 Din.

Histochemical staining of bile canaliculi The adenosine triphosphate (ATPase) method developed by Wachstein and Meisel (16) was employed The sections were fixed in acetone-chloroform, and then stained by the immunofluorescence method and lastly by the ATPase method as previously described (13)

Preparation of actomyosin. Human uterus from non pregnant women was frozen immediately after hysterectomy and used within one month. The tissue was cut into slices and washed two times in distilled water The preparation of actomyosin was done according to *Finck* (8) and *Becker* (1) after the modification by *Scheinmann* (14) The actomyosin was chromatographied on Sephadex G 200 Superfine (Pharmacia Fine Chemicals) packed on siliconized 6 mm beads in a 1 6 × 100 cm closed column (K 16/100 Pharmacia Fine Chemicals) flow rate 9 ml/h, at room temperature. The protein emerged in one peak at the void volume. In sodium dodecyl sulfate (SDS)-polyacrylamide gel electrophoresis (17) *bands corresponding to the* localization of actin and myosin were found.

Affinity chromatography CH Sepharose 4 B (Pharmacia Fine Chemicals) was used. Sera, twelve *and thirty mg actomyosin were coupled to* the Sepharose according to standard procedure *(Pharmacia Fine Chemicals) One ml SMA-con*taining serum diluted 1 8 was added to the column *After* washing the column with *PBS* elution was done with glycine/HCL solution (0,2 M, pH 2,8) containing NaCl (1 M) The eluate was neutralized by adding NaOH (0 1 M) and dialyzed against PBS

RESULTS

In 50 out of 52 patients with cancer IgG immunofluorescent staining was observed corresponding to the periphery of the hepatocytes (Fig 1) Sera from two patients whith cancer gave *hardly any staining* of the periphery of the hepatocytes. All sera from patients with acute hepatitis and from normal blood donors produced peripheral immunofluorescent staining of the hepatocytes. Most fluorescence reactions with sera *from* patients with cancer and from normal donors were weak, whereas the fluorescence reactions with *sera from* patients with acute hepatitis were generally more intense. The results of the tests for IgG SMA are shown in *Table 1* We considered the sera to be positive, if the reaction was (+) or more, with over half the smooth-*muscle fibres of the muscularis* mucosae Sera with weaker reactions than the above were considered as negative they stained a small part of the muscularis mucosae only and the strength was never higher than (+)

IgM immunofluorescence of the periphery of the hepatocytes was produced only with

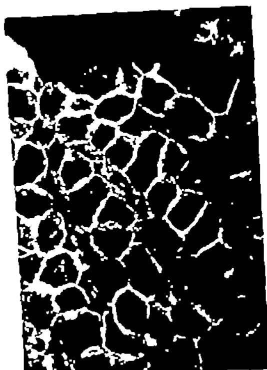


Fig. 1. Immunofluorescence staining of the periphery of hepatocytes. Original magnification × 400

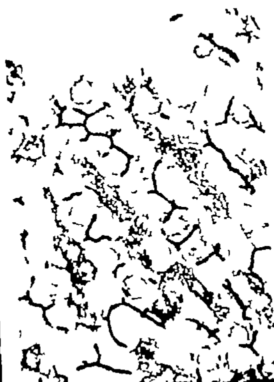


Fig. 2. ATPase staining of bile canaliculi of the same area as Fig. 1. Original magnification × 400

TABLE 1. *IgG SMA in Patients with Cancer and Acute Hepatitis and in Age and Sex Matched Blood Donors*

	Total No.	No. sera with SMA
Cancer	52	15
Matched donors	52	6
Acute hepatitis	21	9
Matched donors	21	1

sera from patients with acute hepatitis (Table 2). The IgM fluorescence pattern resembled completely the IgG fluorescence pattern. All sera producing IgM peripheral fluorescence of the hepatocytes also showed IgM SMA.

Sections presenting immunofluorescent staining of the periphery of the hepatocytes were photographed, then stained for bile canaliculi by the ATPase method and photographs were again taken of the same sites. This procedure

TABLE 2. *IgM peripheral Hepatocyte Staining and IgM SMA in patients with Cancer and Acute Hepatitis and in Age and Sex matched Blood Donors*

	Total No.	No. sera giving peripheral staining of hepatocytes	No. sera with SMA
Cancer	52	0	1
Matched donors	52	0	2
Acute hepatitis	21	3	14
Matched donors	21	0	0

revealed that the pattern obtained by immunofluorescent staining and that produced by ATPase staining were not identical (*Fig. 1* and 2). By way of comparison it is shown that immunofluorescent staining obtained with a serum from a patient with BCA gives the same pattern as that seen in bile canaliculi

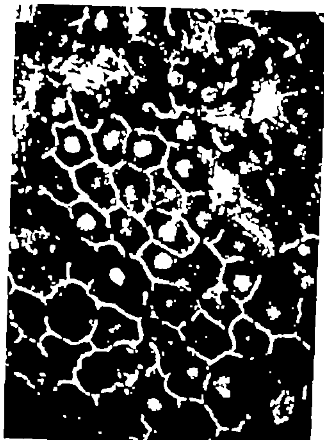


Fig 3 Immunofluorescence staining of bile canaliculi with serum from a patient with chronic active hepatitis. Original magnification × 400



Fig 4 ATPase staining of bile canaliculi of the same area as Fig. 3 Original magnification × 400

stained by the ATPase method (Fig 3 and 4)

When applying rat liver instead of bovine liver identical fluorescence patterns of the periphery of the hepatocytes were obtained

Only one serum obtained from a healthy donor produced immunofluorescence reaction with bile canaliculi. The donor was a 51 year old healthy woman who had never presented symptoms of liver disease and all biochemical tests were normal

Affinity chromatography A serum having IgG SMA against muscularis mucosae and blood vessel walls and giving IgG peripheral hepatocyte staining was used. Eluates obtained at the chromatographies were investigated against liver and stomach by the immunofluorescence method. All three of the eluates reacted with the muscularis mucosae and blood vessels, but none with the hepatocytes.

DISCUSSION

During the present study we found that sera from patients with cancer and with acute hepatitis and from blood donors produced immunofluorescent staining of the periphery of the hepatocytes. This immunofluorescence pattern resembled somewhat that produced by BCA, which has previously been demonstrated in sera from patients with chronic liver disease (3) in that the bile canaliculi in liver sections as shown may in some areas encircle the entire liver cell and thereby resemble the immunofluorescence reaction of the periphery of the hepatocytes. There is a difference between the two fluorescence patterns, in that BCA is somewhat angular whereas the staining of the periphery of the hepatocytes is more smooth. We found another difference between the two patterns of fluorescence during the present study in that the immunofluorescence pattern produced at the

periphery of the hepatocytes was not identical with the ATPase-stained bile canaliculi in the same section of the liver contrary to the BCA fluorescence pattern which has been shown to be identical with ATPase stained bile canaliculi (13).

All the sera examined, except two, from both patients and healthy donors, produced a more or less intense IgG immunofluorescence reaction with the periphery of the hepatocytes, and therefore the occurence of IgG fluorescence of the periphery of the hepatocytes seems to be a non-specific phenomenon or possibly caused by a reaction with several different antigens located at the periphery of the hepatocytes. On the other hand, IgM fluorescence of the periphery of the hepatocytes was produced only by sera from patients with acute hepatitis.

These findings concerning the fluorescence of the periphery of the hepatocytes are contrary to the findings with BCA. BCA was found to be associated with chronic active liver disease (3). It was not found in cases of acute hepatitis (4) and it was not of the IgM class (5).

Holborow et al. have described a polygonal staining pattern surrounding rat hepatocytes (12) produced by sera from patients with chronic hepatitis (9), cancer (18), acute hepatitis (10), and mononucleosis (12) and, in addition, by 20 per cent of the sera obtained from normal individuals (18). The above authors were not able to segregate a special fluorescence pattern with bile canaliculi in sera from patients with chronic hepatitis (11). Further studies led to the conclusion that polygonal fluorescence was produced by SMA, e.g. in hepatitis sera, and that the antibody reacted with a component which resembled smooth-muscle actomyosin on the surface of the liver cells (7). On the other hand, Tannenberg et al. did not observe peripheral hepatocytic staining to be a consistent finding in sera with SMA (15). As regards antibodies of the IgG class, we were unable to demonstrate any relationship between SMA and the capability to produce peripheral hepatocytic staining, even if we compared only sera producing more intense reactions (+ and more) with the periphery of the hepatocytes. On line with this the affinity chromatography IgG anti actomyosin eluates did react with muscularis mucosae but not with hepatocytes. As for IgM antibodies we found on the other hand, only peripheral hepatocytic fluorescence in sera containing IgM SMA when tested with the muscularis mucosae of the stomach, and consequently the peripheral hepatocytic fluorescence might have been produced by SMA in these cases.

Supported by grant from The Danish State Medical Research Council.

REFERENCES

1. *Becker C. G.*: Demonstration of actomyosin in mesangial cells of the renal glomerulus. Am. J. Path. 66: 97–108, 1972.
2. *Diederichsen H.*: Hetero-antibody against bile canaliculi in patients with chronic, clinically active hepatitis. Acta med. scand. 186: 299–302, 1969.
3. *Diederichsen H., Lind N. C. & Møller Nielsen P.*: Antibodies to bile canaliculi in patients with chronic active liver disease. Immunology of the Liver. Edited by M. Smith, R. Williams (Heinemann, London 1971) pp. 82–91.
4. *Diederichsen H.*: Bile canalicular antibody in acute hepatitis. Lancet 2: 326, 1973.
5. *Diederichsen H., Møller Nielsen P. & Linde N. C.*: Antikörper gegen Gallencanaliculi. Probleme des Nachweises und klinische Bedeutung. Bile canalicular antibodies. Problems of detection and clinical significance. Zschr. Gastroenterol. Sonderheft 13: 271–277, 1975.
6. *Farrow L. J., Holborow E. J., Johnson G. D., Lamb S. G., Stewart J. S., Taylor P. E. & Zuckerman A. J.*: Autoantibodies and the hepatitis associated antigen in acute infective hepatitis. Brit. med. J. 2: 693–695, 1970.
7. *Farrow L. J., Holborow E. J. & Brighton W. D.*: Reaction of human smooth muscle antibody with liver cells. Nature 232: 186–187, 1971.
8. *Finck H.*: Immunochemical studies on myosin. I. Effects of different methods of preparation on the immunochemical properties of chicken skeletal muscle myosin. Biochem. Biophys. Acta 111: 208–220, 1965.
9. *Johnson G. D., Holborow E. J. & Glynn L. E.*: Antibody to liver in lupoid hepatitis. Lancet 2: 416–418, 1966.

10 *Holborow E J* Immunological aspects of viral hepatitis. Brit. med Bull *28* 142–144 1972.
11 *Holborow E. J* Smooth muscle autoantibodies, viral infections and malignant disease. Proc. Roy Soc. Med. *65* 481–484 1972
12 *Holborow E. J Hemsted E. H & Mead S* I Smooth muscle autoantibodies in infectious mononucleosis Brit med. J *3* 323–325 1973
13 *Nielsen P M Diederichsen H & Linde N C* Immunofluorescent and enzymatic staining of bile canaliculi in the same sections of the liver Am. J clin. Path. *58* 123–126 1972.
14 *Scheinmann J J Fish A J & Michael A F* The immunohistophatology of glomerular antigens. The glomerular basement membrane collagen, and actomyosin antigens in normal and diseased kidneys J clin. Invest. *54* 1144–1154 1974
15 *Tannenberg A E G., Muller H K Cauchi M N & Nairn R C* Incidence of autoantibodies in cancer patients. Clin. exp. Immunol *15* 153–156 1973
16 *Wachstein M & Meisel E.* Histochemistry of hepatic phosphatases at a physiologic pH. Am J clin. Path. *27* 13–23 1957
17 *Weber K & Osborn M* The relibility of molecular weight determinations by dodecyl sulfate polyacrylamide gel electrophoresis. J biol Chem *244* 4406–4412, 1969
18. *Whitehouse J M A & Holborow E. J* Smooth muscle antibody in malignant disease. Brit. med. J *4* 511–513 1971

Acta path. microbiol. scand. Sect. A, 85: 405–412, 1977

EFFECT OF CELL AGGREGATION ON INTRAVENOUS TUMOR TRANSPLANTATION

W. RYD and B. HAGMAR

Institute of Pathology I, University of Göteborg and
Department of Pathology, Sundsvalls Hospital, Sundsvall, Sweden

Ryd, W. & Hagmar, B. Effect of cell aggregation on intravenous tumor transplantation. Acta path. microbiol. scand. Sect. A, 85: 405–412, 1977.

We have studied how the presence of cell aggregates affects the pattern of intravenously induced "experimental metastases" from two syngeneic murine tumors. Aggregates were produced mechanically by centrifugation, or chemically by a lectin (wheat-germ agglutinin). Compared to well-dissociated suspensions, aggregated suspensions tended to give greater total metastasis volume in the lungs of recipient mice. Disaggregated suspensions, on the other hand, gave rise to more extrapulmonary metastases. Presumably aggregates are preferentially retained in lung vessels, while single cells are let through to other sites. In addition, our results show that tumor aggregates are not necessary to induce metastases. Nor are aggregates superior to single cells in producing tumor growth when the total metastasis yield is considered.

Key words: Tumor transplantation, intravenous; cell aggregation.

W. Ryd, Institute of Pathology I, Sahlgrenska sjukhuset, 413 45 Göteborg, Sweden.

Received 2.xii.76. Accepted 2.iii.76

It is still a matter of controversy whether spontaneous blood-borne metastases arise from single cells or from cell aggregates (*Coman* 1954, *Watanabe* 1954, *Fidler* 1973, *Hagmar & Norrby* 1973, *Liotta et al.* 1974, 1976, *Thompson* 1974).

The problem has been attacked experimentally by *Fidler* (1973), who used *in vitro* cultivated cells for i.v. cell infusion, and *Liotta et al.* (1974, 1976) who used mechanically produced suspensions. They found that cell clumps gave rise to more lung tumors than single cells did. *Thompson* (1974) with mechanical cell suspensions from solid mammary carcinomas, in accordance with *Watanabe* (1954), even found cell aggregates a prerequisite for pulmonary "metastasis" development.

Fidler's (1973), *Thompson's* (1974) and *Liotta's* (1974, 1976) tumors only gave rise to pulmonary metastases. But the amount of lung tumors, determined by gross counts, does not necessarily reflect the distribution of viable cells after i.v. injection. For that purpose tumor systems with extrapulmonary metastases are of course preferable. In one such system *Hagmar & Norrby* (1973) found that aggregation in mechanical suspensions of *in vitro* cultivated cells did not alter the amount of pulmonary metastases. But in comparison to well-dissociated suspensions, aggregates increased the extrapulmonary tumor crop. The results are a little ambiguous, however, for trypsinized, well-dissociated suspensions gave even more extrapulmonary metastases than aggregated, non-trypsinized suspensions.

In the present study we have tried to eva-

TABLE 1 *Number and Size of Aggregates in Suspensions for i.v. Injection. 1000 Particles Counted per Suspension*

	Single cells	Cellularity of aggregates						
	1	2	3	4	5	6–10	11–20	>20
Study I								
Well dispersed susp	905	79	11	5	0	0	0	0
Poorly dispersed susp	878	90	16	9	3	1	2	1
Study II								
Well dispersed susp	852	126	17	4	0	1	0	0
Poorly dispersed susp	813	142	30	12	1	1	1	1
Study III								
Unfiltered susp	839	100	23	6	5	15	10	2
50 µm filter	833	116	27	10	3	10	1	0
10 µm filter	811	144	33	7	2	3	0	0
Study II								
Control	912	73	11	2	1	1	0	0
WGA	545	180	109	59	33	67	7	0
WGA + filtration	676	195	79	28	9	13	0	0

luate the importance of aggregates for i.v. induced metastases. We used suspensions with varied but defined aggregability from two murine tumors which give rise to pulmonary as well as extrapulmonary tumors.

MATERIAL AND METHODS

Tumor

The studies were performed in syngeneic systems with the ascites tumor MCG101 AA in C57BL mice (*Hagmar* 1974 a, b, c) and with the solid sarcoma MCG1 SS in CBA mice (*Mellgren et al.* 1966).

Cell suspensions of MCG1-SS were prepared enzymatically according to *Wijffjes & Prop* (1970). MCG101 AA was havested from the abdomen of routinely transplanted mice and washed twice in Hank's BSS (centrifugation 70 g, 10 min, +4 C). After haemocytometer counts including a trypan blue viability test, both tumors were diluted to the desired cell concentration with Eagle's MEM (MEM).

Induction of Aggregates

Tumour cell aggregates were produced either A/ mechanically by centrifugation or B/ chemically with a lectin (WGA).

A. MCG101 AA cell suspensions were spun down (80 g, 10 min, +4 C) and the resulting cell pellet was dissolved either by i/pipetting or by ii/ filtration.

i/ Three million cells in 3 ml MEM were spun down and the cell pellet was either dissolved completely in the supernatant by repeated pipetting or only slightly dissolved by few pipette strokes. ii/ Ten million cells in 5 ml MEM were spun down and the cell pellet was gently shaken up in the supernatant. The suspensions were then either filtered through nylon filters with 50 or 10 µm mesh openings (Monyl Ruschkon, Switzerland) or left unfiltered. The filters were washed by filtration of additional 5 ml of MEM. Five ml of MEM were also added to the unfiltered suspension. Microscopically we observed no retained cells on the filters. Cell counts after filtration revealed a higher cell number in the 50 µm suspension than in the other suspensions. This was compensated for by appropriate dilution.

B. Wheat-germ agglutinin (WGA), prepared according to *Burger & Goldberg* (1967), was used to aggregate MCG1-SS. Cell suspensions (4×10^6 cells in 2 ml MEM) were incubated for 15 min. at room temperature with approximately 625 µg WGA per ml. Control cells were incubated in MEM only. One part of the WGA treated suspension was filtered through a 10 µm nylon filter (vide supra) and anotehr part was left unfiltered. The filter was washed with 2 ml MEM and the unfiltered suspensions were diluted accordingly.

Prior to i.v. tumor cell injection, samples from all suspensions were filtered onto Millipore filters. The number and cellularity of aggregates in the

TABLE 2. *St dy I MCG101 AA T mor De elopment after i.v. Injection of Poorly and Well Dispersed Suspensions. Observation until Spontaneous D ath*

	Lungs		Extrapulmonary tumors		
	incidence	mean weight (g) (±S.D.)	incidence	number	sites
Poorly dispersed susp.	10/10	1.05 ± 0.31	2/10	2	heart 2
Well dispersed susp.	10/10	0.87 ± 0.25	5/10	7[2]	heart 5 striated muscle 1 lymph node 1

[1] $p < 0.10$ [2] $p < 0.15$

TABLE 3. *Study II MCG101 AA T mor Development in the Lu gs after i.v. I jection of Poorly and Well Dispersed S spensions Observation Time 21 Days*

	incidence	mean weight (g) (±S.D.)	V 10 cm³	$\bar{V}$ 10⁻⁴ cm³	N
Poorly dispersed suspension	10/10	0.39 ± 0.10	0.50	0.0016	199
Well dispersed suspension	10/10	0.34 ± 0.04[1]	0.14[2]	0.0010	178

Planimetric measurement of tumor olume (V) number of metastases (N) and mean tumor olume ($\bar{V}$) per cm tissue.
[1] $p < 0.15$ [2] $p < 0.05$

suspensions were determined from these filters according to *H gmar & Norrby* (1973). WGA-agglutinated cell suspensions were also run in an electronic particle size counter (Celloscope, Ljungberg, Sweden).

I I n Studies

W performed 3 different experiments with MCG101-AA and one with MCG1-SS. In all studies 0.1 ml suspension containing 10⁵ tumor cells was injected into tail ein. When the experiments were terminated the animals were subjected to complet autopsy. Lungs, liver kidneys, heart and any doubtful extrapulmonary tumor were subjected to histological examination according to *Boeryd* (1966). Where not otherwise stated, lung eights were used to measure the amount of lung metastases (*H gmar & Boeryd* 1969).

St dy I Poorly and well pipetted cell suspensions of MCG101 AA (*id supra*) were injected into 10 mice each. The mice were observed unt l they died spontaneously.

St dy II As in I but the animals were killed on day 21 after the tumor cell inj on. The olume and number of lung metastases were measured planimetrically according to *Boeryd et al.* (1965).

Study III An unfiltered suspension of MCG101 AA and suspensions filtered through 50 or 10 μm nylon filters (*vide supr*) were injected i.v. into groups of 10 mice. The mice were observed until spontaneous death.

Study IV The two types of WGA agglutinated MCG1 SS *suspensions and the control suspension* (*id supra*) were injected i.v. into 10 mice each. The mice were observed until spontaneous death. To evaluate any cytotoxic effect of WGA we also injected graded doses of these suspensions s.c. on the back of syngeneic animals. Thus, groups of 4 mice were given 10⁵ 10⁴ or 10³ cells from either of the suspensions. These mice were observed for tumor development.

Statistical Methods

Survival times for spontaneously dying mice, and the lung weights were compared by Fisher's permutation test. The same test was used for evaluation of the number and olumes of metastases in *study IV*. *The numbers of* extrapulmonary metastases were compared according to *Hagmar* and *Boeryd* (1969). The number of aggregates were compared by test for trend in contingency tables (*Maxwell* 1961).

TABLE 4 *Study III MCG101 AA Tumor Development after i.v. Injection of Unfiltered and Filtered Cell Suspensions*

	Lungs		Extrapulmonary tumors		
	incidence	mean weight (g) (±S.D.)	incidence	number	sites
Unfiltered suspension	10/10	0.74 ± 0.18	8/10	14	kidney 1 heart 7 striated muscle 2 lymph nodes 2, ovary 1 pelvic fat 1
50 µm filter	10/10	0.73 ± 0.19	9/10	18	heart 9 striated muscle 4, ovary 2, pelvic fat 3
10 µm filter	9/9*	0.73 ± 0.23	9/9	24[1]	kidney 1 heart 9 striated muscle 2, lymph nodes 2, subcutis 1 pelvic fat 4, ovary 3 adrenal 1

* One mouse developed tumor at injection site and was omitted.
[1] $p<0.05$ (unfiltered suspension – 10 µm filter)

TABLE 5 *Study II MCG1-SS Tumor Development after i.v. Injection of Filtered or Unfiltered WGA-Exposed Cells*

	Lungs		Extrapulmonary tumors		
	incidence	mean weight (g) (±S.D.)	incidence	number	sites
Control	9/9[1]	0.09 ± 0.03[2]	9/9	105	liver 3 kidney 3 heart 7 striated muscle 32 lymph node 37 subcutis 3 pelvic fat 4, mesentery 8, adrenal 4 ovary 3, orbita 1
WGA	10/10	0.09 ± 0.02[4]	10/10	64	kidney 2 heart 7 striated muscle 18 lymph node 22, subcutis 2 pelvic fat 3 mesentery 4 adrenal 3 orbita 1 uterus 2
WGA + filtration	8/8[1]	0.10 ± 0.04[2]	8/8	68 [5]	liver 1 kidney 1 heart 4 striated muscle 19 lymph node 30 subcutis 4 pelvic fat 1 mesentery 7 adrenal 1

[1] Mice excluded because of cannibalism and/or severe autolysis. [2] Lung weights in xylene. [3] Control – WGA $p<0.01$ [4] Control – WGA + filtration $p<0.10$ [5] WGA – WGA + filtration $p<0.10$

RESULTS

Study I The two suspensions were different in aggregability ($p<0.005$) as seen in Table 1 All animals died spontaneously from tumor growth. Autopsy revealed extensive lung metastases, but only few extrapulmonary tumors. In comparison with the disaggregates suspension the poorly pipetted suspension killed the animals earlier ($p<0.0001$) and tended to give rise to more lung metastases



Fig 1 Particle size distribution in filtered and unfiltered suspensions of WGA-agglutinated MCG1 SS cells The differences in particle size are evident even though the larger cell clumps are outside the instrument range.

($p<0.10$) on the other hand, it tended to give fewer extra pulmonary metastases ($p < 0.15$) (Table 2)

Study II The difference in aggregability was similar to that in Study I ($p<0.003$) (Table 1) All animals developed lung metastases but no extrapulmonary tumors were found. The lungs were heavier ($p<0.15$) in the group given the aggregated suspension, and planimetry demonstrated that they held a greater total tumor volume than mice given the disaggregated suspension ($p<0.05$) Neither the number of lung metastases nor the mean tumor volume differed statistically (Table 3)

Study III The control suspension contained more aggregates than the two filtered ones (C 50 µm $p<0.01$ C – 10 µm $p<0.001$) (Table 1) The 50 µm suspension held a higher number of aggregates composed of 4 or more cells ($p<0.10$) than the 10 µm suspension. All animals died spontaneously from tumor growth. The three groups had equal survival times and lung weights. Mice given the 10 µm filtered suspension developed more extrapulmonary tumors than the 50 µm and control groups. The difference was significant only between the unfiltered and 10 µm filter group ($p<0.05$) (Table 4)

Study II The greatest number of cell aggregates was found in the unfiltered WGA suspension, and the smallest number in the control suspension ($p<0.0001$) (Table 1) The results of the electronic particle size analysis are given in Fig. 1 All animals died spontaneously from extensive tumor growth in the lungs and extrapulmonally (Table 5) Mice given the filtered WGA suspension survived somewhat longer than control mice and WGA mice (C – filt. WGA $p<0.10$ WGA – filt. WGA $p<0.15$) The lung weights were similar The control suspension induced the highest number of extrapulmonary metastases, and the unfiltered WGA suspension the lowest number (C – WGA $p<0.01$ C – filt. WGA $p<0.10$ filt. WGA – WGA $p<0.10$)

The subcutaneous transplantability test disclosed no cytotoxic effect by the WGA treatment (Table 6)

TABLE 6. *Study II MCG1-SS Tumor Incidence after s I jection of Filtered and U filtered WGA Agglutinated Cell Suspensions.*

Cell number	Control	WGA	WGA + filtration
10^5	4/4 (8)	3/4 (8)	3/4 (8)
10^4	4/4 (12)	3/4 (12)	4/4 (12)
10	2/4 (13)	4/4 (13)	2/4 (13)

Figure in brackets gives the mean value in days for tumor appearance

DISCUSSION

Cell aggregates for intravenous tumor induction ("experimental metastases") may be

TABLE 4 *Study III MCC101 AA Tumor Development after i.p. Injection of Unfiltered and Filtered Cell Suspensions*

	Lungs		Extrapulmonary tumors		
	incidence	mean weight (g) (±S.D.)	incidence	number	sites
Unfiltered suspension	10/10	0.74 ± 0.18	8/10	14	kidney 1 heart 7 striated muscle 2, lymph nodes 2, ovary 1 pelvic fat 1
50 μm filter	10/10	0.75 ± 0.19	9/10	18	heart 9 striated muscle 4 ovary 2 pelvic fat 3
10 μm filter	9/9*	0.75 ± 0.23	9/9	24[1]	kidney 1 heart 9 striated muscle 2 lymph nodes 2 subcutis 1 pelvic fat 4 ovary 3, adrenal 1

* One mouse developed tumor at injection site and was omitted
[1] $p<0.05$ (unfiltered suspension 10 μm filter)

TABLE 5 *Study II MCG1 SS Tumor Development after i.p. Injection of Filtered or Unfiltered WGA Exposed Cells*

	Lungs		Extrapulmonary tumors		
	incidence	mean weight (g) (±S.D.)	incidence	number	sites
Control	9/9[1]	0.09 ± 0.03[2]	9/9	105	liver 3 kidney 3 heart 7 striated muscle 32 lymph node 37 subcutis 3 pelvic fat 4, mesentery 8 adrenal 4 ovary 3, orbita 1
WGA	10/10	0.09 ± 0.02[2]	10/10	64	kidney 2 heart 7 striated muscle 18 lymph node 22 subcutis 2, pelvic fat 3 mesentery 4 adrenal 3 orbita 1 uterus 2.
WGA + filtration	8/8[1]	0.10 ± 0.04[2]	8/8	68[3,4]	liver 1 kidney 1 heart 4 striated muscle 19 lymph node 30 subcutis 4 pelvic fat 1 mesentery 7 adrenal 1

[1] Mice excluded because of canibalism and/or severe autolysis. [2] Lung weights in xylene [3] Control WGA $p<0.01$ Control WGA + filtration $p<0.10$ [4] WGA WGA + filtration $p<0.10$

RESULTS

Study I The two suspensions were different in aggregability ($p<0.005$) as seen in Table 1 All animals died spontaneously from tumor growth. Autopsy revealed extensive lung metastases, but only few extrapulmonary tumors. In comparison with the disaggregated suspension the poorly pipetted suspension killed the animals earlier ($p<0.0001$) and tended to give rise to more lung metastases

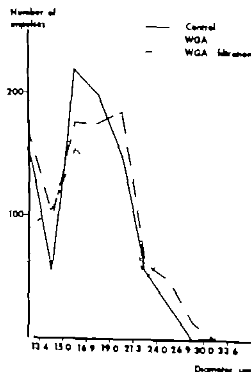


Fig 1 Particle size distribution in filtered and unfiltered suspensions of WGA-agglutinated MCG1 S5 cells. The differences in particle size are evident even though the larger cell clumps are outside the instrument range

($p<0.10$) on the other hand it tended to give fewer extra pulmonary metastases ($p<0.15$) (Table 2)

Study II The difference in aggregability was similar to that in Study I ($p<0.005$) (Table 1) All animals developed lung metastases but no extrapulmonary tumors were found. The lungs were heavier ($p<0.15$) in the group given the aggregated suspension, and planimetry demonstrated that they held a greater total tumor volume than mice given the disaggregated suspension ($p<0.05$) Neither the number of lung metastases nor the mean tumor volume differed statistically (Table 3)

Study III The control suspension contained more aggregates than the two filtered ones (C – 50 µm $p<0.01$ C – 10 µm $p<0.001$) (Table 1) The 50 µm suspension held a higher number of aggregates composed of 4 or more cells ($p<0.10$) than the 10 µm suspension. All animals died spontaneously from tumor growth. The three groups had equal survival times and lung weights Mice given the 10 µm filtered suspension developed more extrapulmonary tumors than the 50 µm and control groups. The difference was significant only between the unfiltered and 10 µm filter group ($p<0.05$) (Table 4)

Study IV The greatest number of cell aggregates was found in the unfiltered WGA suspension and the smallest number in the control suspension ($p<0.0001$) (Table 1) The results of the electronic particle size analysis are given in Fig 1 All animals died spontaneously from extensive tumor growth in the lungs and extrapulmonally (Table 5) Mice given the filtered WGA suspension survived somewhat longer than control mice and WGA mice (C – filt. WGA $p<0.10$ WGA – filt. WGA $p<0.15$) The lung weights were similar Th control suspension induced the highest number of extrapulmonary metastases, and the unfiltered WGA suspension the lowest number (C – WGA $p<0.01$ C – filt. WGA $p<0.10$ filt. WGA – WGA $p<0.10$)

The subcutaneous transplantability test disclosed no cytotoxic effect by the WGA treatment (Table 6)

TABLE 6 *Study IV MCG1-S5 Tumor Incidence after s.c. Injection of Filtered and Unfiltered WGA Agglutinated Cell Suspensions*

Cell number	Control	WGA	WGA + filtration
10^3	4/4 (8)	3/4 (8)	3/4 (8)
10^4	4/4 (12)	3/4 (12)	4/4 (12)
10^5	2/4 (13)	4/4 (13)	2/4 (13)

Figure in brackets gives the mean value in days for tumor appearance.

DISCUSSION

Cell aggregates for intravenous tumor induction ("experimental metastases") may be

TABLE 4 *Study III MCG101 AA Tumor Development after i.v. Injection of Unfiltered and Filtered Cell Suspensions*

	Lungs		Extrapulmonary tumors		
	incidence	mean weight (g) (±S.D.)	incidence	number	sites
Unfiltered suspension	10/10	0.74 ± 0 18	8/10	14	kidney 1 heart 7 striated muscle 2 lymph nodes 2 ovary 1 pelvic fat 1
50 µm filter	10/10	0 73 ± 0 19	9/10	18	heart 9 striated muscle 4, ovary 2, pelvic fat 3
10 µm filter	9/9*	0 ,5 ± 0 25	9/9	24[1]	kidney 1 heart 9 striated muscle 2, lymph nodes 2 subcutis 1 pelvic fat 4 ovary 3 adrenal 1

* One mouse developed tumor at injection site and was omitted
[1] $p<0.05$ (unfiltered suspension – 10 µm filter)

TABLE 5 *Study II MCG1-SS Tumor Development after i.v. Injection of Filtered or Unfiltered WGA-Exposed Cells*

	Lungs		Extrapulmonary tumors		
	incidence	mean weight (g) (±S.D.)	incidence	number	sites
Control	9/9[1]	0 09 ± 0 03[2]	9/9	105	liver 3 kidney 3 heart 7 striated muscle 32 lymph node 37 subcutis 3 pelvic fat 4 mesentery 8 adrenal 4 ovary 3, orbita 1
WGA	10/10	0 09 ± 0 02[2]	10/10	64	kidney 2, heart 7 striated muscle 18 lymph node 22, subcutis 2, pelvic fat 3 mesentery 4 adrenal 3 orbita 1 uterus 2.
WGA + filtration	8/8[1]	0 10 ± 0 04[2]	8/8	68[4,5]	liver 1 kidney 1 heart 4 striated muscle 19 lymph node 30 subcutis 4 pelvic fat 1 mesentery 7 adrenal 1

[1] Mice excluded because of canibalism and/or severe autolysis [2] Lung weights in xylene [3] Control – WGA $p<0.01$ [4] Control WGA + filtration $p<0.10$ WGA WGA + filtration $p<0.10$

RESULTS

Study I The two suspensions were different in aggregability ($p<0.005$) as seen in Table 1 All animals died spontaneously from tumor growth. Autopsy revealed extensive lung metastases, but only few extrapulmonary tumors. In comparison with the disaggregated suspension, the poorly pipetted suspension killed the animals earlier ($p<0.0001$) and tended to give rise to more lung metastases

tumors than the dispersed suspensions. Thus, aggregates seem to favour pulmonary meta stasis formation. This is in agreement with findings in other systems (*Watanabe* 1954 *Fidler 1973 Thompson* 1974 *Liotta* 1974 1976) These systems, however where only lung metastases arise, are unsatisfactory when metastasis distribution is studied. The alleged general superiority of aggregates as a source of metastases therefore seems unfounded. We think the promoted metastasis growth in the lungs is due to an increased retention, per haps by simple filtration of tumor cells in lung vessels. But our experiments do not suggest that aggregates give a great competitive advantage in metastasis formation, compared to single cells. Since aggregability differences may affect metastasis patterns, it should always be controlled in transplantation experiments, however

Intravenous induction of metastases include artifacts compared to spontaneous metastasis formation, which should preclude immediate transfer of findings from one situation to the other Yet the spontaneous spread of MCG1-SS and MCG101 AS (*Hagmar* 1969 *Hagmar* 1974) agrees with the meta stasis pattern after i.v infusion of well-dispersed suspensions of these tumors. This might be taken to indicate that the spontaneous tumor cell release is to a considerable degree monocellular In a wide context it would fit for the hypothesis that meta stasibility and metastasis spread beyond the first capillary bed is determined not only to the quantity of cells released but also by the quality of the cell release, in terms of aggregability

This study was supported by research grant No. 463-B75-06X from the *Swedish Cancer Society* and by grant from the Faculty of Medicine, University of Goteborg.

We thank Miss *Marnes B* [illegible] and Mrs *Ignet Jakobsson* for skillful technical assistance and Mrs *A n-Catrin Olsson* for typing the manuscript.

REFERENCES

Baserga, R & Saffiotti, U Experimental studies on histogenesis of blood-borne metastases. A.M.A. Arch. Path. 59 26–34 1955

Boeryd B & Suurküla M.. Tumor metastasis in mice with reduced immune reactivity I. Studies with two MCA-induced sarcomas in radiation an thymectomized radiation C57BL/6J chimeras. Int. J Cancer *12* 722–727 1973

Coman, D., deLong, R. & McCutcheon M Studies on the mechanism of metastasis. The distribution of tumors in various organs in relation to the distribution of arterial emboli. Cancer Res. *11* 648–651 1951

Coman D R.. Mechanisms responsible for the origin and distribution of blood-borne metastases A review Cancer Res. *13* 397–404 1954

Fidler I The relationship of embolic homogeneity number size and iability to the incidence to experimental metastasis. Europ. J Cancer *9* 223–227 1973

Hagmar B. MCG101-AA, new ascites tumour in C57 mice. 1 I duction procedures and some cytological and physicochemical properties. Acta path. microbiol scand. Sect. A, *92* 358–368, 1974

H gmar B. MCG101-AA, a new ascites tumour in C57 mice. 2. Protocol of fix u transplantation studies in comparison with the solid (SS) and solid ascites (AS) tumours. Acta path. microbiol scand. Sect. A, *82* 369–378 1974

Hagmar B MCG101 AA, a new ascites tumour in C57 mice. 3 Studies of the spontaneous metastasis formation from the resectable solid ascites tumour in comparison with the solid tumour of origin. Acta path. microbiol. scand. Sect A, 82 379–385 1974

Hagmar B & Boeryd B Disseminating effect of heparin on experimental tumor metastases Path. europ *4* 274–282, 1969

Hagmar B. & Norrby K. Influence of cultivation, trypsinization and aggregation on the transplantability of Melanoma B16 cells. Int. J Cancer *11* 663–675 1973

Liotta, L. A Kleinerman J & Saidel G., Quantitative relationships of intravascular tumor cells, tumor vessels, and pulmonary metastases following tumor implantation Cancer Res. *34* 997–1004 1974

Liotta, L. A., Kleinerman J & Saidel G The significance of hematogenous tumor cell clumps in the metastatic process. Cancer Res. *36* 889–894 1976.

Martin W., Wunderlich J Freeman F & Inman, J Enhanced immunogenicity of chemically coated syngeneic tumor cells Proc nat. Acad. Sci. *68* 469–472, 1971

fabricated by different methods. One method implies an incomplete dissociation of cells from solid tumors. If made by mechanical means, as by *Thompson* (1974) and *Liotta et al* (1974 1976) such suspensions are impossible to characterize properly in terms of cell number dead and viable cells or other tissue components *Fidler's* (1973) aggregates, from incompletely separated *in vitro* cultivated cells are more readily characterized but do *not permit adequate cell counts*.

Another method of obtaining cell aggregates is by spontaneous aggregation i e by letting cells in suspension form intercellular *contacts Such a process may be potentiated* mechanically e g by centrifugation We used this method for the ascites tumor MCG101 AA Necessary agitation procedures after centrifugation broke up *some* cell *aggregates and* large cell clumps consequently were rare. Yet the poorly agitated suspensions contained more *small* aggregates than the well agitated ones.

Filtration has been used by others to free mechanical suspensions from cell clumps and debris (*Thompson* 1974 *Liotta et al* 1974 1976 and *Sindelar et al* 1975) We used filtration to obtain well-characterized suspensions. With MCG101 AA the differences between suspensions drawn *through 50* and 10 μm nylon filters were surprisingly small. The 10 μm filter reduced the number of aggregates with more than 3 cells however Small aggregates were present also in the 10 μm filtered suspensions presumable because some small aggregates passed the filters There may also occur cell clumping within *filter pores or from reaggregation after* filtration In addition aggregate counts on filters always represent maximum values, because cells in apposition may be *falsely registered* as aggregates

MCG 101 AA forms relatively few extra pulmonary metastases when *injected* intravenously To evaluate more fully the influence of aggregates on the distribution of metastases we chose the widely metastasizing solid sarcoma MCG1-SS (*Mellgren et al 1966*)

When in practically monodisperse suspension as after our enzymatic dispersion procedure MCG1-SS does not lend itself to mechanical aggregation Istead we induced cell aggregates chemically by a lectin wheat germ agglutinin (WGA) We are aware, of course, of potential hazards inherent in this method. The cells may be damaged by the ligand and/or altered in relation to the host antigenetically or otherwise (*Martin et al 1971 Simmons et al 1975*) We could not detect any cytotoxic effect on MCG1-SS cells, however by our subcutaneous transplantation test

We used *the 10 μm filtration procedure* after agglutination with the aim of obtaining a monocellular suspension of WGA-exposed tumor cells. The cells reaggregated after filtration however giving us a suspension which was intermediate in terms of aggregability In mice receiving this suspension the lung metastases were similar and the amount of extrapulmonary metastases fell in between the two other groups. This finding lead us to believe that WGA *per se* did not influence the metastasis pattern.

With these different experimental designs, we did not disclose any major differences in metastasis yielding capacity between dispersed and aggregated suspensions. In all experiments there was a common pattern, however Dispersed suspens ons gave rise to more extrapulmonary tumor takes than aggregated ones, and if anything less pulmonary tumors. In one experiment, Study II where the metastases were measured planimetrically the difference in lung metastasis volume was significant

These findings strongly support the notion that metastases may arise from single cells. *There is other experimental* (*Coman et al.* 1951) and morphological (*Baserga & Saffiotti* 1955 *Sindelar et al* 1975) evidence to the same effect. Some authors even suggest that most metastases arise from single cells, lodged in capillaries (*Coman* 1954 *Baserga et al* 1960)

In our study aggregated suspensions gave rise to an equal or greater amount of lung

tumors than the dispersed suspensions. Thus, aggregates seem to favour pulmonary metastasis formation. This is in agreement with findings in other systems (*Watanabe* 1954 *Fidler* 1973 *Thompson* 1974 *Liotta* 1974 1976) These systems, however where only lung metastases arise are unsatisfactory when metastasis distribution is studied The alleged general superiority of aggregates as a source of metastases therefore seems unfounded. We think the promoted metastasis growth in the lungs is due to an increased retention perhaps by simple filtration, of tumor cells in lung vessels. But our experiments do not suggest that aggregates give a great competitive advantage in metastasis formation, compared to single cells. Since aggregability differences may affect metastasis patterns, it should always be controlled in transplantation experiments, however

Intravenous induction of metastases include artifacts compared to spontaneous metastasis formation, which should preclude immediate transfer of findings from one situation to the other Yet the spontaneous spread of MCG1 SS and MCG101 AS (*Hagmar* 1969 *Hagmar* 1974) agrees with the metastasis pattern after i.v. infusion of well-dispersed suspensions of these tumors. This might be taken to indicate that the spontaneous tumor cell release is to a considerable degree monocellular In a wide context it would fit for the hypothesis that metastasibility and metastasis spread beyond the first capillary bed is determined not only to the quantity of cells released but also by the quality of the cell release, in terms of aggregability

---

This study was supported by research grant No 465-B75-06X from the *Swedish Cancer Society* and by grant from the Faculty of Medicine, University of Goteborg

We thank Miss *Marianne Brenner* and Miss *Agneta Jakobsson* for skillful technical assistance and Mrs Ann-Catrin Olsson for typing the manuscript

REFERENCES

Baserga R & Saffiotti U.: Experimental studies on histogenesis of blood-borne metastases. A.M.A. Arch. Path. 59 26–34 1955

Boeryd B & S·rhala M Tumor metastasis in mice with reduced immune reactivity I Studies with two MCA-induced sarcomas in radiation an thymectomized radiation C57BL/6J chimeras. Int. J Cancer *12* 722 727 1973

Coman D., dela g R. & McCuthkeon M Studies on the mechanism of metastasis. The distribution of tumors in various organs in relation to the distribution of arterial emboli Cancer Res. *11* 648–651 1951

Coman D R Mechanisms responsible for the origin and distribution of blood-borne metastases: A review Cancer Res. *13* 397–401 1954

Fidler I. The relationship of embolic homogeneity number size and viability to the incidence to experimental metastasis. Europ. J Cancer *9* 223–227 1973

Hagmar B. MCG101 AA, a new ascites tumour in C57 mice 1 Induction procedures and some cytological and physicochemical properties. Acta path. microbiol. scand Sect. A, *92* 358 368 1974

Hagmar B MCG101-AA, a new ascites tumour in C57 mice 2. Protocol of in situ transplantation studies in comparison with the solid (SS) and solid ascites (AS) tumours Acta path. microbiol scand. Sect. A, *82* 369 378 1974

Hagmar B. MCG101-AA, a new ascites tumour in C57 mice. 3 Studies of the spontaneous metastasis formation from the resectable solid ascites tumour in comparison with the solid tumour of origin. Acta path. microbiol scand. Sect. A, *82* 379 385 1974

Hagmar B & Boeryd B Disseminating effect of heparin on experimental tumor metastases. Path. europ. *4* 274 282, 1969

Hagmar B & Norrby K Influence of cultivation, trypsinization and aggregation on the transplantability of Melanoma B16 cells Int J Cancer *11* 663–675 1973

Liotta L. A Kleinerman J & Saidel G. Quantitative relationships of intravascular tumor cells, tumor vessels, and pulmonary metastases following tumor implantation Cancer Res. *34* 997–1004 1974

Liotta L. A., Kleinerman J & Saidel G The significance of hematogenous tumor cell clumps in the metastatic process. Cancer Res. *36* 889–894 1976

Martin W Wunderlich J., Freeman F & I man, J Enhanced immunogenicity of chemically coated syngeneic tumor cells. Proc nat. Acad. Sci. *68* 469–472, 1971

fabricated by different methods. One method implies an incomplete dissociation of cells from solid tumors. If made by mechanical means, as by *Thompson* (1974) and *Liotta et al* (1974, 1976) such suspensions are impossible to characterize properly in terms of cell number, dead and viable cells or other tissue components. *Fidler's* (1973) aggregates, from incompletely separated *in vitro* cultivated cells, are more readily characterized but do not permit adequate cell counts.

Another method of obtaining cell aggregates is by spontaneous aggregation, i.e. by letting cells in suspension form intercellular contacts. Such a process may be potentiated mechanically, e.g. by centrifugation. We used this method for the ascites tumor MCG101 AA. Necessary agitation procedures after centrifugation broke up some cell aggregates and large cell clumps consequently were rare. Yet the poorly agitated suspensions contained more small aggregates than the well agitated ones.

Filtration has been used by others to free mechanical suspensions from cell clumps and debris (*Thompson* 1974, *Liotta et al* 1974, 1976 and *Sindelar et al* 1975). We used filtration to obtain well-characterized suspensions. With MCG101 AA the differences between suspensions drawn through 50 and 10 μm nylon filters were surprisingly small. The 10 μm filter reduced the number of aggregates with more than 3 cells, however. Small aggregates were present also in the 10 μm filtered suspensions, presumable because some small aggregates passed the filters. There may also occur cell clumping within filter pores or from reaggregation after filtration. In addition, aggregate counts on filters always represent maximum values, because cells in apposition may be falsely registered as aggregates.

MCG101 AA forms relatively few extrapulmonary metastases when injected intravenously. To evaluate more fully the influence of aggregates on the distribution of metastases, we chose the widely metastasizing solid sarcoma MCG1-SS (*Mellgren et al* 1966).

When in practically monodisperse suspension as after our enzymatic dispersion procedure, MCG1-SS does not lend itself to mechanical aggregation. Istead, we induced cell aggregates chemically by a lectin, wheat germ agglutinin (WGA). We are aware, of course, of potential hazards inherent in this method. The cells may be damaged by the ligand and/or altered in relation to the host antigenetically or otherwise (*Martin et al* 1971, *Simmons et al* 1975). We could not detect any cytotoxic effect on MCG1-SS cells, however, by our subcutaneous transplantation test.

We used the 10 μm filtration procedure after agglutination with the aim of obtaining a monocellular suspension of WGA-exposed tumor cells. The cells reaggregated after filtration, however, giving us a suspension which was intermediate in terms of aggregability. In mice receiving this suspension the lung metastases were similar and the amount of extrapulmonary metastases fell in between the two other groups. This finding lead us to believe that WGA *per se* did not influence the metastasis pattern.

With these different experimental designs, we did not disclose any major differences in metastasis yielding capacity between dispersed and aggregated suspensions. In all experiments there was a common pattern, however. Dispersed suspensions gave rise to more extrapulmonary tumor takes than aggregated ones and if anything, less pulmonary tumors. In one experiment, Study II, where the metastases were measured planimetrically, the difference in lung metastasis volume was significant.

These findings strongly support the notion that metastases may arise from single cells. There is other experimental (*Coman et al* 1951) and morphological (*Baserga & Saffiotti* 1955, *Sindelar et al* 1975) evidence to the same effect. Some authors even suggest that most metastases arise from single cells, lodged in capillaries (*Coman* 1954, *Baserga et al* 1960).

In our study, aggregated suspensions gave rise to an equal or greater amount of lung

Acta path microbiol. scand. Sect. A, 85 413-420, 1977

ABNORMAL MITOCHONDRIA IN HEPATOCYTES IN HUMAN FATTY LIVER

PALLE PETERSEN

Medical Department A, Division of Hepatology and Medical Department TA, Rigshospitalet, Copenhagen, Denmark

Petersen, P. Abnormal mitochondria in hepatocytes in human fatty liver. Acta path. microbiol. scand. Sect. A, 85: 413-420, 1977.

Liver biopsies from fatty livers in thirty patients whose daily alcohol consumption was excessive or they were in a diabetic state or overweight, and liver biopsies from seven control patients not presenting the above disorders, were studied by light microscopy 0.75 µm EPON embedded, toluidine blue stained sections, and electron microscopy. Abnormal mitochondria were rarely found in normal liver tissue and, if present, they were found only in periportal hepatocytes. The frequency of hepatocytes containing abnormal mitochondria was significantly higher in fatty liver than in normal liver ($p < 0.01$). These cells were usually localized periportally, practically never in the centre of the lobule ($p < 0.01$). The occurrence of abnormal mitochondria was not correlated with the degree of steatosis, and the increase in number of abnormal mitochondria was equally high in alcoholists, diabetics, and overweight subjects. The ultrastructural appearance and the periportal localization suggest a hyperfunction of the mitochondria, which may prevent development of steatosis in these areas.

Key words: Liver; fatty; mitochondria; light microscopy.

P. Petersen, Medical department A, division of hepatology and medical department TA, Rigshospitalet, Copenhagen, Denmark.

Received 12.76 Accepted 28.xii.76

Fatty liver is most frequently associated with one or more of the following three factors: alcohol consumption (1-6), overweight (7-14, 16, 19, 20, 34) and diabetes mellitus of the type maturity onset (2, 3, 9-12, 27, 28, 30, 33). In most clinical series, these three factors interfere with each other and complicate the study of the pathogenetic processes leading to fatty liver (8, 11, 13, 21, 22, 26).

Abnormal mitochondria have been observed both in alcoholic and diabetic fatty livers (17, 23, 29, 32).

The purpose of the present study was to estimate whether the abnormal and misshapen mitochondria are associated with alcohol consumption, overweight, or disturbed glucose assimilation. Moreover it was attempted to find a correlation between the degree of steatosis and the extent of mitochondrial alterations.

MATERIAL AND METHODS

Thirty patients in whom biopsy had verified the presence of fatty liver participated in the study. Since alcohol consumption, overweight and glucose intolerance might be combined, the series was divided into eight groups. As controls served seven patients who did not consume alcohol, whose body weight was normal, whose glucose tolerance was normal, and liver biopsy had showed normal conditions.

Maxwell A E. Analysing quantitative data. Methuen & Co London 1961
Mellgren J Bartholdsson E Boeryd B & Norrby K A spontaneously metastasizing 20 methylcholanthrene induced rhabdomyosarcoma and its transformation to ascites form in the CBA mouse. Acta path. microbiol scand 68 535-546 1966
Simmons R Rios A Toledo-Pereyra L. & Steinmuller D Modifying the immunogenicity of cell membrane antigens Am. J Clin. Path. 63 714-734 1975
Sindelar W Tralka T S & Ketcham A Electron microscopic observations on formation of pulmonary metastases. J Surg. Res. 18 137 161 1975
Thompson S C The colony forming efficiency of single cells and cell aggregates from a spontaneous mouse mammary tumour using the lung colony assay Br J Cancer 30 332 341 1974
Watanabe S The metastatastasizability of tumor cells. Cancer 7 215-223 1954
Wiepjes G J & Prop F J A Improved method for preparation of single-cell suspensions from mammary glands of adult virgin mouse. Exptl. cell res. 61 451-545 1970

ABNORMAL MITOCHONDRIA IN HEPATOCYTES IN HUMAN FATTY LIVER

PALLE PETERSEN

Medical Department A, Division of Hepatology and Medical Department TA, Rigshospitalet, Copenhagen, Denmark

Petersen, P Abnormal mitochondria in hepatocytes in human fatty liver Acta path microbiol. scand. Sect. A, 85 413–420, 1977

Liver biopsies from fatty livers in thirty patients whose daily alcohol consumption was excessive or they were in diabetic state or overweight, and liver biopsies from seven control patients not presenting the above disorders, were studied by light microscopy 0 75 µm EPON embedded, toluidine blue stained sections, and electron microscopy Abnormal mitochondria were rarely found in normal liver tissue and, if present, they were found only in periportal hepatocytes. The frequency of hepatocytes containing abnormal mitochondria was significantly higher in fatty liver than in normal liver ($p < 0.01$) These cells were usually localized periportally practically never in the centre of the lobule ($p < 0.01$) The occurrence of abnormal mitochondria was not correlated with the degree of steatosis, and the increase in number of abnormal mitochondria was equally high in alcoholics, diabetics, and overweight subjects. The ultrastructural appearance and the periportal localization suggest hyperfunction of the mitochondria, which may prevent development of steatosis in these areas.

Key words Liver fatty mitochondria light microscopy

P Petersen, Medical department A, division of hepatology and medical department TA, Rigshospitalet, Copenhagen, Denmark.

Received 12 76 Accepted 28.xii.76

Fatty liver is most frequently associated with one or more of the following three factors alcohol consumption (1 6) overweight (7 14 16, 19 20 34) and diabetes mellitus of the type maturity onset (2, 3 9 12, 27 28, 30, 33) In most clinical series, these three factors interfere with each other and complicate the study of the pathogenetic processes leading to fatty liver (8, 11 13 21 22, 26)

Abnormal mitochondria have been observed both in alcoholic and diabetic fatty livers (17 23 29 32)

The purpose of the present study was to estimate whether the abnormal and misshapen mitochondria are associated with alcohol consumption, overweight, or disturbed glucose assimilation. Moreover it was attempted to find a correlation between the degree of steatosis and the extent of mitochondrial alterations.

MATERIAL AND METHODS

Thirty patients in whom biopsy had verified the presence of fatty liver participated in the study Since alcohol consumption, overweight and glucose intolerance might be combined, the series was divided into eight groups. As control served seven patients who did not consume alcohol whose body weight was normal, whose glucose tolerance was normal, and liver biopsy had showed normal conditions.

Maxwell A E. Analysing quantitative data. Methuen & Co London 1961

Mellgren J Bartholdsson E Boeryd B & Norrby K A spontaneously metastasizing 20-methylcholanthrene induced rhabdomyosarcoma and its transformation to ascites form in the CBA mouse. Acta path. microbiol scand *68* 535–546 1966

Simmons R Rios A Toledo-Pereyra L & Steinmuller D Modifying the immunogenicity of cell membrane antigens. Am. J Clin. Path. *63* 714–734 1975

Sindelar W Tralka T S & Ketcham A Electron microscopic observations on formation of pulmonary metastases. J Surg. Res. *18* 137–161 1975

Thompson S C The colony forming efficiency of single cells and cell aggregates from a spontaneous mouse mammary tumour using the lung colony assay Br J Cancer *30* 332 341 1974

Watanabe S The metastasizability of tumor cells. Cancer *7* 215–223 1954

Wiepjes G J & Prop F J A Improved method for preparation of single-cell suspensions from mammary glands of adult virgin mouse. Expl cell res. *61* 451–545 1970

section. To estimate the extent of the abnormal mitochondria in different zones of the liver lobule, the following definitions were used periportal hepatocytes were defined as liver cells within three cell widths from lamina limitans, and centrilobular as liver cell within three cell widths from the central vein.

The degree of steatosis was estimated in formalin fixed, Gieson stained paraffin sections in which the fatty droplets appeared as lucid holes. In Leitz Classimat distinguishing 10 grey values of the microscopic image, the area of the fatty droplets was given as per cent of the total area of the liver biopsy

Mann-Whitney test was used as statistical method.

RESULTS

In liver biopsies from control patients, 1 1 (0-3.0) per cent of the liver cells contained abnormal mitochondria while the percentage was 16 4 (0.6-77.9) in patients with fatty liver This difference is significant ($p < 0.02$) (Table 2)

On the consideration that the abnormal mitochondria in the control patients occurred close to the portal spaces (3.3 (0-7 7) per cent of the liver cells) and never in the centre of the lobule, periportal areas from patients with fatty liver were compared with periportal areas from control patients the frequency of liver cells with abnormal mitochondria was found to be significantly higher in fatty livers than in normal livers (35.8 (1.3-94.0) per cent) $p < 0.01$) As in the controls, the occurrence of abnormal mitochondria in patients with fatty liver was significantly higher in periportal areas (Fig 1) than in centrilobular areas (Fig 2) (35.8 (1.3-94.0) contra 1 0 (0-6.8) per cent) ($p < 0.01$) (Table 3)

There was no significant correlation between the frequency of hepatocytes containing abnormal mitochondria and alcohol consumption, overweight or diabetic glucose metabolism. Any correlation with the degree of fatty liver was not found

There was no correlation between the frequency of liver cells with abnormal mitochondria and intake of drugs or tobaco smoking time of biopsy as related to time of admission, loss of weight, or sex and age of patients.

Electron microscopic examination of the

TABLE 2. *Per Cent Hepatocytes Containing Abnormal Mitochondria Fatty Liver Compared with Normal Liver*

	Normal liver n = 7	Fatty liver n = 30	
All over the liver lobule	1 1 (0-3.0)	16 4 (0.6-77.9)	$p < 0.02$
Periportal area	3.3 (0-7 7)	35 8 (1.3-94.0)	$p < 0.01$
Centrilobular area	0	1.0 (0.-6.8)	

TABLE 3 *Per Cent Hepatocytes Containing Abnormal Mitochondria. Periportal Areas Compared with Centrilobular Areas*

	Centrilobular area	Periportal area	
Normal liver (7)	0	3.3 (0-7.7)	$p < 0.01$
Fatty liver (30)	1.0 (0-6 8)	35 8 (1.3-94 0)	$p < 0.01$

The alcohol consumption was estimated as grammes of alcohol per day according to the information obtained from the patients

The body weight was calculated as per cent of a normal weight related to sex, age and height (31)

The glucose tolerance was stated as the results of a peroral load of 1 g of glucose per kg body weight, maximum 70 g Blood glucose was estimated half hourly in the fasting patient. The following limits of blood glucose values were used fasting 6 7 mmol/l maximum 10 mml/l 2 h 7 9 mmol/l and 2.5 h 6.7 mmol/l. If patients presented glucosuria of more than 100 mmol/24 h and fasting values above 10 mmol/l they were considered to have manifest diabetes mellitus and were not submitted to the glucose load If patients presented normal fasting values and elevated maximum value 2 h s and 2.5 h s values of blood glucose they were considered to have a diabetic glucose metabolism. None of the patients were at any time suffering from insulin requiring diabetes mellitus or ketonuria

Liver biopsy was performed after an overnight fast, according to Menghini.

For EPON embedding small pieces of the biopsy specimen were fixed in 0.1 m cacodylate-buffered 2.5 per cent glutaraldehyde for 2 h. After washing for a short time in 0 1 M sodium cacodylate the tissue was postfixed in 1 per cent osmium tetroxide, dehydrated in graded ethanol and embedded in EPON 0 75 μm sections were cut from the part next to-the-outermost in the tissue block, at a depth of approximately 30 50 μm. The sectioning was performed at 4 to obtain straight sections even in cases of severe steatosis and numerous fatty vacuoles were present in the liver parenchyma (24) This thin section was stained with toluidine blue and studied by light microscopy Ultrathin sections were studied in a Zeiss electron microscope EM 9 a after staining with uranyl acetate and lead citrate

Mitochondria were defined as abnormal if they were spindle or rod shaped or otherwise of a bizarre form, or if they were greatly enlarged. If only slightly enlarged, round or oval mitochondria would be considered normal since swelling may occur during the preparation (25) Usually 3–10 abnormal mitochondria were found per cell. Cells containing abnormal mitochondria were counted as per cent of the total numbers of cells seen in the

TABLE 1 *Thirty Patients with Fatty Liver and 7 Patients with Normal Liver Tissue Data on the Daily Alcohol Consumption (A) Overweight (O) and Diabetic State (Overt or Latent Diabetes) (D) as Well as the Degree of Steatosis Are Given Together with the Findings of Hepatocytes Containing Abnormal Mitochondria*

	Degree of steatosis in per cent of tissue section (+ range)	Per cent hepatocytes containing abnormal mitochondria (+ range)	
		periportal area	centrilobular area
controls (n = 7)	0	3.3 (0–7 7)	0
— A — O — D (n = 2)	12.4 (4 20 7)	37 1 (35 6–37.5)	0
+ A — O — D (n = 5)	11 3 (0 4 16 8)	16.5 (0 2–25 2)	0
— A + O — D (n = 3)	4.3 (1–10)	20 1 (2 4–48 6)	0
+ A + O — D (n = 6)	7 6 (2 1–15)	41 5 (1.3–86 6)	0 4 (0–1.3)
— A — O + D (n = 5)	8 7 (1–16 6)	4.5 (10 8–68 0)	1 7 (0–6.8)
+ A — O + D (n = 2)	3 9 (3.8–4)	53 9 (47 2 60 6)	1.8 (0–3 6)
— A + O + D (= 3)	9 0 (6–12)	48 8 (24 6 94 0)	3 1 (0–6 3)
+ A + O + D (n = 4)	6.2 (2 1–10)	34 8 (3.8- 82 2)	0

section. To estimate the extent of the abnormal mitochondria in different zones of the liver lobule, the following definitions were used: periportal hepatocytes were defined as liver cells within three cell widths from lamina limitans, and centrilobular as liver cells within three cell widths from the central vein.

The degree of steatosis was estimated in formalin fixed, Gieson stained paraffin sections in which the fatty droplets appeared as lucid holes. In Leitz Classimat distinguishing 10 grey shades of the microscopic image, the area of the fatty droplets was given as per cent of the total area of the liver biopsy.

Mann-Whitney test was used as statistical method.

RESULTS

In liver biopsies from control patients, 1.1 (0–3.0) per cent of the liver cells contained abnormal mitochondria while the percentage was 16.4 (0.6–77.9) in patients with fatty liver. This difference is significant ($p < 0.02$) (Table 2).

On the consideration that the abnormal mitochondria in the control patients occurred close to the portal spaces (3.3 (0–7.7) per cent of the liver cells) and never in the centre of the lobule, periportal areas from patients with fatty liver were compared with periportal areas from control patients: the frequency of liver cells with abnormal mitochondria was found to be significantly higher in fatty livers than in normal livers (35.8 (1.3–94.0) per cent) $p < 0.01$). As in the controls, the occurrence of abnormal mitochondria in patients with fatty liver was significantly higher in periportal areas (Fig. 1) than in centrilobular areas (Fig. 2) (35.8 (1.3–94.0) contra 1.0 (0–6.8) per cent) ($p < 0.01$) (Table 3).

There was no significant correlation between the frequency of hepatocytes containing abnormal mitochondria and alcohol consumption, overweight or diabetic glucose metabolism. Any correlation with the degree of fatty liver was not found.

There was no correlation between the frequency of liver cells with abnormal mitochondria and intake of drugs or tobacco smoking, time of biopsy as related to time of admission, loss of weight, or sex and age of patients.

Electron microscopic examination of the

TABLE 2. *Per Cent Hepatocytes Containing Abnormal Mitochondria. Fatty Liver Compared with Normal Liver*

	Normal liver n = 7	Fatty liver n = 30	
All over the liver lobule	1.1 (0–3.0)	16.4 (0.6–77.9)	$p < 0.02$
Periportal area	3.3 (0–7.7)	35.8 (1.3–94.0)	$p < 0.01$
Centrilobular area	0	1.0 (0–6.8)	

TABLE 3. *Per Cent Hepatocytes Containing Abnormal Mitochondria. Periportal Areas Compared with Centrilobular Areas*

	Centrilobular area	Periportal area	
Normal liver (n = 7)	0	3.3 (0–7.7)	$p < 0.01$
Fatty liver (n = 30)	1.0 (0–6.8)	35.8 (1.3–94.0)	$p < 0.01$

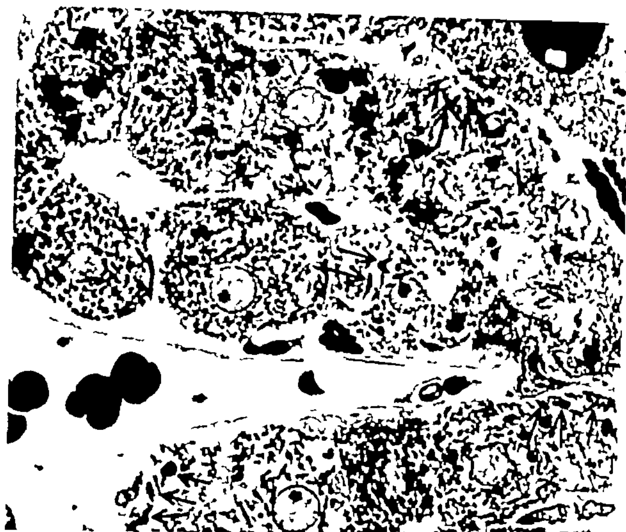


Fig 1 Abnormal mitochondria (arrows) in a periportal area in a patient with fatty liver Light microscopy of a 0 75 μm section of a specimen embedded in EPON and stained with toluidine blue × 1400

abnormal mitochondria (Figs. 3 and 4) showed enlarged irregularly shaped mitochondria generally containing an increased amount of cristae sometimes arranged parallelly vertically towards the double membrane In all patients as well as in controls the abnormal mitochondria contained "paracrystalline inclusions" i e parallelly arranged bundles of filamentous-like formations. The higher the frequency of hepatocytes with abnormal mitochondria, the more frequent the presence of paracrystalline inclusions in the mitochondria studied by electron microscopy The mitochondrial matrix was homogeneously and moderately electron dense. Widening of the intercristal spaces was found only in superficial areas of the tissue blocks and may therefore be an artefact (25)

DISCUSSION

Abnormal mitochondria have been described as a characteristic feature of alcoholic (17 29 32) and diabetic fatty livers (23) In this study abnormal mitochondria in fatty liver have been found to be due either to alcohol consumption overweight or diabetes of the type maturity onset. There was no quantitative or qualitative difference between the three conditions as regard the mithocondrial abnormalities.

Enlarged mitocondria of the type mentioned are conventionally considered to be damaged or hypofunctioning organelles. This is the supported by studies of the function of mitochondria isolated from animals (4 10) *Kiessling* (15) however discovered an increa

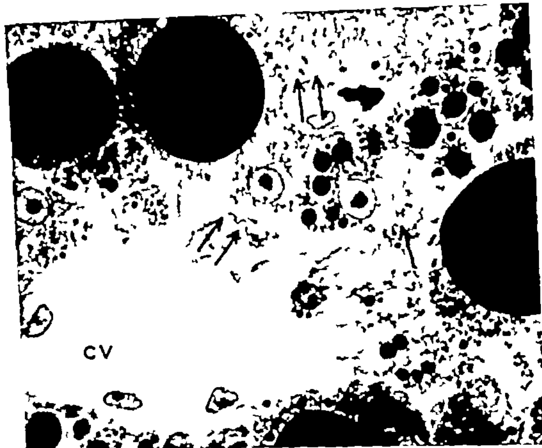


Fig. 2 Normal mitochondria (arrows) in a centrilobular area in a patient with fatty liver The central vein = cv Large black fatty vacuoles are seen in the hepatocytes. Same procedure and magnification as Fig. 1

sed β-hydroxybutyrate oxidation in mitochondria isolated from human alcoholics in whom electron microscopy had revealed a high content of greatly enlarged, elongated mitochondria. If present to the same degree in alcoholic livers, on the one hand, and in diabetic and *obesity fatty livers, on the other. It may* be a result of a similarly altered metabolism of the organelles in all three conditions, and may represent a hyperfunctioning state, and not hypofunctioning as earlier regarded in the case of alcoholic fatty liver

Enlarged irregular liver mitochondria were found in ketotic states produced in alloxan and streptozotocin diabetic rats in which the mitochondria normalized within a few days after insulin treatment (10)

Similar functional changes have been demonstrated in liver mitochondria from rats chronically fed ethanol and from streptozotocin diabetic rats, i.e. increased β-oxydation of fatty acids to acetylCoA (10 4) and changes in the oxydative phosphorylation. This may *result in an impairment of the mitochondrial* oxydation of fatty acids to CO_2. However in these experiments it cannot decided whether centrilobular or periportal mitochondria or mitochondria otherwise placed, dominated the organelles.

Findings in the present study are consistent with the view that abnormal mitochondria in alcoholic, obese and diabetic fatty livers represent hyperfunctioning organelles which eli-

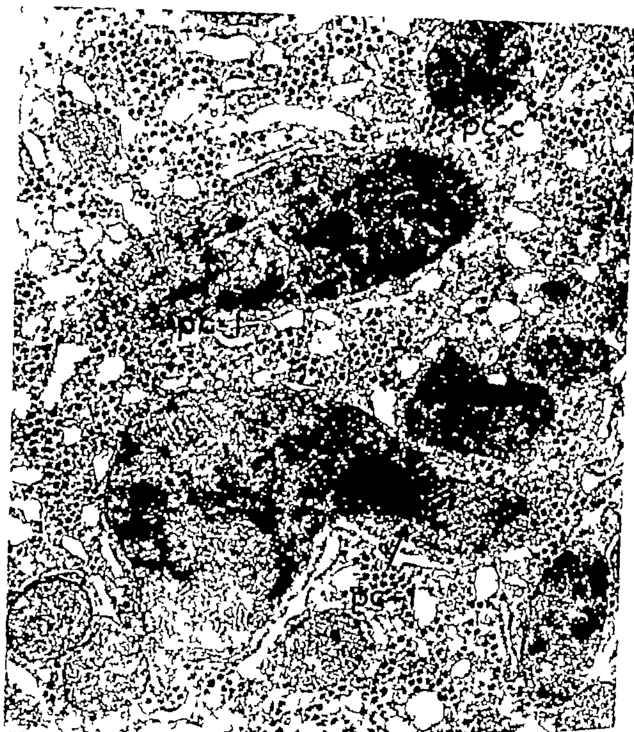


Fig 3 Electronmicrograph showing the ultrastructure of the abnormal mitochondria containing many cristae and paracrystalline inclusions longitudinally sectioned (pc-1) and cross sectioned (pc-c) × 29.500

minate fatty acids and prevent a deposition of triglyceride in this area

---

This study was supported by a grant (51? 3719) from *Danish State Medical Research Council.*

REFERENCES

1 *Addison T* Observations on fatty degeration of the liver Guy's Hosp Rep *1* 476, 1836.
2 *Bauer H Kasch B von der Emden A & Ruckes J* Fettleber Fettsucht und latenter Diabetes. Med. Welt. *35* 1813–1822, 1964



Fig. 4 Higher magnification showing the increased amount of cristae (arrows) and paracrystalline inclusions (pc) × 84,000

3. *Banck K., Krauss B., Pohl, K. & Dempe A.:* Zur Hepatopathie beim Diabetes mellitus. Zschr. in. Med. *30* 61–62, 1975.
4. *Cederbaum A. I., Lieber C. S., Beattie D. S. & Rubin, R.* Effect of chronic ethanol ingestion on fatty acid oxidation by hepatic mitochondria. J. Biol. Chem. *250* 5122–5129, 1975.
5. *Connor C. L.* Fatty infiltration of the liver and the development of cirrhosis in diabetes and chronic alcoholism. Amer. J. Path. *14* 347–364, 1938.
6. *Creutzfeldt W.:* Klinische Beziehungen zwischen *Diabetes mellitus* und Leber. Acta Hepatosplen. (Stuttgart) *6* 156, 1959.
7. *Dittrich H. & Seifert K.:* Klinische und diag



Fig 3 Electronmicrograph showing the ultrastructure of the abnormal mitochondria containing many cristae and paracrystalline inclusions longitudinally sectioned (pc – 1) and cross sectioned (pc – c) × 29.500

minate fatty acids and prevent a deposition of triglyceride in this area.

This study was supported by a grant (512–3719) from *Danish State Medical Research Council*

REFERENCES

1 *Addison T* Observations on fatty degeration of the liver Guy's Hosp. Rep. *1* 476, 1836.
2 *Baser H Knick B von der Emden A & Ruckes J* Fettleber Fettsucht und latenter Diabetes. Med. Welt. *35* 1815–1822, 1964

ULTRASTRUCTURE OF PERIPORTAL AND CENTRILOBULAR HEPATOCYTES IN HUMAN FATTY LIVER OF VARIOUS AETIOLOGY

PALLE PETERSEN

Medical Department A, Division of Hepatology Rigshospitalet, Copenhagen, Denmark

Petersen, P. Ultrastructure of periportal and centrilobular hepatocytes in human fatty liver of various aetiology. Acta path. microbiol. scand. Sect. A, 85 421–427 1977

The ultrastructure of periportal and centrilobular hepatocytes of fatty liver from 2 alcoholic patients, 2 diabetic patients and 2 obese patients is described and compared with that of hepatocytes in 2 patients with normal liver. A striking difference between periportal and centrilobular hepatocytes in all cases of fatty liver is demonstrated. The periportal hepatocytes contain abnormal mitochondria, while centrilobular hepatocytes have normal mitochondria but fatty vacuoles, peroxisomes and lysosomes are more abundant. The nature and degree of ultrastructural changes showed no correlation with aetiology of the fatty liver. The normal livers showed no such changes or distinct differences between periportal and centrilobular hepatocytes.

Key words: Liver fatty; electronmicroscopy; alcoholism; diabetes; obesity.

Palle Petersen, Medical department A, division of hepatology, Rigshospitalet, 2100 Copenhagen, Denmark.

Received 12. 76 Accepted 10.xi.76

Since 1963 numerous papers concerning the ultrastructural aspect of hepatocytes in human alcoholic steatosis have appeared (e.g. 6, 8, 19 20, 21). Electron microscopic studies of diabetic and obese fatty liver are more sparse 1 5 11).

The mitochondrial alterations in the three conditions are described in a previous work (13): the frequency of abnormal mitochondria in periportal areas was found to be significantly higher than that in centrilobular areas. The degree of mitochondrial alterations and steatosis was found to be similar in alcoholic, diabetic and obese fatty livers. By light microscopy the steatosis is found to be most marked in the centre of the lobule. In the present work, the ultrastructure of periportal hepatocytes is compared with that of the centrilobular hepatocytes.

MATERIAL AND METHODS

From among liver biopsies obtained from 30 patients with fatty liver of various origin, two were selected from each of the following groups of patients: high alcohol consumption exclusively, overt diabetes mellitus exclusively and obesity exclusively. Biopsies from two patients without any of the three conditions, in whom the liver tissue was normal, were used as controls. The patients presenting the smallest, and the patient presenting the

nostische Probleme der Fettleber Gastroenterological (Basel 3 123 1964

8. *Fowler G Butterfield W J H & Ackeson R M.* Physique glycosuria und blood glucose levels in Bedford Guy's Hosp Rep *119* 297–314 1970

9 *Hanefeld M Naumann H J & Haller H* Statistische Untersuchungen über den Einfluss des Diabetestyps und der Theraphieform auf die Ausprägung und Frequenz der Leberverfettung bei Diabetes mellitus. Dtsch. Zeitschr f Verdauungs- u. Stoffwechselkrankheiten. *27* 15–19 1967

10. *Herano Y., De Palma R G Lavine L. & Miller M.* Fatty acid oxidation, oxidative phosphorylation and ultrastructure of mitochondria in the diabetic rat liver Diabetes *21* 257–270 1972

11 *Hed R.* Clinical *studies in chronic alcoholism* II Carbohydrate metabolism in chronic alcoholism with particular reference to glucose and insulin tolerances. Acta Med. Scand. *162* 195–202 1958

12. *Kalk H.,* Über die Beziehungen zwischen Fettleber und Diabetes. Deutsch. Med. Wschr *84* 1898, 1959

13 *Karam J H Grodsky G M & Forsham P H* Excessive insulin response to glucose in obese subjects as measured by immunochemical assay Diabetes *12:* 197 1963

14 *Kern W H Heger A H Payne J H & De Wind L T* Fatty metamorphosis of the liver in morbid obesity Arch. Path. *96* 342 346 1973

15 *Kiessling K H & Pilström L.* Ethanol and the human liver Structural and metabolic changes in liver mitochondria. Cytobiologie *4* 339–348, 1971

16 *Kinzlmeier H & Ranft,H* Ätiologische Faktoren und klinische Befunde bei Leberverfettung Z. Gastroenterologie *3* 277 1963

17 *Lane B P & Lieber C S* Ultrastructural alterations in human hepatocytes following ingestion of ethanol with adequate diets. Am. J Path. *49* 593–603 1966

18 *Lieber C S & Schmid R.* The effect of ethanol on fatty acid metabolism, stimulation of fatty acid synthesis in vitro. J Clin. Invest. *40* 394–399 1961

19 *Maruhama, Y Ohneda A Tadaki H Ohtsuki M Yanbe A Abe R & Yamagati S* Hepatic steatosis and the elevated plasma insulin lever in patients with endogenous hypertriglyceridemia. Metabolism *24* 653–664 *1975*

20 *Masserat S Jordan G., Sahrkage G., Kerb G Bode J C & Dölle W* Five-year follow up study of patients with nonalcolic and nondiabetic fatty liver Acta Hepato-Gastroenterol. *21* 176–186 1974

21 *Megyen C Samols E & Marks V.* Glucose tolerance and diabetes in chronic liver disease Lancet *II* 1051–1055 1967

22 *Nikkilä E A & Taskinen M R.* Ethanol-induced alterations of glucose tolerance, post glucose *hypoglycemia and insulin secretion in* normal obese, and diabetic subjects. Diabetes *24 933–943 1975*

23 *Pacel I Bonaparte H., Sdrobici D & Petrovici A* Étude morphologique et physiologique du fois adipeux des diabetiques. Acta Diab. Latina *5* 16–30 1968.

24 *Petersen P* Lipid droplets in fatty liver Acta. Path et Microbiol Scand. Section A, *82* 255–263 1974

25 *Petersen P* Glutaraldehyde fixation for electronmicroscopy *of needle biopsies from human* livers. Acta Path. Microbiol. Scand. Section A, *85* 373–383 1977

26 *Rehfeld J F Juhl E & Hilden M.* Carbohydrate metabolism in alcohol-induced fatty liver Gastroenterology *64* 445–451 1973

27 *Robbers H Strohfeldt P & Krüger C H* Differentialdiagnose der diabetischen und alkoholischen Fettleber Dtsch. med. Wschr *93* 112–113 1968

28. *Sainani G S Choudhary S R. & Grover S* Liver in diabetes mellitus (Histopathological Study) Jr Asso. Phys. Ind. *22* 715–721 *1974*

29 *Schaffner F Loebel A., Weiner H A & Barka T* Hepatocellular *cytoplasmic changes* in acute alcoholic hepatitis. JAMA *183* 131 *134 1964*

30 *Schmidt R. & Tennstedt A* Perkutane Leberbiopsie bei Diabetikern – Erfahrungsbericht der Jahre 1968 bis 1971

31 Society of Actuaries (Hrsg) Build and Blood Pressure Study vol. 1 Chicago 1959

32 *Svoboda, D J & Manning, R. T* Chronic alcoholism with fatty metamorphosis of the liver Mitochondrial alterations in hepatic cells. Am J Path. *44* 645–652 1964

33 *Thaler H* Die Fettleber und ihre Probleme. Internist (Berlin) *7* 21 1966.

34 *Wasastjerna C., Reissell P Karjalainen J & Ekelund P* Fatty liver in diabetes. Acta Med. Scand. *191* 225–228, 1972

Acta path. microbiol. scand. Sect. A, 85: 421–427 1977

ULTRASTRUCTURE OF PERIPORTAL AND CENTRILOBULAR HEPATOCYTES IN HUMAN FATTY LIVER OF VARIOUS AETIOLOGY

PALLE PETERSEN

Medical Department A, Division of Hepatology Rigshospitalet, Copenhagen, Denmark

Petersen, P Ultrastructure of periportal and centrilobular hepatocytes in human fatty liver of various aetiology Acta path. microbiol. scand. Sect. A, 85 421–427 1977

The ultrastructure of periportal and centrilobular hepatocytes of fatty liver from 2 alcoholic patients, 2 diabetic patients and 2 obese patients is described and compared with that of hepatocytes in 2 patients with normal liver A striking difference between periportal and centrilobular hepatocytes in all cases of fatty liver is demonstrated. The periportal hepatocytes contain abnormal mitochondria, while centrilobular hepatocytes have normal mitochondria, but fatty vacuoles, peroxisomes and lysosomes are more abundant. The nature and degree of ultrastructural changes showed no correlation with aetiology of the fatty liver The normal livers showed no such changes or distinct differences between periportal and centrilobular hepatocytes.

Key words Liver fatty electronmicroscopy alcoholism diabetes obesity

Palle Petersen, Medical department A, division of hepatology Rigshospitalet, 2100 Copenhagen, Denmark.

Received 12.v.76 Accepted 10.xi.76

Since 1963 numerous papers concerning the ultrastructural aspect of hepatocytes in human alcoholic steatosis have appeared (e.g 6, 8, 19 20 21) Electron microscopic studies of diabetic and obese fatty liver are more sparse 1 5 11)

The mitochondrial alterations in the three conditions are described in a previous work (15) the frequency of abnormal mitochondria in periportal areas was found to be significantly higher than that in centrilobular areas. The degree of mitochondrial alterations and steatosis was found to be similar in alcoholic, diabetic and obese fatty livers. By light microscopy the steatosis is found to be most marked in the centre of the lobule. In the present work, the ultrastructure of periportal hepatocytes is compared with that of the centrilobular hepatocytes.

MATERIAL AND METHODS

From among liver biopsies obtained from 50 patients with fatty liver of various origin, two were selected from each of the following groups of patients high alcohol consumption exclusively overt diabetes mellitus exclusively and obesity exclusively. Biopsies from two patients without any of the three conditions, in whom the liver tissue was normal, were used as controls. The patients presenting the smallest, and the patient presenting the

nostische Probleme der Fettleber Gastroenterological (Basel *3* 123 1964
8 *Fowler G Butterfield W J H & Acheson R M* Physique, glycosuria und blood glucose levels in Bedford Guy's Hosp Rep *119* 297–314 1970
9 *Hanefeld M Naumann H J & Haller H* Statistische Untersuchungen über den Einfluss des Diabetestyps und der Theraphieform auf die Ausprägung und Frequenz der Leberverfettung bei Diabetes mellitus. Dtsch Zeitschr f Verdauungs- u Stoffwechselkrankheiten. *27* 13–19 1967
10 *Harano Y De Palma R G Lavine L & Miller M* Fatty acid oxidation, oxidative phosphorylation and ultrastructure of mitochondria in the diabetic rat liver Diabetes *21* 257–270 1972
11 *Hed R Clinical studies in chronic alcoholism* II Carbohydrate metabolism in chronic alcoholism with particular reference to glucose and insulin tolerances. *Acta Med Scand. 162* 195–202 1958
12 *Kalk H* Über die Beziehungen zwischen Fettleber und Diabetes. Deutsch. Med. Wschr *84* 1898 1959
13 *Karam J H Grodsky G M & Forsham P H* Excessive insulin response to glucose in obese subjects as measured by immunochemical assay Diabetes *12* 197 1963
14 *Kern W H Heger A H Payne J H & De Wind L T* Fatty metamorphosis of the liver in morbid obesity Arch. Path. *96* 342 346 1973
15 *Kiessling K H & Pilstrom L* Ethanol and the human liver Structural and metabolic changes in liver mitochondria. Cytobiologie *4* *339–348, 1971*
16 *Kunzlmeier H & Ranft,H* Ätiologische Faktoren und klinische Befunde bei Leberverfettung Z. Gastroenterologie *3* 277 1963
17 *Lane B P & Lieber C S* Ultrastructural alterations in human hepatocytes following ingestion of ethanol with adequate diets. Am. J Path. *49* 593–603 1966
18 *Lieber C S & Schmid R* The effect of ethanol on fatty acid metabolism, stimulation of fatty acid synthesis in vitro J Clin. Invest. *40* 394–399 1961
19 *Maruhama Y Ohneda, A Tadaki H., Ohtsuki M Yanbe A Abe R & Yamagati S* Hepatic steatosis and the elevated plasma insulin lever in patients with endogenous hypertriglyceridemia Metabolism *24* 653–664 1975
20 *Massarat S Jordan G Sahrhage G., Korb G Bode J C & Dölle W* Five-year follow-up study of patients with nonalcolic and nondiabetic fatty liver Acta Hepato-Gastroenterol. *21* 176–186 1974
21 *Megyesi C Samols E & Marks V* Glucose tolerance and diabetes in chronic liver disease. Lancet *II* 1051–1055 1967
22 *Nikkilä E A & Taskinen M R.* Ethanol-induced *alterations of glucose tolerance,* post glucose hypoglycemia, and insulin secretion in normal obese and diabetic subjects. Diabetes *24* 933–943 1975
23 *Pavel I Bonaparte H Sdrobici D & Petrovici A* Étude morphologique et physiologique du fois adipeux des diabetiques. Acta Diab Latina *5* 16–30 1968.
24 *Petersen P* Lipid droplets in fatty liver Acta. Path et Microbiol Scand Section A, *82* 255–263 1974
25 *Petersen P* Glutaraldehyde, fixation for electronmicroscopy of needle biopsies from human livers. Acta Path. Microbiol. Scand. Section A, *85* 373–383 1977
26 *Rehfeld J F Juhl E & Hilden M* Carbohydrate metabolism in alcohol-induced fatty liver Gastroenterology *64* 445–451 1973
27 *Robbers H Strohfeldt P & Krüger C H* Differentialdiagnose der diabetischen und alkoholischen Fettleber Dtsch. med. Wschr *93* 112–113 1968.
28 *Sasnani G S., Choudhary S R & Grover S* Liver in diabetes mellitus (Histopathological Study) Jr Asso Phys. Ind. *22* 715–721 *1974*
29 *Schaffner F., Loebel, A Weiner H A & Barka T* Hepatocellular cytoplasmic changes in acute alcoholic hepatitis. JAMA *183* 131 134 1964
30 *Schmidt R & Tennstedt A* Perkutane Leberbiopsie bei Diabetikern – Erfahrungsbericht der Jahre 1968 bis 1971
31 Society of Actuaries (Hrsg) Build and Blood Pressure Study vol. 1 Chicago 1959
32 *Svoboda, D J & Manning, R. T* Chronic alcoholism with fatty metamorphosis of the liver Mitochondrial alterations in hepatic cells. Am J Path. *44* 645–652, 1964
33 *Thaler H* Die Fettleber und ihre Probleme. Internist (Berlin) *7* 21 1966
34 *Wasastjerna, C Reissell P Karjalainen, J & Ekelund P* Fatty liver in diabetes. Acta Med. Scand *191* 225–228 1972.

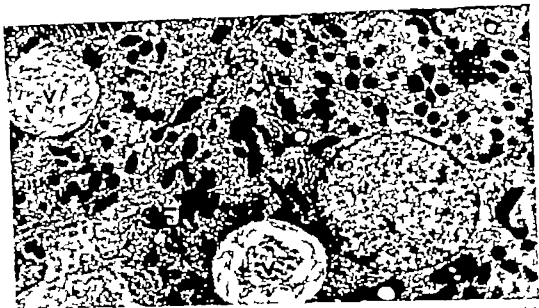


Fig 2 Periportal hepatocyte from an alcoholic fatty liver Inhomogeneous fatty vacuoles are seen (v) The mitochondria are enlarged and of abnormal shapes. Smooth endoplasmic reticulum (SER) is not hypertrophied. ×5.400

Rough endoplasmic reticulum (RER) The cisterns appeared slender especially if present in minor stacks, or slightly dilated, as often seen in liver tissue fixed in glutaraldehyde and they did not differ from those in centrilobular areas or in normal periportal hepatocytes.

Golgi apparatus The cisterns and saccules were not dilated or proliferated. VLDL particles were not a characteristic feature. The appearance of the Golgi complex did not differ from that in normal hepatocytes or centrilobular hepatocytes.

Lysosomes Primary and secondary lysosomes (lipofuscin granules, autophagocytic vacuoles, hemosiderin granules or multivesiculated bodies) were scarce.

Fatty vacuoles represented a rare feature in the periportal hepatocytes and, morphologically they did not differ from those in the centrilobular area (Fig 2)

Nucleus Changes in nuclear envelope or in the appearance and distribution of the chromatin were not found. However intranuclear glycogen was found in the diabetic livers, but was also found in one normal liver

B Centrilobular hepatocytes

Qualitative differences in centrilobular hepatocytes in the three forms of fatty liver were not found.

Mitochondria were normal, as described previously (15)

Peroxisomes A constant feature was the finding of numerous peroxisomes in the centrilobular hepatocytes, especially in cases where centrilobular steatosis was marked. Centrilobular hepatocytes in normal livers contained some peroxisomes, but the latter were more numerous in fatty livers. The appearance of peroxisomes was like that of normal ones, i.e. round organelles containing a loosely arranged matrix and a single membrane. As usual, there was a constant, close relation to some SER cisterns (Fig. 4)

SER was of type 1 Proliferation of hypertrophy was not seen, and any difference between the three forms of steatosis were not found.

RER did not differ either from periportal or from normal centrilobular hepatocytes.

Golgi apparatus appeared like that in the

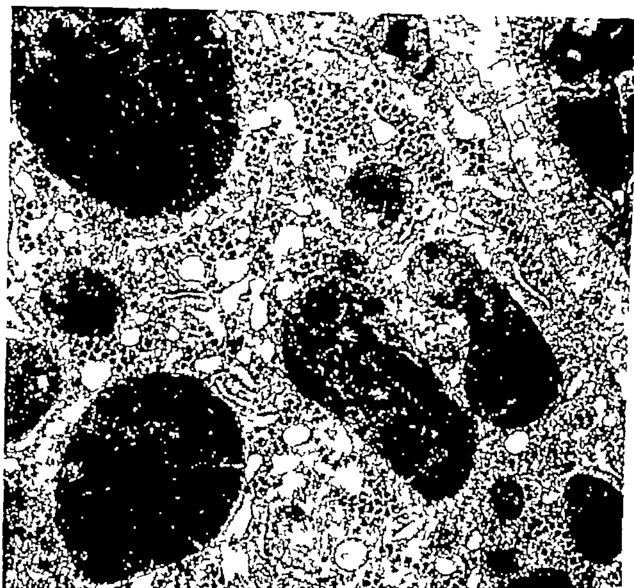


Fig 1 Part of a periportal hepatocyte from a diabetic fatty liver showing the abnormal mitochondria. × 28.500

greatest mitochondrial abnormities (15) were selected from each group.

The alcohol consumption glucose intolerance and over-weight mitochondrial alterations and degree of steatosis were defined as previously described (15) and the same technique was used for the preparation.

RESULTS

A Periportal hepatocytes

No qualitative difference in the ultrastructural appearance in the three forms of fatty liver was found A comparison with periportal hepatocytes in normal livers showed following

Mitochondria were enlarged they were abnormal and of bizarre form they contained an increased amount of cristae and paracrystalline inclusions and a varied amount of mitochondrial matrical granules of different sizes as previously described (15) (Fig 1)

Peroxisomes were rarely found in periportal hepatocytes

Smooth endoplasmic reticulum (SER) was of type 1 i.e vesicles made up of cisterns with a patent lumen of about 1500 Å, diffusely distributed between abundant glycogen (Figs. 2 and 3) Type 2 i.e. the tubular or nonvesicular form was not found No proliferation or hypertrophy were seen.

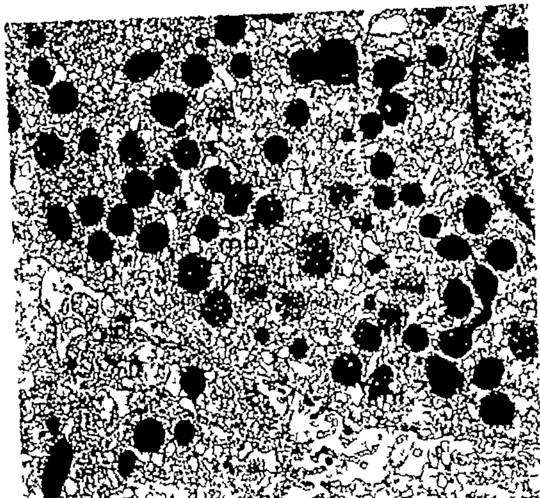


Fig. 4. Centrilobular hepatocyte from an obese fatty liver. The section is taken from a superficial part of the biopsy (i.e. depth of approximately 30 µm). This is responsible for the dilated cisterns of SER and of rough endoplasmic reticulum (RER) and for the more compact matrix of the mitochondria (m) as well as for the more loose matrix of the peroxisomes (mb) making it easy to distinguish between the two organelles. Many peroxisomes are seen. × 13,500.

activity of mitochondrial linked enzymes was found to be irregular (12).

The abnormal mitochondria from alcoholic fatty livers as well as from diabetic and obese fatty livers is a characteristic of the periportal hepatocyte, wheras the steatosis in the mentioned three conditions is centrilobular.

The periportal, enlarged mitochondria have been discussed elsewhere (15).

Many peroxisomes were found in the centrilobular hepatocyte, particularly if the degree of steatosis was high. Peroxisomes of liver cells possess catalase and several H_2O_2-generating oxidases (2, 7, 9), but their function remains unknown. They may play a role in the lipid metabolism (10) and several hypolipidemic drugs have been shown to induce marked proliferation of peroxisomes (16). The increase in number of peroxisomes in the centrilobular hepatocyte containing fatty droplets may indicate some lipolytic function of the organelles.

A proliferated SER in alcoholic fatty livers from animals and man has been observed in

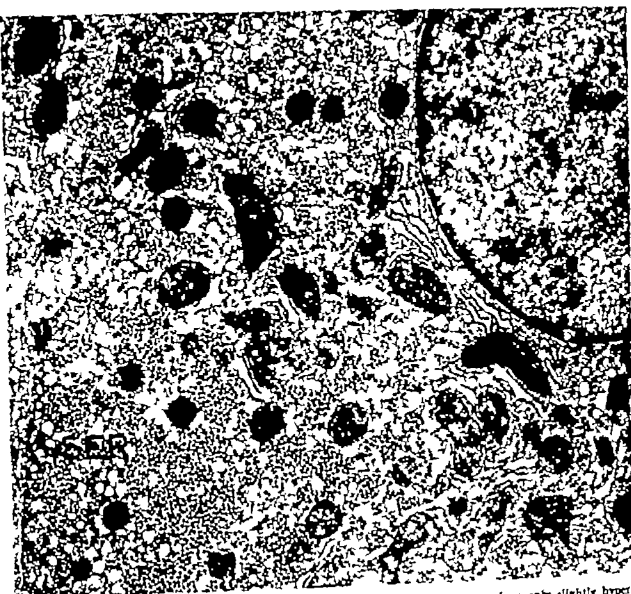


Fig 3 Centrilobular hepatocyte from a diabetic fatty liver The SER is normal or only slightly hypertrophied × 13 500

periportal hepatocyte and in the normal centrilobular hepatocyte.

Lysosomes Lipofuscingranules in considerable amounts were found in centrilobular areas, both in normal and steatotic livers (Fig 5)

Fatty vacuoles were abundant in the centre of the lobule They presented a heterogeneity described previously (13) some were filled with an osmiophilic material supposed to be triglyceride. The presence of smaller or larger 'holes' in this osmiophilic material gave it an appearance of inhomogeneity In some vacuoles, small dark, irregularly shaped granules of sizes from 10 to 100 nm were found. These were often concentrically arranged in the fatty vacuoles, of they might occasionally be sparsely scattered throughout the vacuole (Fig 2)

DISCUSSION

From histochemical studies it is known that zonal differences of the hepatocytes are present in the animal liver lobule (3 22) Such difference has not been found in human hepatocytes, not even in hepatocytes from human alcoholic fatty liver but the enzymatic

cisterns in which the triglyceride accumulation started.

The difference in ultrastructural appearance of the periportal and centrilobular hepatocyte most likely reflects different functional conditions, perhaps dependent on the availability of substrates and oxygen to the cells.

This study was supported by a grant (512-3719) from *Danish State Medical Research Council.*

REFERENCES

1. *Dominici Y & Orlandi F.*: Osservazioni microanalitiche ed ultrastrutturali sul tessuto epatico di sogetti diabetici. Relazione III Simp. Naz. Diabete, Catania, 37–46, 1961
2. *d Duve C & Baudhin P* Peroxisomes (Microbodies and Related Particles) Physiol. Rev 46 323–357 1966
3. *French S W.*: Succinic dehydrogenase histochemical shift" in hepatic lobular distribution induced by ethanol. Lab. Invest. *13* 1051 1056, 1964
4. *Jezequel, A M Koch M & Orlandi F*: A morphometric study of the endoplasmic reticulum in human hepatocytes. Gut. *15* 737 747 1974
5. *Kern W H Heger A. H., Payne J H & De Wind L. T.*. Fatty metamorphosis of the liver in morbid obesity Arch. Pathol. *96* 342 346, 1973.
6. *Lane B P & Lieber C S* Ultrastructural alterations in human hepatocytes following ingestion of ethanol with adequate diets. Am. J Path. *49* 593–603 1966.
7. *Leighton F Poole B., Lazarow P & de Duve C* The synthesis and turnover of rat liver peroxisomes. Cell. Biol. *41* 521–535, 1969
8. *Lieber C S & Rubin E.* Alcoholic fatty liver in man on a high protein and low fat diet. Am. J Med. *44* 200–207 1968.
9. *Mc Groarty E. J & Tolbert N E.* Enzymes in peroxisomes. J Histochem. Cytochem. *21* 949–954 1973
10. *Novikoff A. T & Shin W Y.* The endoplasmic reticulum in the Golgi zone and its relations to microbodies, Golgi apparatus and autophagic vacuoles in rat liver cells. J Microsc. (Paris) *3*: 187 206, 1964
11. *Patel, J., Bonaparte H., Scrobaci, D & Pet e lei A.*: Étude Morphologique et Physiologique de Foie Adipeux des Diabetiques. Acta Diab. Latina *5*: 16–30, 1968.
12. *Petersen, P* Histochemical localization of various enzymes in human fatty liver caused by moderate alcohol consumption. Acta Path. Microbiol. Scand., Sect. A. *78* 161–168, 1970
13. *Petersen P.* Lipid droplets in fatty liver Acta Path. Microbiol Scand. Sect. A, *82*: 255–263 1974
14. *Petersen P.*: Glutaraldehyde fixation for electron microscopy of needle biopsies from human livers. Acta Path. Microbiol. Scand. Sect. A, *85* 373–383 1977
15. *Petersen P.* Abnormal mitochondria in hepatocytes in human fatty liver Acta Path. Microbiol. Scand. Sect. A, *85* 413–420 1977
16. *R ddy J K & Krishnakantha, T P.* Hepatic peroxisomes proliferation Induction by two novel compounds structural unrelated to clofibrate. Science *190*: 787–789 1975
17. *R bin, E. & Lieber C S.* Experimental alcoholic hepatic injury in man ultrastructural changes. Federation Proc. *5*: 1458–1467 1967
18. *Rubin, E. & Lieber C S.* Fatty liver alcoholic hepatitis and cirrhosis produced by alcohol in primates. New Engl. Jr Med. *290* 128–135 1974
19. *Schaffner F S., Loebel, A., Weiner H A. & Barka, T.* Hepatocellular cytoplasmic changes in acute alcoholic hepatitis. JAMA *183* 131–134 1963
20. *Svoboda, D J & Manning R. T.* Chronic alcoholism with fatty metamorphosis of the liver Am. J Path. *44*: 645–662, 1964
21. *Thorpe M E. C & Shorey C D.* Ultrastructural alterations in human liver desease. Amt. Am. Med. *15* 4–16 1966.
22. *Wachstein M.*: Enzymatic histochemistry of the liver Gastroenterology *37* 525–537 1959

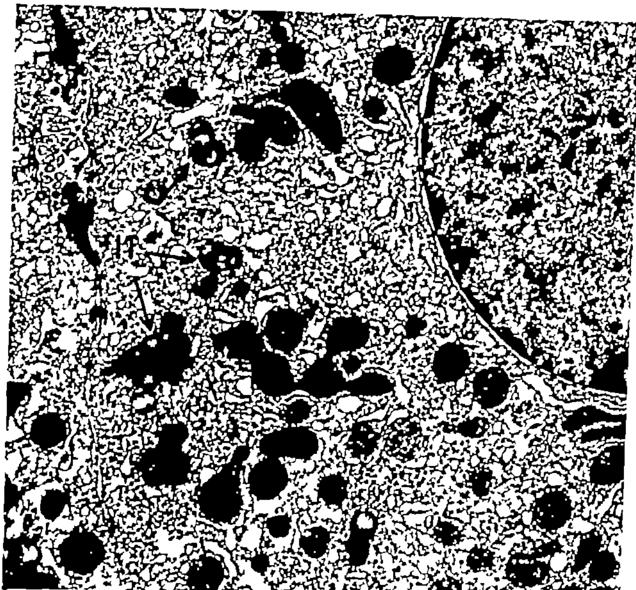


Fig 3 Centrilobular hepatocyte from an obese fatty liver containing many lipofuscin granules (lf) × 13.500

several studies (17 18) As judged from the published electron micrographs, it is a proliferation of type 1 i.e. vesicles made up of cisterns with a patent lumen of about 1500 Å. Such proliferation was not found in the present study of alcoholic diabetic and obese fatty livers or in a study of normal livers. It must be borne in mind that vesiculation of SER may be a result of fixation that is less than optimal (14) In animal and human experiments, an increase of SER is produced by administration of various drugs This type 2 or SER consist of clumps of tubular branching membranes with narrow lumina and is regarded as neoformations, whereas type 1 represent adult" membranes (4) In the present work, proliferation of type 2 SER membranes, was not found in fatty livers of different origin.

The fatty vacuoles have been described elsewhere (13) In the present work they present a heterogeneity regardless of the origin of the fatty liver The "holes in the triglyceride may represent an extraction to occur during the preparation but it may also be a phenomenon which has arisen in vivo. The small dark, irregularly shaped granules may represent remnants of membranes of the SER

the mammary gland in Sprague-Dawley rats are uncommon. *McKenzie & Garner* (3) found only 4 adenocarcinomas of the mammary gland in 1268 rats followed for 2 years. To our knowledge spontaneous ear duct tumours are extremely rare and Magnusson references do not indicate otherwise. It is, however well-known that aromatic amines which are chemically related to aromatic amides can induce ear duct tumours (4). Regretfully we do not understand the purpose of *Magnusson's* reference to *Thompson* (1973).

Magnusson is stressing the difficulties of interpreting results in old experimental animals, since consideration has to be taken to spontaneous disease. These factors have also been stressed in our analysis of both experimental and control groups. As is evident from our paper the demonstrated difference of urothelial hyperplasia of the renal papillae between the groups is valid only concerning the degree of severity and the frequency.

Unfortunately the pharmaceutical companies have shown very little interest in studying possible carcinogenic effects of phenacetin and its main metabolite NAPA (paracetamol). It is our hope that at least pharmaceutical companies manufacturing or selling such compounds would include such studies in their research program.

References: 1. *Magnusson G. & Ramsay C.-H.*, Laboratory Animals 5, 153–162, 1971. —2. *Magnusson G. & Ramsay C.-H.*, Z. Versuchstierk. *17* 185–193 1975.—3. *McKenzie W. F. & Garner F. M.*, J. Natl. Cancer Inst. *50*, 1243–1257 1973. —4. *Shubik P. & Hartwell, J. L.*: Survey of compounds which have been tested for carcinogenic activity. Washington, 1957.

Department of Pathology II
University of Göteborg,
Sweden

S. Johansson
L. Angervall

Acta path. microbiol. scand. Sect. A, 85 428–429 1977

CORRESPONDENCE

FINDINGS IN RATS AFTER ADMINISTRATION OF PHENACETIN

Received 3.iii.77

Sir.—The recent paper by *S. Johansson & L. Angervall* in the Acta path. microbiol. scand. Sect. A, *84* 375–383 1976 deals with findings in rats after long term feeding of phenacetin. The report merits some comments.

Hyperplasia of the epithelium in the renal pelvis is a common disorder in the rat, and it can amount to 30 per cent (3). The epithelial hyperplasia is often accompanied by mineralization and formation of renal calculi, ammonium magnesium phosphate being the most regular constituent of the stones. Besides phenacetin other factors, e.g. dietary magnesium (4), excess sodium chloride (2) and polychlorinated biphenyls (1) can increase the incidence of this epithelial hyperplasia. Thus there is evidence that several factors can influence this epithelial hyperplasia, the mechanism and importance of which is at present not clearly understood.

Furthermore an adenocarcinoma of the mammary gland was observed in five experimental rats and in one control and a squamous cell carcinoma of the ear duct in four experimental animals. Spontaneous neoplasms including mammary adenocarcinoma and squamous cell carcinoma of the ear duct are common findings in old rats (6). An increased number of spontaneous neoplasms can be an indication of a carcinogenic effect but in the reported study the mentioned neoplasms occurred in rather few animals in comparison with the controls. Nor was there any statistical support for an increase of these two types of neoplasm (5).

Hopefully these comments may have contributed to elucidate the difficulties in the interpretation of findings in studies in old experimental animals, when consideration of spontaneous disorders is necessary.

References: 1. *Bruckner J. V., Khanna K. L. & Cornish H. H.*: Toxicol. appl. Pharmacol. *28* 198–199 1974.—2. *Lasek J. J., Paik W. C. W. & Pradhan B.*: Arch. Pathol. *97* 29–32 1974.—3. *Magnusson G. & Ramsay C. H.*: *5* 153–162, 1971.—4. *Magnusson G. & Ramsay C. H.*: Z. Versuchstierk. *17* 185–195 1975.—5. *Thompson S. W.*: Bull. Soc. Pharmacol. Environ. Pathol. *1* 5–7 1973.—6. *Turusov V. S.* ed.: *Pathology of Tumours in Laboratory Animals. IARC Lyon 1973.*

Toxicology Laboratories, Astra Pharmaceuticals AB, Södertälje — GÖRAN MAGNUSSON

Sir.—We are grateful for the attention and regret that *Magnusson's articles* (1, 2) have not been considered by us. This is partly explained by the title of them "Urolithiasis in the rat", a subject outside the frame of our study. Furthermore, the paper from 1975 (2) was not listed in the Index Medicus at the time of finishing our manuscript.

In the study of *Magnusson & Ramsay* (1) 14 per cent (5/35) of the female Sprague-Dawley rats in the control group exhibited epithelial hyperplasia of the renal papillae, 13 of which had urolithiasis. In our control series of female Sprague-Dawley rats 17 per cent (5/30) had epithelial hyperplasia compared with 87 per cent of the rats fed with phenacetin, a highly significant difference. Urolithiasis was not found in our series. As *Magnusson* and we have pointed out many factors may contribute to the development of the urothelial hyperplasia.

The findings of 5 adenocarcinomas of the mammary gland and 4 squamous cell carcinomas of the ear duct are considered by *Magnusson* to be few and points out the lack of statistic analysis. There is only a statistically significant difference between the experimental and control groups for total malignancy (9/?0–1/30, $p<0.05$) but not for each of ear duct and mammary gland tumours. To interpret the biological sense of these results may be difficult and therefore we only stated the presence of a higher incidence of mammary carcinomas and ear duct tumours among the rats fed phenacetin compared with the control rats and drew the conclusion that this observation "may imply a more general carcinogenic effect of phenacetin". In fact, spontaneous adenocarcinomas of

the mammary gland in Sprague-Dawley rats are uncommon. *McKenzie & Garner* (3) found only 4 adenocarcinomas of the mammary gland in 1268 rats followed for 2 years. To our knowledge spontaneous ear duct tumours are extremely rare and Magnusson's references do not indicate otherwise. It is, however, well-known that aromatic amines which are chemically related to aromatic amides can induce ear duct tumours (4). Regretfully we do not understand the purpose of *Magnusson's* reference to *Thompson* (1973).

Magnusson is stressing the difficulties of interpreting results in old experimental animals, since consideration has to be taken to spontaneous disease. These factors have also been stressed in our analysis of both experimental and control groups. As is evident from our paper the demonstrated difference of urothelial hyperplasia of the renal papillae between the groups is valid only concerning the degree of severity and the frequency.

Unfortunately the pharmaceutical companies have shown very little interest in studying possible carcinogenic effects of phenacetin and its main metabolite NAPA (paracetamol). It is our hope that at least pharmaceutical companies manufacturing or selling such compounds would include such studies in their research program.

References: 1. *Magnusson G & Ramsey C.-H.*: Laboratory Animals *5*, 153–162, 1971.—2. *Magnusson G & Ramsey C.-H.*: Z. Versuchstierk. *17*, 185–195, 1975.—3. *McKenzie W. F. & Garner F. M.*: J. Natl. Cancer Inst. *50*, 1243–1257, 1973. —4. *Shubik P & Hartwell, J. L.*: Survey of compounds which have been tested for carcinogenic activity. Washington, 1957.

Department of Pathology II
University of Göteborg,
Sweden

S. Johansson
L. Angervall

Acta path. microbiol scand Sect. A, 85 428–429, 1977

CORRESPONDENCE

FINDINGS IN RATS AFTER ADMINISTRATION OF PHENACETIN

Received 3 iii.77

Sir —The recent paper by *S Johansson* & *L. Angervall* in the Acta path. microbiol. scand. Sect A *84* 375–383 1976 deals with findings in rats after long term feeding of phenacetin. The report merits some comments.

Hyperplasia of the epithelium in the renal pelvis is a common disorder in the rat, and it can amount to 30 per cent (3) The epithelial hyperplasia is often accompanied by mineralization and formation of renal calculi ammonium magnesium phosphate being the most regular constituent of the stones Besides phenacetin other factors e g dietary magnesium (4) excess sodium chloride (2) and polychlorinated biphenyls (1) can increase the incidence of this epithelial hyperplasia. Thus, there is evidence that several factors can influence this epithelial hyperplasia the mechanism and importance of which is at present not clearly understood

Furthermore, an adenocarcinoma of the mammary gland was observed in five experimental rats and in one control and a squamous cell carcinoma of the ear duct in four experimental animals. Spontaneous neoplasms including mammary adenocarcinoma and squamous cell carcinoma of the ear duct are common findings in old rats (6) An increased number of spontaneous neoplasms can be an indication of a carcinogenic effect but in the reported study the mentioned neoplasms occurred in rather few animals in comparison with the controls. Nor was there any statistical support for an increase of these two types of neoplasm (5)

Hopefully these comments may have contributed to elucidate the difficulties in the interpretation of findings in studies in old experimental animals, when consideration of spontaneous disorders is necessary

References 1 *Bruckner J V Khanna K L. & Cornish H H* Toxicol appl Pharmacol. *28* 198–199 1974 —2 *Lalich J J Paik W C W & Pradhan B* Arch Pathol *97* 29–32 1974 —3 *Magnusson G & Ramsay C H* 5 153–167 1971 —4 *Magnusson G & Ramsay C H* Z. Versuchstierk. *17* 185–195 1975.—5 *Thompson S W* Bull Soc. Pharmacol. Environ. Pathol. *I* 5–7 1973 —6 *Turusov V S* ed. *Pathology of Tumours in Laboratory Animals. IARC Lyon 1973*

Toxicology Laboratories, Astra Pharmaceuticals AB Södertälje

GÖRAN MAGNUSSON

Sir —We are grateful for the attention and regret that *Magnusson's* articles (1 2) have not been considered by us. This is partly explained by the title of them Urolithiasis in the rat a subject outside the frame of our study Furthermore the paper from 1975 (2) was not listed in the Index Medicus at the time of finishing our manuscript.

In the study of *Magnusson* & *Ramsay* (1) 14 per cent (5/35) of the female Sprague-Dawley rats in the control group exhibited epithelial hyperplasia of the renal papillae, 13 of which had urolithiasis. In our control series of female Sprague-Dawley rats 17 per cent (5/30) had epithelial hyperplasia compared with 87 per cent of the rats fed with phenacetin a highly significant difference. Urolithiasis was not found in our series. As *Magnusson* and we have pointed out many factors may contribute to the development of the urothelial hyperplasia.

The findings of 5 adenocarcinomas of the mammary gland and 4 squamous cell carcinomas of the ear duct are considered by *Magnusson* to be few and points out the lack of statistic analysis. There is only a statistically significant difference between the experimental and control groups for total malignancy (9/30–1/30 $p<0.05$) but not for each of ear duct and mammary gland tumours. To interpret the biological sense of these results may be difficult and therefore we only stated the presence of a higher incidence of mammary carcinomas and ear duct tumours among the rats fed phenacetin compared with the control rats and drew the conclusion that this observation "may imply a more general carcinogenic effect of phenacetin" In fact, spontaneous adenocarcinomas of

TABLE 1 *Mean Body Weights (± Standard Error of Mean) at Different Times of the Experiment*

Groups		Body weight (g)			
		At alloxan injection "Day 30"	At adrenalectomy "Day 37"	At start of cortisone injection "Day 40"	At autopsy "Day 54"
Co_1	(9)	156 ± 3	191 ± 5	187 ± 5	164 ± 3 P<0.03§
Co_2	(8)	156 ± 4	192 ± 6	185 ± 5	150 ± 5 P<0.001§
$Ax\text{-}Co_1$	(6)	177 ± 2	185 ± 9	193 ± 9	151 ± 9 P<0.01§
$Ax\text{-}Co_2$	(10)	178 ± 2	182 ± 6	187 ± 5	131 ± 3 P<0.001§

Within brackets are given the number of rats in each group.
§ Statistical comparison of body weights at "day 40" and "day 54".

TABLE 2 *Mean Weights (± Standard Error of Mean) of Prostatic Lobes, Seminal Vesicles, Levator Ani Muscle and Thymus in Cortisone Treated Non-Diabetic and Alloxan-Diabetic Rats*

Groups		Ventral prostate (mg)	Dorsolateral prostate (mg)	Coagulating glands (mg)	Seminal vesicles (mg)	Levator ani (mg)	Thymus (mg)
Co	(9)	8.3 ± 0.5 (n.s.)	12.0 ± 0.8 (P<0.02)	6.0 ± 0.7 (P<0.025)	18.5 ± 1.5 (P<0.001)*	32.7 ± 4.4 (n.s.)*	35.6 ± 3.2 (n.s.)
Co_2	(8)	9.3 ± 0.5 (n.s.)§	16.0 ± 1.4 (P<0.001)§	7.4 ± 0.6 (P<0.001)§	26.9 ± 1.8 (P<0.001)§	29.3 ± 3.8 (n.s.)§	31.8 ± 3.6 (n.s.)§
$Ax\text{-}Co_1$	(6)	8.6 ± 0.6	8.9 ± 0.5	3.6 ± 0.3	9.9 ± 0.6	20.4 ± 3.5	28.1 ± 4.5
$Ax\text{-}Co_2$	(10)	8.2 ± 0.6	9.8 ± 0.6	4.0 ± 0.4	12.6 ± 0.8	18.3 ± 3.7	26.3 ± 1.7

* Statistical comparison of group Co and Ax-Co n.s. (not significant)
§ Statistical comparison of group Co_2 and $Ax\text{-}Co_2$

performed. Twelve of these rats were during the experimental period given 3 mg cortisone acetate twice daily. Twelve rats had, besides cortisone acetate protamine zinc insulin in daily doses of 4 to 6 IU.

A commercial cortisone acetate preparation, (Upjohn) 25 mg/ml was used. Cortisone acetate was given as subcutaneous injections on the lower part of the body at 8.30 a.m. and 5.30 p.m. Throughout the experiment all the rats were given a commercial rat diet supplied by Tekmosan AB Malmö, and tap water *ad libitum*. The rats were killed 54 days after castration. The other methods used in this investigation have previously been described (*Tisell & Angervall* 1969 and 1972).

Results

Before the injection period the mean food consumption per 24 h of the non-diabetic rats was about 19 g, and of the diabetic rats about 24 g. Cortisone decreased the daily food consumption a few grams in both diabetic and non-diabetic rats. All the alloxan-diabetic rats had markedly elevated blood glucose values and glucosuria >2 per cent. Body and organ weights are given in Tables 1 and 2 respectively. The value given are mean ± standard error of the mean.

In the group Ax-Co the ventral and dorsolateral prostate, the coagulating glands and the seminal vesicles all had small acini lined with low epithelium which did not exhibit any signs of secretory activity. In the group $Ax\text{-}Co_2$ small and variable signs of stimulation of the growth of the dorsolateral prostate, the coagulating glands and the seminal vesicles were observed. The low columnar epithelium formed some papillary formations and some of the acini contained a small amount of secretion. Distinct signs of secretory activity were not observed.

In the groups Co_1 and Co_2 the growth of the dorsolateral prostate, the coagulating glands and the seminal vesicles was found to be stimulated, in so far as the large acini were lined by high columnar epithelium and contained secretion. The acini were surrounded by smooth-muscle cells

Acta path. microbiol. scand. Sect. A, 85 430–432 1977

BRIEF REPORT

THE PROSTATIC LOBES AND THE SEMINAL VESICLES IN NON DIABETIC AND ALLOXAN DIABETIC CASTRATED ADRENALECTOMIZED RATS INJECTED WITH CORTISONE

Lars Eric Tisell and Lennart Angervall

The Department of Surgery II and the Department of Pathology II
University of Gothenburg, Sweden

Tisell L. E. & Angervall L. The prostatic lobes and the seminal vesicles in non-diabetic and alloxan-diabetic castrated adrenalectomized rats injected with cortisone. Acta path. microbiol. scand. Sect. A, 85: 430–432, 1977

The growth of the prostatic lobes and the seminal vesicles was studied morphologically in alloxan-diabetic and non-diabetic castrated adrenalectomized rats. In non-diabetic but not in alloxan-diabetic rats cortisone in daily doses of 3 or 6 mg induced growth and secretory activity in the epithelium of the dorsolateral prostate, the coagulating glands and the seminal vesicles. Insulin administration to alloxan-diabetic rats could restore the effect of cortisone on these glands. This indicates that insulin deficiency *per se* was the main reason for the failure of cortisone to induce secretory activity of the prostatic lobes and the seminal vesicles of alloxan-diabetic rats.

Key words: Prostatic lobes seminal vesicles morphology alloxan-diabetes cortisone insulin castrated adrenalectomized rats.

L. E. Tisell, Department of Surgery II Sahlgren's Hospital S-413 45 Göteborg, Sweden.

Received 13.vi.75 Accepted 20.II.77

Following studies in castrated adrenalectomized rats treated with cortisone it was proposed that an increased production of insulin may have contributed to the stimulated growth of the prostatic lobes and seminal vesicles (*Tisell 1970*). The result of another study suggests that after hypophysectomy insulin deficiency was partly responsible for the reduced effect of cortisone on the growth of the prostatic lobes and seminal vesicles (*Tisell & Angervall 1972*).

To study the dependence of the cortisone effect on insulin it seems suitable to use diabetic rats. In the present experiments the effect of cortisone on the morphology of the prostatic lobes and the seminal vesicles was studied in castrated adrenalectomized, alloxan-diabetic rats.

Material and Methods

The investigation comprised 33 rats of the *Sprague-Dawley* strain supplied by Anticimex AB, Stockholm. The rats were castrated at a weight of 44 ± 0.3 g (mean and standard error of the mean). Thirty days after castration 16 rats were given alloxan in a single dose of 0.15 mg per g body weight by subcutaneous injection of a freshly prepared 5 per cent alloxan monohydrate solution in physiological saline. After another week all rats were adrenalectomized. Three days after adrenalectomy the rats were divided into the following groups and were given injections during the last fourteen days of the experimental period.

Co_1	Non-diabetic rats injected with 1.5 mg cortisone acetate twice daily	– 9 rats
Co_3	Non-diabetic rats injected with 3 mg cortisone acetate twice daily	– 8 rats
$Ax\text{-}Co_1$	Alloxan-diabetic rats injected with 1.5 mg cortisone acetate twice daily	– 6 rats
$Ax\text{-}Co_3$	Alloxan-diabetic rats injected with 3 mg cortisone acetate twice daily	– 10 rats

A complementary experiment including 24 castrated adrenalectomized, alloxan-diabetic rats was

TABLE 1 *Mean Body Weights (± Standard Error of Mean) at Different Times of the Experiment*

Groups	Body weight (g) At alloxan injection "Day 30"	At adrenalectomy "Day 37"	At start of cortisone injection "Day 40"	At autopsy "Day 54"
Co_1 (9)	156 ± 3	191 ± 5	187 ± 5	164 ± 3 P<0.05§
Co_2 (8)	156 ± 4	192 ± 6	185 ± 5	150 ± 5 P<0.001§
Ax-Co (6)	177 ± 2	185 ± 9	195 ± 9	151 ± 9 P<0.01§
$Ax-Co_2$ (10)	178 ± 2	182 ± 6	187 ± 5	131 ± 3 P<0.001§

Within brackets are given the number of rats in each group.
§ Statistical comparison of body weights at "day 40" and "day 54"

TABLE 2 *Mean Weights (± Standard Error of Mean) of Prostatic Lobes, Seminal Vesicle, Levator Ani Muscle and Thymus in Cortisone Treated Non-Diabetic and Alloxan Diabetic Rats*

Groups	Ventral prostate (mg)	Dorsolateral prostate (mg)	Coagulating glands (mg)	Seminal vesicles (mg)	Levator ani (mg)	Thymus (mg)
Co (9)	8.5 ± 0.5	12.0 ± 0.8	6.0 ± 0.7	18.5 ± 1.5	32.7 ± 4.4	35.6 ± 3.2
	(n.s.)	(P<0.02)	(P<0.025)	(P<0.001)*	(n.s.)	(n.s.)
Co_2 (8)	9.5 ± 0.5	16.0 ± 1.4	7.4 ± 0.6	26.9 ± 1.8	29.5 ± 5.8	31.8 ± 3.6
	(s)§	(P<0.001)§	(P<0.001)§	(P<0.001)§	(n.s.)§	(n.s.)§
Ax-Co (6)	8.6 ± 0.6	8.9 ± 0.5	3.6 ± 0.3	9.9 ± 0.6	20.4 ± 5.5	28.1 ± 4.5
$Ax-Co_2$ (10)	8.2 ± 0.6	9.8 ± 0.6	4.0 ± 0.4	1_.6 ± 0.8	18.5 ± 5.7	26.5 ± 1.7

* Statistical comparison of group Co and $Ax-Co_2$, n.s. (not significant)
§ Statistical comparison of group Co_2 and Ax-Co

performed. Twelve of these rats were during the experimental period given 5 mg cortisone acetate twice daily. Twelve rats had, besides cortisone acetate, protamine zinc insulin in daily doses of 4 to 6 IU.

A commercial cortisone acetate preparation, (Upjohn) 25 mg/ml was used. Cortisone acetate was given as subcutaneous injections on the lower part of the body at 8.30 a.m. and 3.30 p.m. Throughout the experiment all the rats were given commercial rat diet supplied by Tekniaen AB, Malmo, and tap water *ad libitum*. The rats were killed 54 days after castration. The other methods used in this investigation have previously been described (Tisell & Angervall 1969 and 1972).

Result

Before the injection period the mean food consumption per 24 h of the non-diabetic rats was about 19 g, and of the diabetic rats about 24 g. Cortisone decreased the daily food consumption a few grams in both diabetic and non-diabetic rats. All the alloxan-diabetic rats had markedly elevated blood glucose values and glucosuria >2 per cent. Body and organ weights are given in Tables 1 and 2 respectively. The values given are mean ± standard error of the mean.

In the group Ax-Co the ventral and dorsolateral prostate, the coagulating glands and the seminal vesicles all had small acini lined with low epithelium which did not exhibit any signs of secretory activity. In the group $Ax-Co_2$ small and variable signs of stimulation of the growth of the dorsolateral prostate, the coagulating glands and the seminal vesicles were observed. The low columnar epithelium formed some papillary formations and some of the acini contained a small amount of secretion. Distinct signs of secretory activity were not observed.

In the groups Co and Co the growth of the dorsolateral prostate, the coagulating glands and the seminal vesicles was found to be stimulated, in so far as the large acini were lined by high columnar epithelium and contained secretion. The acini were surrounded by smooth-muscle cells

which showed better development than seen in the diabetic rats. The histological signs of stimulation were most apparent in group Co_2 where the lateral part of the dorsolateral prostate showed supranuclear clear zones and the granules in the epithelium of the seminal vesicles were surrounded by light halos. In the non-diabetic rats given daily doses of 6 mg cortisone (group Co) the ventral prostate showed minor signs of stimulation. The acini were larger with higher epithelium than seen in other groups, but the epithelium showed no supranuclear clear zone.

In the complementary experiment with alloxan diabetic rats the combined treatment with cortisone and insulin resulted in higher weights of the dorsolateral prostate the coagulating glands and the seminal vesicles (16 0 ± 1 1 mg 4 2 ± 0 6 mg and 21 0 ± 1 8 mg respectively) than cortisone treatment alone (11 6 ± 2 9 mg 3 0 ± 0.9 and 15 6 ± 4 0 mg respectively) Only four of the rats given cortisone alone survived the experiment and the weight differences did not reach statistically significant levels. The histological examination, however revealed that addition of insulin to the cortisone treatment restored the growth-promoting effect of cortisone on the epithelium of the prostatic lobes and the seminal vesicles of the alloxan-diabetic rats.

Discussion

In rats, cortisone probably increases the production of insulin (*Houssay et al* 1954 *Yoshinaga et al* 1967) and insulin accelerates the protein synthesis (*Lukens* 1964) Hence the growth promoting effect of cortisone on the accessory reproductive glands of the castrated non-diabetic rats may in the present investigation have been mediated in part by endogenous insulin However it was seen in studies on force fed hypophysectiomized castrated, adrenalectomized rats injected with insulin, that insulin alone cannot induce growth and secretory activity in the accessory reproductive organs (*Tisell & Angervall* 1972)

In the alloxan-diabetic rats the effect of cortisone was markedly impaired and definite signs of secretory activity in the epithelial cells of the prostatic lobes and the seminal vesicles were not observed The results of some experiments indicate that alloxan-diabetic rats have an impaired ability to produce growth hormone (*Lawrence et al.* 1958, *Haselwood & Hazelwood* 1964) as well as prolactin (*Ahrén et al* 1963 1965) These observations might imply that the decreased effect of cortisone on the growth of the prostatic lobes and the seminal vesicles of the alloxan-diabetic rats was pituitary dependent. However in an earlier experiment cortisone was found to stimulate prostatic and seminal vesicle growth in hypophysectomized rats, provided insulin was also administered (*Tisell & Angervall* 1972) This finding indicates that in the present study insulin deficiency *per se* was the main reason for the failure of cortisone to induce secretory activity in the epithelium of the prostatic lobes and seminal vesicles of the alloxan-diabetic rats. The fact that insulin administration could restore the growth promoting effect of cortisone on the epithelium of the prostatic lobes and the seminal vesicles strengthens this opinion.

Conclusion

From the results of the present investigation and our previous study on hypophysectomized rats injected with insulin and/or cortisone it is concluded that the cortisone-induced growth of the prostatic lobes and seminal vesicles in rats is markedly dependent on the amount of insulin available.

This study was supported by grants from the *Swedish Medical Research Council* (B74-12X 719-09B)

References Ahrén K. & Angervall L. Acta path microbiol scand. *58* 161–171 1963 — *Ahrén K., Angervall L. & Arvill A* Diabetes *14* 501–506, 1965 — *Hazelwood R L. & Hazelwood B. S* Amer J Physiol *206* 1137–1144 1964 — *Houssay B A Foglia V C & Rodriguez R R.* Acta endocr (Kbh) *17* 146–164 1954 — *Lawrence A M Contopoulos A N & Simpson M E.* Proc. Soc. exp. Biol. (N Y) *99* 35–38, 1958 — *Lukens F D W* Diabetes *13* 451–461 1964 — *Tisell L. E.* Acta endocr (Kbh.) *64* 637–655, 1970 — *Tisell L. E. & Angervall L.* Acta endocr (Kbh.) *62* 694–710 1969 — *Tisell L.-E. & Angervall L.* Acta endocr (Kbh.) *71* 179–190, 1972 — *Yoshinaga, T Katayama, T Nakajima, I & Nishikawa M* Endocrinologie *51* 211 223, 1967

Acta path. microb ol scand. Sect. A, 85 433–446, 1977

THE EFFECT OF IMMUNOTHERAPY WITH BCG ON THE DEVELOPMENT OF RADIOSTRONTIUM (^{90}Sr) INDUCED OSTEOSARCOMA

A Roentgenographical Light Microscopical and Ultrastructural Study in Mice

Sven Erik Larsson Ronny Lorentzon and Lennart Boquist

The Department of Orthopaedic Surgery and Institute of Pathology University of Umeå, Umeå, Sweden

Larsson, S.-E., Lorentzon, R. & Boquist, L. The effect of immunotherapy with BCG on the development of radiostrontium (^{90}Sr)-induced osteosarcoma. A roentgenographical, light microscopical and ultrastructural study in mice. Acta path. microbiol. scand. Sect. A, 85 433–446 1977

The development of radiostrontium-induced osteosarcoma was studied in BCG-treated and in untreated control mice. Within the observation period of 420 days after the administration of radiostrontium there was total tumour-incidence of 89.5 and 90.5 per cent for the respective groups of animals. There was no statistically significant difference between the two groups, neither with regard to the time of the first roentgenographic appearance of the osteosarcoma, nor concerning the total tumour incidence, nor with regard to the distribution of the primary sites of the tumours. The tumours of the BCG-treated animals showed clear tendency to slower growth rate in comparison to that of the tumours in the control animals. This effect was probably immunological in nature. The mortality in osteosarcoma following radiostrontium administration, however showed no significant difference between the two groups. Light microscopical and ultrastructural examination did not disclose any clear structural difference between the tumours from BCG-treated and untreated control animals.

Key words Osteosarcoma, radiostrontium-induced immunotherapy mice.

Sven-Erik Larsson, Department of Orthopaedic Surgery University of Umeå, S-901 85 Umeå, Sweden

Received 28 76 Accepted 8 xii 76

Numerous animal experiments have demonstrated the existence of immunological host reactions to various induced tumours of an antigenic character (cf. *Southam* 1960 *Old & Boyse* 1966 *Klein* 1968). In humans, cell-mediated immunity to neoplasms of various histological types has been demonstrated (cf. *Hellström et al* 1971 *Kumar et al* 1972) and humoral antibodies have also been observed (*Lewis et al.* 1969 *Hellström & Hellström* 1973).

Radiostrontium-induced osteosarcomas in mice show a weak tumour-specific antigenicity (*Moore & Williams* 1972). Treatment with heavily-irradiated tumour cells prior to whole-body irradiation decreases the frequency of progressively-growing transplanted

osteosarcomas, as compared to treatment with heavily irradiated normal tissues (*Nilsson et al* 1972). Furthermore, whole body irradiated mice show a significantly greater incidence of transplanted tumours than unirradiated ones do.

In an attempt to increase immunological reactivity BCG (Bacillus Calmette Guerin) has been administered to tumourbearing animals (cf *Bansal & Sjogren* 1973) and also humans (cf *Mathé et al* 1973). BCG is one of a variety of biological agents which are known to stimulate the reticuloendothelial system and to provide non specific increases in both cell mediated and humoral immunity to a variety of unrelated antigens. Administration of BCG to radiostrontium treated mice at a time close to the expected appearance of the first bone tumours results in a delay of the development and a significant decrease in the total incidence of such tumours (*Nilsson et al* 1965). The present study was undertaken to examine further whether or not BCG treatment of ^{90}Sr injected mice influenced the total tumour incidence, the time of tumour development, the growth rate and the histological character of the tumours.

MATERIAL AND METHODS

Material—A total of forty approximately seventy five-days-old CBA mice[1] of both sexes were used. Their body-weight at the time of injection of ^{90}Sr was 25–30 grams. The animals were kept on a standard pellet diet[2] which, together with drinking water, was supplied without restriction.

Radiostrontium was administered to all the animals at a dose of 0.7 microcurie per gram of body weight. The isotope was given by a single intraperitoneal injection of carrier free sterile water solution of ^{90}Sr $(NO_3)_2$[3] with a specific activity of 100 microcurie per ml.

BCG treatment—Freeze-dried Danish BCG vaccine[4] was injected subcutaneously into nineteen mice. During a period of 70–135 days after the administration of radiostrontium, each animal was given 1.0 mg of dry weight bacterial mass in 0.2 ml of Sauton solution every 3 weeks for 4 times. For each occasion, a single batch of Sauton solution containing BCG was prepared. The remaining twenty-one ^{90}Sr-injected animals constituted the control group and were given Sauton solution with no BCG added.

Roentgenographic examination—Dorso-ventral roentgenograms of the whole skeleton were obtained from all experimental and control animals at monthly and later fourteen-day intervals, commencing on the eightieth day after injection of the radioisotope. The animals were anaesthetized with ether and were placed in a standard position on paper-holder cassettes with Structurix D4P Agfa-Gevaert Roentgen X film. The exposure used was 0.40 seconds at 80 milliamperes and 79 kilovolts peak 30 centimetres from the tube of an Elema Järnh, Triplex Automatic 1000 X ray unit. The roentgenograms were examined at a magnification of 1.5 times. Tumour-size was measured on the films with the aid of a fine caliper.

Light microscopy and histochemistry—On the death of the animals, terminal roentgenograms were made and a complete autopsy was performed. Pathologically-altered hard and soft tissues were removed for light and electron microscopic studies.

Specimens taken for light microscopic examination were fixed for 24 hours in 10 per cent neutral formalin. Decalcification was accomplished in a mixture of equal parts of 20 per cent monosodium citrate and 44 per cent formic acid for 10 to 12 days. The specimens were then immersed for 24 hours in 5 per cent disodium sulphate, washed in water for 24 hours, and dehydrated by successive immersion in 70 per cent, 95 per cent and absolute alcohol (2 changes).

Paraffin-embedded sections were stained with hematoxylin and eosin, van Gieson's stain, periodic acid Schiff (P.A.S.), Laidlaw's silver stain and phosphotungstic acid hematoxylin.

Histochemical demonstration of alkaline phosphatase was carried out, using the calcium-cobalt method after Gomori (*Pearse* 1968).

Electron microscopy—Specimens taken for ultrastructural examination were fixed in 2.5 per cent glutaraldehyde in 0.34 M Veronal acetate buffer adjusted to pH 7.4, followed by postfixation in 1 per cent osmium tetroxide in the same buffer. Embedding was carried out in Epon 812 and thick sections stained with toluidine-blue were used for identification of suitable areas for the thin sections which were stained with uranyl-acetate and lead-citrate prior to examination in a Siemens Elmiscope 101.

Statistical analysis—Data applying to the two groups of animals were compared in pairs and subjected to the Student's t test.

1 Obtained from Karolinska Institutet, Stockholm.
2 Obtained from Ewos Co., Södertalje.
3 Obtained from Institutt for Atomenergi, P.O. Box 40, 2007 Kjeller, Norway.
4 Obtained from Statens Seruminstitut, Amager Boulevard 80, 2300 Copenhagen S, Denmark. The courtesy of Dr. K. *Bunch-Christensen* is acknowledged.

RESULTS

Incidence and Distribution—Seventeen of the nineteen BCG-treated animals and nineteen of the twenty-one control animals developed osteosarcoma within the observation period of 420 days after the administration of radiostrontium (Fig 1) This makes a total tumour-incidence of 89.5 and 90.5 per cent for the respective groups of animals. There was a slight tendency to an earlier tumour incidence among the BCG-treated than among the control animals with a mean time of 283 4 and 296.9 days, respectively However there was no statistically significant difference between the two groups either with regard to the time of the first roentgenographic appearance of the osteosarcoma, or concerning the total tumour-incidence. The earliest time that a tumour was detectable roentgenographically was 174 days after injection of ^{90}Sr and the latest, 368 days.

The distribution of the primary sites of the osteosarcomas showed no notable difference between BCG-treated and control animals (Table 1) Among the former four animals had two primary tumours and among the latter one animal had three and one animal two primary tumours For the combined groups a percentage of 60.5 of the neoplasms occurred in the long bones, followed by 32.5 in the spinal column and 7 0 in the pelvis.

Roentgenographic appearance—Osteosarcomas of the spine had most often a sclerotic appearance and became very radio-dense. A soft-tissue component was usually absent. Tumours of the long bones became generally evident by their soft tissue swelling, usually situated within the metaphysial region of the bone. There was a definite calcification of the tumour and elevation of the adjacent periosteum. Primarily osteolytic neoplasms within the long bones caused a marked loss of bone substance, often with resulting pathologic fracture. Tumours of the pelvic bones had quite a sclerotic appearance and also a soft tissue mass.

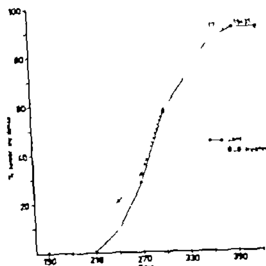


Fig 1 The incidence of osteosarcoma following one intraperitoneal injection of ^{90}Sr at a dose of 0.7 microcurie per gram of body weight in BCG-treated and untreated, control mice.

Among the BCG-treated animals, the roentgenographic appearance of the tumour

TABLE 1 *Distribution of the Primary Site of Osteosarcoma in Thirty-six Animals*

Location	Number of tumours			Distribution (Per cent)
	BCG-treated animals	Control animals	Total	
Spinal column	6	8	14	32.5
Femur	6	6	12	27.9
Tibia	6	4	10	23.3
Humerus	2	2	4	9.3
Pelvis	1	2	3	7.0
Total	21	22	43	100.0

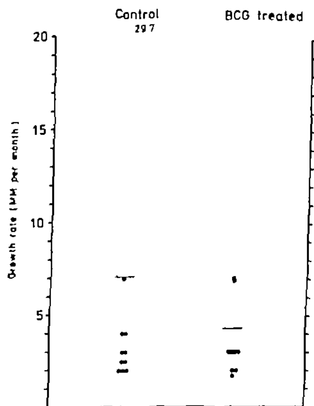


Fig 2 The growth rate of ^{90}Sr induced osteosarcomas in BCG-treated and untreated control mice.

was classified as sclerotic in seventy-one per cent and osteolytic in twenty nine per cent of the lesions. For the control animals, the corresponding figures were sixty three and thirty seven per cent, respectively Roentgenographically no noteworthy difference was found between the two groups of animals.

Tumour growth rate—In comparison to those of the control animals, the tumours of the BCG treated animals showed a clear tendency to a slower growth rate (Fig 2) Statistically the difference was found to be almost significant ($0.01 < p < 0.05$) The values showed large variations, from 1 6 to 29 7 millimetres per 30 days among the control animals and from 0.9 to 9 0 among the BCG-treated animals

Mortality—This was caused by the osteosarcoma in all tumour bearing animals. As shown in Fig. 3 the mortality following radiostrontium administration was slightly higher initially among the BCG-treated animals than among the control animals, but thereafter the mortality curves were almost identical The former survived for a mean of 305 days and the latter for 307 days. In comparison untreated CBA mice lived for a mean of 950 days

The mortality after roentgenologic appearance of the tumour is shown in Fig 4 Animals of both groups died within quite a short period of time after the neoplasm had reached sufficiant size visible roentgenographi-

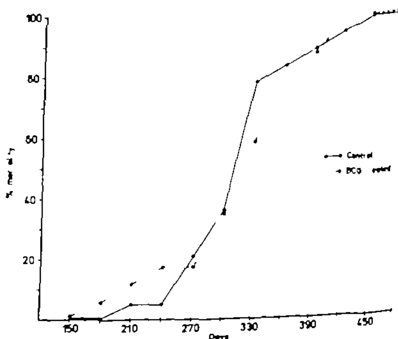


Fig 3 The mortality following ^{90}Sr administration in tumour bearing BCG-treated and untreated, control mice.

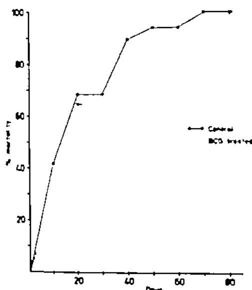


Fig. 4 The mortality after roentgenological tumour appearance in BCG-treated and untreated, control mice.

cally Thus, more than twenty per cent of the animals of both groups died within 20 days. BCG-treated animals showed a tendency to a longer period of survival than that of the control animals, but the difference was not statistically significant.

Light microscopy and histochemistry—All tumours from both the BCG-treated and control animals showed characteristics of osteosarcoma, which could be differentiated into either osteoblastic or fibroblastic types. No chondroblastic tumours were identified. The osteoblastic type predominated both among the BCG-treated and control animals.

The osteoblastic tumours consisted of a malignant stroma and malignant neoplastic osteoid and bone (Figs. 5–7) The degree of atypism varied among the stromal cells. Mitotic figures were seen with a rather low frequency Mono- or multinucleated giant cells occurred, usually collected in groups. In some tumours the osteoid was abundant, whereas others had a moderate or a sparse amount of osteoid No chondromatous components were encountered.

The fibroblastic tumours were mainly composed of spindle-shaped cells, often in parallel bundles (Figs. 8 and 9) and occasionally with a tendency to whorled arrangement. In some areas these tumours consisted of large cells with rounded nuclei showing irregular chromatin distribution and one or more enlarged nucleoli. Mono- or multinucleated giant cells were rather frequently seen usually localized in small groups. Mitotic figures were more often seen in the fibroblastic (Fig 10) than in the osteoblastic tumours. Osteoid, tumour bone, or chondromatous tissue were not seen in the fibroblastic tumours.

In no light microscopically detectable respect was there any clear difference between the tumours from the BCG-treated and control animals.

The alkaline phosphatase activity was strong in the chondroblastic tumours, especially those from the BCG-treated animals (Fig. 11) but weak or absent in the fibroblastic tumours.

Electron microscopy—The findings made by light microscopy were verified by the ultrastructural examinations.

The osteoblastic tumour cells had nuclei with smooth or irregular outline and rather distinct membranes. The chromatin was irregularly dispersed and the nucleoli were large, distinct and often multiple (Fig. 12) The cytoplasm exhibited a moderate electron density The endoplasmic reticulum was of the rough type and moderately or richly

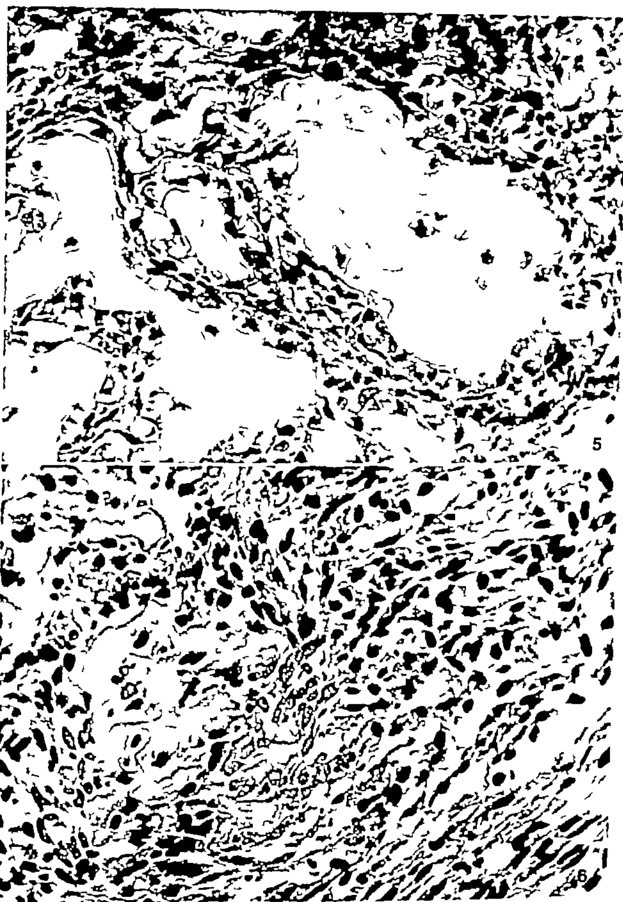
---

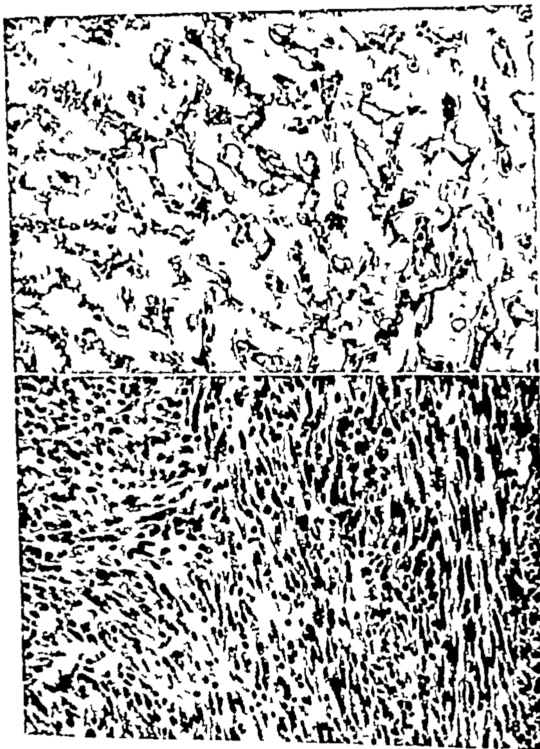
Fig 5 Photomicrograph of ^{90}Sr-induced osteosarcoma of osteoblastic type in BCG-treated mice, showing sarcomatous stroma and osteoid formation. Hematoxylin-eosin × 360

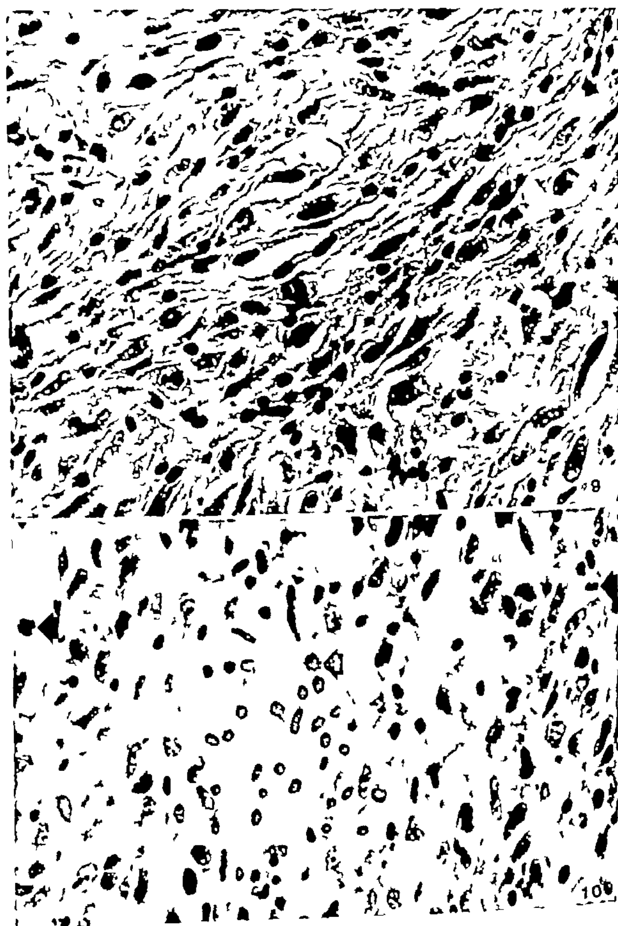
Fig 6 Another ^{90}Sr-induced osteosarcoma of osteoblastic type showing osteoid and sarcomatous stroma composed of hyperchromatic and partly spindle-shaped cells. Hematoxylin-eosin × 340.

Fig 7 Extensive formation of tumour bone in ^{90}Sr induced osteosarcoma of osteoblastic type. van Gieson stain × 170.

Fig 8 ^{90}Sr-induced osteosarcoma of fibroblastic type showing bundles of elongated stromal cells with polymorphous nuclei. No osteoid is seen. Hematoxylin-eosin × 160


5
6


7


8
10

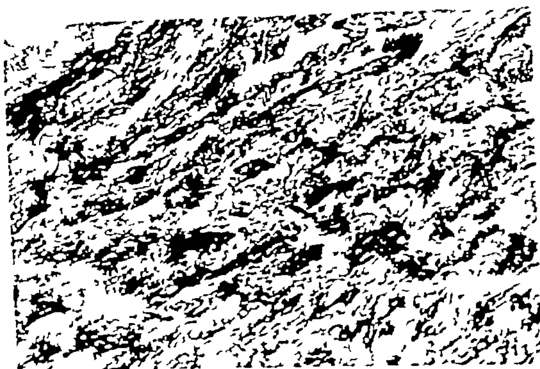


Fig. 11 Histochemical reaction for alkaline phosphatase showing strong reaction in an osteoblastic osteosarcoma from BCG-treated mouse. × 160.

developed (Fig. 13). Free ribosomes were seen in the cytoplasm. The Golgi complex was usually rather small. The mitochondria were rounded, oval, or elongated and had a moderately dense matrix and distinct transverse cristae. Lysosomal bodies and homogenously electron dense rounded bodies were found in the cytoplasm.

Vacuoles containing flocculent material and fibrils of moderate density were identified in the cytoplasm. Collagen fibers (osteoid by light microscopy) occurred extracellularly (Fig. 14). These fibers seemed to originate from the cytoplasm of the tumour cells. Degenerative changes were found in some tumour cells, occasionally in the form of focal cytoplasmic degradation (Fig. 15).

The fibroblastic tumours consisted of spindle-shaped or irregular cells. The nuclei of the former were elongated and showed a rather smooth outline and distinct membranes. The chromatin was either diffusely dispersed, or somewhat irregularly condensed. The nucleoli were moderately large. The nuclei of the irregular cells were usually irregular and had one or more large nucleoli.

The cytoplasm of the fibroblastic tumour cells exhibited a moderate electron density. The endoplasmic reticulum was of the rough type and rather prominent (Fig. 16). The Golgi complex was rather small. Lysosomal bodies and homogenously electron-dense rounded bodies of varying size were occasionally encountered in the cytoplasm. The cellular outline was smooth, or more often irregular and exhibited occasional microvilli (Fig. 17).

The ultrastructural examination could not

Fig. 9 Another [illegible]-induced osteosarcoma of fibroblastic type showing considerable polymorphism among the stromal cells. Hematoxylin-eosin. × 440.

Fig. 10 [illegible]-induced osteosarcoma of fibroblastic type showing mitotic figures (arrow). Hematoxylin-eosin. × 400.



Fig 12 Electron micrograph of a portion of a stromal cell in osteoblastic osteosarcoma of BCG-treated mice, showing a nucleus with rather finely dispersed chromatin a distinct nucleolus and smooth nuclear outline Medium-sized mitochondria and Golgi complex are also seen. × 10 000

Fig 13 Part of another stromal cell from an osteoblastic osteosarcoma showing rounded mitochondria and some strands of rough endoplasmic reticulum Small vesicles containing amorphous moderately dense material are also seen. × 24 000



Fig 14 Portion of a stromal cell in osteoblastic osteosarcoma showing a body with electron-dense granular contents (G), a vacuole with amorphous contents (V) and fibrils (F) in the cytoplasm. Numerous fibres (EF) are seen outside the cell × 27,000

disclose any clear structural difference between the tumours from BCG-treated and untreated control animals.

DISCUSSION

The light and electron microscopic studies clearly showed that the ^{90}Sr-treatment had resulted in the development of osteosarcomas in the experimental animals. The morphological appearance of these tumours was essentially similar to that described in previous studies of ^{90}Sr-induced osteosarcomas in mice (*Sandelin & Nilsson* 1967, *Nilsson et al* 1974). The structural appearance of the tumours also conforms to that of osteosarcoma in man, although no chondroblastic tumours were detected.

Mice of the used CBA strain, in which spontaneously occurring osteosarcomas are very rare, developed radiation-induced osteosarcoma in about ninety per cent of the animals after a mean latency period of 266 days following one intraperitoneal injection of 0.9 microcuries of ^{90}Sr $(NO_3)_2$ per gram body weight, the first tumour being detectable after 90 days (*Nilsson* 1962, *Nilsson et al.* 1965). The lower dose of 0.7 microcuries per gram body weight used in the present study induced osteosarcomas in ninety per cent of the animals after a mean period of 297 days, the first tumour occurring after 174 days and

L

D

L

L

B

15

16

17

the last after 368 days. The longer latency period was apparently dose-related. The mean survival time of untreated mice of this strain is 935±26 days (*Nilsson et al.* 1965).

The distribution of the tumours in the skeleton was similar to that reported by *Nilsson et al.* (1965) with a preponderance of long bones over vertebrae and pelvis. No difference was found in this respect between BCG-treated and control animals.

Comparison between the BCG-treated and control mice did not reveal any obvious differences in the light microscopical or ultrastructural appearance of the tumours. However, the alkaline phosphatase activity in the osteoblastic tumours was more intense in the tumours from the BCG-treated mice than in those from the controls. The present series did not permit any definite appraisal of whether this difference was of a coincidental nature or whether it was of any functional significance. Generally, the results of the studies did not disclose any unequivocal difference between the BCG-treated animals and the controls.

In the present study, treatment with BCG was found to result in a minor suppression of tumour growth-rate. There was no influence by BCG upon the total tumour incidence, nor the time of tumour development. Neither the survival time, nor the distribution in the skeleton, nor the osteogenic or osteolytic character of the tumours was affected by BCG treatment. These findings do not support those reported by *Nilsson et al.* (1965) who found a delay of the development and a significant decrease in the total incidence of radiostrontium-induced osteosarcomas after treatment with BCG. In that study only one dose of BCG was given two hundred and nine days after the administration of ^{90}Sr at the time of the first macroscopical appearance of the bone tumours. In the present study four doses were given every 3 weeks from seventy to one hundred and thirty five days after ^{90}Sr administration to achieve an optimum stimulation of immunological reactivity. As shown by *Nilsson* (1962), the first ^{90}Sr induced tumours can be detected by histological methods within ninety days after injection of radiostrontium. Therefore, we treated our mice with BCG at a time corresponding to the emergence of the first osteosarcoma, to obtain a more efficient suppression of antigenic, potentially neoplastic cells. The different results therefore are not readily explained by the different kinds of BCG treatment given. It seems more likely that the high mortality due to other causes than tumour in the series of *Nilsson et al.* (1965) introduced errors in their interpretation of data. Thus, 40.8 per cent of the deaths among the BCG-treated *experimental animals* were caused by some other damage than tumour and 14.3 per cent among the BCG treated control animals. Because of the short life-span of those animals, the carcinogenic effect of ^{90}Sr could not be studied. The statistical *treatment* of our data was not influenced by unrelated deaths.

The minor suppression of tumour growth rate induced by BCG treatment in the present study might in part be a nonimmunological effect. There is some evidence for such a slight retardive effect on the growth of murine tumours in mice unable to respond immunologically to either BCG or tumour antigens (*Bartlett et al.* 1972). However, in view of the fact that radiostrontium-induced osteosarcomas in mice show a weak tumour-specific antigenicity (*Moore & Williams* 1972), the effect of BCG on tumour-growth observed in the present study is probably immunological in nature, owing to *stimulated* immunological reactivity.

Fig. 15. Area of osteoblastic osteosarcoma, showing stromal cells containing lipoid bodies (L) and areas of degeneration (D) in the cytoplasm. × 25,500.

Fig. 16. Portion of a spindle-shaped cell in fibroblastic osteosarcoma, showing prominent rough endoplasmic reticulum and some mitochondria. The cisternae of the endoplasmic reticulum contain amorphous material of low density. × 14,000.

Fig. 17. Intercellular area in fibroblastic osteosarcoma, showing microvilli. Amorphous material is present extracellularly. × 26,000.

This work was supported by grants from the *Swedish Cancer Society* No 711 B75-03XA and 711 B76-04XB

REFERENCES

Bansal S C & Sjögren H O Correlation between changes in antitumor immune parameters and tumor growth *in vivo* in rats. Federation Proceedings *32* 165 1973

Bartlett G L, Zbar B & Rapp H J Suppression of murine tumour growth by immune reaction to the Bacillus Calmette—Guérin strain of Mycobacterium bovis. J Nat. Cancer Inst. *48* 245 257 1972

Hellström K E, Sjögren H O & Warner G A Demonstration of cell mediated immunity to human neoplasms of various histological types. International Journal of Cancer *7* 1–12, 1971

Hellström K E & Hellström J Lymphocyte mediated cytotoxicity and blocking serum activity to tumor antigens. Advances in Immunology *18* 209–216 1973

Klein G Tumor specific transplantation antigens. G.H.A Clowes Memorial Lecture Cancer Research *28* 625–636 1968

Kumar S Taylor G Steward J K Waghe M A & Pearson A Cellular immunity in Wilms tumor and neuroblastomas, International Journal of Cancer *10* 36–42 1972

Lewis M G Ikonopisov R L Nairn R C Phillips T M Hamilton Fairley G Bodenham D C & Alexander P Tumour specific antibodies in human malignant melanoma and their relationship to the extent of the disease. British Medical Journal *3* 547–555 1969

Mathé G Kamel M Dezfulian M Halle-Pannenko O & Bourut C An experimental screening for "systemic adjuvants of immunity applicable in cancer immunotherapy Cancer Research *33* 1987–1997 1973

Moore M & Williams D E Studies on the antigenicity of radiation-induced murine osteosarcomata. British Journal of Cancer *26* 90–98, 1972

Nilsson A Strontium 90 induced bone and bonemarrow changes. An experimental study with special reference to the histogenesis and histopathology of osteosarcomas. Almqvist & Wiksells Boktryckeri AB Uppsala 1962.

Nilsson A Révész L & Stjernswärd J Suppression of strontium-90-induced development of bone tumours by infection with *Bacillus Calmette Guérin* (BCG) Radiation Research *26* 378–382 1965

Nilsson A, Sundelin P & Sjödén Ultrastructure of ^{90}Sr induced osteosarcomas and early phases of their development Acta radiol. Ther Phys Biol *13* 107–128 1974

Old L J & Boyse E A Specific antigens of tumours and leukaemias of experimental animals. Medical Clinics of North America *50* 901–909 1966

Pearse A G E Histochemistry Theoretical and applied, 3rd Ed., Vol. I J & A Churchill Ltd London 1968 p 710

Southam C M Relationship of immunology to cancer a review Cancer Research *20* 271 282 1960

Sundelin P & Nilsson A Cytoplasmic ultraviolet extinction of strontium-90-induced fibroblastic osteosarcomas correlated to histologic appearance and ultrastructure Acta radiol. Ther Phys. Biol *7* 161–174 1967

Acta path. microbiol. scand. Sect. A, 85 447–454 1977

PRIMARY CEREBRAL MELANOMAS

Report of Six Cases and a Review of the Literature

MARIE BOJSEN-MØLLER

Department of Neuropathology Aarhus Kommunehospital, University of Aarhus, Denmark

Bojsen-Møller M. Primary cerebral melanomas. Report of six cases and a review of the literature. Acta path. microbiol. scand. Sect. A, 85 447–454 1977

Six cases of primary malignant melanoma of the leptomeninges and brain are reported. Three were diagnosed histologically at surgery three at autopsy. Four presented as solitary brain tumours which is unusual compared to other reported cases. In all six there was infiltration of the leptomeninges which must be regarded as the site of origin. Three of the cases have had relatively long survival, two of them have died 2 years after the operation, and the third patient is still alive 18 months after surgery. It is suggested that the frequency of these tumours is underestimated on account of their resemblance to astroblastomas and poorly differentiated astrocytomas, and because biopsies are not always taken from small and atypical haematomas.

Key words: Melanoma; brain; leptomeninges.

Marie Bojsen-Møller Department of Neuropathology Kommunehospitalet, 8000 Aarhus, Denmark.

Received 21.iii.76 Accepted 9.xii.76

Primary melanomas of the central nervous system are considered rare. By 1973 186 cases of primary CNS—melanomas had been described in the literature (6). Six cases were investigated by the author during the period from January 1970 to March 1975 in the Neuropathological Department of Århus Kommunehospital. In none of the six cases was the diagnosis suspected prior to microscopical examination.

The purpose of this paper is to draw attention to the meninges and brain as a primary site of malignant melanoma and to suggest that their frequency is underestimated.

MATERIAL AND METHODS

Three of the six cases both surgical specimens and autopsy material were examined. Two were represented by autopsy material alone. One patient is still alive 18 months after the operation. Further essential data are listed in Table 1 which also gives details regarding examination of the eyes.

Frozen sections were performed on the surgical specimens, and paraffin sections cut from both the surgical and autopsy material.

The following stains were performed: haematoxylin-eosin, van Gieson Hansen, toluidine blue, Weil and Mahon stains for myelin sheaths, Perls stain for haemosiderin and Lillie stain for melanin.

RESULTS

Radiological investigation indicated solitary brain tumours in cases 1, 2, 4 and 6 whereas vascular lesions were suspected in cases 3 and 5.

All patients except one (case 3) underwent surgery and there was no suspicion of melanoma prior to or during operation. In case 1 an intraventricular tumour blocking the foramen Monroi was removed (Fig. 1) and in

This work was supported by grants from the *Swedish Cancer Society* No. 711 B75-03\A and 711 B76-04λB

REFERENCES

Bansal S C & Sjögren H O Correlation between changes in antitumor immune parameters and tumor growth *in vivo* in rats. Federation Proceedings 32 165 1973

Bartlett G L, Zbar B & Rapp H J Suppression of murine tumour growth by immune reaction to the Bacillus Calmette—Guérin strain of Mycobacterium bovis. J Nat. Cancer Inst. *48* 245 257 1972

Hellström K E, Sjogren H O & Warner G A Demonstration of cell-mediated immunity to human neoplasms of various histological types. International Journal of Cancer 7 1–12 1971

Hellström K F & Hellström J Lymphocyte mediated cytotoxicity and blocking serum activity to tumor antigens. Advances in Immunology *18 209-216 1973*

Klein G Tumor specific transplantation antigens. G H.A. Clowes Memorial Lecture Cancer Research *28* 625–636 1968

Kumar S Taylor G., Steward J K Waghe M A & Pearsson A Cellular immunity in Wilms tumor and neuroblastomas International Journal of Cancer *10* 36–42 1972

Lewis M G Ikonopisov R L Nairn R C Phillips T M Hamilton Fairley G Bodenham D C & Alexander P Tumour-specific antibodies in human malignant melanoma and their relationship to the extent of the disease. British Medical Journal 3 547–555 1969

Mathé G Kamel M Dezfulian M, Halle-Pannenko O & Bourut C An experimental screening for "systemic adjuvants of immunity applicable in cancer immunotherapy Cancer Research *33* 1987–1997 1973

Moore M & Williams D E. Studies on the antigenicity of radiation-induced murine osteosarcomata British Journal of Cancer *26* 90-98, 1972.

Nilsson A Strontium 90 induced bone and bone-marrow changes. An experimental study with special reference to the histogenesis and histopathology of osteosarcomas. Almqvist & Wiksells Boktryckeri AB Uppsala, 1962.

Nilsson A Révész L & Stjernswärd J Suppression of strontium-90-induced development of bone tumours by infection with *Bacillus Calmette-Guérin* (BCG) Radiation Research *26* 378 382 1965

Nilsson A Sundelin P & Sjödin Ultrastructure of ^{90}Sr induced osteosarcomas and early phases of their development. Acta radiol Ther Phys Biol *13* 107–128 1974

Old L J & Boyse E. A Specific antigens of tumours and leukaemias of experimental animals Medical Clinics of North America *50* 901–909 1966

Pearse A G E. Histochemistry Theoretical and applied 3rd Ed., Vol. I J & A. Churchill Ltd., London 1968 p 710

Southam C M Relationship of immunology to cancer a review Cancer Research *20* 271 282, 1960

Sundelin P & Nilsson A Cytoplasmic ultraviolet extinction of strontium 90-induced fibroblastic osteosarcomas correlated to histologic appearance and ultrastructure *Acta radiol. Ther.* Phys. Biol *7* 161–174 1967

Fig. 1 (case 1) intraventricular tumour blocking the foramen Monroi, resulting in hydrocephalus (pneumoencephalography)



Fig. 2 Typical histological appearance of a cerebral melanoma. a) many large spheroid cells are seen, some with two nuclei and some pigmented (haematoxylin-eosin × 250) b) heavily pigmented cells are seen together with fine intracytoplasmatic granules and free clumps of melanin (Lillie stain for melanin × 400)

In cases 2, 4 and 6 circumscribed tumours with infiltration of cortex and white matter were found. In case 5 the right temporal lobe was soft, and 75 ml blood aspirated from a deep haematoma but no biopsy was taken. The microscopic examination of the specimens

TABLE 1 *Clinical Data of the Six Cases*

Case	yrs./sex	First symptoms	Duration of symptoms	Opthalmological examination	Radiology	Tumour localization 1) operation 2) autopsy	Melanin	Survival	Comments*
1	19 ♂	Meningitis diplopia headache	6 weeks	Papilloedema, Reduced vision, No tumour	Intraventricular tumour	1) intraventricular (5 cm) 2) ventricular walls, leptomeninges, medulla oblongata	1) 0 2) + + + +	2 yrs.	Primary diagnosis astroblastoma
2	22 ♂	Facial tic dysarthria	6 months	Papilloedema, No tumour	Suspicion of solitary tumour	1) left parietal lobe (4 cm) 2) same site	1) + + + 2) + +	2 mths	
3	44 ♂	Headache paresthesia	4 weeks	Papilloedema, No tumour	Dilated 3rd ventricle	1) no operation 2) leptomeninges	2) + + +	0	Died one day after a pneumography
4	32 ♂	Weakness of right leg	5 weeks	Normal, No tumour	Solitary brain tumour	1) left parietal lobe (3 cm)	1) + + +	18 mths. still alive	
5	55 ♀	Hemiparesis	Few days	Left-sided homonymous, hemianopsia, No tumour	Displacement of right middle cerebral artery	1) right temporal lobe (75 ml "haematoma") 2) cicatrice, ventricles leptomeninges	1) ? 2) + + +	2 yrs.	No biopsy at operation
6	55 ♀	Headache	1 year	Normal No tumour	Solitary brain tumour	1) right temporal lobe (4 cm) 2) same site, insula leptomeninges aqueduct	1) (+) 2) + +	3 mths.	Eyes examined histologically

* Cases 1–6 No melanomas outside the central nervous system.

Fig 1 (case 1) Intraventricular tumour blocking the foramen Monroi, resulting in hydrocephalus (pneumoencephalography)

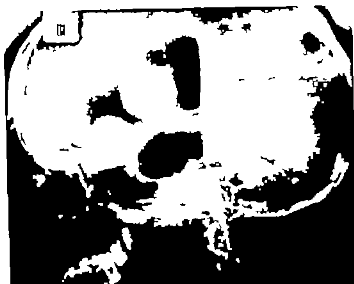


Fig 2 Typical histological appearance of cerebral melanoma. a) many large spheroid cells are seen, some with two nuclei and some pigmented (haematoxylin-eosin × 250) b) heavily pigmented cells are seen together with fine intracytoplasmatic granules and free clumps of melanin (Lillie stain for melanin × 400)

...ses 2, 4 and 6 circumscribed tumours with infiltration of cortex and white matter were found. In case 5 the right temporal lobe was soft, and 75 ml blood aspirated from a deep haematoma but no biopsy was taken. The microscopic examination of the specimens



Fig 3 (case 6) malignant melanoma appearing as a solitary brain tumour A faint pigmentation is seen (O)

from cases 1, 2 4 and 6 revealed highly cellular tumours composed of small round or polyhedral cells with round nuclei and large spheroid cells with peripherally placed often indented nuclei prominent nucleoli and a bulky eosinophilic cytoplasm (Fig 2 a) Several large cells containing 2–3 nuclei were present and mitoses varied from numerous to sparse.

The cells were arranged in compact clusters or small groups with a tendency to a perivascular rosette arrangement In case 1 no pigment was present which was the reason for the primary diagnosis of astroblastoma but in cases 2 4 and 6 varying amounts of melanin were found (Table 1) Some areas were pigmented to such a degree that cellular detail was masked while in other areas small pigment granules could be found in the cytoplasm or between the tumour cells (Fig 2 b)

On account of the biopsy diagnosis of melanoma in these three patients thorough clinical examination was performed but no primary tumour outside the central nervous system could be found. One patient is still alive and well 18 months after the operation.

The autopsy results are seen in Table I and it should be noted that no melanomas were found outside the central nervous system There was no discoloration of the surface of the brain to arouse suspicion of a melanoma not even in those cases previously diagnosed but thickenings of the leptomeninges were noticed in cases 1 3 and 5 A

Fig 4 (case 1) a) remaining tumour on ventricular wall (→) b) heavily pigmented tumour of the leptomeninges. Note the perivascular infiltration of the cortex (→) c) tumour infiltration around cranial nerves (→) d) invasion of vessel wall by melanoma. a, b c and d haematoxylin-eosin × 100

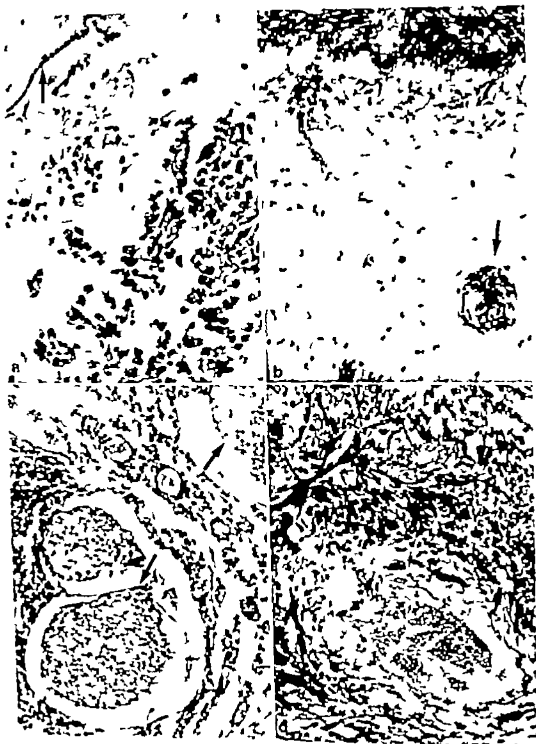

a
b



Fig 5 (case 6) a) growth pattern of tumour from the leptomeninges into the cerebral cortex (haematoxylin-eosin × 100) b) higher magnification of the tumour in the leptomeninges (haematoxylin-eosin × 250)

large residual tumour was seen in case 6 with a faint bluish colour in some areas (Fig 3) and the microscopic examination of all the operated cases revealed tumour infiltration in all the surgical fields with cells identical to those of the surgical specimens and with varying degrees of pigmentation In the tumour infiltrations on the ventricular walls the cellular pattern was the same and the pigment sparse (Fig 4 a) but when the tumour spread along the leptomeninges spindle shaped heavily pigmented cells were dominant in some areas (Fig 4 b c and d) whereas other areas were characterized by spheroid cells (Fig 5 a and b)

In cases 1 3 and 6 tumour cells were seen in the spaces of Robin—Virchow (Fig 4 b and 5 a) which explains the tumour in the central part of the medulla oblongata in case 1 (Fig 6)

DISCUSSION

As the skin is the site of predilection for melanomas and the central nervous system one of the unusual primary sites, caution must be taken in accepting a melanoma as a primary brain tumour (8)

In addition primary cerebral melanomas have the same growth pattern and cellular appearance as melanoma metastases to the brain so that either intense clinical investigation or autopsy must be performed in suspected cases of primary CNS—melanomas in order to rule out melanomas at other sites

If melanomas are found in other organs the author agrees with *Gibson et al* (1957) that such tumours should be rejected as primary CNS—melanomas in as much as brain tumours very seldom spread to other organs

Melanin bearing cells are normally found in the leptomeninges in adults but are seldom



Fig 6 (case 1) central tumour of the medulla oblongata (no myelin sheaths) (→) Mahon's stain for myelin sheaths.

noticed at sites other than the ventral surface of the medulla oblongata and the upper cervical spinal cord (14). However it is a personal experience that sparse amounts of melanin may sometimes be found in the leptomeninges of any of the lobes.

This pigmentation may be pronounced without a coexistent neoplasm as mentioned in the papers on neurocutaneous melanoses by *van Bogaert* (1948) and *Touraine* (1949).

Most papers on malignant melanomas of the central nervous system deal with a diffuse melanosis of the leptomeninges (2, 5, 9 and 10) and some of the reported cases present the neurocutaneous melanosis syndrome.

Circumscribed melanomas of the brain have also been reported (1, 7) but even if a solitary tumour of the brain or spinal cord is found, the origin of the tumour is the melanin bearing cells of the leptomeninges (14) which is illustrated by the growth pattern in Fig. 4 b and 5 a.

Four of the six cases referred to here are unusual because they presented as solitary brain tumours (cases 1, 2, 4 and 6). In addition survival has been relatively long in three of them (case 1, 4 and 5) compared to other reported cases. Only *Christensen* (1941) and *Gibson et al.* (1957) have reported cases of long survival, 2 years and 18 months respectively.

Two cases (1 and 5) deserve special attention. Case 1 because the patient had been admitted to hospital with a suspected meningitis and 6 months later readmitted to the neurosurgical department. Here the primary histological diagnosis was astroblastoma because no melanin pigment was found in the surgical specimen. Amelanotic melanoma should always be considered in the differential diagnosis of astroblastoma and poorly differentiated astrocytoma as emphasized by *Rubinstein* (12, 13).

However the autopsy material revealed

sparse pigment in the remaining tumour on the ventricular wall and extensive pigmentation of the meninges. Moreover this patient had von Recklinghausen's disease and neurofibromas had previously been removed from the skin. This case is very similar to the one reported by *Bjorneboe* (1935) and it is known that this neurocutaneous disorder may be associated with other intracranial neoplasms such as gliomas, meningiomas and acoustic neurinomas (11).

In case 5 no biopsy was taken during the operation for a suspected vascular lesion, but examination of the brain at autopsy revealed a typical pigmented melanoma. Therefore biopsies ought to be taken from small and atypical haematomas as a good deal of melanin may be present even if it cannot be detected macroscopically.

These two cases may explain why primary melanomas of the central nervous system are infrequently diagnosed. When melanomas are only slightly pigmented they may be mistaken for astroblastomas or poorly differentiated astrocytomas, and when haemosiderin is present in the tumours, melanin and melanoma cells are easily overlooked. Thus an iron stain is essential in order to distinguish betaween the two types of pigment and should always be followed by one of the stains for melanin.

REFERENCES

1. *Arnvig J.* & *Christensen E.* Primary benignant intracranial melanoma. Acta Chir. Scand. 82: 218–226, 1939.
2. *Bhatia R.* Primary melanomas of the central nervous system. J. Oslo City Hosp. 24: 57–68, 1974.
3. *Björneboe M.* Primäres Melanosarkom des Gehirns, massenhafte Naevi pigmentosi der Haut, ausgedehnte Neurofibromatose der Hautnerven. Frankfurt. Ztschr. Path. 47: 363–373, 1935.
4. *Bogaert M. L. van.* La Mélanose neurocutanée diffuse hérédofamiliale. Bull. Acad. Roy. Med. Belgique. 13: 397–428, 1948.
5. *Boxton J.* Primary melanoma of the leptomeninges. J. Clin. Path. 11: 12? 127, 1958.
6. *Budka H.* & *Pantucek F.* Primäre diffuse Melanoblastosen der Meningen und neurokutane Melanosen. Neurochirurgia. 16: 90–98, 1973.
7. *Christensen E.* Two cases of primary intracranial melanoma. Acta Chir. Scand. 85: 90–98, 1941.
8. *DasGupta T. K.*, *Brasfield R. D.* & *Paglia, M. A.* Primary melanomas in unusual sites. Surg. Gynec. & Obst. 128: 841–848, 1969.
9. *Gibson J. B.*, *Burrows D.* & *Weir W. P.* Primary melanoma of the meninges. J. Path. & Bact. 74: 419–438, 1957.
10. *Hüning K. J.* Malignant melanoblastosis of the leptomeninx. Beitr. Path. 152: 200–205, 1974.
11. *Rodriguez H. A.* & *Berthrong M.* Multiple primary intracranial tumors in von Recklinghausen's neurofibromatosis. Arch. Neurol. 14: 467–475, 1966.
12. *Rubinstein L. J.* Tumors of the central nervous system. Atlas of tumor pathology, series 2, fasc. 6. Armed Forces Institute of Pathology. Washington, D.C. 1972, p. 49.
13. *Rubinstein L. J.* Tumors of the central nervous system. Atlas of tumor pathology, series 2, fasc. 6. Armed Forces Institute of Pathology, Washington, D.C. 1972, p. 378.
14. *Russell D. S.* & *Rubinstein L. J.* Pathology of tumours of the nervous system, 3rd ed. Edward Arnold (Publishers) Ltd. London 1971, p. 40–41.
15. *Touraine A.* Les Mélanoses Neuro-cutanées. Ann. Dermat. 9: 489–524, 1949.

Acta path. microbiol. scand. Sect. A, 85 455–460, 1977

NUCLEAR DNA CONTENT OF PARATHYROID CELLS IN ADENOMAS HYPERPLASTIC AND NORMAL GLANDS

A. Bengtsson, L. Grimelius, H. Johansson and J. Pontén

Departments of Pathology and Surgery University of Uppsala, Sweden

Bengtsson, A. Grimelius, L., Johansson, H. & Pontén J. Nuclear DNA-content of parathyroid cells in adenomas, hyperplastic and normal glands. Acta path. microbiol. scand. Sect. A, 85 455–460, 1977

Nuclear DNA-content in parathyroid cell imprints from adenomas, hyperplastic and normal glands was determined. Two principally different staining procedures were applied pararosaniline-Feulgen and ethidium-bromide staining. All nuclei, particularly with the ethidium-bromide method were registered as containing even multiples of the normal human diploid DNA-content. Normal and hyperplastic glands showed ≥98 per cent diploid nuclei, the remaining fraction was tetraploid. In adenomas the frequency of diploid nuclei varied from 50–98 per cent the remaining were predominantly tetraploid, but octaploid and higher even ploidy also occurred. A good correlation was found between nuclear DNA-content and nuclear diameter. The findings indicate that determination of nuclear DNA-content of parathyroid cells may be a valuable contribution in the differentiation between hyperplasia and adenoma.

Key words: Parathyroid glands, nuclear DNA, cytofluorescence.

Allan Bengtsson, Department of Pathology, University of Uppsala, P.O. Box 553, S-751 22 Uppsala 1, Sweden.

Received 20.xii.76 Accepted 20.xii.76

In some parathyroid adenomas a pronounced nuclear size variation of the parenchymal cells occurs. Empirically this "atypia" has been found not to be correlated with malignancy, but its cause remains unknown. A slight nuclear size variation can also be seen in hyperplastic glands and rarely in normal parathyroids, but again the significance of these findings was not clear.

One important determinant of nuclear size is DNA-content. The principal aim of the present study is to correlate the nuclear DNA content with the histopathological diagnosis of parathyroid diseases, the clinical symptoms and the glandular weight, since the latter is often used as a simple indicator of endocrine activity. Cytofluorometric technique was used for the DNA-determination. Two principally different staining procedures were applied: pararosaniline Feulgen and ethidium bromide staining. The possibility of replacing the DNA measurements with simple measurements of nuclear diameters was also investigated.

MATERIAL AND METHODS

DNA-analyses of individual cell nuclei were performed on 66 parathyroid glands, including 23 solitary adenomas, 24 hyperplastic glands and 19

glands of normal size and histological appearance. The glandular specimens were from 38 surgical cases and one autopsy case. Of the hyperplastic glands 12 were from patients with primary hyperparathyroidism (HPT) and 12 from patients with secondary HPT (four of these glands were from the autopsy case). The normal-size glands were from patients with parathyroid adenomas or goitre.

The histopathological diagnosis of adenoma was based on the findings of either that there was a remnant of normal glandular tissue outside the connective tissue capsule or that the largest of the non-adenomatous glands showed a normal weight (<50 mg) and histology. The diagnosis of hyperplasia was based on enlargement of all glands and lack or reduction of the fat-cell content. Patients with HPT were followed postoperatively during 1–? years with regard to clinical symptoms, serum calcium and urinary calcium excretion. No relapse occurred.

The removed glandular specimens were weighed and cut into two or more pieces. Imprints were made from moist cut surfaces on five glass slides which were immediately fixed in a mixture of acetone and ethanol (1:1) for 30 min at room temperature. Four of the slides were then air-dried and stored over a desiccant until the DNA staining (see below). The fifth slide was stained with eosin-haematoxylin for light microscopy.

The glands were fixed in 10 per cent neutral formalin, dehydrated and embedded in paraffin. 5 µm thick deparaffinized sections were stained with haematoxylin-eosin according to van Gieson's method.

Cytofluorometric DNA analysis of individual cell nuclei was performed using two different staining procedures.

1. Pararosaniline-Feulgen staining

The cells were hydrolyzed in 4 M HCl at 25 C for 40 min and then washed in 0.1 M HCl and stained for two hours in a 0.2 per cent pararosaniline solution 0.045 M in potassium metabisulphite and 0.3 M in HCl. The slides were then washed three times for five minutes in SO water (10 per cent NaHSO in 0.05 M HCl) and then dehydrated in 50 per cent, 70 per cent, 96 per cent and 99 per cent ethanol, each time for five minutes. The slides were then transferred into a mixture of xylene and ethanol (1:1) and then into pure xylene, each for 5 minutes. The preparations were briefly air-dried and mounted in glycerol.

2. Ethidium bromide staining

The preparations were incubated in ribonuclease from bovine pancreas (30 Kunitz/ml) for one hour at 37 C and then stained in ethidium bromide (10 mg/l, pH 7.5, 0.1 M in Tris and 0.1 M in NaCl) for 30 minutes at 25 C. The solution was renewed after 15 minutes. The preparations were mounted in the staining solution.

The fluorescence measurement was carried out on a Zeiss microscope fluorometer equipped with the following filter combination: exciter filter BP 546, beam splitter FT 580 and barrier filter LP 590. An uranyl glass standard was used for control of the stability of the fluorometer.

The DNA-contents of 50 to 200 non-overlapping randomly selected nuclei were measured in each imprint preparation. Human lymphocytes were used as controls on each staining occasion and given the value 2, denoting the normal human diploid DNA-content.

In imprint preparations from three adenomas DNA and nuclear diameter estimations were performed on the same individual cells. The diameters were measured with an ocular micrometer in a phase-contrast microscope.

RESULTS

Light Microscopy

In most adenomas, hyperplastic and normal glands, chief cells predominated. Two adenomas were of the oxyphil type while another two contained an almost pure population of dark chief cells. The oxyphil and transitional oxyphil cell types were also seen in some adenomas and hyperplastic glands in varying frequency, localized in single positions, groups or nodules. In the normal glands the oxyphil and transitional oxyphil cells were few in number. Transitional water-clear cells were seen in some adenomas and hyperplastic glands.

No mitosis was seen in the examined glands.

The imprint preparations showed in some areas whole cells, in others only nuclei. It appeared that the oxyphil and transitional oxyphil cells often retained the cytoplasm, while the chief cells were sometimes represented as bare nuclei.

Nuclear DNA-determination

The stoichiometry of the DNA staining with ethidium bromide of cells from parathyroids as wells from parathyroid adenomas and hyperplastic glands appeared to be in

Fig 1 Ethidium bromide staining. Histogram of DNA-content in peripheral lymphocytes and in parenchymal cells from three cases of different diagnoses.

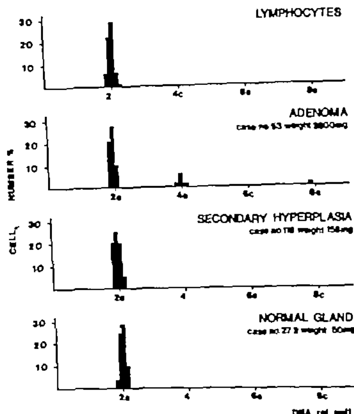


TABLE 1 *Comparison of Ethidium Bromide and Feulgen in Staining Parenchymal Cell Human Peripheral Lymphocytes used as Reference Cells and given the Value 2*

Histopathological diagnosis	Ethidium bromide M ± SD 2 C	4 C	8 C	Feulgen M ± SD 2 C	4 C	8 C
Adenomas	1 93 ± 0 07 n = 36	3 93 ± 0 11 n = 28	7.90 ± 0.50 n = 6	2.48 ± 0.25 n = 19	4.80 ± 0 53 n = 7	10 1 ± 0 9 n = 4
Hyperplastic glands	1 95 ± 0 10 n = 19	–	–	2.30 ± 0.30 n = 8	–	–
Normal glands	1 98 ± 0 02 n = 18	–	–	2.32 ± 0.30 n = 1	–	–

C ploidity n number of specimens

good agreement with the staining of peripheral lymphocytes (Fig 1 Table 1) The corresponding staining according to *Feulgen's* method showed, however a slightly stronger uptake of dye in the parenchymal cells than in the lymphocytes (Fig 2, Table 1) In each case however the staining of tetraploid cells well equalled the double value of diploid cells.

It is notable that even in cases of very high frequency of polyploid cells there were extremely few cells with DNA-contents between even diploid multiples.

In all normal and hyperplastic glands the

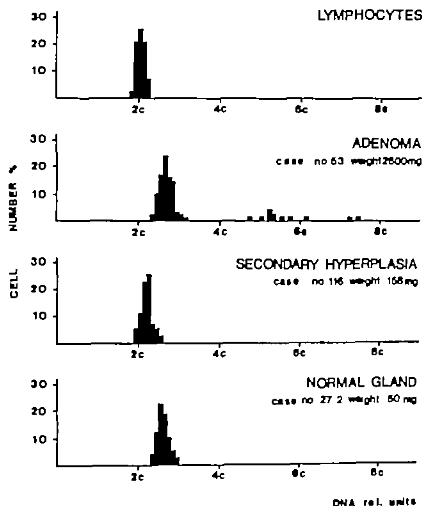


Fig 2 Feulgen staining. Histograms of DNA-content in cells from the same cases as in Fig 1

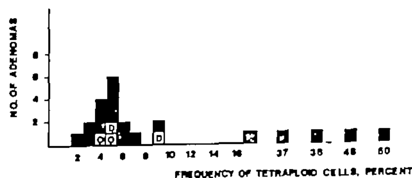


Fig 3 The distribution of the frequency of tetraploid cells in parathyroid adenomas. O means oxyphil adenoma, D means adenoma containing almost a pure population of dark chief cells

diploid cells predominated and the frequency of tetraploid cells was less than 1 per cent with the exception of 2 of 12 hyperplastic glands in patients with secondary HPT where the frequency was about 2 per cent. Also in the adenomas the diploid cells predominated but the frequency of tetraploid cells varied from 2 up to about 50 per cent (Fig 3). The distribution of nuclear DNA in the two oxyphil and the two pure dark cell adenomas fall within the range of the entire groups of adenomas (Fig 3). The frequency of the polyploid cells in the various histopathological groups is shown in Table 2.

Cells of higher ploidity than four were often seen in adenomas, but never in hyperplastic or normal glands.

The frequency of tetraploid cells in adenomas varied in different areas of the glands as evidenced from a comparison between dif

TABLE 2. *The Frequency of Tetraploid (4 C) and Octoploid (8 C) Cells in Different Diagnoses*

Histological diagnosis	Number of specimens	Mean frequency of polyploid cells, per cent	
		4 C	8 C
Adenomas			
Group I	19	5 (range 2 17)	<1
Group II‡	4	44 (range 37 50)	2
Hyperplastic glands			
Primary and	12	<1	0
secondary	10	<1	0
secondary		<2	0
Normal glands	19	<1	0

Group I = adenomas with frequency of tetraploid cells less than 25 per cent.
‡ Group II = adenomas with frequency of tetraploid cells higher than 25 per cent.

ferent imprints from the same lesion. This variation was most pronounced in adenomas with a high frequency of tetraploid cells.

The results of the estimation of the nuclear diameters are given in Table 3. The variation of nuclear diameters of cells of the same ploidity is low compared to the difference in diameters of cells with different ploidity.

TABLE 3. *Nuclear Diameters of Polyploid Cells Compared to Those of Diploid Cells*

Case	Nuclear diameters M ± SD		
	2 C	4 C	8 C
1	1.00±0.06 n=16	1.26±0.07 n=6	
2	1.00±0.04 n=7	1.29±0.06 n=7	–
3	1.00±0.09 n=7	1.28±0.07 n=6	1.70±0.10 n=5

C ploidity n = number of specimens

No correlation was found between the frequency of tetraploid cells and the weight of the adenomas nor to the serum calcium level or the type and duration of the symptoms (kidney-stone disease, tiredness, muscular weakness, mental symptoms).

DISCUSSION

Generally speaking results from cytochemical DNA-determinations are difficult to interpret. The principal reason for this seems to be that the stoichiometry of the staining reactions varies with different types of cells as well as with varying activity states of the cell (6). When comparing our results from the two DNA-techniques of normal and pathologically changed parathyroid glands it was evident that the Feulgen technique gave higher values and larger variation than those of the ethidium-bromide method. The reason for this greater variation with the Feulgen technique is not clear but it may reflect structural variations in the deoxyribonucleoprotein complex at varying cell activity (1 4 5 7).

The most striking result was that the nuclear "atypia" found in varying frequency especially in adenomas appeared to consist of nuclei with higher even ploidity. The frequency of tetraploid cells was, with a few exceptions, higher in the adenomas compared with that of hyperplastic and normal glands. Cells with higher ploidity than tetraploidity were only found in parathyroid adenomas. However it must be pointed out that the rather few cases of hyperplasia have only been of chief cell type.

The mechanism of tetraploidization in parathyroid adenoma is unknown. Our methods do not distinguish between diploid cells

in the G 2 phase of the cell cycle and genuine tetraploids in G 1 The fact that practically no intermediate values were found indicates that the process which led to tetraploidization was either very slow or had already finished at the time of operation

A high proportion of polyploid cells was noted by *Eneroth et al* (2 3) in pleomorphic salivary gland adenomas. These authors found an increasing frequency of polyploid cells with increasing duration of the disease and higher frequency seemed to predispose to a secondary development of salivary gland carcinoma In our study however no such correlations were found

In all hyperplastic and normal glands the frequency of tetraploid cells was low and no differences could be demonstrated between hyperplasia of primary (chief cells) and secondary types. Nor did the normal sized glands removed in connection with thyroid surgery or parathyroid adenomas show any differences in frequency of tetraploid cells as compared with the hyperplastic glands.

In imprint preparations of parathyroid glands the cell nuclei appeared to be spherical and similar in size in the same ploidity This was especially the case if the cells were well separated from each other The DNA-content was strongly correlated to the nuclear diameters. The standard deviation of the diameter for each ploidity was low enough to make it possible to distinguish between cells of different ploidity simply by measuring the diameters.

Sometimes difficulties appear in differentiating a hyperplastic gland from an adenoma where the adenoma criteria (a) normal glandular tissue outside the connective capsel and/or (b) apparent nuclear atypia" are lost. *In such a situation* the determinations of nuclear DNA-content or nuclear diameter might be of value. More than 2 per cent tetraploids strongly favour the diagnosis of adenoma

---

This investigation was supported by the *Swedish Medical Research Council* (Project No. B77 17X 04787-02)

REFERENCES

1 *Bolund L. Ringertz N R. & Harris H* Changes in the cytochemical properties of erythrocyte nuclei reactivated by cell fusion J Cell Sci. *4* 71–87 1969
2 *Eneroth C M & Zetterberg A* Nuclear DNA content as a criterion of malignancy in salivary gland tumours of the oral cavity Acta Otolaryng (Stockh) *75* 296–298 1973.
3 *Eneroth C M & Zetterberg, A.* Microspectrophotometric DNA analysis of malignant salivary gland tumours Acta Otolaryng (Stockh) *77* 289–294 1974
4 *Garcia A M* Studies on deoxyribonucleic acid in leukocytes and related cells of mammals VI The Feulgen-deoxyribonucleic acid content of rabbit leukocytes after hypertonic treatment. J Histochem. Cytochem *17* 47 55 1969
5 *Gledhill B L. Gledhill M P., Rigler R & Ringertz N R* Changes in deoxyribonucleoprotein during spermiogenesis in the bull Exp Cell Res. *41* 652–665 1966.
6 *Ringertz N R* Handbook of Molecular Cytology Ed Lima De-Favia A (Amsterdam, North Holland Co.) 1969 p 656
7 *Ringertz N R & Bolund L.* Activation of hen erythrocyte deoxyribonucleoprotein Exp Cell Res. *55* 205–215 1969

Acta path. microbiol. scand. Sect. A, 85 461–469 1977

PRIMARY CARCINOMA OF THE LIVER

A Histological Study of 27 Cases of Primary Carcinoma of the Liver from Malawi

KAI NØRREDAM

Departments of Medicine, Queen Elizabeth Central Hospital, Blantyre, and Zomba General Hospital, Zomba, Malawi, and University Institute of Pathological Anatomy Copenhagen, Denmark

Nørredam, K. Primary carcinoma of the liver. A histological study of 27 cases of primary carcinoma of the liver from Malawi. Acta path. microbiol. scand. Sect. A, 85 461–469 1977.

Liver biopsies from 27 Bantu patients with primary carcinoma of the liver from Malawi were examined histologically. All the biopsies showed hepatocellular carcinoma (HCC). Structurally the tumours consisted of trabeculae or groups of such, separated by a variable amount of connective tissue which in a few cases was so pronounced that the tumour had a scirrhous character. Estimation of the grade of differentiation showed 3 cases to be of grade I, 10 of grade II, 3 of grade III and 8 of grade IV. The grade could vary in tumour tissue from the same patient, but never extremely so. The histological structure did not differ significantly from that found in other African and Caucasian series. The reticulin structure of tumour tissue was found distinctly different from that of benign tissue and thus an important tool in the differential diagnosis between HCC grade I and normal or cirrhotic liver tissue. Out of 15 patients 12 had cirrhosis which was of the postnecrotic type.

Key words: Malawi; African Bantus; primary carcinoma of the liver; cirrhosis.

Kai Nørredam, Esperance Alle 9, 2920 Charlottenlund, Denmark.

Received 20.iii.76 Accepted 12.i.77

Primary carcinoma of the liver (PCL) is one of the most frequent malignant diseases in the tropics. In subsaharan Africa PCL constitutes from 10 to 30 per cent of all malignant tumours. In Malawi in South East Africa this relative incidence was found to be 15.8 per cent (*Cook & Burkitt* 1971). As there were no other published data about this disease in Malawi, the author decided to undertake a prospective investigation with the purpose of examining some relevant aspects of PCL in that country. Epidemiological, clinical, biochemical and serological data have been published elsewhere (*Nørredam* 1977). The present study describes the histological findings.

MATERIAL AND METHODS

The study comprises of 27 Bantu Africans with PCL, admitted consecutively from March, 1971 to April, 1972 to the Departments of Medicine, Queen Elizabeth Central Hospital and Zomba General Hospital in the southern part of Malawi. There were 21 men and 6 women. The age varied from 21 to 65 years, the average being 42.2 years. Liver biopsies were performed during laparotomy in 5 patients, and percutaneously using the Menghini technique in 22 cases. The following staining techniques were used: Haematoxylin and eosin (H & E), van Gieson-Hansen, periodic acid-Schiff (PAS) before and after digestion with diastase, and staining for reticulin (*Gordon & Sweet* 1936) and iron (*Perls* 1867). In a few cases the Alcian technique was used. The tumours were typed histologically according to *Anthony* (1973). The degree of differentiation of the tumours was estimated using the criteria described by *Edmondson* (1958).

RESULTS

Classification

Histological examination of the biopsies from the 27 patients showed exclusively hepatocellular carcinoma (HCC) There were thus no cases of cholangiocellular carcinoma (CCC) cholangiolocellular carcinoma (CLCC) or mixed HCC and CCC

Histological Structure of HCC

The tumour tissue consisted in most cases of from 4 to about 50 cells thick trabeculae which in longitudinal sections were cylindric ally shaped with blunt ends or irregularly anastomosing and in cross-sections roundish, compact groups of cells. The trabeculae were separated by blood filled cavities. They were always covered on their outer surface with a single layer of endothelial cells (Figs. 1 and 7) and further coated with reticulin fibres (Fig 15) The exact relationship between endothelial cells and reticulin could not be discerned by light microscopy With the exception of the case of haemochromatosis these endothelial cells never showed any signs of phagocytocic activity The trabeculae contained only tumour cells, i.e. neither blood vessels nor connective tissue Very often the centre of the trabeculae was necrotic, containing cell debris and pyknotic tumour nuclei (Fig 1) The necrotic material seemed to disappear gradually forming empty cavities. In some cases these cavities developed into glandular structures, so-called acini (Fig 2) which often contained PAS-positive material In the present study bile could not be identified in the acini The tumour cells, facing the lumen of the acini were often cubic or columnar in shape (Fig 2) and naked on their luminal surface i.e covered with neither endothelial cells nor reticulin fibres. A very characteristic feature was the scarcity of reticulin inside the trabeculae only a few frail fibres being present here and there between the tumour cells, contrasting the elaborate reticulin network of benign liver tissue (Figs. 3 and 4 5 and 6 8 11 and 12 15) Furthermore using the reticulin staining technique the cytoplasm and especially the nuclei were stained rather markedly while benign liver cells were left unstained (Figs. 4 and 8)

In a number of cases one had the immediate impression of a more massive tumour tissue, but a careful study much aided by the reticulin staining technique, showed the tissue to consist of trabeculae as described above but closely packed, being separated from each other only by their endothelial and reticular covering although an occasional small area with loose collagenous connective tissue with small blood vessels was seen (Fig 8) In some cases the tumour contained more connective tissue trabeculae or bundles of trabeculae being separated by a rather abundant, loose collagenous connective tissue containing a fair number of blood vessels (Fig 9) Three cases were characterized by large amounts of dense connective tissue stroma in which trabeculae or small islands of tumour tissue were embedded giving the appearance of a scirrhous cancer (Fig 10)

Using the classification of *Anthony* (1973) the tumours could according to their histological structure, be typed into hepatic (14 cases) pleomorphic (6 cases) adenoid (2 cases) clear-cell (2 cases) and scirrhous (3 cases) varieties

Where tumour tissue bordered on benign tissue the 2 components were often separated

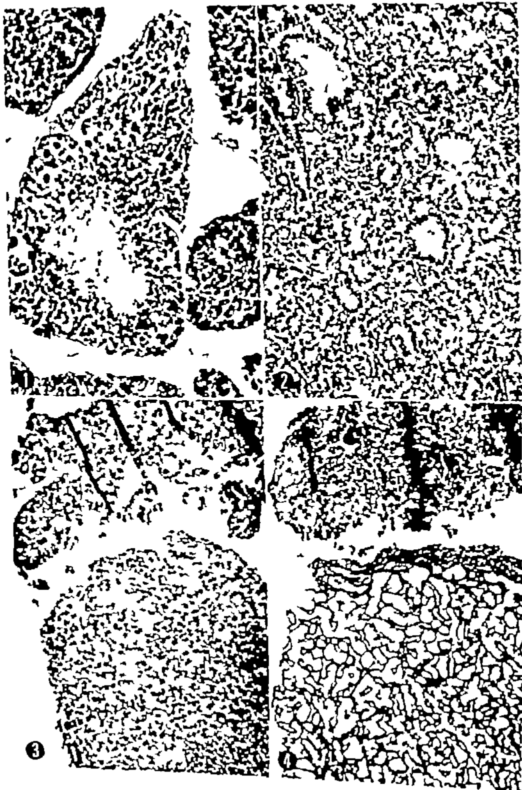
---

Fig 1 HCC, grade II The trabeculae are covered by a single layer of endothelium. In the centre can be seen a necrosis, containing cell debris and pyknotic nuclei H & E, × 210

Fig 2 HCC grade II There are numerous acini H & E × 210

Fig 3 HCC grade I Below a cirrhotic regeneration nodule. Above highly differentiated tumour tissue The vertical lines are artefacts. H & E, × 210

Fig 4 HCC, grade I Same area as Fig 3 The tumour tissue (above) contains very few fine reticulin fibres. The cytoplasm and even more so the nuclei of the tumour cells are stained in contrast with the cells in the regeneration nodule (below) Reticulin stain, × 210


1
2
3
4

RESULTS

Classification

Histological examination of the biopsies from the 27 patients showed exclusively hepatocellular carcinoma (HCC) There were thus no cases of cholangiocellular carcinoma (CCC) cholangiolocellular carcinoma (CLCC) or mixed HCC and CCC

Histological Structure of HCC

The tumour tissue consisted in most cases of from 4 to about 50 cells thick trabeculae which in longitudinal sections were cylindrically shaped with blunt ends or irregularly anastomosing and in cross sections roundish compact groups of cells The trabeculae were separated by blood filled cavities. They were always covered on their outer surface with a single layer of endothelial cells (Figs. 1 and 7) and further coated with reticulin fibres (Fig 15) The exact relationship between endothelial cells and reticulin could not be discerned by light microscopy With the exception of the case of haemochromatosis, these endothelial cells never showed any signs of phagocytocic activity The trabeculae contained only tumour cells, i e neither blood vessels nor connective tissue Very often the centre of the trabeculae was necrotic containing cell debris and pyknotic tumour nuclei (Fig 1) The necrotic material seemed to disappear gradually forming empty cavities. In some cases these cavities developed into glandular structures so-called acini (Fig 2) which often contained PAS-positive material. In the present study bile could not be identified in the acini The tumour cells facing the lumen of the acini were often cubic or columnar in shape (Fig 2) and naked on their luminal surface i e covered with neither endothelial cells nor reticulin fibres. A very characteristic feature was the scarcity of reticulin inside the trabeculae only a few frail fibres being present here and there between the tumour cells, contrasting the elaborate reticulin network of benign liver tissue (Figs. 3 and 4 5 and 6 8 11 and 12 15) Furthermore using the reticulin staining technique the cytoplasm and especially the nuclei were stained rather markedly while benign liver cells were left unstained (Figs 4 and 8)

In a number of cases one had the immediate impression of a more massive tumour tissue but a careful study much aided by the reticulin staining technique, showed the tissue to consist of trabeculae as described above but closely packed, being separated from each other only by their endothelial and reticular covering although an occasional small area with loose collagenous connective tissue with small blood vessels was seen (Fig 8) In some cases the tumour contained more connective tissue trabeculae or bundles of trabeculae being separated by a rather abundant, loose collagenous connective tissue containing a fair number of blood vessels (Fig 9) Three cases were characterized by large amounts of dense connective tissue stroma in which trabeculae or small islands of tumour tissue were embedded giving the appearance of a scirrhous cancer (Fig 10)

Using the classification of *Anthony* (1973) the tumours could according to their histological structure be typed into hepatic (14 cases) pleomorphic (6 cases) adenoid (2 cases) clear-cell (2 cases) and scirrhous (3 cases) varieties.

Where tumour tissue bordered on benign tissue the 2 components were often separated

---

Fig 1 HCC, grade II The trabeculae are covered by a single layer of endothelium. In the centre can be seen a necrosis containing cell debris and pyknotic nuclei *H & E*, × 210

Fig 2 HCC grade II There are numerous acini H & E × 210

Fig 3 HCC grade I Below a cirrhotic regeneration nodule Above, highly differentiated tumour tissue. The vertical lines are artefacts. H & E, × 210

Fig 4 HCC, grade I Same area as Fig 3 The tumour tissue (*above*) contains very few fine reticulin fibres. The cytoplasm and even more so the nuclei of the tumour cells are stained in contrast with the cells in the regeneration nodule (below) Reticulin stain, × 210

by a layer of collagenous connective tissue in such cases compression and atrophy of the benign cells were seen (Figs. 5 and 6). In other cases the normal liver plates were replaced by tumour cells (Figs. 11 and 12).

In biopsies from 2 patients tumour emboli were found in small veins.

In 11 of the biopsies haemorrhages were seen in tumour tissues. This was never a feature of benign liver tissue.

In 12 cases there were necroses in the malignant tissue, usually in the centre of the trabeculae as described above. In other cases necroses of larger tumour masses were observed. Necroses were never found in benign liver tissue.

Accumulation of bile was seen in benign hepatocytes in 4 biopsies, and in malignant cells in 1 case. Bile plugs were found in 2 cases in benign tissue, but never in malignant tissue.

Fatty changes were seen in malignant cells in only one case (Fig. 5) and never in benign liver cells.

There were 2 cases of clear-cell-type tumours. In both, the phenomenon was not uniform, but presented rather as clear-cell areas scattered in tumour tissue of the usual type (Fig. 13). The clear cytoplasm, when stained with the PAS technique showed PAS-positive, fine perinuclear granules.

PAS-positivity of the benign hepatocytes was seen in only 6 cases and was pronounced in only 3 of these. The stain was negative after digestion with diastase. Except for the 2 cases of clear-cell type tumours, malignant cells were in no cases PAS-positive (Fig. 14).

Cytology and Grade of Differentiation

In 26 cases where the biopsy contained sufficient tumour tissue to evaluate the grade of differentiation, the following distribution was found. Grade I (3 cases): The cells resemble normal hepatocytes so much that the diagnosis can only be made on the histological structure and in particular the characteristic composition of the reticulin (Figs. 3 and 4, 5 and 6). Grade II (10 cases): The malignant cells look very much like normal hepatocytes, but the nuclei are larger and more hyperchromatic and the cytoplasm is abundant and eosinophilic; the cell borders are distinct; there may be acini (Fig. 2). Grade III (5 cases): The nuclei are larger and more hyperchromatic, the cytoplasm is less abundant, as well as less granular and acidophilic than in grade II; there are many giant tumour cells (Fig. 7). Grade IV (8 cases): The nuclei are intensely hyperchromatic, there is very little cytoplasm with few granules, and the cell borders are indistinct, often with no cohesion. There may be areas with spindle cells or oat-cells. Tumour thrombi in the blood vessels are most frequent in grade IV (Fig. 10). The cells of grade III and grade IV tumours often contained intranuclear vacuoles (Fig. 11), shown by electron microscopy to be *cytoplasmatic invaginations* (*Nørredam* unpublished work). Quite often the grade of differentiation varied from one area of the biopsy to another, but never extremely so.

The reticulin structure of grade I tumours was distinctly different from the structure in normal and cirrhotic liver tissue, but did not differ in any predictable or regular way in different grades of malignancy.

Fig. 5. HCC, grade I. The highly differentiated tumour tissue (below) is separated from normal liver tissue (above) by a layer of collagenous connective tissue. There is fatty degeneration of some of the malignant cells. H & E, × 210.

Fig. 6. HCC, grade I. Same area as Fig. 5. Tumour tissue (below) is easily distinguishable from benign liver tissue (above). Reticulin stain, × 210.

Fig. 7. HCC, grade III. The surface of the trabecula is covered by a single layer of epithelial cells which do not contain phagocytosed material. Several giant tumour cells are seen. H & E, × 525.

Fig. 8. HCC, grade II. The trabeculae, covered with reticulin, are packed in groups, separated from each other by small amounts of loose, collagenous connective tissue containing blood vessels. The nuclei of the tumour cells are stained rather distinctly. Reticulin stain, × 210.


5
6
7
8



10*

Cirrhosis

The presence of cirrhosis could not be decided in 12 biopsies that were either too small or contained only tumour tissue. Of the remaining 15 patients 12 had cirrhosis while in 3 cases the benign liver tissue was normal. One of the patients with cirrhosis had haemocromatosis. Staining for iron showed pronounced deposition in both hepatocytes and Kuppfer cells in benign tissue but only very little iron in a few of the endothelial cells of the neighbouring malignant tissue.

All cases of cirrhosis were of the macronodular type. In 9 cases of cirrhosis there was a moderate to pronounced infiltration of the portal areas with lymphocytes and plasma cells, and in 7 of these cases there were piecemeal necroses. Focal necroses were seen in biopsies from 7 patients, and confluent necroses in 1 case. Fatty changes, Mallory bodies or acidophilic bodies could not be identified in any of the biopsies.

DISCUSSION

PCL is best classified into 4 histological types: HCC, CCC, mixed tumour with elements of both these types, and finally CLCC (*Edmondson* 1958). In the present material all the biopsies showed HCC exclusively. In his series of 282 cases of PCL from Uganda *Anthony* (1973) found 93.3 per cent to be HCC, the rest was CCC. *Berman* (1941) found 96 per cent HCC and 4 per cent CCC and no other types, in his large series of South African Bantu patients. This is in sharp contrast to Caucasian patient materials where CCC was found to constitute about 25 per cent (*Gustafson* 1937, *Bengmark et al.* 1971, *Glenert* 1961). This discrepancy is explained by the fact that the much higher incidence of PCL in Africa south of Sahara is almost exclusively caused by a higher frequency of HCC (*Higginson* 1956).

The histological structure of HCC in the present material does not differ from the one found by other investigators in Africa (*Anthony* 1973, *Berman* 1941, *Higginson* & *Steiner* 1961) or in the western world (*Edmondson* 1958).

The classification by *Anthony* (1973) was found useful for descriptive purposes. When this classification was compared with the grading of the tumours of the present series, the following approximate correlation was found: Hepatic type tumours corresponded to grade I and II tumours; the adenoid-type tumours with acini were grade II; tumours of the pleomorphic type were grade III and IV; clear-cell type tumours may have any grade, but are most frequently highly differentiated (*Buchanan* & *Huvos* 1974); in the present material the two tumours of this type were both grade II; finally rare varieties, among these the scirrhous form, which in the present study were grade IV.

A supplementary classification suggested here would be to divide HCC into tumours without, with moderate, and with large amounts of connective tissue.

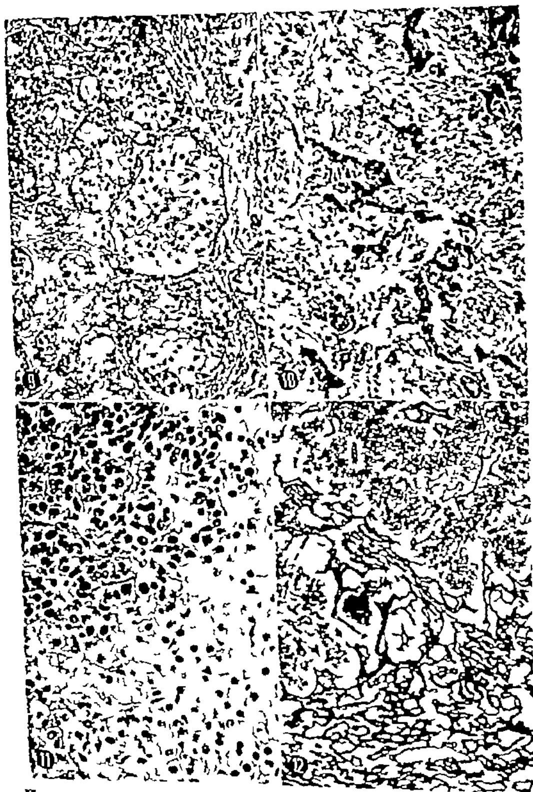
The importance of the reticulin stain cannot be too strongly emphasized. Its value has been mentioned by *Anthony* (1973) but has otherwise passed unnoticed in previous studies. The structure of the reticulin fibres in HCC is distinctly different from that of normal or cirrhotic liver tissue. Moreover, the present study shows that this staining tech-

Fig. 9. HCC Grade II. The trabeculae are separated by rather abundant, loose, collagenous connective tissue, containing blood vessels. *H & E,* × 210.

Fig. 10. HCC, grade IV. The tumour tissue has been split into small islands and thin trabeculae by dense collagenous connective tissue, giving the impression of a scirrhous cancer. H & E, × 210.

Fig. 11. HCC grade III. The tumour cells (upper left) invade the benign liver tissue (lower right) by replacing the normal liver cell plates. Many of the malignant cells contain intranuclear vacuoles. H & E × 210.

Fig. 12. HCC, grade III. Same area as Fig. 11. The reticulin structure of the malignant tissue (upper left) is distinctly different from that of the benign liver tissue (lower right). The cytoplasm of the tumour cells is stained grayish. Reticulin stain, × 210.



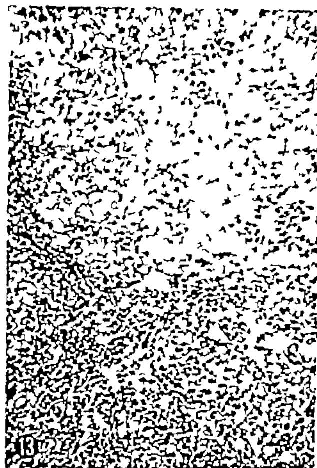






Fig 13 HCC, grade II Above is an area of clear-cell type tumour tissue. H & E, × 84

Fig 14 HCC, grade I Benign liver tissue (lower left) is strongly PAS-positive whereas the tumour cells (above) are unstained. PAS × 210

Fig 15 HCC, grade III The surface of the trabeculae is covered by a thin layer of reticulin Only very few thin reticulin fibres are visible inside the trabeculae Reticulin stain × 525.

nique stains the cytoplasm and the nuclei of the malignant cells, but leaves the benign cells unstained. The reticulin stain is thus a diagnostic tool which is very useful and important in the differential diagnosis between on one side HCC, especially if the tumour is highly differentiated, and on the other side normal liver tissue or cirrhotic regeneration nodules. The reticulin stain does not seem suitable to evaluate the grade of differentiation of HCC, but the present material is too small to allow a definitive conclusion on this point.

The frequency of cirrhosis in PCL of 80 per cent corresponds to that of other African material (*Anthony* 1973 *Berman* 1941). As in other African series (*Anthony* 1973 *Higginson* 1956) the cirrhosis in the present material was of the postnecrotic type. This fact, together with a high prevalence of hepatitis-associated antigen and the absence of alcohol in the history of patients with PCL (*Norredam* 1977) seems to indicate that not alcohol, but rather a hepatitis virus, possibly in conjunction with a carcinogen such as aflatoxin, is the most important cause of cirrhosis and thereby of PCL in Malawi.

REFERENCES

1 *Anthony P. P.*: Primary carcinoma of the liver. A study of 282 cases in Ugandan Africans. J. Path. *110*: 37–48, 1973

2 *Bengmark S., Bö jesson B. & Hafström L.*: The natural history of primary carcinoma of the liver. Scand. J. Gastroenterol. *6*: 351–355 1971

3 *Berman C.*: The pathology of primary carcinoma of the liver in the Bantu races of South Africa. S. Afr. J. Med. Sci. *6*: 11–26, 1941

4 *Buchanan T. F., J. & Huvos A. G.*: Clear cell carcinoma of the liver. A clinicopathologic study of 13 patients. Am. J. Clin. Path. *61*: 529–539 1974

5 *Cook P. J. & Burkitt D. P.*: Cancer in Africa. Brit. Med. Bull. *27*: 14–20 1971

6 *Edmondson H. A.*: Tumors of the liver and intrahepatic bile ducts, 1. ed. Armed Forces Institute of Pathology. Washington, D.C. 1958.

7 *Glenart J.*: Primary carcinoma of the liver. A post-mortem study of 104 cases. Acta path. microbiol. scand. *53*: 50–60 1961

8. *Gordon H. & Sweets H. H.*: A simple method for the silver impregnation of reticulum. Am. J. Path. *12*: 545–551 1936

9 *Gustafson E. G.*: An analysis of 62 cases of primary carcinoma of the liver based on 24 400 necropsies at Bellevue Hospital. Ann. Intern. Med. *11*: 889–900 1937

10. *Higginson J.*: Primary carcinoma of the liver in Africa. Brit. J. Cancer *10*: 609–622, 1956

11 *Higginson J. & Steiner P. E.*: Definition and classification of malignant epithelial neoplasms of the liver. Un. Internat. Cancer. Acta *17*: 593–603 1961

12. *Norredam K.*: Primary carcinoma of the liver. Clinical, biochemical and serological examinations of 24 patients from Malawi with histologically verified primary carcinoma of the liver. Trop. Geogr. Med., 1977

13 *Norredam K.*: To be published.

14 *Perls M.*: Nachweis von eisenoxyd in gewissen Pigmenten. Arch. Pathol. Anat. Phys. *39*: 42–48, 1867

Acta path. microbiol scand. Sect A 85 470–480 1977

FINE STRUCTURE OF EPITHELIAL THYMUS CYSTS IN DOGS

AILI OKSANEN

Department of Pathology College of Veterinary Medicine Helsinki 00550, and Department of Electron Microscopy University of Helsinki, Helsinki 00170

Oksanen A Fine structure of epithelial thymus cysts in dogs. Acta path. microbiol. scand. Sect. A, 85 470–480 1977

Epithelial thymus cysts in dogs were investigated by electron microscopy Epithelial cells from one and the same cyst showed morphological differences. Regular columnar or cuboidal epithelial cells predominated These had an elongated nucleus, poor in chromatin but with abundant cytoplasmic organelles, e g mitochondria and a Golgi region with sacs and vacuoles. Other cells possesed a narrower indented nucleus richer in chromatin a cytoplasm with numerous tonofilaments and cell membranes showing interdigitations with other cell membranes. Some cysts displayed a pseudostratified epithelium In these cells the same organelles were present as were seen in the cuboidal cells. Abundant cilia and microvilli were present in the luminal cells. All these different morphological characteristics were considered to be different functional aspects of the same kind of thymus epithelial cell. The cells had a structure indicating a secretory activity

Key words Thymus cysts ultrastructure dog

A. Oksanen Department of Pathology College of Veterinary Medicine, Helsinki 00550 and Department of Electron Microscopy University of Helsinki, Helsinki 00170

Received 19 xi 76 Accepted 3.i 77

The embryonic thymus is composed of epithelium from the third branchial pouches and branchial clefts (*Cordier & Heremans* 1975) In connection with involution, the reticulum cells in the canine thymus organize themselves into cysts with a ciliated epithelium (*Watney* 1883 *Hammar* 1905 *Marine* 1915 *Bargmann* 1943 *Oksanen* 1968 *Neuman* 1971) The epithelial cells show abundant enzymatic activity and the cysts contain a slightly eosinophilic PAS-positive structureless mass. This mass also stains with Alcian blue (*Oksanen* 1968) and can by immunoelectrophoresis be indentified as an oligomeric IgA (*Sandholm* et al. 1976) Thymus cysts occur spontaneously in laboratory animals (*Erdheim* 1906, *Arnesen* 1936 *Clark* 1963 *Oksanen* 1966, *Thung* 1966) but especially in connection with various stress conditions (*Selye* 1936, *Davidson* 1951) under the influecne of hormonal agents (*Ross & Korenchevsky* 1941 *Plagge* 1946 *Friedman* et al. 1964 *Lukacs & Tóth* 1964 *Cherry* et al. 1967 *Glucksmann & Cherry* 1968 *Ebbesen & Nielsen* 1977 *Bardth & Csaba* 1974) During the cold season thymus cysts are relatively frequent in poikilothermic animals, such as snakes (*Rao*

1955) and frogs (*ver Ecke* 1899) Moreover thymus cysts are often encountered in human autopsy material (*Hesse* 1939 *Crovatto* 1972)

Large epithelial thymus cysts, resting on a basement membrane, have been described in electron-microscopic studies on snakes (*Oksanen* 1972) rats (*Seneral* et al. 1975) and Nude mice (*Cordier* 1974) In all these investigations, high epithelial cells rich in organelles and with a somewhat varying ultrastructure have been described.

It is considered that epithelial cysts are important constituents of the thymus of old dogs (*Oksanen* 1968) and since such cysts have not previously been studied by electron microscopy it was considered worth while to undertake this study

MATERIAL AND METHODS

Specimens for histological and electron microscopical studies were obtained from 11 dogs of various ages and breeds. In all cases the material was obtained immediately after sacrifice of the animal.

Usually glutaraldehyde fixation was followed by osmium fixation, after which the specimens were dehydrated. The material was embedded in Epon 812 and sectioned at 700–900 Å. Sections were lightly stained with uranyl acetate in distilled water and with lead citrate and were examined with a Philips 300 or a Philips 200 electron microscope. Sections approx 2 µm thick were stained with toluidine blue for light microscopic examination.

RESULTS

Thymus cysts were found by electron microscopy of specimens from only four of the dogs. These dogs were old and had suffered from various chronic diseases nephritis, pyometra, thyroid or mammary carcinoma.

In the strongly involuted thymus, light microscopy revealed varying amounts of adipose tissue, lymphocytes and, centrally in the thymus lobule numerous cysts of various sizes. The luminal surfaces of the cysts were often lined with a simple ciliated cuboidal epithelium or a pseudostratified or occasionally a more flattened stratified epithelium (Fig. 1)

Electron microscopy revealed the same morphological variations as were seen with the

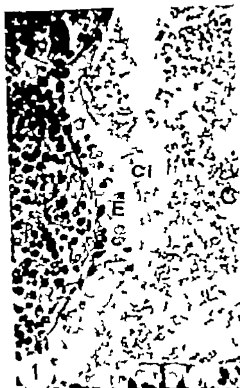


Fig 1 Part of thymus cyst (C) Epithelium (E) mostly ciliated (ci) Reticulum cells and lymphocytes (L) beneath the basement membrane. Light microscopy Glutaraldehyde-osmium fixation. Toluidine blue. × 650.

light microscope. The epithelium, wich rested on a basement membrane varied from columnar to cuboidal and further to a type in which narrow cytoplasmic processes extended far along the luminal surface of the cysts (Fig 2) A high columnar epithelium was often observed, particularly in the large cysts. The elongated nuclei rather poor in chromatin, were situated at the base of the cell. Cell membranes were smooth and joined by desmosomes. The cytoplasm was rich in organelles. The mitochondria were numerous in the apical cytoplasm they were small, oblong and of a regular structure in some cells (Fig 3) distended in others.

Closer to the nuclei an abundant Golgi region with cisternae and sacs was seen (Figs. 3 4 and 8) More apically some larger sacs

Acta path. microbiol. scand. Sect. A 85: 470–480, 1977

FINE STRUCTURE OF EPITHELIAL THYMUS CYSTS IN DOGS

AILI OKSANEN

Department of Pathology, College of Veterinary Medicine, Helsinki 00550 and Department of Electron Microscopy, University of Helsinki, Helsinki 00170

Oksanen, A. Fine structure of epithelial thymus cysts in dogs. Acta path. microbiol. scand. Sect. A 85: 470–480, 1977.

Epithelial thymus cysts in dogs were investigated by electron microscopy. Epithelial cells from one and the same cyst showed morphological differences. Regular columnar or cuboidal epithelial cells predominated. These had an elongated nucleus, poor in chromatin but with abundant cytoplasmic organelles, e.g. mitochondria, and a Golgi region with sacs and vacuoles. Other cells possessed a narrower, indented nucleus richer in chromatin, a cytoplasm with numerous tonofilaments and cell membranes showing interdigitations with other cell membranes. Some cysts displayed a pseudostratified epithelium. In these cells the same organelles were present as were seen in the cuboidal cells. Abundant cilia and microvilli were present in the luminal cells. All these different morphological characteristics were considered to be different functional aspects of the same kind of thymus epithelial cell. The cells had a structure indicating a secretory activity.

Key words: Thymus cysts; ultrastructure; dog.

A. Oksanen, Department of Pathology, College of Veterinary Medicine, Helsinki 00550, and Department of Electron Microscopy, University of Helsinki, Helsinki 00170

Received 19.xi.76 Accepted 3.i.77

The embryonic thymus is composed of epithelium from the third branchial pouches and branchial clefts (*Cordier & Heremans* 1975). In connection with involution the reticulum cells in the canine thymus organize themselves into cysts with a ciliated epithelium (*Watney* 1883, *Hammar* 1905, *Marine* 1915, *Bargmann* 1943, *Oksanen* 1968, *Newman* 1971). The epithelial cells show abundant enzymatic activity and the cysts contain a slightly eosinophilic PAS-positive structureless mass. This mass also stains with Alcian blue (*Oksanen* 1968) and can by immunoelectrophoresis be indentified as an oligomeric IgA (*Sandholm* et al. 1976). Thymus cysts occur spontaneously in laboratory animals (*Erdheim* 1906, *Arnesen* 1956, *Clark* 1963, *Oksanen* 1966, *Thung* 1966) but especially in connection with various stress conditions (*Selye* 1936, *Davidson* 1951) under the influecne of hormonal agents (*Ross & Korenchevsky* 1941, *Plagge* 1946, *Friedman* et al. 1964, *Linker*, *tood* 1964, *Cherry* et al. 1967, *Glucksmann* & *Cherry* 1968, *Ebbesen* & *Nielsen* 1977, *Bardth* & *Csaba* 1974). During the cold season, thymus cysts are relatively frequent in poikilothermic animals, such as snakes (*Roo*

1935) and frogs (*ver Eecke* 1899) Moreover thymus cysts are often encountered in human autopsy material (*Weise* 1939 *Crovallo* 197?)

Large epithelial thymus cysts, resting on a basement membrane, have been described in electron-microscopic studies on snakes (*Oksanen* 1972) rats (*Seneral* et al. 1973) and Nude mice (*Cordier* 1974) In all these investigations, high epithelial cells rich in organelles and with a somewhat varying ultrastructure have been described.

It is considered that epithelial cysts are important constituents of the thymus of old dogs (*Oksanen* 1968) and since such cysts have not previously been studied by electron microscopy it was considered worth while to undertake this study

MATERIAL AND METHODS

Specimens for histological and electron microscopical studies were obtained from 11 dogs of various ages and breeds. In all cases the material was obtained immediately after sacrifice of the animal.

Usually glutaraldehyde fixation was followed by osmium fixation, after which the specimens were dehydrated. The material was embedded in Epon 812 and sectioned at 700–900 Å. Sections were lightly stained with uranyl acetate in distilled water and with lead citrate and were examined with Philips 300 or a Philips 200 electron microscope. Sections approx 2 μm thick were stained with toluidine blue for light microscopic examination.

RESULTS

Thymus cysts were found by electron microscopy of specimens from only four of the dogs. These dogs were old and had suffered from various chronic diseases nephritis, pyometra, thyroid or mammary carcinoma.

In the strongly involuted thymus, light microscopy revealed varying amounts of adipose tissue lymphocytes and, centrally in the thymus lobule numerous cysts of various sizes. The lumenal surfaces of the cysts were often lined with a simple ciliated cuboidal epithelium or a pseudostratified or occasionally a more flattened stratified epithelium (Fig 1)

Electron microscopy revealed the same morphological variations as were seen with the



Fig 1 Part of a thymus cyst (*C*) Epithelium (E) mostly ciliated (cl) Reticulum cells and lymphocytes (L) beneath the basement membrane. Light microscopy Glutaraldehyde-osmium fixation. Toluidine blue. × 650

light microscope. The epithelium, which rested on a basement membrane varied from columnar to cuboidal and further to a type in which narrow cytoplasmic processes extended far along the lumenal surface of the cysts (Fig 2) A high columnar epithelium was often observed, particularly in the large cysts. The elongated nuclei rather poor in chromatin, were situated at the base of the cell. Cell membranes were smooth and joined by desmosomes. The cytoplasm was rich in organelles. The mitochondria were numerous in the apical cytoplasm they were small, oblong and of a regular structure in some cells (Fig 3) distended in others.

Closer to the nuclei an abundant Golgi region with cisternae and sacs was seen (Figs. 3 4 and 8) More apically some larger sacs



Fig 2 A small thymus cyst (C) lined with heterogeneous cells containing cilia (ci) and vacuoles (v) Cytoplasmic protrusions (P) in the apical parts of the cells Nuclei (N) mitochondria (M) and a lymphocyte (L) × 3 000 Insert Cross-sectioned cilia and microvilli. Lead + uranyl × 36 000.

were observed These sacs resembled vacuoles and had either an empty appearance or contained some homogeneous nearly electron-lucent material (Figs. 2 and 3)

The endoplasmic reticulum was studded with ribosomes It consisted mostly of dilated cisternae, rarely narrow tubuli The cytoplasm contained numerous free ribosomes principally polysomes (Fig 8) and microfilaments and microtubules in varying numbers (Fig 4) An intracellular cyst containing cilia and microvilli was sometimes seen in the apical cytoplasm (Figs. 5 and 6) In favourable sections these intracellular cysts were seen to communicate with the lumen of the thymus cysts (Fig 7)

Other epithelial cells in the same thymus cyst contained only few organelles, but their cytoplasm was full of bundles of tonofilaments, which were sometimes continuous with the desmosomes (Figs. 8 and 9) The nuclei of these cells were indented and narrower and more electron-opaque than the nuclei of the cells described previously The plasma membranes often showed interdigitations, and the intercellular spaces were dilated (Fig 9)

Occasionally irregularly shaped electron opaque cells were seen in the apical part of the thymus cyst. Scattered swollen mitochondria and Golgi cisternae and irregular sacs were present in such "dense" cells (Fig 10)

Generally the apical plasma membrane appeared smooth, but in one dog the cytoplasm of some cells formed protuberances of varying shape. These protuberances often contained microfilaments (Fig 11)

Many cilia and microvilli were present in some cells, while other cells showed none of these structures or only a few of them The cilia contained two central microtubules and nine pairs of peripheral tubules. Faint radial spokes extended from the central tubule to the marginal tubules and from them to the ciliary membrane (insert, Fig 2) The ciliary membrane was predominantly regular However the ciliary tubules were occasionally sur



F g 3 Oblique section through the regular cubo.dal epithelium of thymus cyst (C) Numerous cyto-
plasmic organelles are present. Mitochondria (M) Golgi reg ons (G) acuoles ( ) cilia (cl) Ciliary
roots ( ) are seen in cross-section N denotes nuclei. Lead + uranyl. × 8,000.

F g 4 Parts of fix epithelial thymus cells The cell membranes are interdigitated (Id) Numerous
cytoplasmic organelles are present Mitochondria (M) Golgi region (G) rough endoplasmic reticu-
lum (R desmosomes (d) tonofilaments (F) Free ribosomes in the form of polysomes are also pre
sent Lead + uranyl × 30,000

rounded by a relatively broad slightly granular irregular zone and sometimes several cilia were surrounded by one membrane The roots of the cilia extended relatively deeply into the cytoplasm. In longitudinal sections of the roots a bulge with a striated configuration was observed (Fig 11) In cross-section the picture varied with the plane of sectioning Occasionally nine coarsely structured tubule *triplets* were seen from which bundles of filaments extended into the surrounding cytoplasm (Insert Fig 11)

The microvilli were mostly straight occasionally ramified and contained some parallel longitudinally arranged filaments (Fig 11)

DISCUSSION

Epithelial thymus cysts increase in frequency with age (*Thung* 1966 *Cherry* et al 1967 *Oksanen* 1968 *Croxatto* 1972) and stress (*Selye* 1936) Such cysts were subjected to electron microscopical investigation as they were demonstrated in specimens from four diseased dogs.

The epithelium was seen to vary from columnar to flat the columnar cells generally contained elongated nuclei poor in chromatin and a cytoplasm rich in membraneous organelles. Mitochondria were present in the apical cytoplasm, in which a high enzymatic activity has previously been demonstrated by histochemical methods (*Oksanen* 1968)

Another frequently found component was a well-developed Golgi region situated close to the nucleus. In the apical cytoplasm the sacs of the Golgi widened into large vacuoles. Similar structures have been described in previous electron microscopic investigations of individual thymus reticulum cells as "vacuoles" dense bodies or secretory granules" (*Clark* 1963 *Hoshino* 1963 *Kohnen & Weiss* 1964 *Lundin & Schelin* 1965 *Ito & Hoshino* 1966, *van Haelst* 1967 a and b *Cesarini* et al 1968 *Oláh* et al 1968 *Mandel* 1970 *Pfoch* 1971 *Curtis* et al. 1972 *Ebbesen & Nielsen* 1972 *Frazier* 1973) They probably also correspond to the vacuoles demonstrated in cell cultures of thymus reticulum cells where they were



Fig 5 Apically situated intracytoplasmic cyst (IC) containing cilia, microvilli and some osmiophilic structureless materia. Thymus cyst (large C) cilia (ci) mitochondria (M) vacuoles (v) nucleus (N). Lead + uranyl. × 12 000

reported to show active movement within the cytoplasm or out from the cell, and were interpreted as secretory granules (*Kaiserling & Takaoka* 1973)

The intracellular cilia and microvilli-containing cysts in the apical portion of the epithelial cells of the thymus correspond to the intracytoplasmic ciliated cysts previously demonstrated by light microscopy in reticulum cells of the same organ (*ver Eecke* 1899 *Hammar* 1905) and later by electron-microscopy of the thymus (*Hoshino* 1963 *Kohnen & Weiss* 1964 *Lundin & Schelin* 1965 *Ito & Hoshino* 1966, *Mandel* 1970 *Curtis* et al 1972 *Frazier* 1973) The direct communication between the intracellular cyst and the lumen of the thymus cyst demonstrated in the present investigation suggests that the two contain the same substance.

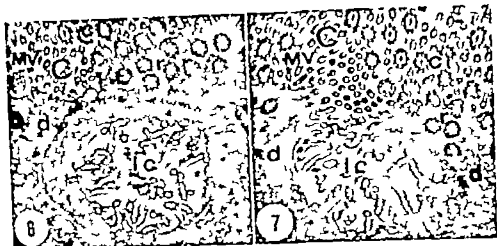


Fig. 6 Apically-situated intracytoplasmic cyst (IC) in an epithelial cell of thymus cyst (C). Note the presence of microvilli (M), cilia (ci) and some cross-sectioned ciliary roots (r) desmosome (d) can also be distinguished. Lead + uranyl. × 18,000

Fig. 7 The same intracytoplasmic cyst as in Fig. 6 but sectioned in different plane. The cyst (IC) is in contact with the large thymus cyst (large C). Cilia (ci) microvilli (M) ciliary roots (r) and desmosomes (d) are still present. Lead + uranyl. × 18,000

In general, the cilia contained two central and nine paired peripheral tubules, and radial spokes, as described for mobile cilia (*Warner* & *Satir* 1974). The cilia were mostly regular in structure but exceptions were observed, as has previously been reported (*Cordier* 1974 a and b). The microvilli were either straight or ramified, as was described in an investigation on the rat (*Seneral* et al. 1973) and contained parallel, longitudinally arranged microfilaments.

The epithelial cells of the thymus cysts with their numerous organelles seemed to be active and functioning. This observation is in agreement with a previous study (*Seneral* et al. 1973) but disagrees with other opinions according to which, the thymus cysts were degenerated structures (*Hammar* 1905 *Bargmann* 1943 *Kohnen* & *Weiss* 1964).

The epithelial cells of the thymus cysts showed wide morphological variations 1) large cells which contained an abundance of cytoplasmic organelles (mitochondria, a Golgi region with sacs and vacuoles, rough endoplasmic reticulum with ribosomes, and free ribosomes) 2) some cells which were rich in cytoplasmic microfilaments and microtubules had an indented and relatively small nucleus and showed interdigitations of their cell membranes, and 3) electron-opaque cells which contained only remnants of cell organelles. In general the filament-containing thymus reticulum cells have been considered to be degenerative forms (*Hoshino* 1963 *Kohnen* & *Weiss* 1964 *Lundin* & *Schelin* 1965 *Toró* et al. 1965 *Ito* & *Hoshino* 1966, *Cesarini* et al. 1968, *Mandel* 1970, *Levine* & *Bensch* 1972, *Frazer* 1973). Lately however an association has been considered to exist between the presence of filaments and tubules on the one hand and cellular movement on the other (*Tilney* 1971). This possibility should also be taken into account, particularly as the microfilaments often originated in large bundles from desmosomes this suggests that the microfilaments and tubules may in some way be involved in the process of organizing the reticulum cells into a cyst, and may even be responsible for the transportation of secretory granules (*Lacy* 1975).

Electron-opaque cells have been described earlier (*Clark* 1963) and considered to be


8
9
10



Fig 11 Detail of Fig. 2 showing irregular cytoplasmic protrusions (P) The protrusions and the apical portion of the cell contain filaments and some microtubuli (t) The various features are marked as follows: Cyst (C) cilia (ci) microvilli (M) desmosomes (d) mitochondria (M) and some obliquely and longitudinally sectioned ciliary roots ( ) × 45,000 Insert Cross-sectioned ciliary roots. Filament bundles originate from the tubule triplets. Lead + uranyl × 56,000.

Fig 8 Four adjacent epithelial thymus cells, one of which (top centre) contains numerous tonofilament bundles (F) The other three are rich in organelles. A prominent Golgi region with sacs (G) and vacuoles ( ) is present in the cell in the lower center of the field of view Lead + uranyl. 24 000.

Fig 9 Prominent membrane interdigitations (id) of adjacent epithelial thymus cells. One cell shows numerous bundles of tonofilaments (F) some of which originate from large desmosomes (d) The cells contain numerous ribosomes and a small amount of rough endoplasmic reticulum (R) Lead uranyl 50,000

Fig 10 An irregular electron-opaque cell (E) in which swollen mitochondria (M) and Golgi cisternae G and sacs are distributed. An adjacent cell contains an elongated nucleus (N) Lead + uranyl. 14,000

degenerated forms of epithelial thymus cells (*Jarplid* 1974)

The reticulum cells of the thymus have been studied by electron microscopy by several authors and have been classified according to the different cell types thus distinguished. In general, the presence of either cytoplasmic vacuoles or of filaments has been used as a distinctive criterion (*Hoshino* 1963 *Lundin* & *Schelin* 1965 *Törö* et al. 1965 *Oláh* et al. 1968, *Mandel* 1970 *Seneral* et al 1973 *Cordier* 1974) However since all kinds of intermediary forms between the extreme types were represented in the present material, a classification into different cell types does not seem justified. Despite the great morphological differences observed, the author is inclined to believe that all varieties are derived from

one and the same celltype and that the morphology of the cell despends on its activity A similar interpretation has been offered previously (*Ito & Hoshino* 1966)

Since epithelial thymus cysts were found neither in the seven healthy young dogs of the present study nor in a larger number of young dogs previously investigated by light microscopy (*Oksanen* 1968), these cysts cannot be embryonic rudiments, as has been suggested (*Nezeman* 1971) they must develop during the life of the individual from some component of the thymus The most probable source is the thymus reticulum cells, which are believed also to form Hassall s bodies (*Hammar* 1905 *Fraser* 1973)

If a thymus cyst is formed by reticulum cells, can it be said that all thymus reticulum cells even those of different morphology and location participate in the process or is it only certain types of cell that do so. As canine thymus cysts are located in the middle of the involuted lobule it seems logical to suggest that the large cells at the cortico-medullary junction might be involved in the process. These cells have been variously described as a) undifferentiated cells (*Mandel* 1970 *Fraser* 1973) b) cells with high enzymatic activity (*Kahri* et al. 1963) and c) cells containing Gomori positive granules (*Csaba* 1973)

The numerous mitochondria present in the epithelial thymus cells suggest an intensive metabolic activity and the prominence of the Golgi region with its sacs and vacuoles indicates a secretory activity Similar conclusions have been drawn from morphological studies of the reticulum cells of the thymus (*Arnesen* 1956 *Ito & Hoshino* 1966 *Cherry* et al 1967 *Kostowiecki* 1967 *Cesarini* et al 1968 *Olah* et al 1968 *Curtis* et al 1972 *Katsuta & Takaoka* 1973, *Rojo-Ortega* et al 1973 *Seneral* et al. 1973)

REFERENCES

Arnesen Kr The secretory apparatus in the thymus of mice Acta path microbiol scand *63* 339–349 1956

Baráth P & Csaba, G Histological changes in the lung thymus and adrenal one and a half year after pinealectomy Acta biol. Acad. Sci. 25 123–125 1974

Bargmann W Handbuch der mikroskopischen Anatomie des Menschen. VI Springer Verlag, Berlin pp 90–92 1943

Cesarini J F Benkoel L. & Bonneau H Ultrastructure comparée du thymus chez le hamster jeune et adulte C.r Soc. Biol. Marseille. *162* II 1975–1979 1968.

Cherry C P., Eisenstein R. & Glücksmann, A Epithelial cords and tubules of the rat thymus. Effects of age sex, castration of sex, thyroid and other hormones on their incidence and secretory activity J exp Path. *48* 90–106 1967

Clark S L. The thymus in mice of strain 129 7 studied with electron microscope. Ann. J Anat. *112* 1–33 1963

Cordier A C Ultrastructure of the thymus in "Nude" mice. J Ultrasctruct. Res. 47 26-44, 1974

Cordier A C Ciliogenesis and ciliary anomalies in thymic cysts of Nude" mice. Cell Tissue Res. *148* 397-406 1974

Cordier A C & Heremans J F Nude mouse embryo ectodermal nature of the primordial thymic defect. Scand. J Immunol. *4* 193–196, 1975

Croxatto O C Cordones epiteliales con aspecto endocrino observados en restos tímicos de adultos, Medicina, B Aires. 3? 203–208, 1972.

Csaba G An attempt to demonstrate endocrine cells in the rat thymus. Endocr exp *7* 99-106, 1973

Curtis Sh K Volpe E P & Cowden R. R. Ultrastructure of the developing thymus of the Leopard frog (Rana pipiens) Z. Zellforsch. mikrosk. Anat. *127* 323–346 1972.

Davidson W M B The development of thymic bodies in rats after fat injection. Br J exp Path. *52* 448–451 1951

Ebbesen P & Nielsen M H Thymic cysts in oestrogenized Balb/c mice. Acta path. microbiol scand. Section A. *80* 211–2?1 1972.

ver Eecke A Structure et modifications fonctionelles du thymus. Bull. Acad. r Méd. Belg. 4 Sér *13* 67–75 1899

Erdheim J Zur Anatomie der Keimenderreste bei Ratte Kaninchen und Igel. Anat. Anz. 29 609–623 1906

Fraser Judith A Ultrastructure of the chick thymus. Z. Zellforsch. mikrosk. Anat. *136* 191 205 1973

Friedman N B Bonice E J & Dratz E. The effect of local hormonal transplants and steroid hormone implants upon the thymus gland Leucopoesis in health and disease. Ann. N.Y Acad. Sci. *113* art 2, 916–932, 1964

Gluckmann A. & Cherry Cor P. The effect of castration, oestrogens, testosterone and the oestrous cycle on the cortical epithelium of the thymus in male and female rats. J Anat. 103 113–115 1968.

Hammar J A g Zur Histogenese und Involution der Thymusdrüse. Anat. Anz. 27 23–30 41 89 1905.

van Haelst U Light and electron microscopic study of the normal and pathological thymus of the rat. The normal thymus. Z. Zellforsch. mikrosk. Anat. 77 534–553 1967 a.

van Haelst U Light and electron microscopic study of the normal and pathological thymus of the rat. II. The acute thymic involution. Z. Zellforsch. mikrosk. Anat. 80 153–182, 1967 b.

Hoshino T Electronmicroscopic studies of the epithelial reticular cells of the mouse thymus. Z Zellforsch. mikrosk. Anat. 59 513–529 1963

Ito T & Hoshino T Fine structure of the epithelial reticular cells of the medulla of the thymus in the golden hamster. Z. Zellforsch. mikrosk. Anat. 69 311–318, 1966.

Järplid B Dark reticular cells in the thymus. Acta radiol. 13 319–328, 1974

Kahri, A. J Hammarkela, M & Karakorpi E. O Succinate tetrazolium reductase activity in the developing rat thymus. Acta endocr (Copenh.) 42 564–570 1963

Katsuta, H & Takaoka, T Rat thymus cells in culture I Peculiar granules in cytoplasm of reticulum cells. Jap J exp. Med 43 247–261 1973

Kohnen P & Weiss L. An electron microscopic study of thymic corpuscles in the guinea pig and the mouse Anat. Rec. 148 29–57 1964

Kostowiecki M Marjan Secretory component in the thymus of the pregnant white rats Jahrb. Morph. mikrosk. Anat. 2 Abt. Z. mikrosk.-anat. Forsch 76 141 183 1967

Lacy P E Endocrine secretory mechanisms. Am. J Path 79 170–187 1975

Le me G D & Bensch, KI. G Epithelial nature of spindle-cell thymomas. Cancer (Philadelphia) 30 500–511 1972

Lindstedt Alena Experimentelle Zystose des Thymus Zentbl allg Path. Anat 105 340–349 1964

Lundin P M & Schelin U Ultrastructure of the rat thymus Acta path. microbiol. scand. 65 379 394 1965

Mandel, T Differentiation of epithelial cells in the mouse thymus Z Zellforsch. mikrosk Anat. 106 498 515, 1970

Mann D The frequency of duct-like spaces in the thymus gland with remarks on the formation and fate of Hassell corpuscles. Cleveland med. J 14 186–193 1915

Neumann A J Cysts of branchial arch origin in the thymus of the Beagle. J small Anim. Pract. 12 681–685 1971

Oksanen Aili A histological and histochemical study on the epithelial rosettes and cysts in the thymus of the rat. Acta histochem 25 267 275 1966

Oksanen Aili The thymus of the adult stressed dog predominantly epithelial organ. Acta path. microbiol. scand. 72 192–204 1968

Oksanen Aili An electron microscopic study on the thymus epithelium of the snake (Vipera berus L.) Ann. Acad. Sci. fenn. A., IV Biologica 189 1–6 1972.

Oláh I., Dunay Csilla Röhlich P & Törő I. A special type of cells in the medulla of the rat thymus. Acta biol. hung. 19 97–113 1968.

Plagge J C. Some effects of prolonged massive estrogen treatment on the rat. Archs. Path. 42 598–609 1946.

Pfeck M Vergleichende elektronen-mikroskopische Untersuchungen an entodermalen Thymus Retikulumzellen neugeborener und alter Wistar Ratten Z. Zellforsch. mikrosk. Anat. 114 271 280 1971

Rao A M The involution of the thymus of the lizard, Calotes Versicolor (Daud.) Proc. natn. Inst. Sci. India. 21 Part B, 10–16 1955.

Rojo-Ortega, J M Yeghiayan E. & Genest J The thymus of spontaneously hypertensive rats Light and electron microscopic studies. Clin. Sci. mol. Med. 45 141–144 1973

Ross M A & Korenchevsky V. The thymus of the rat and sex hormones J Path. Bact. 52 349–360, 1941

Sandholm M., Kaartinen M & Oksanen A. Evidence of oligomeric IgA in canine thymus cysts. Scand. J Immunol. 5 149–154 1976.

Selye H Thymus and adrenals in the response of the organism to injuries and intoxications. Br J exp. Path. 17 234–248 1936

Senteral, R., Cateyee G Escola, R., Escola, M J & Bruno, J P Contribution a letude des kystes épithéliaux du thymus du rat Wistar et de leurs variations. Sous l'influence des hormones sexuelles et thyroidiennes. Path. Biol. (Paris) 21 937–948, 1973

Thung, P J Note on the thymic epithelium in senile mice. Exp. Gerontol. 1 337–340 1966.

Tilney L. G Origin and continuity of microtubules Origin and continuity of cell organelles. Ed J Reinert and H. Ursprung. Springer Verlag. Berlin, Heidelberg, New York. pp. 222 260, 1971

Törő I Röhlich P Oláh I & Pálfy, I Elektronenmikroskopische Untersuchungen an in Vitro gerichteten Thymusepithelzellen und Hassallschen Körperchen. Z. Zellforsch. mikrosk. Anat. 65 915–929 1965

Törő I Fine structure and enzyme cytochemistry

one and the same celltype and that the morphology of the cell despends on its acitivity. A similar interpretation has been offered previously (*Ito* & *Hoshino* 1966).

Since epithelial thymus cysts were found neither in the seven healthy young dogs of the present study nor in a larger number of young dogs previously investigated by light microscopy (*Oksanen* 1968), these cysts cannot be embryonic rudiments, as has been suggested (*Newman* 1971); they must develop during the life of the individual from some component of the thymus. The most probable source is the thymus reticulum cells, which are believed also to form Hassall's bodies (*Hammar* 1905, *Frazier* 1973).

If a thymus cyst is formed by reticulum cells, can it be said that all thymus reticulum cells, even those of different morphology and location, participate in the process, or is it only certain types of cell that do so. As canine thymus cysts are located in the middle of the involuted lobule, it seems logical to suggest that the large cells at the cortico-medullary junction might be involved in the process. These cells have been variously described as a) undifferentiated cells (*Mandel* 1970, *Frazier* 1973), b) cells with high enzymatic activity (*Kahri* et al. 1963) and c) cells containing Gomori positive granules (*Csaba* 1973).

The numerous mitochondria present in the epithelial thymus cells suggest an intensive metabolic activity and the prominence of the Golgi region with its sacs and vacuoles indicates a secretory activity. Similar conclusions have been drawn from morphological studies of the reticulum cells of the thymus (*Arnesen* 1956, *Ito* & *Hoshino* 1966, *Cherry* et al. 1967, *Kostowiecki* 1967, *Cesarini* et al. 1968, *Oláh* et al. 1968, *Curtis* et al. 1972, *Katsuta* & *Takaoka* 1973, *Kojo-Ortega* et al. 1973, *Seneral* et al. 1973).

REFERENCES

Arnesen K.: The secretory apparatus in the thymus of mice. Acta path. microbiol. scand. *63*: 339–349, 1956.

Bardth P. & *Csaba G.*: Histological changes in the lung, thymus and adrenal one and a half year after pinealectomy. Acta biol. Acad. Sci. *25*: 123–125, 1974.

Bargmann W.: Handbuch der mikroskopischen Anatomie des Menschen. VI Springer Verlag, Berlin, pp. 90–92, 1943.

Cesarini J. F., *Benkoel L.* & *Bonneau H.*: Ultrastructure comparée du thymus chez le hamster jeune et adulte. C.r. Soc. Biol. Marseille. *162* II: 1975–1979, 1968.

Cherry C. P., *Eisenstein R.* & *Glucksmann A.*: Epithelial cords and tubules of the rat thymus. Effects of age, sex, castration of sex, thyroid and other hormones on their incidence and secretory activity. J. exp. Path. *48*: 90–106, 1967.

Clark S. L.: The thymus in mice of strain 129/J studied with electron microscope. Ann. J. Anat. *112*: 1–33, 1963.

Cordier A. C.: Ultrastructure of the thymus in "Nude" mice. J. Ultrastruct. Res. *47*: 26–40, 1974.

Cordier A. C.: Cilogenesis and ciliary anomalies in thymic cysts of "Nude" mice. Cell Tissue Res. *148*: 397–406, 1974.

Cordier A. C. & *Heremans J. F.*: Nude mouse embryo: ectodermal nature of the primordial thymic defect. Scand. J. Immunol. *4*: 193–196, 1975.

Croxatto O. C.: Cordones epiteliales con aspecto endocrino observados en restos tímicos de adultos. Medicina, B. Aires. *32*: 203–208, 1972.

Csaba G.: An attempt to demonstrate endocrine cells in the rat thymus. Endocr. exp. *7*: 99–106, 1973.

Curtis Sh. K., *Volpe E. P.* & *Cowden R. R.*: Ultrastructure of the developing thymus of the Leopard frog (*Rana pipiens*). *Z. Zellforsch. mikrosk. Anat.* *127*: 323–346, 1972.

Davidson W. M. B.: The development of thymic bodies in rats after fat injection. Br. J. exp. Path. *32*: 448–451, 1951.

Ebbesen P. & *Nielsen M. H.*: Thymic cysts in oestrogenized Balb/c mice. Acta path. microbiol. scand. Section A. *80*: 211–221, 1972.

van Eecke A.: Structure et modifications fonctionel les du thymus. Bull. Acad. r. Méd. Belg. 4. Sér. *13*: 67–75, 1899.

Erdheim J.: Zur Anatomie der Kiemenderivate bei Ratte, Kaninchen und Igel. Anat. Anz. *29*: 609–623, 1906.

Frazier Judith A.: Ultrastructure of the chick thymus. Z. Zellforsch. mikrosk. Anat. *136*: 191–205, 1973.

Friedman N. B., *Bonner E. J.* & *Dratz E.*: The effect of local hormonal transplants and steroid hormone implants upon the thymus gland. Leucopoesis in health and disease. Ann. N.Y. Acad. Sci. *113*, art. 2: 916–932, 1964.

Acta path. microbiol. scand. Sect. A, 85 481–488 1977

SCANNING ELECTRON MICROSCOPIC SURFACE MORPHOLOGY OF ISOLATED HEPATOCYTES FROM NORMAL AND PREMALIGNANT RAT LIVER

Dag Boman, Trond Berg and Thoralf Christoffersen

Zoological Institute, Institute for Nutritional Research and Institute of Pharmacology
University of Oslo Oslo Norway

Boman, D Berg, T & Christoffersen, T Scanning electron microscopic surface morphology of isolated hepatocytes from normal and premalignant rat liver Acta path. microbiol. scand. Sect. A, 85 481–488 1977

Scanning electron microscopy was performed on hepatocytes isolated after collagenase perfusion of livers from rats fed 2-acetylaminofluorene (AAF) in the diet for 6–8 weeks and on hepatocytes from control rats. The premalignant AAF-cells showed a greater variation in cell size and shape. They also exhibited a reduced number of microvilli and more blebs and other protrusions on the surface than hepatocytes from control animals.

Key words Hepatocytes chemical carcinogenesis scanning electron microscopy

Dag Boman, Zoological Institute, University of Oslo, P O Box 1050 Blindern, Oslo 3 Norway

Received 25. iii.76 Accepted 10.i.77

There is at present a growing interest in various aspects of the cell surface in cancer For example differences between normal and transformed cells have been observed with regard to membrane composition (*Hakomori* 1975) transport functions (*Hatanaka* 1974) cyclic nucleotide formation (*Ryan & Heidrick* 1974) and agglutination in the presence of lectins (*Burger* 1973) Alterations in surface topography as revealed by scanning electron microscopy have been described in hamster embryo cells transformed by irradiation (*Borek & Fenoglio* 1976) in SV 40 transformed fibroblasts (*Collard & Temmink* 1976 and in duct cells from cancerous human breasts (*Spring-Mills & Elias* 1975) So far however there are no such studies of changes occurring during experimental carcinogenesis in vivo

It was previously proposed (*Christoffersen & Berg* 1975) that a combination of experimental liver carcinogenesis *in vivo* followed by cell dispersion of livers from the treated animals, might be useful in the study of the process of tumor development in liver In this way it is possible to obtain cell populations at different stages during carcinogenesis and thus study various aspects of their morphology and functions. Using this approach, evidence has so far been obtained that the hepatocytes acquire an altered regulation pattern of the cyclic AMP formation during 2-acetylaminofluorene carcinogenesis (*Christoffersen & Berg* 1975) and that the increased activity of lysosomal enzymes during the carcinogenesis is due to alterations of the hepatocytes and not the reticuloendothelial cells of the liver (*Berg & Christoffersen* 1974)

of rat thymus cells in situ and in tissue culture Folia Histochem Cytochem. (Krakow) *3* 333-334 1971

Warner Fr D & Satir P The structural basis of ciliary bend formation. J Cell Biol *63* 35-63 1974

Watney H The minute anatomy of the thymus. Phil. Trans R. Soc *173* 1063-1123 1883

Weese H Morphologie und Klinik des Thymus Dt. Z. Chir *253* 145-163 1939

Wetters J M & Macadam R F Fine structural evidence for hormone secretion by the human thymus. J clin. Path. *26* 194 197 1973



Fig. 2. Hepatocytes isolated after collagenase perfusion of the liver as described in Materials and Methods. Millipore filters served as substratum. A: hepatocytes from control animals. B: hepatocytes from AAF-treated animals. Bar represents 10 μm.

hepatocyte fixed *in situ* are shown in Fig. 1. The surface towards the sinusoid has a regular pattern of microvilli. The bile canaliculus runs as a single or branched furrow on the smoother surface towards the neighbouring hepatocyte.

During collagenase perfusion of the isolated liver the hepatocytes progressively become rounded. At the same time the canaliculi disappear (*Boman* unpublished) and there is a regular pattern of microvilli on the entire surface of the cell, as shown in Fig. 2, so that one can no longer recognize the areas which have been in contact with the neighbouring cell *in situ*.

Hepatocytes from Carcinogen Treated Animals

Isolated hepatocytes from normal and carcinogen-treated rats exhibited differences in morphology. The following points may deserve attention.

1. Cell size and shape. As can be seen in Fig. 2 the cells from the AAF-treated rats varied more in size and exhibited a more irregular shape than the normal cells. The maximum and minimum diameters of the cells were measured and calculated from scanning electron micrographs at 4000 × magnification, and the results are presented in Fig. 3. The cells from control animals were roughly normally distributed with respect to size while AAF treated animals showed a higher frequency of smaller cells, possibly reflecting increased rate of cell division in the premalignant liver.

2. Surface structures. It was found that cells from carcinogen-treated animals had a reduced number of microvilli on the surface as compared to control cells (Fig. 4). Counting of the main surface structures per square



Fig 1 Surface of a hepatocyte fixed *in situ* and isolated by gently crushing small osmium-treated liver blocks as described in Materials and Methods. Bar represents 2 µm.

We here present some studies of the surface morphology of hepatocytes isolated after collagenase perfusion of livers from normal rats and from rats fed 2 acetylaminofluorene.

MATERIALS AND METHODS

Male Wistar rats approx. 2 months old at the beginning of the treatment, were fed a diet with the composition described previously (*Christoffersen* 1975) For the experimental group 0 025 per cent 2 acetyl aminofluorene (AAF) was added. Duration of the treatment was 6 8 weeks. Cells from a total of 8 treated and 6 control rats were studied.

Heterogeneous liver cell suspensions were prepared by perfusing the isolated liver *in vitro* with 0 05 per cent collagenase (Sigma) in Hank's solution (*Berg & Boman* 1973) Briefly the liver was perfused through vena portae for 3 min with a calcium free Hanks buffer which then was replaced by the same buffer containing the collagenase and 4 mM calcium. After 7–10 min with this recirculating medium the liver capsules were opened and the cells released into a HEPES buffered Hanks solution This primary cell suspension was incubated at 37 C for 20 min and purified hepatocytes were prepared by low speed centrifugations as described previously (*Berg et al.* 1972) The viability of the purified cells, assessed by the trypan blue method, was 90 95 per cent.

Hepatocytes dispersed in Hanks buffer were fixed in glutaraldehyde at a final conc of 2.5 per cent for a minimum of 24 hours.

Dehydration was done with graded ethanols, increasing to 100 per cent The cells were then dried by the critical point method, using CO_2 (*Anderson* 1951) and coated with 400 Å gold in a Polaron E 5000 diode sputtering system. Millipore or nucleopore filters were used as substratum for the cells during the scanning procedure The cells were examined in a Jeol JSM S1 scanning electron microscope at 10 kV

To study the surface structures of hepatocytes *in situ* we perfused a normal liver with 2.5 per cent glutaraldehyde in Hanks buffer containing 4 per cent polyvinylpyrrolidone (PVP 40) Small blocks were cut from the liver and postfixed in 2 per cent osmium tetroxide for 2 hrs. before dehydration in ethanol and drying in critical point/CO_2. The blocks were then gently crushed with a glass rod and spread on cover slips. The slips had previously been coated with a thin layer of glue made from chloroform and ordinary adhesive tape

Counting of the surface structures of the isolated hepatocytes was performed on high magnification scanning micrographs (× 13 000) from the same sample of cells which was scanned at × 4 000 for size determination. A square field (size 3 × 3 µm) was placed on the picture of the central part of the hepatocyte and the number of structures within this field was evaluated

The hepatocytes shrink during the dehydration and drying procedure for scanning The maximum diameter of control cells in the fixation solution was 23.3 ± 2 2 µm (n = 44) (measured in a light microscope at 320 × with a Zeiss micrometer eyepiece) After dehydration of the same cells in ethanol the diameter had diminished to 18.2 ± 2.7 µm (n = 44)

RESULTS

Normal Hepatocytes

In the normal liver the hepatocytes are polyhedral and have surfaces of three types those exposed to the sinusoid to the adjacent hepatocyte or to the lumen of the bile canaliculus (*Bloom & Fawcett* 1968 *Grisham et al* 1975) These different facets of a

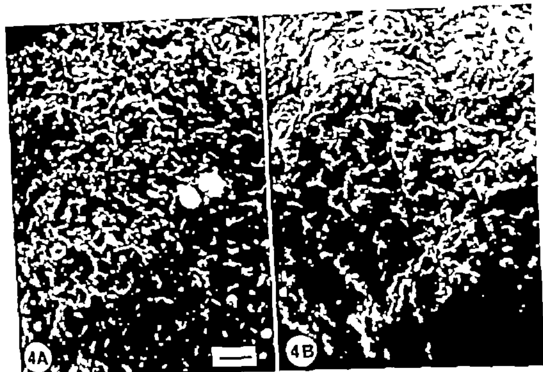


Fig. 4. Surfaces of hepatocytes isolated after collagenase perfusion. A: hepatocytes from control animals with a dense pattern of microvilli on the surface. B: hepatocytes from AAF-treated animals, showing more scanty and irregular pattern of microvilli. Bar represents 1 µm.

trunk-like protrusions, which may have developed from the blebs (Fig. 6). The large protrusions were often connected to the cell by a thin, short stalk, and could easily be removed from the cell by repeated pumping of the cell suspension through a pipette.

DISCUSSION

The present results indicate differences between the cell surface structure of normal and premalignant hepatocytes. There was a reduced number of microvilli and an increased number of surface blebs on the AAF treated cells. It should be stressed that the comparison was performed on suspended cells. Thus, since the cell surface undergoes structural alterations during the cell dispersion procedure (Figs. 1 and 2), the results presented here do not give information on possible differences between the surfaces of the two cell types *in situ*. Our observations are, however, supported by transmission electron microscopical studies of rat liver during AAF feeding, showing anomalies of the surface of hepatocytes fixed *in situ*. The sinusoidal surface of such cells seemed to be more irregular (*Flaks* 1968, 1970) and possessed fewer microvilli which were irregular in form and orientation (*Flaks* 1971).

Alterations in the surface morphology of malignant as well as premalignant cells have previously been reported. Thus, *Spring-Mills & Elias* (1975) found that the duct cells from cancerous human breasts show a greater variation in the number, length and arrangement of the apical microvilli. These cells tended to have fewer microvilli and more knobs or rudimentary microvilli than duct cells from non-cancerous breasts. Interestingly enough, cells from so-called normal areas located several centimeters from the primary

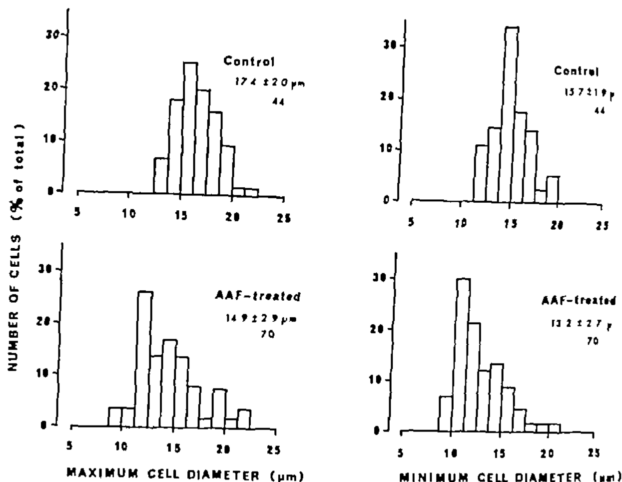


Fig 3 Size distribution of isolated hepatocytes from control and AAF treated animals. The cells were randomly selected on different scanning specimens made from 8 AAF-treated animals and 6 controls. The values are given as mean values ± S D (n = number of cells) *The distinction of the two maximum diameters is highly significant based on Wilcoxon (Mann Whitney) two sample rank test.*

TABLE 1 *Number of Main Surface Structures per Unit Area (see "Materials and Methods") of Isolated Hepatocytes from Control and AAF Treated Animals*

	Microvilli	Protrusions/blebs	Smooth areas
AAF (n = 37)	30.2 ± 11.5	3.6 ± 2.0	2.7 ± 1.6
Control (n = 24)	65.5 ± 10.6	0.9 ± 1.1	0.2 ± 0.4

For all three parameters the observed differences between control and AAF-cells are highly significant (Student t test, $P<0.001$) The values are given as mean values ± S.D n = number of cells.

unit showed that AAF-cells had less than half the number of microvilli and four times more protrusions and blebs than control hepatocytes (Table 1) The microvilli of the control cells were regular and seemed to be situated on a common level while the irregular microvilli of the AAF hepatocyte seemed to protrude from a more ruffled surface (Fig 5) Pinocytotic pits were occasionally observed on the smooth areas between the protruding surface structures of the AAF cells (Fig 5) The AAF-cells also had a greater tendency to form surface blebs, somewhat larger than the microvilli and larger

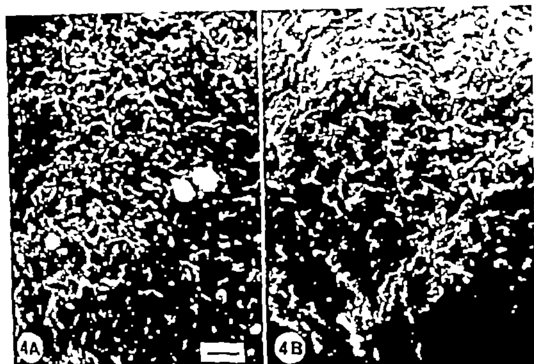


Fig. 4. Surfaces of hepatocytes isolated after collagenase perfusion. A: hepatocytes from control animals with a dense pattern of microvilli on the surface. B: hepatocytes from AAF-treated animals, showing a more scanty and irregular pattern of microvilli. Bar represents 1 µm.

trunk-like protrusions, which may have developed from the blebs (Fig. 6). The large protrusions were often connected to the cell by a thin, short stalk, and could easily be removed from the cell by repeated pumping of the cell suspension through a pipette.

DISCUSSION

The present results indicate differences between the cell surface structure of normal and premalignant hepatocytes. There was a reduced number of microvilli and an increased number of surface blebs on the AAF treated cells. It should be stressed that the comparison was performed on suspended cells. Thus, since the cell surface undergoes structural alterations during the cell dispersion procedure (Figs. 1 and 2), the results presented here do not give information on possible differences between the surfaces of the two cell types *in situ*. Our observations are, however, supported by transmission electron microscopical studies of rat liver during AAF feeding, showing anomalies of the surface of hepatocytes fixed *in situ*. The sinusoidal surface of such cells seemed to be more irregular (*Flaks* 1968, 1970) and possessed fewer microvilli which were irregular in form and orientation (*Flaks* 1971).

Alterations in the surface morphology of malignant as well as premalignant cells have previously been reported. Thus, *Spring-Mills* & *Elias* (1975) found that the duct cells from cancerous human breasts show a greater variation in the number, length and arrangement of the apical microvilli. These cells tended to have fewer microvilli and more knobs or rudimentary microvilli than duct cells from non-cancerous breasts. Interestingly enough, cells from so-called normal areas located several centimeters from the primary

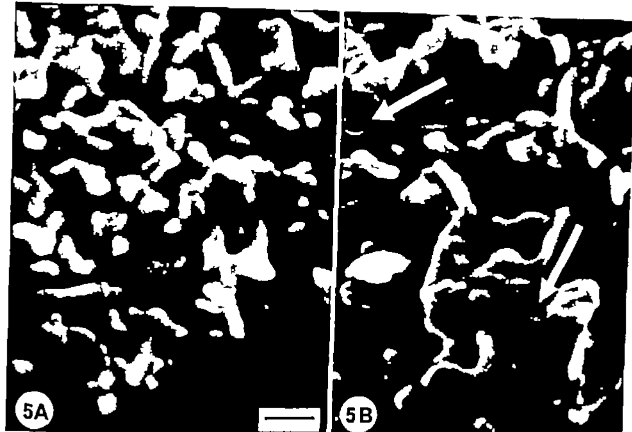


Fig 5 High magnification of the surfaces of hepatocytes isolated after collagenase perfusion. A control cells. B AAF treated cells Arrows indicate pinocytotic pits in the surface. Bar represents 0.5 µm.

lesion in some cancerous breasts also showed these structural characteristics.

The functional significance of the surface alterations is not clear Utilizing morphological studies of various cultured cells, the relationship between cell function and surface topography has been discussed but in many respects these results are discrepant Thus, it has been shown that the density of microvilli on the surface of cultured cells is changing during the cell cycle (*Porter et al* 1973 1974 *Hale et al* 1975) Furthermore the presence of blebs and microvilli is more frequent in transformed (Chinese hamster ovary) cells than in non transformed cells of equivalent type in confluent cultures. (*Porter et al* 1973) *Willingham & Pastan* (1975) also found more microvilli on transformed fibroblasts These results are supported by studies of hamster embryo cells transformed *in vitro* by X irradiation (*Borek & Fenoglio* 1976) showing that the non transformed cells in confluent cultures have a smooth surface while the transformed cells exhibit microvilli blebs and ruffles on their surfaces after transformation On the other hand *Collard & Temmink* (1976) have recently found that simian virus 40-transformed fibroblasts throughout the life cycle have a smoother surface than normal fibroblasts.

Willingham & Pastan (1975) have proposed that there is an inverse relationship between the content of cyclic AMP and the appearance of microvilli on transformed cells. They argued that transformed fibroblasts were highly agglutinable because their low cyclic AMP levels result in the formation of numerous surface microvilli A comparison between these findings and our observations cannot easily be made, since the short microvilli of the hepatocytes are different from the long thin filopodia often observed on the cultured cells. However livers from AAF

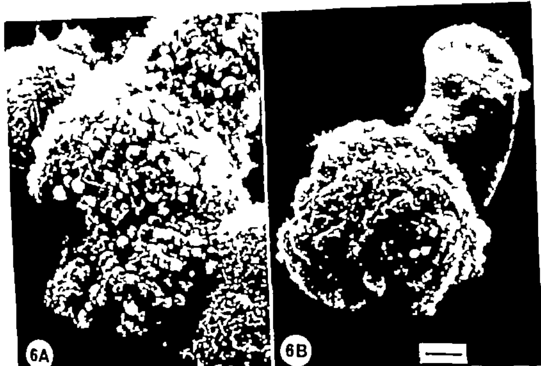


Fig. 6 Surface blebs (A) and larger trunk-like protrusions (B) on hepatocytes isolated from AAF treated animals Bar represents μm.

treated rats have been shown to have increased levels of cyclic AMP as compared to controls (*Christoffersen et al* 1974) Thus, the reduced number of microvilli which we have observed on isolated hepatocytes from AAF-treated rats might be consistent with an inverse relationship between the level of cyclic AMP and the number of microvilli.

We wish to thank Dr *Trond B rkes* at the Electron Microscopical Unit for Biological Sciences, University of Oslo for the use of scanning facilities and advice during the preparation of the specimens.

REFERENCES

Anderson T F Techniques for the preservation of three-dimensional structure in preparing specimens for the electron microscope Trans. N Y Acad. Sci Ser III *13* 130–134 1951

Berg, T Boman D & S glen P O Induction of tryptophan oxygenase in primary rat liver cell suspension by glucocorticoid hormone Expl Cell Res *72* 571 574 1972.

Berg T & Boman D Distribution of lysosomal enzymes between parenchymal and Kupffer cells of rat liver Biochim. Biophys. Acta *321* 585–596 1973

Berg, T & Christoffersen T Early changes induced by 2-acetylaminofluorene in lysosomes in rat liver parenchymal cells. Biochem. Pharmacol. *23* 3323–3329 1974

Bloom W & Fawcett D W A Textbook of Histology pp. 582–613 Saunders, Philadelphia 1968

Bor k C & Fox glo C M Scanning electron microscopy of surface features of hamster embryo cells transformed in vitro by X-irradiation. Cancer Research *36* 1525–1534 1976

Burger M M Surface changes in transformed cells detected by lectins Fed. Proc. *32* 91–101 1976.

Christoffersen T Effect of treatment of rats with some chemical carcinogens on the stimulatory effect of adrenaline on cyclic AMP accumulation in liver slices. Acta Pharmacol. et Toxicol *37* 233–236, 1975.

Christoffersen T Brønstad G O Walstad P & Øye I Cyclic AMP metabolism in rat liver during 2-acetylaminofluorene carcinogenesis Biochim. Biophys Acta *372* 291–303 1974

Christoffersen T & Berg, T Altered hormone

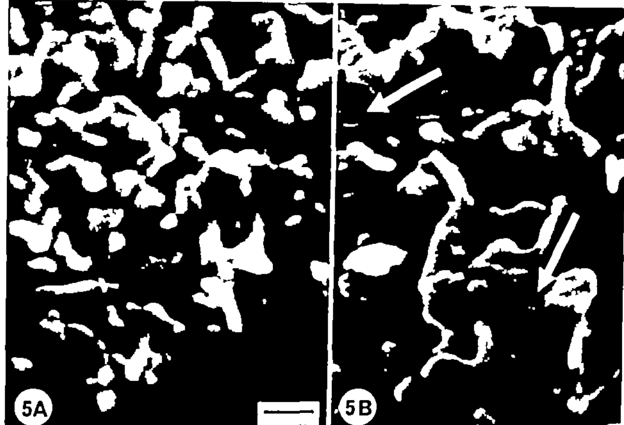


Fig 5 High magnification of the surfaces of hepatocytes isolated after collagenase perfusion. A control cells. B AAF treated cells Arrows indicate pinocytotic pits in the surface. Bar represents 0.5 μm.

lesion in some cancerous breasts also showed these structural characteristics.

The functional significance of the surface alterations is not clear Utilizing morphological studies of various cultured cells, the relationship between cell function and surface topography has been discussed but in many respects these results are discrepant. Thus, it has been shown that the density of microvilli on the surface of cultured cells is changing during the cell cycle (*Porter et al* 1973 1974 *Hale et al* 1975) Furthermore the presence of blebs and microvilli is more frequent in transformed (Chinese hamster ovary) cells than in non transformed cells of equivalent type in confluent cultures. (*Porter et al* 1973) *Willingham & Pastan* (1975) also found more microvilli on transformed fibroblasts. These results are supported by studies of hamster embryo cells transformed *in vitro* by X irradiation (*Borek & Fenoglio* 1976) showing that the non transformed cells in confluent cultures have a smooth surface while the transformed cells exhibit microvilli blebs and ruffles on their surfaces after transformation. On the other hand *Collard & Temmink* (1976) have recently found that simian virus 40-transformed fibroblasts throughout the life cycle have a smoother surface than normal fibroblasts.

Willingham & Pastan (1975) have proposed that there is an inverse relationship between the content of cyclic AMP and the appearance of microvilli on transformed cells. They argued that transformed fibroblasts were highly agglutinable because their low cyclic AMP levels result in the formation of numerous surface microvilli A comparison between these findings and our observations cannot easily be made since the short microvilli of the hepatocytes are different from the long thin filopodia often observed on the cultured cells. However livers from AAF

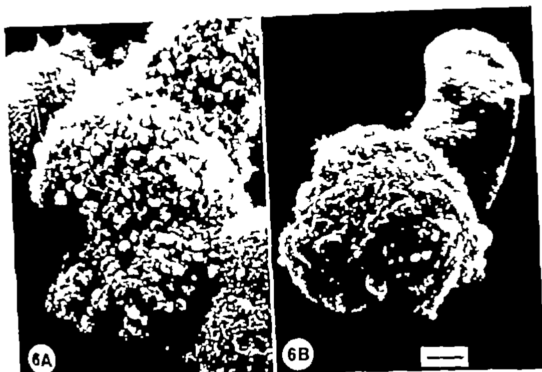


Fig 6 Surface blebs (A) and larger trunk-like protrusions (B) on hepatocytes isolated from AAF-treated animals. Bar represents 2 μm.

treated rats have been shown to have increased levels of cyclic AMP as compared to controls (*Christoffersen et al* 1974). Thus, the reduced number of microvilli which we have observed on isolated hepatocytes from AAF-treated rats might be consistent with an inverse relationship between the level of cyclic AMP and the number of microvilli.

We wish to thank Dr *Trond Brtten* at the Electron Microscopical Unit for Biological Sciences, University of Oslo, for the use of scanning facilities and advice during the preparation of the specimens.

REFERENCES

Anderson T F Techniques for the preservation of three-dimensional structure in preparing specimens for the electron microscope Trans. N.Y. Acad. Sci Ser III *13* 130–134 1951

Berg, T Boman D & Seglen P O Induction of tryptophan oxygenase in primary rat liver cell suspensions by glucocorticoid hormone. Expl Cell Res 72 571 574 1972.

Berg, T & Boman D Distribution of lysosomal enzymes between parenchymal and Kupffer cells of rat liver Biochim. Biophys. Acta *321* 585–596, 1973

Berg, T & Christoffersen T.: Early changes induced by 2-acetylaminofluorene in lysosomes in rat liver parenchymal cells. Biochem. Pharmacol. *23:* 3323 3329 1974

Bloom W & Fawcett D W A Textbook of Histology pp. 582–613 Saunders, Philadelphia 1968.

Borek C & Fenoglio C M Scanning electron microscopy of surface features of hamster embryo cells transformed *in vitro* by X-irradiation. Cancer Research 36 1325–1334 1976

Burger M M Surface changes in transformed cells detected by lectins. Fed. Proc. *32* 91–101 1976

Christoffersen T Effect of treatment of rats with some chemical carcinogens on the stimulatory effect of adrenaline on cyclic AMP accumulation in liver slices. Acta Pharmacol. et Toxicol. *37* 233–236 1975

Christoffersen T., Brønstad G O Walstad P & Øye I Cyclic AMP metabolism in rat liver during 2-acetylaminofluorene carcinogenesis Biochim. Biophys. Acta *372* 291–303 1974

Christoffersen T & Berg, T.: Altered hormone

control of cyclic AMP formation in isolated parenchymal liver cells from rats treated with 2 acetylaminofluorene Biochim. Biophys. Acta *381* 72–77 1975

Collard J G & Temmink J H M Surface morphology and agglutinability with concanavalin A in normal and transformed murine fibroblasts. J Cell Biol *68* 101–112 1976

Flaks B Permanent changes in the fine structure of rat hepatocytes following prolonged treatment with 2 acetylaminofluorene. Europ J Cancer *4* 279–304 1968

Flaks B Changes in the fine structure of rat hepatocytes during the early phases of chronic 2-acetylaminofluorene intoxication. Chem Biol Interacions *2* 129–150 1970

Flaks B Fine structure of rat hepatocytes during the late phase of chronic 2 acetylaminofluorene intoxication Chem Biol. Interactions *3* 157–176 1971

Grisham J W Nopanitaya W Compagno J & Nägel A E H Scanning electron microscopy of normal rat liver The surface structure of its cells and tissue components. Am. J Anat. *144* 295–322 1975

Hakomori S I Structures and organization of cell surface glycolipids dependency on cell growth and malignant transformation. Biochim. Biophys. Acta *417* 55–89 1975

Hale A H., Winkelhake J L. & Weber M J Cell surface changes and Rous sarcoma virus gene expression in synchronized cells. J Cell Biol *64* 398–407 1975

Hatanaka M. Transport of sugars in tumor cell membranes. Biochim. Biophys. Acta *355* 77 104 1974

Porter K Prescott D & Frye J. Changes in surface morphology of Chinese hamster ovary cells during the cell cycle. J Cell Biol. *57* 815–836 1973

Porter K R Fonte V & Weiss G A scanning microscope study of the topography of HeLa cells. Cancer Res *34* 1385–1394 1974

Ryan W L & Heidrick M L Role of cyclic nucleotides in cancer In Advances in Cyclic Nucleotide Research, vol 4 pp 81–116, Raven Press, New York 1974

Spring Mills E. & Elias J J Cell surface differences in ducts from cancerous and noncancerous human breasts. Science *188* 947 948, 1975

Willingham M C & Pastan I. Cyclic AMP modulates microvillus formation and agglutinability in transformed and normal mouse fibroblasts Proc. Nat. Acad. Sci. USA *72* 1263–1267 1975

Acta path. microbiol. scand. Sect. A, 85 489–500 1977

EFFECT OF 1.25-DIHYDROXYCHOLECALCIFEROL ADMINISTRATION ON BLOOD GLUCOSE AND PANCREATIC ISLET MORPHOLOGY IN MICE

L. Boquist, S. Hagström and L. Strindlund

Department of Pathology, University of Umeå, Sweden

Boquist, L., Hagström, S. & Strindlund, L. Effect of 1.25-dihydroxycholecalciferol administration on blood glucose and pancreatic islet morphology in mice. Acta path. microbiol. scand. Sect. A, 85: 489–500, 1977.

1.25-dihydroxycholecalciferol (DHCC) administration to fed and starved mice had no effect on the blood-glucose concentration or the light-microscopic appearance of the endocrine or exocrine pancreas. Electron microscopy, however, disclosed changes which appeared early after the injection and were more marked in starved than in fed animals. The B-cells exhibited mitochondrial hypertrophy studied both by qualitative and quantitative methods, invagination and vacuolation of mitochondrial membranes, increased occurrence of light secretory granules, multiple rough endoplasmic cisternae, multi-lamellar bodies, and a rather rich Ca^{2+}-containing pyroantimonate precipitation mainly localized to nuclei and mitochondria. A tendency to mitochondrial hypertrophy was observed also in some D-cells. The A-cells were unaffected. The findings indicate that the endocrine pancreas (or at least the B-cells) is affected in some way directly or indirectly by DHCC.

Key words: Endocrine pancreas; 1.25-dihydroxycholecalciferol; blood glucose; mitochondrial hypertrophy; multiple rough endoplasmic cisternae.

L. Boquist, Department of Pathology, University of Umeå, S-901 87 Umeå, Sweden.

Received 23.1.77. Accepted 23.1.77

In a parallel study (*Boquist et al.* 1977) pre-administration of 1.25-dihydroxycholecalciferol (DHCC) was found to enhance the diabetogenic action of alloxan in mice. Since there is no previous report on the effect of this vitamin D metabolite on the endocrine pancreas in any species, the present work was carried out to study whether injection of DHCC alone, without alloxan, affects the blood-glucose level and/or islet morphology in mice.

MATERIAL AND METHODS

Animals and Treatment

The animals were adult C57BL-KsJ +/+ mice of both sexes, from a local stock kept under standard laboratory conditions. The following experimental groups were used: I. Fed, treated with 7.5 ng DHCC; II. Starved 24 hrs, treated with 7.5 ng DHCC; III. Fed, treated with 1 ml of saline; IV. Starved 24 hrs, treated with 1 ml of saline. All injections were given intraperitoneally under ether anesthesia.

Blood Glucose

Blood glucose was assayed by the glucose oxidase method, using Glox® (AB Kabi, Stockholm, Swe-

TABLE 1 *Blood Glucose Concentration (mg/100 ml) in Groups of Fed and Starved Mice before (0 Hours) and at Different Intervals after Intraperitoneal Injection of 1,25-Dihydroxycholecalciferol (DHCC) or Saline*

Group	Starvation	Treatment	Blood glucose concentration (mean ± S.E.) Hours 0	1	2	4	24	48
I	No	DHCC	133 ± 6	113 ± 6	107 ± 3	122 ± 7	102 ± 8	103 ± 6
II	Yes	DHCC	89 ± 6	69 ± 5	68 ± 5	56 ± 5	115 ± ?	105 ± 4
III	No	Saline	121 ± 5	118 ± 4	10? ± 3	123 ± 4	114 ± 5	110 ± 6
IV	Yes	Saline	?0 ± 5	74 ± 6	70 ± 4	61 ± 3	109 ± 4	103 ± 5

den). Blood was obtained by cutting the tip of the tail before the injections and 1, 2, 4, 24 and 48 hours after the injections.

Light Microscopy

Mice from the different groups were killed at the following predetermined intervals after the injections: 10, 30 and 60 minutes and 1, 2, 3, 4, 7 and 14 days. Then the pancreas was immediately removed and most of it was fixed in Bouin's fluid. The following stains were applied: hematoxylin eosin, van Gieson's stain, aldehyde fuchsin, and the silver impregnations according to Hellerström and Hellman (1960) and Grimelius (1968).

Qualitative Electron Microscopy

Pyroantimonate Technique and X Ray Analysis

Small pancreatic specimens not used for light microscopy, taken at the same time-intervals as used for light microscopy, were fixed in 2.5 per cent glutaraldehyde in 0.34 M veronal acetate buffer pH 7.4 followed by post fixation in osmium-tetroxide. Embedding was carried out in Epon 812 and thick sections stained with toluidine blue were used for identification of the islets. The thin sections were stained with uranyl-acetate and lead citrate and were then examined in a Siemens Elmiskop 101.

Other specimens, taken at the 10 min., 60 min. and 1 day intervals, were fixed for 2 hours in 3 per cent glutaraldehyde and 2 per cent potassium pyroantimonate adjusted to pH 7.4 with 0.01 M acetic acid, followed by fixation for 1 hour in 1 per cent osmium-tetroxide and 2 per cent potassium pyroantimonate. The sections were either unstained or stained with uranyl acetate and lead citrate, after which they were viewed in a Siemens Elmiskop 101.

The specificity of the pyroantimonate precipitates was investigated by X ray analysis, using an energy dispersive system (Kevex X ray energy spectrometer subsystem 5000 A) combined with a JEOL JSEM 200 scanning-transmission-microscope.

Quantitative Transmission Electron Microscopy

A stereological method (*Ruigrok & Elbers* 1972) was applied for estimation of mitochondrial volume, using a printing frame fitted with a grid of steel wires for production of a square grid of white lines superimposed on the photographs obtained on enlargement of electron micrographs. Ten original micrographs were taken of pancreatic B-, D- and A-cells from each of five animals from the different groups, 1 and 24 hours after the injections. The length fraction of cytoplasmic lines passing through mitochondria was measured, corresponding to the fractional volume of the mitochondria in the cytoplasm.

RESULTS

Blood Glucose

The results of the blood-glucose determinations are given in Table 1. The blood-glucose level after DHCC-treatment did not differ significantly from that recorded before the injections in any of the groups. Nor was any significant difference observed between the DHCC- and saline-treated groups of fed mice or between the corresponding groups of starved mice. The mean blood-glucose level was, however, higher in the fed than in the starved groups, before the injections,

Fig. 1. Mitochondrial hypertrophy in B-cell. Most mitochondria are rounded or oval and possess preserved cristae and moderate density of their matrices. Group II, 30 minutes. × 19 000



TABLE 1 *Blood-Glucose Concentration (mg/100 ml) in Groups of Fed and Starved Mice before (0 Hours) and at Different Intervals after Intraperitoneal Injection of 1,25-Dihydroxycholecalciferol (DHCC) or Saline*

Group	Starvation	Treatment	Blood glucose concentration (mean ± S.E.) Hours 0	1	2	4	24	48
I	No	DHCC	133 ± 6	113 ± 6	107 ± 3	122 ± 7	102 ± 8	103 ± 6
II	Yes	DHCC	89 ± 6	69 ± 5	68 ± 5	56 ± 5	115 ± 2	105 ± 4
III	No	Saline	121 ± 5	118 ± 4	10? ± 3	123 ± 4	114 ± 5	110 ± 6
IV	Yes	Saline	90 ± 5	74 ± 6	70 ± 4	61 ± 3	109 ± 4	103 ± 3

den). Blood was obtained by cutting the tip of the tail before the injections and 1, 2, 4, 24 and 48 hours after the injections.

Light Microscopy

Mice from the different groups were killed at the following predetermined intervals after the injections: 10, 30 and 60 *minutes and* 1, 2, 3, 4, 7 *and* 14 days. Then the pancreas was immediately removed and most of it was fixed in Bouin's fluid. The following stains were *applied*: *hematoxylin* eosin, van Gieson's stain, aldehyde fuchsin and the silver impregnations according to Hellerström and Hellman (1960) and Grimelius (1968).

Qualitative Electron Microscopy

Pyroantimonate Technique and X-Ray Analysis

Small pancreatic specimens not used for light microscopy, taken at the same time-intervals as used for light microscopy, were fixed in 2.5 per cent glutaraldehyde in 0.34 M veronal acetate buffer pH 7.4, followed by post fixation in osmium-tetroxide. Embedding was carried out in Epon 812 and thick sections stained with toluidine blue were used for identification of the islets. The thin sections were stained with uranyl acetate and lead citrate and were then examined in a Siemens Elmiskop 101.

Other specimens, taken at the *10 min., 60 min.* and 1 day intervals, were fixed for 2 hours in 3 per cent glutaraldehyde and 2 per cent potassium *pyroantimonate adjusted to pH 7.4 with 0.01 M* acetic acid, followed by fixation for 1 hour in 1 per cent osmium-tetroxide and per cent potassium *pyroantimonate*. The sections were either unstained or stained with uranyl acetate and lead citrate, after which they were viewed in a Siemens Elmiskop 101.

The specificity of the pyroantimonate precipitates was investigated by X-ray analysis, using an energy dispersive system (Kevex X-ray energy spectrometer subsystem 5000 A) combined with a JEOL JSEM 200 scanning-transmission-microscope.

Quantitative Transmission Electron Microscopy

A *stereological method (Ruigrok & Elbers 1972)* was applied for estimation of mitochondrial volume, using a printing frame fitted with a grid of steel wires for production of a square grid of white lines superimposed on the photographs obtained on enlargement of electron micrographs. Ten original micrographs were taken of pancreatic B-, D- and A-cells from each of five animals from the different groups, 1 and 24 hours after the injections. The length fraction of cytoplasmic lines passing through mitochondria was measured, corresponding to the fractional volume of the mitochondria in the cytoplasm.

RESULTS

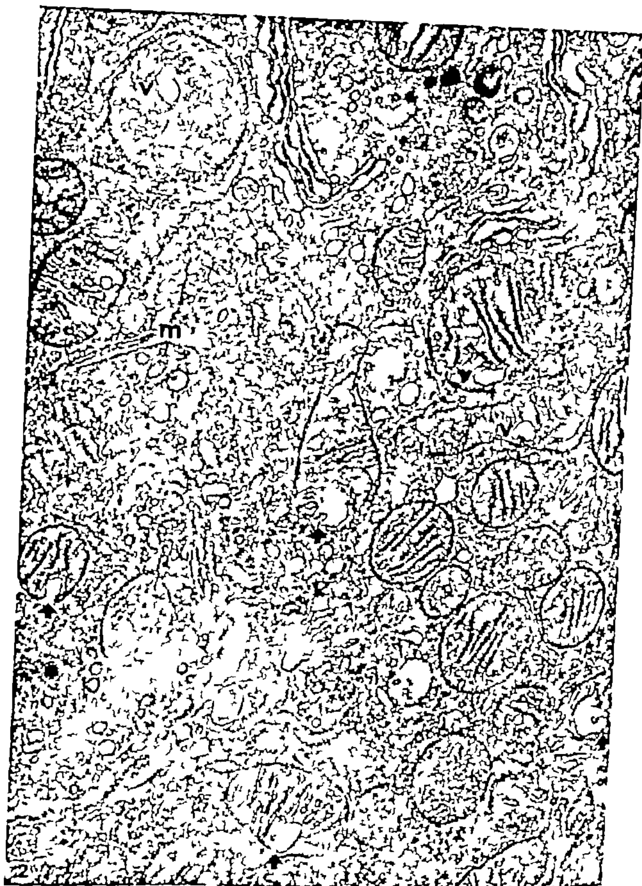
Blood Glucose

The results of the blood-glucose determinations are given in Table 1. The blood-glucose level after DHCC-treatment did not differ significantly from that recorded before the injections in any of the groups. Nor was any significant difference observed between the DHCC- and saline treated groups *of fed* mice or between the corresponding groups of starved mice. The mean blood-glucose level was, however, higher in the fed than in the starved groups, before the injections,

---

Fig. 1. Mitochondrial hypertrophy in *B-cell.* Most mitochondria are rounded or oval and possess preserved cristae and moderate density of their matrices. *Group II, 30 minutes.* × 19 000




m
2

and after the injections until the observation time at 4 hours. Then the starved animals were fed again, and at the following observation times at 24 and 48 hours no difference was recorded between the groups.

Light Microscopy

No light microscopically detectable alterations were found in the endocrine or exocrine pancreas at any observation time in the different groups. Thus, the B-, A- and D-cells appeared normal both as to structure and granulation.

Qualitative Electron Microscopy

At *10 minutes* some B-cells in group II exhibited enlarged mitochondria with preserved cristae and moderate electron density of the matrix apparently representing hypertrophy of these organelles. Most of the hypertrophic mitochondria were rounded or oval. A few secretory granule cores showed an atypical configuration whereas most secretory granules were normal. The endoplasmic reticulum was vesicular and the perinuclear spaces were dilated in some B-cells. The other organelles, as well as the nucleus and plasma membrane, were normal. No alterations were recorded in the A- or D-cells in group II or in any of the islet cells from the other groups. The B-cells mitochondria in these groups were *medium*-sized, most often elongated, and possessed preserved cristae and a moderate electron density of their matrix.

At *30 minutes* still more B-cells in group II showed mitochondrial hypertrophy (Fig 1). The mitochondrial membranes were preserved and the matrix was moderately electron dense. Some hypertrophic mitochondria possessed electron lucent vacuoles in the inner compartment, and at the periphery the mitochondrial membranes showed occasional invaginations with electron lucent interiors (Fig 2).

The endoplasmic reticulum and Golgi complexes were prominent in many B-cells, and signs of granule formation were seen in the Golgi region. Many B-cells also possessed an increased number of so-called light granules, characterized by large rounded, finely granular cores of rather low electron density and often only faintly visible electron lucent halos between the core and the surrounding membrane (Fig 3).

A few D-cells seemed also to possess hypertrophic mitochondria, whereas no other changes were recorded in these cells. The A-cells were unaffected the mitochondria were *medium*-sized and possessed distinct cristae and a matrix of rather high electron density.

Some B-cells in group I also exhibited slight mitochondrial hypertrophy a slightly increased frequency of light granules, and somewhat expanded Golgi complexes. No alterations were recorded in the A- or D-cells from group I, or in any of the cells in group III or IV.

At *60 minutes* similar B-cell changes were observed in the B-cells in group II as at 30 minutes, although the mitochondrial hypertrophy was more marked and an increased number of light secretory granules with more or less prominent halos could be observed.

In addition, an increased number of so-called multiple rough endoplasmic cisternae (MREC) were indentified in the cytoplasm of some B-cells from group II (Fig 4). They consisted of two (Fig 5) or more (Fig 6) closely apposed cisternae separated by narrow spaces of rather uniform width and moderate electron density. The outer membranes possessed ribosomes, whereas the inner membranes were smooth. The lumina of the cisternae were either electron lucent or contained some amorphous or slightly granular substance of low electron density. The MREC were found in any portion of the

---

Fig. 2 Portion of another B-cell showing hypertrophic mitochondria possessing electron lucent vacuoles ( ) and electron-lucent membranous invaginations (arrow) two of which have small polypoid projections of moderate electron density (m) denotes multiple rough endoplasmic cisternae (MREC) and rather prominent Golgi complexes are also demonstrated. Group II; 30 min test × 22,000.

cytoplasm often close to or in direct continuity with rough endoplasmic reticulum or Golgi complex.

Some B-cells also contained cytoplasmic structures tentatively called multi lamellar bodies (ML), consisting of two three or more closely apposed cisternae in a more or less straight semi circular or circular arrangement (Fig 7) The ML were separated by moderately electron-dense narrow spaces of slightly varying width whereas the lumina were usually electron lucent or contained some slightly electron-dense amorphous substance Ribosomes were not seen on the inner or outer membranes (Fig 8) The cisternae constituting the ML were occasionally cystically dilated and spaces were thus formed which were either electron lucent or contained some amorphous moderately electron dense substance (Fig 9) Occasionally two or more cisternae seemed to open into one and the same cystically dilated area. Connections could be seen between the individual cisternae of the ML (Fig 8) No annulate lamellae, however were recorded

Some D-cells in group II exhibited slight mitochondrial hypertrophy whereas the other organelles were normal The A-cells were unaffected

The B-cells in group I showed slight or moderate mitochondrial hypertrophy and a slight or moderate increase in the number of light granules whereas rather few MREC, but no ML, were observed. The A and D cells in group I were normal

At *1 day* qualitatively similar but in some cells more marked alterations were recorded in groups I and II Thus light granules were frequent in some B-cells from both groups.

Some D-cells from group I and II exhibited slight mitochondrial hypertrophy The A-cells were normal

Slight or moderate mitochondrial hypertrophy was also seen in some B-cells from group IV whereas the A and D-cells from this group and all the endocrine cells from group III were normal

At *2 and 3 days* essentially similar findings were made as at 1 day but from the *4th day* on the structural changes described above occurred less regularly and at *1 and 2 weeks* most islets appeared completely normal in all groups.

Pyroantimonate Technique and X Ray Microanalysis

Comparison between the different groups disclosed at all three observation times a more pronounced pyroantimonate precipitate in many B-cells from groups I and II than in those from groups III and IV The precipitates were mainly localized to nuclei and mitochondria (Fig 10) whereas only sparse amounts of precipitates were observed in the secretory granules, the endoplasmic reticulum, the Golgi complexes and the cytoplasmic ground substance An appreciable amount of precipitate was also seen intercellularly in many islets from groups I and II

X ray microanalysis of the precipitates revealed peaks for Ca^{2+} but not for other cations, apart from those associated with the pyroantimonate technique

Quantitative Electron Microscopy

The results of the determination of the fractional volume of the mitochondria in the endocrine cells in tissue taken 1 or 24 hours after the injections are given in Table 2. At *1 hour* the mitochondrial volume was significantly greater in the B-cells from group II than in those from the other groups, whereas this volume was significantly greater in the B-cells from groups I II and IV than

---

Fig 3 B-cell cytoplasm containing two "mature secretory granules (g) Numerous so-called light secretory granules characterized by large rounded, finely granular cores of rather low electron density surrounded by thin electron lucent halos are also present. Group II 30 minutes. × 24 000

Fig 4 B-cell cytoplasm showing enlarged mitochondria of which one has an electron lucent vacuole (v) MREC (arrows) and light secretory granules, some of which (g) are localized to the Golgi area are also shown. Group II 60 minutes. × 12 000

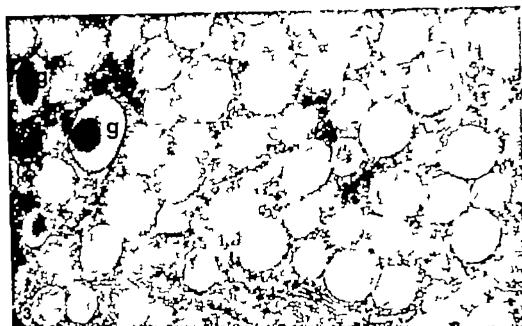

g
3

TABLE 2. *Fractional Volume (Mean ± S.D.) of Mitochondria in the Endocrine Pancreas of Fed and Starved Mice Treated with 1,25-Dihydroxycholecalciferol (DHCC) or Saline (Controls) 1 or 24 Hours before Tissue Sampling*

Group	Starvation	Treatment	B-cells		A-cells		D-cells	
			1 hr	24 hr	1 hr	24 hr	1 hr	24 hr
I	No	DHCC	9.1 ± 0.9	11.1 ± 1.0	7.1 ± 0.5	6.7 ± 0.4	7.0 ± 0.9	8.0 ± 0.8
II	Yes	DHCC	12.1 ± 1.1	12.5 ± 0.9	6.9 ± 0.9	7.2 ± 0.6	7.9 ± 1.2	9.4 ± 0.9
III	No	Saline	8.1 ± 0.5	7.8 ± 0.6	7.4 ± 0.8	6.9 ± 0.7	6.8 ± 0.7	6.9 ± 0.9
IV	Yes	Saline	8.7 ± 0.8	10.8 ± 0.7	7.7 ± 0.6	7.4 ± 0.6	7.3 ± 0.5	7.4 ± 0.7

in those from group III at 24 hours. No difference was observed between the A-cell mitochondria at any observation time. Nor was any significant difference observed at any observation time between the D-cells from the four groups. However, at 24 hours there was a tendency to increased mitochondrial volume in the D-cells from the DHCC-treated groups.

DISCUSSION

The present data show that DHCC injection in fed or starved mice does not affect the blood glucose level at the observation time used here. Nor does this treatment cause any structural alterations that are demonstrated by light microscopy. Ultrastructurally, however, differences were found between the controls and the DHCC-treated mice, suggesting that DHCC in some way, directly or indirectly, affects the islet cells, possibly by interference with the concentration and/or localization of the intracellular biochemical constituents. DHCC is well known to act upon some other kinds of cells, but nothing is so far known about its effects upon the islets.

The ultrastructural alterations were more marked in mice that had been starved before DHCC-injection than in those that were fed before the injection. The cause of this difference is not known. However, since mitochondrial hypertrophy was found at 24 hours also in the B-cells of the starved animals treated with saline, as well as in the B-cells of previously studied starved but non-treated mice (*Boquist* 1977 a), it seems that the effects of starvation and DHCC-treatment upon the B-cells at least in some respects may be similar and thus additive in group II.

Increased mitochondrial volume has previously been observed in the B-cells of islets subjected to low glucose concentrations *in vitro* (*Hultquist & Pontén* 1974, *Borg et al.* 1975, *Boquist* 1977 b) compared with islets exposed to high glucose. Increased mitochondrial volume of unknown significance has also been reported in mice with spontaneous diabetes (*Like et al.* 1965, *Like & Jones* 1967, *Like & Chick* 1970, *Boquist et al.* 1974). It was previously suggested that B-cells with hypertrophic mitochondria, as seen e.g. after starvation, are more easily damaged by alloxan than those with "normal sized" mitochondria (*Boquist* 1977 a). Therefore it is of interest that mitochondrial hypertrophy was observed in the present study already 10

Fig. 5. B-cell cytoplasm containing hypertrophic mitochondria and MREC consisting of two cisternae (arrow). Group II, 60 minutes. × 26,000.

Fig. 6. Two stacks of MREC (arrows) consisting of three closely apposed cisternae separated by narrow spaces of rather uniform width. Group II, 60 minutes. × 28 000.

Fig. 7. Multi-lamellar body in B-cell cytoplasm, consisting of closely apposed smooth cisternae in circular and semicircular arrangement. Group II, 60 minutes. × 28 000.

Fig. 8. Higher magnification of a part of another multi-lamellar body demonstrating closely-apposed smooth cisternae, two of which appear to be in direct continuation with each other (arrow). Group II, 60 minutes. × 60 000.


5
6
8

9

10

minutes after DHCC injection in starved mice since this treatment increases the sensitivity to alloxan (*Boquist et al* 1977)

It is well-known that light secretory granules may occur in the B-cells of many species, in addition to the usually predominating dark ones. A predominance of light β-granules has been reported in conditions with a rapid turnover of insulin (*Greider et al.* 1970) after experimental B-cell stimulation (*Bencosme & Martinez Palomo* 1968, *Williams et al* 1969 *Lazarus & Volk* 1970) and in pregnant rats (*Aerts & Van Assche* 1975) Furthermore, it has been suggested that light β-granules are responsible for the immediate release of insulin, while dark granules represent the insulin reserve (*Shino & Iwatsuka* 1973) Other authors maintain that light β-granules represent proinsulin, while dark granules represent insulin. The results of the present study do not allow any definite conclusion as to the nature of the light β-granules, or the cause of the increased occurrence of these granules in the DHCC-treated mice. However since light β-granules were observed in the Golgi area, both in the present study and in other ultrastructural studies carried out in this laboratory it appears that these granules may represent newly formed insulin. The dark β-granules may then represent a mature storage form of insulin, perhaps differing from newly-formed insulin in respect to the occurrence and/or binding of cations in the granule core.

MREC have previously been described in the B- A and D-cells of the adult rat pancreas, in which they have been ascribed a role in the secretory activity of the endocrine cells (*Wassermann* 1975) In the present study an increased number of MREC were found in some B-cells from the starved DHCC-treated mice In addition, ML without ribosomes on the outermost cisternal membranes were encountered in some B-cells from these mice such structures do not seem to have been previously reported in the endocrine pancreas. The possible functional significance of the MREC and ML, and the cause of the occurrence of ML, and of the increased occurrence of MREC in the B-cells of some DHCC-treated mice is not known. Both structures bear some resemblance to but are in some respects structurally clearly distinguished from, the annulate of unknown significance that have been previously observed in the B-cell cytoplasm of chick embryos (*Benzo* 1974) and in the endocrine cells of the islet organ of the hagfish (*Boquist & Östberg* 1975) Because of the structural similarities between the MREC and ML, these structures might be related developmentally and possibly functionally

Vacuolation and invagination of mitochondrial membranes have previously been observed in pancreatic islet cells in this laboratory (unpublished findings) although at a lower frequency than was found in the present study Similar changes have also been recorded *in vitro* in parathyroid cells in which they are possibly involved in the transport of cations (*Boquist* 1977 c)

Supported by grants from the *Swedish Medical Research Council* (Project No. B76-12X-00718-11B)

Fig. 9 Multi-lamellar body with cystically dilated cisternae. At least two cisternae seem to open into one and the same dilated area (arrows) Group II 60 minutes. × 23,000

Fig 10 Pyroantimonate technique. A pronounced precipitate is present in B-cell mitochondria and nuclei of the B-cell shown. An obvious precipitate is also seen intercellularly whereas the amount of precipitate is sparse in the cytoplasmic ground substance and secretory granules of the B-cells included in the field of view Group II 60 minutes. × 18,000

12*

REFERENCES

Aerts L. & Van Assche F A: Ultrastructural changes of the endocrine pancreas in pregnant rats. Diabetologia *11* 285–289 1975

Bencosme S A & Martinez-Palomo A: Formation of secretory granules in pancreatic islet B cells of cortisone-treated rabbits. Lab. Invest. *18* 746–756 1968

Benzo C A.: Annulate lamellae in hepatic and pancreatic beta cells of the chick embryo. Am. J Anat. *140* 139–143 1974

Boquist L. The endocrine pancreas in early alloxan diabetes. Including study of the alloxan inhibitory effect of feeding and some hexoses. Acta path. microbiol scand Sect. A, *85* 219 229 1977 a

Boquist L. Pancreatic islets subjected to different concentrations of glucose *in vitro* A study with special regard to mitochondrial changes. Virchows Arch Abt. B Zellpath. (In press) 1977 b

Boquist L. Ultrastructural changes in the parathyroids of Mongolian gerbils induced experimentally *in vitro* Effects of variations in Ca^{2+} and Mg^{2+} concentrations Acta path microbiol scand. Sect A *85* 203–218 1977 c

Boquist L. Hagström S & Strandlund L. Effects of 1 25-dihydroxycholecalciferol parathormone and Ca^{+} on the pancreatic B-cell sensitivity to alloxan. Acta path. microbiol scand Sect. A *85* 501–510 1977

Boquist L. Hellman B Lernmark A & Täljedal I B Influence of the mutation diabetes on insulin release and islet morphology in mice of different genetic backgrounds. J Cell Biol. *62* 77–89 1974

Boquist L. & Östberg Y Annulate lamellae and crystalline inclusions in granular endoplasmic reticulum of the islet organ and associated tissue of a cyclostome *Myxine glutinosa*. Cell Tiss Res *158* 75–87 1975

Borg L. A H Andersson A Berne C & Westman J Glucose-dependent alterations of mitochondrial ultrastructure and enzyme content in mouse pancreatic islets maintained in tissue culture A morphometrical and biochemical study Cell Tiss Res. *162* 313–321 1975

Greider M H Bencosme S A & Lechago J The human pancreatic islet cells and their tumors. I The normal pancreatic islets. Lab Invest *22* 344–354 1970

Grimelius L. A silver nitrate stain for α_2 cells in human pancreatic islets. Acta Soc Med Upsal *73* 243–276 1968

Hellerström C & Hellman B Some aspects of silver impregnation of the islets of Langerhans in the rat Acta Endocrinol *35* 518–532, 1960

Hultquist G & Pontén J Ultrastructure of rat pancreatic islets in long-term tissue culture Upsal. J Med Sci. *79* 21–27 1974

Lazarus S S & Volk B W Ultrastructural aspects of the function of rabbit β-cells. *In* The structure and metabolism of the pancreatic islets, Eds. Falkmer S Hellman, B. & Täljedal, I B Oxford Pergamon Press, 1970, pp. 159–170

Like A A & Jones E E Studies on experimental diabetes in the Wellesley hybrid mouse VI Morphological changes in islet tissue. Diabetologia *3* 179–187 1967

Like A A & Chick W L. Studies in the diabetic mutant mouse II Electron microscopy of pancreatic islets. Diabetologia *6* 216–242, 1970

Like A A Steinke J Jones E E & Cahill, G F Jr Pancreatic studies in mice with spontaneous diabetes mellitus. Amer J Path. *46* 621–644 1965

Ruigrok Th J C & Elbers P F The effects of calcium acetate on mitochondria in the perfused rat liver I Accumulation of Ca^{++} and concomitant swelling Cytobiol *5* 51–64 1972

Shino A & Iwatsuka H Histochemistry of the zinc in the pancreatic islets of genetically diabetic yellow KK mice Heterogeneity of B granules. Acta Histochem Cytochem. *6* 275–279 1973

Wassermann D Multiple rough endoplasmic cisternae in the endocrine pancreas of the adult rat. Cell Tiss. Res. *160* 539–549 1975

Wellman K F Volk B W Lazarus S S & Brancato P Pancreatic B cell morphology and insulin content of normal and alloxan-diabetic rabbits and their offspring Diabetes *18* 138–145 1969

Acta path. microbiol. scand. Sect. A, 85: 501–510, 1977

EFFECTS OF 1,25-DIHYDROXYCHOLECALCIFEROL, PARATHORMONE AND Ca^{2+} ON THE PANCREATIC B-CELL SENSITIVITY TO ALLOXAN

L. Boquist, S. Hagström and L. Strindlund

Department of Pathology, University of Umeå, Sweden

Boquist, L., Hagström, S. & Strindlund, L. Effects of 1,25-dihydroxycholecalciferol, parathormone and Ca^{2+} on the pancreatic B-cell sensitivity to alloxan. Acta path. microbiol. scand. Sect. A, 85: 501–510, 1977.

The sensitivity to alloxan was investigated by blood and urine glucose determination and light and electron microscopic study of the endocrine pancreas in groups of mice differing from each other with respect to food ingestion and treatment before alloxan administration. Because of differences in occurrence of glucosuria, degree and duration of hyperglycemia, and severity of structural lesions, it was concluded that starvation increases the alloxan sensitivity and that pre-treatment with 1,25-dihydroxycholecalciferol (DHCC) or parathormone (PTH), but not with Ca^{2+}, enhances the alloxan effect. The serum-calcium concentration determined 10 minutes after pre-treatment was significantly increased in the group given Ca^{2+}, but not in the groups injected with DHCC or PTH. Starved mice injected with DHCC or PTH 10 minutes before alloxan administration exhibited pronounced second hyperglycemia of long duration, and extensive selective B-cell necrosis. Starvation and increased serum concentration of DHCC and PTH are believed, directly or indirectly, to induce B-cell alterations which increase the alloxan sensitivity.

Key words: Alloxan diabetes; 1,25-dihydroxycholecalciferol; parathormone; starvation; islet morphology.

L. Boquist, Department of Pathology, University of Umeå, S-901 87 Umeå, Sweden

Received 23 77 Accepted 23.1.77

Several factors are known that for unknown reasons increase or decrease the sensitivity to alloxan. Thus, e.g. pre-treatment with certain hexoses is known to have a protective effect against alloxan toxicity, which could be verified in a preceding study (*Boquist* 1977 a). In a search for other factors of this kind, an increased sensitivity to alloxan was found in mice pre-treated with 1,25-dihydroxycholecalciferol (DHCC). This effect of DHCC has not been previously reported in any species. Therefore the present study was undertaken to obtain further information about the effects of this vitamin D metabolite for the development, severity and duration of alloxan diabetes, as evidenced by alterations in blood-glucose concentration and B-cell morphology. Since DHCC plays a prominent role in calcium metabolism, the

influence on alloxan-diabetes of administration of Ca^{2+} and parathormone (PTH) was also investigated.

MATERIAL AND METHODS

Animals. Pretreatment and Alloxan Administration

The animals were non-diabetic adult C57BI KsJ mice of both sexes from local stocks kept under standard laboratory conditions. The following experimental groups were used: I. Fed, pre-treated with 1 ml of saline. II. Starved, pre-treated with 1 ml of saline. III. Fed, pre-treated with 7.5 ng DHCC. IV. Starved, pre-treated with 7.5 ng DHCC. V. Fed, pre-treated with 400 U.S.P. Units/kg body weight of PTH. VI. Starved, pre-treated with 400 U.S.P. Unit/kg body weight of PTH. VII. Fed, pre-treated with 0.8 g/kg body weight of Ca^{2+}. VIII. Starved, pre-treated with 0.8 g/kg body weight of Ca^{2+}.

The starved animals were deprived of food for 24 hours before experimentation. The substances used for pre-treatment were administered intraperitoneally 10 minutes before alloxan injection. The alloxan (Alloxan monohydrate, Eastman Kodak Co., Rochester, N.Y.) was dissolved in saline and injected intraperitoneally in all groups at a dose of 200 mg/kg body weight. All injections were carried out under ether anaesthesia.

Blood and Urine Glucose Determination

Blood glucose was assayed by the glucose-oxidase method using Glox® (AB KABI, Stockholm, Sweden) on blood obtained by cutting the tip of the tail before the injections and at the following predetermined intervals after alloxan administration: 1, 2 and 4 hours, and 1, 2, 4, 7 and 14 days, and thereafter once a week (except week 4) in group IV until 10 weeks after alloxan injection.

Qualitative tests for urine glucose were carried out using paper strips (Clinistix, Ames Co., London, England) at the same intervals as above.

Serum Calcium Determination

Serum calcium was determined in some animals from groups II, IV (here called IV a), VI and VIII 10 minutes after injection of the substances used for pre-treatment but before alloxan injection, and in other animals from group IV (here called IV b) 10 minutes after alloxan injection and thus 20 minutes after the administration of DHCC. In addition, serum calcium was assayed in some starved non-pre-treated mice (group IX) 10 minutes after alloxan administration.

Serum calcium was assayed by atomic absorption spectrophotometry on blood obtained in the same way as for blood-glucose determination. Proteins were precipitated with 20 per cent trichloroacetic acid to which $SrCl_2$ was added for depression of the phosphorus interference according to Willis (1961). The absorption was read in a Unicam S.P. 90 B spectrophotometer (Unicam Instruments, Ltd., London).

Tissue Sampling and Light Microscopy

Some of the experimental animals were killed at the following time-intervals after alloxan injection: 5 and 10 minutes, 1, 2 and 4 hours, and 1, 2, 4 and 6 days. Then the pancreas was immediately removed and most of it was fixed in Bouin's fluid. The following stains were applied: hematoxylin-eosin, van Gieson's stain, aldehyde fuchsin, and the silver impregnations according to *Hellerström* and *Hellman* (1960) and *Grimelius* (1968).

Transmission Electron Microscopy

Small pancreatic specimens not used for light microscopy were fixed in 2.5 per cent glutaraldehyde in 0.34 M Veronal acetate buffer pH 7.4, followed by post fixation in osmium tetroxide in the same buffer. Embedding was carried out in Epon 812 and thick sections stained with toluidine blue were used for identification of the islets. The thin sections were stained with uranyl acetate and lead-citrate and were then examined in a Siemens Elmiskop 101.

Some specimens taken at the 1 and 2 day intervals were fixed for 2 hours in 3 per cent glutaraldehyde and 2 per cent potassium-pyroantimonate adjusted to pH 7.4 with 0.01 M acetic acid, followed by fixation for 1 hour in 1 per cent osmium tetroxide and 2 per cent potassium-pyroantimonate. The sections were either unstained or stained with uranyl acetate and lead-citrate, after which they were viewed in a Siemens Elmiskop 101.

The specificity of the pyroantimonate precipitates was investigated by X-ray analysis, using an energy dispersive system (Kevex X-ray energy spectrometer subsystem 5000 A) combined with a JEOL JSEM 200 scanning transmission-microscope.

RESULTS

Symptoms and Course of Alloxan Diabetes

Considerable differences were recorded between the experimental groups as regards the sensitivity towards alloxan, which was roughly estimated by a study of the occurrence and duration of glucosuria, polyuria and polydipsia. Thus, fed animals pre-treated with saline (group I) were more or less insensitive

to alloxan, and the other groups of fed animals exhibited a rather low alloxan sensitivity whereas the groups of starved animals pre-treated with Ca^{2+} showed a moderate sensitivity to alloxan. The groups consisting of starved animals pre treated with DHCC (group IV) or PTH (group VI) on the other hand, were highly sensitive to alloxan. Spontaneous deaths were occasionally found on days 3 to 5 after alloxan administration in groups IV and VI but not in the other groups.

Blood Glucose

Before alloxan injection, the mean blood-glucose level was significantly higher in the fed than in the starved groups (Fig 1) After the administration of alloxan, an initial hyperglycemic phase was recorded in all groups the maximum value was recorded at 1 hour in the fed groups and at 2 hours in most starved groups. Decreasing blood-glu

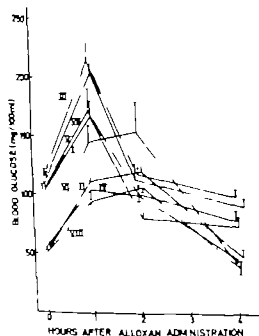


Fig 1 Blood-glucose concentration (mean ± S.E.) in groups of mice before (0 hours) and during the first 4 hours following alloxan injection. Details about the groups are given in the text.

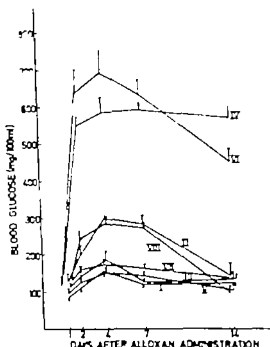


Fig 2 Blood-glucose response (mean ± S.E.) in groups of mice from 1 to 14 days after alloxan injection.

cose concentration was seen in the fed groups after 1 hour and in the starved groups after 2 hours, to levels which at 4 hours were higher in the starved than in the fed mice.

During the second hyperglycemic stage, significant variations were found between the groups as regards the degree and duration of blood glucose elevation (Fig 2) Thus, the blood-glucose concentration was only slightly increased in the groups of fed animals (groups I, III V and VII) whereas a moderate hyperglycemia was observed in the starved animals pretreated with saline (group II) or Ca^{2+} (group VIII) The animals in groups IV and VI, on the other hand, exhibited a pronounced hyperglycemia with significantly higher blood-glucose values in the secondary stage than those in the other groups of mice.

Moreover the duration of the second hyperglycemic stage was longer in groups IV and VI than in the other groups. In the fed groups and in groups II and VIII normo-

glycemia (blood glucose below 140 mg/100 ml) was reached within two weeks after alloxan injection. Group VI was markedly hyperglycemic from 2 until 14 days.

In group IX markedly hyperglycemic values were recorded from 2 until 14 days. This group was the only one followed for more than 2 weeks; the following hyperglycemic values (mg/100 ml; mean ± S.E.) were recorded until the end of the observation period: 3 weeks – 504 ± 21; 5 weeks – 364 ± 18; 6 weeks – 344 ± 12; 7 weeks – 316 ± 15; 8 weeks – 287 ± 20; 9 weeks – 294 ± 11 and 10 weeks 307 ± 19.

Serum Calcium

The results of the serum calcium determinations are given in Table 1. The calcium concentration in groups IV a, IV b, VI and IX did not differ significantly from that recorded in the saline treated mice (group II). The group given Ca^{2+} on the other hand showed a significantly higher serum-calcium concentration than group II.

TABLE 1. *Serum-Calcium Concentration (mmol/l) in Groups of Mice 10 Minutes after Treatment. The Number of Observations is given with Brackets.*

Group	Treatment	Ca (mean ± S.E.)
II	Saline	2.6 ± 0.2 (14)
IV a	DHCC	2.8 ± 0.4 (11)
IV b	DHCC + alloxan	3.0 ± 0.4 (9)
VI	PTH	2.9 ± 0.3 (12)
VIII	Ca^{2+}	3.8 ± 0.4 (14)
IX	Alloxan	2.5 ± 0.3 (12)

Light Microscopy

Five and 10 minutes and 1 hour after alloxan injection the endocrine pancreas was normal in all groups. At 2 hours some B-cells in group IX and VI exhibited slightly vacuolated cytoplasm, whereas the islets in the other groups were normal.

At 4 hours pyknosis and vacuolation and occasionally disintegration were recorded in the cytoplasm of some B-cells in group IX and VI. Cytoplasmic vacuolation was infrequently found in the B-cells of the other groups of starved animals, whereas no changes were recorded in the islets of the other groups.

At day 1 many degenerated and necrotic B-cells were observed in groups IX and VI and some necrotic B-cells were seen also in group II. The other groups exhibited no obvious alterations.

Two days after alloxan injection extensive selective B-cell necrosis was found in the islets from group IX (Fig. 3 A) and VI (Fig. 3 B) leaving central accumulations of cellular debris with scattered inflammatory and stromal cells. In most islets there were no preserved B-cells, whereas a few remaining B-cells could be identified in single islets. The A- and D-cells were unaffected, as was the exocrine parenchyma.

At 2 days some B-cells from groups II and VIII showed pyknosis and cytoplasmic vacuolation and a few B-cells were necrotic (Fig. 2 C). Fed animals pre-treated with DHCC (group III) or PTH (group V) on the other hand showed slight B-cell anisokaryosis and a few B-cells with cytoplasmic vacuolation (Fig. 2 D). In the other groups no changes were recorded in the endocrine or exocrine parenchyma.

At 4 days extensive selective B-cell necrosis was recorded in groups IX and VI and a sparse or moderate amount of degenerated and necrotic B-cells was observed in the islets from the other groups of starved animals. In the other groups the findings were essentially similar to those made at 2 days. At 6 days extensive selective B-cell necrosis was still recorded in the islets from groups IX and VI and rather few necrotic B-cells were observed in groups II and VIII. In the other groups of animals the islets were essentially normal.

Electron Microscopy

At 5 *minutes* some mitochondria in the B-cells from groups IX and VI exhibited swelling and disruption of the inner membranes but no other lesions. Non-damaged mitochondria were often hypertrophic. The A- and

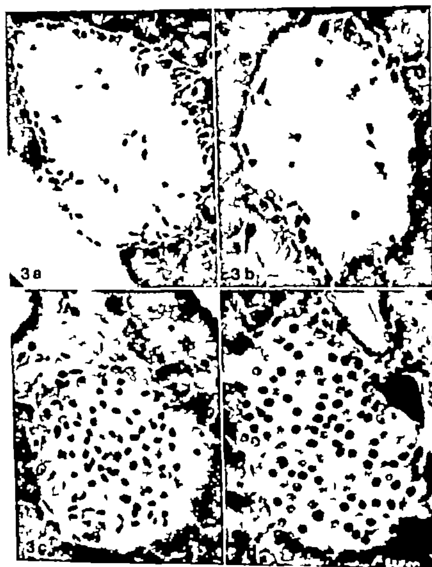


Fig 3 Photomicrographs of mouse pancreas two days after alloxan injection, showing extensive selective B-cell necrosis in group IV (A) and VI (B) moderate degenerat. changes in group II (C) and slight anisokaryosis and some cytoplasmic vacuolation in group V (D) Hematoxylin-Eosin. × 380.

D-cells were unaffected The islets from the other groups were normal.

At *10 minutes* many B-cell mitochondria from groups IV and VI and a few B-cell mitochondria from groups II and VIII showed similar changes as those above (Fig. 4) and some mitochondria in groups IV and VI were disintegrated. Non-damaged mitochondria were often hypertrophic No other changes were recorded in the islets of these or the other groups.

At *1 hour* most mitochondria in the B-cells of groups IV and VI were disintegrated, and the Golgi complex was occasionally distended or disorganized The secretory granules were preserved, but some of them possessed atypical configuration of the cores. Only some few secretory granules were of the so-called light

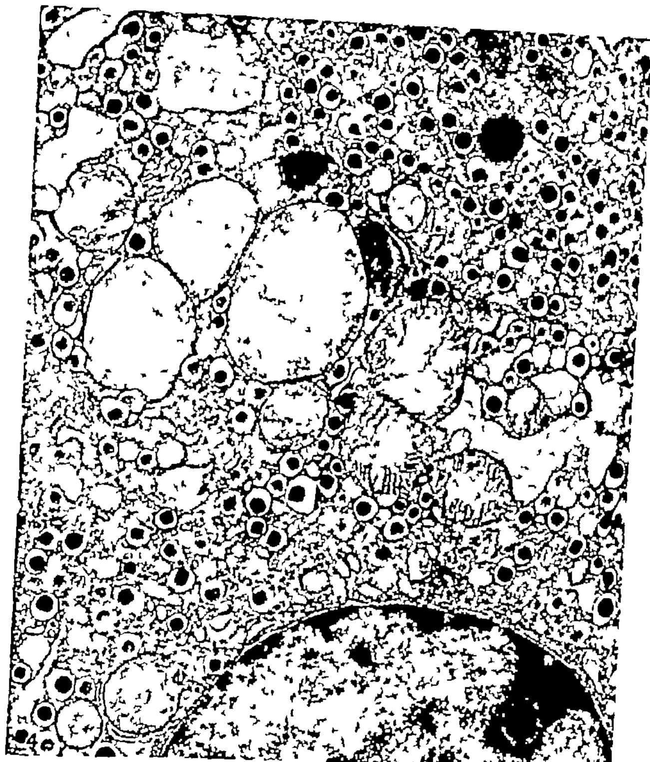


Fig 4 B-cells of mouse from group IV ten minutes after alloxan injection, showing swollen mitochondria with disrupted inner membranes, and numerous normal secretory granules. × 18 000

Fig 5 Portion of an islet of mouse from group II two days after alloxan injection showing undamaged B-cells (B) with small or medium-sized mitochondria and rather few secretory granules, and a severely damaged B-cell (DB) with electron lucent cytoplasm and secretory granules with atypical cores. Varying amounts of pyroantimonate precipitates are observed. Pyroantimonate technique. × 10 000


B
DB
B

type Multiple rough endoplasmic cisternae (MRFC) were only sparsely represented No so-called multi lamellar bodies (ML) were encountered Dilated perinuclear spaces were seen in some B-cells from these groups. Mitochondrial disintegration was also observed although less frequently, in groups II and VIII No other essential findings were made in any group

At 2 *and 4 hours* the degenerative changes in the B-cells were still more marked in groups IV and VI and less marked in groups II and VIII whereas a few mitochondria in the groups of fed mice showed swelling and occasionally disruption of the membranes. Disorganization of the Golgi complex and endoplasmic reticulum was seen in many B-cells from groups IV and VI and in a few B-cells from groups II and VIII In some islets of groups IV and VI there were a few necrotic B-cells As to secretory granules and MREC, similar findings were made as at 1 hour The other groups showed no obvious lesions.

At *1 day* many B-cells in groups IV and VI and a few B-cells in group II and VIII were necrotic whereas no necrosis was seen in the islets from the other groups. At *2 days* almost all B-cells in group IV and VI and some B-cells in group II and VIII were necrotic Degenerative changes of varying severity but no necrosis, were also seen in rather few B-cells in the groups of fed mice Preserved B-cells in the groups of starved animals often showed expanded Golgi complex sparse or moderate amount of secretory granules and small or medium sized mitochondria without degenerative changes (Fig 5) MRFC were still sparsely represented and no MI were found. Rather few light secretory granules were encountered The A and D cells were still unaffected in all groups At *4 and 6 days* the differences between the groups described above were still evident

A study of pyroantimonate treated sections disclosed a varying amount of fine or coarse precipitate in the B-cells of the different groups degenerating cells generally possessed a greater amount of precipitate than non damaged ones. The precipitation was mainly localized to nuclei and cytoplasmic ground substance outside secretory granules and mitochondria X ray analysis of the pyroantimonate precipitates revealed that they contained Ca^{2+} but no other cations, apart from those associated with the technique applied.

DISCUSSION

Preceding studies of experimental diabetes in C57BL-mice have revealed a) that animals not subjected to any pre-treatment are sensitive to alloxan, although the functional and structural changes are of limited severity (*Boquist* 1977 b) b) that starvation increases the alloxan sensitivity both in pre-treated and non pre-treated animals and c) that pre-treatment with glucose, mannose and fructose antagonizes the effect of alloxan upon the B-cells (*Boquist* 1977 a) The results of the present study support the view of an enhancing effect of starvation on the B-cell toxicity of alloxan

The present data also indicate that pre-treatment with DHCC or PTH increases the cytotoxic effect of alloxan Extensive B-cell necrosis and a marked secondary hyperglycemic phase of long duration were found in the animals treated with these substances. This has previously not been reported in any species. It is noteworthy that the enhancing action of DHCC and PTH was evident only in starved animals.

The cause of the enhancing effect of DHCC and PTH on alloxan B-cell toxicity is not known Both substances are intimately involved in calcium-phosphorus metabolism, and calcium is well known to play an important role in the function of the B-cells. Therefore the alloxan enhancing effect of DHCC and PTH might be associated with their action on the serum-concentration of calcium. However with the doses used in the present study no alteration in the serum calcium concentration was observed 10 minutes after the injection of DHCC or PTH corresponding to the time when alloxan is

injected in the alloxan experiments, whereas an enhanced serum-calcium level but no enhancing of the alloxan effect was recorded at that time in animals pre-treated with Ca^{2+}. Therefore it is unlikely that the alloxan-enhancing action of DHCC and PTH is dependent upon the serum calcium concentration.

Another possible cause of the alloxan-enhancing effect of DHCC and PTH may be that these substances directly or indirectly affect the B-cells in some way. In a parallel study (*Boquist et al.* 1977) of C57BL-KsJ +/+ mice treated with DHCC, but not with alloxan, structural changes were observed in the B-cells, suggesting that this metabolite in some way affects the B-cells. In this context it is also of interest that primary hyperparathyroidism is associated with fasting hyperinsulinemia and exaggerated insulin-response to glucose (*Kim et al.* 1971) which has been suggested to be unrelated to abnormalities of A-cell glucagon (*Kalkhoff et al.* 1976). Hypercalcemia *per se* does not enhance insulin secretion in response to glucose over that achieved with physiologic concentrations of the ion (*Curry et al.* 1968, *Kim et al.* 1971).

Since the synthesis of DHCC in the kidneys is feedback regulated by the serum calcium concentration (*Boyle et al.* 1971) and since PTH serves as a tropin for the production of DHCC (*Garabedian et al.* 1972, *Henry & Norman* 1975) the lack of an alloxan-enhancing effect in the Ca^{2+} treated mice, and the presence of such an effect in the animals injected with PTH, might be due to alterations induced by these substances in the synthesis of DHCC: the effect of PTH might then be mediated by DHCC.

It is of interest that hypertrophy of the B-cell mitochondria was observed in DHCC-treated, starved animals in the parallel study (*Boquist et al.* 1977), since enlargement of B-cell mitochondria has previously been observed in starved mice (*Boquist* 1977 a) which are known to be more sensitive to alloxan than fed ones. As a working hypothesis it is suggested that the enhancing effect of DHCC and PTH on B-cell alloxan sensitivity in starved mice is due to a direct or indirect action of these substances upon the B-cells.

In the parallel study mitochondrial hypertrophy was observed in the B-cells shortly after the pre-treatment of starved mice with DHCC or PTH and later these cells also exhibited increased frequency of light granules and MREC, and occurrence of ML. Hypertrophy of B-cell mitochondria was found also in the present study shortly after pre-treatment in the groups of starved mice given DHCC or PTH before alloxan administration, whereas no ML, and no obvious increase in the occurrence of light β-granules or MREC were seen at later observation times. The cause of this difference may be that the B-cells are early damaged by alloxan, which inhibits the possibilities for development of the organelles described above already before marked degeneration and necrosis are structurally evident.

Supported by grants from the *Swedish Medical Research Council* (Project No. B76-12X-00718-11B).

REFERENCES

Boquist L.: The endocrine pancreas in early alloxan diabetes. Including study of the alloxan inhibitory effect of feeding and some hexoses. Acta path. microbiol. scand. Sect. A, *85*: 219–229, 1977.

Boquist L.: Differences in the expressions of spontaneous and induced diabetes in Chinese hamsters, Mongolian gerbils and C57BL-KsJ and C57BL-6J mice. *In*: Proc. XIth Congr. International Diab. Fed., ed. J. S. Bajaj, Exc. Med., Amsterdam, 1977 b.

Boquist L., Hagström S. & Strindlund L.: Effect of 1,25-dihydroxycholecalciferol administration on blood glucose and pancreatic islet morphology in mice. Acta path. microbiol. scand. Sect. A, *85*: 489–500, 1977.

Boyle I. T., Gray R. W. & DeLuca H. F.: Regulation by calcium of in vivo synthesis of 1,25-dihydroxycholecalciferol and 21,25-dihydroxycholecalciferol. Proc. Nat. Acad. Sci. USA *68*: 2131–2134, 1971.

Curry D. L., Bennett L. L. & Grodsky G. M.: Requirement for calcium ion in insulin secretion by the perfused rat pancreas. Am. J. Physiol. *214*: 174–178, 1968.

Garabedian M Holick M F Deluca H F & Boyle I T Control of 25-hydroxycalciferol metabolism by parathyroid glands Proc. Nat. Acad Sci. *69* 1673–1676 1972.

Grimelius L. A silver nitrate stain for A_2 cells in human pancreatic islets. Acta Soc Med. Upsal *73* 243–276 1968

Hellerström C & Hellman B Some aspects of silver impregnation of the islets of Langerhans in the rat Acta Endocr *35* 518–53? 1960

Henry H L & Norman A W Studies on the mechanism of action of calciferol VII Localization of 1,25-dihydroxy vitamin D_3 in chick parathyroid glands. Biochem. Biophys Res Commun *62* 781–788 1975

Kalkhoff R K Gossain V V, Matute M L & Wilson S D Plasma alpha-cell glucagon in primary hyperparathyroidism. Metabolism *25* 769–773 1976

Kim H Kalkhoff R K Costrini N V Cerletty J M & Jacobsen M Plasma insulin disturbances in primary hyperparathyroidism. *J Clin. Invest. 50* 2596–2603 1971.

Willis J B The determination of metals in blood serum by atomic absorption spectroscopy Spectrochim. Acta *16* 259–270 1960.

Acta path. microbiol. scand. Sect. A, 85: 511–518, 1977

LIVER BIOPSIES FROM PSORIATICS RELATED TO METHOTREXATE THERAPY

3. Findings in Post Methotrexate Liver Biopsies from 160 Psoriatics

A. NYFORS

Department of Dermatology, The Finsen Institute, Copenhagen, and Department of Pathology, Hvidovre Hospital, Hvidovre, Denmark

Nyfors, A. Liver biopsies from psoriatics related to Methotrexate therapy. 3. Findings in post Methotrexate liver biopsies from 160 psoriatics. Acta path. microbiol. scand. Sect. A, 85: 511–518, 1977.

The purpose of this paper is to report findings in post MTX liver biopsies from 160 psoriatics treated with Methotrexate (MTX) in single weekly oral doses of 25 mg maximum. The paper comprises two materials: A. 92 patients with a single biopsy and B. 68 patients with serial biopsies. At the time of liver biopsy the 92 patients had received a mean cumulative Methotrexate dose of 2287 mg (range 50–5075 mg). One patient had cirrhosis and six patients had fibrosis. Comparing these 7 patients with patients having normal liver histology (13 patients) revealed no statistically significant difference in cumulative doses of MTX, but a statistically significant higher admitted alcohol intake during MTX therapy ($p < 0.02$) and an older age ($p < 0.01$) in the patients with cirrhosis or fibrosis. In the 68 patients MTX had accumulated to a mean dose of 3940 mg (range 325–8355 mg) at the time the latest liver biopsies were taken. Among the latest liver biopsies were 14 cirrhoses (21 per cent, 95 per cent confidence limits 12–32 per cent) and 16 fibroses (24 per cent, 95 per cent confidence limits 14–35 per cent). The 14 patients with cirrhosis when compared to patients with normal histology (9 patients) had taken an equal total dose of MTX at the latest liver biopsy but had consumed a statistically significant higher amount of alcohol ($p < 0.05$) during MTX therapy and also tended to be older ($p < 0.06$). Comparison of material A and B indicates that the prevalence of cirrhosis and fibrosis among MTX treated psoriatics increases rapidly beyond a cumulative dose of two to four grams of MTX. No MTX treated psoriatics should thus be allowed to pass this dosage range without having a liver biopsy performed.

Key words: Liver damage; post MTX liver biopsies; psoriatics; alcohol; Methotrexate.

A. Nyfors, Department of Dermatology, The Finsen Institute, DK 2100 Copenhagen, Denmark.

Received 9.ii.77. Accepted 9.ii.77.

An increase in the number of pathological findings in liver biopsies from psoriatics, taken before and after Methotrexate (MTX) therapy has been previously described (1, ref. 16, 22, 28, 30).

Many psoriatics have been and are still being given MTX without performance of a liver biopsy prior to MTX therapy. Even in psoriatics who have been on MTX therapy for years it is in the interest of the patient and physician to start liver biopsy controls, as liver function tests are not a reliable enough indicator of liver damage induced by MTX (1, ref. 16, 28).

This paper reports two studies of liver bi-

opsy material taken from psoriatic patients taking MTX A a study of single post MTX liver biopsies from 92 patients, B a prospective study of serial post MTX liver biopsies from another 68 patients

The purpose of study A was to investigate the frequency and severity of pathological findings in liver biopsies after the initiation of MTX therapy for psoriasis

The purpose of study B was to evaluate and compare histological findings in serial liver biopsies from patients with severe psoriasis at varying time intervals after initiation of MTX therapy An attempt was made to correlate possible changes in liver histology with MTX therapy or other factors such as alcohol intake age and obesity

A SINGLE LIVER BIOPSIES

MATERIAL AND METHODS

Selection of patients

The patients included in this study were required to have had

1 Typical and severe psoriasis unresponsive to previous treatment.
2 MTX therapy
3 One post MTX liver biopsy longer than 5 mm.
4 Willingness to cooperate

Material

The study included 92 liver biopsies taken from 92 psoriatics during MTX therapy

The administration of MTX therapy including precautions, and clinical and laboratory controls have been described elsewhere along with the liver biopsy technique and proceedure for evaluation of histological findings (1)

RESULTS

Clinical findings at the time of liver biopsy pertinent to liver histology

The mean age of the 46 males and 46 females was 57 years (range 26–86 years) Table 1 shows the admitted alcohol consumption before and during MTX therapy The men had a statistically significant higher alcohol consumption than the women before as well as during MTX therapy ($p < 0.01$ Chi square test $2\times k$) (1 ref 25)

Jaundice had previously occurred in 12 patients, while 14 patients had had gallstones verified by cholecystography Twenty nine patients were obese. Three patients had mild hepatomegaly while none had ascites.

TABLE 1 *Admitted Alcohol Intake before and during MTX Therapy in 92 patients with Single Post MTX Liver Biopsies*

	Before ♂	Before ♀	During ♂	During ♀
Occasionally	8	32	12	32
1–3 drinks a week	5	9	12	11
1–3 drinks a day	18	5	16	3
More than 3 drinks a day	15	0	6	0

TABLE 2. *Chief Histological Diagnoses in 92 Single Post MTX Liver Biopsies*

Cirrhosis	1	(1 %)
Fibrosis	6	(7 %)
Mixed changes	12	(13 %)
Non specific reactive hepatitis	10	(11 %)
Fatty change	50	(54 %)
Normal	13	(14 %)

Mixed changes non-specific reactive hepatitis + fatty change

Laboratory Findings

Abnormal elevation of SGOT was found only in the patient with cirrhosis.

Liver Histology

Table 2 indicates the chief histological diagnoses of 92 single post MTX liver biopsies.

Table 3 presents the chief clinical and histological features in 7 patients with either cirrhosis or fibrosis in their liver biopsies.

MTX Therapy

The average duration of MTX therapy at the time of liver biopsy was 52 months (range 2–105 months) with a mean cumulative MTX dose of 2287 mg (range 50–5075 mg) During MTX therapy a single weekly oral

TABLE 3. *Clinical and Histological F at   at th Tim of I   Bi psy in 7 Patients ith Cirrh si or Fib sis*

Patient number	Sex	Age	Obesity	Ethanol intake before MTX	Ethanol intake during MTX therapy	MTX total dose (mg)	SGOT	Chief histological diagnosis
304	M	75	0	3	3	1895	normal	fibrosis, moderate
308	M	79	0	1	1	305	normal	fibrosis, mild
318	F	63	+	3	3	1642	normal	fibrosis, mild
321	M	65	0	4	4	1612	abnormal	cirrhosis
345	F	59	0	1	1	2718	normal	fibrosis, mild
378	M	84	+	1	3	1015	normal	fibrosis, mild
388	M	54	0	4	2	2640	normal	fibrosis, mild

1 occasionally 2 1 3 drink week 3 1–3 drinks day 4 more than 3 drink a day

dose of 25 mg MTX maximum had been given continuously in 23 patients. The remaining patients had had MTX therapy discontinued after satisfactory clearing of psoriasis The mean duration of MTX therapy comprised 68 per cent (range 5–100 per cent) of the possible total time between initiation of MTX therapy and the liver biopsy

Correlations

a) before and during MTX therapy The alcohol intake in the 92 patients considered as a group was significantly decreased during MTX therapy ($p < 0.01$) (Wilcoxon matched-pairs signed-ranks test = (Wilcoxon test)) (1 ref 25) while it was unchanged in the seven patients who had cirrhosis or fibrosis in their liver biopsies.

b) comparison between 13 patients with normal histology and 7 patient with cirrhosis or fibrosis There was no significant difference between the total doses of MTX taken by the two groups ($p<0.45$ Mann-Whitney U test) However the latter group was significantly older ($p < 0.002$) and had consumed a statistically higher amount of alcohol than the former group during MTX therapy ($p < 0.016$ Mann-Whitney U test) There was no significant difference between the two groups in either the number of patients with obesity or the distribution of sex (Fisher exact probability test)

B. SERIAL BIOPSIES

MATERIAL AND METHODS

Selection of patient

Patients included in this study were required to have had

1 Typical and severe psoriasis unresponsive to previous therapy
2 MTX therapy
3 At least two liver biopsies longer than 5 mm.
4 Willingness to cooperate

Material

The study included 155 liver biopsies taken from 68 patients during MTX therapy Fifty two patients had two liver biopsies, 13 patients had 3 and 3 patients had 4 biopsies. For each patient histological findings in the latest and earliest liver biopsies were compared.

RESULTS

Clinical findings pertinent to liver histology

The study included 33 males and 35 females with an average age of 57 years (range 23–80 years) The admitted alcohol intake before and during MTX therapy is shown in Table 4 The 68 patients had a statistically significant decreased alcohol intake during MTX therapy ($p < 0.01$ Wilcoxon test) Before and during MTX therapy the men had a statistically significantly higher alcohol consumption than the women ($p < 0.05$ Chi square test $2\times k$) Potentially hepatotoxic medicine (1) was used before MTX therapy

by 35 patients (14 males, 21 females) and during MTX therapy by 28 patients (10 males 18 females) Jaundice had previously occurred in 11 patients, while 8 had gall stones verified by cholecystography and 5 had diabetes mellitus. Twenty three patients were obese. Hepatomegaly was not detected in any of the patients but one patient had mild ascites at the time of the latest liver biopsy (which showed cirrhosis)

Laboratory Tests

At the time of latest liver biopsy the SGOT was normal in 12 of 14 patients with cirrhosis

TABLE 4 *Admitted Alcohol Intake before and during MTX Therapy in 68 Psoriatics with Serial Post MTX Liver Biopsies*

	Before		During	
	♂	♀	♂	♀
Occasionally	8	19	8	20
1–3 drinks a week	8	12	14	12
1–3 drinks a day	15	3	8	3
More than 3 drinks a day	2	1	3	0

TABLE 5 *Pathological versus Normal Findings in Serial Liver Biopsies in 68 psoriatics during MTX Therapy*

	First liver biopsy	Latest liver biopsy
Pathological	53	59
Normal	15	9
Total	68	68

Liver Histology

Table 5 shows the number of pathological and normal liver biopsies taken during MTX therapy with a mean time interval between biopsies of 19 months.

Table 6 indicates the chief histological diagnoses in the first and latest liver biopsies from 68 psoriatics.

The initial post MTX liver biopsies revealed 9 cases of cirrhosis, in contrast to 14 cases of cirrhosis found among the latest liver biopsies The five cases of cirrhosis which developed during MTX therapy were preceeded by normal liver histology in one case, moderate mixed changes in one case and portal fibrosis in 3 patients. There was one case of macronodular cirrhosis evident in both the initial and final liver biopsies from one patient with cirrhosis, while the remaining 21 biopsies showing cirrhosis were micronodular All 23 liver biopsies with cirrhosis also showed mixed changes

TABLE 6 *Chief Histological Diagnoses in Serial Liver Biopsies from 68 Patients*

Diagnosis	First liver biopsy	Latest liver biopsy
Cirrhosis	9 (13 %)	14 (20 %)
Fibrosis	10 (15 %)	16 (24 %)
Mixed changes	20 (29 %)	16 (24 %)
Non-specific reactive hepatitis	6 (9 %)	5 (7 %)
Fatty change	8 (12 %)	8 (12 %)
Normal	15 (22 %)	9 (13 %)
Total	68	68

Seven patients were found to have mild portal fibrosis in their first post MTX liver biopsies. The latest biopsies from these 7 patients showed 1 moderate portal fibrosis, 3 mild portal fibrosis, 1 moderate mixed changes, 1 mild mixed changes and 1 mild non-specific reactive hepatitis. The portal fibrosis thus appeared to have disappeared in liver biopsies from 3 patients while continuing MTX therapy The latest liver biopsies also revealed 12 cases of portal fibrosis, which had been preceeded by biopsies with mixed changes in 6 cases non-specific reactive hepatitis in 2 and normal histology in 4 cases. The same 12 biopsies with portal fibrosis also showed mixed changes in 10 cases and mild non-specific reactive hepatitis in 2 cases.

Comparison of histological findings in the earliest and the latest liver biopsies taken from each of 68 patients during MTX therapy showed that 27 were unchanged, 15 had

TABLE 7 *Clinical and Histological Features in 14 Patients with Cirrhosis*

Patient number	Sex and Age at latest biopsy		Ethanol intake		MTX total dose (mg) at		Time between biopsies (years)	SGOT at latest biopsy	Chief histological diagnosis:	
			before MTX therapy	during MTX therapy	first biopsy	latest biopsy			at first biopsy	latest biopsy
203	M	56	3	3	2994	4469	3	abnormal	cirrhosis	cirrhosis
211	F	71	1	1	2378	2578	1	normal	cirrhosis	cirrhosis
227	M	67	3	1	2510	2610	1	normal	cirrhosis	cirrhosis
235	M	66	2	2	3260	3850	1	abnormal	cirrhosis	cirrhosis
237	F	72	2	2	2500	2500	2	normal	cirrhosis	cirrhosis
241	M	58	2	2	2343	2593	1	normal	cirrhosis	cirrhosis
247	M	59	3	3	2203	2580	1	normal	cirrhosis	cirrhosis
266	F	58	2	2	3408	3423	1	normal	cirrhosis	cirrhosis
260	F	70	1	2	1755	1790	1	normal	cirrhosis	cirrhosis
215	M	64	1	1	2748	3798	4	normal	moderate mixed changes	cirrhosis
216	F	65	2	1	328	4065	4	normal	normal	cirrhosis
246	F	60	4	2	325	523	4	normal	moderate fibrosis	cirrhosis
252	M	61	3	2	3633	4045	1	normal	moderate fibrosis	cirrhosis
257	M	66	3	3	2415	2430	1	normal	moderate fibrosis	cirrhosis
Mean		65			2345	3061	2			

1: occasionally 2: 1–3 drinks a week 3: 1–3 drinks a day; 4: more than 3 drinks a day
Mixed changes: non-specific reactive hepatitis + fatty change

improved and 26 had increased abnormalities (Sign test $p = 0.13$)

Table 7 presents the clinical and histological features of the 14 patients having cirrhosis present in their latest liver biopsies.

MTX Therapy

The average cumulative dose of MTX in all patients was 3940 mg (range 325–8355 mg) at the time of latest liver biopsy compared to 2918 mg (range 175–5568 mg) at the time of the first liver biopsy The mean cumulative dose of MTX at the time of latest liver biopsy in the 14 patients with cirrhosis was 3061 mg while it was 4168 mg in the remaining 54 patients ($p < 0.02$ Mann Whitney U test)

Correlations

a) between histological findings in the first and latest liver biopsies in all 68 patients.

Cirrhosis and/or fibrosis were found to have developed in 14 patients during the study Of 15 patients with normal histology in the initial liver biopsy eight developed pathological liver histology during the study In contrast, only two of the 53 patients with initial pathological liver histology showed normal histology in the latest liver biopsies. The frequencies of 8/15 and 2/53 are significantly different ($p < 0.01$ Fisher exact test)

Cirrhosis and fibrosis were found in 19/68 of initial liver biopsies and in 30/68 of the latest liver biopsies ($p < 0.05$ Fisher exact test)

These findings developed in 12/18 of patients with initially abnormal liver biopsies compared with 5 of 8 patients with normal first biopsies, a difference which is not significant ($p < 0.26$ Fisher exact test)

b) between histological subgroups (cirrhosis/fibrosis/other pathological findings/normal) at the latest biopsy There was no statistically significant difference between MTX cumulative dose in the 9 patients with normal histology (mean 3000 mg) and the 14 patients with cirrhosis (mean 3061 mg) ($p = 0.245$ Mann Whitney U test)

Patients with cirrhosis had a significantly higher alcohol intake during MTX therapy than patients with normal liver histology ($p = 0.041$ Mann Whitney U test) A significantly higher number of patients with cirrhosis were also obese ($p = 0.033$ Fisher exact test) and this group also tended to be older than patients with normal histology ($p = 0.058$) There was no significant correlation between patients in the 4 histological subgroups with respect to distribution of sex or intake of potentially hepatotoxic medicine (Fisher exact test)

DISCUSSION

A Single Biopsies

Several large studies with series of psoriatic patients undergoing one post MTX liver biopsy have been reported. These were previously summarized and analysed according to liver histology total MTX dose, MTX dosage frequency and admitted alcohol intake (1 ref 16 Table 10) The Cooperative study (1 ref 28) with 372 liver biopsies found 2 6 per cent cirrhosis and 34 per cent fibrosis. *Zachariae et al* (1 ref 30) with 96 liver biopsies found 6 per cent cirrhosis. In the present study of 92 liver biopsies was found cirrhosis or fibrosis in 7 per cent of biopsies. These findings agree with the mean incidence of cirrhosis and fibrosis found in psoriatics not previously treated with MTX. However the present figures are smaller than those of either the Cooperative study or the study by *Zachariae et al.* They are also smaller than the average values computed from the eight studies previously summarized, which were 8.7 per cent cirrhosis and 18 per cent fibrosis.

Almeyda et al (1 ref 1) in a study of 4? single post MTX liver biopsies found a statistically significant higher MTX cumulative dose in the patients with cirrhosis or fibrosis ($p = 0.05$) This was not found in the pre-

ent study possibly due to our small number of patients with cirrhosis or fibrosis.

Since concomitant alcohol intake seems to increase liver damage it would seem desirable to forbid such intake, if possible, during MTX therapy According to the Copenhagen Study Group of Liver Diseases (3) cirrhotics may live as long as normal controls if they abstain from any intake of alcohol. Another contributing factor to the development of liver damage appears to be age. Since this factor cannot be changed, it may perhaps be considered that the finding of liver damage is more acceptable in older than in younger age groups since not everyone exposed to hepatotoxic factors develops liver damage Genetic factors may be important (2)

B Serial Biopsies

In the literature there are only 4 studies reporting more than 20 serial post MTX liver biopsies per study The Cooperative study (1 ref. 28) involving 81 patients found no statistically significant changes in either the degree of fibrosis or the number of cases with cirrhosis between the first and latest post MTX liver biopsies. The mean interval between liver biopsies during MTX therapy was 13 months. However they did find a significant increase ($p = 0.038$) in the occurrence of portal inflammation at the time of the latest liver biopsy *Almeyda et al* (1 ref 1) in 30 serial post MTX liver biopsies found 15 normal and 15 pathological liver specimens in initial biopsies compared to findings of 14 normals, 3 with fibrosis and 13 with minor pathological findings in the latest liver biopsies which were taken after a mean interval of 13 months of MTX therapy *Zacharae et al* (1 ref 30) had 3 cases of cirrhosis and 6 cases of fibrosis develop among 28 patients between initial and follow up liver biopsies taken after 3–4 years of MTX therapy *Reese et al* (1 ref 21) found no progression in the fibrosis score in follow-up biopsies among 21 serial liver biopsies taken after an average of 12 months of MTX therapy However they showed a statistically significant ($p < 0.001$) effect of alcohol intake on the histology of the biopsy specimens.

The 21 per cent incidence of cirrhosis among the latest post MTX liver biopsies in the present study agrees most closely with the 11 per cent incidence found by Zacharae et al. The occurrence of cirrhosis during MTX therapy thus seems to be extremely high when compared with the 2-3 per cent incidence of cirrhosis found previously in psoriatics who had never received MTX (1 ref 28)

In this study the cumulative MTX dose was not found to be statistically higher in the group of cirrhotic patients than in the group of patients with normal histology This agrees with findings in the studies mentioned above However the alcohol intake during MTX therapy did correlate significantly with the findings of cirrhosis in liver histology both in the study by Reese et al. and in the present study

The findings of more cases of cirrhosis in this study and in the study of *Zacharae et al.* than in those of *Almeyda et al* and *Reese et al* is difficult to explain, as the cumulative dose of MTX, MTX dosage schedules and alcohol intake during MTX therapy appear to be approximately the same size Possible factors contributing to the differences in findings include previous liver pathology as documented by pre-MTX liver histology age obesity potential hepatotoxic medicines and differences in the type of alcohol consumed. To rule out the first mentioned factor a pre-MTX liver biopsy is mandatory It is probable that at least some of the 14 patients with cirrhosis in their latest liver biopsies had fibrosis or cirrhosis before initiation of MTX therapy

The liver damage demonstrated in parts A and B of this study and in a previous study of post MTX liver biopsies from psoriatics (1 ref 16) suggest a multifactorial aetiology produced by MTX, alcohol, age, obesity and potentially hepatotoxic medicine.

Comparing the two groups of patients A and B in this study the most conspicuous finding is the high incidence of cirrhosis and fibrosis in group B compared to the low in-

improved and 26 had increased abnormalities (Sign test $p = 0.13$).

Table 7 presents the clinical and histological features of the 14 *patients having cirrhosis present in their latest liver biopsies.*

MTX Therapy

The average cumulative dose of MTX in all patients was 3940 mg (range 325–8355 mg) at the time of latest liver biopsy compared to 2918 mg (range 175–5568 mg) at the time of the first liver biopsy. The mean cumulative dose of MTX at the time of latest liver biopsy in the 14 patients with cirrhosis was 3061 mg, while it was 4168 mg in the remaining 54 patients ($p < 0.02$, Mann Whitney U test).

Correlations

a) between histological findings in the first and latest liver biopsies in all 68 *patients.*

Cirrhosis and/or fibrosis were found to have developed in 14 patients during the study. Of 15 patients with normal histology in the initial liver biopsy, eight developed pathological liver histology during the study. In contrast, only two of the 53 patients with initial pathological liver histology showed normal histology in the latest liver biopsies. The frequencies of 8/15 and 2/53 are significantly different ($p < 0.01$, Fisher exact test).

Cirrhosis and fibrosis were found in 19/68 of initial liver biopsies and in 30/68 of the latest liver biopsies ($p < 0.05$, Fisher exact test).

These findings developed in 12/18 of patients with initially abnormal liver biopsies compared with 5 of 8 patients with normal first biopsies, a difference which is not significant ($p < 0.26$, Fisher exact test).

b) between histological subgroups (cirrhosis/fibrosis/other pathological findings/normal) at the latest biopsy. There was no statistically significant difference between MTX cumulative dose in the 9 patients with normal histology (mean 3000 mg) and the 14 patients with cirrhosis (mean 3061 mg) ($p = 0.245$, Mann Whitney U test).

Patients with cirrhosis had a significantly higher alcohol intake during MTX therapy than patients *with normal liver histology* ($p = 0.041$, Mann Whitney U test). A significantly higher number of patients with cirrhosis were also obese ($p = 0.033$, Fisher exact test) and this group also tended to be older than patients with normal histology ($p = 0.058$). There was no significant correlation between patients in the 4 histological subgroups with respect to distribution of sex or intake of potentially *hepatotoxic medicine* (Fisher exact test).

DISCUSSION

A. Single Biopsies

Several large studies with series of psoriatic patients undergoing one post MTX liver biopsy have been reported. These were previously summarized and analysed according to liver histology, total MTX dose, MTX dosage frequency and admitted alcohol intake (1, ref. 16, Table 10). The Cooperative study (1, ref. 28) with 372 liver biopsies found 2.6 per cent cirrhosis and 34 per cent fibrosis. *Zachariae et al.* (1, ref. 30) with 96 liver biopsies found 6 per cent cirrhosis. In the present study of 92 liver biopsies was found cirrhosis or fibrosis in 7 per cent of biopsies. These findings agree with the mean incidence of cirrhosis and fibrosis found in psoriatics not previously treated with MTX. *However, the present figures are smaller than* those of either the Cooperative study or the study by *Zachariae et al.* They are also smaller than the average values computed from the eight studies previously summarized, which were 8.7 per cent cirrhosis and 18 per cent fibrosis.

Almeyda et al. (1, ref. 1) in a study of 42 single post MTX liver biopsies found a statistically significant higher MTX cumulative dose in the patients with cirrhosis or fibrosis ($p = 0.05$). This was not found in the pre-

sent study possibly due to our small number of patients with cirrhosis or fibrosis.

Since concomitant alcohol intake seems to increase liver damage it would seem desirable to forbid such intake, if possible during MTX therapy According to the Copenhagen Study Group of Liver Diseases (3) cirrhotics may live as long as normal controls if they abstain from any intake of alcohol. Another contributing factor to the development of liver damage appears to be age. Since this factor cannot be changed, it may perhaps be considered that the finding of liver damage is more acceptable in older than in younger age groups since not everyone exposed to hepatotoxic factors develops liver damage. Genetic factors may be important (2)

B. Serial Biopsies

In the literature there are only 4 studies reporting more than 20 serial post MTX liver biopsies per study The Cooperative study (1 ref. 28) involving 81 patients found no statistically significant changes in either the degree of fibrosis or the number of cases with cirrhosis between the first and latest post MTX liver biopsies. The mean interval between liver biopsies during MTX therapy was 13 months However they did find a significant increase ($p = 0.038$) in the occurrence of portal inflammation at the time of the latest liver biopsy *Almeyda et al* (1 ref 1) in 30 serial post MTX liver biopsies found 15 normal and 15 pathological liver specimens in initial biopsies compared to findings of 14 normals, 3 with fibrosis and 13 with minor pathological findings in the latest liver biopsies which were taken after a mean interval of 13 months of MTX therapy *Zachariae et al* (1 ref 30) had 3 cases of cirrhosis and 6 cases of fibrosis develop among 28 patients between initial and follow-up liver biopsies taken after 3-4 years of MTX therapy *Reese et al* (1 ref 21) found no progression in the fibrosis score in follow-up biopsies among 21 serial liver biopsies taken after an average of 12 months of MTX therapy However they showed a statistically significant ($p < 0.001$) effect of alcohol intake on the histology of the biopsy specimens.

The 21 per cent incidence of cirrhosis among the latest post MTX liver biopsies in the present study agrees most closely with the 11 per cent incidence found by Zachariae et al. The occurrence of cirrhosis during MTX therapy thus seems to be extremely high when compared with the 2-3 per cent incidence of cirrhosis found previously in psoriatics who had never received MTX (1 ref 28)

In this study the cumulative MTX dose was not found to be statistically higher in the group of cirrhotic patients than in the group of patients with normal histology This agrees with findings in the studies mentioned above However the alcohol intake during MTX therapy did correlate significantly with the findings of cirrhosis in liver histology both in the study by Reese et al. and in the present study

The findings of more cases of cirrhosis in this study and in the study of *Zachariae et al.* than in those of *Almeyda et al* and *Reese et al* is difficult to explain, as the cumulative dose of MTX, MTX dosage schedules and alcohol intake during MTX therapy appear to be approximately the same size Possible factors contributing to the differences in findings include previous liver pathology as documented by pre MTX liver histology age obesity potential hepatotoxic medicines and differences in the type of alcohol consumed. To rule out the first mentioned factor a pre MTX liver biopsy is mandatory It is probable that at least some of the 14 patients with cirrhosis in their latest liver biopsies had fibrosis or cirrhosis before initiation of MTX therapy

The liver damage demonstrated in parts A and B of this study and in a previous study of post MTX liver biopsies from psoriatics (1 ref 16) suggest a multifactorial aetiology produced by MTX, alcohol, age obesity and potentially hepatotoxic medicine.

Comparing the two groups of patients A and B in this study the most conspicuous finding is the high incidence of cirrhosis and fibrosis in group B compared to the low in-

improved and 26 had increased abnormalities (Sign test $p = 0.13$)

Table 7 presents the clinical and histological features of the 14 patients having cirrhosis present in their latest liver biopsies.

MTX Therapy

The average cumulative dose of MTX in all patients was 3940 mg (range 325–8355 mg) at the time of latest liver biopsy compared to 2918 mg (range 175–5568 mg) at the time of the first liver biopsy. The mean cumulative dose of MTX at the time of latest liver biopsy in the 14 patients with cirrhosis was 3061 mg while it was 4168 mg in the remaining 54 patients ($p < 0.02$ Mann Whitney U test)

Correlations

a) between histological findings in the first and latest liver biopsies in all 68 patients.

Cirrhosis and/or fibrosis were found to have developed in 14 patients during the study. Of 15 patients with normal histology in the initial liver biopsy eight developed pathological liver histology during the study. In contrast, only two of the 53 patients with initial pathological liver histology showed normal histology in the latest liver biopsies. The frequencies of 8/15 and 2/53 are significantly different ($p < 0.01$ Fisher exact test)

Cirrhosis and fibrosis were found in 19/68 of initial liver biopsies and in 30/68 of the latest liver biopsies ($p < 0.05$ Fisher exact test)

These findings developed in 12/18 of patients with initially abnormal liver biopsies compared with 5 of 8 patients with normal first biopsies, a difference which is not significant ($p < 0.26$ Fisher exact test)

b) between histological subgroups (cirrhosis/fibrosis/other pathological findings/normal) at the latest biopsy. There was no statistically significant difference between MTX cumulative dose in the 9 patients with normal histology (mean 3000 mg) and the 14 patients with cirrhosis (mean 3061 mg) ($p = 0.245$ Mann Whitney U test)

Patients with cirrhosis had a significantly higher alcohol intake during MTX therapy than patients with normal liver histology ($p=0.041$ Mann Whitney U test) A significantly higher number of patients with cirrhosis were also obese ($p=0.033$ Fisher exact test) and this group also tended to be older than patients with normal histology ($p=0.058$) There was no significant correlation between patients in the 4 histological subgroups with respect to distribution of sex or intake of potentially hepatotoxic medicine (Fisher exact test)

DISCUSSION

A Single Biopsies

Several large studies with series of psoriatic patients undergoing one post MTX liver biopsy have been reported. These were previously summarized and analysed according to liver histology total MTX dose MTX dosage frequency and admitted alcohol intake (1 ref 16 Table 10) The Cooperative study (1 ref 28) with 372 liver biopsies found 2.6 per cent cirrhosis and 34 per cent fibrosis. *Zachariae et al* (1 ref 30) with 96 liver biopsies found 6 per cent cirrhosis. In the present study of 92 liver biopsies was found cirrhosis or fibrosis in 7 per cent of biopsies. These findings agree with the mean incidence of cirrhosis and fibrosis found in psoriatics not previously treated with MTX. However the present figures are smaller than those of either the Cooperative study or the study by *Zachariae et al*. They are also smaller than the average values computed from the eight studies previously summarized, which were 8.7 per cent cirrhosis and 18 per cent fibrosis.

Almeyda et al (1 ref 1) in a study of 42 single post MTX liver biopsies found a statistically significant higher MTX cumulative dose in the patients with cirrhosis or fibrosis ($p = 0.05$) This was not found in the pre-

ent study possibly due to our small number of patients with cirrhosis or fibrosis.

Since concomitant alcohol intake seems to increase liver damage, it would seem desirable to forbid such intake, if possible, during MTX therapy. According to the Copenhagen Study Group of Liver Diseases (3) cirrhotics may live as long as normal controls if they abstain from any intake of alcohol. Another contributing factor to the development of liver damage appears to be age. Since this factor cannot be changed, it may perhaps be considered that the finding of liver damage is more acceptable in older than in younger age groups since not everyone exposed to hepatotoxic factors develops liver damage. Genetic factors may be important (2).

B. Serial Biopsies

In the literature there are only 4 studies reporting more than 20 serial post MTX liver biopsies per study. The Cooperative study (1 ref 28) involving 81 patients found no statistically significant changes in either the degree of fibrosis or the number of cases with cirrhosis between the first and latest post MTX liver biopsies. The mean interval between liver biopsies during MTX therapy was 15 months. However, they did find a significant increase ($p = 0.038$) in the occurrence of portal inflammation at the time of the latest liver biopsy. *Almeyda et al.* (1 ref 1) in 30 serial post MTX liver biopsies found 15 normal and 15 pathological liver specimens in initial biopsies compared to findings of 14 normals, 3 with fibrosis and 13 with minor pathological findings in the latest liver biopsies which were taken after a mean interval of 13 months of MTX therapy. *Zachariae et al.* (1 ref 30) had 3 cases of cirrhosis and 6 cases of fibrosis develop among 28 patients between initial and follow-up liver biopsies taken after 3-4 years of MTX therapy. *Reese et al.* (1 ref 21) found no progression in the fibrous score in follow-up biopsies among 21 serial liver biopsies taken after an average of 12 months of MTX therapy. However, they showed a statistically significant ($p < 0.001$) effect of alcohol intake on the histology of the biopsy specimens.

The 21 per cent incidence of cirrhosis among the latest post MTX liver biopsies in the present study agrees most closely with the 11 per cent incidence found by Zachariae et al.. The occurrence of cirrhosis during MTX therapy thus seems to be extremely high when compared with the 2-3 per cent incidence of cirrhosis found previously in psoriatics who had never received MTX (1 ref 28).

In this study the cumulative MTX dose was not found to be statistically higher in the group of cirrhotic patients than in the group of patients with normal histology. This agrees with findings in the studies mentioned above. However, the alcohol intake during MTX therapy did correlate significantly with the findings of cirrhosis in liver histology both in the study by Reese et al. and in the present study.

The findings of more cases of cirrhosis in this study and in the study of *Zachariae et al.* than in those of *Almeyda et al.* and *Reese et al.* is difficult to explain, as the cumulative dose of MTX, MTX dosage schedules and alcohol intake during MTX therapy appear to be approximately the same size. Possible factors contributing to the differences in findings include previous liver pathology as documented by pre MTX liver histology, age, obesity, potential hepatotoxic medicines and differences in the type of alcohol consumed. To rule out the first mentioned factor a pre MTX liver biopsy is mandatory. It is probable that at least some of the 14 patients with cirrhosis in their latest liver biopsies had fibrosis or cirrhosis before initiation of MTX therapy.

The liver damage demonstrated in parts A and B of this study and in a previous study of post MTX liver biopsies from psoriatics (1 ref 16) suggest a multifactorial aetiology produced by MTX, alcohol, age, obesity and potentially hepatotoxic medicine.

Comparing the two groups of patients A and B in this study, the most conspicuous finding is the high incidence of cirrhosis and fibrosis in group B compared to the low in-

cidence of cirrhosis in group A. The mean cumulative MTX dose in group B was almost the double of that in group A (3940 mg versus 2287 mg MTX) while the number of patients admitting daily alcohol intake during MTX therapy was similar in group A and B (21 per cent versus 27 per cent) The mean patient age was 57 years in both studies.

Comparison of the latest liver biopsy results with the incidence of cirrhosis and fibrosis found in a previous study of 88 psoriatics (1 ref 16) reveals a smaller incidence of cirrhosis and fibrosis (6 per cent each) corresponding to a smaller mean cumulative dose of MTX (1733 mg) This suggests that the hepatotoxic effect of MTX becomes more manifest at cumulative doses of MTX over 2–4 grams.

In conclusion, the finding of cirrhosis in 21 per cent of the latest serial post MTX liver biopsies is alarming and very strongly emphasizes the need of performing control post MTX liver biopsies.

My thanks are due to *Severin Olesen Larsen* cand. polit. Head of department of Biostatistics, The State Serum Institute, Copenhagen, for evaluation of statistical data, by a grant from the *Lægevidenskabelige Forskningsfond* The study was aided by a research grant from Lederle.

REFERENCES

1 *Nyfors A and Poulsen H* Liver biopsies from psoriatics related to Methotrexate therapy 1 Findings in 123 consecutive non-Methotrexate treated patients. Acta path. microbiol. scand. Sect. A *84* 253–261 1976.

2 *Sherlock S* Disease of the liver and biliary system. 5 ed. Blackwell Scientific Publications, Oxford 1975 p. 450

3 *Tygstrup N Juhl E. and The Copenhagen Study Group for Liver Diseases* The treatment of alcoholic cirrhosis. The effect of continued drinking and Prednisone on survival In *Gerok W Sickinger K and Hennekeuser H H* (Ed.) Internationales Symposion 2–4 Oktober 1970 in Freiburg I. Br. Schattauer Verlag Stuttgart, 1971 p. 519–526.

Acta path. microbiol. scand. Sect. A, 85: 519–527, 1977

GASTRIC CARCINOMA I

The Reproducibility of a Histogenetic Classification Proposed by Masson, Rember and Mulligan

P. Stubbe Teglbjærg and M. Vetner

Institute of Pathology, The Central Hospital, 7500 Holstebro and Institute of Pathology, Odense University Hospital, 5000 Odense, Denmark

Stubbe Teglbjærg, P. & Vetner, M. Gastric carcinoma I. The reproducibility of a histogenetic classification proposed by Masson, Rember and Mulligan. Acta path. microbiol. scand. Sect. A, 85: 519–527, 1977.

The purpose of the present paper has been to examine the reproducibility of the classification of gastric carcinomas, as proposed by Mulligan and Rember. Two microscopic slides from each of one hundred randomly selected specimens of gastric carcinoma, obtained by gastrectomy or gastric resection, were classified independently by both authors. Neither of the authors knew which slides originated from the same specimen. The inter-examiner reproducibility rate was 79 per cent. The reproducibility rates of the diagnoses with two independent slides from the same tumour was 74 per cent with examiner I and 80 per cent with examiner II.

Key words: Gastric carcinoma; classification; reproducibility.

P. Stubbe Teglbjærg, Institute of Pathology, Odense University Hospital, 5000 Odense, Denmark.

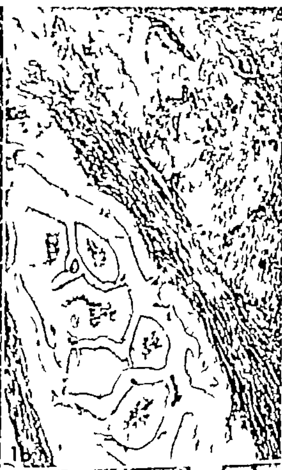
Received 20.x.76. Accepted 11.ii.77

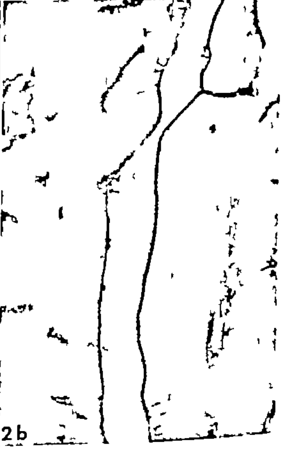
The ideal histological tumour classification requires 1) an adequate knowledge of the etiology and histogenesis of the tumour, 2) that the classification can be reproduced, and 3) that the classification is of prognostic value. There appears to be little agreement in the classification of gastric carcinomas, so much so, that the value of histological diagnoses has been questioned (7). Despite insufficient knowledge of the etiology and histogenesis of gastric carcinoma, attempts have been made, within the last 20 years, to define histogenetic classifications of these tumours (2, 4, 5). These classifications have shown a certain amount of prognostic value (2,4,5,6).

The purpose of this paper has been to examine the reproducibility of the classification of gastric carcinoma, as proposed by *Mulligan and Rember* (4).

MATERIAL AND METHODS

Two randomly selected tissue blocks from 100 randomly selected specimens of gastric carcinomas (gastrectomy or gastric resection specimens) were employed, from the files of the Institute of Pathology of the Odense University Hospital. This selection was carried out by a third party so that neither of the authors had any previous knowledge of the microscopic picture. Two microscopic slides were prepared from each block, one was stained with haematoxylin-eosin and one stained with alcian-blue pH 2.6 PAS according to the method of *Mowry* (3). The microscopic slides were numbered 1 to 200 and classified independently by both authors; neither had any knowledge of which sections were from the same tumour nor had they previously seen these microscopic slides.



1b

2a

2b

Principles of classification

The classification proposed by Mulligan and Rember (4) was used, with the following minor modifications 1) The signet ring cell was considered diagnostic for mucous cell carcinoma 2) We have defined sub-types of pyloro-cardiac gland cell carcinoma and mucous cell carcinoma. In the majority of tumours more than one sub-type is normally present

Intestinal cell carcinoma (IC)

Type I, highly differentiated (Fig 1a, 1b 2a, 2b) High cylindrical epithelium, slim cells with acidophilic cytoplasm. The cellular borders are indistinct, often not recognizable. The nuclei are ovoid, of rather uniform size, hyperchromatic pseudo-stratified, with the long axis perpendicular to the basement membrane. Luminal brush border present at the epithelium of neoplastic glands and/or papilliferous processes. Signet ring cells, surrounded by collagen stroma are not present.

Epithelial cells, desquaminated into the lumen of the glands, or floating in lakes of mucous in the stroma, become rounded in contour but these are not designated signet ring cells. (Fig. 6)

Type II, porly differentiated (Fig. 1a, 1b, 3a, 3b) Cell type as type I but with a more solid growth pattern. The cells are often more polygonal. In some areas small glands with a luminal brush border are seen. Signet ring cells are not present.

Pyloro-cardiac gland cell carcinoma (PC)

Type I highly differentiated "clear-cell"-type (Fig 4a, 4b) High, cylindrical epithelium in one layer the cells being broader than the IC type I. The cytoplasm is clear the cellular borders are distinct. The nuclei are in a basal or central position, orientated in single layer In some areas with the long axis parallel to the basement membrane. The nuclei in these areas are often rather small and uniform. Signet ring cells are not present.

Areas with pseudostratification of the nuclei and eosinophilic cytoplasm often occur These areas are often very difficult to distinguish from IC type I but the cells are broader and the cellular borders distinct. The nuclei in these areas are larger more light and more pleomorphic than the nuclei of IC type I

Type II poorly differentiated (Fig. 5a, 5b) The major part of the tumour is composed of solid nests of poorly differentiated tumour tissue or single neoplastic cells in the stroma. There is pronounced pleomorphism of the nuclei and cells. In some areas, glands with an epithelium similar to PC type I may be found. Signet ring cells are not present.

Mucous cell carcinoma (MC)

The hallmark of this tumour is the signet ring cell, which occurs in all four sub-types.

Type I tubular differentiation (Fig. 7a, 7b) Small, irregular tubular structures having a low cubic epithelium. The nuclei are small, circular with or without pseudostratification. Some signet ring cells are present in the stroma.

Type II signet cell type (Fig. 8a, 8b) This type is dominated by signet ring cells with small, hyperchromatic nuclei displaced to the periphery of the cell by intracellular mucous

Type III diffuse desmoplastic type (Fig. 9a, 9b) This type has single, small neoplastic cells with small hyperchromatic nuclei and sparse cytoplasm without mucous. Some but often few signet ring cells present Pronounced desmoplastic stromal reaction.

Type IV solid anaplastic (Fig. 10a, 10b): The cell type is identical to that of type III. The growth pattern, however is solid Very few signet ring cells present.

NB The occurrence of extracellular mucous located to the lumen of neoplastic glands and/or to the stroma has no differential diagnostic significance All three tumour types (IC, PC and MC) may produce the picture of so-called "colloid carcinoma

---

Fig. 1 and 1b IC type I and II mixed pattern. (Fig. 1 Haematoxylin-eosin, × 100 Fig. 1b Alcianblue pH 2.6 PAS × 100)

Fig 2 and 2b IC type I Highly differentiated adenocarcinoma. Cellular borders are indistinct Nuclei are pseudostratified, rather uniform. Luminal brush border of the neoplastic epithelium. No mucous in the cytoplasm.

Fig 2a Haematoxylin-eosin, × 400 Fig 2b Alcianblue- pH 2.6 PAS, × 400)

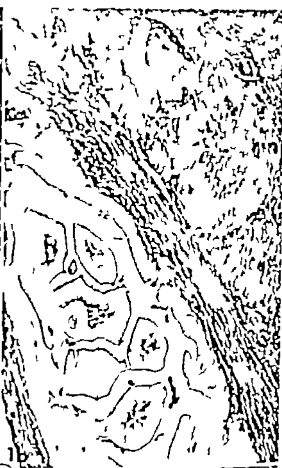
Fig. 3a and 3b IC type II Poorly differentiated, solid carcinoma. Polygonal cells with rather uniform nuclei. No mucous in the cytoplasm and no signet ring cells.

(Fig. 3a Haematoxylin-eosin, × 400. Fig. 3b Alcianblue- pH 2.6 PAS × 400)

Fig 4a and 4b PC type I. Highly differentiated adenocarcinoma The cellular border are distinct. The nuclei are situated in a single layer basally in the cells. Mucous granules in the luminal part of the cytoplasm, but no brush border

(Fig. 4 Haematoxylin-eosin, × 400 Fig. 4b Alcianblue pH 2.6 PAS × 400)




1b


2c


2b

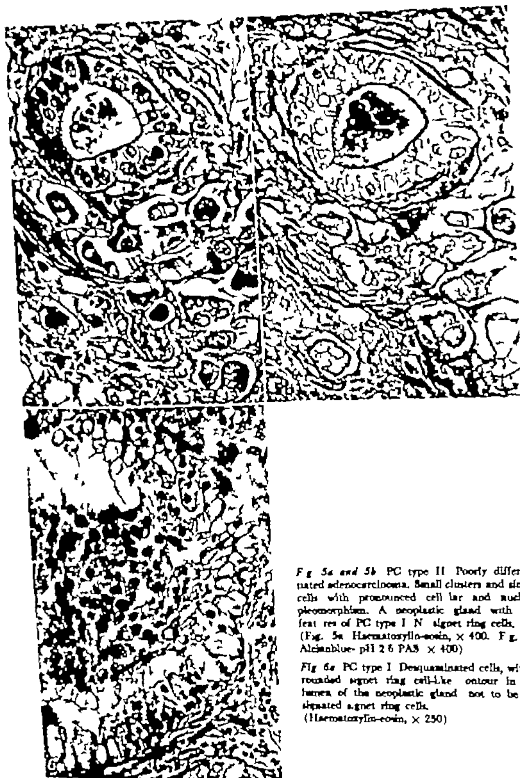


Fig. 5a and 5b PC type II. Poorly differentiated adenocarcinoma. Small clusters and single cells with pronounced cellular and nuclear pleomorphism. A neoplastic gland with the features of PC type I. No signet ring cells.
(Fig. 5a Haematoxylin-eosin, × 400. Fig. 5b Alcianblue- pH 2.6 PAS × 400)

Fig. 6a PC type I. Desquamated cells, with rounded signet ring cell-like contour in the lumen of the neoplastic gland not to be designated signet ring cells.
(Haematoxylin-eosin, × 250)


4a
4b

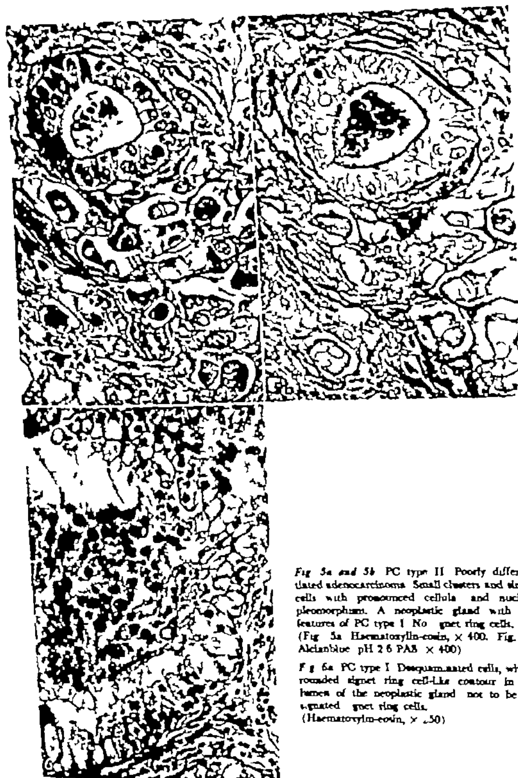


Fig. 5a and 5b PC type II. Poorly differentiated adenocarcinoma. Small clusters and single cells with pronounced cellular and nuclear pleomorphism. A neoplastic gland with the features of PC type I. No signet ring cells.
(Fig. 5a Haematoxylin-eosin, × 400. Fig. 5b Alcianblue pH 2.6 PAS × 400)

Fig. 6a PC type I. Desquamated cells, with rounded signet ring cell-like contour in the lumen of the neoplastic gland not to be designated signet ring cells.
(Haematoxylin-eosin, × 250)


3
b
4a
4b

RESULTS

The variation between the diagnoses made by the two examiners is shown in Table 1

TABLE 1 *The Distribution of the Diagnoses Made Independently by Two Examiners, of 200 Microscopical Slides*

EXAMINER I		EXAMINER II			
	IC	PC	MC	Total	
IC	31	19	2	52	
PC	13	46	4	63	
MC	3	1	81	85	
Total	47	66	87	200	

The same diagnosis was made by both the examiners in 158 slides (79 %)

TABLE 2A. *The Distribution of the Diagnoses Obtained From Two Independent Microscopical Slides From 100 Cases of Gastric Carcinoma Examiner I*

SLIDE I	SLIDE II IC	PC	MC	Total
IC	15	6	1	22
PC	11	21	2	34
MC	4	2	38	44
Total	30	29	41	100

The variation between the diagnoses made on slides I and II from the same tumour by the two examiners is shown in Tables 2A and 2B. The reproducibility of the diagnosis from two independent slides from the same tumour was 74 per cent with examiner I and 80 per cent with examiner II

TABLE 2B. *The Distribution of the Diagnoses Obtained From Two Independent Microscopical Slides From 100 Cases of Gastric Carcinoma. Examiner II*

SLIDE I	SLIDE II IC	PC	MC	Total
IC	18	6	0	24
PC	3	24	4	31
MC	2	5	38	45
Total	23	35	42	100

DISCUSSION

To the best of our knowledge, no investigation of the reproducibility of the present classification has previously been published.

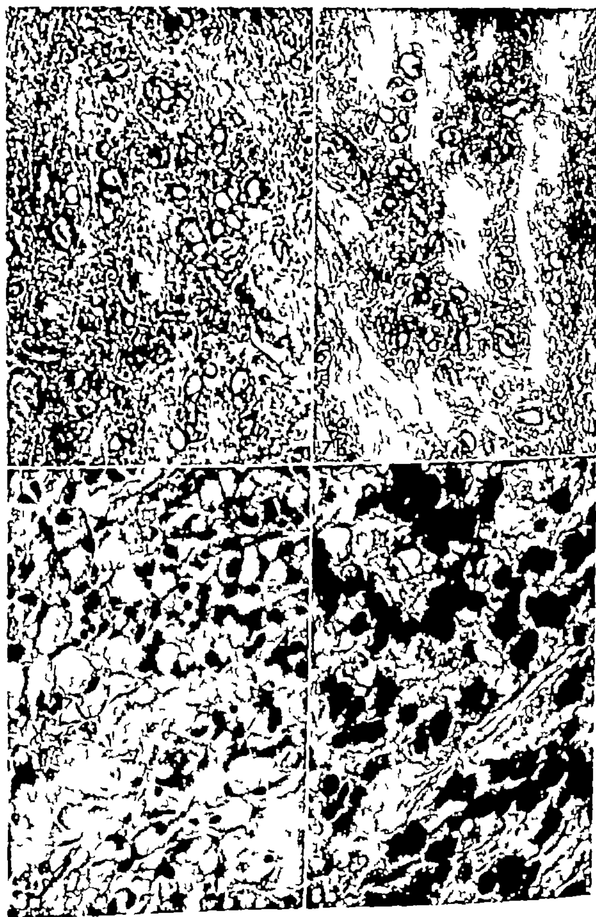
From Table 1 and Tables 2A and 2B it can be seen, that the diagnosis of MC was made with an acceptable reproducibility. We have not been able to distinguish IC from PC, with acceptable accuracy in the present material. However the reproducibility rates for these tumour types are somewhat higher than the random reproducibility rate of 34 per cent. It should be kept in mind, that the present reproducibility rates probably represent minimum rates. Thus a higher reproducibility rate might conceivably be achieved when multiple slides from the same tumour are available which is, of course the normal routine procedure. This applies, in particular when the differential diagnosis is between IC and PC, as this normally requires more than one slide in order to obtain a diagnostic area.

An investigation of the inter-observer difference using *Laurén's* (2) classification of gastric carcinomas has been published by *Kubo* (1). In this paper three pathologists reviewed 100 histological slides of gastric carcinoma and classified these into the following groups Intestinal type (I) Diffuse type (D) and others (O) The results were path-

---

Fig 7 and 7b MC type I. Tubular differentiation. Small irregular glands with low cubic epithelium, intermingled with single, infiltrating cells. Scattered signet ring cells.
(Fig. 7 Haematoxylin-eosin, × 100. Fig 7b Alcianblue pH 2.6 PAS × 100)

Fig 8a and 8b MC type II The signet ring cell type Numerous signet ring cells containing abundant mucous in the cytoplasm. The nucleus is displaced to the periphery of the cell
(Fig. 8a Haematoxylin-eosin, × 400. Fig. 8b Alcianblue pH 2.6 PAS × 400)



RESULTS

The variation between the diagnosis made by the two examiners is shown in Table 1

TABLE 1. *The Distribution of the Diagnoses Made Independently by Two Examiners of 200 Microscopical Slides*

EXAMINER I	EXAMINER II			
	IC	PC	MC	Total
IC	31	19	2	52
PC	13	46	4	63
MC	3	1	81	85
Total	47	66	87	200

The same diagnosis was made by both the examiners in 158 slides (79 %)

TABLE 2A. *The Distribution of the Diagnoses Obtained From Two Independent Microscopical Slides From 100 Cases of Gastric Carcinoma. Examiner I*

SLIDE I	SLIDE II			
	IC	PC	MC	Total
IC	15	6	1	22
PC	11	21	2	34
MC	4	2	38	44
Total	30	29	41	100

The variation between the diagnoses made on slides I and II from the same tumour by the two examiners is shown in Tables 2A and 2B The reproducibility of the diagnosis from two independent slides from the same tumour was 74 per cent with examiner I and 80 per cent with examiner II

TABLE 2B. *The Distribution of the Diagnoses Obtained From Two Independent Microscopical Slides From 100 Cases of Gastric Carcinoma Examiner II*

SLIDE I	SLIDE II			
	IC	PC	MC	Total
IC	18	6	0	24
PC	3	24	4	31
MC	2	5	38	45
Total	23	35	42	100

DISCUSSION

To the best of our knowledge, no investigation of the reproducibility of the present classification has previously been published.

From Table 1 and Tables 2A and 2B it can be seen, that the diagnosis of MC was made with an acceptable reproducibility We have not been able to distinguish IC from PC, with acceptable accuracy in the present material. However the reproducibility rates for these tumour types are somewhat higher than the random reproducibility rate of 34 per cent. It should be kept in mind, that the present reproducibility rates probably represent minimum rates. Thus a higher reproducibility rate might conceivably be achieved when multiple slides from the same tumour are available which is, of course, the normal routine procedure. This applies, in particular when the differential diagnosis is between IC and PC, as this normally requires more than one slide in order to obtain a diagnostic area.

An investigation of the inter-observer difference using *Lauréns* (2) classification of gastric carcinomas has been published by *Kubo* (1) In this paper three pathologists reviewed 100 histological slides of gastric carcinoma, and classified these into the following groups Intestinal type (I) Diffuse type (D) and others (O) The results were path-

Fig 7a and 7b MC type I Tubular differentiation. Small irregular glands with low cubic epithelium, intermingled with single, infiltrating cells. Scattered signet ring cells
(Fig 7 Haematoxylin-eosin, × 100 Fig 7b Alcianblue pH 2 6 PAS, × 100)

Fig 8a and 8b MC type II The signet ring cell type Numerous signet ring cells containing abundant mucous in the cytoplasm The nucleus is displaced to the periphery of the cell.
Fig 8a Haematoxylin-eosin, × 400 Fig 8b Alcianblue pH 2.6 PAS, × 400)

9a

9b

10a

10b

Fig. 9a and 9b MC type III. The diffuse, desmoplastic type. Small, single cells with small, hyperchromatic nuclei. Pronounced desmoplastic stromal reaction. The majority of cells contain no mucous in the cytoplasm. Few signet ring cells.
(Fig. 9a Haematoxylin-eosin, × 100. Fig. 9b Alcianblue- pH 2.6 PAS × 100)

Fig. 10a and 10b MC type IV. The solid anaplastic type. Small cells, with small hyperchromatic nuclei. No signet ring cells in this area.
(Fig. 10 Haematoxylin-eosin, × 400. Fig. 10b Alcianblue- pH 2.6 PAS, × 400)

---

ologist A I 39 D 47 O 14, pathologist B I 53 D 40, O 7 and pathologist C I 45 D 41 O 15. It was further stated that "there was considerable difference when individual cases were compared".

On this basis it can be concluded, that the reproducibility of the present classification is presumable better than that of Laurén.

REFERENCES

1. *Kubo T.* Geographical pathology of gastric carcinoma. Acta path. jap. *24* 465–479 1974
2. *Laurén P.* The two histological main types of gastric carcinoma: diffuse and so-called intestinal-type carcinoma. Acta path. microbiol. scand. *64* 31–49 1965.
3. *Mowry R.W.* The special value of methods that color both acidic and vicinal hydroxyl groups in the histochemical study of mucins. With revised directions for the colloidal iron stain, the use of alcian blue G 8x and their combination with the periodic acid-Schiff reaction. Ann. N.Y. acad. Sci. *106* 402–423 1963
4. *Mulligan R. M. & Rember R. R.* Histogenesis and biologic behavior of gastric carcinoma. Arch. Path. *58* 1–25 1954
5. *Mulligan R. M.* Histogenesis and biologic behavior of gastric carcinoma. Ann. Path. 7 349–415 1972.
6. *Stemmermann G. N. & Brown C.* A survival study of intestinal and diffuse types of gastric carcinoma. Cancer *33* 1190–1195 1974
7. *Stout A. P.* Tumors of the stomach. In: Atlas of tumor pathology. Section VI, fascicle 21 Armed Forces Inst. Path., Washington, D.C. 1953 p. 65–67

Acta path microbiol scand Sect. A, 85 528–534 1977

GASTRIC CARCINOMA 2

An analysis of Morphological and Prognostic Parameters correlated to the Classification Proposed by Masson Rember and Mulligan

P Stubbe Teglbjærg and M Vetner

Institute of Pathology The Central Hospital 7500 Holstebro, Denmark

Stubbe Teglbjærg P and Vetner M. Gastric carcinoma 2 An analysis of morphological and prognostic parameters correlated to the classification proposed by Masson Rember and Mulligan. Acta path. microbiol scand Sect A 85 528–534 1977

One-hundred and fifteen gastric adenocarcinomas were classified according to Mulligan and Rember into one of the following types Intestinal cell carcinoma (IC) pyloro-cardiac gland carcinoma (PC) mucous cell carcinoma (MC) and unclassified The tumour type was correlated to the growth pattern and inflammatory reaction at the margin of the tumour invasion of the veins and nerve sheaths, Dukes stage intra and extracellular mucous production, and occurrence of intestinal metaplasia in the non-tumour bearing parts of the gastric mucosa. MC was the only type of tumour producing the macroscopic picture "linitis plastica" PC was the type of tumour that dominated in the cardiac region. The following parameters showed no relation to tumour type Sex and age size of tumour invasion of lymphatic vessels. This study suggests that the three types of tumour are different entities, MC being the most aggressive and IC the least aggressive of the types of tumour

Key words Gastric carcinoma classification morphology prognosis.

P Stubbe Teglbjærg Institute of Pathology Odense University Hospital 5000 Odense Denmark.

Received 20.x 76 Accepted 12.ii.77

In 1953 *Stout* (23) stated that the microscopic picture of gastric carcinoma is of little significance Up until that time the classification of these tumours had been of a descriptive character without any definite prognostic significance because the major part of these tumours were classified as being of *Broders* (4) grades III and IV

In 1951 *Jarvi and Laurén* (11) showed that some adenocarcinomas of the stomach were related histogenetically to intestinal metaplasia this was later confirmed by others (14 17) A histogenetic classification was published by Mulligan and Rember (19) in 1954 and it was later shown, that this classification could be correlated to the prognosis (20) An identical classification was proposed by Masson (16) as early as in 1923 however this received no international recognition

The purpose of the present study has been

1) to investigate the way in which Mulligan-Rember's 3 types of tumour are correlated to Dukes stage, growth pattern and inflammatory reaction at the tumour margin and tumour invasion of lymphatic vessels, veins and nerve sheaths.

2) to investigate the relation between tumour type and the degree of intestinal metaplasia in the non tumour bearing parts of the gastric mucosa.

3) to collect a material for later survival studies.

MATERIAL AND METHODS

This prospective material comprises 111 consecutive patients, who underwent resection of the stomach or total gastrectomy for gastric carcinoma in 6 County Hospitals during the period Dec. 1st 1972 to Jan. 1st 1975. There were 80 men with 82 gastric carcinomas, and 31 women with 33 tumours. The specimens were fixed for at least 48 hours in 4 per cent aqueous formalin solution. An average of 14 tissue blocks were taken from each tumour for microscopic examination. An average of 15 evenly distributed tissue blocks were taken from the non-tumour bearing parts of the gastric mucosa. Two paraffin sections stained with haematoxylin-eosin and the alcianblue- pH 2.6 PAS procedure (18) respectively were examined by both authors. The following parameters were registered:

1) Growth pattern at the tumour margin (expansive, with clearly defined demarcation between tumour and host, or streaming out, i.e. diffusely infiltrating, without well-defined tumour margins)

2) Inflammatory reaction at the tumour margin (graded semiquantitatively as: None, slight, moderate, or severe)

3) Tumour invasion of lymphatic vessels, vein and nerve sheaths

4) The occurrence of extra- and/or intracellular mucous

5) The occurrence of intestinal metaplasia in the non-tumour bearing parts of the gastric mucosa was estimated (none, less than 50 per cent of the mucosa intestinalized, more than 50 per cent intestinalized)

Fisher exact test and the chi square-test were used in the statistical analysis.

Principle of classification

The tumours were classified according to Mulligan and Rember (19, 20) with some minor modifications as described in a previous paper (24) into one of the following groups: Intestinal cell carcinoma (IC), pyloro-cardiac gland carcinoma (PC) or mucous cells carcinoma (MC).

RESULTS

Table 1 shows the sex distribution of 114 classified tumours. There was no significant difference.

Table 2 shows the age distribution. MC has a tendency to occur more frequently under the age of 60 years, but in the present material this difference is not significant.

The tumours were classified into the following groups according to the largest diameter (LD): LD < 2 cm, 2 cm < LD < 5 cm and LD > 5 cm. There was no significant difference between the frequencies of IC, PC and MC in these groups.

TABLE 1. *The Sex Distribution of 114 Classified Gastric Carcinomas (ns = Non Significant)*

	IC	PC	MC	Total
♂	24	27	30	81
♀	10	7	16	33
Total	34	34	46	114

$x = 1.67$ $p > 0.1$ (ns)
$f = 2$

TABLE 2. *The Age Distribution of 114 Classified Gastric Carcinomas (ns = Non Significant)*

Age	IC	PC	MC	Total
≤ 60 years	4	5	12	21
> 60 years	30	29	34	93
Total	34	34	46	114

= 3.1 $0.1 > p < 0.05$ (ns)
= 2

The majority of the tumours were situated in the antral mucosa or the transition between the antral and body mucosa, defined histologically. In 12 cases of PC the tumour was situated in or bordering the histological cardiac region. One IC was situated in the cardiac region. However, severe chronic atrophic gastritis together with widespread intestinal metaplasia was found in this stomach. There were no cases of MC where the cardiac region alone was affected, but in 10 cases of MC with diffuse involvement of the entire stomach the cardiac region was also affected (Table 3).

The majority of the tumours were ulcerated. MC was the only tumour type that show

Acta path. microbiol scand Sect A, 85 528-534 1977

GASTRIC CARCINOMA 2

An analysis of Morphological and Prognostic Parameters correlated to the Classification Proposed by Masson Rember and Mulligan

P STUBBE TEGLBJÆRG and M VETNER

Institute of Pathology The Central Hospital 7500 Holstebro Denmark

Stubbe Teglbjærg P and Vetner M Gastric carcinoma 2. An analysis of morphological and prognostic parameters correlated to the classification proposed by Masson, Rember and Mulligan. Acta path. microbiol. scand Sect. A 85 528–534 1977

One-hundred and fifteen gastric adenocarcinomas were classified according to Mulligan and Rember into one of the following types Intestinal cell carcinoma (IC) pyloro-cardiac gland carcinoma (PC) mucous cell carcinoma (MC) and unclassified. The tumour type was correlated to the growth pattern and *inflammatory reaction at the margin of the tumour* invasion of the veins and nerve sheaths, Dukes stage intra and extracellular mucous production and occurrence of intestinal metaplasia in the non-tumour bearing parts of the gastric mucosa. MC was the only type of tumour producing the macroscopic picture "linitis plastica" PC was the type of tumour that dominated in the cardiac region. The following parameters showed no relation to tumour type Sex and age size of tumour invasion of lymphatic vessels. This study suggests that the three types of tumour are different entities, MC being the most aggressive and IC *the least aggressive of the types of tumour*

Key words Gastric carcinoma classification morphology prognosis.

P Stubbe Teglbjærg Institute of Pathology Odense University Hospital
5000 Odense Denmark.

Received *20 x 76* Accepted *12 ii 77*

In 1953 *Stout* (23) stated that the microscopic picture of gastric carcinoma is of little significance *Up until that time the classification* of these tumours had been of a descriptive character without any definite prognostic significance, because the major part of these tumours were classified as being of *Broders* (4) grades III and IV

In 1951 *Jarvi and Laurén* (11) showed that some adenocarcinomas of the stomach were *related histogenetically* to intestinal metaplasia this was later confirmed by others (14 17) A histogenetic classification was published by Mulligan and Rember (19) in 1954 and it was later shown, that this classification could be *correlated to the prognosis* (20) An identical classification was proposed by Masson (16) as early as in 1923 however *this received no* international recognition

The purpose of the present study has been

1) to investigate the way in which Mulligan-Rember's 3 types of tumour are correlated to *Dukes stage, growth pattern* and inflammatory reaction at the tumour margin and tumour invasion of lymphatic vessels, veins and nerve sheaths.

2) to investigate the relation between tumour type *and the degree* of intestinal metaplasia in the non tumour bearing parts of the gastric mucosa

quently in PC than in IC (table 11) The occurrence of granulated mucous situated in the luminal part of the cytoplasm was characteristic of PC. Further considerable difficulty was encountered in distinguishing between an area of the PC where only a few mucous granules were present just beneath the cell membrane and a brush-border In addition this gave me to problems in the differential diagnosis between PC and IC. All of the IC cases showed a brush-border Intracellular mucous in IC was sparce diffuse and non-granular when present.

TABLE 8. *The Degree of Inflammatory Reaction at the Tumour Margin of 114 Classified Gastric Carcinomas*

Inflammatory reaction at the tumour margin	IC	PC	MC	Total
None	1	2	25	28
Slight	3	8	15	26
Moderate	3	9	5	17
Severe	27	15	1	43
Total	34	34	46	114

$x = 68.0$ $p < 0.001$
$= 6$

TABLE 9 *The Occurrence of Venous Invasion in 114 Classified Gastric Carcinomas*

Invasion of veins	IC	PC	MC	Total
+	10	25	37	72
−	24	9	9	42
Total	34	34	46	114

$x^2 = 24.4$ $p < 0.001$
2

Extracellular mucous occurred more frequently in IC and PC than in MC (Table 12)

The mucous, in cases of IC and PC, was present in the lumen of the neoplastic glands. If excessive amounts of mucous were present, the glands might rupture displacing the mucous to the stroma. The extracellular mucous in cases of MC was always situated in the stroma, but this originated from ruptured signet ring cells. When intracellular and/or extracellular mucous was present, it could always be stained by means of the PAS-procedure and in most cases some areas were also stained by alcianblue indicating a mixture of neutral and acid mucopolysaccharides.

TABLE 10. *The Occurrence of Invasion of Nerve Sheaths in 114 Classified Gastric Carcinomas*

Invasion of nervesheaths	IC	PC	MC	Total
+	8	21	38	67
−	26	13	8	47
Total	34	34	46	114

$x^2 = 25.4$ $p < 0.001$
$x = 2$

TABLE 11 *The Occurrence of Intracellular Mucous in PC and IC*

Intracellular mucus	IC	PC	Total
+	12	33	45
−	22	1	23
Total	34	34	68

$p < 0.001$

TABLE 12. *The Occurrence of Extracellular Mucous in 114 Classified Gastric Carcinomas*

Extracellular mucus	IC	PC	MC	Total
+	31	33	24	88
−	3	1	22	26
Total	34	34	46	114

$x^2 = 27.2$ $p < 0.001$
$= 2$

The occurrence and degree of intestinal metaplasia in the non-tumour bearing parts of the gastric mucous was significantly more pronounced in IC than in PC and MC (Table 13)

ed the macroscopic picture "linitis plastica" (Table 4)

TABLE 3 *The Tumor Site of 114 Classified Gastric Carcinomas*

Tumorsite	IC	PC	MC	Total
Antrum	31	22	33	86
Corpus	2	–	3	5
Cardia	1	12	–	13
Diffuse	–	–	10	10
Total	34	34	46	114

TABLE 4 *The Macroscopic Presentation of 114 Classified Gastric Carcinomas*

Macroscopic presentation	IC	PC	MC	Total
Ulcerated	25	27	28	80
Ulceropolypous	4	3	1	8
Polypous	5	3	1	9
Linitis plastica	–	–	15	15
No macr changes	–	1	1	2
Total	34	34	46	114

Nine per cent of the tumours were classified as being of Dukes stage A (IC 4 PC 2 MC 4) i.e confined to the stomach without penetration of the muscular coat. Thirty-two per cent were confined to the stomach without (stage A) or with malignant growth into the subserosal or serosal layers (stage B) all without lymph node involvement Metastases to the lymph nodes were only demonstrated in 50 per cent of IC whereas 74 per cent of PC and 78 per cent of MC had spread to the lymph nodes (stage C) (Table 5)

There was no significant difference between IC type I (generally classified as highly differentiated adenocarcinoma) and IC type II (generally classified as solid anaplastic carcinoma) with regard to lymph node involvement (Table 6)

The growth pattern at the tumour margin did show significant differences, as 76 per cent of IC and 53 per cent of PC showed an expansive growth pattern Ninety three per cent of MC had no sharply defined tumour margins ("streaming out") (Table 7)

TABLE 5 *Dukes' Stage of 114 Classified Gastric Carcinomas*

Dukes stage	IC	PC	MC	Total
A + B	17	9	10	36
C	17	25	36	78
Total	34	34	46	114

$x^2 = 7.92$ $0.02 > p > 0.01$
$v = 2$

TABLE 6. *Dukes' Stage of IC Type I Versus Type II (ns = Non Significant)*

Dukes stage	IC type I	IC type II	Total
A + B	8	9	17
C	9	8	17
Total	17	17	34

$p > 0.2$ (ns)

TABLE 7 *The Growth Pattern of the Tumour Margin of 114 Classified Gastric Carcinomas*

Growth pattern at the tumor margin	IC	PC	MC	Total
Expansive	26	18	3	47
Streaming out	8	16	43	67
Total	34	34	46	114

$x^2 = 42.4$ $p < 0.001$
$v = 2$

IC and PC showed a more pronounced inflammatory reaction at the tumour margin than MC (Table 8)

Invasion of the lymphatic vessels was observed in 96 per cent of the total material, and there was no significant difference between the tumour types

PC and MC showed a more pronounced tendency to invade veins (Table 9) and nerve sheaths (Table 10) than IC.

Intracellular mucous occurred more fre-

quently in PC than in IC (table 11). The occurrence of granulated mucous situated in the luminal part of the cytoplasm was characteristic of PC. Further considerable difficulty was encountered in distinguishing between an area of the PC where only a few mucous granules were present just beneath the cell membrane and a brush-border. In addition this gave rise to problems in the differential diagnosis between PC and IC. All of the IC cases showed a brush-border. Intracellular mucous in IC was sparce, diffuse and non-granular when present.

TABLE 8 *The Degree of Inflammatory Reaction at the Tumour Margin of 114 Classified Gastric Carcinomas*

Inflammatory reaction at the tumor margin	IC	PC	MC	Total
None	1	2	25	28
Slight	3	8	15	26
Moderate	3	9	5	17
Severe	27	15	1	43
Total	34	34	46	114

$x = 68.0$ $p < 0.001$
$v = 6$

TABLE 9 *The Occurrence of Venous Invasion in 114 Classified Gastric Carcinomas*

Invasion of veins	IC	PC	MC	Total
+	10	25	37	72
	24	9	9	42
Total	34	34	46	114

$x = 24.4$ $p < 0.001$
$= 2$

Extracellular mucous occurred more frequently in IC and PC than in MC (Table 12).

The mucous, in cases of IC and PC, was present in the lumen of the neoplastic glands. If excessive amounts of mucous were present, the glands might rupture, displacing the mucous to the stroma. The extracellular mucous in cases of MC was always situated in the stroma, but this originated from ruptured signet ring cells. When intracellular and/or extracellular mucous was present, it could always be stained by means of the PAS-procedure and in most cases some areas were also stained by alcianblue indicating a mixture of neutral and acid mucopolysaccharides.

TABLE 10 *The Occurrence of Invasion of Nerve Sheaths in 114 Classified Gastric Carcinomas*

Invasion of nervesheaths	IC	PC	MC	Total
+	8	21	38	67
−	26	13	8	47
Total	34	34	46	114

$= 23.4$ $p < 0.001$
$v = 2$

TABLE 11 *The Occurrence of Intracellular Mucous in PC and IC*

Intracellular mucous	IC	PC	Total
+	12	33	45
−	22	1	23
Total	34	34	68

$p < 0.001$

TABLE 12 *The Occurrence of Extracellular Mucous in 114 Classified Gastric Carcinomas*

Extracellular mucous	IC	PC	MC	Total
+	31	33	24	88
−	3	1	22	26
Total	34	34	46	114

$x^2 = 27.2$ $p < 0.001$
$= 2$

The occurrence and degree of intestinal metaplasia in the non-tumour bearing parts of the gastric mucosa was significantly more pronounced in IC than in PC and MC (Table 13).

TABLE 13 *The Degree of Intestinal Metaplasia in the Non-tumour Bearing Parts of the Gastric Mucosa*

Intestinal metaplasia	IC	PC	MC	Total
None	0	8	14	22
Slight–moderate	11	21	24	56
Severe	23	5	8	36
Total	34	34	46	114

$x^2 = 33.2 \quad p < 0.001$
$v = 4$

One tumour could not be classified. The patient was a 72 year old man with an ulcerated tumour in the antrum the largest diameter of the tumour was 10 cm and it was Dukes stage C The growth pattern at the tumour margin was expansive, with moderate inflammatory reaction. Invasion of the lymphatic vessels, nerve sheaths and veins was present. Intra as well as extracellular mucous occurred. The non tumour bearing parts of the gastric mucosa showed moderate intestinal metaplasia.

DISCUSSION

The present classification divides the adenocarcinomas of the gastric mucosa into three types of tumour having different relationships to the parameters examined

1) IC Characteristically located to the antrum with severe intestinal metaplasia of the gastric mucosa Expansive growth pattern with severe inflammatory reaction at the tumour margin There was rarely invasion of veins or nerve sheaths. Metastases to the lymph nodes was relatively uncommon. The highly and poorly differentiated tumours behaved in the same manner (type I and II respectively)
2) PC *Characteristically located to areas* containing pyloro-cardiac glands No or sparse intestinal metaplasia of the gastric mucosa. Same frequency of expansive and "streaming out" growth pattern at the tumour margin with severe or moderate inflammatory reaction. Invasion of veins and nerve sheaths and metastases to the lymph nodes was frequently present
3) MC Characteristically located to the antrum or of the diffuse type involving the entire stomach The only tumour type producing the macroscopic picture of "linitis plastica" No or sparse intestinal metaplasia of the gastric mucosa. "Streaming out" growth pattern at the tumour margin without inflammatory reaction Tumour invasion of veins and nerve sheaths, together with metastases to the lymph nodes was generally present.

The present material is surgical and therefore selected probably with an under representation of highly malignant tumour types. *Mulligan* (20) in a combined surgical and autopsy material, found 61 IC, 77 PC and 121 MC in a total of 268 tumours leaving 9 cases unclassified as the biopsy specimens were too small or the autopsy material poorly preserved etc

The sex and age distribution of the present material is non-significant. However there seems to be a tendency towards increased occurrence of MC in younger females, as found by *Mulligan* (20) and *Laurén* (14) in larger series.

Laurén (14) describes two main types of gastric carcinoma i e "intestinal type" believed to be derived histogenetically from intestinal metaplastic epithelium and "diffuse" carcinoma originating from the normal gastric epithelium

IC and MC of the present classification are almost identical with *Laurén's* two main types, respectively The occurrence of a brushborder in IC and the strong association of this tumour type with intestinal metaplasia, combined with the morphological picture of IC,

support the view that this tumour type is re lated histogenetically to intestinal metaplastic epithelium. This has also been suggested by others (8, 11 14 15 17 19 20)

PC is the most controversial type of tumour in the present classification. PC has a pecul iar localisation in the stomach, to areas containing pyloro-cardiac glands it also has a low correlation to intestinal metaplasia This, together with the morphological picture and the occurrence of granulated mucous in the luminal portion of the cytoplasm indicates, that this tumour type might be derived histogenetically from the normal gastric mucosa, probably the pyloro-cardiac glands (19 20)

Laurén does not recognize PC as a separate entity but classifies PC type I as "intestinal-type and PC type II as "diffuse" However studies of the enzyme-histochemistry of gastric carcinomas (13 22) have shown that approximately one half of the adenocarcinomas has an intestinal enzyme pattern, while the other half has not. Further studies are necessary to determine whether these adenocarcinomas without an intestinal enzyme pattern and PC are identical.

IC, PC, as well as MC may appear as so-called colloid carcinoma" This term should be abandoned, because it is poorly defined (23) heterogeneous (7) and includes tumours with very varying prognoses (3)

The growth pattern (9 21 25) and inflammatory reaction (1 2, 9 10 21) at the tumour margin, tumour invasion of the lymphatic vessels, veins and nerve sheaths (21) and especially Dukes stage (2, 5 6, 10 12 21 25) have been shown to be of prognostic significance with regard to gastric carcinomas, as well as to colo-rectal and mammary carcinomas.

The tumour types IC PC and MC have in the present material shown significantly dif ferent relationships to these prognostic para meters We must thus expect that IC will have the most favourable and MC the most unfavourable prognosis and that the prognosis of PC will be intermediate

The final evaluation of the prognostic significance of the present classification, i. e. survival studies will be presented in a later paper

We wish to express our gratitude to the Heads of the Department of Pathology of the following Hospitals Hjørring Sygehus, Randers Centralsygehus, Skive Sygehus, Alborg Sygehus and Arhus Amtssygehus for the material kindly placed at our disposal.

REFERENCES

1 *Ackerman L. V & Del Regato J A.:* Cancer Diagnosis treatment and prognosis. 4 ed. C. V Mosby St. Louis 1970 p. 484.

2. *Black M M F eeman C., Mork, T., Harvei S & Cutler S J* Prognostic significance of microscopic structure of gastric carcinomas and their regional lymfnodes. Cancer *27:* 703 –711 1971

3. *Brander W L., Needham, P R. G & Morgan A D* Indolent mucoid carcinoma of the stomach. J clin. Path. *27* 536–541 1974

4 *Broders A C* Carcinoma and other malignant lesions of the stomach pathological considerations in Walters et al. Carcinoma and other malignant lesions of the stomach. W B. Saunders Co., Philadelphia, 1942, p. 127–148.

5 *Dockat G R. & Gray H K.:* Carcinoma of the stomach prognosis bases on a combination of Dukes and Broders methods of grading. Amer J clin. Path *13* 441–449 1943

6. *Dukes C E.* The classification of cancer of the Rectum. J Path. Bact. *35* 323–332, 1932.

7 *Eker R. & Efskind J* The pathology and prognosis of gastric carcinoma. Acta chir scand. Supp. 264 Stockholm, 1960

8. *Goldman, H & Ming, S -C* Fine structure of intestinal metaplasia and adenocarcinoma of the human stomach. Lab. Invest. *18* 203–210, 1968.

9. *Hultborn, K. A & Tornberg, B.,* Mammary carcinoma the biologic character of mammary carcinoma studied in 517 cases by a new form of malignancy grading. Acta Radiol. Suppl. 196, 1960

10 *Inokuchi K., I atraka, S Furusawa M., Soejima, K & Ikeda T.* Stromal reaktion around tumor and metastases and prognosis after curative gastrectomy for carcinoma of the stomach. Cancer *20* 1924–1929 1967

11 *Järvi, O & Laurén P* On the role of heterotopias of the intestinal epithelium in the pathogenesis of gastric cancer Acta path. microbiol. scand. 29 26–44 1951

12. *Kennedy B J.:* TNM classification for stomach cancer Cancer 26 971–983 1970

13 *Kobori O & Oota K* Mucous substance and enzyme histochemistry of non-neoplastic and neoplastic gastric-epithelium in man. Acta path. Jap *24* 119–130 1974
14 *Laurén P* The two histological main types of gastric carcinoma diffuse and so-called intestinal type carcinoma. Acta path. microbiol. scand *64* 31–49 1965
15 *Lev R* The mucin histochemistry of normal and neoplastic gastric mucosa. Lab Invest. *14* 2080–2100 1965
16 *Masson P* Diagnostics de Laboratoire. II Tumeurs. A. Maloine et Fils Paris 1923 p 405–417
17 *Morson B C* Carcinoma arising from areas of intestinal metaplasia in the gastric mucosa. Brit. J Cancer *9* 366–385 1955
18. *Mowry R W* The special value of methods that color both acidic and vicinal hydroxyl groups in the histochemical study of mucins. With revised directions for the colloidal iron stain, the use of alcian blue G 8x and their combination with the periodic acid-Schiff reaction. Ann. N Y acad Sci *106* 40?–423 1963
19 *Mulligan R M & Rember R R* Histogenesis and biologic behavior of gastric carcinoma. Arch. Path *58* 1–25 1954
20 *Mulligan R M* Histogenesis and biologic behavior of gastric carcinoma. Ann. Path. *7* 349–415 1972
21 *Spratt J S & Spjut H J* Prevalence and prognosis of individual clinical and pathologic variables associated with colorectal carcinoma. Cancer *20* 1976–1985 1967
22 *Stemmermann G N* Comparative study of histochemical patterns in non-neoplastic and neoplastic gastric epithelium A study of Japanese in Hawaii. J Nat. Cancer Inst. *39* 375–383 1967
23 *Stout A P* Tumors of the stomach In Atlas of tumor pathology Section VI – fascicle 21 Armed Forces Inst. Path. Washington, D C., 1953 p 65–67
24 *Teglbjerg P S & Vetner M* Gastric Carcinoma I The reproducibility of a histogenetic classification proposed by Masson, Rember and Mulligan Acta path. microbiol. scand. Sect. A *85* 519–527 1977
25 *Urban C H & McNeer G* The relation of the morphology of gastric carcinoma to long and short term survival. Cancer *12* 1158–1162 1959

Acta path. microbiol. scand. Sect. A, 85: 535–538, 1977

TRANSTHORACIC ASPIRATION BIOPSY

Cytological Classification of Aspirated Malignant Tumour Cells

Dorthe Francis

Institute of Pathological Anatomy, Bispebjerg Hospital, Copenhagen

Francis, D. Transthoracic aspiration biopsy. Cytological classification of aspirated malignant tumour cells. Acta path. microbiol. scand. Sect. A, 85: 535–538, 1977.

On correlating our cytological classification of aspirated malignant tumour cells from intrathoracic lesions with the histological classification of the same lesions, agreement was found in 75 per cent. The cytological criteria used for the classification of the differentiated types of tumour cells were convenient. It is proposed to utilize the cytological classification in the planning of an individualized tumour therapy in cases not accessible to pretreatment bioptic histological classification.

Key words: Aspiration biopsies; transthoracic; tumour cells; cytological classification.

Dorthe Francis, Sæbberrisenget 13, DK 2830 Virum.

Received 23.xii.76. Accepted 20.ii.77.

In a recent paper the sensitivity and specificity of the diagnosis of malignant tumour cells in transthoracic aspiration biopsies obtained by our biopsy method were presented (4, 5). With the increasing possibilities for an individual treatment of patients with malignant lung tumours, there is a growing demand for a pretreatment tumour classification.

In the present paper we report results concerning classification of aspirated malignant tumour cells in a consecutive biopsy material of histologically verified malignant intrathoracic tumours.

MATERIAL AND METHODS

During the period, February 1st 1972 to January 31st 1975, 433 transthoracic aspiration biopsies were performed. At the end of the period of investigation histological verification had been obtained in 227 cases. In 180 of these malignant intrathoracic tumours were demonstrated (4). Comparison with the corresponding intrathoracic aspiration biopsies showed that malignant tumour cells had been found in a total of 139 cases. The present material thus comprises these 139 aspiration biopsies with their original cytological classification. As two patients had biopsies performed from malignant tumours in both lungs, the material stems from 137 patients.

The fine needle aspiration biopsies were performed using the Franzén equipment (6, 10). Our biopsy procedure has been described in detail elsewhere (4, 5).

Cytological Investigation

The aspirated material was smeared on at least two glass-slides, of which one was usually fixed immediately in methanol for a Papanicolaou stain, the rest were air dried and stained by the May-Grünwald-Giemsa method.

Based on the cellular characteristics the biopsies were grouped according to the following system.

Epidermoid carcinoma, smears containing malignant tumour cells of which some in May-Grünwald-Giemsa stained specimens appeared with light blue coloured cytoplasm and condensed nuclei. The blue colour was taken to represent cytoplasmic cornification. Likewise, the occurrence of a narrow light blue ring just encircling the nucleus was taken as a sign of epidermoid differentiation.

13 *Kobori O & Oota K* Mucous substance and enzyme histochemistry of non neoplastic and neoplastic gastric-epithelium in man. Acta path. jap *24* 119–130 1974

14 *Laurén P* The two histological main types of gastric carcinoma diffuse and so-called intestinal-type carcinoma. Acta path. microbiol. scand. *64* 31–49 1965

15 *Lev R* The mucin histochemistry of normal and neoplastic gastric mucosa. Lab Invest. *14* 2080–2100 1965

16 *Masson P* Diagnostics de Laboratoire. II Tumeurs. A Maloine et Fils Paris 1923 p 405–417

17 *Morson B C* Carcinoma arising from areas of intestinal metaplasia in the gastric mucosa. Brit. J Cancer *9* 366–385 1955

18 *Mowry R W* The special value of methods that color both acidic and vicinal hydroxyl groups in the histochemical study of mucins. With revised directions for the colloidal iron stain the use of alcian blue G 8x and their combination with the periodic acid-Schiff reaction. Ann. N Y acad Sci. *106* 402–423 1963

19 *Mulligan R M & Rember R R* Histogenesis and biologic behavior of gastric carcinoma. Arch. Path. *58* 1–25 1954

20 *Mulligan R M* Histogenesis and biologic behavior of gastric carcinoma. Ann. Path. *7* 349–415 1972.

21 *Spratt J S & Spjut H J* Prevalence and prognosis of individual clinical and pathologic variables associated with colorectal carcinoma. Cancer *20* 1976–1985 1967

22. *Stemmermann G N.* Comparative study of histochemical patterns in non neoplastic and neoplastic gastric epithelium A study of japanese in Hawaii. J Nat. Cancer Inst. *39* 375–383 1967

23 *Stout A P* Tumors of the stomach In Atlas of tumor pathology Section VI – fascicle 21 Armed Forces Inst. Path., Washington, D.C., 1953 p 65–67

24 *Teglbjærg P S & Vetner M* Gastric Carcinoma I The reproducibility of a histogenetic classification proposed by Masson, Rember and Mulligan. Acta path. microbiol scand. Sect. A, *85* 519–527 1977

25 *Urban C H & McNeer G* The relation of the morphology of gastric carcinoma to long and short term survival Cancer *12* 1158–1162 1959

TABLE 2. *Number of Cytologically Classified Aspiration Biopsies in Agreement with the Histological Classification (Sensitivity of Cytological Classification)*

	Epidermoid carcinomas	Small cell carcinomas	Adeno-carcinomas	Undifferentiated carcinomas	Other malignant neoplasms
Correctly classified biopsies	29	18	28	20	9
Number of positive biopsies	45	19	35	23	17
Sensitivity	0.64	0.95	0.80	0.87	0.53

TABLE 3. *Number of Aspiration Biopsies correctly Classified in Each of the Cytological Groups (Diagnostic Specificity of Cytological Classification)*

	Epidermoid carcinomas	Small cell carcinomas	Adeno-carcinomas	Undifferentiated carcinomas	Other malignant neoplasms
Correctly classified biopsies	29	18	28	20	9
Number of biopsies classified as	34	21	35	39	10
Specificity	0.85	0.86	0.80	0.51	0.90

nocarcinoma, and the sensitivity for this group was 80.0 per cent.

In 39 cases the aspirated tumour cells were classified as originating from large cell or undifferentiated carcinomas. Of these cases 20 were correctly grouped (51.3 per cent) while 13 were found to be epidermoid carcinomas, 4 were adenocarcinomas, and two were mucoepidermoid carcinomas. The group comprised 23 histologically verified cases of large cell or undifferentiated carcinomas, and the sensitivity was 87.0 per cent.

In 10 cases the malignant cells were classified as originating from other malignant tumours, and this was correct in 9 cases (90.0 per cent) since one histologically was found to be an adenocarcinoma. The nine biopsies correctly classified represented one case each of pulmonary blastoma, embryonal carcinoma, mucoepidermoid carcinoma, and mesothelioma, and five different types of sarcomas. Histologically the material comprised 17 cases belonging to this group, the sensitivity thus being 52.9 per cent.

As pointed out in Table 2 the cytological classification was in agreement with the histological in 104 out of 139 cases (74.8 per cent) ranging from 53 to 95 per cent of the different tumour groups represented. The diagnostic specificity (in the following simply designated specificity) of the cytological classification is shown in Table 3.

DISCUSSION

In the present study we have compared our original cytological classification of the malignant tumour cells with the histological classification and found the percentage of correct cytological classification to be 75 per cent. This result is in agreement with results obtained by *Dahlgren* (2) who in a comparable series found a correlation of 77 per cent. Our result is also in agreement with the best results obtained in cytological typing of tumour cells in sputum (9) and bronchial secretions (1, 3, 8).

The specificity of the classification of tumour cells representing an epidermoid carcinoma was found to be very high. This was especially found to be so when also the four cases of mucoepidermoid carcinomas were considered correctly classified as regards their epidermoid components. This high specificity

Small cell anaplastic carcinoma smears containing cells with a barely visible rim of cytoplasm and rather uniform, but very friable nuclei without distinct nucleoli. The tumour cells were most often completely dissociated, and if groups of tumour cells occurred, no glandlike structure could be recognized.

Adenocarcinoma smears containing well demarcated groups of malignant tumour cells arranged in ring or papillary formations or in more or less well shaped "bags.

Large cell or undifferentiated carcinoma smears containing epithelial tumour cells showing no signs of cytoplasmic cornification or arrangement in glandlike structures.

Other malignant tumours smears containing malignant tumour cells which could not unequivocally be placed in the above mentioned groups.

Histological Investigation

Histological specimens from autopsy material, lung resections, and in a few cases from thoracoscopic biopsies were stained with haematoxylin-eosin and by Kreyberg's method (7)

A classification was made according to the following system without any knowledge of the cytological classification

Epidermoid carcinoma primary or metastatic tumours with keratinisation or intercellular bridges.

Small cell anaplastic carcinoma. Identical to WHO type II 1–4 primary bronchogenic small cell anaplastic carcinomas (7)

Adenocarcinoma primary or metastatic tumours with formation of tubules or glandlike structures.

Large cell or undifferentiated carcinoma primary or metastatic large cell epithelial tumours without evidence of epidermization or formation of glandlike structures.

Other malignant tumours primary or metastatic tumours that cannot be placed in any of the type categories described above.

RESULTS

Table 1 shows the cytological classification correlated to the histological diagnosis in the 139 cases of malignant intrathoracic tumours.

In 34 cases epidermoid differentiation was detected in the cytological specimens. This was in agreement with the histological tumour type in 29 cases (85.3 per cent) while four histologically were found to be mucoepidermoid carcinomas, and one a large cell undifferentiated carcinoma. The material comprised 45 histologically verified cases of epidermoid carcinoma, and the sensitivity with regards to classification—malignant tumour cells from epidermoid carcinoma—was thus 64 4 per cent.

In 21 cases the cytological classification stated small cell anaplastic carcinoma This was in agreement with the histology in 18 cases (85 7 per cent) while one case histologically was an epidermoid carcinoma, and two were adenocarcinomas. The material comprised 19 histologically verified cases of small cell anaplastic carcinoma and the sensitivity for this group was 95 per cent.

An adenomatous pattern of the aspirated tumour cells was found in 35 cases, 28 being in agreement with the histology (80 0 per cent) Two were epidermoid carcinomas, two were large cell undifferentiated carcinomas showing mucin formation one was a small cell anaplastic carcinoma and the last two cases were mesotheliomas. The material comprised 35 histologically verified cases of ade-

TABLE 1 *Comparison between Cytological and Histological Classification of 139 Cases of Malignant Intrathoracic Neoplasms*

Cytological classification		Histological classification				
		Epidermoid carcinomas	Small cell carcinomas	Adeno-carcinomas	Undifferentiated carcinomas	Other malignant neoplasms
Epidermoid carcinomas	34	29			1	4
Small cell carcinomas	21	1	18	2		
Adenocarcinomas	35	2	1	28	2	2
Undifferentiated carcinomas	39	13		4	20	2
Other malignant neoplasms	10			1		9
	139	45	19	35	23	17

TABLE 2. *Number of Cytologically Classified Aspiration Biopsies in Agreement with the Histological Classification (Sensitivity of Cytological Classification)*

	Epidermoid carcinomas	Small cell carcinomas	Adeno-carcinomas	Undifferentiated carcinomas	Other malignant neoplasms
Correctly classified biopsies	29	18	28	20	9
Number of positive biopsies	45	19	38	23	17
Sensitivity	0.64	0.95	0.80	0.87	0.53

TABLE 3. *Number of Aspiration Biopsies correctly Classified in Each of the Cytological Groups (Diagnostic Specificity of Cytological Classification)*

	Epidermoid carcinomas	Small cell carcinomas	Adeno-carcinomas	Undifferentiated carcinomas	Other malignant neoplasms
Correctly classified biopsies	29	18	28	20	9
Number of biopsies classified as	34	21	35	39	10
Specificity	0.85	0.86	0.80	0.51	0.90

nocarcinoma, and the sensitivity for this group was 80.0 per cent.

In 39 cases the aspirated tumour cells were classified as originating from large cell or undifferentiated carcinomas. Of these cases 20 were correctly grouped (51.3 per cent) while 13 were found to be epidermoid carcinomas, 4 were adenocarcinomas, and two were mucoepidermoid carcinomas. The group comprised 23 histologically verified cases of large cell or undifferentiated carcinomas, and the sensitivity was 87.0 per cent.

In 10 cases the malignant cells were classified as originating from other malignant tumours, and this was correct in 9 cases (90.0 per cent) since one histologically was found to be an adenocarcinoma. The nine biopsies correctly classified represented one case each of pulmonary blastoma, embryonal carcinoma, mucoepidermoid carcinoma, and mesothelioma and five different types of sarcomas. Histologically the material comprised 17 cases belonging to this group the sensitivity thus being 52.9 per cent.

As pointed out in Table 2 the cytological classification was in agreement with the histological in 104 out of 139 cases (74.8 per cent) ranging from 53 to 95 per cent of the different tumour groups represented. The diagnostic specificity (in the following simply designated specificity) of the cytological classification is shown in Table 3.

DISCUSSION

In the present study we have compared our original cytological classification of the malignant tumour cells with the histological classification and found the percentage of correct cytological classification to be 75 per cent. This result is in agreement with results obtained by *Dahlgren* (2) who in a comparable series found a correlation of 77 per cent. Our result is also in agreement with the best results obtained in cytological typing of tumour cells in sputum (9) and bronchial secretions (1 3 8).

The specificity of the classification of tumour cells representing an epidermoid carcinoma was found to be very high. This was especially found to be so when also the four cases of mucoepidermoid carcinomas were considered correctly classified as regards their epidermoid components. This high specificity

Small cell anaplastic carcinoma smears containing cells with a barely visible rim of cytoplasm and rather uniform but very friable nuclei without distinct nucleoli. The tumour cells were most often completely dissociated and if groups of tumour cells occurred no glandlike structure could be recognized.

Adenocarcinoma smears containing well demarcated groups of malignant tumour cells arranged in ring or papillary formations or in more or less well shaped "bags".

Large cell or undifferentiated carcinoma smears containing epithelial tumour cells showing no signs of cytoplasmic cornification or arrangement in glandlike structures.

Other malignant tumours smears containing malignant tumour cells which could not unequivocally be placed in the above mentioned groups.

Histological Investigation

Histological specimens from autopsy material, lung resections, and in a few cases from thoracoscopic biopsies were stained with haematoxylin-eosin and by Kreyberg's method (7).

A classification was made according to the following system without any knowledge of the cytological classification.

Epidermoid carcinoma primary or metastatic tumours with keratinisation or intercellular bridges.

Small cell anaplastic carcinoma identical to WHO type II 1–4 primary bronchogenic small cell anaplastic carcinomas (7).

Adenocarcinoma primary or metastatic tumours with formation of tubules or glandlike structures.

Large cell or undifferentiated carcinoma primary or metastatic large cell epithelial tumours without evidence of epidermization or formation of glandlike structures.

Other malignant tumours primary or metastatic tumours that cannot be placed in any of the type categories described above.

RESULTS

Table 1 shows the cytological classification correlated to the histological diagnosis in the 139 cases of malignant intrathoracic tumours.

In 34 cases epidermoid differentiation was detected in the cytological specimens. This was in agreement with the histological tumour type in 29 cases (85.3 per cent) while four histologically were found to be mucoepidermoid carcinomas, and one a large cell undifferentiated carcinoma. The material comprised 45 histologically verified cases of epidermoid carcinoma and the sensitivity with regards to classification—malignant tumour cells from epidermoid carcinoma—was thus 64.4 per cent.

In 21 cases the cytological classification stated small cell anaplastic carcinoma. This was in agreement with the histology in 18 cases (85.7 per cent) while one case histologically was an epidermoid carcinoma, and two were adenocarcinomas. The material comprised 19 histologically verified cases of small cell anaplastic carcinoma and the sensitivity for this group was 95 per cent.

An adenomatous pattern of the aspirated tumour cells was found in 35 cases, 28 being in agreement with the histology (80.0 per cent). Two were epidermoid carcinomas, two were large cell undifferentiated carcinomas showing mucin formation, one was a small cell anaplastic carcinoma, and the last two cases were mesotheliomas. The material comprised 35 histologically verified cases of ade-

TABLE 1 *Comparison between Cytological and Histological Classification of 139 Cases of Malignant Intrathoracic Neoplasms*

Cytological classification		Histological classification				
		Epidermoid carcinomas	Small cell carcinomas	Adeno-carcinomas	Undifferentiated carcinomas	Other malignant neoplasms
Epidermoid carcinomas	34	29			1	4
Small cell carcinomas	21	1	18	2		
Adenocarcinomas	35	2	1	28	2	2
Undifferentiated carcinomas	39	13		4	20	2
Other malignant neoplasms	10			1		9
	139	45	19	35	23	17

Acta path. microbiol. scand. Sect. A, 85: 539-547, 1977

THE IMPORTANCE OF THYMUS IN THE PATHOGENESIS OF THE CHRONIC PHASE OF HYPERTENSION IN MICE FOLLOWING PARTIAL INFARCTION OF THE KIDNEY

ULRIK GERNER SVENDSEN

The University Institute for Experimental Medicine, Copenhagen, Denmark

Svendsen, U. G. The importance of thymus in the pathogenesis of the chronic phase of hypertension in mice following partial infarction of the kidney. Acta path. microbiol. scand. Sect. A, 85: 539-547, 1977.

Partial infarction of one kidney and contralateral nephrectomy was followed by a similar initial increase in blood pressure in athymic (nude) and normal mice of the C57/BL/6J strain. The chronic phase of the hypertension was, however, thymus dependent, since the athymic mice failed to maintain an increased blood pressure, in contrast to the normal mice. A response of thymus transplantation in athymic mice was the ability to maintain the blood pressure high in the chronic phase of the hypertension, whereas cyclophosphamide treatment to the normal hypertensive mice decreased the blood pressure in the chronic phase of the hypertension, but not in the early (acute) phase. Some perivascular round cell infiltrations were found in the un-infarcted part of the kidney in normal and thymus-transplanted nude mice *after 80 days of* hypertension, but the degree of cellular reaction was less than previously observed in the NMRI-strain of mice. Substantial perivascular cellular infiltrations, which appeared to be thymus-dependent, occurred in the ischemic border-zone of the infarcted area. Athymic mice of the NMRI-strain were able to develop the usual blood pressure elevation of DOCA/salt hypertension during the chronic phase of Loomis hypertension, in which phase the arterial pressure otherwise would be declining towards normal values.

Key words: Hypertension; thymus; infarction of kidney.

Ulrik Gerner Svendsen, The University Institute for Experimental Medicine, Nørre Allé 71, 2100 Copenhagen Ø, Denmark.

Received 2.5.77. Accepted 25.3.77.

In previous studies on the vascular lesion in various models of experimental hypertension in rats and mice, evidence has been provided to indicate that the perivascular round cell infiltration may be due to a thymus dependent immune reaction (for literature see (4, 5, 10)). Also it has been found that the initial rise in blood pressure within the first month of the development of "Loomis" (10) as well as desoxycorticosterone acetate (DOCA) – salt (11) hypertension is the same in athymic nude and normal-haired mice, and therefore is independent of the thymus. By contrast, in the late phase of these forms of hypertension (i.e. after about two to three months) the mean blood pressure remained elevated in the haired, but declined towards normotensive values in the nude mice, suggesting a thymus-dependency for the main-

is explained by the cytologically stringent demand for a bright blue coloured cytoplasm as a sign of cytoplasmatic cornification. The rather low sensitivity of 64 per cent is explained partly by the stringent cytological criteria partly by the fact that a tumour was histologically classified as an epidermoid carcinoma even in those cases where the amounts of epidermization or monocellular keratinization were very sparse.

The cytological appearance of tumour cells showing uniform and friable nuclei with sparse cytoplasm was highly characteristic of a small cell anaplastic carcinoma. Both the sensitivity and specificity were found to be high. That the sensitivity in this group was especially high, may be explained by these tumours apart from necrotic areas, being uniform throughout.

Adenomatous differentiation was cytologically based on the arrangement of the aspirated tumour cells, not the shape of single cells nor the cytoplasmic contents of secretory vacuoles. That adenomatous formations were registrated in two cases of mesotheliomas can hardly be considered a typing error. Hereby the specificity may be raised from 80 to 86 per cent. This high specificity shows that the above mentioned cytological criterion is useful in cytological classification.

A large number of biopsies were cytologically registered as large cell undifferentiated carcinomas. This cytological group was used when other groups were inapplicable. Not surprisingly this led to a rather low specificity.

The high specificity achieved for the heterogenous group of other malignant tumours showed that it was posible to cytologically distinguish between these tumour cells and cells from the other cytological groups. The low sensitivity is influenced by the difficulty or impossibility of making a correct bioptical identification of tumours as mesotheliomas and mucoepidermoid carcinomas.

The criteria we used for classifying aspirated malignant tumour cells from differentiated neoplasms were feasible. The specificity achieved in classifying differentiated malignant tumours was found to be so high that it seems reasonable to utilize the cytological classification in the planning of an individualized tumour therapy in cases not accessible to pretreatment bioptic histological classification.

REFERENCES

1 *Bibbo M., Fennessy J. J., Lu C. T., Straus F., Vrakopis D. & Wied G. L.* Bronchial brushing technique for the cytologic diagnosis of periferal lung lesion. Acta Cyt. Vol. *17* 245, 1973.

2 *Dahlgren S. E.* Aspiration biopsy of intrathoracic tumours. Acta Path. Microbiol. Scand. *70* 566–576 1967.

3 *Dahlgren S. E. & Lind B.* Transthoracic needle biopsy or bronchoscopic biopsy. Scand. J. Resp. Dis. *50* 265–272 1969.

4 *Francis D.* Transthoracic aspiration biopsy. A histological verified material. Acta path. microbiol. scand. Sect. A, *85* 230–234 1977.

5 *Francis D.* Aspiration biopsies from diagnostically difficult pulmonary lesions. A consecutive case material. Acta path. microbiol. scand. Sect. A *85* 235–239 1977.

6 *Franzén S.* Personal communication.

7 *Kreyberg L., Liebow A. A. & Uehlinger E. A.* Histological typing of lung tumours. WHO, p. 28. Geneve 1967.

8 *Nasiell M.* Diagnosis of lung cancer by aspiration biopsy and a comparison between this method and exfoliative cytology. Acta Cyt. Vol. 11. 2. 114. 1967.

9 *Russel W. O., Neidhardt H. W., Mountain C. F., Griffith K. M. & Chang J. P.* Cytodiagnosis of lung cancer. Acta Cyt. *7* 1–44 1963.

10 *Zajicek J.* Aspiration Biopsy Cytology I. Karger p. 2, Basel 1974.

Acta path. microbiol. scand. Sect. A, 85 539–547 1977

THE IMPORTANCE OF THYMUS IN THE PATHOGENESIS OF THE CHRONIC PHASE OF HYPERTENSION IN MICE FOLLOWING PARTIAL INFARCTION OF THE KIDNEY

ULRIK GERNER SVENDSEN

The University Institute for Experimental Medicine, Copenhagen, Denmark

Svendsen, U. G. The importance of thymus in the pathogenesis of the chronic phase of hypertension in mice following partial infarction of the kidney. Acta path. microbiol. scand. Sect. A, 85: 539–547, 1977.

Partial infarction of one kidney and contralateral nephrectomy was followed by a similar initial increase in blood pressure in athymic (nude) and normal mice of the C57/BL/6J strain. The chronic phase of the hypertension was, however, thymus dependent, since the athymic mice failed to maintain an increased blood pressure, in contrast to the normal mice. A response of thymus transplantation in athymic mice was the ability to maintain the blood pressure high in the chronic phase of the hypertension, whereas cyclophosphamide treatment to the normal hypertensive mice decreased the blood pressure in the chronic phase of the hypertension, but not in the early (acute) phase. Some perivascular round cell infiltrations were found in the uninfarcted part of the kidney in normal and thymus-transplanted nude mice after 80 days of hypertension, but the degree of cellular reaction was less than previously observed in the NMRI-strain of mice. Substantial perivascular cellular infiltrations, which appeared to be thymus-dependent, occurred in the ischemic border-zone of the infarcted area. Athymic mice of the NMRI-strain were able to develop the initial blood pressure elevation of DOCA/salt hypertension during the chronic phase of Loomis hypertension, in which phase the arterial pressure otherwise would be declining towards normal values.

Key words: Hypertension; thymus; infarction of kidney.

Ulrik Gerner Svendsen, The University Institute for Experimental Medicine, Nørre Allé 71, 2100 Copenhagen Ø, Denmark.

Received 23. .77. Accepted 25.i.77

In previous studies on the vascular lesion in various models of experimental hypertension in rats and mice, evidence has been provided to indicate that the perivascular round-cell infiltration may be due to a thymus dependent immune reaction (for literature see (4, 5, 10). Also, it has been found that the initial rise in blood pressure within the first month of the development of "Loomis" (10) as well as desoxycorticosterone acetate (DOCA) – salt (11) hypertension is the same in athymic nude and normal-haired mice, and therefore is independent of the thymus. By contrast, in the late phase of these forms of hypertension (i.e. after about two to three months) the mean blood pressure remained elevated in the haired, but declined towards normotensive values in the nude mice, suggesting a thymus-dependency for the main-

tenance of the hypertensive blood pressure level in the chronic phase. Furthermore, thymus grafting in nude mice conferred the ability to maintain an elevated arterial pressure in the late phase in response to DOCA/salt treatment, and to develop chronic hypertensive vascular disease in the kidneys (11).

The aim of the present study was to test, firstly whether or not the early development and the chronic maintenance of experimental hypertension would be the same as previously observed in a different strain of mice (C57/BL/6J) known to react with minor degrees of perivascular round cell infiltrations than the previously studied strain (NMRI), secondly whether thymus grafting in nude mice would confer the ability to maintain an elevated blood pressure in the late phase also of Loomis" hypertensive mice, thirdly to study whether or not the cytostatic drug cyclophosphamide would influence the blood pressure in the early thymus-independent and/or the late, thymus-dependent phase of hypertension in haired mice. Finally it was investigated whether nude mice were able to develop a different kind of experimental hypertension when superimposed during the chronic phase of the Loomis hypertension, i.e. at a time when the blood pressure is known to decline towards normal values, or whether other defects in these mice prevent the maintenance or establishment of an elevated systemic arterial pressure in this phase.

MATERIAL AND METHODS

Animals. Nude congenital athymic mice carrying the mutant alleles (nu/nu) and their haired litter mates (+/+ or nu/+) of the C57/BL/6J and the NMRI strain (SPF, GL Bomholtgård Ltd., Ry, Denmark) 20–25 g received tetracyclin (Tetracyclin Novo Vet., 100 mg/l) in the drinking water. (For literature on nude mice see (6, 7)).

Thymus transplantation. Subcutaneous whole thymus grafts were made in 6-week old nude C57/BL/6J mice. Donors were C57/BL/6J mice less than 24 hours old. The success of the thymus transplantation was judged after 4 to 6 weeks from the achieved ability to reject a skin allograft (donors C H/Tif/Bom mice).

Skin transplantation was performed as previously described (10). 15 haired and 10 nude C57/BL/6J female mice and all thymus transplanted nude mice were challenged with an allograft (C_3H/Tif/Bom).

The animals were grouped according to the treatment.

Group I (Control C57/BL/6J mice). 20 nude and 25 haired mice 3–6 months of age. The numbers of males and females used were similar. Also included were 4 female nude mice 6–8 months of age, which had been thymus transplanted and thereafter had rejected a skin allograft.

Group II (Loomis hypertensive nude and haired C57/BL/6J mice). 40 nude, 40 haired and 15 nude thymus transplanted female mice with the left kidney partly infarcted and placed subcutaneously and contralateral nephrectomy (3). Randomly selected groups of 5 or 10 mice were investigated after 5, 15, 40, 80 or 120 days, except for thymus transplanted nude mice, which were all investigated after 80 or 120 days.

Group III (Loomis hypertensive haired C57/BL/6J mice treated with cytostatics). 75 haired female mice. Immediately after the Loomis operation 25 mice were treated with a weekly intraperitoneal injection of either 1.4 mg cyclophosphamide (Endoxan Asta®, Asta-Werke AG, Schering Kemi AS, Denmark) (15 mice) or with an equal volume of isotonic saline (10 mice) for 4 weeks. 40 mice were allowed to live for 90 days after the operation. Then systemic arterial pressure was recorded in 5 randomly selected mice. The remaining 35 mice were divided into two groups and treated for 4 weeks with weekly injections of either cyclophosphamide or saline, as described above. 10 *untouched* mice were treated with a weekly intraperitoneal injection of 1.4 mg cyclophosphamide for 4 weeks, whereafter blood pressures were recorded.

Group IV (nude NMRI mice with Loomis and DOCA/salt hypertension). Nude NMRI male mice were made Loomis hypertensive. After 60 days they were treated with a weekly subcutaneous injection of 6 mg DOCA (desoxycorticosterone acetate, Percorten® microcrystalline Ciba) and received 1 per cent saline as drinking water. 21 days later blood pressures were recorded. The mean blood pressures obtained were compared with the mean blood pressures of 20 nude and 20 haired untouched control mice 3–6 months of age, as previously reported (11).

The further treatment was the same for all groups. Systemic arterial pressures were recorded in the conscious mice, as previously described (10). Arterial blood samples were obtained for measurement of haematocrit and the number of circulating lymphocytes. The relative heart weight (heart weight × 100/body weight) was determined. The heart, kidney and spleen were fixed in 4 per cent formalin and embedded in paraffin. Five-

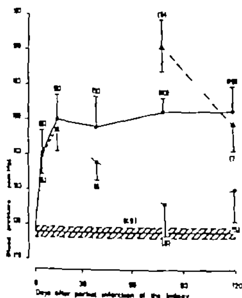


Fig 1 The mean blood pressure ± SEM in nude (○——○) nude thymus transplanted (▲---▲) and haired (●——●) mice with partial infarction of one kidney and contralateral nephrectomy. The scratched area indicates the mean blood pressure in the nude nude thymus-transplanted and the haired control mice ± SEM. After 80 days significant difference ($p < 0.01$) between the mean blood pressure of the nude and the haired mice was observed. Number in brackets number of mice

micron-thick sections were cut and stained with the van Gieson Hansen (VGH) and the periodic acid Schiff (PAS) stain. The round cell infiltrations around arteries in the heart and the arcuate/interlobular arteries in the kidney were graded semiquantitatively according to photographed scales from 1+ to 3+ in which a 1+ cellular reaction includes the sparse number of mononuclear cells in adventitia of normal arteries (8 9). Deposits of amyloid were identified as previously described (1). All mean values are given with standard error of the mean. For comparison of experimental results the students t-test was used. The five per cent level was used as indicator of significance of differences.

RESULTS

A subcutaneous, macroscopically visible thymus was observed in all the thymus transplanted nude mice which rejected the skin allograft within an average of 22 days (range 11–40 days). None of the 10 nude mice without a thymus graft were able to reject the skin allograft, and donor hair grew on the graft by the time the experiment was termin

TABLE 1 *R and Cell Infiltration around Int arenal Arteries*

Day	A. Interlobularis/arcuata		
	Nude mice	Nude mice + thymus	Haired mice
	+		+
	+		+
5	+		+
	+		+
	+		+
	+		+
	+		+
15	+		+ +
	+		+
	+		+
	+		+
	+		+
40	+		+
	+		+
	+		+ + +
	+	+	+ + +
	+	+	+ + +
	+	+ +	+
80	+	+	+ + +
	+	+	+
			+
			+
			+
			+
			+
	+	+ + +	+ +
	+	+	+ +
	+	+ +	+
	+	+ +	+ +
	+	+ +	+
120		+	+ + +
		+ +	+ +
			+
			+ + +
			+

The degree of round cell infiltration around the interlobular/arcuate arteries in the uninfarcted part of the kidney of Loomis hypertensive nude, nude thymus transplanted and haired mice. The day indicates at what time after the partial infarction of the kidney the animals are sacrificed. Increased round cell infiltrations are only found in haired and nude thymus transplanted mice.

tenance of the hypertensive blood pressure level in the chronic phase. Furthermore thymus grafting in nude mice conferred the ability to maintain an elevated arterial pressure in the late phase in response to DOCA/salt treatment and to develop chronic hypertensive vascular disease in the kidneys (11)

The aim of the present study was to test firstly whether or not the early development and the chronic maintenance of experimental hypertension would be the same as previously observed in a different strain of mice (C57/BL/6J) known to react with minor degrees of perivascular round cell infiltrations than the previously studied strain (NMRI) secondly whether thymus grafting in nude mice would confer the ability to maintain an elevated blood pressure in the late phase also of Loomis hypertensive mice thirdly to study whether or not the cytostatic drug cyclophosphamide would influence the blood pressure in the early thymus-independent and/or the late, thymus-dependent phase of hypertension in haired mice Finally it was investigated whether nude mice were able to develop a different kind of experimental hypertension when superimposed during the chronic phase of the Loomis hypertension i e. at a time when the blood pressure is known to decline towards normal values or whether other defects in these mice prevent the maintenance or establishment of an elevated systemic arterial pressure in this phase

MATERIAL AND METHODS

Animals Nude, congenital athymic mice carrying the mutant alleles (nu/nu) and their haired litter mates (+/+ or nu/+) of the C57/BL/6J and the NMRI strain (SPF Gl Bomholtgård Ltd., Ry Denmark) 20–25 g received tetracyclin (Tetracyclin Novo Vet. 100 mg/l) in the drinking water (For literature on nude mice see (6 7))

Thymus transplantation Subcutaneous whole thymus grafts were made in 6-week old nude C57/BL/6J mice Donors were C57/BL/6J mice less than 24 hours old The success of the thymus transplantation was judged after 4 to 6 weeks from the achieved ability to reject a skin allograft (donors C H/Tif/Bom mice)

Skin transplantation was performed as previously described (10) 15 haired and 10 nude C57/BL/6J female mice and all thymus transplanted nude mice were challenged with an allograft (C_3H/Tif/Bom)

The animals were grouped according to the treatment.

Group I (Control C57/BL/6J mice) 20 nude and 25 haired mice, 3–6 months of age. The numbers of males and females used were similar Also included were 4 female nude mice 6–8 months of age, which had been thymus transplanted and thereafter had rejected a skin allograft.

Group II (Loomis hypertensive nude and haired C57/BL/6J mice) 40 nude, 40 haired and 15 nude, thymus transplanted female mice with the left kidney partly infarcted and placed subcutaneously and contralateral nephrectomy (3) Randomly selected groups of 5 or 10 mice were investigated after 5 15 40 80 or 120 days, except for thymus transplanted nude mice, which were all investigated after 80 or 120 days.

Group III (Loomis hypertensive haired C57/BL/6J mice treated with cytostatics) 75 haired female mice Immediately after the Loomis operation 25 mice were treated with a weekly intraperitoneal injection of either 1 4 mg cyclophosphamide (Endoxan-Asta® Asta Werke AG Schering Kemi AS Denmark) (15 mice) or with an equal volume of isotonic saline (10 mice) for 4 weeks 40 mice were allowed to live for 90 days after the operation. Then systemic arterial pressure was recorded in 5 randomly selected mice. The remaining 35 mice were divided into two groups and treated for 4 weeks with weekly injections of either cyclophosphamide or saline as described above. 10 *untouched* mice were treated with a weekly intraperitoneal injection of 1 4 mg cyclophosphamide for 4 weeks, whereafter blood pressures were recorded.

Group IV (nude NMRI mice with Loomis and DOCA/salt hypertension) Nude NMRI male mice were made Loomis hypertensive After 60 days they were treated with a weekly subcutaneous injection of 6 mg DOCA (desoxycorticosterone acetate, Percorten® microcrystalline Ciba) and received 1 per cent saline as drinking water 21 days later blood pressures were recorded The mean blood pressures obtained were compared with the mean blood pressures of 20 nude and 20 haired untouched control mice 3–6 months of age, as previously reported (11)

The further treatment was the same for all groups. Systemic arterial pressures were recorded in the conscious mice as previously described (10) Arterial blood samples were obtained for measurement of haematocrit and the number of circulating lymphocytes. The relative heart weight (heart weight × 100/body weight) was determined The heart, kidney and spleen were fixed in 4 per cent formalin and embedded in paraffin. Five-



Fig 1 The mean blood pressure ± SEM in nude (O——O) nude thymus transplanted (▲- - -▲) and haired (●——●) mice with partial infarction of one kidney and contralateral nephrectomy The scratched area indicates the mean blood pressure in the nude, nude thymus-transplanted and the haired control mice ± SEM. After 80 days a significant difference (p < 0.01) between the mean blood pressure of the nude and the haired mice was observed Number in brackets number of mice

micron-thick sections were cut and stained with the van Gieson Hansen (VGH) and the periodic acid Schiff (PAS) stain. The round cell infiltrations around arteries in the heart and the arcuate/interlobular arteries in the kidney were graded semiquantitatively according to photographed scales from 1+ to 3+ in which a 1+ cellular reaction includes the sparse number of mononuclear cells in adventitia of normal arteries (8, 9) Deposits of amyloid were identified as previously described (12) All mean values are given with standard error of the mean For comparison of experimental results the students t-test was used. The five per cent level was used as indication of significance of differences

RESULTS

A subcutaneous, macroscopically visible thymus was observed in all the thymus transplanted nude mice which rejected the skin allograft within an average of 22 days (range 11-40 days) None of the 10 nude mice without a thymus graft were able to reject the skin allograft, and donor hair grew on the graft by the time the experiment was termin

TABLE 1 *Round Cell Infiltration around Intrarenal Arteries*

	A. Interlobularis/arcuata		
Day	Nude mice	Nude mice + thymus	Haired mice
	+		+
	+		+
5	+		+
	+		+
	+		+
	+		+
	+		+
15	+		+ +
	+		+
	+		+
	+		+
	+		+
40	+		+
	+		+
	+		+ + +
	+	+	+ + +
	+	+	+ + +
	+	+ +	+
80	+	+	+ + +
	+	+	+
			+
			+
			+
			+
			+
	+	+ + +	+ +
	+	+	+ +
	+	+ +	+
	+	+ +	+ +
	+	+ +	+
120		+	+ + +
		+ +	+ +
			+
			+ + +
			+

The degree of round cell infiltration around the interlobular/arcuate arteries in the uninfarcted part of the kidney of Loomis hypertensive nude, nude thymus transplanted and haired mice. The day indicates at what time after the partial infarction of the kidney the animals are sacrificed. Increased round cell infiltrations are only found in haired and nude thymus transplanted mice.

TABLE 2 *Round Cell Infiltration around Intrarenal Arteries in the Ischaemic Area between the Uninfarcted and the Infarcted Area of the Kidney*

Day	A Interlobularis/arcuata Nude mice	Nude mice + thymus	Haired mice
5	+		+
	+		+
	+		+
	+		+
	+		+
15	+		+ +
	+		+
	+		+ + +
	+		+
	+		+
40	+		+
	+		+
	+		+ + +
	+		+
	+		+ +
80	+	+ + +	+ + +
	+	+	+
	+	+	+ + +
	+	+ +	+ + +
	+	+ +	+
			+ + +
			+ + +
			+ +
			+
			+
120	+	+ +	+ + +
	+	+ +	+ +
	+	+ +	+ +
	+	+	+
	+ +	+ + +	+ + +
		+ + +	+ +
			+ +
			+ +
			+ +
			+ + +

The degree of round cell infiltration around intrarenal arteries in the ischaemic borderzone of the kidney of the Loomis hypertensive nude nude thymus transplanted and the haired mice The days indicates at what time after infarction of the kidney the mice are sacrificed Round cells are only found in haired and nude thymus transplanted mice

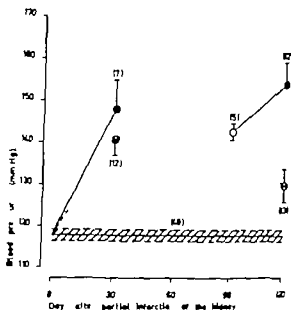


Fig 2 The mean blood pressure ± SEM in haired mice with partial infarction of one kidney and contralateral nephrectomy treated with one weekly intraperitoneal injection of either physiological saline (●) or cyclophosphamide (⊗) for 4 weeks. The group of mice investigated after 90 days was not treated with injections (O) It is seen that only treatment with cyclophosphamide between day 90 and 120 was followed by a fall in the mean blood pressure The scratched area indicates the mean blood pressure in the control mice ± SEM. Number in brackets number of mice.

ated All haired mice rejected the skin allograft within an average of 17 days (range 13–20 days) The haematocrit ranged between 40–45 per cent in all mice.

Group I (Control C57/BL/6J mice) The mean blood pressure in mice of both sexes was the same ($p > 0.5$) in the nude and the haired mice.

The mean relative heart weight in the nude and haired mice was 0.41 ± 0.01 per cent.

Thymus transplanted nude mice had the same mean blood pressure ($p > 0.5$) and the same mean relative heart weight ($p > 0.2$) as the control mice. The mean number of *circulating lymphocytes* was similar in nude (2073 ± 296 per microlitre) and nude thymus-transplanted (3438 ± 520 per microlitre, $p > 0.05$) mice, significantly less than that found in the haired mice (8355 ± 494 per microlitre, $p < 0.001$)

Histological investigation the heart and spleen no vascular disease. No amyloidosis.

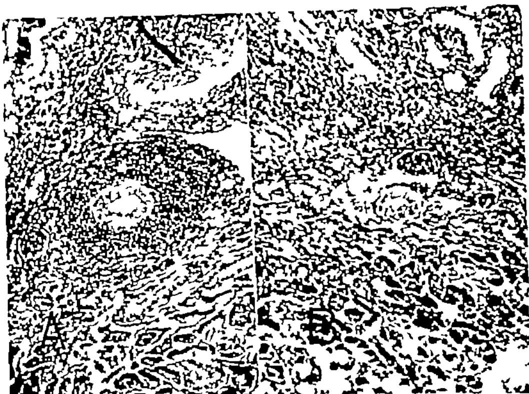


Fig. 3 (A) An artery in the area of the kidney between the infarcted and the uninfarcted part from a haired mouse with Loomis hypertension. In (B) is shown a similar artery from nude mouse. A pronounced round cell infiltration around the artery is observed in (A). No fibrinoid degeneration of the wall is observed. PAS staining, 140 ×

The kidney: no vascular disease, except for 2 of the 4 thymus-transplanted nude mice which were sacrificed 5 months after the grafting. In these two mice a slight increase (less than a 2+ reaction) in round cell infiltrations around the interlobular arteries was found.

Group II (Loomis hypertensive nude and haired C57/BL/6J mice). 5 haired, 15 nude and 3 nude thymus-transplanted mice died spontaneously and are excluded from the following description. Fig. 1 shows *the mean blood pressure.* Infarction of the kidney was followed by a similar and significant ($p < 0.001$) increase in blood pressure, which did not differ significantly before day 80 and day 120 ($p < 0.01$ and $p < 0.025$ respectively). While the mean blood pressure in the haired mice was still significantly elevated ($p < 0.001$ both days) the mean blood pressure in the nude mice decreased to a value close to that obtained in the control mice ($p < 0.1$ and $p < 0.025$ respectively). In thymus-transplanted nude mice the mean blood pressure was significantly higher after 80 days than that obtained both in haired ($p<0.025$) and nude ($p < 0.001$) Loomis-hypertensive mice, but a value similar to the value in the haired mice ($p > 0.5$) was found after 120 days. *The mean relative heart weight* was increased in both nude (0.49 ± 0.02 per cent, $p < 0.001$) and haired mice (0.47 ± 0.03 per cent, $p < 0.001$) already 5 days after the operation, and it remained increased for the rest of the observation period. *Histological investigation: the heart:* fibrinoid degeneration and necrosis in the walls of the arteries, and infarcts of the heart muscle were ob-

served in 5 haired and 5 nude mice until day 40 *after infarction of the kidney* After this time these lesions were only found in 7 haired and 5 nude thymus transplanted mice. An increased number of perivascular round cells was found in 3 haired (all 2+ reactions) mice and in one thymus transplanted mouse (a 2+ reaction) *The kidney* Table 1 shows the number of round cells observed around the arcuate/interlobular arteries. None of the nude mice, but both haired and nude thymus transplanted mice showed increased numbers of round cells. Increased amounts of PAS positive material in the glomerular tufts were often found in both haired and nude thymus transplanted mice 80 and 120 days after the operation These lesions were seldom found in the nude mice. The ischaemic zone between the uninfarcted and the infarcted part of the kidney contained lesions similar to the intrarenal lesions previously described (10) in hypertensive mice with advanced renal disease. Commencing after 15 days pronounced perivascular infiltrations of round cells, but absence of fibrinoid degeneration were found in this area in haired and thymus-transplanted nude mice but in none of the untransplanted nude mice (Table 2, Fig 3A and B) *The spleen* amyloidosis was found commencing 80 days after the operation in 4 haired, 4 nude and one thymus-transplanted nude mouse There was no relationship between the degree of hypertension and amyloidosis

Group III (Loomis hypertensive haired C57/BI/6J mice treated with cytostatica) Treatment of 10 normal mice with cyclophosphamide for 4 weeks was followed by a slight increase in *the mean blood pressure (126 ± 3 mm Hg)* as compared with the mean blood pressure in the control group of mice ($p < 0.025$) In the other mice no difference was observed clinically between those treated with cytostaticum and those treated with saline 7 mice treated with cytostaticum and 9 with saline died and were excluded from the following description Fig 2 shows *the mean blood pressure* in the saline and cyclophosphamide treated series of Loomis-hypertensive mice. In the initial phase after the operation a similar ($p > 0.4$) and significant ($p < 0.001$) increase in blood pressure was observed However when the treatment was delayed to the late phase between day 90 and 120 a significant difference in blood pressure was observed ($p < 0.005$) The mean number of circulating lymphocytes was decreased in cytostatica treated mice (1000 ± 97 per microlitre) as compared with 4528 ± 839 per microlitre in the saline injected mice ($p < 0.001$)

TABLE 3 *Round Cell Infiltrations around Intrarenal Arteries in Cyclophosphamide-Treated or Saline Injected Haired Mice which have been Loomis Hypertensive for 120 Days*

Ischaemic area		Uninfarcted part	
Endoxan	Saline	Endoxan	Saline
+	+	+	+
+ +	+ + +	+	+ +
+	+	+	+
+ +	+	+	+
+ +	+	+	+
+	+ + +	+	+
+	+ +	+ +	+
+	+ + +	+	+ + +
+	+ + +	+	+
+	+ + +	+	+
+ +	+ + +	+	+ +
+ +	+	+	+
+ +		+	

The degree of round cell infiltration around the interlobular/arcuate arteries in the uninfarcted part of the kidney and around similar arteries in the ischaemic borderzone of the kidney Only sa line injected mice have 3+ round cell infiltrations in the ischaemic border zone of the kidney

Histological investigation no vascular disease was found in the normal, cyclophosphamide treated mice, and no amyloidosis. Loomis-hypertensive mice had vascular disease as described above (Group III) in *the heart* and *the kidney* except after treatment with cytostatica in the late phase (90–120 days after the operation) in which series no vascular disease was found in the heart *In the kidneys* of this latter series a less severe degree of perivascular round cell reaction was

found in the ischaemic border-zone (Table 3). Deposits of amyloid were found in the glomeruli and in the basement membranes of the tubules in two cyclophosphamide-treated mice after the late 30-day period of treatment. *The spleen*: perifollicular deposits of amyloid were found after the late 30-day period of treatment in 8 (62 per cent) of the cyclophosphamide-treated mice, and in 2 (17 per cent) of the saline-treated mice.

Group II (Nude NMRI mice with Loomis and DOCA/salt hypertension): 4 mice died in the initial 60-day period of Loomis hypertension, and 9 died after commencement of 21 days of treatment with DOCA/salt. In the remaining 7 mice *the mean blood pressure* was 154 ± 8 mm Hg, similar to the mean blood pressure obtained previously (11) in nude DOCA/salt treated mice after 21 days ($p > 0.5$) and significantly increased as compared with the value in untouched control NMRI mice ($p < 0.001$ (11)). *The mean relative heart weight* was significantly increased (0.55 ± 0.03 per cent, $p < 0.001$) above the value obtained in untreated control NMRI mice (11). The mean number of *circulating lymphocytes* was 514 ± 47 per microlitre. *Histological investigation*: hypertrophia of the media was found in 3 and infarcts of the heart muscle in 4 mice. *The kidney*: the number of perivascular round cells was not increased, neither in the uninfarcted part nor in the ischaemic border zone of the kidney. Glomerular changes, consisting of increased amounts of PAS positive material in the glomerular tufts and dilated tubules with hyaline casts, were found in 5 mice. *The spleen*: one mouse had amyloidosis.

DISCUSSION

It was found in the present study that nude athymic C57/BL/6J mice with their kidneys partly infarcted ("Loomis" hypertension) failed to maintain the initial rise in blood pressure in the chronic phase. Thymus grafting in these nude Loomis-hypertensive mice conferred the ability not only to react with known thymus-dependent immune reactions such as skin allograft rejection, but also to maintain the hypertension in the chronic phase. Furthermore, treatment with cyclophosphamide, an ankylating agent which is known to be effective against diseases in which T-cells are essentially implicated (1), decreased the blood pressure in haired Loomis-hypertensive mice in the chronic phase of the hypertension but not in the initial phase of the hypertension. This difference in effects indicates that the anti hypertensive effect of cyclophosphamide in the chronic phase of the hypertension is not due to an unspecific blood-pressure-decreasing effect, such as deterioration of the general condition of the animals. Similarly it is shown that nude NMRI mice in the chronic phase of Loomis hypertension, in which the arterial blood pressure was declining towards normal values, were able to develop the initial increase in arterial pressure caused by DOCA/salt treatment. This would indicate that unspecific deterioration of the general condition was not responsible for the failure of maintaining a high pressure level in the chronic phase of Loomis hypertension in these athymic mice. It would seem that the secondary arterial-pressure decline is actually related to the absence of the thymus and the ability to develop thymus-dependent immune reactions. Thus, the present investigation has added strong support to the suggestion that there exists an initial, thymus-independent, and a chronic, thymus-dependent phase, also of Loomis hypertension in mice. However, the detailed mechanism by which such relations interfere with systemic arterial-pressure control remains unknown.

It has previously been suggested, as one of several possibilities, that high systemic arterial pressure, combined with thymus-dependent perivascular cellular reactions during prolonged hypertension, might cause progressive ischaemia of the kidney by gradually constricting the intrarenal arteries. In this way it might have pathogenic significance for the development of wedge-shaped infarcted areas and for maintenance, or aggravation, of the

high blood pressure lending to a vicious cycle (10)

An attempt was made to test this hypothesis by using a strain of mice (C57/BL/6J) which develops significantly less perivascular round cell infiltrations than the previously investigated NMRI strain do It was found in contrast to previous observations in haired NMRI mice with Loomis hypertension (10) that haired and nude thymus transplanted C57/BL/6J mice developed only minor degrees of perivascular round cell infiltrations and few degenerative changes in the uninfarcted part of the kidney even 4 months after the rise in systemic arterial pressure yet the blood pressure increased to similar high levels. However this finding is not enough evidence to invalidate the hypothesis, since it remains a possibility that thymus-dependent cellular immune reactions in the ischaemic border zone of the kidney still might have pathogenic significance for the maintenance of the chronic phase of the Loomis hypertension Perivascular round cell infiltrations were frequent in this area And they seemed to be thymus-dependent since they occurred only in the haired and in the thymus transplanted nude mice in the haired mice the perivascular cellular reaction was present already 15 days after the rise in arterial pressure at which time the arterial pressure of the nude athymic mice had risen to equally high levels yet these latter mice had no perivascular cellular reactions Finally treatment with cyclophosphamide in contrast to saline treatment decreased the frequency and degree of perivascular cellular reaction only in this ischaemic area of the kidney This finding might tentatively suggest that ischaemia of the hypertensively-damaged arteries could be responsible for uncovering or creation of antigenic determinants in the vessel walls On the other hand, the short duration of the initial phase of the hypertension in the nude C57/BL/6J mice and the scarcity of perivascular round cell infiltrations outside the ischaemic border zone in the haired Loomis hypertensive mice after 40 days of hypertension prevented the conclusion whether or not the few round cell infiltrations present in the uninfarcted part of the kidney were actually thymus-dependent Finally supporting the hypothesis that the perivascular cellular reaction might influence the blood pressure in the chronic phase by gradually constricting the intrarenal arteries we have the present finding of absence of such perivascular cellular infiltrations and wedge-shaped infarcted areas in nude NMRI mice in which the systemic arterial pressure was maintained elevated for about 80 days by superimposing the early phase of DOCA/salt hypertension during the late phase of Loomis hypertension It has previously been found that such lesions were frequent in haired NMRI mice with either Loomis or DOCA/salt hypertension of 90 and 78 days duration respectively (10 11)

The development of amyloidosis in the hypertensive mice in this study agrees with previous findings in hypertensive mice (12) Treatment with cyclophosphamide was followed by an increased frequency of amyloidosis this agrees with the results obtained with kasein induced amyloidosis in mice treated with different forms of cytostatics (2)

The author is grateful to Miss Lisbeth Olsen for her valuable technical assistance The Percorten® was kindly supplied by Ciba-Geigy Copenhagen. This work was supported by grants from the *Danish Medical Research Council* Ingeniør *Søren Alfred Andersen's* Foundation and *Carl and Ellen Hert* Foundation.

REFERENCES

1 *Back J F* The pharmacological and immunological basis for the use of immunosuppressive drugs. Drugs *11* 1 13 1976
2 *Hardt F* Acceleration of casein induced amyloidosis in mice by immunosuppressive agents. Acta path microbiol scand *79* 1 61–64 1971
3 *Loomis D* Hypertension and necrotizing arteritis in the rat following renal infarction Arch Path. *41* 231 268, 1946.
4 *Okuda T & Grollman A* Passive transfer of autoimmune induced hypertension in the rat by lymph node cell Texas rep. Biol. Med *25* 257 264 1967

5 Olsen F Inflammatory cellular reaction i hypertensi vascular disease. Munksgaard Copenhagen, 1971
6 Rygaard J Thymus & Self Immunobiology of the mouse mutant nude Thesis F.A.D.L. Copenhagen, 1973
7 Rygaard J & Poulsen C O Proceedings of the First International Workshop on Nude Mice. Gustav Fischer Verlag, Stuttgart, 1974
8 S endsen U G Thymus dependency of pe rlarteritis nodosa in DOCA and salt treated m ce Acta path. microbiol scand, 82A 30 34 1974
9. S endsen U G Studies elucidating the importance of thymus on the degree of increased blood pressure and vascular disease in renal hypertens. e m.ce Acta path. microbiol scand. 83A 568–572 1975
10 Svendsen U G The role of thymus for the dev lopment and prognosis of hypertension nd hypertens. vascular d sease in m.c fol lowing renal inf ction. Acta path m crobiol. scand 84A 234 243 1976
11 Svendsen U G E idence for an initial thy mu independent and a chronic, thymus dependent phase of DOCA and salt hypertension n mice. Acta path microbiol scand 84A 523–528, 1976.
12 S endsen U C Occurrence of amyloidosis secondary to the induction of experimental hypertension in mice Acta path. microbiol scand Sect A, 85 263–266 1977

Acta path. microbiol scand, Sect. A 85 548 554 1977

SPONTANEOUS HYPERTENSION AND HYPERTENSIVE VASCULAR DISEASE IN THE NZB STRAIN OF MICE

ULRIK GERNER SVENDSEN

The University Institute for Experimental Medicine Copenhagen Denmark

Svendsen, U G Spontaneous hypertension and hypertensive vascular disease in the NZB strain of mice Acta path microbiol scand Sect A, 85 548–554 1977

NZB mice spontaneously develop a high blood pressure and hypertensive vascular disease in the heart and the kidney Treatment with cyclophosphamide decreased the level of blood pressure congenital athymic nude NZB mice failed to develop a high blood pressure These findings suggest that thymus and the thymus-dependent immune reactions have pathogenic importance for the spontaneous hypertension in these mice

Key words Hypertension spontaneous hypertensive vascular disease NZB mice

Ulrik Gerner Svendsen, The University Institute for Experimental Medicine Nørre Allé 71 2100 Copenhagen Ø Denmark

Received 27.1 77 Accepted 27.1.77

The "auto-immune" New Zealand Black (NZB) strain of mice (for literature see 2 3 9) develop renal disease spontaneously commencing in some mice as early as 3 months of age with proteinuri and cylindruria Chronic renal failure is a common cause of death in adult NZB mice (8 10) Histologically the renal disease is characterized by increased amounts of PAS-positive material in the glomerular tufts, dilated and degenerated tubules with hyaline casts and a perivascular accumulation of lymphoid cells around the arcuate/interlobular arteries of the kidney (6) Similar renal lesions occur in a variety of clinical and experimental conditions, including hypertension in man (5 6) Hybridization studies have shown that the auto-immune disorder is inherited dominantly and is not sex linked although some modification of the disorder occurred in the F hybrids (9) Treatment with cyclophosphamide was found to suppress the development of the renal lesions in F_1 (NZB×NZW (white)) mice and greatly increased life-span of the animals (12)

In previous studies in mice (for literature see 18) it was observed that the perivascular cellular reaction of hypertensive vascular disease as well as the maintenance of elevated systemic arterial pressure in the late phase of various forms of experimental hypertension, was dependent upon the presence of the thymus and could be suppressed by cyclophosphamide suggesting that an "auto-immune" process was involved, at least in this late phase of the hypertensive disease

Because of the similarity between the histopathological changes in the kidneys of NZB mice and experimental hypertensive mice we investigated whether or not the NZB strain of mice developed hypertension spontaneously Since this proved to be the case it was

appropriate to investigate whether the elevated arterial pressure was a cause or an effect of the intrarenal vascular disease, and whether or not the thymus and thymus-derived lymphocytes had any significance for the pathogenesis of the renal disorder

The existence of a nude strain of NZB mice with congenital aplasia of the thymus would seem appropriate and was utilized in this study

MATERIAL AND METHODS

Animals. Inbred SPF NZB/C C57/B1/6J Balb/c/A, C3H/Tif and outbred NMRI mice Furthermore, nude athymic mice, carrying the mutant alleles (nu/nu) from all strains (all strains received the nu/nu alleles from the NMRI strain by back crossing for at least 5 generations (4)) (Gl. Bomholtgaard Ltd Ry Denmark) For literature on nude mice, see (11 13 14)

The investigation was performed in three parts

Part I The mean blood pressure and vascular disease of nude and haired mice of different strains The systemic arterial blood pressure was measured, as previously described (18) in 10 nude and 15 haired male mice from each strain at the age of 2 months After sacrifice, the relative heart-weight (heart-weight x 100/body-weight) was determined The heart, kidney and spleen were fixed, and histological investigations performed, as described previously including semi-quantitative estimation both of the round-cell infiltrations around the arteries in the heart and the interlobular/arcuate arteries of the kidney (15 16) Deposits of amyloid in the spleen were estimated as previously described (19)

Part II The mean blood pressure and vascular disease of haired male and female NZB mice of different ages was measured in 60 males (from 3 weeks to 10 months of age) and 20 females (2 and 6 months of age)

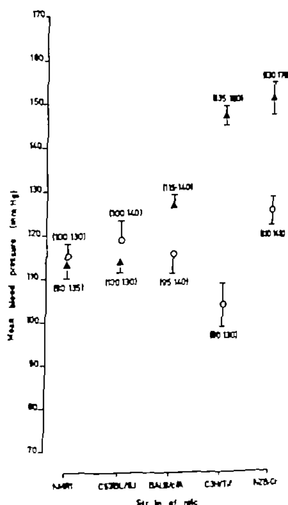
Part III The mean blood pressure and vascular disease in nude and nude thymus-transplanted and haired cyclophosphamide treated NZB mice 2 to 5 months of age 23 haired and 17 nude male mice.

2 nude male mice at the age of 6 weeks were transplanted subcutaneously with thymus grafts from newborn NZB mice as described previously (18) The blood pressure was measured at 5 months of age The other nude mice were investigated at their 2 or 5 months of age respectively The haired NZB mice were divided into two groups at the age of 2 months Each group received for 4 weeks weekly intraperitoneal injection of either cyclophosphamide (Endoxan Asta® Asta Werke AG) 14 mg per mouse dissolved in 0 9 per cent saline, or an equal volume of 0.9 per cent saline thereafter blood pressure determinations and histological investigations were performed. The mean number of circulating lymphocytes and the haematocrite was determined before sacrifice in both groups. All mean values are given with standard error of the mean (SEM) For comparison of experimental results, the students t-test was used. The five per cent level was used as indicator of significance of differences.

RESULTS

Part I (The mean blood pressure and vascular disease of 2 months-old nude and haired mice of different strains) Fig. 1 shows that *the mean blood pressure* obtained in nude and haired mice of the NMRI and the C57/B1/6J strain did not differ significantly ($p > 0.5$) while significant differences were observed between nude and haired mice of the Balb/c/A ($p < 0.025$) the C3H/Tif ($p < 0.001$) and the NZB/Cr ($p < 0.001$) strains. A comparison of the mean blood-pressures of the haired mice shows that the C57/B1/6J mice had a mean blood pressure similar to that of the NMRI mice ($p > 0.05$) while the mean blood-pressures of the other strains were significantly higher particularly in the C3H/Tif and NZB/Cr strains. The mean blood pressures of the nude mice were the same for NMRI C57/B1/6J Balb/c/A and C3H/Tif mice, while a significantly higher mean blood-pressure was found in the nude NZB/Cr mice ($p < 0.025$) Table 1 gives *the mean relative heart-weights.* No relationship was found between the mean relative heart weights and the mean blood-pressures of the haired mice C3H mice had a lower ($p < 0.05$) and NZB mice a higher ($p < 0.001$) mean relative heart-weight than haired NMRI mice, while their mean blood-pressures were similarly ($p > 0.1$) increased as compared with the mean value in the NMRI group of mice ($p < 0.001$ for both groups) The group of nude NZB mice was the only group of nude mice that had a significantly higher ($p < 0.005$) mean relative heart weight than the NMRI group of nude mice also their mean blood-pressure was higher (cf Fig 1)

Fig 1 shows the mean blood pressure ± SEM obtained in groups of 2 months old male mice of different strains ▲ the mean value in 15 haired mice ○ the mean value in 10 nude mice It is seen that both the C3H and the NZB group of haired mice had a high blood pressure Number in brackets the range of blood pressures.



Histological investigation The heart kidney and spleen No vascular disease no amyloidosis, except that 4 haired NZB mice (27 per cent) had 2+ round-cell infiltrations around their arteries in the heart, and fibrinoid degeneration of the media 6 mice had hypertrophia of the media

Part II (The mean blood pressure and vascular disease of haired male and female NZB mice of different ages) Fig 2 shows that *the mean blood pressure* in male mice increased during the first 2 months of life whereafter it reached a hypertensive level which was maintained up to 10 months of age Female mice had a significantly lower mean blood pressure both at 2 and 6 months of age ($p < 0.025$ and $p < 0.005$ respectively) Both male and female NZB mice had a mean blood pressure at 2 months of age which was significantly increased ($p < 0.001$) as compared to the value in the 2 months-old haired male NMRI mice (cf Fig 1) Table 2 shows that *the mean relative heart weight* was invariable with sex and age beyond 3 weeks of age. At 3 weeks of age male mice had a higher value than that of older mice ($p < 0.001$) The haematocrite ranged around 35–45 per cent,

TABLE 1 *The Mean Relative Heart Weight in Nude and Haired Male Mice of Different Strains*

Strain		Mean relative heart-weight ± SEM (per cent)	Range (per cent)	Difference (nude-haired)
NMRI	Haired	0.39 ± 0.05	0.33 – 0.52	p < 0.05
	Nude	0.43 ± 0.04	0.39 – 0.53	
Balb c A	Haired	0.42 ± 0.01	0.37 – 0.47	NS
	Nude	0.45 ± 0.03	0.39 – 0.50	
C3H Tif	Haired	0.36 ± 0.03	0.32 – 0.43	p < 0.005
	Nude	0.40 ± 0.03	0.33 – 0.43	
C57 Bl 6J	Haired	0.40 ± 0.02	0.37 – 0.43	NS
	Nude	0.41 ± 0.03	0.37 – 0.47	
NZB Cr	Haired	0.48 ± 0.02	0.46 – 0.52	NS
	Nude	0.50 ± 0.05	0.43 – 0.52	

Table 1 shows the mean relative heart weight ± SEM in 2 months-old nude and haired male mice of 5 different strains 15 haired and 10 nude mice were investigated in each group Note that the NZB strain of mice had a significantly higher relative heart weight than the other strains of mice

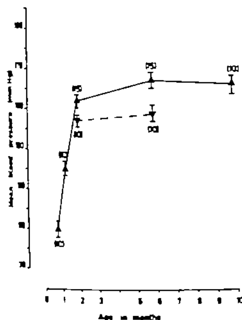


Fig 2 show the mean blood pressure ± SEM in groups of haired male (▲ —▲) and female (▼ ▼) NZB mice
Number in brackets number of mice.

except in 2 male mice, 6 months of age in which values below 29 per cent were found these 2 mice had pronounced vascular disease in their kidneys (both with 3+ cellular reactions) *Histological investigations The heart* No vascular disease was found in the mice beyond the age of *3 and 5 weeks* At *2 months* of age vascular disease as described above was found in males. No vascular disease was found in the female mice At *6 months* of age increased amounts of round-cell infiltrations around the arteries were found in 2 male mice (both 2+ reactions) Fibrinoid degeneration and hypertrophia of the media, and infarcts of the heart muscle were found in 7 male mice and in 3 female mice. At the age of *10 months* 7 mice had hypertrophia of the media and 7 had infarcts of the heart muscle. *The kidney* The degree of perivascular round-cell infiltration around the arcuate/interlobular arteries in the male mice are given in Table 3 Grade 2+ and 3+ were found at 10 months of age None of the female mice showed any increased numbers of perivascular round cells. Increased amounts of PAS-positive material in glomerular tufts were frequently observed beyond the age of 6 months. Dilated tubules with hyaline casts, wedge shaped infarcts and interstitiel fibrosis were observed in 2 male mice at 6 months of age and in one male mouse at the age of 10 months. *The spleen* Amyloidosis was found in one male mouse at the age of 6 months.

Part III (The mean blood pressure and vascular disease in nude nude thymus-transplanted and haired cyclophosphamide treated NZB mice 2 to 5 months of age Fig. 1 shows

TABLE 2. *The Mean Relative Heart Weight in Haired Male and Female NZB Mice of Different Age*

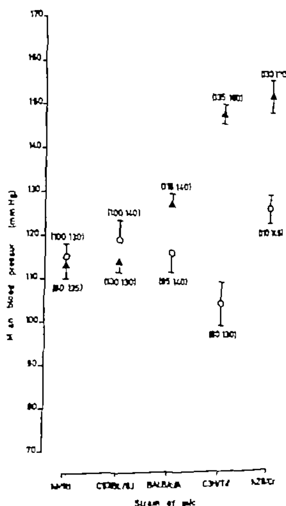
Age	Sex	Mean relative heart-weight ± SEM (per cent)	Range (per cent)
3 weeks	♂	0.58 ± 0.02	0.52 – 0.67
5 weeks	♂	0.46 ± 0.01	0.43 0.49
2 months	♂	0.48 ± 0.02	0.46 – 0.52
	♀	0.47 ± 0.01	0.4 – 0.53
6 months	♂	0.46 ± 0.01	0.38 – 0.55
	♀	0.49 ± 0.02	0.44 0.62
10 month	♂	0.46 ± 0.02	0.37 0.54

TABLE 3 *The Degree of Round-Cell Infiltration around Intrarenal Arteries in Male NZB Mice of Different Ages.*

Age	Degree of cellular reaction 1+	2+	3+
3 weeks	10	0	0
5 weeks	10	0	0
2 months	15	0	0
6 months	12	0	3
10 months	3	4	3

that nude NZB male mice at the age of 2 months had a significantly lower mean blood pressure than the haired male NZB mice of the same age At 5 months of age, no increase had occurred in the mean blood-pressure of male nude NZB mice in 5 mice in-

Fig 1 shows the mean blood pressure ± SEM obtained in groups of 2 months old male mice of different strains ▲ the mean value in 15 haired mice ○ the mean value in 10 nude mice It is seen that both the C3H and the NZB group of haired mice had a high blood pressure Number in brackets the range of blood pressures.



Histological investigation The heart kidney and spleen No vascular disease no amyloidosis, except that 4 haired NZB mice (27 per cent) had 2+ round-cell infiltrations around their arteries in the heart, and fibrinoid degeneration of the media 6 mice had hypertrophia of the media

Part II (The mean blood pressure and vascular disease of haired male and female NZB mice of different ages) Fig 2 shows that *the mean blood pressure* in male mice increased during the first 2 months of life whereafter it reached a hypertensive level which was maintained up to 10 months of age Female mice had a significantly lower mean blood pressure both at 2 and 6 months of age ($p < 0.025$ and $p < 0.005$ respectively) Both male and female NZB mice had a mean blood pressure at 2 months of age which was significantly increased ($p < 0.001$) as compared to the value in the 2 months old haired male NMRI mice (cf Fig 1) Table 2 shows that *the mean relative heart weight* was invariable with sex and age beyond 3 weeks of age At 3 weeks of age male mice had a higher value than that of older mice ($p < 0.001$) The haematocrite ranged around 35–45 per cent.

TABLE 1 *The Mean Relative Heart Weight in Nude and Haired Male Mice of Different Strains*

Strain		Mean relative heart weight ± SEM (per cent)	Range (per cent)	Difference (nude-haired)
NMRI	Haired	0 39 ± 0 05	0 33 – 0 52	$p < 0.05$
	Nude	0 43 ± 0 04	0 39 – 0 53	
Balb/c/A	Haired	0 42 ± 0.04	0 32 – 0 47	NS
	Nude	0 45 ± 0 03	0 39 – 0 50	
C3H/Tif	Haired	0 36 ± 0 03	0 32 – 0 43	$p < 0.005$
	Nude	0 40 ± 0 03	0 35 – 0 43	
C57/Bl/6J	Haired	0 40 ± 0 02	0 37 – 0 43	NS
	Nude	0 41 ± 0 03	0 37 – 0 47	
NZB/Cr	Haired	0 48 ± 0 02	0 46 – 0.57	NS
	Nude	0 50 ± 0 05	0 43 – 0.52	

Table 1 shows the mean relative heart weight ± SEM in 2 months-old nude and haired male mice of 5 different strains 15 haired and 10 nude mice were investigated in each group. Note that the NZB strain of mice had a significantly higher relative heart-weight than the other strains of mice

tion at the age of 5 months. Secondly treatment with cyclophosphamide, an ankylating drug known to be effective in chronic treatment against diseases in which T-cells are essentially implicated (1) resulted in a significant blood pressure decline in the haired (normal) NZB mice.

Thus, these observations might seem to agree with previous observations in other strains of mice with experimental hypertension. However a difference, which may be crucial, was apparent. While the absence of thymus or cyclophosphamide-treatment had no effect in experimental hypertension on the initial rise in blood pressure but only prevented the maintenance of a high pressure level in the chronic phase (18) thymus aplasia did prevent the initial phase of the spontaneous hypertension in NZB mice and cyclophosphamide treatment effectively reduced the arterial pressure early in life i.e. between the age of 2 and 3 months before the renal lesions including vascular disease had become established. The dose of cyclophosphamide was equal to that previously used in our laboratory (20) which also has been found effective in preventing perivascular lymphoid cell-infiltrations in NZB/NZW mice by others (12). This dose has no depressor-effect on the blood pressure in the normal C57/B1/6J strain of mice of about the same age (20). These findings provide the first evidence against the hypothesis that thymus-dependent immune reactions influence the level of systemic arterial pressure solely by constricting the intrarenal arteries focally and progressively due to the perivascular cellular immune reactions. They suggest rather that other thymus-dependent mechanisms might have pathogenic significance for the elevated arterial pressure, at least for the early development of spontaneous hypertension in the NZB mice. Further studies are highly desirable in order to test this suggestion, and if it is verified, to clarify the mechanism(s).

An unexplained result of the present study was the lack of a clear cut relationship between the mean systemic arterial pressure and the mean relative heart-weight. The relative heart-weight of haired and nude NZB mice did not differ from each other and were significantly higher than that of normo-tensive NMRI mice yet, the blood pressure of nude NZB mice, though higher than that of other nude mice, was still within normotensive values. On the other hand, the mean relative heart-weight of C3H mice was lower than that of the control NMRI mice, even though the mean blood-pressure in this group was elevated to a hypertensive level. Another difference between the haired NZB and C3H mice was the absence in C3H mice of vascular disease in the heart at the age of 2 months, despite an arterial pressure level almost as high as that recorded in the haired NZB mice. Further studies are clearly needed to explain these inconsistent observations in the C3H strain of mice.

Haemolytic anaemia has been observed in NZB mice, possibly a result of auto-immune reactions characteristic of this strain (9). The low haematocrite measured in two of the present untreated NZB mice might therefore have been due to such haemolytic anaemia, but this posibility was not further investigated.

The author is grateful to Director *C. W. Friis* Dr. med. vet. who very kindly donated many of the animals for this investigation, and to Miss *Lisbeth Olsen* for her valuable technical assistance. The Percorten® was kindly supplied by Ciba-Geigy Copenhagen. This work was supported by grants from the *Danish Medical Research Council*, *Ingeniør Søren Alfred Andersens Foundation* Frederikssund, and *Carl and Ellen Hertz' Foundation*.

REFERENCES

1 *Bach J F* The pharmacological and immunological basis for the use of immunosuppressive drugs. Drugs *11* 1–13 1976.
2 *Bielschowsky M Helyer B J & Howie J B.* Spontaneous haemolytic anaemia in mice of the NZB/B1 strain. Proc. Univ Otago Med. School. *37* 9–11 1959
3 *DeHeer D H & Edgington T S* Cellular events associated with the immunogenesis of anti-erythrocyte autoantibody responses of NZB mice. Transplant Rev *31* 116–155 1976.

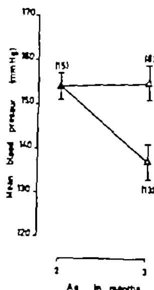


Fig 3 shows the effect in haired NZB mice on the mean blood pressure ± SEM of 4 weeks treatment with either 0 9 per cent saline (Δ) or with cyclophosphamide 1 4 mg/mouse/week injected once weekly intraperitoneally (▲) Number in brackets number of mice (▲) indicates the mean blood pressure of 2 months old untreated male mice.

vestigated after 5 months of age a mean value of 130 ± 7 mm Hg was found ($p > 0.05$) The haematocrite ranged from 40 to 50 in all nude mice the number of circulating lymphocytes ranged from 300 to 1600 per microlitre. One of the 2 nude male mice that were grafted with a *thymus graft* died The other one looked healthy at 5 months of age a microscopically visible thymus was present in the subcutis the blood pressure was 160 mm Hg Treatment of 13 haired NZB mice with *cyclophosphamide* for 4 weeks was followed by a significant fall in the mean systemic arterial pressure as compared to the mean value obtained in 8 saline injected controls ($p < 0.01$ cf Fig 3) One cyclophosphamide treated and one saline-injected mouse died during the treatment The mean number of circulating lymphocytes was 1725 ± 279 per microlitre in saline injected mice significantly higher than the value measured in the cyclophosphamide treated mice (1033 ± 94 per microlitre $p < 0.025$) *Histological investigation 1) nude NZB mice The heart kidney and spleen* No amyloidosis, no vascular disease except for a small increase in PAS-positive material in the glomerular tufts often observed at 5 months of age 2) *The one nude thymus-transplanted NZB mouse The heart and spleen* No vascular disease, no amyloidosis. *The kidney* a 3+ round cell infiltration around the intrarenal arteries and a small increase in PAS-positive material of the glomerular tufts were observed. 3) *Cyclophosphamide and saline injected haired mice The kidney* No vascular disease, no amyloidosis.

DISCUSSION

In previous studies, evidence was provided indicating a thymus-dependency for the maintenance of elevated systemic arterial pressure only in the chronic phase of experimental hypertension in which hypertensive vascular disease was present in varying degrees in the kidney (17 18 20) Various tests have failed so far to invalidate the suggestion that thymus-dependent intrarenal perivascular cellular immune reactions, at least partly are responsible for the maintenance of the arterial pressure in this phase of the disease by causing focal constrictions of the intrarenal arteries (17)

The present study has verified and more firmly established the suggestion from data of other investigators (5) that NZB mice develop hypertension spontaneously Also it has confirmed that the renal disease which is shown to be manifest in the present series not until the age of 6 months, has all the characteristics of hypertensive vascular disease including its secondary parenchymatous lesions, in accordance with the conclusion of other investigators (5 6 7)

Evidence of a pathogenic significance of the thymus and the thymus-derived lymphocytes (T-cells) for the development of the spontaneous hypertension and the vascular disease in the NZB mice was obtained from two observations Firstly all of the 15 athymic nude NZB mice failed to develop either hypertension or vascular disease but the only one thymus-transplanted nude mouse had both hypertension and vascular disease with a 3+ degree of perivascular round-cell infiltra

tion at the age of 5 months. Secondly treatment with cyclophosphamide, an ankylating drug known to be effective in chronic treatment against diseases in which T-cells are essentially implicated (1) resulted in a significant blood-pressure decline in the haired (normal) NZB mice

Thus, these observations might seem to agree with previous observations in other strains of mice with experimental hypertension. However a difference which may be crucial, was apparent. While the absence of thymus or cyclophosphamide treatment had no effect in experimental hypertension on the initial rise in blood pressure but only prevented the maintenance of a high pressure level in the chronic phase (18) thymus aplasia did prevent the initial phase of the spontaneous hypertension in NZB mice and cyclophosphamide treatment effectively reduced the arterial pressure early in life, i.e. between the age of 2 and 3 months before the renal lesions including vascular disease had become established. The dose of cyclophosphamide was equal to that previously used in our laboratory (20) which also has been found effective in preventing perivascular lymphoid cell-infiltrations in NZB/NZW mice by others (12) This dose has no depressor-effect on the blood pressure in the normal C57/B1/6J strain of mice of about the same age (20) These findings provide the first evidence against the hypothesis that thymus-dependent immune reactions influence the level of systemic arterial pressure solely by constricting the intrarenal arteries focally and progressively due to the perivascular cellular immune reactions. They suggest rather that other thymus-dependent mechanisms might have pathogenic significance for the elevated arterial pressure at least for the early development of spontaneous hypertension in the NZB mice. Further studies are highly desirable in order to test this suggestion and if it is verified, to clarify the mechanism(s)

An unexplained result of the present study was the lack of a clear cut relationship between the mean systemic arterial pressure and the mean relative heart-weight. The relative heart-weight of haired and nude NZB mice did not differ from each other and were significantly higher than that of normo-tensive NMRI mice yet, the blood pressure of nude NZB mice though higher than that of other nude mice, was still within normotensive values. On the other hand the mean relative heart weight of C3H mice was lower than that of the control NMRI mice, even though the mean blood pressure in this group was elevated to a hypertensive level. Another difference between the haired NZB and C3H mice was the absence in C3H mice of vascular disease in the heart at the age of 2 months, despite an arterial pressure level almost as high as that recorded in the haired NZB mice. Further studies are clearly needed to explain these inconsistent observations in the C3H strain of mice

Haemolytic anaemia has been observed in NZB mice, possibly a result of auto-immune reactions characteristic of this strain (9) The low haematocrite measured in two of the present untreated NZB mice might therefore have been due to such haemolytic anaemia, but this posibility was not further investigated.

The author is grateful to Director *C W Friis* Dr med vet who very kindly donated many of the animals for this investigation, and to Miss *Lisbeth Olsen* for her valuable technical assistance. The Percorten® was kindly supplied by Ciba-Geigy Copenhagen. This work was supported by grants from the *Danish Medical Research Council*, Ingeniør *Søren Alf & A Andersen Foundation* Frederikssund, and *Carl and Ellen Hertz Foundation*.

REFERENCES

1 *Beck J F* The pharmacological and immunological basis for the use of immunosuppressive drugs. Drugs *11* 1–13 1976

2 *Bielschowsky M Helyer B J & Howie J B.* Spontaneous haemolytic anaemia in mice of the NZB/Bl strain. Proc. Univ Otago Med. School. 37 9–11 1959

3 *DeHeer D H & Edgington T S* Cellular events associated with the immunogenesis of anti-erythrocyte autoantibody responses of NZB mice. Transplant. Rev *31* 116–135, 1976.

4 *Frus C H* Personal Communication.
5 *Hicks J D Giltinan P & Pye J* A new method of measuring blood pressure in mice. Lancet *II* 930–932 1965
6 *Hicks J D & Burnet F M* Renal lesions in the "auto-immune" mouse strains NZB and F1 NZB×NZW J Path. Bact *91* 467–477 *1966*
7 *Hicks J D* Vascular changes in the kidneys of NZB mice and F_1NZB×NZW hybrids J Path. Bact. *91* 479–486 1966
8 *Holmes M C & Burnet F M* The natural history of auto-immune disease in NZB mice Ann. Internat. Med *59* 265–276 1963
9 *Howie J B & Helyer B J* The immunology and pathology of NZB mice. Adv Immunol. *8* 215–266 1968.
10. *Mellors R C* Auto-immune disease in NZB/Bl mice. I Pathology and pathogenesis of a model system of spontaneous glomerulonephritis. J Exp Med *122* 25–40 1965
11 *Raff M C* θ-bearing lymphocytes in nude mice Nature *246* 350–351 1973
12 *Russel P J & Hicks J D* Cyclophosphamide treatment of renal disease in (NZB×NZW) F_1 Hybrid mice. Lancet *I* 440–446 1968
13 *Rygaard J* Thymys & Self Immunobiology of the mouse mutant nude. F.A.D.L. Copenhagen, 1973
14 *Rygaard J & Poulsen C O*.. Proceedings of the first international workshop on nude mice Gustav Fischer Verlag Stuttgart, 1974
15 *Svendsen U G* Thymus dependency of periarteritis nodosa in DOCA and salt treated mice. Acta path. microbiol scand. Sect. A, *82* 30–34 1974
16. *Svendsen U G* Studies elucidating the importance of thymus on the degree of increased blood pressure and vascular disease in renal hypertensive mice. Acta path. microbiol scand. Sect. A, *83* 568–572, 1975
17 *Svendsen U G* The role of thymus for the development and prognosis of hypertension and hypertensive vascular disease in mice following renal infarction. Acta path. microbiol. scand. Sect. A, *84* 235–246, 1976
18 *Svendsen U G* Evidence for an initial, thymus independent and a chronic, thymus dependent phase of DOCA and salt hypertension in mice. Acta path, microbiol scand. Sect. A, *84* 523–528 1976.
19 *Svendsen U G* Occurence of amyloidosis secondary to the induction of experimental hypertension in mice Acta path. microbiol. scand Sect A *85* 263–266 1977
20 *Svendsen U G* The importance of thymus in the pathogenesis of the chronic phase of hypertension in mice following partial infarction of the kidney Acta path microbiol scand. Sect. A *85* 539–547 1977

Acta path. microbiol. scand. Sect. A, 85: 555–557, 1977

BRIEF REPORTS

ESTIMATION OF THE PARENCHYMAL-CELL CONTENT OF THE PARATHYROID GLAND USING DENSITY-GRADIENT COLUMNS

Preliminary Report

Göran Åkerström, Lars Grimelius, Henry Johansson & Hans Lundqvist

Departments of Pathology and Surgery, University Hospital and G. Werner Institute, Uppsala, Sweden

Åkerström, G., Grimelius, L., Johansson, H. & Lundqvist, H. Estimation of the parenchymal-cell content of the parathyroid gland, using density-gradient columns. Acta path. microbiol. scand. Sect. A, 85: 555–557, 1977.

The parenchymal cell mass was measured by the density-gradient technique. The results of this technique were compared with those obtained by an ocular semiquantitative method as described by Gilmour and Martin. In most parathyroid glands good correlation was found between the two methods. In contrast to the method of Gilmour and Martin the density-gradient technique is easy and rapid and therefore seems to be a more convenient tool in intraoperative diagnosis.

Key words: Parathyroid gland; parenchymal cell content; density-gradient columns.

G. Åkerström, Department of Surgery, University Hospital, S-750 14 Uppsala, Sweden.

Received 29.iii.77 Accepted 29.iii.77

The histological evaluation of the parathyroid gland may entail problems. Sometimes it is difficult to differentiate normal from slightly hyperplastic glands. The difficulties in the pathological interpretation may have considerable practical consequences, as the surgeon is dependent on a reliable histopathological diagnosis during the operation for his decision concerning the extent of operation.

In the histological evaluation it is important to consider the total glandular weight and also the amount of parenchymal cell and fat cell tissue. The parenchymal and fat cell distribution in the gland is often irregular (Grimelius et al. 1977) and to some extent age-dependent (*Gilmour & Martin* 1937). A semiquantitative method for estimating the parenchymal cell content has been described by *Gilmour & Martin* (1937). This method is based on ocular estimation of the distribution of parenchymal and fat cell tissue. The subjectivity in the evaluation with this method may give miscalculations. The parenchymal cell distribution can also be estimated more objectively, however, by a method using a TV-image analysing system (*Grimelius et al.* 1977). Both these methods are time-consuming, which makes them less suitable for use during surgery. An objective method of estimating the amount of parenchymal cell tissue for intraoperative use would therefore be of great value.

When the parathyroid glands become more active, fat cells are usually replaced by parenchymal cells. As the specific densities of parenchymal and fat cells differ, the density of the whole parathyroid gland might give some indication as to the amount of parenchymal tissue.

A sensitive and simple method for determining density is the density-gradient column technique. Such a column contains liquids with different densities linearly layered from top to bottom (*Oste* 1965). An object that is dropped in such a column will fall until it reaches its own density. If the column is carefully calibrated, the specific density is easily and very accurately estimated. The density-gradient technique was therefore used for estimating the parenchymal cell content of parathyroid glands and the preliminary findings are reported here.

Material and methods

Density gradients were made with a special pump using mixtures of sucrose and water with a density range of 1 00–1 10 and alcohol and water with a density range of 0 95–1 00.

The density of the parathyroid parenchymal cells was calculated by measuring pieces of parathyroid adenomas containing no fat tissue The density of fat cells was calculated by measuring pieces of fat tissue surrounding the parathyroid glands These values of parenchymal cell density (M = 1 065) and fat cell density (M = 0.945) were used to make a diagram relating density of parathyroid gland to parenchymal cell content (Fig 1)

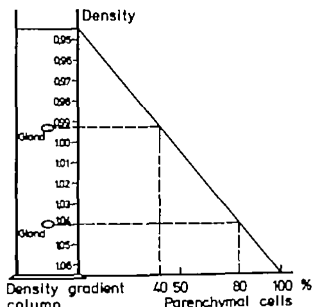


Fig 1 Diagram relating density of parathyroid gland to parenchymal cell content.

Fifteen parathyroid glands were removed from autopsy cases. The glands were carefully dissected free from extra-capsular fat tissue weighed and measured in the density columns. The glands floated at different density levels and the percentage of parenchymal cells was registrated in the diagram in Fig 1 When measurements in the column were repeated, each gland always floated at the same niveau

The results of the density calculations of the parenchymal cell content were compared with those made by conventional ocular estimation (*Gilmour & Martin* 1937) using 10–12 sections at different levels of each gland.

Results

The amount of parenchymal tissue in each gland, calculated from measurements of density is given in Table 1 In most glands these results showed good correlation with the ocular estimation of parenchymal cell content.

TABLE 1 *Parenchymal Cell Content Estimated by Two Techniques*

Glandular weight mg	Glandular density	Density calculation of % parenchymal cell content	Ocular estimation of % parenchymal tissue
29 9	0.965	17	10
12.0	1.002	47	40
18.1	1 008	43	30
37 7	1 017	60	45
28.7	1 025	66	55
18 0	1 018	61	50
21.5	1 019	62	40
21.3	1 036	76	45
149 8	1 054	91	90
19 4	0 995	42	30
19.8	1 012	55	40
42 6	0.995	42	20
19 7	0.965	17	15
11.3	1.025	64	45
34 6	0 995	42	10

Discussion and conclusions

An initial change in parathyroid hyperplasia is an increase of the parenchymal cell content in relation to the fat cells. Therefore the density-gradient column technique could be a useful tool in parathyroid diagnosis, as glands with different parenchymal cell contents will have different densities.

The liquids used in this study are not ideal, as sucrose and alcohol have osmotic effects that disturb density measurements. The values obtained in our measurements cannot therefore be claimed to be absolutely correct. Development of the density gradient technique is necessary It seems possible to improve the density-gradient system and equilibrate this system by using the TV-image analysing technique, which gives objective and reliable information about the parenchymal cell content (*Grimelius et al.* 1977) The aim of this paper however is only to illustrate the possibility of using density measurements in parathyroid diagnosis. As the density-gradient column technique is rapid and easy it could very well be used as an intraoperative procedure to obtain objective information about the parenchymal cell content of an extirpated parathyroid gland.

Supported by the *Swedish Medical Research Council*, project B77 17 04787-02.

References Gilmour J R & Martin W Y.: Pathol Bacteriol. 44 431–468, 1937 — Grimelius L, Johansson, H., Lundqvist H & Åkerström G.: To be published. — Oster G Chemical Reviews 63 257–268, 1963

Acta path. microbiol. scand Sect. A, 85 557–558, 1977

ON THE SPECIFICITY OF MEDIUM-SIZED ISOMARKER CHROMOSOMES IN NON-BURKITT LYMPHOMAS

J Mark

Cytogenetic laboratory Department of Pathology Central Hospital, Fack, Skövde, Sweden

Mark, J On the specificity of medium-sized isomarker chromosomes in non-Burkitt lymphomas. Acta path microbiol scand Sect A, 85 557–558, 1977

The chromosomal observations by G-banding in an intestinal, histiocytic lymphoma are reported. The findings, as those in a series of about 10 other lymphomas, indicate a varying origin of medium-sized isomarkers the results oppose the view that there exists a specific marker of this type in non-Burkitt lymphomas.

Key words Histiocytic lymphoma chromosomes G-banding

J Mark, Cytogenetic laboratory Department of Pathology Central Hospital, Fack, 541 01 Skövde Sweden

Received 26.iv 77 Accepted 26.iv 77

Cytogenetical studies by banding methods of non-Burkitt lymphomas (non-Bl) were first performed by Fleischman et al (1975) They reported one or several similar medium-sized markers with identical arms (but unknown derivation) in 3 different non-Bl. Later on, the authors added a sixth case (*Fleischman et al* 1976) These suggestive observations have not been confirmed by other investigators, and in a recent survey of banding patterns in human lymphomas it was proposed that the above-mentioned marker type was probably a product of different structural rearrangements, involving different chromosomes (*Mark* 1977 a) The cytogenetical findings in the intestinal lymphoma to be described below are in line with this proposal.

Material and Methods

The patient was a 56-year-old female with histiocytic lymphoma involving the small intestine and some of its tributary lymph nodes. The material for the chromosomal studies was taken from the intestinal tumour The chromosomes were studied in direct preparations. The method was described earlier (*Mark* 1975) as was the technique used for G-banding and the nomenclature.

Results

The chromosomes were counted in 55 cells. The numbers ranged from 72 to 98 and there was a flat mode at 89 ± 2. Six cells with the modal numbers could be completely analysed. The karyotypes were closely related, and two cells had the

Material and methods

Density-gradients were made with a special pump using mixtures of sucrose and water with a density range of 1 00–1 10 and alcohol and water with a density range of 0 95–1 00

The density of the parathyroid parenchymal cells was calculated by measuring pieces of parathyroid adenomas containing no fat tissue. The density of fat cells was calculated by measuring pieces of fat tissue surrounding the parathyroid glands These values of parenchymal cell density (M = 1 065) and fat cell density (M = 0.945) were used to make a diagram relating density of parathyroid gland to parenchymal cell content (Fig 1)

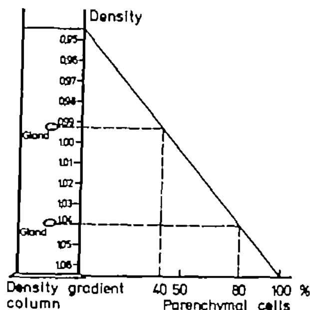


Fig 1 Diagram relating density of parathyroid gland to parenchymal cell content

Fifteen parathyroid glands were removed from autopsy cases. The glands were carefully dissected free from extra-capsular fat tissue weighed and measured in the density columns. The glands float ed at different density levels and the percentage of parenchymal cells was registrated in the diagram in Fig 1 When measurements in the column were repeated each gland always floated at the same niveau

The results of the density calculations of the parenchymal cell content were compared with those made by conventional ocular estimation (*Gilmour & Martin* 1937) using 10–12 sections at different levels of each gland

Results

The amount of parenchymal tissue in each gland, calculated from measurements of density is given in Table 1 In most glands these results showed good correlation with the ocular estimation of parenchymal cell content.

TABLE 1 *Parenchymal Cell Content Estimated by Two Techniques*

Glandular weight mg	Glandular density	Density calculation of % parenchymal cell content	Ocular estimation of % parenchymal tissue
29 9	0 965	17	10
12 0	1 002	47	40
18.1	1.008	43	50
37 7	1 017	60	45
28.7	1.025	66	55
18 0	1 018	61	50
21.5	1 019	62	40
21.3	1 036	76	45
149 8	1 054	91	90
19 4	0 995	42	30
19.8	1 012	55	40
42 6	0 995	42	20
19 7	0.965	17	15
11.3	1 023	64	45
34 6	0.995	42	10

Discussion and conclusions

An initial change in parathyroid hyperplasia is an increase of the parenchymal cell content in relation to the fat cells. Therefore the density-gradient column technique could be a useful tool in parathyroid diagnosis, as glands with different parenchymal cell contents will have different densities.

The liquids used in this study are not ideal, as sucrose and alcohol have osmotic effects that disturb density measurements. The values obtained in our measurements cannot therefore be claimed to be absolutely correct. Development of the density-gradient technique is necessary It seems possible to improve the density-gradient system and equilibrate this system by using the TV-image analysing technique, which gives objective and reliable information about the parenchymal cell content (*Grimelius et al.* 1977) The aim of this paper however is only to illustrate the possibility of using density measurements in parathyroid diagnosis. As the density-gradient column technique is rapid and easy it could very well be used as an intraoperative procedure to obtain objective information about the parenchymal cell content of an extirpated parathyroid gland.

Acta path. microbiol. scand. Sect. A, 85: 559–560, 1977

AGE CHANGES IN THE QUANTITY OF HEMATOPOIETIC TISSUE

U. Schrøder and L. Tougaard

Department of Pathology, Hjørring Sygehus, Hjørring and
Department of Clinical Physiology, Aalborg Sygehus, Denmark

Schrøder, U. and Tougaard, L. Age changes in the quantity of hematopoietic tissue. Acta path. microbiol. scand. Sect. A, 85: 559–560, 1977.

The ratio between hematopoietic tissue and lipoid tissue was determined by histologic planimetry in bone marrow biopsies from 52 persons without bone or blood disorders, aged from 20 to 85 years. The ratio decreased significantly with increasing age, equally in the two sexes. The ratio correlated significantly to the hemoglobin concentration in the blood.

Key words: Hematopoietic tissue; age changes.

U. Schrøder, Nørregade 120, 1, DK-6700 Esbjerg, Denmark.

Received 30. 77   Accepted 15. 77

The activity of the hematopoietic bone marrow is often estimated from the ratio between hematopoietic tissue and lipoid tissue (H/L). It is a general assumption that this ratio decreases with increasing age (1, 2, 3). This assumption has not been confirmed by a systematic study with determination of this ratio from living individuals of varying age. Therefore we have investigated the H/L ratio in bone marrow from normal persons covering a wide span of ages.

Material and Methods

a. *Bone marrow.* Small bone biopsies from the anterior iliac spine were obtained under local anesthesia (4) from 110 patients in the department of internal medicine, Hjørring Sygehus. No patients suffered from malignant neoplasms, bone or blood disorders, or other diseases affecting the hematopoietic tissue. The hemoglobin concentration ranged from 10.8 to 6.9 mmol/liter.

It was necessary to reject 58 biopsies since the marrow was washed out during the preparations. The material consisted hereafter of bone specimens from 52 persons (25 males and 27 females) aged 20 to 86 years (mean 52 years).

b. *Histologic planimetry.* The size of the biopsies used for the determinations ranged from 5 to 20 mm after fixation in formalin. All biopsies were decalcified in RDO®. The duration of the decalcification was from 4 to 24 hours, depending on the amount of corticalis in each biopsy. 3 longitudinal slices were cut at intervals of 50 μm, with corticalis represented in one of the ends, stained with hematoxylin and eosin, microphotographed on colour reversal films and magnified in dark room (total magnification = × 1250). The areas of hematopoietic tissue and lipoid tissue were determined by planimetry.

Results

Fig. 1 shows a highly significant inverse correlation between H/L ratio and age (= −0.49, $p < 0.001$). Mean H/L ratio decreased from 3.35 in the third decennium to 2.11 in the ninth decennium. No difference was found between the lines of regression for females and males. The correlation coefficient between H/L ratio and blood hemoglobin concentration was significant (= 0.33, $p < 0.02$).

Discussion

The biopsies used for the determinations were not only small but also decalcified.

This probably accounts for the high proportion of rejected bone biopsies. However, the unsatisfactory bone specimens turned out to be randomly



Fig 1 a. Partial karyotype of a modal cell showing the 13 markers (= Roman numerals) and the normal chromosomes from which they are derived × 2600

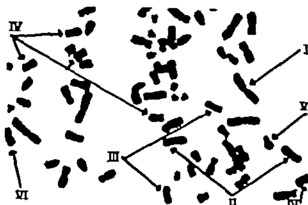


Fig 1 b Part of G-banded modal cell the arrows point at the different marker types (Roman numerals) × 1000

same karyotype viz. 89,XX +1 +2 −3 +4 +5 +5 +7 +7 +7 +7 +8 +9 +10 +10 +11 12 +13 +13 +13 +14 +14 +14 +15 +15 +16 +18 +19 +19 +19 +20 +21 +22 +22 +22 +13 markers (mar) The other modal cells analyzed had the same marker set (as also 5 additional only partially analyzed cells) but deviated by gain and/or loss of 1–2 of one or several of the chromosome types Nos. 3 8 10 14 19 and 22 The marker set included 6 different types (Fig 1) 1 mar I = i(1q) 2 mar II = del(3)(p15p23) 3 mar III = i(mar IIp) 5 mar IV = i[del(10)(q24)] 1 mar V = del(12)(p12) 1 mar VI = i(17q)

Discussion

The modal cells of the present lymphoma contained 13 markers, and 10 of these were isochromosomes. As many as 9 of the isomarkers were medium-sized. The latter group however included 3 types (with dissimilar banding pattern) which were derived from different chromosomes, namely Nos 3 10 and 17 These 3 types of isochromosomes showed banding patterns quite different from that of the only other medium-sized isomarker [derived from a deleted No 13 i(13q-)] found in a series of 10 non Bl (*Mark* 1975 1977 b and unpublished observations) Furthermore none of the 4 types of medium-sized isochromosomes had a banding pattern identical to that of any of the corresponding isomarkers found in 6 cases by *Fleischmann et al.* (1971 1976) Because of these conclusions and also the almost complete lack of similar isomarkers in other series reported in the literature (references in *Mark* 1977 a, and in *Fleischman & Prigogina* 1977) it seems difficult to believe that there actually exists a particular medium-sized isomarker common to at least a subgroup of non-Bl and with significance for their karyotypic evolution (*Fleischmann et al.* 1971 1976)

The present work was supported by grants from the *Swedish Cancer Society*

References 1 *Fleischman E W & Prigogina E L* Humangenetik 35 269–279 1977 —2 *Fleischmann T Håkansson C H & Levan A* Hereditas 69 311–314 1971 —3 *Fleischmann T Håkansson C H & Levan A* Hereditas 83 47 56 1976 —4 *Mark J* Hereditas 81 289 292, 1975 —5 *Mark J* In Advances in Cancer Research" (eds. *Klein G & Weinhouse S*) 74 pp 165–222 Academic Press, New York, 1977 a.—6 *Mark J* Humangenetik 1977 b (in press)

Acta path. microbiol. scand. Sect. A, 85 561–571 1977

CELL TYPES IN MEDULLARY THYROID CARCINOMA

TRINE NORMANN and JAN VINCENT JOHANNESSEN

Department of Pathology The Norwegian Radium Hospital and Norsk Hydro Institute of Cancer Research, Montebello, Oslo, Norway

Normann, T & Johannessen, J V Cell types in medullary thyroid carcinoma. Acta path. microbiol. scand. Sect. A, 85 561–571 1977

Eleven medullary thyroid carcinomas covering a wide variety of histological patterns and cell forms were studied by light and electron microscopy Two tumours without demonstrable amyloid were also included Different histological cell forms and growth patterns were not paralleled by principal differences at the ultrastructural level All tumours were composed of light and dark cells of principally the same type the dark cell variant being interpreted as a degenerated form of the light A finding not previously reported was the presence of a small number of tumour cells exhibiting microvilli and occasionally socalled intracytoplasmic lumina. *Intracellular* amyloid fibrils were not observed in tumour cells, nor in any other cell type In order to identify the ultrastructure of argyrophil and argentaffin cells, ultrathin sections were cut alternating with semithin sections which were "stained" according to *Bodian* or *Fontana-Masson* *Argyrophilia* was demonstrated in primary and metastatic tumour tissue from all cases. Both the light and dark tumour cell variants were "stained" although the staining intensity varied from one cell to another The silver precipitate was finely granular and from corresponding ultrathin sections it was evident that the "staining" intensity depended on the cell' number of secretory granules *Argentaffin* positive cells were also encountered in most primary tumours and in some metastases. The positive granules were larger than the argyrophil ones and found in cells with an abundance of phagolysosomes and residual bodies The argentaffin cells seemed to represent both degenerated tumour cells and macrophages Our findings do not support *Ljungberg* (18) hypothesis that the cells of MCT originate from two different cell populations.

Key words Argentaffin, argyrophil cell types medullary thyroid carcinoma ultrastructure.

Trine Normann, Department of Pathology Ullevål Hospital, Oslo 1 Norway

Received 20 77 Accepted 27 77

Since medullary thyroid carcinoma (MCT) was defined as a separate morphological and clinical entity in 1959 (12) a large number of publications have dealt with its histopathology and ultrastructure The tumour has been shown to develop from the calcitonin-producing parafollicular cells which originate in the neutral crest and accompany the ultimobranchial body into the thyroid gland during embryonic life (16, 22 24) On the basis of cytochemical characteristics, the C-cells have been included in the APUD-cell system and are like many cells of this system, argyrophilic (25)

In 1970 *Ljungberg* (18) demonstrated an additional cell type in MCT which was argentaffin, chromaffin, and showed an ortho-

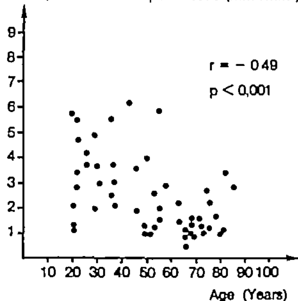


Fig 1 The proportion between hematopoietic and lipoid tissue (mm²/mm²) in the bone marrow of 52 normal persons compared to age

distributed in relation to sex and age. Therefore the results were not biased by the rejection of bone specimens.

It has earlier been found (5 6 7 8) that marrow from the iliac crest is representative of the entire hematopoietic tissue. Therefore the results indicate that the "hematopoietic organ" diminishes with increasing age. This accords with a study on autopsy material previously published (1)

The significant correlation between the hemoglobin concentration in blood and the H/L ratio indicates that this ratio is an index of the hematopoietic activity

References 1 *Hartsock R J Smith E. B., Petty C S* Am. J Clin. Pathol. *43* 326–331 1965 — 2 *Custer R. P* J Lab. Clin. Med. *17* 951–959 1932 — 3 *Custer R P., Florence E., Ahlfeldt E.* J Lab. Clin. Med. *17* 960–962, 1932 — 4 *Tengaard L.* Scan. J Clin. Lab. Invest. *32* 351–355, 1973 — 5 *Rubinstein M A.* JAMA. *137* 1281 1285 1948. — 6 *McFarland W., Dameshek W* JAMA. *166* 1464–1466 1958. — 7 *Allyn R. L., Prendergast R. A* Med. Clin. North Am. *45* 553 –561 1961 — 8 *Brody J J Finch S C* Am. J Med Sci *238* 140–145 1959

Acta path. microbiol. scand. Sect. A, 85 561–571 1977

CELL TYPES IN MEDULLARY THYROID CARCINOMA

Trine Normann and Jan Vincent Johannessen

Department of Pathology The Norwegian Radium Hospital
and Norsk Hydro' Institute of Cancer Research, Montebello Oslo, Norway

Normann, T & Johannessen, J V Cell types in medullary thyroid carcinoma. Acta path. microbiol. scand. Sect. A, 85 561 571 1977

Eleven medullary thyroid carcinomas covering wide variety of histological patterns and cell forms were studied by light and electron microscopy Two tumours without demonstrable amyloid were also included Different histological cell forms and growth patterns were not paralleled by principal differences at the ultrastructural level. All tumours were composed of light and dark cells of principally the same type the dark cell variant being interpreted as a degenerated form of the light. A finding not previously reported was the presence of a small number of tumour cells exhibiting microvilli and occasionally socalled intracytoplasmic lumina. Intracellular amyloid fibrils were not observed in tumour cells, nor in any other cell type In order to identify the ultrastructure of argyrophil and argentaffin cells, ultrathin sections were cut alternating with semithin sections which were "stained" according to Bodian or Fontana-Masson. *Argyrophilia* was demonstrated in primary and metastatic tumour tissue from all cases. Both the light and dark tumour cell variants were "stained" although the staining intensity varied from one cell to another The silver precipitate was finely granular and from corresponding ultrathin sections it was evident that the "staining" intensity depended on the cells' number of secretory granules. *Argentaffin* positive cells were also encountered in most primary tumours and in some metastases. The positive granules were larger than the argyrophil ones and found in cells with an abundance of phagolysosomes and residual bodies The argentaffin cells seemed to represent both degenerated tumour cells and macrophages Our findings do not support *Ljungberg'* (18) hypothesis that the cells of MCT originate from two different cell populations

Key words Argentaffin, argyrophil cell types medullary thyroid carcinoma ultrastructure.

Trine Normann, Department of Pathology Ullevål Hospital, Oslo 1 Norway

Received 20 77 Accepted 27 77

Since medullary thyroid carcinoma (MCT) was defined as a separate morphological and clinical entity in 1959 (12) a large number of publications have dealt with its histopathology and ultrastructure. The tumour has been shown to develop from the calcitonin-producing parafollicular cells which originate in the neural crest and accompany the ultimobranchial body into the thyroid gland during embryonic life (16 22, 24) On the basis of cytochemical characteristics, the C-cells have been included in the APUD-cell system and are, like many cells of this system, argyrophilic (23)

In 1970, *Ljungberg* (18) demonstrated an additional cell type in MCT which was argentaffin, chromaffin, and showed an ortho-

chromatic reaction when stained with certain cationic dyes Though few in number and unevenly distributed they were found in primary as well as metastatic tumours, and later also in normal thyroid and parathyroid tissue (19) On the basis of these findings *Ljungberg* proposed that the cells of MCT originate from two different cell populations. The argentaffin cell was thought to be responsible for the reported monoaminergic function (7 31) and the argyrophil C-cell for the production of calcitonin (CT) The hypothesis of *Ljungberg* has been received with great interest but the two cell types were never ultrastructurally defined. One purpose of the present investigation was to do so The other was to see whether or not the spectrum of growth patterns and cell forms, seen histologically were paralelled by principal ultrastructural differences.

MATERIAL AND METHODS

Surgically removed primary tumours and/or metastases from 11 human cases of MCT were studied The diagnosis was in 9 cases based on histological criteria including a positive amyloid reaction These patients also had hypercalcitoninemia. In 2 cases otherwise histologically consistent with MCT but lacking amyloid high levels of calcitonin were found in both serum and tumour tissue. Calcitonin in serum and tissue was measured by radioimmunoassay as described previously (8) Serum values more than 0 05 ng/ml were considered pathological

Light Microscopy

Histological investigations were performed on paraffin-embedded tumour tissue fixed in 4 per cent buffered formaldehyde and stained with HE and PAS For the demonstration of amyloid Congo red and thioflavin T were used

Combined light and electron microscopy was performed on small cubes of tumour tissue fixed in 2 per cent phosphate-buffered glutaraldehyde immediately after surgical removal and postfixed in osmium tetroxide for 2 hours each dehydrated in graded ethanol and embedded in Epon 812 or Epon/Araldite using propylene oxide as an intermedium *Semithin* sections were cut with glass knives, mounted on an LKB Pyramitome or Ultratome III and stained with toluidine blue

Fontana Masson's method was used for the demonstration of argentaffinity (23) and *Bodian's* silver impregnation for the demonstration of argyrophilia (26) Prior to the silver impregnation Epon was removed from the sections with 1 per cent alcoholic sodium hydroxide for 3-5 min

In order to compare light and electron microscopic findings, consecutive semithin and ultrathin sections were cut from the same blocks The ultrathin sections were made with an LKB Ultratome III equipped with glass knives, mounted on naked copper grids, stained with uranyl acetate and lead citrate and examined in a Philips EM 201 electron microscope.

RESULTS

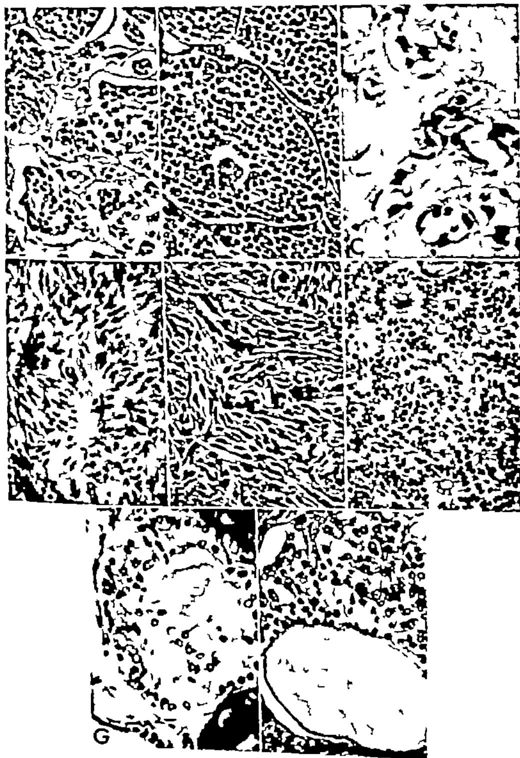
Growth Patterns and Cell Forms

The *formalin fixed paraffin-embedded* tissues showed the following histological growth patterns and cell forms Polyhedral, plasmocytoid or small uncharacteristic tumour cells arranged in micronodules or in small clusters surrounded by amyloid (Fig 1 A-C) spindle shaped cells in streaming patterns with or without palisaded nuclei (Fig 1 D and E) and columnar cells arranged in rosettes (Fig 1 F) Pseudopapillary and pseudofollicular arrangements were in part due to tumour cells surrounding amyloid (Fig 1 C) and in part to tumour infiltration of pre-existing follicles (Fig 1 H) The pseudopapillary arrangement seemed to be due to fixation

---

Fig 1 A-H Light micrographs from 8 different tumours, showing variation in growth patterns and cell types of MCT Hematoxylin and eosin × 100.

- A Sheats of polyhedral tumour cells, sometimes immitating papillary growth.
- B Nodules of plasmocytoid tumour cells surrounded by slender connective tissue septa
- C Small clusters of tumour cells within amyloid stroma
- D Spindle-formed tumour cells with palisading of the nuclei
- E Crossing bundles of spindle-formed tumour cells
- F Columnar tumour cells arranged in rosettes, sometimes with a PAS positive substance in the centre. (From lymph node metastasis)
- G Polyhedral tumour cells in pseudofollicular arrangement around central amyloid
- H Tumour cells infiltrating a pre-existing thyroid follicle Colloid is seen in the lower part of the picture


A
B
C
G

chromatic reaction when stained with certain cationic dyes Though few in number and unevenly distributed they were found in primary as well as metastatic tumours and later also in normal thyroid and parathyroid tissue (19) On the basis of these findings, *Ljungberg* proposed that the cells of MCT originate from two different cell populations. The argentaffin cell was thought to be responsible for the reported monoaminergic function (7 31) and the argyrophil C-cell for the production of calcitonin (CT) The hypothesis of *Ljungberg* has been received with great interest but the two cell types were never ultrastructurally defined. One purpose of the present investigation was to do so. The other was to see whether or not the spectrum of growth patterns and cell forms seen histologically were paralelled by principal ultrastructural differences

MATERIAL AND METHODS

Surgically removed primary tumours and/or metastases from 11 human cases of MCT were studied The diagnosis was in 9 cases based on histological criteria including a positive amyloid reaction These patients also had hypercalcitoninemia. In 2 cases, otherwise histologically consistent with MCT but lacking amyloid, high levels of calcitonin were found in both serum and tumour tissue Calcitonin in serum and tissue was measured by radioimmunoassay as described previously (8) Serum values more than 0 05 ng/ml were considered pathological

Light Microscopy

Histological investigations were performed on paraffin-embedded tumour tissue fixed in 4 per cent buffered formaldehyde and stained with HE and PAS For the demonstration of amyloid Congo red and thioflavin T were used

Combined light and electron microscopy was performed on small cubes of tumour tissue fixed in 2 per cent phosphate-buffered glutaraldehyde immediately after surgical removal and postfixed in osmium tetroxide for hours each dehydrated in graded ethanol and embedded in Epon 812 or Epon, Araldite using propylene oxide as an intermedium *Semithin* sections were cut with glass knives, mounted on an LKB Pyramitome or Ultratome III and stained with toluidine blue

Fontana Masson's method was used for the demonstration of argentaffinity (23) and *Bodian's* silver impregnation for the demonstration of argyrophilia (26) Prior to the silver impregnation Epon was removed from the sections with 1 per cent alcoholic sodium hydroxide for 3–5 min

In order to compare light and electron microscopic findings, consecutive semithin and ultrathin sections were cut from the same blocks. The ultrathin sections were made with an LKB Ultratome III equipped with glass knives, mounted on naked copper grids, stained with uranyl acetate and lead citrate and examined in a Philips EM 201 electron microscope

RESULTS

Growth Patterns and Cell Forms

The *formalin fixed paraffin-embedded* tissues showed the following histological growth patterns and cell forms Polyhedral, plasmocytoid or small uncharacteristic tumour cells arranged in micronodules or in small clusters surrounded by amyloid (Fig 1 A–C) spindle shaped cells in streaming patterns with or without palisaded nuclei (Fig 1 D and E) and columnar cells arranged in rosettes (Fig 1 F) Pseudopapillary and pseudofollicular arrangements were in part due to tumour cells surrounding amyloid (Fig 1 G) and in part to tumour infiltration of pre-existing follicles (Fig. 1 H) The pseudopapillary arrangement seemed to be due to fixation

---

Fig 1 A–H Light micrographs from 8 different tumours, showing variation in growth patterns and cell types of MCT Hematoxylin and eosin × 100.

A Sheets of polyhedral tumour cells, sometimes immitating papillary growth
B Nodules of plasmocytoid tumour cells surrounded by slender connective tissue septa.
C Small clusters of tumour cells within amyloid stroma
D Spindle-formed tumour cells with palisading of the nuclei.
E Crossing bundles of spindle-formed tumour cells
F Columnar tumour cells arranged in rosettes, sometimes with a PAS positive substance in the centre (From lymph node metastasis)
G Polyhedral tumour cells in pseudofollicular arrangement around central amyloid
H Tumour cell infiltrating a pre-existing thyroid follicle Colloid is seen in the lower part of the picture



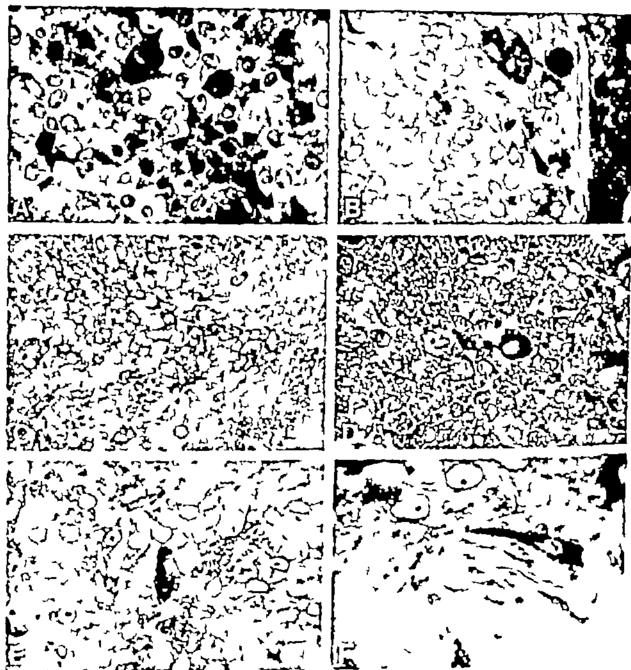


Fig. 2 A) Semithin section from MCT showing light and dark tumour cells. Toluidine blue stain. Magnification of diapositive × 400. B) Semithin section from MCT revealing predominantly light tumour cells and large cells containing yellowish coarse granules. Toluidine blue stain. Magnification of diapositive × 400. C) Semithin section from MCT showing a large number of tumour cells with positive argyrophil reaction. The number of small silver granules varies considerably from one cell to another. Bodian stain. Magnification of diapositive × 250. D) Semithin section from MCT showing one rather large cell with coarse reddish brown granules. Smaller black granules are found within the same cell and in a few of the surrounding tumour cells. Bodian stain. Magnification of diapositive × 400. E) Semithin section from MCT showing argentaffin cell containing coarse black granules. A small number of similar granules are seen in some of the surrounding tumour cells. Fontana-Masson stain. Magnification of diapositive × 400. F) Semithin section from MCT showing slender argentaffin positive cell containing numerous black coarse granules. The cell is situated peripherally in a tumour cell lobule. Fontana-Masson stain. Magnification of diapositive × 650

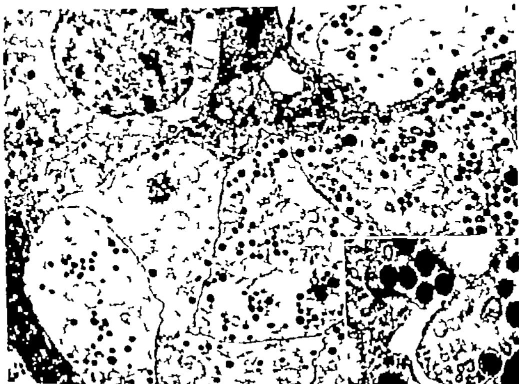


Fig 3 Electron micrograph showing dark tumour cells between light ones Inset Detail from light cell, showing secretory granules. Uranyl acetate and lead citrate stain. Magnification × 6,160 Inset × 44,000

artifacts. Several tumours showed a mixture of patterns and cell forms, and one contained numerous multinucleated tumour cells. Histological atypia was usually modest.

In *semithin* toluidine-blue stained sections from all tumours light and dark tumour cells were seen (Fig 2 A) In one tumour composed of alternating areas of rosettes and micronodules, the light cells were almost exclusively located in the former and the dark cells in the latter This separation was also evident in the lymph node metastases. The calcitonin concentration of tissue dominated by light cells was 540 ng as compared with 40 ng/g wet weight of tissue showing predominantly dark cells. In all the other tumours the light and dark cells were randomly distributed. Many dark cells showed cytoplasmic branchings embracing neighbouring light cells (Fig. 2 A) Between the tumour cells and in the stroma, rather large cells containing coarse yellowish granules were sometimes seen (Fig 2 B)

Semithin sections from all tumours revealed *argyrophil* positive cells. These were found among both light and dark tumour cells, but the staining intensity varied from one cell to another owing to the cell's content of small black cytoplasmic granules (Fig 2 C) The number of granules corresponded to the number of secretory granules seen in the same cells by electron microscopy

Sections treated according to *Fontana-Masson's* method revealed in the majority of tumours and in some lymph node metastases, scattered *argentaffin* cells (Fig. 2 E and F) The positive cells contained coarse black or dark brown granules considerably larger than the argyrophil ones Some argentaffin cells had long cytoplasmic processes (Fig. 2 F) The argentaffin positive cells corresponded to the cells showing yellow granules in the



Fig 4 A) Electron micrograph of dark cells from a medullary carcinoma where one area was dominated by this cell type The cells have dense cytoplasm irregular interdigitating plasma membranes and dilated endoplasmic reticulum. Som contain secretory granules (upper middle part) Stain as Fig. 3 × 7 000 B) Detail from dark cell showing dense core secretory granules similar to those seen in the light cells. Numerous ribosomes, mitochondria and some dilated profiles of the endoplasmic reticulum are also present Stain as Fig 3 × 10,000

toluidine-blue stained sections (Fig 2 B) In silver impregnated (*Bodian* positive) sections these granules were deep purple or brown (Fig 2 D)

Ultrastructurally all tumours including those without demonstrable amyloid and regardless of histological differences, revealed light and dark tumour cells (Fig 3) corresponding to the light and dark cells seen in semithin sections

The *light cell* (Fig 3) contained numerous membrane-bound secretory granules with 120 to 240 nm diameters. The nuclei were usually round or oval and regularly outlined Many cells of this type contained more than one nucleus.

The *dark cell* (Fig 3 and 4 A–B) had a more electron-dense cytoplasmic matrix and often irregular cell membranes interdigitating with neighbouring cells. The rough endoplasmic reticulum (RER) was usually distended and the secretory granules few in number but otherwise similar to those seen in the light cells. The nuclear/cytoplasmic ratio was higher than in the light cells.

A small number of tumour cells exhibited microvilli, and occasionally these were seen in so-called intracytoplasmic lumina (Fig 5) Cells with microvilli were predominantly found in one case which histologically was composed of spindle-shaped cells arranged in a streaming pattern

Ultrastructurally the *argentaffin* cells were found to contain a high number of phagolysosomes and residual bodies. Some were obvious tumour cells (Fig 6 A) containing

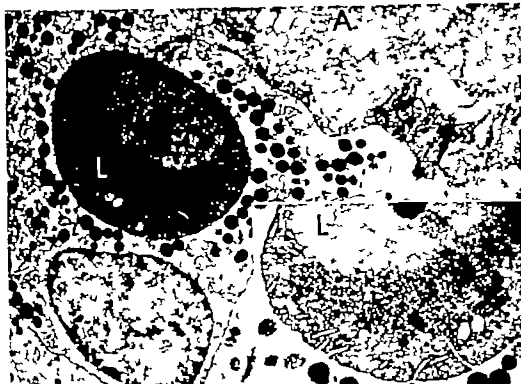


Fig. 5. Tumour cell with so-called intracytoplasmic lumen surrounded by long, slender microvilli. Amyloid (A) stroma with scattered collagen bundles (C) in the upper right corner. Inset show the border of the intracytoplasmic lumen at higher magnification. Stain as Fig. 3. Magnification × 6,800. Inset × 12,900.

secretory granules of the same type as described in non-argentaffin tumour cells. Some argentaffin cells, not containing secretory granules, were interpreted as macrophages (Fig. 6 B).

Extracellular *amyloid* was demonstrated in all but two tumours. The amyloid fibrils were usually intermingled with those of collagen (Fig. 5). In cases where the amyloid was sparse and found in the middle of a pseudofollicle collagen was seldom seen. In such areas membrane fragments and secretory granules were seen among the amyloid fibrils.

DISCUSSION

Considering the wide range of patterns and cell types seen by light microscopy, the ultrastructure of MCT is surprisingly monotonous. All tumours, whether amyloid was present or not, and irrespective of their histological pattern, contained the same light and dark tumour cells. The ultrastructure of the most commonly occurring cell, the light one, has earlier been thoroughly dealt with in the literature (1, 3, 5, 9, 11, 13, 14, 15, 17, 20, 21, 22, 30) and it closely resembles the normal parafillocular cell (4).

The dark tumour cell variant of the present study is probably identical with the dark cells described by *Bord et al.* (3) and *Hackmeister & Zimmermann* (11). It also shares some features with the dark cell containing intracytoplasmic fibrils, which *Ibanez* (15) considered to be the cell responsible for amyloid production; we were however not able to demonstrate intracytoplasmic amyloid fibrils in them. Furthermore, these cells comprised the bulk of one of the tumours which lacked amyloid. We agree with *Meyer* (21)

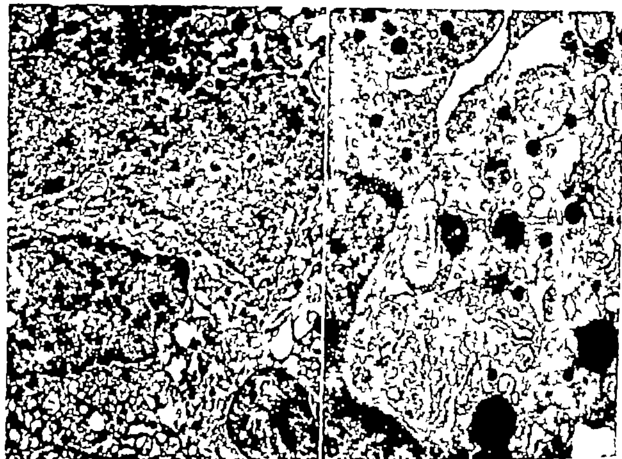


Fig 4 A) Electron micrograph of dark cells from a medullary carcinoma where one area was dominated by this cell type The cells have dense cytoplasm, irregular interdigitating plasma membranes and dilated endoplasmic reticulum. Some contain secretory granules (upper middle part) Stain as Fig. 3, × 7 000 B) Detail from dark cell showing dense core secretory granules similar to those seen in the light cells. Numerous ribosomes, mitochondria and some dilated profiles of the endoplasmic reticulum are also present. Stain as Fig 3 × 10 000

toluidine-blue stained sections (Fig 2 B) In silver impregnated (*Bodian* positive) sections these granules were deep purple or brown (Fig 2 D)

Ultrastructurally all tumours, including those without demonstrable amyloid and regardless of histological differences, revealed light and dark tumour cells (Fig 3) corresponding to the light and dark cells seen in semithin sections.

The *light cell* (Fig 3) contained numerous membrane bound secretory granules with 120 to 240 nm diameters The nuclei were usually round or oval and regularly outlined Many cells of this type contained more than one nucleus

The *dark cell* (Fig 3 and 4 A–B) had a more electron-dense cytoplasmic matrix and often irregular cell membranes interdigitating with neighbouring cells. The rough endoplasmic reticulum (RER) was usually distended and the secretory granules few in number but otherwise similar to those seen in the light cells. The nuclear/cytoplasmic ratio was higher than in the light cells.

A small number of tumour cells exhibited microvilli and occasionally these were seen in so-called intracytoplasmic lumina (Fig 5) Cells with microvilli were predominantly found in one case which histologically was composed of spindle-shaped cells arranged in a streaming pattern.

Ultrastructurally the *argentaffin cells* were found to contain a high number of phagolysosomes and residual bodies. Some were obvious tumour cells (Fig 6 A) containing



Fig. 5 Tumour cell with so-called intracytoplasmic lumen surrounded by long, slender microvilli. Amyloid (A) stroma with scattered collagen bundles (C) in the upper right corner. Inset show the border of the intracytoplasmic lumen at higher magnification. Stain as Fig. 3. Magnification × 8,800 inset × 12,900

secretory granules of the same type as described in non-argentaffin tumour cells. Some argentaffin cells, not containing secretory granules, were interpreted as macrophages (Fig. 6 B).

Extracellular *amyloid* was demonstrated in all but two tumours. The amyloid fibrils were usually intermingled with those of collagen (Fig. 5). In cases where the amyloid was sparse and found in the middle of a pseudofollicle collagen was seldom seen. In such areas membrane fragments and secretory granules were seen among the amyloid fibrils.

DISCUSSION

Considering the wide range of patterns and cell types seen by light microscopy the ultrastructure of MCT is surprisingly monotonous. All tumours, whether amyloid was present or not, and irrespective of their histological pattern, contained the same light and dark tumour cells. The ultrastructure of the most commonly occurring cell, the light one, has earlier been thoroughly dealt with in the literature (1 3 5 9 11 13 14 15 17 20 21 22 30) and it closely resembles the normal parafillocular cell (4).

The dark tumour cell variant of the present study is probably identical with the dark cells described by *Bordi et al* (3) and *Hachmeister & Zimmermann* (11). It also shares some features with the dark cell containing intracytoplasmic fibrils, which *Ibanez* (15) considered to be the cell responsible for amyloid production; we were however not able to demonstrate intracytoplasmic amyloid fibrils in them. Furthermore, these cells comprised the bulk of one of the tumours which lacked amyloid. We agree with *Meyer* (21)



Fig 6

A Large irregular residual bodies of the lipofuscin type (1) are seen in the cytoplasm of an argentaffin tumour cell of the type shown in Figure 2 E. (The cell of the light micrograph seems to contain more granules, owing to the greater thickness of the section) Stain as Fig. 3 Magnification × 12 400.

B Electron micrograph of argentaffin cell situated in th stroma Numerous residual bodies of lipofuscin type are seen in the cytoplasm. This cell may represent a macrophage. Stain as Fig 3 × 5 000

and *Huang & McLeish* (14) that the intracellular fibrils described in this as well as in more fibroblast-like cells (17) represent fibrils unrelated to amyloid. Like *Huang & McLeish* (14) *Bordi et al.* (3) and *Meyer* (21) we found cell organelles, including secretory granules between the extracellular amyloid fibrils. The recent study by *Sletten et al.* (27) has shown that the structure of MCT-amyloid is very similar to that of calcitonin. Amyloid formation in MCT may therefore be initiated by tumour cell necrosis with release of calcitonin-containing granules to the extracellular space

The morphological differences between the light and dark cells may theoretically express differences in origin, differentiation, functional state, or viability In our opinion, the electron-dense cytoplasmic matrix, the dilated RER and the chromatin margination of the dark cells indicate degeneration. Their paucity of secretory granules, as well as the low calcitonin content found in the tumour tissue dominated by dark cells, may also indicate a reduced function, though is it not impossible that the two latter signs may be due to accelerated release of calcitonin-containing granules.

The medullary thyroid carcinoma is included in the APUD tumour group owing to its Amine Precursor Uptake and Decarboxylation ability as well as to its capacity of synthesizing polypeptide hormones (25). Precisely how these two functions are linked is at present not clear and it has been questioned whether the tumour contains two cell types one concerned with the production of polypeptide hormone and one with the amine precursor uptake decarboxylation function.

The gastrointestinal tract harbours both argyrophil and argentaffin APUD cells and both cell types are known to develop into tumours. The normal as well as the neoplastic enterochromaffin (argentaffin) cell preferably produces amines (5-HT) while the argyrophil cell is responsible for the production of polypeptide hormones (as, for instance gastrin and secretin) (6) When *Ljungberg* therefore in addition to the argyrophil C-cells of MCT found a small number of argentaffin cells, these were thought to be responsible for this tumour's monoaminergic function (18, 19)

In the gut ultrastructural studies have revealed that both the argyrophil and argentaffin cells contain endocrine secretory granules, but with differences in size and configuration of the granules (2) By studying alternating semithin and ultrathin sections of MCT we found that the argyrophil cells corresponded to both light and dark tumour cells, and that the number and size of the silver-impregnated granules were equivalent to the number and size of the secretory granules. This finding is in accordance with what *Tateishi et al* (30) found by ultracytochemical methods. The *argentaffin* cells, on the other hand, contained numerous large phagolysosomes and residual bodies and only occasional secretory granules, the size and localization of the argentaffin granules of the semithin sections corresponding with the lysosomes and residual bodies seen by electron microscopy Residual bodies of the lipofuscin type have also been found within the argentaffin cells of another APUD-cell tumour namely the chemodectoma (10)

Since *Ljungberg* used formalin fixed paraffin-embedded material, and we used glutaraldehyde fixation and Epon embedding we have questioned whether the argentaffin and argyrophil cells discussed represent the same cells. By comparing the light micrographs of *Ljungberg* with those of the present study we find, however no reason not to believe that we are discussing the same cells. Furthermore, *Solcia et al.* (28, 29) have shown that both argentaffinity and argyrophilia are just as well demonstrated in glutaraldehyde as in formaldehyde fixed material. On the basis of the present study the argentaffin cells of MCT are interpreted as "old" tumour cells and possible also macrophages.

The authors wish to express their appreciation to *I ge Finseth, Hilde B H* *[illegible]* and *Steinar Hoy-*



Fig 6

A Large irregular residual bodies of the lipofuscin type (1) are seen in the cytoplasm of an argentaffin tumour cell of the type shown in Figure 2 E. (The cell of the light micrograph seems to contain more granules, owing to the greater thickness of the section) Stain as Fig. 3 Magnification × 12 400

B Electron micrograph of argentaffin cell situated in the stroma. Numerous residual bodies of lipofusc n type are seen in the cytoplasm. This cell may represent a macrophage Stain as Fig 3 × 5 000

and *Huang* & *McLeish* (14) that the intracellular fibrils described in this as well as in more fibroblast-like cells (17) represent fibrils unrelated to amyloid. Like *Huang* & *McLeish* (14) *Bordi et al.* (3) and *Meyer* (21) we found cell organelles, including secretory granules between the extracellular amyloid fibrils. The recent study by *Sletten et al.* (27) has shown that the structure of MCT amyloid is very similar to that of calcitonin. Amyloid formation in MCT may therefore be initiated by tumour cell necrosis with release of calcitonin-containing granules to the extracellular space.

The morphological differences between the light and dark cells may theoretically express differences in origin, differentiation, functional state, or viability. In our opinion, the electron-dense cytoplasmic matrix, the dilated RER and the chromatin margination of the dark cells indicate degeneration. Their paucity of secretory granules, as well as the low calcitonin content found in the tumour tissue dominated by dark cells, may also indicate a reduced function though is it not impossible that the two latter signs may be due to accelerated release of calcitonin-containing granules.

The medullary thyroid carcinoma is included in the APUD tumour group, owing to its Amine Precursor Uptake and Decarboxylation ability as well as to its capacity of synthesizing polypeptide hormones (25). Precisely how these two functions are linked is at present not clear and it has been questioned whether the tumour contains two cell types one concerned with the production of polypeptide hormone and one with the amine precursor uptake decarboxylation function.

The gastrointestinal tract harbours both argyrophil and argentaffin APUD cells, and both cell types are known to develop into tumours. The normal as well as the neoplastic enterochromaffin (argentaffin) cell preferably produces amines (5-HT) while the argyphil cell is responsible for the production of polypeptide hormones (as, for instance gastrin and secretin) (6). When *Ljungberg* therefore in addition to the argyrophil C-cells of MCT found a small number of argentaffin cells, these were thought to be responsible for this tumour's monoaminergic function (18, 19).

In the gut ultrastructural studies have revealed that both the argyrophil and argentaffin cells contain endocrine secretory granules, but with differences in size and configuration of the granules (2). By studying alternating semithin and ultrathin sections of MCT we found that the argyrophil cells corresponded to both light and dark tumour cells, and that the number and size of the silver impregnated granules were equivalent to the number and size of the secretory granules. This finding is in accordance with what *Tateishi et al* (30) found by ultracytochemical methods. The *argentaffin* cells, on the other hand, contained numerous large phagolysosomes and residual bodies and only occasional secretory granules, the size and localization of the argentaffin granules of the semithin sections corresponding with the lysosomes and residual bodies seen by electron microscopy. Residual bodies of the lipofuscin type have also been found within the argentaffin cells of another APUD-cell tumour namely the chemodectoma (10).

Since *Ljungberg* used formalin fixed paraffin-embedded material, and we used glutaraldehyde fixation and Epon embedding we have questioned whether the argentaffin and argyrophil cells discussed represent the same cells. By comparing the light micrographs of *Ljungberg* with those of the present study we find, however no reason not to believe that we are discussing the same cells. Furthermore, *Solcia et al* (28, 29) have shown that both argentaffinity and argyrophilia are just as well demonstrated in glutaraldehyde as in formaldehyde fixed material. On the basis of the present study *the argentaffin cells of MCT are interpreted as "old" tumour cells and possible also macrophages.*

The authors wish to express their appreciation to I gn Fraseth Hilde B Helgesen and Steinar Hey-

by for excellent technical assistance, and to *Anne-Brit Lunde* and *Ira Hirsch* for preparing the manuscript.

REFERENCES

1 *Albores Saavedra J Rose G G Ibanez M L. Russell W O Grey C E. & Dmochowski L.* The amyloid in solid carcinoma of the thyroid gland Staining characteristics, tissue culture and electron microscopic observations. Lab. Invest. *13* 77–92 1964
2 *Black W C* Enterochromaffin cell types and corresponding carcinoid tumours. Lab. Invest *19* 473–486 1968.
3 *Bordi C Anversa P & Vitali-Mazza L.* Ultrastructural study of a calcitonin-secreting tumour Typology of the tumour cells and origin of amyloid Virchows Arch Abt A Path. Anat. *357* 145–161 1972
4 *Braunstein H & Stephens C L.* Parafollicular cells of human thyroid Arch Path. *86* 659–666 1968.
5 *Braunstein H Stephens C L. & Gibson R L.* Secretory granules in medullary carcinoma of the thyroid Electron microscopic demonstration. Arch. Path. *85* 306–313 1968.
6 *Dawson I* The endocrine cells of the gastrointestinal tract. Histochem. J *2* 527–549 1970
Falck B Ljungberg O & Rosengren E. On the occurrence of monoamines and related substances in familial medullary thyroid carcinoma with phaeochromocytoma. Acta path. microbiol scand *74* 1–10 1968.
8 *Gautvik K M Normann T Teig I Wille S O Brennhovd I O & Christensen I* Radioimmunoassay of human calcitonin in serum and tissue from healthy individuals and patients with medullary carcinoma of the thyroid gland. Scand J clin. Lab. Invest *36* 324–329 1976
9 *Gonzalez Licea A Hartmann W H & Yardley J H* Medullary carcinoma of the thyroid Ultrastructural evidence of its origin from the parafollicular cell and its possible relation to carcinoid tumours Am. J clin Path *49* 512–520 1968
10 *Grimley P M & Glenner G G* Histology and ultrastructure of carotid body paragangliomas Comparison with the normal gland Cancer *20* 1473–1488 1967
11 *Hachmeister U & Zimmermann H D* Elektronen mikroskopische Untersuchungen an einem C-Zellencarcinom Electron microscopic examination of a C-cell carcinoma Verh Dtsch. Ges Path. *54* 371 375 1970
12 *Hazard J B Hawk W A & Crile G jr* Medullary (solid) carcinoma of the thyroid —a clinicopathologic entity J Clin. Endocrinol *19* 152–161 1959
13 *Horvath E Kovacs K & Ross R C.* Medullary cancer of the thyroid gland and its possible relations to carcinoids. An ultrastructural study Virchows Arch. Abt. A Path Anat. *356* 281–292 1972.
14 *Huang S & McLeish W A* Pheochromocytoma and medullary carcinoma of thyroid. Cancer *21* 302–311 1968.
15 *Ibanez M L.* Medullary carcinoma of the thyroid gland. Path. Ann *9* 263–290 1974
16 *Le Douarin N & Le Lièvre C* Embryologie expérimentale Démonstration de l'origine neurale des cellules à calcitonine du corps ultimobranchial chez l embryon de Poulet. C. R. Acad. Sc. Paris, Série D *270* 2857–2860 1970
17 *Lietz H & Donath K* Zur Ultrastruktur und Entstehung des Amyloides im medullaren Schilddrüsencarcinom. Virchows Arch. Abt. A Path. Anat. *350* 261–274 1970.
18 *Ljungberg, O* Two cell types in familial medullary thyroid carcinoma. A histochemical study Virchows Arch. Abt. A Path. Anat. *349* 312–322 1970
19 *Ljungberg O* Argentaffin cells in human thyroid and their relationship to C-cells and medullary carcinoma. Acta path. microbiol. scand. Section A. *80* 589–599 1972.
20 *McDermott F T & Hart J A L* Medullary carcinoma of the thyroid with hypocalcaemia. Clinical and ultrastructural observations. Brit. J Surg *57* 657-661 1970.
21 *Meyer J S* Fine structure of two amyloid-forming medullary carcinomas of thyroid. Cancer *21* 406–425 1968
22 *Meyer J S & Abdel Bari W* Granules and thyrocalcitonin like activity in medullary carcinoma of the thyroid gland. New Eng. J Med *278* 530–533 1968.
23 *Pearse A G E. Masson Fontana* method Histochemistry Theoretical and applied. 2. ed. J & A Churchill Ltd. London 1960 Appendix 23 p 919
24 *Pearse A G E. & Polak J M* Cytochemical evidence for the neutral crest origin of mammalian ultimobranchial C-cells. Histochemie *27* 96–102 1971
25 *Pearse A G E. & Polak J M* Endocrine tumours of neural crest origin Neurolophomas, apudomas and the APUD concept. Med Biol. *52* 3–18 1974
26. *Romeis B.* Methode von *Bodian.* Mikroskopische technik R Oldenbourg Verlag München—Wien 1968 p. 446.
27 *Sletten K Westermark P & Natvig, J B.* Characterization of amyloid fibril proteins from medullary carcinoma of the thyroid. J. Exp Med. *143* 993–998, 1976.

28 *Solcia, E., Sampietro R & Vassallo G* Indole reactions of enterochromaffin cell and mast cells. J Histochem. Cytochem *14* 691 693 1966.
29 *Solcia, E Vassallo G & Sampietro R* Endocrine cells in the antro-pyloric mucosa of the stomach. Zeitschrift fur Zellforschung *81* 474-486 1967
30 *Tateishi R T k kash Y & N guchi A* Histologic and ultracytochemical studies on thyroid medullary carcinoma. D gnostic significance of argyrophil secretory granules. Cancer 30 755 763 1972.
31 *Williams E. D* Diarrhea and thyroid carcinoma. Proc. roy Soc. Med. 59 602-603 1966.

by for excellent technical assistance and to *Anne Brit Lunde* and *Ira Hirsch* for preparing the manuscript.

REFERENCES

1 *Albores-Saavedra J Rose G G Ibanez M L. Russell W O Grey C E. & Dmochowski L.* The amyloid in solid carcinoma of the thyroid gland Staining characteristics tissue culture and electron microscopic observations. Lab Invest. *13* 77–92 1964
2 *Black W C* Enterochromaffin cell types and corresponding carcinoid tumours. Lab Invest. *19* 473–486 1968
3 *Bordi C Anversa P & Vitali Mazza L.* Ultrastructural study of a calcitonin-secreting tumour Typology of the tumour cells and origin of amyloid Virchows Arch. Abt. A Path Anat. *357* 145–161 1972.
4 *Braunstein H & Stephens C L.* Parafollicular cells of human thyroid Arch Path *86* 659–666 1968.
5 *Braunstein H Stephens C L. & Gibson R L.* Secretory granules in medullary carcinoma of the thyroid Electron microscopic demonstration. Arch. Path *85* 306–313 1968
6 *Dawson I* The endocrine cells of the gastrointestinal tract Histochem J *2* 527–549 1970
7 *Falck B Ljungberg O & Rosengren E.* On the occurrence of monoamines and related substances in familial medullary thyroid carcinoma with phaeochromocytoma. Acta path. microbiol scand *74* 1–10 1968.
8 *Gautvik K M Normann T., Teig V Walle S O Brennhovd I O & Christensen I* Radioimmunoassay of human calcitonin in serum and tissue from healthy individuals and patients with medullary carcinoma of the thyroid gland. Scand J clin Lab. Invest *36* 324–329 1976
9 *Gonzalez Licea A Hartmann W H & Yardley J H* Medullary carcinoma of the thyroid Ultrastructural evidence of its origin from the parafollicular cell and its possible relation to carcinoid tumours. Am J clin. Path. *49* 512–520 1968
10 *Grimley P M & Glenner G G* Histology and ultrastructure of carotid body paragangliomas Comparison with the normal gland. Cancer *20* 1473 1488 1967
11 *Hachmeister U & Zimmermann H D* Elektronenmikroskopische Untersuchungen an einem C Zellencarcinom. Electron microscopic examination of a C-cell carcinoma. Verh Dtsch Ges Path *54* 371–375 1970
12 *Hazard J B Hawk W A & Crile G jr* Medullary (solid) carcinoma of the thyroid —a clinicopathologic entity J Clin. Endocrinol. *19* 152–161 1959
13 *Horvath E. Kovacs K & Ross, R C* Medullary cancer of the thyroid gland and its possible relations to carcinoids. An ultrastructural study Virchows Arch. Abt. A Path Anat. *356* 281–292, 1972
14 *Huang S & McLeish W A.* Pheochromocytoma and medullary carcinoma of thyroid. Cancer *21* 302–311 1968
15 *Ibanez M L* Medullary carcinoma of the thyroid gland. Path. Ann *9* 263–290 1974
16 *Le Douarin N & Le Lièvre C* Embryologie expérimentale Démonstration de l'origine neurale des cellules à calcitonine du corps ultimobranchial chez l'embryon de Poulet. C. R. Acad. Sc. Paris, Série D *270* 2857–2860 1970
17 *Lietz H & Donath K* Zur Ultrastruktur und Entstehung des Amyloides im medullären Schilddrüsencarcinom. Virchows Arch. Abt. A Path. Anat *350* 261–274 1970
18 *Ljungberg O* Two cell types in familial medullary thyroid carcinoma. A histochemical study Virchows Arch. Abt. A Path. Anat. *349* 312–322, 1970.
19 *Ljungberg O* Argentaffin cells in human thyroid and their relationship to C-cells and medullary carcinoma. Acta path. microbiol scand Section A *80* 589 599 1972.
20 *McDermott F T & Hart J A L.* Medullary carcinoma of the thyroid with hypocalcaemia. Clinical and ultrastructural observations. Brit. J Surg *57* 657–661 1970
21 *Meyer J S* Fine structure of two amyloid-forming medullary carcinomas of thyroid Cancer *21* 406–425 1968
22 *Meyer J S & Abdel Bari W* Granules and thyrocalcitonin like activity in medullary carcinoma of the thyroid gland. New Eng J Med *278* 530–533 1968.
23 *Pearse A G E Masson Fontana* method. Histochemistry Theoretical and applied. 2. ed. J & A Churchill Ltd London 1960. Appendix 23 p 919
24 *Pearse A G E. & Polak J M* Cytochemical evidence for the neural crest origin of mammalian ultimobranchial C-cells. Histochemie *27* 96–102 1971
25 *Pearse A G E. & Polak J M* Endocrine tumours of neural crest origin Neurolophomas, apudomas and the APUD concept Med Biol *52* 3–18, 1974
26 *Romeis B* Methode von *Bodian* Mikroskopische technik. R. Oldenbourg Verlag München—Wien 1968, p. 446
27 *Sletten K Westermark P & Natvig J B.* Characterization of amyloid fibril protein from medullary carcinoma of the thyroid. J Exp Med. *143* 993–998 1976.

extravasation the data would suggest that it is one of decreased flow in hyperpermeable regions.

The aim of the present study has been to examine whether it is possible to demonstrate an increased permeability of the cerebral vessels for fluorescent homologous serum proteins and colloidal carbon particles following a few hours of acute angiotensin hypertension in rats, and if so, to identify which types of cerebral vessels become permeable.

MATERIAL AND METHODS

Animals. White female rats weighing about 150 grams were used.

Anaesthesia. A solution of amylobarbitone sodium (Amytal®) 25 mg/ml was injected intraperitoneally at a dose of about ⅓ ml per 100 gram body weight.

Fluorescent serum proteins were produced as previously described (*Olsson* 1968) by a modification of the procedure described by *Nairn* (1962).

Colloidal carbon particles specially manufactured for experimental use (Günther Wagner Pelikan-Werke, Hannover, Germany C 11/1431a).

Angiotensin. Hypertensin CIBA was dissolved in physiological saline.

The experimental technique. Group I. After induction of complete anaesthesia a catheter of polyethylene was placed in the femoral vein of each of four rats, and about 40 mg of Lissamine Rhodamine labelled homologous serum proteins were injected intravenously. About ten minutes later intravenous injections of angiotensin were commenced using doses of about ⅙ microgram every fifth minute over a period of four hours. Using this procedure the blood pressure rises from the normal level (about 90 mm Hg) to 150–160 mm Hg after each injection and normalizes before the next angiotensin injection (Olsson 1968). At the end of the experimental period the rats were killed by injection of a large intraperitoneal dose of amytal and the brain was fixed in a 4 per cent buffered formalin, pH 7.3.

Group II. Four rats were treated identically to those in group I except that instead of the fluorescent proteins, colloidal carbon particles were injected intravenously about ten minutes before the end of the hypertensive period. For two of the rats the hypertensive period lasted half an hour and for the two others it lasted four hours. After the rats had been killed, the mesenteric arterioles were examined under a stereo microscope to ascertain whether the arterial hypertension had increased the permeability for colloidal carbon particles. This was indeed the case in all the rats, indicating that the hypertension had damaged the mesenteric arterioles (*Giese* 1966).

Group III. Four control rats which had otherwise been subjected to the same experimental treatment as the rats in group I were given intravenous injections of physiological saline instead of angiotensin, the volumes being identical.

Group IV. Four control rats treated otherwise in the same way as the rats in group II were given physiological saline injection instead of angiotensin, the volumes being identical.

Microscopical preparation. After fixation, the brain was embedded in paraffin, cut into sections five microns thick and examined under a fluorescence microscope or a light microscope after staining with hematoxylin and eosin. Sections for studies of the vascular permeability under the fluorescence microscope were prepared from all of the cerebral lobes. A total of 200–300 sections from each rat brain were examined.

RESULTS

Group I. Arterioles with a diameter of 50–100 microns, localized in the grey as well as in the white substance of the brain, showed a clear permeability to the fluorescent homologous serum proteins. The degree of deposition of the fluorescent serum proteins varied from only a small part to practically the entire circumference of the arterioles. When a deposition of fluorescent proteins was observed in the wall of the arterioles it was situated in both the tunica intima and the tunica media, and no depositions could be seen in the surrounding part of the cerebral tissue (Fig. 1a).

Arterioles with a diameter larger than 100–150 microns showed a very slight or more typically no permeability for the fluorescent proteins, while in small and large arteries no deposition of fluorescent proteins was observed with the exception of one pial artery in which the fluorescent proteins had penetrated into the tunica intima and the most luminal part of the tunica media (Fig. 1b).

Veins and venules of all sizes located in the grey and white substance of the brain, as well as in the pia, showed a very pronounced permeability of the wall for the fluorescent proteins (Fig. 2) and in some cases the fluorescent proteins had penetrated through the wall of the venule or the vein into the surrounding cerebral tissue.

Acta path. microbiol scand Sect. A, 85 572-576 1977

INCREASED PERMEABILITY FOR PLASMA COMPONENTS OF THE CEREBRAL VESSELS DURING ACUTE ANGIOTENSIN HYPERTENSION IN RATS

FINN OLSEN

Institute of Hygiene University of Copenhagen, Denmark

Olsen, F Increased permeability for plasma components of the cerebral vessels during acute angiotensin hypertension in rats. Acta path. microbiol scand Sect. A 85 572-576 1977

Experimentally induced acute angiotensin hypertension has been shown to increase the permeability of cerebral arterioles, venules and veins to plasma components within a few hours. This increase in permeability was demonstrated by means of circulating homologous fluorescent serum proteins and colloidal carbon particles The results support the view that an increased permeability of the cerebral vessels to plasma components is either a causal or an additional pathogenetic factor in the development of the hypertensive encephalopathy

Key words Angiotensin hypertension cerebral vessels permeability

Finn Olsen, Institute of Hygiene University of Copenhagen,
21 Blegdamsvej DK 2100 Copenhagen Ø

Received 15.x 76 Accepted 29 iii.77

In cases of severe arterial hypertension in man, as well as in acute experimental hypertension in animals it has been demonstrated that the cerebral blood flow is maintained at a relatively constant level due to an autoregulatory constriction of the cerebral resistance vessels following an increase in the blood pressure However when the blood pressure rises beyond a certain limit this autoregulation breaks down resulting in a forced arteriolar dilation and an increase in cerebral blood flow (*Ekström Jodal et al* 1971 *Strandgaard et al* 1973 *Skinhoj & Strandgaard* 1973 *Strandgaard et al* 1975 *Farrar et al* 1976)

This breakdown in the autoregulation is believed to be an important factor in the pathogenesis of acute hypertensive encephalopathy (*Lassen & Agnoli* 1972) *Johansson et al* (1970) demonstrated hypertensive blood brain barrier damage in cats, within a few minutes of a sudden pronounced increase in blood pressure and *Farrar et al* (1976) obtained clear evidence for hyperfusion and plasma protein extravasation in hypertensive cats, indicating overstretching of the cerebral vessels.

In contrast to the theory that hyperfusion followed by plasma protein extravasation is an important factor in the pathogenesis of acute hypertensive encephalopathy it must be mentioned that *Dinsdale et al* (1974) demonstrated that cerebral areas of greatly decreased flow clustered in the same areas where damage to the blood brain barrier and ischemic lesions were found In these studies it was concluded that if there is a correlation between alteration of cortical blood flow and



3

Fig 3 Arteriole showing deposition of colloidal carbon particles in the wall (arrow) Hematoxylin-eosin. Magnification 800 ×

proteins or colloidal carbon particles in the walls of the arterial or venular vessels.

DISCUSSION

The results presented have revealed that in the brain arterioles as well as veins and venules, show a pronounced permeability to plasma components following experimentally induced acute angiotensin hypertension in rats. The increased permeability of the cerebral arterioles was identical to that previously demonstrated in arterioles of the pancreas, the mesentery the kidney and the heart (*Giese* 1966, *Olsen* 1968, *Olsen* 1977)

An increased permeability of the intracerebral vessels with a resulting dysfunction of the blood-brain barrier has been observed previously during acute hypertension (*Johansson* 1974 1975 *Farrar et al* 1976) The majority of the permeable vessels seemed to be pial and cortical arteries and arterioles, but also capillaries and venules appeared to be involved in the vascular permeability although less frequently (*Johansson* 1974) The present results are to a certain extent in agreement with the afore mentioned observations, but with the apparent exception that the permeability of the veins and venules for plasma components seems to be more pronounced than has been described previously (for literature see *Johansson* 1974) Furthermore the increased vascular permeability seems to occur both in the grey and the white substance without any marked difference between these regions, and it has not been possible to recognize any cerebral areas in which fluorescent proteins had been deposited in the tissue to a degree as has been described previously by various authors concerning macroscopic extravasation of Evans blue in the brain in animals in which acute hypertension had been induced (for literature see *Johansson* 1974) The pronounced permeability of the venules and the veins observed in the present study could be due to an increased venous pressure in the brain, as a result of the failure of the autoregulative constriction system of the arterial vessels to prevent the pressure from propagating to the capillaries and the veins (*Häggendal* & *Johansson* 1972) The results support the view that an increased permeability of the cerebral vessels for plasma components is either an additional phatogenetic factor in the development of the hypertensive encephalopathy or may indeed be a causal factor

A comparison of the permeability of the cerebral vessels to fluorescent proteins with the permeability for colloidal carbon particles revealed that the penetration of the latter was very sparse One explanation for this discrepancy in the permeability of the two tracers can be found in the fact that the colloidal carbon particles were circulating in the blood for only a few minutes, while the fluorescent homologous serum proteins were circulating over the entire experimental period. Furthermore, the average size of the carbon particles, or conglomerates of carbon particles, is larger than that of most of the serum proteins. The deposition of colloidal carbon particles in the cerebral arterioles was very sparse when compared with the deposition of carbon in the walls of the mesenteric arterioles. This finding indicates that a possible dilatation of the cerebral arterioles was not as marked as is usually the case for the mesenteric arterioles during a

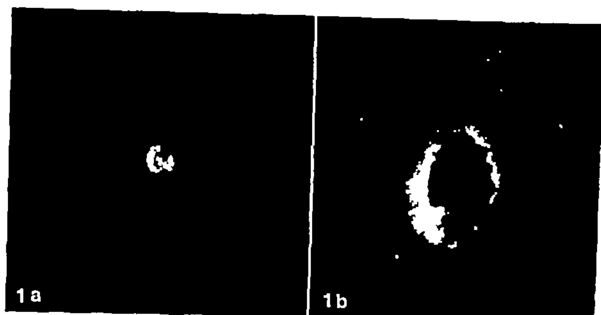


Fig 1 A cerebral arteriole showing deposition of fluorescent proteins in the wall (a) and a pial artery showing deposition of fluorescent proteins in the tunica intima and the most luminal part of the tunica media (b) Magnification 800 ×

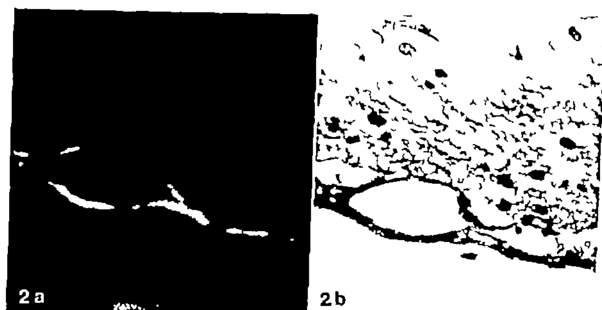


Fig 2 Vein with deposition of fluorescent proteins in the wall (a) The same vein after staining with hematoxylin-eosin (b) Magnification 800 ×

No differences in the permeability of the arterioles and venules of the white and grey substance could be seen, no matter which region of the brain was examined

Group II The rats in which colloidal carbon particles were injected intravenously half an hour and four hours after the beginning of the intravenous injections of angiotensin showed a very sparse deposition of carbon particles in the wall of arterioles, venules and veins (Fig 3) This deposition was not as marked as that seen in group I using fluorescent proteins.

It was surprising to observe that many of the endothelial cells had phagocytized carbon particles.

Groups III and IV The control animals showed no deposition of either fluorescent

Acta path. microbiol. scand. Sect. A, 85: 577-589, 1977

PSEUDOSARCOMATOUS PROLIFERATIVE LESIONS OF SOFT TISSUE WITH OR WITHOUT BONE FORMATION

INGVAR DAHL and LENNART ANGERVALL

Departments of Pathology, University of Gothenburg and Central Hospital, Vänersborg, Sweden

Dahl, I. and Angervall, L. Pseudosarcomatous proliferative lesions of soft tissue with or without bone formation. Acta path. microbiol. scand. Sect. A, 85: 577-589, 1977.

The clinical observations, the structural appearance and the light microscopy of 18 cases of pseudosarcomatous proliferative lesions of soft tissue are described. The study indicates that a close relationship exists between nodular fasciitis, proliferative fasciitis and proliferative myositis. The descriptive term pseudosarcomatous proliferative lesion of soft tissue is proposed for these lesions and mixed forms with or without bone formation. Seven patients were females and 11 were males; the ages ranged between 37 years and 81 years, with a median of 58.5 years. Seven lesions were situated entirely or almost entirely within the subcutaneous tissue, and 11 lesions within striated muscle, with a predilection for muscles of the trunk and proximal regions of the extremities. The predominant proliferating cells were large cells, resembling ganglion cells. The histochemical study of the myxoid matrix indicated the presence of chondroitin 4- and/or 6- sulfates. The gross and the light microscopic appearances of the lesions were compatible with the diagnosis of proliferative fasciitis in 6 cases and proliferative myositis in 9 cases. Four lesions showed mixed forms between proliferative myositis and proliferative fasciitis. Nodular fasciitis-like areas were evident in 14 cases. Four lesions showed bone and cartilage formation. Follow-up information was available in all patients. The follow-up period ranged from 9 months to 17 years, with a median of 11 years. Four patients died from intercurrent diseases; the remaining 14 patients are alive and well, indicating the perfectly benign clinical course. Awareness of the existence of pseudosarcomatous proliferative lesions of soft tissue and a knowledge of their characteristic gross structural and variable light microscopic appearances is mandatory for the avoidance of misinterpreting these lesions as sarcoma.

Key words: Soft tissue tumour; pseudosarcomatous proliferative lesion; nodular fasciitis; proliferative fasciitis; proliferative myositis; myositis ossificans.

Ingvar Dahl, Department of Pathology, Central Hospital, Fack, S-462 01 Vänersborg, Sweden.

Received 20.xii.76. Accepted 14.i.77

Proliferative non-neoplastic mesenchymal lesions occurring in the subcutaneous tissue and voluntary muscle such as nodular fasciitis (Konwaler et al. 1955), proliferative myositis (Kern 1960) and pseudomalignant osseous tumour of soft tissue (Fine & Stout 1957) are considered to be recognizable separate entities. These pseudosarcomatous lesions have frequently been misinterpreted as sarcomas on account of their rapid and often infiltrative manner of growth, polymorphous cellular composition and high mitotic frequency. Recently another pseudosarcomatous

period of acute arterial hypertension (*Giese* 1966)

REFERENCES

1 *Dinsdale H B Robertson D M & Haas R A* Cerebral blood flow in acute hypertension Arch. Neurol *31* 80–87 1974

2 *Ekström Jodal B Häggendal E. Linder L. E & Nilsson N J* Cerebral blood flow autoregulation at high arterial pressures and different levels of carbon dioxide tension in dogs. Europ. Neurol. *6* 6–10 1971

3 *Farrar J K Jones J V Graham D I Strandgaard S & MacKenzie E T* Evidence against cerebral vasospasms during acutely induced hypertension. Brain Res. *104* 176–180 1976

4 *Giese J* The pathogenesis of hypertensive vascular disease Munksgaard Copenhagen, 1966 Thesis.

5 *Häggendal E & Johansson B* Effect of increased intravascular pressure on the blood brain barrier to protein in dogs. Acta Neurol Scand. *48* 271–275 1972.

6 *Johansson B Chok Luh L. Olsson Y & Klatzo I* The effect of acute arterial hypertension on the blood brain barrier to protein tracers. Acta Neuropath. (Berl) *16* 117–124 1970

7 *Johansson B* Blood-brain barrier dysfunction in acute arterial hypertension. Gothenburg 1974 Thesis.

8. *Johansson B* Cerebrovascular permeability after angiotensin-induced blood pressure increase in normotensive and spontaneously hypertensive rats. In *Sharper M Jennett, B Miller D & Rowan J..* Blood flow and Metabolism in the Brain. Churchill Livingstone, Edinburgh (1975) p. 5.3–5 7

9 *Lassen N A & Agnoli A* The upper limit of autoregulation of cerebral blood flow On the pathogenesis of hypertensive encephalopathy Scand. J Clin. Lab. Invest. *30* 113–116 1972

10 *Nairn R. C* Fluorescent protein tracing. Edinburg & London, 1962.

11 *Olsen F* Penetration of circulating fluorescent proteins into walls of arterioles and venules in rats with intermittent acute angiotensin-hypertension. Acta path. microbiol. scand. Sect. *74* 325–332, 1968.

12 *Olsen F.*, Penetration of fluorescent homologous serum proteins into arterial and arteriolar walls of the kidney and the heart in rats with acute angiotensin hypertension Cir Res. 1977 (in press)

13 *Skinhoj E. & Strandgaard S* Pathogenesis of hypertensive encephalopathy Lancet *I* 461–462, 1973

14 *Strandgaard S Olesen J Skinhoj E. & Lassen N A* Autoregulation of brain circulation in severe arterial hypertension. Br Med. J *1* 507–510 1973

15 *Strandgaard S Jones J V., MacKenzie E. T & Harper A M* Upper limit of cerebral blood flow autoregulation in experimental renovascular hypertension in the baboon. Cir Res. *37* 164–167 1975




2




4

lesion, named proliferative fasciitis, involving fascia and interlobular fibrous septa of subcutaneous fat and characterized by the proliferation of large mono- and binucleated cells, has been described (*Chung & Enzinger* 1975) These authors consider proliferative fasciitis to be related to proliferative myositis rather than to nodular fasciitis.

Osteoid bone and/or cartilage have been described in occasional cases of nodular fasciitis, proliferative fasciitis and proliferative myositis (*Stout* 1961 *Hutter et al* 1962 *Kern* 1960 *Enzinger & Dulcey* 1967, *Chung & Enzinger* 1975) These lesions have been considered to be related to pseudomalignant osseous tumour of soft tissue (or so-called pseudomalignant myositis ossificans) a bone-forming lesion characterized histologically by the so-called zonal phenomenon (*Angervall et al* 1969 *Lagier & Cox* 1975) and included in the general category of myositis ossificans. On reviewing the literature the term circumscribed or localized myositis ossificans" has been applied to all forms of intra and extra muscular proliferative, non neoplastic bone-forming soft tissue lesions with or without zonal phenomenon (*Noble* 1924 *Liebig* 1929 *Geschickter & Maseritz* 1938 *Ackerman* 1958 *Gilmer & Anderson* 1959 *Spjut et al* 1970)

This paper presents a clinico-pathological study of 18 cases of pseudosarcomatous proliferative lesions of soft tissue with or without bone-formation

MATERIAL AND METHODS

Nine out of 18 cases in the present series were obtained from a Swedish series comprising some 800 cases of malignant soft tissue tumours reported to the Swedish Cancer Registry during a 6-year period (1958–1963) Four cases were selected after reviewing various soft tissue lesions recorded in the Department of Pathology Sahlgren's Hospital Gothenburg, between the years 1961 and 1969 Three cases examined between 1966 and the present day were primarily diagnosed as pseudosarcomatous proliferative lesions of soft tissue The remaining 2 case were sent to us for consultation from other Departments of Pathology

Histological methods Sections of tissue routinely stained with haematoxylin and eosin and the haematoxylin–van Gieson method were available for review in all cases. In 15 cases, 5 micron thick sections of paraffin-embedded tissue were stained by Masson-trichrome and by Ladewig's modification of Mallory's stain for collagen and Gordon-Sweet for reticulin fibres. The Prussian-blue reaction for iron-containing pigments and the periodic acid Schiff reaction (McManus) with and without prior treatment of the sections with diastase (Merck) was also performed Alcian blue (Chroma-Gesellschaft) stain was used at 2 different pHs (pH 2.5 and 0.5) for the examination of mucosubstances as described previously (*Angervall* et al. 1973 *Kindblom & Angervall* 1975)

RESULTS

Information concerning the age and sex of the patients, anatomical site and location, duration of tumour symptoms, evidence of previous trauma and bone formation as well as follow up information is summarized in Table 1 The youngest patient was 37 years old and the oldest was 81 the median age of the patients was 58.5 years.

Gross Appearance The lesion was estimated to be less than 1 cm in the widest diameter in 2 cases, between 1 and 2 cm in 7 cases, between 2 and 5 cm in 6 cases and larger than 5 cm in 3 cases. The largest les-

Fig 1 Proliferative lesion of soft tissue situated within striated muscle and adjacent subcutaneous tissue with a net-like appearance and a grey white trabecular and scar like cut surface Case 12 × 2.

Fig 2 Proliferative lesion of soft tissue situated entirely within striated muscle. The lesion extends along intramuscular connective tissue septa, around and into bundles of muscle fibres features associated with proliferative myositis. Case 2. Haematoxylin and eosin. × 7

Fig 3 Proliferation of large cells looking like ganglion cells within striated muscle encircling bundles of muscle fibres. Case 2 Haematoxylin and eosin. × 100
Insert Large cells looking like ganglion cells arranged in a small group like a zig-zag pattern. Haematoxylin and eosin. × 250

Fig 4 Proliferation of haphazardly distributed thin spindle-shaped, wavy or stellate-like cells in a mucoid matrix area compatible with the diagnosis of nodular fasciitis. Case 2 Haematoxylin and eosin. × 100


3


2


3


4

les on, named proliferative fasciitis, involving fascia and interlobular fibrous septa of subcutaneous fat and characterized by the proliferation of large mono- and binucleated cells, has been described (*Chung & Enzinger* 1975) These authors consider proliferative fasciitis to be related to proliferative myositis rather than to nodular fasciitis.

Osteoid, bone and/or cartilage have been described in occasional cases of nodular fasciitis, proliferative fasciitis and proliferative myositis (*Stout* 1961 *Hutter et al.* 1962 *Kern* 1960 *Enzinger & Dulcey* 1967 *Chung & Enzinger* 1975) These lesions have been considered to be related to pseudomalignant osseous tumour of soft tissue (or so-called pseudomalignant myositis ossificans) a bone-forming lesion characterized histologically by the so-called "zonal phenomenon" (*Angervall et al* 1969 *Lagier & Cox* 1975) and included in the general category of myositis ossificans. On reviewing the literature the term circumscribed or localized myositis ossificans" has been applied to all forms of intra and extra muscular proliferative non neoplastic bone forming soft tissue lesions with or without zonal phenomenon (*Noble* 1924 *Liebig* 1929 *Geschickter & Maseritz* 1938 *Ackerman* 1958 *Gilmer & Anderson* 1959 *Spjut et al* 1970)

This paper presents a clinico-pathological study of 18 cases of pseudosarcomatous proliferative lesions of soft tissue with or without bone formation.

MATERIAL AND METHODS

Nine out of 18 cases in the present series were obtained from a Swedish series comprising some 800 cases of malignant soft tissue tumours reported to the Swedish Cancer Registry during a 6-year period (1958–1963) Four cases were selected after reviewing various soft tissue lesions recorded in the Department of Pathology *Sahlgren's Hospital* Gothenburg between the years 1961 and 1969 Three cases examined between 1966 and the present day were primarily diagnosed as pseudosarcomatous proliferative lesions of soft tissue The remaining 2 cases were sent to us for consultation from other Departments of Pathology

Histological methods Sections of tissue routinely stained with haematoxylin and eosin and the haematoxylin–van Gieson method were available for review in all cases. In 15 cases, 5 micron-thick sections of paraffin-embedded tissue were stained by Masson-trichrome and by Ladewig's modification of Mallory's stain for collagen and Gordon-Sweet for reticulin fibres. The Prussian blue reaction for iron-containing pigments and the periodic acid Schiff reaction (McManus) with and without prior treatment of the sections with diastase (Merck) was also performed. Alcian blue (Chroma-Gesellschaft) stain was used at 2 different pHs (pH 2.5 and 0.5) for the examination of mucosubstances as described previously (*Angervall* et al. 1973 *Kindblom & Angervall* 1975)

RESULTS

Information concerning the age and sex of the patients, anatomical site and location, duration of tumour symptoms, evidence of previous trauma and bone formation as well as follow up information is summarized in Table 1 The youngest patient was 37 years old and the oldest was 81 the median age of the patients was 58.5 years

Gross Appearance The lesion was estimated to be less than 1 cm in the widest diameter in 2 cases, between 1 and 2 cm in 7 cases, between 2 and 5 cm in 6 cases and larger than 5 cm in 3 cases. The largest les-

---

Fig 1 Proliferative lesion of soft tissue situated within striated muscle and adjacent subcutaneous tissue with a net like appearance and a grey-white trabecular and scar-like cut surface. Case 12 × 2.

Fig 2 Proliferative lesion of soft tissue situated entirely within striated muscle The lesion extends along intramuscular connective tissue septa, around and into bundles of muscle fibres features associated with proliferative myositis. Case 2 Haematoxylin and eosin. × 7

Fig 3 Proliferation of large cells looking like ganglion cells within striated muscle encircling bundles of muscle fibres. Case 2. Haematoxylin and eosin. × 100
Insert Large cells looking like ganglion cells arranged in a small group like a zig-zag pattern. Haematoxylin and eosin. × 250.

Fig 4 Proliferation of haphazardly distributed thin, spindle-shaped, wavy or stellate-like cells in a mucoid matrix area compatible with the diagnosis of nodular fasciitis. Case ? Haematoxylin and eosin. × 100.

5





TABLE 1 *Clinical Features in 18 Patients with Proliferative Pseudosarcomatous Lesions of Soft Tissue*

Patient Code Nr	Sex	Age in Years	Anatomical Site	Anatomical Location	Duration of Tumour Symptoms	Bone Formation	Trauma	Duration of Follow-up (Years)
1	M	71	Thigh	Subcutaneous tissue	2 weeks	No	No	8
2	M	40	Upper arm (brachial m.)	Striated muscle	1 week	No	No	15
3	F	47	Forearm	Subcutaneous tissue	1 month	Yes	Yes	3
4	F	37	Thigh	Subcutaneous tissue	1 week	No	No	10
5	M	53	Thigh	Subcutaneous tissue	1 day	No	No	2
6	F	81	Thigh (quadriceps m.)	Striated muscle	3 months	Yes	No	12 (dead)
7	M	61	Upper arm (deltoid m.)	Striated muscle	2 weeks	Yes	No	8.5 (dead)
8	M	63	Back (latissimus dorsi m.)	Striated muscle and subcut tissue	1 week	No	Yes?	0.8 (dead)
9	M	43	Chest (pectoralis major m.)	Striated muscle	1 week	No	No	15 (dead)
10	M	50	Back (latissimus dorsi m.)	Striated muscle	2 weeks	No	No	12.5
11	F	63	Chest	Subcutaneous tissue	2 weeks	No	No	13.5
12	F	60	Upper arm (deltoid m.)	Striated muscle and adjacent subcut. tissue	1 week	Yes	Yes	6.5
13	M	59	Chest (pectoralis major m.)	Striated muscle	5 days	No	No	16
14	F	61	Thigh (quadriceps m.)	Striated muscle and subcut. tissue	2 weeks	No	No	13.5
15	M	69	Chest (pectoralis major m.)	Subcut. tissue and adjacent striated muscle	1 week	No	No	15
16	M	47	Thigh	Subcutaneous tissue	1 week	No	No	10
17	F	44	Forehead	Striated muscle	2 months	No	Yes	3
18	M	58	Back (latissimus dorsi m.)	Striated muscle	1 week	No	No	17

Fig 5 Subcutaneously situated proliferative lesion of soft tissue extending along fascial planes and interlobular fibrous septa a in proliferative fasciitis Case 1 Haematoxylin and eosin. × 7

Fig 6 Mixture of collagen rich (black) and myxomatous areas surrounding fat lobules and groups of fat cells Case 1 Haematoxylin–van Gieson × 40

Fig 7 Proliferation of large cells looking like ganglion cells surrounding fat cells showing atrophy and lipophagocytosis. Such an area is easily misinterpreted as sarcoma Case 1 Haematoxylin and eosin × 100

lon was approximately 7 cm in the widest diameter

Ten of the 11 intramuscularly-situated lesions were diffusely growing affecting principally the inter and intramuscular connective tissue, giving the cut surface a characteristic net-like appearance (Fig 1) Three of these lesions extended outwards into the adjacent subcutaneous tissue (Fig 13) One of the intramuscularly situated lesions was rather well-demarcated but not encapsulated. Six of the 7 lesions situated within the subcutaneous tissue were poorly demarcated, extending along fascial planes and interlobular fibrous septa and affecting the residual adipose tissue (Fig. 5) One of these lesions involved the underlaying muscle (Fig 8) The remaining lesion was well-demarcated and nodular

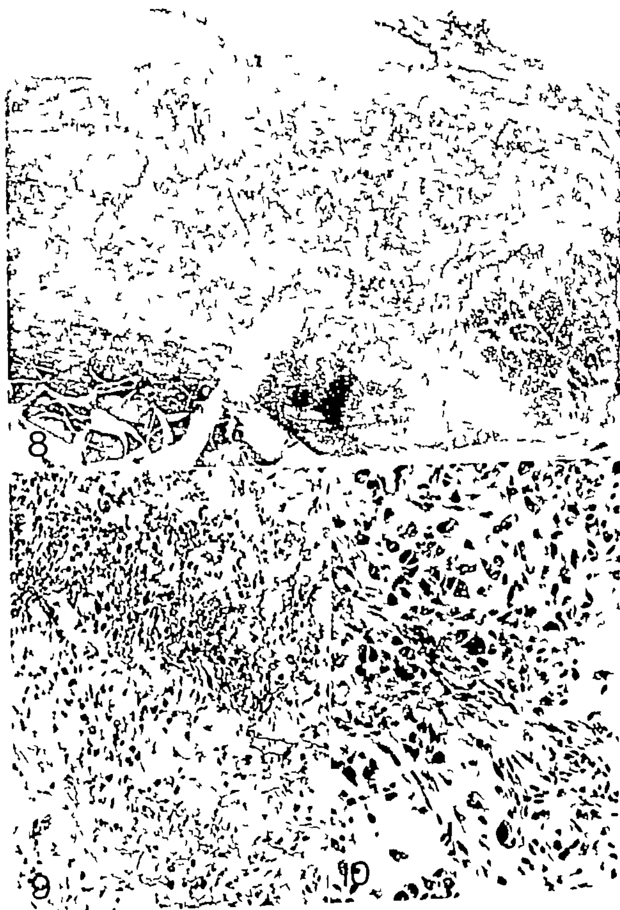
Microscopic Findings The microscopic appearance of the lesions fulfilled the criteria for the diagnosis of proliferative myositis (Figs. 3 and 11) and proliferative fasciitis (Figs. 6, 7 9 and 10) in 9 and 6 cases, respectively In 4 of these 15 lesions, there were areas with a proliferative fasciitis-like component in the subcutaneous tissue and a proliferative myositis-like component in the striated muscle (Figs. 8 and 13)

The predominant proliferating cells were large, mono- and binucleated, occasionally multinucleated (Figs. 3 9 10 and 11) The mononucleated cells were large, resembling ganglion cells. They were rounded or polygonal with thin cytoplasmic protrusions. The cytoplasm was abundant, weakly basophilic or amphophilic, rather homogeneous with well-demarcated borders and in some cells slightly granular The nuclei were large, with a distinct nuclear membrane. The chromatin pattern was delicate, with a few small chromatin clumps. One large nucleolus or a few smaller nucleoli were visible. These large cells were randomly distributed within a mucoid matrix. In places the cells were arranged in small groups or in nests, forming a zig zag pattern (Fig 3 insert) In other areas there were proliferations of plump fibroblast-like, spindle-shaped cells with elongated cytoplasm and an oval nucleus. Mitoses were frequently encountered both in the large "ganglion cell-like" and the plump fibroblast like cells. Atypical mitoses were not observed Collagen and reticulin fibres were seen in close proximity to the proliferating cells, and 6 lesions were rich in collagen (Fig. 6) with areas of hyalinization. Areas typical of nodular fasciitis (Figs. 4 and 12) were easily demonstrated in 14 lesions which showed proliferations of elongated, thin S-formed or wavy spindle shaped cells, separated by small clefts or slit like spaces. In places there were proliferations of stellate-like cells haphazardly arranged in a mucoid matrix alternating with proliferations of radiating capillaries with extravasated erythrocytes and inflammatory cells.

The arrangement of the cells within the lesions was characteristic in 16 out of the 18 cases, regardless of whether they were situated in the subcutaneous tissue or within striated muscle. In the muscle tissue, the cells were arranged around individual muscle fibres, bundles of fibres or varying sizes, intramuscular connective tissue septa and fascia (Figs. 2, 3 and 11) The surrounded muscle fibres seemed virtually uninvolved but areas with atrophy and rounded muscle fibres were evident however there was no proliferation of the sarcolemma nuclei. The same type of cell distribution within the lesions was seen in the subcutaneous tissue, with involvement of fascial planes and interlobular septa (Figs. 5 and 6) The cells also radiated into the adipose tissue and surrounded fat cells (Fig 7) which focally exhibited signs of lipophagocytosis. The osteoid tissue, cartilage and/or bone trabeculae, whether subcutaneously or intramuscularly situated, were similarly distributed (Figs. 14 and 15)

Fig 8 Proliferative lesion of soft tissue situated in the subcutaneous tissue Note the involvement of the underlying striated muscle suggestive of proliferative myositis Case 15 Haematoxylin and eosin. × 7

Figs 9 and 10 Areas compatible with the diagnosis of proliferative fasciitis Case 15 Haematoxylin and eosin. × 100 and × 250


8
9
10

13

14

15



Fig. 11. Area compatible with the diagnosis of proliferative myositis. Case 15. Haematoxylin and eosin. × 100

Fig. 12. Area compatible with the diagnosis of nodular fasciitis. Case 15. Haematoxylin and eosin. × 250

The mucoid matrix showed alcianophilia at pH 2.5 as well as at pH 0.5, and testicular hyaluronidase, which digests hyaluronic acid as well as chondroitin 4- and 6- sulfates (*Zugibe* 1970), reduced the alcianophilia at pH 2.5 and abolished it at pH 0.5. These staining reactions indicated the presence of chondroitin 4- and/or 6- sulfates but gave no information about the possible presence of hyaluronic acid (*Kindblom* & *Angervall* 1975).

In 12 lesions, 4 subcutaneously and 8 predominantly intramuscularly situated, there were areas of loosening of collageneous fascial and septal planes, and a tendency to cyst formation was observed in 6 of them. In these areas the alcianophilia was reduced and a diastase resistant staining reaction with the PAS-method was evident. A fibrillary fibrinous material giving a bright orange-red stain with the Ladewig stain was observed in these areas, and the collageneous septa or fascia adjacent to the lesion showed extravasated erythrocytes and reduced staining reaction with the trichrome stains. Deposition of haemosiderin was not evident in any lesion.

Fig. 13. Proliferative lesion of soft tissue growing diffusely within striated muscle as can be seen in proliferative myositis and extending into the adjacent subcutaneous tissue in a manner suggestive of proliferative fasciitis. Case 12. Haematoxylin and eosin. × 7

Figs. 14 and 15. Bone formation within the subcutaneous tissue and within striated muscle. The bone trabeculae surround single or small groups of fat cells and muscle fibres. Case 12. Haematoxylin-van Gieson and haematoxylin and eosin. × 40

13

14

15



Fig 11 Area compatible with the diagnosis of proliferative myositis Case 15 Haematoxylin and eosin. × 100

Fig 12 Area compatible with the diagnosis of nodular fasciitis. Case 15 Haematoxylin and eosin. × 250

The mucoid matrix showed alcianophilia at pH 2.5 as well as at pH 0.5 and testicular hyaluronidase which digests hyaluron c acid as well as chondroitin 4 and 6- sulfates (*Zugibe* 1970) reduced the alcianophilia at pH 2.5 and abolished it at pH 0.5 These staining reactions indicated the presence of chondroitin 4 and/or 6- sulfates but gave no information about the possible presence of hyaluronic acid (*Kindblom* & *Angervall* 1975)

In 12 lesions, 4 subcutaneously and 8 predominantly intramuscularly situated there were areas of loosening of collageneous fascial and septal planes and a tendency to cyst formation was observed in 6 of them. In these areas the alcianophilia was reduced and a diastase-resistant staining reaction with the PAS-method was evident. A fibrillary fibrinous material giving a bright orange-red stain with the Ladewig stain was observed in these areas, and the collageneous septa or fascia adjacent to the lesion showed extravasated erythrocytes and reduced staining reaction with the trichrome stains. Deposition of haemosiderin was not evident in any lesion.

Fig 13 Proliferative lesion of soft tissue growing diffusely within striated muscle as can be seen in proliferative myositis and extending into the adjacent subcutaneous tissue in a manner suggestive of proliferative fasciitis. Case 12 Haematoxylin and eosin. × 7

Figs 14 and 15 Bone formation within the subcutaneous tissue and within striated muscle The bone trabeculae surround single or small groups of fat cells and muscle fibres. Case 12 Haematoxylin- van Gieson and haematoxylin and eosin. × 40.

In 4 lesions there were areas containing osteoid tissue, cartilage and/or bone trabeculae (Figs. 14 and 15). In areas with cartilage there were hyaluronidase-resistant alcian ophilia at pH 0.5 indicating the presence of sulfated mucosubstances other than chondroitin 4- and 6- sulfates, probably keratan sulfates (*Kindblom & Angervall* 1975). One lesion (case 6) situated within striated muscle was particularly interesting because the whole lesion showed osteoid tissue, cartilage and bone formation (Figs. 16, 17 and 18). Marginally in these lesions there were proliferations of spindle-shaped fibroblast like cells encircling individual muscle fibres and bundles of muscle fibres.

Primary diagnoses. In 11 of the 13 retrospectively collected cases, the primary histological diagnosis was sarcoma. Four of them had been diagnosed as fibro- or fibromyxosarcoma, 2 as neurofibrosarcoma, 3 as rhabdo- or myosarcoma, and 2 as unspecified sarcoma. The remaining 2 tumours, both with bone formation, were diagnosed as myositis ossificans and osteochondroma.

Treatment and follow-up. In 16 patients local excision of the tumour was performed, which in 5 of them was immediately followed by wide surgical excision and in another followed by radiotherapy because of the initial diagnosis of sarcoma. Regional lymph node excision was performed in one of these patients. In 3 patients, in whom the tumour was initially diagnosed as sarcoma, only local excision was performed and no further treatment given. In one patient, wide surgical excision was performed after an initial biopsy suggestive of fibrosarcoma, and in another after cytological examination of an aspiration-biopsy suggestive of "fibromyxosarcoma".

Follow-up information was obtained in all patients. The length of the follow-up period in these patients ranged from 9 months to 17 years, with a median of 11 years. Four patients died, all of intercurrent diseases. In 3 of them an autopsy was performed. The remaining patients are alive and well, without signs of recurrences or metastases.

DISCUSSION

This study shows that there exists a close relationship between nodular fasciitis, proliferative fasciitis and proliferative myositis with the presence of mixed forms. We therefore propose that nodular fasciitis, proliferative fasciitis and proliferative myositis should be grouped under a more general descriptive term pseudosarcomatous proliferative lesions of soft tissue. However the terms nodular fasciitis, proliferative myositis and proliferative fasciitis may be retained as subtypes, with different gross structural patterns, light microscopic appearance and age-distribution within the spectrum of pseudosarcomatous proliferative lesions of soft tissue.

Proliferative myositis and proliferative fasciitis are considered distinguishable from nodular fasciitis, not only because of their gross structural appearance, but also because of their light microscopic appearance with large mono- and binucleated cells as predominating cell types. However nodular fasciitis is not always nodular: in approximately half the cases (*Dahl*, personal observations, 112 cases) the lesion is indistinctly delineated, extending along *fascial* planes or subcutaneous septa and radiating into the fat lobules as in the so-called repair variant of nodular fasciitis (*Allen* 1972). Furthermore, in classical forms of nodular fasciitis it is almost always possible to identify a few large mono- and binucleated cells (*Allen* 1972, *Dahl et al.* 1972) which are indistinguishable from those seen in proliferative fasciitis and proliferative myositis.

In 6 lesions in the present series, there were slit-like spaces or a tendency to cyst-forma-

Fig. 16. Proliferative lesion of soft tissue with bone formation within striated muscle. Case 6. Haematoxylin and eosin. × 2.

Figs. 17 and 18. The entire lesion shows bone trabeculae distributed in a manner suggestive of proliferative myositis surrounding single and small groups of muscle fibres. Case 6. Haematoxylin and eosin. × 6 and × 100.

16

17

18

In 4 lesions there were areas containing osteoid tissue, cartilage and/or bone trabeculae (Figs. 14 and 15). In areas with cartilage there were hyaluronidase-resistant alcianophilia at pH 0.5 indicating the presence of sulfated mucosubstances other than chondroitin 4- and 6- sulfates, probably keratan sulfates (*Kindblom* & *Angervall* 1975). One lesion (case 6) situated within striated muscle was particularly interesting because the whole lesion showed osteoid tissue, cartilage and bone formation (Figs. 16, 17 and 18). Marginally in these lesions there were proliferations of spindle-shaped fibroblast like cells encircling individual muscle fibres and bundles of muscle fibres.

Primary diagnoses. In 11 of the 13 retrospectively collected cases, the primary histological diagnosis was sarcoma. Four of them had been diagnosed as fibro- or fibromyxosarcoma, 2 as neurofibrosarcoma, 3 as rhabdo- or myosarcoma, and 2 as unspecified sarcoma. The remaining 2 tumours, both with bone formation, were diagnosed as myositis ossificans and osteochondroma.

Treatment and follow-up. In 16 patients local excision of the tumour was performed which in 5 of them was immediately followed by wide surgical excision and in another followed by radiotherapy because of the initial diagnosis of sarcoma. Regional lymph node excision was performed in one of these patients. In 3 patients, in whom the tumour was initially diagnosed as sarcoma, only local excision was performed and no further treatment given. In one patient, wide surgical excision was performed after an initial biopsy suggestive of fibrosarcoma, and in another after cytological examination of an aspiration-biopsy suggestive of "fibromyxosarcoma".

Follow-up information was obtained in all patients. The length of the follow-up period in these patients ranged from 9 months to 17 years, with a median of 11 years. Four patients died, all of intercurrent diseases. In 3 of them an autopsy was performed. The remaining patients are alive and well, without signs of recurrences or metastases.

DISCUSSION

This study shows that there exists a close relationship between nodular fasciitis, proliferative fasciitis and proliferative myositis with the presence of mixed forms. We therefore propose that nodular fasciitis, proliferative fasciitis and proliferative myositis should be grouped under a more general descriptive term pseudosarcomatous proliferative lesions of soft tissue. However the terms nodular fasciitis, proliferative myositis and proliferative fasciitis may be retained as subtypes, with different gross structural patterns, light microscopic appearance and age-distribution within the spectrum of pseudosarcomatous proliferative lesions of soft tissue.

Proliferative myositis and proliferative fasciitis are considered distinguishable from nodular fasciitis, not only because of *their* gross structural appearance, but also because of their light microscopic appearance with large mono- and binucleated cells as predominating cell-types. However nodular fasciitis is not always nodular: in approximately half the cases (*Dahl* personal observations, 112 cases) the lesion is indistinctly delineated, extending along fascial planes or subcutaneous septa and radiating into the fat lobules as in the so-called repair variant of nodular fasciitis (*Allen* 1972). Furthermore, in classical forms of nodular fasciitis it is almost always possible to identify a few large mono- and binucleated cells (*Allen* 1972, *Dahl et al.* 1972) which are indistinguishable from those seen in proliferative fasciitis and proliferative myositis.

In 6 lesions in the present series, there were slit like spaces or a tendency to cyst-forma-

Fig. 16. Proliferative lesion of soft tissue with bone formation within striated muscle. Case 6. Haematoxylin and eosin. × 2.

Figs. 17 and 18. The entire lesion shows bone trabeculae distributed in a manner suggestive of proliferative myositis surrounding single and small groups of muscle fibres. Case 6. Haematoxylin and eosin. × 6 and × 100.

16

17

18

teogenic sarcoma must always be excluded. In contrast to pseudosarcomatous proliferative lesions of soft tissue with bone formation, extra-skeletal osteogenic sarcomas are poorly differentiated (*Allan* & *Soule* 1971) and characterized by the formation of osteoid by anaplastic tumour cells. Furthermore, in none of our cases atypical mitoses, a frequent finding in extra-skeletal osteogenic sarcoma (*Enzinger* 1969) were present.

The study points out the difficulties in differentiating betwen the various forms of pseudosarcomatous proliferative, non-neoplastic soft tissue lesions, and emphasizes that accurate categorisation is of less importance than the recognition of the whole spectrum of these lesions, hence the avoidance of erroneous sarcoma diagnosis.

Supported by a research grant from the *Swedish Cancer Society* 530-K73-02X.

REFERENCES

Ackerman, L. V Extra-osseus localized non-neoplastic bone and cartilage formation (so-called myositis ossificans) J Bone Jt Surg 40 A 279–298, 1958

Allan C J & Soule E H Osteogenic sarcoma of the somatic soft tissue. Clinicopathologic study of 26 cases and review of literature. Cancer (Philad) 27 1121–1133 1971

Allen, P W Nodular fasciitis Pathology 4 9–26 1972

Angervall, L. Enerbäck L & K ... H Chondrosarcoma of soft tissue origin. Cancer (Philad) 32 507 513 1973

Angervall L Stener B Stener I & Ah ... C Pseudomalignant osseous tumour of soft tissue. A clinical, radiological and pathological study of five cases J Bone Jt Surg 51 B 634–663 1969

Burne J F On myositis ossificans traumatica. Ann. Surg 37 423–440 1903

Chung E B. & Enzinger F M Proliferative fasciitis Cancer (Philad) 36 1450–1458, 1975

Dahl I Angervall, L. Magnusson S & Stener B Classical and cystic nodular fasciitis. Pathol. Eur 7 211 221 1972.

Dahlin D C., Bone tumors. 2. ed. Charles C. Thomas, Springfield, Illinois, 1967 p. 246.

Enzinger F M Syllabus of miscellaneous soft tissue tumors. Who-reference set no. VIII Armed Forces Institute of Pathology Washington, 1969

Enzinger F M & Dulcey F., Proliferative myositis. Report of thirty-three cases. Cancer (Philad.) 20 2213–2223, 1967

Fine G & Stout A P., Osteogenic sarcoma of the extraskeletal soft tissues. Cancer (Philad.) 9 1027 1043 1956

Geschickter C F & Maseritz, I H: Myositis ossificans. J Bone Jt Surg 20 661–674 1938.

Gilmer W S Jr & Anderson L D. Reactions of soft somatic tissue which may progress to bone formation circumscribed (traumatic) myositis ossificans. Sth. med J (Bgham, Ala.) 52 1432 1448 1959

Hutter R V P., Stewart F W & Foot F W J., Fasciitis. A report of 70 cases with follow-up proving the benignity of the lesion. Cancer (Philad.) 15 992–1003 1962.

Kern W H Proliferative myositis a pseudosarcomatous reaction to injury A report of seven cases Arch. Path. 69 97–104 1960

Kindblom L-O & Angervall L. Histochemical characterization of mucosubstances in bone and soft tissue tumors. Cancer (Philad.) 36 985–994 1975.

Konwaler B E. Keasbey L. & Kaplan L. Subcutaneous pseudosarcomatous fibromatosis (fasciitis) Report of 8 cases. Amer J clin. Path. 25 241–252, 1955.

Lagier R & Cox J N Pseudomalignant myositis ossificans. A pathological study of eight cases. Hum. Pathol. 6 653–665 1975

Liebig, F Die Myositis ossificans circumscripta. Ergebn. Chir Orthop 22 501–584 1929

Noble T P Myositis ossificans. A clinical and radiological study Surg. Gynec. Obstet. 39 795–802, 1924

Solomon M P Rosen Y & Delman, A. Intraoral submucosal pseudosarcomatous fibromatosis Oral Surg 38 264 269 1974

Spjut H J., Dorfman H D Fechner R E. & Ackerman L V Tumors of bone and cartilage, second series, fascicle 6 AFIP Washington, D C., 1971

Stout A P.: Pseudosarcomatous fasciitis in children. Cancer (Philad.) 14 1216–1222, 1961

Tenstedt ... en A.: Beitrag zur proliferativen Myositis, einer wahrscheinlichen Variante der pseudosarkomatösen Fasciitis. Zbl. allg. Path. path. Anat. 116 364–371 1972.

Zugibe F T Diagnostic Histochemistry Mosby St Louis 1970, p. 298.

tion, so that the lesion resembled the so-called cystic nodular fasciitis (*Dahl et al.* 1972) a form of nodular fasciitis in which prolifera tion of large, plump mono- and binucleated cells are frequently encountered Moreover 2 lesions characterized histologically by proliferations of large mono- and binucleated cells, were rounded or almost nodular in structure, thus possessing the histologic but not the gross structural appearance, of proliferative fasciitis and proliferative myositis.

In contrast to nodular fasciitis which occurs in all ages (*Allen* 1972) all patients in the present series were 37 years old or more. This is in agreement with the observation that unlike nodular fasciitis, proliferative myositis and proliferative fasciitis do not affect children (*Enzinger & Dulcey* 1967 *Chung & Enzinger* 1975) This difference in age of the patient may be a reason for distinguishing proliferative fasciitis and proliferative myositis from nodular fasciitis. It is possible, however that it merely reflects different age-linked types of reaction to the same basic stimulus (*Tennstedt* 1972)

Four lesions in the present series showed a variable degree of bone formation In our opinion there are the following reasons for not including these lesions in the general category of myositis ossificans. The lesions showed a gross structural and/or a microscopic appearance of proliferative myositis and proliferative fasciitis with respect to the structural arrangement of the bone trabeculae furthermore the term is a misnomer (*Dahlin* 1967 *Spjut et al.* 1971) particularly if used for bone-forming non neoplastic lesions appearing outside skeletal muscles as in two of our cases (cases 3 and 12) Pseudomalignant osseous tumour of soft tissue is a term proposed by *Fine and Stout* (1956) for bone-forming lesions sometimes occurring in the subcutaneous tissue Pseudomalignant osseous tumour of soft tissue has been believed to be of infectious origin and considered to be closely related to proliferative myositis and nodular fasciitis (*Angervall et al* 1969 *Lagier & Cox* 1975) In the present cases, however the bone trabeculae were haphazardly arranged throughout the lesions, in contrast to the zoning phenomenon which characterizes pseudomalignant osseous tumour of soft tissue Furthermore clinical signs of infection, such as preceding respiratory throat infection, raised body temperature and elevated sedimentation rate, which have been described in pseudomalignant osseous tumour of soft tissue (*Angervall et al* 1969) were not known to be present in any of our patients. Case 6 is of particular interest since the entire lesion showed bone trabeculae distributed in a manner suggestive of proliferative myositis, surrounding single muscle fibres and bundles of fibres. Such lesions have probably earlier been described as myositis ossificans, and as early as 1903 *Binnie* described and sketched such a lesion. This type of ossifying lesion of soft tissue, lacking zonal phenomenon, seem to us related to proliferative myositis, and we think it preferable to include such lesions under the general term pseudosarcomatous proliferative lesion of soft tissue.

As in previous surveys, only a few patients in the present series spontaneously reported or recalled trauma in the area, prior to the appearance of the lesion (*Kern* 1960 *Enzinger & Dulcey* 1967 *Chung & Enzinger* 1975) The histogenesis of these pseudosarcomatous proliferative lesions of soft tissue has been ascribed to a reparative response to local nutritional or mechanical events caused by injury or a degenerative process (*Solomon et al.* 1974 *Enzinger & Dulcey* 1967 *Chung & Enzinger* 1975 *Lagier & Cox* 1975) The loosening and other degenerative tissue reactions of fascial or septal planes observed in 12 lesions in the present series seem to support this opinion.

In order to avoid an erroneous diagnosis of sarcoma 2 factors should be emphasized firstly that the pathologist is aware of the existence of these pseudosarcomatous proliferative lesions, and secondly that the gross structural appearance and the low-power view of the lesion in the light microscope is often conclusive in distinguishing the lesion from sarcoma In dealing with lesions of soft tissue with bone formation, extra skeletal os-

teogenic sarcoma must always be excluded. In contrast to pseudosarcomatous proliferative lesions of soft tissue with bone formation, extraskeletal osteogenic sarcomas are poorly differentiated (*Allen* & *Soule* 1971) and characterized by the formation of osteoid by anaplastic tumour cells. Furthermore, in none of our cases atypical mitoses, a frequent finding in extra-skeletal osteogenic sarcoma (*Enzinger* 1969) were present.

The study points out the difficulties in differentiating between the various forms of pseudosarcomatous proliferative non neoplastic soft tissue lesions, and emphasizes that accurate categorization is of less importance than the recognition of the whole spectrum of these lesions hence the avoidance of erroneous sarcoma diagnoses.

Supported by research grant from the *Swedish Cancer Society* 330-K73-02X.

REFERENCES

Ackerman, L. V. Extra-osseous localized non-neoplastic bone and cartilage formation (so-called myositis ossificans) J Bone Jt Surg 40 A 279–298, 1958.

Allen C J & *Soule E H* Osteogenic sarcoma of the somatic soft tissue. Clinicopathologic study of 26 cases and review of literature. Cancer (Philad) 27 1121 1133 1971

Allen P W Nodular fasciitis, Pathology 4 9–26 1972

Angervall, L. Enerback L & *Knutson H* Chondrosarcoma of soft tissue origin. Cancer (Philad) 32 507 515 1973

Angervall, L. Stener B Stener I & *Ahrén C* Pseudomalignant osseous tumour of soft tissue A clinical, radiological and pathological study of five cases J Bone Jt Surg 51 B 654–663 1969

Baume J P On myositis ossificans traumatica. Ann. Surg 37 423–440, 1903

Chung, E B & *Enzinger F M* Proliferative fasciitis Cancer (Philad) 36 1450–1458, 1975

Dahl I Angervall, L Magnusson S & *Stener B* Classical and cystic nodular fasciitis Pathol. Eur 7 211 221 1972

Dahlin D C. Bone tumors. 2. ed. Charles C. Thomas, Springfield, Illinois 1967 p 246.

Enzinger F M Syllabus of miscellaneous soft tissue tumors. Who-reference set no. VIII Armed Forces Institute of Pathology Washington. 1969

Enzinger F M & *Dulcey F* Proliferative myositis. Report of thirty-three cases. Cancer (Philad.) 20 2213–2223 1967

Fine G & *Stout A P* Osteogenic sarcoma of the extraskeletal soft tissues. Cancer (Philad.) 9 1027–1043 1956.

Geschickter C F & *Maseritz I H* Myositis ossificans. J Bone Jt Surg 20 661–674 1938.

Gilmer W S J & *Anderson L D* Reactions of soft somatic tissue which may progress to bone formation circumscribed (traumatic) myositis ossificans. 8th. med. J (Bgham, Ala.) 52 1432 1446, 1959

Hutter R V P., Stewart F W & *Foote F W Jr* Fasciitis. A report of 70 cases with follow-up proving the benignity of the lesion. Cancer (Philad.) 15 992 1003 1962.

Kern W H Proliferative myositis a pseudosarcomatous reaction to injury A report of seven cases. Arch. Path. 69 97–104 1960.

Kindblom L-G & *Angervall L.* Histochemical characterization of mucosubstances in bone and soft tissue tumors. Cancer (Philad.) 36 985–994 1975

Konwaler B. E., Keasbey L. & *Kaplan L.* Subcutaneous pseudosarcomatous fibromatosis (fasciitis) Report of 8 cases. Amer J clin. Path. 25 241-252, 1955.

Lagier R. & *Cox J N* Pseudomalignant myositis ossificans. A pathological study of eight cases. Hum. Pathol. 6 653–665 1975

Liebig, F Die Myositis ossificans circumscripta. Ergebn. Chir Orthop. 22 301–384 1929

Noble T P Myositis ossificans. A clinical and radiological study Surg Gynec. Obstet. 39 795–802, 1924

Solomon, M P Rosen Y & *Delman A* Intraoral submucosal pseudosarcomatous fibromatosis. Oral Surg. 38 264–269 1974

Spjut H J Dorfman, H D Fechner R. E. & *Ackerman L. V* Tumors of bone and cartilage second series, fascicle 5, AFIP Washington, D.C., 1971

Stout A P Pseudosarcomatous fasciitis in children. Cancer (Philad.) 14 1216–1222, 1961

Tenstedt ex A.: Beitrag zur proliferativen Myositis, einer wahrscheinlichen Variante der pseudosarkomatösen Fasciitis. Zbl. allg. Path. path. Anat. 116 364 371 1972.

Zugibe F T. Diagnostic Histochemistry Mosby St Louis, 1970. p. 298.

Acta path microbiol. scand. Sect. A 85 590–602 1977

COMPUTER ASSISTED IMAGE ANALYSIS OF FEULGEN-STAINED CELL NUCLEI FROM TRANSITIONAL CELL CARCINOMA OF THE HUMAN URINARY BLADDER

SOPHIE DOROTHEA FOSSÅ and OLAV KAALHUS

General Department and Department of Pathology The Norwegian Radium Hospital, and Department of Tissue Culture Norsk Hydro's Institute for Cancer Research, The Norwegian Radium Hospital Oslo, Norway
Department of Biophysics, Norsk Hydro's Institute for Cancer Research, The Norwegian Radium Hospital Oslo, Norway

Fosså S D and Kaalhus, O Computer assisted image analysis of Feulgen-stained cell nuclei from transitional cell carcinoma of the human urinary bladder Acta path. microbiol. scand. Sect A, 85 590–602 1977

Computer assisted image analysis was performed in Feulgen-stained cell nuclei from 117 transitional cell carcinomas of the human urinary bladder The results were compared to corresponding findings from a control group consisting of 27 specimens from non-malignant urothelium. Generally the mean nuclear area in carcinoma specimens was found to be increased as compared to the control group both in diploid and non-diploid tumours. The concentration and the distribution of nuclear chromatin, and the relative area and content of non-condensed chromatin were dependent on nuclear DNA-content and nuclear area. These nuclear parameters did not give supplementary information which could be used in discriminating benign urothelial cell nuclei from malignant ones. A multiple regression analysis, performed for diploid and non-diploid tumours separately did not show any significant correlation between the considered nuclear parameters and clinical stage of the tumour or the patient's survival.

Key words Urinary bladder transitional cell carcinoma computerized cell analysis.

Sophie Dorothea Fosså, The Norwegian Radium Hospital, Montebello, Oslo 3 Norway

Received 18 ii 77 Accepted 18.ii 77

A previous paper (*Fosså et al* in press) dealt with the clinical and histopathological significance of measurements of nuclear DNA-content in individual cells from human bladder carcinomas. Patients with non-diploid tumours had a worse prognosis than those with diploid carcinomas Decreasing histological differentiation and increasing clinical stage were associated with increased occurrence of non-diploid DNA values, indicating an unstable cell population.

In the present paper we discuss the histopathological and clinical relevance of cytological features such as nuclear size chromatin concentration, chromatin distribution and the area and content of non-condensed chromatin (*Fosså & Kaalhus 1976*) The prognostic value of these parameters is compared to the prognostic significance of determina

tion of the DNA-stemline ploidy clinical staging and histopathological grading

MATERIAL AND METHODS

A tumour biopsy ("actual biopsy") was taken from each of 117 patients (32–81 years old, mean age 64.2) with histologically proven bladder carcinomas admitted to the Norwegian Radium Hospital, during the year 1974 and from October 1st 1975 to March 31st 1976. Clinical staging of the bladder tumours was performed according to the TNM system (*UICC* 1974) slightly adjusted to the present study (*Fosså et al.* in press)

All bladder tumours revealing cellular anaplasia were denominated as carcinomas regardless of whether infiltrative growth was demonstrated or not. Histological grading was done according to *Mostofi* (1962) using the following system: Grade I = well differentiated tumours. Grade II = moderately differentiated tumours. Grade III = poorly differentiated tumours with preserved transitional cell character. Grade IV = undifferentiated tumours without transitional cell character. Table 1 summarises the relationship between clinical stage and histological grade in the 117 patients included in the study.

Follow-up was continued until July 1st 1976.

A control group consisted of urothelial biopsies from 24 patients with non-malignant urological disease and from 3 patients who died without urological disease; these specimens were taken immediately after death.

The technique of imprint preparation and Feulgen staining has been described previously (*Fosså* 1975). Selection of different regions in the imprints followed a definite random number system, measuring up to 10 non-clustering tumour cell nuclei within each region. The scanning cytophotometric measurements were performed in 100 cell nuclei in each specimen by means of SMP 05 (Zeiss, Oberkochen, W. Germany) connected to a Wang Desk Computer 720 B (objective Plan 100/1.25 oil condensor 40/0.6 diameter of the scanning unit 0.7 µm distance between centres of the two neighbouring scanning units 0.5 µm wavelength 570 nm). The computer program Areascan (Zeiss, Oberkochen, W. Germany) provided the scanning procedure and the light transmission measurements, and furthermore the nuclear parameters.

Figures 1 A and 1 B show the printed images of one Feulgen-stained diploid and one tetraploid cell nucleus. Each figure in the demonstrated nuclear area represents the extinction value ( ) measured in the actual scanning unit with the area a = 1 AU (AU = arbitrary units). For each scanning unit the extinction value given in arbitrary units, was calculated from the transmission value per scanning unit (t) based on the relationship

$$= -\log t$$

The following nuclear parameters were evaluated

Nuclear size ( ). Number of all scanning units in the extinction class 0.02–1.5

Mean nuclear size (A). Mean size of 100 measured cell nuclei per specimen.

Total nuclear extinction (te). Sum of all extinction values within the nuclear area. This so-called *Feulgen DNA-value* was taken as a quantitative expression of the nuclear DNA-content (*Swift* 1950, *Leuchtenberger et al.* 1954)

Mean nuclear extinction (TE). Mean of 100 measured nuclear Feulgen DNA-values per specimen.

The specimen DNA stemline was determined from the 100 DNA-values per specimen (*Fosså* 1975)

The *diploid DNA-value* was defined as the mean of 30 Feulgen DNA-values measured in polymor

TABLE 1 *Number of Patients with Diploid and Non-Diploid Bladder Carcinoma Related to Histological Grade and Clinical Stage*

DNA-stemline ploidy	Grade I			Grade II			Grade III			Grade IV			Total		
	Dipl.	Non-dipl.	All	Dipl.	Non-dipl.	All	Dipl.	Non-dipl.	All	Dipl.	Non-dipl.	All	Dipl.	Non-dipl.	All
Clinical stage: Stage I	25	2	27	14	7	21	2	9	11				41	18	59
Stage II III	2		2	1	1	2	5	13	18		2	2	8	16	24
Stage IV	2		2	3	4	7	2	15	17	5	3	8	12	22	34
Total	29	2	31	18	12	30	9	37	46	5	5	10	61	56	117

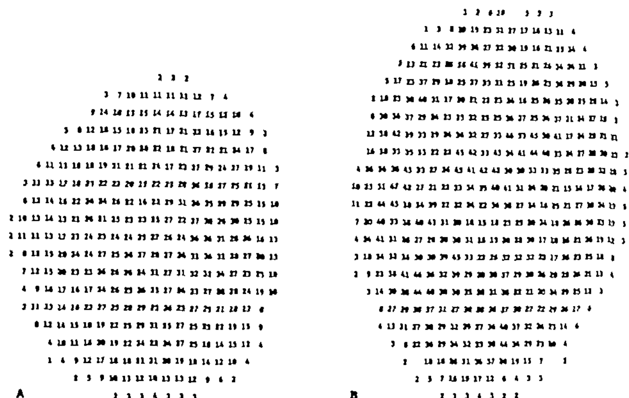


Fig 1 Print-out of computerized image analysis of a diploid (A) and a tetraploid (B) cell nucleus. Each figure represents the extinction value in a scanning unit.

phonuclear leukocytes in the actual specimen (internal standard)

Nuclear chromatin concentration (me) Mean extinction within a cell nucleus ($me = \frac{te}{a}$) measured in arbitrary units.

Mean chromatin concentration (ME) Mean of 100 me-values per specimen.

Difference value (di) This parameter represented the sum of all differences between two neighbouring transmission values (t_{i+1} and t_i) divided by the nuclear area ($di = \frac{\Sigma | t_{i+1} - t_i |}{a}$) This parameter yielded information about the chromatin structure of the Feulgen-stained nucleus. A homogeneous chromatin distribution in a cell nucleus gave a lower di-value than that obtained in a cell nucleus with coarse chromatin

Mean difference value (DI) Mean of 100 di values per specimen

Relative nuclear area of non-condensed chromatin ($r_{non-cond.}$) Relationship between area of non-condensed chromatin (= chromatin within the extinction class 0 02–0 22) and total nuclear area (*Fosså & Kaalhus* 1976) ($r_{non-cond.} = a_{non-cond.}/a$)

Mean relative nuclear area of non-condensed chromatin ($R_{non-cond.}$) Mean of 100 $r_{non-cond.}$ values per specimen

Relative nuclear content of non-condensed chromatin ($t_{non-cond.}$) Relationship between the amount of non-condensed chromatin and total nuclear extinction ($t_{non-cond.} = te_{non-cond.}/te$)

Mean relative nuclear content of non-condensed chromatin ($S_{non-cond.}$) Mean of 100 $t_{non-cond}$ values per specimen.

The above parameters were given the suffix e and l to indicate measurements of epithelial cell nuclei and leukocyte nuclei, respectively

Variation coefficient of nuclear area per specimen (Var coeff a)

Variation coefficient of nuclear chromatin concentration per specimen (Var coeff me)

The primary figures of the specimen mean values of the nuclear parameters were corrected to make allowances for unavoidable variations in the imprint, fixation and staining technique using the following correction procedure

$$X' = X \left(1 - \frac{X_i - \bar{X}_i}{\sqrt{X_i \cdot X}}\right)$$

Here

X' = corrected mean value per specimen

X = observed non-corrected mean value per specimen

$\bar{X}$ = observed non-corrected mean value in the complete study

(X = the particular parameter under discussion.)

To arrive at a numerical expression of the cell population DNA-deviation from the mean DNA-content of a non-proliferating diploid cell population, the *diploid deviation quotient DDQ* was defined as $DDQ = \frac{TE}{\text{diploid DNA-value}}$

In addition to the above-mentioned parameters, the number of *giant cell nuclei* (a > 700 AU) and *hyperchromatic cell nuclei* (me > 0.23 AU) in each specimen were recorded.

Statistical Evaluation

The significance of the difference between calculated means was tested by the Student t test. Differences were regarded as statistically significant if $p < 0.05$.

A multiple regression analysis of the above cytophotometric data was performed to test the prognostic significance of these parameters. The regression analysis was made separately for tumours with diploid and non-diploid DNA-stemline. Independent variables were the patient' age and all nuclear parameters listed above. Two dependent variables were considered:

1) *Observed death rate q*. This was the inverse lifetime of a patient after the actual biopsy. This part of the multiple regression analysis comprised only those patients who died during the observation period, t (75 patients). The observation period for each of these patients equalled the lifetime. The observed death rate was computed as $q = \frac{1}{t}$

2) *Clinical stage*. In order to quantitate clinical stage, stage I, stage II/III and stage IV were given the values 1, 2.5 and 4 respectively. All the 117 patients were included in this part of the multiple regression analysis.

The survival of the patients was computed according to the life table method (*Cutler & Ederer* 1958).

RESULTS

Sixty-one bladder carcinomas with diploid DNA-stemlines, and 56 with non-diploid DNA-stemlines were found.

The frequency distributions of the corrected mean nuclear area (A) in normal urothelium and carcinoma specimens are shown in Fig. 2a. Figure 2b demonstrates the histograms of the values of A for diploid and non-diploid tumours separately. A considerable overlap between the corrected mean nuclear area of diploid and non-diploid tumours is obvious.

Table 2 summarizes the numerical results of the cytophotometric image analysis considering DDQ and the corrected means of the investigated nuclear parameters with Var.coeff a and Var.coeff me.

The mean value of DDQ was increased in the carcinoma group compared to the control group. The upper 99 per cent confidence limit of DDQ-values in the control group was DDQ = 1.25.

The mean values of A in the carcinoma specimens was larger than that in the control group. The upper 99 per cent confidence limit for the corrected mean nuclear area in the control group was A = 321.1 AU.

The corrected mean nuclear area in 1619 diploid normal urothelial cell nuclei was compared to that in 935 diploid carcinoma cell

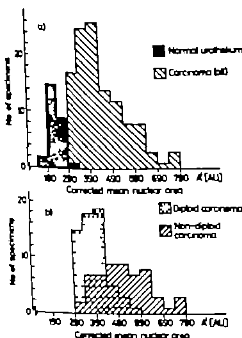


Fig. 2. Frequency distributions of corrected mean nuclear area (A) in 27 specimens from normal urothelium and 117 specimens from bladder carcinoma ( ) and from 61 specimens with diploid carcinoma and 56 specimens with non-diploid carcinoma (b).

A

B

Fig 1 Print-out of computerized image analysis of a diploid (A) and a tetraploid (B) cell nucleus. Each figure represents the extinction value in a scanning unit.

phonuclear leukocytes in the actual specimen (internal standard)

Nuclear chromatin concentration (me) Mean extinction within a cell nucleus ($me = \frac{te}{a}$) measured in arbitrary units.

Mean chromatin concentration (ME) Mean of 100 me-values per specimen.

Difference value (di) This parameter represented the sum of all differences between two neighbouring transmission values (t_{i+1} and t_i) divided by the nuclear area ($di = \frac{\Sigma |t_{i+1} - t_i|}{a}$). This parameter yielded information about the chromatin structure of the Feulgen-stained nucleus. A homogeneous chromatin distribution in a cell nucleus gave a lower di value than that obtained in a cell nucleus with coarse chromatin.

Mean difference value (DI) Mean of 100 di values per specimen

Relative nuclear area of non-condensed chromatin ($r_{non\text{-}cond}$) Relationship between area of non condensed chromatin (= chromatin with in the extinction class 0.02–0.22) and total nuclear area (Fosså & Kaalhus 1976) ($r_{non\text{-}cond} = a_{non\text{-}cond} / a$)

Mean relative nuclear area of non-condensed chromatin ($R_{non\text{-}cond}$) Mean of 100 $r_{non\text{-}cond}$ values per specimen

Relative nuclear content of non-condensed chromatin ($s_{non\text{-}cond}$) Relationship between the amount of non-condensed chromatin and total nuclear extinction ($s_{non\text{-}cond} = te_{non\text{-}cond} / te$)

Mean relative nuclear content of non-condensed chromatin ($S_{non\text{-}cond}$) Mean of 100 $s_{non\text{-}cond}$ values per specimen.

The above parameters were given the suffix e and l to indicate measurements of epithelial cell nuclei and leukocyte nuclei, respectively

Variation coefficient of nuclear area per specimen (Var coeff a)

Variation coefficient of nuclear chromatin concentration per specimen (Var coeff me)

The primary figures of the specimen mean values of the nuclear parameters were corrected to make allowances for unavoidable variations in the imprint, fixation and staining technique using the following correction procedure

$$X' = X \left(1 - \frac{X_l - \bar{X}_l}{\sqrt{X_l \cdot X}}\right)$$

Here

X' = corrected mean value per specimen

X = observed non-corrected mean value per specimen

$\bar{X}$ = observed non-corrected mean value in the complete study

(X = the particular parameter under discussion)

T arme t numerical expression of the cell population's DNA-deviation from the mean DNA content of non-proliferating diploid cell population, the *diploid deviation quotient DDQ* was defined as DDQ = $\frac{TE}{\text{diploid DNA-value}}$

In addition to the above-mentioned parameters, the number of *giant cell nuclei* (a > 700 AU) and *hyperchromatic cell nuclei* (me > 0.25 AU) in each specimen were recorded.

Statistical Evaluation

The significance of the difference between calculated means was tested by the Student' *t* test. Differences were regarded as statistically significant if $p < 0.01$

A multiple regression analysis of the above cytophotometric data was performed to test the prognostic significance of these parameters. The regression analysis was made separately for tumours with diploid and non-diploid DNA-stemline. Independent variables were the patient' age and all nuclear parameters listed above. Two dependent variables were considered

1) *Observed death rate q*. This was the inverse lifetime of a patient after the actual biopsy. This part of the multiple regression analysis comprised only those patients who died during the observation period, t (75 patients). The observation period for each of these patients equalled the lifetime. The observed death rate was computed as

$q = \frac{1}{t}$

2) *Clinical stage*. In order to quantitate clinical stage: stage I, stage II, III and stage IV were given the values 1, 2.5 and 4 respectively. All the 117 patients were included in this part of the multiple regression analysis.

The survival of the patients was computed according to the life table method (*Cutler & Ederer* 1958)

RESULTS

Sixty-one bladder carcinomas with diploid DNA-stemlines, and 56 with non-diploid DNA-stemlines were found.

The frequency distributions of the corrected mean nuclear area (A) in normal urothelium and carcinoma specimens are shown in Fig 2a. Figure 2b demonstrates the histograms of the values of A for diploid and non-diploid tumours separately. A considerable overlap between the corrected mean nuclear area of diploid and non-diploid tumours is obvious.

Table 2 summarizes the numerical results of the cytophotometric image analysis considering DDQ and the corrected means of the investigated nuclear parameters with Var coeff. a and Var.coeff. me

The mean value of DDQ was increased in the carcinoma group compared to the control group. The upper 99 per cent confidence limit of DDQ-values in the control group was DDQ = 1.23

The mean values of A in the carcinoma specimens was larger than that in the control group. The upper 99 per cent confidence limit for the corrected mean nuclear area in the control group was A = 321.1 AU

The corrected mean nuclear area in 1619 diploid normal urothelial cell nuclei was compared to that in 935 diploid carcinoma cell

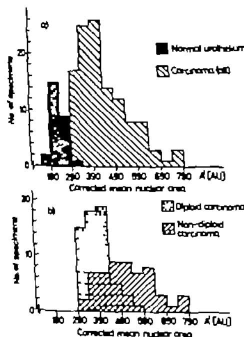


Fig 2. Frequency distributions of corrected mean nuclear area (A) in 27 specimens from normal urothelium and 117 specimens from bladder carcinoma ( ) and from 61 specimens with diploid carcinoma and 56 specimens with non-diploid carcinoma (b)

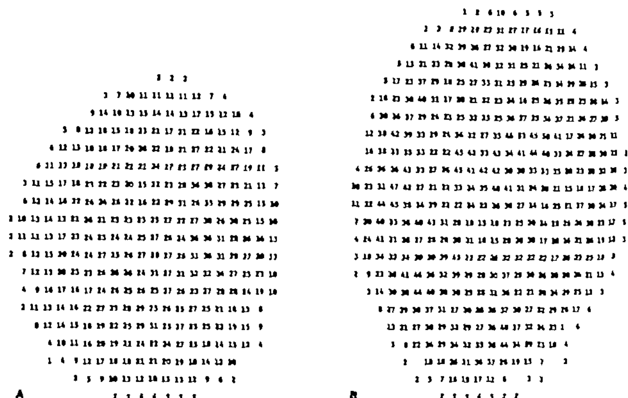


Fig 1 Print-out of computerized image analysis of a diploid (A) and a tetraploid (B) cell nucleus. Each figure represents the extinction value in a scanning unit.

phonuclear leukocytes in the actual specimen (internal standard)

Nuclear chromatin concentration (me) Mean extinction within a cell nucleus ($me = \frac{te}{a}$) measured in arbitrary units.

Mean chromatin concentration (ME) Mean of 100 me-values per specimen.

Difference value (di) This parameter represented the sum of all differences between two neighbouring transmission values (t_{i+1} and t_i) divided by the nuclear area ($di = \frac{\Sigma|t_{i+1}-t_i|}{a}$). This parameter yielded information about the chromatin structure of the Feulgen-stained nucleus. A homogeneous chromatin distribution in a cell nucleus gave a lower di value than that obtained in a cell nucleus with coarse chromatin.

Mean difference value (DI) Mean of 100 di-values per specimen.

Relative nuclear area of non-condensed chromatin ($r_{non-cond}$) Relationship between area of non condensed chromatin (= chromatin within the extinction class 0.02–0.22) and total nuclear area (*Fossâ & Kaalhus* 1976) ($r_{non\text{-}cond} = a_{non\text{-}cond}/a$).

Mean relative nuclear area of non-condensed chromatin ($R_{non-cond}$) Mean of 100 $r_{non\text{-}cond}$ values per specimen.

Relative nuclear content of non-condensed chromatin ($s_{non-cond}$) Relationship between the amount of non-condensed chromatin and total nuclear extinction ($s_{non\text{-}cond} = te_{non\text{-}cond}/te$).

Mean relative nuclear content of non-condensed chromatin ($S_{non-cond}$) Mean of 100 $s_{non\text{-}cond}$ values per specimen.

The above parameters were given the suffix e and l to indicate measurements of epithelial cell nuclei and leukocyte nuclei respectively.

Variation coefficient of nuclear area per specimen (Var coeff a)

Variation coefficient of nuclear chromatin concentration per specimen (Var coeff me)

The primary figures of the specimen mean values of the nuclear parameters were corrected to make allowances for unavoidable variations in the imprint, fixation and staining technique using the following correction procedure

$$X' = X\left(1 - \frac{X_l - \bar{X}_l}{\bar{X}_l \cdot X}\right)$$

Here

X' = corrected mean value per specimen

X = observed non-corrected mean value per specimen

$\bar{X}$ = observed non-corrected mean value in the complete study

(A the particular parameter under discussion)

T serves as a numerical expression of the cell population DNA-deviation from the mean DNA-content of non-proliferating diploid cell population, the *diploid deviation quotient DDQ* was defined as $DDQ = \frac{TE}{\text{diploid DNA-value}}$

In addition to the above-mentioned parameters, the number of giant cell nuclei (a > 700 AU) and hyperchromatic cell nuclei (me > 0.25 AU) in each specimen were recorded.

Statistical Evaluation

The significance of the difference between calculated means was tested by the Student' t test. Differences were regarded as statistically significant if $p < 0.05$

A multiple regression analysis of the above cytophotometric data was performed to test the prognostic significance of these parameters. The regression analysis was made separately for tumours with a diploid and non-diploid DNA-stemline. Independent variables were the patient age and all nuclear parameters listed above. Two dependent variables were considered

1) *Observed death rate q*. This was the inverse lifetime of a patient after the actual biopsy. This part of the multiple regression analysis comprised only those patients who died during the observation period, t (75 patients). The observation period for each of these patients equalled the lifetime. The observed death rate was computed as

$$q = \frac{1}{t}$$

2) *Clinical stage*. In order to quantitate clinical stage, stage I, stage II–III and stage IV were given the values 1, 2.5 and 4 respectively. All the 117 patients were included in this part of the multiple regression analysis.

The survival of the patients was computed according to the life table method (*Cutler & Ederer* 1958).

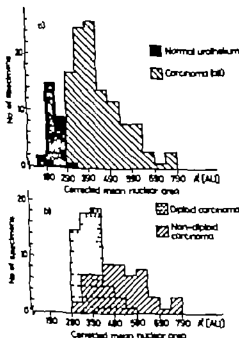


Fig. 2. Frequency distributions of corrected mean nuclear area (A) in 27 specimens from normal urothelium and 117 specimens from bladder carcinoma ( ) and from 61 specimens with diploid carcinoma and 56 specimens with non-diploid carcinoma (b).

RESULTS

Sixty-one bladder carcinomas with diploid DNA-stemlines, and 56 with non-diploid DNA-stemlines were found.

The frequency distributions of the corrected mean nuclear area (A) in normal urothelium and carcinoma specimens are shown in Fig. 2a. Figure 2b demonstrates the histograms of the values of A for diploid and non-diploid tumours separately. A considerable overlap between the corrected mean nuclear area of diploid and non-diploid tumours is obvious.

Table 2 summarizes the numerical results of the cytophotometric image analysis considering DDQ and the corrected means of the investigated nuclear parameters with Var. coeff. a and Var.coeff. me.

The mean value of DDQ was increased in the carcinoma group compared to the control group. The upper 99 per cent confidence limit of DDQ-values in the control group was DDQ 1.25.

The mean values of A in the carcinoma specimens was larger than that in the control group. The upper 99 per cent confidence limit for the corrected mean nuclear area in the control group was A = 321.1 AU.

The corrected mean nuclear area in 1619 diploid normal urothelial cell nuclei was compared to that in 935 diploid carcinoma cell

TABLE 2. *Numerical Results of the Cytophotometric Image Analysis in Feulgen-stained Cell Nuclei from Normal Urothelium and Bladder Carcinomas in Relation to the Tumours DNA-Stemline Ploidy*

Nuclear parameter	Control	Diploid tumours	Non-diploid tumours	All tumours
DDQ	1 06 ±0 066	1.21 ±0 204	2.14 ±0 764	1.65 ±0.717
A' [AU]	234.2 ±33.8	384 8 ±57.3	514.3 ±114.5	446 7 ±104.5
ME' [AU]	0 28 ±0 034	0 19 ±0 034	0 25 ±0.053	0.21 ±0 053
DI' [AU]	10.8 ±1.38	8 00 ±1.37	8.2 ±1.39	8.1 ±1.38
$R'_{non-cond.}$	0 63 ±0 087	0 82 ±0 166	0.75 ±0 123	0 79 ±0 150
$S'_{non-cond.}$	0 60 ±0 136	0.92 ±0.237	0 79 ±0 173	0.86 ±0.217
Var.coeff a	28 6 ±6.58	31 8 ±11 10	38.3 ±9.83	34 9 ±10.90
Var.coeff me	26 7 ±3 64	29 6 ±7 24	30 7 ±8.57	30 1 ±7.89

DDQ Diploid deviation quotient A corrected mean nuclear area ME corrected mean chromatin concentration DI corrected mean difference value $R_{non-cond.}$ corrected mean relative area of non-condensed chromatin $S'_{non-cond.}$ corrected mean relative content of non-condensed chromatin Var coeff.a Variation coefficient of nuclear area Var coeff.me Variation coefficient of nuclear chromatin concentration AU arbitrary units. (The figures refer to mean ± standard deviation within each group)

TABLE 3 *Corrected Mean Nuclear Area and Chromatin Concentration in Normal Urothelial Cell Nuclei and Cell Nuclei from Bladder Carcinomas*

	Nuclear area			Nuclear chromatin concentration		
	Diploid	Tetraploid	Octoploid	Diploid	Tetraploid	Octoploid
No. of nuclei	1619	51	4	1619	51	4
Control cell nuclei	228 4 ±69 4	462.9 ±180 6	517 0 ±170.2	0 28 ±0 07	0.30 ±0 04	0 45 ±0 1?
No. of nuclei	935	316	220	935	316	220
Carcinoma cell nuclei	349.3 ±89 6	586 9 ±192.6	784.3 ±304.5	0 16 ±0 05	0.20 ±0 07	0.29 ±0 10

nuclei (Table 3) The difference was statistically significant ($p < 0.05$) A similar difference was found between the corrected mean nuclear area of tetraploid normal and tetraploid carcinoma cell nuclei.

The mean chromatin concentration was lower in tumour cell nuclei than in normal cells within the same ploidy class (Table 3) In polyploid cells the nuclear size was increased to a lesser degree than the DNA content resulting in a slight increase of the mean chromatin concentration in polyploid cell nuclei compared to diploid cells.

The values showing the relationship between nuclear area (a) and chromatin concentration (me) (Fig 3a) were nearly ident

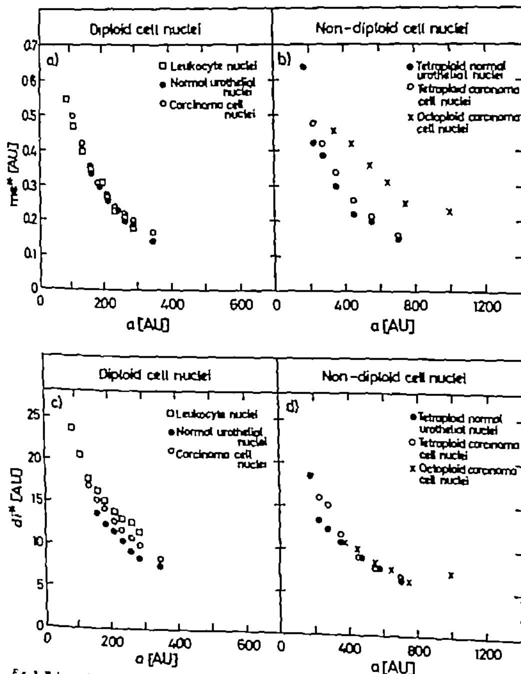


Fig. 3 Relationship between nuclear area and nuclear chromatin concentration (a, b), difference value (c, d) and relative area (e, f)/content (g, h) of non-condensed chromatin averaged per area interval (me* di* f*non-cond, i*non-cond) a nuclear area AU arbitrary units.

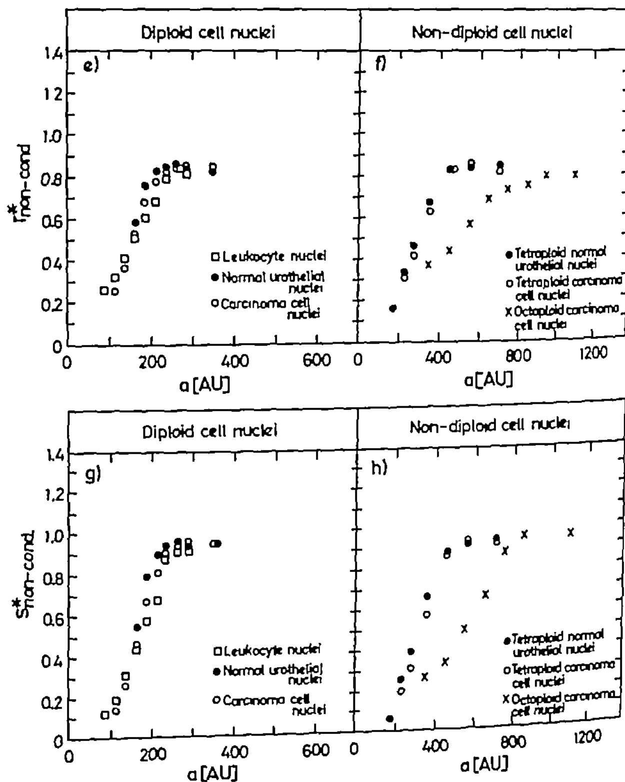


Fig 3 cont

ical for leukocyte nuclei, diploid normal urothelial and diploid carcinoma cell nuclei The same type of curve was found in tetraploid and octoploid nuclei (Fig 3b)

Figure 3c and Fig 3d show that the difference value (di) was influenced by nuclear area (a) in the same way as nuclear chromatin concentration (mc) *Increase of nuclear area without simultaneous DNA increase resulted in a decrease of the difference value*

TABLE 4 *Corrected Mean Nuclear Area (A) in Bladder Carcinomas Related to Clinical Stage Histological Grade and DNA-Stemline Ploidy*

DNA-stemline ploidy	Histological grade: Grade I			Grade II			Grade III			Grade IV			Total		
	Dipl	Non-dipl.	All	Dipl.	Non-dipl.	All	Dipl.	Non-dipl.	All	Dipl.	Non-dipl.	All	Dipl.	Non-dipl.	All
Stage I	369.9	575.7	385.1	391.0	540.4	440.8	406.9	522.5	501.4				378.9	535.3	426.5
Stage II–III	336.0		336.0	364.0	359.4	361.7	395.4	554.0	509.8		576.5	576.5	376.6	544.6	484.4
Stage IV	396.4		396.4	366.5	418.8	396.5	344.6	482.3	466.1	469.9	516.4	487.5	410.9	475.3	452.5
Total	369.5	575.7	382.6	385.4	484.7	425.1	386.6	517.2	491.6	469.9	540.4	505.1	384.8	514.3	446.7

TABLE 5 *Diploid Deviation Quotient (DDQ) in Bladder Carcinomas Related to Clinical Stage Histological Grade and DNA-Stemline Ploidy*

DNA-stemline ploidy	Histological grade: Grade I			Grade II			Grade III			Grade IV			Total		
	Dipl.	Non-dipl	All	Dipl.	Non-dipl.	All	D pl.	Non-dipl.	All	Dipl.	Non-dipl.	All	Dipl.	Non-dipl.	All
Stage I	1.11	1.80	1.16	1.22	2.27	1.57	1.27	2.14	1.98				1.15	2.15	1.45
Stage II III	1.18		1.18	1.20	1.60	1.40	1.37	2.42	2.12		2.18	2.18	1.30	2.33	1.98
Stage IV	1.14		1.14	1.24	1.61	1.45	1.44	2.06	1.98	1.49	2.23	1.76	1.36	2.00	1.77
Total	1.12	1.80	1.16	1.22	1.99	1.52	1.36	2.20	2.03	1.49	2.21	1.85	1.21	2.14	1.65

(di) The di-values for diploid normal urothelial cell nuclei in general seemed to be slightly lower than the di-values for carcinoma cell nuclei and leukocyte nuclei within the same area class. In non-diploid cell nuclei the di-values were only moderately increased as compared to corresponding diploid cell nuclei.

The dependency of $r_{non-cond}$ on nuclear area is shown in Fig. 3e and Fig. 3f. Correspondingly Fig. 3g and Fig. 3h give the values for $a_{non-cond}$. The values for relative area and content of non-condensed chromatin were nearly identical for leukocytes normal diploid urothelial cells and diploid cells from bladder carcinoma. The corresponding values of $r_{non-cond}$ and $a_{non-cond}$ tended to decrease proportionally to 1:0.5-0.25 in diploid, tetraploid and octoploid cell nuclei respectively.

The mean value of the variation coefficient of nuclear area (Var.coeff a) showed a slight increase in tumour specimens compared to the control group, more pronounced in non-diploid than in diploid tumours (Table 2). The differences, however were not statistically significant.

Tumour specimens showed a slightly increased mean value of the variation coefficient of chromatin concentration (Var.coeff me) compared to normal urothelium. Almost no difference was found between diploid and non-diploid carcinomas.

Table 4 and Table 5 show the parameters A and DDQ in diploid tumours compared to those in non-diploid tumours related to histological grade and clinical stage. In almost all subgroups non-diploid tumours had larger values of A and DDQ than the cor

TABLE 6 *Mean Percentage of Giant Cell Nuclei (a > 700 AU) and Hyperchromatic Cell Nuclei (me > 0.25 AU) in Normal Urothelium and Bladdder Carcinomas Related to Histological Grade and DNA-Stemline Ploidy*

		Diploid tumours					Non-diploid tumours					Total				
	Control	Grade I	Grade II	Grade III	Grade IV	All	Grade I	Grade II	Grade III	Grade IV	All	Grade I	Grade II	Grade III	Grade IV	All
No of giant cell nuclei %	0.4	1.3	3.4	2.7	12.6	3.1	27.0	13.2	17.7	12.4	16.6	3.0	6.9	14.9	12.5	9.5
No of hyperchromatic cell nuclei %	35.7	17.3	19.0	23.7	18.6	18.9	25.5	44.4	44.1	49.8	44.0	17.9	29.2	40.1	34.2	30.9

responding diploid ones With decreasing histological differentiation DDQ in both groups tended to increase Within the same histological grade there was no evident correlation of DDQ to clinical stage.

Table 6 gives the mean percentage of giant and hyperchromatic cell nuclei in the control group compared to that in diploid and non diploid tumours. In the diploid tumours an increasing number of giant cell nuclei was found in the more dedifferentiated carcinomas. In non-diploid tumours the number of giant cell nuclei was about 5 times higher than in diploid carcinomas but no increase was found with decreasing histological differentiation More hyperchromatic cell nuclei were observed in the non-diploid tumours than in the diploid ones, without clear correlation to histological grade in any group

By multiple regression analysis, made separately for diploid and non-diploid tumours, a weak positive correlation between the observed death rate and DDQ was found (correlation coefficient $r \approx 0.2$) The correlation was of the same magnitude as that between the patient's age and death rate No other criterium of prognostic value could be obtained from correlating the cytophotometric data with the patient's death rate.

Correlating the independent variables to clinical stage, only DDQ and the patient's age showed a positive correlation ($r \approx 0.2$)

In Table 7 the 117 patients are classified according to clinical stage DNA stemline ploidy and histological grade. The number of patients and the 20-month survival rate with its standard deviation are given for each subgroup separately Differences in cummulative survival rates of all patients belonging to stage I stage II III and stage IV were statistically significant ($p<0.01$) When further subdivision according to DNA-stemline ploidy was made, these differences were found both in patients with diploid and non diploid tumours, although not statistically significant in all groups.

The survival rates shown in Table 7 were at all clinical stages lower for the non-diploid cases than for the corresponding diploid ones, but only for stages IV was this difference statistically significant. The difference between survival rates was also statistically significant in favour of the diploid patients when combining all clinical stages ($p < 0.01$) Comparing Grade I and II carcinomas to Grade III and IV ones, histopathological evaluation seemed to have the same prognostic value as the DNA-stemline ploidy classification.

TABLE 7 *Cumulative Survival Rates (± Standard Deviation) at 20 Months in 117 Patients with Bladder Carcinoma Related to Clinical Stage (a), DNA-Stemline Ploidy (b) and Histological Grade (c)*

a)

	Stage I	Stage II–III	Stage IV	Stage II–III Stage IV	Total
	59* 0.90 ± 0.04	24 0.57 ± 0.11	34 0.17 ± 0.07	58 0.32 ± 0.07	117 0.61 ± 0.05

b)

DNA-stemline ploidy	Clinical stage				
	Stage I	Stage II–III	Stage IV	Stage II–III Stage IV	Total
Diploid	41 0.92 ± 0.05	8 0.57 ± 0.19	12 0.38 ± 0.15	20 0.45 ± 0.12	61 0.76 ± 0.06
Non-diploid	18 0.82 ± 0.13	16 0.57 ± 0.14	22 0.05 ± 0.05	38 0.25 ± 0.08	56 0.43 ± 0.07

c)

Histological grade	Clinical stage				
	Stage I	Stage II–III	Stage IV	Stage II–III Stage IV	Total
Grade I Grade II	48 0.90 ± 0.05	4 0.25 ± 0.22	9 0.11 ± 0.11	13 0.15 ± 0.10	61 0.73 ± 0.06
Grade III Grade IV	11 0.91 ± 0.09	20 0.65 ± 0.12	25 0.19 ± 0.09	45 0.39 ± 0.08	56 0.47 ± 0.07

* Number of patients within each group.

DISCUSSION

The program Areascan is a modification of the TICAS program which was developed by *Wied et al.* (1968) for cytophotometric image analysis of exfoliated Papanicolaou-stained cells from the female genital tract. By means of the Areascan program it is possible to quantitate nuclear size, chromatin concentration and chromatin distribution in individual Feulgen-stained cells. In addition, the area and content of non-condensed chromatin can be estimated.

During scanning cytophotometry visual control of the individual cell to be measured can be obtained, and obvious sources of error can be avoided, e.g. by ignoring overlapping and destroyed cell nuclei. When using the mean value of a nuclear parameter as a discriminator between different cell populations it would be desirable to perform a large number of observations per specimen. As the cytophotometric method is time-consuming, however, in practice only a limited number of cell nuclei can be examined. In this study it has been assumed that the mean value of a nuclear parameter calculated from 100 cells per specimen could be considered representative of the cell population and might be used to compare different cell populations. Contrary to other authors (*Böhm et al.* 1971, *Nodskov Pedersen* 1971, *Zetterberg & Esposti* 1976) we used an at random selection procedure by

which all non-clustering cell nuclei with intact nuclear envelope were measured not only those with obviously malignant appearance. However to discriminate between diploid tumour cell nuclei and nuclei from non tumour cells, for example macrophage nuclei (*Evans* 1972) may be difficult and this factor must be regarded as a possible methodological source of error

The technique of taking the biopsy specimens and preparing the imprints are detailed procedures Due to unavoidable methodological variations, small but registrable variations of the cytophotometric results will often be observed In order to obtain more homogeneous results we therefore introduced a correction procedure to make allowance for such variations.

As preliminary studies have shown (*Fossd* unpublished results) non proliferating granulocytes in carcinoma patients do not seem to change their mean nuclear area in contrast to what is to be expected in lymphocytes, due to their increased DNA synthesis found in carcinoma patients (*Huber et al* 1971 *Heier & Godal* 1977) Any variations of the mean nuclear area of Feulgen-stained granulocyte nuclei were therefore most likely due to methodological variation We have therefore used granulocyte nuclei as an internal standard in each specimen assuming that the variations from technical reasons influence granulocyte and epithelial cell in the same way

The normal transitional epithelium shows marked morphological variation in the thickness of the epithelium and in the size and the chromatin concentration of the cell nuclei (*Starklint et al* 1976) *Koss* (1975) suggested that normal urothelium may show variants which may be misinterpreted as due to proliferative changes. The relatively high mean values of the variation coefficients for nuclear size and chromatin concentration found in our control group confirm the above cited authors' opinion that normal urothelium may show remarkable intercellular variations In addition hyperchromatic cell nuclei were frequently found in the control group (35 7 per cent) No difference was noted in the above parameters between the 24 surgical biopsies and the 3 post mortem specimens in the control material.

We found that the mean nuclear size of most of the malignant bladder tumours increased compared to that of normal urothelium The upper 99 per cent confidence limit for mean nuclear size in the control group was 321 1 AU A value A > 321 1 AU therefore strongly indicates that the considered specimen represents a bladder carcinoma biopsy Mean nuclear sizes below A = 321 1 AU may refer either to normal urothelium or to carcinoma specimens. *Koss et al* (1975) however found no statistically significant difference between the size of cell nuclei in normal urothelium and bladder carcinoma. It seems most likely that the discrepancy between these authors results and our findings can be explained by differences in the procedure of selection of the cell nuclei to be measured and by the limited number of cell nuclei measured by *Koss et al* (1975)

We observed nuclear enlargement both in diploid and polyploid carcinoma cells compared to normal urothelial cell nuclei in the same ploidy class (Table 3) confirming our previous observations (*Fossd & Kaalhus* 1976) It should be emphasized however that nuclear enlargement has also been described in non malignant conditions such as benign hypertrophy (*Avtandilov & Nesterov* 1970) in benign tumours (*Avtandilov & Kazantseva* 1973) during DNA synthesis (*Andersson & Agrell* 1972) after irradiation (*Capoferro* 1973) in association with inflammatory processes (*Nilsson* 1976) and in association with increased nuclear function (*Schneider et al* 1973)

As many as 39 of 117 carcinoma specimens —mostly from well differentiated tumours—showed DDQ-values below the upper 99 per cent confidence limit of normal urothelium (DDQ = 1 23) DDQ seemed therefore to be a poor discriminator when differentiating between normal urothelial and carcinoma specimens.

Like the nuclear chromatin concentration

the nuclear parameters d_l, $r_{max-cond}$ and $s_{max-cond}$ were all functions of nuclear DNA content and nuclear area. The corresponding mean nuclear parameters ME, DI, $R_{max-cond}$ and $S_{max-cond}$ did therefore not give supplementary information for discrimination between cells from normal urothelium and bladder carcinoma.

We found that the occurrence of giant cell nuclei was more closely correlated to the diploid tumours histological grade than was the occurrence of hyperchromatic cell nuclei. Furthermore a similar mean percentage of hyperchromatic cell nuclei was observed in the control group and in the carcinoma group (Table 6). These observations and the results concerning the variation coefficients a and me (Table 2) might suggest that histological grading of bladder carcinoma is based on changes of nuclear size to a larger degree than on changes of nuclear chromatin concentration. However one may discuss the justification of comparing the results from measuring Feulgen-stained imprints to findings made in haematoxylin-eosin-stained histological sections. The basic principles of the two staining procedures differ essentially and the morphological appearances of cell nuclei in an imprint may vary considerably from those found in histological sections.

The results of the multiple regression analysis, done separately from diploid and non diploid tumours, showed that the presented cytophotometric parameters did not correlate significantly to the patient's survival, or to the clinical stage. DNA-stemline ploidy, clinical stage and histopathological grade, however did have definite prognostic significance confirming the authors' previous observations (*Fosså et al.* in press).

This work was supported by grants from Grosserer N. A. Stang, *Legat til Kreftsykdommens Bekjempelse*, *K. og K. Olsens O.A.S. fond for Kreftforskning, Nansenfond* and the *Norwegian Cancer Society*.

REFERENCES

Andersson G. K. A. & Agrell I. P. S.: Cytoplasmic and nuclear growth during the proliferation of Ehrlich ascites tumour cells in mice. Virchows Arch. Abt. B. Zellpath. *11* 11-19, 1972.

Artandilov G. G. & Kazantseva I. A.: Comparative microspectrophotometric study of the DNA content in the diagnosis of pre-tumorous processes and cancer. Virchows Arch. Abt. A. Path. Anat. 359 289-297, 1973.

Artandilov G. G. & Nesterov E. N.: Reversibility of experimental hypertrophy of the myocardium of the right ventricle. Bull. exp. Biol. Med. 69 401-404, 1970.

Böhm N., Roka S., Sprenger E. & Wagner D.: Absorptions- und fluoreszenzcytophotometrische DNS-Bestimmungen an vaginal-cytologischem Material. Acta histochem. (Jena) Suppl. *10* 233-242, 1971.

Capoferro R.: Increased nuclear diameter of gastric parietal cells after X irradiation in the guinea pig. Acta path. microbiol. scand. Sect. A, *81* 591-592, 1973.

Cutler S. J. & Ederer F.: Maximum utilization of the life table method in analyzing survival. J. chron. Dis. *8* 699-712, 1958.

Evans R.: Macrophages in syngeneic animal tumours. Transplantation *14* 468-473, 1972.

Fosså S. D.: Feulgen-DNA-values in transitional cell carcinoma of the human urinary bladder. Beitr. Path. *155* 44-55, 1975.

Fosså, S. D. & Kaalhus, O.: Nuclear size and chromatin concentration in transitional cell carcinoma of the human urinary bladder. Beitr. Path. *157* 109-125, 1976.

Fosså, S. D. & Kaalhus O.: "Non-condensed" and condensed" chromatin in transitional cell carcinoma of the human urinary bladder. Beitr. Path. *158* 241-254, 1976.

Fosså S. D., Kaalhus O. & Scott-Knudsen O.: The clinical and histopathological significance of Feulgen DNA-values in transitional cell carcinoma of the human urinary bladder. Europ. J. Cancer, in press.

Høst H. E. & Godal T.: DNA synthesis in unstimulated blood lymphocytes of patients with untreated malignant lymphomas or other malignant tumors. Scand. J. Haematol. *18* 149-153, 1977.

Huber C., Huber H., Gföller A., Michlmayr G. & Braunsteiner H.: DNS-synthetisierende Blutlymphocyten bei Karzinompatienten. Med. Klin. *66* 1441-1445, 1971.

Koss, L. G.: Tumors of the urinary bladder. Atlas of tumor pathology. Second Series, Fascicle 11. AFIP, Washington D.C. 1975, p. 64.

Koss, L. G., Bartels P. H., Bibbo M., Freed S. Z., Taylor J. & Wied G. L.: Computer discrimination between benign and malignant urothelial cells. Acta cytol. *19* 378-391, 1975.

Leuchtenberger C., Leuchtenberger R. & Davis, A. M.: A microspectrophotometric study of the

which all non-clustering cell nuclei with intact nuclear envelope were measured not only those with obviously malignant appearance. However to discriminate between diploid tumour cell nuclei and nuclei from *non tumour cells*, for example macrophage nuclei (*Evans* 1972), may be difficult and this factor must be regarded as a possible methodological source of error

The technique of taking the biopsy specimens and preparing the imprints are detailed procedures Due to unavoidable methodological variations, small but registrable variations of the cytophotometric results will often be observed In order to obtain more homogeneous results we therefore introduced a correction procedure to make allowance for such variations.

As preliminary studies have shown (*Fosså* unpublished results) non proliferating granulocytes in carcinoma patients do not seem to change their mean nuclear area in contrast to what is to be expected in lymphocytes, due to their increased DNA synthesis found in carcinoma patients (*Huber et al* 1971 *Heier & Godal* 1977) Any variations of the mean nuclear area of Feulgen stained granulocyte nuclei were therefore most likely due to methodological variation We have therefore used granulocyte nuclei as an internal standard in each specimen assuming that the variations from technical reasons influence granulocyte and epithelial cell in the same way

The normal transitional epithelium shows marked morphological variation in the thickness of the epithelium and in the size and the chromatin concentration of the cell nuclei (*Starklint et al* 1976) *Koss* (1975) suggested that normal urothelium may show variants which may be misinterpreted as due to proliferative changes The relatively high mean values of the variation coefficients for nuclear size and chromatin concentration found in our control group confirm the above cited authors' opinion that normal urothelium may show remarkable intercellular variations In addition hyperchromatic cell nuclei were frequently found in the control group (35 7 per cent) No difference was noted in the above parameters between the 24 surgical biopsies and the 3 post mortem specimens in the control material.

We found that the mean nuclear size of most of the malignant bladder tumours increased compared to that of normal urothelium. The upper 99 per cent confidence limit for mean nuclear size in the control group was 321 1 AU A value A > 321 1 AU therefore strongly indicates that the considered specimen represents a bladder carcinoma biopsy Mean nuclear sizes below A = 321 1 AU may refer either to normal urothelium or to carcinoma specimens *Koss et al* (1975) however found no statistically significant difference between the size of cell nuclei in normal urothelium and bladder carcinoma. It seems most likely that the discrepancy between these authors results and our findings can be explained by differences in the procedure of selection of the cell nuclei to be measured and by the limited number of cell nuclei measured by *Koss et al.* (1975)

We observed nuclear enlargement both in diploid and polyploid carcinoma cells compared to normal urothelial cell nuclei in the same ploidy class (Table 3) confirming our previous observations (*Fosså & Kaalhus* 1976) It should be emphasized however that nuclear enlargement has also been described in non malignant conditions such as benign hypertrophy (*Avtandilov & Nesterov* 1970) in benign tumours (*Avtandilov & Kazantseva* 1973) during DNA synthesis (*Andersson & Agrell* 1972) after irradiation (*Capoferro* 1973) in association with inflammatory processes (*Nilsson* 1976) and in association with increased nuclear function (*Schneider et al* 1973)

As many as 39 of 117 carcinoma specimens —mostly from well differentiated tumours— showed DDQ values below the upper 99 per cent confidence limit of normal urothelium (DDQ = 1 23) DDQ seemed therefore to be a poor discriminator when differentiating between normal urothelial and carcinoma specimens.

Like the nuclear chromatin concentration,

Acta path. microbiol. scand. Sect. A, 85: 603–610 1977

DNA VARIATIONS IN NEIGHBOURING EPITHELIUM IN PATIENTS WITH BLADDER CARCINOMA

SOPHIE DOROTHEA FOSSÅ

General Department and Department of Pathology, The Norwegian Radium Hospital and Department of Tissue Culture, Norsk Hydro's Institute for Cancer Research, Oslo, Norway

Fosså, S. D. DNA-variations in neighbouring epithelium in patients with bladder carcinoma. Acta path. microbiol. scand. Sect. A, 85: 603–610, 1977.

Histologically atypical urothelium taken from bladder mucosa neighbouring transitional cell carcinoma showed similar, though less marked DNA-changes as observed in the corresponding tumours. A definite increase in the number of non-diploid DNA-values was found in 6 (of 12) urothelial specimens. The clinical significance of urothelial DNA-changes is discussed.

Key words: Bladder carcinoma; epithelium; DNA-variations.

Sophie Dorothea Fosså, The Norwegian Radium Hospital, Montebello, Oslo 3, Norway.

Received 18.i.77. Accepted 18.ii.77

Nuclear DNA-changes in bladder carcinoma demonstrated by quantitative cytophotometry have been described previously (*Tavares et al.* 1966, *Levi et al.* 1969a, *Lederer et al.* 1972, *Fosså* 1975) and are in good agreement with findings from chromosome studies (*Shigematsu* 1965, *Lamb* 1967, *Falor* 1971, *Spooner & Cooper* 1972).

The non-tumour-bearing urothelium in patients with bladder carcinoma quite often shows histopathological changes, varying from hyperplasia to definite carcinoma *in situ* (*Eisenberg et al.* 1960, *Schade & Swinney* 1973). Furthermore urothelial carcinoma *in situ* has been found to precede an invasive carcinoma by several years (*Schade & Swinney* 1973).

The aim of the present study was to investigate to what extent nuclear DNA-changes are present in the urothelium in patients with bladder carcinoma.

MATERIAL AND METHODS

The material comprised 11 patients with histologically proven bladder carcinoma, 7 males and 4 females, identified by the numbers 1–11. The patients were clinically staged according to a modified TNM system (*UICC* 1974) in that stage II and stage III were grouped as a combined stage II/III (*Fosså et al.* in press). The Bristol Bladder Tumour Registry's definition of multiple versus single tumours was applied (*Miller et al.* 1969).

Specimens of bladder mucosa appearing normal to inspection and preferably taken near by the bladder tumour were obtained from the patients. In 4 patients the biopsy specimen was taken by transurethral resection, and total cystectomy specimens provided the biopsy material in 7. Simultaneous tumour biopsies were obtained in all patients except one. This patient (No. 10) had been treated by bladder wall resection two years previously and had now disseminated disease. At the time of the urothelial biopsy no locally recurrent bladder tumour could be found. In one patient (No. 11) who had multiple bladder tumours, mucosal and tumour biopsies were taken from both the right and the left side of the bladder wall.

The control group comprised 8 cystotomy specimens of the bladder mucosa, 7 from males and one

desoxyribose nucleic acid (DNA) content in cells of normal and malignant human tissues. Amer J Path. 30 65–85 1954

Mostofi F K Pathology of cancer of bladder Acta Un. int. Cancer *18* 611–615 1962.

Nilsson G Nuclear size classes in the follicular epithelium of lymphoid thyroiditis. Acta path. microbiol. scand. Sect. A *84* 165–171 1976.

Nedskov-Pedersen S Degree of malignancy of cancer involving the cervix uteri judged on the basis of clinical stage histology size of nuclei, and content of DNA. Acta path. microbiol. scand. Sect. A *79* 617–628 1971

Schneider E Henkamp U & Pera F Loss of heteropycnosis of the constitutive heterochromatin in specifically activated cells of the thyroid gland of *Microtus agrestis*. Chromosoma (Berl.) *41* 167–173 1973

Starklint H Jensen N K & Thybo E. The extent of carcinoma *in situ* in urinary bladders with primary carcinomas. Acta path. microbiol. scand Sect. A, *84* 130–136 1976

Swift H H. The desoxyribose nucleic acid content of animal nuclei. Physiol Zool. *23* 169–200 1950

UICC TNM classification of malignant tumours, 2 ed. International Union Against Cancer Geneva 1974 p 79–83

Wied G L Bartels P H Bahr G F & Oldfield D G Taxonomic intra-cellular analytic system (TICAS) for cell identification. Acta cytol. *12* 180–204 1968.

Zetterberg A & Esposti, P L Cytophotometric DNA-analysis of aspirated cells from prostatic carcinoma. Acta cytol. *20* 46–57 1976

Acta path. microbiol. scand. Sect. A, 85: 603–610, 1977

DNA VARIATIONS IN NEIGHBOURING EPITHELIUM IN PATIENTS WITH BLADDER CARCINOMA

Sophie Dorothea Fosså

General Department and Department of Pathology, The Norwegian Radium Hospital, and Department of Tissue Culture, Norsk Hydro's Institute for Cancer Research, Oslo, Norway

Fosså, S. D. DNA-variations in neighbouring epithelium in patients with bladder carcinoma. Acta path. microbiol. scand. Sect. A, 85: 603–610, 1977.

Histologically atypical urothelium taken from bladder mucosa neighbouring transitional cell carcinoma showed similar, though less marked, DNA-changes as observed in the corresponding tumours. A definite increase in the number of non-diploid DNA-values was found in 6 (of 12) urothelial specimens. The clinical significance of urothelial DNA-changes is discussed.

Key words: Bladder carcinoma; epithelium; DNA-variations.

Sophie Dorothea Fosså, The Norwegian Radium Hospital, Montebello, Oslo 3, Norway.

Received 18.ii.77. Accepted 18.ii.77.

Nuclear DNA-changes in bladder carcinoma demonstrated by quantitative cytophotometry have been described previously (*Tavares et al.* 1966, *Levi et al.* 1969a, *Lederer et al.* 1972, *Fosså* 1975) and are in good agreement with findings from chromosome studies (*Shigematsu* 1965, *Lamb* 1967, *Falor* 1971, *Spooner & Cooper* 1972).

The non-tumour-bearing urothelium in patients with bladder carcinoma quite often shows histopathological changes, varying from hyperplasia to definite carcinoma *in situ* (*Eisenberg et al.* 1960, *Schade & Swinney* 1973). Furthermore, urothelial carcinoma *in situ* has been found to precede an invasive carcinoma by several years (*Schade & Swinney* 1973).

The aim of the present study was to investigate to what extent nuclear DNA-changes are present in the urothelium in patients with bladder carcinoma.

MATERIAL AND METHODS

The material comprised 11 patients with histologically proven bladder carcinoma, 7 males and 4 females, identified by the numbers 1–11. The patients were clinically staged according to a modified TNM system (*UICC* 1974) in that stage II and stage III were grouped as a combined stage II/III (*Fosså et al.*, in press). The Bristol Bladder Tumour Registry' definition of multiple versus single tumours was applied (*Muller et al.* 1969).

Specimens of bladder mucosa appearing normal to inspection and preferably taken near by the bladder tumour were obtained from the patients. In 4 patients the biopsy specimen was taken by transurethral resection, and total cystectomy specimens provided the biopsy material in 7. Simultaneous tumour biopsies were obtained in all patients except one. This patient (No. 10) had been treated by bladder wall resection two years previously and had now disseminated disease. At the time of the urothelial biopsy no locally recurrent bladder tumour could be found. In one patient (No. 11) who had multiple bladder tumours, mucosal and tumour biopsies were taken from both the right and the left side of the bladder wall.

The control group comprised 8 cystotomy specimens of the bladder mucosa, 7 from males and one

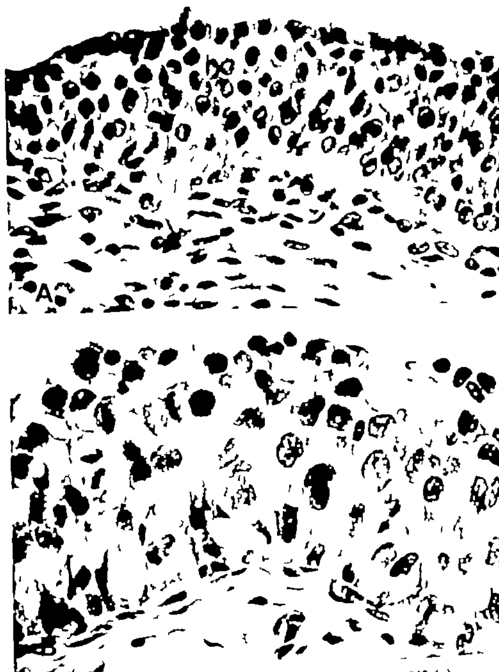


Fig 1 Urothelial specimen from the control group Haematoxylin-eosin. × 540 (a) Moderately atypical hyperplasia of the urothelium in a patient with bladder carcinoma (No 8) Haematoxylin-eosin × 540 (b)

from a female. Five specimens were taken from patients with benign prostatic hyperplasia. Three specimens were taken immediately after death from patients who died without urological disease

All biopsy specimens were divided into two parts one for imprint preparation the other for preparation of histological sections Imprints from each biopsy were made on two fatfree glass slides The glass slides were touched several times with a freshly cut tumour surface or with the mucosal surface of the urothelium specimen. The imprints were fixed and stained by Feulgen's method as described previously (*Fosså* 1975) In each imprint 100 randomly chosen cell nuclei were measured by absorption cytophotometry (*Fosså et al.* in press) taking the total nuclear extinction (te) given in arbitrary units (AU) as an expression of the nuclear DNA-value. The mean total nuclear extinction of 30 polymorphonuclear leukocytes yielded the diploid DNA-value used as an internal stand-

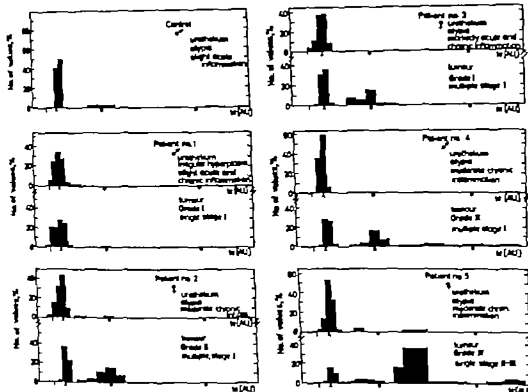


Fig. 2 DNA-frequency distributions (m) in a urothelial biopsy from the control group and in the urothelium and in a tumour biopsy in patients with bladder carcinoma. Normal DNA-frequency distribution in the urothelial biopsy (AU arbitrary units) × diploid DNA-value ○ tetraploid DNA-value ● octoploid DNA-value

ard for each preparation (*Böhm & Sandritter* 1975)

The DNA-stemline for each specimen was established from the frequency distribution of the measured DNA-values. The presence of more than 15 per cent non-diploid DNA-values was taken as evidence of abnormal DNA-changes in the urothelium (*F ... et al*, in press)

Histological sections were cut from paraffin embedded material, and were stained with haematoxylin-eosin. The histological evaluation of the tumour specimens was based on the grading system proposed by *M ...* (1962) defining well differentiated tumours (Grade I) moderately differentiated tumours (Grade II) poorly differentiated tumours with preserved transitional cell character (Grade III) and undifferentiated tumours with loss of transitional cell character (Grade IV). All epithelial bladder tumours revealing cellular anaplasia were designated as carcinomas regardless of whether they showed infiltrative growth or not. The mucosal biopsies were recorded as normal urothelium or as urothelium showing either simple, irregular moderately typical or markedly typical hyperplasia (Fig 1). Furthermore, the degree of the acute or chronic inflammatory changes was recorded as slight, moderate or marked.

RESULTS

In all specimens of the control group the DNA histograms showed a diploid DNA stemline with 8–10 per cent non-diploid DNA-values. These were usually found within the tetraploid range, although infrequent octoploid and intermediate values were also recorded (Fig 2). There was no difference between the results from urothelial biopsies obtained from patients with prostatic hyperplasia and the post-mortem specimens.

Histologically five specimens from the control group showed normal bladder mucosa.

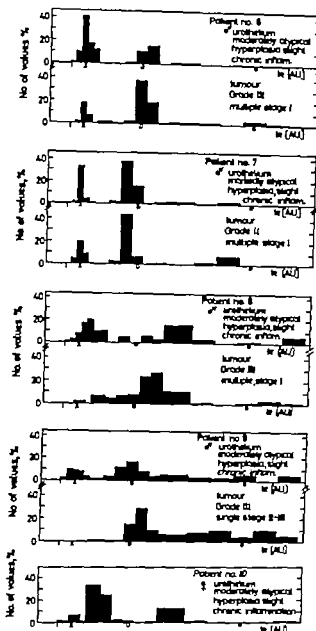


Fig 3 DNA frequency distributions (te) in biopsies from patients with bladder carcinoma Abnormal DNA frequency distribution in the urothelial biopsy (AU arbitrary units) × diploid DNA value ○ tetraploid DNA value ● octoploid DNA value

Two specimens, both taken from patients with prostatic hyperplasia, showed a slight degree of mucosal inflammation In one control specimen slight mucosal inflammation combined with simple urothelial hyperplasia was recorded.

DNA-distributions of the same kind as in the control group were found in the mucosal biopsies from 5 tumour-bearing bladders (Fig 2) Histologically irregular urothelial hyperplasia was recorded in one of these patients (No 1) while no urothelial irregularities were observed in the other 4 All biopsies showed inflammatory changes of varying degree. Two patients had single tumours, one of these a well differentiated diploid stage I carcinoma (No 1) the other a non-diploid stage II–III tumour of Grade IV (No. 5) *Three patients had multiple stage I tumours of Grade I (No 3) and Grade II (Nos. 2 and 4) The DNA frequency distribution in* one of the *multiple tumours in each of these* three patients revealed a diploid DNA-stemline with an increased number of non-diploid DNA values as compared with the control group

Abnormal DNA frequency distributions in the mucosal biopsies were found in 5 patients (Fig 3) One patient showed a diploid DNA stemline with 29 per cent non-diploid DNA values (No 6) In another the DNA frequency distribution was bimodal (diploid and *tetraploid DNA-stemline) (No. 7) while 3 patients revealed a non-diploid DNA stemline (Nos. 8 9 10)*

Histologically the urothelial biopsy from these 5 patients showed either moderately or markedly atypical urothelial hyperplasia. Signs of mucosal inflammation were noted in all specimens.

In each of the 4 patients with a simultaneous tumour biopsy a non-diploid tumour DNA stemline was observed *(Nos. 6 7 8, 9) (Fig 3)* Three patients had *multiple stage I disease (Nos. 6 7 8) of Grade* II and Grade *III while 1 patient (No 9)* had a single poorly differentiated stage II–III tumour The previously resected tumour in the fifth patient within this group (No 10) had been recorded as a single poorly differentiated stage II–III carcinoma.

Patient No 11 *(Fig 4) had multiple stage* I tumours (Grade *II* and *Grade III)* The urothelium from *the right bladder wall* showed *11 per cent non-diploid* DNA values. The *poorly differentiated* tumour from the right bladder wall revealed a diploid DNA-stem-

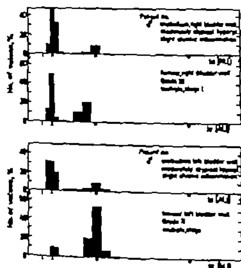


Fig. 4 DNA-frequency distributions (%) in urothelial biopsies from the right and left bladder wall and the corresponding primary tumours in patient with bladder carcinoma (No 11) (AU arbitrary units) × diploid DNA-value ○ tetraploid DNA-value ● octoploid DNA-value

line with 31 per cent tetraploid cell nuclei The urothelium from the left bladder wall showed 18 per cent tetraploid DNA-values. The corresponding moderately differentiated tumour showed a tetraploid DNA stemline. Histologically both mucosal biopsies showed markedly atypical urothelial hyperplasia with a slight degree of chronic inflammation.

DISCUSSION

It is difficult to obtain a completely normal control material of human bladder mucosa. The control material in this study was provided by either in vivo excision of bladder mucosa from patients undergoing surgery for prostatic hyperplasia, or by taking mucosal specimens immediately after death from patients deceased without urological disease. In these preparations 8–10 per cent of the urothelial cells were found to be non-diploid, most of these in the tetraploid range. No difference was found between the two types of control specimens. In the biopsy specimens taken from patients with prostatic hyperplasia, it was necessary to accept some degree of mucosal inflammation, which may be attended with slight nuclear abnormalities (*Koss* 1975) This may in particular lead to loss of the characteristic superficial polyploid surface cells of the normal urothelium and result in an underestimation of the number of non-diploid DNA values in the controls. Urothelial cells rapidly undergo autolysis. Nevertheless, *Koss et al.* (1975) claimed that post mortem specimens of the bladder mucosa may be used for cytophotometric studies of normal human urothelium.

With the corresponding findings in the two groups of our controls we believe that, with some reservation for the problems discussed the results may be taken as representative of normal urothelium. The number of non-diploid DNA values in our control group is lower than given by *Levi et al.* (1969a) On the other hand, it fits well with *Frenz's et al.* (1975) DNA measurements of scraped smeared cells from normal human urothelium and with cytophotometric DNA-studies in histological sections of normal urothelium (*Fossa et al.* unpublished results) In our opinion *Levi's et al.* (1969a) finding of about 25 per cent polyploid cell nuclei in normal urothelium is too high. The different authors deviating results may be explained by different methods used to select the cell nuclei to be measured.

Based on *Frenz's et al.* (1975) and our own observations we assumed that normal urothelium does not contain more than 15 per cent non-diploid cell nuclei, and that about 10 per cent non-diploid DNA-values are most commonly found in normal human urothelium obtained under optimal conditions.

The presence of histological changes in the non-tumour-bearing urothelium in patients with bladder carcinoma is well known (*Eisenberg et al.* 1960 *Schade* & *Swinney* 1973 *Koss* 1975 *Riddle et al.* 1976) Atypical urothelium can most frequently be observed nearby the bladder tumour and, particularly neighbouring histologically dedifferentiated carcinomas (*Starklint et al.* 1976)

We found a close correlation between urothelial atypia and abnormal patterns of the DNA histograms. Normal DNA histograms were found in all our biopsies without histologically demonstrable urothelial atypia. A definitely abnormal increase in the number of non-diploid DNA values was found in 6 out of 7 specimens showing moderately or markedly atypical urothelial hyperplasia. Such an increase in the number of non-diploid DNA values may be taken as an indication of either an increased growth fraction in the cell population or presence of quantitative chromosomal changes, or both (*Fosså et al.* in press).

Three urothelial biopsies showed a marked increase in the number of DNA values in the triploid and hexaploid regions. These specimens were taken from bladders giving rise to poorly differentiated and undifferentiated carcinomas. No increase in the number of triploid and hexaploid DNA values was observed in urothelium neighbouring well differentiated tumours.

None of the 5 diploid bladder carcinomas had definite increase in the number of non-diploid DNA values in the corresponding urothelium. Of 6 non-diploid tumours one corresponded with normal urothelium while the other 5 showed an abnormally increased number of non-diploid DNA values in the neighbouring urothelium. The number of non-diploid cells, however, was usually lower in the urothelium than in the corresponding bladder tumour. These observations suggest that similar DNA variations as observed in bladder carcinomas, although less marked, may also be present in the neighbouring bladder urothelium.

Lamb (1967) performed chromosome analyses in 8 specimens of urothelial carcinoma in situ, all of which had near-diploid stemlines. The number of cells within the stemline tended to decrease with decreasing histological differentiation. The present results are in agreement with these findings. In the available literature we have not found any other studies concerning chromosomal aberrations or DNA-changes in premalignant human urothelial lesions.

It is well known that cells with non-diploid DNA-content are frequently observed in premalignant lesions of the human uterine cervix (*Sandritter* 1964, *Wagner et al.* 1972). *Wagner et al.* (1976) have pointed out that the finding of cells in the triploid and hexaploid regions in such lesions indicates irreversible epithelial changes and implies a particularly high risk of development of invasive carcinoma. An increase of non-diploid DNA-values has also been demonstrated in other types of human premalignant lesions, e.g. in the larynx and in the skin (*Steele et al.* 1963, *Ehlers* 1971, *Avtandilov & Kazantseva* 1973). Furthermore corresponding results are known from experimental studies on carcinogenesis (*Meek* 1963, *Levi et al.* 1969b, *Wiest* 1972, *Herzog et al.* 1973). By analogy it seems justifiable to assume that the finding of an abnormally increased number of non-diploid DNA values also in urothelial biopsies may indicate increased risk of tumour development in the actual region of the bladder mucosa, in particular if numerous triploid and hexaploid DNA values are found.

The present study shows that the same type of DNA variations as observed in bladder tumours may be found in the urothelium in patients with bladder carcinoma. Though it is difficult to define the clinical significance of such DNA variations in the urothelium based on a study of only 12 specimens, we suggest that patients with abnormal DNA histograms in the urothelial specimens should be regarded as belonging to a high risk group. Changes of the DNA frequency distribution in the urothelium should therefore be taken into account when treatment and control in patients with bladder carcinoma are discussed. Further the observation of abnormal DNA histograms in urothelial biopsies may be of importance for the health control in individuals exposed to industrial carcinogens known to increase the risk of bladder carcinoma (*Koss et al.* 1969).

This ork was supported by grants from Grosserer *N A. Stang' Legat til Kreftsykdommers Bekjempelse*, *Kent Kenters' O.A.S. fond for Kreftforsk ning*, *Vanssfondet* and the *Norwegian Can r Society*

The author wants to thank *Per F Marton* MD for help with evaluation of the histopathological sections and for valuable criticism of the manuscript.

REFERENCES

Attendilov G G. & Kasentse a, I A Comparative microspectrophotometric study of the DNA content in the diagnosis of pre-tumorous processes and cancer Virchows Arch. Abt. A. Path Anat. 359 289–297 1973

Böhm N & Sandritter W. DNA in tumors cytophotometric study Corr Top. Path. 60 151 219 1975

Ehlers, G. DNS-Gehalt on Haut Prakanzerosen Ein Beitrag zur Frage der nosologischen Sonderstellung kutaner Präkanzerosen. Fortschr Med. 89 1042 1045 1971

Eisenberg, R. B. Roth R B & Schmmasberg, M H Bladder tumors and associated proliferative mucosal lesions. J Urol. (Baltimore) 84 544–550, 1960

Falor W H Chromosomes in noninvasive papillary carcinoma of the bladder J Amer med. Ass 216 791–794 1971

Fosså, S D Feulgen-DNA-values in transitional cell carcinoma of the human urinary bladder Beitr. Path. 155 44–55 1975

F sså S D Kaalhus O & S ott K adsen O The clinical and histopathological significance of Feulgen DNA-values in transitional cell carcinoma of the human urinary bladder Europ. J Cancer in press.

Frost, S C Reynders-Warner O de Voogt H J Beyer-Boon M E. & Brusset J A. M Flow fluorophotometry on urinary cells compared with conventional cytology In *Hermen C A. M Hillen H F P & W ssels J M C* (Eds) First I t. Symp Pulse-Cytophotometry Part III. Europ Press Medicon, Ghent, Belgium 1975, p. 194–203

Herting, R Grimm H & Sandritter W Das experimentelle Portiokarzinom der Maus unter der Einwirkung on Norhydroxyprogesteroncaproat Beitr Path. 148 230–241 1973

Kos L G Tumors of the urinary bladder Atlas of tumor pathology Second Series, Fascicle 11 AFIP Washington D C 1975 p 64

Kos L G Melamed M R. & Kelly R E. Further cytologic and histologic studies of bladder lesions in workers exposed to para-aminodiphenyl: progress report, J nat. Cancer Inst. 43 253–243 1969

Koss L G Bartels P H., Bibbo M., F eed S Z., Taylor J & Wied G L. Computer discrimination between benign and malignant urothelial cells. Acta cytol. 19 378–391 1975

Lamb D Correlation of chromosome counts with histological appearances and prognosis in transitional-cell carcinoma of bladder Brit. med. J 1 273–277 1967

Lederer B., Mikus, G., Gütter W & zur Nedden G Zytophotometrische Untersuchungen on Tumoren des Übergangsepithels der Harnblase. Vergleich zytophotometrischer Untersuchungsergebnisse mit dem histologischen Grading. Beitr Path. 147 379–389 1972.

Levi P E., Cooper E. H., Anderson C K., Path, M C & Williams R. E. Analyses of DNA content, nuclear size and cell proliferation of transitional cell carcinoma in man. Cancer (Philad.) 23 1074 1085, 1969a.

Le P E. Cowen D M & Cooper E. H. Induction of cell proliferation in the mouse bladder by 4-ethylsulphonylnaphthalene-1-sulphonamide. Cell Tiss. Kinet. 2 249–262, 1969b.

M k E. S Changes in cellular deoxyribonucleic acid in mouse skin following pplication of tumor-promoting agent. Exp Cell Res. 29 389–393 1963

Mills A., Mit hell, J P & Brow A J. The B istol Bladder Tumour Registry Brit. J Urol. 41 Suppl. 1–64 1969

M st fi, F K. Pathology of cancer of bladder. Acta Un. Int. Cancr 18 611–615 1962.

Riddle P R., Chisholm G D., Trott P A. & P gh R C B Flat carcinoma in situ of bladder Brit J Urol. 47 829–833 1976.

Sandritter W Cytophotometrische Untersuchungen am Portiocarcinom und seinen Vorstufen. Verh. dtsch. Ges. Path. 48 34–43 1964

Schade R. O K. & Swinney J. The association of urothelial atypism with neoplasia: its importance in treatment and prognosis. J Urol. (Baltimore) 109 619–622 1973

Shigematsu S Significance of the chromosome in esical cancer Int. Soc. Urol. 13th Congr., London 1964 ol. 2. E. & S Livingstone London 1965 p. 111 121

Spooner M E. & Cooper E. H Chromosome constitution of transitional cell carcinoma of the urinary bladder Cancer (Philad.) 29 1401–1412, 1972.

Starklint H Jensen V K. & Thybo E. The extent of carcinoma in situ in urinary bladders with primary carcinomas. Acta path. microbiol scand. Sect. A, 84 130–136 1976.

Steele H D., Manocha, S L. & Stich H F. Deoxyribonucleic acid content of epidermal in-situ carcinomas. Brit. med. J 2 1314–1315 1963

Tavares A S Costa J de Carvalho A & Reis M Tumour ploidy and prognosis in carcinomas of the bladder and prostate Brit J Cancer *20* 438–441 1966

UICC TNM classification of malignant tumours. 2 ed International Union Against Cancer Geneva 1974 p 79–83

Wagner D Sprenger E & Blank M H DNA content of dysplastic cells of the uterine cervix Acta cytol *16* 517–52? 1972

Wagner D Sprenger E & Merkle D Cytophotometric studies in suspicious cervical smears. Acta cytol. *20* 366–371 1976

West L The effect of diethylnitrosamine on the distribution of cell classes in the parenchyma of the liver of newborn rats Europ J Cancer *8* 121–125 1972.

Acta path. microbiol. scand. Sect. A, 85 611-624 1977

ULTRASTRUCTURAL AND IMMUNO CYTOCHEMICAL CHARACTERIZATION OF CIRCULATING MONONUCLEAR CELLS IN PATIENTS WITH MYELOMATOSIS

PETER BIBERFELD, HÅKON MELLSTEDT and DAGNY PETTERSSON

Department of Pathology Karolinska Hospital, and
Department of Immunology National Bacteriological Laboratory Stockholm, and
Department of Medicine, Seraphimer Hospital, Stockholm, Sweden

Biberfeld, P Mellstedt, H. & Pettersson, D Ultrastructural and immunocytochemical characterization of circulating mononuclear cells in patients with myelomatosis Acta path. microbiol. scand Sect. A, 85 611-624 1977

The ultrastructure of blood mononuclear cells from two IgG myeloma patients was studied, and cells reacting with anti-idiotypic serum and polyspecific anti-Ig serum were characterized by immunoperoxidase techniques. Abnormal, mononuclear cells were present in the blood of both patients, which morphologically were classified as atypical small to medium-sized lymphocytes, polymorphic immature lymphocytes (lymphoblasts) predominantly of the lymphoplasmocytic type and atypical, plasmocytic cells or myeloma cells. Immunocytochemical observations showed that most of the abnormal cells, including atypical small to medium-sized lymphocytes, reacted with anti-idiotypic and polyspecific anti-Ig serum. Periods of relapse and remission were correlated with an increase and decrease, respectively of the number of abnormal cells and cells which reacted with anti-idiotype and anti-Ig serum. The observations indicate that circulating lymphoid cells are part of the myeloma clone.

Key words Myeloma electron microscopy immunofluorescence immunoperoxidase.

P Biberfeld, Department of Pathology Karolinska Sjukhuset, 10401 Stockholm 60 Sweden.

Received 14 iii 77 Accepted 14 iii.77

Many cases of myeloma develop relative lymphocytosis with a variable proportion of immature lymphocytic and plasmacytic forms (17) It is generally believed that these immature cells are derived from the bone marrow and represent a displacement phenomenon (15) By immunofluorescence studies using anti-idiotype serum against myeloma protein it has been demonstrated that many of these circulating mononuclear cells expressed myeloma specific protein determinants on their surface membrane or contained myeloma protein intracellularly (1 7 9 12, 13 14 *Kunkel*, personal communication) It was also shown that the size of this population of circulating abnormal cells apparently belonging to the myeloma clone was correlated with the dissemination of the disease, decreasing during induction therapy and during remission but increasing again at relapse (13 14) By following the size of the monoclonal subpopulation it was possible in some cases to predict a relapse several months

before it was clinically evident (14) At the light microscopical level the cells with myeloma surface protein sometimes had an atypical lymphocytic morphology and cytoplasmic staining for myeloma protein was observed in larger lymphocytic cells. These observations support the assumption that circulating myeloma cells constitute a morphologically heterogeneous population To elucidate this point further blood lymphoid cells from two myeloma patients were studied on several occasions during relapse periods by ultrastructural and immunocytochemical methods.

MATERIAL AND METHODS

Two patients with IgG myeloma without Bence-Jones proteinuria were studied different stages of the disease After diagnosis the patients were treated with an intermittent high dosage melphanprednisolone therapy for four days. The courses were repeated every sixth week Studies on blood lymphocytes were performed immediately before a new course of therapy to avoid acute toxic effects of the drugs.

Isolation of Lymphocytes

Defibrinated venous blood was mixed with gelatine and allowed to sediment (5) Phagocytic cells were allowed to ingest colloidal iron and were removed by a magnet (10) Non-phagocytic cells were then centrifuged through a Ficoll Isopaque gradient to remove remaining red blood cells (4) This procedure resulted in lymphocyte preparations virtually free from monocytes and granulocytes (5 12)

Antisera

A polyvalent rabbit antiserum containing antibodies against human γ α μ κ and λ chains was used (Cappel Lab Inc Downingtown USA) The preparation of individual (idiotypic) specific antisera against myeloma proteins has been described previously in detail (12) The anti myeloma sera were extensively adsorbed with human Ig Each antiserum was also tested for non-specific reactivity with human lympocytes. In the IFI and IEM tests antiserum dilutions were chosen within a plateau where the serum did not react with normal lymphocytes (12)

Immunofluorescence Staining (IFI)

Membrane staining Lymphocytes stained by indirect immunofluorescence were incubated with rabbit anti-human Ig serum or the idiotypic antiserum for 45 min at 4 C and after thorough washing incubated with sheep anti-rabbit Ig serum conjugated with fluorescein isothiocyanate (National Bacteriological Lab., Stockholm, Sweden) The percentage of stained lymphocytes was determined by counting 200 cells under a Zeiss fluorescence microscope (8 12)

Cytoplasmic staining Lymphocytes were resuspended in bovine serum albumin and cytocentrifuged on glass slides. After fixation with methanol, one drop of the appropriate antiserum dilution was added onto the cells. The slides were incubated in a wet chamber at room temperature for 30 min, washed in phosphate buffered saline and further incubated for 30 min with the conjugate After washing cells were mounted in phosphate buffered glycerol and examined in UV light (13)

Electron Microscopy (EM)

Cells from both patients on three different occasions, week 90 99 102 and 108, 113 120 (See Table 1) respectively were processed for electron microscopy and immune electron microscopy Preparations of isolated lymphocytes were fixed for 20 to 45 min in 3 per cent glutaraldehyde in cacodylate buffer when in suspension, osmicated in 1 per cent OsO_4 and embedded in Spurr low viscosity medium as previously described (3) Ultrathin sections were examined in a Siemens Elmiscop

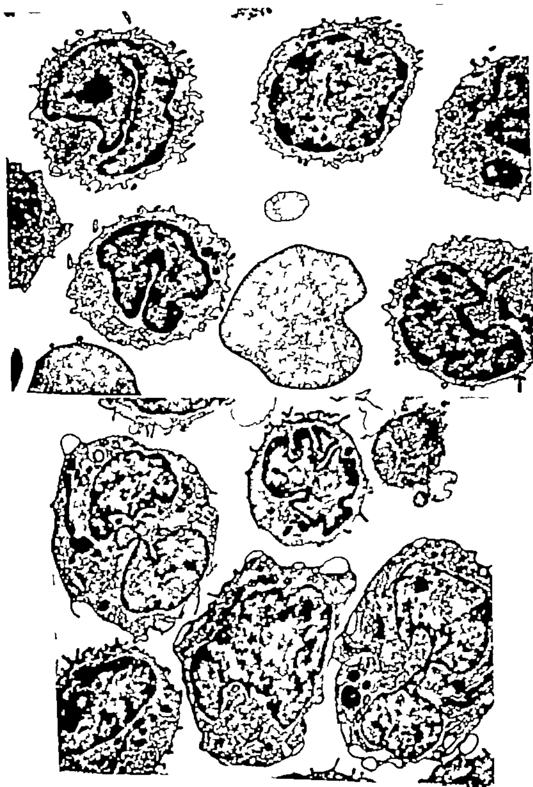
Immunoelectron Microscopy (IEM)

Isolated lymphocytes were "stained" by an indirect technique using the same primary rabbit antisera as for IFL, i.e polyspecific antihuman Ig (Cappel) and two idiotypic antimyeloma protein sera. After incubation for 30 to 60 min at 4 C with respective (primary) antiserum, rabbit antibodies bound to cells were detected by antirabbit Ig (sheep) antibody coupled to horse-radish peroxidase (HRP) After washing the cells were briefly fixed in 0.5 per cent glutaraldehyde The bound HRP was visualized by treatment with a

---

Fig 1 Blood mononuclear cells from patient W The cells show features of small to medium-sized lymphocytes some with atypical indented nuclei and rather villous surfaces. × 6 000

Fig 2 Mononuclear cell preparation from patient A. Most cells are atypical, large with irregular or lobated euchromatic nuclei and varying amounts of cytoplasm rich in ER-profiles and conspicuous Golgi zones. Note also vesicle formation at the surface of these cells. × 5,500



before it was clinically evident (14) At the light microscopical level the cells with myeloma surface protein sometimes had an atypical lymphocytic morphology, and cytoplasmic staining for myeloma protein was observed in larger lymphocytic cells These observations support the assumption that circulating myeloma cells constitute a morphologically heterogeneous population To elucidate this point further blood lymphoid cells from two myeloma patients were studied on several occasions during relapse periods by ultrastructural and immunocytochemical methods.

MATERIAL AND METHODS

Two patients with IgG myeloma without Bence-Jones proteinuria were studied different stages of the disease After diagnosis the patients were treated with an intermittent high dosage melphanprednisolone therapy for four days The courses were repeated every sixth week. Studies on blood lymphocytes were performed immediately before a new course of therapy to avoid acute toxic effects of the drugs.

Isolation of Lymphocytes

Defibrinated venous blood was mixed with gelatine and allowed to sediment (5) Phagocytic cells were allowed to ingest colloidal iron and were removed by a magnet (10) Non-phagocytic cells were then centrifuged through a Ficoll Isopaque gradient to remove remaining red blood cells (4) This procedure resulted in lymphocyte preparations virtually free from monocytes and granulocytes (5 12)

Antisera

A polyvalent rabbit antiserum containing antibodies against human γ α μ, κ and λ chains was used (Cappel Lab Inc., Downingtown, USA) The preparation of individual (idiotypic) specific antisera against myeloma proteins has been described previously in detail (12) The anti myeloma sera were extensively adsorbed with human Ig. Each antiserum was also tested for non-specific reactivity with human lympcocytes. In the IFL and IEM tests antiserum dilutions were chosen within a plateau where the serum did not react with normal lymphocytes (12)

Immunofluorescence Staining (IFL)

Membrane staining Lymphocytes stained by indirect immunofluorescence were incubated with rabbit anti human Ig serum or the idiotypic antiserum for 45 min at 4 C and after thorough washing incubated with sheep anti-rabbit Ig serum conjugated with fluorescein isothiocyanate (National Bacteriological Lab., Stockholm, Sweden) The percentage of stained lymphocytes was determined by counting 200 cells under a Zeiss fluorescence microscope (8 12)

Cytoplasmic staining Lymphocytes were resuspended in bovine serum albumin and cytocentrifuged on glass slides. After fixation with methanol, one drop of the appropriate antiserum dilution was added onto the cells. The slides were incubated in a wet chamber at room temperature for 30 min, washed in phosphate buffered saline and further incubated for 30 min with the conjugate After washing cells were mounted in phosphate buffered glycerol and examined in uv light (13)

Electron Microscopy (EM)

Cells from both patients on three different occasions, week 90 99 10? and 108, 113 120 (See Table 1) respectively were processed for electron microscopy and immune electron microscopy Preparations of isolated lymphocytes were fixed for 20 to 45 min in 3 per cent glutaraldehyde in cacodylate buffer when in suspension, osmicated in 1 per cent OsO_4 and embedded in Spurr low viscosity medium as previously described (5) Ultrathin sections were examined in a Siemens Elmiscop.

Immunoelectron Microscopy (IEM)

Isolated lymphocytes were "stained" by an indirect technique using the same primary rabbit antisera as for IFL, i e. polyspecific antihuman Ig (Cappel) and two idiotypic antimyeloma protein sera. After incubation for 30 to 60 min at 4 C with respective (primary) antiserum, rabbit antibodies bound to cells were detected by antirabbit Ig (sheep) antibody coupled to horse-radish peroxidase (HRP) After washing the cells were briefly fixed in 0.5 per cent glutaraldehyde The bound HRP was visualized by treatment with

---

Fig 1 Blood mononuclear cells from patient W The cells show features of small to medium-sized lymphocytes, some with atypical indented nuclei and rather villous surfaces. × 6 000

Fig 2 Mononuclear cell preparation from patient A Most cells are atypical large with irregular or lobated euchromatic nuclei and varying amounts of cytoplasm rich in ER profiles and conspicuous Golgi zones. Note also vesicle formation at the surface of these cells. × 5,500

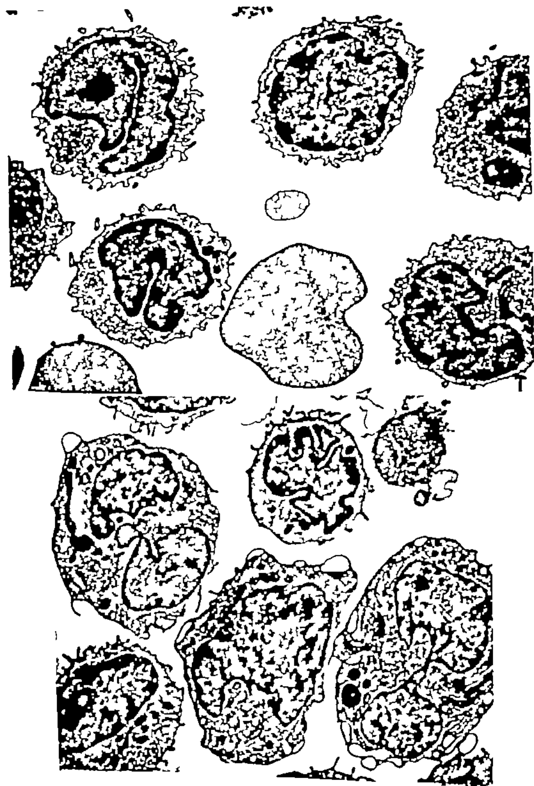


TABLE 1 *Differentiation of Mononuclear Cells Isolated from Peripheral Blood of Two Myeloma Patients during Relapse Periods in May-Grünwald Giemsa Stained Films and Electron Microscope*

	Weeks after institution of therapy	Total lymphocytes per µl	Normal lymphocytes (per cent)	Atypical cells: Total LM[1])	lymphocytic LM	lymphocytic EM[2])	lymphoblastic lymphoplasmocytic LM	lymphoblastic lymphoplasmocytic EM	plasmocytic LM	plasmocytic EM
Pat. A	0	2800	62	38	12	ND	26	ND	0	ND
	90	900*	73	27	6	+	21	++	0	+++
	99	900**	72	27	21	+	7	++	0	+++
	102	1300*	33	67	36	+	22	+	9	++++
Pat. W	0	1400	89	11	0	ND	11	ND	0	ND
	108	1100*	69	31	0	+	31	+++	0	+
	113	1100	81	19	0	+	19	++++	0	+
	120	1100*	75	25	0	ND	25	ND	0	ND

ND = not done
* = relapse
** = peripheral (blood) remission
1) = LM = light microscopic calculation in per cent.
2) = Subjective estimations by EM of respective cell frequency on untreated cell preparations + a few +++ approx. half ++++ most cells.

solution of diaminobenzidine 5 0 mg/ml hydrogen peroxide 0 005 per cent in Tris-HCL buffer After treatment with the substrate medium the cells were fixed in 3 per cent glutaraldehyde followed by treatment with 1 per cent OsO_4 and further processed for electron microscopy as described above The conjugation of immunoglobulin with HRP was essentially done according to the two-step technique described by *Avrameas* (14) The following controls were also performed treatment with normal rabbit serum treatment with only HRP conjugate (negative controls) and treatment with anti-Hela cell serum (positive control)

On two occasions intracellular staining was attempted by incubating cells which had been prefixed in 1 per cent paraformaldehyde (PFA) and 0.5 per cent glutaraldehyde and subsequently freeze-thawed four times.

RESULTS

Two patients (A and W) with IgG κ myeloma were studied Both patients were examined several times during 102 and 120 weeks, respectively before they died They had both a classical case history with clinical manifestations related to marrow infiltration and bone destruction by neoplastic plasma cells and presence of M type protein in the serum Patient A showed signs of partial remission in the blood after 99 weks, but not in the bone marrow

Hematological observations by light microscopy are shown in Table 1 The mononuclear cells were classified into four different morphological variants. However considerable morphological overlapping of atypical cells did not allow a distinct segregation into different cell populations Usually normal-looking small lymphocytes constituted the majority of the mononuclear cells, but during the progress of the disease varying numbers of atypical—immature lymphocytic cells were usually observed Classical plasmacytic cells were only observed in the blood of patient A after 102 weeks. Among the atypical—

Fig 3 Plasmacytic cell from patient A. The cell contains abundant ER profiles and cytofibrils. × 17 000

Fig 4 Part of a plasmacytic cell in the blood of patient W with arrays of ER profiles, a large Golgi zone and bundles of cytofibrils. Note vesicles with tubular structures (arrows) × 21 600.

3





Serum treatment	L[1]	LB+LP	P
Anti - idiotypic serum	+[2]	++	+ — ++
Anti - Ig (polyspecific) serum	+ — ++	+++	++

1) L = lymphocytic LB = lymphoblastic LP = lymphoplasmacytic P = plasmacytic

2) + = a few ++ = approx half +++ = most cells within respective category

Subjective estimation of staining frequency

6

TABLE 2. *Blood Lymphocytes Stained for Immunoglobulin by Indirect Immunofluorescence*

	Weeks after institution of therapy	Polyvalent antiserum		Idiotypic antiserum	
		surface staining (per cent)	*cytoplasmic staining* (per cent)	*surface staining* (per cent)	*cytoplasmic staining* (per cent)
Pat. A	0	44	34	39	26
	90*	62	44	53	36
	99**	18	14	15	9
	107*	50	68	44	56
Pat. W	0	50	2	47	2
	106*	33	4	24	3
	113	36	ND	28	ND
	120*	33	7	ND	6

* = relapse.
** = peripheral (blood) remission.
ND = not done.

immature lymphocytic cells at least two different and frequent variants could be distinguished one lymphocytic, the other lymphoblastic or lymphoplasmacytic. These cells varied considerably in size (7 to 20 μm) nuclear polymorphism, chromatin pattern and size of nucleoli.

Ultrastructural Observations

The vast majority of the cells were mononuclear with lymphocytic, lymphoplasmacytic or atypical plasmacytic features. Only rarely were the preparations contaminated with granulocytes.

The heterogeneous morphology of the mononuclear cells was more evident at the EM level than by light microscopy. On the basis of their content of ergastoplasm (ER) and its organization, three different categories of cells could be distinguished.

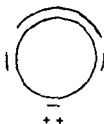
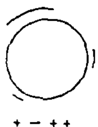
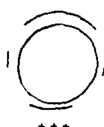
Cells with no or only one or two short profiles of ER had mostly the features of small to medium-sized lymphocytes (Fig. 1) with high nucleocytoplasmic ratio and, if present, an inconspicuous rounded nucleolus, a poorly-developed Golgi zone, few mitochondria, and a cytoplasm rich in single, free ribosomes (monosomes). Rather often these lymphocytes had a distinctly villous surface topography (Fig. 1). Some of them had an atypical, irregular nucleus (Fig. 1) and corresponded to the atypical lymphocytic variant observed by light microscopy.

With respect to ER content, the extreme opposite to these small and medium-sized lymphocytic cells were cells with a well-developed ergastoplasm organized circumferentially around the nucleus in long, single profiles or as arrays of parallel ER profiles (Fig. 2). However apart from a common denominator of a well-developed ER, these cells varied considerably with respect to size, nuclear form and cytoplasmic features. Thus, the size of these cells ranged from approximately 7 to 20 μm, and some of the cells were rounded whereas others were irregular (Figs. 2, 3). Nuclear polymorphism from

Fig. 3. Two cells of lymphoplasmocytic type from the blood of patient W. Note the moderate amounts of short ER-profiles, the relatively large Golgi zones and the irregular or lobated nuclei. In addition, the surface villousness of the cells is obvious. × 10,000

Fig. 4. A schematic representation of the reactions of atypical blood mononuclear cells from myeloma patients with anti-idiotypic or anti-Ig antibody as revealed by indirect immunoperoxidase staining and electron microscopy. The cell type and range of reactivity observed is illustrated.

5

Serum treatment	L[1]	LB+LP	P
Anti - idiotypic serum	 + [2]	 ++	 + – ++
Anti - Ig (polyspecific) serum	 + – ++	 +++	 ++

1) L = lymphocytic LB = lymphoblastic LP = lymphoplasmacytic P = plasmacytic

2) + = a few ++ = approx half, +++ = most cells within respective category

Subjective estimation of "staining frequency

6

rounded to highly-indented or lobated nuclei was frequently observed (Figs. 2, 3). Conspicuous cytoplasmic features in many of these cells were well-developed Golgi zones and large bundles of cytofibrils (Figs. 3, 4). Adjacent to or within the Golgi zone of these cells usually several types of vesicular structures were observed, which mostly appeared to be of a lysomal nature. In the cells from one patient (W) tubular material was consistently seen in lysomal structures (Figs. 4). The surface of these cells was usually villous and also displayed vesicular structures which might indicate either clasmatosis or exocytosis (Figs. 2, 3). These cells were designated atypical plasmacytic or myeloma cells.

The third category of cells was intermediate between the other two types described above with respect to their content of ER. Thus, most of these cells had a few irregularly distributed ER profiles. Also these cells varied in size and form and showed nuclear polymorphism (Fig. 5). Furthermore the Golgi (zone) varied from inconspicuous to prominent, and lysosomal structures also varied considerably in number. These cells showed a varying degree of surface villousness. These cells were designated atypical, lymphoblastic and lymphoplasmacytic.

Table 1 shows the proportion of cells with in the different categories observed in the patients' blood on several occasions. It was noticed that in patient A the proportion of lymphoplasmacytic and atypical plasmacytic cells increased with the progress of the disease and was roughly correlated to the percentage of cells with surface and/or cytoplasmic myeloma protein (Table 2). Patient W had a small proportion of atypical plasmacytic cells at the ultrastructural level compared to patient A, but most of the lymphocytes were classified as atypical, lymphoblastic lymphoplasmacytic cells and lymphocytic cells.

The pronounced cell polymorphism of atypical lymphocyte types shown at the ultrastructural level did not allow a direct and easy correlation with observations by light microscopy (differential counts).

Immunofluorescence Observations

A large proportion of the isolated mononuclear cells from both patients showed an intense, dotted and/or segmental, membrane staining with both the polyspecific and the anti-idiotypic antisera. Patient A also had a relatively large population of cells which could be stained in their cytoplasm. In control lymphocyte preparations from healthy donors, about 10 to 20 per cent lymphocytes showed membrane staining with polyspecific serum (11) and only a few per cent (2 per cent) were stained with the anti-idiotypic sera at plateau dilutions (3). The percentage of stained cells from both patients on four different occasions is shown in Table 2. As can be seen, membrane staining with both types of antisera stained a large proportion of the isolated mononuclear cells during relapse periods, whereas cytoplasmic fluorescence was much more frequent in cells of patient A. When tested under partial remission, patient A showed a clear decrease in cells with membrane and cytoplasmic fluorescence after staining with either polyspecific or anti-idiotypic sera. The percentage of cells showing membrane fluorescence usually exceeded that of cells with cytoplasmic reactivity (after 102 weeks). On all test occasions, cells showing membrane or cytoplasmic reaction with polyspecific antiserum were slightly more numerous than cells stained with anti-idiotypic serum. The membrane stained cells that reacted exclusively with the polyspecific antiserum probably represent

Fig. 7. Cells with features of small to medium-sized lymphocytes. The cells were processed immunocytochemically for the demonstration of surface Ig. Both cells show patchy or segmental surface deposits of enzyme reaction product, indicative of the presence of surface Ig determinants on these cells. × 10,500

Fig. 8. Plasmocytic cell showing only small areas (delineated) with surface reaction for Ig. × 21,000

7

8

9

10

normal B-cells. However it is unlikely that normal B-cells can account for the slight surplus in cytoplasmic stainable cells in patient A at week 102

Immune Electron Microscopical (IEM) Observations

The ultrastructure of cells processed for IEM was clearly less wellpreserved than that of the non treated ones (Figs. 7–12) However in general the cells could be classified according to the same criteria as the non treated ones (cf above) Attempts to perform intracellular staining of cells were unsuccessful, irrespective of antiserum used including cells incubated with anti HeLa serum. This was probably due to insufficient penetration of sera and conjugates.

The observations on membrane staining were derived from 3 different experiments respectively with cells from patients A and W From each experiment and patient approximately 500 cells incubated by either antiserum were analyzed. In most sections examined irrespective of antiserum used a varying degree of cell agglutination was observed This seemed to affect to some extent the outcome of the peroxidase reaction since cells within larger clumps were usually less stained than marginal cells Thus, estimations of frequency of staining with either antiserum was not attempted The observations were essentially similar with cells from both patients and are schematically summarized in Fig 6 With both anti idiotypic antisera and the polyspecific antiserum stained cells showed a dotted patchy or occasionally segmental distribution of reaction product on their membranes (Figs. 7–12) In general the reaction with anti idiotypic serum was weaker than with the polyspecific serum (cf Figs 7 10) The atypical lymphoblastic lymphoplasmacytic cells usually showed the strongest membrane staining with either anti idiotypic or polyspecific serum (Figs. 11) whereas the atypical plasmacytic cells were usually somewhat less stained (Figs. 8–12) In addition some small lymphocytes with more or less atypical ultrastructural features were in small numbers but consistently found reacting with either the anti idiotypic or polyspecific serum, although weakly (Figs. 7, 10) Such cells were most frequently seen in patient A at week 90 In the negative control preparations, only occasional cells of any type were weakly stained Most cells treated with anti HeLa serum showed segmental or a ring type of surface staining pattern.

DISCUSSION

The present observations extend to the ultrastructural level our previous IFL observations that lymphocytic (B) cells in myeloma patients express myeloma proteins on their surface (12 13 14)

In both cases examined in this study atypical circulating mononuclear cells were found which displayed ultrastructural features ranging from small to medium-sized lymphocytes, immature lymphoblasts, lymphoplasmacytic cells to classical myeloma cells (atypical plasmacytic) In patient A more mature" variants predominated whereas in patient W the opposite was observed. All these types of cells were shown by immunoelectron microscopy to express, to a varying extent myeloma protein determinants on their surface The concomitant immunofluorescence studies showed corresponding findings of lymphoid cells which expressed membrane-bound myeloma protein. In one patient (A) a sizeable population of the cells was shown by immunofluorescence to contain cytoplasmic inclusions of myeloma protein. These cells were roughly correlated to the presence of relatively mature atypical plasmacytic cells in the electron microscopical pre-

---

Fig 9 Medium-sized atypical lymphocytic cell with conspicuous Golgi zone, cytofibrils and rather extensive reaction with anti-idiotypic serum × 16 000

Fig 10 A small or medium-sized atypical lymphocytic cell stained with anti idiotypic serum. Its surface shows patchy and spotty reaction with the antiserum. × 20,000

parations Using the indirect immunoperoxidase technique with complete Ig preparations, we did not succeed in demonstrating the presence of myeloma protein in the various cell types. Studies in progress using Fab-conjugates of anti-idiotype serum will, we hope, allow direct ultrastructural identification of various cell types containing myeloma protein. In previous experiments we have demonstrated that the cells which show membrane immunofluorescence staining with idiotypic antiserum re-express the monoclonal protein after tryptic digestion, indicating *de novo* production of myeloma protein by these cells (12) Furthermore, lymphocytes incubated in myeloma protein do not absorp the protein onto their surface, according to immunofluorescence studies (12) Thus, myeloma protein determinants on cells demonstrated in the present study do indeed identify cells belonging to the myeloma-protein-producing clone. A possible contribution of non-specific staining of individual cells in the immunoperoxidase test canot be completely eliminated, since occasional cells in control tests showed minimal amounts of reaction product on their surface However the very weak reaction on these cells was easy to distinguish from that of clearly positive cells. Furthermore, the control tests with normal lymphocytes by IFL clearly showed, on a quantitation basis, that non-specific staining, e.g. due to Fc receptors, was negligible if present.

Quantitative and cytological aspects of the immunofluorescence studies indicate that cells with surface staining and cells with cytoplasmic staining overlap The immune-electron microscopical observations indicate that the atypical plasmacytic cells, which are part of the intracytoplasmatic stained cells, were less extensively and less often or faintly stained on their surface by the anti-idiotypic serum. This seems to indicate that maturing myeloma cells only transitionally express the myeloma protein on their surface, which is analogous to the fate of the membrane Ig on normal B-cells maturing to plasma cells (6, 16) It is also clear from the present studies that differential counts, immunofluorescence and EM were not always well correlated to the demonstration of circulating lymphoid cells belonging to the myeloma cell population. Thus, on some occasions (week 90 patient A week 0 patient W) the immunofluorescence and the immune-electron microscopical observations indicated that a relatively large fraction of small to medium-sized lymphocytic cells were probably included among the membrane reactive cells. Furthermore, morphologically normal lymphocytes at the light microscope level were evidently at the ultrastructural level rich in ER, indicative of active protein synthesis. Thus, the use of anti idiotypic antiserum seems to be a more sensitive technique for the demonstration of pathognomonic cells, particularly at early stages (14) and for an evalution of degree of remission. It is also obvious that immunofluorescence studies should include both membrane and cytoplasmic reactive cells when evaluating the total population of myeloma-protein-producing cells.

The ultrastructure of myeloma cells in the bone marrow has previously been described in several studies and in general the more mature variants have been emphasized as characteristic of myeloma cells (11)

These cells, in the present study mostly correspond to atypical plasmacytic cells. However the immuno-electron microscopical observations show that immature variants and small to medium-sized lymphocytes must be taken into account as potential myeloma cells, if these are evaluated by cytological criteria.

According to the present concepts of tumoral monoclonality it would seem that the demonstration of the presence of endogenous,

---

Fig 11 Atypical medium to large lymphocytic cell with relatively large cytoplasm and Golgi zone and rather conspicuous surface reaction with anti-idiotyp antiserum 19,000

Fig 12 Atypical plasmocytic cell from patient A. The cell show patchy surface reaction with anti-idiotypic antiserum 16,000

11

12

Acta path. microbiol. scand. Sect. A, 85: 625–639, 1977

CYTOPLASMIC EFFECTS OF X-IRRADIATION ON CULTURED CELLS IN A NON-DIVIDING STAGE

2. *Alterations in Lysosomes, Plasma Membrane, Golgi Apparatus and Related Structures*

HANS HAMBERG, ULF BRUNK, JAN L. E. ERICSSON and BO JUNG

Department of Pathology at Sabbatsberg Hospital, Karolinska Institutet, Stockholm, and The Departments of Pathology and Radiophysics, University of Uppsala, Uppsala, Sweden

Hamberg, H., Brunk, U., Ericsson, J. L. E. and Jung, B. Cytoplasmic effects of X-irradiation on cultured cells in a non-dividing stage. 2. Alterations in lysosomes, plasma membrane, Golgi apparatus, and related structures. Acta path. microbiol. scand. Sect. A, 85: 625–639, 1977.

Topoinhibited human glia cells *in vitro* were exposed to X-radiation generated by an 8-MeV linear accelerator at a dose of 20,000 rad. Transmission electron microscopy of irradiated cells at intervals varying between 30 min and 3 days following irradiation revealed alterations mainly in the plasma membrane and the lysosomal vacuome. Increased ruffling of plasma membranes, augmented endocytosis and extensive intracellular autophagy developed within 24 hours after irradiation. The implications of the plasma membrane alterations are discussed, and a tentative model covering possible mechanisms involved in the development of autophagic vacuoles is presented. The possibility is entertained that alternative mechanisms may be operative during the formation of the autophagic vacuole in irradiated glia cells. The origin of the isolation membrane appears to be (*a*) preexisting lysosomes and (*b*) flattened vacuolar cytoplasmic elements.

Key words: X-irradiation; lysosomes; cultured cells; autophagic vacuoles; plasma membrane.

H. Hamberg, Department of Pathology, Sabbatsberg Hospital, Box 6401, 113 82 Stockholm.

Received 1.xii.76 Accepted 24.ii.77

The mechanisms involved in radiation-induced interphase-cell damage are still largely unknown. It has been suggested that structural and functional derangements in various organelles would be responsible for the degenerative cytoplasmic changes observed. Ultrastructural analysis of radiation-induced cytoplasmic alterations can be expected to supply increased knowledge about the processes involved.

We have recently reported on a suitable experimental model for elucidating morphologically the sequential development of radiation-induced damage of interphase cells (*Hamberg et al.* 1976). In this model, utilizing strictly topoinhibited human glia cells *in vitro*, the most conspicuous radiation-induced modifications occurred in the lysosomal vacuome. Lysosomal alterations appear to be common in irradiated cells and it seems possible that such alterations are of a pathogenetic significance in the development of radiation-induced interphase cell death (for a discussion, see *Watkins* 1975). Current knowledge suggests that lysosomes are intimately

idiotypic myeloma protein determinants in or on cells qualifies these cells as belonging to the tumor clone. Thus, the observed lymphocytic variants may represent an immature pool of dividing cells, which for unknown reasons are made to mature.

This study was supported by the *Swedish Cancer Society*. The skilled technical assistance of *Marianne Ekman*, *Göran Utter* and *Walter Schilling* is gratefully acknowledged.

REFERENCES

1. *Abdou N I & Abdou N L.* The monoclonal nature of lymphocytes in multiple myeloma. Ann. Intern Med. *83* 42–45 1975
2. *Avrameas S & Ternynck T* Peroxidase labelled antibody and Fab conjugates with enhanced intracellular penetration. Immunochemistry *8* 1175 1971
3. *Biberfeld P & Mellstedt H* Selective activation of human B-lymphocytes by suboptimal doses of pokeweed mitogen (PWM) Quantitation and ultrastructure of the stimulated cells. Ex. Cell Res. *89* 377–388 1974
4. *Bøyum A* Separation of lymphocytes and erythrocytes by centrifugation Scand. J Clin. Lab. Invest. *21* 77–89 1968.
5. *Coulson A S & Chalmers D G* Separation of viable lymphocytes from human blood. Lancet *I* 468–469 1969
6. *Fu S M Winchester R J Feizi T., Walzer P D & Kunkel H G* Idiotypic specificity of surface immunoglobulin and the maturation of leukemic bone marrow-derived lymphocytes. Proc. Natl. Acad. Sci. USA *71* 4487–4490 1974
7. *Holm G Mellstedt H Pettersson D & Biberfeld P* Idiotypic immunoglobulin structures on blood lymphocytes in human plasma cell myeloma. Immunolog. Rev *34* 139–164 1977
8. *Holm G Pettersson D Mellstedt H., Hedfors E. & Bloth B.*, Lymphocyte subpopulations in peripheral blood of healthy donors. Characterization by surface markers and lack of selection during purification. Clin. exp. Immunol. *20* 443–457 1975
9. *Lindström F D Hardy W R. Eberle B J & Williams R C jr* Multiple myeloma and benign monoclonal gammopathy: differentiation by immunofluorescence of lymphocytes. Ann. Intern. Med. *78* 837–844 1973
10. *Lundgren G., Zukoski C F & Möller G* Differential effects of human granulocytes and lymphocytes on human fibroblasts in vitro. Clin. exp. Immunol. *3* 817–836, 1968.
11. *Maldonado J E., Brown A L. jr., Bayrd E. D & Pease G L.* Ultrastructure of the myeloma cell. Cancer (Philad.) *19* 1613–1627 1966
12. *Mellstedt H Hammarström S & Holm G* Monoclonal lymphocyte population in human plasma cell myeloma. Clin. exp. Immunol. *17* 371–384 1974
13. *Mellstedt H Pettersson D & Holm G* "Monoclonal" B-lymphocytes in peripheral blood of patients with plasma cell myeloma. Relation to activity of the disease. Scand. J Haematol. *16* 112–120 1976.
14. *Mellstedt H Pettersson D & Holm G* Monoclonal B-lymphocytes in myelomatosis. Relation to activity of the disease. In Proceedings Third International Symposium on Detection and Prevention of Cancer 1976 (in press)
15. *Ossermann E. F & Farhangi M.* Plasma cell myeloma. In Hematology By W J Williams E Beutler A J Erslev & R. W Rundles. McGraw Hill Book Co. 1972, pp. 956–968.
16. *Vitetta E S & Uhr J W* Immunoglobulin-receptors revisited. A model for the differentiation of bone marrow-derived lymphocytes is described. Science *189* 964–969 1975.
17. *Wallgren A* Untersuchungen über die Myelomkrankheit. Uppsala Läkareförenings Förhandlingar *25* 113–263 1920

CYTOPLASMIC EFFECTS OF X-IRRADIATION ON CULTURED CELLS IN A NON DIVIDING STAGE

2. *Alterations in Lysosomes, Plasma Membrane, Golgi Apparatus and Related Structures*

HANS HAMBERG, ULF BRUNK, JAN L. E. ERICSSON and BO JUNG

Department of Pathology at Sabbatsberg Hospital, Karolinska Institutet, Stockholm, and The Departments of Pathology and Radiophysics, University of Uppsala, Uppsala, Sweden

Hamberg, H., Brunk, U., Ericsson, J. L. E. and Jung, B. Cytoplasmic effects of X-irradiation on cultured cells in a non-dividing stage. 2. Alterations in lysosomes, plasma membrane, Golgi apparatus, and related structures. Acta path. microbiol. scand. Sect. A, 85: 625–639, 1977.

Topoinhibited human glia cells in vitro were exposed to X-radiation generated by an 8-MeV linear accelerator at a dose of 20 000 rad. Transmission electron microscopy of irradiated cells at intervals varying between 30 min. and 5 days following irradiation revealed alterations mainly in the plasma membrane and the lysosomal vacuome. Increased ruffling of plasma membranes, augmented endocytosis and extensive intracellular autophagy developed within 24 hours after irradiation. The implications of the plasma membrane alterations are discussed, and a tentative model covering possible mechanisms involved in the development of autophagic vacuoles is presented. The possibility is entertained that alternative mechanisms may be operative during the formation of the autophagic vacuole in irradiated glia cells. The origin of the isolation membrane appears to be (a) preexisting lysosomes and (b) flattened vacuolar cytoplasmic elements.

Key words: X-irradiation; lysosomes; cultured cells; autophagic vacuoles; plasma membrane.

H. Hamberg, Department of Pathology, Sabbatsberg's Hospital, Box 6401, 113 82 Stockholm.

Received 1.xii.76. Accepted 24.ii.77.

The mechanisms involved in radiation-induced interphase-cell damage are still largely unknown. It has been suggested that structural and functional derangements in various organelles would be responsible for the degenerative cytoplasmic changes observed. Ultrastructural analysis of radiation-induced cytoplasmic alterations can be expected to supply increased knowledge about the processes involved.

We have recently reported on a suitable experimental model for elucidating morphologically the sequential development of radiation-induced damage of interphase cells (*Hamberg et al.* 1976). In this model, utilizing strictly topoinhibited human glia cells in vitro, the most conspicuous radiation-induced modifications occurred in the lysosomal vacuome. Lysosomal alterations appear to be common in irradiated cells and it seems possible that such alterations are of a pathogenetic significance in the development of radiation-induced interphase cell death (for a discussion, see *Watkins* 1975). Current knowledge suggests that lysosomes are intimately



b
MP
U
L
1

associated with the Golgi apparatus there is also a close connection between the plasma membrane and lysosomes, since—following endocytosis—part of the plasma membrane becomes incorporated in the bordering membrane of the lysosomes following fusion events.

The aim of the present study is to describe in some detail the ultrastructural alterations in the lysosomal system and associated changes of the Golgi apparatus plasma membrane and related structures that occur in the irradiated glia cells. Since autophagic vacuoles were a conspicuous feature of the cytoplasm of irradiated cells, and different developmental stages in the formation of these vacuoles were frequently observed, the experimental model appeared to be suitable for elucidating the mechanisms underlying the creation of the autophagic vacuole membrane. Included in this report—and partly based on the findings—is a scheme of possible pathways involved in the formation of the autophagic vacuole.

MATERIALS AND METHODS

Cell culture procedures, irradiation conditions, and methods used in the preparation for transmission electron microscopy were as described earlier (*Hamberg et al.* 1976)

All experiments were performed on diploid human glia cells in phase II cultured *in situ*. The cells were harvested for irradiation when they had formed a confluent monolayer and were in a state of topoinhibition of cell division and movement.

The cultures were exposed to X radiation generated by 8 MV electrons in a linear accelerator (MEL SL 75 Super). The radiation dose was 20,000 rad given at a rate of 1 700 rad/min. Cells were harvested for examination at intervals varying between 30 min. and 5 days following irradiation.

Fig. 1 48 hours after irradiation. Glia cell with numerous endocytotic vesicles both along the upper (U) and lower (L) cell border MP microprecipitate on which the cells grow × 33,000

Inset a. Vesicles appear to fuse to form large, vacuolar structures in the cytoplasm. × 40,000.

Inset b. A vacuole surrounded by vesicles and appearing to fuse with 3 of the latter (*arrow*). × 26,000

The cells were fixed *in situ* in 2 per cent glutaraldehyde in 0.1 M Na-cacodylate-HCl buffer with 0.1 M sucrose (pH 7.2 total osmolality ~ 510 mOsmol, vehicle osmolality ~ 300 mOsmol) post fixed in 2 per cent OsO_4 in s-collidine buffer (pH 7.2) dehydrated in ethanol and embedded in Epon 812. Ultrathin sections, cut on an LKB ultrotome, were examined in a Jeol 100C transmission electron microscope

RESULTS

Controls

The fine structure of contact inhibited glia cells in phase II has been described previously (*Brunk et al.* 1971) The cells studied in this investigation showed a similar morphology They were flattened with a centrally placed nucleus. The upper surface was smooth lacking cytoplasmic or membranous projections except for a variable amount of microvilli. Along the lower surface, the cells were supplied with foot-processes anchoring them to the microprecipitate on which they had grown Endocytotic vacuoles were rather unfrequent and occurred mostly at the lower surface of the cell. The cytoplasm contained few lysosomes and only occasional autophagic vacuoles and residual bodies. The Golgi apparatus consisted of stacks of cisternae with peripheral coated vesicles occurring abundantly in some areas. No conspicuous "GERL" (structurally specialized Golgi-endoplasmic reticulum-lysosome region) was noted Endoplasmic reticulum (ER) consisted mainly of scattered cisternae of rough ER. The cytoplasmic ground substance contained microtubules, microfilaments and free ribosomes.

This report will be confined to the alterations in plasma membranes, the lysosomal system and the Golgi apparatus. Other components of the cell such as nuclei mitochondria and endoplasmic reticulum show ultrastructural modifications only at a later postirradiation stage (*Hamberg et al.* 1976)

Irradiated Cells

Plasma membranes At 6 and 12 hours post irradiation, a slight increase in the occurrence of micropinocytotic vacuoles at the cell

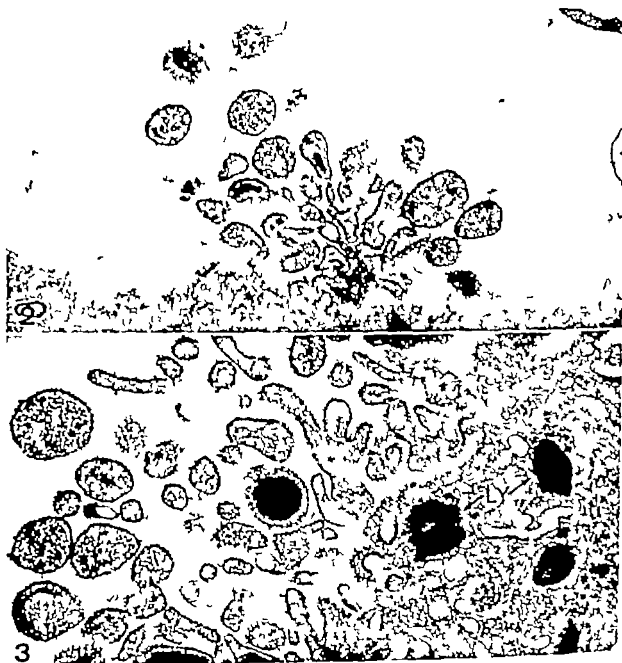


Fig 2 48 hours after irradiation. Superficial portion of cell forming numerous blunt extrusions with narrow stalks (probably a vertical ruffle from the upper cell surface) × 18 000

Fig 3 96 hours after irradiation Section through exuberant ruffle composed of abundant thin sheets, folds and blunt projections from the cell surface Endocytotic vacuoles appear numerous in the cytoplasm adjacent to the projection on the surface LY lysosomes. × ?8.000

surface was noted At 24 hours and onward the endocytotic activity appeared markedly increased in some cells. Contrary to the control cells, the irradiated ones displayed a high endocytotic activity all around the cell surface (Fig 1) In the cytoplasm vacuoles of variable size and shape were often surrounded by swarms of vesicles, some of which appeared to be in continuity with the vacuoles (Fig 1 insets) Some cells formed cytoplasmic and membranous projections similar to those found at the border of sparsely growing ruffling cells in culture Occasionally such projections occurred along the upper cell sur

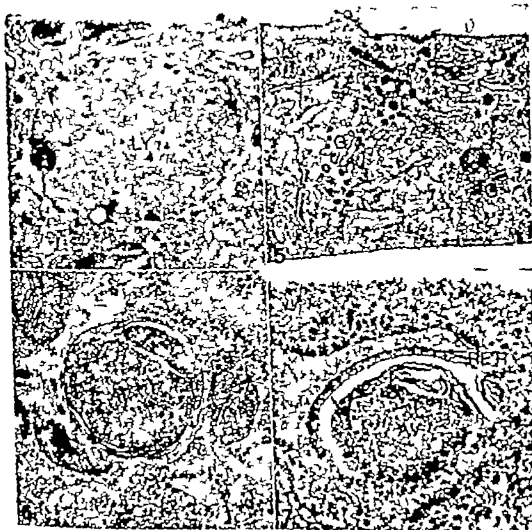


Fig. 4 6 hours after irradiation. Picture illustrating the appearance of giant lysosome (LY) × 50,000.

Fig. 5 12 hours after irradiation. A large Golgi apparatus (G) is surrounded by several coated vesicles (arrows) × 52,000.

Fig. 6 24 hours after irradiation. Portion of cell with an autophagic vacuole (AV) containing ground cytoplasm × 46,000

Fig. 7 12 hours after irradiation. An autophagic vacuole (AV) closely associated with rough surfaced endoplasmic reticulum (RER). Note that the wall of the vacuole (arrows) is smooth-surfaced, and not in continuity with the RER × 80,000

face also in the vicinity of the nucleus—and not only at the periphery of the cell (Figs. 2 and 3

Lysosomes No obvious changes in the lysosomal vacuome were noted before 6 hours post irradiation. At this time occasional, unusually big, lysosomes were observed (Fig. 4). These lysosomes contained a homogeneous or partially dissolved matrix which was less electron dense than in normal lysosomes

From approximately 12 hours onward, numerous lysosomes of unusual configuration

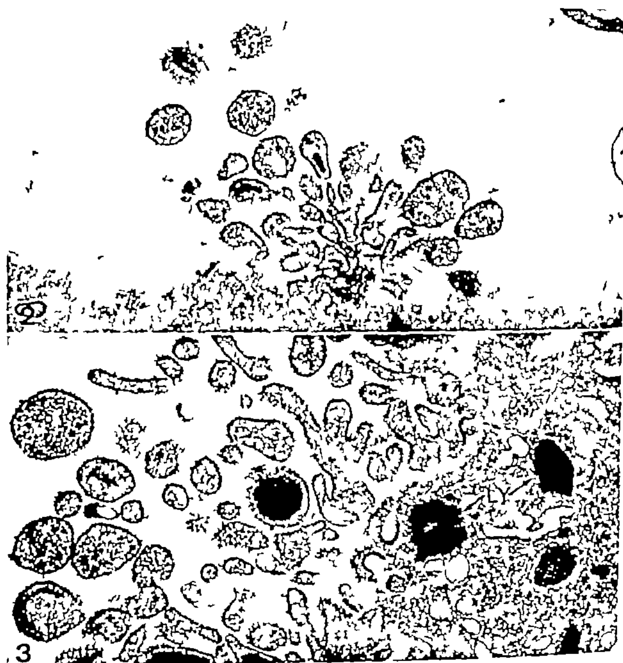


Fig 2 48 hours after irradiation. Superficial portion of cell forming numerous blunt extrusions with narrow stalks (probably a vertical ruffle from the upper cell surface) × 18.000

Fig 3 96 hours after irradiation. Section through exuberant ruffle composed of abundant thin sheets, folds and blunt projections from the cell surface Endocytotic vacuoles appear numerous in the cytoplasm adjacent to the projections on the surface. LY lysosomes. × 28.000

surface was noted At 24 hours and onward, the endocytotic activity appeared markedly increased in some cells Contrary to the control cells the irradiated ones displayed a high endocytotic activity all around the cell surface (Fig 1) In the cytoplasm vacuoles of variable size and shape were often surrounded by swarms of vesicles, some of which appeared to be in continuity with the vacuoles (Fig 1 insets) Some cells formed cytoplasmic and membranous projections similar to those found at the border of sparsely growing ruffling cells in culture Occasionally such projections occurred along the upper cell sur



Fig. 4 6 hours after irradiation. Picture illustrating the appearance of giant lysosome (LY) × 30,000

Fig. 5 12 hours after irradiation. A large Golgi apparatus (G) is surrounded by several coated vesicles (arrows) × 32 000.

Fig. 6 24 hours after irradiation. Portion of cell with an autophagic vacuole (AV) containing ground cytoplasm × 46,000

Fig. 7 12 hours after irradiation. An autophagic vacuole (AV) closely associated with rough surfaced endoplasmic reticulum (RER) Note that the wall of the vacuole (arrows) is smooth-surfaced, and not in continuity with the RER × 80,000.

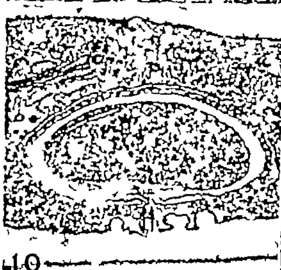
face also in the vicinity of the nucleus—and not only at the periphery of the cell (Figs. 2 and 3

Lysosomes No obvious changes in the lysosomal vacuome were noted before 6 hours post irradiation At this time occasional, unusually big lysosomes were observed (Fig. 4) These lysosomes contained a homogeneous or partially dissolved matrix which was less electron dense than in normal lysosomes.

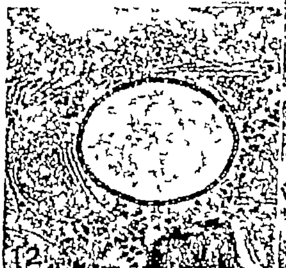
From approximately 12 hours onward, numerous lysosomes of unusual configuration


8


9


10




12


13

were seen. Very often these lysosomes contained slender attenuated parts connecting rounded areas resulting in the creation of dumbbell-shaped "goggles-like" lysosomes. Some of these lysosomes appeared to be attenuated to a considerable lenght (Figs. 14–16). Other lysosomes showed a ring-like structure with cytoplasmic areas seemingly sequestered in the "ring" (Figs. 17 and 18). However since serial sections have not been studied, it is not clear whether or not the images observed represent sections through cup-shaped areas of attenuated lysosomes or through completely walled-off portions of cytoplasm. Configurational changes in the lysosomes of the aforementioned type might represent the initial phase in an autophagic process.

The number of autophagic vacuoles was markedly increased from 12 hours onward until 2–3 days after irradiation. Different kinds of autophagic vacuoles and their presumed precursors were observed (Figs. 6–13). Some were constituted by a piece of cytoplasm surrounded by a circular cleft-like space lined by two separated membranes (Fig. 11). Other vacuoles appeared to be bordered by smooth-surfaced membranes showing close spatial relationship to rough ER (Figs. 7 and 10). However the rough-surfaced and smooth membranes were never seen to fuse or connect, and no evidence was obtained of cytoplasmic sequestration by wrapping into smooth ER. In some instances, cytoplasmic areas appeared partially wrapped by semicircular membrane pairs either arranged as flattened attenuated cisternae or cleft-like spaces in the cytoplasm (Fig. 8). Occasional vacuoles appeared to be lined by a 5-layered membrane array (Figs. 12 and 13).

Initially most autophagic vacuoles contained well recognizable ground cytoplasm or organelles such as mitochondria. After an additional day or two, many vacuoles contained material in a more or less advanced stage of degradation and structural reorganization and showed the appearance of residual bodies. At 2–5 days post irradiation, a marked increase in the number of residual bodies dominated the picture in most cells, although autophagic vacuoles in different developing stages still were to be seen and in some cells occurred with considerable frequency. The residual bodies were *evenly* distributed through the cytoplasm and at 5 days post irradiation, a great proportion of the cell volume appeared to be occupied by these organelles (Fig. 20). The residual bodies found in irradiated cells were of approximately the same shape and appearance as those accumulating in glia cells which had been kept as a stable monolayer for long periods of time (*Brunk et al.* 1973).

Golgi area. The Golgi area of the irradiated cells appeared to occupy a greater part of the cytoplasm than in control cells (Fig. 5). The apparent Golgi proliferation was first noted at the 12 hour interval post irradiation, *i. e.* at about the same time as the beginning of increased autophagy. Although the in-

---

Fig. 8. 12 hours after irradiation. Picture suggestive of an early phase in an autophagic process involving a cleft-like membrane bound structure. × 50,000.

Fig. 9. 12 hours after irradiation. Suggested further development in isolation procedure outlined in Figure 8. × 70,000.

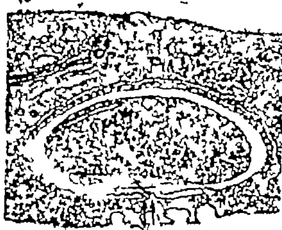
Fig. 10. 24 hours after irradiation. Vacuole containing membrane-bound part of the ground cytoplasm. The structure is suggestive of an almost completed isolation of cellular cytoplasm, the earlier phases of which are indicated in Figs. 8 and 9. *Double arrows* indicate point of apparent detachment site. × 40,000.

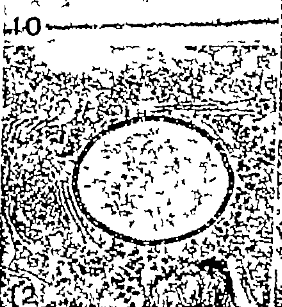
Fig. 11. 12 hours after irradiation. A vacuole containing an—at the level of the section—unattached membrane-bound portion of cytoplasm. × 60,000.

Fig. 12. 24 hours after irradiation. Apparently double-walled vacuole containing granular and flocculent material of uncertain origin. × 58,000.

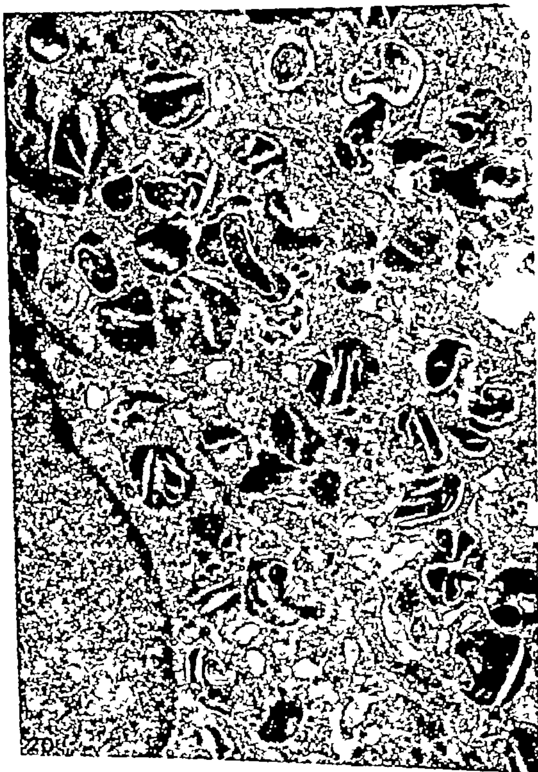
Fig. 13. 96 hours after irradiation. High magnification picture of a vacuole similar to the previous one (Fig. 12). At this magnification, the five-laminar structure of the vacuolar wall is clearly shown. The total thickness (between arrows) of the wall is approximately 200 Å. × 90,000.

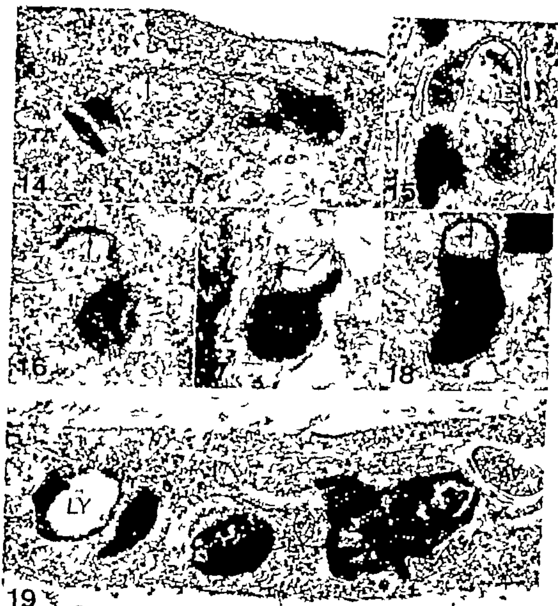

8

9

10


12

13





Figs 14–18 Intervals varying from 12–24 hours after irradiation. Pictures illustrating apparent mode of formation of autophagic vacuoles by stretching out and attaining sheet or cup-shape of preexisting lysosomes. LY lysosomes Arrows indicating sheet-like parts of lysosomes. Fig 14 × 40 000 Fig 15 × 54 000 Fig 16 × 46,000 Fig 17 × 35 000 Fig 18 × 60 000

Fig 19 48 hours after irradiation Portion of cell cytoplasm containing an autophagic vacuole (AV) and lysosomes (LY) of different appearance. × 35 000

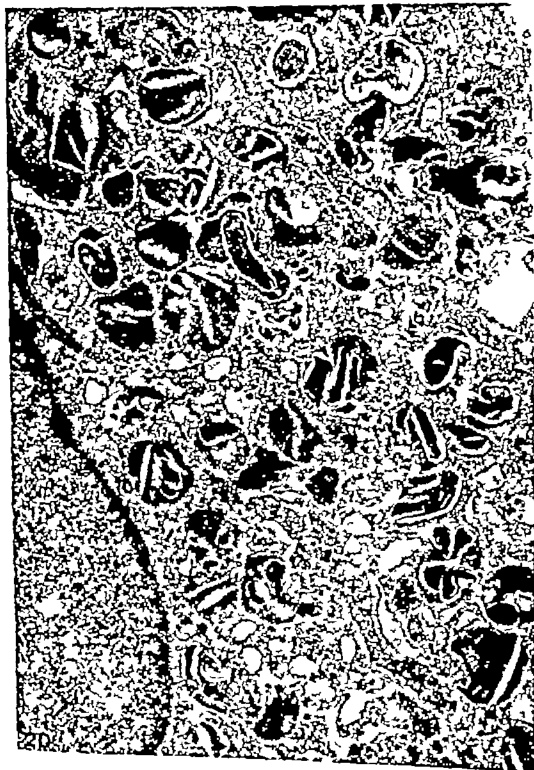
Fig 20 96 hours after irradiation. Glia cell with a great part of the cytoplasm occupied by residual bodies × 19 000

crease in size was considerable in some cells, the configuration of the individual saccules and cisternae appeared unaltered (no dilatation or addition of contents of these components was observed) Golgi associated coated vesicles were abundant in some areas, but might be equally frequent in controls.

DISCUSSION

I *Plasma Membranes and Associated Structures*

Lateral ruffling is a normally occurring phenomenon in sparse cultures of normal human glia cells. However such ruffling is not





Figs 14–18 Intervals varying from 12–24 hours after irradiation Pictures illustrating apparent mode of formation of autophagic vacuoles by stretching out and attaining sheet or cup-shape of preexisting lysosomes. LY lysosomes Arrows indicating sheet-like parts of lysosomes. Fig. 14 × 40 000 fig. 15 × 54 000 Fig 16 × 46 000 Fig. 17 × 35 000 Fig 18 × 60 000.

Fig 19 48 hours after irradiation. Portion of cell cytoplasm containing an autophagic vacuole (AV) and lysosomes (LY) of different appearance. × 33 000

Fig 20 96 hours after irradiation Glia cell with a great part of the cytoplasm occupied by residual bodies. × 19 000

crease in size was considerable in some cells, the configuration of the individual saccules and cisternae appeared unaltered (no dilatation or addition of contents of these components was observed) Golgi associated coated vesicles were abundant in some areas, but might be equally frequent in controls.

DISCUSSION

I Plasma Membranes and Associated Structures

Lateral ruffling is a normally occurring phenomenon in sparse cultures of normal human glia cells. However such ruffling is not

II *Mechanism of Autophagy*

A. *Theoretical Considerations*

Current knowledge of autophagocytosis is incomplete as to the origin of the isolation membranes and the source of the lytic enzymes in the autolysosomes. The different hypotheses which have been proposed concerning the origin of the membranes limiting the autophagic vacuoles have been reviewed by *Ericsson* (1969) and later by *Holtzman* (1976) and are summarized below

(1) The membranes are *de novo* synthesized when the autophagic vacuole is created (*Ashford and Porter* 1962). According to one theory the segregation of cytoplasm is accomplished by local accumulation of a lipid substance in the cytoplasm, whereafter membranes are organized at the borders of the lipid (*Pfeifer* 1971)

(2) The autophagic vacuoles are formed from preexisting membranes. These may be constituted by plasma membranes (by way of endocytosis) (*Miller and Palade* 1964). Golgi membranes (*Fedorko et al.* 1968, *Locke and Sykes* 1975) rough or smooth endoplasmic reticulum (*Novikoff and Shin* 1964 *Arstila and Trump* 1968 *Ericsson* 1969) or lysosomal membranes (*Sato and Ogawa* 1974). The suggested mechanisms have been wrapping of cytoplasm in flattened out, sheet-like membranes of the aforementioned origin, or extrusion of part of the cytoplasm into preformed vacuoles in a process that has been termed exotropy (*Trump* 1975)

Labelling experiments (*Ericsson* 1969) have demonstrated that once the autophagic vacuole is formed fusion occurs with preexisting lysosomes, at least as far as the hepatic parenchymal cell is concerned. From the data so far available it is entirely feasible that variable mechanisms for the formation of the autophagic vacuole may be operative in different cell types.

All conceivable alternatives regarding the origin of the isolation membranes and the sources of the hydrolytic enzymes in the newly formed autophagic vacuole are summarized in Fig. 21 and Table 1

B. *Suggested Origin of Isolation Membranes based on Observations of Irradiated Glia Cells*

(*1*) *From lysosomes.* A common mechanism of autophagocytosis in the irradiated glia cells seemed to be isolation of portions of cytoplasm by flattened or tail-equipped lysosomes (Figs 14–18). Often a stretched out, sheet like portion was seen to connect two rounded parts of a lysosome thus creating a dumbbell- or goggles-like appearance. A similar "plasticity" of the lysosomal vacuoles in liver cells has been described by *Pfeifer* (1971). According to Pfeifer's theories, the alterations in lysosomal morphology would

TABLE 1 *Summary of possible pathways during the formation of the isolation membrane with scheme of expected hydrolytic enzyme content of the primary vacuole and expected thickness of isolation membrane*

Pathway	A	B	C	D	E
Origin of isolation membrane	De novo synthesis	Plasma membrane via endocytosis	Lysosomes	Golgi membranes	ER
Expected hydrolytic enzyme content of the initial vacuole	—	—	+	— or +	— or +
Expected thickness of primary isolation membrane	60–100 Å	100 Å	100 Å	60–100 Å	60 Å

seen in crowded cultures under monolayer topo inhibited conditions. Ruffles emerging from the upper cell surface ("atypical ruffling") have never been encountered in normal cells (sparsely or densely distributed) under standard culture condition However atypical ruffling is frequently seen in crowded cultures of malignant glioma cells (*Forsby and Collins* 1974) Furthermore this type of ruffling has been observed in cultures of glia cells exposed *to isolated mitochondria added* to the growth medium (*Collins et al* 1976)

Formation of large pinocytotic vacuoles (macropinocytosis) is closely associated with ruffling membranes and implies internalisation into the cytoplasm of the plasma membrane in the ruffling area. Therefore cells showing macropinocytosis and ruffling probably have a high plasma membrane turnover While macropinocytosis seems to be bound to ruffles, micropinocytosis may occur from the plasma membrane without any undulating activity of the latter

In the irradiated cells, atypical ruffling and associated macropinocytosis was only occasionally observed The amount of endocytotic vesicles *of micropinocytotic type however* was markedly increased in many cells within 24 hours post irradiation, an observation also made on irradiated rat glia cells by *Ostenda* (1973) From the images obtained it appeared that some of these vesicles merged to form big vacuoles within the cytoplasm Many of the micropinocytotic vesicles were associated *with the upper surface of the cells.* This localization of endocytosis is often seen in malignant glioma cells but is rather uncommon in the normal benign *in vitro* cultured glia cells where the majority of this type of vesicles is confined to the lower cell surface (*Brunk et al* 1971) The observations suggest that radiation directly or via mediators, affected the plasma membrane in such a way that atypical *ruffling and increased endocy*tosis ensued These modulations of plasma *membrane* activity observed in the irradiated cells would probably imply an increased turnover of the plasma membrane. It should be noted in this connection that *Collins et al.* (1976) have described increased ruffling resulting from exposure of glia cells *to suspen*sions of mitochondria these mitochondria are taken up by the cells by way of endocytosis. In the present study atypical ruffling might have been induced by presence of damaged cells and organelles in the medium. However in areas with ruffling such structures were not present

The functional significance of the increased endocytosis could be manifold Augmented uptake of molecules from the growth medium into the cell internalization and degradation of pieces of injured or otherwise altered plasma membranes diminution of the total cell surface and/or supplementation of membrane material to autophagic processes in the cytoplasm.

In some situations, cells displaying extensive endocytotic activity also show a high autophagic activity This has been interpreted as a stimulation of *autophagocytosis by endo*cytosis (*Plattner et al* 1975) It does not *seem, however* that autophagy is a generally occurring phenomenon in endocytotically active cells (*Ericsson* 1969)

Among the earliest detectable alterations in the lysosomal system was the occurrence of giant lysosomes. Enlarged lysosomes seem to be a common finding in irradiated cells (for references, see *Hamberg et al 1976) and the* enlargement has sometimes been found to be paralleled *by an increase in* cytochemically detectable intralysosomal hydrolytic enzymes (*René et al* 1971) In the absence of quantitative biochemical measurements of lysosomal enzymes in the human glia cells, it is presently not known whether or not these cells display augmented activity of these enzymes following irradiation. *Taking into* account the greatly increased endocytosis in the irradiated cells, *another* possibility would be that the giant lysosomes are formed by fusion *of multiple* endocytotic vesicles with lysosomes shortly after irradiation.

II Mechanism of Autophagy

A. Theoretical Considerations

Current knowledge of autophagocytosis is incomplete as to the origin of the isolation membranes and the source of the lytic enzymes in the autolysosomes. The different hypotheses which have been proposed concerning the origin of the membranes limiting the autophagic vacuoles have been reviewed by *Ericsson* (1969) and later by *Holtzman* (1976) and are summarized below

(1) The membranes are *de novo* synthesized when the autophagic vacuole is created (*Ashford and Porter* 1962) According to one theory the segregation of cytoplasm is accomplished by local accumulation of a lipid substance in the cytoplasm, whereafter membranes are organized at the borders of the lipid (*Pfeifer* 1971)

(2) The autophagic vacuoles are formed from preexisting membranes. These may be constituted by plasma membranes (by way of endocytosis) (*Miller and Palade* 1964) Golgi membranes (*Fedorko et al.* 1968 *Locke and Sykes* 1975) rough or smooth endoplasmic reticulum (*Novikoff and Shin* 1964 *Arstila and Trump* 1968, *Ericsson* 1969) or lysosomal membranes (*Saito and Ogawa* 1974) The suggested mechanisms have been wrapping of cytoplasm in flattened out, sheet-like membranes of the aforementioned origin, or extrusion of part of the cytoplasm into preformed vacuoles in a process that has been termed exotropy (*Trump* 1975)

Labelling experiments (*Ericsson* 1969) have demonstrated that once the autophagic vacuole is formed fusion occurs with preexisting lysosomes, at least as far as the hepatic parenchymal cell is concerned. From the data so far available it is entirely feasible that various mechanisms for the formation of the autophagic vacuole may be operative in different cell types.

All conceivable alternatives regarding the origin of the isolation membranes and the sources of the hydrolytic enzymes in the newly formed autophagic vacuole are summarized in Fig. 21 and Table 1

B. Suggested Origin of Isolation Membranes based on Observations of Irradiated Glia Cells

(1) From lysosomes. A common mechanism of autophagocytosis in the irradiated glia cells seemed to be isolation of portions of cytoplasm by flattened or tail-equipped lysosomes (Figs. 14–18) Often a stretched out, sheet like portion was seen to connect two rounded parts of a lysosome, thus creating a dumbbell- or goggles-like appearance. A similar "plasticity" of the lysosomal vacuoles in liver cells has been described by *Pfeifer* (1971) According to Pfeifer's theories, the alterations in lysosomal morphology would

TABLE I *Summary of possible pathways during the formation of the isolation membrane with scheme of expected hydrolytic enzyme content of the primary vacuole and expected thickness of isolation membrane*

Pathway	A	B	C	D	E
Origin of isolation membrane	De novo synthesis	Plasma membrane via endocytosis	Lysosomes	Golgi membranes	ER
Expected hydrolytic enzyme content of the initial vacuole		—	+	— or +	— or +
Expected thickness of primary isolation membrane	60–100 Å	100 Å	100 Å	60–100 Å	60 Å

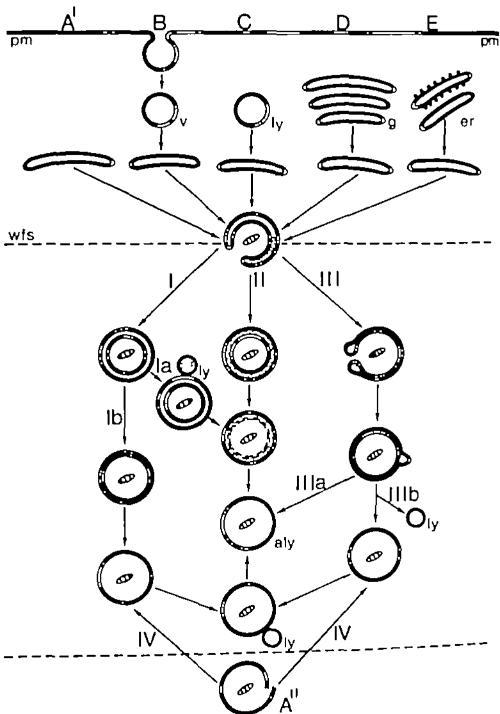


Fig 21 Schematic summary of the possible origin of isolation membranes modes of formation of auto-phagic vacuoles a d distribution of lysosomal enzyme activity during the development of an "autolyso-some

Five different pathways (A–E) for the origin of the isolation membrane are indicated (cf Table 1) In the case of *de novo* synthesis, two variants are conceivable direct formation of a closed vacuole (v pathway A) or formation of a wrapping sheet of unit membrane which ultimately closes to form an isolation membrane (pathway A line of development IV) Segregation via a wrapping flattened sac (stage wf) can occur along three different lines (I II and III) Lysosomal enzyme (indicated by dots) may or may not be present in the cavity of the wrapping flattened sac. The drawing shows the possible ways by which enzyme—preexisting within the sac or in lysosomes (ly)—can gain access to the endo-genous substrate (a mitochondrion) Pathways Ib and III involve "compaction" of the two limiting membranes, pathways Ia and II dissolution of the inner membrane. The final stage is represented by the single unit membrane-limited autolysosome (aly) Conventional lysosomes are indicated by ly er en-doplasmic reticulum (rough and/or smooth surfaced) g, Golgi apparatus pm, plasma membrane

merely reflect an altered lysosomal surface/volume ratio. However *Saito and Ogawa* (1974) in an enzyme-histochemical study suggested that such lysosomes participated in the autophagic process.

(2) *From nonlysosomal cytoplasmic vacuoles.* Vacuoles were common in the irradiated cells. Pictures suggestive of autophagy by exotropy into preformed, flattened vacuoles were often obtained (Fig. 8). These vacuoles were observed to be lined by a membrane approximately 100 Å thick. Since the lumen between the flattened membranes was devoid of the finely granular material observed in the lysosomes, and as endocytotic vacuoles were common in the irradiated cells, these vacuoles are presumed to originate from the cell membrane (although some of them might possibly stem from the Golgi apparatus).

In the present study autophagic vacuoles were of a highly variable appearance. Some were surrounded by a cleft-like space in the cytoplasm with bordering membranes of obscure origin (Fig. 11). In some instances, these membranes were in close vicinity to rough endoplasmic reticulum. By close examination, however, it became apparent that continuity between these membranes and endoplasmic reticulum was lacking (Figs. 7 and 10). On the basis of the fine structural appearance alone, it does not seem possible to determine whether these membranes originally were derived from the rough surfaced endoplasmic reticulum (*Holtzman* 1976), from membranes of other organelles such as Golgi cisternae (*Locke and Collins* 1965), or were formed *de novo* (*Pfeifer* 1971). Autophagy utilizing membranes belonging to the smooth endoplasmic reticulum—commonly seen in e.g. liver cells (*Ericsson* 1969)—were not evident in the glia cells which almost completely lack this type of endoplasmic reticulum.

III. *Development and Fate of Autophagic Vacuoles*

Early after irradiation, the cells contained a great amount of autophagic vacuoles, often lined by a pair of unit membranes. Later on, secondary lysosomes and residual bodies lined by a single membrane dominated. Thus, it would seem that the autophagic vacuoles loose one of their limiting membranes in the course of development into secondary lysosomes and residual bodies. Theoretically this could be accomplished in different ways.

(*1*) Following fusion with a lysosome the space between the two limiting membranes of the autophagic vacuole might be filled by hydrolytic enzymes and the inner membrane digested (*Arstila and Trump* 1968). However, this theory suffers from the difficulties in explaining why only the inner membrane is digested.

(*2*) The inner and outer membranes of the autophagic vacuole might melt together to form a single membrane in a process termed "compaction" (*Novikoff and Shin* 1964). Figure 13—showing a vacuole surrounded by a 5-layered 200 Å membrane—may illustrate an intermediary step in the presumed compaction procedure. In this case, the vacuole is likely to have originated from a lysosome or an endocytotic vacuole.

The proposed mechanism of compaction is outlined in Fig. 21. Theoretically the compaction of membranes in an autophagic vacuole derived from a lysosome could yield a vacuole containing lysosomal matrix (with enzymes) attached to the autophagic vacuole. In a further step this imagined vacuole could either fuse with the autophagic vacuole or be pinched off attaining the features of a small lysosome (Fig. 21).

In the case of an autophagic vacuole formed by a lysosome the hydrolytic enzymes that are to be added to the segregated material would evidently be present from the beginning of the autophagic process. This may theoretically hold true even in the case of a vacuole formed by Golgi membranes or smooth surfaced endoplasmic reticulum. In the case of an autophagic vacuole formed *de novo* or originating from an endocytotic vacuole the hydrolytic enzymes would have to be added by fusion of the autophagic vacuole with a primary or a secondary lysosome (Table 1, Fig. 21).

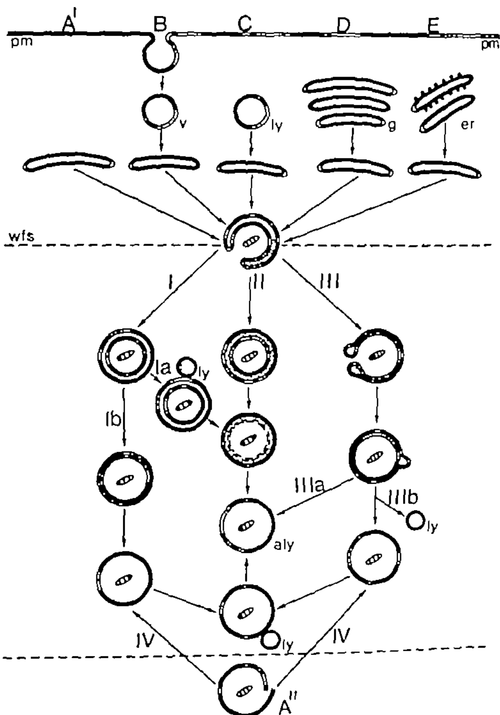


Fig 21 Schematic summary of the possible origin of isolation membranes modes of formation of autophagic vacuoles and distribution of lysosomal enzyme activity during the development of an "autolysosome"

Five different pathways (A–E) for the origin of the isolation membrane are indicated (cf Table I) In the case of *de novo* synthesis two variants are conceivable direct formation of a closed vacuole (r pathway A) or formation of a wrapping sheet of unit membrane which ultimately closes to form an isolation membrane (pathway A line of development IV) Segregation via a wrapping flattened sac (stage wf) can occur along three different lines (I II and III) Lysosomal enzyme (indicated by dots) may or may not be present in the cavity of the wrapping flattened sac The drawing shows the possible ways by wh ch enzym —preexisting within the sac or in lysosomes (ly)—can gain access to the endogenous substrate (a mitochondrion) Pathways Ib and III involve "compaction" of the two limiting membranes, pathways Ia and II dissolution of the inner membrane. The final stage is represented by the single unit membrane-limited "autolysosome" (aly) Conventional lysosomes are indicated by *ly* er endoplasmic reticulum (rough and/or smooth surfaced) g Golgi apparatus pm, plasma membrane.

merely reflect an altered lysosomal surface/volume ratio. However *Saito and Ogawa* (1974) in an enzyme-histochemical study suggested that such lysosomes participated in the autophagic process.

(2) *From nonlysosomal cytoplasmic vacuoles* Vacuoles were common in the irradiated cells. Pictures suggestive of autophagy by exotropy into preformed, flattened vacuoles were often obtained (Fig. 8) These vacuoles were observed to be lined by a membrane approximately 100 Å thick. Since the lumen between the flattened membranes was devoid of the finely granular material observed in the lysosomes, and as endocytotic vacuoles were common in the irradiated cells, these vacuoles are presumed to originate from the cell membrane (although some of them might possibly stem from the Golgi apparatus)

In the present study autophagic vacuoles were of a highly variable appearance. Some were surrounded by a cleft-like space in the cytoplasm with bordering membranes of obscure origin (Fig 11) In some instances these membranes were in close vicinity to rough endoplasmic reticulum. By close examination, however it became apparent that continuity between these membranes and endoplasmic reticulum was lacking (Figs. 7 and 10) On the basis of the fine structural appearance alone, it does not seem possible to determine whether these membranes originally were derived from the rough surfaced endoplasmic reticulum (*Holtman* 1976) from membranes of other organelles such as Golgi cisternae (*Locke and Collins* 1965) or were formed *de novo* (*Pfeifer* 1971) Autophagy utilizing membranes belonging to the smooth endoplasmic reticulum—commonly seen in g liver cells (*Ericsson* 1969)—were not evident in the glia cells which almost completely lack this type of endoplasmic reticulum.

III *Development and Fate of Autophagic Vacuoles*

Early after irradiation the cells contained a great amount of autophagic vacuoles, often lined by a pair of unit membranes Later on, secondary lysosomes and residual bodies lined by a single membrane dominated. Thus, it would seem that the autophagic vacuoles loose one of their limiting membranes in the course of development into secondary lysosomes and residual bodies. Theoretically this could be accomplished in different ways

(1) Following fusion with a lysosome, the space between the two limiting membranes of the autophagic vacuole might be filled by hydrolytic enzymes and the inner membrane digested (*Arstila and Trump* 1968) However this theory suffers from the difficulties in explaining why only the inner membrane is digested.

(2) The inner and outer membranes of the autophagic vacuole might melt together to form a single membrane in a process termed "compaction (*Novikoff and Shin* 1964) Figure 13—showing a vacuole surrounded by a 5-layered 200 Å membrane—may illustrate an intermediary step in the presumed compaction procedure. In this case, the vacuole is likely to have originated from a lysosome or an endocytotic vacuole.

The proposed mechanism of compaction is outlined in Fig 21 Theoretically the compaction of membranes in an autophagic vacuole derived from a lysosome could yield a vacuole containing lysosomal matrix (with enzymes) attached to the autophagic vacuole. In a further step, this imagined vacuole could either fuse with the autophagic vacuole or be pinched off attaining the features of a small lysosome (Fig 21)

In the case of an autophagic vacuole formed by a lysosome, the hydrolytic enzymes that are to be added to the segregated material would evidently be present from the beginning of the autophagic process. This may theoretically hold true even in the case of a vacuole formed by Golgi membranes or smooth surfaced endoplasmic reticulum. In the case of an autophagic vacuole formed *de novo* or originating from an endocytotic vacuole, the hydrolytic enzymes would have to be added by fusion of the autophagic vacuole with a primary or a secondary lysosome (Table 1 Fig. 21)

IV Residual Body Formation and Proliferation of Golgi Areas

The evidently increased number of autophagic vacuoles present in the irradiated cells does not necessarily imply an increased formation of autophagic vacuoles. A decreased turnover rate of autophagic vacuoles, due to e g enzyme inhibition would also result in a high prevalence of vacuoles However the greatly increased amount of residual bodies observed after irradiation indicates an absolute increase in the formation of autophagic vacuoles followed by degradation of vacuolar contents by active hydrolytic enzymes.

It appears unlikely that the residual bodies result from heterophagocytosis of organelles from the medium since endocytosis of such organelles has never been observed Further more residual bodies are known to accumulate in contact inhibited monolayers of human glia cells when they are kept without subcultivation for prolonged periods of time (*Brunk et al* 1973) In such cultures there is no apparent cell death

The consequenses of accumulation of residual bodies are not fully known. However it seems likely that a massive occurrence of such organelles, occupying a great proportion of the cell volume, would adversely affect different cell functions, *e g* in aged neurons filled with lipofuscin pigment granules or cells affected by lysosomal storage diseases.

Accumulation of residual bodies is seen in ageing *in vitro* cultured glia cells and so is proliferation of Golgi regions (*Brunk et al* 1973) These observations are also valid for *e g* cultured fibroblasts (*Lipetz and Cristofaly 1972)* The Golgi proliferation and residual body accumulation has also been reported to occur in irradiated cells other than glia cells (for references see *Hamberg et al* 1976) It is tempting to assume that the Golgi proliferation may reflect an increased synthesis of enzymes to be distributed to autophagic vacuoles and secondary lysosomes of different kinds.

CONCLUSIONS

Following irradiation glia cells react by increased cytoplasmic membrane ruffling and enhanced endocytotic activity Obviously this results in internalization of plasma membranes into the vacuolar system of the cytoplasm The cells also exhibit a markedly enhanced autophagocytotic activity It seems possible that these morphologic alterations are indications of a reparative process in which damaged organelles and membranes are eliminated and their constituents reutilized In heavily irradiated glia cells, however it can be expected that the reparative measures are unsuccessful and cell death ensues.

The ultrastructural features of autophagy in the irradiated cells suggest the existence of alternate sources of the isolation membranes viz. lysosomes and endocytotic vesicles and/or —possibly—Golgi elements (vacuoles, cisternae) These observations, in the light of earlier studies suggesting smooth endoplasmic reticulum as the origin of the isolation membrane (*Ericsson* 1969) not only indicate that mechanisms operative in the formation of the membranes bordering autophagic vacuoles vary with the cell type they also make it likely that in a given cell alternate routes may be used during the sequestration process. In order to further elucidate to what extent different membrane structures in the glia cells are involved in autophagy supplementary experiments including histochemical identification of these membranes are needed. The possible role for endocytotic vacuoles and preexisting secondary lysosomes in autophagy in these cells also needs to be investigated, preferably by the use of marker molecules introduced into endocytotic vacuoles and the lysosomal vacuome

---

This work was supported by a grant from the *Swedish Medical Research Council* (project number B77 12X-01006-12C)

REFERENCES

Arstila, A. U & *Trump B F.*, Studies on cellular autophagocytosis. The formation of autophagic vacuoles in the liver after glucagon administration. Am. J Path. 53 687–733 1968.

Ashford T P & *Porter K. R.*, Cytoplasmic components in hepatic cell lysosomes. J Cell Biol. *12* 198–202, 1962

Brunk, U Ericsson, J L. E., Ponten J & *Westermark B.*: Specialization of cell surfaces in contact-inhibited human glia-like cells *in vitro* Exptl. Cell Res 67 407–415, 1971

Brunk, U Ericsson J L. E., Ponten, J & *Westermark B* Residual bodies and "aging" in cultured human glia cells. Effect of entrance into phase III and prolonged periods of confluence. Exptl Cell Res 79 1–14 1973

Collins V P Arborgh, B., Brunk U T & *Fredriksson, B. A* The phagocytosis of mitochondria by *in vitro* cultivated diploid human glia cells. In O Johari and R. P Becker (Eds.) Proc 9th Annual Scanning Electron Microscope Symposium, pp. 187–194 Vol. 2., IIT Research Institute, Chicago, 1976

Ericsson J L E., Mechanism of cellular autophagy In J T Dingle & H. B. Fell (Eds.) Lysosomes in Biology and Pathology North Holland, Amsterdam & London, 1969 Vol. 2.

Fedorko M E Hirsch J G & *Cohn Z. A* Autophagic vacuoles produced *in vitro* II Studies on the mechanism of formation of autophagic vacuoles produced by chloroquine, J Cell Biol. *38* 392–402 1968

Forsby N & *Collins, P* Ultrastructural studies of *in vitro* cultivated normal and malignant cells. Abstracts of the XIth International Cancer Congress, Florence Oct. 1974

Hamberg, H Brunk U T Ericsson J L. E. & *Jung B* Cytoplasmic effects of X-irradiation on cultured cells in a non-dividing stage. I. Establishment of an experimental model. Acta path. microbiol scand. Sect A, *84* 201 214 1976.

Holtzman E. Lysosomes A survey Springer Verlag, New York, Vienna, 1976

Lipetz J & *Cristofalo V J.*, Ultrastructural changes accompanying the ageing of human diploid cells in culture. J Ultrastr Res. 39 43–56 1972.

Locke M & *Collins J V.*, The structure and formation of protein granules in the fat body of an insect. J Cell Biol. 26 857–884 1965.

Locke M & *Sykes A K.*, The role of the Golgi complex in the isolation and digestion of organelles. Tissue & Cell 7 143–158, 1975

Miller F & *Palade G E.*, Lytic activities in renal protein absorption droplets. J Cell Biol. 23 519–552, 1964.

Novikoff A. B & *Shin W Y.*, The endoplasmic reticulum in the Golgi zone and its relations to microbodies, Golgi apparatus, and autophagic vacuoles in rat liver cells. J Microscopie 3 187–206 1964

Ostenda M Ultrastructure of glial cells irradiated *in vitro* with gamma rays. Neuropath. Pol. *11* 405–410 1973.

Pfeifer U., Probleme der cellulären Autophagie. Advances in Anatomy Embryology and Cell Biology *44* Heft 4 1971

Plattner H., Henning, R. & *Brauser B.* Formation of Triton WR 1339-filled rat liver lysosomes. II Involvement of autophagy and of pre-existing lysosomes. Exptl. Cell Res. *94* 377–391 1975

René A A., Darden J H & *Parker J L.*, Radiation-induced ultrastructural and biochemical changes in lysosomes. Lab. Invest. *25* 230–239 1971

Sato T & *Ogawa K.*, Lysosomal changes in rat hepatic parenchymal cells after glucagon administration. Acta Histochem. et Cytochem. *7* 1 18, 1974

Trump B F The network of intracellular membranes In G Weismann & R. Claiborne (Eds.) Cell Membranes – Biochemistry Cell Biology & Pathology HP Publish. New York, 1975, pp 123 133.

Watkins D K.: Lysosomes and irradiation injury In J T Dingle & R. T Dean (Eds.) Lysosomes in Biology and Pathology North Holland/Amer Elsevier publ., Amsterdam—New York, 1975 Vol. 4 147–166

IV Residual Body Formation and Proliferation of Golgi Areas

The evidently increased number of autophagic vacuoles present in the irradiated cells does not necessarily imply an increased formation of autophagic vacuoles. A decreased turnover rate of autophagic vacuoles, due to *e g* enzyme inhibition would also result in a high prevalence of vacuoles. However the greatly increased amount of residual bodies observed after irradiation indicates an absolute increase in the formation of autophagic vacuoles followed by degradation of vacuolar contents by active hydrolytic enzymes.

It appears unlikely that the residual bodies result from heterophagocytosis of organelles from the medium since endocytosis of such organelles has never been observed Furthermore residual bodies are known to accumulate in contact inhibited monolayers of human glia cells when they are kept without subcultivation for prolonged periods of time (*Brunk et al* 1973) In such cultures there is no apparent cell death

The consequenses of accumulation of residual bodies are not fully known However it seems likely that a massive occurrence of such organelles, occupying a great proportion of the cell volume would adversely affect different cell functions, *e g* in aged neurons filled with lipofuscin pigment granules or cells affected by lysosomal storage diseases.

Accumulation of residual bodies is seen in ageing *in vitro* cultured glia cells and so is proliferation of Golgi regions (*Brunk et al* 1973) These observations are also valid for *e g* cultured fibroblasts (*Lipetz and Cristofaly 1972*) The Golgi proliferation and residual body accumulation has also been reported to occur in irradiated cells other than glia cells (for references, see *Hamberg et al* 1976) It is tempting to assume that the Golgi proliferation may reflect an increased synthesis of enzymes to be distributed to autophagic vacuoles and secondary lysosomes of different kinds

CONCLUSIONS

Following irradiation glia cells react by increased cytoplasmic membrane ruffling and enhanced endocytotic activity Obviously this results in internalization of plasma membranes into the vacuolar system of the cytoplasm. The cells also exhibit a markedly enhanced autophagocytotic activity It seems possible that these morphologic alterations are indications of a reparative process in which damaged organelles and membranes are eliminated and their constituents reutilized. In heavily irradiated glia cells, however it can be expected that the reparative measures are unsuccessful and cell death ensues.

The ultrastructural features of autophagy in the irradiated cells suggest the existence of alternate sources of the isolation membranes *viz* lysosomes and endocytotic vesicles and/or —possibly—Golgi elements (vacuoles, cisternae) These observations, in the light of earlier studies suggesting smooth endoplasmic reticulum as the origin of the isolation membrane (*Ericsson* 1969) not only indicate that mechanisms operative in the formation of the membranes bordering autophagic vacuoles vary with the cell type they also make it likely that in a given cell alternate routes may be used during the sequestration process. In order to further elucidate to what extent different membrane structures in the glia cells are involved in autophagy supplementary experiments including histochemical identification of these membranes are needed. The possible role for endocytotic vacuoles and preexisting secondary lysosomes in autophagy in these cells also needs to be investigated, preferably by the use of marker molecules introduced into endocytotic vacuoles and the lysosomal vacuome

---

This work was supported by a grant from the *Swedish Medical Research Council* (project number B77 12X-01006-12C)

ed to be a form of multicentric, focal, mesenchymal dysplasia developing during the last few months of intra-uterine life (*Enzinger* 1965). In most reported cases, the multinodular lesions of predominantly fibroblastic mesenchymal tissue involved the subcutaneous tissue and/or skeletal muscle and viscera and/or skeleton, and have often proved fatal (*Williams & Schrum* 1951, *Stout* 1954, *Schlosser & Rotzler* 1952, *Grotton* 1955, *Shnitka et al.* 1958, *Bartlett et al.* 1961, *Christensen et al.* 1961, *Condon & Allen* 1961, *Beatty* 1962, *Teo & Teoh* 1963, *Enzinger* 1965, *Streit & Kirsch* 1967, *Daudet et al.* 1969, *Morettin et al.* 1972, *Autine et al.* 1974, *Dehner et al.* 1976). Complete or partial spontaneous regression has been described (*Holt & Wright* 1948, *Legall et al.* 1962, *Teng et al.* 1963, *Mande et al.* 1966, *Schaffzin et al.* 1972, *Plaschkes* 1974). In several published cases the multiple lesions have been restricted to the subcutaneous tissue and/or skeletal muscle (*Bartlett et al.* 1961, *Kauffman & Stout* 1965, *Enzinger* 1965). None of these cases were fatal. Occasional cases with multiple lesions histologically indistinguishable from congenital generalized fibromatosis were restricted to the skeleton and showed spontaneous regression (*Zeisel & Helbig* 1955, *Jaffe* 1958, *Heiple et al.* 1972). To our knowledge, a solitary form of congenital generalized fibromatosis has not been described in the literature. However *Enzinger* (a. 196.) mentioned that among his series of unclassified solitary fibromatoses in infancy there were cases which appeared histologically similar to congenital generalized fibromatosis.

This paper presents 2 cases of congenital solitary fibromatosis and describes their clinical course, light microscopic apperance and, in one case, the ultrastructural findings.

CASE REPORTS

Case 1. – A 10-day-old boy was subjected to surgery because of a tumour in the right gluteal region. The tumour was noticed immediately after a straight-forward delivery and seemed to enlarge slowly during the following 10 days. At operation, the tumour appeared partly encapsulated and was found to be intermuscularly situated close to the deeper portion of the fascia of the gluteus maximus muscle. The tumour was excised with the adjacent fascia and a margin of surrounding muscle. There was no family history of congenital tumours. Over the next 21 years no new tumours developed, nor were there any signs of recurrences or metastases.

Case 2. – A previously healthy $3^{10}/_{12}$-year-old girl was admitted to hospital with a painless lump in the right thigh, which had been noticed a week earlier by her mother. The tumour situated within the rectus muscle was excised with the surrounding skeletal muscle. The patient has a healthy sister and there is no history of congenital tumours in the rest of her family. One year after the operation there were no signs of other tumours, recurrences or metastases.

PATHOLOGY

Light Microscopy

The surgical specimens were fixed in 4 per cent formaldehyde solution and embedded in paraffin. Fi... µm-thick sections were stained according to the haematoxylin-van Gieson method and with haematoxylin and eosin. Gordon's silver impregnation was used for the demonstration of reticulin fibres and Palmgren's silver impregnation to demonstrate the presence of axons. The periodic acid-Schiff reaction (McManus) with or without prior diastase digestion was used to study glycogen, and Luxol fast blue to demonstrate the presence of myelin sheats. For the demonstration of calcium, an Kossa-staining was performed.

Electron Microscopy

Only paraffin-embedded material was available in case 2. Small tumour pieces from selected areas of 6–20 µm-thick sections from the paraffin blocks were carefully deparaffinized in xylene, dehydrated in decreasing concentrations of ethanol and finally washed in cacodylate buffer. Thereafter the tissue was fixed in 1 per cent osmium tetroxide in cacodylate buffer pH 7.2 for 2 hours, dehydrated in ethanol and embedded in Epon 812. Ultrathin sections were cut in an LKB Ultrotome III, stained with uranyl acetate and lead citrate, examined and photographed in a Philips EM 200 electron microscope.

Case 1

Gross Appearance. The surgical specimen consisted of a 5×4×2.5 cm lobulated tumour weighing 120 g. The tumour appeared predominantly well-delineated and partly encapsulated, but in some areas there was no distinct demarcation between the fascia and the tumour. The cut surface of the tumour was mottled light-brown and grey-red, with necrotic areas centrally.

Acta path. microbiol scand Sect A 85 640 648 1977

CONGENITAL SOLITARY FIBROMATOSIS OF SOFT TISSUES, A VARIANT OF CONGENITAL GENERALIZED FIBROMATOSIS

2 Case Reports

LARS-GUNNAR KINDBLOM GUNNAR TERMÉN
JOHAN SAVE SÖDERBERGH and LENNART ANGERVALL

Department of Pathology II University of Göteborg Sweden

Kindblom L.-G., Termén G Säve-Söderbergh, J & Angervall L. Congenital solitary fibromatosis of soft tissues, a variant of congenital generalized fibromatosis. 2 case reports. Acta path. microbiol scand Sect A 85 640–648 1977

A report of 2 cases of solitary fibromatosis in a 10-day-old boy and a girl 3 years and 10 months old is presented Both lesions were deep-seated and showed a nodular and infiltrating growth predominantly built-up by immature fibroblast like cells and including hemangiopericytoma like areas. One of the lesions also showed leiomyoma like areas. An ultrastructural study however revealed no intra-cytoplasmatic myofilaments. At follow-up examinations after 21 years and 1 year respectively there were no signs of recurrences or metastases. These 2 cases are considered to represent a solitary form of congenital generalized fibromatosis. The differential diagnosis from infantile hemangiopericytoma and fibrous lesions seen in infancy and early childhood such as infantile fibrosarcoma, diffuse infantile fibromatosis, extra-abdominal desmoid fibrous hamartoma of infancy and juvenile aponeurotic fibroma, is discussed.

Key words Congenital fibromatosis fibromatosis infancy soft tissue tumour

L.-G Kindblom, Department of Pathology Vasa Hospital, S-411 33 Göteborg, Sweden

Received 3 i 77 Accepted 12 iv 77

Among mesenchymal tumours there is a large complex group of fibrous proliferations occurring in infancy and early childhood (*Stout* 1954 *Enzinger* 1965 *Macken ie* 1972 *Dehner et al* 1976) The incidence of fibromatosis in neonates is second only to that of vascular tumours (*Kauffman & Stout* 1965) Among the congenital or infantile fibromatoses may be included fibromatosis colli (*Coventry et al.* 1960 *Iwahara & Ikeda* 1962 *Mackenzie 1970 Rosai & Ackerman* 1974) recurrent digital fibromatosis (*Reye* 1965) fibrous hamartoma of infancy (*Enzinger 1965*) diffuse infantile fibromatosis (*Enzinger* 1965) fibromatosis hyalinica multiplex juvenilis (*Drescher et al* 1967 *Woyke et al* 1970) juvenile aponeurotic fibroma (*Keasbey* 1953, *Kindblom* 1970 *Allen & Enzinger 1970*) hereditary gingival fibromatosis (*Rushton* 1956) and congenital generalized (multiple) fibromatosis.

Congenital generalized fibromatosis, a rare lesion described by *Stout* (1954) is consider

3

4

5

6

Light microscopic appearance There was considerable variation in the microscopic appearance of different areas of the tumour The cells at the periphery of the tumour contained elongated or oval fibroblast like nuclei within a fusiform faintly eosinophilic, poorly-outlined cytoplasm (Fig 1) In the central parts of the tumour the cells were immature-looking with rounded or oval chromatin-rich nuclei and a weakly eosinophilic granular cytoplasm There was no distinct fascicular arrangement of cells except at the periphery of the tumour where only scattered collagen fibres were found. Mitotic figures were exceedingly rare The tumour vessels most abundant peripherally were predominantly capillary like or sinusoidal These vessels were frequently angulated and surrounded by proliferating tumour cells giving these areas of the tumour a pericytoma-like appearance (Fig 2) Neither axons nor myelin sheaths suggestive of a neurogenic origin were found nor were significant amounts of glycogen or intracytoplasmic fibrils, suggestive of a muscle tumour observed.



Fig 1 The peripheral part of the tumour (left) shows cell with elongated nuclei and a tendency to fascicular arrangement the highly cellular central parts (right) show partly a pericytoma like pattern H & E × 90



Fig 2 Case 1 Highly cellular areas with a pericytoma like pattern and multiple small foci of calcification. H & E × 90

Centrally there were necrotic areas. Widespread foci of calcification were found within the tumour frequently adjacent to the irregular vascular spaces. Haemosiderin pigment was found both intra and extracellularly in the tumour tissue adjacent to the necrotic areas and the calcifications. Peripherally the tumour showed a nodular

---

Fig 3 Case 2. A leiomyoma like area showing a fascicular intertwining arrangement. van Gieson × 120

Fig 4 Case 2 Fibroblast-like fusiform tumour cells with a tendency to fasciular arrangement. H & E × 180

Fig 5 Irregularly-arranged delicate collagen fibre bundles within the tumour van Gieson × 225

Fig 6 Closely-arranged angulated sinusoidal vascular spaces giving a pericytoma like pattern. H & E × 180

3







growth pattern and infiltrated the surrounding connective tissue and skeletal muscle.

Case 2

Gross appearance At operation the tumour appeared to be fairly well demarcated and measured 1.5×1.5×1 cm after fixation

Light microscopic appearance The tumour was partly composed of fusiform cells with oval or elongated nuclei and faintly picrinophilic and eosinophilic cytoplasm, cytologically similar to leiomyblasts The leiomyoma like character of the tumour was further enhanced by a fascicular intertwining of the cells (Fig. 3) However fuchsinophilic fibrils within the cytoplasm of the tumour cells were not observed, and the nuclei were pale staining and more vesicular than the nuclei usually seen in leiomyomatous tumours. Collagen fibres were abundant both in these areas of the tumour and in areas composed of more immature-looking or fibroblast like cells Bundles of collagen fibres were frequently seen separating the tumour cell fascicles or enclosing clumps of cells. Centrally the tumour cells were more plump the nuclei were rounded and in some cells stained darker (Figs. 4 & 5) Occasional mitotic figures were observed. Within the central parts of the tumour were several cleft like angulated spaces, some of which were distinct sinusoidal blood filled vessels, giving a pericytoma-like appearance (Fig 6) As in case 1 there was no encapsulation the tumour showed a nodular growth pattern at the periphery and infiltration of skeletal muscle tissue (Fig 7)

Electron microscopic appearance The cellular appearance of the paraffin-embedded tumour tissue of case 2 was sufficiently well preserved to allow ultrastructural examination after reprocessing and osmium fixation. Myofibrils were for example easily identifiable in the adjacent striated muscle tissue.

The tumour tissue was highly cellular composed of closely arranged cells with pale cytoplasm and ill-defined cytoplasmic membranes (Fig 8) The cells were elongated with several fusiform extensions, usually appearing in the sections as small round parts of cells without nuclei The nuclei were elongated with smooth outlines and distinct nucleoli small invaginations were seen in some cells. The cytoplasm contained few organelles. Several uncharacteristic, very fine short filaments were dispersed in a clear cytoplasm (Fig 9) containing few parallel membranes of endoplasmic reticulum Shadows of a few mitochondria were seen No myofilaments or basement membranes could be demonstrated. A few collagen fibres with characteristic crossbanding were found intercellularly



Fig 7 Case 2. Atrophic muscle fibres split-up by the infiltrating tumour tissue and surrounded by mononuclear inflammatory cells. H & E × 170.

DISCUSSION

The tumours in both these cases had several clinical and histological features in common the deep intra or intermuscular location, the nodular and infiltrating growth pattern, the predominantly or partly immature fibroblast like cell population the pericytoma like areas and a clinical course free from recurrences or metastases The histological appearance of both the tumours has been described as being typical of congenital generalized fibromatosis (*Shnitka et al* 1958 *Teng et al* 1963 *Enzinger* 1965 *Schaffzin et al.* 1972) The microscopic appearance of the two present cases corroborates Enzinger's observations (1965) that it is impossible to distinguish histologically between solitary and generalized fibromatosis, and suggests that the clinical picture



Fig. 8. Cellular tumour tissue with elongated tumour cells and numerous cut cytoplasmic extensions × 16,200.

of congenital fibromatosis varies widely and ranges from a fatal generalized form to a solitary form with benign course. The infiltrating growth-pattern, the highly cellular tumour tissue and the sometimes prominent mitotic figures may lead to misinterpretation of the tumour as a sarcoma. In fact, the tumour in case 2 was sent to us for consultation with the suggested diagnosis rhabdomyosarcoma, and case 1 had originally been diagnosed as a locally malignant neurogenic tumour.

Malignant fibrous tumours in neonates and infants have been described (*Stout* 1962, *Goslee et al* 1964, *Balsaver et al* 1967, *Soule et al* 1968, *Gonzales-Crussi* 1970, *Dahl et al* 1973, *Chung & Enzinger* 1976). Infantile fibrosarcoma may resemble congenital solitary fibromatosis: both tumours infiltrate surrounding tissue and are predominantly composed of immature spindle-shaped fibroblast-like cells. Furthermore, a pericytoma-like pattern such as was found in both the present cases may also occasionally be seen in infantile fibrosarcoma (*Chung & Enzinger* 1976). However, infantile fibrosarcoma differs histologically in its greater cellularity, higher mitotic activity and cellular atypia (*Dahl et al* 1973, *Chung & Enzinger* 1976). Furthermore, infantile fibrosarcoma has a rather homogeneous cell structure devoid of the leiomyoma-like areas found in case 2.

Diffuse infantile fibromatosis, not yet a fully established entity, is usually a solitary fibroblastic growth predominantly involving voluntary muscle. The multicentric and diffuse growth of fibroblastic proliferations enclosing individual muscle fibres may extend



Fig 9 Tumour cell with atypical intracytoplasmic *fine filaments and extracellular collagen fibres.* × 60 000

along fasciae and the presence of mature fat and aggregates of lymphocytes seems to distinguish this lesion from congenital solitary fibromatosis (*Enzinger* 1965)

Extra abdominal desmoid rarely seen in early childhood and only occasionally in infancy should be included in the differential diagnoses of intramuscular fibrous lesions (*Das Gupta et al* 1969) Occasionally the extra abdominal desmoid may contain myxoid areas and metaplastic bone (*Enzinger & Shiraki* 1967 *Das Gupta et al* 1969) Usually however extra abdominal desmoid can be clearly distinguished from solitary congenital fibromatosis by its monotonous desmoplastic appearance with evenly-distributed collagen and elongated slender cells forming interlacing bundles or fascicles Moreover the vasculature predominantly consists of small thick walled vessels, and there is no hemangiopericytoma like pattern.

Fibrous hamartoma of infancy is clearly distinguished from congenital solitary fibromatosis by the characteristic organoid arrangement of traversing bundles of dense fibrocollagenous tissue immature-appearing *mucoid loose-textured* cellular areas and mature fat. Moreover these lesions are situated in the lower dermis or subcutaneous fat (*Reye* 1956 *Enzinger* 1965)

Juvenile aponeurotic fibroma may because *of its infiltrative growth pattern of a cellular* fibrous tissue possess some features similar to *those seen in the two present cases.* Histologically juvenile aponeurotic fibroma contains, however calcified foci surrounded by radiating columns of cells in a chondroid matrix and multinucleated giant cells adjacent to the calcium deposits (*Keasbey* 1953, *Allen & Enzinger* 1970 *Kindblom* 1970) Juvenile aponeurotic fibromas are located in the hand wrist, or sole of the foot a characteristic that may be helpful in the differential diagnoses.

The 2 cases differed from each other firstly in the age of the patient at discovery and secondly in the more mature histological appearance of the tumour in case 2 The more mature cellular appearance in case 2 may be related to the fact that the patient was older at removal of the tumour *Congenital fibromatosis* has been considered to be a mesenchymal dysplasia Differentiation into non fibroblastic mesenchymal tissue has seemingly been found in previously reported cases (*Bartlett et al* 1961 *Beatty* 1962 *Enzinger* 1965) and the term generalized hamartomatosis has been suggested (*Morettin et al* 1972)

In case 2, areas within the tumour had a histological appearance suggestive of leiomyomatous differentiation, and both tumours showed *pericytoma* like areas. Infantile hemangiopericytoma has some histological characteristics in common *with congenital* generalized fibromatosis, but apart from the pericytoma pattern both tumours reveal a multinodular growth variable mitotic activity and

occasional necroses (*Enzinger* & *Smith* 1976) However in contrast to congenital generalized fibromatosis, infantile hemangiopericytoma is characterised by a prominent pericytoma pattern throughout the whole lesion a frequent endothelial proliferation suggesting a relationship with hemangioendothelioma and an exclusively subcutaneous location of the tumour (*Enzinger* & *Smith* 1976)

The only previously reported case of congenital generalized fibromatosis studied by electron microscopy revealed intracytoplasmic filaments interpreted as myofilaments (*Morrison et al.* 1972) In the present study however the electron microscope examination of case 2 revealed neither myofilaments such as those found in smooth muscle cells nor any basement membrane like structures such as seen in neurogenic tumours and sometimes in hemangiopericytomas (*Fisher* & *Vuzevski* 1968, *Battifora* & *Hines* 1971 *Spence* & *Rubinstein* 1975)

The clinical course without recurrences, despite the infiltrative growth in the 2 cases presented suggests that complete surgical removal is the treatment of choice.

REFERENCES

Ackerman, L. V. & *Rosai, J.* Surgical pathology The C V Mosby Co pp 1118–1119 St Louis, 1974

Allen, P W & *Enzinger F M* Juvenile aponeurotic fibroma Cancer *26* 857–867 1970

Anita B E Brown F M & *Anson M J* Fibroma of the cornea Report of case associated with congenital generalized fibromatosis Archives of Opthalmology *91* 278–280 1974

Balsaver A M Butler J J & *Martin R G* Congenital fibrosarcoma Cancer *20* 1607 1616, 1967

Bartlett R C Otis R D & *Laakso A O* Multiple congenital neoplasms of soft tissues Report of 4 cases in 1 family Cancer 14 913–920 1961

Battifora H & *Hines J R* Recurrent digital fibromas of childhood, an electron microscope study Cancer 27 1530 1536 1971

Beatty E C J Congenital generalized fibromatosis in infancy Am Journal of Diseases of Children *103* 620–624 1962

Christensen E Hjgaard K & *Winkel-Smith* C C Congenital malignant mesenchymal tumors in two month old child. Acta path. et microbiol. scand. *53*: 237–242, 1961

Chung, E. B. & *Enzinger F M.* Infantile fibrosarcoma. Cancer *38*: 729–739 1976

Condon V R. & *Allen R. P.* Congenital generalized fibromatosis. Case report. Roentgen Manifestations, Radiology *76* 444–448, 1961

Coventry M B. Harris L. E., Bianc A J & *Bulbulian A H* Congenital muscular torticollis (wryneck) Postgraduate Medicine *28* 383 392 1960

Dahl, I., Save-Söderbergh J & *Angervall L.* Fibrosarcoma in early infancy Path. Europ. *8*: 193–209 1973

Das Gupta T K Brasfield M D & *O Hara J.* Extra-Abdominal Desmoids A clinicopathological Study Ann. Surg. *170* 109 121 1969

Daudet M Chappuis B S Rosenberg D & *Monnelle J C* Fibromatose congénitale multiple. Ann. de chir infantile *10* 273–282, 1969.

Dehner L. P & *Askin F B* Tumors of fibrous tissue origin in childhood. A clinicopathologic study of cutaneous and soft tissue neoplasms in 66 children. Cancer *38* 888–900, 1976.

Drescher E Woyke S Markiewicz C & *Tegi S* Juvenile fibromatosis in siblings (*fibromatosis hyalinica multiplex juvenilis*) J Pediatr Surg 2 427–430 1967

Enzinger F M Fibrous hamartoma of infancy Cancer *18* 241 248 1965 b.

Enzinger F M. Fibrous tumors of infancy In Tumors of bone and soft tissue. pp 375–396. Chicago. Year book Medical Publishers Inc., 1965 a.

Enzinger F M & *Smith, B* Hemangiopericytoma. An analysis of 106 cases. Human Path. 7 61–82, 1976

Gonzalez-Crussi F. Ultrastructure of congenital fibrosarcoma. Cancer 26 1289–1299 1970.

Goder L., Clermont V Bernstein J & *Welley P V J* Superficial connective disease in early infancy J Pediatrics *65* 377–387 1964

Grotten H A Sarkom der Haut. Hautarzt 4 1–11 1953

Heiple K G Perrin E. & *Aikawa M* Congenital generalized fibromatosis. A case limited to osseous lesions. J Bone & Joint Surg. 54-A 665–669 1972.

Holt J F & *Wright E. M* The radiologic features of neurofibromatosis Radiology *51* 647–663 1948.

Iwahara T & *Ikeda, A* On the ipsilateral involvement of congenital muscular torticollis and congenital dislocation of the hip Journal of the Japanese Orthopaedic Association *35* 1221 1226 1962

Jaffe H L. Tumors and tumorous conditions of the bones and joints, p. 249 Philadelphia, Lea and Febiger 1958.

Kauffman S L & Stout A P Congenital mesenchymal tumors Cancer *18* 160–176 1965

Keasbey L E Juvenile aponeurotic fibroma (calcifying fibroma) Cancer *6* 338–346 1953

Kindblom L-G Juvenilt aponeurotiskt fibrom. Kort översikt över fibrösa tumörer hos barn jämte en fallbeskrivning Särtryck ur Opuscula Medica Bd 15 nr *8* 295–300 1970

Legall Y Schneegans E & Buck P Les tumeurs fibromateuses de la première enfance Ann. Chir Infantile *3* 105–114 1962.

Luck J V Dupuytren's contracture. J Bone Jt. Surg *41* A 635 1959

Mackenzie D H The differential diagnosis of fibroblastic disorders, pp 72–75 Blackwell Scientific Publications Oxford and Edinburgh, 1970

Mackenzie D H The fibromatoses —A clinicopathological concept. Br Med J *4* 277–280 1972

Mande R Hennequet A., Loubry P Cloup M & Marie J Fibromatose congénitale diffuse du nouveau-né à évolution régressive Ann. Pediat (Paris) *12* 692–701 1965

Morettin L B Mueller E & Schreiber M Generalized hamartomatosis (congenital generalized fibromatosis) Am. J Roentgenol. Radium Ther Nucl. Med. *114* 722–734 1972

Pickren J W Smith A G Stevenson T W Jr & Stout A P Fibromatosis of the plantar fascia. Cancer *4* 846–856 1951

Plaschkes J Congenital fibromatosis.—Localized and generalized forms. J Pediatr Surg *9* 95–101 1974

Reye R D K Recurring digital fibrous tumors of childhood. Arch. Pathol. *80* 228–231 1965

Rushton M A Hereditary or idiopathic hyperplasi of the gums Dent Practit. dent. Rec. *7* 136 1956

Schaffzin P A Chung S M K & Kaye R Congenital generalized fibromatosis with complete spontaneous regression. A case report. J Bone Joint. Surg (Am.) *54* 657–662, 1972.

Schlösser W & Rotzler A Zur Kasuistik angeborener Geschwülste Spindelzelliges Sarkom mit ausgedehnter Metastasierung. Zentralbl allg Path. *88* 161–163 1952

Shnitka T K Asp D M & Horner R H Congenital generalized fibromatosis. Cancer *11* 627–639 1958.

Soule E H Mahour H G Mills S D & Lynn H D Soft-tissue sarcomas of infants and children A clinicopathologic study of 135 cases. Mayo clin Proc. *43* 313–326 1968

Spencer A M & Rubinstein L J Cerebellar capillary hemangioblastoma Its histogenesis studied by organ culture and electron microscopy Cancer *35* 326–341 1975.

Stout A P Juvenile fibromatoses. Cancer *7* 953–978 1954

Stout A P Fibrosarcoma in infants and children. Cancer *15* 1028–1040 1962

Streit W & Kirsch W Multiple fibroblastische Proliferationsherde bei einer Neugeborenen Helvet paediat acta *22* 271–277 1967

Teng P Warden H J & Cohn W L Congenital generalized fibromatosis (renal and skeletal) with complete spontaneous regression. J Pediat. *62* 748–753 1963

Ts o T O T & Teoh T B Fibromatosis in an infant. J Pathol. Bacteriol. *85* 521–525 1963.

Williams J O & Schrum D Congenital fibrosarcoma. Arch. Path. *51* 548–552 1951

Woyke S Domagala W & Olszewski W Ultrastructure of a fibromatosis hyalinica multiplex juvenilis. Cancer *26* 1157–1168, 1970

Zeisel H & Helbig G Polyostische polytope, fast systematisierte Skeletaffektion mit paraossalen Herden beim Säugling Zeitsch. Kinderh *76* 379–388 1955

Acta path. microbiol. scand. Sect. A 85 649–655 1977

ALPHA 1 ANTITRYPSIN DEFICIENCY

Experience from an Autopsy Material

INGERMARIE REINTOFT

The Pathology Department, Esbjerg Central Hospital, Esbjerg, Denmark.

Reintoft, I. Alpha-1-antitrypsin deficiency. Experience from an autopsy material. Acta path. microbiol. scand. Sect. A, 85: 649–655, 1977.

Alpha-1-antitrypsin deficiency of genotype PiZ was found in 15 persons (6.3 per cent) out of an autopsy series of 238. The hepatic tissue was screened after diastase digestion and PAS staining. The globules demonstrated thereby showed by the immunoperoxidase reaction an antigenic identity with alpha-1-antitrypsin. It is estimated that one of the persons was homozygous, the others heterozygous. Among the latter, pulmonary emphysema was rather more common than found previously, whereas the hepatic changes were not quite so pronounced.

Key words: Antitrypsin alpha 1 deficiency; autopsy.

Ingermarie Reintoft, Retsmedicinsk Institut, 17 J. B. Winsløwsvej, DK 5000 Odense, Denmark.

Received 30.ii.77 Accepted 20. i.77

Alpha-1-antitrypsin (A 1-AT) is an enzyme formed in the liver. It makes up about 90 per cent of the protease inhibitor capacity of the serum. There are many molecular variants of A 1 AT, which is also called Pi (Protease inhibitor); in the presence of most, the serum concentration of A 1-AT is normal. Persons having the Z gene (PiZ) are characterized by a low serum level of A 1 AT. Homozygous PiZZ have a serum concentration of 10–15 per cent, heterozygous PiMZ about 60 per cent of that in normals. The Z gene causes the formation of an abnormal A 1 AT analo-antitrypsin (2, 10) which accumulates in the hepatocytes where it is demonstrable as diastase resistant, periodic acid-Schiff (PAS) positive globules. They occur particularly in the periportal areas and peripherally in regeneration nodules (2, 18). Frequently they are multiple and measure 1–40 µ (2).

In 1963 *Laurell & Eriksson* (12) discovered the A 1 AT defect (A 1 ATD), and in 1964 *Eriksson* (5) demonstrated that it was associated with emphysema of the lung. In 1969 *Sharp* (17) pointed out that infants with A-1 ATD of the PiZ type often develop neonatal cholestasis and hepatic cirrhosis. Subsequent studies have shown that cirrhosis also occurs in adults having A 1 ATD of genotype PiZ. Most recently it has been found by *Cox & Huber* (4) that in patients with rheumatoid arthritis the prevalence of the PiZ gene is increased and that in such patients the rheumatoid arthritis is of a more severe degree than in patients of other genotypes within the A 1 AT system.

The object of the present study was to demonstrate the incidence of A 1-ATD in an autopsy material and to discuss its clinical significance.

MATERIAL AND METHOD

The investigation was performed in the Pathology Department of the Central Hospital, Esbjerg, Denmark. The material consists of hepatic tissue re-

moved at autopsies carried out in 1975 and 1976. In 1975 when 434 autopsies were performed liver tissue was removed in 100 as a rule only one specimen for microscopic examination. In 1976 a prospective study was made of hepatic tissue from 138 consecutive autopsies. In these cases two blocks were removed from each liver one from the edge of the right lobe and one from its centre. The autopsies were routine autopsies, and data were collected in retrospect from the clinical case records and the autopsy reports. In half the cases lung tissue had been studied histologically.

The hepatic tissue was fixed in formalin embedded in paraffin and cut into 2 μ sections. Thereupon, it was screened for intracytoplasmic globules after diastase digestion and PAS staining of the sections.

In cases where diastase-resistant, PAS-positive globules were found the study was supplemented by immunoperoxidase examination of the hepatic tissue. The technique used was a 3-layer immunoenzyme bridge technique recommended by *Palmer et a.,* (15) for demonstrating A 1 AT in hepatic tissue (Sera rabbit antihuman A 1 AT normal hog serum, and hog anti-rabbit IgG as well as the peroxidase (PAP) were obtained from Dacopatts Ltd Copenhagen). The dilutions and time units were the same as used by *Palmer et al* (15). Prior to investigating the reaction the tissue sections were post fixed in Bouin's fluid and the peroxidase present was blocked by methanol hydrogen peroxide treatment of the sections. 0 O_4 was used as an accelerator for the stain reaction. Control staining was done on some of the above mentioned preparations by omitting rabbit antihuman A 1-AT. Besides, positive control staining was done on two patients previously described by Brandrup (3) and negative control staining on liver tissue without diastase-resistant PAS-positive globules.

*The quantity of hepatocytes containing diastase-*resistant PAS-positive globules is indicated by crosses, + meaning less than 5 per cent, + + 20–40 per cent, and + + + more than 40 per cent hepatocytes with globules. *It was endeavoured to* assess the genotype by the course of the disease the number *of hepatocytes with globules, and labor*atory findings.

RESULTS

Among 238 autopsy cases 15 persons (5 among 100 studied in 1975 and 10 among *138* studied in 1976) had diastase-resistant, PAS-positive globules (Fig 1) as well as a positive *immunoperoxidase* reaction (Fig 2). The latter manifests itself partly in a diffuse intracellular granular staining partly *in an intra*cellular annular very dark brown to black staining presumably *representing staining of* the rim of the globules found on PAS staining (Fig 3). There was a good correlation between immunoperoxidase and PAS staining (16). Control staining done on hepatic tissue from the two *patients reported previously* was positive while in all other cases it was negative.

Thus, 6.3 per cent of the persons studied had A 1 ATD. *These 15 persons fall into three groups according to the quantity of* globules. 12 persons had less than 5 per cent positive hepatocytes and therefore must be classified as heterozygotes with respect to the Z gene. *Aagenaes et al.* (1). One person had *40–80 per cent positive hepatocytes and there*fore must be considered a homozygote with regard to the Z gene. Two persons had 20–40 per cent positive hepatocytes. Their genotype is uncertain.

Table 1 lists the main symptoms, clinical findings, and autopsy findings in the 15 persons. The age range is from 44 to 87 years. 10 out of the 15 exhibited post mortem signs of chronic pulmonary disease of varying severity. *Six had signs of* parenchymal hepatic diseases one having severe steatosis, one cirrhosis, and four portal fibrosis. This *last* mentioned group includes Case 9 who had extrahepatic occlusion of the bile ducts. The *serum* level of A 1 AT was measured in Case 12 in whom it was 100 units (N 61/145 U).

DISCUSSION

Diastase-resistant, PAS-positive globules are found within hepatocytes *in* patients who have the PiZ gene. However they have also been demonstrated int. al. in two patients with hepatic cirrhosis (19). These two patients were of normal phenotype PiMM and had a normal *serum concentration* of A 1 AT. The authors, therefore, recommended using immunofluorescence or *immunopero*xidase reaction to demonstrate whether the globules are antigenically identical with *A 1 AT. The latter method* is said to be technically superior to the former (15 19). The de-



Fig. 1 Liver tissue with intracytoplasmic diastase-resistant, PAS-positive globules. Case 4 × approx. 500

Fig. 2 General view of liver tissue after immunoperoxidase reaction. Same case. × approx. 50

Fig. 3 High-power view of the liver cells shows dark, annular staining presumably representing the rim of the intracytoplasmic globules and liver cells with diffuse granular cytoplasmic reaction. Same case (A 1-AT immunoperoxidase reaction, × approx. 900)

TABLE 1 *Main Symptoms clinical Findings Autopsy Findings Quantity of Globules and Presumed Genotype*

Case	Age	Sex	Clinical symptoms and signs of pulmonary and hepatic diseases as well as other important diseases and findings	Lungs X ray findings	Lungs post mortem findings	Liver post mortem findings	α glob N 0 9–2.7 g/l	Quantity of globules	Presumed genotype
1	F	54	Dyspnoea and cough for about 10 yrs	Pulm. fibrosis, emphysema, in particular basally	Emphysema, severe chronic congestion	Acute congestion		+	MZ
2	F	53	Dyspnoea and peripheral oedema for about 6 mo.	Pulm. fibrosis, emphysema	Emphysema mod chronic congestion	Mild chronic congestion	2.4	+	MZ
3	M	44	Cancer of the urinary bladder with metastases	No abnormality 2 mo before death	Acute bronchitis, metastases	Numerous metastases		+	MZ
4	F	81	Productive cough for years. Decompensated heart disease for 1 yr., haematemesis 2 mo before death prepyloric ulcer	No abnormality	Nothing striking	Cirrhosis	1.6	+ + +	ZZ
5	M	73	Bronchitis for at least 6 yrs Weight loss, poor general condition for 4 mo., cancer of the biliary tract	–	Marginal emphysema	Acute and chronic congestion, no cirrhosis, large neoplastic masses in R.lobe	2.3	+ +	MZ?
6	F	82	Fatigue altered defaecation habits for 3 mo., endometrial carcinoma with metastases	Mild pulm congestion	Mild emphysema	No metastases, severe steatosis		+ +	MZ?

7	F	74	Heart disease and hypertension for 2 yrs	Pulm. fibrosis	Mild fibrosis	Acute congestion, steatosis, mild portal fibrosis	1.9	+	MZ
8	F	71	Hypertension recognized for 2 weeks		Nothing striking	Multiple cysts, otherwise normal		+	MZ
9	M	62	Jaundice for 3 mo. cancer of the pancreas with metastases	No abnormality	Oedema, no metastases	Acute congestion, no metastases, severe portal fibrosis		+	MZ
10	F	58	Recurrent cancer 4 yrs, previously breast cancer with metastases	Metastases?	Pulm. carcinosis	Mild acute congestion, metastases		+	MZ
11	M	44	Bronchial asthma, brought in dead acute myocardial infarction		Bronchiectases, emphysema, mod. chronic and mild acut congestion	Mild acute congestion		+	MZ
12	M	47	Increasing dyspnoea for 3 yrs	Mild pulm. congestion. (About 1 yr before death)	Chronic bronchitis, emphysema, mild chronic congestion	Acute and mild chronic congestion	$\frac{N:1.8\text{–}3.0\ g/l}{3.4}$	+	MZ
13	F	87	Dyspnoea on exertion for 2 yrs., rheumatoid arthritis for 3 yrs.		Mild emphysema	Acute congestion, mild portal fibrosis, artheritis of intimal proliferation type		+	MZ
14	M	79	Myocardial infarction 2 yrs. previously admitted with cardiac arrest		Severe, emphysema, acute congestion	Acute + chronic congestion		+	MZ
15	F	78	Bronchitis for 15 yrs.	Sequelae to bilat. pulm. tuberculosis	Emphysema, sequelae to apical pulm. tuberculosis	Mild steatosis, acute congestion, mod. portal fibrosis		+	MZ

monstration of diastase resistant PAS-positive globules and a positive immunoperoxidase reaction are considered diagnostic of A 1 ATD (19) According to *Lunis et al* (2) A 1 AT like other serum proteins is synthesized in the rough endoplasmic reticulum where it accumulates owing to a coupling defect in the *smooth endoplasmic reticulum* For this reason an oligosaccharide with sialic acid will not be coupled to the glycoprotein and the normal speed of transporting A 1 AT out of the cell will be reduced

In Sweden and Norway homozygotes (PiZZ) occur at the ratio 1 1500–2000 whereas heterozygotes make up 3–4 per cent of the population (6 9) A population study in Arizona U.S.A. revealed 1 250 presumed to be homozygous with respect to the defect and 6 2 per cent had an intermediate concentration of A 1 AT (14) In the U.S.A the prevalence of *intermediate* A 1 AT concentration ranges from 5–12 per cent and the defect is found particularly in persons of Northern European descent (13)

Among homozygotes over 40 years of age *Eriksson* (6) found that all the males and two-thirds of the females exhibited signs of obstructive pulmonary disease Frequently these patients die before the age of 50 (11) About 10 per cent of homozygotes develop rapidly progressing hepatic cirrhosis after the age of 50 and often also carcinoma of the liver (7)

In an autopsy series of persons who must be presumed to have been heterozygous, pulmonary emphysema was found in 50 per cent and hepatic fibrosis with nodular regeneration or cirrhosis in 25 per cent (8) The mean lifetime was the same as that in a control series. The incidence of hepatic carcinoma was not increased among the heterozygotes.

Aagenaes et al (1) quantitated the amount of hepatocytes with globules and determined the genotype in 10 persons having A 1 ATD Among them the heterozygotes had a maximum of 5 per cent hepatocytes with globules the homozygotes 20–70 per cent These workers also found a reverse relationship between the serum level of A 1 AT and the percentage of hepatic cells showing fluorescence in the immunofluorescence study According to *Berg & Eriksson* (2) the amount of globules increases with advancing age A 1 AT makes up 80 90 per cent of the alpha 1 globulin and is an acute phase reactant. *Triger et al* (19) doubt the validity of quantitative A 1 AT especially if the patients are heterozygous.

Of the present patients presumably only Case 4 with cirrhosis was homozygous, as more than 40 per cent of her hepatocytes contained globules In Case 5 there was only a small amount of liver tissue which was affected with neoplastic infiltration, and this rendered it difficult to assess the hepatocytes with globules. Case 5 as well as Case 6 are among the oldest ones of the entire series. This perhaps contributes to their making up an intermediate group with regard to granular hepatocytes. That 6.3 per cent of the patients had A 1 ATD probably does not differ definitely from the approx. 4 per cent found in Sweden and Norway The occurence of emphysema in the present series is somewhat higher than that found by *Eriksson et al* (8) whereas the hepatic changes were not as pronounced

---

For the loan of case records thanks are due to the consultants in the Esbjerg Central Hospital and in the Spangsbjerg Hospital and for that of control preparations to the chief pathologists in the Odense University Institute of Pathology Odense Hospital The technical assistance of *Jane Hede Delboe* is acknowledged

REFERENCES

1 *Aagenaes O Fagerhol M Elgjo K Munthe E & Hovig T* Pathology and pathogenesis of liver disease in alpha 1-antitrypsin deficient individuals Postgrad med. J *50* 365 375 1974

2 *Berg N O & Eriksson S* Liver disease in adults with alpha$_1$ antitrypsin deficiency New Engl J Med. *287* 1264–1267 1972

3 *Brandrup F O* Leverforandringer hos voksne med alfa 1-antitrypsinmangel og svært emfysem Ugeskr Læg *135* 2513–2517 1973

4 *Cox D W & Huber O* Rheumatoid ar

thritis and alpha-1-antitrypsin. Lancet i 1216 1217, 1976.

5. *Eriksson S* Pulmonary emphysema and α_1 antitrypsin deficiency Acta med. scand. *175* 197 205 1964

6 *Eriksson, S* Studies in $\alpha_1$antitrypsin deficiency Acta med. scand. Suppl. 432, 1965

7 *Eriksson, S & Hägerstrand I.* Cirrhosis and malignant hepatoma in α-antitrypsin deficiency Acta med scand. *195* 451 458, 1974

8 *Eriksson S Moest p T & Hägerstrand I* Liver Lung and malignant disease in heterozygous (Pi MZ)α_1-antitrypsin deficiency Acta med scand. *198* 243–247 1975

9 *Fagerhol M K.* Serum P types in Norwegians. Acta path. microbiol. scand. *70* 421–428, 1967

10. *Feldmann G Bignon J Chahinian P Degott C & Benhamou J-P* Hepatocyte ultrastructural changes in -antitrypsin deficiency Gastroenterology *67* 1214–1224 1974

11 *Jensen K* Alfa$_1$-antitrypsin. Ugeskr. Laeg. *132* 2167–2170 1970.

12 *Laurell, C B. & Eriksson S* The electrophoretic α_1-globulin pattern of serum in α antitrypsin deficiency Scand J clin. Lab Invest. *15* 132–140, 1963.

13 *Lieberman J* Alpha$_1$-antitrypsin deficiency and chronic pulmonary disease. N Y St. J Med. *76* 181–186, 1976.

14 *Morse J O., Lebowitz M D Knudson, R J & Burrows B.* A community study of the relation of alpha$_1$-antitrypsin levels to obstructive lung diseases. New Engl. J Med. *291* 278–281 1975

15 *Palmer P E. DeLellis R. A. & Wolfe H J.* Immunohistochemistry in alpha$_1$-antitrypsin deficiency Am. J clin. Path. *62* 350–354 1974

16. *Reintoft I* Unpublished work.

17 *Sharp H L., Bridges R. A Krivit W & Freier E. F.* Cirrhosis associated with alpha-1-antitrypsin deficiency: a previously unrecognized inherited disorder J Lab. clin. Med. *73* 934–939 1969

18 *Sharp H L.* Alpha-1-antitrypsin deficiency Hosp. Pract. *92* 83–96 1971

19 *Triger D R Millward-Sadler G H Czaykowski, A A Trowel J & Wright R.* Alpha-1-antitrypsin deficiency and liver disease in adults. Quart. J Med. *45* 351–372 1976

20 *Yunis E J., Agostini, R. M & Glew R. H* Fine structural observations of the liver in α-1 antitrypsin deficiency Amer J Path. *82* 265–272, 1976

monstration of diastase-resistant PAS-positive globules and a positive immunoperoxidase re action are considered diagnostic of A 1 ATD (19) According to *Yunis et al* (2) A 1 AT like other serum proteins is synthesized in the rough endoplasmic reticulum where it ac cumulates, owing to a coupling defect in the smooth endoplasmic reticulum. For this rea son an oligosaccharide with sialic acid will not be coupled to the glycoprotein and the normal speed of transport ng A 1 AT out of the cell will be reduced

In Sweden and Norway homozygotes (PiZZ) occur at the ratio 1 1500-2000 whereas heterozygotes make up 3-4 per cent of the populat on (6 9) A population study in Arizona, U.S.A revealed 1 250 presumed to be homozygous with respect to the defect, and 6 2 per cent had an intermediate concen tration of A 1 AT (14) In the U.S.A the prevalence of intermediate A 1 AT concen tration ranges from 5-12 per cent and the defect is found particularly in persons of Northern European descent (13)

Among homozygotes over 40 years of age *Eriksson* (6) found that all the males and two-thirds of the females exhibited signs of obstructive pulmonary disease. Frequently these patients die before the age of 50 (11) About 10 per cent of homozygotes develop rapidly progressing hepatic cirrhosis after the age of 50 and often also carcinoma of the liver (7)

In an autopsy series of persons who must b presumed to have been heterozygous pul monary emphysema was found in 50 per cent and hepatic fibrosis with nodular regenera tion or cirrhosis in 25 per cent (8) The mean lifetime was the same as that in a control series The incidence of hepatic carcinoma was not increased among the heterozygotes.

Aagenaes et al (1) quantitated the amount of hepatocytes with globules and determined the genotype in 10 persons having A 1 ATD Among them the heterozygotes had a maxi mum of 5 per cent hepatocytes with globules the homozygotes 20-70 per cent These work ers also found a reverse relationship between the serum level of A 1 AT and the percentage of hepatic cells showing fluorescence in the immunofluorescence study According to *Berg & Eriksson* (2) the amount of globules in creases with advancing age A 1 AT makes up 80-90 p r cent of the alpha 1-globulin and is an acute phase reactant. *Triger et al* (19) doubt the validity of quantitative A 1-AT especially if the patients are heterozygous.

Of the present patients presumably only Case 4 with cirrhosis, was homozygous, as more than 40 per cent of her hepatocytes con tained globules In Case 5 there was only a small amount of liver tissue which was af fected with neoplastic infiltration, and this rendered it difficult to assess the hepatocytes with globules. Case 5 as well as Case 6 are among the oldest ones of the entire series. This perhaps contributes to their making up an intermediate group with regard to gran ular hepatocytes. That 6.3 per cent of the patients had A 1 ATD probably does not dif fer definitely from the approx. 4 per cent found in Sweden and Norway The occurence of emphysema in the present series is some what higher than that found by *Eriksson et al* (8) whereas the hepatic changes were not as pronounced.

For the loan of case records thanks are due to the consultants in the Esbjerg Central Hospital and in the Spangsbjerg Hospital and for that of con trol preparations to the chief pathologists in the Odense University Institute of Pathology Odense Hospital The technical assistance of *Jane Hede Delboe* is acknowledged

REFERENCES

1 *Aagenaes O Fagerhol M Elgjo K Munthe E. & Hovig T* Pathology and patho genesis of liver disease in alpha-1-antitrypsin deficient individuals Postgrad. med. J *50* 365–375 1974

2 *Berg N O & Eriksson S* Liver disease in adults with alpha$_1$-antitrypsin deficiency New Engl J Med *287* 1264–1267 1972.

3 *Brandrup F O* Leverforandringer hos ob ne med alfa 1-antitrypsinmangel og svært em fysem. Ugeskr Læg *135* 2515–2517 1973.

4 *Cox D W & Huber O* Rheumatoid ar

and infiltration by mononuclear inflammatory cells (*Pearson et al.* 1960 *Verity et al.* 1963 *Dolan et al.* 1966, *Arkin & Masi* 1975). Histochemical studies revealing decreased basophilia, Alcian blue affinity and metachromasia have suggested a loss of glucosaminoglycans from the cartilage matrix (*Verity et al.* 1963 *Hughes et al.* 1972).

This paper reports the clinical features and results of a morphologic and histochemical investigation of the cartilage lesions in 2 patients with relapsing polychondritis. Material was obtained by biopsies, as well as at autopsy in one. Refined histochemical techniques involving staining with Alcian blue at controlled pH levels, with and without pretreatment with bacterial chondroitinase ABC, and with controlled electrolyte concentrations, which may help to characterize the glucosaminoglycans in tissues, were utilized on the cartilage lesions (*Kvadblom & Angervall* 1975. *Kvadblom & Karlsson* 1977).

CASE REPORTS

Case 1. — A 57-year-old man, who had had an operation for nasal septal deviation in 1968. In 1969 some weeks after an attack of influenza (Hongkong) associated with high fever and intense cough, he developed arthralgias and severe respiratory symptoms mainly of an obstructive type. These symptoms subsided when he was admitted to hospital and given high doses of prednisolone. Some months later after reduction in the corticosteroid dosage, he was again hospitalized with generalized arthralgias and hacking cough. Two months later he developed nasal pain, impaired hearing and painful swelling of the right external ear. On examination he had pronounced obstructive respiratory symptoms, generalized arthritis and saddle-nose deformity. The diagnosis at this stage was rheumatoid arthritis (collagenosis?) bronchial asthma and bilateral hearing impairment.

Because of depression in late 1969 he was admitted to the department of internal medicine at ... mental hospital. He then presented the picture of advanced respiratory insufficiency with dyspnoea, cyanosis, severe cough and an obstructive state differing from that of asthmatic bronchitis as breath sounds resembled air blowing through sheet-metal tubes. There was pulmonary emphysema, and the tracheal lumen was the width of a lead-pencil, with calcifications in tracheal ring cartilages. He had active arthritis of small and large joints, a saddle-nose, deformed external ears with granular swellings at the edges, narrow external auditory meatus and conjunctivitis. The urinary excretion of glucosaminoglycans was slightly increased. A biopsy from the ear cartilage showed inflammatory and degenerative changes. A diagnosis of relapsing polychondritis was made, based upon the clinical picture. The patient was treated with prednisolone in doses of about 30 mg daily. Reducing the dose resulted in relapses of eye symptoms (conjunctivitis, iridocyclitis) and arthritic exacerbations. For a short while azathioprine therapy was tried without any noticeable clinical effect.

In July 1971 he was re-admitted with pleuropneumonia. At this time there were ECG-changes and elevated LDH-isoenzymes, though whether on an ischemic or myocarditic basis could not be determined.

Because of respiratory distress he was again admitted to hospital in April 1972 and improved after temporary increase of the corticosteroid dosage.

After a rapid deterioration over a few days he was finally hospitalized in September 1973 with severe bronchial insufficiency, hypoxia and circulatory failure. In spite of intensive treatment with high doses of corticosteroids, antibiotics and tracheostomy the patient died within four days. Death was apparently due to bronchial collapse terminally.

Case 2. — A woman now 70-years old, previously in good health apart from suspected rheumatic fever without obvious cardiac involvement in 1947. She was admitted to hospital because of fever and muscle pain. Laboratory tests showed a moderate anemia, thrombocytosis and an elevated erythrocyte sedimentation rate (130 mm in the first hour). Serum protein analysis showed hypoalbuminemia and increased gamma globulins. Liver function tests were normal except for elevation of serum alkaline phosphatases. Investigations for malignancy were negative. She was thought to have a polymyalgia arteritica although biopsy from one temporal artery showed no signs of arteritis. Institution of corticosteroid (prednisolone 10–15 mg daily) was followed by a decline in the fever and the patient became free from pain. One year later she developed symptoms of significant osteoporosis, and radiographic examination revealed multiple thoracic vertebral compressions.

During 1975 and early 1976 the prednisolone dose was slowly diminished to 5 mg daily. During mid 1976 the patient had a non-productive cough and in September developed obstructive respiratory

A brief clinical report has previously been given on this case while the patient was still alive (Dalén & Kjellbo, 1973).

Acta path. microbiol scand. Sect. A 85 656–664 1977

RELAPSING POLYCHONDRITIS

A Clinical Pathologic Anatomic and Histochemical Study of 2 Cases

LARS-GUNNAR KINDBLOM PER DALÉN, GUNNEL EDMAR and HANS KJELLBO

Department of Pathology II and Medicine III Sahlgren s Hospital and
Department of Medicine St. Jörgen Hospital, University of Göteborg Sweden

Kindblom, L.-G., Dalén, P., Edmar G & Kjellbo H Relapsing polychondritis. A clinical, pathologic-anatomic and histochemical study of 2 cases. Acta path. microbiol scand Sect. A, 85 656–664 1977

A 57-year-old man and a 70-year-old woman with *relapsing polychondritis* are reported. The man, suffering from arthralgias, respiratory obstruction external ear and saddle-nose deformities conjunctivitis and irido-cyclitis died after 4 years from airway obstruction because of tracheal and bronchial collapse. The woman is alive 8 months after the development of *respiratory obstruction* probably caused by radiographically demonstrated tracheal obstruction, a saddle nose deformity and hearing impairment. Microscopically the involved cartilages showed degenerative and slight inflammatory changes and were eventually replaced by fibrous tissue Histochemical studies, utilizing staining with Alcian blue at controlled electrolyte concentrations (Scott technique) and at controlled pH s, with or without digestion with bacterial chondroitinase ABC and staining with the PAS-method, with or without diastase digestion, revealed a complete or relative loss of glucosaminoglycans and glycogen. A biosynthetic defect is considered unlikely to be the primary pathogenetic mechanism of relapsing polychondritis. Histological and histochemical examination of biopsies from involved cartilages contribute to a definite diagnosis.

Key words Relapsing polychondritis glucosaminoglycan.

L.-G Kindblom, Department of Pathology Vasa Hospital, S-411 33 Göteborg, Sweden.

Received 4.iii 77 Accepted 17.iii.77

Relapsing polychondritis is a rare disorder characterized by recurrent multiple lesions in which inflammation and degeneration in cartilage chiefly affects the external ears nose upper respiratory passages and articular cartilages (*Pearson et al* 1960 *Dolan et al* 1966 *Arkin & Masi* 1975) Hearing impairment vestibular dysfunction and ocular involvement as well as abnormalities of the aorta and heart valves have also been described in association with this condition (*Hemry et al* 1972, *Arkin & Masi* 1975) Since *Jaksch Wartenhorst* (1923) described the disease about 130 cases have been reported

The etiology and pathogenesis of relapsing polychondritis has not been established although several hypotheses have been put forward. A causative infectious agent has been proposed as well as theories of a biosynthetic defect, increased enzymatic proteolysis or an autoimmune defect (*Bean et al* 1958, *Dolan et al* 1966 *Hughes et al* 1972 *Arkin & Masi* 1975) Involved cartilage has been reported to show diffuse destruction focal calcification, bone formation, fibrous tissue replacement

and infiltration by mononuclear inflammatory cells (*Pearson et al.* 1960, *Verity et al.* 1963, *Dolan et al.* 1966, *Arkin & Masi* 1975). Histochemical studies revealing decreased basophilia, Alcian blue affinity and metachromasia have suggested a loss of glucosaminoglycans from the cartilage matrix (*Verity et al.* 1963, *Hughes et al.* 1972).

This paper reports the clinical features and results of a morphologic and histochemical investigation of the cartilage lesions in 2 patients with relapsing polychondritis. Material was obtained by biopsies, as well as at autopsy in one. Refined histochemical techniques involving staining with Alcian blue at controlled pH levels, with and without pretreatment with bacterial chondroitinase ABC, and with controlled electrolyte concentrations, which may help to characterize the glucosaminoglycans in tissues, were utilized on the cartilage lesions (*Kindblom & Angervall* 1975, *Kindblom & Karlsson* 1977).

CASE REPORTS

Case 1. – A 57-year-old man, who had had an operation for nasal septal deviation in 1968. In 1969 some weeks after an attack of influenza (Hongkong) associated with high fever and intensive cough, he developed arthralgias and severe respiratory symptoms mainly of an obstructive type. These symptoms subsided when he was admitted to hospital and given high doses of prednisolone. Some months later after a reduction in the corticosteroid dosage he was again hospitalized with generalized arthralgias and a hacking cough. Two months later he developed nasal pain, impaired hearing and a painful swelling of the right external ear. On examination he had pronounced obstructive respiratory symptoms, generalized arthritis and a saddle-nose deformity. The diagnosis at this stage was rheumatoid arthritis (collagenosis), bronchial asthma and bilateral hearing impairment.

Because of depression in late 1969 he was admitted to the department of internal medicine at a mental hospital. He then presented the picture of advanced respiratory insufficiency with dyspnoea, cyanosis, severe cough and an obstructive state differing from that of asthmatic bronchitis as breath sounds resembled air blowing through sheet-metal tubes. There was pulmonary emphysema, and the tracheal lumen was the width of a lead-pencil, with calcifications in tracheal ring cartilages. He had active arthritis of small and large joints, a saddle nose, deformed external ears with granular swellings at the edges, a narrow external auditory meatus and conjunctivitis. The urinary excretion of glucosaminoglycans was slightly increased. A biopsy from the ear cartilage showed inflammatory and degenerative changes. A diagnosis of relapsing polychondritis was made, based upon the clinical picture. The patient was treated with prednisolone in doses of about 30 mg daily. Reducing the dose resulted in relapses of eye symptoms (conjunctivitis, irido-cyclitis) and arthritic exacerbations. For a short while azathioprine therapy was tried without any noticeable clinical effect.

In July 1971 he was re-admitted with pleuropneumonia. At this time there were ECG-changes and elevated LDH-isoenzymes, though whether on an ischemic or myocarditic basis could not be determined.

Because of respiratory distress he was again admitted to hospital in April 1972 and improved after temporary increase of the corticosteroid dosage.

After a rapid deterioration over a few days he was finally hospitalized in September 1973 with severe bronchial insufficiency, hypoxia and circulatory failure. In spite of intensive treatment with high doses of corticosteroids, antibiotics and tracheostomy the patient died within four days. Death was apparently due to bronchial collapse terminally.

Case 2. – A woman now 70-years old, previously in good health apart from suspected rheumatic fever without obvious cardiac involvement in 1947. She was admitted to hospital because of fever and muscle pain. Laboratory tests showed a moderate anemia, thrombocytosis and an elevated erythrocyte sedimentation rate (130 mm in the first hour). Serum protein analysis showed hypoalbuminemia and increased gamma globulins. Liver function tests were normal except for elevation of serum alkaline phosphatases. Investigations for malignancy were negative. She was thought to have a polymyalgia arteritica although a biopsy from one temporal artery showed no signs of arteritis. Institution of corticosteroids (prednisolone 10–15 mg daily) was followed by a decline in the fever and the patient became free from pain. One year later she developed symptoms of significant osteoporosis, and radiographic examination revealed multiple thoracic vertebral compressions.

During 1975 and early 1976 the prednisolone dose was slowly diminished to 5 mg daily. During mid-1976 the patient had a non-productive cough and in September developed obstructive respiratory

A brief clinical report has previously been given on this case while the patient was still alive (Dalén & Kjellbo 1973).

Acta path. microbiol scand Sect. A, 85 656–664 1977

RELAPSING POLYCHONDRITIS

A Clinical Pathologic Anatomic and Histochemical Study of 2 Cases

LARS-GUNNAR KINDBLOM PER DALÉN GUNNEL EDMAR and HANS KJELLBO

Department of Pathology II and Medicine III Sahlgren's Hospital and
Department of Medicine St. Jörgen Hospital, University of Göteborg, Sweden

Kindblom L.-G Dalén, P., Edmar G & Kjellbo, H Relapsing polychondritis. A clinical, pathologic anatomic and histochemical study of 2 cases. Acta path. microbiol. scand Sect. A, 85 656–664 1977

A 57 year-old man and a 70-year-old woman with relapsing polychondritis are reported. The man suffering from arthralgias, respiratory obstruction, external ear and saddle-nose deformities, conjunctivitis and irido-cyclitis, died after 4 years from airway obstruction because of tracheal and bronchial collapse. The woman is alive 8 months after the development of respiratory obstruction, probably caused by radiographically demonstrated tracheal obstruction, a saddle-nose deformity and hearing impairment. Microscopically the involved cartilages showed degenerative and slight inflammatory changes and were eventually replaced by fibrous tissue Histochemical studies, utilizing staining with Alcian blue at controlled electrolyte concentrations (Scott technique) and at controlled pH s, with or without digestion with bacterial chondroitinase ABC and staining with the PAS-method, with or without diastase digestion, revealed a complete or relative loss of glucosaminoglycans and glycogen. A biosynthetic defect is considered unlikely to be the primary pathogenetic mechanism of relapsing polychondritis. Histological and histochemical examination of biopsies from involved cartilages contribute to a definite diagnosis.

Key words Relapsing polychondritis glucosaminoglycan.

L.-G Kindblom, Department of Pathology Vasa Hospital, S-411 33 Göteborg Sweden.

Received 4.iii 77 Accepted 17.iii.77

Relapsing polychondritis is a rare disorder characterized by recurrent, multiple lesions in which inflammation and degeneration in cartilage chiefly affects the external ears nose upper respiratory passages and articular cartilages (*Pearson et al* 1960 *Dolan et al* 1966 *Arkin & Masi* 1975) Hearing impairment vestibular dysfunction and ocular involvement as well as abnormalities of the aorta and heart valves have also been described in association with this condition (*Hemry et al* 1972, *Arkin & Masi* 1975) Since *Jaksch Wartenhorst* (1923) described the disease about 130 cases have been reported.

The etiology and pathogenesis of relapsing polychondritis has not been established although several hypotheses have been put forward A causative infectious agent has been proposed as well as theories of a biosynthetic defect increased enzymatic proteolysis or an autoimmune defect (*Bean et al* 1958 *Dolan et al* 1966 *Hughes et al* 1972 *Arkin & Masi* 1975) Involved cartilage has been reported to show diffuse destruction focal calcification, bone formation, fibrous tissue replacement



Fig 2 Case 1 Biopsy from the pinna. Cartilage showing degenerative changes of chondrocytes, focal inflammatory cell infiltration and loss of usual hyaline and lacunar structure (bottom) The cartilage is partly replaced by fibrous tissue (top) H & E, × 90

Fig 3 A weakly basophilic cartilage island (bottom) within the fibrous tissue showing groups of mononuclear inflammatory cells. H & E, × 120

sized bronchi of both lungs showed patchy widenings of the lumen, resembling bronchiectasis The cut-surfaces of the lungs showed signs of congestion and moderate vesicular emphysema

Microscopic Appearance

Case 1 The biopsy from the helix of the left ear taken in 1969 showed pronounced degenerative changes of the cartilage There was an indistinct demarcation between the cartilage and the perichondrial fibrous and elastic tissue In most regions the cartilage lacked the usual basophilia seen in hematoxylin-eosin stained sections and was patchily replaced by partly fibrillary pale eosinophil matrix which contained cells, either single or in small groups some of them resembling chondrocytes and lying in lacunae

At the periphery of the preformed cartilage there was a dense fibrous matrix mainly built up of traversing collagen fibre bundles and fusiform cells resembling fibroblasts. Basophilic cartilage was seen centrally and in small areas within the fibrous tissue (Fig 2) Within these islands of cartilage most lacunae contained normal chondrocytes but there were also empty lacunae and some containing ghost-cells. Small foci of plasma cells and lymphocytes, frequently adjacent to proliferating capillaries, were seen within and around the degenerating cartilage (Figs 2 & 3)

The biopsy from the tracheal cartilage, obtained at tracheostomy and material obtained at autopsy from various levels in the trachea, main bronchi, and several medium-sized bronchi, showed microscopic changes similar to those in the biopsy from the external ear However in this material there were only few foci of basophilic cartilage within the fibrous tissue which had replaced the tracheal and bronchial cartilage (Fig 4) Most of these few small islands of basophilic cartilages lacked

symptoms. She also had a stuffy feeling in her right ear associated with hearing impairment and over a few days a prominent saddle-nose deformity developed. There was no evidence of infection and no history of previous trauma.

In October 1976 she was admitted to hospital because of increasing respiratory distress. Her obstructive symptoms were unchanged by giving bronchodilating drugs. She was moderately hoarse and had a right-sided serous otitis media. After myringotomy her hearing was restored. There was no ocular or external ear involvement and no arthritic changes were noted. Laboratory findings were similar to those of 1972 except that she now had a mild diabetes mellitus. Urinary analysis for glucosaminoglycans was negative. Spirometric examination revealed features characteristic of obstruction and the readings were not significantly changed by inhalation of bronchodilators. Tracheal tomogram revealed a severe narrowing of the lumen to less than 6 mm in diameter in the intrathoracic region. A biopsy specimen from the deformed nasal septum helped to confirm the diagnosis of relapsing polychondritis. After elevation of the corticosteroid doses (prednisolone 30 mg daily) she improved and is now treated as an out patient. Azathioprine has recently been given to reduce if possible the maintenance dose of corticosteroids because of the advanced osteoporosis.



Fig 1 Case 1 Dorsal aspect of the lungs with opened tracheobronchial tree showing severe narrowing of the trachea and the proximal main bronchi. Some large distal bronchi show irregular widening of the lumen, resembling bronchiectasis.

PATHOLOGY

Materials and Methods

The material consisted of biopsies from the left external ear and trachea as well as materials obtained at autopsy from the trachea, large and medium-sized bronchi. Several samples of adult and foetal tracheal and articular cartilage taken at autopsy served as controls. The specimens were fixed in 4 per cent formaldehyde solution and embedded in paraffin. Five-micron thick sections were routinely stained according to the hematoxylin-van Gieson method, and with hematoxylin and eosion. Weigert's elastin stain was used for studying elastic tissue.

For the examination of glucosaminoglycans Alcian blue was used at pH 2.5 and 0.5 as described previously (Kindblom & Angervall 1975) with and without prior treatment with bacterial chondroitinase ABC (Seikagaku Chemical Industry) (Kindblom & Karlsson, 1977). Staining was also performed according to Scott & Dorling (1965) at pH 5.6 with 0.5 per cent Alcian blue in 0.025 M acetate buffer with the addition of increasing concentrations of $MgCl_2$ in order to determine the "critical electrolyte concentration" (CEC) of the dye polymer binding in the mucoid material. The following series of $MgCl_2$ concentrations was used: 0.0 M, 0.025 M, 0.05 M, 0.1 M, 0.25 M, 0.35 M, 0.45 M, 0.55 M, 0.65 M, 0.75 M, 0.85 M and 1.0 M. Staining time was 16 hours.

In order to classify the results of the Alcian blue staining procedure in control tissues and the cartilage lesions, a five-step scale was introduced: negative, feeble or doubtful, weak, moderate and strong. The slides were examined at the same magnification (× 50) and with the same light intensity.

For the demonstration of vicglycols, the periodic acid-Schiff (PAS) reaction (McManus) was performed with and without prior treatment of the sections with diastase (Merck, 2800 E/g).

Autopsy Findings

Case 1 Post mortem findings included cardiomegaly (435 g) with gross thickening of the left ventricular wall, atheromatosis of the coronary arteries and atrophic adrenal glands. Gross examination of the trachea and bronchial airways revealed an almost complete loss of the ordinary cartilaginous rings, with collapse of the trachea and proximal main bronchi (Fig 1). The larynx appeared normal. The lumen of the intrathoracic part of the trachea was less than 5 mm in diameter. The mucosa was edematous and the lumen contained abundant mucinous secretions. Large and medium-



Fig. 2 Case 1. Biopsy from the pinna. Cartilage showing degenerative changes of chondrocytes, focal inflammatory cell infiltration and loss of usual hyaline and lacunar structure (bottom). The cartilage partly replaced by fibrous tissue (top). H & E, × 90.

Fig. 3 A weakly basophilic cartilage island (bottom) within the fibrous tissue showing groups of mononuclear inflammatory cells. H & E, × 120.

sized bronchi of both lungs showed patchy widening of the lumen, resembling bronchiectasis. The cut-surfaces of the lungs showed signs of congestion and moderate vesicular emphysema.

Microscopic Appearance

Case 1. The biopsy from the helix of the left ear taken in 1969 showed pronounced degenerative changes of the cartilage. There was an indistinct demarcation between the cartilage and the perichondrial fibrous and elastic tissue. In most regions the cartilage lacked the usual basophilia seen in haematoxylin-eosin stained sections and was patchily replaced by partly fibrillary pale eosinophil matrix which contained cells, either single or in small groups, some of them resembling chondrocytes and lying in lacunae.

At the periphery of the preformed cartilage there was dense fibrous matrix mainly built up of traversing collagen fibre bundles and fusiform cells resembling fibroblasts. Basophilic cartilage was seen centrally and in small areas within the fibrous tissue (Fig. 2). Within these islands of cartilage most lacunae contained normal chondrocytes but there were also empty lacunae and some containing ghost-cells. Small foci of plasma cells and lymphocytes, frequently adjacent to proliferating capillaries, were seen within and around the degenerating cartilage (Figs. 2 & 3).

The biopsy from the tracheal cartilage obtained at tracheostomy and material obtained at autopsy from various levels in the trachea, main bronchi, and several medium-sized bronchi, showed microscopic changes similar to those in the biopsy from the external ear. However, in this material there were only a few foci of basophilic cartilage within the fibrous tissue which had replaced the tracheal and bronchial cartilage (Fig. 4). Most of these few small islands of basophilic cartilages lacked

symptoms. She also had a stuffy feeling in her right ear associated with hearing impairment and over a few days a prominent saddle-nose deformity devel oped There was no evidence of infection and no history of previous trauma

In October 1976 she was admitted to hospital because of increasing respiratory distress. Her obstructive symptoms were unchanged by giving bronchodilating drugs. She was moderately hoarse and had a right-sided serous otitis media. After myringotomy her hearing was restored There was no ocular or external ear involvement and no ar thritic changes were noted Laboratory findings were similar to those of 1972 except that she now had a mild diabetes mellitus. Urinary analysis for glucosaminoglycans was negative. Spirometric ex amination revealed features characteristic of obstruction and the readings were not significantly changed by inhalation of bronchodilators. Tracheal tomogram revealed a severe narrowing of the lumen to less than 6 mm in diameter in the intra thoracic region. A biopsy specimen from the deformed nasal septum helped to confirm the diag nosis of relapsing polychondritis. After elevation of the corticosteroid doses (prednisolone 30 mg daily) she improved and is now treated as an out patient. Azathioprine has recently been given to reduce, if possible the maintenance dose of corticosteroids because of the advanced osteoporosis.



Fig 1 Case 1 Dorsal aspect of the lungs with opened tracheobronchial tree, showing severe nar rowing of the trachea and the proximal main bron chi Some large distal bronchi show irregular widening of the lumen resembling bronchiectasis.

PATHOLOGY

Materials and Methods

The material consisted of biopsies from the left external ear and trachea as well as materials obtained at autopsy from the trachea, large and medium-sized bronchi. Several samples of adult and foetal tracheal and articular cartilage taken at autopsy served as controls. The specimens were fixed in 4 per cent formaldehyde solution and embedded in paraffin. Five-micron thick sections were routinely stained according to the hematoxylin-van Gieson method, and with hematoxylin and eosin. Weigert's elastin stain was used for studying elastic tissue

For the examination of glucosaminoglycans Al cian blue was used at pH 2.5 and 0.5 as described previously (Kindblom & Angervall, 1975) with and without prior treatment with bacterial chon droitinase ABC (Seikagaku Chemical Industry) (Kindblom & Karlsson, 1977) Staining was al so performed according to Scott & Dorling (1965) at pH 5 6 with 0 5 per cent Alcian blue in 0 025 M acetate buffer with the addition of increasing con centrations of $MgCl_2$ in order to determine the critical electrolyte concentration" (CEC) of the dye polymer binding in the mucoid material. The following series of $MgCl_2$ concentrations was used 0 0 M 0 025 M 0 05 M, 0 1 M, 0 25 M 0.35 M 0 45 M, 0 55 M 0 65 M 0 75 M 0.85 M and 1 0 M Staining time was 16 hours.

In order to classify the results of the Alcian blue staining procedure in control tissues and the carti- lage lesions, a five-step scale was introduced nega- tive feeble or doubtful weak, moderate and strong The slides were examined at the same magnifica- tion (× 50) and with the same light intensity

For the demonstration of glycols, the periodic acid-Schiff (PAS) reaction (McManus) was per formed with and without prior treatment of the sections with diastase (Merck, 2800 E/g)

Autopsy Findings

Case 1 Post mortem findings included cardiom- egaly (435 g) with gross thickening of the left ventricular wall, atheromatous of the coronary ar- teries and atrophic adrenal glands. Gross examina- tion of the trachea and bronchial airways revealed an almost complete loss of the ordinary cartilagin- ous rings, with collapse of the trachea and proximal main bronchi (Fig 1) The larynx appeared nor- mal. The lumen of the intrathoracic part of the trachea was less than 5 mm in diameter The mu- cosa was edematous and the lumen contained abundant mucinous secretions. Large and medium-



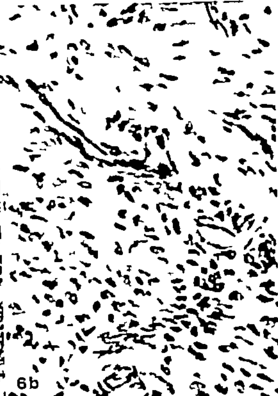


Fig 6 Case 2. Biopsy from the nasal septum. A Small irregular foci of degenerate altered cartilage with fibrous tissue H & E, × 90. B Cartilage area with reduced basophilia, proliferating capillaries and nuclear fragmentation and degeneration H & E, × 180

brin ne haracter there were no distinct lacunae the chondrocytes frequently showed an extended cytoplasm and were enclosed by wavy bundles of collagenous fibres, thereby imposing an appearance similar to that of fibrous cartilage (Fig 4 B) In the trachea and main bronchi abundant metaplastic bone was seen within the fibrous tissue adjacent to the preserved cartilage islands (Figs 4 A, 5 A & B Marrow cavities among the bone trabeculae

Fig 4 Case 1 Trachea A Most of the normal cartilage ring is replaced by metaplastic bone fatty marrow and fibrous tissue A th m of weakly basophil cartilage remain H & E, 30 B Higher magnification of residual cartilage island partly showing absence basophilia (top left and fibrocartilage-like appearance (bottom H & E, 60)

Fig 5 Case 1 A & B Mainstem bronchus with small foci of cartilage with only partly retained basophilia and with metaplastic bone formation and marrow H & E, 60

were predominantly filled by fat cells (Fig. 5 A & B) but occasionally small hematopoetic foci were encountered Lymphocytes and plasma cells were seen in small groups within the fibrous tissue which had replaced the cartilage

Case 2 The biopsy from the nasal septum showed sparsely cellular fibrous tissue with collagen fibres arranged in traversing bundles. Within the fibrous tissue were small poorly-delineated non-basophilic cartilage islands (Fig 6 A) The chondrocytes often had pyknotic nuclei, the pale staining cytoplasm was vacuolated in some cells, and only few were lying in distinct lacunae Delicate collagen fibres were seen within these cartilage zones Many proliferating capillaries were found with the cartilage and fibrous tissue (Fig 6 B) Small foci of lymphocytes and plasma cells were frequently seen adjacent to capillaries within the fibrous tissue

Histochemical Study

Control The adult tracheal and articular cartilages used control were strongly stained both





4a



4b



5a



5b

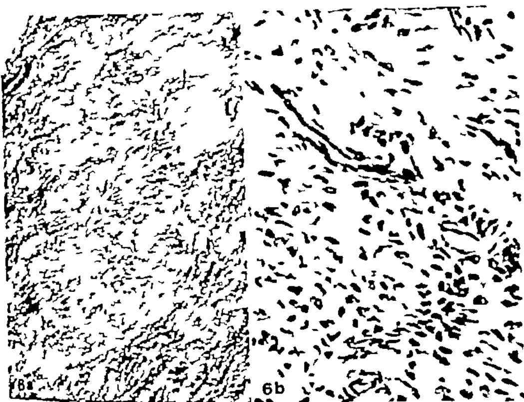


Fig 6 Case 2. Biopsy from the nasal septum. A Small irregular foci of degenerate altered cartilage in the fibrous tissue H & E, × 90 B. Cartilage area with reduced basophilia, proliferating capillaries and nuclear fragmentation and degeneration H & E, 180

line in character there were no distinct lacunae the chondrocytes frequently showed an extended cytoplasm and were enclosed by wavy bundles of collagenous fibres, thereby imposing an appearance similar to that of fibrous cartilage (Fig. 4 B In the trachea and main bronchi abundant metaplastic bone was seen within the fibrous tissue adjacent to the preserved cartilage islands (Figs 4 A, 5 A & B) Marrow cavities among the bone trabeculae were predominantly filled by fat cells (Fig 5 A & B but occasionally small hematopoietic foci were encountered Lymphocytes and plasma cells were seen in small groups within the fibrous tissue which had replaced the cartilage

Case 2 The biopsy from the nasal septum showed sparsely cellular fibrous tissue with collagen fibres arranged in traversing bundles. Within the fibrous tissue were small poorly-delineated non-basophilic cartilage islands (Fig 6 A The chondrocytes then had pyknotic nuclei the pale staining cytoplasm was vacuolated in some cells, and only a few were lying in distinct lacunae Delicate collagen fibres were seen within these cartilage zones Many proliferating capillaries were found within the cartilage and fibrous tissue (Fig 6 B) Small foci of lymphocytes and plasma cells were frequently seen adjacent to capillaries within the fibrous tissue

Fig 4 Case 1 Trachea A Most of the normal cartilage ring is replaced by metaplastic bone, fatty marrow and fibrous tissue A thin zone of weakly basophilic cartilage remains H & E, × 30 B Higher magnification of residual cartilage island, partly showing absence of basophilia (top, left) and fibrocartilage-like appearance (bottom) H & E, × 90

Fig 5 Case 1 A & B Main bronchus with small foci of cartilage with only partly retained basophilia and with metaplastic bone formation and fatty marrow H & E, × 90

Histochemical Study

Controls The adult tracheal and articular cartilages used as controls were strongly stained both




4a


4b


5a


5b

islands of basophilic cartilage remained which showed retention of chondroitin -4 and -6 sulphate and in case 1 also of keratan sulphate although in a reduced quantity. The loss of all classes of glucosaminoglycans, the presence of retained cartilage islands, the lack of involvement of several cartilages in the body as well as the benefit of corticosteroid administration, would together seem to rule out a biosynthetic defect as the primary pathogenetic mechanism of relapsing polychondritis.

The complete absence of intracytoplasmic glycogen in the chondrocytes as well as PAS-positive diastase-resistant neutral mucosubstances (ne-glycols) in the matrix in the areas with loss of glucosaminoglycans is at variance with the observation of *Verity et al.* (1963). They found retained intracytoplasmic glycogen and an increased PAS reactivity of the residual cartilage matrix. The intracytoplasmic glycogen is presumed to be a store of raw material for the synthesis of glucosaminoglycans (*Pritchard* 1952, *Schajowicz & Cabrini* 1958). It is interesting that glycogen disappears rapidly from ear cartilage cells in experimental animals after intravenous papain administration which causes matrix dissolution and apparently stimulates glucosaminoglycan synthesis by chondrocytes (*McElligot & Potter* 1960). The loss of intracytoplasmic glycogen in the residual cartilage islands of the present cases might therefore be due to a stimulation of the chondrocytes rather than caused by degenerative changes.

In case 1 urinary analysis for glucosaminoglycans according to *Di Ferrante* (1967) showed slightly increased values. The diagnostic value of urinary analysis for glucosaminoglycans has been reported by some authors (*Kaye & Sones* 1964). However it may be normal during exacerbations of relapsing polychondritis (*Hemry et al* 1972, *Strann & Strand* 1972) as in our case 2. Both our patients were taking corticosteroids at the time of urinary analysis. The loss of glucosaminoglycans as detected by urinary analyses probably depends on the amount of cartilage involved, the stage of the disease and the treatment given. This analysis may therefore aid diagnosis when positive, while a negative finding does not exclude the possibility of relapsing polychondritis.

Radiologic examination of the trachea in both cases revealed severe narrowing of the lumen and in case 1 also foci of calcification within the cartilage rings. Tracheal stenosis and cartilage calcification have previously been reported as characteristic of patients with relapsing polychondritis involving the tracheobronchial tree (*Dolan et al* 1966). Radiologic examination of the trachea, therefore, seems to be of value in the differential diagnosis of obstructive respiratory symptoms, and we feel it should always be done in patients with asthma-like symptoms which are unchanged by conventional anti-asthmatic drugs or have simultaneous symptoms from involvement of extra-respiratory cartilage, as in both the present cases.

Relapsing polychondritis usually follows a low-grade and "smouldering" course over many years (*Dolan et al* 1966, *Hughes et al.* 1972, *Arkin & Masi* 1975). However the disease may be fatal as in 29 out of the 132 previously reported cases (*Arkin & Masi* 1975). Respiratory involvement, as in both the present cases, may cause airway collapse, the commonest cause of death (*Arkin & Masi* 1975). Corticosteroids have been reported to be most efficient for laryngo-tracheo-bronchial manifestations of the disease (*Dolan et al* 1966). It is interesting that one of our patients (case 1) treated with prednisolone lived for more than 4 years after the onset of obstructive symptoms and radiologic demonstration of severe tracheal stenosis. An early diagnosis based on clinical, morphologic, radiologic and possibly laboratory findings, followed by prompt corticosteroid administration and, if necessary, tracheotomy may be life saving (*Dolan et al.* 1966, *Hughes et al.* 1972, *Arkin & Masi* 1975).

REFERENCES

1. *Arkin C. R. & Masi A. T.*: Relapsing polychondritis: review of current status and case report. Seminars in Arthritis and Rheum. 5: 41–62, 1975.

at pH 2.5 and 0.5 The staining reaction was not significantly changed by pretreatment with bacterial chondroitinase ABC The cartilage stained strongly with Alcian blue up to a $MgCl_2$-concentration of 0 75 M with a moderate staining at 1 0 M These results agree well with the known presence of keratan sulphate in adult cartilage (Mathews 1967 *Meyer et al* 1958) *The* cytoplasm of chondrocytes contained abundant glycogen (PAS positive and diastase sensitive) and the *hyaline matrix contained PAS-positive diastase* resistant material

Foetal tracheal articular and costal cartilage were strongly stained with Alcian blue as was adult cartilage, at pH 2 5 and 0.5 but the staining was completely abolished by pretreatment with chondroitinase ABC. The cartilage stained strongly up to 0.35 M $MgCl_2$ and the CEC was 0.55 M $MgCl_2$. *These results* are compatible with a known presence of chondroitin -4 and -6 sulphate but not keratan sulphate in foetal cartilage There was only a slight amount of glycogen in chondrocytes and PAS-positive diastase-resistant material in the foetal cartilage matrix.

Case 1 Areas within the fibrous cartilage and the dense fibrous tissue which had replaced most of the ordinary hyaline cartilage of the external ear trachea and bronchi stained with Alcian blue both at pH 2 5 and 0.5 However the staining was *weak compared to control adult cartilage. The* weak alcianophilia was completely abolished by pretreatment of the sections with bacterial chondroitinase ABC. Staining with Alcian blue at controlled electrolyte concentrations revealed alcianophilia up to 0 55 M These results indicate the presence of chondroitin sulphates but not of keratan sulphate and the weak staining compared to controls suggests decreased amounts of the former Some areas within the fibrous tissue were only weakly stainable with Alcian blue at pH 2.5 and *not at all at pH 0.5 chondroitinase* ABC digestion did not change this staining and the CEC was 0 1 M $MgCl_2$ indicating a complete loss of chondroitin sulphates as well as keratan sulphate

The cartilage foci which retained a hyaline character stained strongly with Alcian blue at pH 2 5 and 0 5 pretreatment with chondroitinase ABC reduced the Alcian blue affinity but only in some areas completely abolished staining With the Scott and Dorling technique a weak staining remained at 1 0 M $MgCl_2$ in most of the hydraline cartilage These result nd at the presence of both chondroitin ulphates nd ke atan sulphate within the retained hyal n rt lage although compared to *control* th w ak *i ning* with Alcian blue after chondro tinase ABC d gestion and at 1 0 M $MgCl_2$ suggest reduced quantities of keratan sulphate *Only the cartilage areas with retained basophilia* and hyaline character staining with Alcian blue at pH 0.5 and above 0 65 M $MgCl_2$ revealed intracytoplasmic glycogen and PAS-positive diastase resistant material in the matrix, as seen in control adult cartilage.

Case 2 The biopsy which mostly resembled fibro-cartilage and was *without a distinct hyaline* character showed a moderate alcianophilia at pH 2.5 and also patchily at pH 0.5 the staining was *completely* abolished by chondroitinase ABC digestion. A weak staining remained up to 0.65 M $MgCl_2$ most clearly seen in some perilacunar zones *These results* indicate the presence of chondroitin sulphates but not of keratan sulphate, and the staining intensity compared to controls suggests decreased amounts of chondroitin sulphate. There was no glycogen within the cytoplasm of the chondrocytes and no PAS-positive diastase-resistant material could be found in the matrix.

DISCUSSION

Relapsing polychondritis is a rare disorder which may be diagnosed on the typical clinical findings associated with destruction of multiple cartilages. Initially however the symptoms may be localized for example to the external ear or nasal cartilage, and may then be regarded as traumatic or infectious in origin Involvement of the tracheobronchial tree leading to obstructive symptoms may be interpreted as bronchial asthma as in both the present cases, and arthropathy may be considered as rheumatoid arthritis, as in case 1 The morphologic changes in involved hyaline cartilage including inflammatory cell infiltration degeneration and loss of the hyaline character and glucosaminoglycans, followed by replacement by fibrocartilage or dense fibrous tissue, seem to be constant and characteristic of relapsing polychondritis. A biopsy from involved cartilage may help to establish the diagnosis, as in case 2 This might also have occurred with the primary biopsy in case 1 if the pathologist had been aware of the disease

Most of the cartilage lesions in both the cases presented revealed histochemical characteristics compatible with a complete, or almost complete loss of chondroitin -4 and -6 sulphate and keratan sulphate This loss of glucosaminoglycans and the subsequent fibrous replacement seem to be responsible for the structural collapse. However in both cases

Acta path. microbiol. scand. Sect. A, 85 665-670 1977

DIFFERENTIAL STAINING OF GLYCOSAMINOGLYCANS UTILIZING BACTERIAL CHONDROITINASE AND CHONDROSULPHATASE

Lars-Gunnar Kindblom and Karin Karlsson

Department of Pathology University of Göteborg, Sweden

Kindblom, L.-G & Karlsson, K. Differential staining of glycosaminoglycans, utilizing bacterial chondroitinase and chondrosulphatase Acta path. microbiol. scand Sect. A, 85 665-670 1977

A histochemical method for the differentiation of glycosaminoglycans, utilizing bacterial chondroitinase ABC and chondro-4 and -6 sulphatases, and staining with Alcian blue is presented. The method is applied on human tissues with known glycosaminoglycan content (ganglion cyst, umbilical cord, foetal cartilage adult cartilage) and the results are compared with the results obtained by staining with Alcian blue at controlled pH levels, with or without prior digestion with bovine testicular hyaluronidase and the Scott method utilizing Alcian blue at varying concentrations of $MgCl_2$ It is concluded that chondroitinase ABC digest chondroitin-4 and -6 sulphate and to some extent also hyaluronic acid and dermatan sulphate, but not heparin and keratosulphate

Key words Glycosaminoglycans staining chondroitinase chondrosulphatase.

Kindblom, L.-G Department of Pathology Vasa hospital, S-411 33 Göteborg, Sweden.

Received 4 xi 77 Accepted 5 iv 77

Histochemical differentiation of glycosaminoglycans has been performed by staining with basic dyes, mainly Alcian blue and toluidine blue, at different pH levels (*Spicer et al* 1967 *Lima* 1968 *Angervall et al.* 1973) With this method, acid non-sulphated and sulphated mucosubstances can be distinguished (*Quintarelli et al.* 1964) Glycosaminoglycans, being polyanions, may be bound and precipitated by cationic substances and can be differentiated from each other according to the salt concentration necessary to dissolve the precipitate (*Scott* 1960 *Laurent & Scott* 1964) Making use of these properties, Scott and *Dorling* (1965) described a histochemical method by which the different glycosaminoglycans could be further distinguished from each other by determining the critical electrolyte concentration (CEC) needed to abolish their staining with Alcian blue.

Bovine testicular and bacterial hyaluronidase have been used in histochemical studies to differentiate between hyaluronic acid and sulphated mucosubstances (*Leppi et al.* 1961 *Zugibe* 1961 *Yamada* 1974 *Kindblom & Angervall* 1975) Diastase (amylase) digestion of sections, followed by staining according to the PAS-method, has been used

2 *Bean W B Derrets C C & Chapman J S* Chronic atrophic polychondritis. Medicine *37* 353–363 1958
3 *Dalén P & Kjellbo H* Relapsing polychondritis Sv Läkartidn. *70* 927–928 1973
4 *Di Ferrante N* The measurement of urinary mucopolysaccharides. Anal Biochem *21* 98 1967
5 *Dolan D L Lemmon G B & Teitelbaum S L* Relapsing polychondritis. Analytical literature reviews and studies on pathogenesis. Am. J Med. *41* 285–299 1966
6 *Hemry D A Moss A I & Jacox R F* Relapsing polychondritis, a "floppy" mitral valve and migratory polytendonitis. Ann. Intern Med *77* 576–580 1972
7 *Hughes R A Berry C L, Seifert M & Lessof M A* Relapsing polychondritis Three cases with a clinico-pathological study and literature review Quart. J Med. New York Series *41* 363–380 1972
8 *Jaksch Wartenhorst R* Polychondropathia. Wien Arch Inn Med *6* 93 1923
9 *Kaye R L & Sones, D A* Relapsing polychondritis. Clinical and pathologic features in fourteen cases. Ann. Intern. Med *60* 653–664 1964
10 *Kindblom L.-G & Angervall L.* Histochemical characterization of mucosubstances in bone and soft tissue tumors. Cancer *36* 985–994 1975
11 *Kindblom L. G & Karlsson K* Differential staining of glucosaminoglycans utilizing bacterial chondroitinase and chondro sulphatase. Acta path microbiol. scand. Sect A *85* 665–670 1977
12. *Mathews M B.* Biophysical aspects of acid mucopolysaccharides relevant to connective tissue structure and function. In The Connective Tissue International Academy of Pathology Monograph No 7 Baltimore William and Wilkins, 1967 pp. 304–329
13 *McElligott T F & Potter J L* Increased fixation of sulphur[35] by cartilage in vitro following depletion of the matrix by intravenous papain. J exp. Med. *112* 743 1960
14 *Meyer K Hoffman P & Linker A* Mucopolysaccharides of costal cartilage Science *128* 896 1958
15 *Pearson C M., Kline H M & Newcomer V D* Relapsing polychondritis. N Engl. J Med. *263* 51–58, 1960
16. *Pritchard J J* A cytological and histochemical study of bone and cartilage formation in the rat. J Anat. *86* 259 1952
17 *Schajowicz F & Cabrini R. L.* Histochemical distribution of succinic dehydrogenase in bone and cartilage Science *131* 1043 1958.
18. *Scott J E & Dorling J* Differential staining of acid glycosaminoglycans (mucopolysaccharides) by Alcian blue in salt solution. Histochemie *5* 221–233 1965
19 *Swain R E & Stroud M H* Relapsing polychondritis. Laryngoscope *82* 891–898, 1972
20 *Verity M A Larson W M & Madden S C* Relapsing polychondritis. Report of two necropsied cases, with histochemical investigation of the cartilage lesion. Am. J Pathol. *42* 251–269 1963

Digestion with CHase ABC		Digestion with 4-Sase and/or 6-Sase		Digestion with CHase ABC + 4-Sase + 6-Sase	
AB (pH 2.5)	AB (pH 0.5)	AB (pH 2.5)	AB (pH 0.5)	AB (pH 2.5)	AB (pH 0.5)
—	—	+ +	—	—	—
—	—	+ +	±	—	—
+	+	+ +	+ +	+ +	+ +
+ + +	+ + +	+ + +	+ + +	+ + +	+ + +
—	—	+ + +	+ + +	—	—
+ + +	+ + +	+ + +	+ + +	+ + +	+ + +

…schaft) was performed at pH 2.5 (1 per cent in 3 per cent acetic acid, staining time 30 minutes) and pH 0.5 (1 per cent in 0.5 M HCl, staining time 30 minutes). The sections stained at pH 0.5 were blotted dry without rinsing in water. All sections were then dehydrated in ethanol, cleared in xylene and mounted in Pertex (Bethlehem Trading Company).

Enzyme Digestion

Hyaluronidase. After deparaffinisation and hydration the sections were incubated in 0.1 M phosphate buffer pH 6.0 containing testicular hyaluronidase (hyaluronidase from bovine testes, type IV, Sigma Chemical Company) 0.3–0.6 mg/ml (the enzyme activity was 750 units/mg). Enzyme digestion was performed at room temperature for 6 hours.

Chondroitinase ABC. After deparaffinisation and hydration the sections were allowed to dry. They were then incubated in Tris-HCl buffer pH 8, containing 1.25 units chondroitinase ABC/ml (Seikagaku Chemical Industry) at 37° C for 2 hours.

Chondroitinase ABC—Chondro-4 sulphatase—Chondro-6 sulphatase. The sections were treated as for chondroitinase ABC digestion. The enzyme solution contained chondroitinase ABC, 1.25 units/ml, chondro-4 sulphatase (Seikagaku Chemical Industry) 1.2 units/ml and chondro-6 sulphatase (Seikagaku Chemical Industry) 1.2 units/ml.

Chondro-4 sulphatase—Chondro-6 sulphatase. The sections were treated as for chondroitinase ABC digestion. The enzyme solution contained chondro-4 sulphatase 1.2 units/ml and chondro-6 sulphatase, 1.2 units/ml.

In order to classify the results of the Alcian-blue staining procedure on tissues, a five-step scale was introduced: + + + = strong, + + = moderate, + = weak, ± = feeble or doubtful, and — = negative. All standard tissues were examined at the same magnification (× 50) and at the same light intensity.

RESULTS

(Summarized in Tabl 1)

Synovial fluid of ganglion cysts stained with Alcian blue up to 0.1 M MgCl showed a moderately strong staining at pH 2.5. Lowering of the pH and/or digestion with hyaluronidase and chondroitinase ABC with or without the addition of chondro-4 and -6 sulphatase abolished the reaction. Digestion with chondro-4 and -6 sulphatase alone did not affect the staining.

Umbilical Cord

Wharton's jelly of the umbilical cord stained with Alcian blue up to 0.35 M $MgCl_2$. The staining was moderately strong at pH 2.5 and was completely abolished or doubtful at pH 0.5. Hyaluronidase digestion and digestion with chondroitinase ABC with or without addition of chondro-4 and -6 sulphatase completely abolished the alcianophilia. Treatment with chondro-4 and -6 sulphatase had no effect on the staining.

The inner third of the *arterial walls* showed a CEC of 0.55 M $MgCl_2$. A moderately strong

	CEC* (molarity of $MgCl_2$)	AB (pH 2.5)	AB (pH 0.5)	Digestion with hyaluronidase AB (pH 2.5)	AB (pH 0.5)
Ganglion					
Synovial fluid	0 1	+ +	—	—	—
Umbilical cord					
Wharton's jelly	0.35	+ +	±	—	—
Arterial walls	0.55	+ +	+ +	+ +	+ +
Mast cells	0.85	+ + +	+ + +	+ + +	+ + +
Foetal cartilage	0.55	+ +	+ + +	—	—
Adult cartilage	1 0	+ + +	+ + +	+ + +	+ + +

* Abbreviations CEC = Critical Electrolyte Concentration AB (pH 2.5) = Alcian blue pH 2.5 AB (pH 0.5) = Alcian blue pH 0.5 CHase ABC = Chondroitinase ABC 4-Sase = Chondro-4-sulphatase 6-Sase = Chondro-6-sulphatase Intensity of staining reaction + + + = strong + + = moderate + = weak ± = feeble or doubtful — = negative

to identify glycogen (*Lillie* & *Greco* 1947) Histochemical identification of sialic acid has been performed using neuraminidase (*Spicer* & *Warren* 1960 *Quintarelli* 1963 *Jensen* 1970) Chondroitinase ABC and chondrosulphatases have been purified from extracts of *Proteus vulgaris* which was adapted on a medium containing chondroitin 6-sulphatase (*Yamagata et al* 1968) The optimal pH for chondroitinase ABC for degradation of chondroitin 4-sulphate dermatan sulphate and chondroitin 6-sulphate (chondroitinsulphate A B and C respectively) was found to be approximately 8 0 By contrast the maximal rates of degradation of chondroitin and hyaluronic acid ocurred near pH 6 2 and 6 8 respectively Maximal effect of chondro-4 sulphatase and chondro-6 sulphatase were obtained at pH 7 5 (*Yamagata et al* 1969 *Suzuki et al* 1968) Enzymatic methods for the biochemical demonstration of small quantities of isomeric chondroitin sulphates have been described (*Saito et al* 1968) To our knowledge no histochemical method using the now commercially available chondrosulphatases has appeared in the literature Only one report on the use of chondroitinase ABC and chondroitinase AC on human umbilical cord and various animal tissues has been published (*Yamada* 1974)

The present report describes a histochemical method for the differentiation of glycosaminoglycans and presents the results obtained using condroitinase and chondrosulphatase on human tissues. These results are compared with the well-established histochemical methods for the differentiation of glycosaminoglycans.

MATERIALS AND METHODS

The glycosaminoglycan content of certain human tissues has been isolated and biochemically identified. In the present investigation, tissues with known glycosaminoglycan content were studied histochemically umbilical cord (*Wharton's* jelly containing hyaluronic acid, arterial walls containing dermatan sulphate mast cells containing heparin) foetal cartilage (chondroitin-4 and -6 sulphate) adult cartilage (chondroitin-4 and -6 sulphate and keratosulphate) and synovial fluid of ganglion cysts (hyaluronic acid) (*Szirmai* 1956, *Zugibe* 1962, *Fitton Jackson* 1964 *Spicer et al* 1967) The tissues were fixed in 4 per cent formaldehyd embedded in paraffin and cut into 5 μ thick sections The CEC's were determined according to *Scott and Dorling* (1965)

Staining with Alcian blue (8 GS, Chroma Ge-

Hyaluronidase as well as chondroitinase ABC with or without chondro-4 and -6 sulphatase completely abolished the staining (Fig. 1). Chondrosulphatases alone had no effect on the dye binding.

Adult cartilage showed a CEC of 1.0 M $MgCl_2$. As for foetal cartilage, the staining was stronger at pH 0.5 than at pH 2.5. Digestion with hyaluronidase or with chondroitinase ABC with or without chondro-4 and -6 sulphatase or chondrosulphatase did not decrease the staining reaction (Fig. 2).

COMMENTS

In biochemical studies, chondroitinase ABC from Proteus vulgaris has been shown to degrade chondroitin-4 and -6 sulphate, dermatan sulphate and to some extent hyaluronic acid, yielding Δ 4, 5-unsaturated disaccharides, while it does not digest keratosulphate, heparin or heparin sulphate (*Yamagata et al.* 1968, *Seno et al.* 1974, *Thurston et al.* 1975). The chondro-4 and -6 sulphatases are required for the hydrolytic desulphation of these disaccharides but have no influence on the intact polymers (*Yamagata et al.* 1968, *Seno et al.* 1974). The value of staining with basic dyes at varying pH's with or without prior digestion with testicular hyaluronidase and staining at varying electrolyte concentrations for histochemical differentiation of glycosaminoglycans has already been emphasized (*Scott & Dorling* 1965, *Kindblom & Angervall* 1975). Knowledge of the histochemical properties of chondroitinase ABC is very slight and the histochemical properties of chondrosulphatases are completely unknown (*Yamada* 1974).

The results of the present study indicate that chondroitinase ABC digests hyaluronic acid (as in synovial fluid) sufficiently to abolish completely the alcianophilic reaction. Chondroitinase ABC also completely abolishes the staining of chondroitin-4 and -6 sulphate as in foetal cartilage. Although *Yamagata et al.* (1968) have reported that this enzyme also digests dermatan sulphate, a weak staining remained in arterial walls of umbilical cord known to contain dermatan sulphate. *Thurston et al.* (1975) have shown that the catalytic effect of this enzyme was much less efficient with dermatan sulphate than with the chondroitin-4 and -6 sulphatase. This might explain the weak effect of chondroitinase ABC on the staining of dermatan sulphate in the arterial walls.

The absence of effect of chondroitinase ABC on the staining of adult cartilage (containing keratosulphate) and mast cells (containing heparin) is in agreement with the known inability of the enzyme to digest keratosulphate and heparin (*Yamagata et al.* 1968, *Thurston et al.* 1975).

The complete loss of staining of chondroitin-4 and -6 sulphate (as in foetal cartilage) after chondroitinase ABC digestion, known to yield sulphated disaccharides, is probably due to a dissolution of these disaccharides from the tissue.

The lack of change of alcianophilia after digestion with chondro-4 and/or -6 sulphatases of tissues known to contain chondroitin-4 and -6 sulphate agrees well with the biochemical observation that these enzymes bring about desulphation only after prior degradation into disaccharides (*Yamagata et al.* 1968, *Seno et al.* 1974).

The present results indicate that chondroitinase ABC may be of value in the histochemical characterization of glycosaminoglycans because of its definite selective effect on chondroitin-4 and -6 sulphates, somewhat lesser effect on dermatan sulphate and hyaluronic acid, and total lack of effect on heparin and keratosulphate. The present study also indicates that chondroitin-4 and -6 sulphatases probably do not give further information in the histochemical differentiation of glycosaminoglycans when studied by Alcian blue at controlled pH's.

REFERENCES

Angervall L., Enerbäck L. & Knutson H.: Chondrosarcoma of soft tissue origin. Cancer 32: 507–515, 1973.



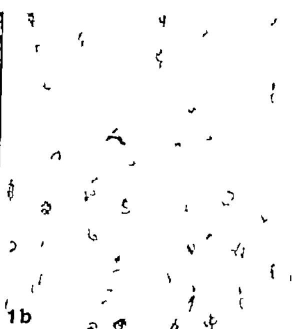


Fig 1 Foetal cartilage. A Alcian blue pH 0 5 B Digestion with chondroitinase ABC, Alcian blue





Fig 2 Adult cartilage A Alcian blue pH 0.5 B Digestion with chondro tinase ABC Alcian blue

staining with Alcian blue was found both at pH 2 5 and 0 5 which was not altered by hyaluronidase digest on Chondro tinase ABC decreased the alcianophilia but a weak staining remained both at pH 2 5 and 0 5 The addition of chondrosulphatases did not alter further the dye polymer interaction. No change in sta ning was noticed after digestion with chondrosulphatases alone.

Mast cells within the umbilical cord had a CEC of 0 85 M $MgCl_2$ and stained strongly at both pH 2.5 and 0 5 The staining was not influenced by digestion with hyaluronidase, chondroitinase ABC or chondro-4 and -6 sulphatase

Foetal cartilage possessed a CEC of 0.55 M $MgCl_2$ The moderate alcianophilia at pH 2.5 was increased by lowering the pH to 0.5

Acta path. microbiol. scand. Sect. A, 85 671–682, 1977

ENDOTHELIAL STRUCTURE IN RABBITS WITH MODERATE HYPERCHOLESTEROLAEMIA

A Scanning Electron Microscopic Study

ANDERS BYLOCK, SÖREN BJÖRKERUD, RALPH BRATTSAND, GÖRAN K. HANSSON, HANS-ARNE HANSSON and GÖRAN BONDJERS

Departments of Medicine and Histology, University of Göteborg, Göteborg, Sweden

Bylock, A., Björkerud, S., Brattsand, R., Hansson, G. K., Hansson, H.-A. & Bondjers, G. Endothelial structure in rabbits with moderate hypercholesterolaemia. A scanning electron microscopic study. Acta path. microbiol. scand. Sect. A, 85 671–682, 1977

The aortic surface of rabbits given a supplement of 0.1–0.3 per cent cholesterol to the diet was studied by scanning electron microscopy. In regions where increased haemodynamic strain was anticipated, similar structural changes were observed in normal and hypercholesterolaemic rabbits. However, changes indicating cell injury were more wide-spread in cholesterol-fed animals. This suggests that hypercholesterolaemia may increase cell susceptibility to injury. In the same regions, the development of intimal thickenings was observed in cholesterol-fed rabbits. The central parts of such thickenings had been reendothelialized, whereas a region with cell injury surrounded each lesion. In regions with low haemodynamic strain, a loss of fine-structural details was observed in hypercholesterolaemic rabbits. It is suggested that these changes may be related to the deteriorated functional properties of the intact endothelium in such rabbits. In view of these data it is suggested that the interrelationship between hypercholesterolaemia and atherosclerotic arterial disease may partly be due to a deleterious effect of hypercholesterolaemia on the functional and structural integrity of the arterial endothelium.

Key words: Endothelial structure; hypercholesterolaemia; scanning electron microscopy.

Anders Bylock, Department of Histology, University of Göteborg, 400 33 Göteborg 33, Sweden.

Received 28.x.76 Accepted 22.iii.77

Clinical as well as experimental studies indicate that increased serum cholesterol levels are connected with an increased incidence of atherosclerotic lesions (reviews *Adams* 1967, *Key* 1967). However, decreased endothelial integrity appears to be an equally significant factor in atherogenesis (review *Björkerud* 1975). Even in the normolipidaemic animal, atherosclerosis-like lesions develop under experimentally induced endothelial defects of sufficient size and duration (*Björkerud* 1969, *Bondjers & Björnheden* 1970, *Moore* 1973). In cholesterol-fed animals, the atherosclerosis-like lesions mostly develop in regions where spontaneous endothelial defects are found (*Bondjers et al.* 1977). Furthermore, endothelial integrity is decreased in clinical

Fitton Jackson S Connective tissue cells. In The Cell vol. 6 New York, Academic Press 1964 pp 387–520

Fisher E R Histochemical observations on an alveolar soft part sarcoma with references to histogenesis. Am J Pathol *32* 721–737 1956

Jensen O A Mucosubstances of mixed tumours of the human lacrimal gland Histochemical and histogenetic aspects. Acta Path. Microbiol Scand Section A *78* 110–126 1970

Kindblom L-G & Angervall L Histochemical characterization of mucosubstances in bone and soft tissue tumors Cancer *36* 985–994 1975

Laurent T C & Scott J E Molecular weight fractionation of polyanions by cetylpyridinium chloride in salt solutions. Nature *202* 661–662 1964

Lillie R D & Greco J Malt diastase and ptylin in place of saliva in the indentification of glycogen Stain Tech *22* 67–70 1947

Ludowig J Vennesland B & Dorfman A. The mechanism of action of hyaluronidases J Biol Chem. *236* 333–339 1961

Luna L G Manual of histologic staining methods of the Armed Forces Institute of Pathology 3d ed., New York McGraw—Hill Book Company 1968.

Quintarelli G Histochemical identification of salivary mucins Ann. N Y Acad. Sci *106* 339–363 1963

Quintarelli G Scott J E. & Dellovo M C The chemical and histochemical properties of Alcian blue. II Dye binding of tissue polyanions. Histochemie *4* 86–89 1964

Saito H Yamagata T & Suzuki S Enzymatic methods for the demonstration of small quantities of isomeric chondroitin sulphates. J Biol. Chem. *243* 1536–1542 1968

Scott J E. Aliphatic ammonium salts in the assay of acidic polysaccharides from tissues Methods Biochem. Anal *8* 145–197 1960

Scott J E & Dorling J Differential staining of acid glycosaminoglycans (mucopolysaccharides) by Alcian blue in salt solutions. Histochemie *5* 221–233 1965

Seno N Akiyama F & Anno K Substrate specificity of chondrosulphatases from P vulgaris for sulphated tetrasaccharides. Biochem. & Biophys. Acta *362* 290–298 1974

Spicer S S & Warren L. The histochemistry of sialic acid containing mucoproteins. J Histochem Cytochem. *8* 135–137 1960

Spicer S S Horn R G & Leppi T J Histochemistry of connective tissue mucopolysaccharides. In The Connective Tissue, International Academy of Pathology Monograph No. 7 Baltimore, Williams and Wilkins, 1967 pp 251 303

Suzuki S., Saito H., Yamagata T., Anno K Seno N Kawai Y & Furuhashi, T Formation of three types of disulphated disaccharides from chondroitin sulphates by chondroitinase digestion. J Biol Chem. *243* 1543–1550, 1968.

Szirmai J A Studies on the connective tissue of the cock comb—I Histochemical observation on the ground substance. J Histochem Cytochem. *4* 96–105 1956

Thurston C Hardingham T & Muir H The kinetics of chondroitin sulphates and hyaluronic acid by chondroitinase from P vulgaris. J Biochem. *145* 397–400 1975

Yamada K The effect of digestion with chondroitinase upon certain histochemical reactions of mucosaccharide-containing tissues. J Histochem. Cytochem. *22* 266—275 1974

Yamagata T Saito H Habuchi O & Suzuki S Purification and properties of bacterial chondroitinases and chondrosulphatases. J Biol. Chem. *243* 1523–1535 1968

Zugibe F T The demonstration of the individual acid mucopolysaccharides in human aorta, coronary arteries and cerebral arteries. I The methods. J Histochem. Cytochem. *10* 441 447 1962

Acta path. microbiol. scand. Sect. A, 85: 671–682, 1977

ENDOTHELIAL STRUCTURE IN RABBITS WITH MODERATE HYPERCHOLESTEROLAEMIA

A Scanning Electron Microscopic Study

ANDERS BYLOCK, SOREN BJÖRKERUD, RALPH BRATTSAND, GORAN K. HANSSON, HANS-ARNE HANSSON and GÖRAN BONDJERS

Departments of Medicine and Histology, University of Göteborg, Göteborg, Sweden

Bylock, A., Björkerud, S., Brattsand, R., Hansson, G. K., Hansson, H.-A. & Bondjers, G. Endothelial structure in rabbits with moderate hypercholesterolaemia. A scanning electron microscopic study. Acta path. microbiol. scand. Sect. A, 85: 671–682, 1977.

The aortic surface of rabbits given a supplement of 0.1–0.3 per cent cholesterol to the diet was studied by scanning electron microscopy. In regions where increased haemodynamic strain is anticipated, similar structural changes were observed in normal and hypercholesterolaemic rabbits. However, changes indicating cell injury were more wide-spread in cholesterol-fed animals. This suggests that hypercholesterolaemia may increase cell susceptibility to injury. In the same regions, the development of intimal thickenings was observed in cholesterol-fed rabbits. The central parts of such thickenings had been reendothelialized, whereas a region with cell injury surrounded each lesion. In regions with low haemodynamic strain, a loss of fine-structural details was observed in hypercholesterolaemic rabbits. It is suggested that these changes may be related to the deteriorated functional properties of the intact endothelium in such rabbits. In view of these data it is suggested that the interrelationship between hypercholesterolaemia and atherosclerotic arterial disease may partly be due to a deleterious effect of hypercholesterolaemia on the *functional* and structural integrity of the arterial endothelium.

Key words: Endothelial structure; hypercholesterolaemia; scanning electron microscopy.

Anders Bylock, Department of Histology, University of Göteborg, 400 33 Göteborg 33, Sweden.

Received 28.x.76. Accepted 22.iii.77.

Clinical as well as experimental studies indicate that increased serum cholesterol levels are connected with an increased incidence of atherosclerotic lesions (reviews: *Adams* 1967, *Key* 1967). However, decreased endothelial integrity appears to be an equally significant factor in atherogenesis (review: *Björkerud* 1975). Even in the normolipidaemic animal, atherosclerosis-like lesions develop under experimentally induced endothelial defects of sufficient size and duration (*Björkerud* 1969, *Bondjers & Björnheden* 1970, *Moore* 1973). In cholesterol-fed animals, the atherosclerosis-like lesions mostly develop in regions where spontaneous endothelial defects are found (*Bondjers et al.* 1977). Furthermore, endothelial integrity is decreased in clinical

Fitton Jackson S Connective tissue cells. In The Cell vol. 6 New York, Academic Press 1964 pp 387–520

Fisher E R Histochemical observations on an alveolar soft part sarcoma with references to histogenesis. Am J Pathol. *32* 721–737 1956

Jensen O A Mucosubstances of mixed tumours of the human lacrimal gland. Histochemical and histogenetic aspects. Acta Path Microbiol Scand Section A *78* 110–126 1970

Kindblom L.-G & Angervall L. Histochemical characterization of mucosubstances in bone and soft tissue tumors. Cancer *36* 985–994 1975

Laurent T C & Scott J E. Molecular weight fractionation of polyanions by cetylpyridinium chloride in salt solutions. Nature *202* 661–662, 1964

Lillie R D & Greco J Malt diastase and ptylin in place of saliva in the indentification of glycogen Stain Tech *22* 67–70 1947

Ludowieg J Vennesland B & Dorfman A The mechanism of action of hyaluronidases. J Biol Chem. *236* 333–339 1961

Luna L. G Manual of histologic staining methods *of the Armed Forces Institute of Pathology* 3d ed., New York McGraw—Hill Book Company 1968.

Quintarelli G Histochemical identification of salivary mucins. Ann. *N Y* Acad. *Sci* *106* 339–363 1963

Quintarelli G Scott J E. & Dellovo M C The chemical and histochemical properties of Alcian blue II Dye binding of tissue polyanions. Histochemie *4* 86–89 1964

Saito H Yamagata T & Suzuki S Enzymatic methods for the demonstration of small quantities of isomeric chondroitin sulphates. J Biol. Chem. *243* 1536–1542 1968

Scott J E Aliphatic ammonium salts in the as*say of acidic polysaccharides from tissues* Methods Biochem. Anal. *8* 145–197 1960

Scott J E. & Dorling J Differential staining of acid glycosaminoglycans (mucopolysaccharides) by Alcian blue in salt solutions. Histochemie *5* 221–233 1965

Seno N Anyama F & Anno K. Substrate specificity of chondrosulphatases from P vulgaris for sulphated tetrasaccharides. Biochem. & Biophys. Acta *362* 290–298 1974

Spicer S S & Warren L. The histochemistry of sialic acid containing mucoproteins. J Histochem. Cytochem. *8* 135–137 1960

Spicer S S Horn R G & Leppi T J Histochemistry of connective tissue mucopolysaccharides. In The Connective Tissue, International Academy of Pathology Monograph No. 7 *Baltimore* Williams and Wilkins, 1967 pp 251 303

Suzuki S., Saito H Yamagata T., Anno K Seno N., Kawai Y & Furuhashi T Formation of three types of disulphated disaccharides from chondroitin sulphates by chondroitinase digestion. J Biol Chem. *243* 1543–1550, 1968.

Szirmai J A Studies on the connective tissue of the cock comb—I Histochemical observation on the ground substance. J Histochem. Cytochem. *4* 96–105 1956

Thurston C Hardingham T & Muir H The kinetics of chondroitin sulphates and hyaluronic acid by chondroitinase from P vulgaris. J Biochem. *145* 397–400 1975

Yamada K The effect of digestion with chondroitinase upon certain histochemical reactions of mucosaccharide-containing tissues. J Histochem Cytochem. *22* 266—275 1974

Yamagata T Saito H Habuchi O & Suzuki S Purification and properties of bacterial chondroitinases and chondrosulphatases. J Biol. Chem. *243* 1523–1535 1968.

Zugibe F T The demonstration of the individual acid mucopolysaccharides in human aortas, coronary arteries and cerebral arteries. I The methods. J Histochem. Cytochem. *10* 441 447 1962

Acta path. microbiol. scand. Sect. A, 85 671–682, 1977

ENDOTHELIAL STRUCTURE IN RABBITS WITH MODERATE HYPERCHOLESTEROLAEMIA

A Scanning Electron Microscopic Study

ANDERS BYLOCK, SÖREN BJÖRKERUD, RALPH BRATTSAND, GÖRAN K. HANSSON, HANS-ARNE HANSSON and GÖRAN BONDJERS

Departments of Medicine and Histology, University of Göteborg, Göteborg, Sweden

Bylock, A., Björkerud, S., Brattsand, R., Hansson, G. K., Hansson, H.-A. & Bondjers, G. Endothelial structure in rabbits with moderate hypercholesterolaemia. A scanning electron microscopic study. Acta path. microbiol. scand. Sect. A, 85 671–682, 1977

The aortic surface of rabbits given a supplement of 0.1–0.3 per cent cholesterol to the diet was studied by scanning electron microscopy. In regions where increased haemodynamic strain was anticipated, similar structural changes were observed in normal and hypercholesterolaemic rabbits. However, changes indicating cell injury were more widespread in cholesterol-fed animals. This suggests that hypercholesterolaemia may increase cell susceptibility to injury. In the same regions, the development of intimal thickenings was observed in cholesterol-fed rabbits. The central parts of such thickenings had been reendothelialized, whereas a region with cell injury surrounded each lesion. In regions with low haemodynamic strain, a loss of fine-structural details was observed in hypercholesterolaemic rabbits. It is suggested that these changes may be related to the deteriorated functional properties of the intact endothelium in such rabbits. In view of these data it is suggested that the interrelationship between hypercholesterolaemia and atherosclerotic arterial disease may partly be due to a deleterious effect of hypercholesterolaemia on the functional and structural integrity of the arterial endothelium.

Key words: Endothelial structure; hypercholesterolaemia; scanning electron microscopy.

Anders Bylock, Department of Histology, University of Göteborg, 400 33 Göteborg 33, Sweden.

Received 28. 76   Accepted 22.iii.77

Clinical as well as experimental studies indicate that increased serum cholesterol levels are connected with an increased incidence of atherosclerotic lesions (reviews: *Adams* 1967, *Keys* 1967). However, decreased endothelial integrity appears to be an equally significant factor in atherogenesis (review: *Björkerud* 1973). Even in the normolipidaemic animal, atherosclerosis-like lesions develop under experimentally induced endothelial defects of sufficient size and duration (*Björkerud* 1969, *Bondjers & Björnheden* 1970, *Moore* 1973). In cholesterol-fed animals, the atherosclerosis-like lesions mostly develop in regions where spontaneous endothelial defects are found (*Bondjers et al.* 1977). Furthermore, endothelial integrity is decreased in clinical

conditions characterized by an increased incidence of atherosclerotic manifestations, such as heavy smoking (*Kjeldsen et al* 1972) stress (*Bjorkerud* 1974) or hypertension (*Bjorkerud & Eriksson* 1975) It has been suggested that hypercholesterolaemia too might be related to deteriorated cell structure and function (*Papahadjopoulos* 1974) Therefore the present study was planned to investigate the relationship between moderate degrees of hypercholesterolaemia and endothelial surface ultrastructure.

MATERIALS AND METHODS

Male albino rabbits of the Swedish country strain were obtained from the same local breeder They were kept and fed a diet with 0 1–0.3 per cent cholesterol for 6 months, under the conditions described in detail previously (*Brattsand* 1974) Serum cholesterol levels were controlled at bi weekly intervals and the cholesterol supplement to the diet was adjusted according to these measurements to maintain stable and individually different serum cholesterol levels. One week before the animals were killed the range of serum cholesterol levels of the animals was 71 to 866 mg per cent.

After an over night fast, the animals were anaesthetised with sodium pentobarbital A thoracotomia was made and a catheter was introduced through the left ventricle into the aorta. The animals were killed by exsanguination after incision into the right ventricle, during continuous perfusion with Ringer's glucose solution at 100 mm Hg After 5 minutes perfusion with this solution a 4 per cent formaldehyde solution in buffer was introduced into the aorta Great care was taken never to let the intraluminal pressure in the aorta fall to a value below the in vivo diastolic pressure After fixation in situ under these conditions for one hour 2 cm portions of the aorta were carefully excised Fat and periadventitial tissue was removed by microdissection under a dissecting microscope The aorta was cut open, and the specimens were dehydrated in a graded series of ethanol The dehydrated tissue samples were dried according to the critical-point method as described by *Andersson* (1951) with amyl acetate as intermediate fluid and carbon dioxide as transitional fluid After mounting on specimen holders, the samples were coated with copper in a vacuum evaporator and studied in a JEOL JSM 35 scanning electron microscope at a maximal accelerating voltage of 25 kV

In the design of the present study we planned to combine freeze-drying and critical-point drying of the tissue Previous studies (*Bylock et al.,* unpublished) suggest that each of these methods provides separate advantages. Freeze-drying gives less tissue-shrinkage in non fat-fed animals but the results are more difficult to reproduce than after critical-point drying. It is not possible to use freeze-drying after glutaraldehyde fixation, as the endothelial surface is covered with an amorphous layer after such fixation. Therefore, a pure formaldehyde fixative was chosen in preference to a combination with glutaraldehyde. The formaldehyde fixative was prepared fresh from paraformaldehyde and buffered with sodium cacodylate as described by *Karnovsky* (1965)

After freeze-drying of the tissue, the general endothelial surface structure in non fat-fed animals was similar to that described below However in hypercholesterolaemic animals the surface was covered with a layer of amorphous substance obscuring all finer details. The structure of this layer changed during observation in the scanning electron microscope Therefore the description is confined to preparations where critical-point drying has been employed At present we feel uncertain about the biological significance of the amorphous layer but we are inclined to believe that it is due to the exposure of the lipid-rich tissue to heat during copper evaporation and scanning electron microscopy

RESULTS

Regardless of the serum cholesterol level, marked and characteristic regional differences in aortic microtopography were observed in each animal. Regions in the vicinity of branching points had an endothelial ultrastructure that was quite different from that of regions more remote from aortic branches. In order to simplify the description of specific morphological characteristics at different serum cholesterol levels, the structure of these regions will be described separately

---

Fig 1 Scanning electron micrograph. The luminal surface of the aorta of a rabbit, with normal serum cholesterol Borders between individual endothelial cells are seen as microvillous structures projecting into the lumen. × 800

Fig 2 Scanning electron micrograph. The luminal surface of the aorta of a rabbit, with normal serum cholesterol. Nuclei, (N) of the endothelial cells are seen bulging into the lumen. The cytoplasmic surface is quite irregular × 1500

1

2

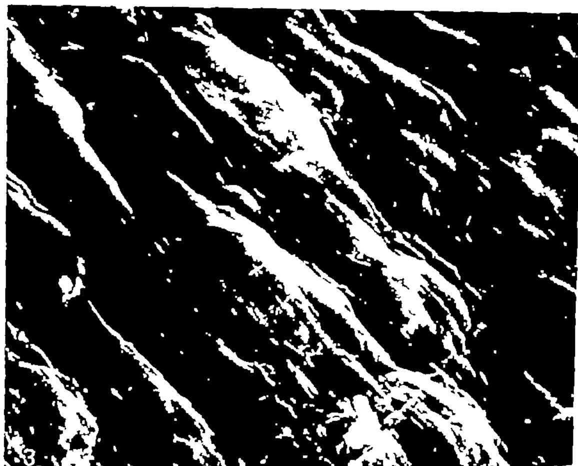


Fig 3 Scanning electron micrograph The luminal surface of the aorta of a rabbit with an Increased serum cholesterol level The surface is rather smooth and the endothelial cells are large and distended. × 1000

Regions remote from branching points In rabbits with normal serum cholesterol levels individual endothelial cells were well demarcated in such regions. Cell borders could be identified by the presence of a thin row of villous structures or folds projecting into the lumen (Fig 1) The cells were 20–70 μm long and 10–25 μm wide They were oriented with the longitudinal axis in the flow direction or at an angle of 10–20 to the flow direction The position of the cell nucleus was recognized as a gentle bulging in the central part of the cell (Fig 2) In the more peripheral parts of the cells the surface was rougher and more irregular (Fig 2)

With increasing serum cholesterol levels more elaborate structural modifications of the endothelial cell surface were rare (Fig 3) Individual cells looked larger and more distended (Fig 3) Owing to the decreased frequency of villous structures in hypercholesterolaemic rabbits, cell borders were, however difficult to identify At serum cholesterol levels above 600 mg per cent, the aortic surface was smooth and looked as if it was covered with a layer of amorphous substance (Fig 3)

Thrombotic material was rarely observed on the aortic surface, and we do not feel that it is possible to draw any conclusions concerning its frequency at different serum cholesterol levels

Regions in the vicinity of branching points Irrespective of serum cholesterol levels, a zonal arrangement of cells with differing surface structure was observed. Approaching a branching point from the unbranched segment, four different zones with individually different microtopography were regularly found

Fig. 4 Scanning electron micrographs. The aortic luminal surface of rabbit, with normal serum cholesterol. Gradual changes of the surface are seen in the locality of branching points.

Fig. 4a. Cells which re smaller and more irregular than ordinary cells. × 1200



Fig. 4b. The surface is more rough closer to the branching point. × 1200

1 Close to the more uniform structure of the lls covering regions remote from branching points, smaller endothelial cells were found (Fig. 4a). They were about half the size of ordinary endothelial cells. The position of this zone was further away from the branching points in rabbits with higher serum cholesterol levels.

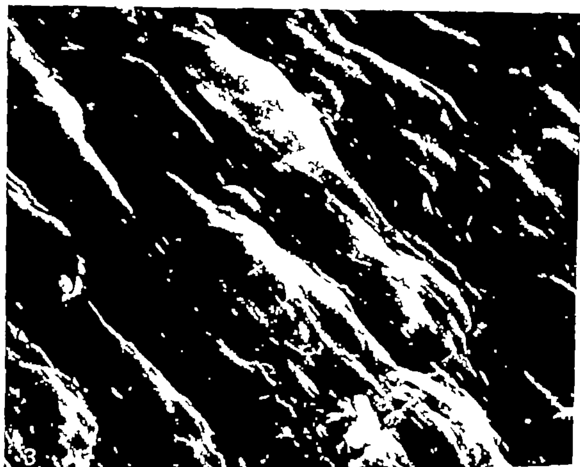


Fig 3 Scanning electron micrograph. The luminal surface of the aorta of a rabbit, with an increased serum cholesterol level The surface is rather smooth and the endothelial cells are large and distended × 1000

Regions remote from branching points In rabbits with normal serum cholesterol levels individual endothelial cells were well demarcated in such regions. Cell borders could be identified by the presence of a thin row of villous structures or folds projecting into the lumen (Fig 1) The cells were 20–70 μm long and 10–25 μm wide They were oriented with the longitudinal axis in the flow direction or at an angle of 10–20 to the flow direction The position of the cell nucleus was recognized as a gentle bulging in the central part of the cell (Fig 2) In the more peripheral parts of the cells the surface was rougher and more irregular (Fig 2)

With increasing serum cholesterol levels, more elaborate structural modifications of the endothelial cell surface were rare (Fig 3) Individual cells looked larger and more distended (Fig 3) Owing to the decreased frequency of villous structures in hypercholesterolaemic rabbits, cell borders were however difficult to identify At serum cholesterol levels above 600 mg per cent, the aortic surface was smooth and looked as if it was covered with a layer of amorphous substance (Fig 3)

Thrombotic material was rarely observed on the aortic surface and we do not feel that it is possible to draw any conclusions concerning its frequency at different serum cholesterol levels

Regions in the vicinity of branching points irrespective of serum cholesterol levels, a zonal arrangement of cells with differing surface structure was observed Approaching a branching point from the unbranched segment, four different zones with individually different microtopography were regularly found

4d

4e

2) Slightly nearer the branching point a zone containing cells with a more elaborate surface structure was present. The cells were covered with transverse folds, bridging from side to side (Fig 4b). Occasional cell bodies projected into the lumen but the cell borders were still in continuity with neighbouring cells (Fig 4c).

3) A gradual transition to areas with partially detached cells was observed. Such cells were spindle-shaped and one end of the cells adhered to the underlying surface. Their longitudinal axes were often oriented at an acute angle to the longitudinal axis of the aorta. Beneath these cells, the surface was rather smooth. However borders between individual cells could still be identified by the increased frequency of surface projections (Fig 4d, e).

4) Distended and round cells were present between partially detached cells. Such cells were common close to the branches. The size of these cells was significantly larger than that of other surface cells. In certain preparations, varying numbers of holes with a diameter of 2–10 μm were observed on the surface of distended cells (Fig 5).

In hypercholesterolaemic rabbits (serum cholesterol levels of approximately 300 mg per cent or more) intimal thickenings were observed in the centre of the zones described above. The cells covering these thickenings were more similar to the cells remote from the branching points, but they were often polyhedral without any specific orientation. Owing

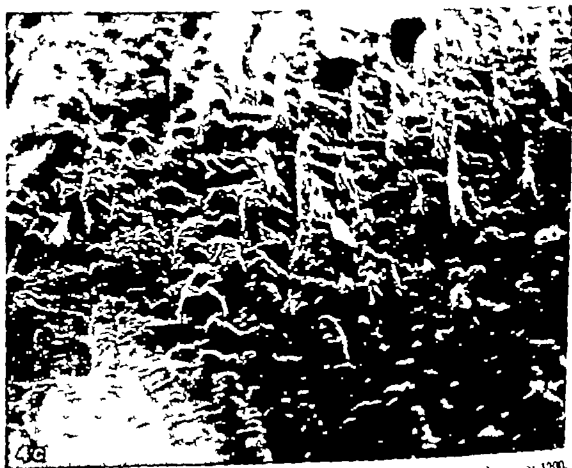


Fig 4c Very close to the branching point. One end of these cells projects into the lumen. × 1000.

Fig 4d A low power micrograph showing the elevated ends of the endothelial cells close to a branching point. × 400

Fig 4e Elevated ends of endothelial cells at a branching point. × 2000

4d

4e

Fig 5 Scanning electron micrograph The aortic luminal surface of a rabbit with normal serum cholesterol A zone of smaller cells borders a zone of larger more distended cells, closer to the branching point Note the holes of 2–3 μm in diameter in the distended cells × 500

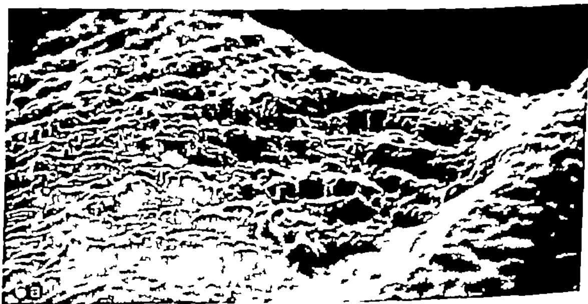


Fig 6 Scanning electron micrographs. The aortic luminal surface of a rabbit, with serum cholesterol level above 300 mg per cent

Fig 6a An intimal thickening at a branching point in a hypercholesterolaemic rabbit × 250

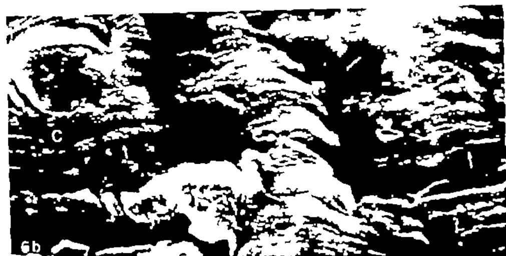


Fig. 6 b. The surface of the area in 6 a. Polyhedral, irregular cells are seen covering the area. Endothelial cell borders indicated by arrows. The folding is due to the underlying tissue structures. The crack (C) to the left is an artefact. × 1000

to the underlying structures, the surface of these lesions were quite irregular with folds and rifts (Fig. 6a, b). Rifts sometimes seemed to interrupt the structure of the covering endothelial cell layer. Occasional distended endothelial cells, sometimes with surface holes, were scattered over the lesion.

DISCUSSION

The endothelial surface as revealed in the scanning electron microscope forms a most pictorial landscape. However much of the topographical variation seen in the literature is apparently due to inadequate preparation procedures (see *Clark & Glagov* 1975, *Davies & Bowyer* 1975). It has been pointed out that a number of processing artefacts are easy to induce unless careful precautions are taken (*Clark & Glagov* 1975, *Davies & Bowyer* 1975, *Bylock et al.* 1976). In a comparative methodological study we found that fixation at normal arterial blood pressure, followed by critical-point dehydration, gives optimal reproducibility (*Bylock et al* 1976). Nevertheless, the possibility that the *in vivo* topography is distorted during preparation should always be kept in mind. In the present series of preparations we observed a variation in the frequency of holes in endothelial cells. This variation was more pronounced among different specimens from the same animal than it was between the animals. Obviously this suggests that the holes may not have been present *in vivo*. On the other hand, when they occurred, they were reproducibly confined to large distended endothelial cells. Such cells have also been observed by interference contrast microscopy (*Bjorkerud & Bondjers* 1972). Dye exclusion tests indicate that they are injured or dead cells. Therefore it is uncertain whether the holes in the surface of such cells are due to a decreased resistance to the preparation strain, with artefactual formation of defects, or whether they actually occur *in vivo*.

Spindle-like artefacts appear after mechanical manipulation of the artery before fixation, during fixation if the distending pressure is inadequate or after fixation if volatile agents are not adequately removed before coating (*Clark & Glagov* 1975). The presence of similar structures in spite of the precautions taken in the present study to prevent the formation of the artefacts may seem puzzling.

However the frequency of spindle-shaped

Fig 5 Scanning electron micrograph. The aortic luminal surface of a rabbit, with normal serum cholesterol A zone of smaller cells borders a zone of larger more distended cells, closer to the branching point Note the holes of 2–3 μm in diameter in the distended cells. × 500

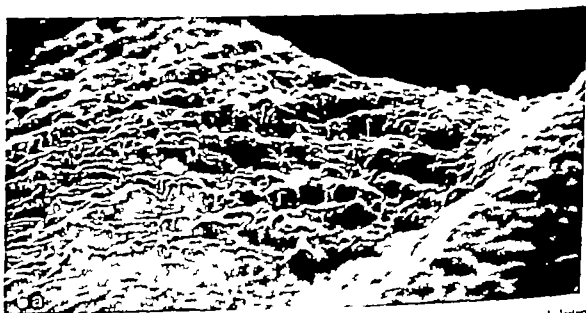


Fig 6 Scanning electron micrograph The aortic luminal surface of a rabbit, with serum cholesterol level above 300 mg per cent.

Fig 6a An intimal thickening at a branching point in a hypercholesterolaemic rabbit × 250

plaque growth are mediated by decreased endothelial integrity re-endothelialization of dietarily induced experimental atherosclerotic lesions follows soon after the formation of an intimal thickening.

In regions remote from branching points and not subjected to increased haemodynamic strain, marked structural changes were seen in experimental animals with serum cholesterol of 500 mg per cent and more. A complete loss of all fine structural details was observed, giving the impression of an amorphous layer covering the endothelial surface. Such observations were previously reported by *Weber & Tosi* (1971 a, b) in hypercholesterolaemic rabbits and guinea-pigs. The functional implications of these changes are not clear but it should be emphasized once more that the arterial endothelium exerts significant regulatory influences on the underlying smooth muscle tissue (review *Björkerud* 1975). Cholesterol deposition is counteracted by active barrier functions of the intact endothelium (*Bondjers & Björkerud* 1973, *Bondjers et al* 1976). In rabbits with marked hypercholesterolaemia the potentials of this barrier may be exceeded (*Bondjers et al* 1976). The simultaneous obscuration of fine structural detail suggests an interrelationship between surface ultrastructural modifications and the functional properties of the cells. Such evidence for cellular dysfunction related to membrane changes gives further support to the idea that increased membrane cholesterol concentrations in hypercholesterolaemia may provide a basis for the development of arterial disease (*Papahadjopoulos* 1974).

An increasing body of evidence casts doubt upon the view that atherosclerosis is simply a reaction to an increased concentration of cholesterol in serum filtered into the arterial tissue. The significance of endothelial integrity for cholesterol transfer in normo- and hyperlipoproteinaemic animals has been pointed out (*Bondjers & Björkerud* 1973, *Bondjers et al* 1976). The present results suggest that cholesterol deposition is not simply due to preexisting endothelial defects in hypercholesterolaemic rabbits. The hypercholesterolaemia *per se* may also lead to decreased endothelial integrity at least in two respects. (i) The normal haemodynamic strain induces a more pronounced injurious effect. (ii) Even in areas where haemodynamic strain is low evidence of endothelial cell dysfunction may be observed.

REFERENCES

Anderson, T. F.: Techniques for preservation of the fine structure in preparing specimens for the electron microscope. Trans. N Y Acad. Sci. *13* 130–134 1951

Adams, C. W. M. Vascular Histochemistry. London Lloyd-Luke 1967

Björkerud, S. Atherosclerosis initiated by mechanical trauma in normolipidemic rabbits. J Atheroscler Res. 9 209–213 1969

Björkerud, S.: Effect of adrenocortical hormones on the integrity of rat aortic endothelium. In *Schettler, G. & Weizel, A.* (Eds.) Atherosclerosis III. Berlin, Springer 1974 pp. 245–248.

Björkerud, S.: Relationship of endothelium to smooth muscle-overview. Adv. Exp. Med. Biol. *57* 180–204 1975

Björkerud, S. & Bondjers, G. Endothelial integrity and viability in the aorta of the normal rabbit and rat as evaluated with dye exclusion tests and interference contrast microscopy. Atherosclerosis *15* 285–300 1972.

Björkerud, S. & Eriksson, L.-O.: Strain, injury adaption and repair in hypertensive macroangiopathy. *In* "The Arterial Hypertensive Disease. A Symposium." *Rorive, G. & van Cauwenberg, H.* (Eds.) Masson Inc., New York, Paris, Barcelona, Milan 1976 pp. 39–49

Bondjers, G. & Björkerud, S.: Cholesterol accumulation and content in regions with defined endothelial integrity in the normal rabbit aorta. Atherosclerosis 17 71–83 1973

Bondjers, G. & Björkheden, T.: Experimental atherosclerosis induced by mechanical trauma in rats. Atherosclerosis *12* 301–306, 1970

Bondjers, G., Brattsand, R., Bylock, A., Hansson, G. K. & Björkerud, S. Endothelial integrity and atherogenesis in rabbits with moderate hypercholesterolemia. Artery in press, 1977

Bondjers, G., Brattsand, R., Hansson, G. K. & Björkerud, S.: Cholesterol transfer and content in aortic regions with defined endothelial integrity from rabbits with moderate hypercholesterolaemia. Nutr. Metabol. 20 452–460 1976

Brattsand, R. Studies on the prophylactic action of nicotinol and nicotinic acid on experimental hyperlipidemia and atherosclerosis in rabbits. Linköping University Medical Dissertation. No. 34 1976.

cells was rather constant in different preparations, and in different animals Furthermore they were always found in the same position i e close to branching points. In these regions flow disturbances are likely to occur (e g *Texon* 1967) If the spindle shaped structures do develop primarily in response to different mechanical manipulations *in vitro* it is possible that similar conditions *in vivo* may induce similar structural alterations. The present results do not allow any conclusions on this point However it is possible that the formation of spindle-shaped cells in response to haemodynamic strain may represent an intermediate stage in the progression to definite cell death as manifested in the "swollen" cells.

A zone of markedly smaller cells was identified in the vicinity of the injured cells. With ^{3}H thymidine incorporation techniques it has been observed that not only endothelial cell injury but also endothelial cell replication is increased in the vicinity of aortic branching points (*Payling-Wright* 1972) Therefore it is possible that the very distinct population of smaller cells may be young cells. Perhaps they are a source for restitution of the rapid decimation in the endothelial cell population induced by haemodynamic injury

Scanning electron microscopy has also previously been employed to study endothelial ultrastructure in dietarily induced experimental atherosclerosis (*Weber & Tosi* 1971a b *Weber et al* 1974 1975 *Still* 1974 *de Bruijn & van Mourik* 1975) However when these studies were performed attention had not yet been called to the ready production of artefacts in the preparation procedure for scanning electron microscopy Therefore the present results cannot be directly compared with previous results Furthermore earlier studies have been performed with a 1 per cent cholesterol supplement to the diet. This is a method that rapidly produces atherosclerosis-like lesions, but it leads to undue elevations of the serum cholesterol levels, and generalized tissue cholesterol deposition. It has been demonstrated that if only 0 1–0 3 per cent cholesterol is added to the diet, the serum cholesterol levels are more similar to those in man and after sufficient time atherosclerous-like lesions develop in rabbits with serum cholesterol above approx 300 mg per cent (*Brattsand* 1976) In view of these data, a small supplement of cholesterol to the diet has been used in the present study

Previous investigators have reported seemingly discrepant results concerning the endothelial ultrastructure over the lesions. *Weber* and collaborators (*Weber & Tosi* 1971 a, b *Weber et al* 1975) and *de Bruijn* and *van Mourik* (1975) described endothelial discontinuities on the top of the lesions, whereas *Still* (1974) found that the centre of the lesions was covered with endothelial cells *Shimamoto et al* (1971) state that the lesions were covered with abnormal endothelium whereas more normal endothelium was found in the periphery of the lesions. Their pictures, however, permit the opposite interpretation to be made In a previous study with SEM immunofluorescence microscopy and dye exclusion test, we also observed that the endothelial integrity was greater in the centre of the lesions than in the periphery (*Bondjers et al* 1977) It was concluded that plaque formation and plaque growth might be mediated by the formation of endothelial defects and that re-endothelialization followed soon after the formation of an intimal thickening (*Bondjers et al* 1977) In view of this it is possible to comprehend data suggesting that endothelial integrity is decreased in the centre of lesions. Investigators presenting such data have studied very early lesions (*Weber & Tosi* 1971 a, b *Weber et al* 1974 *de Bruijn & van Mourik* 1975) It is possible that re-endothelialization may not yet have occurred in such lesions. In a later study *Weber et al* (1975) found that 4 months after the cessation of cholesterol feeding a complete endothelial lining had formed on top of the lesions. In the periphery of the dietarily induced experimental atherosclerotic lesions, *Still* (1974) observed "bulbous cells. In view of our data these cells may be classified as non-viable, injured cells. In conclusion, most previous data can fit in with the idea that although plaque formation and

Acta path. microbiol. scand. Sect. A, 85: 683–690, 1977

CAUSE OF THE CONTINUOUS RISE IN PLASMA RENIN CONCENTRATION AFTER REMOVAL OF MANIPULATED SUBMAXILLARY GLANDS IN NEPHRECTOMIZED MICE

JENS BING, CHRISTIAN MALLING and KNUD POULSEN

The University Institute for Experimental Medicine
Nørre Allé 71, 2100 Copenhagen Ø, Denmark

Bing, J., Malling, C. & Poulsen, K. Cause of the continuous rise in plasma renin concentration after removal of manipulated submaxillary glands in nephrectomized mice. Acta path. microbiol. scand. Sect. A, 85: 683–690, 1977.

After gentle manipulation with subsequent removal of the submaxillary glands in nephrectomized mice there is a vast increase in the concentrations of high molecular weight renin ("prorenin") as well as active renin in plasma. The increase in active renin is continuous even after removal of glands as well as kidneys. Using in vitro incubation and replacement transfusion experiments, the continuous rise was found not to be due to activation of the high molecular weight renin. The continuous increase could instead be shown to be due to a rapid transfer of submaxillary lymph and (or) interstitial fluid to the surrounding tissues, with a subsequent slower release from these tissues to the blood. Continued release of renin from extra-submaxillary tissue-depots is probably also the cause of the continuance of the high plasma renin concentrations for several hours after the removal of the manipulated glands, which contrasts with the much more rapid decline in the concentration after injection of extracts of submaxillary glands as well as after injection of pure submaxillary renin.

Key words: Plasma renin; submaxillary gland; prorenin.

J. Bing, The University Institute for Experimental Medicine,
Nørre Allé 71, 2100 Copenhagen Ø, Denmark.

Received 6.ii.77 Accepted 6.iv.77

Gentle manipulation of the submaxillary glands of nephrectomized mice results in a 10–20 fold increase in plasma renin concentration, with no or only slight increase in blood pressure. If the glands are removed after the manipulation an apparently paradoxical continued rise in plasma renin is observed, which could be due to a release of inactive renin ("prorenin") that was activated with time (Bing & Poulsen 1976).

The aim of the present study was to find out whether the continued increase in plasma renin after removal of kidneys as well as submaxillary glands is due to activation of "prorenin" released during the manipulation, or whether it can be explained by other mechanisms. This question was elucidated by 1)

de Bruijn H C & van Mourik H Scanning electron microscopic observations of endothelial changes in experimentally induced atheromatosis of rabbit aortas. Virch Arch. Abt A. Path. Anat. *365* 23–40 1975

Bylock A Hansson H A Bondjers G & Björkerud S Scanning electron microscopy of the arterial endothelium—a methodological study Manuscript 1976

Clark J J & Glagov S Luminal surface of distended arteries by scanning electron microscopy eliminating contiguational and technical artefacts. Br J Exp Path *57* 129–135 1975

Davies P F & Bowyer D E Scanning electron microscopy arterial endothelial integrity after fixation at physiological pressure. Atherosclerosis *21* 463–470 1975

Karnovsky M J A formaldehyde-glutaraldehyde fixative of high osmolality for use in electron microscopy J Cell Biol. *27* 137A 1965

Keys A Dietary factors in atherosclerosis In *Blumenthal H T* (Ed) Cowdry's Arteriosclerosis, 1967 p 376

Kjeldsen K Astrup P & Wanstrup J Ultrastructural intimal changes in the rabbit aorta after a moderate carbon monoxide exposure *Atherosclerosis 16* 67–82 1972

Moore S Thromboatherosclerosis in normolipidemic rabbits a result of continued endothelial damage Lab Invest. *29* 478–487 1973

Papahadjopoulos O Cholesterol and cell membrane function a hypothesis concerning the etiology of atherosclerosis. J Theor Biol. *43* 329–341 1974

Payling-Wright H Mitosis patterns in aortic endothelium. Atherosclerosis *15* 93–100 1972.

Shinamoto T., Yamashita Y., Numano F & Sunaga T Scanning and transmission electron microscopic observation of endothelial cells in the normal condition and initial stages of atherosclerosis. Acta Path. Jap *21* 93–119 1971

Still W J S The topography of cholesterol-induced fatty streaks. Exp Mol. Path. *20* 374 386 1974

Texon M Mechanical factors involved in atherosclerosis. In *Brest A N & Moyer J H* (Eds.) Atherosclerotic Vascular Disease. London, Butterworth, 1967 p 23–42

Weber G & Tosi P Observations with the scanning electron microscope on the development of cholesterol atherosclerosis in the guinea pig Virch Arch. Abt. A Path. Anat. *353* 325–329 1971 a.

Weber G & Tosi P Some observations with the scanning electron microscope on the rabbit. Pathol. Europ *6* 407–410 1971 b.

Weber G Fabbrini P & Resi L Scanning and transmission electron microscopic observations on the surface of aortic intimal plaques in rabbits on a hypercholesterolic diet. Virch. Arch. Abt. A Path. Anat *364* 325–331 *1974*

Weber G Fabbrini P Capacciolì E. & Resi L. Repair at early cholesterol-induced aortic lesions in rabbits after withdrawal from short term atherogenic diets. Atherosclerosis *22* 565–572 1975

Acta path. microbiol. scand. Sect. A 85: 683–690, 1977

CAUSE OF THE CONTINUOUS RISE IN PLASMA RENIN CONCENTRATION AFTER REMOVAL OF MANIPULATED SUBMAXILLARY GLANDS IN NEPHRECTOMIZED MICE

Jens Bing, Christian Malling and Knud Poulsen

The University Institute for Experimental Medicine,
Nørre Allé 71, 2100 Copenhagen Ø, Denmark

Bing, J., Malling, C. & Poulsen, K. Cause of the continuous rise in plasma renin concentration after removal of manipulated submaxillary glands in nephrectomized mice. Acta path. microbiol. scand. Sect. A, 85: 683–690, 1977.

After gentle manipulation with subsequent removal of the submaxillary glands in nephrectomized mice there is a fast increase in the concentrations of high molecular weight renin (prorenin) as well as active renin in plasma. The increase in active renin is continuous even after removal of glands as well as kidneys. Using in vitro incubation and replacement transfusion experiments, the continuous rise was found not to be due to activation of the high molecular weight renin. The continuous increase could instead be shown to be due to a rapid transfer of submaxillary lymph and (or) interstitial fluid to the surrounding tissues, with a subsequent slower release from these tissues to the blood. Continued release of renin from extra-submaxillary tissue-depots is probably also the cause of the continuance of the high plasma renin concentrations for several hours after the removal of the manipulated glands, which contrasts with the much more rapid decline in the concentration after injection of extracts of submaxillary glands as well as after injection of pure submaxillary renin.

Key words: Plasma renin; submaxillary gland; prorenin.

J. Bing, The University Institute for Experimental Medicine,
Nørre Allé 71, 2100 Copenhagen Ø, Denmark

Received 6.iv.77. Accepted 6.iv.77.

Gentle manipulation of the submaxillary glands of nephrectomized mice results in a fast increase in plasma renin concentration, with no or only slight increase in blood pressure. If the glands are removed after the manipulation an apparently paradoxical continued rise in plasma renin is observed, which could be due to a release of inactive renin ("prorenin") that was activated with time (*Bing & Poulsen* 1976).

The aim of the present study was to find out whether the continued increase in plasma renin after removal of kidneys as well as submaxillary glands is due to activation of "prorenin" released during the manipulation, or whether it can be explained by other mechanisms. This question was elucidated by 1)

de Bruijn W C & van Mourik W Scanning electron microscopic observations of endothelial changes in experimentally induced atheromatosis of rabbit aortas. Virch. Arch. Abt. A Path. Anat. *365* 23–40 1975

Bylock A Hansson H A Bondjers G & Björkerud S Scanning electron microscopy of the arterial endothelium—a methodological study Manuscript 1976

Clark J J & Glagov S Luminal surface of distended arteries by scanning electron microscopy eliminating configuational and technical artefacts. Br J Exp Path. *57* 129–135 1975

Davies P F & Bowyer D E Scanning electron microscopy arterial endothelial integrity after fixation at physiological pressure Atherosclerosis *21* 463–470 1975

Karnovsky M J A formaldehyde-glutaraldehyde fixative of high osmolality for use in electron microscopy J Cell Biol. *27* 137A 1965

Keys A Dietary factors in atherosclerosis. In *Blumenthal H T* (Ed) Cowdry's Arteriosclerosis, 1967 p 576.

Kjeldsen K Astrup P & Wanstrup J Ultrastructural intimal changes in the rabbit aorta after a moderate carbon monoxide exposure Atherosclerosis *16* 67–82 1972

Moore S Thromboatherosclerosis in normolipidemic rabbits a result of continued endothelial damage. Lab Invest *29* 478–487 1973

Papahadjopoulos O Cholesterol and cell membrane function a hypothesis concerning the etiology of atherosclerosis. J Theor Biol *43* 329–341 1974

Payling-Wright H Mitosis patterns in aortic endothelium Atherosclerosis *15* 93–100 1972.

Shimamoto T Yamashita Y Numano F & Sunaga T Scanning and transmission electron microscopic observation of endothelial cells in the normal condition and initial stages of atherosclerosis. Acta Path. Jap. *21* 93–119 1971

Still W J S The topography of cholesterol-induced fatty streaks. Exp Mol Path. *20* 374–386 1974

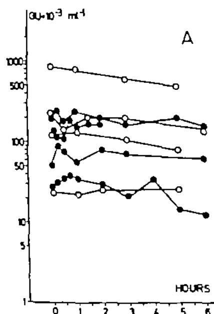
Texon M Mechanical factors involved in atherosclerosis. *In Brest A N & Moyer J H* (Eds.) Atherosclerotic Vascular Disease. London Butterworth 1967 p 23–42

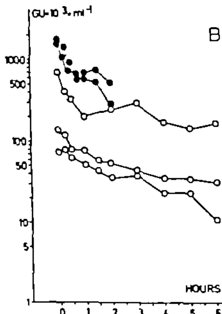
Weber G & Tosi P Observations with the scanning electron microscope on the development of cholesterol atherosclerosis in the guinea pig Virch. Arch. Abt A Path. Anat. *353* 325–329 1971 a.

Weber G & Tosi P Some observations with the scanning electron microscope on the rabbit. Pathol Europ. 6 407–410 1971 b.

Weber G Fabbrini P & Resi L Scanning and transmission electron microscopic observations on the surface of aortic intimal plaques in rabbits on a hypercholesterolic diet. Virch. Arch. Abt. A Path. Anat. *364* 325–331 1974

Weber G Fabbrini P., Capaccioli E. & Resi, L. Repair at early cholesterol-induced aortic lesions in rabbits after withdrawal from short term atherogenic diets. Atherosclerosis *22* 565–572 1975





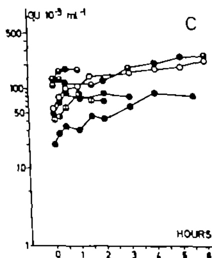


Fig. 1. Effect on plasma renin concentration in G.U. $\times 10^{-3} \times ml^{-1}$ with time *A* after *in vitro incubation* at 37 °C of blood (●) or plasma (○) taken immediately after manipulation of the submaxillary glands of nephrectomized mice, *B* after [illegible] *replacement transfusion* of blood from nephrectomized donors with manipulated submaxillary glands bled several hours (●) or immediately (○) after sialoadenectomy to sialoadenectomized as well as nephrectomized recipients, and *C* after *replacement transfusion* with blood from sialoadenectomized as well as nephrectomized donors to nephrectomized recipients immediately after their manipulated glands had been removed. In C the values are given with different symbol for each individual mouse.

continuous fall in the plasma renin concentration (Fig. 1B). The opposite way of replacement transfusion was performed with blood from sialoadenectomized as well as nephrectomized donors given to nephrectomized recipients after they had been manipulated (method 1) and immediately thereafter sialoadenectomized. In 6 such experiments (Fig. 1C) it was found that there was a continuous rise in plasma renin concentration.

3. Concentration and enzymatic activity of high and low molecular weight forms of renin in serum immediately after manipulation of the submaxillary glands of previously nephrectomized mice. These studies were performed on two pools of serum from in one case 2 and in the other 4 mice, the blood of which was taken immediately after their submaxillary glans had been manipulated (method 1) and removed. The renin concen

incubation in vitro 2) replacement transfusion of blood taken immediately after the manipulation and 3) by determination of its relative content of high molecular weight renin (*Malling & Poulsen* 1977) A further study (4) was made to see whether the degree of the lesion of the glands by the manipulation plays any role and 5) whether the time course of the changes in plasma renin concentration after injection either of crude extracts of submaxillary glands or of pure submaxillary renin is the same or differs from that found after the manipulations. Finally a study 6) was made to see whether the manipulation causes renin release to the extra submaxillary tissues.

MATERIAL AND METHODS

Animals male albino mice of Danish Serum Institute strain weight about 50 g

Anaesthesia while most experiments were performed on *conscious mice after insertion of catheters* in the femoral arteries during a short term ether anaesthesia intraperitoneal injection of amylobarbitone sodium (amytal®) in a dose of 60 to 120 mg/kg was used for the anaesthesia in the replacement transfusion experiments. *Blood sampling* was as previously described (1976) *In vitro incubation* was performed by placing the blood to which 10 µl 300 mM EDTA was added per ml or plasma in a rotating holder at 37 C

Replacement transfusion took about 9 min and was performed by simultaneous removal and infusion of about 2.5–3 ml blood pooled from 2 donors through catheters in a carotic and a femoral artery of the recipient.

Manipulation of the submaxillary glands was performed by 3 different methods The first was the same as previously described (1976) the glands being lifted up from their normal position by grasping them with pincettes placed approximately around the middle of the glands, whereafter they were manually gently compressed once per 10 seconds for one minute before removal The second was an even gentler method the lifting of the glands being performed by grasping only the most peripheral ends of the glands before the manipulation and removal By the third method not only the submaxillary gland but also the surrounding tissue including connective tissue fat lymph nodes and in some cases parts of the parotis were lifted up as a connected whole by grasping with pincettes in the same way as used by method 1 before manipulating and removing both glands and surrounding tissue

Extraction of tissue renin and determination of *renin concentration* in extracts and in plasma were performed as described by *Poulsen & Jørgensen* (1974) using their capture radioimmunoassay for angiotensin I Determination of the *fractions of renin with different molecular weight* was performed with the methods used by *Malling & Poulsen* (1977b)

Peri submaxillary gland tissues for histology and determination of renin content were in several mice removed from 0 to 7 hours after manipulation, which in some cases was followed by sialoadenectomy In the controls with previously untouched glands the glands were cautiously lifted and the peri-glandular tissues quickly removed. In some of these mice (marked ● in fig 4) a forceps was placed on the pedicle of the glands 10 to 15 seconds after they were lifted, after which the tissues were quickly removed For comparison inguinal fat tissue from some of the mice was removed and its renin content determined

Histological examination immediate fixation in neutral 4 per cent formalin solution embedding in paraffin and staining about 5 µ thick sections with the periodic acid Schiff stain.

RESULTS

1 In vitro incubation of blood or plasma taken after manipulation In 8 experiments, the results of which are given in Fig 1A blood (●) or plasma (○) taken immediately after manipulation (method 1) was incubated at 37° C *in vitro* in order to see if a continuous increase in renin concentration parallel to that found in the in vivo experiments (Fig 3A) could be demonstrated. The figure shows that this was not the case the renin concentration being constant or slightly falling during 5 to 6 hours.

2 Replacement transfusion experiments. These experiments were performed in order to elucidate whether the continuous rise in plasma renin concentration after manipulation by method 1 and subsequent sialoadenectomy is due to a factor in the blood or is caused by release of renin found in extra submaxillary tissues. In 5 replacement transfusion experiments, in which blood from donors with manipulated submaxillary gland was transfused to recipients that had previously been sialoadenectomized as well as nephrectomized there was not only absence of a continuous rise but on the contrary a

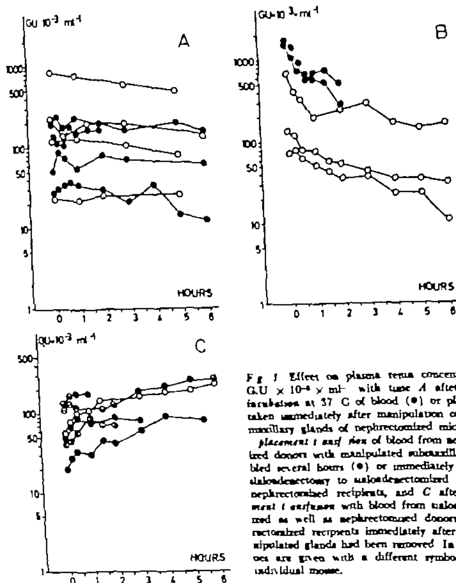


Fig 1 Effect on plasma renin concentration in G.U $\times 10^{-3} \times ml^{-1}$ with time *A* after *in vitro incubation* at 37 °C of blood (●) or plasma (○) taken immediately after manipulation of the submaxillary glands of nephrectomized mice, *B* after *replacement transfusion* of blood from nephrectomized donors with manipulated submaxillary glands bled several hours (●) or immediately (○) after sialoadenectomy to sialoadenectomized as well as nephrectomized recipients, and *C* after *replacement transfusion* with blood from sialoadenectomized as well as nephrectomized donors to nephrectomized recipients immediately after their manipulated glands had been removed In C the values are given with a different symbol for each individual mouse.

continuous fall in the plasma renin concentration (Fig 1B) The opposite way of replacement transfusion was performed with blood from sialoadenectomized as well as nephrectomized donors given to nephrectomized recipients after they had been manipulated (method 1) and immediately thereafter sialoadenectomized. In 6 such experiments (Fig 1C) it was found that there was a continuous rise in plasma renin concentration.

3 Concentration and enzymatic activity of high and low molecular weight forms of renin in serum immediately after manipulation of the submaxillary glands of previously nephrectomized mice These studies were performed on two pools of serum from in one case 7 and in the other 4 mice, the blood of which was taken immediately after their submaxillary glands had been manipulated (method 1) and removed. The renin concen-

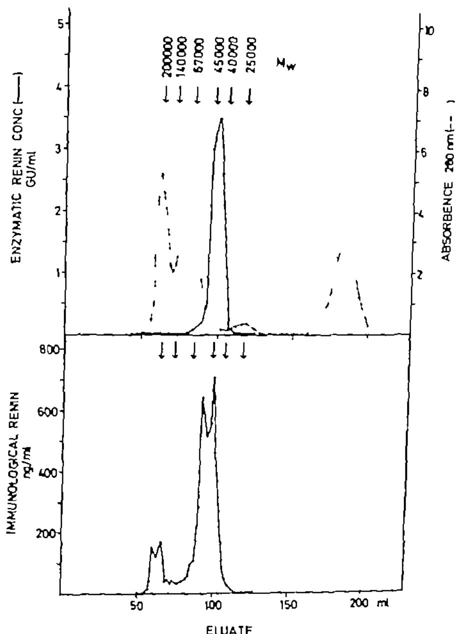


Fig 2 Gel filtration on sephadex G-100 of serum from nephrectomized mice bled immediately after manipulation of the submaxillary glands The top figure shows the protein (--) and the enzymatic reactivity of renin (——) measured by the antibody trapping method. The bottom figure shows the direct radioimmunoassay for the enzyme molecule by using an antirenin-antiserum The arrows and the figures at the top indicate the molecular weights.

tration determined by the enzymatic method, was markedly increased in both pools (0 2 and 1 4 GU/ml respectively) This was found to be due to increases in both the high and low molecular weight forms of renin (Fig 2) the relative amounts of these fractions being not significantly different from those found by *Malling & Poulsen* (1977) in serum from normal mice.

4 *Importance of the degree of the lesion of the submaxillary glands for the appearance of a continuous rise in plasma renin concentration after manipulation of the glands.* The finding of a continuous increase in plasma renin after removal of gently manipulated submaxillary glands in nephrectomized mice (1976) was confirmed in a re-investigation, using 10 mice in which the glands were lifted

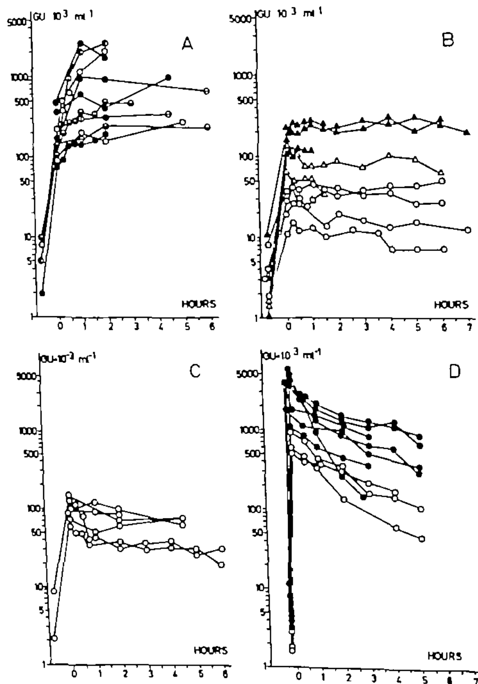


Fig. 3. Effect on plasma renin concentration in G U × 10^{-3} × ml^{-1} with the time after different forms of manipulation of the submaxillary glands (A–B–C) and (D) after injection of extracts of submaxillary glands (●) or pure submaxillary renin (○) in previously nephrectomized mice. The methods used in A, B and C are method 1, 2 and 3 respectively (see material and methods). In A the values are given with different symbols in order to illustrate the continuous rise in plasma renin in the single animal. In B the symbol ○ marks experiments when sialoadenectomy was performed after 1 minute's manipulation, while it was performed 3 (△) and 6 (▲) min. after the manipulation in some experiments.

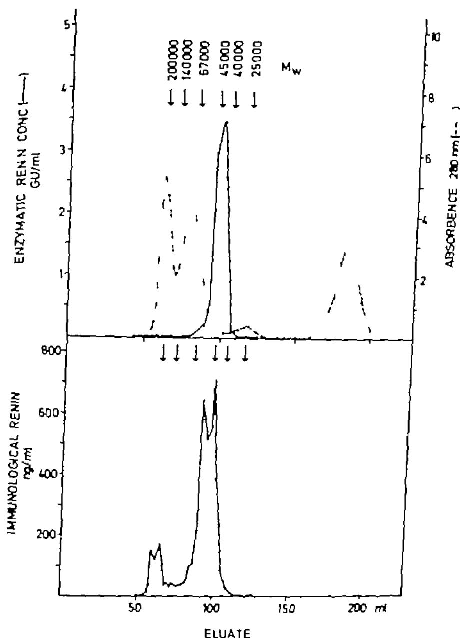


Fig 2 Gel filtration on sephadex G-100 of serum from nephrectomized mice bled immediately after manipulation of the submaxillary glands. The top figure shows the protein (– – –) and the enzymatic reactivity of renin (——) measured by the antibody trapping method. The bottom figure shows the direct radioimmunoassay for the enzyme molecule by using an antirenin-antiserum The arrows and the figures at the top indicate the molecular weights.

tration determined by the enzymatic method was markedly increased in both pools (0.2 and 1 4 GU/ml respectively) This was found to be due to increases in both the high and low molecular weight forms of renin (Fig 2) the relative amounts of these fractions being not significantly different from those found by *Malling & Poulsen* (1977) in serum from normal mice

4 Importance of the degree of the lesion of the submaxillary glands for the appearance of a continuous rise in plasma renin concentration after manipulation of the glands The finding of a continuous increase in plasma renin after removal of gently manipulated submaxillary glands in nephrectomized mice (1976) was confirmed in a re-investigation, using 10 mice in which the glands were lifted

the controls, those of the *mice with manipulated glands* all contained from 1000 to 30,000 GU × 10^{-6} per gram. This pronounced scatter of the values depended neither on the degree of manipulation (method 1 or 2) the time from manipulation to removal of the tissues, which differed from 0 to 7 hours, nor on the post-manipulation procedure about equally high values being found in the mice in which the glands were removed and in those where they were replaced. The renin content of *inguinal fat tissue* (marked △ in Fig. 4) of 5 of the mice, including 2 with manipulated glands and high renin content in the periglandular tissue (360 and 2,300 GU × 10^{-6} per g respectively) was in all cases lower than that of all but one of the samples from periglandular tissues of the controls.

Histological examination of the peri-submaxillary tissue was performed in 18 mice It contained connective tissue, fat and often also pieces of the parotid glands, but never any submaxillary tissue.

DISCUSSION

The present study shows that manipulation of the submaxillary glands causes a vast release of high molecular weight renin with low renin activity as well as of active renin (Fig 2) The continuous rise in plasma renin concentration after removal of manipulated glands in previously nephrectomized mice could thus be due to an activation of the high molecular weight renin (prorenin?) That this, however is *not* the cause of the continuous rise is seen both from the results of the in vitro incubation experiments (Fig 1A) and from the replacement transfusion experiments, in which blood from donors with manipulated glands was transfused to nephrectomized as well as sialoadenectomized recipients (Fig 1B) the result in both cases being not a continuously increasing but a constant or falling plasma renin In accordance with these findings, transfusion of blood from nephrectomized as well as sialoadenectomized donors to nephrectomized recipients shortly after manipulation and subsequent removal of their glands resulted in a continuous increase in plasma renin (Fig 1C) similar to that found after manipulation of the glands and subsequent sialoadenectomy (Fig 3A) It is, therefore, probable that the continued rise in plasma renin is due to lymphogenous (?) release of submaxillary renin to the peri-submaxillary tissue, from where renin is subsequently released to plasma. Further evidence for this explanation is given by experiments showing that if the tissue lying closest around the glands is removed together with the manipulated glands, there is no continuous rise in plasma renin (Fig. 3C) In accordance with this explanation there is the direct finding of very high renin concentrations in the peri-submaxillary tissue after manipulation of the glands, while much lower values were found in most control experiments, in which the tissue was removed quickly after the glands had been gently lifted, making removal of the peri-glandular tissue possible (Fig 4) The fact that a few of the controls had higher renin concentration than the majority shows how easily and quickly (in less than 15 seconds) renin passes from the glands to the surrounding tissue. Inguinal fat tissue, analyzed as control (△ in Fig. 4) contained about the same low renin concentration as normal plasma.

Release of glandular renin to the surrounding tissue and from there more slowly to the blood is not only the cause of the continued rise in plasma renin after manipulation followed by sialoadenectomy it is probably also the cause of the prolonged continuance of the high plasma renin concentration (Fig 3A) which is found even after so gentle a manipulation that no continued rise is found after sialoadenectomy (Fig 3B) That these continued high values can be due to continued renin release from peri-submaxillary depots seems likely according to a comparison with the much more rapid decrease in renin concentration with time found after injection of extracts of submaxillary glands and of pure submaxillary renin (Fig. 3D) this agrees with previous studies on disappearance

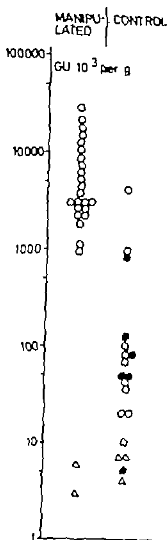


Fig 4 Comparison between the renin concentration in G U × 10⁻³ per g perisubmaxillary tissue after manipulation of the submaxillary glands of nephrectomized mice (left row) with that of nephrectomized controls, in which the tissue was removed after gentle *lifting of the glands In some* cases (marked ●) a forceps was placed on the pedicle of the glands 10 to 15 sec. after the glands were lifted For comparison some estimations of the renin concentration in fat tissue from the inguen are given (Δ)

up by grasping with pincettes around the middle of them (method 1) before the manipulation (Fig 3A) Such a continuous rise was, however either only slight or absent in 9 experiments (Fig 3B) in which the glands were lifted up by grasping only their most peripheral ends (method 2) In 6 experiments performed by method 3 by which not only the glands but also the surrounding tissues were removed as a whole after having been lifted and manipulated as the glands (without surrounding tissue) were by method 1 there was in no case a significant increase in plasma renin concentration, but constant or falling values (Fig 3C) The figures further show that higher renin concentrations were reached when the manipulation was performed by method 1 than when the two other methods were used

5 *Time course of changes in plasma renin concentration after injection of crude extracts of submaxillary glands or of pure submaxillary renin* In 6 nephrectomized mice which received injection of *crude extracts* of submaxillary glands the plasma renin concentration *measured 2 min after the injection* was about 1200 GU × 10^{-3} × ml^{-1} in one which received extracts containing about 11 GU *and about 3000 to 5000 in the other* five each of which received about 23 GU renin These values are thus the same or *somewhat higher than those found after* manipulation of the glands by method 1 (Fig. 3A) Contrary to the findings after all three *types of manipulation (Fig 3A, B and C)* the plasma renin was, however more or less rapidly falling with time in the mice which received injections of extracts (● Fig. 3D) reaching values which after 3 hours were about 25 per cent and after 5 hours about 15 per cent of the initial high value A few *experiments (marked ○ in Fig 3D)* in which the mice were injected with about 6 GU *pure submaxillary renin showed* a similar decline of the plasma renin concentration from the high post injection values

6 *Release of renin to extra submaxillary tissues after manipulation of the submaxillary glands* In the *controls* in which the submaxillary glands were *not* manipulated but only cautiously lifted in order to allow removal of peri submaxillary tissues, the renin concentration was *in most cases* between *10 and 100* GU × 10^{-3} per gram but in some cases—even in one of those (marked ●) where a forceps was placed on the pedicle of the glands less than 15 seconds after they were lifted—much higher values were found (Fig 4) Contrary to the peri glandular tissues of

Acta path. microbiol. scand. Sect. A, 85: 691–698, 1977

CAUSE OF THE DISPROPORTION BETWEEN THE VAST INCREASE IN PLASMA RENIN AND THE ONLY SMALL (IF ANY) INCREASE IN BLOOD PRESSURE AFTER MANIPULATION OF THE SUBMAXILLARY GLANDS

JENS BING and KNUD POULSEN

The University Institute for Experimental Medicine, Copenhagen, Denmark

Bing, J. & Poulsen, K. Cause of the disproportion between the vast increase in plasma renin and the only small (if any) increase in blood pressure after manipulation of the submaxillary glands. Acta path. microbiol. scand. Sect. A, 85: 691–698, 1977.

The cause of the disproportion between the vast increase in plasma renin concentration and the small, if any, increase in blood pressure after manipulation of the submaxillary glands in mice is complex. The increase in plasma renin was found to cause a marked depletion of renin substrate, which, however, was relatively so much less than the increase in renin that the (calculated) renin activity was markedly increased. The sensitivity of the vessels to angiotensin had only decreased in about half the animals studied, and even here the tachyphylaxis could not cope with the pronounced increase in plasma renin activity, as shown by a marked decrease in the blood pressure after blockade of the renin system. The finding that blockade of the renin system lowered the blood pressure below the pre-manipulation level made it probable that the vast release of submaxillary renin is followed by release of a depressor substance. The glands are known to contain kallikrein, but with the methods used it was neither proved nor disproved that the manipulation causes a release of kallikrein. Besides the factors studied, compensatory cardiovascular reflexes can play a role for the disproportion between plasma renin and blood pressure.

Key words: Plasma renin; blood pressure; renin substrate.

J. Bing, The University Institute for Experimental Medicine, Nørre Allé 71, 2100 Copenhagen Ø, Denmark.

Received 6.x.77. Accepted 6.iv.77.

Although there is a vast increase in the plasma renin concentration after gentle manipulation of the submaxillary glands of previously nephrectomized mice there is no, or only a small, increase in their blood pressure (*Bing & Poulsen* 1976). The aim of the present study was to elucidate the cause(s) of this disproportion. For this purpose it was first studied 1) whether the increased plasma renin results in depletion of renin substrate and if so whether this depletion results in normal renin activity, 2) whether the increased renin activity results in changes in the

of renin from the blood (*Lee* 1969 *Yoshida et al* 1975) A comparison between this rapid decrease with the more constantly high renin concentration with time in the mice whose glands as well as parts of their surrounding tissue were removed (Fig 3C) shows that the depots of renin are not limited to these tissue lying closest to the glands.

It is known that *renal* renin is released to renal lymph as well as to the blood (*Lever & Peart* 1963 *Skinner et al* 1963 and *Horie et al* 1970) and it has been suggested that renin released into the interstitial space plays a role for a local action in the kidney (*Morgan & Davis* 1975) Similar studies on the relation between *submaxillary* renin release to lymph and blood have not been performed It is, however known that numerous lymphatic vessels accompany the intralobular ducts and communicate freely with extensive lymph spaces that lie between the delicate interlobular connective tissue and the secretory end pieces (*Leeson* 1967) It is probably from these lymph vessels and spaces, that renin so rapidly can gain access to the periglandular tissues. It cannot be ruled out that such a release takes place through fine macroscopically invisible ruptures of the capsule through which even renin containing granules may be expelled Similarly rapid transfer of renin from an organ to the surrounding tissues has apparently not previously been found but *Eskildsen* (1973) showed that experimentally induced contact between rabbit uterine tissue and different types of autologous tissues after 1 day (or more) resulted in increased renin concentration in these tissues.

This study was supported by grants from the *Danish Heart Foundation F L. Smidth & Co Foundation King Christian X Foundation* and the *Foundation of the Insurance Companies of 1952*

The Selektronic Analyser Model 45-23 used for the radioimmunoassay is a gift from the *Danish State Medical Research Council*.

REFERENCES

Bing J & Poulsen K Vast and apparently paradoxical continuous rise in plasma renin after removal of gently manipulated submaxillary glands in nephrectomized mice Acta path. microbiol scand *84 A* 285–290 1976.

Eskildsen P C Transfer of rabbit uterine renin to autologous tissues placed in contact with the uterus. Acta path. microbiol scand *81 A* 125-136 1973

Horie K F., Brown J J Harper A M Lever A F MacGregor J & Robertson J I S The release of renin into the renal circulation of the anaesthetized dog Clin. Sci *38* 154-174 1970

Lee M R Renin and Hypertension. London 1969 page 11

Leeson C R Structure of salivary glands. In Handbook of Physiol (Ed. W Heidel) Section 6 vol. II

Lever A F & Peart W S Renin and angiotensin like activity in renal lymph. J Physiol *160* 548–563 1962

Malling Chr & Poulsen K A direct radioimmunological assay for plasma renin in mice and its evaluation. Biochem. Biophys. Acta *491* 532–541 1977

Malling Chr & Poulsen K Direct measurement of high molecular weight forms of renin in plasma. Biochim Biophys. Acta *491* 542-550, 1977

Morgan T & Davis J M Renin secretion at the individual nephron level Pflügers Arch. *359* 23–31 1975

Poulsen K & Jorgensen J An easy radioimmunological microassay of renin activity concentration and substrate in human and animal plasma and tissues based on angiotensin I *trapping* by antibody J Clin. Endocrin. Metabol *39* 816–825 1974

Skinner S L. McCubbin J W & Page I H Angiotensin in blood and lymph. Circ Res. *13* 336–345 1963

Yoshida H Menzie J & Michelakis A Distribution and disappearance rate of submaxillary renin. Proc. Soc. Exp *Biol. Med* *150* 451-456 1975

Acta path. microbiol. scand. Sect. A, 85: 691–698, 1977

CAUSE OF THE DISPROPORTION BETWEEN THE VAST INCREASE IN PLASMA RENIN AND THE ONLY SMALL (IF ANY) INCREASE IN BLOOD PRESSURE AFTER MANIPULATION OF THE SUBMAXILLARY GLANDS

Jens Bing and Knud Poulsen

The University Institute for Experimental Medicine, Copenhagen, Denmark

Bing, J. & Poulsen, K. Cause of the disproportion between the vast increase in plasma renin and the only small (if any) increase in blood pressure after manipulation of the submaxillary glands. Acta path. microbiol. scand. Sect. A, 85: 691–698, 1977.

The cause of the disproportion between the vast increase in plasma renin concentration and the small, if any, increase in blood pressure after manipulation of the submaxillary glands in mice is complex. The increase in plasma renin was found to cause a marked depletion of renin substrate, which, however, was relatively so much less than the increase in renin that the (calculated) renin activity was markedly increased. The sensitivity of the vessels to angiotensin had only decreased in about half the animals studied, and even here the tachyphylaxis could not cope with the pronounced increase in plasma renin activity, as shown by a marked decrease in the blood pressure after blockade of the renin system. The finding that blockade of the renin system lowered the blood pressure below the pre-manipulation level made it probable that the [illegible] release of submaxillary renin is followed by release of a depressor substance. The glands are known to contain kallikrein, but with the methods used it was neither proved nor disproved that the manipulation causes a release of kallikrein. Besides the factors studied, compensatory cardiovascular reflexes can play a role for the disproportion between plasma renin and blood pressure.

Key words: Plasma renin; blood pressure; renin substrate.

J. Bing, The University Institute for Experimental Medicine, Nørre Allé 71, 2100 Copenhagen Ø, Denmark.

Received 6.iv.77. Accepted 6.iv.77.

Although there is a vast increase in the plasma renin concentration after gentle manipulation of the submaxillary glands of previously nephrectomized mice there is no, or only a small, increase in their blood pressure (*Bing & Poulsen* 1976). The aim of the present study was to elucidate the cause(s) of this disproportion. For this purpose it was first studied 1) whether the increased plasma renin results in depletion of renin substrate and if so, whether this depletion results in normal renin activity. 2) whether the increased renin activity results in changes in the

sensitivity of the vessels, resulting in tachyphylaxis to angiotensin II It was further investigated 3) whether the rather unchanged blood pressure was due to a combined effect of release of submaxillary pressor and depressor substances this was elucidated by means of blockers of the renin system and of the kallikrein system

MATERIAL AND METHODS

Material and methods were on the whole identical with those described in the preceding paper While all other studies were performed on conscious mice amylobarbitone anaesthesia, as described in the preceding paper was used in studies on the sensitivity to angiotensin II and noradrenaline *Blood pressure* determination and blood sampling from catheters in the femoral arteries as previously described (1976) Determination of *plasma renin* and *renin substrate* concentration with the capture radioimmunoassay as described by *Poulsen & Jørgensen* (1974) In order to be able to calculate the *plasma renin activity* from the concentrations of renin and renin substrate the following experiments were performed a pool of plasma was obtained from sialo-adenectomized as well as nephrectomized mice A series of dilutions of this *pool with a final renin-substrate concentration* varying between zero and 1160 ng/ml (measured as angiotensin I) was incubated with a fixed concentration of mouse renin The incubations were performed as described by *Poulsen & Jørgensen* (1974) in order to study the kinetics of the reaction. The mouse renin used was pure submaxillary renin with a specific enzymatic activity of 0 41 $\times$ 10^{-3} GU per ng of pure renin (*Malling & Poulsen* 1977) The *renin was used in a* final concentration of 9 $\times$ 10^{-3} GU $\times$ ml^{-1} incubated with the dilutions of renin-substrate for 1 h at 37 C. The reaction rate was found to be proportional to the renin-substrate concentration, suggesting 1 order reaction rate with respect to renin-substrate up to at least 1160 ng $\times$ ml^{-1} The plasma renin activity could then be calculated from the already measured renin and renin-substrate *concentrations* by using the following equation Plasma renin activity (ng $\times$ ml^{-1} $\times$ h^{-1}) = constant $\times$ renin concentration (GU $\times$ 10^{-3} $\times$ ml^{-1}) $\times$ renin substrate concentrations (ng $\times$ ml^{-1}) the constant being 0 0015 (ml $\times$ GU $\times$ 10^{-3} $\times$ h^{-1})

Sensitivity of the vessels to angiotensin II was estimated by *comparison of* the blood pressure responses to injections of angiotensin II (synthetic Asp¹-Ile⁵ angiotensin II Schwartz Bio Research, New York) and noradrenaline *Blockade of the renin system* was performed by intra-arterial infusion of 1 to 4 mg/kg/hour of the competitive angiotensin II inhibitor Saralasin (Norwich Pharm. Comp) or injection of 3 mg/kg of the nonapeptide SQ20 881 (Squibb Corp) which inhibits both the angiotensin I converting enzyme and bradykininases. *Blockade of the kallikrein-system* was tried by injection of aprotinin giving 10–20,000 KIU Trasylol® (Bayer) (batch 056N and 4796P) which is known to inactivate kallikrein in several species of animals and in man.

RESULTS

1 Changes with time in concentration of plasma renin substrate (and renin) after the manipulation In seven mice, 1 normal and 6 previously binephrectomized, in which the submandibular glands had been manipulated (method 1) and either replaced (in 5) or removed (in 2) the plasma renin substarte as well as renin concentrations were followed for from 2 to 6 hours. In all cases it was found that the concentration of renin substrate, which at the start of the experiment was about 1000 ng angiotensin/ml plasma, was decreasing with increasing renin concentration. Fig 1 A gives the changes with time in one experiment, the blood pressure curve of which shows normal values with a slight fall with time which could be due to the repeated blood-samplings. The relation between corresponding values of renin and renin substarte concentration in all samples thoughout the experiment from the 6 binephrectomized mice is shown in Fig 1 B, which shows that the renin substrate is only a little depleted when the renin-concentration is about 100-fold increased, but that the substrate concentrations thereafter decrease with increasing renin concentrations reaching values about 10 ng angiotensin or less. Before the manipulation the *calculated renin activity* was between 2 and 7 ng angiotensin I/ml/hour After the manipulation there was a vast increase in the values, which rose to about 50-fold the pre manipulation value (reaching about 100 to 400 ng/ml/h) and thereafter more or less slowly after 1 to 3 hours, fell to values about 20-fold the initial value. Only in one case (shown in Fig 1 A) the activity

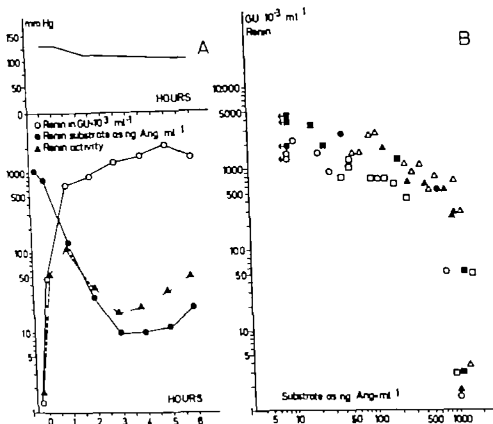


Fig 1 A. Effect of manipulation of the submaxillary glands on blood pressure, plasma renin concentration (○), renin substrate (●) and calculated renin activity (▲) with time in a nephrectomized mouse. Although the increase in renin is followed by depletion of substrate the renin activity is markedly increased. *Fig 1 B.* Relation between the concentrations of plasma renin and renin substrate in 6 nephrectomized mice before and after manipulation of their glands, both values given on a logarithmic scale here as in fig 1 A, and each mouse having its own symbol.

went lower but even here it was about 10-fold the pre-manipulation value.

2 *Vascular sensitivity to the pressor actions of angiotensin and noradrenaline before and after manipulation of the submaxillary glands.* The *sensitivity of the vessels to angiotensin II* (as measured by a comparison of the pressor effect of angiotensin II and noradrenaline) was measured in 15 normal and 10 nephrectomized amytal anaesthetized mice.

A In *mice with untouched submaxillary gland* a pressor response of about 25 mmHg (range 20 to 30 mm) was obtained with 5 ng angiotensin in 11 of the 15 *normal* mice, while 3 needed a dose of 10 ng and 1 mouse 20 ng in order to obtain a pressor response of about 25 mm. The corresponding equipressor doses of noradrenaline were 30 to 60 ng in the mice reacting to 5 ng angiotensin, and 60 to 90 ng in those who needed 10 to 20 ng angiotensin II. In seven of these mice a second and in 3 a third test was performed with 1 hour or more between the tests. In all of these repeated tests the same ratio was found between the dose of angiotensin II and noradrenaline as that found in the first test. The pressor response was also the same as in the first test in all but 2 mice, in one of which the pressor response to both angiotensin and noradrenaline changed from 27 to 16 and again to 28 mmHg while it was 26

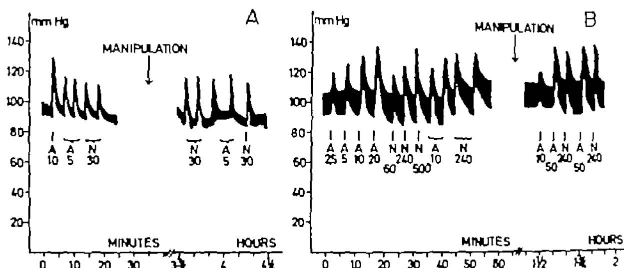


Fig 2 The sensitivity of the vessels to the pressor action of angiotensin (A) as compared to that of noradrenaline (*N*) before and after manipulation. Fig. 2 A shows a case where the sensitivity was unchanged, fig 2 B a case where the sensitivity to angiotensin was markedly decreased, while that of noradrenaline was unchanged after the manipulation. The doses are given in ng After the manipulation the plasma renin concentration was about 600 and 1500 GU $\times 10^{-4} \times ml^{-1}$ respectively in cases A and B.

and 17 mmHg in the other The sensitivity to angiotensin II of the 10 *nephrectomized* was about the same as in the normal mice the doses needed to get a pressor response of about 25 mmHg being from 5 to 20 ng angiotensin II Their sensitivity to noradrenaline showed however more scatter than in the normal ones, the doses varying from 30 to 960 ng These differences did not run parallel to the variations in the doses of angiotensin II The ratio noradrenaline/angiotensin which in normal mice varied between 3 and 12 was accordingly more varying between 3 and 96 in the nephrectomized

B From 1 to 4 hours after manipulation of the submaxillary glands the pressor effect of angiotensin II and noradrenaline was retested in 13 (3 normal and 10 nephrectomized) of the above-mentioned mice 7 (the 3 normal and 4 nephrectomized) of these 13 mice reacted with the same pressor responses to angiotensin II and noradrenaline as before the manipulation (Fig 2 A) although the plasma renin concentration was from 10 to well over 200-fold the normal reaching more than 2 GU/ml in one mouse. In the 6 other mice which all had renin concentrations above 1 GU/ml, there was, however decreased sensitivity to angiotensin II so that the dose had to be increased about 8-fold (range 4 to 16-fold) in order to obtain the same pressor response as before the manipulation (Fig 2 B) In 4 of these 6 mice with decreased sensitivity to angiotensin II the sensitivity to noradrenaline was quite the same as before the manipulation, while 2 (which needed 10 and 16-fold increased doses of angiotensin) needed 3-fold the dose of noradrenaline given before the manipulation to reach the premanipulation pressor response

3 Effect on the blood pressure of blockade of the renin system in conscious nephrectomized mice

A Studies in which the blockade was performed at various times (most often 1 to ? hours) after the manipulation including studies on controls which either had untouched glands or previously had been adenectomized In 8 experiments it was found that the nonapeptide SQ20.881 which inhibits the angiotensin I converting enzyme as well as bradykininases, lowers the blood pressure of the mice when injected in a dose of 3 mg/kg from 1 to well over 5 hours after manipulation of the glands. Repeated injections of the blocker showed that a max-

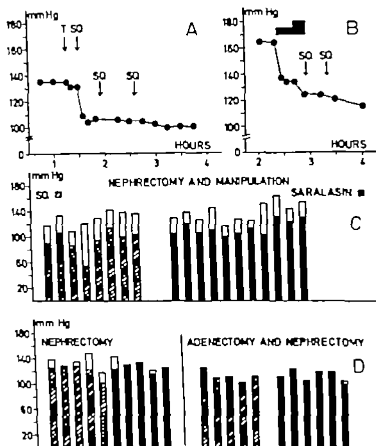


Fig. 3A shows the blood pressure of a nephrectomized mouse from about 1 to 4 hours after manipulation of its submaxillary glands. Injection of 1000 KIU *aprotinin* (Trasylol®) marked *T* gives no increase in blood pressure. Injection of 3 mg *SQ20 881* (SQ) causes a marked fall in blood pressure, this dose giving maximum effect, as seen by the lack of effect of the two following doses of 3 mg each. *Fig. 3B* shows the blood pressure of a nephrectomized mouse from about 2 to 4 hours after manipulation. It is seen that infusion of 1.2 mg/kg/h *Saralasin* was followed by a marked fall in blood pressure, which was augmented by doubling of the dose, while the blood pressure was not significantly changed by the following two injections of 3 mg *SQ20 881*. *Fig. 3C* shows the result of the blockade with *SQ20 881* (left) and *Saralasin* (right) in all the experiments on mice with manipulated glands, the blood pressure in mmHg before the treatment being given by the top of the white part of the columns, while the markedly depressed blood pressure found after the blockade is shown by the top of the hatched and black columns. *Fig. 3D* gives the much less, if any, depression of the blood pressure after blockade of the renin system with the two blockers on non-manipulated nephrectomized mice (left) and on sialoadenectomized as well as nephrectomized mice (right part).

imum effect was obtained with the primary dose (Fig. 3A). The result of the blockade in all 8 mice is given in Fig. 3C, in which each experiment is marked by a column, the top of the white part of which indicates the blood pressure before the treatment while the top of the hatched part gives the level reached after the blockade. It is seen that the blood pressure from values between about 120 to 140 mmHg fell to values about 90 to 110, in one case even to 55 mmHg.

When the blockade was performed by infusion of the competitive angiotensin inhibitor *Saralasin* in a dose of 1.2 mg/kg/h, a very similar result to that found after blockade with SQ, was obtained. The results are

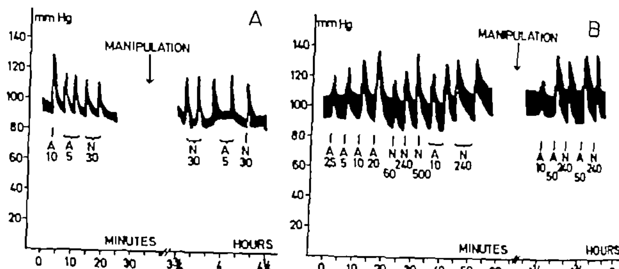


Fig 2 The sensitivity of the vessels to the pressor action of angiotensin (A) as compared to that of noradrenaline (N) before and after manipulation. Fig 2 A shows a case where the sensitivity was unchanged, fig 2 B a case where the sensitivity to angiotensin was markedly decreased, while that of noradrenaline was unchanged after the manipulation The doses are given in ng After the manipulation the plasma renin concentration was about 600 and 1500 GU × 10^{-3} × ml^{-1} respectively in cases A and B.

and 17 mmHg in the other The sensitivity to angiotensin II of the 10 *nephrectomized* was about the same as in the normal mice the doses needed to get a pressor response of about 25 mmHg being from 5 to 20 ng angiotensin II Their sensitivity to noradrenaline showed however more scatter than in the normal ones, the doses varying from 30 to 960 ng These differences did not run parallel to the variations in the doses of angiotensin II The ratio noradrenaline/angiotensin which in normal mice varied between 3 and 12 was accordingly more varying between 3 and 96 in the nephrectomized

B From 1 to 4 hours after manipulation of the submaxillary glands the pressor effect of angiotensin II and noradrenaline was retested in 13 (3 normal and 10 nephrectomized) of the above mentioned mice 7 (the 3 normal and 4 nephrectomized) of these 13 mice reacted with the same pressor responses to angiotensin II and noradrenaline as before the manipulation (Fig 2 A) although the plasma renin concentration was from 10 to well over 200-fold the normal, reaching more than 2 GU/ml in one mouse. In the 6 other mice which all had renin concentrations above 1 GU/ml there was, however decreased sensitivity to angiotensin II so that the dose had to be increased about 8-fold (range 4 to 16-fold) in order to obtain the same pressor response as before the manipulation (Fig 2 B) In 4 of these 6 mice with decreased sensitivity to angiotensin II the sensitivity to noradrenaline was quite the same as before the manipulation, while 2 (which needed 10 and 16-fold increased doses of angiotensin) needed 3-fold the dose of noradrenaline given before the manipulation to reach the premanipulation pressor response.

3 Effect on the blood pressure of blockade of the renin system in conscious nephrectomized mice

A Studies in which the blockade was performed at various times (most often 1 to ? hours) after the manipulation including studies on controls which either had untouched glands or previously had been sialoadenectomized In 8 experiments it was found that the nonapeptide SQ20.881 which inhibits the angiotensin I converting enzyme as well as bradykininases, lowers the blood pressure of the mice when injected in a dose of 3 mg/kg from 1 to well over 5 hours after manipulation of the glands. Repeated injections of the blocker showed that a max-

renin system was started before and continued after the manipulation including controls which either were manipulated but not treated with blocker or neither manipulated nor treated with blocker The results of these studies are given in Fig 4 which shows the mean blood pressure in mmHg of 5 mice which after the end of ether anaesthesia with insertion of catheters had the usual increase in blood pressure to a plateau (○) This plateau was not changed after the start of continous infusion of 2.4 mg Saralasin/kg/h (● in the figure) After manipulation of the glands in the second short ether anaesthesia there is a significant ($p < 0.001$ Students t test) fall in blood pressure which with time, although slightly increasing continues to be significantly lower ($p < 0.01$) than before the manipulation The blood pressure of the mice that received no blocker (△ in Fig 4) was not significantly different from the Saralasin-treated before, and fell in the same significant way ($p < 0.001$) immediately after the manipulation but contrary to that of the blocker-treated mice it rose quickly reaching the pre-manipulation value after about 15 minutes, and further rising above this value, this rise being, however statistically non-significant ($p > 0.1$) In a later control material in which 5 mice were neither manipulated nor treated with blocker it was found that the second ether anaesthesia performed at the same time as in the two groups shown in Fig 4 did give a slight but not significant change in the mean blood pressure which fell from 112 ± 5 to 105 ± 7 mmHg (p being > 0.05) and stayed at this level.

4 *Effect on the blood pressure of aprotinin (Trasylol®)* 4 conscious mice received injections of from 500 to 2000 KIU of Trasylol® at least 2 hours after manipulation followed by replacement of the glands. In none of these mice did aprotinin cause any increase in the blood pressure which was either uninfluenced or slightly decreased (Fig 3 A) A similar lack of blood-pressure-increasing effect of aprotinin was found in a further 5 mice which besides being treated in the same way as the previously mentioned had been pretreated with 500 to 1000 KIU before the manipulation.

DISCUSSION

The disproportion between the vast increase in plasma renin and the only small, if any increase in blood pressure after manipulation of the submaxillary glands is, according to the results of the present study not due to a single cause but is the result of several different factors. It was found that the increase in plasma renin is followed by *depletion of renin substrate* which from post nephrectomy values of more than 1000 ng angiotensin/ml plasma falls, in some cases reaching less than 1 per cent of the pre-manipulation value. As this high-graded depletion of substrate, which shows that the renin system is very active does not equal the rise in plasma renin the *calculated renin activity* remains highly increased (Fig 1 A) The disproportion could also be due to *tachyphylaxis to angiotensin II* caused by the high renin activity (for literature, see *Page & McCubbin* 1968 and *Michelakis et al.* 1974) Such tachyphylaxis was, however *only* found in about half of the cases studied (Fig 2 A and B) and even in the cases where the sensitivity had *fallen* to 6 to 25 per cent of the pre-manipulation sensitivity the 20 to 50-fold increase in the calculated renin activity would counteract the decreased sensitivity *That this is the case* was shown by the pronounced decrease in blood pressure which was found in all mice with manipulated glands when the renin system was blocked with SQ20.881 or with Saralasin (Fig 3 A, B and C) When the renin system was blocked before as well as after the manipulation by continuous infusion of Saralasin, the manipulation resulted in a persistent *decrease in* blood pressure, which stayed significantly lower than before the manipulation, while in non-blocked mice (after a short decrease) *it resulted* in a slight increase in blood pressure (Fig. 4) This finding suggests that the manipulation of the submaxillary glands

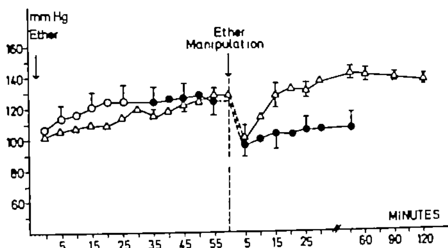


Fig 4 shows the mean effect of manipulation of the submaxillary glands on the blood pressure in nephrectomized untreated mice (Δ) and in nephrectomized mice that had been pretreated with 2 4 mg *Saralasin*/kg/h and were continously treated with this dose after the manipulation (○ and ● giving the values before and after the start of the blockade) It is seen that the blockade does not influence the blood pressure before the manipulation which in both groups causes a primary marked fall in blood pressure but while the blood pressure stays low in the Saralasin treated mice it quickly rises to the pre manipulation value in the untreated mice.

given by the 11 columns in the right parts of Fig 3 C and in Fig 3 B which further shows that in some cases a doubling of the dose resulted in a further decrease in blood pressure In the last 7 experiments shown in Fig 3 C the blockade was performed by *infusion of Saralasin followed by injection of SQ* Saralasin was infused in a dose of first 1.2 mg/kg/h for 20 min followed by a dose of 2 4 mg for 10 min (and in one case a further dose of 4 8 mg for 10 min) at the end of which injections of 3 mg SQ were given In 3 of these experiments the injection of SQ did not cause any further decrease in blood pressure than that obtained by the previous Saralasin infusion (Fig 3 B) and in the other 4 experiments there was only a further mean decrease of 5 mmHg (individ ual values 2 4 5 and 10 mmHg) There was no relation between the plasma renin concentration at the time before the treat ment with the blockers and 1) the initial blood pressure level or 2) the degree of de crease in blood pressure after the treatment

Control experiments showed that the blood pressure of nephrectomized mice with un touched submaxillary glands was in most cases much less reduced after treatment with SQ20 881 and after infusion of Saralasin (left part of Fig 3 D) than that of the mice with manipulated glands (Fig 3 C) the most pronounced effect being found in the only two mice with initial blood pressure above 140 mmHg It was further found that the blood pressure of nearly all sialo-adenec tomized as well as nephrectomized mice was unaffected by the treatment (right part of the Fig 3 D) When the blood pressure of the mice with manipulated glands (Fig 3 C) is compared with the non manipulated (left part of Fig 3 D) it is seen that in both groups most mice have values between 130 and 140 mm before treatment with blocker After this treatment there is, however a difference between the two groups, the val ues falling only to about 125 mmHg in most of the controls, while they are less than 105 mmHg in all but one of the SQ treated and less than 120 mm in the Saralasin treated mice The difference between the effect of the two blockers is probably due to the previously mentioned finding that while the dose of SQ gives a maximum effect, this is not always the case with the dose of Sara lasin

3 B Studies in which the blockade of the

renin system was started before and continued after the manipulation including controls which either were manipulated but not treated with blocker or neither manipulated nor treated with blocker. The results of these studies are given in Fig. 4 which shows the mean blood pressure in mmHg of 5 mice, which after the end of ether anaesthesia with insertion of catheters had the usual increase in blood pressure to a plateau (○). This plateau was not changed after the start of continuous infusion of 2.4 mg Saralasin/kg/h (● in the figure). After manipulation of the glands in the second short ether anaesthesia there is a significant ($p < 0.001$ Students t test) fall in blood pressure which with time, although slightly increasing, continues to be significantly lower ($p < 0.01$) than before the manipulation. The blood pressure of the mice that received no blocker (△ in Fig. 4) was not significantly different from the Saralasin-treated before, and fell in the same significant way ($p < 0.001$) immediately after the manipulation but contrary to that of the blocker-treated mice it rose quickly reaching the pre-manipulation value after about 15 minutes, and further rising above this value, this rise being however statistically non-significant ($p > 0.1$). In a later control material, in which 5 mice were neither manipulated nor treated with blocker it was found that the second ether anaesthesia performed at the same time as in the two groups shown in Fig. 4 did give a slight but not significant change in the mean blood pressure which fell from 112 ± 5 to 105 ± 7 mmHg (p being > 0.05) and stayed at this level.

4. Effect on the blood pressure of aprotinin (Trasylol®). 4 conscious mice received injections of from 500 to 2000 KIU of Trasylol® at least 2 hours after manipulation followed by replacement of the glands. In none of these mice did aprotinin cause any increase in the blood pressure, which was either uninfluenced or slightly decreased (Fig. 5 A). A similar lack of blood-pressure-increasing effect of aprotinin was found in a further 5 mice which besides being treated in the same way as the previously mentioned had been pretreated with 500 to 1000 KIU before the manipulation.

DISCUSSION

The disproportion between the vast increase in plasma renin and the only small, if any increase in blood pressure after manipulation of the submaxillary glands is, according to the results of the present study not due to a single cause but is the result of several different factors. It was found that the increase in plasma renin is followed by *depletion of renin substrate* which from post nephrectomy values of more than 1000 ng angiotensin/ml plasma falls, in some cases reaching less than 1 per cent of the pre manipulation value. As this high-graded depletion of substrate, which shows that the renin system is very active does not equal the rise in plasma renin, the *calculated renin activity* remains highly increased (Fig. 1 A). The disproportion could also be due to *tachyphylaxis to angiotensin II* caused by the high renin activity (for literature, see *Page & McCubbin* 1968 and *Michelakis et al.* 1974). Such tachyphylaxis was, however only found in about half of the cases studied (Fig. 2 A and B) and even in the cases where the sensitivity had fallen to 6 to 25 per cent of the pre-manipulation sensitivity the 20 to 50-fold increase in the calculated renin activity would counteract the decreased sensitivity. That this is the case was shown by the pronounced decrease in blood pressure which was found in all mice with manipulated glands when the renin system was blocked with SQ20.881 or with Saralasin (Fig. 3 A, B and C). When the renin system was blocked before as well as after the manipulation by continuous infusion of Saralasin, the manipulation resulted in a persistent *decrease* in blood pressure, which stayed significantly lower than before the manipulation, while in non-blocked mice (after a short decrease) it resulted in a slight increase in blood pressure (Fig. 4). This finding suggests that the manipulation of the submaxillary glands

besides renin release causes *release of a vasodepressor substance* As the submaxillary glands of mice have a high content of kallikrein (*Webster* 1970) which as renin is located in the granules of the granular ducts (*Chiang et al* 1968) the effect of a kallikrein inhibitor aprotinin (Trasylol[R]) (for literature see *Vogel & Werle* 1970) was studied Trasylol[R] however was found not to give any rise in the blood pressure of mice with manipulated glands (Fig 3 A) This finding does not rule out that the depressor substance may be kallikrein as it has been found that the effect of aprotinin which in the available preparations is of bovine origin has some species specificity and by *Chiang et al* (1968) was found not to act on kallikrein from mice The finding that blockade of bradykininases with SQ20 881 after previous blockade of the renin system with Saralasin did not give any significant change in blood presure (Fig 3 A) points against but does *not exclude, kallikrein as the vasodepressor* substance which counteracts the pressor effect of renin A further cause of the disproportion between the vast increase in plasma renin as well as in (calculated) renin activity and the small if any increase in blood pressure may be found in *compensatory cardiovascular reflexes* which have been found to suppress the response to infusion of high *concentrations of angiotensin* (*Day et al* 1965)

This study was supported by grants from the *Danish Heart Foundation F I Smidt & Co Foundation King Christian X Foundation* and the *Foundation of the Insurance Companies of 1952* The authors are also grateful to Dr *Alan W Castellion The Norwich Pharmacal Co* New York, to Dr *S J Lucania The Squibb Institute for Medical Research* New Jersey U.S.A and to *Bayer Farma* Copenhagen for generous gifts of Saralasin, the nonapeptide SQ20 881 and aprotinin, Trasylol[R] respectively The Selektronic Analyser Model 45-23 used for the radioimmunoassay is a gift from the *Danish State Medical Research Council* Dr *Ole Frederiksen* kindly performed the statistical calculations.

REFERENCES

Bing J & Poulsen K Vast and apparently paradoxical continuous rise in plasma renin after removal of gently manipulated submaxillary glands in nephrectomized mice Acta path. microbiol scand *84 A* 285–290 1976

Chiang Tsu S Erdös E. G., Miwa I Tague L. L. & Coalson J J Isolation from a salivary gland of granules containing renin and kallikrein Circ. Res. *23* 507–517 1967

Day M D McCubbin J W & Page I H Limited hypertensive effect of infusion of angiotensin Am. J Physiol *209* 264–268, 1965

Malling C & Poulsen K. A direct radioimmunological assay for plasma renin in mice and its evaluation. Biochim. Biophys Acta *491* 532 541 1977

Michelakis A M Cohen S Taylor J Murakami K & Inagami T Studies on the characterization of pure submaxillary gland renin Proc. Soc Exp Biol Med *147* 118–121 1974

Page I H & McCubbin J W Renal hypertension, page 115 Chicago 1968 Year book medical publishers.

Poulsen K & Jorgensen J An easy radioimmunological microassay of renin activity concentration and substrate in human and animal plasma and tissues based on angiotensin I trapping by antibody J Clin. Endocrinol. Metab *39* 816–825 1974

Vogel R & Werle E. Kallikrein inhibitors. In E G Erdös Bradykinin Kallidin and Kallikrein. Handbuch der exp. Pharm. Berlin 1970 page *213*

Webster M E Kallikreins in glandular tissues Ibidem page 131

Acta path. microbiol. scand. Sect. A, 85 699–706, 1977

AN AUTOPSY STUDY OF THE ISLETS OF LANGERHANS IN ACUTE-ONSET JUVENILE DIABETES MELLITUS

KARSTEN JUNKER, JOHN EGEBERG, HANS KROMANN, JØRN NERUP

Medical Department F Gentofte Hospital
Anatomy Department B, University of Copenhagen
Steno Memorial Hospital
Laboratory of Pediatric Pathology State University Hospital, Copenhagen

Junker K., Egeberg, J., Kromann, Hans & Nerup Jørn. An autopsy study of the islets of Langerhans in acute-onset juvenile diabetes mellitus. Acta path. microbiol. scand. Sect. A, 85 699–706, 1977

The existence of lymphocytic inflammation of the islets of Langerhans—insulitis—in the early stages of juvenile diabetes mellitus (j.d.m.) has been matter of discussion. In order to evaluate the possible occurrence of insulitis in early j.d.m. the present autopsy study was performed. From the years 1945 to 1974 blocks of pancreatic tissue were collected from 11 juvenile diabetics aged less than 30 years and dying within 2 months after the onset of diabetic symptoms. Pancreatic tissue blocks from 22 age-and-sex-matched sudden, unexpected deaths served as control material. 3-micron thick sections from the 33 blocks were stained with hematoxylin-eosin, aldehyde-fuchsin and silver. 1-micron sections were stained with toluidine blue. Islets were found in all the control cases, and A- and B-cell granulations were distinct. Insulitis was absent. Islets were also present in all the diabetic cases. No difference in islet number between the controls and the diabetics was apparent. The diabetic islets were morphologically heterogeneous. No difference between controls and diabetics could be demonstrated in respect of A-cell number and granulation. However B-cell granulation was demonstrable in only 1 case, and in that case in extremely reduced proportion. Insulitis was present to varying degrees in 6 of the diabetics. In this material, like others, insulitis seems most frequent in the diabetics aged less than 10 years. No conclusion can be drawn from this study about whether an infectious agent, an autoimmune process, or a combination of these, causes the insulitis. However the findings presented suggest the existence of lymphocytic insulitis as a feature of early j.d.m.

Key words: Diabetes mellitus, juvenile; islets of Langerhans; autopsy study

J. Nerup, Steno Memorial Hospital, 2820 Gentofte, Denmark.

Received 13.ii.77 Accepted 13.ii.77

If morphological studies of the islets of Langerhans might be of any help in the understanding of the etiology and/or the pathogenesis of juvenile diabetes mellitus (j.d.m.) the pathological findings in early stages of the disease call for the greatest interest.

A summary of these findings has been given by *Warren et al.* (26)

Quantitative studies have shown normal weight of pancreas, normal or reduced number of islets, reduced proportion of insular tissue due to a reduced mass of B-cells, but an

besides renin release causes *release of a vasodepressor substance*. As the submaxillary glands of mice have a high content of kallikrein (*Webster* 1970) which as renin is located in the granules of the granular ducts (*Chiang et al* 1968) the effect of a kallikrein inhibitor aprotinin (Trasylol[R]) (for literature see *Vogel* & *Werle* 1970) was studied. Trasylol[R] however was found not to give any rise in the blood pressure of mice with manipulated glands (Fig 3 A). This finding does not rule out that the depressor substance may be kallikrein as it has been found that the effect of aprotinin which in the available preparations is of bovine origin has some species specificity and by *Chiang et al* (1968) was found not to act on kallikrein from mice. The finding that blockade of bradykininases with SQ20 881 after previous blockade of the renin system with Saralasin did not give any significant change in blood pressure (Fig 3 A) points against but does not exclude, kallikrein as the vasodepressor substance which counteracts the pressor effect of renin. A further cause of the disproportion between the vast increase in plasma renin as well as in (calculated) renin activity and the small if any increase in blood pressure may be found in *compensatory cardiovascular reflexes* which have been found to suppress the response to infusion of high concentrations of angiotensin (*Day et al* 1965).

This study was supported by grants from the *Danish Heart Foundation*, *F. L. Smidt & Co Foundation*, *King Christian X Foundation* and the *Foundation of the Insurance Companies of 1952*. The authors are also grateful to Dr *Alan W Castellion*, *The Norwich Pharmacal Co*, New York, to Dr *S J Lucania*, *The Squibb Institute for Medical Research*, New Jersey, U.S.A. and to *Bayer Farma*, Copenhagen for generous gifts of Saralasin, the nonapeptide SQ20 881 and aprotinin, Trasylol[R] respectively. The Selektronic Analyser Model 45-23 used for the radioimmunoassay is a gift from the *Danish State Medical Research Council*. Dr *Ole Frederiksen* kindly performed the statistical calculations.

REFERENCES

Bing J & *Poulsen K*. Vast and apparently paradoxical continuous rise in plasma renin after removal of gently manipulated submaxillary glands in nephrectomized mice. Acta path microbiol. scand *84 A* 285–290 1976

Chiang Tzu S, *Erdös E. G*, *Miwa I*, *Tague L. L.* & *Coalson J J*. Isolation from a salivary gland of granules containing renin and kallikrein. Circ. Res. *23* 507–517 1967

Day M D, *McCubbin J W* & *Page I H*. Limited hypertensive effect of infusion of angiotensin. Am. J Physiol *209* 264–268, 1965

Malling C & *Poulsen K*. A direct radioimmunological assay for plasma renin in mice and its evaluation. Biochim. Biophys Acta *491* 532–541 1977

Michelakis A M, *Cohen S*, *Taylor J.*, *Murakami K* & *Inagami T*. Studies on the characterization of pure submaxillary gland renin. Proc. Soc Exp Biol Med *147* 118–121 1974

Page I H & *McCubbin J W*. Renal hypertension page 113 Chicago 1968 Year book medical publishers.

Poulsen K & *Jorgensen J*. An easy radioimmunological microassay of renin activity concentration and substrate in human and animal plasma and tissues based on angiotensin I trapping by antibody. J Clin. Endocrinol. Metab *39* 816–825 1974

Vogel R & *Werle E*. Kallikrein inhibitors. *In* E. G. Erdös Bradykinin Kallidin and Kallikrein. Handbuch der exp Pharm. Berlin 1970 page *213*

Webster M F. Kallikreins in glandular tissues. Ibidem, page 131

Acta path. microbiol. scand. Sect. A, 85: 699–706, 1977

AN AUTOPSY STUDY OF THE ISLETS OF LANGERHANS IN ACUTE-ONSET JUVENILE DIABETES MELLITUS

KARSTEN JUNKER, JOHN EGEBERG, HANS KROMANN, JØRN NERUP

Medical Department F, Gentofte Hospital
Anatomy Department B, University of Copenhagen
Steno Memorial Hospital
Laboratory of Pediatric Pathology, State University Hospital, Copenhagen

Junker K., Egeberg, J., Kromann, Hans & Nerup, Jørn. An autopsy study of the islets of Langerhans in acute-onset juvenile diabetes mellitus. Acta path. microbiol. scand. Sect. A, 85: 699–706, 1977.

The existence of lymphocytic inflammation of the islets of Langerhans—insulitis—in the early stages of juvenile diabetes mellitus (j.d.m.) has been a matter of discussion. In order to evaluate the possible occurrence of insulitis in early j.d.m. the present autopsy study was performed. From the years 1945 to 1974 blocks of pancreatic tissue were collected from 11 juvenile diabetics aged less than 30 years and dying within 2 months after the onset of diabetic symptoms. Pancreatic tissue blocks from 22 age-and-sex-matched sudden, unexpected deaths served as control material. 5-micron thick sections from the 33 blocks were stained with hematoxylin-eosin, aldehyde-fuchsin and other 1-micron sections were stained with toluidine blue. Islets were found in all the control cases, and A- and B-cell granulations were distinct. Insulitis was absent. Islets were also present in all the diabetic cases. No difference in islet number between the controls and the diabetics was apparent. The diabetic islets were morphologically heterogeneous. No difference between controls and diabetics could be demonstrated in respect of A-cell number and granulation. However, B-cell granulation was demonstrable in only 1 case and in that case in extremely reduced proportion. Insulitis was present to varying degrees in 6 of the diabetics. In this material, like others, insulitis seems most frequent in the diabetics aged less than 10 years. No conclusion can be drawn from this study about whether an infectious agent, an autoimmune process, or a combination of these causes the insulitis. However, the findings presented suggest the existence of a lymphocytic insulitis as a feature of early j.d.m.

Key words: Diabetes mellitus, juvenile; islets of Langerhans; autopsy study.

J. Nerup, Steno Memorial Hospital, 2820 Gentofte, Denmark.

Received 13.iv.77   Accepted 15.vi.77

If morphological studies of the islets of Langerhans might be of any help in the understanding of the etiology and/or the pathogenesis of juvenile diabetes mellitus (j.d.m.) the pathological findings in early stages of the disease call for the greatest interest.

A summary of these findings has been given by *Warren et al.* (26)

Quantitative studies have shown normal weight of pancreas, normal or reduced number of islets, reduced proportion of insular tissue due to a reduced mass of B-cells, but an

besides renin release causes *release of a vasodepressor substance* As the submaxillary glands of mice have a high content of kallikrein (*Webster* 1970) which as renin is located in the granules of the granular ducts (*Chiang et al* 1968) the effect of a kallikrein inhibitor aprotinin (Trasylol[R]) (for literature see *Vogel & Werle* 1970) was studied Trasylol[R] however was found not to give any rise in the blood pressure of mice with manipulated glands (Fig 3 A) This finding does not rule out that the depressor substance may be kallikrein as it has been found that the effect of aprotinin which in the available preparations is of bovine origin has some species specificity and by *Chiang et al* (1968) was found not to act on kallikrein from mice The finding that blockade of bradykininases with SQ20 881 after previous blockade of the renin system with Saralasin did not give any significant change in blood presure (Fig 3 A) points against but does not exclude kallikrein as the vasodepressor substance which counteracts the pressor effect of renin A further cause of the disproportion between the vast increase in plasma renin as well as in (calculated) renin activity and the small if any increase in blood pressure may be found in *compensatory cardiovascular reflexes* which have been found to suppress the response to infusion of high concentrations of angiotensin (*Day et al* 1965)

This study was supported by grants from the *Danish Heart Foundation F L. Smidt & Co Foundation King Christian X Foundation* and the *Foundation of the Insurance Companies of 1952* The authors are also grateful to Dr *Alan W Castellion The Norwich Pharmacal Co* New York, to Dr *S J Lucania The Squibb Institute for Medical Research* New Jersey U.S.A. and to *Bayer Farma* Copenhagen for generous gifts of Saralasin, the nonapeptide SQ20 881 and aprotinin, Trasylol[R] respectively The Searle Analyser Model 45-23 used for the radioimmunoassay is a gift from the *Danish State Medical Research Council*. Dr *Ole Frederiksen* kindly performed the statistical calculation

REFERENCES

Bing J & Poulsen K Vast and apparently paradoxical continuous rise in plasma renin after removal of gently manipulated submaxillary glands in nephrectomized mice Acta path. microbiol scand *84 A* 285–290 1976

Chiang Tzu S Erdős E. G., Miwa I., Tague L. L. & Coalson J J Isolation from a salivary gland of granules containing renin and kallikrein. Circ. Res. *23* 507–517 1967

Day M D McCubbin J W & Page I H Limited hypertensive effect of infusion of angiotensin. Am J Physiol *209* 264–268 1965

Malling C & Poulsen K A direct radioimmunological assay for plasma renin in mice and its evaluation Biochim. Biophys. Acta *491* 532–541 1977

Michelakis A M Cohen S Taylor J Murakami K & Inagami T Studies on the characterization of pure submaxillary gland renin Proc. Soc Exp Biol. Med *147* 118–121 1974

Page I H & McCubbin J W Renal hypertension page 113 Chicago 1968. Year book medical publishers.

Poulsen K & Jorgensen J An easy radioimmunological microassay of renin activity concentration and substrate in human and animal plasma and tissues based on angiotensin I trapping by antibody J Clin Endocrinol. Metab *39* 816–825 1974

Vogel R & Werle E. Kallikrein inhibitors. In E G Erdős Bradykinin, Kallidin and Kallikrein. Handbuch der exp. Pharm. Berlin 1970 page *213*

Webster M E. Kallikreins in glandular tissues Ibidem, page 131

penhagen (Table 3) The control persons were previously healthy and died unexpectedly The times from death to autopsy ranged from 12 to 36 hours. In 11 cases no cause of death was apparent at autopsy 3 controls died violently (traffic accident, strangulation, battered baby) 3 had cerebral hemorrhage 2 were poisoned and 3 died during narcosis I no cases were signs of local or systemic infection demonstrated at autopsy

Neither the weight of the pancreas nor records of the site in the pancreas from which the block had been taken were available in the diabetic cases. Details about the initial fixation procedures were also lacking

The total of 33 blocks of pancreas were reembedded in paraffin and sectioned at 5 microns. These sections were stained with hematoxylin-eosin, Gomori s aldehyde-fuchsin for B-granules and Grimelius silver-staining for A-cells 5 sections from each staining procedure representing different levels of the block were examined. Islets were counted on one of the silver-stained sections from each block by drawing a circle of diameter 5 millimeters on the coverglass of the preparation and counting all islets within this circle. A part of each block was embedded in epon and sectioned at 1 micron. These sections were stained w th toluidine blue

TABLE 3 22 *Controls*

Case number	Sex	Age (years)
1a	M	1
1b	M	1 4/12
2a	F	2 /12
2b	F	2 4/
3a	M	2
3b	M	2
4a	F	9 4/12
4b	F	10 /
5a	F	10 9/
5b	F	10 9/12
6a	F	13 /12
6b	F	13 /12
7	F	18 4/12
7b	F	18 10/
8a	M	21 10/12
8b	M	25
9a	M	28 /12
9b	M	29 4/12
10a	M	29 9/12
10b	M	30 4/
11	M	30 6/12
11b	M	31

RESULTS

Islets were present in all 22 control specimens. The islets were rather well preserved. The number of islets ranged from 5 to 62 islets per circle. The A-cells were clearly seen in all islets. The B-granules stained well with

Onset Juvenile Diabetes Mellitus

Case Number	Plasma-bicarbonate at the admission meq/l	Serum-potassium at the admission meq/l	Insulin-dose (I U Regular) given during the first 24 hours of the admission	Hours from admission to death	Infectious focus Cause of death
1	12	?	?	26	Otitis media. Thrombosis of cerebral vein
2	1?	?	48	7	Aspiration
3	8	5 1	96	16	Hemorrhagic disease
4	6	?	180	34	Hypoglycemia
5	8	3 7	72	72	Hypopotassemia
6	8	3.2	100	216	Cerebral edema
7	4	?	120	1	Pneumonia Tracheobronchitis
8	12	5 0	160	1	Ketoacidosis Tracheobronchitis
9	8	2.0	160	3	Hypopotassemia
10	9	2 8	80	3	Hypopotassemia Tracheobronchitis
11		2.4	220	24	Hypopotassemia Hypopotassemia

almost normal A-cell mass and hence a reduced B/A-cell *ratio*.

Qualitative changes include variations in islet size and morphology and presence of inflammatory cells, *predominantly lymphocytes*, in the islets. This lymphocytic cell infiltration of the islets—insulitis—was described more than *seventy years ago as a rare* but specific lesion in early j.d.m. However the existence of insulitis in j.d.m. has been a matter of discussion (6–10).

In order to evaluate the possible occurence of insulitis, the present autopsy material was collected.

MATERIAL AND METHODS

A material of paraffin-embedded pancreatic tissue from patients with j.d.m. aged 30 years or less and dying within one year after the onset of the disease, *was collected in the following way*.

From The Central Registry of Death Certificates in Denmark were collected all death certificates registered under the diagnoses diabetes mellitus, diabetic coma or hypoglycemia from the years *1943* to 1974. Of a total of 357, 47 patients fulfilled the above mentioned criteria and the hospital records from the respective hospital departments were reviewed. Inquiries on autopsy material were sent but pancreatic tissue was available from only 11 of these patients.

Details of the years of death, age, sex and clinical characteristics are shown in Tables 1 and 2. All the patients had an acute onset of diabetic *symptoms (thirst, polyuria, loss of weight)* within less than two months prior to the terminal admission. No patient was treated with insulin before the terminal admission. The clinical picture was that of precoma or coma. All patients were treated with insulin during their final admission. No patient was treated with potassium. The survival periods in hospital ranged from 1 to 216 hours. The times from death to autopsy ranged from 12 to 36 hours.

TABLE 1. *Years of Death for 11 Juvenile Diabetics*

Years	Number of cases
1943–1950	0
1951–1960	5
1961–1970	4
1971–1974	2

Pancreas blocks *from two* age-and-sex-matched controls were collected for each diabetic at the Institute of Forensic Medicine at the University of Copenhagen and the Laboratory of Pediatric Pathology at the State University *Hospital* in Co-

TABLE 2. *11 Cases of Acute-*

Case Number	Sex	Age Years	Duration of symptoms Weeks	Degree of consciousness at the admission	Temperature at the admission. °C	Glucosuria Ketonuria	Blood glucose at admission mg/100 ml
1	M	1 $^{1}/_{12}$	1	Precoma	38.6	+/+	832
2	F	1 $^{11}/_{12}$	4	Coma	"Fever"	+/+	1184
3	M	2 $^{7}/_{12}$	4	Coma	37.3	+/+	386
4	F	9 $^{8}/_{12}$	8	Coma	36.5	+/+	412
5	F	11	3	Coma	37.3	+/+	488
6	F	14 $^{10}/_{12}$	8	Coma	37.6	+/+	450
7	F	17	$^{1}/_{2}$	Coma	39.0	+/+	1000
8	M	25 /	1	Coma	40.9	+/+	1585
9	M	25 $^{10}/_{12}$	1	Coma	37.1	+/+	1048
10	M	29 $^{8}/_{12}$	3	Coma	40.3	+/+	549
11	M	30 $^{0}/_{12}$	1	Coma	36.5	+/+	364

type II (larger cells with large round nuclei with more loose chromatin and abundant cytoplasma without granules) were most common. Very few islets looked normal (type III). The islet pattern could differ from one part of a section to another. Hyalinization of a few islets was present in one case.

A morphologic qualitative evaluation of the silver-stained sections revealed no difference between the controls and the diabetics in respect of the A-cell number and granulation.

In aldehyde fuchsin stainings the B-cell granulation was not detectable in 10 cases. In only one case was granulation present, but in extremely reduced proportion.

Insulitis characterized by infiltration of mononuclear cells, predominantly lymphocytes, was found in all hematoxylin-eosin stained preparations from 6 of 11 cases of j.d.m. The extent of insulitis differed from one patient to another involving from / to / of the islets in each section. The number of lymphocytes in each islet and the degree of islet destruction varied widely from a most discrete cell infiltration (Fig 1) to a most heavy one with complete displacement of normal islet cells (Fig 2). Most of the involved islets showed slight infiltration. The lymphocytic cell infiltration did not involve the exocrine pancreatic tissue. In none of the cases was the insulitis mentioned in the original autopsy records.

The patients showing insulitis were 3 females and 3 males. Insulitis was found in 4 of 4 patients aged 0–10 years, 1 of 3 patients in the second decade and 1 of 4 in the third decade. 3 patients with insulitis were febrile at the admission 3 were not.

The findings of paraffin sections were confirmed in studying the 1 micron sections in epon, but further characterization of the pathology was not obtained.



Fig 2 Another islet from the same patient. In this case the lymphocytic infiltration is so massive that the islet cells almost have disappeared. Hematoxylin-eosin 300 ×

TABLE 4 *Summary of Findings in 11 Acute Onset Juvenile Diabetics*

Case number	Islets present	A-cells	B-cells	Insulitis
1	+	Normal	Degranulated	+
2	+	Normal	Degranulated	+
3	+	Normal	Degranulated	+
4	+	Normal	Degranulated	+
5	+	Normal	Degranulated	+
6	+	Normal	Degranulated	—
7	+	Normal	Degranulated	—
8	+	Normal	Degranulated	+
9	+	Normal	Degranulated	—
10	+	Normal	B-granules extremely reduced	—
11	+	Normal	Degranulated	—

aldehyde fuchsin in all islets of all the controls. Insulitis was absent.

Islets were also present in all cases of j.d.m., and the findings are summarized in Table 4. The islet number ranged from 3 to 70 islets per circle, and no significant difference between controls and diabetics could be demonstrated. Islet hypertrophy was recognized in a few cases, but not as a major feature. The morphological islet types described by *Gepts* (10) were recognizable, but in our material intermediate forms between type I (small-sized islet cells with small nuclei with dense chromatin and scanty cytoplasma) and

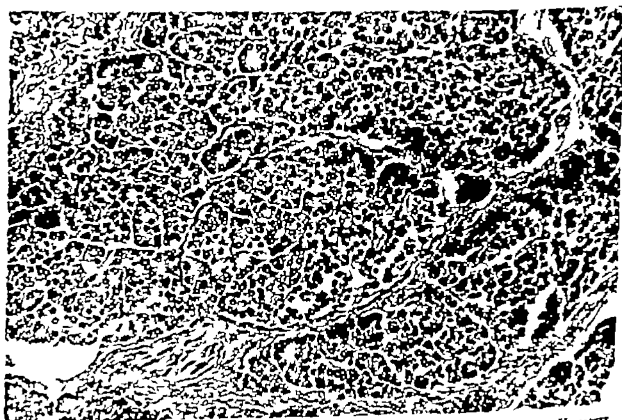


Fig. 1 Islet from 2½ year-old boy. Lymphocytes have invaded approximately ⅓ of the islet. Hematoxylin-eosin. 300 ×

pancreas, as insulitis also has been demonstrated in diabetics from ten to seventy-four years of age (10 18)

Essential information about insulitis is lacking The lesion seems to be transient as it has not been described in the later stages of j.d.m. Not all islets are affected at the same time (26) If insulitis is not an obligatory lesion in j.d.m., we cannot know which patients will be prone to insulitis.

The cause of insulitis is still obscure The presence of lymphocytic cell infiltration might be explained in many ways, but most likely it indicates an immunological process going on. This could be due to an infectious agent invading the islets, an autoimmune reaction, or a combination of these.

The idea of the infectious genesis of insulitis would be supported by the frequent association of some infection with the onset of diabetic symptoms, especially in children (7 14) Association between mumps and the incidence of diabetes has been claimed (12, 15) Increased titres of antibodies to Coxsackie virus B (type B in particular) have been found in juvenile diabetics (9) and this virus, like the other picorna virus encephalomyocarditis virus (5) has been found to be diabetogenic in mice (4) 6 of our patients were febrile, and although other infectious foci were detected a direct invasion of the islets cannot be ruled out

An autoimmune cause of insulitis would be in accordance with experimental animal models. *Renold et al.* (22) produced insulitis, but no diabetes, in cows with high doses of insulin in Freund's adjuvant. *Toreson et al.* (24) made rabbits diabetic with beef insulin and found insulitis. An allergic insulitis and pancreatitis was produced by *Lacy and Wright* (16) in rats with guinea pig anti-insulin serum, and in mice immunized with homologous islets a transient diabetic state and insulitis was described by *Nerup et al* (20) Diabetes in man is often associated with other endocrinopathies and autoimmune diseases. Cell-mediated hypersensitivity against pancreatic antigens (21) and islet-cell antibodies (2, 19) was recently reported in j.d.m.

A combination of infectious and autoimmune mechanisms seems most likely as an explanation of insulitis, but from the present study no conclusion can be drawn in this respect. However the findings presented support the idea of the existence of a diffuse lymphocytic insulitis as a feature of early j.d.m.

Our thanks are due to colleagues at the Institute of Forensic Medicine at the University of Copenhagen for providing us with most of the control material. We are also grateful to the Heads of all departments who kindly provided us with hospital records and autopsy material.

REFERENCES

1 *Bell E. T* The incidence and significance of degranulation of the beta cells in the islets of Langerhans in diabetes mellitus. Diabetes 2 125–129 1953

2 *Bottazzo G F., Florin-Christensen A & Doniach D* Islet-cell antibodies in diabetes mellitus with auto-immune polyendocrine deficiencies. Lancet ii 1279-1282, 1974

3 *Cecil, R. L.* A study of the pathological anatomy of the pancreas in ninety cases of diabetes mellitus J Exp Med. *11* 266–290, 1909

4 *Coleman T J., Taylor K. W & Gamble D R.* The development of diabetes following Coxsackie B virus infection in mice. Diabetologia *10* 755–759 1974.

5 *Craighead J E. & M Lean M F.* Diabetes mellitus. Induction in mice by encephalo-myocarditis virus. Science *162* 913–914 1968.

6. *Doniach, I & Morgan A G.* Islets of Langerhans in juvenile diabetes mellitus. Clin. Endocr 2 233–248 1973

7 *Ferrell, H W Hand A M & Newcomb A. L.* Infantile diabetes. Diabetes 2 85–89 1953

8. *Fischer B.* Pancreas and Diabetes. Frankfurt. Ztschr Path *17* 218–275 1915

9 *Gamble D R., Kinsley M L. Fitzgerald M G., Bolton R. & Taylor K. W.* Viral antibodies in diabetes mellitus. Brit. Med. J 3 627–630 1967

10. *Gepts, W* Pathologic anatomy of the pancreas in juvenile diabetes mellitus. *Diabetes 14* 619–633 1965

11 *Grimelius L.:* A modified silver protein method for studying the argyrophil cells of the islets of Langerhans. I *Brolin S E., Hellman B. & Knutson H* (Eds.) The structure and metabolism of the pancreatic islets. Wenner

DISCUSSION

In this autopsy study no pancreatic tissue had been stored for more than 21 years. For this reason the 11 diabetics were clinically and biochemically well characterized. The causes of death listed in Table 2 were decided upon by taking into account the clinical signs and the biochemical data as well as the autopsy findings. The patients who died from hypopotassemia were 3 patients with hypopotassemia on admission and 2 patients who developed ecg signs of hypopotassemia during the treatment. Since none of the diabetics treated for coma received potassium this material stresses the importance of initiating the supply of potassium from the very beginning of the treatment of diabetic ketoacidosis.

In dealing with these autopsy specimens we had to face the above mentioned fact that no information was available on the size of the pancreata, on the site within the pancreas for the tissue sample or the initial fixation procedure. It is wellknown that the number of islets varies from the cauda to the caput of the pancreas, and the staining procedures may vary with the method of tissue fixation. As minor quantitative differences between the controls and the diabetics might reflect different topography or different initial fixation rather than true differences, we did not apply rigorous quantitative morphologic methods on this material, which however furnished characteristic qualitative morphologic data in the diabetic cases.

The control material differs from those of previous investigators. *Gepts* (10) and *Doniach and Morgan* (6) used non-diabetics suffering from a wide scala of acute and chronic diseases. We collected material from previously healthy persons in order to get a homogeneous group and to avoid non specific inflammation of the pancreatic gland. However, insulitis was not detected in any of the 3 control materials.

The staining procedures were identical for the diabetics and the controls. The A-cell staining, a Grimelius silver staining, showed us distinct A-cell granulation, although *Grimelius* in the original presentation of the method did not find it suitable for autopsy studies (11).

B-cell granules were only detectable in one diabetic and in that case in a reduced proportion. This is in accordance with *Bell* (1) who in a series of 995 pancreata from diabetic subjects found B-cell degranulation in all cases less than 20 years old and in 82 per cent of patients aged 20 to 30 years. The duration of diabetes was not mentioned in his work. *Gepts* (10) however found preserved but reduced numbers of B-granules in 16 of his 22 short term patients, and *Doniach and Morgan* (6) found no B-cells in 2 of their 13 patients. In these three investigations, B-cell staining showed B-cells in respective control groups. Whether the B-cell degranulation is a primary lesion or secondary to hyperglycemia, starvation or increased growth hormone levels (1) is unknown. Insulin treatment degranulates B-cells in the rat, but it takes from 1 to 2 weeks to produce complete degranulation. Only one of our patients was treated for more than 3 days with insulin, so it seems unlikely that insulin treatment could be responsible for the B-cell degranulation demonstrated in the present study.

Infiltration of lymphocytes in the islets of juvenile diabetics was described by the early students of diabetes (3, 8, 13, 23, 25) and was looked upon as a rare but specific finding in young patients dying shortly after the onset of the disease. *Warren* (27) called new attention to the feature (17), and *Gepts* (10) found insulitis in 15 of 22 cases of j.d.m.. The existence of insulitis was questioned, however, by *Doniach and Morgan*, who in a series of 13 diabetic cases found no insulitis (6).

In our study, 6 of 11 cases of j.d.m. showed insulitis. A partial explanation of these conflicting results might be differences in the age-distribution of the materials. *Gepts* (10) had 10 patients aged less than ten years, 9 of them showing insulitis. *Doniach and Morgan* (6) had only one patient less than ten years. 4 patients in our material were aged less than ten years, and all showed insulitis. However age differences cannot account for all discre-

pancreas, as insulitis also has been demonstrated in diabetics from ten to seventy four years of age (10 18)

Essential information about insulitis is lacking. The lesion seems to be transient as it has not been described in the later stages of j.d.m. Not all islets are affected at the same time (26) If insulitis is not an obligatory lesion in j.d.m., we cannot know which patients will be prone to insulitis.

The cause of insulitis is still obscure. The presence of lymphocytic cell infiltration might be explained in many ways, but most likely it indicates an immunological process going on. This could be due to an infectious agent invading the islets, an autoimmune reaction, or a combination of these.

The idea of the infectious genesis of insulitis would be supported by the frequent association of some infection with the onset of diabetic symptoms, especially in children (7 14) Association between mumps and the incidence of diabetes has been claimed (12, 15) Increased titres of antibodies to Coxsackie virus B (type B in particular) have been found in juvenile diabetics (9) and this virus, like the other picorna virus encephalomyocarditis virus (5) has been found to be diabetogenic in mice (4) 6 of our patients were febrile, and although other infectious foci were detected a direct invasion of the islets cannot be ruled out.

An autoimmune cause of insulitis would be in accordance with experimental animal models *Renold et al* (22) produced insulitis, but no diabetes, in cows with high doses of insulin in Freund's adjuvant. *Toreson et al* (24) made rabbits diabetic with beef insulin and found insulitis. An allergic insulitis and pancreatitis was produced by *Lacy and Wright* (16) in rats with guinea pig anti-insulin serum, and in mice immunized with homologous islets a transient diabetic state and insulitis was described by *Nerup et al.* (20) Diabetes in man is often associated with other endocrinopathies and autoimmune diseases. Cell-mediated hypersensitivity against pancreatic antigens (21) and islet-cell antibodies (2, 19) was recently reported in j.d.m.

A combination of infectious and autoimmune mechanisms seems most likely as an explanation of insulitis, but from the present study no conclusion can be drawn in this respect. However the findings presented support the idea of the existence of a diffuse lymphocytic insulitis as a feature of early j.d.m.

Our thanks are due to colleagues at the Institute of Forensic Medicine at the University of Copenhagen for providing us with most of the control material We are also grateful to the Heads of all departments who kindly provided us with hospital records and autopsy material.

REFERENCES

1 *Bell, E. T* The incidence and significance of degranulation of the beta cells in the islets of Langerhans in diabetes mellitus. Diabetes 2 125–129 1953
2. *Bottazzo G F., Florin-Christensen A & Doniach D* Islet-cell antibodies in diabetes mellitus with autoimmune polyendocrine deficiencies. Lancet ii 1279–1282, 1974
3 *Cecil, R. L.:* A study of the pathological anatomy of the pancreas in ninety cases of diabetes mellitus. J Exp. Med. *11:* 266–290, 1909
4. *Coleman, T J Taylor K W & Gamble D R.* The development of diabetes following Coxsackie B virus infection in mice. Diabetologia *10* 755–759 1974
5 *Craighead J E. & McLane M F.:* Diabetes mellitus. Induction in mice by encephalo-myocarditis virus. Science *162* 913–914 1968.
6. *Doniach, I & Morgan, A. G.* Islets of Langerhans in juvenile diabetes mellitus. Clin. Endocr 2 233–248, 1973
7 *Farrell H W Head A. M & Newcomb A. L.* Infantile diabetes. Diabetes 2 83–89 1953
8. *Fischer B.* Pancreas und Diabetes. Frankfurt. Ztschr Path. *17* 218–275 1915
9 *Gamble D R., Kinsley M L., Fitzgerald M G., Bolton R. & Taylor K. W.:* Viral antibodies in diabetes mellitus. Brit. Med. J 3 627–630, 1967
10. *Gepts, W.* Pathologic anatomy of the pancreas in juvenile diabetes mellitus. Diabetes *14* 619–633, 1965
11 *Grimelius L.:* A modified silver protein method for studying the argyrophil cells of the islets of Langerhans. In *Brolin S E., Hellman B. & Knutson H (Eds.)* The structure and metabolism of the pancreatic islets. Wenner

DISCUSSION

In this autopsy study no pancreatic tissue had been stored for more than 21 years. For this reason the 11 diabetics were clinically and biochemically well characterized. The causes of death listed in Table 2 were decided upon by taking into account the clinical signs and the biochemical data as well as the autopsy findings. The patients who died from hypopotassemia were 3 patients with hypopotassemia on admission and 2 patients who developed ecg signs of hypopotassemia during the treatment. Since none of the diabetics treated for coma received potassium this material stresses the importance of initiating the supply of potassium from the very beginning of the treatment of diabetic ketoacidosis.

In dealing with these autopsy specimens we had to face the above-mentioned fact that no information was available on the size of the pancreata, on the site within the pancreas for the tissue sample or the initial fixation procedure. It is wellknown that the number of islets varies from the cauda to the caput of the pancreas, and the staining procedures may vary with the method of tissue fixation. As minor quantitative differences between the controls and the diabetics might reflect different topography or different initial fixation rather than true differences, we did not apply rigorous quantitative morphologic methods on this material, which however furnished characteristic qualitative morphologic data in the diabetic cases.

The control material differs from those of previous investigators. *Gepts* (10) and *Doniach and Morgan* (6) used non-diabetics suffering from a wide scala of acute and chronic diseases. We collected material from previously healthy persons in order to get a homogeneous group and to avoid non-specific inflammation of the pancreatic gland. However, insulitis was not detected in any of the 3 control materials.

The staining procedures were identical for the diabetics and the controls. The A-cell staining, a Grimelius silver staining, showed us distinct A-cell granulation, although *Grimelius* in the original presentation of the method did not find it suitable for autopsy studies (11).

B-cell granules were only detectable in one diabetic and in that case in a reduced proportion. This is in accordance with *Bell* (1) who in a series of 995 pancreata from diabetic subjects found B-cell degranulation in all cases less than 20 years old and in 82 per cent of patients aged 20 to 30 years. The duration of diabetes was not mentioned in his work. *Gepts* (10) however found preserved but reduced numbers of B-granules in 16 of his 22 short term patients, and *Doniach and Morgan* (6) found no B-cells in 2 of their 13 patients. In these three investigations, B-cell staining showed B-cells in respective control groups. Whether the B-cell degranulation is a primary lesion or secondary to hyperglycemia, starvation, or increased growth hormone levels (1) is unknown. Insulin treatment degranulates B-cells in the rat, but it takes from 1 to 2 weeks to produce complete degranulation. Only one of our patients was treated for more than 3 days with insulin, so it seems unlikely that insulin treatment could be responsible for the B-cell degranulation demonstrated in the present study.

Infiltration of lymphocytes in the islets of juvenile diabetics was described by the early students of diabetes (3, 8, 13, 23, 25) and was looked upon as a rare but specific finding in young patients dying shortly after the onset of the disease. *Warren* (27) called new attention to the feature (17), and *Gepts* (10) found insulitis in 15 of 22 cases of j.d.m. The existence of insulitis was questioned, however, by *Doniach and Morgan*, who in a series of 13 diabetic cases found no insulitis (6).

In our study, 6 of 11 cases of j.d.m. showed insulitis. A partial explanation of these conflicting results might be differences in the age-distribution of the materials. *Gepts* (10) had 10 patients aged less than ten years, 9 of them showing insulitis. *Doniach and Morgan* (6) had only one patient less than ten years. 4 patients in our material were aged less than ten years, and all showed insulitis. However age differences cannot account for all discre-

Acta path. microbiol. scand. Sect. A, 85 707–712 1977

RE APPRAISAL OF MALIGNANT MELANOMA DIAGNOSIS IN THE SWEDISH CANCER REGISTRY

ELISABETH MALEC, GUNNAR EKLUND and BENGT LAGERLÖF

Department of Plastic Surgery Karolinska sjukhuset, Stockholm
Statistical Institution, University of Stockholm
Department of Pathology Karolinska sjukhuset, Stockholm

Malec, E., Eklund, G. & Lagerlöf B. Re-appraisal of malignant melanoma diagnosis in the Swedish Cancer Registry Acta path microbiol. scand. Sect. A, 85 707–712, 1977

In many countries the registration of malignant melanoma of the skin show an increased incidence this may partially be due to an over-diagnosis. From the group of 3,268 adults and 21 children classified as suffering from malignant melanoma of the skin in the Swedish Cancer Registry between 1959–1968, one-in-ten systematic sample survey was the object of a retrospective examination. 349 adults and 2 children had a uniform histopathological evaluation performed by one of the authors (B.L.) Slides were not available in 8 cases (2 per cent) and in the remaining 343 the diagnosis was regarded as incorrect in 13 (3.7 per cent) All these 13 cases, (2 children and 11 adults) showed no special predilection as to age, sex, location, or year of registration. In view of such a slight degree of error the Swedish Cancer registry melanoma group from 1959–1968 would seem suitable for further epidemiological studies.

Key words Malignant melanoma diagnosis Swedish Cancer Registry

Elisabeth Malec, Dept. of Plastic Surg Karolinska sjukhuset
S-104 01 Stockholm 60 Sweden.

Received 31 iii.1977 Accepted 17.iv 1977

Several reports (2, 3 8, 9 11) indicate an increasing incidence of malignant melanoma of the skin, in Sweden and other countries. We suspected that the increase might be due, at least in part, to an over-diagnosis, as previous reports had shown this to be the case in children (25 28) The aims of the present study were to answer the following questions

1 To what extent were there errors in the registration of adult malignant melanoma of the skin in the Swedish Cancer Registry from 1959–1968 (over-registration)?
2. To what extent were there failures to diagnose these tumours during the same period (under registration)?

MATERIAL AND METHOD

Altogether 3,289 cases of malignant melanoma of the skin, 1,534 males and 1 755 females, both adults and children (0–14 years) had been reported to The Swedish Cancer Registry between 1959–1968. The distribution according to sex and age is shown in Fig. 1

A systematic selection was made from the total material (3,289 cases) of those born on the 10th,

gren Center Internat. Symp Series vol. 3 Pergamon Press London 1964 p 99–104

12 *Gundersen F* Is diabetes of infectious origin? J Infect. Dis. *41* 197–202 1927

13 *Heiberg K A* Über Diabetes bei Kindern. Arch Kinderh *56* 403–411 1911

14 *John H J* Diabetes mellitus in children. J Pediat. *35* 723–744 1949

15 *Kremer H U* Juvenile diabetes as a sequel to mumps. Am J Med *3* 257–258 1947

16 *Lacy P E & Wright P H* Allergic pancreatitis in rats injected with guinea pig anti insulin serum. Diabetes *14* 634–642 1965

17 *LeCompte P M* "Insulitis" in early juvenile diabetes Arch. Path *66* 450–457 1958

18. *LeCompte P M & Legg M A* Insulitis (lymphocytic infiltration of pancreatic islets) in late-onset diabetes. Diabetes *21* 762–769 1972

19 *Landrum R Walker G & Gamble D R* Islet-cell antibodies in juvenile diabetes mellitus of recent onset. Lancet *i* 880–883 1975

20 *Nerup J Andersen O O Bendixen G Egeberg J Gunnarson R. Kromann H & Poulsen J E.* Glucose intolerance and islet damage in mice immunized with homologous endocrine pancreas. Horm. Metab. Res. *6* 173–175 1973

21 *Nerup J Andersen O O Bendixen G Egeberg J Gunnarson R. Kromann H & Poulsen J E* Cell-mediated immunity in diabetes mellitus. Proc. Roy Soc. Med. *67* 506–513 1974

22 *Renold E. E Soeldner J S & Steinke J* Immunological studies with homologous and heterologous pancreatic insulin in the cow In Etiology of diabetes mellitus and its complications, Ciba Foundation Colloquium, vol. 15. Churchill London 1964 p. 122–134

23 *Schmidt M B* Über die Beziehung der Langerhans schen Inseln des Pancreas zum Diabetes mellitus. München med. Wochenschr *49* 51–54 1902.

24 *Toreson W E. Feldman R. Lee J C & Grodsky G M.*. Pathology of diabetes mellitus in rabbits by means of immunization with beef insulin. Am. J Path. *42* 531 1964

25 *von Meyenburg H* Über "Insulitis" bei Diabetes. Schweiz. med. Wochenschr *21* 554–557 1940

26 *Warren S LeCompte P M & Legg M A* The pathology of diabetes mellitus. 4th ed. Lea and Febiger Philadelphia 1966. pp. 53–101 and 351–354

27 *Warren S* The pathology of diabetes in children. J.A.M.A. *88* 99–101 1927

TABLE 2. *Distribution of Erroneously Classified Cases according to Age and Sex*

Age	–14	15–19	20–29	30–39	40–49	50–59	60–69	70–79	80–
Male	1	–	–	1	–	1	3	–	–
Female	1	–	–	1	1	2	–	2	–
Total	2	–	–	2	1	3	3	2	–

TABLE 3. *The Distribution of Erroneously Classified Case according to Year of Registration*

Year	59	60	61	62	63	64	65	66	67	68
Errors/total sample	1/31	1/31	2/30	1/25	2/29	0/33	4/43	0/41	1/46	1/42

TABLE 4. *The Distribution of Erroneously Classified Cases according to Body-site*

Site	Number Errors/total sample
Head & Neck	5/74
Trunk	1/114
Arm	3x/40
Leg	4x/93
Unknown	2/30
Total	15/351

x = child

Sweden and other countries has been given several explanations. One criticism of most incidence-trend studies concerned the accuracy of diagnosis. Very few re-examinations and re-classifications of the original specimens have been performed. The epidemiological studies of *Macdonald* (16, 18), *Lee* (14, 15) and *Ericsson et al.* (9) were based on information from The Cancer Registry of Texas and other American states, of Sweden and of England and Wales, without any attempt to perform histological re-examinations. *Truax et al.* (32) performed histopathological re-examinations of 247 survivors of malignant skin melanoma and found that an incorrect diagnosis had been made in no less than 62 cases (25 per cent). In the present selected material only 9 cases were incorrectly diagnosed amongst the survivors; this would represent 5 per cent of the whole material—a figure drastically lower than Truax's.

Iversen et al. (12) made a randomly-selected histopathological study of 1,521 cases from The Norwegian Cancer Registry. They could confirm a histological diagnosis of primary malignant melanoma or metastases of malignant melanoma in 72 per cent of the cases. In 19 per cent the material was insufficient for diagnosis, and in 9 per cent they found an incorrect diagnosis. As *Saxén* (29) remarked, quality-control of the Cancer Registries from various countries is essential before they can be used as a basis for epidemiological studies.

One aim of the present study was to see if the 351 systematically selected cases fulfilled the histopathological criteria for malignant melanoma of the skin (4, 5, 6, 7). No attempt has been made to use new principles of classification (4, 6, 20, 21), but only to confirm the diagnosis of malignant melanoma.

Previous re-examinations of 26 cases registered as malignant melanoma in children (0–14 years) in the Swedish Cancer Registry between 1959–1971 revealed that 25 of the 26 cases (95 per cent) had been wrongly diagnosed originally (2, 25), and only one fulfilled the criteria for melanoma. Even in the present study the two children in the selected group were found on re-examination

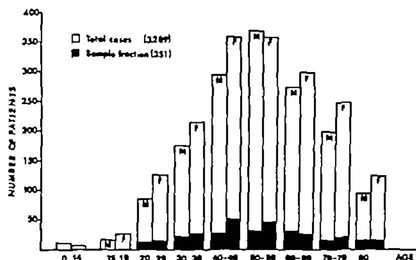


Fig 1 Total distribution of malignant melanoma of the skin year 1959–1968 according to age and sex.

20th or 30th of each month, giving an almost one-in ten (35/365 25) sample fraction (22, 33) There were 349 adults and two children. Details of the composition of the sample are shown in Fig 1

The various hospitals were asked to lend us their histological specimens of the selected 351 cases. Satisfactory responses were obtained in 343 cases (98 per cent) Specimens were not sent in 3 cases because of failure in identification. In five cases the original slides could not be found.

The original sections were stained with htx-eosin or van Gieson. If difficulties were encountered in making a definite diagnosis from the original sections, the blocks were asked for and new sections made. When paraffin blocks were available new sections were made and stained with htx-eosin.

The commonly applied criteria for the differentiation of malignant melanoma from benign naevi and other tumours included the presence of atypia mitotic figures and invasion into the upper cell layers of the epidermis (7) Identification of the melanomocytoma of Spitz ("juvenile melanoma") was made by applying the differential diagnostic criteria she proposed (1 31)

RESULTS

A total of 11 adults and 2 children had been incorrectly diagnosed (Table 1)

The method of selection used would correspond to an error in diagnosis of 2 per cent –6.3 per cent in the whole material (95 per cent interval of confidence) These errors did not predominate in any special adult age or sex (Table 2)

The distribution of these errors was fairly even throughout the years of registration (Table 3)

TABLE 1 *Final Diagnosis of Erroneous Cases*

Lentigo maligna	1
Dermatofibroma	1
Junction naevus	2
Melanocytoma of Spitz	3 (2 children)
Atypical melanocytic hyperplasia	1
Squamous cell cancer	1
Metastases from renal cancer	1
Undifferentiated tumour	3
Total	13

Errors in diagnosis were not confined to special body-sites, but had an even distribution as shown in Table 4

With the exception of an increase in erroneous diagnoses in children no other statistically significant (χ^2 test) correlation was found.

It is possible that during the same period of time, some cases of malignant melanoma of the skin escaped diagnosis. This difficulty will be further considered in the discussion.

DISCUSSION

The apparent increase in the incidence of cutaneous malignant melanoma observed in

they must constitute an extremely small proportion of the total cases in the Registry

It should therefore be accepted that the number of reported cases of malignant melanoma of the skin have shown a real increase between 1959 and 1968. Taking into consideration the small proportion of incorrect diagnosis (3 7 per cent) and the estimated infrequency of "missed" or non-registered melanoma cases, the material in the Swedish Cancer Registry may be regarded as suitable and reliable for an epidemiological study of cutaneous malignant melanoma in adults.

Supported by grants from *The Swedish Cancer Society* (Grant no 72 117) and *Konung Gustaf V's Jubileumsfond* (Grant no 76 27)

REFERENCES

1 *Allen, A. C & Spitz, S* Malignant Melanoma. A clinicopathological analysis of the criteria for diagnosis and prognosis. Cancer 6 1-45 1953

2. Cancer Incidence in Sweden 1959-1968. Publications of the Swedish National Board of Health and Welfare. 1962-1971

3 Cancer incidence in Sweden 1959-1965, National Board of Health and Welfare. The Cancer Registry Stockholm, 1971

4 *Clark W H J* The Classification of Human Primary Malignant Melanoma. American Joint Committee for Cancer Staging and End Results Reporting, Jan. 1975

5. Clark W H J *Ainsworth A M Bernardino E A., Yang, C-H Mihm M C. & Reed R. J* The developmental Biology of Primary Human Malignant Melanomas. Seminars in Oncology 2 83-103, 1975

6 *Clark W H From, L. Bernardino E. A & Mihm M C* The Histogenesis and Biologic Behavior of Primary Human Melanomas of the skin. Cancer Res. 29 705-726, 1969

7 Clark W H J & Mihm M C.: Moles and Malignant Melanoma In *T B. Fitzpatricks* Dermatology in general medicine, 491-511 New York, 1971

8 Doll, *R Muir* C & *Waterhouse J.* Cancer Incidence in Five Continents Vol. 2 UICC, Lyon, 1970.

9 *Ericsson J Kerastrom, L., Mattson, B & Wallgren J* Maligna Hudmelanom – epidemiologiska och statistiska aspekter Läkartidningen 73 516-518, 1976.

10 *Ericsson, J Ringertz, N., Sjöström, A. & Swensson D.:* Svenska Cancerregistret 10 år Läkartidningen 65 1648-1653 1968.

11 *Ericsson J & Ringertz N.* Trender i cancerincidensen i Sverige 1959-1968 och jämförelse med mortaliteten. Läkartidningen 69 5907-5916 1972.

12. *Iversen, O H., Larsen, T E. Grude T H & Mogens,K.* Histological classification of malignant melanoma in relation to prognosis and cytogenesis. Excerpta Medica International Congress Series *375* 260-273 1975.

13. *Körlof B., Anker O., Jacobson, P., Malec E., Moberger G., Nylén B. & Werdlll, J.:* Primär bedömning och behandling av maligna melanom. Nord. Med. 86 907-908 1971

14 *Lee J A. H & Carter A. P.* Secular Trends in Mortality from Malignant Melanoma. Journal of the National Cancer Institute. *45*: 91-97 1970.

15 *Lee J A. H & Issenberg, H J.:* A Comparison between England and Wales and Sweden in the Incidence and Mortality of Malignant Skin Tumours. Br Journ. Cancer 26 59-66, 1972.

16. *Macdonald E. J* The Epidemiology of melanoma. Annals New York Academy of Sciences. 4-17 1963.

17 *Macdonald E. J.* Epidemiology of Melanoma. In Irving M. Ariel (Ed.): Progress in Clinical Cancer 6 Ed. Grune and Stratton, Inc., 1975

18. *Macdonald E. J McGuffee V & White E.* Status of Epidemiology of Melanoma 1971. Pigment Cell. Vol. *1* 222-228, Karger Basel 1973

19 *MacDougal B A., Weeks P M & Wray R., Jr.* Spontaneous regression of the primary lesion of a metastatic malignant melanoma. Plastic & Reconst. Surg. *57*: 355-358 1976.

20 *McGovern, V J* The classification of melanoma and its relationship with prognosis. Pathology 2 85-98 1970.

21 *McGovern, V J., Mihm M C., Jr., Bailly C., Booth J C., Clark W H., J., Cochran A J., Hardy E. G Hicks J D., Levene A., Lewis M G., Little J H & Milton G.W.* The classification of malignant melanoma and its histologic reporting. Cancer 6 1446-1457 1973

22. *MacMahon B & Pugh T F.* Epidemiology —principles and methods. First Ed. Third printing. Published in Great Britain by Churchill, Livingstone, Edinburg and London, 1970.

23 Malec, E. Maligna melanoma – en analys av Cancerregistret i Sverige. Nord. Med. 84 1377-1378, 1970.

24 *Malec, E.* Statistiska synpunkter på maligna melanom i Sverige. Nord. Med. 84 1340 1970.

to have been wrongly diagnosed and could be re-classified as melanocytoma of Spitz.

In spite of the high degree of diagnostic inaccuracy in the case of children, since they compose only a very small proportion of the total material (and fraction sample) they would not affect the conclusions of an epidemiological analysis. The degree of incorrect diagnosis in the adult material was low (3.7 per cent), in spite of earlier suspicions of over-diagnosis (lower and upper limits of 95 per cent interval of confidence are 2 per cent and 6.3 per cent respectively). The general spread of these incorrectly diagnosed cases indicated that no special factor was involved.

An analysis of the erroneous diagnosis, according to age, sex, geographical distribution, year of discovery or body-site, did not show any special predilection.

The errors seem to have been exceptions occurring in randomly distributed departments of pathology.

An analysis of Swedish publications (10, 13, 23, 24) indicated an increase in the frequency of melanoma cases registered. The present study shows this to be a real incidence increase and not due to more accurate pathological diagnosis (Table 3). By this demonstration of the low frequency of mistaken diagnoses and the absence of systematic errors, the use of the Swedish Cancer Registry for epidemiological studies is considerably enhanced. The occurrence of melanoma in various subgroups of age, sex, special geographical regions, different body sites and in those practising various trades and professions, can thus be investigated with the help of the Registry.

The frequency of failures to recognize and report malignant skin melanomas to the Registry (under-diagnosis) can be only roughly estimated, but a previous study of the Swedish Cancer Registry (27) showed the total of non reported cases to be between 2.5 per cent – 3.5 per cent.

The following mistakes (under registration) are possible:

1. A reported melanoma inadvertently not included in the Registry.
2. A reported melanoma *wrongly* registered as another tumour.
3. An incorrect registration because of an inaccurate report from the surgeon or pathologist.
4. The failure to report a known malignant melanoma to the Registry either unintentionally or, as in the case of private and some general practitioners in Sweden, the absence of any obligation to report such cases.

5a. When the diagnosis of malignant melanoma was not made during the patient's lifetime and no post mortem examination was performed. The patient may have died of melanoma without consulting a physician, or died of another disease before the melanoma became apparent. Some patients can survive with a localized less malignant non-metastasizing form of the disease.

5b. When radically operated cases are either not sent for histological examination, or if an incorrect report is received from the pathologist. Follow up of these patients may then be incomplete.

6. Occasional cases of spontaneous regression. Several cases have been reported where a malignant melanoma of the skin has first been diagnosed on lymph gland involvment. The primary tumour was never discovered and may have spontaneously healed (19, 30). It can be assumed that in same rare cases a spontaneous regression of the primary tumour may have taken place without lymph gland spread and thus have escaped detection.

Because of the Swedish system of double registration, both by the clinician and the pathologist to the Cancer Registry, mistakes of types 1, 2, 3, 4, 6 could be subsequently rectified. Therefore only those types of cases discussed in 5a, 5b and 6 may fail to be registered as malignant melanoma and therefore be omitted from epidemiological studies.

Most of these errors, however, are more hypothetical than real and even if other types of incorrect registration are possible,

Acta path. microbiol. scand. Sect. A, 85: 713–720, 1977

NITROFURANTOIN INDUCED ALTERATIONS IN PULMONARY TISSUE

A Report on Five Patients with Acute or Subacute Reactions

E. TASKINEN, P. TUKIAINEN and A. R. A. SOVIJÄRVI

Department of Pulmonary Diseases, Helsinki University Central Hospital and
Department of Pathology, Aurora Hospital, Helsinki, Finland

Taskinen, E., Tukiainen, P. & Sovijärvi, A. R. A. Nitrofurantoin-induced alterations in pulmonary tissue. Acta path. microbiol. scand. Sect. A, *85*: 713–720, 1977.

Three patients with acute and two with subacute nitrofurantoin-induced pulmonary reactions were studied clinically and by examining microscopically needle biopsy specimens of their lungs. In all fiv patients slight vasculitis and a few interstitial eosinophils were found in the pulmonary tissue 1–2 weeks after the withdrawal of nitrofurantoin therapy. Alveolitis, fibrinous alveolar exudate and perivascular granulomas were also seen in some specimens. The patients with acute reactions had marked blood eosinophilia. In all patients, pulmonary diffusing capacity (DL_{CO}) was below normal, but entilatory function was not appreciably affected. Withdrawal of nitrofurantoin resulted in complete or partial improvement in 4–8 weeks. Our clinical and histological findings support the suggestion that a type III immune-complex-mediated reaction is involved in acute and subacute hypersensitivity reactions to nitrofurantoin.

Key words: Nitrofurantoin; pulmonary reactions; histology; cytology; diffusion capacity of lung.

E. Taskinen, Department of Pathology, Aurora Hospital, SF-00250 Helsinki 25, Finland.

Received 4.ii.77. Accepted 19.iv.77.

In 1962 *Israel & Diamond* (10) described a patient who reacted to nitrofurantoin therapy with chills, fever, dyspnea, cough and cyanosis, and whose chest radiograph showed lung infiltrates and a pleural reaction. When the drug was withdrawn the clinical and radiographic signs disappeared. Since then, many similar acute cases have been reported (8, 14, 22), and long term nitrofurantoin therapy has been implicated as a cause of a subacute or chronic interstitial lung disease (3, 6, 7, 11, 12, 18, 19, 21, 22).

Several studies have shown that when the reaction is chronic, lung biopsy specimens display a non-specific pattern of chronic interstitial pneumonitis with fibrosis, difficult to distinguish from fibrosing alveolitis (18, 20). We have found, however, only one report on tissue alterations in acute or subacute reactions to nitrofurantoin. *Ochsner et al.* (15) described a subacute reaction with granulomatous vasculitis.

We report here the clinical and lung biopsy findings in five patients with acute or subacute pulmonary reactions induced by nitrofurantoin.

MATERIAL AND METHODS

Our test subjects were five women, aged 33 to 78 yr (mean 57), who were part of a series of 300 patients with diffuse lung disease, from whom lung biopsy specimens were taken for histological examination.

25 *Malec E & Lagerlöf B* Malignant melanoma of the skin in children. In manuscript.

26 *Malec E & Eklund G* The changing incidence of malignant melanoma. In manuscript.

27 *Mattsson B* Personal communication 1976

28 *Saksela E & Rintala A* Misdiagnosis of prepubertal malignant melanoma. Reclassification of Cancer Registry Material Cancer *22* 1308–1314 1968

29 *Saxén E* Third international symposium on detection and prevention of Cancer New York 1976 DePCa. Abstract.

30 *Smith J L & Stehlin J S*. Spontaneous regression of primary malignant melanomas with regional metastases. Cancer *18* 1399–1415, 1965

31 *Spitz S* Melanomas of childhood, Am. J Path. *24* 591–609 1948

32 *Truax H Barnett R N Hukill P B, Campbell P C & Eisenberg H* The effect of inaccurate pathological diagnosis and survival statistics for melanoma. Cancer *19* 1543–1547 1966

33 *Wallis W A & Roberts H V* Statistics—A new approach The Free Press, Glencoe, Illinois USA 1956

TABLE 2. *Findings in Needle Biopsy Specimens of Pulmonary Tissue from Fu Patients with Nitrof rantoin Hypersensitivity*

Patient	Type of reaction	Duration from w thdrawal of nitrofurantoin to lung biopsy	Histopathological findings		
			Interstitium	Vascular walls	Al eolar spaces
EM	Acute	2 wk	Some eosinophils, one perivascular granuloma, a few plasma cells	Slight lymphocyte infiltration with a few eosinophils nd plasma cells	Some macrophages and erythrocytes
KE	Acute	1 wk	A few eosinophils	Capillary endothelial proliferation	Free
PB	Acute	1 wk	A few eosinophils, neutrophils and lymphocytes	Infiltration by lymphocytes and few plasma cells	Free
AA	Subacute	2 wk	Moderat lymphocyte and plasma cell infiltration, few eosinophils, a perivascular "loose granuloma, slight fibroblastic proliferation	Lymphocyt and plasma cell infiltration	Some macrophages
KA	Subacute	2 wk	A few eosinophils, fibrinous exudate slight fibrosis	Slight intimal proliferation and vascular sclerosis	Some macrophages and slight fibrinous exudate

TABLE 1 *Clinical Details of Five Patients with Nitrofurantoin Induced Hypersensitivity Reactions of the Lungs*

	Patient KE	Patient PB	Patient FM	Patient AA	Patient KA
Type of reaction	acute	acute	acute	subacute	subacute
Sex	female	female	female	female	female
Age (yr)	48	63	64	78	35
Duration of nitrofurantoin therapy before symptoms	3 wk	1 wk	1 wk	4 yr	4 mo
Duration of symptoms before admission to hospital	1 wk	1 wk	1 wk	1 mo	2 mo
Symptom	fever dyspnea cough chest pain	fever dyspnea vomiting	fever dyspnea, muscle pains	fever dyspnea cough chest pain, vomiting	fever dyspnea cough
Signs	crepitant rales	crepitant rales	crepitant rales	crepitant rales	crepitant rales
Blood eosinophils/mm³	1600	860	1480	222	111
Latex fixation test	negative	negative	negative	negative	negative
Antinuclear antibodies	negative	negative	negative	+ 1:10 (IgG)	negative
Anti-red cell antibodies	negative	negative	negative	negative	+ (IgG)
Serum gammaglobulins (g/l)	normal (< 1 6)	normal (< 1 6)	normal (< 1 6)	17.5	16.8
Parenchymal changes in chest radiograph	mild fine mottling	moderate fine mottling	moderate coarse mottling	moderate patchy clouding	moderate fine mottling
VC (per cent of predicted)*	82	85	94	100	80
FEV_1/FVC, per cent	81	47	80	76	96
DL_{CO} (per cent of predicted)**	65	68	76	47	52

* Predicted values according to Berglund et al (2)
** Predicted values according to Cotes (5)

TABLE 2. *Findings in Needle Biopsy Specimens of Pulmonary Tissue from Five Patients with Nitrofurantoin Hypersensitivity*

Patient	Type of reaction	Duration from withdrawal of nitrofurantoin to lung biopsy	Histopathological findings		
			Interstitium	Vascular walls	Alveolar spaces
EM	Acute	2 wk	Some eosinophils, one perivascular granuloma, few plasma cells	Slight lymphocyte infiltration with few eosinophils and plasma cells	Some macrophages and erythrocytes
KE	Acute	1 wk	A few eosinophils	Capillary endothelial proliferation	Free
PB	Acut	1 wk	A few eosinophils, neutrophils and lymphocytes	Infiltration by lymphocytes and a few plasma cells	Free
AA	Subacute	2 wk	Moderate lymphocyte and plasma cell infiltration, a few eosinophils, perivascular "loose" granuloma, slight fibroblastic proliferation	Lymphocyte and plasma cell infiltration	Some macrophages
KA	Subacute	2 wk	A few eosinophils, fibrinous exudate slight fibrosis	Slight intimal proliferation and vascular sclerosis	Some macrophages and slight fibrinous exudate



Fig 1 Patient AA Interstitial inflammatory reaction involving lymphocytes and a few plasma cells. Alveolar septae are slightly thickened and fibroblastic proliferation is scanty (H & E) × 660.

In three patients acute symptoms developed after nitrofurantoin had been administered for 1–3 wk (Table 1) The duration of the symptoms before admission to hospial was about 1 wk. In the two patients with subacute reactions the duration of nitrofurantoin therapy before onset of symptoms was 4 mo and 4 yr respectively and the duration of symptoms before admission to hospital 1 mo and 2 mo respectively

Immediately on admission, nitrofurantoin was withdrawn. According to all patients this had been their first course of treatment with nitrofurantoin. Because the initial clinical condition of the patients was poor lung biopsies were not performed until 1–2 wk after admission

Biopsies were performed with a TruCut cutting needle (24) Tissue specimens were fixed in *10* per cent formaldehyde solution embedded in paraffin and stained with Prussian blue van Gieson, periodic acid Schiff (PAS) diastase PAS hematoxylin-eosin and methyl-green pyronin. Histological examination was carried out by conventional light microscopy

The pulmonary diffusing capacity for carbon monoxide (DL_{CO}) was determined by using a single breath method (Morgan Mark 4) (16)

RESULTS

Clinical and Laboratory Findings

The symptoms (Table 1) of the patients with acute reactions were more intense and disabling than those with the subacute ones. On admission to hospital, crepitant rales were heard in all patients. One patient with an acute reaction also had cyanosis and exanthema.

The three patients with acute reactions had marked blood eosinophilia (Table 1) Both patients with subacute reactions had raised serum gammaglobulin concentrations (> 1 6 g/l) One of these (AA) had an anti



Fig. 2 Patient AA. Slight vasculitis lymphocytes and plasma cells have infiltrated the vascular wall. Arrow points to the vascular lumen. (H & E) × 660.

nuclear antibody titer (IgG) of 1 10 and in the other (KA) a direct Coombs test was positive (IgG) Results of the latex fixation test were normal in all five patients.

Radiographic examination revealed mild or moderate diffuse lung infiltrations in all patients. The parenchymal changes consisted of fine or coarse mottling one patient with a subacute reaction also had patchy clouding The acute reaction of patient EM was accompanied by a temporary pleural effusion.

On admission to hospital, patients had normal ventilatory function, except one (PB) whose obstructive ventilatory impairment was caused by chronic bronchitis. When measured about 1 wk after admission the diffusion capacity for carbon monoxide (DL_{co}) was below normal (< 80 per cent of predicted value) in all patients (mean 61 per cent, range 47–76)

Biopsy Findings

The lung biopsy specimens varied in size from 2.5 × 0.5 mm (about 100–200 alveoli) to 5 × 1.5 mm (about 700–800 alveoli) The specimen of one patient was fragmented.

The general structure was preserved in all specimens except in that of patient AA, which also showed the most prominent histological changes (Fig 1) In all others the alterations in pulmonary tissue were slight (Table 2) The most frequent changes were a slight inflammation of the vascular wall (Fig. 2) and the invasion of the interstitium by a few eosinophils. In three patients alveolar spaces contained some macrophages. The specimens of two patients (EM and AA) showed a perivascular granuloma (Fig. 3) Both patients with subacute reactions had slight interstitial fibrosis and thickening of the alveolar



Fig 1 Patient AA Interstitial inflammatory reaction involving lymphocytes and a few plasma cells. Alveolar septae are slightly thickened and fibroblastic proliferation is scanty (H & E) × 660.

In three patients acute symptoms developed after nitrofurantoin had been administered for 1–3 wk (Table 1) The duration of the symptoms before admission to hospital was about 1 wk. In the two patients with subacute reactions, the duration of nitrofurantoin therapy before onset of symptoms was 4 mo and 4 yr respectively and the duration of symptoms before admission to hospital 1 mo and 2 mo respectively

Immediately on admission, nitrofurantoin was withdrawn. According to all patients this had been *their first course of treatment with nitrofurantoin* Because the initial clinical condition of the patients was poor lung biopties were not performed until 1–2 wk after admission.

Biopsies were performed with a TruCut cutting needle (24) Tissue specimens were fixed in 10 per cent formaldehyde solution, embedded in paraffin, and stained with Prussian blue, van Gieson periodic acid-Schiff (PAS) diastase PAS hematoxylin-eosin and methyl-green pyronin Histological examination was carried out by conventional light microscopy

The pulmonary diffusing capacity for carbon monoxide (DL_{CO}) was determined by using a single breath method (Morgan Mark 4) (16)

RESULTS

Clinical and Laboratory Findings

The *symptoms* (Table 1) of the patients *with acute reactions* were more *intense* and *disabling than those with the subacute ones.* On admission to hospital, crepitant rales were heard in all patients. One patient with an acute reaction also had cyanosis and exanthema

The three patients *with acute reactions* had marked blood eosinophilia (Table 1) Both patients with subacute reactions had *raised serum gammaglobulin concentrations* (> 16 g/l) One of these (AA) had an anti-



Fig 2 Patient AA Slight vasculitis lymphocytes and plasma cells have infiltrated the vascular wall. Arrow points to the vascular lumen (H & E) × 660.

nuclear antibody titer (IgG) of 1 10 and in the other (KA) a direct Coombs test was positive (IgG) Results of the latex fixation test were normal in all five patients.

Radiographic examination revealed mild or moderate diffuse lung infiltrations in all patients. The parenchymal changes consisted of fine or coarse mottling one patient with a subacute reaction also had patchy clouding The acute reaction of patient EM was accompanied by a temporary pleural effusion.

On admission to hospital, patients had normal ventilatory function, except one (PB) whose obstructive ventilatory impairment was caused by chronic bronchitis. When measured about 1 wk after admission the diffusion capacity for carbon monoxide (DL_{CO}) was below normal (< 80 per cent of predicted value) in all patients (mean 61 per cent, range 47–76)

Biopsy Findings

The lung biopsy specimens varied in size from 2.5 × 0.5 mm (about 100–200 alveoli) to 5 × 1.5 mm (about 700–800 alveoli) The specimen of one patient was fragmented.

The general structure was preserved in all specimens except in that of patient AA, which also showed the most prominent histological changes (Fig. 1) In all others the alterations in pulmonary tissue were slight (Table 2) The most frequent changes were a slight inflammation of the vascular wall (Fig. 2) and the invasion of the interstitium by a few eosinophils. In three patients alveolar spaces contained some macrophages. The specimens of two patients (EM and AA) showed a perivascular granuloma (Fig 3) Both patients with subacute reactions had slight interstitial fibrosis and thickening of the alveolar



Fig 3 Patient EM A perivascular granuloma. (H & E) × 165

septae Most changes, however were inflammatory The histological picture remained nonspecific

Follow-up

All patients except one (EM) were treated with prednisolone for 4–8 wk After that period chest radiographs and measurements of DL_{co} of all patients showed that the acute reactions had been completely reversed and the subacute reactions partly reversed

DISCUSSION

The principal responses evoked in pulmonary tissue by nitrofurantoin seemed to be alterations in the interstitial space and in the walls of capillaries and arterioles (Table 2) The inflammatory reaction in the interstitium involved lymphocytes and some plasma cells and eosinophils. We interpret these histological changes to be signs of an immune-complex reaction. Such an inflammatory reaction might gradually subside without causing permanent damage, as radiographic and pulmonary function tests have shown (22) but in some cases interstitial inflammation, fibrosis and vascular degeneration may become chronic Most such chronic reactions may develop insidiously without acute episodes (11 18)

In our patients the histological changes, including eosinophilia, were slight owing in part to some improvement having taken place during the 1–2 wk interval between drug withdrawal and lung biopsy In addition, that the slightness of the tissue alterations was at variance with the initial moderate radiographic opacities was probably also the result

of some spontaneous healing having occurred in the interval between radiographic examination and lung biopsy (about 1 wk). Furthermore, the needle biopsy specimen may not have been representative, especially in patients whose pulmonary reaction was patchy. Contrasting with our modest findings is the report by *Carrington et al.* (4) of a patient with chronic eosinophilic pneumonia induced by nitrofurantoin. Eosinophilia is known to be a non-specific phenomenon associated with immune-complex reactions (25).

In a nitrofurantoin hypersensitivity reaction the functional disturbance—a gas transfer defect—is probably caused by the vascular changes and septal thickening.

According to some investigators (3 13 22) the clinical findings in acute pulmonary reactions to nitrofurantoin reflect a type III (immune-complex-mediated) hypersensitivity reaction. The clinical and histological observations reported here support this view.

It has been suggested that nitrofurantoin acts as a hapten (15). Interestingly IgG autoantibodies against normal human albumin (tailing albumin) and nuclear material were recently identified in the serum of patients treated with nitrofurantoin, many of whom had radiographically-detectable pulmonary changes (9 23). Long-term treatment with nitrofurantoin might therefore induce a B-cell response to normal autologous structures. The exact nature of the immunologic reaction induced by nitrofurantoin is, however, still obscure.

Supported by grants from the *Finnish Anti-Tuberculosis Association*.

REFERENCES

1. *Allison A C.* Mechanism of tolerance and autoimmunity. Ann. rheum. Dis. 32 283–293 1973.
2. *Berglund, E. Birath G., Bjure J. Grimby G. Kjellman I. Sandq ist L. & Söderholm K.* Spirometric studies in normal subjects. I. Forced expirograms in subjects between 7 and 70 years of age. Acta med. Scand. 173 185–192, 1963.
3. *Brander L. & Selroos O.* Pulmonary reaction to nitrofurantoin. Acta med. Scand. 185 215–220 1969.
4. *Carrington C B., Addington, W W., Goff A M., Madoff I M. Marks A., S hwaber J R. & Gaensler A E.* Chronic eosinophilic pneumonia. New Eng. J Med. 280 787–798, 1969.
5. *Cotes J E.* Lung function. Assessment and application in medicine. Blackwell Scientific Publications, London, 1965.
6. *David R. B., Andersen H A. & Stickler G. B.* Nitrofurantoin sensitivity. Report of a child with chronic inflammatory lung disease. Amer. J. dis. Child. 116 418–421 1968.
7. *Haas W., Muntermeier R & Loew K. R.* Beitrag zur Frage der nitrofurantoin-induzierte chronische Lungenfibrose. Dtsch Med. Wschr 98 1867–1971 1973.
8. *Hailey F J. Glascock H W & Hewitt W F.* Pleuropneumonic reactions to nitrofurantoin. New Eng. J Med. 281: 1087–1090 1969.
9. *Hällén, K., Rådman J., Wager O & von Essen R.* Tailing albumin associated with antinuclear antibodies. Scand. J clin. Lab. Invest. 29 Suppl. 122 58, 1972.
10. *Israel H L. & Diamond P.* Recurrent pulmonary infiltration and pleural effusion due to nitrofurantoin sensitivity. New Eng. J Med. 266 1024–1026, 1962.
11. *Israel, K S., Brashear R. E., Sharma, H M., Yum M N & Glover J L.* Pulmonary fibrosis and nitrofurantoin. Amer Rev resp. Dis. 108 353–356, 1973.
12. *Lundgren R., Bäck O & Wiman L.-G.* Pulmonary lesions and autoimmune reactions after long-term nitrofurantoin treatment. Scand J resp. Dis. 56 208–216, 1975.
13. *McCombs R. P.* Diseases due to immunological reactions in lungs. (Second of two parts). New Eng. J Med. 286 1245–1252, 1972.
14. *Murray M J & Kronenberg, R.* Pulmonary reactions simulating cardiac pulmonary edema by nitrofurantoin. New Eng. J Med. 273 1185–1187 1965.
15. *O kner S F Hatch, H B. & Leonard G L.* Hypersensitivity and the lung. Amer J Roentgen. 107 290–293, 1969.
16. *Ogilvie C. M. Forster R. E., Blakemore W S & Morton J W.* A standardized breath holding technique for the clinical measurement of the diffusing capacity of the lung for carbon monoxide. J Clin. Invest. 36 1–17 1957.
17. *Roitt I.* Essential immunology. Blackwell Scientific Publications, Second Edition, Oxford, 1974.
18. *Rosenow E. C. DeRemee R. A. & Dines*

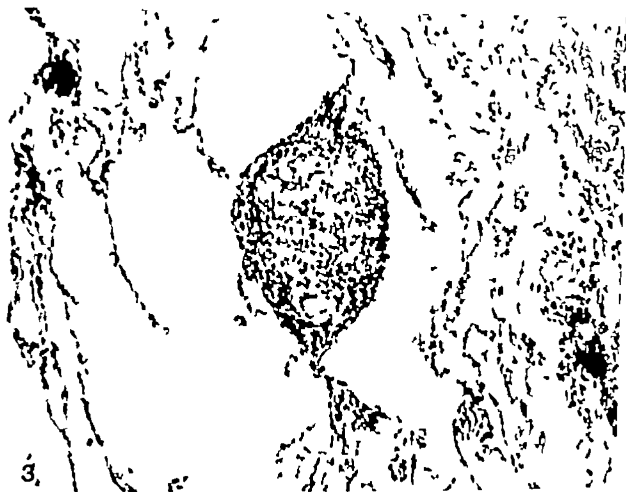


Fig 3 Patient EM A perivascular granuloma. (H & E) × 165

septae Most changes, however were inflammatory The histological picture remained nonspecific.

Follow-up

All patients except one (EM) were treated with prednisolone for 4–8 wk. After that period chest radiographs and measurements of DL_{CO} of all patients showed that the acute reactions had been completely reversed and the subacute reactions partly reversed.

DISCUSSION

The principal responses evoked in pulmonary tissue by nitrofurantoin seemed to be alterations in the interstitial space and in the walls of capillaries and arterioles (Table 2) The inflammatory reaction in the interstitium involved lymphocytes and some plasma cells and eosinophils. We interpret these histological changes to be signs of an immune-complex reaction. Such an inflammatory reaction might gradually subside without causing permanent damage, as radiographic and pulmonary function tests have shown (22) but in some cases interstitial inflammation, fibrosis and vascular degeneration may become chronic. Most such chronic reactions may develop insidiously without acute episodes (11 18)

In our patients the histological changes, including eosinophilia, were slight owing in part to some improvement having taken place during the 1–2 wk interval between drug withdrawal and lung biopsy In addition, that the slightness of the tissue alterations was at variance with the initial moderate radiographic opacities was probably also the result

of some spontaneous healing having occurred in the interval between radiographic examination and lung biopsy (about 1 wk) Furthermore, the needle biopsy specimen may not have been representative, especially in patients whose pulmonary reaction was patchy Contrasting with our modest findings is the report by *Carrington et al.* (4) of a patient with chronic eosinophilic pneumonia induced by nitrofurantoin. Eosinophilia is known to be a non-specific phenomenon associated with immune-complex reactions (25)

In a nitrofurantoin hypersensitivity reaction, the functional disturbance—a gas transfer defect—is probably caused by the vascular changes and septal thickening.

According to some investigators (3 13 22) the clinical findings in acute pulmonary reactions to nitrofurantoin reflect a type III (immune-complex-mediated) hypersensitivity reaction. The clinical and histological observations reported here support this view

It has been suggested that nitrofurantoin acts as a hapten (15) Interestingly IgG autoantibodies against normal human albumin (tailing albumin) and nuclear material were recently identified in the serum of patients treated with nitrofurantoin, many of whom had radiographically-detectable pulmonary changes (9 23) Long term treatment with nitrofurantoin might therefore induce a B-cell response to normal autologous structures. The exact nature of the immunologic reaction induced by nitrofurantoin is, however still obscure.

Supported by grants from the *Finnish A ti-T berculosis Association.*

REFERENCES

1 *Allison A. C* Mechanism of tolerance and autoimmunity Ann. rheum. Dis. 32 283–293 1973

2. *Bergl ad E Birath G Bjur J Grimby G Kjellmon, I Sandqvist L. & Söderholm K* Spirometric studies in normal subjects. I Forced expirograms in subjects between 7 and 70 years of age. Acta med. Scand. *173* 185–192, 1963

3 *Bruuder L. & Selroos O.*. Pulmonary reaction to nitrofurantoin. Acta med. Scand. *185* 215 220, 1969

4 *Carrington C B Addington W W., Goff A. M Madoff I M., Marks A., S hwaber J R. & Gaensler A. E.*. Chronic eosinophilic pneumonia. New Eng. J Med. *280* 787–798, 1969

5 *Cotes, J E.:* Lung function. Assessment and pplication in medicine. Blackwell Scientific Publications, London, 1965

6. *David R B., Andersen H A. & Stickler G B* Nitrofurantoin sensitivity Report of a child with chronic inflammatory lung disease. Amer. J dis. Child. *116:* 418–421 1968.

7 *Haas W., Mentenmeier R. & Loew K. R.*. Beitrag zur Frage der nitrofurantoin-induzierte chronische Lungenfibrose. Dtsch Med, Wschr *98* 1867–1971 1973

8. *Hailey F J., Glascock H W & Hewitt W F* Pleuropneumonic reactions to nitrofurantoin. New Eng. J Med. *281* 1087–1090, 1969

9 *Hallie K Räsänen J., Wager O & von Essen, R.* Tailing albumin associated with antinuclear antibodies. Scand. J clin. Lab. Invest. 29 Suppl. *122* 58, 1972.

10. *Israel H L. & Diamond P.*. Recurrent pulmonary infiltration and pleural effusion due to nitrofurantoin sensitivity New Eng. J Med. *266* 1024–1026, 1962.

11 *Israel, K S Brashear R. E., Sharma H M., Y m, M N & Glover J L.:* Pulmonary fibrosis and nitrofurantoin. Amer Rev resp. Dis. 108 353–356, 1973.

12. *Lundgren R., Bäck O & Wiman L.-G.*. Pulmonary lesions and autoimmune reactions after long-term nitrofurantoin treatment. Scand. J resp. Dis. 56 208–216, 1975

13 *McComb R. P.*. Diseases due to immunological reactions in lungs. (Second of two parts) New Eng. J Med. *286* 1245–1252, 1972.

14 *Murray M J & Kronenberg, R.*. Pulmonary reactions simulating cardiac pulmonary edema by nitrofurantoin. New Eng. J Med. *273* 1185–1187 1965.

15 *Ochsner S F., Hatch H B. & Leonard G L.:* Hypersensitivity and the lung. Amer J Roentgen. *107* 290–299 1969

16. *Ogilvie C. M Forster R. E., Blakemore W S & Morton J W* A standardized breath holding technique for the clinical measurement of the diffusing capacity of the lung for carbon monoxide. *J Clin. Invest. 36* 1–17 1957

17 *Roitt I.*. Essential immunology Blackwell Scientific Publications, Second Edition, Oxford, 1974

18. *Rosenow E. C., D Remee R. A & Dines*



Fig 3 Patient EM A perivascular granuloma (H & E) × 165

septae. Most changes, however were inflammatory The histological picture remained nonspecific

Follow-up

All patients except one (EM) were treated with prednisolone for 4–8 wk. After that period chest radiographs and measurements of DL_{CO} of all patients showed that the acute reactions had been completely reversed and the subacute reactions partly reversed

DISCUSSION

The principal responses evoked in pulmonary tissue by nitrofurantoin seemed to be alterations in the interstitial space and in the walls of capillaries and arterioles (Table 2) The inflammatory reaction in the interstitium involved *lymphocytes and some plasma* cells and eosinophils. We interpret these histological changes to be signs of an immune-complex reaction. Such an inflammatory reaction might gradually subside without causing permanent damage, as radiographic and pulmonary function tests have shown (2?) but in some cases interstitial inflammation, fibrosis and vascular degeneration may become chronic Most such chronic reactions may develop insidiously without acute episodes (11 18)

In our patients the histological changes, including eosinophilia, were slight owing in part to some improvement having taken place during the 1–2 wk interval between drug withdrawal and lung biopsy In addition, that the slightness of the tissue alterations was at variance with the initial moderate radiographic opacities was probably also the result

of some spontaneous healing having occurred in the interval between radiographic examination and lung biopsy (about 1 wk) Furthermore, the needle biopsy specimen may not have been representative, especially in patients whose pulmonary reaction was patchy Contrasting with our modest findings is the report by *Carrington et al.* (4) of a patient with chronic eosinophilic pneumonia induced by nitrofurantoin. Eosinophilia is known to be a non-specific phenomenon associated with immune-complex reactions (23)

In a nitrofurantoin hypersensitivity reaction, the functional disturbance—a gas transfer defect—is probably caused by the vascular changes and septal thickening.

According to some investigators (3 13 22) the clinical findings in acute pulmonary reactions to nitrofurantoin reflect a type III (immune-complex-mediated) hypersensitivity reaction. The clinical and histological observations reported here support this view

It has been suggested that nitrofurantoin acts as a hapten (13) Interestingly IgG autoantibodies against normal human albumin (tailing albumin) and nuclear material were recently identified in the serum of patients treated with nitrofurantoin, many of whom had radiographically-detectable pulmonary changes (9 23) Long term treatment with nitrofurantoin might therefore induce a B-cell response to normal autologous structures. The exact nature of the immunologic reaction induced by nitrofurantoin is, however still obscure.

Supported by grants from the *F ssih Anti-T ber culoss Association.*

REFERENCES

1 *Allison A C* Mechanism of tolerance and autoimmunity Ann. rheum Dis. *32* 283–293 1973

2 *Bergland E Birath, G Bjure J Grimby G Kjellman I Sandqvist L. & Söderholm, K* Spirometric studies in normal subjects. I Forced expirograms in subjects between 7 and 70 years of age. Acta med. Scand. *173:* 185–192, 1963

3. *Brander L. & Selroos O* Pulmonary reaction to nitrofurantoin. Acta med. Scand. *185* 215 220 1969

4 *Carrington G. B., Addington, H W., Goff A M Madoff I M Marks A., Schwaber J R. & Gaensler A E.* Chronic eosinophilic pneumonia. New Eng J Med. *280* 787–798, 1969

5 *Cotes J E.* Lung function. Assessment and pplication in medicine. Blackwell Scientific Publications, London, 1965

6. *David R. B., Andersen H A & Stickler G B.* Nitrofurantoin sensitivity Report of a child with chronic inflammatory lung disease. Amer J dis. Child. *116* 418–421 1968.

7 *Haas, W., Munzenmaier R. & Loeme K. R.* Beitrag zur Frage der nitrofurantoin-induzierte chronische Lungenfibrose. Dtsch Med. Wschr *98* 1867–1971 1973

8. *Hailey F J Glascock H W & Hewitt W F* Pleuropneumonic reactions to nitrofurantoin. New Eng. J Med. *281* 1087–1090 1969

9 *Haltia, K. Räsänen J., Wager O & von Essen R.:* Tailing albumin associated with antinuclear antibodies. Scand. J clin. Lab. Invest. 29 Suppl. *122:* 58, 1972.

10. *Israel H L. & Diamond P.:* Recurrent pulmonary infiltration and pleural effusion due to nitrofurantoin sensitivity New Eng. J Med. 266 1024–1026, 1962.

11 *Israel, K S Brashear R. E., Sharma, H M., Y m M N & Glover J L.* Pulmonary fibrosis and nitrofurantoin. Amer Rev resp. Dis. *108* 353–356 1973

12. *Lundgren R., Bäck O & Wiman L.-G.* Pulmonary lesions and autoimmune reactions after long-term nitrofurantoin treatment. Scand. J resp. Dis. *56* 208–216 1975.

13 *McCombs, R. P.:* Diseases due to immunological reactions in lungs. (Second of two parts) New Eng. J Med. *286* 1245–1252, 1972.

14 *Murray M J & Kronenberg R.* Pulmonary reactions simulating cardiac pulmonary edema by nitrofurantoin. New Eng. J Med. *273:* 1185–1187 1965.

15. *Ochsner S F., Hatch, H B & Leonard G L.:* Hypersensitivity and the lung Amer J Roentgen. *107* 290–299 1969

16 *Ogilvie C. M., Forster R. E., Blakemore W S & Morton J W.* A standardized breath holding technique for the clinical measurement of the diffusing capacity of the lung for carbon monoxide. J Clin. Invest. *36* 1–17 1957

17 *Roitt I* Essential immunology Blackwell Scientific Publications, Second Edition, Oxford, 1974

18. *Rosenow E. C D Remee R. A. & Dines*

D E. Chronic nitrofurantoin pulmonary reaction. Report of five cases. New Eng J Med *279* 1258–1262 1968.

19 *Ruikka I Laustalo T & Saarimaa H* Progressive pulmonary fibrosis during nitrofurantoin therapy Scand J resp Dis *52* 162–166 1971

20 *Scadding J G & Hinson F N* Diffuse fibrosing alveolitis (diffuse interstitial fibrosis of the lung): Correlation of histology at biopsy with prognosis. Thorax *22* 291–304 1967

21 *Sollaccio P A Ribaudo C A & Grace W J* Subacute pulmonary infiltration due to nitrofurantoin. Ann. Int Med. *65* 1284–1286 1966

22 *Sovijärvi A R A Lemola M Stenius B & Idänpää Heikkilä J.* Nitrofurantoin-induced acute, subacute and chronic pulmonary reactions. A report of 66 cases. Scand. J resp Dis. *58* 41–50 1977

23 *Teppo A M Haltia K & Wager O* Immunoelectrophoresis "tailing" of albumin line due to IgG antibody complexes. A side effect of nitrofurantoin Scand. J Immunol. *5* 249–261 1976

24 *Tukiainen P* Needle biopsy in diffuse lung manifestations. An analysis of 145 consecutive cases. Scand. J resp Dis. Suppl. *94* 1–110, 1975

25 *Udwadia F E.* Pulmonary eosinophilia. Progress in Respiration Research, Vol. *7* S. Karger Basel 1975

Acta path. microbiol. scand. Sect. A, 85 721–730 1977

GLIAL CHANGES IN PIGS WITH PORTO-CAVAL ANASTOMOSIS AND TEMPORARY OR TOTAL HEPATIC ARTERY CLAMPING

N H Diemer and K. Tønnesen

Institute of Neuropathology University of Copenhagen, and
Department of surgical gastroenterology C, Rigshospitalet, Copenhagen, Denmark

Diemer N. H. & Tønnesen, K. Glial changes in pigs with porto-caval anastomosis and temporary or total hepatic artery clamping Acta path microbiol scand. Sect. A, 85 721–730 1977

The number and size of astrocyte, oligodendrocyte, and neurone nuclei were determined in cortex and corpus striatum (putamen) of pigs with porto-caval anastomosis (PCA) and total or temporary clamping of the hepatic artery Animals with PCA and total clamping became comatose and died on average 18½ hours postoperatively Their brains showed slight oedema but no changes in the glial and neurone nuclear numbers. Animals with PCA and temporary clamping of the hepatic artery (30–60 min.) all survived without clinical symptoms of encephalopathy However the brains showed vacuolization of the deeper cortical layers, diffuse occurrence of Alzheimer type II astrocytes, and the counts revealed an increased number of astrocytic nuclei The total number of glial cells decreased due to loss of oligodendrocytes, but the number of neurones was unchanged. The findings indicate that the neuropathological changes after PCA and temporary hepatic artery clamping are concerned primarily with changes of the glial cells.

Key words Porto-caval anastomosis hepatic artery clamping encephalopathy glial nuclei morphometry

N H Diemer Institute of Neuropathology University of Copenhagen, 11 Frederik V' V J DK 2100 Copenhagen Ø Denmark.

Received 22.iii.77 Accepted 21.iv.77

Astrocyte proliferation and Alzheimer type II changes are the most common neuropathological findings in patients with acute or chronic liver diseases (*von Hösslin & Alzheimer* 1912, *Adams & Foley* 1953 *Victor et al.* 1965)

This widespread proliferation of astrocytes has been ascribed to amitotic astrocyte divisions as no mitoses are found.

Earlier investigations on rats with CCl_4-induced hepatic encephalopathy (*Diemer* 1977 a, b) and rats with porto-caval anastomosis (*Diemer et al* 1977) revealed in both instances an approx. 25 per cent increase in the number of astrocytes, but also a corresponding decrease in the number of oligodendrocyte nuclei, leaving the total glial number constant. It was postulated that a transformation of astrocyte nuclei took place in both forms of encephalopathy

This theory which eliminates the possibility

D E. Chronic nitrofurantoin pulmonary reaction. Report of five cases. New Eng J Med. *279* 1258–1262 1968

19 *Ruikka I Vaissalo T & Saarimaa H* Progressive pulmonary fibrosis during nitrofurantoin therapy Scand J resp. Dis. *52* 162–166 1971

20 *Scadding J G & Hinson F K* Diffuse fibrosing alveolitis (diffuse interstitial fibrosis of the lung) Correlation of histology at biopsy with prognosis. Thorax *22* 291–304 1967

21 *Sollaccio P A Ribande C A & Grace W J* Subacute pulmonary infiltration due to nitrofurantoin. Ann. Int. Med. *65* 1284–1286 1966

22 *Sovijärvi A R A Lemola M Stenius B & Idänpää Heikkilä J* Nitrofurantoin-induced acute subacute and chronic pulmonary reactions. A report of 66 cases. Scand. J resp. Dis. *58* 41–50 1977

23 *Teppo A M Haltia K & Wager O* Immunoelectrophoresis "tailing" of albumin line due to IgG antibody complexes. A side effect of nitrofurantoin. Scand J Immunol. *5* 249–261 1976

24 *Tukiainen P* Needle biopsy in diffuse lung manifestations. An analysis of 145 consecutive cases. Scand. J resp Dis. Suppl. *94* 1–110, 1975

25 *Udwadia F E* Pulmonary eosinophilia. Progress in Respiration Research, Vol 7 S. Karger Basel 1975

RESULTS

Clinical and General Pathological Findings

Eight to 10 hours after the operation the animals with total devascularization of the liver became lethargic and during a period lasting 6 to 8 hours with increasing drowsiness they became comatose. The mean survival time was 18½ hours and death was due to intractable cardiovascular collapse.

The animals with PCA and temporary hepatic artery clamping showed no clinical abnormalities. Especially ataxia, seizures, or bizarre behaviour were not observed. Liver biopsy at sacrifice showed no pathological changes.

Neuropathological Findings

Mean brain weight was 95.4 g with no significant differences between the groups. The brains from the group with total hepatic devascularization showed no haemorrhages, thrombi or emboli and the vessels appeared normal. Microscopically there were slight signs of edema. There were no significant nerve cell changes.

The astrocytes showed no nuclear or cytoplasmic changes and Alzheimer type II nuclei were not found despite careful searching. Abnormal granules were not seen. The oligodendrocytes were normal and there were no changes of the myelin.

The 4 brains from the animals with PCA and temporary hepatic ischemia showed no macroscopically changes. Microscopically 3 brains (nos. 138, 119 and 125) showed mild to moderate spongiform changes most pronounced in brain no. 125. The vacuolization was localized to the cortical U fibres, to the adjoining grey matter (Fig. 1) and to the white matter of corpus striatum as seen on Fig. 2. One animal (no. 125) had also vacu-

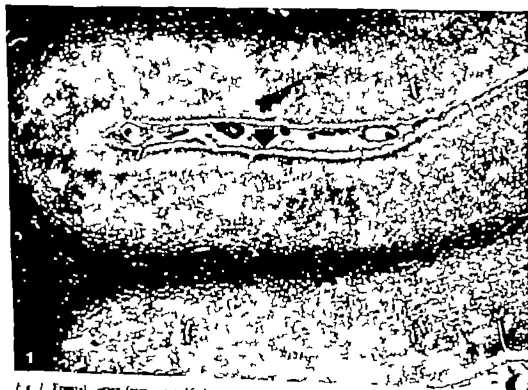


Fig. 1. Frontal cortex from pig 16 days after PCA. Vacuolization (status spongiosus) is seen corresponding to the U-fibres and in the adjoining grey matter. The arrow in the coronal fissure indicates the position of the counting area in cortex. Haematoxylin-eosin × 68.

of a real astrocyte proliferation has to be further consolidated by performing cell quantifications under standardized conditions in other species than the rat.

In the present investigation differential counts of glial and nerve cells were done in cortex and corpus striatum of pigs with acute encephalopathy due to devascularization of the liver and in pigs with porto-caval anastomosis (PCA) and temporary clamping of the hepatic artery.

MATERIAL AND METHODS

The material comprised 20 pigs of Danish landrace weighing between 35 and 45 kg. All animals were anaesthetized with Halothane® oxygen and nitrous oxide through an endotracheal cuffed tube.

Eight animals served as controls. They were killed by bleeding through the common carotid artery.

In 8 animals total devascularization of the liver has previously been described (*Tønnesen* 1976 a). The liver was mobilized by transsecting and ligating all peritoneal adhesions, a porto-caval anastomosis was performed and the hepatic artery ligated and transsected. During the experimental period glucose (0.25 g/kg/hour) was administrated intravenously.

Four animals were subjected to partial anoxia of the liver as earlier described (*Tønnesen* 1976 b). After mobilization of the liver a porto-caval anastomosis were performed and the hepatic artery was temporarily clamped.

The duration of the clamping and the experimental period was as follows:

Pig no. 106 30 min. clamping sacrif. 9 days later
Pig no. 119 30 min. clamping sacrif. 20 days later
Pig no. 138 60 min. clamping, sacrif. 7 days later
Pig no. 125 60 min. clamping sacrif. 16 days later

Shortly after sacrifice the animals were decapitated and the head stored for 24 hours at 4° C.

Histological Technique

After removal the brain was weighed and fixed in *Lillie's* (1954) phosphate buffered formalin for 14 days. The cerebellum and brain stem were divided from the cerebrum with a cut through the mesencephalon. Both the left cerebral and cerebellar hemispheres were cut frontally in 5 mm thick slices. These were dehydrated in graded ethanols, cleared in xylene and embedded in paraffin wax. From each block 7 µm thick sections were cut and stained with haematoxylin eosin, cresyl violet, PAS, Alcian Blue and a.m. van Gieson, Kluver Barrera and Bodian.

Differential Counts of Astrocyte, Oligodendrocyte and Neurone Nuclei in Cortex and Putamen

The counts were performed in 4 controls, 4 animals with total devascularization of the liver and in the 4 animals with PCA and temporary hepatic artery clamping. In the cortex counts took place in the frontal and parietal region. At the lateral side of the coronal fissure halfway between the crest and depth of the gyrus, the thickness of ten hematoxylin eosin stained sections from each region was measured using the micrometer screw method (*Brattgård* 1954, *Pakkenberg* 1960). From each cortical region the two sections with a mean thickness closest to the average thickness in the material (7.54 µm) were chosen for quantitation. At the place marked with an arrow in Fig. 1 and perpendicular to the surface, the glial and nerve cell nuclei were counted in the two cortical areas in 6 (frontal) or 2 (parietal) rows, respectively (*Pakkenberg* 1966, *Haug* 1972).

In the putamen the counts were performed in the anterior part of this structure in the grey matter between the myelin bundles. Two Klüver Barrera stained sections were selected in the way as described earlier and glial and neuronal nuclei were quantitated in 20 counting fields in each section.

Both in cortex and putamen, the differential counts were performed at × 500 magnification using an ocular grid subdivided into 100 squares covering an area of 0.01 mm. The number of glial nuclear pairs were registered separately. The frequency of nuclear pairs was tested with a χ^2-test.

The counted nuclear density was corrected for section thickness and different nuclear diameters by *Floderus* correction formula (*Floderus* 1944) as earlier described (*Diemer* 1977 a).

Nuclear Diameter Determinations

The nuclear diameters were measured by means of an electronic image analyzer (Leitz Classimat®) using an × 100 oil immersion objective and a × 16 ocular (*Diemer & Laursen* 1977). The diameter of 25 neurone nuclei, 25 oligodendrocyte nuclei, and 50 astrocyte nuclei were determined in each section used for differential counts from each animal.

The nuclear diameters were corrected for constraining by section thickness using *Sholpos* formula (1957).

In concordance with earlier determinations of nuclear density and size, the values were expressed as median value with 25- and 75- percentiles. The total number of glial nuclei was also calculated as the median value of the group and this value does thus not appear as the arithmetic sum of the number of oligodendrocyte and astrocyte nuclei in the tables 2, 3 and 4. For statistical evaluation Mann Whitneys rank sum test was used (*Diemer* 1977 a, b).

RESULTS

Clinical and General Pathological Findings

Eight to 10 hours after the operation the animals with total devascularization of the liver became lethargic and during a period lasting 6 to 8 hours with increasing drowsiness they became comatose. The mean survival time was 18½ hours and death was due to intractable cardiovascular collapse.

The animals with PCA and temporary hepatic artery clamping showed no clinical abnormalities. Especially ataxia, seizures, or bizarre behaviour were not observed. Liver biopsy at sacrifice showed no pathological changes.

Neuropathological Findings

Mean brain weight was 95.4 g with no significant differences between the groups. The brains from the group with total hepatic devascularization showed no haemorrhages, thrombi or emboli and the vessels appeared normal. Microscopically there were slight signs of edema. There were no significant nerve cell changes.

The astrocytes showed no nuclear or cytoplasmic changes and Alzheimer type II nuclei were not found despite careful searching. Abnormal granules were not seen. The oligodendrocytes were normal and there were no changes of the myelin.

The 4 brains from the animals with PCA and temporary hepatic ischemia showed no macroscopically changes. Microscopically 3 brains (nos. 138, 119 and 125) showed mild to moderate spongiform changes, most pronounced in brain no. 125. The vacuolization was localized to the cortical U fibres, to the adjoining grey matter (Fig. 1) and to the white matter of corpus striatum as seen on Fig. 2. One animal (no. 125) had also vacu

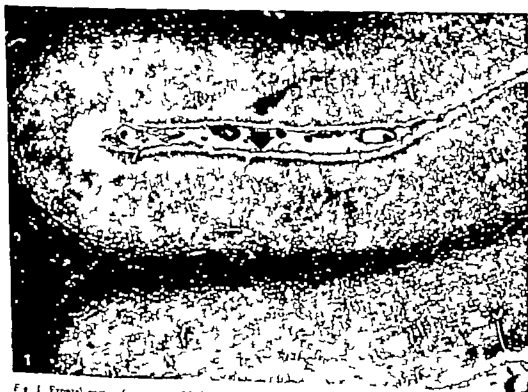


Fig. 1. Frontal cortex from pig 16 days after PCA. Vacuolization (status spongiosus) is seen corresponding to the U-fibres and in the adjoining grey matter. The arrow in the coronal fissure indicates the position of the counting area in cortex. Haematoxylin-eosin × 68.



Fig 2 Vacuolization of the white matter in the putamen of a pig 16 days after PCA Haematoxylin-eosin × 170

oles in the central parts of the white matter Vacuoles were not found in the corpus callosum of any animal In one animal (no 138) a few small vacuoles were found in the central white matter of the cerebellum but otherwise the brains showed no vascuolization in the cerebellum or brain stem The vacuoles measured from 25 to 200 μm in diameter They had a clear rim and were empty In some of the larger vacuoles, membraneous septae were seen crossing the lumen

At low power magnification of the cortex these animals had more conspicuous astrocyte nuclei than the controls (Fig 3) Their nuclei were often watery and obviously enlarged with a distinct nuclear membrane and a peripheral nucleolus (occasionally two) In contrast to the controls a watery cytoplasmic space were often visible sometimes containing a finely granular substance best seen in the haematoxylin-eosin stain. The Klüver Barrera stain revealed a few grey blue granules in the cytoplasm but PAS-positive granules were not observed.

The oligodendrocytes of the white matter were swollen, and sporadically small, dark and irregular nuclei were seen

The neurones showed no obvious changes from those of the control brains. There were no chromatolysis or changes of the nucleoli. Increased satellitosis or neuronophagia were not found

Nuclear Diameter Determinations

In the two experimental groups the neurone diameters did not differ significantly from those of the control group In the frontal and parietal cortex the median neurone nuclear diameter was 12.5 (12.2–12 8) μm (25 and 75 percentiles) after correction with

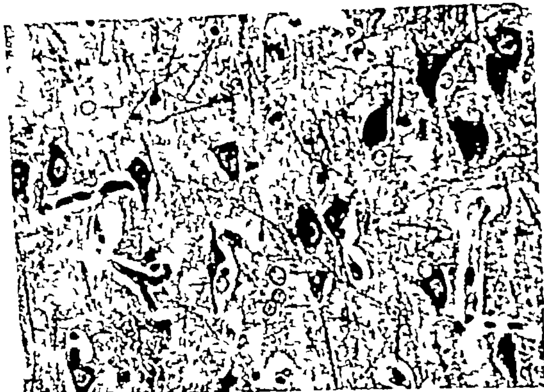


Fig. 3. Frontal cortex from a pig 20 days after PCA. Enlarged astrocyte nuclei with prominent nucleoli and watery cytoplasm are seen (arrows). Klüver Barrera × 685

Sholpo factor. In the corpus striatum the mean neurone nuclear diameter was 10.1 (9.7–11.1) μm.

Similarly, no significant differences in oligodendrocyte nuclear diameter was found between the groups. In cortex the median oligodendrocyte nuclear diameter was 4.8 (4.6–5.3) μm, and in the corpus striatum (putamen) it was 4.3 (4.2–4.9) μm.

However, the astrocyte nuclear diameters differed significantly between the groups, as shown in Table 1. The animals with PCA had a significantly larger astrocyte nuclear diameter both in cortex and in corpus striatum.

The diameter distribution of cortical astrocyte nuclei is shown in Fig. 4, which represents about 300 diameters from the PCA group and 300 from the controls. The plot shows the electronically determined values before *Sholpos* correction. Thus the controls have a peak at about 6 μm, whereas the PCA animals have one about 8 μm. Sectioning of the nuclei (mean section thickness 7.54 μm) contributes to the skewness of the curves.

TABLE 1. *Astrocyte Nuclear Diameters in Cortex and Putamen*

	Cortex	Putamen
Control	7.4 (7.[illegible]–7.8)	7.2 (6.9–7.5)
Sholpo factor	1.12	1.1[illegible]
Acute (n = 4)	7.3 (7.0–7.[illegible])	7.1 (6.8–[illegible].4)
Sholpo factor	1.1	1.1
PCA (n = 4)	9.0 (8.3–9.9)*	7.9 (7.3–8.5)**
Sholpo factor	1.13	1.13

* $p < 0.01$
** $p < 0.0?$ Mann Whitney's rank sum test

The measured values are corrected by Sholpo factor. All values are median values with 25- and 75- percentiles.



Fig 2 Vacuolization of the white matter in the putamen of a pig 16 days after PCA Haematoxylin-eosin × 170

oles in the central parts of the white matter Vacuoles were not found in the corpus callosum of any animal In one animal (no 138) a few small vacuoles were found in the central white matter of the cerebellum, but otherwise the brains showed no vascuolization in the cerebellum or brain stem. The vacuoles measured from 25 to 200 μm in diameter They had a clear rim and were empty In some of the larger vacuoles, membraneous septae were seen crossing the lumen

At low power magnification of the cortex these animals had more conspicuous astrocyte nuclei than the controls (Fig 3) Their nuclei were often watery and obviously enlarged with a distinct nuclear membrane and a peripheral nucleolus (occasionally two) In contrast to the controls a watery cytoplasmic space were often visible sometimes containing a finely granular substance best seen in the haematoxylin-eosin stain. The Klüver Barrera stain revealed a few grey blue granules in the cytoplasm but PAS-positive granules were not observed.

The oligodendrocytes of the white matter were swollen and sporadically small, dark and irregular nuclei were seen

The neurones showed no obvious changes from those of the control brains. There were no chromatolysis or changes of the nucleoli Increased satellitosis or neuronophagia were not found

Nuclear Diameter Determinations

In the two experimental groups the neurone diameters did not differ significantly from those of the control group In the frontal and parietal cortex the median neurone nuclear diameter was 12.5 (12.2–12.8) μm (25 and 75 percentiles) after correction with

TABLE 3 *Density of Astrocyte- Oligodendrocyte- and Neurone Nuclei/0.1 mm² of Parietal Cortex*

	Astrocyte nuclei	Oligodendrocyte nuclei	Neurone nuclei	Total glial nuclei
Control	7.3 (5.5– 8.6)	31.7 (29.6–34.3)	11.9 (10.8–13.3)	39.0 (36.4–41.5)
Acute	6.2 (5.9– 8.0)	31.4 (28.8–39.7)	12.5 (10.3–14.6)	37.6 (34.9–47.6)
PCA	10.5 (8.6–11.6)	24.0 (23.2–28.1)	12.1 (11.2–13.3)	33.8 (32.6–39.4)
Mann-Whitneys rank sum test				
Con./acute	n.s.	n.s.	n.s.	n.s.
Con./PCA	n.s.	n.s.	n.s.	n.s.
Con. + acute/PCA	$p < 0.05$	$p < 0.05$	n.s.	$p < 0.02$

All values are median values with 25- and 75- percentiles.

TABLE 4 *Density/0.05 mm² of Astrocyte- Oligodendrocyte- and Neurone Nuclei in Putamen*

	Astrocyte nuclei	Oligodendrocyte nuclei	Neurone nuclei	Total glial nuclei
Control	9.2 (8.8–10.5)	53.8 (48.8–58.7)	25.4 (23.2–25.8)	62.7 (59.2–68.5)
Acute	9.7 (8.9–11.5)	48.0 (44.4–56.0)	25.6 (24.5–27.8)	59.4 (55.2–64.6)
PCA	13.5 (11.7–15.8)**	39.7 (35.0–42.7)**	27.5 (24.8–29.6)	51.4 (47.6–54.1)

$p < 0.05$
** $p < 0.01$ Mann-Whitneys rank sum test

All values are median values (50-percentile) with 25- and 75- percentiles.

dendrocyte nuclei and a reduced total number of glial nuclei in the putamen.

In the frontal cortex, the control animals had 18 nuclear pairs per 250 astrocyte nuclei, and the animals with temporary hepatic ischemia had 29 pairs per 417 astrocyte nuclei. In putamen the corresponding numbers were 8 nuclear pairs per 142 astrocyte nuclei and 17 nuclear pairs per 202 astrocyte nuclei, respectively. For both regions, the χ^2-test showed no differences in the frequency of nuclear pairs compared to the observed number of astrocyte nuclei.

DISCUSSION

The present neuropathological investigation showed no glial or nerve cell changes in the animals with total hepatic devascularization, whereas pigs with porto-caval anastomosis (7–20 days) and temporary clamping of the hepatic artery (30–60 min.) had a 40 per cent increase in the number of astrocyte nuclei and a 15 per cent decrease in the number of oligodendrocyte nuclei. Three of the 4 animals in this group showed vacuolization of the white matter.

In the acute model, the clinical course and the duration of the devascularized state (about 18½ hours) are consistent with the literature on similar experiments with dogs, monkeys and pigs (*Rappoport et al.* 1953, *Giges et al.* 1955, *Benson et al.* 1970, *Fischer et al.* 1976).

Norenberg et al. (1972) found a significant increase of astrocytes, and paired nuclear forms were frequently seen. Ultrastructurally

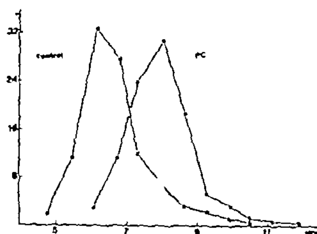


Fig. 4. Percentage distribution of astrocyte nuclear diameters in the frontal cortex of controls and pigs with PCA. Total number of nuclear diameter determinations: 600

Nuclear Density Determinations

The mean section thickness was 7.54 μm (240 sections). This value was used in the correction of the nuclear counts by *Floderus* formula.

Table 2 shows the number of astrocyte, oligodendrocyte, neurone and total glial nuclei in frontal cortex. The density of the different nuclei in the acute animals was not significant different from that of the controls. The group with temporary hepatic ischemia, however, had a significantly higher astrocyte density and a lower oligodendrocyte density. The total number of glial cells in this group was reduced but not significantly. Since the acute and control animals did not deviate from one another, their values were pooled. The Mann-Whitney rank sum test then revealed a significantly lower number of glial cells in the group with temporary hepatic ischemia compared with the two other groups.

Table 3 shows the values from parietal cortex after counting only 2 vertical columns of cells. No significant differences were found between the individual groups. But after pooling the values for control and acute animals, significance testing against the group with temporary hepatic ischemia showed the same pattern as for frontal cortex.

The number of counting fields (100 × 100 μm) in each column of the sections was used to calculate the cortical thickness. No difference was found between the groups. The mean thickness for all groups was 1.5 ± 0.2 mm (s.d.).

Table 4 shows the density of astrocyte, oligodendrocyte and neurone nuclei as well as the total number of glial cells/0.05 mm³ in the corpus striatum. The acute group (animals with total hepatic ischemia) showed no significant differences from the control group.

On the other hand, and similar to the cortical counts, the group with temporary hepatic ischemia had an increased number of astrocyte nuclei, a decreased number of oligo-

TABLE 2. *Density of Astrocyte, Oligodendrocyte and Neurone Nuclei/0.1 mm³ of Frontal Cortex*

	Astrocyte nuclei	Oligodendrocyte nuclei	Neurone nuclei	Total glial nuclei
Control	4.9 (4.5–5.3)	34.2 (29.5–40.9)	12.5 (11.2–13.9)	38.7 (34.1–45.7)
Acute	5.7 (5.0–7.5)	30.1 (25.6–35.5)	11.1 (10.0–14.8)	35.7 (33.0–40.7)
PCA	7.9 (6.6–9.8)	23.2 (20.9–24.9)	11.8 (9.9–12.3)	31.1 (27.8–34.3)
Mann-Whitney rank sum test				
Con/acute	n.s.	n.s.	n.s.	n.s.
Con/PCA	$p < 0.05$	$p < 0.05$	n.s.	n.s.
Con. + acute/PCA	$p < 0.05$	$p < 0.01$	n.s.	$p < 0.01$

All values are median values with 25- and 75-percentiles.

TABLE 3. *Density of Astrocyte- Oligodendrocyt and Neurone N clei/0 1 mm² of Parietal Corte*

	Astrocyte uclei	Oligodendrocyte nuclei	Neurone nuclei	Total glial nuclei
Control	7.5 (5.5– 8.6)	31 7 (29.6–34.5)	11.9 (10 8–15.5)	39.0 (36 4–41.5)
Acute	6 2 (5.9– 8.0)	31 4 (28.8–39 7)	12.5 (10.5–14.6)	37.6 (34.9–47.6)
PCA	10 5 (8 6–11.6)	24.0 (23.2–28.1)	12.1 (11.2–13.5)	33.8 (32.6–39 4)
Mann-Whitneys rank sum test				
Con./acute	n s.	n.s.	n.s.	n.s.
Con./PCA	s	n.s.	n.s.	n.s.
Con. + acute/PCA	$p < 0.05$	$p < 0.05$	n.s.	$p < 0.02$

All values are median alues with 25- and 75- percentiles.

TABLE 4 *Density/0 05 mm² of Ast ocyte- Oligodendrocyte- and Neurone N clei in Putamen*

	Astrocyte nuclei	Oligodendrocyte nuclei	Neurone nuclei	Total glial nuclei
Control	9.2 (8.8–10.5)	53 8 (48.8–58.7)	25 4 (23.2–25 8)	62.7 (59.2–68.5)
Acute	9 7 (8.9–11.5)	48 0 (44 4–56.0)	25.6 (24.5–27.8)	59 4 (55.2–64.6)
PCA	13.3 (11 7–13.8)**	39 7 (35 0–42.7)**	27.5 (24 8–29 6)	51 4 (47.6–54 1)

 $p < 0.05$
** $p < 0.01$ Mann-Whitneys rank sum test

All alues are median alues (50-percentile) with 25- and 75- percentiles.

dendrocyte nuclei and a reduced total number of glial nuclei in the putamen.

In the frontal cortex, the control animals had 18 nuclear pairs per 250 astrocyte nuclei, and the animals with temporary hepatic ischemia had 29 pairs per 417 astrocyte nuclei. In putamen the corresponding numbers were 8 nuclear pairs per 142 astrocyte nuclei and 17 nuclear pairs per 202 astrocyte nuclei respectively For both regions, the χ^2-test showed no differences in the frequency of nuclear pairs compared to the observed number of astrocyte nuclei.

DISCUSSION

The present neuropathological investigation showed no glial or nerve cell changes in the animals with total hepatic devascularisation, whereas pigs with porto-caval anastomosis (7–20 days) and temporary clamping of the hepatic artery (30–60 min.) had a 40 per cent increase in the number of astrocyte nuclei and a 15 per cent decrease in the number of oligodendrocyte nuclei. Three of the 4 animals in this group showed vacuolization of the white matter

In the acute model, the clinical course and the duration of the devascularized state (about 18½ hours) are consistent with the literature on similar experiments with dogs, monkeys and pigs (*Rappoport et al.* 1953 *Giges et al.* 1955 *Benson et al.* 1970 *Fischer et al.* 1976)

Norenberg et al (1972) found a significant increase of astrocytes, and paired nuclear forms were frequently seen. Ultrastructurally

the paired nuclei were separated by a set of apposing cytoplasmic membranes Mitotic figures were not found, but centrioles associated with complex structures procentrioles, and microtubules were often seen in the astrocytes.

Our study revealed no *increase in the number* of astrocyte nuclei and the frequency of nuclear *pairs* was the same as in the control animals. This is consistent with the calculated cycle period of 20 hours for glial cells (*Korr et al* 1976) First after this period of time it seems can astrocyte mitoses be observed Furthermore *Cavanagh* (1970) has shown in rats that after a brain wound which represents a strong stimulus to astrocyte proliferation the earliest astrocyte mitoses are seen on the second day

The neuropathological changes in the animals with PCA and temporary hepatic artery clamping correspond partly to those of patients with *hepatic encephalopathy* Thus, *Adams* & *Foley* (1953) and *Victor et al* (1965) described enlarged astrocyte nuclei increased numbers of astrocytes, and also in some patients status spongiosus (microvacuolization)

Concerning the status spongiosus which was only found in areas containing myelin sheaths, different pathogenetic possibilities exist and "status spongiosus" covers a wide range of ultrastructural lesions in different cells (*Hooper* 1975 *Blakemore* 1972 *McC Howell et al* 1974)

In our material rats with porto-caval anastomosis develop vacuolization in the molecular layer of the cerebellum (*Cavanagh et al* 1972 *Diemer et al* 1977) The ultrastructural correlate to this was membrane bound swellings in the astrocyte processes adjacent to dendrites. A direct relationship probably exists between the occurrence of the vacuoles and the plasma NH N level (*Cavanagh et al* 1972) That such astrocyte swellings should be due to altered glial transport mechanisms is not unlikely as increased astrocyte membrane permeability to horse-radish peroxidase has been observed in rats after porto-caval anastomosis (*Laursen* & *Westergaard* 1977)

The occurrence of enlarged astrocyte nuclei and increased numbers of astrocytes has previously been described both *in animals* (*Kline et al* 1966 1971 *Norenberg et al.* 1972) and in patients with porto-systemic encephalopathy (*Victor et al* 1965)

It has been shown by *Cavanagh* & *Kyu* (1970) that most of the nuclear enlargement is an artifact due to immersion fixation. In rats, however some astrocyte nuclear enlargement is also present after perfusion fixation (*Diemer et al* 1977) This is probably a sign of nuclear hyperfunction in the astrocytes and this hypothesis is supported by ultrastructural investigations of rats with PCA, which have shown an increased number of organelles in the astrocytes (*Cavanagh et al* 1972, *Norenberg* & *Lapham* 1974) indicating cellular hyperactivity

Earlier investigations of rats with PCA have shown that the increased number of astrocyte nuclei is not due to astrocyte division but probably to a transformation of nuclei normally regarded as oligodendroglial (*Diemer* 1977 a, *Diemer et al* 1977)

The present investigation supports this theory as neither increase in the total glial number nor increase in the frequency of astrocyte nuclear pairs or mitoses were observed Actually the total glial number decreased in all animals with PCA due to loss of oligodendrocytes.

Differential counts of glial cells have rarely been performed in liver encephalopathy Loss of oligodendrocytes in patients with hepatic coma has only been described by *Victor et al* (1965) However a pattern somewhat similar to the present was found in PCA rats (*Diemer et al.* 1977) A 15 per cent decrease in the number of glial cells, due to loss of oligodendrocytes were found in the animals with the heaviest liver damage These animals had also a 15 per cent nerve cell loss, and the experimental period was longer (7–15 weeks) than that of the actual study This could indicate that the glial changes precede the nerve cell changes.

These findings support the theory that glial cells are the primary affected cells in porto-

systemic encephalopathy In the pathogenetic considerations, the disturbed ammonia metabolism has played an important role Thus, plasma ammonia is increased 3–5 fold in PCA rats (*Cavanagh & Kyu* 1972, *Laursen & Westergaard* 1977 *Diemer et al.* 1977) and the glutamine concentrations in the spinal fluid is increased (*Cremer et al* 1975) *Norenberg* (1976) found an increased activity of glutamate dehydrogenase in the glial cells. However hyperammoniemia (induced by urease) results only in a reversible transformation of the glial nuclei, and causes no nuclear enlargement or loss of glial cells (*Diemer & Laursen* 1977) *Hooper* (1975) found spongy degeneration in sheep after infusion of ammonium acetate but hyperammonia does not increase the permeability of the blood-brain barrier to horse-radish peroxidase (*Laursen & Westergaard* personal communication) and it does not cause the disturbances in microtubular function seen in mitotic astrocytes after PCA (*Diemer & Laursen* 1977) Thus, other factors besides ammonia must contribute to the development of porto-systemic encephalopathy

REFERENCES

Adams, R D & Foley J M The neurological disorder associated with liver disease. Res. publ. Ass nerv ment. dis. 32 198–237 1953

Brusen R W May A, O Norenberg M & Lapham L W Protoplasmic astrocytosis of the brain in experimental hepatic coma. Surgical Forum 21 357–359 1970

Blakemore W F Observations on oligodendrocyte degeneration, the resolution of status spongiosus and remyelination in cuprizone intoxication in mice J Neurocytology *1* 413–426, 1972

Breitig d S -O X Microscopical determinations of the thickness of histological sections. J roy micr Soc. 74 113–122 1954

Cavanagh J B. & Kyu M H Type II Alzheimer change experimentally produced in astrocytes in the rat. J neurol. Sci *12* 63–75, 1971

Cavanagh J B Lewis P D., Blakemore W F & Kyu M H Changes in the cerebellar cortex in rats after porto-caval anastomosis. J neurol. Sci *15* 13–26, 1972.

Cremer J E., Heath D F T al H M., Woods, M S & Cavanagh J B Some dynamic aspects of brain metabolism in rats given porto-caval anastomosis. Neuropath. Appl. Neurobiol *1* 293–311 1975

Diemer N H Glial and neuronal alterations in the corpus striatum of rats with CCl-induced liver disease A quantitative morphological study using an electronic image analyzer Acta neurol. Scand. *55* 16–32, 1977 a.

Diemer N H Number of Purkinje cell and Bergmann astrocytes in rats with CCl -induced liver disease Acta neurol Scand. *55* 1 15, 1977 b.

Diemer N H & Laursen H. Glial cell reactions in rats with hyperammonemia induced by urease or porto-caval anastomosis. Acta neurol. Scand. 55 425–442 1977

Diemer N H Kl. J., Schröder H & Klinken L. Glial- and nerve changes in rats with porto-caval anastomosis. Acta Neuropath. 39 59–68 1977

Fischer M., Stätter L., Schmahl, W., Gartmaier P., Eckardt W & D pic H. Acute liver failure due to temporary hepatic Ischemia in the pig. Acta Hepato-Gastroenterol. *23* 241 249 1976.

Floderus S. Untersuchungen über den Bau der menschlichen Hypophyse mit besonderen Berücksichtigung der quantitativen mikromorphologischen Verhältnisse Acta path. microbiol. Scand. suppl. *53* 1944

Gilgers, B., Drin H L. Sherer I M., Seligson D & Howard J M. Experimental hepatic coma. Surg Gynecol. Obstet. 97 763–768 1953

Haug H Stereological methods in the analysis of neuronal parameters in the central nervous system. J micr *95* 165–180 1972.

Hooper P T.: Spongy degeneration in the central nervous system of domestic animals. Acta Neuropath. 31 325–334 1975

Kline D G Doberneck R, C Chan B K & Rutherford R B Encephalopathy in graded porto-caval shunts Ann. surg. *164* 1003–1012, 1966

Kline D G Cook J N & Nan F C. Eck fistula encephalopathy long term studies in primates. Ann. surg. *173* 97–103 1971

Kerr H., Schultze B. & Maurer W. Autoradiograph investigations of glial proliferation in the brain of adult mice. J Comp. Neur *160* 477–490 1976

Laursen H & Westergaard E.: Enhanced permeability to horseradish peroxidase across cerebral vessels in the rat after portocaval anastomosis. Neuropath. Appl Neurobiol. *3* 29–43 1977

Lillie R D in Histopathologic technic and practical histochemistry Blakiston Co. Inc., Philadelphia, 1954

McC Howell J Blakemore W F Gopinath C., Hall G A & Parker J H. Chronic copper poisoning and changes in the central nervous

system of sheep Acta Neuropath. *29* 9–24 1974

Norenberg M D Lapham L W Eastland M W & May A G Division of protoplasmic astrocytes in acute experimental hepatic encephalopathy Am J Path. *67* 403–408, 1972

Norenberg M D Histochemical studies in experimental portal-systemic encephalopathy I Glutamic dehydrogenase Arch neurol. *33* 265–269 1976

Pakkenberg H Cytoplasmic basophilia in the nerve cells of the cerebral cortex. Thesis. Copenhagen Vald. Pedersens bogtrykkeri 1960

Pakkenberg H The number of nerve cells in the cerebral cortex of man. J Comp Neurol. *128* 17–20 1966

Rappaport A M MacDonald M H & Borowy Z J Hepatic coma following ischemia of the liver Surg Gynecol Obstet. *97* 748–762 1953

Sholpo A E Cited in Blinkov S M & Glezer I J The human brain in figures and tables. A quantitative handbook. Basic Books, Inc. Publishers. Plenum Press. New York, 1968.

Tønnesen K Total devascularization of the liver Scand J Gastroent. suppl. *37* 23–26 1976.

Tønnesen K Total and partial anoxia of the liver Scand. J Gastroent. suppl. *37* 27–31 1976

Victor M Adams R D & Cole M The acquired (non Wilsonian) type of chronic hepatocerebral degeneration. Medicine (Balt.) *44* 345–396 1965

von Hösslin C & Alzheimer A Ein Beitrag zur Klinik und Pathologischen Anatomie der Westphal-Strümpellschen Pseudosclerose Z. ges Neurol. Psychiat. *8* 183–209 1912.

Acta path. microbiol. scand. Sect. A, 85: 731-738, 1977

CUTTING FLUIDS AND THEIR EFFECTS ON THE SKIN OF MICE

An Experimental Study with Special Reference to Carcinogenicity

JORGEN R. JEPSEN, STEPHAN STOYANOV, MOGENS UNGER, JORGEN CLAUSEN and HANS EWALD CHRISTENSEN

The Institute of Public Health, Hygiene and Environmental Science, Odense University and The Institute of Pathology, Odense University, DK-5000 Odense, Denmark

Jepsen, J. R., Stoyanov, S., Unger, M., Clausen, J. & Christensen, H. E. Cutting fluids and their effects on the skin of mice. An experimental study with special reference to carcinogenicity. Acta path. microbiol. scand. Sect. A, 85: 731-738, 1977.

Reports of skin malignancies due to occupational exposure have decreased since the introduction of solvent-refining of mineral oil fraction in the manufacture of oil based cutting fluids. Commercial mineral oil based cutting fluids caused local and general pathological changes after repeated application to the skin of mice in the present study. Forty-eight per cent of the mice exposed to oils showed severe dysplasia or malignancy of the skin on histological examination. The corresponding figure for the control group, where various additives were used, was 8 per cent. The frequency of papillomas was also increased in the mice exposed to oils. The systemic lesions included focal necrosis of the liver associated with amyloid deposition, as well as amyloidosis of the skin, spleen and kidneys. The substances responsible for these apparent carcinogenic properties of the complex mixtures may be polycyclic hydrocarbons; the latter are still present in the commercial products despite solvent refining; on the other hand the carcinogens may be the additives to the cutting oils the composition of which is generally trade secret.

Key words: Cutting oils; carcinogenesis; skin.

Jørgen R. Jepsen, The Institute of Public Health, Hygiene and Environmental Science, Odense University, DK-5000 Odense, Denmark.

Received 22. xi.76 Accepted 25.iv.77

Cutting oils are carcinogenic and can induce skin cancers as well as bronchial carcinomas (*Cruickshank & Squire* 1950, *Mastromatteo* 1955, *Gilman & Vesselinovitch* 1955, *Finnie* 1960, *Bingham et al.* 1965, *Thony & Thony* 1969, *Ely et al.* 1970, *Holmes et al.* 1970, *Lee et al.* 1972, *Wahlberg* 1972). *Cadwpole et al.* (1971) demonstrated that some oils cause skin tumours in mice.

The carcinogenic factors of mineral oils may be polycyclic aromatic hydrocarbons; other hydrocarbons, not in themselves carcinogenic, might modify the carcinogenic potency of the polycyclic aromatics. Solvent refining reduces the carcinogenic effects on mouse skin by eliminating part of the high boiling aromatic polycyclic fraction. Additives have been increasingly used in recent years, but the compounds added are generally a trade secret. The authors of the present communication have only found a few studies of

system of sheep Acta Neuropath 29 9 24 1974
Norenberg M D Lapham I W Eastland M W & May A G Division of protoplasmic astrocytes in acute experimental hepatic encephalopathy Am J Path. 67 403-408 1972
Norenberg M D Histochemical studies in experimental portal-systemic encephalopathy I Glutamic dehydrogenase Arch. neurol 33 265-269 1976
Pakkenberg H Cytoplasmic basophilia in the nerve cells of the cerebral cortex Thesis, Copenhagen, Vald Pedersens bogtrykkeri 1960
Pakkenberg H The number of nerve cells in the cerebral cortex of man. J Comp. Neurol 128 17-20 1966
Rappaport A M MacDonald M H & Borowy Z J Hepatic coma following ischemia of the liver Surg Gynecol. Obstet 97 748-762 1953
Sholpo A E Cited in Blinkov S M & Glezer I J The human brain in figures and tables A quantitative handbook Basic Books, Inc. Publishers Plenum Press, New York, 1968.
Tonnesen K Total devascularization of the liver Scand J Gastroent. suppl 37 23 26 1976.
Tonnesen K Total and partial anoxia of the liver Scand J Gastroent suppl 37 27 31 1976
Victor M Adams R D & Cole M The acquired (non Wilsonian) type of chronic hepatocerebral degeneration. Medicine (Balt.) 44 345-396 1965
von Hösslin C & Alzheimer A Ein Beitrag zur Klinik und Pathologischen Anatomie der Westphal-Strümpellschen Pseudosclerose Z. ges Neurol. Psychiat. 8 183-209 1912.

TABLE 1 *The Occurrence of Local Skin Reactions Induced by Skin Application of Cutting Oils and Their Additives on Mice*

Group	No. of animals	No. of animals with visible growth (papilloma)	Mean time for appearance of visible growth (papilloma) (days)	Duration of treatment (weeks)	Number of survivors	Grading of epidermal changes 0	I	II	III	IV	V	No. of animals with mastocytomas	No. of animals with mastocytomas associated with papillomas
A	11	5	214	31	9	–	1	3	6	1		3	1
B	9	0	–	31	7	–	1	3	3	–	–	1	0
C	10	7	235	31	7	–	–	4	5	1	–	2	0
D	10	4	231	31	5	–	2	5	3	–	–	1	0
E	9	9	227	31	7		1	2	2	4	–	5	4
F	10	8	233	31	8	–	2	3	5	–	–	4	3
G	8	0	–	31	8	8	–	–		–	–	0	0
H	11	0	–	31	10	11	–	–	–	–	–	0	0
I	10	0	–	31	10	9	1	–	–	–	–	0	0
J	9	0	–	31	8	–	7	2	–	–	–	0	0
K	10	2	155	1	9	1	1	4	4	–	–	0	0
L	8	1	156	31	5	2	3	1	–	–	–	0	0
M	10	0	–	31	8	9	–	–	–	1	–	0	0
N	9	0	–	21	9	8	1	–	–	–	–	0	0
O	10	0	–	21	8	10	–	–	–		–	0	0

The type of oil respective additive applied appears in the Text, page 732.

the carcinogenicity of modern brands of commercial cutting fluids in the literature (*Brown et al* 1975)

The object of the present investigation has been to determine the ability of certain commercial cutting oils and some additives used in commercial cutting fluids to induce tumours in the skin of mice

MATERIALS AND METHODS

Individual Oils and Additives Used for Application

Three different cutting oils were employed. These three were used in various forms.

The first was a commercial paraffin based straight cutting oil which had been solvent extracted It contains vegetable oils and traces of fatty aliphatic acid the manufacturers state that no biocides or extreme pressure additives (i e lead naphthenate) are present however it contains traces of corrosion inhibitors (aliphatic acid-alcohol esters) in fractions of a per cent Three variations of this oil were employed *A* the clean unused oil *B* used oil, previously utilized for metal working purposes (milling and turning) and *C* the supernatant of the used and centrifugated specimen

The second oil was a naphthalene based straight cutting oil containing oil from animal fat, but no biocides or corrosion inhibitors. This was employed in two forms *D* the clean unused oil and *E* the same brand but used

The third oil was a naphthalene based cutting oil emulsifiable with water containing sulphonated soap butyl-cellosolve (ethylene glycol monobutyl ether) (concentration 12 per cent) oleic acid and surplus of sodium hydroxide, silicone antifoam (polydimethyloxysilicone) and biocides (a mixture of hexahydrotriazine and n-oxy-methylamino derivatives) This was used as *F* the concentrated commercial stock and *G* the diluted emulsion of the oil in water

Additives Used in Cutting Oils

Six additives were employed

The first was the biocide hexahydro-1 3,5 tris-(2 hydroxyethyl)-S-triazine (*Watson & Sowden* (1972)) It bacteriocidal action is based on an interference of the protein synthesis It was used in three different concentrations *H* 0 15 per cent (w/v) *I* 1 5 per cent and *J* 15 per cent

The second was an additive composed of fatty alcohol amide and is termed in the present investigation *K*

The third was an additive composed of sulphonated oxidized fatty acid sodium salt termed *L*.

The *fourth* was ethylene-diamino-tetra acetic acid tetra-sodium salt and termed *M*

The fifth was polypropylenoxide, called *N*

The sixth was benzoic acid amino salt and termed *O*

Animal Material

Samples of the cutting fluids were tested on female NMRI mice aged 6 weeks (average weight 25 g) at the beginning of the study The animals were kept in groups of 8 to 11 in Macrolone cages (III/420/MAh, measuring 420×270×150 mm) with a galvanized cover

They were given an ad libitum diet of laboratory chow optimal in every respect, and water

Skin Application and Method of Evaluation

The exposure to different types of cutting oils and additives consisted of painting the skin thrice weekly The application during the experiment was of an average of 50 mg per application per animal. This was carried out with a soft brush on a shaved area of the upper part of the back, approximately the size of a finger nail

Sixty seven animals were painted with cutting oils (groups A G) while 77 animals in the additive painted groups served as controls for the evaluation of epidermal changes. The X-square test was used for the estimation of the difference in the incidence of visible exophytic growth and epidermal dysplasia or malignancy

Histological Methods

Routine assays were made on paraffin sections (thickness 3–4 μm) Staining with haematoxylin eosin and alkaline Kongo were routine on all sections.

In addition classical staining with van Gieson, Unna Pappenheim PAS and Toluidine blue were used on some sections.

Histological Grading of Epidermal Changes

Grade 0 No epidermal change

Grade I Hyperplasia. The number of epidermal cells was increased but the stratification and the cytological structures were unaltered

Grade II Slight dysplasia. The epidermal cells were enlarged with an associated lack of differentiation of the usual cell layers There was marked acidophilia of the cytoplasm, and bizarre nuclear figures were visible in the deeper layers (Fig 1)

Grade III Severe dysplasia. The epidermal cells had lost their polarity and a general disarrangement of the growth pattern was prominent. The cellular alterations, nuclear hyperchromasia and mitosis

TABLE I *The Oc rrenc of Local Skin R ction I d d by Skin Applicatio f Cutting Oils and Their Additi s in Mi*

Group	No. of animals	N of animals with lable growth (papilloma)	Mean time for appearance of ubl growth (papilloma) (days)	Duration of treatment (weeks)	Number of survivors	Grading of epidermal changes 0	I	II	III	IV	V	No. of animals w th mastocytomas	No. of nimals with mastocytomas associated with papillomas
A	11	5	214	31	9	–	1	3	6	1		3	1
B	9	0		31	7	–	1	3	3	–	–	1	0
C	10	7	235	31	7	–	–	4	5	1	–	2	0
D	10	4	231	31	5	–	2	3	3	–	–	1	0
E	9	9	227	31	7		1	2	2	4	–	5	4
F	10	8	233	31	8		2	3	3	–	–	4	3
G	8	0	–	31	8	8	–			–	–	0	0
H	11	0	–	31	10	11	–	–	–	–	–	0	0
I	10	0	–	31	10	9	1	–	–	–	–	0	0
J	9	0	–	31	8	–	7	2	–	–	–	0	0
K	10	2	155	21	9	1	1	4	4	–	–	0	0
L	8	1	156	31	5	2	3	1	–	–	–	0	0
M	10	0	–	31	8	9	–	–	–	1	–	0	0
N	9	0	–	21	9	8	1	–	–	–	–	0	0
O	10	0	–	21	8	10	–	–	–	–	–	0	0

The type of oil respective additi pplied ppears in the Text page 732

the carcinogenicity of modern brands of commercial cutting fluids in the literature (*Brown et al* 1975)

The object of the present investigation has been to determine the ability of certain commercial cutting oils and some additives used in commercial cutting fluids to induce tumours in the skin of mice

MATERIALS AND METHODS

Individual Oils and Additives Used for Application

Three different cutting oils were employed. These three were used in various forms.

The first was a commercial paraffin based straight cutting oil which had been solvent extracted. It contains vegetable oils and traces of fatty aliphatic acid the manufacturers state that no biocides or extreme pressure additives (i.e. lead naphthenate) are present however it contains traces of corrosion inhibitors (aliphatic acid alcohol esters) in fractions of a per cent Three variations of this oil were employed *A* the clean unused oil *B* used oil, previously utilized for metal working purposes (milling and turning) and *C* the supernatant of the used and centrifugated specimen

The second oil was a naphthalene based straight cutting oil containing oil from animal fat, but no biocides or corrosion inhibitors. This was employed in two forms *D* the clean unused oil and *E* the same brand but used.

The third oil was a naphthalene based cutting oil, emulsifiable with water containing sulphonated soap butyl-cellosolve (ethylene glycol monobutyl ether) (concentration 12 per cent) oleic acid and surplus of sodium hydroxide silicone antifoam (polydimethylsiloxysilicone) and biocides (a mixture of hexahydrotriazine and n-oxy-methylamino derivatives) This was used as *F* the concentrated commercial stock, and *G* the diluted emulsion of the oil in water

Additives Used in Cutting Oils

Six additives were employed

The first was the biocide *hexahydro-1,3,5-tris* (2 hydroxyethyl)-S-triazine (*Watson & Sowden* (1972)) Its bactericidal action is based on an interference of the prot n synthe i It was used in three different concentrations *H* 0 15 per cent (w/v) *I* 1 5 per ent and *J* 15 per cent

The second was an additive composed of fatty alcohol amide and i termed in the present investigation *K*

The third was an additive composed of sulphonated oxidized fatty acid sod um salt, termed *L*.

The fourth was ethylene-diamino-tetra-acetic acid tetra sodium salt and termed *M*

The fifth was polypropyleneoxide called *N*

The sixth was benzoic acid amino salt and termed *O*

Animal Material

Samples of the cutting fluids were tested on female NMRI mice aged 6 weeks (average weight 25 g) at the beginning of the study The animals were kept in groups of 8 to 11 in "Macrolone" cages (III/420/MAK, measuring 420×270×150 mm) with a galvanized cover

They were given an ad libitum diet of laboratory chow optimal in every respect, and water

Skin Application and Method of Evaluation

The exposure to different types of cutting oils and additives consisted of painting the skin three weekly The application during the experiment was of an average of 50 mg per application per animal. This was carried out with a soft brush on a shaved area of the upper part of the back, approximately the size of a finger nail.

Sixty seven animals were painted with cutting oils (groups A–G) while 77 animals in the additive painted groups served as controls for the evaluation of epidermal changes The X square test was used for the estimation of the difference in the incidence of visible exophytic growth and epidermal dysplasia or malignancy

Histological Methods

Routine assays were made on paraffin section (thickness 3–4 μm) Staining with haematoxylin-eosin and alkaline Kongo were routine on all sections.

In addition, classical staining with van Gieson, Unna Pappenheim, PAS and Toluidine blue were used on some sect ons.

Histological Grading of Epidermal Changes

Grade 0 — No epidermal change

Grade I — Hyperplasia. The number of ep dermal cells was increased but the stratification and the cytological structures were unaltered.

Grade II — Slight dysplasia The epidermal cells were enlarged with an associated lack of differentiation of the usual cell layers. There was marked acidophilia of th cytoplasm, and bizarre nuclear figures were visible in the deeper layers. (Fig. 1)

Grade III — Severe dysplasia. The ep dermal cells had lost their polarity and a general disarrangement of the growth pattern was prominent. The cellular alterations, nuclear hyperchromasia and mitosis

TABLE 2. *The Number of Animals with Amyloid Deposition in Organs.*

Group	A	B	C	D	E	F	G	H	I	J	K	L	M	N	O
Liver	3	2	1	0	1	0	0	0	0	0	7	2	2	0	0
Spleen	4	3	4	0	1	0	0	0	0	0	8	3	2	0	1
Kidney	1	0	0	0	5	1	0	0	0	3	5	2	2	0	1
No of animals	11	9	10	10	9	10	8	11	10	9	10	8	10	9	10

For the type of oil respective additive applied see page 732.

were present in half the thickness of the epidermis. (Fig 2)

Grade IV Carcinoma in situ (Disease of Bowen). The epidermis was characterized by complete loss of stratification, loss of polarity and disarrangement of the cells. Individual cell keratinization, multiple nuclei, nuclei in large pale cells, variable chromatin pattern and mitosis were seen in all cell layers. (Fig 3)

Grade V Invasive carcinoma. The same characteristics as Grade IV. In addition, invasion through the basement membrane and/or regional or distant metastases.

RESULTS

Pathological Changes of the Skin

The skin changes had similar features in each of the groups of animals painted with oil. Ulceration and squamous cell hyperplasia of the epidermis was prominent in most animals and various degrees of papillomatous exophytic growth, as well as acanthosis were

---

Fig 1 Hyperkeratotic papilloma with slight dysplasia of the epidermis. Hematoxylin-eosin (group F). Magnification × 40.

Fig 2 Severe dysplasia and acanthosis of the epidermis (group E). Hematoxylin-eosin. Magnification × 150.

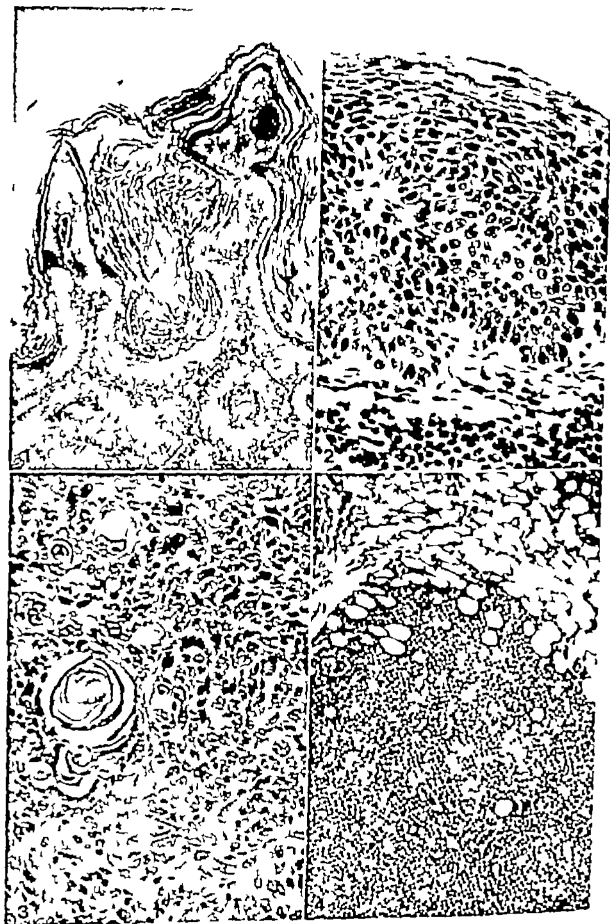
Fig 3 Area of papillomatous growth with severe dysplasia, keratine-pearls, and individual keratinization of epidermal cells. This was part of the epidermis with Bowenoid changes (group E). Hematoxylin-eosin. Magnification × 150.

Fig 4 Mastocytoma of the subcutaneous tissue (group E). Toluidine blue. Magnification × 150.

encountered (Table 1). The histological grading of the dysplastic epidermal changes ranged from 0 to IV (carcinoma in situ); this was observed in 4 animals of group E and one in each of groups A and C. The mean grading of the dysplasia was 2.2 based on all the animals in the various groups; however this figure was influenced by the animals in group G, as these had no dysplastic epidermal *changes at all.*

Forty-eight per cent of the animals in the oil exposed groups showed severe dysplasia or even more severe epidermal changes. In comparison, 8 per cent of the control group exposed to additives showed similar changes ($X^2 = 29.4$, $p < 0.001$). Forty nine per cent of the animals in the oil exposed groups showed *macroscopically visible* exophytic growth (papillomas) at the site of application. The mean time *prior to the* appearance of the papilloma was 229 days. In comparison 4 per cent of the control group showed similar exophytic growth after a mean period of 155 days. The incidence of papilloma bearing animals was higher in the oil treated groups ($X^2 = 59.3$, $p < 0.001$)

Various degrees of inflammatory reaction were observed. Application of used oils (groups B, C, E) tended to increase the inflammatory response. Severe subacute to chronic inflammation was found in the corium and subcutaneous tissue; this consisted of mononuclear and polymorphonuclear cells. Some of the latter were eosinophils. *Pyoderma*, subcorneal bullae and vasculitis were observed in most of these animals. Only *group F* of the animals exposed to unused oils (groups



2
3
4

sure additives (lead naphtenate sulphur chlorinated fats, paraffin oils and sulpho-chlorinated fats) corrosion inhibitors (secondary or tertiary hydroxylamines) dyes (i.e. fluorescein) water conditioners (polyphosphates, trisodium phosphate, borax and sodium carbonates) buffer components (i.e. aliphatic primary amines) and emulsifiers (sulphonates and soaps) (*Keys et al.* 1966))

Known toxic effects including carcinogenic potency have been reported with regard to some of the above mentioned components (*Wiebel et al.* 1975 *Irving* 1973 *Kriek* 1974 and *Stoltz et al.* 1974)

In the present communication death occurred in 24 per cent of the oil painted animals in contrast to 13 per cent in the additive painted animals during a period of thirty-one weeks. The surviving animals showed signs of local as well as systemic changes. Severe dysplasia of the epidermis was the most common finding together with the sporadic occurrence of carcinoma in situ in the groups where undiluted oils were employed. A high frequency of carcinoma in situ, as observed with used oil of type E, may suggest that more carcinogenic compounds are formed during metal processing, i.e. changes in naphtenic components or biocides. This oil gave a high incidence of papillomas (9/9). The present data indicate that skin lesions are more pronounced with straight cutting oils than with soluble oils in dilution, as oil G gave no epidermal dysplasia. However no significant differences could be seen when paraffin based oils were compared to those having a naphtalene base.

Paraffin based straight cutting oils were found to be more liable to induce amyloid deposition than naphtalene based oils. The association of transplantable mastocytomas and amyloidosis has previously been observed by *Rask Nielsen & Christensen* (1963). A possible explanation of this occurrence of mastocytosis (and mastocytomas) is a protective effect of heparin its antimitotic properties acting against the development of cancer.

With regard to the additives, the fatty alcoholamide was especially prone to cause the development of amyloid changes. This additive also induced epidermal dysplasia.

Desoille et al. (1973) have also described cutting oils as being inducers of benign papilloma, dysplasia and carcinoma. Similarly they reported cases of leucemia and bronchogenic carcinoma.

The findings of our present investigation are in agreement with occupational and carcinogenetic studies carried out previously (*Tourenc* 1964 *Carteaud* 1964 *Rivoire et al.* 1965 *Brown et al* 1975 and also literature loc. cit.)

Conclusion 1) The tested commercial cutting oils proved able to induce epidermal dysplastic changes in mice. 2) The substances responsible of the apparent carcinogenic properties of the cutting oils may be polycyclic aromatic hydrocarbons, remaining in the commercial products despite solvent refining, or may be found among the additives, the composition of which are generally a trade secret. 3) A similar effect on the skin of man must be considered probable. 4) Oil manufacturing companies should perform carcinogenic tests on their products, and a declaration as to the quality and quantity of additives should be compulsory.

The authors are very grateful to Danfoss A/S and Lubricor whose donation of funds enabled them to complete these studies.

REFERENCES

Bingham E., Horton A. W & Tye R. The carcinogenic potency of certain oils. AMA Arch. Environ Health *10* 449–451 1965

Brown A. J., Waldron H A & Waterhouse J A H Report on a study of occupational skin cancer with special reference to scrotal cancer by the Unesco References of Birmingham-Institute of Petroleum 1975.

Carteaud A. Cancer du scrotum du au goudron a ses dérivés Presse Medicale *72* 2355–2360 1964

Catchpole W M Macmillan, E. & Powell H: Specification for cutting oils with special reference to carcinogenicity Ann. Occup. Hyg. *14* 171–179 1971



Fig 5 Broad amyloid rings around splenic follicle. (Group O) Magnification × 150

A, D F) showed similar changes to those mentioned above while the inflammatory response in groups A and G was slight or absent. Groups D and E were characterized by slightly increased fibrosis

A large number of mast cells were present in the corium of groups A–F and these mast cells were marked by dense granulation. Apart from the above a high proportion of the animals in these groups revealed benign tumour like formations in the subcutaneous tissue These consisted of uniform cells arranged in chords, and on staining with toluidine blue appeared to be mastocytomas (Fig 4) Mastocytomas and papillomas were observed concomitantly in groups E and F

In mice treated by cutaneous application of oils the systemic findings consisted of varying degrees of sinus reticulosis in the *inguinal* lymph nodes. This was more pronounced and sometimes appeared rather *immature* in animals in which the inflammatory changes in the skin sections were prominent. A malignant mesenchymal tumour had spread to the liver and spleen in one animal of group A.

Eosinophilic necrosis and sinusoidal cell proliferation were prominent in the liver focal necrosis of the animals in groups A to F Slight to moderate degenerative changes in the liver were seen in some of the animals in groups G to O Various degrees of amyloid deposition was prominent in the kidney and spleen, as well as in the liver of the oil painted animals as well as in the additive painted groups (Fig 5 and Table 2)

DISCUSSION AND CONCLUSION

Many new formulas have been developed for the purpose of ameliorating the technical properties of cooling lubricating, inhibiting corrosion and the flushing away of metal chips, since the introduction of cutting oils in metal processing (*Taylor* 1907) A contamination of the skin and air passages of the machinist must be expected owing to evaporation and splashing The temperature at the tool edge reaches 800 C, which permits of evaporation and cracking reactions.

The principal composition of cutting fluids has been reported by *Key et al* (1966) Solvent refining of mineral oil based cutting fluids reduces the content of polycyclic aromatic hydrocarbons which are considered to be responsible for the carcinogenic properties of the oils. Subsequent to this, solvent refining has been widely introduced in the oil manufacturing industry

Modern brands of cutting fluids are interesting to study per se as a variety of additives are used for technical reasons. (Bactericides (cresylic acid, orthophenylphenol tris (hydroxymethyl) nitromethan)) extreme pres-

Acta path. microbiol. scand. Sect. A, 85: 739–744, 1977

IN VITRO ESTABLISHMENT AND SOME PROPERTIES OF AKR THYMOMA CELL LINES

Ingor Riesenfeld, Gunnar Tufveson and Gunnar V. Alm

Department of Virology, Institute of Medical Microbiology, University of Uppsala, Uppsala, Sweden

Riesenfeld, I., Tufveson, G. & Alm, G. V. *In vitro* establishment and some properties of AKR thymoma cell lines. Acta path. microbiol. scand. Sect. A, 85: 739–744, 1977.

Lymphoid cell lines could easily be directly established *in vitro* from spontaneous thymomas of aged AKR mice. The established lines all carried the Thy 1.1 antigenic marker of T lymphocytes. They differed markedly, however, from one another in several respects. Thus, they showed high or low quantity of Thy-1.1 antigens per cell, high or low sensitivity to cortisone and thymidine, as well as differing morphology and growth rate. The observed heterogeneity suggests that such AKR thymoma cell lines may provide a valuable tool to study T lymphocyte properties and the biology of the AKR thymoma, in particular non-immune and immune mechanisms influencing thymoma cell growth.

Key words: Thymoma, spontaneous; cell lines; *in vitro* establishment; mice.

I. Riesenfeld, Department of Virology, Biomedical Center, Box 584, 751 23 Uppsala 1, Sweden.

Received 9.ii.77. Accepted 26.iv.77.

The thymus is of critical importance to the high incidence of spontaneous lymphomas in the AKR mouse strain (7, 9). Lymphoma cells carry T cell markers (8) and are usually first demonstrated in the thymus (2, 7, 9). It is reasonable to assume that they actually originate in this organ.

Analysis of properties of such spontaneous thymomas of aged AKR mice may indicate whether they carry antigenic or funtional markers of any described subpopulation (1, 3, 10) of thymic lymphocytes. Such work may also provide a useful basis for studies of immune and non-immune regulatory mechanisms that may inhibit or promote lymphoma growth.

In the present communication we demonstrate that lymphoid cell lines are easily directly established *in vitro* from individual spontaneous AKR thymomas. The obvious advantage of this approach is that it eliminates the adaptive selection of lymphoma cells for growth in the presence of immune and non immune selective factors during conventional *in vivo* passage. Preliminary characterization of such AKR thymoma cell lines also revealed that they all carried the Thy 1.1 antigen but differed with respect to quantity of antigen expressed, morphology, growth rate and ability to grow in the presence of cortisone and thymidine.

MATERIALS AND METHODS

Animals. Female AKR/A mice (Gl. Bomholtgard, Ry, Denmark) were sacrificed at 6–8 months of age and examined for thymomas.

Preparation of thymoma cells. Thymoma tissue was passed through 60-mesh stainless steel wire screens with the continuous addition of a mixture

Cruickshank C N D & Squire J R Skin cancer in the engineering industry from the use of mineral oil Brit. J industr Med *7* 1–11 *1950*

Desoille H Philbert M Ripault G Carigneaux A & Rossignoli H Action cancérogene des huiles minérales utilisées en métallurgie. Arch. Mal Prof *34* 46 1973

Ely T S Scott F P Hearne F T & Stille W T A study of mortality symptoms and respiratory function in humans occupationally exposed to oil mist. J Occup Med. *12* 253–261 1970

Finnie J S Oil folliculitis. A study of 200 men employed in an engineering factory Brit. J industr Med. *17* 130–140 1960

Gilman J P W & Vesselinovitch S D Cutting oils and Squamous-cell carcinoma. Part II An experimental study of the carcinogenicity of two types of cutting oils Brit. J industr Med *12* 244–248 1955

Holmes J G Kipling M D & Waterhouse J A H Subsequent malignancies in men with scrotal epithelioma. The Lancet, July 25 214–215 1970

Irving C C Interaction of chemical carcinogens with DNA in "International Academy of Environmental Safety from International Symposium, Susono Japan (1973)

Key M M Ritter E J & Arndt K A Cutting and grinding fluids and their effects on the skin. American Industr Hyg Assoc Journal *27* 423–427 1966

Kriek E Carcinogenesis by aromatic amines. Biochimica et Biophysica Acta *355* 177–203 1974

Lee W R Alderson M R & Downes J E. Scrotal cancer in the north-west of England, 1962–68. Brit. J industr Med. 29 188–195 *1972*

Mastromatteo E Cutting oils and squamous-cell carcinoma. Part I Incidence in a plant with a report of six cases. Brit. J industr Med *12* 240–243 1955

Rask Nielsen R & Christensen H E. Studies on a transplantable mastocytoma in mice I Origin and general morphology J Nat. Cancer Inst. *30* 743–761 1963

Rivoire J Pommier A & Robillard J A propos des cancers cutanés chez les ouvriers décolleteurs, Bulletin de la Société française de dermatologie et de syphiligraphie *72* 322–324 1965

Stoltz D R Poirier L A Irving C C Stich, H F Weisburger J H & Grice H C Evaluation of short-term tests for carcinogenicity Toxicol. Appl Pharmacol *29* 157–180 1974

Taylor F W On the art of cutting metals. Trans. Am. Soc. Mech. Eng. *28* 31–58, 1907

Thony C & Thony J Enquete epidemiologique sur le cancer des huiles de coupe. In Proceedings of the XVI International congress on Occupational Health, p 655–657 Tokyo (1969)

Tourence R Le cancer du crotum chez les décolleteurs, La press Médicale *72* 2009–2012, *1964*

Wahlberg J E Skrotal-cancer och olja profylaktiska åtgärder Läkartidningen *69* 3044–3048 1972

Wallcave L Garcia H Feldman R Lijinsky W & Shubik P Skin tumourigenesis in mice by petroleum asphalts and coal tar pitches of known polynuclear aromatic hydrocarbon content. Toxicol. Appl. Pharmacol. *18* 41–52 1971

Watson E T & Scowden R H The way gray products meets customer requirements in the field of industrial biocides. Journal of the Institute of Petroleum *58* 263–267 *1972.*

Wiebel F J Leutz J C & Gelboin H V. Aryl hydrocarbon (benzo(A)pyrene) hydroxylase A mixed function oxygenase in mouse skin. J Invest. Dermatol. *64* 184–189 1975

reducing the ^{3}H TdR uptake by 50 per cent as compared to untreated controls.

RESULTS

In vitro initiation of AKR thymoma cell lines. No systematic study of the technique for establishment of thymoma cell lines was performed. It was found, however, that the establishment *in vitro* of lymphoid lines from individual thymomas was successful in approximately 50 per cent of the attempts. Contributing factors to this were the initial high cell density and the resulting rapid formation of a "feeder" layer of adherent thymic non-lymphoid cells. Lower cell densities (10^6 cells/ml) or absence of adherent cells resulted in poor or no take *in vitro* (results not shown).

TABLE 1. *Morphology and Growth Rate of AKR Thymoma Cell Lines*

Cell line	Morphology	Growth rate
I-8	Large, round	High
I 10	Small, round	Medium
I 15	Medium, round	Medium
I-45	Medium, polar	High
I 51	Small, round	Medium
I 521	Small, round	Medium
I 522	Medium, polar	High
I 57	Medium, round	Low
I 529	Medium, polar	High

Observations on morphology and growth rate. The different thymoma lines showed considerable differences in morphology and growth rate. The observations are merely summarized in Table 1 and detailed data are not included in this report. The morphology observed in the inverted phase-contrast microscope at 37 C ranged from small or large mainly round cells to medium-sized cells with "hand mirror shape", i.e. one uropode-like projection of the cytoplasm (see Fig. 1 for example). Also the growth rate and saturation densities of the lines varied.

Thy-1.1 antigens. As indicated in Table 2 all tested established cell lines carried Thy 1.1 antigens. The cytotoxic indices determined were between 0.90 and 1.00 using the qualitative trypan blue cytotoxicity assay (results not shown). The quantity of expressed Thy 1.1 antigens per cell was determined by the capacity to absorb diluted anti-Thy 1.1 antiserum. Table 2 gives the calculated number of absorbing cells of the different lines that gave a 50 per cent reduction of the anti Thy 1.1 induced lysis of ^{51}Cr labelled I 529 target cells.

It is clear that the quantity of Thy 1.1 antigens per cell varied for the thymoma lines. Lines I-8, I 10 and I 15 expressed much antigen, whereas the others, especially I 521, I 522, I 57 and I 529, considerably less antigen, per cell. The Thy 1.2 positive YAC lymphoma cell line, which is of A mouse

TABLE 2. *Expression of Thy-1.1 Antigen and Sensitivity to Cortisone and Thymidine of AKR Thymoma Cell Lines*

Parameter measured	Cell lines I-8	I 10	I 15	I-45	I 51	I 521	I 522	I 57	I 52[illegible]
Thy 1.1 antigens[1]	14	6	18	62	78	115	141	115	100
Cortisone sensitivity[2]	$10^{-[illegible]}$	$10^{-[illegible]}$	$10^{-[illegible]}$	$10^{-[illegible]}$	$10^{-[illegible]}$	$10^{-[illegible]}$	$10^{-[illegible]}$	–	$10^{-[illegible]}$
Thymidine sensitivity[3]	10^{-4}	$10^{-[illegible]}$	10^{-4}	10^{-4}	$10^{-[illegible]}$	$10^{-[illegible]}$	$10^{-[illegible]}$	–	$10^{-[illegible]}$

[1] Expressed as the number of absorbing cells (× 10) that caused a 50 per cent inhibition of the anti-Thy-1.1 antiserum. Cells of the Thy-1.2 positive YAC line caused no absorption in the test.
[2] Expressed as the cortisone concentration (M) causing 50 per cent inhibition of ^{3}H TdR uptake.
[3] Expressed as the concentration of thymidine during the pre-incubation causing 50 per cent inhibition of subsequent ^{3}H TdR uptake.

of equal parts of Hank's balanced salt solution and Dulbecco phosphate buffered saline (HPBS). Tissue fragments were removed by sedimentation and the cells were then centrifuged and washed once in HPBS. They were re-suspended in RPMI 1640 medium (Flow Laboratories, Irvine U.K.) supplemented with penicillin (100 U/ml) streptomycin (100 µg/ml) and 10 per cent heat inactivated (30 min at 56 C) foetal calf serum (FCS Flow Laboratories). The cell concentration was adjusted to 10^7 cells per ml.

Culture of thymoma cells. 2 ml of the cell suspension were added to 35 × 10 mm tissue culture treated Petri dishes (Flow Laboratories). The cultures were maintained stationary at 37 C in a water saturated atmosphere of 5 per cent CO_2 in air. Half of the medium was replaced daily initially without removing cells. When a layer of adherent cells had established non adherent thymoma cells were removed if necessary. At intervals, when growth of thymoma cells was found, cells were transferred to 25 cm^2 bottom area plastic culture bottles (Nunc, Roskilde Denmark) containing 3 ml medium. For production of larger quantities of cells, 90 cm^2 bottom area bottles (Nunc) with 20–30 ml medium were used. Cells used for experiments were harvested during exponential growth, at a density of approximately 0.8×10^6 cells per ml. All lines were kept *in vitro* for at least half a year and were sub-cultured every second day.

Dye exclusion cytotoxicity assay. Qualitative assay of Thy 1.1 antigens on thymoma cells was performed by means of a conventional trypan blue dye exclusion test. The anti Thy 1.1 antiserum was produced in CBA/J mice immunized with AKR/A thymocytes. Absorbed fresh frozen rabbit serum was used at the source of complement.

Quantitation of Thy-1.1 antigens. ^{51}Cr-labelled thymoma line I 529 cells were used as target cells. 5×10^6 cells in 1.0 ml of HEPES-RPMI 1640 supplemented with 10 per cent FCS were labelled with 300 µCi $Na_2{}^{51}CrO_4$ (Amersham-Searle Amersham, U.K.) for 4 hrs at 37 C in 35 × 10 mm culture dishes on a slowly rocking platform (2 cycles per min). The labelled cells were washed twice in medium and re-suspended to 1×10^6 cells per ml in complete medium.

The anti Thy 1.1 was titrated against the ^{51}Cr labelled target cells, and the antiserum dilution that gave 50–75 per cent lysis (see below) was used in the further test. A volume of 0.025 ml of such diluted anti Thy 1.1 was added to each of the wells of round bottomed microtiter plates (Linbro IS-MRC-96) and then two-fold dilutions of unlabelled thymoma cells of the different lines in 0.0125 ml medium were added in duplicates starting with 4×10^5 cells. The plates were incubated for 30 min at 4 C, with frequent mixing. Then, 2.5×10^4 ^{51}Cr-labelled I 529 cells in 0.025 ml medium were added per well, and the incubation proceeded for another 30 min at 4 C. As complement source there was added 0.0125 ml of a ½ dilution of rabbit serum per well followed by incubation for 30 min at 37 C. The microtiter plates were finally centrifuged at 4 C for 10 min at 600 × g and 0.0375 ml of the supernatants was removed for radioactivity determination in a Wallac gamma counter.

The percent inhibition of the lysis of ^{51}Cr labelled target cells caused by addition of unlabelled adsorbing cells from the various cell lines was calculated as follows:

$$\text{per cent inhibition} = 1 - \frac{\left(\begin{array}{c}\text{c.p.m. re-}\\\text{leased in the}\\\text{presence of}\\\text{absorb. cells}\end{array} - \begin{array}{c}\text{c.p.m.}\\\text{released}\\\text{without}\\\text{antibody}\end{array}\right)}{\left(\begin{array}{c}\text{c.p.m. re-}\\\text{leased in the}\\\text{absence of}\\\text{absorb. cells}\end{array} - \begin{array}{c}\text{c.p.m.}\\\text{released}\\\text{without}\\\text{antibody}\end{array}\right)} \times 100$$

The absorbing capacity of the cells from the different thymoma cell lines was expressed as the number of absorbing cells in the test that caused a 50 per cent inhibition of the lysis induced by antiserum.

Cortisone sensitivity. Cells of the different thymoma cell lines were cultured in flat-bottomed tissue culture plates (Linbro IS-FB-96-TC) in 0.1 ml volumes per well with an initial cell concentration of 0.2×10^6 *cells per ml.* HEPES (10 mM)-buffered RPMI 1640 medium with 10 per cent FCS was used. Hydrocortisone succinate (Solu-Cortef Upjohn, Kalamazoo Mich., U.S.A.) was added in 0.010 ml volumes to final concentrations of hydrocortisone ranging from 10^{-9} to 10^{-4} *M in the* medium. The cells were cultured for 24 hrs, the final 4 hrs in the presence of ^{3}H thymidine (^{3}H TdR) (New England Nuclear Boston Mass., U.S.A.) specific activity 0.8 Ci/mM, 0.25 µ Ci per culture. The pulsed cultures were harvested with a multiple cell culture harvester (Skatron, Lierbyen Norway) and the radioactivity collected on the glass-fiber filters was determined in a liquid scintillation counter. The sensitivity to cortisone was expresed as the concentration of cortisone reducing the ^{3}H TdR uptake by 50 per cent as compared to untreated controls.

Thymidine sensitivity. The sensitivity to unlabelled thymidine (Sigma, St Louis, Mo U.S.A.) was evaluated in the same way as for cortisone with thymidine concentrations ranging from 10^{-6} to 10^{-3} M. The only exception was that the cells in the microtiter plates were centrifuged and washed once in complete medium prior to the addition of the ^{3}H thymidine. The sensitivity to thymidine was expressed as the concentration of thymidine

origin, was included as a control and did not absorb significantly at any tested cell concentration.

Sensitivity to cortisone and thymidine Thymoma cell lines were tested for their ability to grow in the presence of cortisone or thymidine. The concentrations of the respective agent giving a 50 per cent reduction in ³H-thymidine incorporation were calculated. They are given in Table 2.

All thymoma lines were inhibited by cortisone but to a highly varying extent. The three lines I-45, I 522 and I 529 were relatively insensitive. This group included also I 10, which was slightly less resistant. The remaining lines were much more sensitive to growth inhibition by cortisone. The differences in the cortisone concentrations causing 50 per cent inhibition were approximately 1000-fold between the most sensitive and the resistant cell lines.

High concentrations of thymidine markedly inhibited the subsequent incorporation of ³H TdR of all cell lines. At low thymidine concentrations the lines separated into two main groups. Those that were highly sensitive were I 10, I 15, I 51 and I 521. Four lines were markedly less sensitive to thymidine, namely I-45, I 522, I 529 and I-8.

DISCUSSION

The present investigation demonstrates that *in vitro* lymphoid cell lines are easily established from the spontaneous thymomas of aged AKR mice. Critical in the adaption process to *in vitro* growth was an initially high cell density and at least one important consequence of this was the rapid formation of a feeder layer of non-lymphoid adherent cells. The thymoma cells eventually adapted to growth also in the absence of adherent cells.

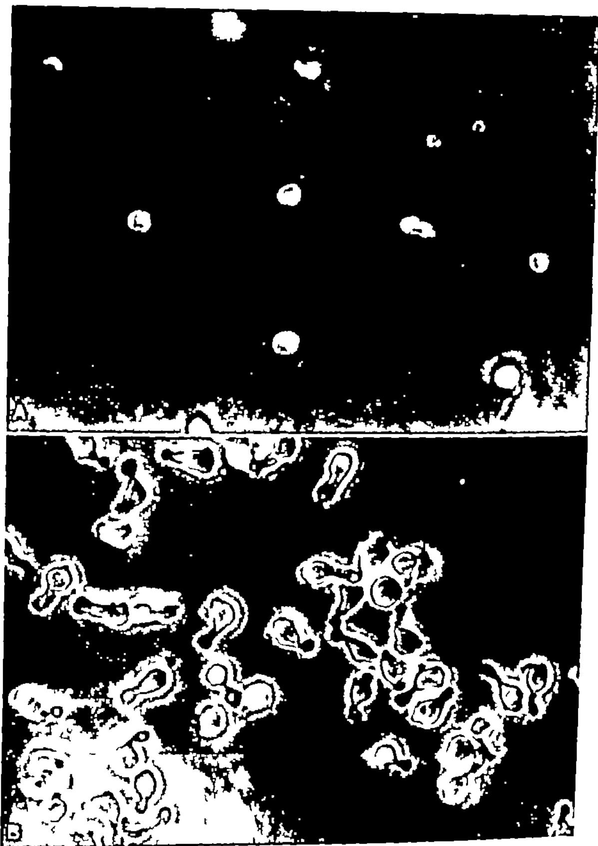
All established AKR thymoma cell lines carried the Thy 1.1 antigen suggesting their T-cell origin. However, as assessed by a number of criteria, they were markedly heterogeneous. These criteria included morphology, growth rate, quantity of Thy 1.1 antigen per cell, as well as sensitivity to cortisone and thymidine. Three lines showed similarities with regard to these rather crude parameters, while the remaining six were clearly unique in one or several respects.

Cortisone and thymidine were used in our study because of their documented inhibitory effect of the growth of lymphoma cells *in vitro* (4, 5, 6). Although they were primarily used as a tool to reveal heterogeneity within the group of established thymoma cell lines, it is clear that the concentrations of cortisone affecting the most sensitive thymoma cell lines are well within the physiological range.

In the present investigation we used localized thymomas as the source of tumor cells. The rationale was that such lymphoma cells taken at their probable site of origin and directly established *in vitro* had a minimal chance of adapting to host immune and non-immune resistance. Although we do not know whether the considerable differences between cell lines reflected corresponding differences between the original thymomas, this is at least one obvious possibility. Another is that these differences occurred during the adaptation to *in vitro* culture. It is likely that this at least decided what cells were permanently capable of *in vitro* growth. Thus, the thymoma I 529 was simultaneously established directly *in vitro* and as an *in vivo* passaged line. The *in vivo* variant failed to grow directly *in vitro*, while the *in vitro* established cell line after passage *in vivo* could easily be re-established *in vitro* (unpublished results).

We have thus established marked differences between *in vitro* AKR thymoma lines by several means, but we still do not know the reason for this heterogeneity. It may represent differences conserved from the originally transformed T lymphocytes, that have arisen at and after transformation *in vivo* or as a result of adaption to *in vitro* growth.

It is, however, a clear possibility that some of the AKR thymoma lines express T-cell receptors for antigen and perhaps also T-cell functions, and may thus be valuable models for the analysis of normal T-cell activities.



Example of easily-detected morphologic differences between the small, round *I 51* cell-line (A) and the medium-sized polar-shaped I 529 cell line (B) as observed in the inverted phase-contrast microscope (400 ×)

Acta path. microbiol. scand. Sect. A, 85 745–750 1977

TRANSPLANTABILITY AND METASTASIBILITY OF AN MCA INDUCED SARCOMA IN NUDE MICE

Influence of Transfer of Thymus Cells and Adoptive Immunity

BERNT BOERYD and MART SUURKÜLA

Department of Pathology I University of Linköping, Linköping,
and Department of Pathology I University of Göteborg, Göteborg, Sweden

Boeryd, B. & Suurkula, M. Transplantability and metastasibility of an MCA-induced sarcoma in nude mice. Influence of thymus cells and adoptive immunity Acta path. microbiol. scand. Sect. A, 85 745–750 1977

Challenge of C57/(nu/nu) mice with an MCA-induced sarcoma, MCG101 induced in C57BL/6J mice, disclosed higher resistance subcutaneously and intravenously than in syngenic C57/(+/+) mice. Transfer of 5 × 10 thymus cells to the nude mice brought their resistance to subcutaneously injected tumour cells back to the level of the C57/(+/+) mice, but only with the highest tumour cell doses tested, i.e. 5 × 10⁴ and 10⁵ cells. Against intravenously injected tumour cells similar effect by the thymus cells was only suggested. Spontaneous metastases from the same tumour transplanted to the tail did occur in the nude mice and were possibly facilitated by specifically sensitized spleen cells. The results indicate that the resistance to subcutaneously injected tumour cells in nude mice may well be dependent on their incapability to develop thymus-dependent immuno-responses and that spontaneous metastases can be facilitated by a weak immuno-response.

Key words Nude mice transplantable tumour spontaneous metastasibility thymus cell adoptive immunity

Bernt Boeryd, Department of Pathology I Regionsjukhuset, 581 85 Linköping, Sweden.

Received 27.ix 77 Accepted 31 77

It was shown in a previous communication that spontaneous metastasis formation did not increase in thymectomized, bone-marrow substituted, radiation chimeras (*Boeryd & Suurküla* 1973) but did so in less heavily immunosuppressed, thymectomized and sublethally irradiated mice (*Suurküla & Boeryd* 1974 1975a) These observations may indicate that some immuno-reactivity may be favourable for tumour spread. If so, the immuno-stimulation theory concerning tumour growth can be extended to the process of tumour spread, too.

The congenitally athymic nude mice offer a further possibility of evaluating the role of the thymus-dependent immune response to tumour growth and spread. They have a few T-cells (*Raff* 1973 *Prichard & Micklem* 1974) but are incapable of developing thymusdependent immuno-responses. This incapability can, however at least partly be restituted by thymus cells (*Pantelouris* 1971

Furthermore in our own current work they have been of immediate use because thymoma lines that show either high or low sensitivity to various factors influencing lymphoma cell growth *in vivo* and *in vitro* can be selected

---

This study was supported by grants from the *Swedish Cancer Society* and the *Medical Faculty of the University of Uppsala* We are grateful for the competent technical assistance of Mrs *Marianne Carlsson* and Miss *Ann Trönnberg*

REFERENCES

1 *Cantor H* & *Weissman I L.* Development and function of subpopulations of thymocytes and T lymphocytes. Prog Allergy *20* 1–64 1976

2 *Declève A Travis M Weissman I L. Lieberman M* & *Kaplan H S* Focal infection and transformation *in situ* of thymus cell subclasses by a thymotropic murine leukemia virus. Cancer Res. *35* 3585–3595 1975

3 *Droege W* & *Zucker R* Lymphocyte subpopulations in the thymus. Transpl Rev *25* 3–25 1975

4 *Harris A W* Differentiated functions expressed by cultured mouse lymphoma cells. I. Specificity and kinetics of cell responses to corticosteroids. Exp Cell Res. *60* 341–353, 1970

5 *Harris A W Bankhurst A D Mason S* & *Warner N L.* Differentiated functions expressed by cultured mouse lymphoma cells. II θ antigen surface immunoglobulin and a receptor for antibody on cells of a thymoma cell line J Immunol. *110* 431–438, 1973

6 *Horibata K* & *Harris A W* Mouse myelomas and lymphomas in cultures. Exp. Cell Res. *60* 61–77 1970

7 *Kaplan H S* Leukemia and lymphoma in experimental and domestic animals. Ser Haematol. *7* 94–163 1974

8 *Krammer P H., Citronbaum R Read S E., Forni L.* & *Lang R* Murine thymic lymphomas as models for T-cell studies T-cell markers, immunoglobulin and Fc receptors on AKR thymomas Cellular Immunol *21* 97 111 1976

9 *Metcalf D.*, The thymus Springer Verlag Berlin, 1966 p. 89–118

10 *Shortman K Von Boehmer H Lipp J* & *Hopper R* Subpopulations of T-lymphocytes Transpl Rev *25* 163–210 1975

Acta path. microbiol. scand. Sect. A, 85 745–750 1977

TRANSPLANTABILITY AND METASTASIBILITY OF AN MCA-INDUCED SARCOMA IN NUDE MICE

Influence of Transfer of Thymus Cells and Adoptive Immunity

BERNT BOERYD and MART SUURKÜLA

Department of Pathology I University of Linköping, Linköping
and Department of Pathology I University of Göteborg, Göteborg, Sweden

Boeryd, B. & Suurküla M. Transplantability and metastasibility of an MCA-induced sarcoma in nude mice. Influence of thymus cells and adoptive immunity Acta path. microbiol. scand. Sect. A, 85 745–750 1977

Challenge of C57/(nu/nu) mice with an MCA-induced sarcoma, MCO101 induced in C57BL/6J mice, disclosed higher resistance subcutaneously and intravenously than in syngeneic C57/(+/+) mice. Transfer of 5×10^7 thymus cells to the nude mice brought their resistance to subcutaneously injected tumour cells back to the level of the C57/(+/+) mice but only with the highest tumour cell doses tested, i.e. 5×10^4 and 10^5 cells. Against intravenously injected tumour cells a similar effect by the thymus cells was only suggested. Spontaneous metastases from the same tumour transplanted to the tail did occur in the nude mice and were possibly facilitated by specifically sensitized spleen cells. The results indicate that the resistance to subcutaneously injected tumour cells in nude mice may well be dependent on their incapability to develop thymus-dependent immuno-responses and that spontaneous metastases can be facilitated by a weak immuno-response

Key words Nude mice transplantable tumour spontaneous metastasibility thymus cells adoptive immunity

Bernt Boeryd, Department of Pathology I Regionsjukhuset, 581 85 Linköping, Sweden.

Received 27.ii.77 Accepted 31 77

It was shown in a previous communication that spontaneous metastasis formation did not increase in thymectomized, bone-marrow substituted, radiation chimeras (*Boeryd & Suurküla* 1973) but did so in less heavily immunosuppressed, thymectomized and sublethally irradiated mice (*Suurküla & Boeryd* 1974 1975a) These observations may indicate that some immuno-reactivity may be favourable for tumour spread. If so, the immuno-stimulation theory concerning tumour growth can be extended to the process of tumour spread, too.

The congenitally athymic nude mice offer a further possibility of evaluating the role of the thymus-dependent immune response to tumour growth and spread. They have a few T-cells (*Raff* 1973 *Prichard & Micklem* 1974) but are incapable of developing thymus-dependent immuno-responses. This incapability can, however at least partly be restituted by thymus cells (*Pantelouris* 1971

Kindred 1971 *Kindred & Schreffler* 1972) or by grafting neonatal thymus (*Kindred & Loor* 1974 *Loor et al* 1976)

Although transplanted tumours, even xenogenic ones, grow in nude mice they are said not to metastasize spontaneously (*Rygaard* 1973) However *Maguire et al* (1976) noted spontaneous metastates in nude mice from a Syrian hamster tumour and *Stutman* has described spontaneous metastases from autochthonous tumours, MCA induced lung adenomas (1974) and polyoma induced tumours (1975) in these mice The reasons for the resistance to spontaneous metastasis formation from transplanted tumours in nude mice are not clear It may depend on the described reluctance of the tumours to infiltrate (*Rygaard* 1973) on the immune deficiency of those mice or on other factors.

In pilot studies the growth of the MCA induced sarcoma MCG101 transplantated as small solid pieces to the tail was similar in C57/(nu/nu) and syngenic C57/(+/+) mice viz. the strong antigenic tumour (*Boeryd & Suurküla* 1973) grew equally in the nude mice who lack a thymus as in their normal counterparts (unpublished results) In the same pilot study spontaneous metastases developed only occasionally in the nude mice

The aim of this preliminary investigation was to study a) Whether in nude mice spontaneous metastasis formation from transplanted tumour could be facilitated by transfer of immuno-competent cells. For this part of the study we used low doses of specifically sensitized spleen cells This approach is in part similar to that of *Prehn* (1972) who demonstrated that small numbers of specifically sensitized spleen cells added to a tumour cell suspension faciliated the tumour growth subcutaneously in thymectomized sublethally irradiated mice The spontaneous metastasibility in the nude mice was compared with that in thymectomized sublethally irradiated C57/(+/+) mice

b) Whether in nude mice the transplantability of tumour cells subcutaneously or intravenously could be influenced by transfer of thymus cells from C57/(+/+) mice

MATERIAL AND METHODS

Animals and tumours C57BL/6J/Bom/(nu/nu) mice from Bomholtgård Denmark, and inbred C57BL/6J/(+/+) 10–12 weeks old were used The nude mice were in their 4–5 back-cross generation. The MCA induced sarcomas MCG101 and MCG102 syngenic in the C57/(+/+) mice (*Boeryd & Suurküla* 1973) were used in their 4–6 transfer generations. MCG101 was used for the metastases and transplantation studies, MCG-102 only for non-specific sensitization of spleen cell donors Monodisperse tumour cell suspensions were prepared as described previously (*Boeryd & Suurküla* 1973) Immunization of spleen cell donors, 3–4 months old C57/(+/+) mice was done by transplanting vital tumour tissue subcutaneously into the flank 10 days before harvesting the spleens. Thymectomy and sublethal irradiation (560 R) of the C57/(+/+) mice were performed as described previously (*Boeryd & Suurküla* 1973 *Suurküla & Boeryd* 1974)

Preparation of thymus and spleen cells Thymuses and spleens were minced and pressed through a sterile steel mesh. The resulting suspensions were allowed to sediment in tubes for a few minutes. The cells in the supernatant were washed three times in Hanks BSS and re-suspended in Parker 199 The concentration was determined in a Bürker chamber

Tumour transplantation For the study of spontaneous metastasis formation a piece of solid tumour was transplanted subcutaneously in the tail as described previously (*Hagmar & Boeryd* 1968) For the study of the transplantability of tumour cells the cell suspensions were injected subcutaneously into the flank or intravenously into a tail vein in 0 1 ml Parker 199

Registration of tumour growth and metastases. The tumour growth at the subcutaneous transplantation site was evaluated by weighing the tumour The tail tumours including 2 cm of the tail were weighed 17 days after transplantation and the subcutaneous tumours resulting from the injected tumour cell suspensions were weighed after 18 days. Gross spontaneous metastases were noted at autopsy Pulmonary metastases were noted after histological investigation of step sections from the lungs prepared according to *Boeryd* (1965)

Statistical methods Differences in tumour weight were tested by *Wilcoxon's* two-sample rank test. Differences in incidences of metastases were tested by Fisher's exact test $P < 0.05$ was accepted as significant

RESULTS

The tumour growth from transplanted solid pieces was similar in nude mice and in thymectomized, irradiated mice irrespective of

TABLE 1. *Spontaneous Metastasis Formation from MCG101 in Nude Mice and Thymectomized C57/(+/+) Mice after Transfer of Non-Specifically and Specifically Sensitized Spleen Cells. Thymectomy 16 Days, Irradiation 8 Days and Spleen Cells Given Intraperitoneally the Day before Tumour Transplantation. Amputation of Tail Tumours 17 Days after Transplantation. Observation Period 47 Days*

Groups	Treatment	No. of spleen cells: Non-specif. sensitized (MCG102)	No. of spleen cells: Specif. sensitized (MCG101)	Average tumour weight	Incidence of metastases: to lymph-nodes	to lungs	total
C57/(+/+)				0.70	0/8	0/8	0/8
Nude mice		10^4		0.77	0/9	0/9	0/9
		10^8		0.80	0/9	1/9	1/9
–			10^4	0.71	1/7	0/7	1/7
–			10^8	0.75	1/8	1/8	2/8
C57/(+/+)	Tx + 560R	10^4		0.54	3/6	3/6	4/6
–	–	10^8		0.75	3/3	1/3	3/3
–	– –		10^4	0.63	5/10	0/10	5/10
	– –		10^8	0.75	4/10	1/10	4/10

TABLE 2. *Metastases from Intravenously Injected MCG101 Cells in C57/(+/+) Mice and Nude Mice Untreated or Transfused Intraperitoneally with 5 × 10⁷ Thymus Cells 8 Days before Tumour Cell Challenge. Observation Period 18 Days*

Groups	Thymus cells	Tumour challenge dose	Incidence of metastases: to lungs	to extrapulm. organs	total
C57/(+/+)	—	5 × 10	6/9	–	6/9
Nude mice	—	– –	0/5	–	0/5
–	+	– –	2/5	–	2/5
C57/(+/+)	—	7.5×10^5	10/10	10/10	10/10
Nude mice	—	–	1/5	1/5	2/5
	+		5/5	2/5	4/5

the type of lymphoid cell treatment, and not significantly different from that in C57/(+/+) mice (Table 1).

Spontaneous metastases did not develop in C57/(+/+) mice. Only one of 18 nude mice given non-specifically sensitized spleen cells had metastases, while metastases occurred in 3 of 15 such mice given specifically sensitized spleen cells. Metastases were more frequent in thymectomized, sublethally irradiated C57/(+/+) mice than in nude mice. The incidence of pulmonary metastases tended to be reduced in thymectomized, irradiated mice given specifically sensitized spleen cells, 1/20 (0/10 + 1/10) compared to those given non-specifically sensitized spleen cells 4/9 (3/6 + 1/3) ($P = 0.10$). In thymectomized irradiated mice given non-specifically sensitized spleen cells, the total incidence of metastases was higher than in similarly treated nude mice (7/9 (4/6 + 3/3) compared to 1/18 (0/9 + 1/9) ($P < 0.002$). However this difference between thymectomized irradiated mice and nude mice was abolished after transfer of specifically sensitized spleen cells 9/20 compared to 3/15 ($P < 0.20$) (Table 1).

The nude mice were more resistant to sub-

TABLE 3 *Subcutaneous and Intravenous Challenge with MCG101 Cells in C57/(+/+) Mice and Nude Mice Untreated or Given 5×10⁷ Thymus Cells Intravenously 13 Days before Challenge Subcutaneous Tumours Weighed 18 Day and Intravenously Challenged Mice Observed for 19 Days after Challenge*

Groups	Tumours challenge dose									
	10^3		10^4		5×10^4			10^5		
	Incidence of takes and average tumour weight (g)									
	s.c.		s.c.		s.c.		i.v.	s.c.		i.v.
C57/(+/+)	5/5	0 04	5/5	0.38	5/5	0 64	7/8	5/5	0 68	8/8
Nude mice	4/5	0 01	5/5	0 19	4/4	0.33¹)	1/8	5/5	0.35²)	7/8
Nude mice thymus cells	0/5	–	4/4	0 05	5/5	0 88	2/7	5/5	0.55³)	2/8

¹) 0.33 # 0 64 $P < 0.05$
²) 0.35 # 0 68 $P < 0.15$
³) 0.55 # 0.35 $P < 0.15$

cutaneously as well as to intravenously injected tumour cells than the C57/(+/+) mice. Transfer of thymus cells to nude mice possibly reduced their resistance to intravenoulsly injected tumour cells up to cell doses of 7.5×10⁴ (Table 2) and reduced it against subcutaneously injected tumour cells, but only in doses of 5×10⁴ and 10⁵ However with near threshold doses subcutaneously 10³ and 10⁴ cells thymus cell transfer to the nude mice had no effect compared to C57/(+/+) mice. (Table 3)

DISCUSSION

The nude mice were more resistant to intravenously as well as to subcutaneously injected tumour cells than the C57/(+/+) mice Similar findings concerning intravenously transfused tumour cells have recently been reported by *Skow et al* (1976) and concerning subcutaneously transplanted tumour cells by *Maguire et al* (1976) On the contrary in the present study the tumour growth from transplanted solid pieces of tumour in nude mice was not different from that in C57/(+/+) mice In previous *experiments with* heavily immuno-suppressed mice thymectomized chimeras, the tumour growth from subcutaneously challenged as well as from solid pieces of MCG101 was slower than in normal mice (*Boeryd & Suurkula* 1973) Thus, the tumour growth from subcutaneously challenged tumour cells in the nude mice and in the thymectomized chimeras differed from the controls in a similar way while the growth from transplants of solid pieces differed from the controls *only in* the thymectomized chimeras There are probably some differences between these two types of "B-mice" in their ability to resist tumour growth Thus, *Stanbridge et al* (1975) found lesser sensitivity to transplanted HeLa cells in nude mice than in thymectomized chimeras

It is known that transfer of thymus cells to nude mice partly restores their T-cell reactivity (*Pantelouris* 1971 *Kindred 1971 Kindred* & *Schreffler* 1972) In these experiments the transfer of thymus cells brought the resistance of the nude mice to subcutaneously injected tumour cells to the level of the normal mice, noted first, however when the cell dose equalled or exceeded 5×10⁴ while a similar effect on intravenously injected tumour cells was only suggested in some experiments. These effects of the thymus cell transfer indicate that the transplantation resistance in nude mice to dissociated tumour cells subcutaneously and possibly intravenously is,

in fact, caused by the lack of T-cell-dependent immune reactivity. Such a conclusion is compatible with the immuno-stimulation theory (*Prehn* & *Lappé* 1971, *Prehn* 1976). The lack of effect of thymus cell transfer on the tumour growth from the lowest tumour cell doses, 10^3 and 10^4 given subcutaneously possibly reflects a mechanism related to the "sneaking through" phenomenom (*Old et al* 1962).

The other aim of the present work was to study whether small doses of immuno-competent cells, specifically sensitized spleen cells, could facilitate spontaneous metastasis formation in nude mice. The results suggest such a facilitation. Previously we observed higher spontaneous metastatibility of the same tumour in thymectomized, sublethally irradiated mice (*Suurküla* & *Boeryd* 1974) than in thymectomized chimeras (*Boeryd* & *Suurküla* 1973). The suggested facilitation of tumour spread by immuno-competent cells in the present study supports the conclusion that some, but weak, immunity could enhance the spontaneous metastasis formation. The effect of transferred thymus cells on spontaneous tumour spread in nude mice will be investigated.

Specifically sensitized spleen cells tended to inhibit the spontaneous metastasis formation to the lungs in thymectomized irradiated mice, an effect similar to that described in a previous communication (*Suurküla* & *Boeryd* 1975b).

It seems reasonable to interpret the results of the experiments in nude mice in terms of immunological mechanisms. However, the nude mice may have other unknown, non-immunological properties of importance for tumour growth and spread, different from those in normal mice.

The present preliminary study comprises experiments with a limited number of mice and experimental groups. Nevertheless, the results indicate that the nude mice are valuable tools for the investigation of possible differences in the effect of immune mechanisms on local tumour growth, chanlleged tumour cells, and metastasis formation.

This investigation was supported by research grants from the *Swedish Cancer Society* (Project Number 136-B76-10XA). We wish to thank Miss *Anita Osbeck* and Miss *Barbro Melin* for skillful technical assistance.

REFERENCES

Boeryd B.: Action of heparin and plasminogen inhibitor (EACA) on metastatic tumour spread in an isologous system. Acta path. microbiol. scand. 65: 395–404, 1965.

Boeryd B. & *Suurküla M.*: Tumour metastasis in mice with reduced immune reactivity. I. Studies with two MCA-induced sarcomas in radiation and thymectomized radiation C57BL/6J chimeras. Int. J. Cancer *12*: 722–727, 1973.

Hagmar B. & *Boeryd B.*: Effect of heparin, ε-aminocaproic acid and protamine on spontaneous metastasis formation from resectable tail tumours. Pat. europ. *3*: 509–520, 1968.

Kindred B.: Antibody response in genetically thymus-less nude mice injected with normal thymus cells. J. Immunol. *107*: 1291–1295, 1971.

Kindred B. & *Schreffler D. C.*: H-2 dependence of co-operation between T and B cells *in vivo*. J. Immunol. *109*: 940–943, 1972.

Kindred B. & *Loor F.*: Activity of host-derived T-cells which differentiate in nude mice grafted with co-isogenic or allogenic thymuses. J. exp. Med. *139*: 1215–1227, 1974.

Loor F., *Kindred B.* & *Hägg L.-B.*: Incomplete restoration of T-cell reactivity in nude mice after neonatal allogenic thymus grafting. Cell Immunol. 26: 29–46, 1976.

Mogul H. J., *Cutera H. C.*, *C. dar R. P.* & *Prehn R. T.*: Invasion and metastasis of a xenogenic tumour in nude mice. J. Nat. Cancer Inst. 57: 439–442, 1976.

Old L. J., *Boyse E. A.*, *Clark D. A.* & *Carswell E. A.*: Antigenic properties of chemically induced tumours. Ann. N.Y. Acad. Sci. *101*: 80–106, 1962.

Pantelouris E. M.: Observations on the immunobiology of "nude mice". Immunology *20*: 247–252, 1971.

Prehn R. T.: The immune reaction as a stimulator of tumour growth. Science *176*: 170–171, 1972.

Prehn R. T.: Do tumours grow because of the immune response of the host? Transpl. rev. *28*: 34–42, 1976.

Prehn R. T. & *Lappé M. A.*: An immunostimulation theory of tumour development. Transpl. rev. *7*: 26–54, 1971.

Prichard H. & *Micklem, H. S.*: The nude (nu/nu) mouse as a model of thymus and T-lymphocyte deficiency. In Proceedings of the first international workshop on nude mice, pp. 127–

139 *Rygaard J & Povlsen C O* (Ed.) Gustav Fisher Verlag Stuttgart, 1974

Raff M C Θ-bearing lymphocytes in nude mice Nature *246* 350–351 1973

Rygaard J Thymus & Self Immunobiology of the mouse mutant nude F.A.D L. Copenhagen, 1973

Skov C B Holland J M & Perkins E H Development of fewer tumor colonies in lungs of athymic nude mice after intravenous injection of tumor cells. J Nat Cancer Inst *56* 193–195 1976

Stanbridge E J Boulger L R Franks C R Garret J A Reeson D E Bishop D & Perkins F T Optimal conditions for the growth of malignant human and animal cell populations in immunosuppressed mice. Cancer Res. *35* 2203–2212 1975

Stutman O Tumor development in immunologically deficient nude mice after exposure to chemical carcinogens. In Proceedings of the first international workshop on nude mice pp. 257–264 *Rygaard J & Povlsen C O* (Eds.) Gustav Fisher Verlag, Stuttgart, 1974

Stutman O Tumor development after polyoma infection in athymic nude mice J Immunol. *114* 1213–1217 1975

Suurküla M & Boeryd B Tumour metastasis in mice with reduced immune reactivity II Studies with a highly antigenic MCA induced sarcoma in thymectomized and/or sub-lethally irradiated C57BL/6J mice Int. J Cancer *14* 633–641 1974

Suurkula M & Boeryd B Tumour metastases in mice with reduced immune reactivity III Studies with three weakly antigenic tumours in thymectomized and/or sublethally irradiated mice Int. J Cancer *16* 404–412 1975a.

Suurküla M & Boeryd B Tumour metastasis in mice with reduced immune reactivity IV Restoration of relative resistance to metastasis formation in thymectomized sublethally irradiated mice by spleen cells. Path. europ. *10* 299–305 1975b.

Acta path. microbiol. scand. Sect. A, 85 751–760, 1977

THE NEPHROTOXIC EFFECT OF THE OTOTOXIC COMPOUND ATOXYL

M. Anniko and A. Ljungqvist

Departments of Otolaryngology and Pathology Karolinska Sjukhuset, and King Gustaf V Research Institute Karolinska Institutet, Stockholm, Sweden

Anniko, M. & Ljungqvist, A. The nephrotoxic effect of the ototoxic compound atoxyl. Acta path. microbiol. scand. Sect. A, 85 751–760, 1977

The arsenical compound atoxyl has been used in labyrinthine research because of its documented effects both on cells engaged in an active transport of ions (secretory epithelia) and sensory epithelia (cochlear hair cells and vestibular sensory cells type I and type II). In the present experiments both the kidney and the structures of the inner ear were studied. The renal tubules were damaged by exposure to atoxyl. Tubular casts, haemorrhages (both in the tubules and in the renal calices) and tubular epithelial cell necrosis occurred. A common denominator in the ototoxic and the nephrotoxic actions of acute atoxyl poisoning might be disturbance of the very active ion transport systems of the cells involved.

Key words: Atoxyl; ototoxicity; nephrotoxicity; correlation inner ear-kidney

M. Anniko, Department of Otolaryngology, Karolinska Sjukhuset, 10401 Stockholm 60, Sweden.

Received 5. 77 Accepted 5. 77

A variety of pathologic conditions exists in which the inner ear and the kidney are simultaneously affected (*Alport* 1927, *Hognestad* 1967, *Winter et al.* 1968, *Merck et al.* 1976). In patients with chronic renal insufficiency and impaired hearing, *Kopsa et al.* (1972) demonstrated damage to the cochlear hair cells. An association between impaired renal function and drug-induced ototoxicity has also been shown under controlled laboratory conditions (*McCrudy et al.* 1974).

When damage to both organs occurs, the relation between ototoxicity and nephrotoxicity indicates that the two processes may have a similar biochemical basis. The renal tubules and the secretory tissues of the inner ear are both engaged in the active transport of ions, and both can be damaged by the accumulation of toxic substances such as strongly basic aminoglycoside antibiotics. Thus *Hawkins* (1968) reported that kanamycin, viomycin, and in particular neomycin, are both ototoxic and nephrotoxic, causing the destruction of the epithelium of the renal proximal tubules. This may however regenerate if the drug is withdrawn.

The ototoxic effect of the arsenical compound atoxyl (sodium arsanilicum, Pro Gen® Sodium) was experimentally described by *Miyamoto* (1931) and later used as a tool in the study of cochlear hair cell pathology by *Rüedi* (1951) and *Nassaphus* (1951). *Anniko & Wersäll* (1975, 1977) have documented the ultrastructural changes in the sensory and secretory epithelia in the vestibular and cochlear labyrinths following atoxyl administration.

The aim of the present study was to investigate whether or not a cell damage will

appear in the kidney as well as in the cochlea following the administration of atoxyl

MATERIAL AND METHODS

Seventy-two healthy young guinea-pigs (250–350 g) were used in the experiment. The control group consisted of five healthy untreated animals.

A 2 per cent solution of atoxyl in sterile water was administrated subcutaneously to each animal during a certain period of time. The atoxyl was administered daily and only if the guinea pig showed signs of severe intoxication was the interval between the injections lengthened to avoid animal death.

The injected dose of atoxyl on each occasion varied from 20 to 140 mg/kg b w administered during 1–81 days. The animals were examined 1–54 days after the last injection The longest time elapsing from the first injection until sacrificing the animal was 108 days. *Anniko* (1976 a) has published a complete table showing the amounts of atoxyl mg/kg b w administered to each guinea-pig in the experiment group

The methods used for the fixation and preparation of materials for light and electron microscopy of the cochlea and the cristae ampullares have been described previously by *Wersäll* (1956) *Anniko* & *Wersäll* (1975) and *Anniko* (1976 a b)

For the examination of the renal tissue, both kidneys of each animal were removed and placed in an ice-cold (+ 4 C) 10 per cent formaldehyde solution for fixation Histological sections were prepared and stained with haematoxylin and eosin

RESULTS

The Labyrinth

Light and Electron Microscopy

The cochlea. The cochlear alterations depended on whether or not the animals were chronically (20–40 mg/kg/day during several weeks) or acutely (at least 140 mg/kg b w within 24–36 hours) intoxicated. The chronically poisoned group of animals showed a degeneration of both the outer (OHC) and the inner (IHC) hair cells starting at the apical region of the cochlea (Fig 1) The distribution of hair-cell damage depended on the treatment period, but the dose at each injection was also *of importance* (increased hair-cell loss following higher *amounts*) No damage was observed in the metabolically active cells of the stria vascularis (Fig 2)

Acute atoxyl poisoning caused cellular alterations among both sensory and secretory epithelia (Fig 3 4) Also in this case the degeneration started in the apical region of the cochlea. The normally smooth surface of the stria vascularis became uneven and marginal and intermediate cells were rejected from the strial surface into the endolymphatic space (Fig 4 5)

The cristae ampullares The sensory and the secretory epithelia of the cristae ampullares reacted in a similar way as those of the cochlea to the atoxyl poisoning. No individual difference occurred between the three separate cristae of the inner ear in the same guinea pig

Chronic atoxyl intoxication caused damage mainly to the hair cells of type I although hair cells of type II were also affected, but to a less extent Acute poisoning resulted initially in severe primary changes in the *secretory epithelia (Fig 6)*

Fig 1 Transmission electron microscopy (TEM) Chronic atoxyl intoxication. *Disarrangement* of the normally regular three rows of cochlear outer hair cells (OHC) is an early sign of toxic damage.

Fig 2 Light microscopy (LM) Chronic intoxication Stria vascularis. Normal morphology

Fig 3 TEM Tangential section. Acute atoxyl poisoning Reissner's membrane (RM) *is depressed over the tectorial membrane (TM) which is tightly lying over the organ of Corti.* Severe degeneration of an outer hair cell (OHC) with vesiculation of the cytoplasm and disarrangement of mitochondrial cristae. The nuclear chromatin is fragmented. Arrow *debris from an adjacent outer* hair cell.

Fig 4 LM *Acute atoxyl intoxication. Stria vascularis. The normally smooth surface is disintegrating with rejection of strial cells. Inset* TEM. Detail from an intermediate cell in the stria vascularis. The cristae mitochondriales are separated from each other

1 OHC OHC OHC 10 µm

2 40 µm

3 RM TM OHC 5 µm

4 40 µm

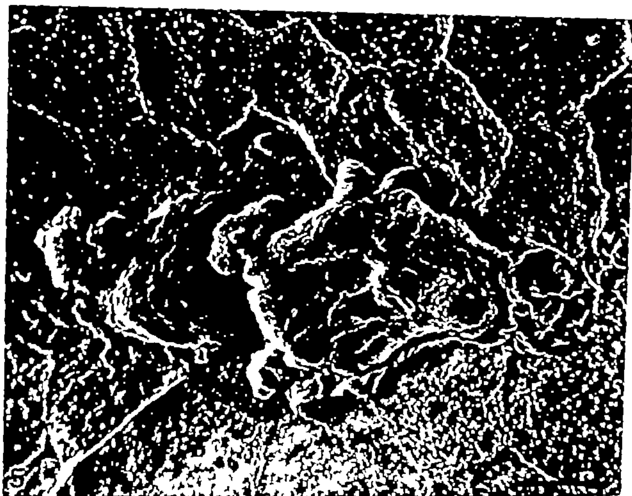


Fig 5 Scanning electron microscopy (SEM) Acute atoxyl intoxication. Stria vascularis. Protrusions (P) which may include several adjacent strial cells extrude into the endolymphatic space.

The Kidneys

Macroscopic Findings

Acute atoxyl intoxication (a total dose of at least 140 mg/kg b. w within 24–36 hours) caused swelling of the kidney The outer surface appeared haemorrhagic after removing the capsule When the kidney was divided into pieces, haemorrhages in the renal parenchyma were observed

In chronic intoxication no lesion was found macroscopically

Light Microscopy

The kidneys from two of the five control animals showed a normal histological picture whereas a certain degree of nephrocalcinosis was found in the other three animals

Nephrocalcinosis including signs of non specific pyelonephritis, was also seen in eleven experimental animals Ten of these were examined after a prolonged period following the last injection of atoxyl whereas one animal was examined the day after the last injection This latter animal belonged to the group receiving the lowest amount of atoxyl at each injection (20 mg/kg b w)

Animals with obvious signs of toxic renal damage could all be included in the group of acute poisoning The changes were rather typically localized to the cortico-medullary zone and could be classified into three degrees (+ ++ and +++) depending on the severity of the renal damage (Table 1) The degree of renal damage was found to be related to the amount of atoxyl at each injection the interval between the administrations, the total dose and the length of

TABLE 1 *Table Illust ating the D gr of Damage to the I er Ear and t the Kid ey Following Atoxyl Treatment*

	Mg/kg on each occasion	Preyer's reflex	Kidney morphology			
			Normal	Toxic damage		
				+	+ +	+ + +
Acute intoxication	70	+ (+) or —	×)		(×)	× ²)
	80	+ (+) or —	×)			
	100	(+) or —			×	×
	140	(+) or —				×
Chronic intoxication	20	+	×			
	40	+	×			
	60	+ or —	×)			

) The specimens were investigated long time after the last atoxyl injection.
) Most specimens following acute intoxication belonged to this group.
The Preyer's reflex was sed to clinically estimate the affection of hearing (classified + (+) — indicating a normal hearing, impairment and complete loss respectively) The toxic renal damage was quantified a × ×× or ×××

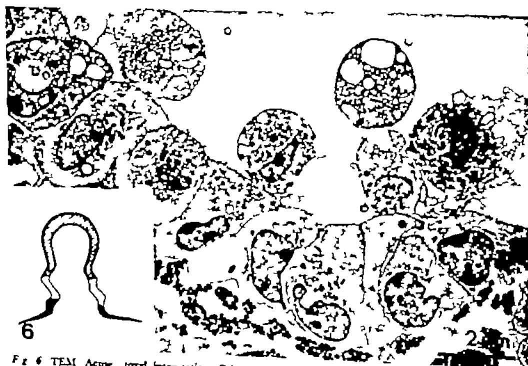
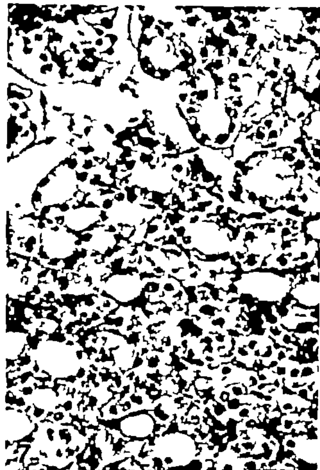


Fig 6 TEM Acute toxyl intoxication. Crista ampullaris. Degeneration of light and dark cells of the secretory region. Some of the damaged cell are expelled into the endolymphatic space Inset Schema tic drawing illustrating the different regions of the crista ampullaris. Dark grey sensory epithelium light grey intermediate zone of the planum semilunatum black: secretory epithelium.


7


8


9


10

the period that had elapsed between the last treatment and the sacrifice of the guinea pig On increasing the dose on each occasion and decreasing the interval between the injections the renal lesion became more severe It therefore appeared that the degrees of renal damage recorded were, in fact, various stages in the evolution of a renal lesion.

The first stage of the renal lesion (classified as +) included a heavy congestion of the renal parenchyma and hyperemia of the cortico-medullary zone, and occasional tubule cells in the cortico-medullary zone showed necrosis (Fig. 7)

In the intermediate stage of the renal lesion (classified as + +) there were changes such as those observed in the first stage, but the areas of tubule cell necrosis were larger and more numerous (Fig 8) Hyaline and granular casts occurred particularly in the distal part of the nephron and were thus found both in the cortical and medullary areas of the kidney Dilated tubules frequently occurred in the striae medullare of the cortex.

The most severe renal changes (classified as + + +) included congestion and hyperemia as well as large areas of necrosis (Fig. 9 10) Often the entire tubule system in the cortico-medullary zone showed necrosis,



Fig 11 Section from kidney a prolonged period after injection of toxic doses of atoxyl. There are features of regeneration of tubules with large hyperchromatic nuclei and occasional tubule cell mitosis (arrow) Hematoxylin-eosin. × 250

which in many places extended into the cortical area along the striae medullare Tubular casts were found both in the medullary and in the cortical zones of the kidney Non-necrotic tubules mostly appeared dilated.

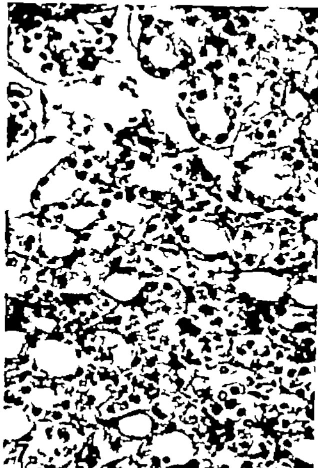
A number of the experimental animals were devoid of renal change. These animals had either been given small amounts of atoxyl over a prolonged period of time (chronic intoxication) or large amounts within a brief period (acute intoxication) and their kidneys had been removed for examination several weeks after the final injection. In many areas these kidneys showed large nuclei of the tubule cells and occasional tubule cell mitosis (Fig. 11) indicating tubular regeneration.

Fig 7 Section from the cortico-medullary border from kidney with lesion classified as + I the upper half of the picture there is necrosis of number of tubule cells. Hematoxylin-eosin. × 150.

Fig 8 Section showing the cortico-medullary zone of kidney with lesion classified as + + There are large areas of necrosis (upper half of picture) Hematoxylin-eosin. × 40.

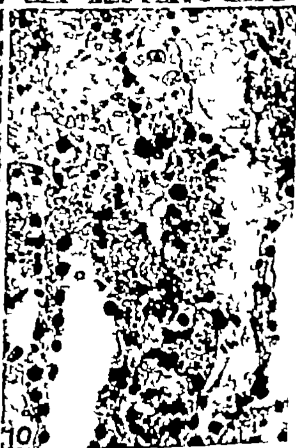
Fig 9 Section showing the cortico-medullary zone of kidney with lesion classified as + + + There is necrosis along the border and extending both into the medulla (top) and cortex (bottom) Tubules within the medullary ray are dilated (bottom left) Hematoxylin-eosin. × 40

Fig 10 Higher magnification of a + + + lesion showing necrosis of the tubular system in the cortico-medullary zone Hematoxylin-eosin. × 250.


7


8


9


10

the period that had elapsed between the last treatment and the sacrifice of the guinea-pig. On increasing the dose on each occasion and decreasing the interval between the injections the renal lesion became more severe. It therefore appeared that the degrees of renal damage recorded were in fact, various stages in the evolution of a renal lesion.

The first stage of the renal lesion (classified as +) included a heavy congestion of the renal parenchyma and hyperemia of the cortico-medullary zone, and occasional tubule cells in the cortico-medullary zone showed necrosis (Fig. 7)

In the intermediate stage of the renal lesion (classified as + +) there were changes such as those observed in the first stage, but the areas of tubule cell necrosis were larger and more numerous (Fig 8) Hyaline and granular casts occurred particularly in the distal part of the nephron and were thus found both in the cortical and medullary areas of the kidney Dilated tubules frequently occurred in the striae medullare of the cortex.

The most severe renal changes (classified as + + +) included congestion and hyperemia as well as large areas of necrosis (Fig. 9 10) Often the entire tubule system in the cortico-medullary zone showed necrosis,



Fig 11 Section from kidney a prolonged period after injection of toxic doses of atoxyl. There are features of regeneration of tubules with large hyperchromatic nuclei and occasional tubule cell mitosis (arrow) Hematoxylin-eosin. × 250.

which in many places extended into the cortical area along the striae medullare Tubular casts were found both in the medullary and in the cortical zones of the kidney Non necrotic tubules mostly appeared dilated.

A number of the experimental animals were devoid of renal change. These animals had either been given small amounts of atoxyl over a prolonged period of time (chronic intoxication) or large amounts within a brief period (acute intoxication) and their kidneys had been removed for examination several weeks after the final injection. In many areas these kidneys showed large nuclei of the tubule cells and occasional tubule cell mitosis (Fig. 11) indicating tubular regeneration.

Fig 7 Section from the cortico-medullary border from a kidney with lesion classified as + In the upper half of the picture there is necrosis of number of tubule cells. Hematoxylin-eosin. × 150.

Fig 8. Section showing the cortico-medullary zone of kidney with lesion classified as + + There are large areas of necrosis (upper half of picture) Hematoxylin-eosin. × 40.

Fig 9 Section showing the cortico-medullary zone of kidney with lesion classified as + + + There is necrosis along the border and extending both into the medulla (top) and cortex (bottom) Tubules within the medullary ray are dilated (bottom left) Hematoxylin-eosin. × 40

Fig 10 Higher magnification of a + + + lesion showing necrosis of the tubular system in the cortico-medullary zone. Hematoxylin-eosin. × 250

Correlation of Renal Damage to Preyer's Reflex Changes

The change of the Preyer's reflex following atoxyl administration was used as a parameter of hearing (normal hearing, impairment or total loss, respectively).

In acute poisoning the Preyer's reflex usually was impaired or totally lost. The change could be correlated to the occurrence of cochlear damage. In these animals morphological signs of toxic renal damage were also obvious (Table 1). However, if the cochlear and renal specimens were investigated a considerable time after the last atoxyl injection, no change in the kidney morphology was detected, whereas the Preyer's reflex was impaired or lost and the neuroepithelia of the cochlea often showed signs of toxic damage by loss of hair cells which were replaced by phalangeal scarring.

Loss of cochlear hair cells could also be found in animals with a preserved Preyer's reflex (chronic intoxication).

DISCUSSION

A relationship may exist between cochlear and renal reactions under both clinical and experimental conditions (*Quick et al.* 1973, *Arnold et al.* 1976).

The present investigation has shown that atoxyl poisoning may cause damage to both the labyrinth and the kidneys and that the cochlear and renal lesions show parallell dose response relationships.

Thus, acute atoxyl intoxication (the animal was examined within a few days following the onset of poisoning) caused changes in both the cochlear (sensory and secretory cells) and the renal (tubular epithelia) structures to an increased degree with increased dosage. However kidney specimens examined a considerable time following the last atoxyl injection (several weeks or months) showed a normal renal morphology with features indicative of a tubular regeneration suggesting that damaged tubules will regenerate when the drug is withdrawn. The damaged hair cells in the cochlea, on the other hand, were not replaced when the drug was withdrawn, and the extent of inner ear damage could be recognized by the appearance of phalangeal scars at the former sites of the cochlear hair cells.

Clinically, the Preyer's reflex was used to estimate the affection of hearing, indicating a sensorineural damage when it was impaired or lost. The correlation to toxic renal damage was good in acute intoxication where an impairment or a total loss of the reflex occurred. Such a correlation did not exist if a long time had elapsed from the last atoxyl injection to the sacrifice of the animal, in which case the Preyer's reflex often was lacking but the renal morphology essentially normal, again indicating that, unlike the renal lesion, that in the inner ear is irreversible.

The elimination of atoxyl (an arsenic compound) from the body takes place via the kidneys (*Hunter et al.* 1942, *Talley et al.* 1960, *Moody & Williams* 1964) without a degrative metabolism (*Overby & Straube* 1965). *Anniko & Plantin* (1977) reported that following a single subcutaneous injection the main part of atoxyl was rapidly excreted within 5–12 hours via the kidneys.

Atoxyl was retained in the cochlea for a long time after its administration into the body, and atoxyl showed a delayed elimination rate from the inner ear compared with other body tissues. The inner ear became thereby exposed to a higher atoxyl concentration than the rest of the body, except the kidneys, after only a few hours.

A renal lesion, when it occurs, is likely to cause impairment of kidney function with a decrease in atoxyl excretion. The toxic effect of atoxyl on both the kidney and the inner ear would thereby increase.

Physiologically there are functional characteristics common to the kidney and the labyrinth. Both the renal tubules and the secretory tissues of the inner ear have a very active ionic transport system. A common denominator in the ototoxic and nephrotoxic actions of atoxyl might be the disturbance of the

complex mechanism involved in the active transport of sodium and potassium ions (*Anniko & Wersäll* 1975) for the preservation of a normal composition of endolymph (*Smith et al.* 1954 *Rauch* 1964—guinea-pig Na 15.8 mEq and K 144.4 mEq) and intravascular body fluid (*Rauch & Köstlin* 1958 —guinea-pig serum Na 138.6 mEq and K 4.5 mEq)

Following acute intoxication, both the secretory tissues of the kidney and the labyrinth and the cochlear hair cells became morphologically damaged. A less degree of interference with vital enzyme functions in both types of the secretory tissues occurred during chronic poisoning, probably because of a certain reserve capacity of the secretory cell metabolism (normal morphology) The cochlear hair cells, however with a far less energy metabolism than the stria vascularis (*Thalmann et al* 1970) and a highly specialized membrane receptor function, were morphologically damaged at a lower concentration of the noxious agent than the other structures of the inner ear and the renal parenchyma.

The authors wish to express their appreciation to Professor *Jan Wersäll* for valuable discussions and for his never failing interest in this work. The technical assistance of Mrs. *Marie-Louise Spångberg*, Mrs *Sonja Björdahl* and Mr *Bengt Hedberg* is gratefully acknowledged. The manuscript was linguistically reviewed by Mrs *Ann K mpe*

Supported by grants from *Karolinska Institutet* and the *Swedish Medical Research Council* (project No B75-12X 716)

REFERENCES

Alport A C Hereditary Familial Congenital Haemorrhagic Nephritis Brit Med. Jour *1* 504 506 1927

Anniko M & Wersäll, J Damage to the stria vascularis in the guinea pig cochlea by acute atoxyl intoxication Acta Otolaryngol (Stockh.) *80* 167 179 1975

Anniko M The cytocochleogram in atoxyl-treated guinea-pigs Acta Otolaryngol. (Stockh.) *82* 70–81 1976

Anniko M Surface structure of stria vascularis in the guinea-pig cochlea. Normal Morphology and Atoxyl-induced Pathologic changes. Acta Otolaryngol. (Stockh.) *82* 343–353 1976 b.

Anniko M & Wersäll, J Experimentally (atoxyl) induced Ampullar Degeneration and Damage to the Macula Utriculi. Acta Otolaryngol. (Stockh.) *83* 429–440, 1977

Anniko M & Plantin L-O. Delayed elimination of the ototoxic compound atoxyl from the inner ear Arch. Oto-Rhino-Laryng *215* 81–89 1977

Arnold W., Weidauer H & Seelig, H P. Experimenteller Beweis einer gemeinsamen Antigenizität zwischen Innenohr und Niere Arch. Oto-Rhino-Laryng. *212* 99 177 1976

Hawkins J E jr Biochemical Aspects of Ototoxicity In *Michael M Paparella* Ed. Biochemical Mechanisms in Hearing and Deafness. Charles C. Thomas Publisher Springfield, Ill. USA. 1968 pp. 323–339

Hungerstad S. Hereditary nerve deafness associated with diabetes. Acta Otolaryngol. (Stockh.) 64 219–225 1967

Hunter F T., Kip A F & Irvine J W. Radioactive tracer studies on arsenic injected as potassium arsenite. I Excretion and localization in tissues. J Pharmacol. exp. Ther *76* 207–220 1942.

Kupper H Kotzerek R Mitscke H & Schmidt P. Hörstörungen bei chronischer Niereninsuffizienz. Monatschr Ohrenheilkd. Laryngorhinol *106* 332 339 1972.

McCrady A McCormick J G. & Harrill, J A Ototoxicity of Ethacrynic Acid in the Anuric Guinea Pig. Arch. Otolaryngol. *100* 143–147 1974

Merck W H ppe-Seyler G & Chrisen I Ultrastrukturelle Veränderungen an der Stria Vascularis und dem Ligamentum spirale bei chronisch – urämischen Ratten Arch. Oto-Rhino-Laryng *214* 63–70, 1976.

Murayama T. Experimentelle Untersuchungen über die Schädigung des Gehörorgans durch die Giftwirkung der Arzneimittel Die Wirkung des Atoxyls auf das Gehörorgan. Arb d. Med. Univ. Okayama 2 212–435, 1931

Moody J P & Williams T. The Fate of Arsanilic Acid and Acetylarsanilic Acid in Hens. Fed Cosmet. Toxicol. 2. Pergamon Press. 1964 pp. 687–693

Naumphlis, P Die Wirkung des Atoxyls auf das Innenohr Arch Ohr Nas u. Kehlk. Heilk. *117* 394 636 1931

Overby L. R. & Straube L. Metabolism of Arsanilic Acid Toxicology and Applied Pharmacology *7* 850–854 1965

Quick, C A Fish A & Brown C. The relationship between cochlea and kidney Laryngoscope *83* 1469 1482 1973

Rauch S Biochemie des Hororgans. Georg Thieme Verlag. Stuttgart, 1964

Rauch S & *Köstlin A* Aspects chimiques de l endolymphe et de la périlymphe. Pract oto-rhino-laryng (Basel) *20* 287 1958

Rüedi L. Some animal experimental findings on the functions of the iner ear The Scientific Papers of the American Otological Society LXXXCIII 993 1951

Smith C A Lowry O H & *Wu M L.* The electrolytes of the labyrinthine fluids. Laryngoscope *64* 141–153 1954

Thalmann I Matschinsky F M & *Thalmann R* Quantitative study of selected enzymes involved in energy metabolum of the cochlear duct. Ann. Otol. *79* 12–29 1970

Valley B L. Ulmer D D & *Wacker W E. C* Arsenic Toxicology and Biochemistry Arch. Industr Health *21* 13?–151 1960

Wersäll J Studies on the structure and innervation of the cristae ampullares in the guinea pig Acta Otolaryngol. (Stockh.) Suppl. *126* 1–85 1956

Winter L. E Cram B M & *Bonecets J B.* Hearing Loss in Hereditary Renal Disease Arch Otolaryngol. *88* 238–241 1968.

Acta path. microbiol. scand. Sect. A, 85 761–767 1977

AMYLOIDOSIS IN AGEING OBESE HYPERGLYCEMIC MICE AND THEIR LEAN LITTER-MATES

A Morphological Study

PETER NAESER and PER WESTERMARK

The Departments of Histology Ophthalmology and Pathology University of Uppsala, Uppsala, Sweden

Naeser P & Westermark, P Amyloidosis in ageing obese-hyperglycemic mice and their lean litter-mates A morphological study Acta path. microbiol. scand. Sect. A, 85 761–767 1977

The occurrence of amyloidosis in obese-hyperglycemic mice (genotype *obob*) about 18 months old and their lean litter-mates was studied. Amyloidosis of varying degrees was found in 60 per cent of the mice and was equally common in both groups. Large amounts of amyloid were usually seen in the adrenal glands, liver spleen and kidneys In the kidneys, the amyloid was found mainly in the glomeruli, in the mesangial region. Electron microscopy of isolated amyloid fibrils showed that these consisted of two filaments about 40 Å thick, twisted around each other It is concluded that the distribution of the amyloidosis in these mice is similar to that seen in secondary or experimental murine amyloidosis.

Key words Amyloidosis ageing mice; obese-hyperglycemic mice.

Peter Naeser Department of Ophthalmology Akademiska sjukhuset, S-750 14 Uppsala, Sweden.

Received 17.iii.77 Accepted 2.v.77

Mice with the obese-hyperglycemic syndrome (gene symbol *ob*) have been used extensively in studies of diabetes mellitus (cf 16) The main interest in these animals has centred upon the function of the endocrine pancreas and the development of the obese-hyperglycemic syndrome. The occurrence of so-called diabetic complications has attracted little attention. However glomerular lesions with hyalinization have been described in ageing obese hyperglycemic mice, though the nature of these changes has not been clarified (20 10)

In a recent study amyloid deposits were found in the adrenal glands of old obese hyperglycemic mice (9) The aim of the present investigation was to determine whether such deposits are part of a systemic amyloidosis. The occurrence of amyloid and its distribution were also studied in old obese and lean mice of this strain

MATERIAL AND METHODS

Twenty-two male obese-hyperglycemic mice (genotype *obob*) and 25 male lean litter-mates (genotype *Obob* *ObOb*) were used in these studies. They were from a colony originating from the Jackson Laboratory Bar Harbor Maine, USA. This non-inbred colony has been kept at the Department of Histology University of Uppsala, Sweden, since 1959 under conditions described previously (cf. 9) The animals were killed at the age of 18 months, and pieces from the spleen, liver kidneys, pancreas, adrenal glands and brain were

TABLE 1 *Frequency of Amyloid Deposits in Various Organs*

	Liver	Spleen	Kidneys		Pancreas		Adrenals
			Glomeruli	Medulla	Exocrine tissue	Islets	
Obese hyperglycemic mice (n = 13)	10	7	10	7	8	2	12
Lean mice (n = 15)	8	8	7	8	9	4	10

removed for histological examination. The specimens were fixed in a 4 per cent neutral formaldehyde solution. After dehydration in graded ethanols and clearance in xylene, they were embedded in paraffin and sectioned Five-μ thick sections were stained with alkaline Congo red (13) and studied in polarized light.

Small pieces of renal cortex were taken for electron microscopic examination. The specimens were fixed in 2.5 per cent glutaraldehyde in 0 1 M phosphate buffer (pH 7 4) postfixed in 1 per cent osmium tetroxide in 0 1 M phosphate buffer and embedded in Epon. Ultra thin sections were contrast-stained with uranyl acetate and lead citrate and studied in a Zeiss Em 9 or a Jeol 100 C electron microscope

Splenic tissue was immediately frozen and stored at —20 C for subsequent isolation of amyloid fibrils. Five spleens rich in amyloid as estimated on Congo red stained sections, were used for this purpose. After homogenization in normal saline amyloid fibrils were extracted with destilled water as described by *Pras et al* (12) A microdroplet of a dilute suspension of amyloid fibrils was dried on a Formvar-coated grid and studied in the electron microscope after being negatively contrast--stained with phosphotungstic acid

TABLE 2 *The Occurrence of Amyloidosis in Obese-Hyperglycemic Mice and Their Lean Litter Mates*

	Obese-hyperglycemic mice (n = 22)	Lean mice (n = 25)
Amyloidosis of moderate to severe degree	8 (36 %)	8 (32 %)
Amyloidosis of all degrees	13 (59 %)	15 (60 %)

RESULTS

In most of the animals the degree of amyloidosis was equal in the different organs. In a few cases, however one or more organs, e.g the spleen were spared. Table 1 shows the frequency with which the various organs displayed amyloid deposition As seen in Table 2 amyloidosis was found in 60 per cent of the animals and was equally frequent in obese and lean mice In both types of mice the degree of amyloidosis varied greatly among the animals with no apparent difference between the two groups.

In the liver amyloid was located mainly in the periportal areas, surrounding the portal venules. The periportal arterioles and central veins were less often affected. In more severe cases, depositions also occurred along the sinusoids and often formed characteristic rounded spiny figures (Fig 1)

The splenic amyloidosis appeared to be perifollicular Some mice only had patches of amyloid in the boundary zone between the red and the white pulp Others exhibited ring like infiltrations surrounding the follicles (Fig 2) In a few cases there was extensive deposition in the red pulp The central arteries were hardly involved.

Amyloid was found most constantly in the adrenal glands. Here the deposits were seen in the perimedullary connective tissue zone in cases with slight amyloidosis these occurred as patches, and in severe cases as strands, sometimes extending deeply into the cortex between the cells (Fig 3) Generally there was no infiltration of the medulla. In a few

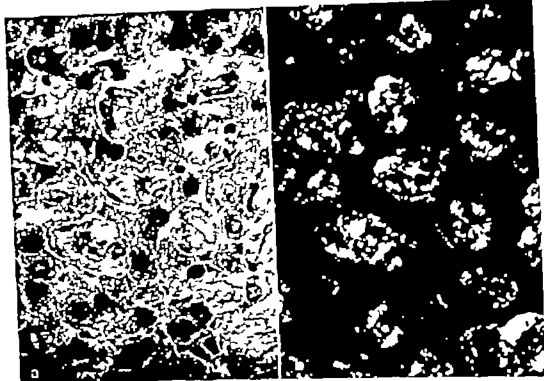


Fig 1 Liver Amyloid deposits between liver cells. The deposits form rounded, spiky figures. Congo red, a) ordinary light and b) between crossed polars. × 500

cases, a discrete deposition was found surrounding the small medullary vessels.

In cases where amyloid was present in the kidney the glomeruli were almost always affected. Large amounts of amyloid were present as nodular deposits in the glomerular tufts (Fig. 4) In the cortex, amyloid was seen around the tubules and in the walls of small vessels. Small to moderate deposits were also found between the cortex and the medulla and in the papillae. No papillary necrosis was found. In two mice no amyloid was found in the glomeruli although the medulla displayed amyloid deposits. The opposite was seen in three mice, with glomerular amyloidosis but no deposits in the medulla.

The amyloidosis of the pancreas was most often slight and usually limited to the walls of small veins of the exocrine part. Some mice, however showed widespread interstitial deposition, with involvement of vessels of all sizes In such cases, small amyloid deposits were found in some islets of Langerhans, usually along the capillaries (Fig. 5) There was no difference between the obese-hyperglycemic mice and their lean litter-mates.

Amyloid was often observed in the adipose tissue. In three mice deposits were only found in this tissue. The amyloid was located mainly around the fat cell membranes in ring-like deposits, but also in the walls of small vessels.

The brain, with its membranes and vessels, was free from amyloid.

Electron microscopy of the glomeruli revealed deposits of fine fibrils located on the capillary side of the basement membrane close to the mesangial cells (Fig 6) The fibrils showed no preferential orientation and were approximately 100 Å in width. The isolated amyloid fibrils were "rigid" and non-branching, and consisted of two filaments, about 40 Å thick, twisted around each other (Fig. 7)

47*











Fig. 6. Electron microscopic picture of a glomerulus. Amyloid fibrils (A) are seen on the capillary (C) side of the basement membrane (arrows) and close to a mesangial cell (M). Uranyl and lead. × 40,000

Fig. 2. Spleen. Deposits of birefringent amyloid are seen in the perifollicular area. Congo red between crossed polars. × 125

Fig. 3. Adrenal gland. Amyloid deposits are present mainly in the perimedullary zone. Congo red between crossed polars. × 50.

Fig. 4. Kidney. Large amounts of amyloid are located in the glomeruli, seen in the picture as small birefringent balls. Congo red between crossed polars. × 50

Fig. 5. Islet of Langerhans. Very discrete deposits of amyloid occur along a capillary. Congo red between crossed polars. × 500.

DISCUSSION

This investigation has shown that systemic amyloidosis is quite common in old obese-hyperglycemic mice and their lean litter mates. Furthermore, the amyloid deposition is not correlated to the presence of a manifest obese-hyperglycemic syndrome.

Recently *Page & Glenner* (11) in a study on spontaneous amyloidosis in mice, noted a considerable strain variability in the frequency of amyloidosis and also pointed out that this condition only occurred in mice that were submissive or wounded. The non-fighting fo-



Fig 7 Isolated amyloid fibrils usually consisting of two filaments, about 40 Å thick, twisted around one another
Negatively contrasted with phosphotungstic acid. × 130,000

male mice usually showed no amyloidosis. The authors thus suggested that in their strains amyloidosis was secondary rather than inherited The mice in the present study were all males but showed little tendency to fight. At sacrifice they did not display any signs of wounds or other diseases. This is remarkable, since the amylo d distribution was the same as that seen in mice with secondary amyloid osis Furthermore, amyloid fibrils obtained from this strain of mice have been found to contain mouse amyloid protein AA (19) homologous to human protein AA (7) which is seen mainly in secondary amyloidosis (1)

In the present study the organ distribution of amyloid varied considerably among different animals Usually the kidneys, spleen and liver were affected in a way similar to that seen in experimentally induced murine amyloidosis (3) However in contrast to the comparably rare glomerular lesions in spontaneous amyloidosis in other strains of mice (5 6 11 14 15) the present investigation showed that glomerular deposition is an almost constant feature in renal amyloidosis in obese-hyperglycemic mice and their lean litter mates. Deposits in the renal medulla and in the tips of the papillae, which have been observed as a major lesion in spontaneous amyloidosis in other strains of mice (5 6 11 14 15) also occurred in these mice but to a much lesser extent

In the hyaline glomerular lesions in ageing obese-hyperglycemic mice described previously (10) the Congo red reaction was negative. The present study however showed a positive amyloid reaction in the same type of mice. This may be explained by the use of different staining methods. It is well known that the introduction of the alkaline Congo red stain in combination with polarization microscopy has markedly improved the possibility of detecting amyloid (4) The electron microscopic findings are also quite typical for the renal lesions reported in systemic amyloidosis in mice (3) This is further emphasized by the morphological features of the individual amyloid fibrils, which were very similar to those described for other mouse strains (8)

It is noteworthy that amyloid deposits in the islets of Langerhans were rare and small, and only present around the capillary vessels. The same pattern of deposition is also seen in experimental murine amyloidosis (18) and in human systemic amyloidosis (17)

The present study has shown that the previously described hyaline glomerular lesions (2 10) and the renal amyloid deposits (9) are manifestations of a systemic amyloidosis in old obese-hyperglycemic mice and their

lean litter-mates. The amyloid occurs in the same organs as are involved in secondary or experimental murine amyloidosis. The deposition of amyloid in the kidneys differs from that in other known spontaneous amyloidoses through its location which is mainly in the glomeruli.

Supported by the *Swedish Medical Research Council* (Projects No.s 102 and 109) the *Swedish Diabetes Association*, the *Swedish Medical Society* and the *Research Fund of King Gustaf V*. Thanks are due to *Margareta Asplund* and her pupils for skilled technical help.

REFERENCES

1 *Benditt E. P & Eriksen, N.*: Chemical classes of amyloid substance. Amer J Path. 65: 231–249 1971

2. *Bergstrand A. Nathorst Wilkadahl G & Hellman, B.* The electron microscopic appearance of the glomerular lesions in obese-hyperglycemic mice. Acta path. microbiol. scand. 74 161–168, 1968.

3 *Cohen A. S & Cathcart E. S.*: Casein-induced experimental amyloidosis. In: Meth. Achiev. exp. Path. Vol. 6. *Bajusz E. & Jasmin, G.* (eds.) p. 207 Basel Karger 1972.

4 *Cooper J H.* An evaluation of current methods for the diagnostic histochemistry of amyloid. J clin. Path. 22 410–413 1969

5. *Cornelius E. A.*. Amyloidosis and renal papillary necrosis in male hybrid mice. Amer J Path. 59 317–325 1970

6. *Dunn, T B.* Amyloidosis in mice. In Pathology of laboratory rats and mice. *Cotchin E. & Roe F J C* (eds.) p 181 Philadelphia F A. Davis Co., 1967

7 *Eriksen, N Ericsson L. H., Pearsall, N., Lagunoff D & Benditt E. P* Mouse amyloid protein AA Homology with non-immunoglobulin protein of human and monkey amyloid substance. Proc. Nat. Acad. Sci. USA 73 964–967 1976

8. *Glenner G G Page D., Isersky C Harada M Cuatrecasas P., Eanes E. D., DeLellis R. A., Bladen, H A & Keiser H R* Murine amyloid fibril protein Isolation, purification and characterization. J Histochem. Cytochem. 19 16–28, 1971

9 *Naeser P.*. Structure of the adrenal glands in mice with the obese-hyperglycemic syndrome (gene symbol *ob*) Acta path. microbiol. scand. Sect. A. 83 120–126, 1976.

10. *Nathorst-Windahl, G & Hellman B.*. Lipohyalin glomerular lesions in ageing obese-hyperglycemic mice. Med. Exp. 10 67–71 1964

11 *Page D L. & Glenner G G.*. Social interaction and wounding in the genesis of "spontaneous" murine amyloidosis. Amer J Path. 67 555–570 1972.

12. *Pras M., Schubert M., Zucker-Franklin D., Rimon A. & Franklin, E. C.* The characterization of soluble amyloid prepared in water J clin. Invest. 47 924–933 1968.

13 *Puchtler H., Sweat F & Levine M.* On the binding of Congo red by amyloid. J Histochem. Cytochem. 10 355–364 1962.

14 *Schwinberg, M A., Cathcart E. S Eastcott J W., Skinner M., Benson M Shirahama T & Bennett M.*: The SJL/J mouse a new model for spontaneous age-associated amyloidosis. I. Morphological and immunological aspects. Lab invest. 35 47–54 1976.

15 *West W T & Murphy E. D.*: Sequence of deposition of amyloid in strain A mice and relationship to renal disease. J Nat. Cancer Inst. 35 167–174 1965

16. *Westman S.*: The obese-hyperglycemic syndrome in mice (*ob/ob*) In Les mutants pathologiques chez l'animal. Sabourdy M., ed. p 155 Paris Centre national de la recherche scientifique 1970

17 *Westermark, P.*. The pancreatic islets in systemic amyloidosis. The occurrence of two different types of amyloid. Virchows Arch. Abt. A. 363 179–182, 19974

18. *Westermark P.* The nature of amyloid in islets of Langerhans in old age. In Amyloidosis. *Wegelius O & Pasternak A.* (eds.) New York Academic Press, 1977

19 *Westermark P., Sletten, K., Anders R., Natvig, J B.* and *Naeser P* To be published.

Acta path. microbiol scand. Sect. A 85 768-774 1977

TUMOURS OF URINARY BLADDER AND URETER ASSOCIATED WITH ABUSE OF PHENACETIN-CONTAINING ANALGESICS

SONNY JOHANSSON and LENNART WAHLQVIST

Department of Pathology II University of Göteborg, Sweden and
Department of Urology University of Umeå Sweden

Johansson, S & Wahlqvist, L. Tumours of urinary bladder and ureter associated with abuse of phenacetin-containing analgesics. Acta path. microbiol. scand Sect. A, 85 768-774 1977

Forty two patients with a bladder tumour and 4 patients with a ureteral tumour and a history of abuse of phenacetin-containing analgesics were studied. The sex ratio was 1 1 and the mean age 63 years. The estimated amount of ingested phenacetin was 7 1 kg, the estimated mean exposure time 21 years, and the estimated mean induction time 30 years. Renal papillary necrosis and impaired renal function were found in 34 patients A history of recurrent urinary tract infection was found in 80 per cent of the patients, suggesting that the combination of phenacetin-abuse and chronic inflammation might be responsible for the localization of the tumours to the bladder The majority of the bladder tumours were of low grade (1 and 2) muscular invasion was seldom found and metastases were rare The patients were followed for 1.5-15 years. Twenty-six patients died the mean survival time was 46 months. Uremia due to analgesic nephropathy was the main cause of death in 14 patients and contributed *to death in another 7 patients. Three of the patients with ureteral tumours had received* radiological treatment against the pelvic region 15-20 years prior to the diagnosis of the ureteral tumour

Key words Phenacetin bladder and ureteral tumours.

S Johansson, Department of Pathology Vasa Hospital S-411 33 Göteborg, Sweden.

Received 5.iv 77 Accepted 10 v 77

The association between abuse of phenacetin-containing analgesics in humans and the development of renal pelvic tumours has been demonstrated in several studies, particularly from Sweden (*Hultengren et al* 1965 *Bengtsson et al* 1968 *Angervall et al* 1969 *Johansson et al* 1974) Small series have also been reported from other countries (*Kung* 1976) Experimental studies support the opinion that phenacetin or metabolites of phenacetin can induce proliferation of the urothelium and can also be carcinogenic (*Nery* 1971 *Eisenbrand & Preussmann* 1975 *Calder et al* 1976 *Johansson & Angervall* 1976)

In the series of phenacetin abusers reported by *Bengtsson et al.* (1968) 9 patients developed renal pelvic tumours and 2 patients primary tumours of the urinary bladder A review of the literature concerning urinary tract tumours in phenacetin-abusers was performed by *Küng* (1976) He collected 11 cases of primary bladder tumours from the literature and added 11 cases of his own 4 of these had also renal papillary necrosis. Ureteral tumours in phenacetin-abusers have not, as far as we

know been reported without associated lesions in the renal pelvis or bladder The present study presents a review of 46 patients with abuse of phenacetin-containing analgesics and primary urothelial tumour of the urinary bladder or ureter

MATERIAL AND METHODS

The series consists of 46 patients treated at Sahlgren hospital Göteborg. The tumours were diagnosed between 1962 and 1975 by histological examination of an operative specimen. Forty-two patients had a bladder tumour and 4 patients a tumour of the ureter All of the patients had a history of abuse of phenacetin-containing analgesics.

Clinical Methods

The diagnosis of nephropathy and renal papillary necrosis was based on clinical and roentgenological or histopathologic examination. Serum creatinine determination, microscopic examination of urinary sediment and bacterial culture of urine were routinely performed in all patients. Biopsy made by a transureteral resection (TUR) was performed for an extirpation of tumour and tumour base, whenever possible.

Analgesic Abuse

As in previous studies (*Bengtsson et al.* 1968, *Angervall et al* 1969 *Johansson et al.* 1974) the patients were classified as analgesic-abusers if they had consumed at least 1 gram of phenacetin per day for 1 year or if the total consumption of phenacetin exceeded 1 kg.

Morphological Methods

Urine cytology was performed on 16 patients. The Millipore technique on olded urine was used (*Eriksson & Johansson* 1975)

The size and localization of the tumour was determined by radiological and endoscopic findings.

Paraffin blocks from all the patients were collected and 5 μm-thick new sections were made and stained with hematoxylin and eosin and according to Weigert-van Gieson method. Histologic grading of malignancy was done with respect to cell differentiation as described by *Bergkvist et al.* (1965) The extent of infiltration into the bladder wall was histologically determined in all cases.

RESULTS

Sex and Age

Twenty-one of the patients with bladder tumours were males, 21 females. The mean age was 63 years, the range being 36 to 84 years. Two patients with ureteral tumours were males, 2 females. The mean age was 63 years, the range being 55 to 68 years.

Analgesic Abuse

The analgesic compositions used by the majority of the patients contained 0.5 g of phenacetin, 0.5 g of phenazone and 0.1 g of caffeine. The other patients had taken similar preparations although the dose relation of phenacetin, phenazone and caffeine varied somewhat. In 23 patients detailed data concerning the analgesic abuse was available (Table 1) The estimated total average dosage of phenacetin was 7.1 kg the estimated mean exposure time 21 years, and the estimated mean induction time 30 years. In the remaining patients it could only be stated that there had been a heavy abuse of analgesics containing phenacetin over a long period of years, although it was not possible to calculate the total dosage of drugs, since this study was retrospective

TABLE 1 *Estimated Consumption of Phenacetin in 23 Patients with Urothelial Bladder Tumours*

	Consumption (kg)	Exposure time (yrs)	Induction time (yrs)
Mean	7.1	21	30
Range	1.4–18.5	4–40	16–47

Radiological Treatment

Three of the 4 patients with ureteral tumours had received radioactive irradiation against the pelvic region because of tumours in the genital tract 15 to 20 years prior to the diagnosis of the ureteral tumours.

Occupation

One patient had been working in a chemical plant manufacturing organic chemicals. No other patient had been working in dye stuff, leather or rubber industries, viz. industries known to be associated with an increased risk of developing carcinoma of the bladder

Smoking Habits

Information concerning smoking habits was available in 19 men and 20 women. Fifteen of the men and 3 of the women were smokers

Clinical Findings

Thirty six of the 42 patients with bladder tumours had had gross hematuria and 2 patients microscopic hematuria All the patients with ureteral tumours had had gross hematuria. Eighty per cent of the patients with bladder tumours had a history of recurrent urinary tract infection

Twenty-seven of the patients with bladder tumours (13 men 14 women) and 3 of the patients with ureteral tumours were found to have renal papillary necrosis. Eighteen of the patients with bladder tumours had arterial hypertension. The renal function measured as serum creatinine was reduced in 30 of the patients with bladder tumours before the operation (Table 2) Thirteen patients had serum creatinine values higher than 2 0 mg per cent. Three of the patients with ureteral tumours had a serum creatinine of 1 3–1 5 mg per cent and one patient 6 mg per cent

Two patients had a radiologically "silent" kidney on the tumour side and 7 patients had signs of partial ureteral obstruction on the tumour side All of these patients except one had invasive tumours, the latter having a large (about 8 cm in diameter) papillary tumour

All the ureteral tumours were localized in the distal part of the ureter The sites of the bladder tumours were as follows. The tumour or a part of the multiple tumours were localized in the trigone near the ureteral orifices in 34 patients. Ten patients had initially multiple tumours Three patients had diffuse papillomatosis involving the entire bladder and in 3 patients the tumour was found in the dome the remaining 2 patients had their tumour localized in the lateral wall.

In 16 patients the tumours were estimated to be smaller than 1.5 cm in diameter in another 16 patients between 1.5–3.5 cm, and in the remaining 10 patients larger than 3.5 cm.

TABLE 2 *Renal Function as Estimated from Serum Creatinine Concentration in 42 Patients with a Urothelial Tumour of the Urinary Bladder and 4 Patients with a Tumour of the Ureter and Abuse of Phenacetin-Containing Analgesics*

	Serum creatinine mg %			
	≤ 1.2	1.3–2.0	2 1–4 0	> 4 0
Number of patients	12	17(3)	8	5(1)

The numbers in brackets concern patients with ureteral tumours.

Microscopic Findings

The tumour structure was papillary in 30 patients, solid in 7 patients, and mixed papillary and solid in the remaining 5 patients. All the tumours were urothelial and in 4 tumours areas of squamous differentiation were found. The histologic grading of the tumours, as well as the depth of invasion, is given in Table 3

TABLE 3 *The Frequency of Tumour Grade and Invasive Growth in 42 Patients with a Primary Tumour of the Urinary Bladder and 4 Patients with a Ureteral Tumour Associated with Abuse of Phenacetin-Containing Analgesics*

	Histological grade									
	1		2		3			4		
	non invasive	non invasive	mucosal invasion	muscular invasion	non invasive	mucosal invasion	muscular invasion	mucosal invasion	muscular invasion	Total
No of patients	12	9(2)	4	1	3	4(1)	3	3	3(1)	42

The numbers in brackets concern patients with ureteral tumours.

Twenty-eight patients had low grade tumours (grade 1 and 2) and 18 patients had high grade tumours (grade 3 and 4). Twenty-six tumours were non-invasive, 12 infiltrated into the mucosa and 8 tumours infiltrated into the smooth muscle layers. Nine of the patients who underwent cytological examination had positive cytologic findings. Two of the 4 patients with ureteral tumours had low grade tumours (grade 2) and 2 patients high grade tumours (grade 3 and 4) the latter invading the mucosa and muscular layer.

Treatment

Table 4 gives the different types of initial treatment in 42 patients with urinary bladder tumours. The reduced kidney function influenced the choice of treatment in many patients. In 29 of the patients the treatment consisted of transuretral resection (TUR). Six patients were treated with full-dose supervoltage irradiation (6500 rad). In 2 patients total cystectomy with uretero-ileal conduit was performed. Two of the patients with ureteral tumours underwent partial resection of the ureter and 2 complete nephroureterectomy including a cuff of the bladder wall.

TABLE 4. *Types of T[illegible]atment in 42 Patients with Primary Bladder Tumour and Abuse of Phenacetin-Containing Analgesics*

Type of treatment	No of patients
TUR	29
Partial resection of the bladder wall	4
Partial resection of the bladder wall + cutaneous ureterostomy	1
Total cystectomy + uretero-ileal conduit	1
Radioactive irradiation (6500 rad)	4
Radioactive irradiation (6500 rad) + cutaneous ureterostomy	1
Radioactive irradiation (6500 rad) + uretero-ileal conduit	1
Radioactive irradiation (5000 rad) + total cystectomy + uretero-ileal conduit	1

Follow-up and Survival

The patients with bladder tumours were followed from 1.5 to 13 years. Twenty-two patients had recurrent tumour disease in the bladder and were treated with TUR up to 18 times. In 19 patients the recurrent tumours were of the same grade as the initial tumour, in 3 patients they were of a higher grade.

Two of the patients developed a renal pelvic tumour 1 and 5 years, respectively, after the initial bladder tumour and were nephrectomized. The mean survival time was 46 months, the range being 1 to 152. The 5-year survival rate was 63 per cent for the 19 patients observed for more than 5 years. Twenty-six of the patients with bladder tumours (13 men and 13 women) died, and 18 of them were autopsied. Table 5 gives the pattern of tumour spread in the 18 operated and later autopsied patients with a primary bladder tumour. In 12 patients local recurrences were found. Metastatic spread was found in 3 cases, 2 of them with disseminated disease. In 10 cases no tumour spread outside the bladder was demonstrated at the autopsy.

TABLE 5. *The Pattern of Tumour-Spread in 18 Operated and Autopsied Patients with a Primary Bladder Tumour and Abuse of Phenacetin-Containing A[illegible]algesic*

Site of tumour spread	No of patients (n = 18)
Local recurrence	12
Liver	2
Lymph nodes	3
Lungs	2
Adrenals	1
Ureter	3
N[illegible] tumour spread	6

TABLE 6. *The Cause [illegible] Death in 18 Operated and Autopsied Patients with a Primary Bladder Tumou[illegible] and Abuse of Phenacetin-Containing Analgesics*

Cause of death	No of patients (n = 18)
Uremia	10
Tumour + uremia	3
Tumour only	2
Cardiac insufficiency	3

The cause of death in 18 operated and autopsied patients with a primary bladder tumour and abuse of phenacetin-containing analgesics is shown in Table 6 Ten patients died from uremia only 3 patients from tumour disease and uremia, and 2 patients from tumour disease only Three patients died from cardiac insufficiency Among the 8 patients who were not subjected to autopsy 4 died from uremia and 4 from uremia and metastatic tumour disease Thus, 21 patients were uremic at the time of death Two of the 4 patients with ureteral tumours developed later tumours in the urinary bladder They died with metastatic disease after one year both of them being uremic at the time of death The other 2 patients with ureteral tumours survived for more than 5 years

DISCUSSION

It is quite reasonable to assume that a chemical which is known to induce tumours in the renal pelvis also would be carcinogenic to the ureter and urinary bladder since the urinary tract from the calyces to the proximal urethra is covered with a histologically identical lining namely the urothelium showing local variation only in its thickness (*Melicow* 1945) Bladder tumours are 15 times more common than renal pelvic tumours in Sweden (The Swedish Cancer Registry) However in phenacetin abusers renal pelvic tumours seem to be more frequent than bladder tumours The N hydroxyesters of aromatic amides are highly reactive in the renal pelvis but short lived (*Miller* 1970) and may thus be less carcinogenically active by the time they reach the bladder This, in combination with a lower amount of ingested phenacetin in the patients with bladder tumours compared with the patients with renal pelvic tumours (*Johansson et al* 1974) may explain the longer induction time for the bladder tumours. The induction time for the bladder tumours was estimated to be 30 years, compared with 22 years for the renal pelvic tumours the latter being close to the induction time for occupational bladder tumours (*Case et al.* 1954)

The role of smoking is difficult to evaluate, since the majority of the men smoked but very few women did Occupational exposure did not seem to play a role in the development of bladder tumour in the present series, since only one male patient had a history of such occupational exposure. A combination of radioactive irradiation and phenacetin-abuse was found in 3 patients with tumours of the distal ureter Radioactive irradiation of the ureter was perhaps of importance for the development of the tumour The short exposure-time in the ureter for the highly reactive N hydroxyesters may explain why so few ureteral tumours have been found in phenacetin abusers.

Chronic inflammation of the urinary tract was found in 80 per cent of the patients in the present study This factor may have contributed to the development of bladder tumours in phenacetin-abusers and their localization in these patients to the urinary bladder Chronic inflammation is of etiological significance for the development of squamous cell carcinoma of the bladder in patients with schistosomiasis (*Dimmette et al* 1956)

The majority of the patients (71 per cent) had their tumour localized in the trigone area close to the ureteral orifices. This is in accordance with the experience of *Mostofi* & *Leestma* (1971) who found 60 per cent of the bladder tumours originated in the trigone. The dominating localization in the trigone area in the present study may be explained by the carcinogenic activity of phenacetin, or perhaps phenacetin metabolites were strongest close to the ureteral orifices

While the clinical picture of the patients in the present study is strikingly similar to the one in the series of analgesic-abusers with renal pelvic tumours (*Johansson et al* 1974) it differs in the following ways from the regular series of patients with bladder tumours.

1 The sex ratio (male to female) was 1 1 in the present series, compared with 2.5 1 in other series (The Swedish Cancer Registry) This may be explained by the fact that all the patients in the present study were phenacetin-abusers, and women were preponderant

in this group of patients (*Hornberger et al.* 1958, *Bengtsson* 1962, and *Dubach et al.* 1966)

2 The mean age was 67 years in the Swedish National Series of bladder cancer diagnosed between 1958–1965 comprising 5151 patients (The Swedish Cancer Registry) The mean age in the present study was 4 years lower The age difference is almost the same as the one seen in patients with renal pelvic tumours with and without phenacetin-abuse (*Johansson et al.* 1974)

3 The majority of the patients in the present study suffered from impaired renal function and/or bilateral renal papillary necrosis. This is not the case in the ordinary patient with a bladder tumour except for patients with obstruction of the ureters (*Ackerman* 1975) In the present study signs of unilateral renal obstruction were seen in 9 patients, but this does not explain the reduced function. The nephropathy with reduced renal function is considered to be associated with the abuse of phenacetin-containing analgesics. This view is supported by the presence of bilateral renal papillary necrosis in most patients.

The distribution of tumour grades in the present study is similar to the one described by *Bergkvist et al.* (1965) comprising 300 cases However among the renal pelvic tumours in phenacetin-abusers (*Johansson et al.* 1974) 68 per cent were of high grade (grade 3 and 4) compared with 38 per cent in the present series This difference may be explained by the fact that the carcinogenic activity of phenacetin is weaker in the bladder than in the renal pelvis. Although 18 patients had invasive tumours, metastases were comparatively rare, possibly because most of the invading tumours had only a superficial invasion. Nephropathy with uremia was the main cause of death in 14 patients and contributed to death in another 7 patients. Thus the analgesic nephropathy was largely responsible for the poor prognosis among the patients in the present series.

REFERENCES

1 *Ackerman L. V & Rosai J.* Surgical pathology p. 681–682. C. V Mosby Company St. Louis, 1974
2. *Angervall, L. Bengtsson U., Zetterlund C G & Zsigmond M.* Renal pelvic carcinoma in a Swedish district with abuse of a phenacetin-containing drug Br J Urol. *41*: 401–405 1969
3 *Bengtsson U.*: A comparative study of chronic non-obstructive pyelonephritis and renal papillary necrosis. Acta Med. Scand. (Suppl.) 388, 1962.
4 *Bengtsson U Angervall L., Ekman H & Lehman L.*: Transitional cell tumours in analgesic abusers. Scand. J Urol. Nephrol. 2 145–150, 1968.
5. *Bergkvist A Ljungqvist A & Moberger G* Classification of bladder tumours based on the cellular pattern. Acta Chir Scand. 130 371–378 1965
6 *Calder J C., Goss D E. Williams P J., Funder C C., Green C R., Ham K N & Tange J D* Neoplasia in the rat induced by N-hydroxyphenacetin, a metabolite of phenacetin, Pathology *8* 1–6, 1976.
7 *Case R. A M Hosker M E., McDonald D B & Pearson J T.* Tumours of the urinary bladder in workmen engaged in the manufacture and the use of certain dye-stuff intermediates in the British chemical Industry – I The role of aniline benzidine alfa-napthylamine and beta-napthylamine. Br J Ind. Med. 2 75–104 1954
8. *Dimmette R. M Sproat H F & Sayegh E. S* The classification of carcinoma of the urinary bladder associated with schistosomiasis and metaplasia. J Urol. *75* 680–686, 1956.
9 *Dubach U C., Minder F & Gsell O R.* An epidemiological study of analgesic abuse. Proc. 3rd Int. Congr Nephrol. Washington 1966 Vol. 2 Basel Karger 1967: p. 300–305
10. *Eisenbrand G & Preussmann R* Nitrosation of phenacetin Arzneim. Forsch. (Drug. Res.) 25 1472–1475 1975.
11 *Eriksson O & Johansson S* Urothelial neoplasms of the upper urinary tract. A correlation between cytological and histologic findings in 43 patients with urothelial neoplasms of the renal pelvis and ureter Acta Cytol 20 20–25 1976.
12. *Hornberger B., Grandjean, E & Lanz, F.*, Untersuchungen über den Medikamentenmissbrauch in einem Grossbetrieb der schweizerischen Uhrenindustrie Schweiz. Med. Wochenschr *88* 920–926, 1958.
13 *Hultengren, N., Lagergren C & Ljungqvist A* Carcinoma of the renal pelvis in renal

papillary necrosis. Acta Chir Scand. *130* 314–320 1965

14 *Johansson S Angervall L. Bengtsson U & Wahlqvist L.* Uroepithelial tumours of the renal pelvis associated with abuse of phenacetin-containing analgesics. Cancer *33* 743–753 1974

15 *Johansson S & Angervall L.* Urothelial hyperplasia of the renal papillae in female Sprague Dawley rats induced by long term feeding of phenacetin Acta pathol microbiol. scand Sect. A *84* 353–354 1976

16 *Johansson S & Angervall L.* Urothelial changes of the renal papillae in Sprague-Dawley rats induced by long term feeding of phenacetin. Acta path microbiol scand. Sect A *84* 375–383 1976

17 *Küng L. G.*. Hypernephroides Karzinom und Karzinom der ableitenden Harnwege nach Phenacetin-abusus. Schweiz. Med. Wschr *106* 47–51 1976

18. *Melicow M M* Tumours of the urinary drainage tract. Urothelial tumours. J Urol. *54* 186–193 1945

19 *Miller J A* Carcinogenesis by chemicals – G H A. Clowes memorial lecture Cancer Research *30* 559–576 1970

20 *Mostofi F K. & Leestma J E.* In Pathology W *A D Anderson* (Ed.) The C. V Mosby Company p 840 1971

21 *Nery R.* The possible role of N hydroxylation in the biological effects of phenacetin. Xenobiotica *1* 339–343 1971

22 The Cancer Incidence in Sweden The National Board of Health Stockholm 1958–1970.

Acta path. microbiol. scand. Sect. A, 85 775–786 1977

MEDULLARY THYROID CARCINOMA IN NORWAY

Epidemiological and Genetic Data

TRINE NORMANN

The Department of Pathology The Norwegian Radium Hospital

Normann, T Medullary thyroid carcinoma in Norway Epidemiological and genetic data. Acta path. microbiol. scand. Sect. A, 85 775–786, 1977

Fifty-four primary cases of medullary carcinoma of the thyroid (MCT) traced in Norway 1960–74 were studied. The mean annual incidence rate was 0.1 per 100,000 the frequency of the tumour among all thyroid carcinomas registered in Norway was 3.4 per cent. The study of the geographical distribution of cases revealed a significantly higher proportion in rural than in urban areas, and in coastal as compared with inland counties. There was also an unexpected accumulation of cases in a few sparsely inhabited valleys in the southern and western part of the country The familial occurrence of the disease was investigated by means of the family history pedigree studies and measurement of immuno-reactive calcitonin (ICT) in serum of relatives. The family history was found to be of limited value in discriminating between familial and sporadic cases. Family screening with serum calcitonin measurements revealed hypercalcitonaemia in relatives of 4 probands, 2 of which were apparently sporadic. Through pedigree studies it became evident that 15 probands were distantly releated to one or two of the others, and the study of grandparents' origin revealed that 16 additional probands had one or more grandparents originating in the same rural municipality as the grandparents of at least one of the others. The high degree of inbreeding in these areas makes it possible that some if not all, of these 16 probands in fact are genetically related. The pattern of inheritance was in one, possibly in two kindreds, consistent with autosomal dominance. I three other kindreds an autosomal recessive trait is discussed. The familial and also the geographical relationships demonstrated in the other probands may also be an expression of genetic etiology The nature of this is not clear but it does not fit in with simple Mendelian inheritance.

Key words Medullary thyroid carcinoma epidemiological and genetic data.

Trine Normann, Department of Pathology Ullevål Hospital Oslo Norway

Received 25.iv 77 Accepted 10. 77

A number of studies on the clinicopathological and genetic aspects of medullary carcinoma of the thyroid (MCT) have been published since *Hazard et al.* (14) recognized this tumour as a distinct entity in 1959 (2–4 6–11 13 16–20 23 25 31 32, 36, 37) Except for one report from Finland (10) these studies have not dealt with the occurrence of the tumour in a total population. It has been generally accepted that MCT occurs in one sporadic and one familial form that the latter comprises approximately 10 per cent of the cases, usually (or perhaps always) associated with other endocrine tumours, such as phaeochromocytoma and/or parathyroid hyperplasia/adenoma, and that the trait is of autosomal dominant type with varying,

but generally high degrees of penetrance The separation of familial and sporadic cases has been based on the family history and/or on the presence or absence of associated endocrine disorders.

In 1971 *Tashjian and co-workers* (33) introduced a reliable method for measuring tumour produced calcitonin in serum and in the last 5 years this method has repeatedly been used in tracing occult MCT in kindreds with known familial type of the disease (3 20 24 33 35) Apart from two small series, however, calcitonin screening of MCT kindreds has not been performed in kindreds with apparently sporadic disease.

The aim of the present investigation was to study epidemiological and genetic aspects of MCT in a stable population. The material comprises 54 probands born in Norway biopsied or treated surgically during the 15-year period 1960–1974

MATERIAL AND METHODS

Ascertainment and Proband Studies

During the 15-year period 1960 through 1974 1670 cases of thyroid carcinoma were reported to The Norwegian Cancer Registry Of these the histological slides were reviewed from all carcinomas indexed as medullary solid, anaplastic, not specified metastatic, and from papillary and follicular carcinomas if the histological description was equivocal Histological slides were reviewed from a total of 807 cases. Of 42 tumours primarily diagnosed as MCT the diagnosis was confirmed in 33 cases, and of 765 cases originally diagnosed as other types 19 were found to be of the medullary type Five additional cases were found by reviewing tumours from the files of the Norwegian Radium Hospital primarily diagnosed as atypical adenomas. A total of 57 patients were thus traced 3 were born in other countries, leaving 54 probands for epidemiological and genetic studies.

In all cases the diagnosis was based upon histological examination In 12 cases where tumour amyloid was lacking elevated levels of serum immuno-reactive calcitonin (12) and/or electron microscopically demonstrable secretory granules served as additional diagnostic criteria (28)

Clinical data were obtained from the files of the Cancer Registry and the hospital records. Details have been given in a previous publication (27)

The *mean annual incidence rate* was defined as the mean number of new cases diagnosed yearly per 100 000 of the population. Age-adjusted incidence rates were also calculated. The population used in these calculations was that of 1967

The *observed number* of cases of MCT was recorded for urban and rural areas as well as for each county The *expected number* of cases in each geographical group was estimated by direct standardization (15) using age-specific rates (1967 census) for the whole country as standard rates. The χ^2-test was applied to test the significance of the difference in urban vs. rural distribution of the cases.

Family Studies

Special *questionnaires* asking for information about familial occurrence of disease, with special regard to thyroid disease other endocrine disorders, peptic ulcer and kidney stones, were sent to the patients or their close relatives. The questionnaires were answered in 52 cases. Kindreds of probands revealing bilateral presence of MCT young onset age pheochromocytoma hyperparathyroidism, and peripheral neuromas were considered genetically at "high risk" for MCT

Genealogical studies were performed partly by trained genealogists and partly by the author The sources were church records, national census data and local histories. All birthplaces were registered by a 4-digit code number the first two indicating county the last two municipality

Serum immuno-reactive calcitonin was measured in 300 relatives of 43 probands, according to the method described by Gautvik et al. (12) Of these, 184 were relatives of the first degree, while the total number of first-degree relatives was 240 The upper normal limit of the hormone was set at 0.50 ng/ml. Twelve of the iCT tested individuals had a positive history of thyroid disease. Details on the family screening program are given separately (26)

RESULTS

Proband Studies

Age and sex Fig 1a shows the age at diagnosis and the sex distribution of the 54 probands The mean age at diagnosis was 56.3 years the youngest patient was 16 the eldest 86 years. The peak incidence was in the sixth and seventh decades. Thirty-three were females and 21 males, giving a female/male ratio of 1 6.

Mean annual incidence rate The annual number of new primary cases of MCT in Norway 1960–1974 ranged from 1 to 9 with

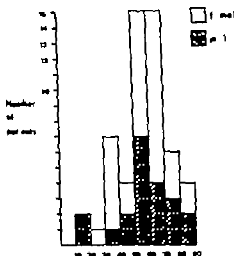


Fig. 1 a. The age and sex distribution of 54 primary cases of MCT diagnosed in Norway 1960–74

a mean of 3.8 cases, giving a mean annual incidence rate for detected MCT of approximately 0.1 per 100,000. The age-specific incidence rate rose evenly with advancing age (Fig. 1b) and the peak (0.3 per 100,000) was reached in the 7th decade. The number of new cases registered per year is too small to permit an estimate of any possible change in incidence rate during the actual 15-year period.

The average annual number of new cases of all types of thyroid carcinoma in the same period was 110, which means that the *relative frequency* of MCT among thyroid carcinomas was approximately 3.4 per cent.

Kindreds of 12 of the probands were considered at *high risk for familial occurrence* of MCT. In the majority of cases *only one* "high risk factor" was present (most frequently bilateral presence of the tumour) but 2 probands (nos 25 and 50) presented 3 and 4 factors, respectively. Details have been given in a previous publication (26).

Geographical distribution. Norway is divided into 20 counties* two of which are larger cities (Oslo 03 and Bergen 13), leaving 18 mainly rural counties with 443 municipalities, including 45 urban ones. Apart from Oslo and Bergen, Norway in 1967 had only one other city (Trondheim) with a population above 100 000. The populations of the remaining 44 urban municipalities ranged from approximately 2 000–80,000. The urban/rural

* Owing to the fusion of 2 counties, the total number of Norwegian counties was reduced to 19 in 1972.

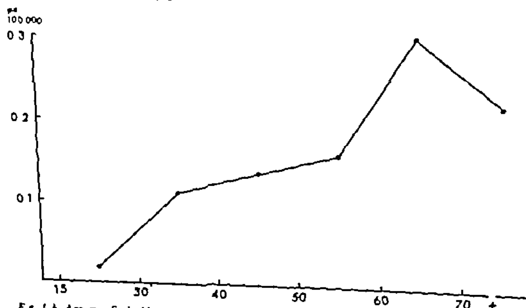


Fig. 1 b. Age specific incidence rates for *MCT* in Norway (1960–74)

but generally high degrees of penetrance. The separation of familial and sporadic cases has been based on the family history and/or on the presence or absence of associated endocrine disorders.

In 1971 *Tashjian and co-workers* (33) introduced a reliable method for measuring tumour produced calcitonin in serum and in the last 5 years this method has repeatedly been used in tracing occult MCT in kindreds with known familial type of the disease (3 20 24 33, 35) Apart from two small series, however, calcitonin screening of MCT kindreds has not been performed in kindreds with apparently sporadic disease

The aim of the present investigation was to study epidemiological and genetic aspects of MCT in a stable population. The material comprises 54 probands born in Norway biopsied or treated surgically during the 15-year period 1960–1974

MATERIAL AND METHODS

Ascertainment and Proband Studies

During the 15 year period 1960 through 1974 1670 cases of thyroid carcinoma were reported to The Norwegian Cancer Registry Of these, the histological slides were reviewed from all carcinomas indexed as medullary solid anaplastic, not specified metastatic, and from papillary and follicular carcinomas if the histological description was equivocal. *Histological slides* were reviewed from a total of 807 cases. Of 42 tumours primarily diagnosed as MCT the diagnosis was confirmed in 33 cases and of 765 cases originally diagnosed as other types, 19 were found to be of the medullary type. Five additional cases were found by reviewing tumours from the files of the Norwegian Radium Hospital primarily diagnosed as atypical adenomas. A total of 57 patients were thus traced 3 were born in other countries, leaving 54 probands for epidemiological and genetic studies.

In all cases the diagnosis was based upon histological examination. In 12 cases where tumour *amyloid was lacking elevated levels of serum* immuno-reactive calcitonin (12) and/or electron microscopically demonstrable secretory granules served as *additional diagnostic criteria* (28)

Clinical data were obtained from the files of the Cancer Registry and the hospital records. Details have been given in a *previous publication* (27)

The *mean annual incidence rate* was defined as the mean number of new cases diagnosed yearly per 100 000 *of the population.* Age-adjusted incidence rates were also calculated. The population used in these calculations was that of 1967

The observed number of cases of MCT was recorded for urban and rural areas as well as for each county The *expected number* of cases in each geographical group was estimated by direct standardization (15) using age-specific rates (1967 census) for the whole country as standard rates. The χ^2-test was applied to test the significance of the difference in urban vs. rural distribution of the cases

Family Studies

Special *questionnaires* asking for information about familial occurrence of disease, with special regard to thyroid disease, other endocrine disorders, peptic ulcer and kidney stones, were sent to the patients or their close relatives. The questionnaires were answered in 52 cases. Kindreds of probands revealing bilateral presence of MCT young onset age pheochromocytoma, hyperparathyroidism, and peripheral neuromas were considered genetically at "high risk" for MCT

Genealogical studies were performed partly by trained genealogists and partly by the author The sources were church records, national census data and local histories. All birthplaces were registered by a 4-digit code number the first two indicating county the last two municipality

Serum immuno-reactive calcitonin was measured in 300 relatives of 43 probands, according to the method described by Gautvik et al. (12) *Of these 184 were relatives of the first degree,* while the total number of first-degree relatives was 240 The upper normal limit of the hormone was set *at 0.50 ng/ml. Twelve of the* ICT tested individuals had a positive history of thyroid disease Details on the family screening program are given separately (26)

RESULTS

Proband Studies

Age and sex Fig 1a shows the age at diagnosis and the sex distribution of the 54 probands. The mean age at diagnosis was 56.3 years the youngest patient was 16 the eldest 86 years The peak incidence was in the sixth and seventh decades. Thirty three were *females* and 21 males, giving a female/male *ratio of 1 6*

Mean annual incidence rate The annual number of new primary cases of MCT in Norway 1960–1974 ranged from 1 to 9 with

Symbols of figures 2-8

- Verified MCT
- Probable MCT by family history
- Serum ICT elevated
- —— —— normal
- —— —— not tested
- Number of individuals
- Proband

Fig 2-7 Pedigrees of 15 probands with MCT found to have a common ancestors. The figures also show the extent and results of ICT screening of first-degree relatives. From Fig 2 3 it is evident that 10 of the related probands originated in the same county while Figs. 6 and 7 reveal that the remaining 5 related probands were born in different counties.

Fig. 4 also includes the pedigree of case no 58, where parental consanguinity was demonstrated (the parents were first cousins) More distant relationship was demonstrated between the parents of cases 1 and 28 (Fig. 7)

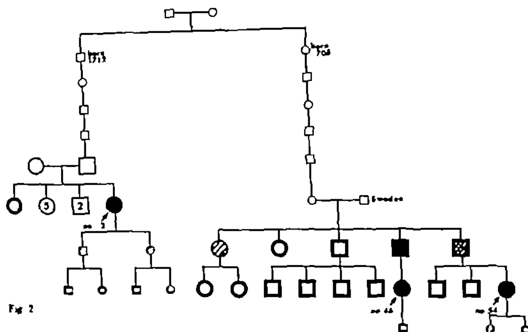


Fig 2

In another family a brother of the proband (no 28) was known to suffer from malignant thyroid disease, which proved to be an anaplastic thyroid carcinoma A positive family history of thyroid disease was elicited in 17 individuals from 9 families. Reviews of the histological slides from 8 of these cases revealed benign disorders. In 8 of the persons not operated, serum values of ICT were measured and found normal In one person the nature of the thyroid disease is completely unknown. In none of the families was it possible to elicit a positive history of pheochromocytoma or parathyroid disease.

Pedigree studies were possible in 46 of the 54 probands information beyond the 4th generation was available in 39 In all, 15 probands were found to be related to one or two of the others. Figs. 2, 3 and 7 show the pedigrees of cases where 3 probands were found to belong to the same pedigree Fig 4 5 and 6 show the pedigrees of those cases where 2 probands belonged to the same pedigree. Apart from the two first cousins shown

50*

TABLE 1 *Observed and Expected Numbers of Patients with MCT according to County and Urban/Rural Residence in Norway during 1960-1974*

County no	Obs. no	Urban Obs. no.	Urban Exp. no.	Urban Ratio obs/exp	Rural Obs. no.	Rural Exp. no	Rural Ratio obs/exp
01		1	1.3	0.8	0	1.6	0
02					3	3.5	0.8
03		2	8.0	0.2			
04	0.7 per	1	0.4	2.5	0	2.1	0
05	100 000	0	0.6	0	4	1.9	2.1
06		1	1.4	0.7	1	1.4	0.7
07		0	0.7	0	1	1.6	0.6
08		0	1.3	0	0	1.0	0
09		1	0.3	3.3	2	0.9	2.2
10		1	1.1	0.9	3	0.5	6.0
11		1	1.9	0.5	3	1.4	2.1
12					2	3.6	0.6
13	2.0 per	1	1.8	0.6			
14	100 000	0	0.1	0	5	1.4	3.6
15		0	0.8	0	4	3.0	1.3
16		2	1.7	1.2	2	1.5	1.3
17		0	0.4	0	4	1.2	3.3
18		1	0.3	3.3	5	2.7	1.8
19	2.0 per	0	0.7	0	2	1.0	2.0
20	100 000	0	0.2	0	1	0.7	1.4
Total		12	23.0	0.5	42	31.0	1.4

Counties 01–08 are inland counties, while the remainder (09–20) all have a coastline.

distribution of the Norwegian population in 1967 was 41/59. The counties are numbered consecutively from the southeastern corner towards the north. Those with numbers below 09 are mainly inland counties, while the remainder all have a coastline.

Table 1 shows the observed and expected numbers of patients with MCT according to county and residence at the time of diagnosis. (Eighty per cent of the patients lived at their birthplaces.) As will be seen, 42 of the 54 patients lived in rural districts, an accumulation of cases which was statistically significant ($p < 0.01$). Furthermore the number of cases observed in the 3 Norwegian cities with populations above 100 000 was 0.7 per 100 000 as compared with 1.6 per 100 000 for the rest of the country.

Table 1 also indicates *regional variation*. While the number of observed cases in the typical inland counties (01–08) was 0.7 per 100 000, the number occurring in counties with a coastline was 2.0 per 100,000. No difference in occurrence was observed between the three northern most counties (18–20) and the other counties with coastlines (09–17). The highest O/E ratios were registered in the rural areas of county 10 (Vest Agder), county 14 (Sogn og Fjordane) and county 17 (Nord Trøndelag). The number of patients is small, however, and tests for statistical significance of the O/E ratios have not been performed.

Family Studies

The questionnaires revealed that very few persons were able to give information about the illnesses of their relatives outside the immediate family. Two probands (nos 46 and 54) were first cousins and knew each other

Symbols of figures 2-8

- ■ ● Verified MCT
- ▨ ◍ Probable MCT by family history
- ■ ● Serum iCT elevated
- ◻ ○ —— —— normal
- □ ○ ——"—— not tested
- [2] ⑤ Number of individuals
- ↗ Proband

Fig 2–7 Pedigrees of 15 probands with MCT found to have common ancestors. The figures also show the extent and results of iCT screening of first-degree relatives. From Fig. 2 5 it is evident that 10 of the related probands originated in the same county while Figs. 6 and 7 reveal that the remaining 5 related probands were born in different counties.

Fig. 4 also includes the pedigree of case no 38, where parental consanguinity was demonstrated (the parents were first cousins) More distant relationship was demonstrated between the parents of cases 1 and 28 (Fig 7)

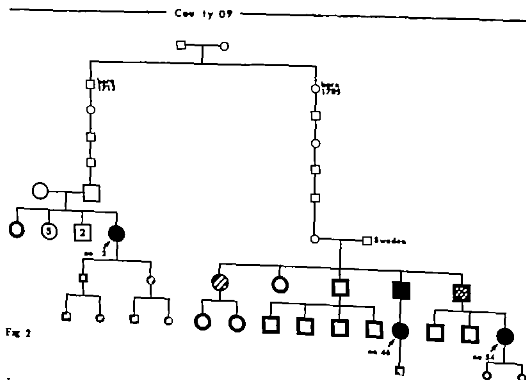


Fig 2

In another family a brother of the proband (no 28) was known to suffer from malignant thyroid disease, which proved to be an anaplastic thyroid carcinoma. A positive family history of thyroid disease was elicited in 17 individuals from 9 families. Reviews of the histological slides from 8 of these cases revealed benign disorders. In 8 of the persons not operated, serum values of iCT were measured and found normal. In one person the nature of the thyroid disease is completely unknown. In none of the families was it possible to elicit a positive history of pheochromocytoma or parathyroid disease.

Pedigree studies were possible in 46 of the 54 probands information beyond the 4th generation was available in 39 In all, 15 probands were found to be related to one or two of the others. Figs. 2, 3 and 7 show the pedigrees of cases where 3 probands were found to belong to the same pedigree Fig 4 5 and 6 show the pedigrees of those cases where 2 probands belonged to the same pedigree. Apart from the two first cousins shown

TABLE 1 *Observed and Expected Numbers of Patients with MCT according to County and Urban/Rural Residence in Norway during 1960-1974*

County no.	Obs. no	Urban Obs. no	Urban Exp. no	Urban Ratio obs/exp	Rural Obs. no.	Rural Exp. no	Rural Ratio obs/exp
01		1	1.3	0 8	0	1 6	0
02					3	3.5	0 8
03		2	8.0	0.2			
04	0 7 per	1	0 4	2.5	0	2 1	0
05	100 000	0	0 6	0	4	1 9	2.1
06		1	1 4	0 7	1	1 4	0 7
07		0	0 7	0	1	1 6	0 6
08		0	1.3	0	0	1 0	0
09		1	0.3	3.3	2	0 9	2.2
10		1	1 1	0 9	3	0.5	6 0
11		1	1 9	0.5	3	1 4	2.1
12					2	3 6	0.6
13	2 0 per	1	1 8	0 6			
14	100 000	0	0 1	0	5	1 4	3 6
15		0	0 8	0	4	3 0	1.3
16		2	1 7	1.2	2	1.5	1.3
17		0	0 4	0	4	1.2	3.3
18		1	0 3	3.3	5	2 7	1.8
19	2.0 per	0	0 7	0	2	1 0	2.0
20	100 000	0	0 2	0	1	0 7	1 4
Total		12	23 0	0.5	42	31 0	1 4

Counties 01–08 are inland counties, while the remainder (09–20) all have a coastline.

distribution of the Norwegian population in 1967 was 41/59 The counties are numbered consecutively from the southeastern corner towards the north Those with numbers below 09 are mainly inland counties, while the remainder all have a coastline.

Table 1 shows the observed and expected numbers of patients with MCT according to county and residence at the time of diagnosis. (Eighty per cent of the patients lived at their birthplaces) As will be seen 42 of the 54 patients lived in rural districts an accumulation of cases which was statistically significant ($p < 0\ 01$) Furthermore the number of cases observed in the 3 Norwegian cities with populations above 100 000 was 0 7 per 100 000 as compared with 1 6 per 100 000 for the rest of the country

Table 1 also indicates *regional variation* While the number of observed cases in the typical inland counties (01–08) was 0 7 per 100 000 the number occurring in counties with a coastline was 2.0 per 100 000 No difference in occurrence was observed between the three northern most counties (18–20) and the other counties with coastlines (09–17) The highest O/E ratios were registered in the rural areas of county 10 (Vest Agder) county 14 (Sogn og Fjordane) and county 17 (Nord Trøndelag) The number of patients is small, however and tests for statistical significance of the O/E ratios have not been performed

Family Studies

The questionnaires revealed that very few persons were able to give information about the illnesses of their relatives outside the immediate family Two probands (nos 46 and 54) were first cousins and knew each other

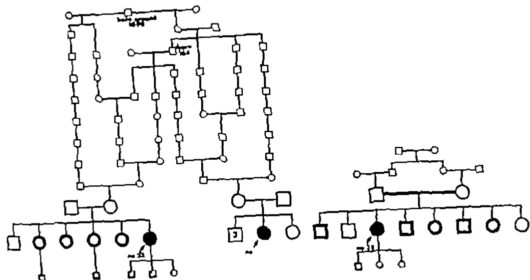


Fig. 4

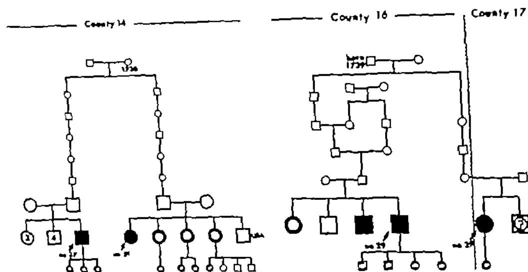


Fig 5

Fig. 6

western counties 14 and 15 and along the coast of Nordland (county 18)

Measurement of serum calcitonin in relatives. Persistently raised values (> 0.30 ng/ml) were found in 5 persons (from 3 families) out of 300 tested. Two individuals belonged to the family of probands nos 46 and 54 and pedigree studies revealed that these two were distantly related to a third proband (Fig 2) Two were relatives of case no 12, about whom no genealogical information was available (Fig 8 A) The fifth person with persistent hypercalcitoninemia was a brother of case no 36 Pedigree studies in this family failed to demonstrate a relationship to any of the other probands (Fig. 8b)

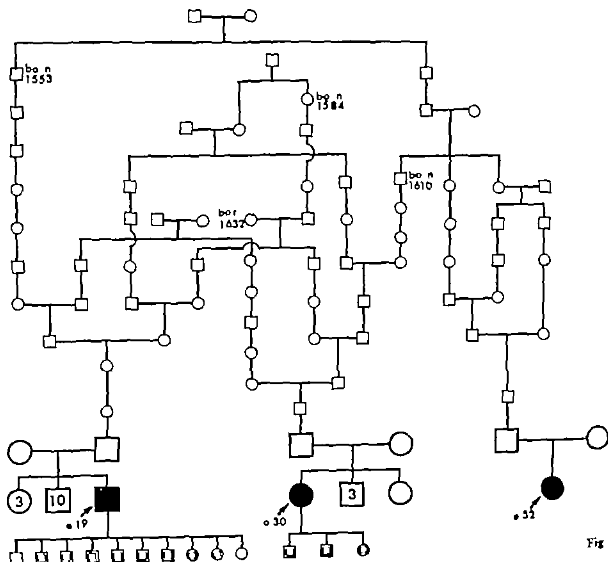


Fig 3

in Fig 2 all the registered relationships were of a distant character

Consanguineous marriages between parents of the patients were demonstrated in families nos 1 28 and 38 (Fig 4 and 7)

By comparing code numbers for *grand parents birthplaces* it became evident that one or more of the grandparent of 26 of the 46 proband investigated originated in the same rural municipality as the grand parents of from one to four other probands In 10 of these cases it was possible to prove familial relationship as well (Fig 2-5)

In the remaining 16 kindreds it has not been possible to demonstrate familial relations but in many of these cases the genealogical information is incomplete

The places of common origin showed no clearcut concentration in any special part of the country (Fig 9) but they were all rural municipalities, and apart from a concentration in one of the large central valleys of Norway (in county 5) all were small and sparsely inhabited. There appeared to be some concentration in the three south western counties 9 10 and 11 the two north

The screening comprised members of all but 4 of the 26 kindreds where familial and/or geographical relationships had been demonstrated. In all, 211 persons from these kindreds were tested All individuals with persistent elevation of serum calcitonin belonged to kindreds considered at high risk for familial occurrence of the disease. On the other hand, the screening was negative in 7 other high risk families and equivocal in two Two families (nos 1 and 51) at high risk, but with negative screening results, belonged to the group in which distant relationship to other probands was demonstrated (Fig 5 and 7)

DISCUSSION

Continuity of settlement since the Viking age some 1000 years ago, and rather good access to genealogical material, makes Norway—with its 4 million inhabitants—suitable for genealogical and epidemiological studies. In addition, when cancer is the topic, The Norwegian Cancer Registry to which all cases of malignant diseases diagnosed in Norway have been reported since 1952, constitutes a valuable source of information.

The present study on MCT in Norway revealed that the mean annual incidence rate of new histologically-verified cases during the 15-year period 1960 through 1974 was 0 1 per 100,000 The tumour constituted 3 4 per cent of all thyroid carcinomas registered in Norway in the same period. In a study of thyroid carcinomas diagnosed in Finland 1958–62, *Franssila* (10) found that MCT comprised 4 4 per cent of all types. The incidence figures in both series surely represent minimum figures, since MCT usually presents itself as an oligo-symptomatic, slowly-growing tumour with late onset age (the highest incidence rate of the disease (0.3 per 100,000) was in the 7th decade) and relatively good prognosis (27) A number of persons may therefore have lived and died with undiagnosed disease. Furthermore, pathologists still seem to have problems in recognizing this tumour (28) *Williams* (37) declares that in order to give a correct incidence figure of MCT examples of practically every type of thyroid tumour benign or malignant, primary or secondary should be reviewed. By reviewing all Norwegian cases of those malignant tumours most commonly harbouring misinterpreted MCT and probably more than half of the atypical adenomas, the majority of biopsied or surgically treated MCT cases in Norway from the actual period have probably been traced. The female/male ratio of 1.6 in the present study corresponds well with the findings of others (13 14 16 18 23 36)

It has been widely accepted that MCT occurs in one sporadic and one hereditary form, the hereditary form comprising from 3 to 20 per cent in different materials (3 7 13 16, 18, 23) The two forms are not separable with regard to histological picture or prognosis, but bilaterality of the thyroid tumour young onsetage and association with other endocrine tumours (pheochromocytoma, parathyroid hyperplasia/adenoma) or peripheral neurogenic tumourlike conditions are considered "high risk" factors and indicative of genetic etiology (1 7 16 18, 23 36) In the present study it was not possible to demonstrate familial occurrence in more than approximately half of the kindreds considered genetically at high risk for MCT

By the introduction of raised serum calcitonin as a tumour marker for MCT (33) a considerably more reliable marker of genetic etiology was obtained However apart from the small series presented by *Jackson et al.* (19) and *Telenius-Berg* (34) the reported iCT screenings of MCT families have been restricted to kindreds with a positive family history and/or genetically at high risk (3 20 24 33 35) The present investigation, which includes serum iCT measurements in relatives of both familial and apparently sporadic cases, has so far led to the discovery of persistently elevated serum iCT levels in relatives of 4 probands, whereof 2 are considered to be of the sporadic type. Relatives of 4 additional probands with apparently sporadic disease are under current control for transitory hypercalcitoninemia (26)

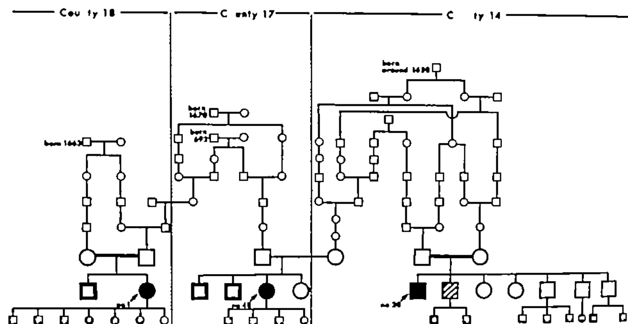


Fig 7

Seven members of 4 additional families (of probands nos 11 23 29 and 34) had slightly elevated serum levels of the hormone on one occasion Their iCT values will therefore be re-examined The significance of one moderately raised iCT value is not clear

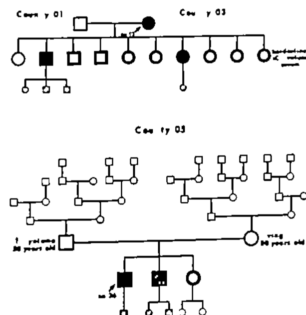


Fig 8 A–B Pedigrees of 2 probands with MCT whose first-degree relatives showed persistent elevation of serum iCT levels In case no 12 it was not possible to obtain reliable information about the ancestors



Fig 9 Birthplaces of grandparents of 46 primary cases of MCT marked ● (The father was unknown in one family the grandfather in another Six grandparents were born in Sweden) In 8 cases no information about grandparents was available. In these cases the patients' own birthplace is marked ▲

I gratefully acknowledge the valuable ad ice and criticism received in discussions with *Carl Berger sen der Hagen Tobias Gedde-Dahl, Letten Fåger ster Saugstad* and *Knut M gnus*. I also wish to thank *Einar P dersen*, Head of The Norwegian Cancer Registry for placing the data of the Reg stry at my disposal, and *Torberg Iversen, Jan H Olstad Per Seland, Egil Iversen Tor L. Lar sen Sig Engen* and *Anne-Brit Lande* for their assistance in collecting the genealogical data. The work was financially supported by the Norwegian Radium Hospital.

REFERENCES

1. *Baylin S B.*, Medullary carcinoma of the thyroid gland Use of biochemical parameters in detection and surgical management of the tumour Surg. clin. North Am. *54* 309–323 1974
2. *Beaugie J M., Belchetz P E., Brown, C L. Froebel R. J & Lloyd M H* Report of family with inherited medullary carcinoma of the thyroid and phaeochromocytoma. Br J Surg 62 264–268 1975
3. *Block, M A Jackson C. E. & Tashjian A. H* Medullary thyroid carcinoma detected by serum calcitonin assay Arch Surg *104* 579–586, 1972.
4. *Block M A., Miller J M & Horn R. C jr* Medullary carcinoma of the thyroid Surgical implications Arch. Surg. 96 521–526, 1968.
5. Cancer registration in Norway The incidence of cancer in Norway 1964–1966 p 44 The Norwegian Cancer Society Oslo 1969
6. *Catalona, W J E gelman K., Ketcham, A S & Hammond W G* Familial medullary thyroid carcinoma, pheochromocytoma, and parathyroid adenoma (Sipple' syndrome) Study of kindred. Cancer *28* 1245–1253 1971
7. *Chong G C Beahrs O H Sizemore G W & Woolner L H* Medullary carcinoma of the thyroid gland Cancer 35 695–704 1975
8. *Cushman P jr* Familial endocrine tumors Report of two unrelated kindred affected with pheochromocytomas, one also with multiple thyroid carcinomas. Am J Med. 32 352 360 1962.
9. *D n E L., Nishiyama, R. H & Thompson N W* Medullary carcinoma of the thyroid gland. Surg. 73 848–858, 1973.
10. *Franssila K* Value of histologic classification of thyroid cancer Acta path. et microbiol. scand. Sect A 1971 Suppl. no. 223 p 22.
11. *Freeman D & Lindsey S* Medullary carcinoma of the thyroid gland. A clinicopathological study of 33 patients. Arch Path. *80* 575–582 1965
12. *Gautvik K M., Vermann T., Teig, I., Wille S O., Brennhovd I O & Christensen I* Radioimmunoassay of human calcitonin in serum and tissue from healthy individuals and patients with medullary carcinoma of the thyroid gland. Scand. J clin. Lab Invest. *36* 323–329 1976.
13. *Gordon, P R., Huvos A G & Strong E. W.*, Medullary carcinoma of the thyroid gland. A clinicopathologic study of 40 cases. Cancer *31* 915–924 1973
14. *Hazard, J B Hawk W A & Crile G jr.*, Medullary (solid) carcinoma of the thyroid —a clinicopathologic entity J clin. Endocrinol. *19* 152 161 1959
15. *Hill, A B.*, Standardised death-rates and indices. In Principles of Medical Statistics. The Lancet Ltd. London 1971 p. 203–210
16. *Hill, C S jr., Ibanez M L., Samaan N A., Ahearn M J & Clark R. L.*, Medullary (solid) carcinoma of the thyroid gland An analysis of the M. D Anderson Hospital experience with patients with the tumor its special features, and its histogenesis. Medicine 52 141 171 1973
17. *Huang, S N & M Leith, W A.*: Phaeochromocytoma and medullary carcinoma of thyroid. Cancer *1* 302–310 1968.
18. *Ibanez M L.* Medullary carcinoma of the thyroid gland. In Path. Annual 1974 ed. Sheldon C. Sommers, M. D p. 263–290.
19. *Jackson C. E., Tashjian A H jr & Block M A* Detection of medullary thyroid cancer by calcitonin assay in families. Ann. Int. Med. *78* 845–852, 1973.
20. *Keiser H R.*, Sipple s syndrome Medullary thyroid carcinoma, pheochromocytoma, and parathyroid disease. Studies in a large family Ann. Int. Med. *78* 561 579 1973
21. *Knudson A G. jr.*, Heredity and human cancer Am. J Pathol. 77 77–84 1974
22. *Knudson A G jr.*, The genetics of child hood cancer Cancer 35 1022–1026, 1975
23. *Ljungberg, O* On medullary carcinoma of the thyroid. Acta path. et microbiol. scand. Sect. A 1972. Suppl. no 231
24. *Melvin, K. E. W., Tashjian A H jr & Miller H H* Studies in familial (medullary) thyroid carcinoma. Recent Progr Hormone Res. *28* 399–470, 1972.
25. *Muller M.*, Etude clinique et anatomo-pathologique de 31 carcinomes médullaires stroma amylo de de la thyroïde Schweiz. med. Wschr 99 433–439 1969.
26. *Vermann T & Gautvik K. M.*, Medullary

In addition to the cases in which familial occurrence was diagnosed by iCT screening pedigree studies demonstrated that 13 probands were related to one or two of the others 16 additional probands were found to have grandparents originating in the same rural municipality as the grandparents of one or more of the others. It seems to be a reasonable assumption that at least some of these 16 may in fact represent familial cases with a common genetic origin. The rate of *consanguineous marriages* (between 2nd cousins or closer) in rural areas was, according to the 1881 census, 8 1 per cent and in some municipalities as high as 10 7 per cent (30) Consanguineous marriages between more distant relatives must have been even more frequent. Thus, *Saugstad and Ødegaard* (*Saugstad* personal *communication*) in a study of the marriage pattern in one rural district of Norway (*Vang & Slidre*) between 1600 and 1850 found that 60 per cent of the marriages were contracted between partners living less than 9 farms apart, and only 1 2 per cent of the partners came from outside the district.

Until now it has been commonly accepted that in its familial form MCT is inherited as an *autosomal dominant* trait with a relatively high degree of penetrance (3 6 8 19 20 23 24 31 32) In the present study at least one family (of probands nos 46 and 54) and possible one other (of proband no 12) fit in with such a pattern *An autosomal recessive* trait must be considered in the 3 probands whose parents were inbred (proband no 38 in Fig 4 and probands nos 1 and 28 in Fig 7) One other pedigree (proband no 48) may also point to autosomal recessive inheritance. The frequency of inbreeding for the total series of probands was however not higher than could be expected considering the rural preponderance of the material Furthermore if the familial and/or geographical relationships demonstrated in the other kindreds of this investigation involve a genetic predisposition the frequency of affected individuals judged by iCT family screening is extremely low and not in accordance with simple Mendelian inheritance.

Also in other dominantly inherited tumours, such as retinoblastoma, neuroblastoma, and Wilms tumour a low number of affected persons has been noted in kindreds of apparently sporadic cases (22) Utilizing the study of these childhood tumours, *Knudson* (21 22) has presented a two-step model *for cancer development in dominantly inherited cases* the first step is a mutation where the mutated gene is carried in the germ line. In the apparently sporadic cases, the first step is also thought to be a mutation, but in a somatic cell In both forms, a second mutation in somatic cells is necessary for the development of cancer If this theory is applied to the development of MCT the *distant relationship and/or common origin of* many probands may indicate that these probands carry a common genetic predisposition for this type of cancer with a somatic mutation as a precipitating event. The results of the study give no answer to the question of whether a mutation or another secondary event eventually leads to cancer development. Common enviromental factors may come into *consideration since there was a significant* accumulation of cases in rural areas, and especially along the coastline *In Norway* thyroid carcinoma generally occurs more frequently in coastal areas but apart from this, the geographical distribution of *MCT did not* follow the overall tendency for distribution of thyroid carcinomas in Norway which shows a significant accumulation in the *northernmost part* (29) and only a slight predominance in rural areas (5)

Based on the study of the Norwegian population, a genetic etiology of MCT seems considerably more frequent than previously assumed. The pattern of inheritance is not fully clarified in all cases, but the study sheds serious doubt on the statement that in its familial form MCT is always inherited as an autosomal dominant trait. In the majority of cases in the present series, the pattern of *inheritance is not* consistent with a simple Mendelian trait.

Acta path. microbiol. scand. Sect. A, 85 787–800 1977

LIVER ULTRASTRUCTURE IN PSORIATICS RELATED TO METHOTREXATE THERAPY

1 A Prospective Study of Findings in Hepatocytes from 24 Patients before and after Methotrexate Treatment

A. Nyfors and D. Hopwood

Department of Dermatology The Finsen Institute, Copenhagen, Denmark and Department of Pathology Ninewells University Hospital, Dundee, Scotland

Nyfors, A & Hopwood, D Liver ultrastructure in psoriatics related to methotrexate therapy 1 A prospective study of findings in hepatocytes from 24 patients before and after methotrexate treatment. Acta path. microbiol. scand. Sect. A, 85 787–800 1977

To show what damage occurs in the hepatocytes of psoriatics receiving Methotrexate (MTX) therapy liver biopsies from 24 psoriatics with severe psoriasis before and after MTX therapy were studied blind by light and electron microscopy We also aimed to determine the severity of lesions and find possible correlations, and to seek a relationship of these observations with light microscopical and clinical findings. The present study has shown that MTX probably caused damage to the hepatocytes reflected in the membrane whorls ($p < 0.05$) and the accumulation of lipid droplets ($p < 0.05$) There was an increase ($p < 0.05$) in autophagic vacuoles, which mostly contained glycogen and cell sap with residual bodies. These residual bodies were then found in an increased number in the nearby Kupffer cells. Crystals were found in megamitochondria in most patients before and after MTX therapy Some of these crystals were found free in the cytoplasm. Mitochondria containing crystals were shown in autophagic vacuoles, representing possible pathways of their breakdown, Bile canaliculi commonly contained debris but only one patient had evidence of cholestasis. There was no significant change in nuclei, Golgi apparatus, or the endoplasmic reticulum and no statistically significant correlation between the shown changes and the total dose of MTX given

Key words Methotrexate therapy; psoriasis ultrastructure liver

A. Nyfors, Department of Dermatology The Finsen Institute, Copenhagen, DK 2100 Denmark.

Received 8 iii.76 Accepted 24 v 77

Methotrexate has been used since 1955 to an increasing extent in the treatment of the most severe cases of psoriasis. MTX therapy has been reported to clear recalcitrant psoriasis vulgaris in 60–70 per cent of cases (14 20) Case reports of liver disease, particularly cirrhosis, observed during MTX therapy have aroused concern (5 12) Prospective studies including liver biopsy in psoriatics before MTX therapy and in the same patient at intervals during MTX therapy have been undertaken (17 25) They revealed an increase in the number of pathological findings in the post MTX liver biopsies.

There appears to be no detailed information on the ultrastructural findings in the livers of psoriatics treated with MTX There

carcinoma of the thyroid gland in Norway Serum calcitonin screening in 300 members of 42 kindreds. Ann. Chir Gyn. In press.

27 *Normann T Gautvik K M Johannessen J V & Brennhovd I O* Medullary carcinoma of the thyroid in Norway Clinical course and endocrinological aspects. Acta Endocrinol *83* 71–85 1976

28 *Normann T Johannessen J V Gautvik K M Olsen B R & Brennhovd I O* Medullary carcinoma of the thyroid Diagnostic problems Cancer *38* 366–377 1976

29 *Pedersen E & Haugen A* Thyroid cancer in Norway UICC Monograph Series, Vol 12 p. 71–74 1967

30 *Saugstad L F The relationship between inbreeding migration and population density in Norway Ann. hum. Genet *40* 331–341 1976

31 *Schimke R N & Hartmann W H* Familial amyloid producing medullary thyroid carcinoma and pheochromocytomas. A distinct genetic entity Ann. Int. Med *63* 1027–1039 1965

32 *Steiner A L, Goodman A D & Powers S R* Study of a kindred with pheochromocytoma, medullary thyroid carcinoma hyperparathyroidism and Cushing's disease Multiple endocrine neoplasia, Type 2[1] Medicine *47* 371–409 1968.

33 *Tashjian A H jr Howland B G Kenneth, B A Melvin E W & Hill C S jr* Immunoassay of human calcitonin, Clinical measurement, relation to serum calcium and studies in patients with medullary carcinoma. New Eng J Med. *283* 890–895 1970

34 *Telenius-Berg M* Diagnostic studies in medullary carcinoma of the thyroid. New methods for early diagnosis in families with Sipple's syndrome. Acta Med. Scand. suppl. no 597 1976

35 *Wells S A jr Ontjes D A Cooper C W, Hennessy J F Ellis G J McPherson H T & Sabiston D C jr.*. The early diagnosis of medullary carcinoma of the thyroid gland in patients with multiple endocrine neoplasia Type II Ann. Surg *182* 362–370 1975

36 *Williams E D* Medullary carcinoma of the thyroid. Rec Adv path. *9* 156–182 1975

37 *Williams E. D Brown C L & Doniach I* Pathological and clinical findings in a series of 67 cases of medullary carcinoma of the thyroid. J clin Path *19* 103–113 1966

TABLE I *Semi-quantitat A pe t of Ult astruct ral Findings in Hepatocytes Psoriatics befor and after Methotre ate Ther py*

Liver biopsy no.	Interval last MTX last l.b. (days)	Cumulative dose of MTX (mg)	Megamitochondria with crystals		Increase in SER		Increase in lysosomes + autophagic vacuoles (APV)		Pigment		Fat		Bile canaliculi debris		Membrane whorls	
			pre	post	pre	post	pre	post	pre	post	pre	post	pre	post	pre	post
270	1	1493	+	+	0	+	0	0	+ +	+ +	+ +	+ + +	0	+	+	+
292	1	3218	+	+	+	0	0	APV	+ +	+ +	+	+	0	+	+	+
308	1	1800	0	0	0	0	0	0	+ +	+ +	+	+ +	+	0	0	+
321	1	1383	+	+	0	+	0	0	+	+ +	+	+	0	+	0	+
294	2	2830	0	0	0	+	0	+	+	+	+ +	+ + +	0	0	0	+
299	2	1074	0	+	+	+	0	0	+ +	+ +	+	+	0	+	0	+
295	4	2330	0	+	0	0	0	0	+ + +	+	+	+	+	+	+	+
296	4	895	+	+	0	0	0	APV	+ + +	+ +	+	+ +	0	+	0	+
293	5	2290	0	0	0	+	0	0	+ +	+ +	+	+	0	+	+	0
349	5	1905	+	+	+	0	0	APV	+ +	+ +	+	+ +	0	+	0	+
233	6	2233	+	+	0	0	0	+	+	+ +	+	+ +	+	+	+	+
301	15	2517	+	+	+	0	0	0	+ +	+ +	+ +	+ +	0	+	0	+
258	39	5040	+	0	0	+	0	0	+ +	+ +	+	+ +	0	0	0	0
249	122	2100	0	0	+	+	0	0	+ +	+ +	+ + +	+	0	0	0	0
302	151	1960	+	+	+	0	+	APV	+ +	+ +	+	+	0	0	+	+
239	168	2833	+	+	0	+	0	0	+	+ +	+	+ +	0	0	0	+
311	183	765	0	+	+	0	0	0	+ +	+	+	+	0	0	0	+
307	240	873	0	0	+	+	0	APV	+	+	+ +	+ +	+	0	0	+
291	455	1183	0	+	0	0	0	0	+	+ +	+ +	+	0	0	+	0
303	600	490	+	+	0	+	0	APV	+ +	+	+ +	+ +	0	0	0	+
254	670	1450	+	0	+	0	+	0	+	+ +	+	+	0	0	0	0
308	731	735	0	+	0	+	0	APV	+	+ +	+ +	+ +	0	0	0	0
281	785	1193	+	+	0	0	0	APV	+ +	+ +	+	+	0	0	+	0
256	1120	5 8	0	0	0	0	0	0	+	+	+	+	0	+	0	+

have been two brief reports. *Nyfors et al* (1971) noted changes in some organelles and the accumulation of lipid droplets *Horvath et al* (1973) confirmed these observations and also found an increase in the number of Ito cells present. We have confirmed those last two observations (5) We have also demonstrated elsewhere fine structural changes in the bile ducts of MTX treated psoriatics (7)

The aims of this study are to show what damage occurs in hepatocytes of psoriatics on MTX to determine the severity of the lesions and find possible correlates to seek a relationship of these observations with the light microscopical and clinical findings.

MATERIAL AND METHODS

Patients

The material comprises 24 pairs of Menghini needle biopsies which were taken both before and after MTX therapy from each consenting patient with disabling psoriasis The liver biopsies were performed during the period August 1969 to March 1974 To be included in the study the patients had to fulfil the following criteria typical severe psoriasis with no lasting effect of other dermatological treatments Clinical features concerning the patients are described in detail elsewhere (16 17) MTX was given orally once a week in a single dose of up to 25 mg

Laboratory Tests

Liver function tests and other blood and urine tests taken at control visits and at liver biopsy are described elsewhere (16)

Light Microscopy

Part of each liver biopsy was fixed in 4 per cent formaldehyde and processed for light microscopy

Electron Microscopy

The remainder of the biopsy was cut into 1 mm cubes, fixed in 4 per cent glutaraldehyde at pH 7.2 and post osmicated and embedded in Araldite Thin section were cut with an LKB ultramicrotome stained with lead citrate and uranyl acetate and examined with an AEI 801 B electron microscope at 60 kV

The microscopical studies were done blind without knowledge of the clinical data.

Statistics

The significance of differences between the post MTX and the pre-MTX values of the various findings were evaluated by either the Sign test (data in nominal scale) or the Wilcoxon matched pairs signed ranks test (data in ordinal (rank) scale) while the significance of associations between the electron microscopical findings were estimated by means of the Spearman rank correlation coefficient (22)

RESULTS

Patients

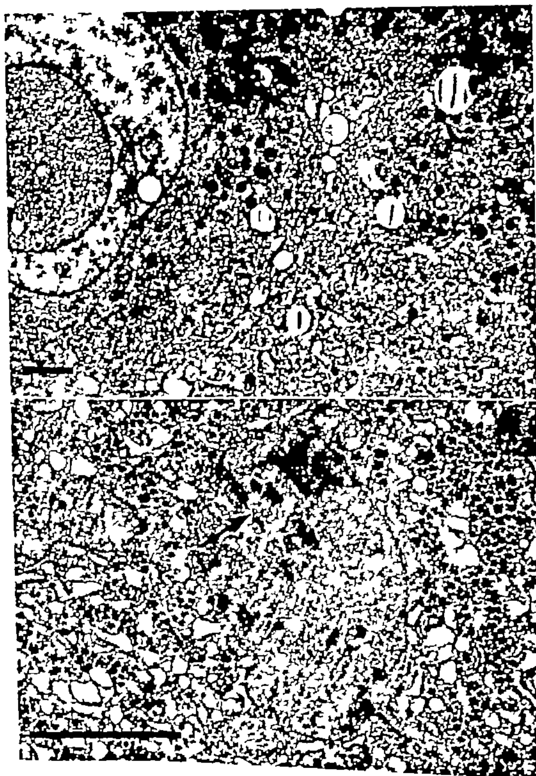
The average age of the patients (8 males, 16 females) was 47 years (range 25–77 years) at the first liver biopsy where the mean duration and extent of psoriasis (per cent of body surface involved) was 21 years (range 3–37 years) and 27 per cent (range 4–95 per cent) respectively The mean cumulative dose of MTX was 1810 mg (range 528–3218 mg) while the average duration of MTX therapy was 28 months (range 4–51 months) The interval between the last intake of MTX and the second liver biopsy was less than 1 week in 11 less than 1 month in 1 between 1–4 months in 2 while it in the remaining patients varied from 151–1120 days.

Light Microscopy

Results of the light microscopy are described in detail elsewhere (17) A statistical worsening of the light microscopy findings was found by the Sign test (1–9 p = 0 11) as 14 sets of liver biopsies remained unchanged 1 set improved and 9 sets developed more pathological findings during MTX therapy

Electron Microscopy
Semi quantitative Aspects

The results of the quantitative study are indicated in Table 1 Besides the data reported there, the nucleus, the Golgi apparatus, glycogen the space of Disse and cell membrane showed no change during MTX therapy in all 24 patients (95 per cent confidence limits 86–100 per cent) In patient



307 the RER increased in amount between the two liver biopsies while it was found to be increased in both liver b opsies in patient 254

Analysis by the Sign test showed in the 24 patients statistically significant increase in lysosomes ($p < 0.05$) and in membrane whorls ($p < 0.05$) while the increase in lipid droplets was found statistically significant ($z = 2.20$ $p = 0.014$ $p < 0.05$) by the Wilcoxon test in the 11 patients with an interval between the last dose of MTX and the second liver biopsy *shorter than 1 week.*

Qualitative Aspects

Nuclei Most of the nuclei observed under the electron microscope were within normal limits. In 3 patients nuclear pseudo-inclusions were found (Fig 1) These were also observed at the light microscopic level with *Araldite and paraffin sections.*

Mitochondria Abnormalities were found in the mitochondria at some time in 18 of the 24 patients. The changes took the form of irregular megamitochondria which invariably contained crystals (Figs. 2 and 3) The megamitochondria appeared to be budding The crystalline arrays were composed of *collections of rods sometimes shown* longitudinally and at other times seen in cross sections. In the more bizarre mitochondrial form the crystals run in all directions and the cristae are reduced in number In the simply elongated mitochondria the crystals run longitudinally sometimes obliterating the cristae The distribution of megamitochondria and crystals varied from patient to patient. In 4 patients (259 279 296 321) they were found in most cells. At the other extreme *a diligent search revealed only* a few in an occasional hepatocyte A few mitochondria had membranes which were incomplete and crystals were apparently present in the gaps (Fig 4)

Rough and smooth endoplasmic reticulum There was no overall change in the amount of rough or smooth endoplasmic reticulum present in the biopsy material In 5 patients (256 293 308 311 349) who admitted taking alcohol daily *there was an increase* in the smooth endoplasmic reticulum in 2, a decrease in 2 and normal amounts of SER in 1 patient (see Table 1)

The lysosomal apparatus The autophagic vacuoles and residual bodies (lipofuscin of light microscopy) were found to increase in a statistically significant way comparing hepatocytes in the pre-MTX and post MTX liver Autophagic vacuoles had a typical appearance containing organelles. In some *instances these* were mitochondria with crystals (Fig 5) The residual bodies varied from cell to cell in any one biopsy and were found chiefly around the bile canaliculi (Figs. 1 6 and 9)

Golgi apparatus There were no changes in the hepatocyte Golgi apparatus in the patients receiving MTX therapy compared with the pre MTX biopsies (Fig 6)

All illustrations are electron micrographs of hepatocytes from psoriatics treated with methotrexate.

Fig 1 The nucleus of the hepatocyte contains pseudo inclusions (P) The cytoplasm contains a number of residual bodies (arrow head) × 7 000. Scale = 2 µm

Fig 2 Bizarrely shaped mitochondrion containing many crystalline arrays (arrow) in different directions. × 40 000 Scale = 1 µm.

Fig 3 Mitochondrion containing crystals which are mostly cross sectioned (arrow *head) showing* various arrays. × 40 000 Scale = 1 µm.

Fig 4 Mitochondrion with inner and outher membranes apparently incomplete and the crystals project into the cytoplasm (arrow) × 45 000 Scale = 1 µm

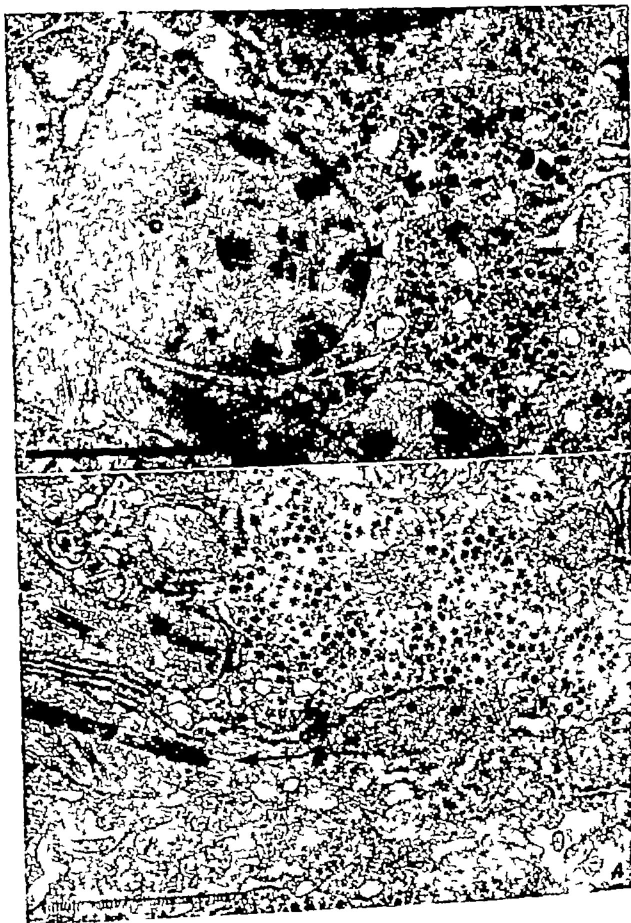
Fig 5 Autophagic vacuole (arrow) in a hepatocyte which contains a crystal bearing mitochondrion and other *organelles.* Another mitochondrion in the field contains crystals. × 45 000 Scale = 1 µm.

Fig 6 Two hepatocytes containing residual bodies (arrow heads) and Golgi apparatus (arrow) and a forming fat droplet (F) × 33 000. Scale = 1 µm.

A



34 Arta pech. mucosal gland. Sect. A, 83, 6


A



31

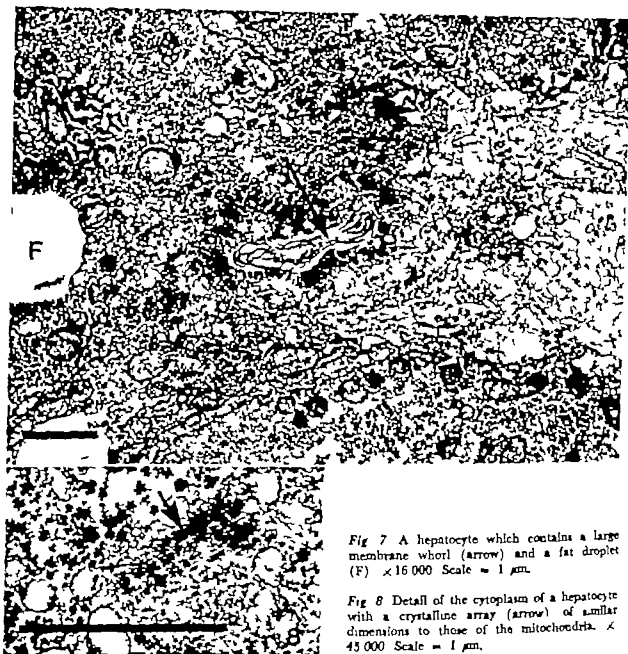


Fig 7 A hepatocyte which contains a large membrane whorl (arrow) and a fat droplet (F) ×16 000 Scale = 1 μm.

Fig 8 Detail of the cytoplasm of a hepatocyte with a crystalline array (arrow) of similar dimensions to those of the mitochondria. × 45 000 Scale = 1 μm.

Cytoplasm Membrane whorls (Fig 7) were found in the cytoplasm of the hepatocytes, most commonly in those patients who had had a liver biopsy shortly after the last dose of MTX (Table 1) They were found less frequently in those patients in whom some time had elapsed between the last dose of MTX and the subsequent liver biopsy The number varied from cell to cell The cytoplasm of one cell also contained a naked crystal of the same form and dimensions to those found in the megamitochondria (Fig 8)

Glycogen was found in the cytoplasm in all the biopsies before and after MTX therapy with no appreciable change in quantity

Lipids Lipid droplets were found in most hepatocytes. In 10 patients they occupied much of the cytoplasm. Some of the lipid droplets were homogenous and others contained membrane profiles (Figs 6 7 and 9)

Cell membrane The cell membranes, space of Disse and bile canaliculi in the hepatocyte were normal in all the liver biopsies. There were abnormalities, however associated with the content of the bile canali-

Fig. 9 Hepatocyte with lipid droplets (F) some containing membranes and some apparently being incorporated into residual bodies (arrow) The mitochondria contain crystals. × 7,500. Scale = 2 μm.

Fig. 10 Bile canaliculus containing particulate debris (arrow head) The microvilli (arrow) contain central fibrils derived from terminal web in the hepatocytes. × 35,000 Scale = 0.5 μm.

Fig. 11 Bile canaliculus containing membranous debris (m) × 21,000. Scale = 1 μm.

Fig. 12 Parts of three hepatocytes (h) with membrane whorls in the intercellular space (arrows) between them. × 30,000 Scale = 1 μm.

culi. In 11 patients (Table 1) these contained membrane and/or particulate debris (Figs. 10 and 11) In liver biopsy 279 membrane whorls were found between hepatocytes (Fig 12)

Other cells Although attention was chiefly paid to the hepatocytes in this study other cells were noted. Councilmanlike bodies, or apoptotic bodies were noted in the post MTX liver biopsy of one patient (254) and a mitosis observed in a hepatocyte at ultrastructural level in another (298) The normal type of littoral cells were observed (the Ito cells are described elsewhere (6)) Kupffer cells were observed to contain residual bodies. Kupffer cell proliferation was noted in the post MTX liver biopsies of 3 patients (255 259 281)

DISCUSSION

Some of our findings in the post MTX compared with the pre MTX liver biopsies are new others confirm those described in brief reports (8, 15) We have shown that there is damage to the hepatocytes, which results in the formation of membrane whorls Related to this is the increase in the number of residual bodies. The appearance of numbers of residual bodies in the Kupffer cells is part of the same process. We have also found membrane profiles and particulate debris commonly in the bile canaliculi. In one patient we found membrane profiles between cells. Our observation of Councilman-like bodies and hepatocytes in mitosis probably reflects the number of patients we studied.

Possible pathways for the breakdown of mitochondrial crystals were also found The presence of crystalline bodies in human liver mitochondria was noted some years ago. Since this time there have been reviews of conditions in which these mitochondrial crystals appeared, in experimental animals and Man (21 23) From these reports there appears to be no common denominator in their genesis.

These previous accounts have been largely concerned with the presence of the crystals within mitochondria and there has been no information on the natural history of these crystals and/or their biochemistry

Our observations can advance knowledge on various fronts. We found mitochondrial crystals in 13 of 24 patients before they began MTX therapy and whose liver function test and light microscopy (16) did not suggest hepatic disease. The 5 of the remaining 11 patients subsequently developed mitochondrial crystals during MTX therapy and two patients lost theirs. Clearly MTX therapy would appear to play no major role in their pathogenesis. Indeed, finding the crystals in so large a number of the patients suggest they may be quite widespread in their occurrence In another study where a moderate number of liver biopsies from patients with biliary lithiasis were examined ultrastructurally 14 out of 17 had crystals in megamitochondria (10) They have also been reported in clinically normal patients (26) in studies where single biopsies are taken. This makes their significance of some doubt.

There are apparently no descriptions of the formation or destruction of these mitochondrial crystals in the literature We have seen two possible ways they may be broken down. The simplest is that they are deposited in the cytoplasm as naked crystals. In this study there has been various examples where crystals have been present in apparently incomplete mitochondria (Fig. 4) From here they


m
h
h
h

bile canaliculi in 12 patients, but only one of these had any evidence of cholestasis (raised alkaline phosphatase). The presence of debris in one canaliculus and its absence from the next has been described before (4, 19).

We did not find any statistical significant correlation between cumulative dose of MTX and liver damage by the Spearman rank correlation coefficient test. As indicated in a previous article (17) the increased of pathological findings in the post MTX liver biopsies seem to be due to a multifactorial action of MTX, alcohol, age with more.

Conclusions

In psoriatics who had received MTX within a few days of the last liver biopsy we found evidence of damage in the hepatocytes compared with their first pretherapy biopsy.

1. Membrane whorls were commonly found in the cytoplasm.
2. There was an increase in the cellular lipid ($p < 0.05$).
3. Megamitochondria were seen.
4. There was an increase in the number of residual bodies present.
5. Membrane and particulate debris was found in the bile canaliculi.

The mitochondria of most patients contained crystals at some time during the study. We found evidence which suggests at least two pathways for the degradation of the crystals. Some nuclei contained pseudoinclusions.

No significant changes were found in the other organelles.

In patients who had received the last MTX treatment some time before the last liver biopsy there were changes in the hepatocytes, although to a lesser degree.

There was no statistically significant correlation between the cumulative dose of MTX and the ultrastructural changes.

In some instances we found incomplete membranes around the crystal containing mitochondria and naked crystals in the cytoplasm. We also found evidence of the inclusion of megamitochondria with crystal within autophagic vacuoles.

We would like to thank Mr *G. Milne* for his help with the preparation for the electron microscopy, Mr *R. Fawkes* and Miss *Shiela Nisbet* for photography and *Lederle* for a research grant.

This paper was compiled during the appointment of Dr Nyfors to the Department of Dermatology, Hvidovre Hospital, Copenhagen.

REFERENCES

1. *Arstila, A. U. & Trump, B. F.*: Studies on cellular autophagocytosis. The formation of autophagic vacuoles in the liver after glucagon administration. Amer. J. Path. *53*: 687–734, 1968.
2. *Burns, W. A., Vander Welde, G., Goldstein, L. I. & Chan, C. H.*: Cytoplasmic crystalline regions in hepatocytes of liver biopsy specimens. Arch. Path. *97*: 43–45, 1974.
3. *Coe, R. O. & Ball, F. E.*: Cirrhosis associated with Methotrexate treatment of psoriasis. JAMA *206*: 1515–1520, 1968.
4. *Hopwood, D., Reid, A. E. & Williams, R.*: Ultrastructural findings in idiopathic recurrent cholestasis. Gut *13*: 986–995, 1972.
5. *Hopwood, D. & Nyfors, A.*: Effects of Methotrexate therapy for psoriasis on the liver. J. Path. *116*: 1977 a (in press).
6. *Hopwood, D. & Nyfors, A.*: Effect of methotrexate therapy in psoriatics on the Ito cells in liver biopsies, assessed by point-counting. J. Clin. Path. *29*: 698–703, 1976.
7. *Hopwood, D. & Nyfors, A.*: Liver ultrastructure in psoriatics related to methotrexate therapy. 2. Findings in bile ducts from 11 methotrexate treated psoriatics and 2 controls. Acta path. microbiol. scand. Sect. A, *85*: 801–811, 1977.
8. *Horvath, E., Kovacs, K. & Ross, R. C.*: Liver ultrastructure in methotrexate treatment of psoriasis. Arch. Derm. *108*: 427–428, 1973.
9. *Isselbacher, K. J. & Alpert, D. H.*: Fatty liver. Biochemical and clinical aspects. In: Schiff, L. (Ed.) Diseases of the liver, 3. ed. Lippincott, Philadelphia 1969, p. 672–688.
10. *Lamme, C. O., Caro-Paton, A., Prieto, J. & Coca, M. C.*: Intramitochondrial paracrystalline inclusions in hepatocytes of patients with biliary lithiasis. Lancet *2*: 1417–1418, 1972.
11. *McDonald, C. J. & Bertino, J. R.*: Parenteral methotrexate in psoriasis. Arch. Derm. *100*: 655–668, 1969.
12. *Muller, S. A., Farrow, G. M. & Martalock, D. L.*: Cirrhosis caused by methotrexate in the treatment of psoriasis. Arch. Derm. *100*: 523–530, 1969.
13. *Newbold, P. C. H.*: Experimental studies on methotrexate and rat liver. Brit. J. Derm. *89*: 343–349, 1973.

could either be injected into the cytoplasm possibly by mitochondrial contractions or the mitochondrion may lyse Free crystals are occasionally described in the hepatocyte cytoplasm (2) The other pathway for the destruction of mitochondrial crystals is by uptake into autophagic vacuoles. It is surprising that in spite of the relative abundance of these crystals even in this study there are relatively few examples of these processes. This must imply the relatively short time during which the crystals remain recognizable either naked or within the lysosomal apparatus. Alternatively the crystals may be degraded within the mitochondria The nature and the function of the crystals remain obscure. Our observations show many mega mitochondria to have bizarre structures suggesting budding This may relate to the effects of MTX in inhibiting replication, there being an inhibition of mitochondrial nuclei acids. Experiments on yeasts show that MTX may produce alteration in oxidative activity and mitochondrial form (27) Although we have sequential liver biopsies from patients with mitochondrial crystals from 1 day to 785 days after last MTX intake it is not possible to be certain about how long livers contain crystals bearing mitochondria

Smooth endoplasmic reticulum When all the patients were considered together there was no significant change in the amount of rough endoplasmic reticulum in agreement with the previous brief reports (8 15) The chronic administration of MTX has been found to increase the dihydrofolate reductase activity a cytoplasmic enzyme with which MTX specifically combines (13)

Lysosomal apparatus We found statistically significant increase in the number of autophagic vacuoles and residual bodies in the cytoplasm of the hepatocytes of the MTX treated patients compared with the pre MTX controls This suggests that the cytoplasm is showing an increased turnover This may be due to binding to the dihydrofolate reductase (13) Over 90 per cent of MTX is excreted from Man unmetabolized (11)

Membrane whorls also appeared commonly in the hepatocyte cytoplasm of the MTX treated patients. Membrane whorls too, may become incorporated in the autophagic vacuoles which in turn may give rise to the increase in the number of residual bodies. Cytoplasmic membrane whorls usually reflect cell damage (24) in this case most likely due to the MTX. Some residua may find their way out of the hepatocytes into the bile canaliculi or intercellular spaces (1) Those leaving by this last route may well be taken up by the Kupffer cells. We have observed some of these cells to contain an increased number of residual bodies in the post MTX liver biopsies.

In our material the use of MTX did not produce any change in the hepatocyte Golgi apparatus. *Horvath et al* (1973) however found some hypertrophy and dilation of this organelle in the hepatocytes of their 9 post MTX liver biopsies from psoriatics.

There was no change in the presence of glycogen in the hepatocytes of the patients in this study with the use of MTX.

Lipids Light microscopy analysis of the sequential liver biopsies from the patients biopsied in this study showed that there was no statistically significant increase in the hepatocyte lipid in the post MTX biopsy compared with the pre MTX biopsy However statistical analysis of the ultrastructural findings showed a significant increase in lipids. The form of the lipid droplets varied some being uniform and others containing membrane profiles Such differences have been commented on recently by *Petersen* (1974)

The development of excess lipids in the liver has been discussed by *Isselbacher & Alpers* (1969)

There were no changes found in the *cell membrane* and its areas of specialization in the *bile canaliculi* and the microvilli of the *space of Disse* following MTX therapy However changes were noted within the *lumen of bile canaliculi* We found membrane profiles or particulate debris in some

Acta path. microbiol. scand. Sect. A, 85 801-811 1977

LIVER ULTRASTRUCTURE IN PSORIATICS RELATED TO METHOTREXATE THERAPY

2 Findings in Bile Ducts from 11 Methotrexate Treated Psoriatics and 2 Controls

D. Hopwood and A. Nyfors

Department of Pathology Ninewells University Hospital, Dundee, Scotland
and Department of Dermatology The Finsen Institute Copenhagen, Denmark

Hopwood, D. & Nyfors, A. Liver ultrastructure in psoriatics related to methotrexate therapy 2 Findings in bile ducts from 11 methotrexate treated psoriatics and 2 controls. Acta path. microbiol. scand. Sect. A, 85 801-811 1977

To determine what damage occurred in the bile ducts of psoriatics receiving Methotrexate (MTX) therapy liver biopsies from 11 patients were studied with the light and electron microscope and compared with normal material. Thick sections (1 µm) showed light and dark cells in biliary epithelium and lipofuscin granules. At the ultrastructural level these were confirmed. The lumen of the bile ducts contained debris. The microvilli were decreased in number and damaged forms appeared. Damage to the biliary epithelial mitochondria was widespread and there were foci of intracellular oedema. The Golgi apparatus was hypertrophied and dilated. Atrophic cells were seen. The lateral intercellular spaces were dilated and contained debris and the basement membrane showed zones of duplication. Similar changes were found in the ducts of Hering.

Key words: Liver ultrastructure bile ducts psoriasis Methotrexate therapy

A. Nyfors, Department of Dermatology The Finsen Institute, Copenhagen, DK 2100 Denmark.

Received 8 xi 76 Accepted 24 ... 77

Most studies of agents which effect the liver concentrate on the hepatocyte. In man where only a small portion of a liver biopsy is available for ultrastructural analysis it is not possible to guarantee the presence of a bile duct. The present series of cases is taken from a study of psoriatic patients who had pre and post Methotrexate (MTX) therapy liver biopsies (5 ref 6). The effect of MTX in psoriasis and the precautions necessary with this therapy are mentioned in a previous paper (5 ref 16). It is not possible for the patients to act as their own controls with the present material. There are, however published accounts of normal human biliary epithelium (6, 7 8 9) and comparison may be made with those.

It is the aim of the present study to describe the ultrastructure in biliary epithelium in psoriatics who have received MTX therapy and to see if any changes may be related to the fibrosis and cirrhosis which have been reported to occur after certain therapeutic schemes (2) (5 ref. 16 24)

14 *Nyfors A & Brodthagen H* Methotrexate for psoriasis in weekly oral doses without any adjunctive therapy Dermatologica *140* 345–355 1970

15 *Nyfors A Lee J C & Mabeck H I* Light and electron microscopy of liver biopsies from longterm methotrexate treated psoriatics and controls. In Proceedings of the 19th meeting of the Scandinavian Dermatological Association Oslo June 10–12 1971 p 21–22

16 *Nyfors A & Poulsen H* Liver biopsies from psoriatics related to methotrexate therapy 1 Findings in 123 consecutive non methotrexate treated patients. Acta path microbiol scand. Sect A *84* 253-261 1976

17 *Nyfors A & Poulsen H* Liver biopsies from psoriatrics related to methotrexate therapy 2 Findings before and after methotrexate therapy in 88 patients. A blind study Acta path, microbiol scand. Sect, A, *84* 262-270 1976

18. *Petersen P* Lipid droplets in fatty liver Acta path. microbiol scand Sect A *82* 255–263 1974

19 *Popper H & Schaffner F* Pathophysiology of cholestasis. Human Path *1* 1–24 1970

20 *Roenigk H H Fowler Bergfeld W & Curtis G H* Methotrexate for psoriasis in weekly oral doses. Arch. Derm *99* 86–93 1969

21 *Shiraki K & Neustein H B* Intramitochondrial crystalloids and amorphous granules. Arch. Path. *9* 32–40 1971

22 *Siegel S* Nonparametric statistics for the behavioral sciences. McGraw Hill, New York 1956

23 *Spycher M A & Rüttner J R* Kristalloide Einschlüsse in menchlichen Lebermitochondrien. Virchows Arch. (B) *1* 211–221 1968.

24 *Trump B F Valigorsky J M Dees J H., Mergner W J Kim K M., Jones R T Pendergrass R E Garbus J & Cowley R.A* Cellular change in human disease Human Path *4* 89 109 1973

25 *Weinstein G Roenigk H., Maibach H Cosmides J Halprin K Millard M Almeyda J Auerbach R Tobias H Bergfeld W Clyde D Dahl M Frost P Schiff E., Krueger R Tindall J Lee J., Lundquist A Schaffner F Scheuer P & Zacharias H* Psoriasis Liver Methotrexate-Interactions. Arch. Derm. *108* 36–42, 1973

26 *Wills F J* Crystalline structures in the mitochondria of normal human liver parenchymal cells J Cell Biol *24* 511–514 1965

27 *Wintersberger U & Hirsch J* Induction of cytoplasmic respiration deficient mutants in yeast by the folic acid analogue Methotrexate. J Molec. gen. Genet. *126* 61–70, 1973

TABLE 1 *Clinical and Histological Features*

	Before MTX		Within 4 days after MTX							Varying time after MTX			
Liver biopsy no.	278	296	298	306	321	68	29	38	295	259	303	308	256
Sex	F	F	M	M	M	M	M	M	F	F	F	M	M
Age (years)	44	33	74	52	54	64	84	38	65	49	53	65	31
Duration of psoriasis (years)	33	27	58	27	32	14	30	22	38	8	35	40	14
Extent of psoriasis (per cent)	12	91	30	10	4	8	1	26	2	38	3	10	46
Alcoholic intake	A	A	A	A	B	A	A	A	A	A	A	C	C
Possible hepatotoxic medicine	+	—	+	+	+	+	—	—	+	—	—	—	+
MTX cumulative dose (mg)	0	0	2463	1800	1385	5778	3748	7405	2330	2833	990	735	328
Duration of MTX therapy (months)	0	0	43	33	21	68	84	80	39	36	16	12	5
Time last MTX – last l.b. (days)			1	1	1	2	4	4	4	168	600	731	1120
Chief histological diagnosis	mild f.c.	mild n.s. r.h.	norm	norm	mild f.c	mild cir	norm	mild f.b.	mild cir	mild fib	mild f.c.	mild f.c.	mild f.c.

Alcoholic intake: A = occasionally B = 1–3 drinks weekly C = 1–3 drinks daily
cirr: cirrhosis, f.c: fatty change fib.: fibrosis, l.b.: liver biopsy n.s.r.h.: non-specific reactive hepatitis,
norm: normal = n, elev: elevated no.: number F: female M: male

MATERIAL AND METHODS

Patients

The material comprises firstly 24 pairs of Menghini needle biopsies which were taken both before and after MTX therapy from each consenting patient with disabling psoriasis and secondly 7 post MTX liver biopsies from similar patients.

Clinical Features MTX Dosage and Laboratory Investigations

They are described previously (5 ref 6)

Light Microscopy

Araldite sections 1 µm thick from the material for electron microscopy stained with Toluidine Blue were examined with the light microscope

Electron Microscopy

The preparation of material for E.M is described in a previous paper (5 ref 16)

RESULTS

Clinical Features

They are shown in Table 1

Laboratory Investigations

Serum aspartate transaminase was elevated in patient 66 at the post MTX liver biopsy while it together with alkaline phosphatase and serum bilirubin were normal in all other patients.

Light Microscopy

Among the 24 sets of pre and post MTX liver biopsies portal tracts were found in 2 pre MTX liver biopsies and 7 post MTX liver biopsies, while portal tracts were seen in 4 of the seven post MTX liver biopsies. In none of the 24 sets of biopsies were portal tracts present in both the pre and post MTX liver biopsy from the same patient

Bile ducts were made up of epithelial cells which varied somewhat in size. There were light and dark cells Pigment granules were seen in the epithelium (Fig 1) Chief histological diagnoses are given in Table 1

Electron Microscopy

In the bile duct lumen and in the intercellular spaces between bile duct epithelial cells were found particulate debris in all 11 MTX treated patients. In the bile duct epithelium in these patients mitochondria were damaged in 11 and the Golgi apparatus was increased and dilated in 9 not seen in 1 and normal in 1 patient. Microvilli were decreased in number or changed in 10 of 11 MTX treated patients. In the two controls the mentioned structures were normal.

In the liver biopsy specimens from the 11 MTX treated patients no changes were found in the following organelles of the bile duct epithelium cilia abnormal fibers, pinocytotic vesicles, light and dark cells, cell atrophy lysosomes, membrane whorls, basement membrane The nucleus of the epithelial cells was found within normal limits in all patients. Residual bodies were increased in number in 11 specimens and normal only in one of the pre MTX liver biopsies (276)

The bile duct lumens examined from the post MTX patients contained debris mostly particulate but some membranous (Fig 2) This was not present in the bile ducts of patients biopsied before MTX therapy Cilia were generally present and increased in number although there was variation in the number of fibrils contained (Fig 3) Microvilli varied considerably (Figs. 2 and 3) In the patients who had recently received MTX there was a decrease in the number of microvilli some oedema and a few microvilli were branched. These changes were present to a lesser extent in those patients who had received their last MTX dose several months previously

The bile duct epithelium showed certain changes in those patients who had received their last MTX treatment within a few days of the liver biopsy Many mitochondria were damaged (Figs. 2 and 4) Autophagic vacuoles were in evidence There was an increase in the number of lysosomes and residual bodies (Fig 5) In some patients membrane whorls were evident and in one there were lipid droplets in the cytoplasm (295) (Fig 6) There was cytoplasmic oedema (Fig 7) light and dark cells were common. Some cells had become atrophic (Fig. 8) and the

All illustrations show liver tissue from psoriatics after Methotrexate therapy. Figure 1 is a light micrograph, while the remaining figures are electron micrographs.

Fig. 1. Toluidine blue stained 1 μm section in Araldite. Section of bile duct (B) show pigment granule (arrowhead) × 1,000. Scale = 10 μm.

Fig. 2. Electron micrograph of part of bile duct. The lumen contains particulate and membranous debris. There is a decrease in the number of microvilli. The mitochondria show little damage. × 20,000. Scale = 1 μm.

lateral intercellular spaces greatly increased with some cytoplasmic blebbing into them (Figs. 6 and 8). These changes were most marked in patients 295 and 306. There was some evidence of extracellular debris. Of the other organelles the Golgi apparatus was generally prominent, hypertrophied and showed some dilation (Fig. 9). Some nuclei were oval, others had an undulating membrane. The endoplasmic reticulum appeared normal. The glycogen was scanty. Free ribosomes were found generally. Microfibrils were seen in all the biopsies. In one (38) there was some tendency to their clumping at the base of the cell. There was a small increase in the number in two other patients (293 and 298). Pinocytotic vesicles were commonly seen at the bases of the cells, but rarely elsewhere.

The cells were attached by well developed desmosomes which were situated between adjacent cell membranes as they abutted by the lumen. The lateral cell membranes were plicated in some areas but generally showed some areas of dilatation. This increased intercellular space contained particulate matter in the treated patients and in one case membrane profiles (Fig. 6) (293). The basement membrane from some of the treated patients showed reduplication. The ultrastructural findings in the ducts of Hering where they were found mirrored those in the biliary epithelium (Fig. 10).

The findings from the patients who had received MTX more than a week before liver biopsy showed some of these features, although to a lesser extent. Few of the abnormalities were noted in the biopsies from patients who had not received MTX—no abnormalities were found in patient 276, while 296 had decreased forked microvilli, and increased intercellular space between bile duct epithelial cells.

DISCUSSION

There are few papers concerned mainly with pathological changes in bile ducts at the ultrastructural level (1-6). Our material does not allow the patients to act as their own controls, but it may be fruitfully compared with published accounts of normal bile ducts (6, 7, 8, 9).

The appearance of particulate debris in the lumen of the bile ducts is similar to that found in bile canaliculi in cholestasis (5, ref 4, 18). The membrane profiles may represent debris from the damaged hepatocytes (5) which may enter the bile canaliculi (5, ref 1). The loss of microvilli and their oedema is associated with cholestasis, although there is little clinical or biochemical evidence in our patients of this. The variation of the fibrils

Fig. 3. The lumen of the bile duct contains particulate debris. Several cilia are cut transversally. The number of fibrils they contain varies. The number of microvilli lining the lumen is decreased. The Golgi apparatus is dilated and the mitochondria damaged. × 40,000. Scale = 1 μm.

Fig. 4. Biliary epithelial cells show damage to their mitochondria in contrast to the mitochondria of the nearby hepatocytes (H). The bile duct basement membrane (arrowhead) shows duplication. × 13,000. Scale = 2 μm.

Fig. 5. Part of biliary epithelial cell containing residual bodies (arrow), the largest of which has particulate structure. The microfibrils typical of these cells, are easily seen. × 70,000. Scale = 0.5 μm.

Fig. 6. Biliary epithelium showing membranous (m) and particulate (p) debris between the cells. The cytoplasm contains damaged mitochondria (M), autophagic vacuoles (arrowhead), residual bodies (RB) and possible lipid droplets (L). × 20,000. Scale = 1 μm.

B

5

P

L

m

M

RB

A

4

P

L

m

M

RB

H

4







53 Acta path. microbiol. scand. Sect. A 83 6



m the number of microvilli lining the lumen, and of those remaining some were oedematous and the others forked.

2. The bile duct epithelium showed an increased number of dark cells and atrophic change. A large proportion of the mitochondria were damaged. The cytoplasm contained some membrane whorls and there were areas of oedema. Residual bodies were increased in number and the Golgi apparatus was hypertrophied and dilated.

3. The lateral intercellular spaces were dilated and filled with particulate and membranous debris and received blebs from the adjacent epithelial cells. The basement membrane showed areas of duplication.

Similar changes were found in the ducts of Hering.

In the patients who had received MTX some time prior to liver biopsy the above changes were much less marked. In those patients who had not received MTX therapy one showed a patchy loss of microvilli and an increase in residual bodies and the other some particulate debris in the bile duct lumen.

This paper was compiled during the appointment of Dr Nyfors to the Department of Dermatology Hvidovre Hospital, Copenhagen.

REFERENCES

1. *Chedid A., Spellberg, M A. & DeBeer R. A.*: Ultrastructural aspects of primary biliary cirrhosis and other types of cholestatic liver disease. Gastroenterol. 67 858–869 1974
2. *Dahl M G C., Gregory M M & Scheuer P J.*: Liver damage due to methotrexate in patients with psoriasis. Brit. Med. J 1: 625–630, 1971
3. *Dubowitz, V & Brooke M H.*: Muscle biopsy A modern approach. Saunders, London 1973 p 386.
4. *Genot C E. & Moses H L.*: Light and dark cells as artifacts of liver fixation. Lab. Invest. 18 740–745 1968.
5. *Nyfors, A. & Hopwood D.*: Liver ultrastructure in psoriatics related to methotrexate therapy 1 A prospective study of findings in hepatocytes from 24 patients before and after methotherxate treatment. Acta path. microbiol. scand. Sect. A, 85 787–800, 1977
6. *Sasaki, H., Schaffner F & Popper H.*: Bile ductules in cholestasis morphologic evidence for secretion and absorption in man. Lab Invest. 16 84–95 1967
7. *Steiner J W & Carruthers J S.*: Studies on the fine structure of the terminal branches of the biliary tree. I The morphology of normal bile canaliculi, bile pre-ductules (ducts of Hering) and bile ductules. Amer J Path. 38 639–661 1961
8. *Sternlieb I.*: Electron microscopic study of intrahepatic biliary ductules. J Microsc. (Paris) 4 71–80 1965
9. *Sternlieb I.*: Special article Functional implications of human portal and bile ductular ultrastructure. Gastroenterol. 63 321–327 1972.

within the cilia is of interest. The normal findings are 9 peripheral plus 2 central fibrils The variations noted may further represent cellular damage as may the forked microvilli.

In our material there was no evidence of micropinocytosis at the bases of the microvilli which has been described in cholestasis (6) In some of our patients there were relatively large numbers of pinocytotic vesicles at the bases of the cells.

The most striking pattern of change following MTX therapy is the damage to various organelles. The mitochondria showed a number of damaged appearances Membrane profiles and fat droplets appeared in the cytoplasm and there was an increase in the number of autophagic vacuoles and residual bodies These may reflect the destruction of effete and damaged mitochondria Areas of cytoplasmic oedema were found and blebs appeared along the lateral intercellular membranes This may be related to falling cellular ATP levels resulting from mitochondrial damage (5 ref 23) The hypertrophy and dilation of the Golgi apparatus is not easy to interpret. This organelle is concerned with the packaging of secretions and the addition of a carbohydrate moiety

The appearance of particulate debris in the increased lateral intercellular space is of interest The membrane profiles may represent damaged material from the bile duct epithelium There is no morphological evidence of any directional movements of this material which is contained basally by the basement membrane The basement membrane showed duplication in some MTX treated patients, again in accord with cholestasis (6) This duplication, however may be related to the atrophy of the bile duct epithelium and it has been described in primary biliary cirrhosis (1) and atrophic situations e.g muscle (3) Intercalated cells were found in MTX treated patients.

Light and dark cells were commonly found. In the liver those are said to be a fixation artefact (4) Even if this was the case it would seem likely that it reflected some underlying difference between the cells. There was evidence of cellular atrophy with the appearance of wide spaces between the cells. It is possible that there may be leakage of small quantities of bile from time to time which may induce fibrosis, which has been reported (5 ref 16 24) These findings have a counterpart at light microscopy where light and dark cells were seen in the bile ducts along with lipofuscin granules. These were not noted in paraffin sections (5 ref 15 16) which are thicker than the Araldite ones.

These findings in the bile ducts are indicative of damage and atrophy Some of these changes may induce fibrosis by repeated small leaks of bile There are also changes which show some similarities to cholestasis. One may speculate that the changes in the biliary epithelium which is known to modify bile (9) may produce changes in the bile composition during MTX therapy

Conclusions

In psoriatics whose liver was biopsied within a few days of receiving Methotrexate therapy the bile ducts differed from normal bile ducts in the following ways

1 The lumen of the bile ducts contained membranous and particulate debris Cilia appeared more often Their central fibres varied in number There was a decrease

←

Fig 7 Section through a bile duct One cell shows focal oedema with damage to the mitochondria. One of the other cells shows a membranous whorl × 10 000 Scale = 1 μm.

Fig 8 Biliary epithelium showing light and dark cells with exaggerated lateral intercellular spaces (arrowhead) between the atrophic cells. × 15 000 Scale = 1 μm.

Fig 9 Part of a biliary epithelial cell showing damaged mitochondria near a dilated and hypertrofied Golgi apparatus (arrowhead) × 30 000 Scale = 1 μm

Fig 10 Section through part of duct of Hering (arrow) with epithelial cell (E) to one side and the hepatocyte (H) to the other Note the oedema of the microvilli. × 20 000 Scale = 1 μm.

the Department of Pathology, Sahlgren's Hospital, Gothenburg, and the Central Hospital, Vänersborg. Three cases were primarily diagnosed as ancient neurilemmoma.

Histological methods. Sections of tissue routinely stained with haematoxylin and eosin and/or haematoxylin—van Gieson method were available for review in all cases. In 9 cases, 5 micron thick sections of paraffin-embedded tissue were stained with Luxol fast blue and Palmgren silver impregnation, for the demonstration of myelin sheaths and axis cylinders respectively. Gordon's and Sweet's silver impregnation for the demonstration of reticulin fibres, the Prussian blue reaction for iron-containing pigments and the periodic acid-Schiff reaction (McManus) with and without prior treatment of the sections with diastase (Merck) were also performed. Alcian blue (Chroma-Gesellschaft) stain was used at pH's 2.5 and 0.5 for the examination of mucosubstances, as described previously (*Angervall et al.* 1973, *Kindblom & Angervall* 1975).

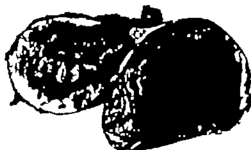


Fig. 1. Large solitary extremely cystic ancient neurilemmoma. The tumour is well-demarcated and encapsulated.

RESULTS

The sex and age of the patient, anatomical location of the tumour, duration of tumour symptoms, size of the tumour as well as duration of follow-up are shown in Table 1. The median age of the patients was 59 years. All tumours were solitary and no signs of Recklinghausen's disease were evident in any patient.

Gross appearance. All tumours were well-demarcated and encapsulated, being rounded or oval. The cut surfaces were grey-white and firm. 5 tumours showed glistening and gelatinous areas. Signs of haemorrhage with red to yellow-brown areas were evident in 5 tumours, and one tumour was for the most part cystic (Fig. 1).

Microscopic findings. All tumours showed a mixture of Antoni type A and type B tissues (Fig. 2). The Antoni type A tissue was cellular with nuclear atypia and polymorphism. The tumour cells were spindle-shaped and arranged in interlacing bundles or fascicles (Fig. 2). The oval or elongated nuclei with variable amounts of chromatin showed a tendency to palisade (Fig. 4). All tumours exhibited areas with polymorphous and hy

TABLE 1. *Clinical Findings in 11 Patients with Ancient Neurilemmoma (Schwannoma)*

Patient code nr	Sex	Age in years	Anatomical location	Duration of tumour symptoms (years)	Widest diameter of tumour (cm)	Duration of follow up (years)
87	F	64	Neck	12	6	6 (dead)
00	F	59	Thigh	not known	5	15 (dead)
03	F	60	Back	4	4	10.5
14	F	48	Leg	2	1	14
15	F	49	Neck	5	4	12.5
16	M	48	Chest	6	1.5	13.5
23	M	39	Leg	1	2.5	14.5
85	F	89	Back	2	17	2.5
33	F	37	Arm	1	1	4
94	M	72	Back	10	2.5	3.5 (dead)
94	M	70	Arm	0.5	1	3 (dead)

Acta path microbiol scand. Sect A *85* 812–818 1977

ANCIENT NEURILEMMOMA (SCHWANNOMA)

Ingvar Dahl

Departments of Pathology University of Gothenburg and Central Hospital Vänersborg, Sweden

Dahl I Ancient neurilemmoma (schwannoma) Acta path. microbiol scand. Sect. A, 85 812–818 1977

A clinical and light microscopic study of 11 patients with ancient neurilemmoma is presented. Ancient neurilemmoma is a cellular form of ordinary neurilemmoma showing nuclear polymorphism and hyperchromasia. Seven patients were female and 4 were male their ages ranged between 37 years and 81 years, with a median of 59 years. Seven tumours were 2.5 cm or larger in the widest diameter and had been slowly enlarging for one year or more. All tumours were solitary encapsulated showing nuclear polymorphism and hyperchromasia without any mitotic activity The differential diagnosis is discussed Follow up information available on all patients confirmed that the clinical course is benign.

Key words Soft tissue tumour pseudosarcomatous lesion neurilemmoma (schwannoma) ancient solitary

Ingvar Dahl, Department of Pathology Central Hospital Fack, S-462 01 Vänersborg, Sweden.

Received 2 vi 77 Accepted 14 vi.77

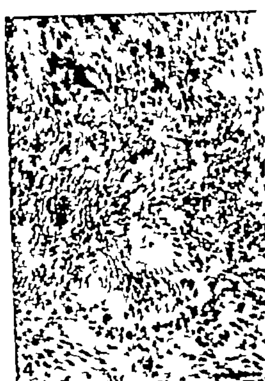
Histologically solitary benign neurilemmoma (schwannoma) may be cellular and show nuclear polymorphism and hyperchromasia, and hence be erroneously diagnosed as sarcoma. *Ackerman & Taylor* (1951) in a series of 31 tumours of nerve sheath origin within the thorax, described 10 tumours which they named ancient neurilemmoma Histologically these tumours contained cellular areas suggestive of fibrosarcoma but the clinical course was perfectly benign in all cases. Other authors (*Erlich & Martin* 1943 *Godwin* 1952 *Kragh et al* 1960 *Oberman & Abell* 1960 *D Agostino et al* 1963 *Oberman & Sullenger* 1967) have mentioned the existence of cellular neurilemmomas exhibiting nuclear hyperchromasia and polymorphism which were initially misinterpreted as sarcoma but had a benign clinical course

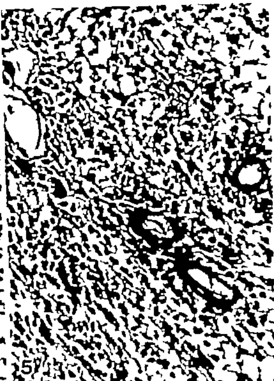
It is evident from a retrospective review of some 800 tumours reported as soft tissue sarcoma to the Swedish Cancer Registry over a 6-year period that ancient neurilemmoma may present diagnostic problems. In this review there were 81 cases of apparently benign lesions originally interpreted as sarcomas. Seven of these were ancient neurilemmomas, 4 peripherally and 3 retroperitoneally located (*Dahl & Angervall* in preparation)

A clinico-pathological study with a long term follow up of *11* patients with ancient neurilemmoma is presented. An attempt is made to establish criteria for the diagnosis of ancient neurilemmoma and to discuss the differential diagnosis.

MATERIAL AND METHODS

Four of the *11* cases in the whole series were taken from a Swedish series comprising some 800 cases of malignant soft tissue tumours reported to the Swedish Cancer Registry during a 6-year period (1958–1963) Four cases were selected after reviewing various soft tissue tumours recorded at


4


5


6

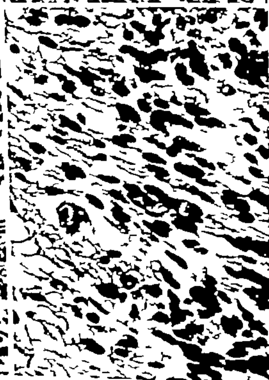

7




Fig 2 Ancient neurilemmoma with a mixture of Antoni type A and B tissue, showing hyperchromatic nuclei. The Antoni type A tissue is cellular with spindle-shaped cells arranged in bundles or fascicles. Haematoxylin—van Gieson, × 100

Fig 3 Antoni type A tissue in ancient neurilemmoma showing spindle-shaped schwann cells with indistinct cell borders and polymorphic nuclei These cells mingle with clusters of small, lymphocytoid cells, giving the area a cellular impression Haematoxylin & eosin, × 100

perchromatic nuclei containing vacuoles or Kern loche (Figs. 6 and 7) The Antoni type B tissue was loose textured and oedematous with elongated, thin tumour cells with hyperchromatic irregular nuclei arranged haphazardly or forming thin tortuous cords (Fig 2) The abundant oedematous matrix in these areas separated the cells and fibres and in 5 tumours formed cystic spaces so-called microcystic degeneration The matrix did not stain with the PAS-method or with Alcian blue except in small perivascular areas where a hyaluronidase-resistant alcianophilia was evident at both pHs, indicating the presence of acid sulphated mucosubstances probably keratan and/or dermatan sulphates Area composed of small tumour cells resembling lymphocytes (lymphocytoid cells) were observed in 9 tumours (Figs 3 and 5) Mitoses were not observed in any tumour Collagen and reticulin fibres were arranged parallel to the

---

Fig 4 Cellular and polymorphic Antoni type A tissue in ancient neurilemmoma. Spindle-shaped tumour cells with a tendency to nuclear palisading Haematoxylin & eosin, × 100

Fig 5 Prominent vessels with thick hyalinized walls in ancient neurilemmoma. Clusters of small lymphocytoid cells are seen around the vessels Haematoxylin—van Gieson, × 250

Figs 6 and 7 Ancient neurilemmoma, showing extreme nuclear polymorphism and hyperchromasia. Some nuclei show vacuoles and karyorrhexis. Haematoxylin—van Gieson, × 250 and haematoxylin & eosin, × 400.

the tumour cells, the cytoplasmic tincturophilia in trichrome stains as well as the blunt ended nuclei, often arranged in rows or in tandem position in leiomyosarcoma seem fairly characteristic, enabling the recognition of this form of sarcoma (*Stout* & *Hill* 1958 *Dahl* & *Angervall* 1974)

Rounded or well-demarcated forms of pseudosarcomatous proliferative lesions of soft tissue such as nodular fasciitis (*Dahl* & *Angervall* 1977) may be confused with ancient neurilemmoma (*Stout* 1960 *Price et al.* 1961 *Allen* 1972) However the proliferating cells in nodular fasciitis are frequently s-formed or wavy enclosing small clefts or slits, and differ from the cells seen in ancient neurilemmoma. Furthermore, mitoses, areas containing proliferating capillaries and extravasated erythrocytes as well as inflammatory cells are frequent findings in nodular fasciitis and may assist in arriving at the correct diagnosis (*Allen* 1972 *Dahl et al* 1972)

Awareness of the existence of cellular neurilemmomas showing extreme nuclear polymorphism and hyperchromasia, but with a perfectly benign clinical course, is mandatory in order to avoid misinterpretation as sarcoma.

Supported by a research grant from the *Swedish Cancer Society* 530-K73-02X.

REFERENCES

Ackerman L. V & *Taylor F H* Neurogenous tumors within the thorax. A clinicopathological evaluation of forty-eight cases Cancer (Philad.) 4 669-691 1951

Allen P W Nodular fasciitis Pathology 4 9-26, 1972

Angervall L., Dahl I Kindblom L.-G & *Säve-Söderbergh J* Spindle cell lipoma. Acta path. microbiol scand. Sect. A, 84 477-487 1976.

Angervall L Enerbäck L. & *Knutson H* Chondrosarcoma of soft tissue origin. Cancer (Philad.) 32 507 513 1973

Compagno J Hyams V J & *Lepore M L.* Nasal polyposis with stromal atypia. Review and follow-up study of 14 cases. Arch. Path. Lab. Med. 100 224 226, 1976.

Dahl, I & *Angervall, L.* Cutaneous and subcutaneous leiomyosarcoma A clinicopathologic study of 47 patients. Pathol. Eur 9 307-315 1974

Dahl, I & *Angervall L.* Pseudosarcomatous proliferative lesions of soft tissue with or without bone formation. Acta path. microbiol. scand. Sect. A, 85 577-589 1977

Dahl, I & *Angervall, L.:* Pseudosarcomatous lesions of the soft tissues reported as sarcoma during a 6-year period (1958-1963) Acta path. microbiol. scand. Sect. A, 85 917-930, 1977

Dahl I., Angervall L., Magnusson S & *Stener B.,* Classical and cystic nodular fasciitis. Pathol. Eur 7 211 221 1972.

D'Agostino A N Soule E H & *Miller R H.,* Primary malignant neoplasms of nerves (malignant neurilemomas) in patients without manifestations of multiple neurofibromatosis (von Recklinghausen's disease) Cancer (Philad.) 16 1005-1014 1963.

Das Gupta, T K., Brasfield R. D., Strong E W & *Hajdu S I* Benign solitary schwannomas (neurilemomas) Cancer (Philad.) 24 355-366 1969

Ehrlich H E. & *Martin H.,* Schwannomas (neurilemomas) in the head and neck. Surg. Gynec. Obstet. 76 577-583 1943

Enzinger F M.: Syllabus of tumours of neural tissues. WHO-Reference Set No VI Armed Forces Institute of Pathology Washington. 1969

Enzinger F M Lattes R & *Torloni H* Histological typing of soft tissue tumours. International histological classification of tumours. N 3 Geneva. WHO 1969

Ghosh B. C., Ghosh L., Huvos A. G. & *Fortner J G* Malignant schwannoma. A clinicopathologic study Cancer (Philad.) 31 184-190 1973

Godwin J T Encapsulated neurilemoma (schwannoma) of the brachial plexus. Report of eleven cases. Cancer (Philad.) 5 708-720 1952.

Harkin, J C & *Reed R. J.:* Tumors of the peripheral nervous system. Atlas of tumor pathology Second series, fascicle 3. AFIP Washington D C. 1969

Kindblom L.-G & *Angervall L.* Histochemical characterization of mucosubstances in bone and soft tissue tumors. Cancer (Philad.) 36 985-994 1975

Kragh, L. V., Soule E. H & *Masson J K.:* Benign and malignant neurilemmomas of the head and neck. Surg. Gynec. Obstet. 111 211-218 1960

Norris H J & *Taylor H B* Polyps of the vagina. A benign lesion resembling sarcoma botryoides. Cancer (Philad.) 19 227-232, 1966.

Obermann, H A & *Abell, M R.:* Neurogenous

tumour cells. Areas rich in collagen with hyalinization were evident in 4 tumours All tumours contained prominent blood vessels with thick hyalinized walls (Fig 5) Thrombosed vessels were observed focally in one tumour Haemorrhage with haemosiderin laden macrophages as well as areas with lipid filled foam-cells (*pseudoxanthoma cells*) were encountered in 5 tumours. A few inflammatory cells, mast cells and lymphocytes were seen in 5 tumours The nerve of origin was identifiable in 2 tumours but neither myelinated nor unmyelinated axons were seen in any tumour

Primary diagnoses Four of the 8 retrospectively collected tumours (all from the Swedish National series) were primarily diagnosed as sarcoma one as neurosarcoma one as neurofibrosarcoma and 2 as malignant neurilemmoma. Two of the 4 reviewed tumours were considered to be cellular and polymorphic, probably malignant with a high risk of recurrence The additional 2 tumours were diagnosed as neurofibroma and neurinoma.

Treatment and follow-up All tumours were removed by local excision In one case where the primary diagnosis was sarcoma, wide surgical excision of the area was performed The other patients in which the tumours were primarily diagnosed as sarcoma or probable sarcoma received no further treatment

Follow up information was available on all patients. The length of the follow up period ranged from 2 5 to 15 years with a median of 10 5 years. Four patients died all of intercurrent disease On one of these an autopsy was performed The remaining 7 patients are alive and well without any sign of recurrences or metastases.

DISCUSSION

All tumours in the present series were cellular and exhibited severe nuclear polymorphism and hyperchromasia. The tumours were encapsulated and showed the basic features of an ordinary neurilemmoma with a mixture of Antoni type A and type B tissues A constant and important finding was the prominent nuclear polymorphism and hyperchromasia without any mitotic activity Occasionally the nuclei showed vacuoles or signs of karyorrhexis, which could be misinterpreted as mitoses.

Nucelar changes similar to those found in the neurilemmomas of the present series have been described in other benign soft tissue tumours such as ancient spindle-cell lipoma (*Angervall et al* 1976) myxoid polyps of the vagina (*Norris & Taylor* 1966) and antrochoanal nasal polyps-polyposis (*Smith et al* 1974 *Compagno et al.* 1976) and confused with sarcoma These nuclear changes without mitotic activity seem to be regressive in nature A diagnosis of malignancy or probable malignancy should not as obviously was the case in 6 tumours in the series be based on these nuclear changes

It is of interest in this connection that malignant schwannoma originating within a pre-existent neurilemmoma appears to be extremely rare if it ever occurs (*Savén* 1948, *Vieta & Pack* 1951 *D Agostino et al* 1963 Das *Gupta et al* 1969) Some forms of malignant schwannoma exhibiting so-called schwann-cell differentiation with densely packed often palisading short spindle-cells may show some resemblance to ancient neurilemmoma These sarcomas, however show mitoses and infiltrative growth, which distinguishes them from neurilemmoma (*Enzinger* 1969) Most malignant schwannoma neurofibrosarcoma possess the basic features of a spindle-cell sarcoma (*D Agostino et al* 1963 *Harkin & Reed* 1969 *Enzinger et al.* 1969 *White 1971 Ghosh et al 1973*) and can hardly be confused with ancient neurilemmoma.

It is not always easy to distinguish between subcutaneous leiomyosarcoma and ancient neurilemmoma. Subcutaneously situated leiomyosarcoma is frequently nodular and well-circumscribed showing areas of hyalinization, palisading of the nuclei polymorphism, hyperchromasia and vacuolization (*Dahl & Angervall* 1974) However the arrangement of

the tumour cells, the cytoplasmic tincturophilia in trichrome stains as well as the blunt ended nuclei, often arranged in rows or in tandem position in leiomyosarcoma seem fairly characteristic, enabling the recognition of this form of sarcoma (*Stout* & *Hill* 1958, *Dahl* & *Angervall* 1974).

Rounded or well-demarcated forms of pseudosarcomatous proliferative lesions of soft tissue such as nodular fasciitis (*Dahl* & *Angervall* 1977) may be confused with ancient neurilemmoma (*Stout* 1960 *Price et al* 1961 *Allen* 1972). However the proliferating cells in nodular fasciitis are frequently s-formed or wavy enclosing small clefts or slits, and differ from the cells seen in ancient neurilemmoma. Furthermore, mitoses, areas containing proliferating capillaries and extravasated erythrocytes as well as inflammatory cells are frequent findings in nodular fasciitis and may assist in arriving at the correct diagnosis (*Allen* 1972, *Dahl et al.* 1972).

Awareness of the existence of cellular neurilemmomas showing extreme nuclear polymorphism and hyperchromasia, but with a perfectly benign clinical course, is mandatory in order to avoid misinterpretation as sarcoma.

Supported by research grant from the *Swedish Cancer Society* 330-K73-07X.

REFERENCES

Ackerman L V & Taylor F H: Neurogenous tumors within the thorax. A clinicopathological evaluation of forty-eight cases. Cancer (Philad.) *4* 669–691 1951.

Allen, P W: Nodular fasciitis. Pathology *4* 9–26, 1972.

Angervall L, Dahl, I., Kindblom L.-G & Säve-Söderbergh, J: Spindle cell lipoma. Acta path. microbiol. scand. Sect A, *84* 477–487 1976.

Angervall L, Enerbäck L. & Knutson H: Chondrosarcoma of soft tissue origin. Cancer (Philad.) *32* 507–513 1973.

Compagno J, Hyams V J & Lepore M L: Nasal polyposis with stromal atypia. Review and follow-up study of 14 cases. Arch. Path. Lab Med *100* 224–226, 1976.

Dahl I & Angervall, L.: Cutaneous and subcutaneous leiomyosarcoma. A clinicopathologic study of 47 patients. Pathol. Eur *9* 307–315, 1974.

Dahl I & Angervall, L.: Pseudosarcomatous proliferative lesions of soft tissue with or without bone formation. Acta path. microbiol. scand. Sect. A, *85*: 577–589 1977.

Dahl, I & Angervall, L.: Pseudosarcomatous lesions of the soft tissues reported as sarcoma during a 6-year period (1958–1963). Acta path. microbiol. scand. Sect. A, *85*: 917–930, 1977.

Dahl, I., Angervall, L. Magnusson S & Stener B.: Classical and cystic nodular fasciitis. Pathol. Eur *7* 211–221 1972.

D'Agostino A N., Soule E. H & Miller R. H.: Primary malignant neoplasms of nerves (malignant neurilemomas) in patients without manifestations of multiple neurofibromatosis (von Recklinghausen disease). Cancer (Philad.) *16* 1003–1014 1963.

Das Gupta T K., Brasfield R. D., Strong, E. W & Hajdu S I.: Benign solitary schwannomas (neurilemomas). Cancer (Philad.) *24*: 355–366, 1969.

Ehrlich H E. & Martin H.: Schwannomas (neurilemomas) in the head and neck. Surg. Gynec. Obstet. *76*: 577–583 1943.

Enzinger F M.: Syllabus of tumours of neural tissues. WHO-Reference Set No VI Armed Forces Institute of Pathology Washington. 1969.

Enzinger F M Lattes R. & Torloni H.: Histological typing of soft tissue tumours. International histological classification of tumours. No 3 Geneva. WHO 1969.

Ghosh, B. C., Ghosh L., Huvos, A. G & Fortner J G.: Malignant schwannoma. A clinicopathologic study. Cancer (Philad.) *31* 184–190, 1973.

Gedulx J T.: Encapsulated neurilemoma (schwannoma) of the brachial plexus. Report of eleven cases. Cancer (Philad.) *5* 708–720, 1952.

Harkin, J C & Reed R. J: Tumors of the peripheral nervous system. Atlas of tumor pathology. Second series, fascicle 3. AFIP Washington D C. 1969.

Kindblom L.-G & Angervall, L.: Histochemical characterization of mucosubstances in bone and soft tissue tumors. Cancer (Philad.) *36* 985–994 1975.

Kragh, L V., Soule E. H & Masson J K.: Benign and malignant neurilemmomas of the head and neck. Surg. Gynec. Obstet. *111*: 211–218 1960.

Norris H J & Taylor H B.: Polyps of the vagina. A benign lesion resembling sarcoma botryoides. Cancer (Philad.) *19* 227–232 1966.

Oberman H A & Abell M R.: Neurogenous

neoplasms of the mediastinum. Cancer (Philad.) *13* 882–898 1960

Oberman H A & Sullenger G Neurogenous tumors of the head and neck. Cancer (Philad.) *20* 1992–2001 1967

Price E B Jr Sulliphant W M & Shuman R. Nodular fasciitis A clinicopathologic analysis of 65 cases. Am J Clin Path. *35* 122–136 1961

Saxén E Tumours of the sheaths of the peripheral nerves. Acta path. microbiol. scand. Suppl 79 1948

Smith C J Echevarria R & McLelland C A Pseudosarcomatous changes in antrochoanal polyps. Arch. Otolaryngol *99* 228–230 1974

Stout A P In Tumor seminar—part III Penn Med. J *63* 715–720 1960

Stout A P & Hill W T Leiomyosarcoma of the superficial soft tissues. Cancer (Philad.) *11* 844–854 1958

Vieta J O & Pack G T Malignant neurilemomas of peripheral nerves. Am. J Surg *82* 416–431 1951

White H R Survival in malignant schwannoma. An 18-year study Cancer (Philad.) *27* 720–729 1971

Acta path. microbiol. scand. Sect. A, 85 819–825, 1977

EPITHELIAL MUCOSUBSTANCES AND ARGYROPHIL CELLS IN BRENNER TUMOURS

PEKKA J KLEMI

Department of Pathological Anatomy University of Turku, Turku, Finland

Klemi, P J Epithelial mucosubstances and argyrophil cells in Brenner tumours. Acta path. microbiol. scand. Sect. A, 85 819–825 1977

Brenner tumours of various degree of malignancy were investigated by histochemical methods. The cells lining the cystic cavities in the benign Brenner tumours contained various amounts of PAS-positive diastase resistant secretory material mixed with small amounts of sulpho- and carboxymucin. The borderline and malignant tumours contained more acidic mucins than the benign tumours. All tumours contained glycogen Argyrophil and argentaffin cells have not earlier been detected in the Brenner tumours but in this study they were detected in twelve of the 18 Brenner tumours. These cells were not proliferating and therefore Brenner tumour should not be included in the group of APUDomas.

Key words Brenner tumours epithelial mucosubstances argyrophil cells.

P J Klemi, Department of Pathological Anatomy University of Turku, Kiinamyllynkatu 10 20520 Turku 52, Finland

Received 7 iv 77 Accepted 24 77

The well demarkated Brenner tumour nest of the ovary consists of ovoid or elongated cells, often with coffee bean nucleus. The name "Brenner tumour" was introduced by *Meyer* (1932) They are usually benign and have been considered to be relative rare constituting in a recent study 1.2 per cent of 3112 ovarian tumours (*Carpen* 1975) Some tumours show proliferating activity but no invasive growth is observed and such tumours are called "proliferating Brenner tumours" (*Roth & Sternberg* 1971) or in the WHO classification, tumours of borderline malignancy (*Serov et al* 1973) Malignant Brenner tumours also exist in the literature since year 1945 (*von Numers* 1945) and about 30 cases have been published (*Carpen* 1975) Many benign Brenner tumours are cystic and sometimes the cells are secreting. The secretory product contains in addition to neutral, PAS-positive and diastase resistant material (*Lauchlan* 1966) also sulpho- and carboxy mucin (*Ruckhaberle et al* 1973) The rare Brenner tumours of borderline malignancy and the malignant tumours also contain secreting cells (*Reel* 1938 and *Hallgrimsson & Scully* 1972) but the character of the secretion has not yet been analysed histochemically

Argyrophil and argentaffin cells have never been identified in Brenner tumours. One case has been reported where in the same ovary there was a carcinoid tumour a mucinous cystadenoma and a benign Brenner tumour (*Evans et al.* 1959)

This study will characterize the epithelial secretions and the distribution of argyrophil and argentaffin cells in benign, borderline and malignant Brenner tumours.

TABLE 1 *Age and Some Gynecological Findings of the Patients Having Brenner Tumours*

Tumours	Age	Lesions in the same ovary	Other lesions in the genital tract
Benign			
1	61	mucinous cystadenoma of borderline malignancy	endometrial atrophy carcinoma in situ in cervical canal
2	64	—	endometrial atrophy *benign endometrial polyp*
3	53	—	leiomyoma of the uterus
4	42	—	leiomyoma of the uterus
5	69	benign mucinous cystadenoma	endometrial atrophy
6	47	—	serous benign cystadenoma of the ovary
7	47	—	leiomyoma of the uterus
8	48	—	leiomyoma of the uterus, endometrial atrophy
9	58	—	cystic glandular hyperplasia of the endometrium
10	50	—	—
11	51	—	—
12	69	—	endometrial atrophy
13	39	—	estrogenic effect in the endometrium
14	50	—	thecoma of the other ovary
15	72	benign mucinous cystadenoma	endometrial atrophy
16	69	—	leiomyoma of the uterus
Borderline tumour			
17	70	benign mucinous cystadenoma	endometrial atrophy
Malignant tumour			
18	65	—	endometrial atrophy

MATERIAL AND METHODS

Material for this study was obtained from 16 benign, one borderline and one malignant Brenner tumours that had been diagnosed at the department of pathological anatomy at the University of Turku Turku, Finland between years 1961–1975 The age and some gynecological findings of the patients are shown in Table 1 The blocks were sectioned serially at 5 micron and stained with van Gieson method and various other methods for *characterization of epithelial mucosubstances* and detection of argyrophil and argentaffin cells. The following methods were from the book of A F I P (*Luna* 1968) if not otherwise indicated Periodic acid-Schiff staining with and without diastase digestion (dPAS and PAS) was used for the detection of glycogen PAS-staining also indicated the presence of 1 2 hydroxyl groups. Acid mucins were demonstrated with the high iron diamine-Alcian blue (HID AB pH 2 5) method in which sulphate (black) and carboxyl (blue) radicals could be differentiated (*Spicer* 1965) In AB pH 1 0 *only sulphate groups* are stained S alidase digestion before HID-AB pH 2.5 was performed in order to demonstrate sialic acid residues. Testicular hyaluronidase digestion before AB pH 2.5 staining was done for demonstration of hyaluronic acid and chondroitin sulphates A and C The Bodian-protargol and *Grimelius* (1968) methods were used for identification of argyrophil granules and Fontana Masson of argentaffin granules.

RESULTS

Benign Brenner Tumours

Twelve of the 16 benign Brenner tumours contained cell nests with central cavities. The secretion in the cavities and in the cells lining the cavities was PAS-positive and diastase resistant. A small part of it was acidic. With HID AB pH 2.5 it stained mostly blue in every tumour but some black staining was also noted A small portion of carboxymucin was removed by sialidase digestion in half of the 16 benign Brenner tumours. *The lumenal* border of the cell stained blue as often as black with HID AB pH 2.5 Almost every tumour cell contained glycogen. Hyaluronidase digestion did not diminish the blue staining with AB pH 2.5 The summary of the stainings is given in Table 2

Ten of the 16 benign Brenner tumours

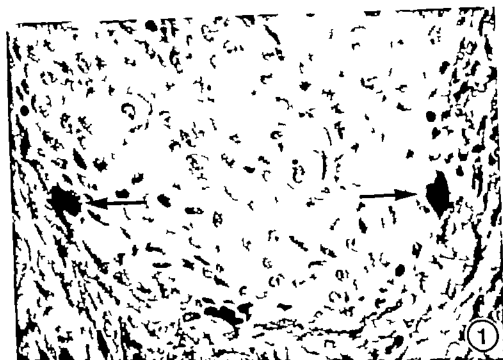


Fig. 1. Two argentaffin-cells (arrows) on the basal lamina in the benign Brenner tumour nest (Fontana-Masson × 630)

TABLE 2. *Staining Results of the Brenner Tumours*

Tumours	Number of cases	Mucosubstances, groups 1.2-hydroxyl	–O–SO	–COO	Glycogen	Argyrophil cells
Benign	16	+ (16)	+ (6)	+ (16)	+ (16)	+ (10)
Borderline	1	+	+ +	+	+	+
Malignant	1	+	+ +	+	+	+

Symbols: + sparse, + + moderate. Number in parenthesis indicates the positive cases.

contained one or more argyrophil cells, located on the basal membrane (Fig. 1) between the Brenner cells. The cells stained equally often with the Bodian-protargol and Grimelius methods, but only 4 of the ten tumours had cells which also stained with the Fontana Masson method.

Borderline and Malignant Brenner Tumours

The Brenner tumour of borderline malignancy was cystic. The epithelium formed papillae lined by cells, which resembled the transitional type. No invasive growth was observed. Superficial cells were either ciliated or nonciliated and the latter sometimes secreting. The ultrastructure of this tumour is described in the accompaning paper (*Klemi & Nevalainen* 1977). The malignant Brenner tumour also contained large cystic cavities bordered by the same type of epithelium as described above, but papillae formation was a more characteristic feature for this tumour (Fig. 2). Invasive growth was observed spo-

Fig 2 Malignant Brenner tumour Mucus in the lumen stained with PAS (dark staining in the picture) (PAS × 345)



Fig 3 C liated and nonciliated superficial cells of the epithelium in the borderline Brenner tumour The nonciliated cells contain acid mucin (dark staining in the picture) (HID-AB pH 2.5 × 375)



Fig 4 Two argyrophil-cell (arrow) on the basal lamina in the borderline Brenner tumour (Bodian × 665)

radically and mitoses were noted frequently but cellular and nuclear atypia was moderate. The malignant part of the tumour was similar to the papillary transitional cell carcinoma of the bladder There were many small typical Brenner cell nests in the vicinity of both tumours. The cells in these nests showed the same staining characteristics as in the benign Brenner tumours.

The staining results for epithelial mucosubstances in the two tumours were similar enough to be described together Some cells were rich in glycogen and in addition there was PAS-positive diastase resistant material in the cytoplasm. The secretion became more visible towards the luminal parts of the epithelium. A small amount of the secretion stained with HID-AB pH 2.5 indicating the presence of acidic groups. Some superficial cells contained much PAS-positive, diastase resistant material but were also rich in acidic radicals (Fig 3) There were more sulphate groups than carboxyl groups The free luminal border of the superficial cells stained blue as often as black with the HID-AB pH 2.5 method. Only weak staining was noted with the AB pH 1.0 method. Sialidase or hyaluronidase digestion did not eliminate the acidic staining of the cells. The secretion in the cavities contained PAS-positive diastase resistant material mixed with some sulpho- and carboxymucins.

Both tumours contained some agyrophil cells, which sometimes were mixed with tumours cells (Fig 4) The cells stained well with the Bodian protargol and Grimelius methods but failed to stain with the Fontana Masson method.

DISCUSSION

The benign Brenner tumour cells contained various amounts of PAS-positive, diastase resistant material indicating the presence of 1 2 hydroxyl groups. This is in accordance with the findings of others (*Christian & Janowski* 1962, *Meiling et al* 1963 *Jopp* 1964 *Lauchlan* 1966 and *Ruckhaberle et al* 1973) Acid mucins have been demonstrated before by AB-staining (*Christian & Janowski* 1962) Benign Brenner tumours contained residues of sialomucin in addition to the sulpho- and carboxymucins shown by *Ruckhaberle et al* (1973) Hyaluronic acid chondroitin sulphate A and C were not present

The staining reactions for borderline and malignant Brenner tumours were similar to the reactions in the benign Brenner tumours except that sialidase labile material did not exist. The secretion was most pronounced in the superficial cells lining the cystic cavities.

Glycogen was detected in every tumour This agrees with the earlier findings of others e g (*Berge* 1967 and *Teilum* 1971) Glycogen has been demonstrated also at the ultrastructural level (*Roth* 1971 *Silverberg & Wilson* 1972, *Merkow et al* 1972 *Cummins et al.* 1973 and *Bransilver et al* 1974)

The epithelium of the Brenner tumour resembled the transitional epithelium of the urinary tract. Especially the epithelium of the borderline and malignant Brenner tumours was similar to that of the papillary transitional cell carcinoma The transitional epithelium in the bladder can differentiate into glandular epithelium as in cystitis cystica, originally described by *von Limbeck* (1887) The transitional epithelium has a high potential for undergoing metaplasia into either glandular or squamous epithelium (*Mostofi* 1954) or into intestinal type epithelium with goblet, Paneth argyrophil and argentaffin cells (*Gordon* 1963) Argyrophil cells were observed in 12 of the 18 Brenner tumours in the present investigation The cells were present in small amounts and did not seem to be proliferating Therefore it is not justified to include Brenner tumours in the APUD series (*Pearse* 1969) The presence of such cells in the Brenner tumours is not surprising since also normal endocervical epithelium (*Tateishi et al* 1975) and mucinous ovarian cystadenomas contain such cells. In an unpublished study argyrophil cells were present in 59 per cent in 179 ovarian mucinous cystadenomas of varying degree of malignancy (*Klemi* 1977) Endocervical epithelium is of Muellerian i e coelomic origin but the origin of mucinous ovarian cystadenomas is still unresolved. A combination of Brenner tumour and mucinous cystadenoma in the same ovary was found in this study in 22.2 per cent. The finding is similar to the figure of an other study where 21 4 per cent of 74 cases contained both type of tumours (*Carpen* 1975) The borderline and malignant Brenner tumours contained ciliated cells which are commonly found in the fallopian tube and in tumours of Muellerian origin such as serous ovarian cystadenomas (*Serov et al* 1973) All the foregoing observations support a common origin for these tumours and tubular structures of Muellerian derivation i e. coelomic origin The histogenesis of Brenner tumours is discussed in more detail in the following paper in this issue (*Klemi & Nevalainen* 1977)

REFERENCES

1 *Berge Th & Borglin N E.* Brenner tumours histogenetic and clinical studies. Cancer (Philad.) 20 308–318, 1967

2 *Bransilver B R Ferenczy A & Richart R M* Brenner tumour and Walthard cell nests. Arch Path 98 76–86, 1974

3 *Carpen E* Brenner tumours of the ovary A clinicopathological study Thesis, University of Helsinki, Helsinki, 1975 p. 30–35

4 *Cummins P A Fox H & Langley F A* An ultrastructural study of the nature and origin of the Brenner tumour of the ovary J Pathol 110 167–176 1973

5. *Christian C D & Jaworski A A* Bilateral Brenner tumour Amer J Obstet. Gynec. *83* 103–106, 1962.
6. *Evans R. W., Harris H R & M Dougall, D M* Argentaffin carcinoma (carcinoid tumour) of ovary J Clin. Path. *12* 183–187 1959
7. *Gordon A* Intestinal metaplasia of the urinary tract epithelium. J Path. Bact. *85* 441 444 1963
8. *Grimelius L.* A silver nitrate stain for alfa 2 cells in human pancreatic islets. Acta Soc. Med. upsalien. *73* 247–270 1968
9. *Hallgrimsson J & Scully R.* Borderline and malignant Brenner tumours of the ovary Acta path. microbiol. scand. Sect. A *80* suppl. 233 56–66 1972.
10. *J pp H.* Histochemischer Beitrag zur Frage der Hormonaktivität von Brenner tumoren. Arch. Gynak. *199* 459–467 1964
11. *Klemi P J & Nevalainen T J* Ultrastructure of the benign and borderline Brenner tumours Acta path. microbiol. scand. Sect. A. *85* 83 —838 1977
12. *Klemi, P J* Epithelial mucosubstances and argyrophil cells in ovarian mucinous cystadenomas In preparation, 1977
13. *Lauchlan S C* Histogenesis and histogenetic relationship of Brenner tumours. Cancer (Philad.) *19* 1628–1643 1966.
14. *von Limbeck R.* Zur Kenntniss der Epithelcysten der Harnblase und der Ureteren. Z. Heilk. *8* 55–66, 1887
15. *Luna, G L* Manual of histological staining methods of the A.F.I.P 3rd ed McGraw–Hill Book Co New York and Toronto and London and Sidney 1968.
16. *Mell g, R L Bourstein J G Teterus Y J., Ullery J C & George O T* Histochemical observations of Brenner cell tumour with masculinization. Amer J Obstet. Gynec. *87* 463–470 1963
17. *Merkow L P Salazar H & Pardo M* Human ovarian neoplasms, light and electron microscopic correlations I Brenner tumour Obstet and Gynec. *40* 667–680 1972.
18. *Meyer R* Ueber verschiedene Erscheinungsformen der als Typus Brenner bekannten Eierstockgeschwulst, ihre Absonderung von den Granulosazelltumoren und Zoordnung unter andere Ovarialgeschwulste. Arch. Gynäk. *148* 541–596 1932.
19. *Mostofi, F K.* Potentialities of the bladder epithelium. J Urol. (Baltimore) *71* 705–714 1954
20. *von N mers C* Contribution to the case knowledge and histology of the Brenner tumor Do malignant forms of the Brenner tumor also occur? Acta obstet. gynec. scand. *25* suppl. 2 114–127 1945
21. *P arse A G E.* The cytochemistry and ultrastructure of polypeptide hormone-producing cells of the APUD series and the embryologic, physiologic and pathologic implications of the concept. J Histochem. Cytochem. *17* 303–313 1969
22. *R l P J.* Malignant Brenner tumour of the ovary with the report of one case Amer J Obstet. Gynec. *76* 872–876 1958
23. *Roth L. M.* Fine structure of the Brenner tumor Cancer (Philad.) 27 1482–1488, 1971
24. *Roth L. M & Sternberg W H.* Proliferating Brenner tumors. Cancer (Philad.) 27 687–693 1971
25. *R ckkäberle K E., Bilek K. & R ckkäberle B* Histochemische Untersuchungen an Brenner tumore Zbl. Gynäk. 95 1148–1154 1973
26. *Silverberg, S G & Willson M S.* Ultrastructure of the Brenner tumour Amer J Obstet. Gynec. *112* 91–100, 1972.
27. *Serov S F., Scully R. E. & Sobin, L. H.* Histological typing of ovarian tumours. WHO Geneve pp. 37–41 1973
28. *Spicer S S* Diamine methods for differentiating mucosubstances histochemically J Histochem. Cytochem. *13* 211–234 1965
29. *Tateishi R., Wada, A., Hayakawa, K Hongo J Ishii S & Terakawa, N* Argyrophil cell carcinomas (apudomas) of the uterine cervix. Light and electron microscopic observations of 5 cases. Virchows Arch. Abt. A *366* 257–274 1975
30. *Teilum G* Special tumors of ovary and testis. Munksgaard, Copenhagen, pp. 236–242, 1971

Acta path. microbiol scand. Sect. A 85 826–838 1977

ULTRASTRUCTURE OF THE BENIGN AND BORDERLINE BRENNER TUMOURS

PEKKA J KLEMI and TIMO J NEVALAINEN

Department of Pathological Anatomy and Laboratory of Electron Microscopy
University of Turku Turku Finland

Klemi, P J & Nevalainen, T J Ultrastructure of the benign and borderline Brenner tumours. Acta path. microbiol. scand Sect. A 85 826–838 1977

One benign Brenner tumour and one Brenner tumour of borderline malignancy were investigated by electron microscopy The cells of the benign Brenner tumour nests and the cells in the borderline tumour were similar in ultrastructure. The intercellular spaces were large and reinforced by a moderate number of desmosomes. The nuclei were round or oval. The nuclear membrane was irregular in shape with deep infoldings corresponding to the characteristic nuclear groovings seen by light microscopy Only few secreting cells could be found in the benign Brenner tumour The cystic cavities of the borderline Brenner tumour were lined by nonciliated secreting and ciliated nonsecreting cells. The secretory granules were PAS-positive and diastaseresistant. The granules stained homogeneously and strongly with the PASM method at the electron microscopical level indicating the presence of 1.2 hydroxyl groups. The Brenner tumours have many similarities to the transitional epithelium and to the Muellerian-derived tubular structures. The findings support the theory that Brenner tumours are of coelomic origin and develop by direct metaplasia from the ovarian surface epithelium.

Key words Brenner tumours ultrastructure.

P J Klemi, Department of Pathological Anatomy University of Turku, Kiinamyllynkatu 10 20520 Turku 52 Finland

Received 7 iv 77 Accepted 24 v 77

In the histological classification of ovarian tumours by WHO Brenner tumours belong to the common epithelial tumours of the ovary and are divided into benign tumours, tumours of borderline malignancy and malignant ones (*Serov et al* 1973) The benign Brenner tumour is a rather common lesion and there are several descriptions of its ultrastructure in the literature (*Philipp & Overbeck* 1970 *Roth* 1971 *Hameed* 1972 *Langley et al* 1972 *Merkow et al* 1972 *Silverberg & Willson* 1972 *Cummins et al* 1973 and *Bransilver et al* 1974) Borderline tumours are rare (*Roth & Sternberg* 1971 and *Hallgrimsson et al.* 1972) and there are no reports on the ultrastructure of borderline and malignant Brenner tumours. The ultrastructure of the Brenner tumour of borderline malignancy is described in this study and compared to that of the benign Brenner tumour Some aspects of the histogenesis of the Brenner tumours are also discussed.

MATERIAL AND METHODS

Two cases of Brenner tumours were studied by light and electron microscopy Representative samples of each tumour removed during surgery were processed for light microscopy by fixation in

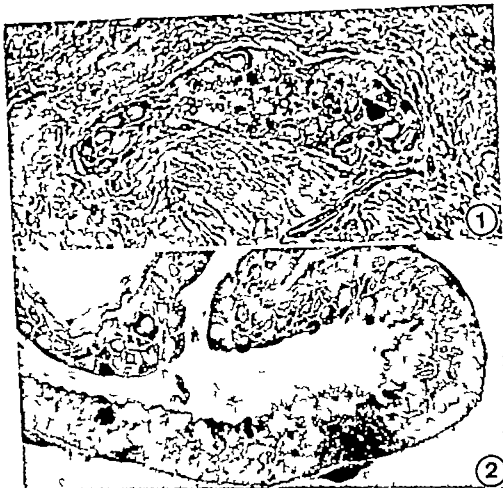


Fig. 1. A cell nest of the benign Brenner tumour. Some cells contain deeply stained granules. Light micrograph of PAS-stained semithin Epon section. Mag. 445 ×

Fig. 2. Wall of large cyst in the Brenner tumour of borderline malignancy lined by ciliated and non-ciliated columnar cells. Beneath the superficial columnar cell layer the intercellular spaces are distended. Light micrograph of PAS-stained semithin Epon section. Mag. 445 ×

neutral buffered formalin, embedded in paraffin, sectioned semiserially and stained with the [illegible] (…eosin-haematoxylin and periodic acid-Schiff (PAS) methods, the latter with and without diastase digestion. The Grimelius silver method was used to detect argyrophil cells (*Grimelius* 1968).

For electron microscopy small pieces (1 mm³) from both tumours were fixed in 3 per cent glutaraldehyde in 0.1 M cacodylate buffer at pH 7.3 (*Sabatini et al.* 1963) for 3 hours and postfixed in 1 per cent osmium tetroxide in the same buffer for 2 hours. Semithin sections from tissues embedded in Epon 812 (*Luft* 1961) were stained with alkaline toluidine blue (*Trump et al.* 1961). PAS and Alcian blue pH 2.5 (AB) stainings were performed following removal of Epon by NaOH in absolute ethanol (*Litwin & Kasprzyk* 1976). Thin sections of silver to gold interference colour were stained with uranyl acetate (*Watson* 1958) and lead citrate (*Venable & Coggeshall* 1965) and studied by JEOL JEM 100C electron microscope. Cellular mucosubstances were demonstrated at the electron microscopical level by the periodic acid silver methenamine (PASM) technique (*Ver lei-nen & Klemi* 1976).

Acta path microbiol scand Sect. A 85 826 838 1977

ULTRASTRUCTURE OF THE BENIGN AND BORDERLINE BRENNER TUMOURS

PEKKA J KLEMI and TIMO J NEVALAINEN

Department of Pathological Anatomy and Laboratory of Electron Microscopy
University of Turku, Turku, Finland

Klemi P J & Nevalainen, T J Ultrastructure of the benign and borderline *Brenner tumours.* Acta path microbiol scand Sect. A 85 826–838 1977

One benign Brenner tumour and one Brenner tumour of borderline malignancy were investigated by electron microscopy The cells of the benign Brenner tumour nests and the cells in the borderline tumour were similar in ultrastructure. The intercellular spaces were large and reinforced by a moderate number of desmosomes The nuclei were round or oval The nuclear membrane was irregular in shape with deep infoldings corresponding to the characteristic nuclear groovings *seen by light microscopy Only few secreting cells could be found in the* benign Brenner tumour The cystic cavities of the borderline Brenner tumour were lined by *nonciliated* secreting and ciliated nonsecreting cells. The secretory granules were *PAS*-positive and diastaseresistant. The granules stained homogeneously and strongly with the PASM method at the electron microscopical level indicating the presence of 1,2 hydroxyl groups. The Brenner tumours have many similarities to the transitional epithelium and to the Muellerian-derived tubular structures. The findings support the theory that Brenner tumours are of coelomic origin and develop by direct metaplasia from the ovarian surface epithelium.

Key words Brenner tumours ultrastructure

P J Klemi Department of Pathological Anatomy University of Turku Kiinamyllynkatu 10 20520 Turku 52 Finland.

Received 7.iv 77 Accepted 24 v 77

In the histological classification of ovarian tumours by WHO Brenner tumours belong to the common epithelial tumours of the ovary and are divided into benign tumours tumours of borderline malignancy and malignant ones (*Serov et al* 1973) The benign Brenner tumour is a rather common lesion and there are several descriptions of its ultrastructure in the literature (*Philipp & Overbeck* 1970 *Roth* 1971 *Hameed* 1972 *Langley et al* 1972 *Merkow et al* 1972 *Silverberg & Willson* 1972 *Cummins et al* 1973 and *Bransilver et al* 1974) Borderline tumours are rare (*Roth & Sternberg* 1971 and *Hallgrimsson et al* 1972) and there are no reports on the ultrastructure of borderline and malignant Brenner tumours. The ultrastructure of the Brenner tumour of borderline malignancy *is described in this study* and compared to that of the benign Brenner tumour Some *aspects of the histogenesis of* the Brenner tumours are also discussed.

MATERIAL AND METHODS

Two cases of Brenner tumours were studied by light and *electron* microscopy Representative samples of each tumour removed during surgery were *processed for* light microscopy by fixation in

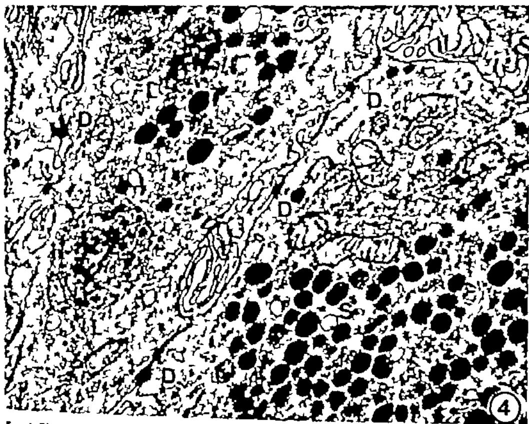


Fig. 4 Electron micrograph of the secretory cells in the benign Brenner tumour. The round homogeneously electron opaque secretory granules (S) are approximately 0.2–0.5 µm in diameter and bounded by a membrane. The lysosomal dense bodies (*L*) are approximately 1 µm in diameter and contain granular and amorphous material. There are cytoplasmic projections into the intercellular *space* (*I*) and numerous desmosomes (D) between adjacent tumour cells. Mag. 20 000 ×

contained PAS-positive, diastase—resistant granular material (Fig. 1). The granules did not stain with AB or Grimelius methods. Glycogen was present in some cells.

The Brenner tumour of borderline malignancy was cystic. Sometimes the epithelium resembled closely that of the urinary tract, especially the transitional cell papilloma. The great majority of the epithelial cells in the Brenner tumour of borderline malignancy were similar to those in the benign tumour but the superficial cells lining the large [illegible] spaces were columnar or flattened [illegible] and sometimes ciliated. The non-[illegible]lated cells often contained PAS-positive diastase resistant material which stained also with AB pH 2.5. Many cells contained glycogen. The superficial cells did not stain with the Grimelius silver method.

Electron Microscopy

Benign Brenner tumour. The cell nests were surrounded by a regular basal lamina (Fig. 3). The cells were round, oval or elongated and the plasma membrane was folded considerably. The intercellular space was irregular and often distended (Figs. 3 and 4). The cells were attached to each other by a *moderate* number of well developed desmosomes (Fig. 4). The nuclei were round or oval with numerous deep indentations in the nuclear membrane. The chromatin was usually dispersed throughout the



Fig 3 Electron micrograph of the benign Brenner tumour The cell nest is surrounded by a regular basal lamina (B) The nuclei (N) are irregularly oval and the nuclear membranes are invaginated. The nucleoli are relatively large. There are numerous small, round secretory (S) and large lysosomal dense bodies (L) in the cytoplasm The intercellular spaces (I) are slightly distended Stained with uranyl acetate (UA) and lead citrate (Pb) Mag 4,380 ×

RESULTS

Light Microscopy

The benign and borderline Brenner tumours investigated in the present study fulfilled the histological criteria of the WHO classification (*Serov et al* 1973) The main gynecological features of these tumours are also dealt with in the preceding article in this issue benign = case 2 and borderline = case 17 (*Klemi* 1977) Only a short comment on the histology is given here

In the benign Brenner tumour in the cell nests there were some cystic spaces filled with secretory product which stained red with PAS The cells were round, oval or elongated The nuclei were ovoid or round with a longitudinal groove Nuclear grooving was not a constant feature. Neither goblet nor ciliated cells were present but some cells



Fig. 6 Electron micrograph of the Brenner tumour of borderline malignancy The intercellular spaces are dilated with numerous microvilli projecting into them The nuclei (N) are oval and deeply idented. The relatively scanty cytoplasm contains profiles of the Golgi apparatus (G) mitochondria (M) and occasional lipid droplets (LI) UA Pb Mag. 5 030 ×

omplex was well developed (Fig. 6) The endoplasmic reticulum was mostly of the rough variety A moderate amount of free ribosomes was present. Some cells contained glycogen particles There were small scattered bundles of microfilaments and occasional microtubules in the cytoplasm. Some cells contained lipid droplets (Fig. 6) Secretory granules similar to those found in the benign Brenner tumour were also occasionally found in the borderline tumour Lysosomes were found relatively frequently The nuclei were mostly slightly elongated and the nuclear membrane was often irregular in shape with deep infoldings. The chromatin was usually evenly distributed (Fig. 6)

The superficial cells on the luminal border were of two types, either ciliated or non ciliated (Fig 7) The latter often contained secretory granules.

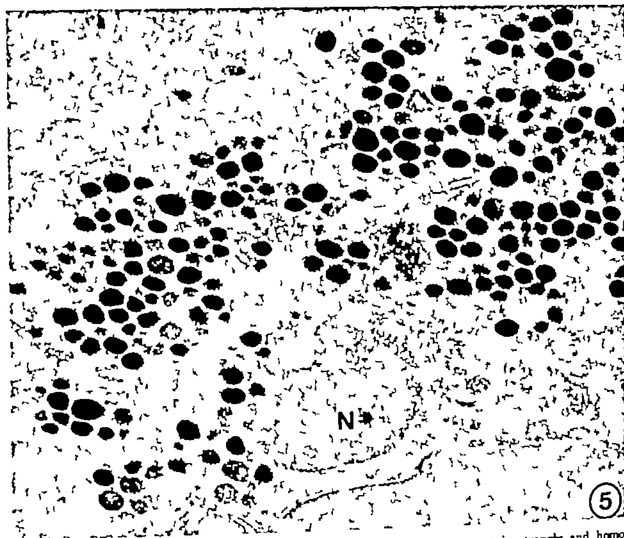


Fig 5 The secretory granules in the cells of the benign Brenner tumour stain strongly and homogeneously with the periodic acid-silver methenamine (PASM) reaction N nucleus. Mag. 17 600 ×

nuclei and the nucleoli were relatively large (Fig 3) The cytoplasm contained numerous free ribosomes and few profiles of the granular endoplasmic reticulum. Profiles of the smooth endoplasmic reticulum were observed only sporadically Mitochondria were of medium size oval or round and not especially numerous (Fig 4) Usually only few and inconspicuous profiles of the Golgi apparatus were present but in cells containing secretory material the Golgi apparatus was more prominent The secretory granules were approximately 0 2 0 3 μm in diameter dense and homogeneous and surrounded by membranes (Fig 4) The granules stained strongly with the PASM method (Fig 5) but did not stain without previous periodic acid oxidation. Glycogen granules were uncommon Lysosomal dense bodies were approximately 1 μm in diameter and contained heterogenous granular and amorphous material (Fig 4)

Borderline Brenner tumour The epithelial cells of the borderline Brenner tumour great ly resembled the cells in the benign Brenner tumour They made up the great majority of the tumour cells and were round elong ated or oval in shape. The plasma membrane was folded and the intercellular space was large (Fig 6) There were cytoplasmic projections into the intercellular space but there were few desmosomal juntions between the cells The cytoplasm contained a number of round or elongated mitochondria The Golgi

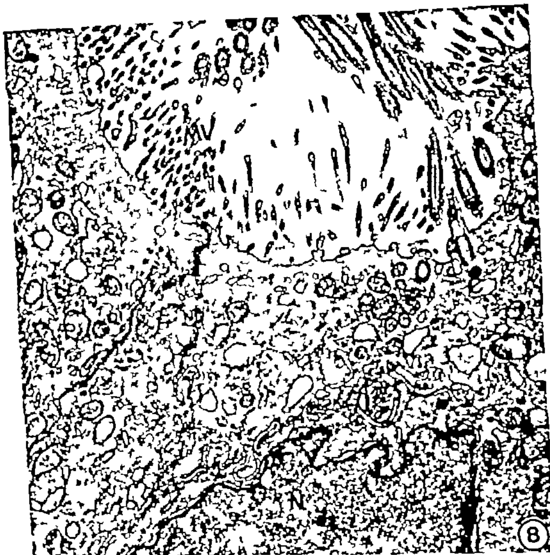


Fig 8 Electron micrograph of two superficial cells. The apical cytoplasm of ciliated cell on the right contains mitochondria and small vesicles but no secretory granules. The cilia appear in longitudinal and cross sections in the cyst lumen (C) basal body of cilium (MV) microvilli (N) nucleus. UA Pb Mag 14,500 ×

m x t al. 1973 and *Braunlcer et al* 1974) The epithelial cells in the Brenner tumour of borderline malignancy closely resembled the cells of the benign tumour The border line tumour most probably develops from its benign counterpart by cellular proliferation. On the other hand the Brenner cells resemble the cells of the transitional epithelium in their morphology (*Batt fora et al.* 1964 *Falk et al* 1971 C *mmins et al.* 1973 and *Braunlcer et al.* 1974) In the common urinary bladder condition, cystitis cystica or cystitis glandularis, the transitional epithelium can differentiate into gland-like structures, which contain mucin secreting cells. This is the end result of the metaplastic changes of the transitional epithelium as originally described by *von Limbeck* (1887) and by *von Brunn* (1893) The same process may occur in the Brenner tumours.

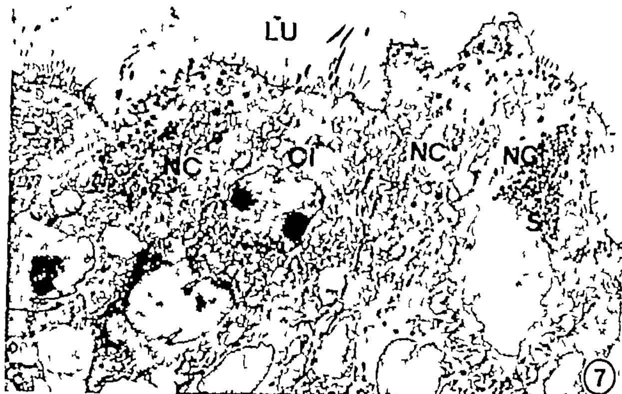


Fig 7 Electron micrograph of ciliated (CI) and nonciliated (NC) superficial cells lining a cyst lumen (LU) of the borderline Brenner tumour There are variable amounts of secretory granules (S) in the nonciliated cells. UA Pb Mag 3 420 ×

The ciliated cells in the epithelium lining the cyst lumen were columnar in shape Every cilium contained 1 central and 9 peri feral pairs of microtubules (Fig 8) The plasma membrane was relatively smooth The cytoplasm contained moderate amounts of round or elongated mitochondria and small vesicles but no secretory granules (Fig 8) The Golgi complex was not as prominent as in the nonciliated secretory cells. There were small glycogen granules in some cells. The oval or elongated nuclei contained dispersed chromatin and 1-2 nucleoli

The secretory granules in the nonciliated superficial cells were confined to the supra nuclear (apical) cytoplasm. They were surrounded by a membrane and contained homogeneous dense material (Fig 9) The secretory granules stained strongly and evenly with the PASM reaction as was the case in the benign tumour Extensive Golgi cisternae were often closely associated with the secretory granules (Fig. 9) There were some short microvilli on the lumenal cell surface. The lateral plasma membrane was relatively complicated and the extracellular space was relatively wide (Fig 9) There were desmosomes between adjacent superficial cells. There were only few oval or elongated mitochondria in the cytoplasm. Occasional microfilaments and free ribosomes were present in the cytoplasm. Profiles of both smooth and rough endoplasmatic reticulum were present but inconspicuous The nuclei were similar to those of the other epithelial cells.

DISCUSSION

The ultrastructural observations on the benign Brenner tumour in the present study confirm largely earlier findings of others (*Philipp & Overbeck* 1970 *Roth* 1971 *Hameed* 1972 *Langley et al* 197? *Merkow et al* 1972 *Silverberg & Wilson* 1972, *Gum*

e.g. serous tumours of the ovary (*Seroo et al.* 1975). The cells in the fallopian tube exhibit signs of secretory activity after treatment with estrogen (*Fredricsson & Björkman* 1973). Ciliated cells may by found in the glandular epithelium of the endometrium during the follicular phase and in cystic glandular hyperplasia (*Maddi & Papanicolau* 1961 and *Schueller* 1968). Estrogen is needed to maintain these functional states. Estrogen influences also the ciliogenesis in the fallopian tube of the Rhesus monkey where the cilia are shed during the luteal phase and regenerate during the follicular phase (*Brenner* 1969). The nature of the cytoplasmic granules in Brenner tumour cells is a very interesting question. Earlier they were considered degenerative products, probably lysosomal in nature (*Philipp & Overbeck* 1970, *Hameed* 1972 and *Langley et al.* 1972). The granules have membranes and are homogeneously electron opaque and thus distinctly different in ultrastructure from the mucous granules in the epithelial cells of the endocervical canal (*Philipp* 1972), the gastric mucosa of rat and man (*Yeomans* 1974 and *Vesalainen & Järvi* 1977) or the ovarian mucinous cystadenomas (*Klemi & Nevalainen* 1977). It was shown in the present study that the granules in the benign and borderline Brenner tumour cells were PAS-positive and diastase resistant and reacted homogeneously and strongly in the PASM treated sections which indicate the presence of 1,2 hydroxyl-groups. At the light microscopical level in the semithin sections they did not stain with the Grimelius stain and thus are not argyrophil-granules. In another study (*Klemi & Nevalainen* 1977) it was found that argyrophil-granules did not stain with the PAS-method in semithin Epon sections. In addition to these secretory granules the cell cytoplasm in both Brenner tumours contained some primary and large secondary lysosomes which result from the degenerative process in the cells.

There are many theories on the origin of the Brenner tumours. A granulosa cell-origin for Brenner tumours has been suggested e.g. (*Brenner* 1907) but in spite of such similarities as nuclear groovings, desmosomes, and Call-exner bodies (*Bjersing* 1967) which sometimes resemble the cystic Brenner tumours, there are so many dissimilarities, that a granulosa cell-origin for Brenner tumours is unlikely (*Bransilver et al.* 1974).

A Walthard cell nests (WCN)-origin for Brenner tumours was first proposed by *Meyer* (1932) and later supported and thoroughly discussed by e.g. *Bransilver et al.* (1974). WCNs are solid or cystic cell populations in the ovarian cortex, mesovarium or hilus. They are very similar to the Brenner tumours both at the light and electron microscopic level. WCNs originate from the ovarian cortical epithelium and some Brenner tumours may originate from WCNs (*Bransilver et al.* 1974).

Rete ovary is the remmants of the mesonephric ducts and originate from the intermediate mesoderm by a somewhat different mechanism than the Muellerian duct but primarily both the Muellerian and mesonephric ducts are mesodermal in origin (*Warwick & Williams* 1973). The transitional epithelium of the urinary tract is of mesonephric derivation and thus the remnants of the mesonephric ducts have been suggested as the origin for Brenner tumours e.g. *Schiller* (1934). Rete ovary is located in the ovarian hilus and some Brenner tumours may originate from it, but this would not explain the origin of those Brenner tumours that are located cortically.

If the Brenner tumours originate from teratomas, there should be more often than presented also other teratomatous elements close to Brenner tumours. A cystic teratoma and 2 dermoid cysts have contained Brenner tumours (*Jondahl* 1950) and this has given rise to speculation about a teratomatous origin for Brenner tumours, there is not any further support for this theory. Some Brenner tumours contain argyrophil cells (*Klemi* 1977), which are also present in about 60 per cent of ovarian mucinous cystadenomas (*Klemi* 1977). The presence of argyrophil cells alone is not sufficient evidence for tera



Fig 9 A higher magnification of part of figure 7 The apical cytoplasm of a nonciliated superficial cell contains abundant secretory granules in the vicinity of the Golgi cisternae (G) MV short microvilli projecting into the cyst lumen (I) lateral intercellular space (N) nucleus. UA Pb, Mag 13 050 ×

The cells lining the cystic cavities in the borderline Brenner tumours were either ciliated and nonsecreting or nonciliated and secreting Both types of cells are found in epithelia of Muellerian derivation such as in the fallopian tube endometrium and cervical canal (*Bloom & Fawcett* 1975) and in tumours derived from coelomic epithelium

e.g. serous tumours of the ovary (*Serov et al.* 1973). The cells in the fallopian tube exhibit signs of secretory activity after treatment with estrogen (*Fredricsson & Björkman* 1973). Ciliated cells may by found in the glandular epithelium of the endometrium during the follicular phase and in cystic glandular hyperplasia (*Maddi & Papanicolau* 1961 and *Schueller* 1968). Estrogen is needed to maintain these functional states. Estrogen influences also the ciliogenesis in the fallopian tube of the Rhesus monkey where the cilia are shed during the luteal phase and regenerate during the follicular phase (*Brenner* 1969). The nature of the cytoplasmic granules in Brenner tumour cells is a very interesting question. Earlier they were considered degenerative products, probably lysosomal in nature (*Philipp & Overbeck* 1970, *Hameed* 1972 and *Langley et al.* 1972). The granules have membranes and are homogeneously electron opaque and thus distinctly different in ultrastructure from the mucous granules in the epithelial cells of the endocervical canal (*Philipp* 1972), the gastric mucosa of rat and man (*Yeomans* 1974 and *Nevalainen & Järvi* 1977) or the ovarian mucinous cystadenomas (*Klemi & Nevalainen* 1977). It was shown in the present study that the granules in the benign and borderline Brenner tumour cells were PAS-positive and diastase resistant and reacted homogeneously and strongly in the PASM treated sections which indicate the presence of 1.2 hydroxyl-groups. At the light microscopial level in the semithin sections they did not stain with the Grimelius stain and thus are not argyrophil-granules. In another study (*Klemi & Nevalainen* 1977) it was found that argyrophil-granules did not stain with the PAS-method in semithin Epon sections. In addition to these secretory granules the cell cytoplasm in both Brenner tumours contained some primary and large secondary lysosomes which result from the degenerative process in the cells.

There are many theories on the origin of the Brenner tumours. A granulosa cell-origin for Brenner tumours has been suggested e.g. (*Brenner* 1907) but in spite of such similarities as nuclear groovings, desmosomes and Call-exner bodies (*Bjersing* 1967) which sometimes resemble the cystic Brenner tumours, there are so many dissimilarities, that a granulosa cell-origin for Brenner tumours is unlikely (*Bransilver et al.* 1974).

A Walthard cell nests (WCN)-origin for Brenner tumours was first proposed by *Meyer* (1932) and later supported and thoroughly discussed by e.g. *Bransilver et al.* (1974). WCNs are solid or cystic cell populations in the ovarian cortex, mesovarium or hilus. They are very similar to the Brenner tumours both at the light and electron microscopic level. WCNs originate from the ovarian cortical epithelium and some Brenner tumours may originate from WCNs (*Bransilver et al.* 1974).

Rete ovary is the remnants of the mesonephric ducts and originate from the intermediate mesoderm by a somewhat different mechanism than the Muellerian duct but primarily both the Muellerian and mesonephric ducts are mesodermal in origin (*Warwick & Williams* 1973). The transitional epithelium of the urinary tract is of mesonephric derivation and thus the remnants of the mesonephric ducts have been suggested as the origin for Brenner tumours e.g. *Schiller* (1934). Rete ovary is located in the ovarian hilus and some Brenner tumours may originate from it, but this would not explain the origin of those Brenner tumours that are located cortically.

If the Brenner tumours originate from teratomas, there should be more often than presented also other teratomatous elements close to Brenner tumours. A cystic teratoma and 2 dermoid cysts have contained Brenner tumours (*Jondahl* 1950) and this has given rise to speculation about a teratomatous origin for Brenner tumours, there is not any further support for this theory. Some Brenner tumours contain argyrophil cells (*Klemi* 1977) which are also present in about 60 per cent of ovarian mucinous cystadenomas (*Klemi* 1977). The presence of argyrophil cells alone is not sufficient evidence for tera

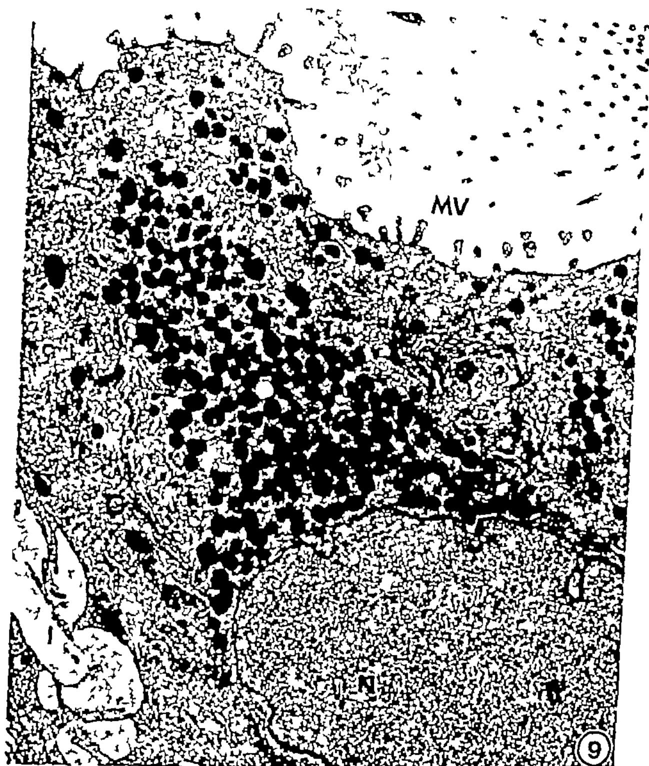


Fig 9 A higher magnification of part of figure 7 The apical cytoplasm of a nonciliated superficial cell contains abundant secretory granules in the vicinity of the Golgi cisternae (G) MV short microvilli projecting into the cyst lumen (I) lateral intercellular space (N) nucleus UA Pb Mag 15 050 ×

The cells lining the cystic cavities in the borderline Brenner tumours were either ciliated and nonsecreting or nonciliated and secreting Both types of cells are found in epithelia of Muellerian derivation such as in the fallopian tube endometrium and cervical canal (*Bloom & Fawcett* 1975) and in tumours derived from coelomic epithelium

Proliferation and ultrastructure of papillary transitional cell carcinoma of the human bladder Cancer (Philad.) 27: 71–82, 1971
12. Greene R. R. The diverse origins of Brenner tumours. Amer J Obstet. Gynec. 64 878–898, 1952.
13. Grimelius L. A silver nitrate stain for alfa-2 cells in human pancreatic islets. Acta Soc. Med. upsalien. 273 247–270, 1968.
14. Hallgrimsson, J & Scully R. Borderline and malignant Brenner tumours of the ovary. Acta path. microbiol. scand. Sect. A. 80 suppl. 233 56–66, 1972.
15. Hameed K. Brenner tumour of the ovary with Leydig cell hyperplasia. A histologic and ultrastructure study. Cancer (Philad.) 30 945–952, 1972.
16. Jondahl, W H., Dockerty M B. & Randall, L M. Brenner tumour of the ovary. A clinicopathological study of 31 cases. Amer J Obstet. Gynec. 60 160–167 1950
17. Klemi, P J. Epithelial mucosubstances and argyrophil cells in Brenner tumours. Acta path. microbiol. scand. Sect. A 85 819–825 1977
18. Klemi, P J. Epithelial mucosubstances and argyrophil cells in ovarian mucinous cystadenomas. In preparation, 1977
19. Klemi, P J & Nevalainen, T J. Ultrastructure of the mucinous ovarian cystadenomas. In preparation, 1977
20. Langley F A. Cummins P A & F H. An ultrastructural study of mucin secreting epithelia in ovarian neoplasms. Acta path. microbiol. scand. Sect. A. 80 suppl. 233 76–86, 1972.
21. Lauchlan S C. Histogenesis and histogenetic relationship of Brenner tumours. Cancer (Philad.) 19 1628–1634 1966.
22. von Limbeck, R. Zur Kenntniss der Epithelcysten der Harnblase und der Ureteren. Z. Heilk. 8 55–66 1887
23. Litwin J A. & Kasprzyk, J M. PAS reactions performed on semithin Epon sections following removal of the resin by NaOH in absolute ethanol. Acta histochem. (Jena) 55 98–103 1976.
24. Luft J H. Improvements in epoxy resin embedding methods. J biophys. biochem. Cytol 9 409–414 1961
25. Maddi, F V & Papanicolaou G N. Diagnostic significance of ciliated cells in human endometrial tissue cultures. Amer J Obstet. Gynec 82 99–101 1961
26. Merkow L. P. Slifkin H & Pardo M. Human ovarian neoplasms, light and electron microscopic correlations. I Brenner tumour. Obstet and Gynec 40 667–680, 1972.
27. Meyer R. Ueber verschiedene Erscheinungsformen der als Typus Brenner bekannten Eierstockgeschwulst, ihre Absonderung von den Granulosazell-tumoren und Zuordnung unter anderen Ovarialgeschwülste. Arch. Gynäk. 148 541–596, 1932.
28. Nevalainen T J & Järvi O H. Ultrastructure of intestinal and diffuse type gastric carcinomas. J Pathol. 122 129–137 1977
29. Nevalainen T J & Klemi P J. Improved periodic-acid-silver methenamine staining procedure for electron microscopy. Acta histochem. (Jena) 56 335–337 1976
30. von Numers C. Observations on metaplastic changes in the germinal epithelium of the ovary and on the etiology of ovarian endometriosis. Acta obstet. gynec. scand. 44 107–116, 1965
31. Philipp E. Über den granulofilamentären Umbau von Secretgranula im schleimbildenden Epithel der Endocervix der Frau. Z. Zellforsch 134 555–563 1972
32. Philipp E. & Overbeck L. Zur ultrastructur der Brenner Tumours. Z. Geburtsh. Gynaekol. 173 196–203 1970
33. Roth L. M. Fine structure of the Brenner tumor. Cancer (Philad.) 27 1482–1488, 1971
34. Roth L. M. & Sternberg W. H. Proliferating Brenner tumours. Cancer (Philad.) 27 687–693 1971
35. Sabatini D D., Bensch K & Barrnett R J. Cytochemistry and electron microscopy. The preservation of cellular ultrastructure and enzymatic activity by aldehyde fixation. J Cell Biol. 17 19–58, 1963
36. Schiller W. Zur Histogenese der Brennerschen Ovarialtumore. Arch. Gynäk. 157: 65–85 1934
37. Schueller E. F. Ciliated epithelia of the human uterine mucosa. Obstet. Gynec. 31 215–223 1968.
38. Serov S F., Scully R. E. & Sobin L. H. Histological typing of ovarian tumours. WHO Geneva, 1973
39. Silverberg S G. Brenner tumor of the ovary. Cancer (Philad.) 28 588–596 1971
40. Silverberg S G & Willson M S. Ultrastructure of the Brenner tumor. Amer J Obstet. Gynec. 112 91–100 1972
41. Tateishi R., Wada, A. Hayakawa, K., Hongo J. Ishii S & Terakawa, N. Argyrophil cell carcinomas (apudomas) of the uterine cervix. Light and electron microscopic observations of 5 cases. Virchows Arch. Abt. A 366 257–274 1975
42. Trump B F., Smuckler E. A. & Benditt E. P. A method for staining epoxy sections for light microscopy. J Ultrastruct. Res. 5 343–348, 1961
43. Warwick, R. & Williams P L. Gray's anatomy 35th ed. Longman group Ltd., Edinburg 1973 p. 183–186

tomatous origin because such cells are also present in the normal endocervical canal (*Tateishi et al* 1976)

The epithelium of Brenner tumours cannot be of stromal origin e g (*Greene* 1952) because between Brenner cells there are plenty of desmosomes, which are lacking between stromal cells but are very characteristic for epithelial cells. Also there is no continuity from the stromal cells to the Brenner cells on the contrary there are very clear basal lamina around the Brenner cell nests

The ovarian cortical epithelium which is of coelomic origin has an enormous potential to differentiate to serous, mucinous or endometrioid type of epithelium as shown e. g by *von Numers* (1965) and *Lauchlan* (1966) The theory that Brenner tumours originate from the epithelium of the ovarian cortex is based on the studies by *Arey* (1961) and later has been accepted generally

The following conclusions can be drawn from the foregoing observations The benign and borderline Brenner tumours have so many similarities that they must originate from the same type of cells. The borderline tumours may originate from its benign counterparts by cellular proliferation The Brenner cells are epithelial and thus they can not originate from stromal cells The epithelium of the Brenner tumours has many similarities to the epithelia of the tubular structures of Muellerian derivation and to the transitional epithelium The borderline Brenner tumour resemble the low grade papillary carcinoma of the transitional epithelium. Normally there are no transitional epithelium close to the ovary Rete ovary which is located in the ovarian hilus has some relationship to the transitional epithelium and could be a possible origin for Brenner tumours. The epithelium which covers the ovarian cortex and all structures close to the ovary is coelomic and originally mesodermal like the mesonephric ducts The latter give rise to the urinary tract and its transitional cell epithelium We can assume that the cells in the ovarian epithelium have preserved the ability to differentiate into serous, mucinous or endometrioid type i e. to cells of Muellerian derivation, but also have the ability to differentiate into transitional cell type. The Brenner tumours may originate directly from the epithelial cells of the ovarian cortex or from the cells of inclusion cysts, which are formed by invagination of the ovarian cortical epithelium. These observations support the theory previously presented by several authors e. g (*Arey* 1961 *Lauchlan* 1966, *Roth* 1971 *Silverberg* 1971, *Merkow et al.* 1972 *Silverberg & Willson* 1972 *Gummins et al* 1973 and *Bransilver et al* 1974) that Brenner tumours originate from the ovarian coelomic surface epithelium. This theory explains well the existence of Brenner tumours everywhere in the ovarian cortex.

REFERENCES

1 *Arey L. B* The origin and form of the Brenner tumour Amer J Obstet. Gynec. *81* 743–751 1961

2 *Battifora H., Eisenstein R & McDonald J M* The human urinary bladder mucosa. An electron microscope study Invest. Urol. *1* 354–361 1964

3 *Bjersing L.* On the ultrastructure of granulosa lutein cells in porcine corpus luteum. With special reference to endoplasmic reticulum and steroid hormone synthesis. Z. Zellforsch *82* 187–211 1967

4 *Bloom W & Fawcett D W* Textbook of histology W B Saunders comp 10 ed. Philadelphia, London, Toronto. *1975* p. *881–897*

5 *Bransilver B R Ferenczy A & Richart R M* Brenner tumour and Walthard cell nest Arch. Path. *98* 76–86 1974

6. *Brenner F* Das Oophoroma folliculare Frankf Z. Path. *1* 150–171 1907

7 *Brenner R M* Renewal of oviduct cilia during the menstrual cycle of the Rhesus monkey Fertil and Steril. *20* 599–611 1969

8. *von Brunn A* Ueber drusenahnliche Bildungen in der Schleimhaut des Nierenbeckens des Ureters and der Harnblase beim Menschen. Arch mikr Anat. *41* 294–302 1893

9 *Cummins P A Fox H & Langley F A* An ultrastructural study of the nature and origin of the Brenner tumour of the ovary J Pathol. *110* 167–176, 1973

10 *Fredricsson B & Björkman N* Morphologic alterations in the human oviduct epithelium induced by contraseptive steroids. Fertil. and Steril *24* 19 30 1973

11 *Fulker M J Cooper E H & Tanaka T*

Proliferation and ultrastructure of papillary transitional cell carcinoma of the human bladder Cancer (Philad.) 27 71–82, 1971
12. *Gr ene R R.*. The diverse origins of Brenner tumours. Amer J Obstet. Gynec 64 878–898, 1952.
13. *Grimelius L.* A silver nitrate stain for alfa 2 cells in human pancreatic islets. Acta Soc. Med. upsalien. 273 247 270 1968
14 *Hallgrimsson J & Scully R* Borderline and malignant Brenner tumours of the ovary Acta path microbiol scand. Sect. A. 80 suppl. 233 56–66 1972.
15. *Hameed K.* Brenner tumour of the ovary with Leydig cell hyperplasia. A histologic and ultrastructure study Cancer (Philad.) 30 945–952, 1972
16. *Jondahl W H Dockerty M B & Randall, L M* Brenner tumour of the ovary A clinicopathological study of 31 cases. Amer J Obstet. Gynec. 60 160–167 1950
17 *Klemi P J* Epithelial mucosubstances and argyrophil cells in Brenner tumours. Acta path. microbiol scand Sect. A. 85 819–825 1977
18 *Klemi, P J* Epithelial mucosubstances and argyrophil cells in ovarian mucinous cystadenomas In preparation. 1977
19 *Klemi, P J & N telainen T J* Ultrastructure of the mucinous ovarian cystadenomas. In preparation. 1977
20 *Langley F A., Cummins P A & F H* An ultrastructural study of mucin secreting epithelia in ovarian neoplasms. Acta path. microbiol scand Sect A 80 suppl. 233 76–86 1972
21 *Lee Hsu, S C* Histogenesis and histogenetic relationship of Brenner tumours Cancer (Philad.) 19 1628–1634 1966.
22 *en Limbe k R* Zur Kenntniss der Epithelcysten der Harnblase und der Ureteren, Z. Heilk 8 55–66 1887
23 *Litwin J A & Kasprzyk J M* PAS reaction performed on semithin Epon sections following removal of the resin by N OH in absolute ethanol Acta histochem. (Jena) 55 98–103 1976
24 *Luft J H* Improvements in epoxy resin embedding methods. J biophys. biochem. Cytol 9 409–414 1961
25 *Maddi F V & P panicolau G N* Diagnostic significance of ciliated cells in human endometrial tissue cultures Amer J Obstet Gynec 82 99–101 1961
26 *Markow L P Salazar H & Pardon M* Human ovarian neoplasms light and electron microscopic correlations. I Brenner tumour Obstet and Gynec. 40 667–680, 1972.
27 *Meyer R* Ueber verschiedene Erscheinungsformen der als Typus Brenner bekannten Eierstockgeschwulst, ihre Absonderung von den Granulosazell-tumoren und Zuordnung unter anderen Ovarialgeschwulste Arch. Gynäk. 148 541–596, 1932.
28. *Nevalainen T J & Järvi O H.* Ultrastructure of intestinal and diffuse type gastric carcinomas. J Pathol. 122 129–137 1977
29 *Nevalainen T J & Klemi P J.* Improved periodic-acid-all er methenamine staining procedure for electron microscopy Acta histochem. (Jena) 56 333 337 1976
30. *von Numers C.* Observations on metaplastic changes in the germinal epithelium of the ovary and on the etiology of ovarian endometriosis. Acta obstet. gynec. scand. 44 107–116 1965
31 *Philipp E.* Über den gran lofilamentaren Umbau on Secretgranula im schleimbildenden Epithel der Endocervix der Frau Z. Zellforsch 134 555–563 1972.
32 *Philipp E. & Ov beck L.* Zur ultrastructur der Brenner Tumours. Z. Geburtsh. Gynaekol. 173 196–203 1970.
33 *Roth L. M* Fine structure of the Brenner tumor Cancer (Philad.) 27 1482–1488, 1971
34 *Roth L. M & Sternberg W H.* Proliferating Brenner tumours. Cancer (Philad.) 27 687–693 1971
35 *Sabatini D D Bensch K & Barrnett R J* Cytochemistry and electron microscopy The preservation of cellular ultrastructur and enzymatic activity by aldehyde fixation. J Cell Biol 17 19–58, 1963
36. *S hiller W* Zur Histogenese der Brennerschen Ovarialtumore. Arch. Gynäk. 15 65–83 1934
37 *S hueller E. F.*. Ciliated epithelia of the human uterine mucosa. Obstet. Gynec. 31 215–223 1968.
38 *Serov S F Scully R. E. & Sobi L. H.*. Histological typing of ovarian tumours. WHO Geneva, 19 3
39. *Silverberg, S G* Brenner tumor of the ovary Cancer (Philad.) 28 588–596 1971
40 *Silverberg, S G & Wilson M S.*. Ultrastructure of the Brenner tumor Amer J Obstet. Gynec. 112 91 100 1972.
41 *Tateishi R Wada, A Hayakawa, K. Hongo J Ishu S & Terakawa N* Argyrophil cell carcinomas (apudomas) of the uterine cervix. Light and lectron microscopic observations of 5 cases. Virchows Arch. Abt. A 366 257– 4 1975.
42. *Trump B F Smuckler E A & Bendit E. P* A method for staining epoxy sections for light microscopy J Ultrastruct. Res. 5 343 348, 1961
43 *Warwick R. & William P L.* Gray's anatomy 35th ed., Longman group Ltd., Edinburg 1973 p. 183–186

44 *Watson M L.* Staining of tissue sections for electron microscopy with heavy metals. J biophys. biochem Cytol *4* 727–730 1958
45 *Venable J H & Coggeshall R* A simplified lead citrate stain for use in electron microscopy J Cell Biol *25* 407–408 1965
46 *Yeomans N D* Ultrastructural and cytochemical study of mucous granules in surface and crypt cells of rat gastric mucosa. Biol. Gastroenterol. *7* 285–290 1974

Acta path. microbiol. scand. Sect. A, 85: 839–849, 1977

THE EFFECT OF D-GALACTOSAMINE ON LCAT SECRETION AND ULTRASTRUCTURE OF ISOLATED RAT HEPATOCYTES

Grete Nordby, Berit Schreiner, Trond Berg and Kaare R. Norum

Institute for Nutrition Research, School of Medicine,
University of Oslo, Blindern, Oslo, Norway

Nordby, G., Schreiner, B., Berg, T. & Norum, K. R. The effect of D-galactosamine on LCAT secretion and ultrastructure of isolated rat hepatocytes. Acta path. microbiol. scand. Sect. A, 85: 839–849, 1977.

The effect of D-galactosamine on secretory activity and morphology of isolated rat hepatocytes was investigated. Galactosamine was found to reduce the secretion of lipoproteins (as indicated by the release of free cholesterol and triacylglycerol) as well as the secretion of lecithin: cholesterol acyltransferase (LCAT) and [14C]-labelled proteins from the isolated cells. The secretion of LCAT was inhibited much more than that of the other secretory products studied. Transmission electron microscopy revealed that galactosamine induced morphological changes in RER, mitochondria and nucleoli. The most striking feature of galactosamine-treated hepatocytes, however, was the appearance of swollen lysosomes. Some of these organelles measured up to 5 μm in diameter. Uridine did not abolish the effect of galactosamine upon the secretory activity of hepatocytes. The most conspicuous ultrastructural feature in cells that had been incubated with both uridine and galactosamine was the appearance of large amounts of glycogen. The possibility that galactosamine inhibits glycogenolysis is discussed. The rather selective effect of galactosamine on LCAT secretion suggests the use of this compound for the study of the interrelationship between LCAT and lipoprotein secretion.

Key words: D-galactosamine; hepatocytes; lecithin:cholesterol acyltransferase; ultrastructure.

Trond Berg, Institute for Nutrition Research, School of Medicine, University of Oslo, Blindern, Oslo 3, Norway

Received 27. ?. 77. Accepted 27. ?. 77.

Isolated rat hepatocytes are able to secrete lecithin: cholesterol acyltransferase (LCAT) at a rate which is comparable to that seen in in vivo studies (11). LCAT is associated with high density lipoproteins (HDL, α-lipoproteins) in the blood and is thought to play an important role in the metabolism of plasma lipoproteins by facilitating the exchange of unesterified cholesterol and cholesteryl esters between lipoproteins (5).

Little is known about the regulation of LCAT synthesis and secretion. Liver parenchymal cells in addition to LCAT also secrete lipoproteins (VLDL, HDL) and it is of interest to get information about the relationship between LCAT secretion and lipoprotein secretion. Isolated rat hepatocytes should provide a useful model for such studies, since the rate of secretion is more easily measured in an in vitro system than in experiments on living animals.

In rats, intraperitoneal injection of D galactosamine leads to a marked decrease in LCAT activity (6 13) D-galactosamine treatment also causes changes in plasma lipoproteins, including absence of HDl and presence of lipoproteins rich in phospholipids and unesterified cholesterol but deficient in cholesteryl esters (13) It has been suggested that all the lipoprotein changes could be due to LCAT deficiency (13)

D-galactosamine provides an experimental model with which to study the relationship between LCAT and lipoprotein secretion. The present report describes data on the effect of D-galactosamine on LCAT and lipoprotein secretion from isolated rat hepatocytes. The results of our electronmicroscopic studies on galactosamine treated rat hepatocytes are also given.

Several of the observed effects of galactosamine on the liver seem to be due to a hepatic UTP-deficiency (3) We therefore tried to find out whether the changes we observed in isolated rat hepatocytes could be reversed by the addition of uridine

MATERIALS AND METHODS

Chemicals

[7α-³H] Cholesterol specific activity 12.6 Ci/mmol and [U¹⁴C] protein hydrolysate were purchased from Radiochemical Center Amersham England The cholesterol was purified before use by thin layer chromatography on silica gel H (obtained from Merck, Darmstadt Germany) with petroleum ether/diethylether/acetic acid (85/15/3) in the developing system

Radioactivity was measured in a Packard Tri-Carb liquid scintillation pectrometer using either Permablend III or Diluene (both from Packard Instrument CO., Ill. USA) as liquid scintillator medium Counting fficiency was determined by the channels ratio method Essentially fatty acid free bovine serum album n prepared from fraction V collagenase Type 1 HEPES (N 2 hydroxethyl piperazine N 2 ethane ulfonic acid) galactosamine and ur din were obtained from Sigma Chemicals Co St Louis, Mo., USA.

Cholesterol b ochemical standard and mercaptoethanol were p r hased from British Drugstore Chemical Poole England Stigmasterol was obtained from Koch-Light Lab. Colnbrooke England

Preparation and Incubation of Rat Hepatocytes

Hepatocytes were prepared as described earlier (11) from male Wistar rats weighing 200-250 g. The animals were given ordinary lab chow and water ad libitum.

The hepatocytes (5×10^6 cells/ml) were incubated in 100 ml Erlenmeyer flasks in a shaking water bath at 37 C. The total volume of the cell suspension was 5–10 ml. The incubation medium contained per l 6 7 g NaCl 0 06 g NaH_2PO_4 $2H_2O$ 0 06 g K_2HPO_4 $2H_2O$ 0 4 g $CaCl_2$ $2H_2O$ 0 2 g $MgSO_4$ $7H_2O$ 0 4 g KCl, 10 g bovine serum albumin and 14.30 g HEPES. The osmolality of the incubation medium was 298 mOsm. pH was adjusted to 7.5 by the addition of NaOH In some experiments 25 per cent rat serum was added. The serum was heated before use at 59 C for one hour to inactivate the LCAT

The viability of the cells as judged by the trypan blue exclusion test was about 95 per cent throughout the incubations.

Protein Secretion

was measured with the following procedure

[U¹⁴C] protein hydrolysate was added to the incubation medium 500 µl samples of cell suspension were taken at different time intervals and cells and medium were separated by centrifugation (500 g for 5 min)

The proteins in the medium were precipitated with 10 per cent trichloracetic acid. The precipitate was washed three times with 5 per cent trichloracetic acid. The radioactivity in the precipitate was thereafter counted. Counting efficiency was the same in all the vials.

Biochemical Determinations

The activity of the secreted lecithin cholesterol acyltransferase (LCAT) was measured as described previously (4) Unesterified and total cholesterol was determined by gas liquid chromotography (4)

The glycerol of the triacylglycerol was determined according to the method of Wieland (23) and measured fluorimetrically

Electron Microscopy

The isolated hepatocytes were processed for electron microscopy either at the end of the cell purification procedure, after incubation for 3 h with or without galactosamine (2 mg/ml or 5 mg/ml) or after incubation for 3 h with uridine alone (30 mg/ml) or a mixture of uridine (30 mg/ml) and galactosamine (5 mg ml) Samples of control hepatocytes, i e cells incubated without galactosamine were also examined after 30 min, 1 h and 2 h.

The cells were fixed according to A borgh et al

(1) and embedded in Epon 812. Sections were stained with lead citrate or treated according to the periodic acid-thiosemicarbazide-silverproteinate (PA-TSC-Prot.) procedure for demonstration of glycogen (20) and examined in a Siemens Elmiskope 1 A electronmicroscope at 80 kV

RESULTS

Fig. 1 shows that the secretion of LCAT from isolated hepatocytes was almost completely blocked when galactosamine (5 mg/ml) was added to the incubation medium. The inhibitory effect was measurable after incubation of the hepatocytes for 30 min, but much more pronounced after incubation for 3 or 5 hours. The effect of galactosamine was not due to an influence upon the method for measuring the LCAT activity since the addition of galactosamine to the LCAT assay system did not lower the LCAT activity

The action of galactosamine on the secretion of lipoproteins from hepatocytes was studied by measuring free cholesterol, cholesteryl ester and triacylglycerol in media from cells incubated in the presence and absence of galactosamine. Fig. 2 shows that after about 3 hours of incubation there was a slightly lowered secretion of both free cholesterol and triacylglycerol when galactosamine was added to the incubation medium The amount of cholesteryl ester present in the incubation medium was—on the other hand—unaffected by the presence of galactosamine (data not given)

The addition of uridine to the incubation medium did not abolish the effect of galactosamine upon the secretion of LCAT and lipids from the hepatocytes (data not given) Galactosamine also inhibited the secretion of [^{14}C] labelled proteins from the hepatocytes (Fig 3) The secretion of labelled proteins, measured as acid-precipitable radioactive material, started in both galactosamine-treated and control cells about 20 min after the addition of [U ^{14}C] labelled protein hydrolysate After the initial lag phase, the secretion of labelled proteins became linear with time and remained linear for the

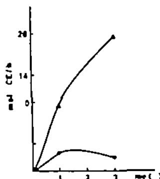


Fig 1 The effect of D-galactosamine on the secretion of LCAT from the hepatocytes.

Isolated rat hepatocytes (5×10^6 cells/ml) were incubated in presence of 5 mg galactosamine/ml. LCAT activity was measured in samples of the medium removed at different time intervals following the start of the incubation, and was calculated as LCAT activity (in nmoles cholesteryl ester/hr per liver) It was assumed that 1 g of liver contains 125×10^6 hepatocytes, and that the liver weight is 3.5 g/100 g of body weight.

Control △ Galactosamine 5 mg/ml 0.

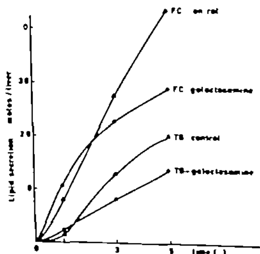


Fig 2 The effect of D-galactosamine on lipoprotein secretion. The concentrations of cholesterol and triacylglycerol were determined in samples from the medium from suspensions of rat hepatocytes (5×10^6 cells/ml) incubated in the presence and absence of D-galactosamine (5 mg/ml)

The amounts of lipids secreted by hepatocytes corresponding to whole liver (see legend to Fig 1) are presented as a function of time (in hrs.)

Cholesterol control △ cholesterol, galactosamine 0 triacylglycerol, control △ triacylglycerol, galactosamine 0

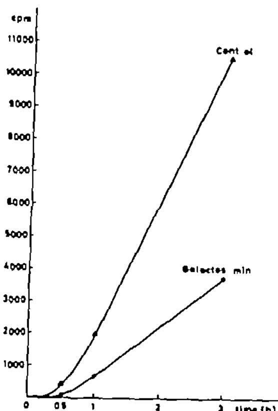


Fig 3 The effect of D galactosamine on the secretion of [^{14}C] labelled proteins. Hepatocytes (5×10^6 cells/ml) were incubated with [^{14}C] labelled amino acids in the medium in the absence (Δ) and presence (0) of 5 mg/ml of D-galactosamine in the medium Trichloracetic acid precipitable radioactivity was measured at different time-intervals following the start of the incubation (see Method section)

remainder of the experimental period (3 hours) The initial lag phase probably corresponds to the time needed for the synthesis and intracellular transport of secretory proteins in liver cells. Similar time intervals have been reported for this process earlier (17 21) Galactosamine (5 mg/ml) inhibited the secretion of labelled proteins to about the same extent as it inhibited the release of triacylglycerol and cholesterol 3 hours after the addition of [U^{14}C] labelled protein hydrolysate the control cells had secreted approximately three times as much labelled proteins as cells incubated in the presence of galactosamine. During the same period control cells had secreted at least 15 times more LCAT than the galactosamine-treated cells.

The viability of the hepatocytes measured as resistance to uptake of trypan blue, was unaffected by the addition of galactosamine. However, when examined in the light microscope the hepatocytes incubated with galactosamine seemed to be filled with vacuoles. This observation led us to undertake a more thorough histological study of the hepatocytes by using electron microscopy

Electron Microscopy

Control hepatocytes Freshly isolated hepatocytes showed the same general ultrastructure as liver cells *in situ* with occasional autophagic vacuoles and secondary lysosomes. Golgi cisternae and vesicles with lipoprotein (nascent VLDL) were frequently seen. Glycogen was present, dispersed in the cytoplasm or packed in larger masses or areas. After 30 min or 1 hour of incubation the picture was relatively unchanged as to autophagic vacuoles or lipoprotein-containing vesicles Little or no glycogen was found.

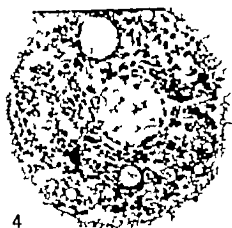
There was a marked increase in the number of autophagic vacuoles after 2 or 3 hours of incubation. The lipoprotein particles (VLDL) showed two types of appearance Some cells contained lipoprotein particles with a uniform and high degree of electron density In most of the cells, however the lipoprotein particles had an electron dense *membrane with a less electron dense content.* Vesicles with lipoprotein of either type were

Figs 4 and 5 Isolated hepatocytes incubated for 3 hrs at 37 C without (Fig. 4) and with (Fig 5) galactosamine (5 mg/ml) Note increase in number and size of secondary lysosomes in cell incubated with galactosamine. × 3000

Figs 6 and 7 Golgi saccules with lipoprotein (VLDL) in control hepatocytes incubated for 2 hrs. VLDL appear as particles that are highly electron dense (Fig 6) or less electron dense (Fig 7) × 48,000 and × 45,000

Fig 8 Higher magnification of Golgi apparatus with VLDL present in a control hepatocyte. × 66 000

Fig 9 Vesicles with VLDL present close to the cell surface of control hepatocyte. × 42,000




4

5




found pinching off from the Golgi apparatus as well as located close to the plasmalemma (Figs. 6–9). Some of the autophagic vacuoles contained remainders of lipoprotein particles. No glycogen was found. The mitochondria, rough endoplasmic reticulum (RER) and microvilli had a normal appearance. Usually a few large lipid droplets were seen.

Galactosamine-treated hepatocytes. a) *2 mg/ml.* There was an increasing amount of autophagic vacuoles and secondary lysosomes. The lysosomes had a dilated appearance. Distinct lipoprotein particles were not seen in the Golgi cisternae although vesicles with lipoprotein particles were common. Several of these vesicles, however, seemed to be in the process of being broken down (Fig. 10). Many of the cells contained concentric whorls of RER. The bulk of the mitochondria was localized around the nucleus, while the RER occupied the area close to the plasmalemma. The mitochondria were condensed with a dark matrix and expanded intracristal spaces. There were fewer microvilli than normal.

b) *5 mg/ml.* The amount and individual size of the secondary lysosomes were highly increased (cf. Figs. 4 and 5). Many lysosomes measured up to 3 μm in diameter. Their interior was relatively electron translucent containing cell debris (membranous elements from mitochondria, RER, etc. (see Fig. 11). Vesicles with a content which resembled lipoprotein were pinched off from the Golgi cisternae. These vesicles were often seen in close contact with, or seemed to coalesce with dilated or swollen lysosomes. The nucleus contained several nucleolar bodies which were predominantly composed of fibrillar material. There were few and short microvilli. Glycogen was found dispersed in the cytoplasm.

Uridine- and uridine/galactosamine-treated hepatocytes. The hepatocytes incubated with uridine in the medium showed a normal appearance with a relatively large amount of glycogen dispersed in the cytoplasm.

Cells which had been incubated in a mixture of uridine and galactosamine also had a conspicuous number of large secondary lysosomes. The most striking feature, however, was the presence of large areas or "lakes" with glycogen. There also appeared to be a distribution of organelles and inclusions in zones within the cytoplasm of the cells. Moving from the plasmalemma towards the nucleus there was first a zone filled with glycogen, free ribosomes and a few secondary lysosomes, then a zone which mainly consisted of RER, then a zone with mitochondria, glycogen accumulations and secondary lysosomes, and finally a perinuclear zone of RER (Fig. 12).

DISCUSSION

The effects of galactosamine seen on isolated rat liver cells in the present study are to some extent qualitatively comparable to those observed in *in vivo* studies. Thus, our finding that galactosamine depresses the rate of total protein secretion from hepatocytes is in agreement with the observation that treatment of rats with galactosamine leads to reduced synthesis of plasma proteins in general and glycoproteins in particular (3, 12). Such *in vivo* effects have been attributed to a hepatic action of galactosamine since this compound is selectively concentrated in the liver (3). Some of the ultrastructural changes seen in isolated hepatocytes have also been observed in *in vivo* studies, e.g. increased formation of autophagic vacuoles (8, 14), changes in the endoplasmic reticulum (8, 9, 14), dispersed and fragmented nucleoli (9). The use of isolated liver cells makes it possible, however, to quantitate the hepatic effects more precisely than in *in vivo* studies. The levels of plasma proteins of hepatic origin are determined not only by the rate of hepatic secretion but also by the rate of removal from the circulation. The reduced levels of plasma LCAT found in rats treated with galactosamine (6, 13) could for instance conceivably both be the result of an increased rate of removal and/or a decreased secretion of this enzyme. It is reasonable to assume that the catabolic component in the



Fig 10 Hepatocyte incubated with galactosamine (2 mg/ml) for 3 hrs. Several vesicles with VLDL are present. Some of the vesicles seem to be in the process of autolysis (arrowheads). Autophagic vacuole (AV) mitochondrion (M) peroxisomes (P) × 18,000.


LY
LY
11
12

turnover of secretory proteins is absent, at least initially in a system of isolated hepatocytes. Hence the use of isolated liver cells makes it possible to measure the effects of galactosamine on the initial rates of protein secretion without the concurrent interference of protein degradation. This is, for several reasons, difficult in an *in vivo* system.

Our data demonstrate clearly that the rate of secretion of active LCAT from isolated hepatocytes is decreased in the presence of galactosamine. The reduced secretion is seen very early after the addition of galactosamine. This might indicate that the effect of galactosamine is on LCAT activation, or LCAT secretion *per se* rather than on LCAT synthesis. Galactosamine inhibits protein synthesis (10) but this would not lead to an immediate effect on LCAT secretion, since we have shown that cycloheximide, which inhibits protein synthesis completely in hepatocytes, does not lead to reduced LCAT secretion until about 90 min after addition of the inhibitor (*Nordby* unpublished observations) It is known that galactosamine injected into rats reduces the levels of plasma glycoproteins (including LCAT) particularly effectively (3 12) This effect has been ascribed not only to reduced protein synthesis but also to an interference of galactosamine with glycosylations in the Golgi vesicles of the hepatocytes—possibly as a result of uridylate trapping in the form of uridine diphosphate hexosamines (3, 7) Although we cannot exclude the possibility that the effect of galactosamine on LCAT secretion is due to an action of this compound on the Golgi apparatus, we find it unlikely that such an effect should be spontaneous since it would take time to exhaust the intracellular pool of uridylate and the preformed intracellular LCAT "ready for export" Moreover we could not reverse the galactosamine effects on LCAT secretion by the addition of excess uridine

It is noticeable that lipoprotein secretion, as evidenced by cholesterol and triglyceride release is not reduced to the same extent as LCAT secretion early after the addition of galactosamine. If the *in vitro* effects of galactosamine apply to the *in vivo* situation, then the differential effects of galactosamine on LCAT and lipoprotein release suggest that an early consequence of galactosamine treatment would be a LCAT-deficient plasma with normal amounts of total lipids. Therefore, our data seem to support the contention that lipoprotein abnormalities observed in rats treated with galactosamine are secondary to LCAT deficiency (13)

A striking feature of galactosamine-treated hepatocytes was the appearance of dilated lysosomes Similar lysosomes have been seen in cells treated with ammonium chloride (16) or chloroquine (2) and may have been caused by the sequestration of osmotically active molecules (ammonium ions, chloroquine) within the lysosomes. The swollen lysosomes seen in the present study could have been formed by the selective uptake into these organelles of galactosamine or a metabolite (ammonium ions?) of galactosamine.

Our electron microscopic studies indicated that lipoprotein-containing vesicles seemed to fuse with lysosomes in galactosamine-treated hepatocytes. Furthermore, several of the lipoprotein-containing vesicles were in the process of being broken down. Earlier morphological studies have indeed suggested that a structural relationship can be established between VLDL-containing vesicles and lysosomes (19) and that lipoprotein-containing secretory granules may receive lysosomal hydrolases and thereby be broken down (12) A similar process (termed crinophagy) has been observed in other secretory organs (e. g the pituitary gland) where, under certain circumstances, hormone-containing secretory granules instead of being released from the

Fig. 11 Vesicles with lipoprotein (VLDL) (arrow) present in hepatocyte incubated for 3 hrs with galactosamine (5 mg/ml) Dilated secondary lysosomes (LY) are also present. × 36,000

Fig. 1 Part of hepatocyte incubated with galactosamine and uridine for 3 hrs. Note the large aggregates of glycogen present. Section treated with PA-TSC-Prot. × 18,000

cells are transported to the lysosomal apparatus and thereby degraded (18)

Ultrastructural studies revealed that hepatocytes treated simultaneously with both galactosamine and uridine appeared to have much more glycogen than cells treated with only one of these compounds or than freshly isolated control cells. This was unexpected since galactosamine is known to reduce glycogen synthesis, probably because the levels of UDP glucose are reduced secondary to uridylate-trapping Our seemingly paradoxical finding may however, be explained by a recent observation of *Wagle et al* (22) These investigators found that galactosamine not only inhibits glycogen formation by reducing UDP-glucose but also inhibits glycogenolysis in isolated rat hepatocytes possibly by inhibiting the production of glucose-1 phosphate from glycogen. Uridine added to hepatocytes increases the levels of UDP glucose and thereby makes available substrate for glycogen formation The net production of glycogen may be higher if galactosamine, which inhibits glycogenolysis, is present simultaneously It is well known that isolated hepatocytes in suspension normally have a high rate of glycogenolysis (15)

Galactosamine-treated rat hepatocytes may represent a useful model for the study of the interrelationships between LCAT secretion and lipoprotein-secretion. LCAT in plasma is bound to high density lipoproteins (HDL) It may be of particular interest to find out whether LCAT secretion is synchronized with the hepatic release of HDL or other lipoprotein-classes (e g VLDL) Treatment of hepatocytes with galactosamine is one means by which this may be done Further work, particularly on the characterization of lipoprotein classes and apolipoproteins is obviously needed to clarify the point.

The authors are grateful to *Margareta Nilsson* for excellent assistance. The work has been supported by the *Norwegian Council for Science and the Humanities.*

REFERENCES

1 *Arborgh B Bell P Brunk U & Collins V P* The osmotic effect of glutaraldehyde during fixation A transmission electron microscopy scanning electron microscopy and cytochemical study J Ultrastruct. Res. *56* 339-350 1976

2 *De Duve C De Barsy T Poole B Trouet A., Tulkens P & Van Hoof F* Lysosomotropic agents. Biochem. Pharmacol. *23* 2495-2531 1974

3 *Decker K & Keppler D* Galactosamine induced liver injury In *Popper H & Schaffner F* (Eds.) Progress in Liver Diseases, 1 ed., vol. 4 Grune & Stratton, Inc. 1972, p. 183–199

4 *Drevon C A & Norum K R.* Cholesterol esterification and lipids in plasma and liver from newborn and young guinea pigs raised on milk and non milk diet. Nutr Metabol *18* 137–151 1975

5 *Glomset J A & Norum K R* The metabolic role of lecithin cholesterol acyltransferase Perspectives from pathology In *Paoletti R & Kritchevsky D* (Eds.) Advances in Lipid Research 1 ed. vol. 11 Academic Press, New York and London 1973 p. 1–65.

6. *Kattermann R & Wolfrum D I* Cholesterin-stoffwechsel und lecithin-Cholesterin Acyltransferase im Plasma bei experimenteller Hepatitis und Cholestase an der Ratte Z Klin. Chem. *8* 413–419 1970

7 *Keppler D O R Pausch J & Decker K.* Selective uridine triphosphate deficiency induced by D-galactosamine in liver and reversed by pyrimidine nucleotide precursors. J biol. Chem. *249* 211–216, 1974

8 *Koff R S Gordon G & Sabesin S M* D galactosamine hepatitis. I Hepatocellular injury and fatty liver following a single dose Proc. Soc. Exp Biol. Med. *137* 696–701 1971

9 *Medline A Schaffner F & Popper H* Ultrastructural features in galactosamineinduced hepatitis. Exp Molec. Path *12* 201–211 1970

10 *Mosier D & Wagle S R* Study of protein synthesis in galactosamine hepatitis. Fed. Proc. *30* 1186 1971

11 *Nordby G Berg T Nilsson M & Norum K R* Secretion of Lecithin Cholesterol Acyltransferase from isolated rat hepatocytes. Biochim. Biophys. Acta *450* 69–77 1976

12 *Reutter W Keppler D Lesch R & Decker K* Zum Glycoproteidstoffwechsel bei der Galaktosamin-induzierten Hepatitis. Verh Deutsch. Ges. Med. *75* 363–365 1969

13 *Sabesin S M Kuiken L B & Ragland J B* Lipoprotein and lecithin cholesterol acyl-

transferase changes in galactosamine-induced rat liver injury Science 190 1302–1304 1975

14 Schaenke L, H S haffner F., Kepple D & Decker K. Ultrastructural studies of the effect of choline orotate on galactosamine induced hepatic injury in rats. Exp. Molec. Path 16 33–46, 1972.

15 Seglen P O Autoregulation of glycolysis, respiration, gluconeogenesis and glycogen synthesis in isolated rat liver parenchymal cells under aerobic and anaerobic conditions. Biochim. Biophys. Acta 338 317–336 1974

16 Seglen, P O & Reith A. Ammonia inhibition of protein degradation in isolated rat hepatocytes. Quantitative ultrastructural alterations in the lysosomal system. Exp. Cell. Res. 100 276–280 1976.

17 Seglen P O & Reith A Ammonia inhibits protein secretion in isolated rat hepatocytes. Biochim. Biophys. Acta 496 29–35 1977

18 Smith R. E. & Farquhar M G Lysosome function in the regulation of the secretory process in cells of the anterior pituitary gland. J. Cell. Biol 31 319–347 1966

19 Stäubli W & Hess R. Lipoprotein formation in the liver cell. Ultrastructural and functional aspects relevant to hypolipidemic action. In: Kritchevsky D (Ed.) Handbook of Experimental Pharmacology Hypolipidemic Agents, 1 ed. vol. 41 Springer Verlag, Berlin, Heidelberg, New York 1975 p. 229–289

20 Thiery J P. Mise en évidence des polysaccharides sur coupes fines en microscopie électronique. J Microscopie 6 987–1018, 1967

21 Van Bezooijen C F A., G ell, T & Knook D L. Albumin synthesis by liver parenchymal cells isolated from young, adult and old rats. Biochem. Biophys. Res. Comm. 71 513–519 1976

22. Wegle S R., Stermann R & Decker K. Studies on the inhibition of glycogenolysis by D-galactosamine in rat liver hepatocytes. Biochem. Biophys. Res. Comm. 71 622–628, 1976.

23. Wieland O Glycerol UV Method In Bergmeyer H U (Ed.) Methods of Enzymatic Analysis 2. ed. vol. 3 Academic Press, New York, 1974 p 1404–1409

Acta path microbiol scand Sect. A 85 850–858 1977

NASOPHARYNGEAL CANCER IN GREENLAND

The Incidence in an Arctic Eskimo Population

NILS HOJGAARD NIELSEN FLEMMING MIKKELSEN and JENS PEDER HART HANSEN

Department of Pathology Rigshospitalet Copenhagen, Ministry of Greenland, Copenhagen, and Department of Pathology Copenhagen County Hospital in Gentofte, Denmark

Nielsen, N Hojgaard, Mikkelsen, F & Hansen, J P Hart Nasopharyngeal cancer in Greenland The incidence in an Arctic Eskimo population. Acta path microbiol. scand. Sect. A, 85 850–858 1977

Nasopharyngeal cancer is very common among the Chinese in various parts of the world, particularly Southern China, and frequent in certain other Mongoloid groups in Southeast Asia. Also, the incidence among the Eskimos of the western Canadian Arctic and Alaska is considerably higher than would be expected This paper reports for the first time the incidence of nasopharyngeal cancer among native Greenlanders, an Eskimo population with some admixture of Caucasian blood. During 1955–1976 thirty five cases of nasopharyngeal cancer were diagnosed Ninety four per cent (33 cases) were squamous cell carcinomas, including lymphoepitheliomas. Incidence rates 1965–1976 age adjusted to the "world" population distribution, were 12.3 and 8.5 per 100 000 per annum for males and females respectively These rates are among the highest recorded in the world and significantly higher than among the Caucasian population in Denmark. Compared with other high risk populations nasopharyngeal cancer among Greenlanders had an older age distribution and a lower male to-female sex ratio An additional 11 cases with malignant involvement seemingly confined only to cervical lymph nodes, may have included some undiagnosed nasopharyngeal cancers. Thus the calculated incidence rates of this study could represent only minimum rates. Further research is needed especially with regard to the HL-A profile and to possible traces of Epstein Barr virus infection.

Key words Nasopharyngeal cancer Eskimo Greenland.

Nils Hojgaard Nielsen University Institute of Forensic Medicine, Frederik V's vej 11 DK 2100 Copenhagen Ø Denmark.

Received 26 v 77 Accepted 12 vi.77

Epidemiological studies have demonstrated an unusual ethnic and geographical distribution of nasopharyngeal cancer While rare in most areas including Europe and the U S this distinctive neoplasm occurs with exceptionally high incidence rates in Southern Chinese whether living in South China or elsewhere (*Muir* 1975) It is also well established that other Mongoloid populations in South East Asia such as Malays, Thais, Javanese and Vietnamese are populations-at risk (*Muir* 1971 1975) but the disease seems to be uncommon in North China (*Ho* 1972) and very rare in Japan (*Miyaji* 1967)

Recently a high relative frequency has been found in Eskimos of Northern Canada ethnically a Mongoloid population (*Schaefer et al* 1975 *Mallen & Shandro* 1974) This paper presents the occurence of nasopharyn

geal cancer in native Greenlanders, racially an Eskimo-caucasian mixture in the 22 year period 1955–1976.

Population and Medical Facilities

Greenland, formerly a Danish colony, aquired status as a more integrated part of the Kingdom of Denmark in 1953. Its population of native Greenlanders increased from 23,000 in 1955 to 35,000 in 1965 and reached 40,000 in 1975 (*Ministry of Greenland* 1976). The two sexes are equally represented. The native Greenland population is predominantly of Eskimo origin, although studies of genetic markers, such as blood groups and HL-A profiles, have revealed an average Caucasian admixture of 25–30 per cent (*Persson* 1970, *Kissmeyer-Nielsen et al.* 1971). The Danish population group amounted to 1 700 persons in 1955 and 8,000 in 1975 with a male predominance. Seventy-five per cent of the population reside in the 16 municipal towns which each has a small hospital. All medical service is free. Dronning Ingrids Hospital, established 1957 in Greenlands largest town, Godthåb, is the only hospital with a surgical department and a department of internal medicine. This referral center has no units for otorhinolaryngology or radiotherapy. However since 1954 otorhinolaryngologists from Denmark each summer visit most of the towns and settlements. A considerable proportion of patients with malignant diseases are transferred to referral centers in Denmark, mainly in Copenhagen.

MATERIAL AND METHODS

In the 22-year period under study nearly all patients with suspected or verified malignant disease were referred either to Dronning Ingrids Hospital or directly to Denmark. All files from Dronning Ingrids Hospital and from the municipal hospitals in Greenland were reviewed. Data, including diagnosis, concerning all patients transferred from Greenland to Denmark was obtained from the Ministry of Greenland in Copenhagen. Hospital records on [illegible] Greenland patients with suspected or proved malignancy from the referral centers in Denmark were reviewed. Files of all surgical biopsy specimens from Greenland in the 22-year period were examined and death certificates reviewed. Before 1967 death certificates were not required by law in Greenland but were nevertheless often made out when patients died in hospitals. After January 1 1967 certificates cover all deaths. Since malignant cases from Greenland have with some consistency been reported to the Danish Cancer Registry during the latter half of the period under study files from this registry were examined.

In addition to cases of nasopharyngeal cancer all patients with cervical lymph node metastases from unknown primaries and all cases of lymphomas in cervical lymph nodes were registered. Surgical biopsy specimens and records from these patients were reviewed.

All histological material from patients with cancer of the nasopharynx was examined and a reclassification made according to the criteria of *WHO* (*WHO et al.* 1971). Incidence rates, age adjusted to the "World standard population (*Doll et al.* 1970), were calculated for the two periods 1955–1964 and 1965–1976, based respectively on the 1960 census and on the census of December 31 1970. Rates are understood to be per 100,000 population per annum.

Age-specific incidence rates for nasopharyngeal cancer in Denmark 1968–1972 were supplied by the Danish Cancer Registry. By applying these rates to the Greenland population 1965–1976 the expected number of nasopharyngeal cancers thus obtained could be compared to the numbers actually observed.

Ninety f[illegible] per cent confidence limits for incidence rates were calculated according to Haenszel, Loveland & Sirken. A chi square test was used in order to evaluate the statistical significance of Observed/Expected ratios.

RESULTS

Thirty five cases of nasopharyngeal cancer were diagnosed in Greenland in the 22-year period 1955–1976 (Table 1), all occurring in the native population. No case was found in the small group of pure Caucasians (Danes). The youngest patient was 21 years old, the oldest 74, both males. All cases were histologically confirmed. In 27 patients the biopsies were taken from the primary tumor, in the remaining 8 cases from metastases in cervical lymph nodes only. These 8 cases combined, however, the rather characteristic histological picture of secondary nasopharyngeal carcinoma with convincing clinical and

TABLE 1 *Nasopharyngeal Cancer Greenland 1955–1976 Number of Cases by Age and Sex Crude Rate per 100,000 and Age Adjusted Rate (World Population) Ninety-five per Cent Confidence Limits in Parenthesis*

Age	1955–1964		1965–1976	
	M	F	M	F
20–24	–	–	1	–
25–29	–	–	–	–
30–34	1	–	–	–
35–39	–	–	–	–
40–44	1	1	1	1
45–49	2	–	1	1
50–54	–	1	2	3
55–59	1	–	3	1
60–64	–	–	2	1
65–69	–	–	2	3
70–74	–	–	2	1
75 +	–	–	1	–
	–	–	–	–
Total	5	2	15	13
Crude rate	3.0 (1 0–7 0)	1 2 (0 2–4.3)	6 4 (3 6–10 6)	5 6 (3 0–9.6)
Age adjusted rate	4 3 (1 4–10 0)	1 8 (0 2–6.5)	12 3 (6.9–20.3)	8.5 (4.5–14.5)

TABLE 2 *Nasopharyngeal Cancer in Greenland 1955–1976 Distribution by Histology*

	Number of cases	Per cent
Squamous cell carcinoma (high differentiated)	1	3
Squamous cell carcinoma (low differentiated)	32	91
Lymphoepitheliomas	20	57
Other low differentiated squamous cell carcinomas	12	34
Lymphomas	2	6
Total	35	100

radiological findings of tumor in the nasopharynx.

Thirty three cases (94 per cent) were found to be tumors of squamous epithelium, the majority (91 per cent) being low differentiated squamous cell carcinomas, including 20 lymphoepitheliomas (57 per cent) (Table 2) Two cases (6 per cent) were malignant lymphomas

Forty three per cent originated in the lateral walls of the nasopharynx including the fossa of Rosenmüller and the Eustachian cushion (Table 3) Thirty four per cent were located in the superoposterior wall and the rest either in the anterior part (6 per cent)

TABLE 3 *Cancer of the Nasopharynx Greenland 1955–1976 Localization in the Nasopharyngeal Region*

	Cases	Per cent
Right lateral wall	8	23
Left lateral wall	7	20
Posterior wall and roof	12	34
Anterior part		6
Diffuse	6	17
Total	35	100

TABLE 4 *Age-specific Incidence Rates for Nasopharyngeal Cancer i Greenland 1965–1976. Comparison with Rates from Denmark 1968 1972 (S pplied by the Danish Cancer R gistry) and with Rat s from Si gapore 1950–1961* (Muir & Shanmugaratnam 1967)

Age	Greenland		Denmark		Singapore			
					Chinese		Malay	
	M	F	M	F	M	F	M	F
10–14	–	–	0.2	0.2	0.2	0 7	–	–
15–19	–	–	0.2	0 2	2.4	0.3	–	1.9
20–24	6.1			0.2	6 1	2.3	–	–
25–29	–	–	–	–	7 4	5 0	1.8	–
30–34	–	–	0.2		18.3	8 0	4.3	–
35–39	7.9	6.1	0.7	0.3	32.3	12.6	2.5	3.7
40–44	8.9	8.5	0.7	0 7	45.4	17 7	1 9	5.3
45–49	27.5	32.2	0.9	0.5	40.2	17.6	5.0	6 4
50–54	45.4	15.0	0 9	0 3	52.8	19.8	13.3	13.9
55–59	39 1	16.1	1.8	0.4	46.2	12.0	19 1	13.9
60–64	50 7	56 3	1.8	0 7	41.8	11 4	8 0	9.3
65–69	67.2	25 4	3.2	0.5	30.5	9.2	15.0	–
70–74	49.3	–	3.2	1 2	} 10.5	6.2	–	–
75–79		–	3.3	2.1				
80+	–	–	1 0	1.0				
Crude rate all ages	6.4	5 6	0.8	0.3	13.2	5 1	2.0	1.3
Age adjusted to World pop.	12.3	8.5	0 6	0.3	17.0	6.2	3.2	2.7
Cases (observed)	15	13	92	46	839	309	23	14
Cases (expected)	0.78	0.46						
O/E ratio	19.2*	28 3**						

y) number of cases expected if age-specific incidence rates for Denmark 1968–1972 are applied to the Greenland population.

or diffusely spread (17 per cent) Twenty three of the 35 cases (66 per cent) were registered in the Danish Cancer Registry

In the two periods 1955–1964 and 1965–1976 age adjusted incidence rates for males were 4 3 and 1?.3 respectively and for fe males 1 8 and 8.5 (Table 1) Male-female ratio was 2.4 in 1955–1964 and 1 4 in 1965–1976 Age-specific incidence rates for males and females in the 12-year period 1965–1976 are given in Table 4 The rates are compared with rates from Denmark 1968–1972 and with minimum rates for Chinese and Malays in Singapore 1950–1961 Peak incidence for Greenland males was found in the age group 65–69 for females in the age group 60–64 with a lower peak from age 45–49

The numbers of nasopharyngeal cancers expected in Greenland 1965–1976 if age-specific incidence rates for Denmark 1968–1972 were applied to the Greenland popula tion are given in Table 4 O/E ratio was 19.2 for males and 28.3 for females ($P < 0.01$) cancer of the nasopharynx thus being significantly commoner in Greenland than in Denmark.

In addition to the 35 cases of nasopharyngeal cancer another 11 patients had malig nant involvement (lymphomas or low differ entiated, solid carcinomas) seemingly only of cervical lymph nodes (Table 5) In 6 of these patients the nasopharynx had not been examined and 4 patients died with symptoms of pharyngeal obstruction.

DISCUSSION

Histologically the commonest form of nasopharyngeal cancer is squamous cell carcinoma (*Shanmugaratnam* 1971) Ultrastruc

TABLE 1 *Nasopharyngeal Cancer Greenland 1955–1976 Number of Cases by Age and Sex Crude Rate per 100,000 and Age Adjusted Rate (World Population) Ninety-five per Cent Confidence Limits in Parenthesis*

Age	1955–1964		1965–1976	
	M	F	M	F
20–24	–	–	1	–
25–29	–	–	–	–
30–34	1	–	–	–
35–39	–	–	1	1
40–44	1	1	1	1
45–49	2	–	2	5
50–54	–	1	3	1
55–59	1	–	2	1
60–64	–	–	2	3
65–69	–	–	2	1
70–74	–	–	1	–
75+	–	–	–	–
Total	5	2	15	13
Crude rate	3.0 (1 0–7 0)	1.2 (0 2–4.3)	6 4 (3 6–10 6)	5 6 (3 0–9.6)
Age adjusted rate	4.3 (1 4–10 0)	1.8 (0 2–6.5)	12 3 (6 9–20.3)	8.5 (4.5–14.5)

TABLE 2 *Nasopharyngeal Cancer in Greenland 1955–1976 Distribution by Histology*

	Number of cases	Per cent
Squamous cell carcinoma (high differentiated)	1	3
Squamous cell carcinoma (low differentiated)	32	91
Lymphoepitheliomas	20	57
Other low differentiated squamous cell carcinomas	12	34
Lymphomas	2	6
Total	35	100

radiological findings of tumor in the nasopharynx.

Thirty three cases (94 per cent) were found to be tumors of squamous epithelium the majority (91 per cent) being low differentiated squamous cell carcinomas, including 20 lymphoepitheliomas (57 per cent) (Table 2) Two cases (6 per cent) were malignant lymphomas.

Forty three per cent originated in the lateral walls of the nasopharynx including the fossa of Rosenmuller and the Eustachian cushion (Table 3) Thirty four per cent were located in the superoposterior wall and the rest either in the anterior part (6 per cent)

TABLE 3 *Cancer of the Nasopharynx Greenland 1955–1976 Localisation in the Nasopharyngeal Region*

	Cases	Per cent
Right lateral wall	8	23
Left lateral wall	7	20
Posterior wall and roof	12	34
Anterior part	2	6
Diffuse	6	17
Total	35	100

rates for nasopharyngeal cancer are given in Table 6. Except in Singapore and Hong Kong calculated rates are often based on small numbers. In a survey of the age adjusted incidence of nasopharyngeal cancer from 67 different parts and population groups in the world (*Muir* 1971) only 29 rates for males and 14 rates for females were based on more than 10 cases. In most countries the disease is rare and age adjusted rates are below 1 per 100,000 per annum (*Doll et al.* 1970). Male:female ratio is usually over 2, the male preponderance being highest in the Chinese reports (*Clifford* 1970). Age specific rates for Chinese in Hong Kong and Singapore show a peak incidence for both sexes in the age group 50–54 following a rapid uninterrupted increase in incidence after age 20–24 (*Ho* 1972) (Table 4). In Denmark peak incidence occurs in older age groups (65–79) and rates are very low under the age of 35 (Table 4). In Sudan and Tunisia 15–20 per cent of patients with nasopharyngeal cancer have been reported under 20 years of age (El Hassan, quoted by *Muir* 1971, *Zaouche* 1970).

The above mentioned incidence and frequency patterns suggest environmental factor(s) working on genetically susceptible populations. The genetic predisposition may be represented by a specific HL-A profile as found in Chinese in Singapore (*Simons et al.* 1974), where case-control studies have demonstrated a significant elevation among the nasopharyngeal patients of the frequency of HL-A and a deficit of detectable second locus antigens. This deficit was filled in with the detection of a new second locus antigen, called SIN (*Simons et al.* 1975), associated with a high risk of nasopharyngeal cancer. No association between HL-A, and nasopharyngeal cancer has been found in Malays in Singapore or in Tunisians, and the deficit in the antigens of the second sublocus is less pronounced in Tunisian patients (*Betuel et al.* 1975). Genetic markers associated with risk of nasopharyngeal cancer may therefore differ in different populations. The basis most often proposed for an HL-A tumor association is that a disease susceptibility (immune response) allele at a neighbouring locus is in linkage disequilibrium with an HL-A allele (*Mc Devitt & Bodmer* 1974). These IR genes may play an important role in the association of nasopharyngeal carcinoma with the herpes virus of Epstein Barr EBV. This association is based on elevated antibodies against a variety of EBV coded antigens, on cell mediated immune reactions and on the regular presence of viral DNA and nuclear antigen, EBNA, in the epithelial tumor cells (*de-Thé* 1975). Although the virus has an oncogenic potential, transforming human lymphocytes B in vitro (*Pattengale et al.* 1974) and inducing lymphomas in marmosets in vivo (*Shope et al.* 1973), a causal relation between EBV infection and nasopharyngeal carcinoma is not established. The similarity of the immune response to EBV antigen in nasopharyngeal carcinoma patients regardless of race and geographical locality seems to indicate a specific role of this virus in the malignant development. EBV is however a ubiquitous lymphotrope virus, which could be naturally present in the nasopharyngeal mucosa and cause secondary infection in the tumor. It is in this respect interesting, that 66 per cent of Chinese in Singapore have converted to EBV positive by the age of five years (*Muir* 1976).

No other environmental carcinogen has been substantiated with any degree of certainty (*Mallen & Shandro* 1974, *Clifford* 1970, *Shanmugaratnam* 1971).

In the present study age adjusted incidence rates in the 12-year period 1965–1976 are 12.5 per 100,000 Greenland males and 8.5 per 100,000 Greenland females (Table 1). These rates are among the highest on record (Table 6) exceeded only by rates among Chinese in Hong Kong and Singapore and among Chinese males in California. Caution, however, must be exercised in the interpretation of results based on 28 cases in a 12 year observation period (Table 1), although the number of diagnosed cases per year was fairly constant.

In 1955–1964 age adjusted incidence rates

TABLE 5 *Greenland 1955–1976 Cases with Secondary Low Differentiated Solid Carcinoma in Cervical Lymph Nodes Primary Tumor Unknown (Group I)*

Cases with Lymphomas (Reticulosarcomas) in Cervical Lymph Nodes (Group II)

	Total	Nasopharynx examined	Radio-therapy	Dead with symptoms of pharyngeal obstruction	Dead. No information on final symptoms
Group I	7	2	2	4	2
Group II	4	3	3	–	4
Total	11	5	5	4	6

tural evidence of squamous differentiation is consistently found in the undifferentiated carcinomas including lymphoepithelioma transitional cell carcinoma and spindle cell carcinoma (*Svoboda et al* 1967) These different forms are therefore considered subtypes of squamous cell carcinoma by many pathologists (*Wahi et al* 1971) while others still regard lymphoepithelioma as a true entity to be preserved (*Michaud* 1975) In areas with high incidence of nasopharyngeal cancer nearly all cases are variants of squamous cell carcinoma (*Shanmugaratnam & Muir* 1967 *Yeh* 1967) whereas in low incidence areas 10–50 per cent are malignant lymphomas (*Godtfredsen* 1944 *Lederman* 1961 *Fletcher & Million* 1965 *Lewis* 1966 *Bertelsen et al* 1976)

Nasopharyngeal cancer is rare in most parts of the world except in China and in many parts of South East Asia inhabited largely by people of Mongoloid stock, who have had close relationship with Southern Chinese for many centuries. Emigrant Chinese are high risk population groups. In multiracial Singapore the age adjusted rates are highest for Chinese and lowest for Indians and Pakistanis, those for Malays being in between (*Muir & Shanmugaratnam* 1967 *Ho* 1972) In Hong Kong Chinese originating from the province of Kwantung in South China have the highest rates in the world (*Ho* 1972) Studies based mainly on the relative frequency of the nasopharyngeal cancer have demonstrated that the disease is common in other Mongoloid populations of South East Asia like the Thais (*Garnjana Coonchorn & Chantarakul* 1967) the Vietnamese (*Huong et al* 1969) the Javanese (*Djojopranoto & Soesilowati* 1967) and the Filipinos (*Pantangco et al* 1967) The neoplasm is reported to be rare in Japan (*Miyaji* 1967) but seems to be rather frequent in the various ethnic groups of Hawaii (Table 6), in the Arab populations of Tunisia (*Cammoun et al* 1971 *Zaouche* 1970) Algeria and Morocco (*Muir* 1975) in parts of Kenya (*Clifford* 1970) in certain tribes in Sudan and Uganda (*El Hassan et al* 1968, *Schmauz & Templeton* 1972) and in Alaskan natives including Eskimos (*Blot et al* 1975) In Israel immigrants from Africa and Asia have a higher risk than immigrants from Europe and the U S (*Muir* 1975) For Chinese born in the U S the risk of nasopharyngeal cancer is lower in the third generation than in the second, although still ten times higher than in Caucasians (*Buell* 1974)

Recent reports from Arctic Canada have pointed to a high relative frequency of nasopharyngeal cancer in the Eskimo population. *Mallen & Shandro* (1974) reported 8 cases from the western Arctic portion of Canada in a population of approximately 4,500 *Schaefer et al* (1975) found 18 histologically verified cases in the North West territories 1950–1974 which made nasopharyngeal cancer the most common malignant tumor among Eskimo males.

Some of the highest recorded incidence

rates for nasopharyngeal cancer are given in Table 6. Except in Singapore and Hong Kong calculated rates are often based on small numbers. In a survey of the age adjusted incidence of nasopharyngeal cancer from 67 different parts and population groups in the world (*Muir* 1971) only 29 rates for males and 14 rates for females were based on more than 10 cases. In most countries the disease is rare and age adjusted rates are below 1 per 100,000 per annum (*Doll et al.* 1970) Male:female ratio is usually over 2, the male preponderance being highest in the Chinese reports (*Clifford* 1970) Age-specific rates for Chinese in Hong Kong and Singapore show a peak incidence for both sexes in the age group 50–54 following a rapid uninterrupted increase in incidence after age 20–24 (*Ho* 1972) (Table 4) In Denmark peak incidence occurs in older age groups (65–79) and rates are very low under the age of 35 (Table 4) In Sudan and Tunisia 15–20 per cent of patients with nasopharyngeal cancer have been reported under 20 years of age (El Hassan, quoted by *Muir* 1971 *Zaouche* 1970)

The above mentioned incidence and frequency patterns suggest environmental factor(s) working on genetically susceptible populations. The genetic predisposition may be represented by a specific HL-A profile as found in Chinese in Singapore (*Simons et al.* 1974) where case-control studies have demonstrated a significant elevation among the nasopharyngeal patients of the frequency of $HL\text{-}A_2$ and a deficit of detectable second locus antigens This deficit was filled in with the detection of a new second locus antigen called SIN_2 (*Simons et al.* 1975) associated with a high risk of nasopharyngeal cancer No association between $HL\text{-}A_2$ and nasopharyngeal cancer has been found in Malays in Singapore or in Tunisians, and the deficit in the antigens of the second sublocus is less pronounced in Tunisian patients (*Betuel et al.* 1975) Genetic markers associated with risk of nasopharyngeal cancer may therefore differ in different populations. The basis most often proposed for an HL-A tumor association is that a disease susceptibility (immune response) allele at a neighbouring locus is in linkage disequilibrium with an HL-A allele (*Mc Devitt & Bodmer* 1974) These IR genes may play an important role in the association of nasopharyngeal carcinoma with the herpes virus of Epstein-Barr EBV This association is based on elevated antibodies against a variety of EBV coded antigens, on cell mediated immune reactions and on the regular presence of viral DNA and nuclear antigen, EBNA in the epithelial tumor cells (*de Thé* 1975) Although the virus has an oncogenic potential, transforming human lymphocytes B in vitro (*Pattengale et al.* 1974) and inducing lymphomas in marmosets in vivo (*Shope et al* 1973) a causal relation between EBV infection and nasopharyngeal carcinoma is not established. The similarity of the immune response to EBV antigen in nasopharyngeal carcinoma patients regardless of race and geographical locality seems to indicate a specific role of this virus in the malignant development. EBV is however a ubiquitous lymphotrope virus, which could be naturally present in the nasopharyngeal mucosa and cause secondary infection in the tumor It is in this respect interesting, that 66 per cent of Chinese in Singapore have converted to EBV positive by the age of five years (*Muir* 1976)

No other environmental carcinogen has been substantiated with any degree of certainty (*Mallen & Shandro* 1974 *Clifford* 1970, *Shanmugaratnam* 1971)

In the present study age adjusted incidence rates in the 12 year period 1965–1976 are 12.3 per 100,000 Greenland males and 8.5 per 100,000 Greenland females (Table 1) These rates are among the highest on record (Table 6) exceeded only by rates among Chinese in Hong Kong and Singapore and among Chinese males in California. Caution, however must be exercised in the interpretation of results based on 28 cases in a 12 year observation period (Table 1) although the number of diagnosed cases per year was fairly constant.

In 1955–1964 age adjusted incidence rates

TABLE 6 *Incidence Rates for Nasopharynx Cancer in High Risk Populations Age Adjusted to World Standard Population*

	Period	Number of cases		Rates		Reference
		M	F	M	F	
Hong Kong	1965–1969	1980	875	24.7	10.4	*Ho* 1972
Singapore Chinese	1960–1964	442	202	20.2	9.0	*Muir* 1971
California Chinese	1960–1964	5	1	12.4	5.4	*Muir* 1971
Greenland Eskimos	1965–1976	15	13	12.3	8.3	
Hawaii Chinese	1960–1964	12	5	10.4	4.6	*Doll et al.* 1970
Hawaii Hawaiian	1960–1964	7	1	7.8	0.7	*Doll et al.* 1970
Singapore Malays	1950–1961	23	14	3.2	2.7	*Muir and Shanmugaratnam* 1967
Hawaii Filipino	1960–1964	8	0	3.1	–	*Doll et al.* 1970
Israelis born in Africa and Asia	1960–1966	38	23	1.8	1.0	*Doll et al.* 1970

for Greenland males (4.3 per 100 000) and females (1.8 per 100 000) are based on only 5 + 2 cases (Table 1) thus making a comparison of the incidence in the two periods 1955–1964 and 1965–1976 less valid. Moreover calculated rates for both periods may only represent minimum incidence rates, as illustrated in Table 5. It is well known that cancer of the nasopharynx, especially lymphoepithelioma can manifest itself by large metastatic deposits in the cervical lymph nodes, with a primary tumor of only pin head size easily overlooked (*de Thé* 1975). Subsequent radiotherapy may obscure the diagnosis, and some of the cases in Table 5 may well have been secondary cancer of nasopharyngeal origin. Further, in a study of parotid gland tumors in Greenlanders (*Nielsen et al.*) metastatic deposits in intraparotid lymph nodes from a primary undetected nasopharyngeal carcinoma could not always be excluded.

These possible sources of bias also necessitate some caution in the interpretation of the particular age and sex distribution in this study which appear to be influenced by the substantial Caucasian genetic material in the Greenland population. Nasopharyngeal cancer in Greenlanders, as in Caucasians, seems to occur in older age groups than among the Chinese. The male preponderance is less pronounced than in most other series, very different from the high male:female ratio (8:1) reported among Canadian Eskimos (*Schaefer et al.* 1975) but more in accordance with findings in Denmark (Table 4).

The epithelial origin in 94 per cent of nasopharyngeal tumors in the present study (Table 2) is consistent with the general pattern in other high-risk populations. The localization of the tumors in the nasopharyngeal region (Table 3) is in agreement with general findings (*Shanmugaratnam* 1971).

The association between genetic factors, a herpes virus and a human tumor makes nasopharyngeal carcinoma a unique model in human cancer research. This study has demonstrated a high risk of nasopharyngeal carcinoma in native Greenlanders. Further studies are necessary to elucidate whether Greenlanders with the neoplasm have the same HL-A profile as Chinese patients in Singapore and/or a profile markedly different from Greenlanders not having the disease. Determination of the serological EBV profile in patients and non patients is equally important. A possible role of other exogenous factors of nutritional, endocrine or thermal character should be investigated. If the cold Arctic climate causes metaplastic changes in the nasopharyngeal mucosa, this could prove to be an important carcinogenic co-factor.

In view of the significance of lymphocytes in immunological response it might be interesting to have further studies into the share

of lymphoepitheliomas in nasopharyngeal carcinomas in various environments.

CONCLUSION

The incidence of nasopharyngeal cancer in native Greenlanders is, for both sexes, significantly higher than in Denmark and, although based on small numbers, among the highest in the world. Nearly all neoplasms are of epithelial origin. Further studies, especially regarding HL-A profile and serological EBV profile would be of importance

REFERENCES

1. *Bertelsen K, Andersen A P, Elb and O & Lund, C.* Cancer rhinopharyngis. Ugeskr Læg. *138* 3342–3347 1976.
2. *Betuel H, Camoun, M., Colombani, J., Day N E, Ellouz R. & de-Thé G.* The relationship between nasopharyngeal carcinoma and the HL-A system among Tunisians. Int. J Cancer *16* 249–254 1975
3. *Blot W J, Lanier A, Fraumeni J F & Bender T R.* Cancer mortality among Alaskan natives, 1960–1969. J nat. Cancer Inst. *55* 547 554 1975.
4. *Buell, P.* The effect of migration on the risk of nasopharyngeal cancer among Chinese. Cancer Res *34* 1189–1191 1974
5. *Cammoun M, Vogt-Hoerner G & Mourali N.* Les tumeurs du naso-pharynx en Tunisie. Étude anatomo-clinique de 143 observations. Tunis méd *49* 131 141 1971
6. *Clifford P.* On the epidemiology of nasopharyngeal carcinoma. Int. J Cancer 5 287 309 1970
7. *de-Thé G.* Facteurs immuno-virologiques dans les épithéliomas d rhinopharynx. Bull Cancer 62 265–276 1975
8. *Djojopranoto M & Soesilowati.* Nasopharynx cancer in East Java (Indonesia). In *Muir C S & Shanmugaratnam K* (Eds.) Cancer of the nasopharynx. UICC Monograph Series, 1st ed. vol. 1 Munksgaard Copenhagen 1967 pp 43–46
9. *Doll R, Muir C S & Waterhouse J A H.* Cancer incidence in five continents Vol. 2. Springer Verlag Berlin 1970
10. *El Hassan A M, Milosev B., Daoud E H & Kerkam A.* Malignant disease of the upper respiratory tract in Sudan. In *Clifford P, Linsell C A & Timms G L.* (Eds.) Cancer in Africa, 1st ed. East African Publishing House Nairobi 1968 pp. 307–314
11. *Fletcher G H & Million R. R.:* Malignant tumors of the nasopharynx. Amer J Roentgenol. *93:* 44 55 1965
12. *Garnjana-Goonchorn S & Chantrakul V.:* Nasopharyngeal cancer at Siriraj Hospital Dhonburi, Thailand. In *Muir C S & Shanmugaratnam K* (Eds.) Cancer of the nasopharynx. UICC Monograph Series, 1st ed. vol. 1 Munksgaard, Copenhagen 1967 pp 33–37
13. *Godtfredsen E.:* Ophthalmologic and neurologic symptoms at malignant nasopharyngeal tumors: clinical study comprising 454 cases, with special reference to histopathology and possibility of earlier recognition. Acta psychiat. Suppl. *34* 1–323 1944
14. *Ho J H C.* Nasopharyngeal carcinoma (NPC). Advanc. Cancer Res. *15* 57–92, 1972
15. *Hoang, B. Q., Bui-Joi, V P., Duong P N, Ta N H & Hoang D D.* Les cancers du nasopharynx au Vietnam. Epidemiologie aspects cliniques, facteurs étiologiques possibles. Ann. Oto-laryng (Paris) *86* 267–278 1969
16. *Kissmeyer-Nielsen F., Andersen, H., Hauge M, Kjerbye K E., Mogensen B. & Svejgaard A.* HL-A types in Danish Eskimos from Greenland. Tissue Antigens *1* 74–80 1971
17. *Lederman H.* Cancer of the nasopharynx. Its natural history and treatment. Thomas, Springfield Illinois 1961 p. 62.
18. *Lewis J S.* Cancer of the nasopharynx. Trans. Pacif Cst. oto-ophthal Soc. 47 69–75 1966
19. *Mallen R W & Shandro W G.* Nasopharyngeal carcinoma in Eskimos. Canad. J Otolaryng. *3* 175–179 1974
20. *McDevitt H O & Bodmer W F.* HL-A, immune response genes, and disease. Lancet *1* 1269–1275 1974
21. *Micheau C.* Anatomie pathologique et essai de classification des épithéliomas du nasopharynx. Bull. Cancer *62* 277–286 1975
22. *Ministry of Greenland.* Greenland 1975 Annual report. Copenhagen 1976, p. 19
23. *Miyaji T.* Carcinoma of the nasopharynx and related organs in Japan based on mortality morbidity and autopsy studies. In *Muir C S & Shanmugaratnam K* (Eds.): Cancer of the nasopharynx. UICC Monograph Series, 1st ed. vol. 1 Munksgaard, Copenhagen 1967 pp. 29–32
24. *Muir C S & Shanmugaratnam K.* The incidence of nasopharyngeal cancer in Singapore. In *Muir C S & Shanmugaratnam K* (Eds.) Cancer of the nasopharynx. UICC Monograph Series, 1st ed. vol. 1 Munksgaard, Copenhagen 1967 pp. 47–53
25. *Muir C S.* Nasopharyngeal carcinoma in

non Chinese populations with special reference to South East Asia and Africa. Int. J Cancer *8* 351–363 1971

26 *Muir C S* L epidemiologie du cancer du cavum, Bull Cancer *62* 251–264 1975

27 *Muir C S* Personal communication, 1976.

28 *Nielsen N H Mikkelsen F & Hansen J P H* Salivary gland tumors in Greenland. In preparation

29 *Pantangco E E. Basa G F & Canlas M* A survey of nasopharyngeal cancers among Filipines. A review of 203 cases. In *Muir C S & Shanmugaratnam K* (Eds) Cancer of the nasopharynx. UICC Monograph Series, 1st ed vol 1 Munksgaard, Copenhagen 1967 pp 38–42

30 *Pattengale P K Smith R W & Gerber P* B-cells characteristics of human peripheral and cord blood lymphocytes transformed by Epstein Barr virus J nat Cancer Inst. *53* 1031–1086 1974

31 *Persson I* Anthropological investigations of the population of Greenland. Medd Gronland *180* 21–49 1970

32 *Schaefer J Hildes J A Medd L M & Cameron D G* The changing pattern of neoplastic disease in Canadian Eskimos. Canad med Ass. J *112* 1399–1404 1975

33 *Schmaus R & Templeton A C* Nasopharyngeal cancer in Uganda Cancer (Philad) *29* 610–621 1972.

34 *Shanmugaratnam K & Muir C S* Nasopharyngeal carcinoma origin and structure. In *Muir C S & Shanmugaratnam K* (Eds) Cancer of the nasopharynx. UICC Monograph Series, 1st ed vol 1 Munksgaard Copenhagen 1967 pp 153–162

35 *Shanmugaratnam K* Studies on the etiology of nasopharyngeal carcinoma. In *Richter G W & Epstein M A* (Eds) International review of experimental pathology 1st ed. vol. 10 Academic Press, New York and London *1971 pp 361–413*

36 *Shope T., Dechairo D & Miller G* Malignant lymphoma in cottontop marmosets after inoculation with Epstein-Barr virus. Proc. nat. Acad Sci. (Wash) *70* 2487–2491 1973

37 *Simons M J Wee G B. Day N E de Thé G Morris J P & Shanmugaratnam K.* Immuno-genetic aspects of nasopharyngeal carcinoma I Differences in HL-A antigen profiles between patients and comparison groups. Int J Cancer *13* 122–134 1974

38 *Simons M J Wee G B Day N E, Chan, S H Shanmugaratnam K & de-Thé G B.* Immuno-genetic aspects of nasopharyngeal carcinoma (NPC) IV Probable identification of an HL-A second-locus antigen associated with a high risk of nasopharyngeal carcinoma Lancet *I* 142–143 1975

39 *Svoboda D Kirchner F & Shanmugaratnam K* The fine structure of nasopharyngeal carcinomas. In *Muir C S & Shanmugaratnam K* (Eds.) Cancer of the nasopharynx UICC Monograph Series, 1st ed. vol. 1 Munksgaard, Copenhagen 1967 pp 163–171

40 *Wahi P N., Cohen B. Luthra U K & Torloni J* Histological typing of oral and oropharyngeal tumors. International histological classification of tumors. 1st ed. Vol 4 World Health Organization, Geneva 1971 pp. 23–24

41 *Yeh S* Histology of nasopharyngeal cancer In *Muir C S & Shanmugaratnam K* (Eds.) Cancer of the nasopharynx. UICC Monograph Series, 1st ed. vol 1 Munksgaard, Copenhagen 1967 pp. *147–152.*

42 *Zaouche A* Les tumeurs malignes de la sphère ORL en Tunisie. (A propos de 644 tumeurs de voies aéro-digestives supérieures observées a l'Institut National de Carcinologie de Tunis du 1 10-67 au 15-8-69) Thèse Faculté de Médecine Paris 1970

Acta path. microbiol. scand. Sect. A, 85: 859–863 1977

A MALIGNANT *BRENNER* TUMOUR OF THE OVARY WITH SUBCUTANEOUS METASTASES

HENNING BECK, DENNIS RAAHAVE and POUL BOESEN

Institute of Pathological Anatomy, Kommunehospitalet, Copenhagen, and Surgical Department, Sct. Josephs Hospital, Copenhagen

Beck, H., Raahave, D. & Boesen, P. A malignant *Brenner* tumour of the ovary with subcutaneous metastases. Acta path. microbiol. scand. Sect. A 85: 859–863, 1977.

The rare, malignant *Brenner* tumour of the ovary was removed in a 67-year old woman. The tumour was of the epidermoid-transitional-cell type and is in particular remarkable because subcutaneous metastases occurred.

Key words: *Brenner* tumour; subcutaneous metastases; ovary.

Dennis Raahave, Anemonevej 24, 2970 Hørsholm, Denmark.

Received 1.x.77 Accepted 1. .77

The ovarian *Brenner* tumour is almost exclusively benign, but a malignant form is being increasingly reported. The diagnostic criteria for this form, however, have varied since its first description in 1945 (*Von Numers* 1945, *Novak & Woodruff* 1967, *Roth & Sternberg* 1971, *Helgrimsson & Scully* 1972) and recently the diagnostic criteria have been tightened (*Hull & Campbell* 1973). We report a case with subcutaneous metastases.

CASE REPORT

History. A 67-year old woman was admitted with acute urinary retention. The patient had been operated on for duodenal ulcer 4 years previously and a hard tumour of the size of a coconut was felt in the female pelvis and taken for a uterine fibroma. During the last 3 years she had lost 17 kg in weight.

Physical examination. Her general condition and nutritional state were poor. Gynecological and rectal exploration revealed that a hard and bulging tumour mass occupied the pelvis, not allowing the internal genitalia to be differentiated.

Laboratory investigations. Blood pressure was 130/170 mm Hg, pulse rate 80/min, temperature 36.9 °C and weight 33.0 kg. Haemoglobin was 6.8 mmol/l (reference 7.0–10.0), ESR 38 mm/h (reference 2–20), serum bilirubin 10 µmol/l (reference 5—17), serum creatinine 45 µmol/l (reference 50–120), serum protein 67 g/l (reference 60–80) and microscopy of the urinary specimen revealed 35–40 leucocytes and 0–1 erythrocytes.

An abdominal roentgenogram showed a soft tissue shadow localized to the minor pelvis, containing calcifications (*Fig. 1*). Intravenous urography showed the right ureter dilated up to the renal pelvis and the bladder irregularly shaped, especially on the right side. A specimen of the uterine mucosa was normal, the uterine cavity measuring 7 cm.

Surgical findings and procedure. A right-sided partly twisted ovarian tumour occupied the whole pelvis. There was no ascites and the uterus, adnexa and left ovary were normal. The iliac or para-aortic lymphnodes were not enlarged and the liver and alimentary tract were without pathological changes, except for a single nodular lesion in the mesentery. Frozen section microscopy of the tumour was characteristic of a malignant *Brenner* tumour. The tumour was removed together with the adnexa, uterus, left ovary and the nodular mesenterial lesion.

Course. The immediate postoperative course was uncomplicated. At the 20th and 70th postoperative



Fig 1 A roentgenogram of the abdomen showing a soft tissue shadow in the minor pelvis, containing calcifications.

day respectively subcutaneous lesions were removed from the inner and outer aspect of the left thigh, approximately 10 cm below Poupart's ligament.

The patient was re-admitted with subcutaneous metastases (left thigh and inguinal region and right lumbar region) These tumours were resected but the patient expired 15 days after re-admission.

PATHOLOGY

Gross appearance The operation specimens consisted of a right-sided ovarian tumour (Fig 2) apparently encapsulated, measuring 13–14 cm, with an irregular and lobulated surface which was smooth and shiny Cut sections showed alternating hard and soft areas changing from greyish to yellowish. Small calcifications were present in a few areas, but no cyst The left ovarian tube and ovary were normal while the uterus contained small intramural fibroids. Biopsies from the peritoneum and the small intestinal mesentery were also examined together with the subcutaneous nodules

Microscopic appearance The ovarian tumour revealed a very variegated histological picture In some areas a dense fibrous stroma was found with islands of epithelial cells, occasionally with central cystic areas containing cell debris, all of this being characteristic of a benign *Brenner* tumour In other areas there was a gradual transition to more pleomorphic epithelial components with darker staining cells and more nuclear irregularity (Fig 3) In most areas, however including the associated capsule the picture was extremely pleomorphic. The fibrous stroma was greatly reduced and the epithelial components showed an admixture of transitional and epidermoid features, mostly dom-

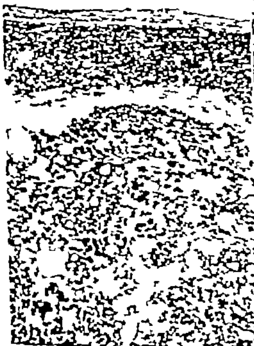
Fig 2 Ovarian *Brenner* tumour with malignant and benign areas

Fig 3 Photomicrograph of part of *Brenner* tumour with transition from typical benign elements to more pleomorphic epithelial structures.

Fig 4 Photomicrograph of subcapsular malignant component with great cellular pleomorphism.

Fig 5 Photomicrograph of metastatic tumour tissue (thigh) showing the same great pleomorphism as in the primary *Brenner* tumour


2




inated by the latter occasionally with mononuclear keratinization but without epithelial pearl formation Furthermore many giant cells occurred and many abnormal configurations were found among the abundant mitoses (Fig. 4) The picture was characteristic of a malignant *Brenner* tumour

The subcutaneous nodules (Fig 5) contained metastatic tumour tissue of the malignant *Brenner* type as did the peritoneal and mesenterial biopsies

Autopsy-findings There was no local ovarian tumour growth but an intraabdominal spread to para aortical lympnodes together with subcutaneous metastases. The histological pattern of the lymphnodes was the same as for the primary tumour

DISCUSSION

The criteria used for the diagnosis of the malignant *Brenner* tumour has been debated for many years. The common finding of the *Brenner* tumour with other tumours in the ovary has obviously led to the diagnosis of a malignant *Brenner* tumour in cases of malignancy of these associated tumours. *Idelson* (1963) and *Novak* & *Woodruff* (1967) excluded these tumours, and the latter accepted a division into an adenocarcinomatous type a mixed type and an epidermoid type In recent years, however the malignant *Brenner* tumour appears as a transitional-cell or as an epidermoid-cell carcinoma. A group of proliferative *Brenner* tumours (*Roth* & *Sternberg* 1971) or *Brenner* tumours of borderline malignancy (*Halgrimsson* & *Scully* 1972) have been separated characterized by cellular dedifferentation with lack of stromal invasion and with a clinical benign course This subdivision has been accepted and included in *WHO s* international classification (1973)

In the present case the appearance of a typical benign *Brenner tumour* with transition to malignant tissue of transitional-cell and epidermoid-cell type together with subcutaneous metastases presenting the same microscopic picture as the malignant part of the ovarian tumour favours the diagnosis of a malignant *Brenner* tumour this is in line with the diagnostic criteria of *Hull* & *Campbell* (1973) all the more since no cystadenoma was seen in any part of the tumour

As mentioned by *Teilum* (1971) the *Brenner* tumour can be developed from a variety of ovarian components, while other investigators assume the tumour to originate from mesonephrogenic remnants or by uroepithelial metaplasia from the coelomic epithelium or from the rete ovarii (*Greene* 1952 *Stohr* 1956 *Ehrlich* & *Roth* 1971 *Fox et al.* 1972) In our case, no morphologic features were found which could contribute to one histogenetic theory or another

The clinical features of the malignant *Brenner* tumour do not differ from malignant ovarian tumours in general However a difference in the prognosis of the malignant *Brenner* tumour has been suggested, depending on whether benign elements are present or not (*Halgrimsson* & *Scully* 1972) This is to some degree contradicted by the fatal course of the present case Our case is remarkable for metastasizing outside the abdominal cavity after removal of the malignant *Brenner* tumour The subcutaneous metastases, which do not seem to have been described earlier may have originated from tumour tissue either from peritoneum or from para aortic lymphnodes.

REFERENCES

1 *Ehrlich C E* & *Roth L M* The Brenner tumour A clinicopathologic study of 33 cases. Cancer 27 332–342 1971

2 *Fox H Cummins P A* & *Langley F A* An ultrastructural study of the histogenesis of the Brenner tumour of the ovary J Path. Bact. *107* pxl–pxli 1972

3 *Greene R R* The diverse origin of Brenner tumours. Amer J Obstet. Gynec. *64* 878–898, 1952

4 *Halgrimsson J* & *Scully R E* Borderline and malignant Brenner tumours of the ovary A report of 15 cases. Acta path. microbiol scand. Sect. A *80* suppl. *233* 56–66 1972.

5 *Hull M G R* & *Campbell G R* The malignant Brenner tumour Obstet. and Gynec 42 527–534 1973

6 *Idelson M G* *Malignancy in* Brenner tumours of the ovary with comments on histiogenesis and possible estrogen production. Obstet. gynec. Surv *18* 246–267 1963

7 *Novak E R* & *Woodruff J D* Brenner tumours of the ovary In Novaks gynecologic and obstetic pathology Saunders, Philadelphia and London 1967 pp 379–389

8. *Roth, L. M. & Sternberg, W. H.* Proliferating Brenner tumours. Cancer 27 687–693 1971
9. *Stohr G.* The relationship of the Brenner tumour to the rete ovarii. Amer J Obstet. Gynec. 72 389–399 1956.
10. *Teilum G.* Brenner tumour In Special tumours of the ovary and testis. Munksgaard, Copenhagen, 1971 pp. 236–249
11. *von Numers C.* A contribution to the case knowledge and histology of the Brenner tumour Acta obstet. gynec. scand 25 Suppl. 2 114–127 1945
12. *World Health Organization* Histological typing of ovarian tumours, Geneva, 1973 pp. 40–41

Acta path. microbiol. scand. Sect. A 85 864–868 1977

MUSCLE CHANGES IN PATIENTS WITH VARICOSE VEINS

JUKKA MÄKITIE

Department of Neurology University Central Hospital
Helsinki Finland

Mäkitie J Muscle changes in patients with varicose veins. Acta path. microbiol. scand. Sect. A, 85 864–868 1977

Gastrocnemius muscle specimens from 19 patients with varicose veins without clinical neuropathy were examined with a light microscope after staining fresh frozen sections with modified Gomori trichrome and after histochemical reactions for NADH diaphorase ATPases and phosphorylase. Only four muscle specimens from these 19 patients were regarded as completely normal In five of the patients (26 per cent) a combination of fiber type grouping and small group atrophy and in nine patients (47 per cent) fiber type grouping with occasional small angulated fibers were observed These changes were less frequent in nine biopsies from brain death control patients (11 per cent) Various forms of abnormalities in the distribution of NADH diaphorase were seen in 13 patients with varicose veins (68 per cent) and in one of the controls (11 per cent) Necrosis and phagocytosis of the muscle fibers were present in three biopsies from patients with varicose veins (16 per cent) and in one of the controls (11 per cent)

J Mäkitie Department of Neurology University Central Hospital Helsinki, Finland.

Received 20 vii 76 Accepted 25 v 77

The present study was originally started to obtain control material for various muscle studies. I thought that the material would represent the normal variation of muscle alterations, because histopathological studies on varicose veins have not yet been made and because the disease is generally considered mild and harmless. However pathological muscle alterations falling outside the range of the normal variation (9 11) were observed. Considering the very common occurrence of varicose veins (1 6 10) and the possible importance of these alterations when interpreting the findings in muscle histopathology these changes seemed to be worth describing

PATIENTS AND METHODS

The material consisted of biopsy specimens from the gastrocnemius muscle of 18 females and two males between 32 and 65 years of age (mean 46.1) with varicose veins of the legs. The patients had no known neuromuscular diseases in their previous history It was difficult to estimate accurately the duration of the disease because of its insidious onset or the absence of symptoms. In general, the patients had been suffering for 1–5 years from cosmetic disturbances, from feelings of heaviness and fatigue and/or from swelling of the legs Patients with complicated varicosities or previous cardiovascular or other manifest diseases, were not operated at the Out Patients Department of Surgery University of Helsinki Hospital H lsinki and thus they were not included in this study Numerous granulomatous infiltrations were seen among muscle fibers in a 32 year-old female (later found to have sarcoidosis) therefore she is not included in the comparison of the results shown in Table I

TABLE 1 *Abnormalities of Muscle in Patients with Varicose Veins Compared to Those of the Controls*

Patients	Fiber type grouping + group atrophy	Fiber type grouping + sporadic atrophy	Changes in NADH distribution	Central nuclei > 3 per cent	Fiber necrosis or phagocytosis
With varicose veins (n = 19) age 32–65 years (mean 47.0)	5 (26 per cent)	9 (47 per cent)	13 (68 per cent)	7 (37 per cent)	3 (16 per cent)
Controls (n = 9)* age 18–45 years (mean 33.8)	1 (11 per cent)	1 (11 per cent)	1 (11 per cent)	2 (22 per cent)	1 (11 per cent)

*from Mikkus and Mustonen, 1978 (9)

The biopsy specimens were taken during the operation for varicose veins from the medial head of the gastrocnemius, about 1 cm below the surface of the muscle. The muscle piece was immediately trimmed and frozen in isopenthane pre-cooled in liquid nitrogen. Serial transverse sections of 10 microns were cut in a cryostat at — 25 C and thawed and dried at room temperature on glass slides. Modified Gomori trichrome (4) was employed to show possible alterations in the cytoplasm and nuclei of the fibers. The activity of NADH diaphorase was demonstrated by incubation at 37° C, with nicotinamide dinucleotide as substrate for 60 minutes (11) to demonstrate alterations in intermyofibrillar network distribution. The ATPase reaction was performed with ATPase disodium salt as substrate after pre-incubation in either alkaline (pH 10.2) or acid media (pH 4.3) before incubation at pH 9.4 for 90 minutes at + 37° C, the original reaction (5) being slightly modified. The ATPase reactions were used to type the fibers to type 1 and type 2 fibers. The fiber type grouping was estimated visually. The phosphorylase reaction (12) was carried out in order to detect the presence of damaged fibers, the reaction being known to be sensitive for early demonstration of fiber dysfunction (2). The nomenclature for muscle pathology used by *Dubowitz & Brooke* (3) is employed in this study.

The results were compared to gastrocnemius biopsies from nine living patients between 18 and 45 years of age (mean 33.4) who were brain-dead owing to accidental craniocerebral trauma prior to the termination of artificial ventilation (9).

RESULTS

Simultaneous occurrence of fiber type grouping (Fig 1) and small angular atrophic muscle fibers in small groups was present in five of the biopsy specimens. In nine patients, fiber type grouping combined with sporadic small angular fibers was present, but there was no group atrophy. The atrophic fibers had intense NADH diaphorase activity (Fig 2 A–B).

Alterations from the normal intermyofibrillar distribution of NADH diaphorase were present in 13 of the patients, the most common forms being "moth-eaten" or whorled fibers (Fig 2 C–F). With Gomori trichrome staining necrotic fibers undergoing phagocytosis were observed in three of the patients. Being devoid of the phosphorylase enzyme the fibers were also easily distinguished from the living muscle fibers. A slight increase in the number of fibers with central nuclei (to 5–10 per cent) was present in these three biopsies. In addition, an increase in the number of fibers with central nuclei (to 4–5 per cent) was present in four other biopsy specimens.

DISCUSSION

Distally located muscles are more frequently affected than the proximal muscles of the leg (7). One explanation is that distal muscles are subjected to direct or indirect damage more often than proximally located muscles, owing, for example, to nerve compression or circulatory disturbances in relatively common diseases, such as sciatica and atherosclerosis. Varicosities may also be a reason for the

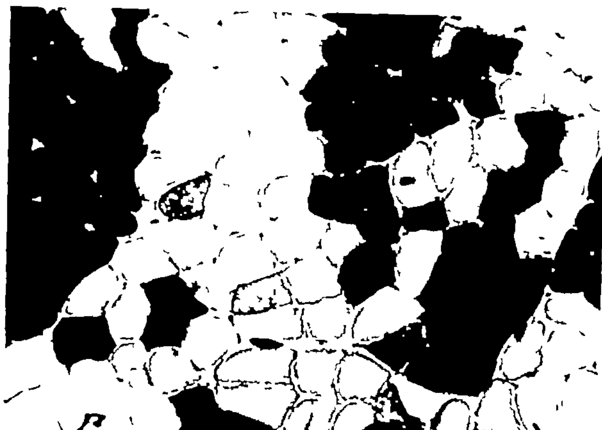


Fig 1 Micrograph illustrative of fiber type grouping in a biopsy specimen from the gastrocnemius muscle of a 42 year-old female with varicose veins. Several groups of dark type I fibers among groups of less reactive type II fibers have replaced the normal checkerboard pattern of fiber distribution. Incubated for ATPase with acid pre-incubation at pH 4.3 × 80

changes observed in the muscles of the lower leg since in the present study there were less changes in individual muscle fibers of the same muscle in the reference group

It is possible that the difference in the frequencies of the observed changes between the patients with varicosities and the reference group are due to the age difference the age of the reference group being lower (33.8 ± 2 9 years mean ± S D) than that of the patients with varicose veins (47 0 ± 8.5 years mean ± S D) Fiber type grouping and group atrophy were observed in $^{8}/_{\ 9}$ and type grouping with sporadic atrophic fibers in $/_{1}$ biopsy specimens. The most frequent change however was the one observed in the NADH diaphorase distribution present in $^{13}/_{19}$ of the biopsy specimens. *Jennekens et al.* (7) have studied gastrocnemius muscles biopsied postmortem from patients with a mean age of 79 8 years using similar histochemical techniques to those used in the present study They observed group atrophy in $^{4}/_{16}$, type grouping in $^{9}/_{16}$ and structural changes in $^{4}/_{1}$ of the gastrocnemius biopsies. Comparing these with the present results, it appears that structural alterations as reflected by NADH distribution were clearly more frequent (68 per cent) in the present series of patients although they were younger Because neurogenic changes tend to *increase* with age (7) the mean age of the patients with and without changes attributable to subclinical neuropathy was calculated The mean age of the patients with fiber type grouping and group atrophy was 47 0 ± 7 4 years (mean ± S D) of those with fiber type grouping and single atrophic fibers 50.3 ± 9 7 years (mean ± S D) and of those with completely normal structure 44 4 ± 6 0 years (mean ± S D) *None of these groups*

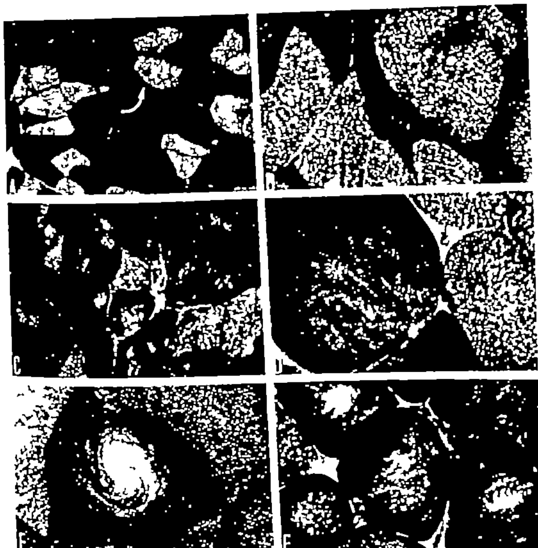


Fig 2 Some of the changes observed in the distribution of the NADH diaphorase within the muscle fibers.

A Specimen from 53-year-old female with normal NADH diaphorase distribution type I fibers stain darkly and type II fibers are lightly stained. Some scattered small angular fibers with intense NADH diaphorase activity can be seen (arrow) × 60 B Group atrophy × 120 C to F Examples of NADH distribution differing from the normal distribution, seen e g in figure A. C Several fibers of moth-eaten or whorled appearance are seen. × 85 Figure D illustrates diffuse "mitochondrial disorganization within the fibers × 225 E A fiber of whirlpool appearance and devoid of NADH diaphorase in its central area × 225 F Several fibers with central areas devoid of NADH diaphorase. 120

differed significantly from one another Thus, in our patients, age did not seem to be the decisive factor for the presence of neurogenic changes

It has been previously shown that ligation of the caudal veins in the rat leads to degeneration and necrosis of the muscle fibers of the leg (8) similar to those we observed in

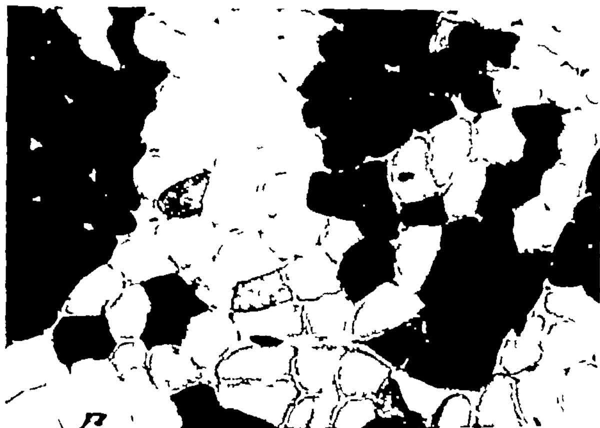


Fig 1 Micrograph illustrative of fiber type grouping in a biopsy specimen from the gastrocnemius muscle of a 42 year-old female with varicose veins. Several groups of dark type I fibers among groups of less reactive type II fibers have replaced the normal checkerboard pattern of fiber distribution. Incubated for ATPase with acid pre incubation at pH 4.3 × 80

changes observed in the muscles of the lower leg since in the present study there were less changes in individual muscle fibers of the same muscle in the reference group

It is possible that the difference in the frequencies of the observed changes between the patients with varicosities and the reference group are due to the age difference the age of the reference group being lower (33.8 ± 2.9 years mean ± S D) than that of the patients with varicose veins (47.0 ± 8.5 years mean ± S D) Fiber type grouping and group atrophy were observed in 8/16 and type grouping with sporadic atrophic fibers in 9/ biopsy specimens. The most frequent change however was the one observed in the NADH diaphorase distribution present in 11/16 of the biopsy specimens. *Jennekens et al.* (7) have studied gastrocnemius muscles biopsied postmortem from patients with a mean age of 79.8 years, using similar histochemical techniques to those used in the present study They observed group atrophy in 4/16, type grouping in 8/16 and structural changes in 4/16 of the gastrocnemius biopsies. Comparing these with the present results, it appears that structural alterations as reflected by NADH distribution were clearly more frequent (68 per cent) in the present series of patients although they were younger Because neurogenic changes tend to increase with age (7) the mean age of the patients with and without changes attributable to subclinical neuropathy was calculated The mean age of the patients with fiber type grouping and group atrophy was 47.0 ± 7.4 years (mean ± S D) of those with fiber type grouping and single atrophic fibers 50.3 ± 9.7 years (mean ± S D) and of those with completely normal structure 44.4 ± 6.0 years (mean ± S D) None of these groups

Acta path. microbiol. scand. Sect. A, 85 869–874 1977

LÖFFLER'S ENDOCARDITIS AND ENDOMYOCARDIAL FIBROSIS —A NOSOLOGIC ENTITY?

ULRIK BAANDRUP

The University Institute of Pathology
University of Aarhus, Kommunehospitalet, 8000 Aarhus C, Denmark

Baandrup, U. Löffler' Endocarditis and Endomyocardial Fibrosis—a Nosologic Entity? Acta path. microbiol. scand. Sect. A, 85 869–874 1977

The problem whether Löffler' endocarditis and endomyocardial fibrosis belong to the same disease spectrum or are separate entities is still under debate. Until recently it was believed that endomyocardial fibrosis was disorder restricted to tropical areas. Three Danish patients are presented, two showing a continuous disease spectrum, one patient showing the fully developed endomyocardial fibrosis which is indistinguishable from endomyocardial fibrosis described from the tropical areas. Eosinophilia was present in all three patients. The findings described in these three patients lend support to the unitarian hypothesis that Löffler' endocarditis and endomyocardial fibrosis belong to the same disease spectrum, and that the eosinophilic granulocyte may be the underlying cause.

Key words Löffler' endocarditis parietalis fibroplastica endomyocardial fibrosis eosinophilia cardiomyopathy

Ulrik Baandrup University Institute of Pathology Kommunehospitalet, DK-8000 Arhus C, Denmark

Received 13.vi.77 Accepted 13 77

In 1936 *Löffler* (9) described endocarditis parietalis fibroplastica in patients with eosinophilic leucocytosis, but the disorder was morphologically recognized by *Reinbach* (16) in 1893 in a patient dying from lymphosarcoma with eosinophilic leukemoid reaction

In 1948 *Davies* (5) initiated the reporting of a large number of endomyocardial fibrosis (EMF from Uganda Half of the cases had known eosinophilia.

Gerbeux et al (7) proposed that Löffler's endocarditis and EMF were essentially the same disorder and this is the leading perception at the moment (2, 10) Löffler's endocarditis correlates with the acute/necrotic and thrombotic stage and EMF with the fibrotic stage of a graduated disease spectrum (Table 1) (12) but still some claim they are distinct entities (14) A few scandinavian cases have been published under a variety of names (1 6, 11 15 20 21)

The following three cases are presented because they contribute to the unitarian theory on morphological grounds. Eosinophilia was present in all three patients.

CASE REPORTS

Case 1 This case has been published before under the diagnosis eosinophilic myocarditis (21)

The patient was 9 years old boy who 3½

three of the present patients Venous pressure after ligation of the veins in the experimental animals is presumably greater than in the patients with varicose veins, which may explain the quantitatively more severe changes in the experimental animals (8) The reason for the changes is still uncertain even though changes in the venous pressure, or secondary disturbances in blood flow, in the tissue oxygen and in its metabolites are presumably the most likely causes.

I want to thank A. *Asp* M.D Head of the Out Patients Department of Surgery University Central Hospital Helsinki, for clinical discussions and for making the biopsy specimens available The skilful technical assistance of Miss *Anne Manninen* and Mrs *Eija Vuorio* is gratefully acknowledged.

REFERENCES

1 *Asp A. & Aromaa U* Suonikohjukirurgia lyhytjälkihoitoisena – toiminnan edellytykset Suom Lääk. L. *30* 1906–1909 1975

2 *Dahlbäck L. O* Effects of temporary tourniquet ischemia on striated muscle fibers and motor end plates. Scand J plast. reconstruct. Surg 1–91 Suppl 7 1970

3 *Dubowitz V & Brooke M H* Muscle Biopsy A Modern Approach, Saunders, London. 1973

4 *Engel W K & Cunningham G* Rapid examination of muscle tissue Neurology *13* 919–923 1963

5 *Guth L. & Samaha F J* Procedure for histochemical demonstration of actomyosin ATPase Exp. Neurol. *28* 365–367 1970

6. *Haeger K* Venous and Lymphatic Disorders of the Leg Scandinavian University Books, Lund 1966

7 *Jennekens F G I Tomlinson B. E. & Walton J N* Histochemical aspects of five limb muscles in old age An autopsy study J neurol. Sci *14* 259–276 1971

8 *Kery L. & Wouters H W* Effect of venous stasis on striated muscles and its relation to the anterior tibial syndrome. An experimental study Acta chir Acad. Sci. hung *12* 151–157 1971

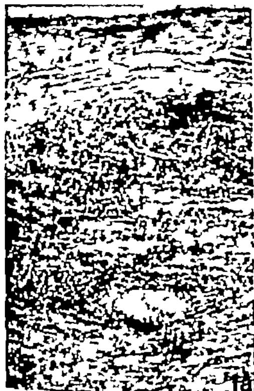
9 *Mäkitie J & Mustonen T* Normal human muscle. A morphometric histochemical and ultrastructural biopsy study *1978, to be published.*

10. *Pirnat L.* Systematic untersuchungen des varikösen Symptomenkomplexes in der Industrie. Zbl Phlebol. *6* 265–271 1967

11 *Pearse A G* (ed.) Histochemistry III ed. Churchill, London, 1972 Vol. II p. 1342.

12. *Rebeiz J Moore M., Holden E. & Adams R* Variations in muscle status with age and systemic diseases. Acta Neuropath. *19* 51–69 1971

13 *Takeuchi T & Kuriaki H.* Histochemical detection of phosphorylase in animal tissues. J Histochem. Cytochem. *3* *153–160, 1955*


1a




2a

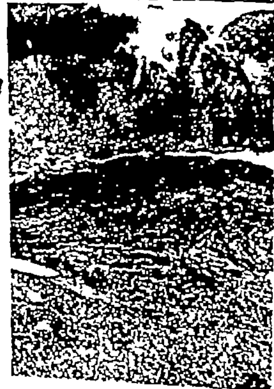


TABLE 1 *Spectrum of Löffler's Endocarditis and Endomyocardial Fibrosis*

Acute/necrotic stage	Thrombotic stage	Fibrotic stage
eosinophilic pancarditis	endocardial thickening	severe endocardial thickening (zonal layering)
muscle necrosis, arteritis	parietal thrombus	fibrotic septa into inner 1/3 of the myocardium
average length of symptoms 5.5 weeks	average length of symptoms 10 months	average length of symptoms 24.5 months

years old had poliomyelitis paralytica but had completely recovered by the age of 4. 7 years old symptoms of asthma bronchiale developed.

The boy deteriorated rather suddenly with gastric pain, dyspnoe and cyanosis. He was treated with digitalis, diuretics, penicillin and actocortin without effect.

Shortly before death eosinophilia of 7 per cent was found. 2 and 5 months earlier it had been 9 and 34 per cent.

ECG showed sinustachycardia, accentuated P waves and extra systoles. Stetoscopically a smooth systolic murmur at apex and galop rhythm devel oped few days before death. Chest X rays showed left sided pleuropneumonia.

Autopsy. The pericardium showed fibr nous and delicate fibrous adhesions but no fluid. The heart weighed 250 gs. Right ventricle was hypertrophic and dilated and in both ventricles the endocardium was yellowishly discoloured. Thrombi were not found.

Histology. The whole myocardium showed extensive granulocytic infiltration, especially eosinophils. Muscle necroses were frequently demonstrated and arteritis was seen (Fig. 1 a + b). The endocardium was patchily thickened and infiltrated by eosinophils. Other organs were acutely and chronically congested and often eosinophilic infiltration was met.

This case represents the acute stage of the disorder.

No. 2. 29 years old woman who in 1969—22 years old—developed rhinitis and since 1974 asthma bronchiale. After a few days admission in October 1976 with febrilia, joint pain, slight erythema and edema, she was found dead. The treatment had consisted in prednison and a purine.

During admission 5 months earlier eosinophilia of 14 per cent was noted and in June and September 1975 values of 27 and 41 per cent were found. ECG showed periodic extra-systoles and chest X ray diffuse infiltrates of the lungs and moderately enlarged heart.

Autopsy. The pericardial sac contained 200 mls of serous fluid and scanty fibrinous deposits were seen. The heart was hypertrophic and dilated weighing 380 gs. Large parietal thrombi were present in the right side of the heart (Fig. 2 a). The endocardium was thickened and endocardium and myocardium were yellowishly discoloured. On the tricuspid valve small thrombotic excrescenses were seen.

Histology. Parietal thrombi and pancarditic changes with muscle necroses were prominent (Fig. 2 b). Most of the inflammatory cells were eosinophils. The alterations seemed to be of older age in the left ventricle as some fibrous healing was found here. Besides that bronchopneumonia with heavy eosinophilia, embolic small lung infarcts and bilateral pleuritis were present.

The findings are consistent with the early thrombotic stage.

No. 3. 31 years old woman by whom acute intermittent porphyria was diagnosed at the age of 20. 7 years later extensive polyneuropathy developed with almost complete paralysis of the lower extremities. From now on respiratory difficulties and cardial incompensation progressed. On the day of her last admission she died suddenly.

During hospitalization 7 years earlier eosinophilia was noted: 17–33–39–6 per cent. Two leucocytic counts later on did not show any eosinophilia. ECG from the period with eosinophilia showed tachycardia but no further abnormalities.

Autopsy. The pericardium was normal. The heart weighed 3 5 gs. The endocardium was thickened in both ventricles and low in the anterior wall of left ventricle endocardial calcification was present.

Histology. The severely thickened endocardium was zonally layered (Fig. 3 a) and consisted predominantly of fibrous tissue with much collagen and varying amounts of elastic tissue. In some areas. The fibrous tissue showed numerous fibroblastic nuclei and in this layer calcification might be found. A hyaline layer was not evident but the layer adjacent to the myocardium revealed numerous blood vessels and chronic inflammatory cells, but no eosinophils (Fig. 3 b). From this layer

Fig. 1. Case no. 1. Myocardial arteritis and necrosis (H & E, a) × 400, b) × 1000).

Fig. 2. Case no. 2. a) Right ventricle of the heart showing large parietal thrombi. b) Myocardium infiltrated by eosinophils, thickened and destroyed endocardium with overlying thrombus (Elastic V G., × 100).

strated in a variety of disorders accompanied by eosinophilia status asthmaticus, poly arteritis nodosa, sensitivity to antituberculous drugs, bronchial carcinoma and tropical eosinophilia associated with chronic infestations including filariasis.

Eosinophilia may be missing at the onset of the cardiac symptoms although present in other stages of the disease, as exemplified by case no 3

The eosinophilic leucocyte differs considerably from the neutrophil concerning its content of enzymes (22) Electron microscopy has shown specific osmophilic cytoplasmic inclusions or granules in the eosinophils of patients with this kind of cardiomyopathy and in patients with marked eosinophilia (18) Several substances have chemotactic activity for eosinophils, e. g histamine, some antigen-antibody complexes, and components of human complement. Eosinophils can phagocytose immune complexes and thus may produce vacuolization and degranulation of the cells. *Spry & Tai* (18) have shown that some circulating eosinophils in patients with Löffler's endocarditis posess receptors for rabbit IgG coated erythrocytes and phagocytose lymphocytes coated with rabbit IgG or human C_3B. These eosinophils therefore have characteristics of mature or stimulated eosinophils able to respond to soluble substances in the blood by forming endocytic vacuoles and degranulation. The material formed in this way may itself produce cardiac injury Alternatively it is possible that these eosinophils act in an entirely beneficial fashion through fagocytosis. The research along these lines may turn out to let EMF be the first disorder to leave the exclusive group of cardiomyopathies.

In general the results of treatment have been disappointing but cytostatics and surgery seem to be promising.

The usefulness of echocardiographic studies following the patients is great and the potential usefulness of endomyocardial biopsy as a diagnostic tool has been demonstrated on several occasions by excellent correlations between the biopsy and autopsy findings (4 8, 13)

The present three case stories are characterized by heart failure and eosinophilia. Autopsy and microscopical investigation have revealed a continous spectrum of a heart disorder in keeping with the theory that Löffler's endocarditis and EMF are stages of a nosologic entity

For the use of the material I owe my gratitude to the physicians at the Institute of Pathology Randers Centralsygehus and Skive Sygehus, and at the Department of Internal Medicine, Viborg Sygehus. Dr *E. G. J Olsen* National Heart Hospital, London, has given me most invaluable help.

REFERENCES

1 *Amtes, S & Fischer-Hansen J.:* Endomyokardial fibrose. Ugeskr Laeg *138* 101–103 1976.

2 *Brockington I F & Olsen E. G J* Löffler's endocarditis and Davies endomyocardial fibrosis. Am. Heart J *85* 308–322, 1973

3 *Chew C Y C., Ziady G M., R phael M J., N llen M & Oakley C M* Primary restrictive cardiomyopathy non-tropical endomyocardial fibrosis and hyper-eosinophilic heart disease Brit. Heart J *39* 413–427 1977

4 *Chusid M J., Dale D C., West B. C. & Wolff S M.:* The hypereosinophilic syndrome Medicine *54* 1 27 1975

5 *Davies J N P* Endocardial fibrosis in africans. East Afric. Med. J *25* 10–14 1948.

6 *Engfeldt B. & Zetterström R.:* Disseminated eosinophilic collagen disease" Acta Med. Scand. *153* 337 353 1956.

7 *Gerbeaux A D Brux J., Bonnacez M & Lenègre J* L endocardite pariétale fibroplastique avec éosinophilie sanguine (endocardite de Löffler) Bulletins et Mémoires de la Société Medicale des Hopiteaux de Paris *72* 456, 1956.

8. *Hall, J S W., Theologides A From A. H L., Gobel, L., Fortuny I Lawrence C J & Edwards, J E.,* Hypereosinophilic syndrome with biventricular involvement. Circulation *55* 217–222 1977

9. *Löffler W* Endocarditis parietalis fibroplastica mit Bluteosinophilie, ein eigenartiges Krankheitsbild. Schweiz. Med. Wschr *66* 817–820 1936.

10 *Oakley C M & Olsen E. G J* Eosinophilia and heart disease (Editorial) Brit. Heart J *39* 233–237 1977

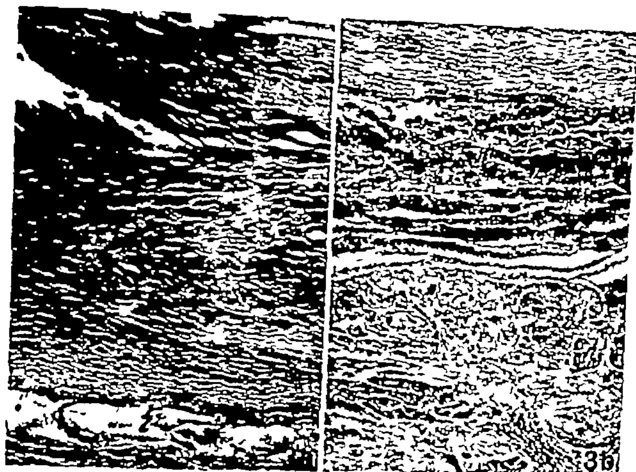


Fig 3 Case no 3 a) Thickened fibrous endocardium with calcification. b) Granulation tissue between *endo- and myocardium Fibrous septum extending from here into the myocardium* (H & E × 200)

fibrous septa extented into the underlying $^{1}/_{3}$ of the myocardium Other findings were bronchopneumonia, signs of polyneuropathy and consequently neurogenic muscle degeneration

This case represents the fibrotic stage

DISCUSSION

Patients suffering from Löffler's endocarditis and EMF are usually young adults with male preponderance Nothing can be said about incidence

EMF was originally thought to be a disease occurring exclusively in Africa and South America, but some cases have emerged from North America Asia and Europe one case has been reported in Scandinavia (1)

The onset is often indefinite febrile disease going on to heart failure through an unpredictable course of time Embolic phenomena are common Hemodynamically it is a restrictive/obliterative heart disease

Usually the disorder is confined mainly to one of the ventricles, but may be bilateral

There are *four sites of election within the* heart the mitral valve the apex of the left ventricle the tricuspid valve and the body of the right ventricle. The outflow tracts are usually spared although a few cases with this involvement have been described (17)

Classified as a cardiomyopathy this indicates a disorder of unknown cause or association Many *hypotheses have been raised re*garding the cause dietary causes, lymphatic obstruction filariasis etc but they *all seem* to be incomplete (2) The current view shared by most—but not all—*investigators is* that *the disease is caused by the* eosinophilic granulocyte per se

Chusid et al (4) have claimed *that* 93 per cent of patients with a hypereosinophilic *syndrome had clinical* or necropsy evidence *of myocardial disease as* has been demon

strated in a variety of disorders accompanied by eosinophilia status asthmaticus, poly arteritis nodosa, sensitivity to antituberculous drugs, bronchial carcinoma and tropical eosinophilia associated with chronic infestations including filariasis.

Eosinophilia may be missing at the onset of the cardiac symptoms although present in other stages of the disease, as exemplified by case no 3

The eosinophilic leucocyte differs considerably from the neutrophil concerning its content of enzymes (22) Electron microscopy has shown specific osmiophilic cytoplasmic inclusions or granules in the eosinophils of patients with this kind of cardiomyopathy and in patients with marked eosinophilia (18) Several substances have chemotactic activity for eosinophils, e. g histamine, some antigen-antibody complexes, and components of human complement. Eosinophils can phagocytose immune complexes and this may produce vacuolization and degranulation of the cells. *Spry* & *Tai* (18) have shown that some circulating eosinophils in patients with Löffler's endocarditis possess receptors for rabbit IgG coated erythrocytes and phagocytose lymphocytes coated with rabbit IgG or human C_3B. These eosinophils therefore have characteristics of mature or stimulated eosinophils able to respond to soluble substances in the blood by forming endocytic vacuoles and degranulation. The material formed in this way may itself produce cardiac injury Alternatively it is possible that these eosinophils act in an entirely beneficial fashion through fagocytosis The research along these lines may turn out to let EMF be the first disorder to leave the exclusive group of cardiomyopathies

In general the results of treatment have been disappointing but cytostatics and surgery seem to be promising.

The usefulness of echocardiographic studies following the patients is great and the potential usefulness of endomyocardial biopsy as a diagnostic tool has been demonstrated on several occasions by excellent correlations between the biopsy and autopsy findings (4 8, 13)

The present three case stories are characterized by heart failure and eosinophilia. Autopsy and microscopical investigation have revealed a continuous spectrum of a heart disorder in keeping with the theory that Löffler's endocarditis and EMF are stages of a nosologic entity

---

For the use of the material I owe my gratitude to the physicians at the Institute of Pathology Randers Centralsygehus and Skive Sygehus, and at the Department of Internal Medicine, Viborg Sygehus. Dr *E. G J Olsen* National Heart Hospital, London, has given me most invaluable help.

REFERENCES

1 *Amtas, S & Fischer-Hansen J.*. Endomyokardial fibrose Ugeskr Læg *138* 101–103, 1976.

2. *Brockington, I F & Olsen E. G J.*. Löffler's endocarditis and Davies endomyocardial fibrosis. Am. Heart J *85* 308–322, 1973

3 *Chew C Y C., Ziady G M Raphael, M J., Nellen M & Oakley C M.*. Primary restrictive cardiomyopathy non-tropical endomyocardial fibrosis and hyper-eosinophilic heart disease Brit. Heart J *39* 415–427 1977

4 *Chusid M J Dale D C., West B. C & Wolff S M* The hypereosinophilic syndrome. Medicine *54* 1–27 1975

5 *Davies J N P.*. Endocardial fibrosis in africans. East Afric. Med. J *25* 10–14 1948.

6 *Engfeldt B & Zetterström R.*. Disseminated eosinophilic "collagen disease Acta Med. Scand. *153* 337–353 1956

7 *Gerbeux A D Brux J Bonnecour M & Lenègre J* L endocardite pariétale fibroplastique avec éosinophilie sanguine (endocardite de Löffler) Bulletins et Mémoires de la Société Médicale des Hopitaux de Paris 72 456 1956.

8. *Hall, J., S W., Theologides A., Frem A-H L., Gobel, L. Fortuny I., Lawrenc C J & Edwards J E.* Hypereosinophilic syndrome with biventricular involvement Circulation *55* 217–222 1977

9 *Löffler W* Endocarditis parietalis fibroplastica mit Bluteosinophilie ein eigenartiges Krankheitsbild. Schweiz. Med. Wschr *66* 817–820 1936.

10. *Oakley C M & Olsen E. G J.*. Eosinophilia and heart disease (Editorial) Brit. Heart J *39* 233–237 1977

11 *Odeberg B* Eosinophilic leukemia and disseminated eosinophilic collagen disease—a disease entity Acta Med. Scand *177* 129–144 1965

12 *Olsen E G J* Löffler's endocarditis and endomyocardial fibrosis. Path. Microbiol. *43* 104–106 1975

13 *Olsen E. G J* Personal communication 1977

14 *Patel A K D'Arbela P G & Somers K* Endomyocardial fibrosis and eosinophilia. Brit. Heart J *39* 238–241 1977

15 *Pedersen H* Endocarditis parietalis fibroplastica (Löffler) med overvejende cerebrale initialsymptomer Ugeskr Laeg *126* 274–279 1964

16 *Reinbach G* Über das Verhalten der Leukocyten bei malignen Tumoren Arch Klin Chir *46* 486–562, 1893

17 *Shaper A G Hutt M S R & Coles R M* Necropsy studies of endomyocardial fibrosis and rheumatic heart disease in Uganda 1950–1965 Brit Heart J *30* 391–401 1968.

18. *Solley G O Maldonado J E., Gleich G J., Giuliani E. R Moagland H C Pierre R V & Brown Jr A L.* Endomyocardiopathy with eosinophilia. Mayo Clin. Proc. *51* 697–708 1976

19 *Spry C J F & Tai P C* Studies on eosinophils II Patients with Löffler's cardiomyopathy Clin. Exp Immun. *24* 423–434 1976

20 *Thomsen S & Plum P* Eosinophilic leukemia. Acta Med. Scand *101* 116–137 1939

21 *Thorsen K & Thorborg J I* "Eosinofil" myocarditis ved asthma bronchiale. Ugeskr Laeg *123* 614–617 1961

22 *West B C Gelb N A & Rosenthal A S* Isolation and partial characterization of human eosinophil granules. Comparison to neutrophils. Am. J Pathol *81* 575–588, 1975

Acta path. microbiol. scand. Sect. A, 85 875–888, 1977

NAPHTHYLAMIDASE USED AS A LYSOSOME MARKER IN THE STUDY OF ACUTE SELECTIVE NECROSIS OF THE INTERNAL GRANULAR LAYER OF CEREBELLUM

REIDAR ALBRECHTSEN

Department of Pathology Rigshospitalet, University of Copenhagen, Denmark

Albrechtsen, R. Naphthylamidase used as a lysosome marker in the study of the pathogenesis of acute selective necrosis of the internal granuar layer of cerebellum. Acta path. microbiol. scand. Sect. A, 85 875–888, 1977

Histochemical examination of the activity of naphthylamidase (LNAse) in the cerebellar cortex of 70 human autopsies consistently revealed a marked activity mainly in the internal granular layer with pH optimum of 5.8. Slight enzyme activity was also localized in sites corresponding to lipofuscin deposits and areas of acid phosphatase activity in the Bergmann glial cells, Purkinje cells and in perivascular cells. The histochemical findings support the LNAse reaction as a lysosome marker. Differences in localization of LNAse and acid phosphatase could possibly be due to prior release of the latter enzyme from the internal granular layer. Significant correlation between demonstrable loss of granule cell nuclei (the so-called acute, selective necrosis of the granular layer) and low pH of the cerebellar tissue could be demonstrated in 21 cases. The present findings support the hypothesis that an enzymatic disintegration of the granule cells takes place in postmortem cerebella with low pH simulating a necrotic tal phenomenon.

Key words: Cerebellum granular layer naphthylamidase lysosomes autolysis.

R. Albrechtsen, Department of Pathology Rigshospitalet, Frederik d. V' v J 11 DK 2100 Copenhagen, Denmark.

Received 21 77 Accepted 21 1.77

The so-called "acute selective necrosis of the granular layer" (NGL) frequently encountered in routine examination of human cerebella (*Olsen* 1959 *Okazaki et al.* 1961 *Albre htsen* 1977 b) has been shown to be a postmortem occurring phenomenon (*Ikuta et al.* 1963 *Albrechtsen* 1975 *Albrechtsen* 1977 a, *Alb chtsen* 1977 b) and enzyme dependent factors—such as tissue temperature (*Ikuta et al.* 1963) and the presence of increased postmortem cerebellar acidity (*Albrechtsen* 1977 a)—are important for its development.

It is not completely clear how large a part the enzymatic process plays in the total autolytic process. However it is generally accepted, that the lysosomes are the only cell organelles that contain the necessary enzymes for the complete breakdown of most of the complex molecules of cells and tissues (*Barrett* 1969)

The histochemical demonstration of the enzyme naphthylamidase (LNAse) at pH 5.5–5.8 has been used as an indicator for lysosomes (*Niemi and Sylvén* 1969). Employing this method it has been possible to demonstrate LNAse activity with a pH optimum of 5.5 mainly in the *internal granular layer* in the cerebellum of rats (*Albrechtsen & Jensen* 1975).

The purpose of the present study is to demonstrate that similar LNAse activity is present in the internal granular layer of cerebellum in human autopsies and to consider the role of the lysosomes in the development of autolysis.

MATERIAL AND METHODS

Cerebella from 70 human subjects were obtained at necropsy by cutting through the cerebral peduncles. pH measurements of the cerebellum were carried out immediately after the necropsy according to the methods previously described (*Albrechtsen* 1977 a). From the geriatric hospitals (De Gamles By and Norre Hospital) mainly cases with pH < 6.0 were collected due to an anticipated high incidence of NGL in these patients (*Albrechtsen* 1977 a). There were 28 cases (16 females and 12 males) with ages ranging from 63–93 years (mean 80.9 years). The time interval from death to necropsy varied from 12–68 hrs. (mean 38.7 hrs.). The most frequent causes of death were arteriosclerotic disorders or neoplasia.

From the Medico-Legal Institute, University of Copenhagen, 42 cases (19 females and 23 males) with age ranging from 7–80 years (mean 44.4 years) were examined. The time lapse from death to necropsy varied from 9–271 hrs. (mean 91.8 hrs.). The causes of death were violent accidents (33 cases), homicides (3 cases), suicides (4 cases) and natural causes (2 cases). Of these 25 subjects died instantly either by total rupture of heart wall or aorta (23 cases) or total rupture of the atlanto-occipitol membrane (2 cases).

Bilateral portions of cerebellar hemisphere measuring about 10 × 5 × 5 mm were excised from anterior and posterior lobes, immediately placed in isopentane cooled to −80 C by a freezing mixture of acetone and solid carbon dioxide and stored at −70 C. The remaining cerebellum was then fixed for at least 15 days at room temperature in a 10 per cent buffered (pH 7.2) formalin solution with glycerin added. After fixation 2 pieces from both cerebellar hemispheres were dehydrated in alcohol and embedded in paraffin wax by the method previously described (*Albrechtsen* 1977 a). Six µm thick sections were stained with Carazzi haematoxylin-eosin (10 min haematoxylin, 4 min eosin).

The evaluation of NGL was based on the histopathologic criteria given by *Steen Olsen* (1961).

Histochemical Procedure

With a drop of tissue-tek the frozen cerebellar tissue was firmly fixed to the top of a cooled metal chuck, which was then attached to the microtome in a Pearse's cryostat, Slee Type HS. The cerebellar tissue was sectioned at −20 C, 15 µm thick sections being used for enzymatic investigations and 6 µm sections being stained with Carazzi haematoxylin-eosin for histological examination.

The sections were studied for LNAse enzyme activity according to the method of *Nachlas et al.* (1957), but without potassium cyanide according to *Barka & Anderson* (1963). The incubation period was 120 min, which gave the optimum of enzyme activity, the incubation temperature was 37 C and the pH varied from 5.5–6.8 (0.1 M acetate buffer) being adjusted approximately to the previously measured pH of the cerebellum under examination.

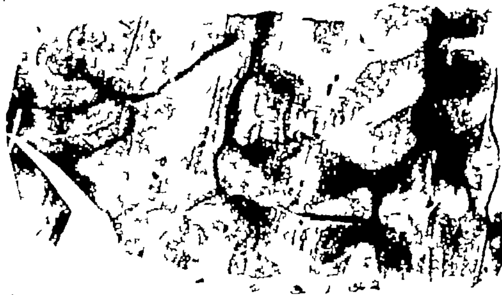
After incubation the sections were washed in distilled water and embedded in glycerin gelatine or coupled with Cu^{++} according to *Barka & Anderson* (1963). In the enzyme reaction the substrate is hydrolyzed with release of betanaphthyl amine which is converted to a reddish azo-compound when coupled to Fast Blue B salt (no. 250 Microne). This reaction product is not stable for any length of time and to prevent diffusion Cu^{++} can be added, resulting in the formation of a more stable copper chelate, which is deep purple in colour (*Pearse* 1972).

Only a water soluble mounting medium (glycerol/gelatine) was used in the present study because the red reaction product becomes more diffuse and the colour fades in alcohol (*Chennoy et al.* 1964).

In order to examine the reproducibility of the enzyme activity, LNAse reaction was performed in consecutive sections.

Histochemical investigations for acid phosphatase were carried out in 24 cases according to the method of *Barka & Anderson* (1963) and autofluorescent microscopy examination in ten cases was carried out on a Reichert fluorescence microscope modified with a wide-angle darkfield oil immersion condenser (light source—Osram HBO 200 lamp).

In order to eliminate the apparent changes of enzyme activity caused by the inevitable variation of section thickness, the cover slips with the mounted sections were cut into two halves. The two parts of the tissue sections having the same thickness were then incubated at different pH



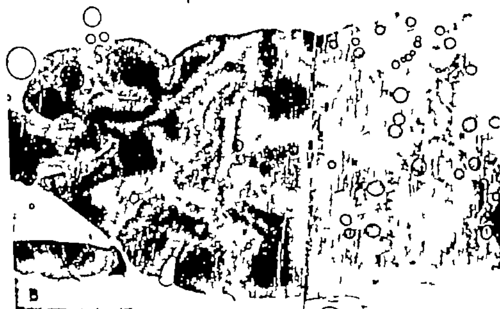


Fig 1 Frozen section of cerebellar cortex. A stained with haematoxylin/eosin B. The coverslip with the mounted section is cut before incubation into two halves and thereafter mounted close together on same glass slide. LNAse activity after incubation for 120 mins at pH 5.8 for the left half and 6.5 for the right half. The highest enzyme activity is seen on the left half and mainly confined to the granular layer × 6

The histochemical demonstration of the enzyme naphthylamidase (LNAse) at pH 5.5–5.8 has been used as an indicator for lysosomes (*Niemi and Sylvén* 1969). Employing this method it has been possible to demonstrate LNAse activity with a pH optimum of 5.5 mainly in the internal granular layer in the cerebellum of rats (*Albrechtsen & Jensen* 1975).

The purpose of the present study is to demonstrate that similar LNAse activity is present in the internal granular layer of cerebellum in human autopsies and to consider the role of the lysosomes in the development of autolysis.

MATERIAL AND METHODS

Cerebella from 70 human subjects were obtained at necropsy by cutting through the cerebral peduncles. pH measurements of the cerebellum were carried out immediately after the necropsy according to the methods previously described (*Albrechtsen* 1977 a). From the geriatric hospitals (De Gamles By and Norre Hospital) mainly cases with pH $<$ 6.0 were collected due to an anticipated high incidence of NGL in these patients (*Albrechtsen* 1977 a). There were 28 cases (16 females and 12 males) with ages ranging from 63–95 years (mean 80.9 years). The time interval from death to necropsy varied from 12–68 hrs. (mean 38.7 hrs.). The most frequent causes of death were arteriosclerotic disorders or neoplasia.

From the Medico-Legal Institute, University of Copenhagen, 42 cases (19 females and 23 males) with age ranging from 7–80 years (mean 44.4 years) were examined. The time lapse from death to necropsy varied from 9–271 hrs. (mean 91.8 hrs.). The causes of death were violent accident (33 cases), homicides (3 cases), suicides (4 cases) and natural causes (2 cases). Of these 25 subjects died instantly either by total rupture of heart wall or aorta (23 cases) or total rupture of the allanto-occipital membrane (? cases).

Bilateral portions of cerebellar hemisphere measuring about $10 \times 5 \times 5$ mm were excised from anterior and posterior lobes, immediately placed in isopentane cooled to −80 C by a freezing mixture of acetone and solid carbon dioxide, and stored at −70 C. The remaining cerebellum was then fixed for at least 15 days at room temperature in a 10 per cent buffered (pH 7.2) formalin solution with glycerin added. After fixation, 2 pieces from both cerebellar hemispheres were dehydrated in alcohol and embedded in paraffin wax by the method previously described (*Albrechtsen* 1977 a). Six µm thick sections were stained with Carazzi haematoxylin-eosin (10 min haematoxylin, 4 min eosin).

The evaluation of NGL was based on the histopathologic criteria given by *Steen Olsen* (1961).

Histochemical Procedure

With a drop of tissue-tek the frozen cerebellar tissue was firmly fixed to the top of a cooled metal chuck, which was then attached to the microtome in a Pearse's cryostat, Slee Type HS. The cerebellar tissue was sectioned at −20 C, 15 µm thick sections being used for enzymatic investigations and 6 µm sections being stained with Carazzi haematoxylin-eosin for histological examination.

The sections were studied for LNAse enzyme activity according to the method of *Nachlas et al.* (1957) but without potassium cyanide according to *Barka & Anderson* (1963). The incubation period was 120 min, which gave the optimum of enzyme activity, the incubation temperature was 37 C, and the pH varied from 5.3–6.8 (0.1 M acetate buffer) being adjusted approximately to the previously measured pH of the cerebellum under examination.

After incubation the sections were washed in distilled water and embedded in glycerin gelatine or coupled with Cu^{++} according to *Barka & Anderson* (1963). In the enzyme reaction the substrate is hydrolyzed with release of betanaphthylamine, which is converted to a reddish azo-compound when coupled to Fast Blue B salt (no. 250 Microne). This reaction product is not stable for any length of time and to prevent diffusion Cu^{++} can be added, resulting in the formation of a more stable copper chelate, which is deep purple in colour (*Pearse* 1972).

Only a water soluble mounting medium (glycerol/gelatine) was used in the present study because the red reaction product becomes more diffuse and the colour fades in alcohol (*Chauncey et al.* 1964).

In order to examine the reproducibility of the enzyme activity LNAse reaction was performed in consecutive sections.

Histochemical investigations for acid phosphatase were carried out in 24 cases according to the method of *Barka & Anderson* (1963) and autofluorescent microscopy examination in ten cases was carried out on a Reichert fluorescence microscope, modified with a wide-angle darkfield oil immersion condenser (light source—Osram HBO 200 lamp).

In order to eliminate the apparent changes of enzyme activity caused by the inevitable variation of section thickness, the cover slips with the mounted sections were cut into two halves. The two parts of the tissue sections having the same thickness were then incubated at different pH

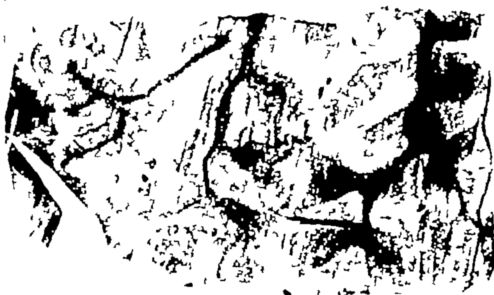




Fig. 1 Frozen section of cerebellar cortex. A. stained with haematoxylin/eosin. B. The coverslip with the mounted section is cut before incubation into two halves and thereafter mounted close together on same glass slide. LNAse activity after incubation for 120 min. at pH 5.8 for the left half and 6.5 for the right half. The highest enzyme activity is seen on the left half and mainly confined to the granular layer × 6

The histochemical demonstration of the enzyme naphthylamidase (LNAse) at pH 5.5–5.8 has been used as an indicator for lysosomes (*Niemi and Sylvén* 1969). Employing this method it has been possible to demonstrate LNAse activity with a pH optimum of 5.5 mainly in the internal granular layer in the cerebellum of rats (*Albrechtsen & Jensen* 1975).

The purpose of the present study is to demonstrate that similar LNAse activity is present in the internal granular layer of cerebellum in human autopsies and to consider the role of the lysosomes in the development of autolysis.

MATERIAL AND METHODS

Cerebella from 70 human subjects were obtained at necropsy by cutting through the cerebral peduncles. pH measurements of the cerebellum were carried out immediately after the necropsy according to the methods previously described (*Albrechtsen* 1977 a). From the geriatric hospitals (De Gamles By and Nørre Hospital) mainly cases with pH < 6.0 were collected due to an anticipated high incidence of NGL in these patients (*Albrechtsen* 1977 a). There were 28 cases (16 females and 12 males) with ages ranging from 63–93 years (mean 80.9 years). The time interval from death to necropsy varied from 12–68 hrs. (mean 38.7 hrs.). The most frequent causes of death were arteriosclerotic disorders or neoplasia.

From the Medico-Legal Institute, University of Copenhagen, 42 cases (19 females and 23 males) with age ranging from 7–80 years (mean 44.4 years) were examined. The time lapse from death to necropsy varied from 9–271 hrs. (mean 91.8 hrs.). The causes of death were violent accidents (33 cases), homicides (3 cases), suicides (4 cases) and natural causes (2 cases). Of these 25 subjects died instantly either by total rupture of heart wall or aorta (23 cases) or total rupture of the allanto-occipital membrane (2 cases).

Bilateral portions of cerebellar hemisphere measuring about 10 × 5 × 5 mm were excised from anterior and posterior lobes, immediately placed in isopentane cooled to −80 C by a freezing mixture of acetone and solid carbon dioxide and stored at − 70 C. The remaining cerebellum was then fixed for at least 15 days at room temperature in a 10 per cent buffered (pH 7.2) formalin solution with glycerin added. After fixation, 2 pieces from both cerebellar hemispheres were dehydrated in alcohol and embedded in paraffin wax by the method previously described (*Albrechtsen* 1977 a). Six µm thick sections were stained with Carazzi haematoxylin-eosin (10 min haematoxylin, 4 min eosin).

The evaluation of NGL was based on the histopathologic criteria given by *Steen Olsen* (1961).

Histochemical Procedure

With a drop of tissue-tek the frozen cerebellar tissue was firmly fixed to the top of a cooled metal chuck, which was then attached to the microtome in a Pearse's cryostat *Slee Type HS*. The cerebellar tissue was sectioned at −20 C. 15 µm thick sections being used for enzymatic investigations and 6 µm sections being stained with Carazzi haematoxylin-eosin for histological examination.

The sections were studied for LNAse enzyme activity according to the method of *Nachlas et al.* (1957), but without potassium cyanide according to *Barka & Anderson* (1963). The incubation period was 120 min, which gave the optimum of enzyme activity, the incubation temperature was 37 C, and the pH varied from 5.3–6.8 (0.1 M acetate buffer) being adjusted approximately to the previously measured pH of the cerebellum under examination.

After incubation the sections were washed in distilled water and embedded in glycerin gelatine or coupled with Cu^{++} according to *Barka & Anderson* (1963). In the enzyme reaction the substrate is hydrolyzed with release of betanaphthylamine which is converted to a reddish azo-compound, when coupled to Fast Blue B salt (no. 250 Michrome). This reaction product is not stable for any length of time and to prevent diffusion Cu^{++} can be added, resulting in the formation of a more stable copper chelate, which is deep purple in colour (*Pearse* 1972).

Only a water soluble mounting medium (glycerol/gelatine) was used in the present study because the red reaction product becomes more diffuse and the colour fades in alcohol (*Chauncey et al.* 1964).

In order to examine the reproducibility of the enzyme activity LNAse reaction was performed in consecutive sections.

Histochemical investigations for acid phosphatase were carried out in 24 cases according to the method of *Barka & Anderson* (1963) and autofluorescent microscopy examination in ten cases was carried out on a Reichert fluorescence microscope modified with a wide-angle darkfield oil immersion condenser (light source—Osram HBO 200 lamp).

In order to eliminate the apparent changes of enzyme activity caused by the inevitable variation of section thickness, the cover slips with the mounted sections were cut into two halves. The two parts of the tissue sections having the same thickness were then incubated at different pH

2

PB

B

B

B

levels, and the enzyme activity could be compared after the incubation by *mounting the paired* cover slips close together on the same glass slide (Fig 1 B)

The enzyme activity was evaluated semiquantitatively immediately after the incubation by assessing the intensity grading from 0–4 as previously described (*Albrechtsen & Jensen* 1973) Control sections were incubated as above but without the specific substrate.

RESULTS

LNAse in Cerebella without NGL

The distribution of LNAse activity was the same in all normal cerebella (49 cases) The staining intensity varied according to the pH of the incubation medium with an only slight individual variation The hight enzyme activity was mainly confined to the internal granular layer (Fig 1B 2)

A marked LNAse activity was seen as 5–10 circular red granules 0.5 μm in diameter surrounding the nuclei of the granule cells (Fig 4) The enzyme activity was also noted as a few red granules corresponding to glomeruli cerebelli Slight diffuse LNAse reaction could be seen in the granular layer Slight enzyme activity was seen localized to the same sites, as the lipofuscin deposits in the cytoplasm of Bergmann glial cells (B) in the perivascular beds (PB) mainly in leptomeninges but also in a few glial cells and perivascular cells within the internal granular layer (Fig 3, 4 and 5 A)

A LNAse *activity was also found in the Purkinje cells (P) seen as small granules* scattered randomly in the cytoplasm and extending into the apical dendrites (Fig 4 5A)

The activity of LNAse coincided with the localization of acid *phosphatase* and autofluorescence of lipofuscin in the Purkinje cell layer (Fig 5) In the granular layer autofluorescent granules were found in the granule cell cytoplasm and also in perivascular cells (Fig 5 C and D)

No acid phosphatase activity was seen in the granule cells (Fig 5 B) Slight LNAse activity was constantly seen in the cytoplasm of the central neurons of cerebellum whereas slight enzyme activity in the central spines was inconsistant. In contrast the molecular layer was almost without any enzyme reaction. Regardless of the cause of death LNAse activity was found in all cases throughout the granular layer without *any demonstrable* variation in the loss of activity in the central and peripheral parts. No cases were found without enzyme activity Cerebella from patients less than 1–2 years old (not included in the present material) however did not reveal any LNAse activity until this layer had been developed (*Albrechtsen* in preparation)

The LNAse activity at different pH levels revealed that the strongest reaction was found at pH 5 8 (Fig. 1 B) with marked activity of the granules surrounding the nuclei of the granule cells. Enzyme activity decreased progressively until pH 4.0 where no activity could be demonstrated Estimated enzyme activity started to fall at pH values greater than 6.0 the colour of the reaction product became less intense and changed from red to yellow

At pH 6.5 an increasing yellowish colouration of all the tissue was found and at pH 7 0 the histochemical reaction was unreadable. No nuclear staining was found.

Cerebella with NGL

The histological examinations showed 21 cases with NGL. The pH of the postmortem

---

Fig 2 LNAse activity after 120 mins incubation at pH 5.8. The darkest zone corresponding to the granular layer represent the highest enzyme activity × 150

Fig 3 LNAse activity after 120 mins incubation at pH 5.8 Slight enzyme activity is seen localized to the same sites, as the lipofuscin deposits in the Bergman glial cells (B) and in the perivascular beds (PB) mainly in leptomeninges, but also in the granular layer (G) × 250.

Fig 4 A marked LNAse activity is seen as circular black granules surrounding the nuclei of the granule cells (arrow) Enzyme activity is also *found in Purkinje cells (P)* and corresponding to lipofuscin deposits both in the Purkinje cell layer (B) and the granular layer (G) *120 mins incubation* at *pH* 5 8 × 480

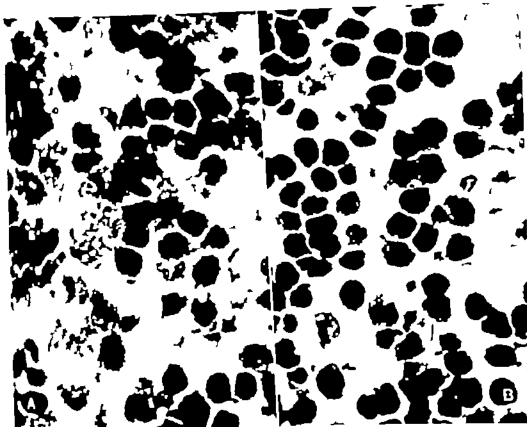


Fig. 6 A. Frozen section from cerebellar cortex. Granule cells with intra- and extra nuclear vacuole-formation. *Fig. B.* Areas with granule cells without vacuoles. Haematoxylin/eosin. × 1000

cerebella of all these cases was less than 6.0, significantly lower than the mean pH (6.4) of the cases without NGL ($p < 0.00003$ Mann-Whitney U-test).

All but one of the 21 cases showed both intra and extranuclear vacuole formation in the granule cells with early destruction of the nuclei. This was apparent in several frozen sections, but only in small areas (Fig. 6). Vacuole formation was significantly more frequent in cerebella with NGL compared with those without NGL ($p < 0.0005$ Chi-square-test) where minimal vacuole formation was only identified in 7 of the 49 cases.

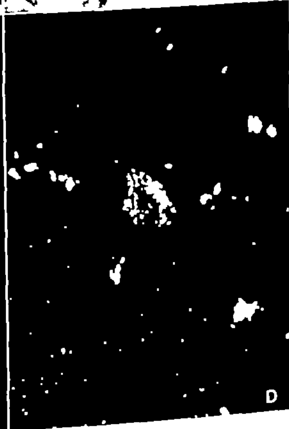
The diagnosis of NGL could be made by frozen sections in only 5 cases at the time of the autopsy and 19 cases with NGL was first revealed in the conventional formalin fixed paraffin sections mainly in the central part of cerebellum (Fig. 7A, C). In 2 cases NGL was found only in frozen sections and not in the paraffin sections. NGL was expected, but not observed in 9 cases with $pH < 6.0$

According to increasing activity at low pH a marked LNAse in the granular layer was found in 19 out of the 21 cases with NGL. In the four cases where NGL changes were

Fig. 5 A. LNAse activity in Purkinje cell (P) and the granule cells (G) after incubation for 120 mins at pH 5.8. *Fig. 5 B.* Acid phosphatase activity localized in Purkinje cell (P) as small black granules scattered randomly in the cytoplasm. Lipofuscin deposits are enzyme positive in a glial cell (B) left for the Purkinje cell. × 810.

Fig. 5 C D. Autofluorescent granules in Purkinje cell, Bergman glial cells and granule cells × 950 (C) × 600 (D)


C


D

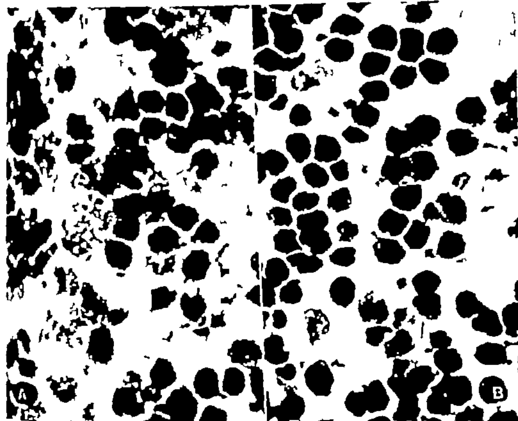


Fig 6 A. Frozen section from cerebellar cortex. Granule cells with intra- and extra nuclear vacuole-formation. *Fig B* Areas with granule cells without vacuoles Haematoxylin/eosin. × 1000

cerebella of all these cases was less than 6.0 significantly lower than the mean pH (6.4) of the cases without NGL ($p < 0.00003$ Mann-Whitney U-test)

All but one of the 21 cases showed both intra- and extranuclear vacuole formation in the granule cells with early destruction of the nuclei. This was apparent in several frozen sections, but only in small areas (Fig. 6) Vacuole formation was significantly more frequent in cerebella with NGL compared with those without NGL ($p < 0.0005$ Chi-square-test) where minimal vacuole formation was only identified in 7 of the 49 cases.

The diagnosis of NGL could be made by frozen sections in only 5 cases at the time of the autopsy and 19 cases with NGL was first revealed in the conventional formalin fixed paraffin sections mainly in the central part of cerebellum (Fig. 7A, C) In 2 cases NGL was found only in frozen sections and not in the paraffin sections. NGL was expected, but not observed in 9 cases with $pH < 6.0$

According to increasing activity at low pH a marked LNAse in the granular layer was found in 19 out of the 21 cases with NGL. In the four cases where NGL changes were

---

Fig. 5 A LNAse activity in Purkinje cell (P) and the granule cells (G) after incubation for 120 mins at pH 5.8 *Fig 5 B.* Acid phosphatase activity localized in Purkinje cell (P) as small black granules scattered randomly in the cytoplasm. Lipofuscin deposits are enzyme positive in glial cell (B) left for the Purkinje cell. × 810

Fig. 5 C D Autofluorescent granules in Purkinje cell, Bergmann glial cell and granule cells × 950 (C) × 600 (*D*)

apparent in the frozen sections, histochemistry showed a decreased and more diffuse LNAse activity, while at the same time intranuclear enzyme activity occurred. In some of the vacuoles slight LNAse activity could be demonstrated (Fig 8 C)

Supplementary experiments of cerebella without NGL changes showed a similar increase in LNAse activity in the granular layer when incubation was carried out at pH 5.8 The semiquantitative evaluation of mean LNAse activity of the internal granular layer in all 70 cases can be seen in Fig 9 The enzyme activity is shown as the mean value of the two cerebellar hemispheres. A significant negative correlation coefficient was found between LNAse activity and increasing pH ($R(S) = -0.542$ $T = -5.312$ 68 degrees of freedom $p < 0.001$ Spearman rank correlation)

After 24 hours formalin fixation persistent LNAse activity was found in one undissected cerebellum with NGL (not included in the present 70 cases) except for the granular layer near the surface, where only inconspicuous enzyme activity could be demonstrated (Fig 10)

The control sections were all without LNAse activity

Only insignificant diffusion was observed to the molecular layer in the first 2 days after incubation, if the sections were preserved in a refrigerator

Preservation for more than a month disclosed a decreased LNAse activity mainly in the sections incubated at low pH (< 6.0) whereas the slides incubated at higher pH was more unchanged

DISCUSSSION

The histochemical findings in the present study show a distinct LNAse activity with a low pH optimum of 5.8 predominantly localized in the internal granular layer of cerebellum.

Adams & Glenner (1962) investigated the LNAse localization in the central nervous system but found that the method using Garnet GBC as diazo-compound was not applicable (*Adams* 1966 pp 289 367) This may explain why only a few reports on histochemical demonstration of LNAse in central nervous system have been published since then (*Glussc* 1963 *Vanha Perttula & Hopsu* 1966 *Fischer* 1970 *Cabrielescu & Bordianu* 1971 *Poberai et al* 1972 (peripheral nerves) and *Albrechtsen & Jensen* 1975) and none concerning human cerebellum.

Biochemical investigations have generally revealed a separate naphthylamidase present in the lysosome fraction (*Sylvén & Bois-Svensson* 1964 *Mahadevan & Tappel* 1967 *Idal & Taljedal* 1968)

Cytochemically *Glussc* (1963) showed increased LNAse activity in areas of degenerations in relation to tumours of the central nervous system The pattern of this enzyme activity in the degenerative areas was found to be similar to that of acid phosphatase and non specific esterase, but *Glussc* did not mention the consequence of this observation. *McCape & Chayen* (1965) demonstrated LNAse activity akin to lysosomal particles in rat liver kidney and small intestine finding increased activity after pretreatment with acetate buffer at pH 5.0 Sylvén and coworkers showed in a series of reports (see *Pearse* 1972 p 197) that the LNAse-reaction, carried out at pH 5.5 could reveal cytochemically both lysosomes and autolytic vacuoles (*Niemi & Sylvén* 1969) In the present report the LNAse properties are characterized

---

Fig 7 A Conventional formalin fixed paraffin section from cerebellar hemisphere Paling of the granular layer indicating NGL is found increasing toward the deeper portion of the cerebellum with sparring of the most peripheral part of the section. × 76

Fig 7 C Well preserved granule cells from the peripheral part of Fig 7 A × 300

Fig 7 C From the deeper portion of Fig 7 A. Demonstrating "Status bullosus" Most of the nuclei of the granul cells have disappeared and the remainder are greatly altered with a large number of vacuoles Haematoxylin/eosin × 300



B

apparent in the frozen sections histochemistry showed a decreased and more diffuse LNAse activity while at the same time intra nuclear enzyme activity occurred. In some of the vacuoles slight LNAse activity could be demonstrated (Fig 8 C)

Supplementary experiments of cerebella without NGL changes showed a similar increase in LNAse activity in the granular layer when incubation was carried out at pH 5.8 The semiquantitative evaluation of mean LNAse activity of the internal granular layer in all 70 cases can be seen in Fig. 9 The enzyme activity is shown as the mean value of the two cerebellar hemispheres. A significant negative correlation coefficient was found between LNAse activity and increasing pH ($R(S) = -0.542$ $T = -5.312$ 68 degrees of freedom, $p < 0.001$ Spearman rank correlation)

After 24 hours formalin fixation persistent LNAse activity was found in one undissected cerebellum with NGL (not included in the present 70 cases) except for the granular layer near the surface where only inconspicous enzyme activity could be demonstrated (*Fig 10*)

The control sections were all without LNAse activity

Only insignificant diffusion was observed to the molecular layer in the first 2 days after incubation, if the sections were preserved in a refrigerator

Preservation for more than a month disclosed a decreased LNAse activity mainly in the sections incubated at low pH (< 6.0) whereas the slides incubated at higher pH was more unchanged.

DISCUSSSION

The histochemical findings in the present study show a distinct LNAse activity with a low pH optimum of 5.8 predominantly localized in the internal granular layer of cerebellum.

Adams & Glenner (1962) investigated the LNAse localization in the central nervous system but found that the method using Garnet GBC as diazo-compound was not applicable (*Adams* 1966 pp 289 367) This may explain why only a few reports on histochemical demonstration of LNAse in central nervous system have been published since then (*Glussc* 1963 *Vanha Perttula & Hopsu* 1966 *Fischer* 1970 *Gabrielescu & Bordianu* 1971 *Poberai et al* 1972 (peripheral nerves) and *Albrechtsen & Jensen* 1975) and none concerning human cerebellum.

Biochemical investigations have generally revealed a separate naphthylamidase present in the lysosome fraction (*Sylvén & Bois-Svensson* 1964 *Mahadevan & Tappel* 1967 *Idal & Taljedal* 1968)

Cytochemically *Gluszcz* (1963) showed increased LNAse activity in areas of degenerations in relation to tumours of the central, nervous system. The pattern of this enzyme activity in the degenerative areas was found to be similar to that of acid phosphatase and non specific esterase, but *Gluszcz* did not mention the consequence of this observation *McCabe & Chayen* (1965) demonstrated LNAse activity akin to lysosomal particles in rat liver kidney and small intestine finding increased activity after pretreatment with acetate buffer at pH 5.0 Sylvén and coworkers showed in a series of reports (see *Pearse* 1972 p 197) that the LNAse-reaction, carried out at pH 5.5 could reveal cytochemically both lysosomes and autolytic vacuoles (*Niemi & Sylvén* 1969) In the present report the LNAse properties are characterized

---

Fig 7 A Conventional formalin fixed paraffin section from cerebellar hemisphere Paling of the granular layer indicating *NGL is found increasing* toward the deeper portion of the cerebellum with sparring of the most peripheral part of the section. × 76

Fig 7 C Well preserved granule cells from the peripheral part of Fig 7 A × 300

Fig 7 C From the deeper portion of Fig 7 A. Demonstrating "Status bullosus" *Most of the nu*clei of the granule cells have disappeared and the remainder are greatly altered with a large number of vacuoles. Haematoxylin/eosin × 300

by the following findings, which suggest a lysosomal localization.

1. the enzyme optimum was found at low pH about 5.8.
2. enzyme localization was focally confined to small particles in the cytoplasm
3. enzyme reaction was also found in the same sites as lipofuscin deposits, which are known to be engulfed in lysosomes, and in the same sites as acid phosphatase (*Olsen & Petri* 1963)
4. long incubation time (60–120 mins) was necessary to obtain optimal enzyme activity this being the length of time required for the substrate to pass through the lysosomal membrane.
5. the LNAse activity was preserved with unchanged activity even many hours after death. Lysosomal enzymes similarly share an unusual resistance to autolysis (*de Duve & Beaufay* 1959)

Olsen & Petri (1963) demonstrated acid phosphatase localized in cerebella from human autopsies in the same place as LNAse distribution, but found activity in the granule cells in only a few cases The difference between the distribution of two lysosome markers could be explained by acid phosphatase being released earlier from the lysosomes in the granule cells than from the Purkinje cells and Bergmann glial cells. In experimental autolysis, acid phosphatase had already been released after 30 mins in biochemical studies (*van Lancker & Holtzer* 1959) and after 4–24 hours in histochemical studies (*Lazarus et al.* 1962) Another factor which precluded a direct comparison between the two lysosome markers is the variation in the

Fig. 8 A Frozen section with vacuole formation and slight necrosis of the granular layer Haematoxylin/eosin × 1000

Fig. 8 B. LNAse activity from same area as Fig A. with decreased enzyme reaction. 120 mins incubation at pH 5.8 × 1000

Fig. 8 C Alteration of the LNAse activity pattern with several LNAse positive vacuoles (V) × 1300.

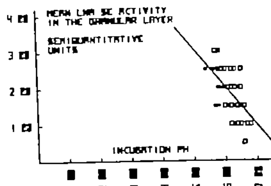


Fig 9 Semiquantitative evaluation of mean LNAse activity of the granular layer in 70 cases. The enzyme activity is shown as the mean value of the two cerebellar hemispheres Negative correlation coefficient was found between LNAse activity and increasing pH ($p < 0.001$ R(S) = —0.542, T = —5.312, 68 degrees of freedom, Spearman rank correlation) • cases with NGL. ▫ cases without NGL

type of hydrolytic enzymes in brain lysosomes in different areas, as demonstrated by *Sellinger & Hiatt* (1968)

Electron microscopical investigations of human cerebellar cortex has confirmed the presence of lysosome-like bodies around the granule cell nuclei (*Dahl et al.* 1962)

The use of LNAse as a lysosome marker should therefore be the enzyme of choise in histochemical studies of the internal granular layer

Biochemical studies of naphthylamidase in cerebellum have been carried out (*Marks* 1968, *Marks et al* 1968) but without isolation of a particularly well defined LNAse in lysosomes of the granule cells.

The findings of NGL predominantly in the conventional formalin fixed tissue and not in the frozen sections at the time of the autopsy is in accordance with the previous experiments (*Albrechtsen* 1975) showing development of NGL during formalin fixation mainly in the regions which are furthest away from the fixative. This change could, however be prevented by cutting the cerebellar tissue before fixation, thus explaining the small number of cases with NGL in the present series (absence of NGL in 9 cases with

B

V

V

C

ly the following findings, which suggest a lysosomal localization.

1 the enzyme optimum was found at low pH about 5.8.
2 enzyme localization was focally confined to small particles in the cytoplasm.
3 enzyme reaction was also found in the same sites as lipofuscin deposits, which are known to be engulfed in lysosomes, and in the same sites as acid phosphatase (*Olsen & Petri* 1963)
4 long incubation time (60–120 mins) was necessary to obtain optimal enzyme activity this being the length of time required for the substrate to pass through the lysosomal membrane.
5 the LNAse activity was preserved with unchanged activity even many hours after death. Lysosomal enzymes similarly share an unusual resistance to autolysis (*de Duve & Beaufay* 1959)

Olsen & Petri (1963) demonstrated acid phosphatase localized in cerebella from human autopsies in the same place as LNAse distribution, but found activity in the granule cells in only a few cases The difference between the distribution of two lysosome markers could be explained by acid phosphatase being released earlier from the lysosomes in the granule cells than from the Purkinje cells and Bergmann glial cells. In experimental autolysis, acid phosphatase had already been released after 30 mins in biochemical studies (*van Lancker & Holtzer* 1959) and after 4–24 hours in histochemical studies (*Lazarus et al.* 1962) Another factor which precluded a direct comparison between the two lysosome markers is the variation in the

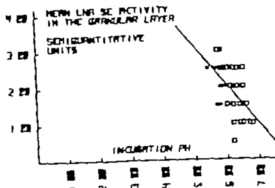


Fig 9 Semiquantitative evaluation of mean LNAse activity of the granular layer in 70 cases. The enzyme activity is shown as the mean value of the two cerebellar hemispheres. Negative correlation coefficient was found between LNAse activity and increasing pH ($p < 0.001$ R(S) = −0.542, T = −5.312, 68 degrees of freedom, Spearman rank correlation) * cases with NGL, ◻ cases without NGL

type of hydrolytic enzymes in brain lysosomes in different areas, as demonstrated by *Sellinger & Hiatt* (1968)

Electron microscopical investigations of human cerebellar cortex has confirmed the presence of lysosome-like bodies around the granule cell nuclei (*Dahl et al.* 1962)

The use of LNAse as a lysosome marker should therefore be the *enzyme of choise in* histochemical studies of the internal, granular layer

Biochemical studies of naphthylamidase in cerebellum have been carried out (*Marks* 1968, *Marks et al* 1968) but without isolation of a particularly well defined LNAse in *lysosomes of the granule cells.*

The findings of NGL predominantly *in the* conventional formalin fixed tissue and not in the frozen sections at the time of the autopsy is in accordance with the previous experiments (*Albrechtsen* 1975) showing development of NGL during formalin fixation mainly in the *regions* which are furthest away from the fixative. This change could, however be prevented by cutting the cerebellar tissue before fixation, thus explaining the small number of cases with NGL in the present series (absence of NGL in 9 cases with

Fig 8 A Frozen section with vacuole formation and slight necrosis of the granular layer Haematoxylin/eosin. × 1000

Fig 8 B. LNAse activity from same area as Fig A. with decreased enzyme reaction. 120 mins incubation at pH 5.8 × 1000

Fig 8 C Alteration of the LNAse activity pattern with several LNAse positive vacuoles (V) × 1500

B

C

e Acid phosphatase failed to demonstrate lysosomes in the internal granular layer possibly due to early release from these organelles.

Considering the correlation of NGL to higher postmortem acidity and temperature (*Ikuta et al.* 1963) the present findings suggest that this phenomenon, like other types of autolysis, is caused by the action of different proteolytic enzymes released from the lysosomes in the internal granular layer.

REFERENCES

Adams, C W M Neurochemistry Elsevier Publishing Company Amsterdam, London, New York 1965 p. 140 289 312, 367

Adams, C W M & Glenner G G Histochemistry of myelin-IV Aminopeptidase activity in CNS and PNS. J Neurochem 9 233–239 1962.

Albrechtsen, R. Loss of nuclear density of the granule cell of cerebellum during conventional immersion fixation simulating acute selective necrosis of the granular layer Proc. VIIth Intern. Congr Neuropath Budapest 1974 Excerpta medica Amsterdam II, pp 269–272, 1975.

Albrechtsen, R. The pathogenesis of acute selective necrosis of the granular layer of the human cerebellar cortex. Acta neuropath (Berl) 37 31 34 1977 a.

Albrechtsen, R. The incidence of the so-called acute selective necrosis of the granular layer of cerebellum in 1000 autopsied patients Acta path. microbiol scand Sect A, 85 193–202 1977 b.

Albrechtsen, R. & Jensen H Histochemical demonstration of an LNA-splitting enzyme in the cerebellum of the rat Acta path. microbiol. scand. Sect A, 83 503 510, 1975

Barrett A J Peptidases and amidases In Dingle, J T & Fell, H B (Ed) Lysosomes in biology and pathology ol 2 North-Holland publishing company Amsterdam, London 1969 p. 282 312

Barka, R. & A derson P J Histochemistry Hoeber New York 1963

Bradley H C Studies of autolysis VIII The nature of autolytic enzymes J biol. Chem 52 467–484 1922

Bradley H C Autolysis and atrophy Physiol. Rev 18 173 196 1938.

Chauncey H H Smarsh A & Kronman J H False cellular localization of aminopeptidase caused by reamous mounting media. Stain Technol 39 131 134 1964

Dahl, I., Olsen, S & Birch-Andersen A. The fine structure of the granular layer in the human cerebellar cortex. Acta Neurol. Scand 38 81–97 1962.

De Duve C & Beaufay H. Tissue fractionation studies. 10 Influence of ischaemia on the state of some bound enzymes in rat liver J Biochem. 73 610–616 1959

Duren K C Events in dying cells. Proc. roy Soc. Med. 60 271—275 1967

Fischer F E Lokalisation der leucyl-aminopeptidase (LAP) beim blutegel (Hirudo medicinalis L.) und beim pferdeegel (Haemopis sanguisuga L) Acta histochem. 37 170–175 1970.

Gabrielescu E & Bordeianu A La réactivité des cathepsines du tissu nerveux et leur intégration dans les mécanismes cellulaires d'adaptation au stress. Ann, Histochim. 16 119–128, 1971

Glenner A A histochemical study of some hydrolytic enzymes in tumours of the nervous system. Acta Neuropath. 3 184–201 1963

Idahl L Å & Täljedal, I B Leucyl-β-naphthylamide-Splitting enzymes in the mammalian endocrine pancreas Biochem. J 106 161–163 1968.

Ikuta F., Hirano A & Zimmerman H M An experimental study of postmortem alterations in the granular layer of the cerebellar cortex. J Neuropath. exp. Neurol. 22 581–593 1963

Koenig, R S & Koenig, H An experimental study of post mortem alterations in neurons of the central nervous system J Neuropath. exp. Neurol. 11 69–78, 1952.

Lazarus S S Wallace B. J Edgar G W F & Volk B W. Enzyme localization in rabbit cerebellum and effect of post mortem autolysis. J Neurochem. 9 227–232, 1962.

Lindenberg, R Morphotrophic and morphostatic necrobiosis. Investigation on nerve cells of the brain Amer. J Path. 32 1147–1177 1956.

Mahadevan, S & Tappel A. L. Arylamidase of rat liver and kidney J Biol. Chem. 242 2369–2374 1967

Marks N Exopeptidases of the nervous system. International review of neurobiology Academic press New York and London. 11 57–97 1968.

Marks N., Datta, R K & Lajtha A. Partial resolution of brain arylamidases and aminopeptidases. J Biol. Chem. 243 2882–2889 1968.

M Cabe M & Chayen J. The demonstration of latent particulate aminopeptidase activity J Roy Microscop. Soc. 84 361–371 1965

Nachlas M N., Crawford D T & S Eymen A M. The histochemical demonstration of leucine aminopeptidase. J Histochem. Cytochem. 5 264–278, 1957

Nemes, M & Sylvén B. The naphthylamidase reaction as a diagnostic tool for the demonstra-

pH < 6 0) because it was necessary to cut the cerebellum on both sides in order to remove tissue for histochemical investigation of LNAse activity The NGL is nearly preceeded by the presence of small vacuoles in the granule cells previously found in the frozen sections. Similar changes are often mentioned as the first sign in the development of autolysis shown in experimental studies (*Koenig & Koenig* 1952, *Lindenberg* 1956 *Pribor* 1956 *Dixon* 1967) and in human material (*Pakkenberg & Vraa Jensen* 1964 *Albrechtsen* 1977 b) *Lindenberg* (1956) found such vacuole formation absent or only slight developed in autolytic cells previously made anoxic in vivo

Bradley (1922 1938) demonstrated the importance of tissue acidity to accelerate autolysis in liver and explained that it was caused by increased proteolytic activity

The postmortem acidity of cerebellum has been demonstrated previously (*Albrechtsen* 1977 a) and in the present study to be the most decisive factor in the production of NGL

In the later stages of development of NGL thus autodigestion will be enhanced by the increasing acidity of the tissue, and protein breakdown will continue possibly for several days even during the conventional formalin fixation Hence the most severe changes of NGL will be found in the central part of the cerebellum (*Albrechtsen* 1975) as in the present material

CONCLUSION

Lysosome-like bodies mainly localized in the internal granular layer of cerebellum were demonstrated by the use of LNAse as a mark





Fig 10 A LNAse activity (120 mins incubation at pH 5 8) after 24 hours formalin fixation of an uncuted cerebellum A Area from the peripheral part of the cerebellar cortex with remaining LNAse activity only corresponding to lipofuscin deposits.

Fig 10 B Areas from the deeper portion of the cerebellar hemisphere with well preserved *enzyme*

Acta path. microbiol. scand. Sect. A, 85 889–896 1977

TRANSTHORACIC ASPIRATION BIOPSY

A Study on Diagnostic Reproducibility

DORTHE FRANCIS and KNUD HØJGAARD

Institute of Pathological Anatomy Bispebjerg Hospital, Copenhagen

Francis, D & Højgaard, K. Transthoracic aspiration biopsy A study on diagnostic reproducibility Acta path. microbiol. scand. Sect. A, 85 889–896, 1977

Based on a randomized material of 100 histologically verified transthoracic aspiration biopsies an inter and intraobserver variation study was carried out by the two investigators. The results showed a high degree of diagnostic reproducibility pointing towards the value of the aspiration biopsy *per se* It is concluded that this diagnostic method is reliable in the hands of the expert and useful even in the hands of a pathologist only given a short introduction to—and a reasonable amount of correction within—this special field.

Key words Aspiration biopsy transthoracic reproducibility

Dorthe Francis, Snebærvænget 13 DK-2850 Virum.

Received 24.iii.77 Accepted 26.vi.77

In previous reports (2, 3) concerning transthoracic aspiration biopsies we have described the sensitivity and the specificity of our results regarding the diagnosis malignant tumour cells When introducing, and especially when recommending, a diagnostic method reproducibility of the results is a reasonable requirement (6) The reproducibility has naturally been continually controlled. However the present study represents a systematic inter and intraobserver variation investigation applied to a randomized material of 100 histologically verified transthoracic aspiration biopsies.

By interobserver variation is understood the discrepancies in diagnostic results between the two investigators

By intraobserver variation is understood the discrepancies in diagnostic results obtained at two different readings of the same material by the same investigator (6)

MATERIAL AND METHODS

The present material consists of 100 biopsies from our previously reported material of 227 histologically verified transthoracic aspiration biopsies (2) The selection was performed at random from Geigy's tables (1)

From each of the 100 cases an independent pathologist with experience in cytology chose one or two of the most suitable smears. To secure objectivity only May-Grünwald-Giemsa and Papanicolaou stained smears were made available.

All identification marks on the glass-slides were sufficiently covered and each biopsy was renumbered in casual order before they were handed over to the authors.

Both authors are specialists in pathology One (DF) has worked with diagnostic aspiration cytology for 5 years, the other (KH) is experienced in exfoliative cytology The latter's knowledge concerning aspiration cytology was limited to an introduction to this special subject lasting two weeks. This introduction covered cases not included in the present investigation.

When the authors had independently reviewed the material, the biopsies were renumbered for a second reading starting one month later

tion of cellular injury and autophagy Histochemie *18* 40–47 1969

Okazaki H Aroka I & Aronson S M Acute selective necrosis of the cerebellar internal granular layer Trans. Am. neurol Ass. *86* 181–183 1961

Olsen S Acute selective necrosis of the granular layer of the cerebellar cortex. J Neuropath exp Neurol. *18* 609—619 1959

Olsen S & Petri C Histochemical localization of acid phosphatase in the human cerebellar cortex. Acta Neurol scand *39* 112–122 1963

Pakkenberg H & Vraa-Jensen J Cytoplasmic basophilia in the nerve cells of the cerebral cortex. V Autolysis of RNA and inhibition of glycolysis. Acta Neuropath. *3* 211–?16 1964

Pearse A G E Histochemistry theoretical and applied. 3 ed Churchill Livingstone Edinburgh and London 1972 p 962–980

Poberai M Sávay G & Csillik B Function-dependent proteinase activity in the neuromuscular synapse Neurobiology *2* 1–7 1972

Pribor H C Post mortem alterations in autonomic ganglion. J Neuropath exp Neurol *15* 79–84 1956

Sellinger O Z & Hiatt R A Cerebral lysosomes. IV The regional and intracellular distribution of arylsulfatase and evidence for two populations of lysosomes in rat brain. Brain Research. 7 191–200 1968

Sylvén B & Bois-Svensson I Studies on the histochemical "leucine aminopeptidase" reaction. IV Chemical and histochemical characterization of the intracellular and stromal LNA reactions in solid tumor transplants. Histochemie *4* 135–149 1964

Van Lancker J L & Holtzer R L The release of acid phosphatase and beta-glucuronidase from cytoplasmic granules in the early course of autolysis. Amer J Path. *35* 563–573 1959

Vanha-Perttula T P J & Hopsu V K Esterolytic and proteolytic enzymes of the rat adenohypophysis. II Chromatographic fractionation and characterization of enzyme activities hydrolysing leucyl β-naphtylamide. Ann. Med exp. Fenn *43* 32–39 1965

TABLE 1 *Relevant Probabilities Concerning the Accuracy of Diagnosing Malignant Tumour Cells, Inter- and Intraobserver Variation Study in 100 Cases of Randomized Transthoracic Aspiration Biopsies*

	DF 1 reading	DF 2' reading	KH 1 reading	KH 2' reading
True Positive Biopsy (TP)	71	71	60	61
False Positive Biopsy (FP)	0	0	2	1
True Negative Biopsy (TN)	19	19	17	18
False Negative Biopsy (FN)	10	10	21	20
Sensitivity $\frac{TP}{TP+FN}$ per cent	71/81 87.7 (78.47–93.92)	71/81 87.7 (78.47–93.92)	60/81 74.1 (63.14–83.18)	61/81 75.3 (64.47–84.22)
Specificity $\frac{TN}{TN+FP}$ per cent	19/19 100 (82.35–100)	19/19 100 (82.35–100)	17/19 89.5 (66.86–98.70)	18/19 94.7 (73.97–99.87)
PV positive $\frac{TP}{TP+FP}$ per cent	71/71 100 (94.94–100)	71/71 100 (94.94–100)	60/62 96.8 (88.83–99.61)	61/62 98.4 (91.34–99.96)
PV negative $\frac{TN}{TN+FN}$ per cent	19/29 65.5 (45.67–82.06)	19/29 65.5 (45.67–82.06)	17/38 44.8 (28.62–61.70)	18/38 47.4 (30.98–64.18)

PV positive being the predictive value of a positive result.
PV negative being the predictive value of a negative result.
Figures in brackets being the 95 per cent confidence limits.

The biopsies were grouped as follows

I Biopsies containing malignant tumour cells
  a) epidermoid carcinoma
  b) small cell anaplastic carcinoma
  c) adenocarcinoma
  d) undifferentiated carcinoma
  e) tumours other than a b, c and d
II Biopsies containing cells suspected of malignancy
III Biopsies containing benign tumour cells.
IV Biopsies containing cells from granulomatous lesions
V Biopsies containing cells from acute inflammation.
VI Biopsies containing miscellaneous material excluded from the above groups. Included were also biopsies with non-diagnostic material.

Each biopsy was registered in only one of the six main groups, group I being superior to group II etc.

For each biopsy in group I a cytological classification of the malignant tumour cells was carried out following the system previously reported (4)

In the present investigation restaining for identification of microorganisms did not take place due to lack of available cytological specimens

The 100 biopsies represent 100 patients. Based on the histological findings there were 81 cases of malignant intrathoracic tumours and five cases of benign tumours In seven cases granulomatous lesions were found and the last seven cases comprised the following lesions abscess (two cases) pneumocystis carinii (one case) pulmonary infarction (one case) and localized fibrosis (three cases)

The original cytological diagnoses were malignant tumour cells in 68 cases cells suspected of malignancy in 6 cases, benign tumour cells in 4 and no tumour cells in 22 cases. The 68 biopsies positive for malignant tumour cells were in agreement with the histological diagnoses. The sensitivity and the specificity for this part of the total material of 22 biopsies (2) thus being 84 and 100 per cent respectively

The interobserver variation study is based on the results from the first reading of each investigator The significance of the results will be expressed in the terms of Vecchio (5 6)

RESULTS

Interobserver Variation Study

Malignant tumour cells As shown in *Table 1* and Fig 1 a the experienced investigator (DF) had more biopsies with malignant tumour cells than did the inexperienced (KH) The sensitivity and the specificity are higher for DF than for KH the difference however being insignificant ($p > 0.05$)

Overreading KH found malignant tumour cells in two instances of histologically benign tumours (false positives) DF having no false positives

Underreading False negatives in 10 instances with DF (12 per cent) and in 21 with KH (25 per cent) the difference being insignificant ($p > 0.05$)

Cells suspected of malignancy Based on the first readings, cells suspected of malignancy were diagnosed in three biopsies by DF and in four by KH. The biopsies represent six patients with histologically malignant tumours, agreement between the investigators being found in one case.

Benign tumour cells DF found benign tumour cells in four cases of histologically benign tumours. KH had no such diagnosis.

Granulomatous lesion DF had five biopsies with this cytological diagnosis.

KH had no such diagnosis.

Cells from acute inflammation This cytological diagnosis was used in two biopsies by DF and in two biopsies by KH agreement being found in one instance

Miscellaneous cytological diagnosis (numbers in brackets being false negative biopsies) This diagnosis was used in the first reading by DF in 15 (7) biopsies, and by KH in 32 (15) biopsies agreement was found in 14 (6) biopsies.

Intraobserver Variation Study

Malignant tumour cells Full agreement between the first and the second readings by DF is shown in Fig 1 b

Comparison between the first and the second readings by KH shows that the 62 biopsies with malignant tumour cells in the first reading were registered in the second reading as 56 biopsies with malignant tumour cells and six without (Fig 1 c) Of the six biopsies diagnosed as negative in the second reading five were false negatives. One biopsy registered as positive in both readings was histologically a benign tumour (fibrous tumour)—false positive The 38 biopsies

Fig 1 Results of inter- and intraobserver study in 100 cases of randomized transthoracic aspiration biopsies.

The biopsies are in addition registered according to the final histological diagnoses, using the following signatures ● = malignant tumour ○ = benign tumour. ▲ = granulomatous lesion. △ = acute inflammation. □ = others (pneumocystic carini, pulmonary infarction and localized fibrosis)

---

without malignant tumour cells in the first reading were in the second registered as 32 biopsies without malignant tumour cells and six biopsies with malignant tumour cells. These six biopsies being false negatives in the first reading. Full agreement was obtained by DF, an 82 per cent agreement by KH, the difference being significant ($p < 0.05$)

Consistency in the malignant tumour cell diagnosis was obtained by DF in 71 biopsies out of the 81 histologically malignant cases (88 per cent) for KH the consistence being 55 out of 81 (68 per cent) The difference was significant ($p < 0.05$)

The number of positive biopsies in at least one of the readings was for KH 66 (81 per cent) the number of false positives unchanged.

Cells suspected of malignancy In the first reading DF found cells suspected of malignancy in three biopsies, in the second reading the corresponding diagnoses were suspected cells in one biopsy and no tumour cells in two biopsies. In the second reading suspected cells were found in two biopsies, the corresponding diagnoses in the first reading being suspected cells in one and no tumour cells in the other agreement thus being found in one instance. All the biopsies mentioned were from malignant tumours.

In the first reading KH found cells suspected of malignancy in four biopsies, which in the second were diagnosed in two instances as malignant tumour cells and as no tumour cells in two. In the second reading KH found suspected cells in two biopsies, both having been found negative in the first reading. No agreement was found. The six biopsies represented six cases of tumours, five malignant and one benign (histiocytoma)

Presuming that biopsies containing cells suspected of malignancy had been included as positive, the number of true positive biopsies found in at least one of the readings of DF would increase from 71 to 75 out of the 81 malignant cases (93 per cent) for KH the number would increase from 55 to 70 (86 per cent) This presumption would cause no false positives for DF while in the case of KH one false positive would be added.

Benign tumour cells In both readings DF found benign tumour cells in the same four biopsies agreement in 100 per cent. The four biopsies originated from four patients with benign tumours

The benign tumour cell diagnosis was not used by KH in first reading, twice in the second no agreement. The histological diagnosis in these two cases were benign tumour in one and malignant tumour in one (false negative)

Granulomatous lesion In both readings DF had five biopsies with this cytological diagnosis. These biopsies represented seven cases, agreement been found in three cases, two of which were histologically granulomatous lesions, one a localized fibrosis. The four cases showing inconsistance represented two cases of granulomatous lesions and two cases of malignant tumours.

Cells from acute inflammation DF found acute inflammation in the same two biopsies in both readings full agreement. In both cases the histological diagnosis was abscess without malignancy.

KH used this diagnosis twice in the first reading, both being reproduced in the second. In the second reading KH diagnosed one more which in the first reading was diagnosed as no tumour cells. Agreement was thus found in two out of three cases. The three biopsies represented one case of an abscess (full agreement) and two cases of malignant tumours.

Miscellaneous cytological diagnosis (numbers in brackets being false negative biopsies) The miscellaneous diagnosis was used by DF in the first reading in 15 (7) biopsies which in the second reading had the

a INTEROBSERVATION DF$_1$ KH$_1$

DF$_1$ \ KH$_1$	Malignant Tumour Cells	Cells Suspected of Malignancy	Benign Tumour Cells	Granulomatous Lesion	Acute Inflammation	Miscellaneous Cyt Diagnosis
Malignant Tumour Cells	● 60	● 3				● 8
Cells Suspected of Malignancy		● 1				● 2
Benign Tumor Cells	○ 2					○ 2
Granulomatous Lesion						▲ 4 □ 1
Acute Inflammation					△ 1	△ 1
Miscellaneous Cyt Diagnosis					● 1	● 6 □ 4 ○ 1 ▲ 3

b INTRAOBSERVATION DF$_1$ DF$_2$

DF$_1$ \ DF$_2$	Malignant Tumour Cells	Cells Suspected of Malignancy	Benign Tumour Cells	Granulomatous Lesion	Acute Inflammation	Miscellaneous Cyt Diagnosis
Malignant Tumour Cells	● 71					
Cells Suspected of Malignancy		● 1		● 1		● 1
Benign Tumour Cells			○ 4			
Granulomatous Lesion				▲ 2 □ 1		▲ 2
Acute Inflammation					△ 2	
Miscellaneous Cyt Diagnosis		● 1		● 1		● 5 ▲ 3 ○ 1 □ 4

c INTRAOBSERVATION KH$_1$ KH$_2$

KH$_1$ \ KH$_2$	Malignant Tumour Cells	Cells Suspected of Malignancy	Benign Tumour Cells	Granulomatous Lesion	Acute Inflammation	Miscellaneous Cyt Diagnosis
Malignant Tumour Cells	● 55 ○ 1		○ 1			● 5
Cells Suspected of Malignancy	● 2					● 2
Benign Tumour Cells						
Granulomatous Lesion						
Acute Inflammation					△ 1 ● 1	
Miscellaneous Cyt Diagnosis	● 4	● 1 ○ 1	● 1		● 1	● 9 ▲ 7 □ 5 ○ 2 △ 1

Fig 1. Results of inter- and intraobserver study in [illegible] cases of randomised transthoracic aspiration biopsies.

The biopsies are in addition registered according to the final histological diagnoses, using the following signatures: ● = malignant tumour. ○ = benign tumour. ▲ = granulomatous lesion. Δ = acute inflammation. □ = others (pneumocystic ...a, pulmonary infarction and localised fibrosis)

...without malignant tumour cells in the first reading were in the second registered as 52 biopsies without malignant tumour cells and ...x biopsies with malignant tumour cells. There six biopsies being false negatives in the first reading. Full agreement was obtained by DF an 82 per cent agreement by KH the difference being significant ($p < 0.05$)

Consistency in the malignant tumour cell diagnosis was obtained by DF in 71 biopsies out of the 81 histologically malignant cases (... per cent) for KH the consistence being ...5 out of 81 (68 per cent) The difference was significant ($p < 0.05$)

The number of positive biopsies in at least one of the readings was for KH 66 (81 per cent) the number of false positives unchanged.

Cells suspected of malignancy In the first reading DF found cells suspected of malignancy in three biopsies, in the second reading the corresponding diagnoses were suspected cells in one biopsy and no tumour cells in two biopsies. In the second reading suspected cells were found in two biopsies, the corresponding diagnoses in the first reading being suspected cells in one and no tumour cells in the other agreement thus being found in one instance. All the biopsies mentioned were from malignant tumours.

In the first reading KH found cells suspected of malignancy in four biopsies, which in the second were diagnosed in two instances as malignant tumour cells and as no tumour cells in two. In the second reading KH found suspected cells in two biopsies, both having been found negative in the first reading. No agreement was found. The six biopsies represented six cases of tumours, five malignant and one benign (histiocytoma)

Presuming that biopsies containing cells suspected of malignancy had been included as positive, the number of true positive biopsies found in at least one of the readings of DF would increase from 71 to 75 out of the 81 malignant cases (93 per cent) for KH the number would increase from 55 to 70 (86 per cent) This presumption would cause no false positives for DF while in the case of KH one false positive would be added.

Benign tumour cells In both readings DF found benign tumour cells in the same four biopsies agreement in 100 per cent. The four biopsies originated from four patients with benign tumours.

The benign tumour cell diagnosis was not used by KH in first reading, twice in the second no agreement. The histological diagnosis in these two cases were benign tumour in one and malignant tumour in one (false negative)

Granulomatous lesion In both readings DF had five biopsies with this cytological diagnosis. These biopsies represented seven cases, agreement been found in three cases, two of which were histologically granulomatous lesions, one a localised fibrosis. The four cases showing inconsistance represented two cases of granulomatous lesions and two cases of malignant tumours.

Cells from acute inflammation DF found acute inflammation in the same two biopsies in both readings full agreement. In both cases the histological diagnosis was abscess without malignancy

KH used this diagnosis twice in the first reading, both being reproduced in the second. In the second reading KH diagnosed *one* more which in the first *reading* was diagnosed as no tumour cells. Agreement was thus found in two out of three cases. The three biopsies represented one case of an abscess (full agreement) and two cases of malignant tumours.

Miscellaneous cytological diagnosis (numbers in brackets being false negative biopsies) The miscellaneous diagnosis was used by DF in the first reading in 15 (7) biopsies which in the second reading had the

a INTEROBSERVATION DF$_1$ KH$_1$

DF$_1$ \ KH$_1$	Malignant Tumour Cells	Cells Suspected of Malignancy	Benign Tumour Cells	Granulomatous Lesion	Acute Inflammation	Miscellaneous Cyt Diagnosis
Malignant Tumour Cells	● 60	● 3				● 8
Cells Suspected of Malignancy		● 1				● 2
Benign Tumor Cells	○ 2					○ 2
Granulomatous Lesion						▲ 4 □ 1
Acute Inflammation					△ 1	△ 1
Miscellaneous Cyt Diagnosis					● 1	● 4 □ 4 ○ 1 ▲ 3

b INTRAOBSERVATION DF$_1$ DF$_2$

DF$_1$ \ DF$_2$	Malignant Tumour Cells	Cells Suspected of Malignancy	Benign Tumour Cells	Granulomatous Lesion	Acute Inflammation	Miscellaneous Cyt Diagnosis
Malignant Tumour Cells	● 71					
Cells Suspected of Malignancy		● 1		● 1		● 1
Benign Tumour Cells			○ 4			
Granulomatous Lesion				▲ 2 □ 1		▲ 2
Acute Inflammation					△ 2	
Miscellaneous Cyt Diagnosis		● 1		● 1		● 5 ▲ 3 ○ 1 □ 4

c INTRAOBSERVATION KH$_1$ KH$_2$

KH$_1$ \ KH$_2$	Malignant Tumour Cells	Cells Suspected of Malignancy	Benign Tumour Cells	Granulomatous Lesion	Acute Inflammation	Miscellaneous Cyt Diagnosis
Malignant Tumour Cells	● 55 ○ 1		○ 1			● 5
Cells Suspected of Malignancy	● 2					● 2
Benign Tumour Cells						
Granulomatous Lesion						
Acute Inflammation					△ 1 ● 1	
Miscellaneous Cyt Diagnosus	● 4	● 1 ○ 1	● 1		● 1	● 9 ▲ 7 □ 5 ○ 2 △ 1

Table. Inter and Intraobserver Variation Study of 81 Transthoracic Aspiration Biopsies Representing a Randomized Material of 100 Biopsies

Adeno-carcinoma	Undifferentiated carcinoma	Other malignant neoplasms	Total
20	11	7	81
16/20 = 80 0 (56 34–94.27)	6/11 = 54.5 (23.38–83.25)	3/7 = 42.9 (9.90–81.59)	50/81 = 61 7 (50.26–72.31)
16/19 = 84.2 (60 42 96 6.)	6/19 = 31.6 (12.58–56 55)	3/3 = 100.0 (29.24–100.0)	50/71 = 70.4 (58.41–80.67)
17/20 = 85 0 (62 11 96.79)	7/11 = 63 6 (30 79–89.07)	3/7 = 42.9 (9.90–81.59)	55/81 = 67.9 (56.60–77.85)
17/20 = 85 0 (62.11 96.79)	7/16 = 43.8 (19 73–70.12)	3/3 = 100 0 (29.24–100.0)	55/71 = 77.5 (66.00–86.54)
8/20 = 40.0 (19 12–63 95)	2/11 = 18.2 (2 28–51 78)	1/7 = 14.3 (0 36–57 87)	36/81 = 44 44 (33.40–55.91)
8/12 = 66.7 (34 89–90 08)	2/10 = 20 0 (2.57–55 61)	1/1 = 100 0 ---------	36/62 = 58.1 (44.85–70.89)
7/20 = 35 0 (15 39–59 22)	1/11 = 9 1 (0 23–41 28)	0/7 = 0.0 (0 00–40 96)	31/81 = 38 3 (27.69–49 74)
7/10 = 70 0 (34 75–93 33)	1/6 = 16.7 (0.42–64 12)	0/0 = --- ---------	31/62 = 50 0 (37 02–62.98)

different interobserver variations from the table We have, however chosen to only compare the results obtained by the two investigators in the first readings.

In short, discrepancies are seen between the two investigators in nearly all of the five histological groups, but these are in none of the cases significant

DISCUSSION

Reproducibility of the diagnostic results is a reasonable requirement when introducing and recommending a diagnostic method.

The present investigation shows that there is a high degree of reproducibility of the aspiration cytological diagnoses and of the classification of aspirated malignant tumour cells from intrathoracic tumours, and this is so independent of the second reading being carried out by the same reader or another

Without knowledge of any clinical or radiological findings the readings were carried out on a randomized material of 100 histologically verified transthoracic aspiration biopsies.

With reference to the sensitivity and the diagnostic specificity the presented results are in accordance with those obtained by the original cytological reading which were made with knowledge of clinical and radiological findings.

This correlation shows the value of the aspiration biopsy diagnosis *per se*

TABLE 2 *Reproducibility of Classification of Aspirated Malignant Tumour Cells Expressed in the T[...] Malignant Tumours out [...]*

	Epidermoid carcinoma 30	Small cell carcinoma 13
DF		
1 reading Sensitivity	19/30 = 63.3 (43 86–80 07)	6/13 = 46.2 (19 22–74 87)
1 reading Specificity (diagnostic)	19/23 = 82.6 (61.22–95 05)	6/7 = 85 7 (42.13–99 64)
2 reading Sensitivity	19/30 = 63.3 (43.86–80 07)	9/13 = 69.2 (38.57–90.91)
2 reading Specificity (diagnostic)	19/23 = 82 6 (61.22–95 05)	9/9 = 100.0 (66.37–100.0)
KH		
1 reading Sensitivity	18/30 = 60.0 (40 60–77 34)	7/13 = 53.8 (25 13–80 78)
1 reading Specificity (diagnostic)	18/29 = 62 1 (42.26–79.31)	7/10 = 70.0 (34 75 93.33)
2 reading Sensitivity	19/30 = 63 3 (43.86–80 07)	4/13 = 30 8 (9 09–61 43)
2 reading Specificity (diagnostic)	19 40 = 47 5 (31 51–63.87)	4/6 = 66.7 (22.28–95.67)

Figures in brackets being the 95 per cent confidence limits.

diagnosis suspected malignant cells in one biopsy granulomatous lesion in one and agreement in 13 biopsies In the second reading the diagnosis was used in 16 (5) biopsies Inconsistence was found in three biopsies, the diagnoses being suspected malignant cells in one and granulomatous lesion in two biopsies

For KH the diagnosis was used in 32 (15) biopsies in the first reading the corresponding diagnoses in the second reading being malignant tumour cells in four suspected malignant tumour cells in two benign tumour cells in one acute inflammatory cells in one and agreement in 24 In the second reading there were 31 such diagnoses, in consistence being found in seven biopsies, the diagnosis being malignant tumour cells in five and suspected malignant cells in two

Reproducibility of the Cytological Classification of Malignant Tumour Cells

Table 2 shows the results of the cytological classification correlated to the histological diagnosis expressed as the sensitivity and the diagnostic specificity* in the 81 cases of malignant intrathoracic tumours.

It is quite possible to draw out several

* The term diagnostic specificity being preferred for PV positive cf *Wulff* (6)

Acta path. microbiol. scand. Sect. A, 85 897-906, 1977

CLINICAL, HISTOLOGICAL AND ULTRASTRUCTURAL FEATURES OF A POSSIBLY VIRUS-INDUCED ORAL LEUKOPLAKIA

O. Fejerskov, B. Roed-Petersen and J. J. Pindborg

Departments of Dental Pathology and Operative Dentistry and Electron Microscopy, Royal Dental College, Aarhus
Department of Oral Pathology, Royal Dental College, Copenhagen, and
Department of Oral Medicine and Oral Surgery, University Hospital (Rigshospitalet), Copenhagen, Denmark

Fejerskov, O., Roed-Petersen, B. & Pindborg, J. J. Clinical, histological and ultrastructural features of a possibly virus-induced oral leukoplakia. Acta path. microbiol. scand. Sect. A, 85: 897-906, 1977.

Two male patients with oral leukoplakias exhibiting a peculiar type of apparent dysplastic changes have been followed for 4 and 6 years, and a series of biopsies has been examined by light and electron microscopy. The apparent lack of normal epithelial stratification below the keratinized cell layers was mainly caused by the frequent appearance of large ballooned cells and multinuclear giant cells. The centre of the large ballooned cells contained aggregations of chromatin and evenly-dispersed microtubulus surrounded by a thick rim of tonofibril bundles. In the peripheral cytoplasm large numbers of smooth-surfaced endoplasmic reticulum were found, but no Golgi apparatus was observed. In addition, several autophagocytic bodies were recorded. Along the cell membrane only a few desmosomes were present, whereas aggregations of digested desmosomes were found in the cytoplasm. On the basis of the ultrastructural findings, it is suggested that the large ballooned cells represent epithelial cells arrested in early stages of mitotic division. The epithelial cells in interphase exhibited a normal ultrastructure except for large nucleoli with varying degrees of condensation of nucleolonema and vacuolization. Further, atypical dense granular aggregations and strands of fine fibrillar material were recorded in the nuclei. It is suggested that this new type of oral leukoplakia has a viral etiology.

Key words: Oral leukoplakia; virus-induced; histology; ultrastructure.

Ole Fejerskov, Department of Dental Pathology and Operative Dentistry, Royal Dental College, DK-8000 Aarhus C, Denmark.

Received 9.iii.77. Accepted 26.vi.77

Oral leukoplakia is a purely descriptive clinical diagnosis used for white patches of the oral mucosa which cannot be rubbed off or diagnosed as another lesion. Histologically these lesions mostly show either a hyperortho- or hyperparakeratosis (20). Malignant transformation occurs in 2–4 per cent of oral leukoplakias (21). If the epithelium shows dysplastic changes, it is believed that this is in-

Our investigation do contain an opportunity to compare the results obtained by an experienced aspiration cytologist with those obtained by a pathologist without this experience. Of all the comparable results only the difference in consistency of the malignant tumour cell diagnosis was significant, and this difference may be explained by the intended omission of a correction between the readings.

It is our belief that the presented results will make it clear that this diagnostic method is useful and reliable even in the hands of a trained pathologist given a short introduction to—and a reasonable amount of correction within—this special field.

REFERENCES

1. Documenta Geigy. Scientific tables, 7. ed. Basel 1968, pp. 85–101, 131.
2. *Francis D.* Transthoracic fine-needle aspiration biopsy. A histologically verified material. Acta path. microbiol. scand. Sect. A. *85*: 230–234, 1977.
3. *Francis D.* Aspiration biopsies from diagnostically difficult pulmonary lesions. A consecutive case material. Acta path. microbiol. scand. Sect. A. *85*: 235–239, 1977.
4. *Francis D.* Transthoracic aspiration biopsy. Cytological classification of aspirated malignant tumour cells. Acta path. microbiol. scand. Sect. A. *85*: 535–538, 1977.
5. *Iecchio T. J.* Predictive value of a single diagnostic test in unselected populations. New Engl. J. Med. *274*: 1171–1173, 1966.
6. *Wulff H. R.* Rational diagnosis and treatment. Blackwell, Oxford, 1976, p. 93.

Acta path. microbiol. scand. Sect. A, 85 897–906 1977

CLINICAL HISTOLOGICAL AND ULTRASTRUCTURAL FEATURES OF A POSSIBLY VIRUS-INDUCED ORAL LEUKOPLAKIA

O Fejerskov B. Roed-Petersen and J J Pindborg

Departments of Dental Pathology and Operative Dentistry and Electron Microscopy
Royal Dental College, Aarhus
Department of Oral Pathology Royal Dental College, Copenhagen, and
Department of Oral Medicine and Oral Surgery University Hospital (Rigshospitalet)
Copenhagen, Denmark

Fejerskov O Roed-Petersen, B & Pindborg, J J Clinical, histological and ultrastructural features of a possibly virus-induced oral leukoplakia. Acta path. microbiol. scand. Sect. A, 85 897 906 1977

T male patients with oral leukoplakias exhibiting a peculiar type of apparent dysplastic changes have been followed for 4 and 6 years, and a series of biopsies have been examined by light and electron microscopy The apparent lack of normal epithelial stratification below the keratinized cell layers was mainly caused by the frequent appearance of large ballooned cells and multinuclear giant cells The centre of the large ballooned cells contained aggregations of chromatin and evenly-dispersed microtubules surrounded by a thick rim of tonofibril bundles In the peripheral cytoplasm large numbers of smooth-surfaced endoplasmic reticulum were found, but no Golgi apparatus was observed. In addition, several autophagocytic bodies were recorded. Along the cell membrane only a few desmosomes were present, whereas aggregations of digested desmosomes were found in the cytoplasm. On the basis of the ultrastructural findings, it is suggested that the large ballooned cells represent epithelial cells arrested in early stages of mitotic division The epithelial cells in interphase exhibited a normal ultrastructure except for large nucleoli with varying degrees of condensation of nucleolonema and vacuolization Further atypical dense granular aggregations and strands of fine fibrillar material were recorded in the nuclei It is suggested that this new type of oral leukoplakia has viral etiology

Key words Oral leukoplakia virus-induced histology ultrastructure

Ole Fejerskov Department of Dental Pathology and Operative Dentistry
Royal Dental College, DK-8000 Aarhus C, Denmark.

Received 9.iii.77 Accepted 26.x. 77

Oral leukoplakia is a purely descriptive clinical diagnosis used for white patches of the oral mucosa which cannot be rubbed off or diagnosed as another lesion. Histologically these lesions mostly show either a hyperortho- or hyperparakeratosis (20) Malignant transformation occurs in 2–4 per cent of oral leukoplakias (21) If the epithelium shows dysplastic changes, it is believed that this is m-

dicative of premalignancy (17). However it is still unknown to what extent dysplastic oral leukoplakias undergo malignant transformation. One of the reasons for this uncertainty may be that the *diagnosis epithelial dysplasia*, covers several diseases of different etiology.

The purpose of the present study has been to present clinical, histopathological and ultrastructural features of a peculiar, newly recognized type of leukoplakia, which on the basis of routine histopathological examination was originally classified as a dysplastic lesion or carcinoma in situ. However, the ultrastructural observations to be presented indicate that the cellular changes which occur in this type of leukoplakia are different from those usually occurring in dysplastic lesions.



Fig. 1. Oral leukoplakia on the commissure of the left buccal mucosa.

MATERIAL AND METHODS

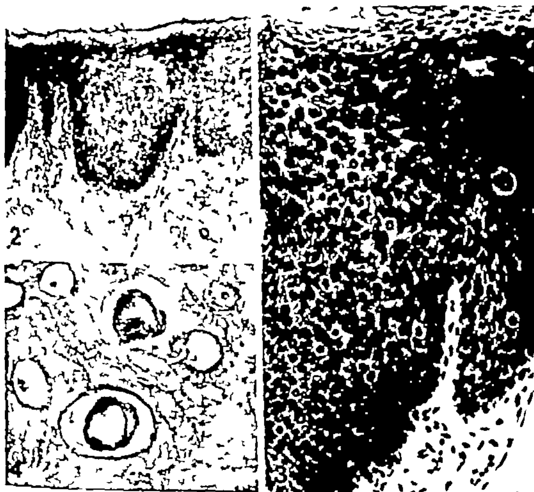
Case histories. In 1970 a 47-year-old man suffering from oral leukoplakias located in both commissures and extending backwards unto the buccal mucosa (Fig. 1) was referred to the University Hospital in Copenhagen. According to the medical *history the lesions* had recurred *with varying* intensity throughout the previous 25 years. *Clinically* the lesion confirmed to the left buccal mucosa was most extensive covering an area of 2 × 1 cm. It was slightly elevated from the surrounding mucosa of normal appearance and presented small erythematous areas concomitant with greyish white areas. During a 5-year period, punch biopsies were taken regularly for routine histopathological examination. In addition, material from a *lesion at the inferior surface of the tongue* was fixed in a combined glutaraldehyde and paraformaldehyde fixative (13), embedded in Epon and *processed for electron microscopical examination.*

Case 2. A 72-year-old man exhibited a white non-elevated and apparently homogeneous leukoplakia on the lower lip. The lesion was biopsied in 1974 and one year later the remaining lesion was surgically removed and the material processed for light and electron microscopical examination.

RESULTS

Light microscopical examination. The oral epithelium was hyperortho- or hyperparakeratotic with a distinct stratum granulosum. The epithelial ridges exhibited acanthosis, occasionally with drop-shaped rete pegs. The epithelium appeared highly cellular with a change in nuclear-cytoplasmic ratio and some disorganization of stratification (Figs. 2 and 3). Mitotic figures were found 6 to 7 cell layers above the basal cell layer and through*out the stratum spinosum and stratum granulosum* individual large ballooned cells (Fig. 4) and multinuclear epithelial giant cells were frequently encountered. In all specimens a distinct basement membrane separated the epithelium from the underlying connective tissue, which exhibited a slight to moderate infiltration of lymphocytes and plasma cells.

Electron microscopical examination. The large ballooned cells located in the spinous cell layer demonstrated characteristic, uniform changes. The plasma membrane was usually in close apposition to that of the neighbouring cells only leaving an intercellular space of 10–30 nm in width (Figs. 5 and 6). A few typical desmosomes were recorded along the plasma membrane of the ballooned cells, and no other types of cell junctions were observed. The content of the cells was divided into a peripheral rim of cytoplasm and a large central portion by a thick ring



Figs 2 & 3 Micrographs of paraffin-embedded material, demonstrating an increased density of cells in the epithelium. Several mitoses ppear high p in the non-proliferativ e layers. Throughout the epithelium, large ballooned cells re seen. The epithelium is either hyperortho- or hyperparakeratinized. × 90, × 210

F g 4 Micrograph of the large ballooned cells surrounded by ep thelial cells of normal appearance. The large cells re devoid of ucleus, with central thick ring of tonofibril bundles. No typical desmosomes can be found surround ng the large cells, contrary to what is seen in the intercellular spaces between the cells of normal ppearance × 1 000

of tonofibr l bundles (Fig 5) No individual tonofibril were lying free in the cytoplasm. *I th entral part* of the cells, large round or irregular areas of varying density were found cons sting of either clusters of dense coarse granules or a fine fibrillar material very milar to heterochromatin (Fig 6) The chromat n was embedded in a ground substance of the same density as the cytoplasm, containing ev enly-dispersed ribosome like granules Further bundles of microtubles were intermingled with the chromatin areas (Fig. 6) and occas onally a centriole was found. A nuclear env e.ope and distinct nucleolar material were never observed.

The peripheral cytoplasm contained mitochondria often irregular in outline and a well-developed complex of mainly smooth-

dicative of premalignancy (17) However it is still unknown to wha extent dysplastic oral leukoplakias undergo malignant transforma tion. One of the reasons for this uncertainty may be that the diagnosis ep thelial dyspla sia, covers several diseases of different eti ology

The purpose of the present study has been to present clinical histopathological and ul trastructural features of a peculiar newly recognized type of leukoplakia, wh ch on the basis of routine histopathological examina tion was originally classified as a dysplastic lesion or carcinoma in situ. However, the ul trastructural observations to be presented in dicate that the cellular changes which occur in this type of leukoplakia are different from those usually occurring in dysplastic lesions.



Fig 1 Oral leukoplakia on the commissure of the left buccal mucosa.

MATERIAL AND METHODS

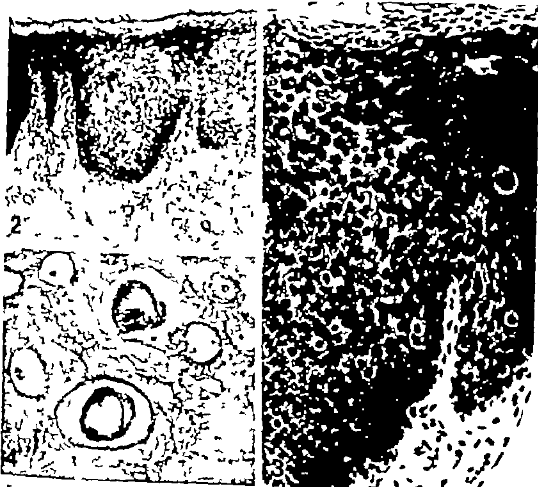
Case histories In 1970 a 47 year-old man suffer ing from oral leukoplakias located in both commissures and ext nding backwards unto the buccal mucosa (Fig 1) was referred to the University Hospital in Copenhagen. According to the medical history the lesions had recurred with varying intensity throughout the previous 25 years. *Clinically* the lesion confirmed to the left buccal mu cosa was most extensive, cover ng an area of 2×1 cm It was slightly elevated from the surrounding mucosa of normal appearance and presented small erythematous areas concomitant with greyish white areas During a 5-year period punch biopsies were taken regularly for routine histopathological examination. In addition material from a lesion at the inferior surface of the tongue was fixed in a combined glutaraldehyde and paraformaldehyde fixative (13) embedded in Epon and processed for electron microscopical examination

Case 2 A 7? year-old man exhibited a white non-elevated and apparently homogeneous leukoplakia on the lower lip The lesion was biopsied in 1974 and one year later the remaining lesion was surgically removed and the material processed for light and electron microscopical examination.

RESULTS

Light microscopical examination The oral epithelium was hyperortho- or hyperparakeratotic with a distinct stratum granulosum The epithelial ridges exhibited acanthosis, occasionally with drop-shaped rete pegs. The epithelium appeared highly cellular with a change in nuclear-cytoplasmic ratio and some disorganization of stratification (Figs. 2 and 3) *Mitotic figures* were found 6 to 7 cell layers above the basal cell layer and throughout the stratum spinosum and stratum granulosum individual large ballooned cells (Fig 4) and multinuclear epithelial giant cells were *frequently encountered* In all speci mens a distinct basement membrane separat ed the ep thelium from the underlying con nective tissue, which exhibited a slight to moderate infiltration of lymphocytes and plasma cells

Electron microscopical examination. The large ballooned cells located in the spinous cell layer demonstrated characteristic, uni form changes The plasma membrane was usually in close apposition to that of the neighbouring cells only leaving an intercellu lar space of 10–30 nm in width (Figs 5 and 6) A few typical desmosomes were recorded along the plasma membrane of the ballooned cells and no other types of cell junctions were observed. The content of the cells was divided into a peripheral rim of cytoplasm and a large central portion by a thick ring



Figs 2 & 3 Micrographs of paraffin-embedded material, demonstrating an increased density of cells in the epithelium. Several mitoses appear high up in the non-proliferative layers. Throughout the epithelium, large ballooned cells are seen. The epithelium is either hyperortho- or hyperparakeratinized. × 90 × 210

Fig. 4 Micrograph of the large ballooned cells surrounded by epithelial cells of normal appearance. The large cells are devoid of nucleus, with central thick ring of tonofibril bundles. N typical desmosomes can be found surrounding the large cells, contrary to what is seen in the intercellular spaces between the cells of normal appearance × 1,000

of tonofibril bundles (Fig. 5). No individual tonofibrils were lying free in the cytoplasm.

In the central part of the cells, large round or irregular areas of varying density were found consisting of either clusters of dense coarse granules or a fine fibrillar material very similar to heterochromatin (Fig. 6). The chromatin was embedded in a ground substance of the same density as the cytoplasm, containing evenly-dispersed ribosome like granules. Further bundles of microtubles were intermingled with the chromatin areas (Fig 6) and occasionally a centriole was found. A nuclear envelope and distinct nucleolar material were never observed.

The peripheral cytoplasm contained mitochondria often irregular in outline and a well-developed complex of mainly smooth



Fig 5 Electron micrograph of a typical large ballooned cell. In the center of the cell aggregations of varying density are seen surrounded by a ring of tonofibril bundles. In the surrounding epithelial cells of normal appearance the cytoplasm is characterized by numerous, evenly-dispersed tonofibril bundles. To the left a lymphocyte is seen × 6 000

surfaced endoplasmic reticulum (Fig 6) The cisternae were running an irregular course, giving the appearance of numerous elongated vesicles located like pearls on a string In several areas the endoplasmic reticulum enclosed part of the cytoplasm including mitochondria exhibiting different stages of structural disintegration (Fig 7) The mitochondrial cristae appeared as slender tubules or vesicles before total disappearance of the organelles leaving empty membrane-bound vesicles in the cytoplasm Aggregations of small often polymorphic, vesicles of varying size were recorded between the evenly-dispersed ribosomes (Fig 8) Further small membrane bound structures having a homogeneous dense centre appeared, but typical Golgi complexes were never observed

In every ballooned cell one or more electron-dense areas devoid of ribosomes were found (Fig 9) containing clusters of desmosomes seemingly at different stages of breakdown At both ends of the desmosomes the trilaminar plasma membranes coalesced, or casionally forming a small vesicle (Figs 10 and 11) but the complex structure of the desmosomes was preserved In other areas the attachment plaques and the outer dense condensations were partly lost, leaving a membrane-bound elongated structure containing only the original intercellular desmosome disk with the dense contact layer in the middle.



Fig 6 Part of the central and peripheral cytoplasm of ballooned cell Note the even and narrow intercellular spaces with no desmosomes. In the peripheral cytoplasm, numerous smooth-surfaced endoplasmic reticulum cisternae are found. Chromatin aggregations are seen centrally Part of the chromatin is distinctly fibrillar (inset upper right) Numerous microtubules are evenly dispersed in the central part of the cell (inset upper left) × 7,600 Inserts × 75,000

The ultrastructural examination of the apparently normal cells in the different epithelial stratae showed that in principle the structure of these cells appeared very similar to what has been described previously for different types of keratinized epithelia, except that many nuclei exhibited changes in the structural composition of the nucleoli (Figs. 12 and 13).

In the basal and spinous cell layers the nucleoli were often very large, dominated by a granular material. The network of the fibril-containing nucleolonema appeared denser than usual, and was often aggregated (Fig. 13) Vacuolization of the nucleoli was frequently observed. Occasionally strands of a fine-fibrillar material were recorded lying free in the euchromatin of the nuclei (Fig 14) which further contained atypical electron-dense granular aggregations.



Fig 7 Autophagocytic body containing mitochondrion with cristae appearing as numerous vesicular figures. × 67 200

Fig 8 Part of cytoplasm containing numerous, irregular membrane-bound bodies, some of which appear electron dense (inset lower left) × 54 000

DISCUSSION

The present study has demonstrated that this newly recognized type of oral leukoplakia differs histopathologically from other types previously described (20) The examination of 1 μm thick sections of material processed for electron microscopy gave valuable additional information as this material exhibits less shrinkage than that processed for routine paraffin sectioning This was particularly evident when dealing with the ballooned cells, as the almost total lack of intercellular junctions around these cells made them much more susceptible to shrinkage artifacts.

The electron microscopical examination has demonstrated that the differentiation pattern as reflected by cytoplasmic changes from the basal cell layer towards the keratinized surface is very similar to that of normal human keratinized oral epithelium (16) The disturbance is thus a result of the increased number of cells, the increased nucleus/cytoplasm ratio and the disturbance in layering caused by pressure from the large cells.

In the paraffin-embedded material mitoses were recorded several cell layers above the basal layer indicative of epithelial dysplasia or carcinoma in situ. These mitotic figures are probably examples of the large ballooned cells which have been sectioned so that they appear as a stage in cell division. This view is supported by the electron microscopical examination of the ballooned cells, suggesting that these cells are squamous epithelial cells arrested in an early stage of the mitotic cyclus, probably late prophase. Little is known about the ultrastructural features of squamous epithelial cells during cytokinesis, but the structural appearance of the ballooned cells observed in the present study is very similar to that reported for other mammalian cells in late prophase (25) In general, the nuclear components are rather uncharacteristicly



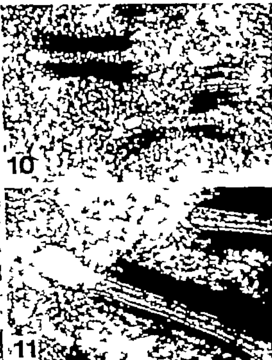


Fig. 9 Part of the cytoplasm with tonofibril bundles and an electron-dense area consisting of desmosomes. × 25,200

Figs 10 & 11 Cytoplasmic desmosomes with coalescent plasma membranes at the end of the desmosomes often forming small circles. Attachment plaques and the characteristic structure of the desmosomes are illustrated. × 100,000, × 120,000

preserved when using conventional electron microscopical methods (1) but the size of the particles, as well as the presence of thin filaments in the dense areas of the present cells, is in accordance with the general description of chromatin material (1, 26).

Some of the distinct round areas may, however, represent disintegrated parts of the nucleolus, since remnants of this structure may remain as several small irregular bodies after nucleoli disintegration in late prophase (11, 12). The large number of mainly smooth-surfaced endoplasmic reticulum cisternae in the surrounding cytoplasm is another typical feature of dividing cells (26) and may present remnants of the nuclear membrane. Squamous epithelial cells in interphase very seldom contain smooth-surfaced endoplasmic reticulum cisternae and never in a number like that presented in the large cells.

Whilst the surrounding interphase cells contained one or more large Golgi complexes, it was characteristic that this organel was missing in the ballooned cells. This observation is also indicative of a cell in mitosis, as *Reith & Jokelainen* (24) did not observe any organized Golgi apparatus in stratum intermedium cells of rat molar enamel organ in metaphase. In other mammalian cells, *Robbins & Gonatas* (26) have stressed that the Golgi complex disappears both morphologically and histochemically during mitosis.

In the present study, large areas of the cytoplasm were filled with small polymorphic membraneous cisternae and vesicles often intermingled with microtubules. A similar arrangement is never observed in interphase squamous epithelial cells (7) but this is a persistent feature in other mammalian cells in metaphase (15, 27), particularly as polar



Figs 12 & 13 Nuclei changes in stratum spinosum The nucleolonema appear fragmented and condensed surrounded by granular areas. Small vesicles containing a less dense material are seen. In the nucleoplasm aggregations of atypical electron dense particles are seen × 21 000
Fig 14 Nuclei containing strands of fine fibrillar material in the nucleoplasm. × 80,000

aggregations (26) Also the clusters of small membrane bound bodies with an electron dense matrix described in the present study are reported as typical in HeLa cells during mitosis being of lysosome origin (26) Different types of lysosome like bodies appear regularly in keratinizing squamous epithelia (7) whereas lysosome-like bodies of the autophagocytic type predominated the large cells. The significance of this observation is unknown however

The significance of the intracellular aggregation and apparent digestion of desmosomes is unknown Similar observations have been reported in epithelial cells in a variety of lesions such as carcinomas (14) carcinoid papillomatosis (3) keratoacanthoma (2) focal epithelial hyperplasia (23) and benign pleomorphic adenoma and ameloblastoma (5)

The etiology of this type of oral leukoplakia is unknown We have not been able, either in the large ballooned cells or in the epithelial cells in interphase, to observe virus-like particles. Nevertheless it seems reasonable to suggest a viral origin of this type of lesion for the following reasons. The nuclear changes observed are indicative of a virus infection and particularly the nucleolar changes may be induced by infections with both RNA and DNA virus (1)

The occasional findings of intranuclear fil

ments further supports the hypothesis of a virus infection. Similar intranuclear filaments have been shown in human oral papillomas (9) and human genital warts (6) and described by *Smith et al.* (29) as closely associated with typical papilloma virus particles.

In focal epithelial hyperplasia, large ballooned cells have been examined, which are very similar to those here described (4 23) and in one case (20) virus-like particles have been reported in interphase nuclei of this oral disease.

Finally it is important to note that virus-induced lesions do not necessarily contain virus when examined in the electron microscope (6, 18) Thus, virus-induced brain tumors in dogs do not contain morphologic evidence of virus particles (10) In an electron microscopical study of 12 specimens of human genital warts, condylomata acuminata, particles that had the morphology typical of papilloma virus were recorded in one specimen only and in a very limited number (6) Furthermore great variations in the development of the same wart virus in different situations in papillomas of domestic and wild rabbits have been described (19)

In conclusion, it is suggested that this new type of oral leukoplakia has a viral etiology The viral nuclei acid ("masked virus") may stimulate cell proliferation, leading to increased density of cells, multinuclear cells, and to accumulations of cells which are arrested in an early stage of mitosis and located throughout the nonproliferative layers of the epithelium

---

This study was supported by grants No. 512-4064 and N 512 3151 from the *Danish Medical Research Council* The authors wish to thank Miss *Ulla Ka dsen* for skilful technical assistance

REFERENCES

1 *Bernhard W & Gra boulan A* Electron microscopy of the nucleolus in vertebrate cells. I The nucleus Dalton, A J & Haguenau, F (eds. New York, Academic Press, 1968
2 *Balow M & Klingmüller G* Elektronenmikroskopische Untersuchungen des Keratoakanthoms. Arch. Derm. Forsch. *241* 292–304 1971
3 *Caput C & P ands, G.* Intracytoplasmic desmosomes. J Ultrastruct. Res. *41* 358–368, 1972.
4 *Clausen F Praetorius* Histopathology of focal epithelial hyperplasia. Tandlaegebladet *73* *1015–1022, 1969*
5 *Cutler L. S* Intracytoplasmic desmosomes in human oral neoplasms. Arch. Oral Biol. *21* 221–226 1976.
6. *Dunn A. E. G & Oglsle M M* Intranuclear irus particles in human genital wart tissue Observations on the ultrastructure of the epidermal layer J Ultrastruct. Res. 22 282–295 1968.
7 *Fejerskov O* Keratinized squamous epithelium of normal and wounded palatal mucosa in guinea pigs. J Periodont. Res. supplement no. *11* 1973
8. *Fischer E. R., McCoy M M & W kler H L.* Analysis of histopathologic and electron microscopic determinants of keratoacanthoma and squamous cell carcinoma. Cancer 29 1387–1397 1972.
9 *Frithiof L. & Wersäll J.* Virus-like particles in papillomas of the human oral cavity Arch. Ges. Virusforschung *21* 32–44 1967
10. *H ganam F* Personal communication.
11 *Hensen W K & Nichols W W.:* Persistence of nucleoli in short term and long-term cell cultures and in direct bone marrow preparations in mammalian materials. J Cell Biol. *31* 343–361 1966
12. *Hsu T C., Arrighi, F E. & Klevecz, R. R.:* The nucleoli in mitotic divisions of mammalian cells in vitro J Cell Biol. *26* 539–553 1965.
13 *Karnovsky M J.:* A formaldehyde-glutaraldehyde fixative of high osmolarity for use in electron microscopy J Cell Biol. *27* 137A–138A, 1965
14 *Klingmüller G., Klehr H U & Ishibashi Y.* Desmosomen im Cytoplasma entdifferenzierter Keratinocyten des Platten epithelcarcinoms. Arch. Klin. Exp. Dermatol. *238* 356–365 1970
15 *McIntosh, J R. & Landis S C* The distribution of spindle microtubules during mitosis in cultured human cells. J Cell Biol. *49* 468–497 1971
16 *Meyer M & Schroeder H E.* A quantitative electron microscopic analysis of the keratinizing epithelium of normal human hard palate. Cell Tis. Res. *158* 177–203 1975
17 *Mincer H H Coleman S A & H pkins K P.* Observations on the clinical characteristics of oral lesions showing histologic epithelial dysplasia. Oral Surg. *33* 389–399 1972.

18 *Nasemann T* Viruskrankheiten der Haut der Schleimhäute und des Genitales. Georg Thieme Verlag Stuttgart 1974
19 *Noyes W F & Mellors R C* Fluorescent antibody detection of the antigens of the shope papilloma virus in papillomas of the wild and domestic rabbit. J Exp Med *106* 555-562 1957
20 *Pindborg J J* Oral leukoplakia Austr Dent J *16* 83-93 1971
21 *Pindborg J J Jölst O Renstrup G & Roed Petersen B.* Studies in oral leukoplakia. A preliminary report on the period prevalence of malignant transformation in leukoplakia based on a follow-up study of 248 patients. J Am. Dent. Assoc. *76* 767-771 1968.
22 *Prætorius-Clausen F & Willis J M* Papova virus-like particles in focal epithelial hyperplasia. Scand. J Dent Res. *79* 362-365 1971
23 *Prætorius-Clausen F & Fejerskov O* Unpublished observation 1973
24 *Reith E. J & Jokelainen P T* Cytokinesis in the stratum intermedium of the rat molar enamel organ. J Ultrastruct. Res. *42* 51-65 1973
25 *Rhodin J A G* Histology New York, Oxford University Press, London, Toronto 1974
26 *Robbins E. & Gonatas N K* The ultrastructure of mammalian cell during the mitotic cycle. J Cell Biol *21* 429-463 1964
27 *Robbins E & Jentzsch G* Ultrastructural changes in the mitotic apparatus at the metaphase to anaphase transition. J Cell Biol. *40* 678-691 1969
28 *Roed Petersen B. Banoczy J & Pindborg J J* Smoking habits and histological characteristics of oral leukoplakias in Denmark and Hungary Brit J Cancer *28* 575-579 1973
29 *Smith K O Dougherty E., Melnick J L & Rapp F* Fine structure of unassembled viral subunits from human warts. J Bacteriol. *90* No. 1 pp 2 8-281 1965

Acta path. microbiol. scand. Sect. A, 85 907–910 1977

AMYLOID TUMOUR OF THE LUNG

Report of a Case and a Short Review of the Literature

JUDIT MÄKINEN, JUHA NICKELS and PAAVO E. A. HALTTUNEN

Central Laboratory of Pathology, University of Helsinki, and Department of Thoracic Surgery, Helsinki University Central Hospital, Helsinki, Finland

Mäkinen, J., Nickels, J. & Halttunen, P. E. A. Amyloid tumour of the lung. Report of a case and short review of the literature. Acta path. microbiol. scand. Sect. A, *85* 907–910 1977

A 67-year-old woman who had earlier suffered from rheumatic fever and a persistently elevated sedimentation rate, was operated on for a right pulmonary tumour which was shown clinically, light and electron microscopically to be primary nodular isolated amyloid tumour.

Key words: Lung tumour; amyloid.

Judit Mäkinen, Central Laboratory of Pathology, Haartmaninkatu 3, SF-00290 Helsinki 29, Finland

Received 13. i.77   Accepted 30. i.77

Systemic, primary amyloidosis is a very uncommon condition, the lung being involved in from 30 to 50 per cent of the cases (9). In the form of isolated, nodular tumour of the lung, primary amyloidosis is still more rarely diagnosed, especially from biopsy specimens. Up to 1974 there were only 35 cases reported in the literature (3, 7).

Amyloid deposits may occur as masses in the alveolar walls, and/or in the pulmonary arteries, forming either single or multiple nodules located centrally or peripherically (2, 10).

The purpose of the present paper is to report a case of primary amyloid tumour of the lung examined by light and electron microscope, with a brief review of the literature.

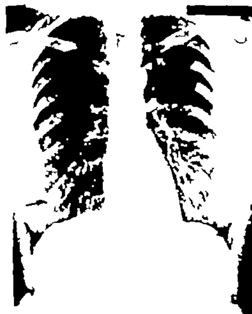


Fig. 1. Chest roentgenogram illustrating the tumour-like infiltration in the lower lobe of the right lung (arrow).

CASE REPORT

The patient, born in 1909, contracted rheumatic fever at the age of 17 after an acute tonsillitis



Fig 2 Part of the amyloid mass with thick blood vessels (H & E × 240)



Fig 3 Masses of eosinophilic material surrounded by inflammatory cells Focal calcification. (H & E × 240)

thereafter she had a raised sedimentation rate varying between 50 and 100 mm/h In 1939 tonsillectomy was performed Afterwards the patient had several fever attacks with pain in the joints. In 1976 a chest roentgenogram showed a tumour like infiltration in the lower lobe of the right lung (Fig 1) which enlarged during the next four months The laboratory data revealed only a raised sedimentation rate (50 mm/h) but a Waaler Rose test was negative and no antinuclear antibodies or leucocytosis were found By thoracotomy the tumour was found to be approximately 3 cm in diameter slightly yellow and necrotic with no visible tract res within it The postoperative course was uneventful A rectal biopsy was performed, but no amyloid material was found Three months after the operation the sedimentation rate was still 45 mm h

Light microscopical findings In the paraffin embedded sections, hyaline eosinophilic material with an ill-defined capsule was seen Within this mass and partly in the adjacent lung tissue thick blood vessels were noticed with slightly eosinophilic deposits in the wall (Fig 2) Congo-red stain revealed the typical green birefringence of amyloid when viewed with polarized light. Focal calcification lymphocytic infiltration and occasional foreign-body giant cells were seen, especially near the periphery of the lesion (Fig 3)

Electron microscopical findings The formalin fixed paraffin-embedded material was deparaffinized with xylol, passed through decreasing alcoholic grades, postfixed in osmium tetroxide and embedded in Epon The ultra thin sections were stained with uranyl acetatae and examined with a Jeol 100 S electron microscope The hyaline eosinophilic material seen in the light microscope was found to consist of loosely-arranged and haphazardly

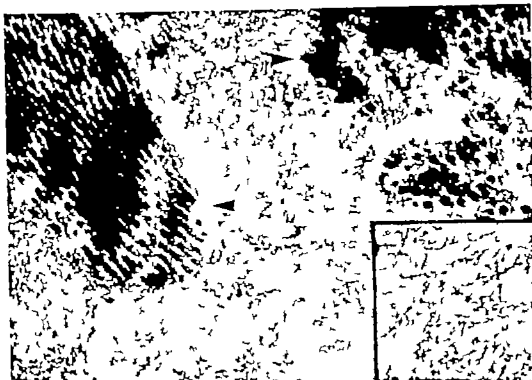


Fig 4 Electron microscopically amyloid material can be seen between bundles of collagen fibres (arrow) × 25,000. In the inset, amyloid fibrils are shown at higher magnification. × 42,000

oriented fibrils with the ultrastructural appearance of amyloid (Fig 4) Scattered within this were a few entrapped degenerated cells and fibres of mature collagen The diameter of the amyloid fibrils varied between 7 12 mμ, corresponding to earlier observations on amyloid with variation within the range of 5 to 17 mμ (6)

DISCUSSION

We consider our case an example of isolated primary nodular pulmonary amyloidosis, which is an extremely rare disease occurring especially in elderly patients, regardless of sex (7 Our patient had suffered from rheumatic fever which has been reported in association with amyloidosis (1) To rule out the more common secondary amyloidosis, generalized primary amyloidosis and amyloidosis associated with myelomatosis, the search for an infectious disease or malignancy in these cases is of great importance. Congo-red staining of rectal biopsy which was negative in our case indicates the presence of amyloid in generalized involvement in 75 per cent of the cases (7)

The prognosis is usually favourable, except for those patients with massive, bilateral lung involvement (7 8 11) There is only one reported case of a recurrent amyloid tumour in the same lobe as previously operated on (2)

It has been suggested that the presence of inflammatory cells is a helpful morphologic sign in distinguishing the deposits of primary from secondary amyloid (5) These cells may also have a disordered protein synthesis resulting in the local deposition of amyloid (2) Other authors stress the fact that the deposition of amyloid mass was preceded by a tumour probably an angioma or hamartoma (4)

The presence of calcification and foreign-body giant cells in this case may suggest the possible role of a previous haemorrhage or

an old inflammatory focus in the development of amyloid deposits

REFERENCES

1 *Cohen A S* Laboratory diagnostic procedures in the rheumatic diseases. 1st ed J & A Churchill Ltd., London 1967 p 333

2 *Dyke P C Demeray M J Delaven J W & Rasmussen R A* Pulmonary amyloidoma. Amer J clin. Path. *61* 301–305 1974

3 *Firestone F N & Joison J* Amyloidosis a cause of primary tumours of the lung J Thorac. Cardiovasc. Surg *51* 292–299 1966

4 *Fors B & Rudén L.* Tumoral amyloidosis of the lung Acta path. microbiol Scand *61* 1–12 1964

5 *Hayes W & Bernhardt H* Solitary amyloid mass of the lung Cancer *24* 820–825 1969

6 *Lehner T Nunn R E. & Pearse E.* Electron microscopy of paraffin-embedded material in amyloidosis J path. Bact. *91* 297–300, 1966

7 *Saab S B Burke J Hopeman A & Almond C* Primary pulmonary amyloidosis Report of two cases. J Thorac. Cardiovasc. Surg *67* 301–307 1974

8 *Skagseth R & Normann T* Localised amyloid tumour of the lung. Scand. J Thorac. Cardiovasc. Surg *4* 135–138 1970

9 *Thomsen O* Primary amyloidosis in lungs and heart. Acta Med. Scand. *184* 125–128, 1968

10 *Weiss L.* Isolated multiple nodular pulmonary amyloidosis. Amer J clin. Path *33* 318–329 1960

11 *Zundel W E. & Prior A P.* An amyloid lung Thorax *26* 357–363 1971

Acta path. microbiol. scand. Sect. A, 85: 911–916, 1977

A QUANTITATIVE STUDY OF GLOMERULI IN IDIOPATHIC NEPHROSIS WITH MINIMAL OR NO GLOMERULAR LESIONS

ERIK LUDWIGSEN, FINN HANBERG SØRENSEN and STEEN OLSEN

The University Institute of Pathology, University of Aarhus, Kommunehospitalet, Århus, Denmark

Ludwigsen, E., Hanberg Sørensen, F. & Olsen, S. A quantitative study of glomeruli in idiopathic nephrosis with minimal or no glomerular lesions. Acta path. microbiol. scand. Sect. A, 85: 911–916, 1977.

A quantitative investigation was performed of glomeruli in renal biopsies from patients with nephrotic syndrome or persisting proteinuria associated with normal light microscopic findings or slight changes not considered significant ("minimal change disease", lipoid nephrosis). The mesangial area was widened (+ 26 per cent, $p < 0.05$) and there was an increase in the mean of the total number of cellular nuclei per glomerulus, the number of mesangial (+ 19 per cent) and endothelial nuclei (+ 23 per cent), but of these only endothelial hypercellularity was significant ($p < 0.025$).

Key words: Nephrosis; renal biopsy; minimal change disease; cellular count; morphometry.

Erik Ludwigsen, University Institute of Pathology, Kommunehospitalet, DK-8000 Aarhus C, Denmark.

Received 30.?.77. Accepted 30.?.77

It is generally recognized that monosymptomatic proteinuria and nephrotic syndrome may be associated with a variety of glomerular lesions as well as with glomeruli which are virtually normal on light microscopy (*Pollak et al.* 1968). In the latter cathegory (Lipoid nephrosis, "minimal change disease") changes are present on electron microscopy (retraction of epithelial foot processes) which most authors consider to be secondary to proteinuria, but immunodeposits have not been detected by either electron microscopy or immunofluorescence (*Drummond et al.* 1966, *Jao et al.* 1973).

The histologic diagnosis of normal glomerular structure or minimal glomerular lesions has nearly always been based on subjective judgement, and precise quantitative investigations are few and partially contradictory. One group found a significant mesangial hypercellularity (*Wehner* 1974) and therefore regarded the disease as a mild proliferative glomerulonephritis. Another group of investigators (*Kawano et al.* 1971) found that the glomeruli from patients with lipoid nephrosis had fewer cells as compared with normal looking glomeruli in biopsies from patients with focal glomerulonephritis. The problem is unsettled at the moment and is

an old inflammatory focus in the development of amyloid deposits.

REFERENCES

1 *Cohen A S* Laboratory diagnostic procedures in the rheumatic diseases. 1st ed J & A Churchill Ltd. London 1967 p 333
2. *Dyke P C Demaray M J Delaney J W & Rasmussen R A* Pulmonary amyloidoma. Amer J clin Path 61 301–305 1974
3 *Firestone F N & Joison J* Amyloidosis a cause of primary tumours of the lung J Thorac. Cardiovasc. Surg. 51 292–299 1966
4 *Fors B & Rudén L.* Tumoral amyloidosis of the lung Acta path. microbiol. Scand. 61 1–12 1964
5 *Hayes W & Bernhardt H* Solitary amyloid mass of the lung Cancer 24 820–825 1969
6 *Lehner T Nunn R E & Pearse E* Electron microscopy of paraffin-embedded material in amyloidosis. J path. Bact. 91 297–300, 1966
7 *Saab S B Burke J Hopeman A & Almond C* Primary pulmonary amyloidosis. Report of two cases. J Thorac. Cardiovasc. Surg 67 301–307 1974
8. *Skagseth E & Normann T* Localised amyloid tumour of the lung Scand. J Thorac. Cardiovasc. Surg 4 135–138, 1970
9 *Thomsen O.* Primary amyloidosis in lungs and heart Acta Med. Scand 184 125–128, 1968.
10 *Weiss L.* Isolated multiple nodular pulmonary amyloidosis. Amer J clin. Path. 33 318–329 1960
11 *Zundel W E. & Prior A P* An amyloid lung. Thorax 26 357–363 1971

RESULTS

The mean values for total and differential counts of cell nuclei and the determination of total glomerular and mesangial areas appear from Table 1 which for comparison also contains the normal values of these parameters provided from a study of persons without renal disease investigated by the same technique as in the present study (*Hanberg Sorensen* 1977) Of the 12 patients one patient was omitted from the statistic estimations because of age (eight years old) Two patients were excluded from the age related differential nuclear counts because they were past 45 years (62 and 66 years old) and six patients were omitted from area related estimations because their biopsies were fixed in formaldehyde.

The main results of the comparison can be summarized as follows. The deviations from normal values were small or minimal. The most conspicuous feature was an increase in the number of glomerular cell nuclei. Thus the endothelial cells were increased by 23 per cent, the mesangial cells by 19 per cent and the total number by 10 per cent. However due to a rather large inter individual variation in some of the counts, only endothelial hypercellularity was significant ($p < 0.025$) The observed changes of absolute counts can probably explain the significant increase in the relative number of endothelial nuclei and decrease in the relative number of epithelial nuclei. The mean value of the mesangial area was increased by 25 per cent ($p < 0.05$) No changes were observed concerning the total glomerular area, the number of nuclei per unit area and the number of mesangial nuclei per unit mesangial area. Of course these last mentioned results must be evaluated very cautiously due to the small number of test objects. The quantitative glomerular changes in each biopsy are presented in a diagram designed for individual biopsies (*Hanberg Sorensen* 1977) which demonstrates the same trends as described above (Fig. 1) The patient with a total cell count exceeding the upper normal limit (95 per cent confidence limit) did not present special clinical or laboratory features and electron microscopical examination was normal.

TABLE 1 *Quantitative Glomerular Findings in "Minimal Change Disease" (M C.D)*

Parameters	Number of kidneys		Mean values and variances of means				Level of significance of difference
	M C.D	Normals	M.C.D		Normals		
			$\bar{x}$	s^2	$\bar{x}$	s^2	
Number of mesangial nuclei Age < 45 years.	9	10	29.8	7.0770	25.0	0.7674	
Number of endothelial nuclei All ages	11	22	58.0	20.1818	47 7	2.8585	$p < 0.025$
Number of epithelial nuclei Age < 45 years	9	10	32.9	1.8457	34 1	1 4476	
Mesangial nuclei % of total nuclei Age < 45 years	9	10	24.5	2.7747	23 7	0 6592	
Endothelial nuclei % of total nuclei All ages	11	22	47	3.0997	43.2	0 3648	$p < 0.0125$
Epithelial nuclei % of total nuclei Age < 45 years	9	10	27.8	3.0567	32.6	0 1807	$p < 0.01$
Total glomerular nuclei All ages	11	22	120 4	34.0231	110 0	14.6995	
Total glomerular area μm² 1,000 All ages	5	12	18.9	6.8071	18.5	1.0417	
Mesangial area % of total area Age < 45 years	4	6	10 8	1.2026	8 6	0.0333	$p < 0.05$
Total nuclei per 1,000 μm² of total area All ages	5	12	6.3	0.0625	6.3	0.0334	
Mesangial nuclei per 1,000 μm² of mesangial area Age < 45 years	4	6	16 6	2.0138	16.6	0.5156	

generally regarded as having implications for pathogenesis and classification We therefore undertook a quantitative study of renal biopsies from a series of patients with this disease

MATERIAL AND METHODS

Criteria for selection of specimens Percutaneous renal biopsies were selected from our files on the basis of the following criteria Biopsies from patients with nephrotic syndrome or persisting proteinuria without significant hematuria or elevation of blood pressure and with normal renal function were considered and selected for further study if no light microscopical abnormalities of the glomeruli were present or if only slight and probably insignificant changes such as minimal hypercellularity or mesangial widening were noted on initial examination of the biopsy Furthermore the biopsies included in the quantitative examination fulfilled the technical criteria of having at least 10 undamaged glomeruli not situated near the outer surface of the biopsy specimen and it being possible to study 30 serial sections of each of these glomeruli to be sure that only central sections were used for the quantitative investigation (*Hanberg Sorensen* & *Ledet* 1972 *Hanberg Sorensen* 1972)

The patients One biopsy from each of 12 patients, six males and six females fulfilled these criteria. The mean age was 34 4 years (range 8–66 years) The known duration of the proteinuria at the time of biopsy was 0–½ year in seven patients 1 to 12 years in five patients. Ten had a nephrotic syndrome two had persisting proteinuria without edema. One patient received steroids with temporary effect on proteinuria the others had not been treated earlier Serological investigation for streptococcal infection was performed in nine patients. It was negative in all patients investigated The proteinuria at the time of biopsy was 1 g/day in one patient 11 patients had more than 5 g/day maximum 19 6 g/day Microscopic hematuria was found in one patient, the others had no hematuria. All patients had normal blood pressure. The serum creatinine was in one patient 3 0 mg% at biopsy but it decreased to 1 2 mg% at discharge from the hospital This patient had only one kidney All the other patients had serum creatinine below 1 1 mg%

Six patients were not treated after the biopsy one of them showed spontaneous remission, four had persistent slight proteinuria 1 2 years later and no information was available from one. Four patients were treated with steroids three with good response (no proteinuria on to two years later) one without. Two patients received Endoxan® (one of them in addition to steroid) Both these patients responded satisfactorily with disappearance of the proteinuria.

The biopsy specimens Light microscopy showed normal glomeruli or insignificant mesangial hypercellularity and/or mesangial broadening. Segmental sclerosis or hyalinosis or spike formations were not present Tubules and interstitium were normal Immunofluorescence investigation was performed in 5 biopsies. Immunoglobulins, C3 and fibrinogen were not detected in the glomeruli or elsewhere. Electron microscopical study of 5 biopsies showed normal findings apart from fusion (retraction) of epithelial foot processes. No deposits were seen.

Methods The quantitative examination of the biopsies was carried out as a blind study The specimens were investigated together with renal biopsies from other renal diseases, the quantitative examinator (E L.) being unaware of clinical data and histological diagnosis.

The biopsy specimens were fixed in Carnoy's fluid (5 patients) or 4 per cent aqueous formaldehyde (ph 7) (7 patients) Thirty serial sections of each paraffin embedded biopsy were cut on a microtome adjusted to 2 μm, the staining method being periodic-acid-Schiff-hematoxylin

In each biopsy the quantitative examination was carried out on central sections of ten different glomeruli (*Hanberg Sorensen* & *Ledet* 1972) If more than ten glomeruli were available three glomeruli situated most subcapsularly three others most juxtamedullarly and four glomeruli placed in the midcortical zone were examined.

The quantitative examination included total and differential counts of nuclei in all biopsies. Determination of mesangial and total glomerular areas (i.e areas delineated by Bowman's capsule) was carried out only on biopsies fixed in Carnoy's fluid because these parameters are dependent on fixation and the normal material used for comparison was fixed in Carnoy's fluid (*Hanberg Sorensen* 1977) The quantitative methods used in this study have previously been described in detail (*Hanberg Sorensen* & *Ledet* 1972, *Hanberg Sorensen* 1977) Point counting was used for determination of total glomerular and mesangial areas, the point spacing being 17 μm. The total—and differential counts were carried out on projected glomeruli with marking of each nucleus counted. A Leitz Ortolux microscope was used with a mirror for projection. The objective was a Leitz FL Apo 40/075 Total magnification of the projected glomerulus was × 920

Statistical methods. Estimation of means and the variances of means was performed in the way described in a previous paper (*Hanberg Sorensen* 1977) Comparison of the parameter means of biopsies with minimal change disease and normal was done by a modified t test (*Hald* 1952)

paring their patients (who were mostly children) with their previously published normal values which were obtained from adults (*Kazeno et al.* 1971). However their cell counts from patients with lipoid nephrosis were constantly lower than those from microscopically normal-looking glomeruli from patients with a focal glomerulonephritis, which led them to disregard the concept of an inflammatory lesion forming the base of lipoid nephrosis. It is obvious, that this approach does not permit to detect small deviations from normal values.

The technique used by *Wehner* (1974) varies in several important details from that used by us (thickness of sections, embedding medium, staining method and selection of sections). No comparison can therefore be made concerning the absolute figures for measurements or counts. When comparing with his own control material, Wehner found an increase in the total number of glomerular cells by 21 per cent due to hypercellularity of all three cell types. The mesangial and epithelial proliferation were both significant, the mesangial count being most increased (55 per cent). The relative mesangial area was not found to be increased in this study.

Thus, a glomerular hypercellularity was demonstrated in the study by Wehner as well as in the present study but there is not unanimity concerning the cell type which is most increased in number. In part this difference might come from difficulties in distinguishing mesangial cells from endothelial cells, but differences in the population of patients investigated might also influence the results. The age of the patients studied by Wehner was generally higher than ours and it was in the group of patients with hematuria that Wehner found the greatest differences as compared with his normal material.

Based on the results of Wehner and our group we regard it as probable that the nephrotic syndrome with no or minimal glomerular lesions on conventional light microscopy is associated with hypercellularity of mesangial or endothelial cells or both. However the cell proliferation is rather slight and single cases will often show values not exceeding the 95 per cent confidence limits of a normal material. Cellular proliferation has long been regarded as a sign of an inflammatory reaction. This has led Wehner to postulate that lipoid nephrosis in fact is a minimal proliferative glomerulonephritis. We are not convinced that slight hypercellularity tells anything about pathogenesis. The constant absence of immunodeposits in this disease seems to us to be sufficient reason to exclude it from the group of glomerulonephritides. The etiology and pathogenesis of the disease are still quite unknown.

We wish to thank *Claus Brun* M.D., Department of Clinical Pathology, Municipal Hospital, Copenhagen, for accession to his material and for providing us with three biopsies.

REFERENCES

1. *Drummond K. N., Michael A. F., Good R. A. & Vernier R. L.* The nephrotic syndrome of childhood: Immunologic, clinical and pathologic correlations. J. Clin. Invest. 45 620–630 1966.
2. *Grishman E. & Churg J.* Pathology of nephrotic syndrome with minimal or minor glomerular changes. In *Kincaid-Smith P., Mathew T. H. & Becker E. L.* (Ed.): Glomerulonephritis, part 1. John Wiley & Sons, New York, London, Sydney and Toronto, 1972 pp. 165–181.
3. *Hald A.* Statistical theory with engineering applications. John Wiley & Sons, London, New York, Tokyo, 1952, pp. 397–398.
4. *Hanberg Sørensen F.* Quantitative studies of the renal corpuscles I. Intraglomerular, interglomerular and interfocal variation in the normal kidney. Acta path. microbiol. scand. Sect. A. 80 115–124 1972.
5. *Hanberg Sørensen F.* Quantitative studies of the renal corpuscles IV: determination of normal values in various age categories, and an analysis of the possible influence of physiological degrees of arteriolosclerosis. Acta path. microbiol. scand. Sect. A. 85 356–366 1977.
6. *Hanberg Sørensen F.:* A quantitative study of the renal corpuscles in acute renal allograft

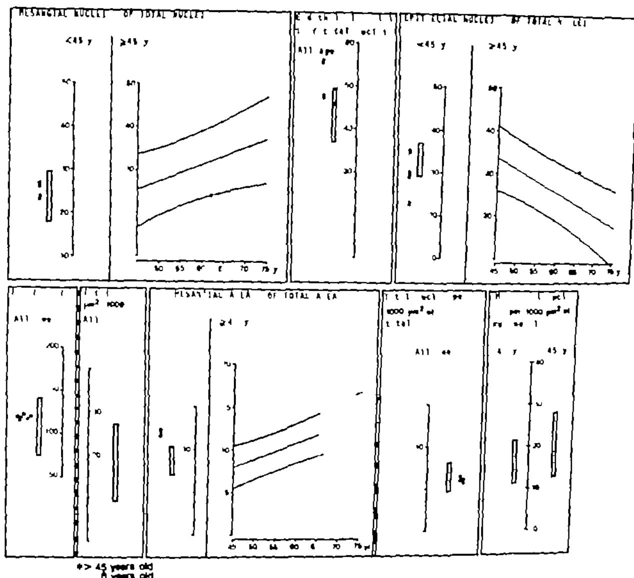


Fig 1 Mean values in biopsies from patients with minimal glomerular lesions in relationship to 95 per cent prediction limits for normal renal biopsies.

DISCUSSION

The distinction between virtually normal or only slightly altered glomeruli and glomerular alterations of abnormal character presents severe difficulties. Here as in other fields of pathology the dividing line between normality and slight degrees of abnormality cannot be drawn precisely by subjective judgement (*Jao et al* 1973). In the case of patients with a nephrotic syndrome this distinction has important prognostic implications. The proteinuria in patients with few or no changes will *most often* respond to steroid while a *significant* number of patients with suspected or distinct glomerular pathology will show resistency toward treatment and eventually develop an irreversible renal failure (*Jao et al* 1973, *Grishman & Churg* 1973). It is therefore surprising that so few quantitative investigations have been performed (*Wehner* 1968, *Kawano et al* 1971) even if the technique for such studies is cumbersome and time consuming.

Kawano et al (1971) in their study used central sections and almost the same section thickness as we did and the general level of their normal values corresponds acceptably with ours. They abstained from com-

ing their patients (who were mostly children) with their previously published normal values which were obtained from adults (Larsen et al. 1971). However their cell counts from patients with lipoid nephrosis were unexpectedly lower than those from microscopically normal-looking glomeruli from patients with a focal glomerulonephritis, which led them to disregard the concept of an inflammatory lesion forming the base of lipoid nephrosis. It is obvious, that this approach does not permit to detect small deviations from normal values.

The technique used by *Wehner* (1974) differs in several important details from that used by us (thickness of sections, embedding medium, staining method and selection of glomeruli). No comparison can therefore be made concerning the absolute figures for measurements or counts. When comparing with his own control material, Wehner found an increase in the total number of glomerular cells by 21 per cent due to hypercellularity of all three cell types. The mesangial and epithelial proliferation were both significant, the mesangial count being most increased (55 per cent). The relative mesangial area was not found to be increased in this study.

Thus, a glomerular hypercellularity was demonstrated in the study by Wehner as well as in the present study but there is not unanimity concerning the cell type which is most increased in number. In part this difference might come from difficulties in distinguishing mesangial cells from endothelial cells, but differences in the population of patients investigated might also influence the results. The age of the patients studied by Wehner was generally higher than ours and it was in the group of patients with hematuria that Wehner found the greatest differences as compared with his normal material.

Based on the results of Wehner and our group we regard it as probable that the nephrotic syndrome with no or minimal glomerular lesions on conventional light microscopy is associated with hypercellularity of mesangial or endothelial cells or both. However the cell proliferation is rather slight and single cases will often show values not exceeding the 95 per cent confidence limits of a normal material. Cellular proliferation has long been regarded as a sign of an inflammatory reaction. This has led Wehner to postulate that lipoid nephrosis in fact is a minimal proliferative glomerulonephritis. We are not convinced that slight hypercellularity tells anything about pathogenesis. The constant absence of immunodeposits in this disease seems to us to be sufficient reason to exclude it from the group of glomerulonephritides. The etiology and pathogenesis of the disease are still quite unknown.

We wish to thank *Claus Brun* M.D. Department of Clinical Pathology Municipal Hospital, Copenhagen, for accession to his material and for providing us with three biopsies.

REFERENCES

1. *Drummond K. N., Michael A. F., Good R. A. & Vernier R. L.* The nephrotic syndrome of childhood: immunologic, clinical and pathologic correlations. J. Clin. Invest. 45: 620–630, 1966.
2. *Grishman, E. & Churg, J.* Pathology of nephrotic syndrome with minimal or minor glomerular changes. In *Kincaid-Smith P., Mathew T. H. & Becker E. L.* (Ed.) Glomerulonephritis, part 1. John Wiley & Sons, New York, London, Sydney and Toronto, 1973, pp. 165–181.
3. *Hald A.* Statistical theory with engineering applications. John Wiley & Sons. London, New York, Tokyo. 1952, pp. 397–398.
4. *Hanberg Sørensen F.* Quantitative studies of the renal corpuscles I. Intraglomerular, interglomerular and interfocal variation in the normal kidney. Acta path. microbiol. scand. Sect. A. 80: 115–124. 1972.
5. *Hanberg Sørensen F.* Quantitative studies of the renal corpuscles IV. determination of normal values in various age categories, and an analysis of the possible influence of physiological degrees of arteriolosclerosis. Acta path. microbiol. scand. Sect. A. 85: 356–366, 1977.
6. *Hanberg Sørensen F.* A quantitative study of l corpuscles in acute renal allograft

rejection Acta path microbiol scand Sect. A. 85 367–372 1977

7 *Hanberg Sorensen F & Ledet T* Quantitative studies of renal corpuscles II a methodological study Acta path microbiol. scand. Sect A. 80 721–728 1972

8 *Jao W Lewy P Norris S H Pollak V E & Pirani C L.* Lipoid Nephrosis A reassessment. In *Kincaid-Smith P Mathew T H & Becker E L.* (Ed.) Glomerulonephritis, part 1 John Wiley & Sons, New York London Sydney and Toronto 1972 pp 165–181

9 *Kawano K Wenzl J McCoy J Porch J & Kimmelstiel P* Lipoid nephrosis. A multifold blind study including quantitation Lab Invest. 24 499–503 1971 a.

10 *Kawano K McCoy J Wenzl J Porch J Howard D Goddard M & Kimmelstiel P.* Quantitation of glomerular structure. A study of methodology Lab Invest. 25 343–348 1971 b

11 *Pollak V E Rosen S M Pirani C L. Muehrcke R C & Kark R M* Natural history of lipoid nephrosis and of membranous glomerulonephritis. Ann. Int. Med 69 1171–1196 1968.

12 *Wehner H* Zur Frage der glomerulären Zellproliferation bei akuter membranöser Glomerulonephritis. Verh. dtsch. Ges. Path. *52* *288–293 1968* b.

13 *Wehner H* Quantitative Pathomorphologie des Glomerulum der menschlichen Niere. Veröffentlichungen aus der Pathologie 95 1–67 1974

Acta path. microbiol. scand. Sect. A, 85 917–930 1977

PSEUDOSARCOMATOUS LESIONS OF THE SOFT TISSUES REPORTED AS SARCOMA DURING A 6 YEAR PERIOD (1958–1963)

INGVAR DAHL and LENNART ANGERVALL

Departments of Pathology University of Gothenburg and Central Hospital, Vänersborg, Sweden

Dahl, I. & Angervall, L. Pseudosarcomatous lesions of the soft tissues reported as sarcoma during a 6-year period (1958–1963). Acta path. microbiol. scand. Sect. A, 85 917–930 1977

Pseudosarcomatous lesion of the soft tissues is a term used in the present study for various soft tissue lesions and tumours easily clinically or histologically or both, misinterpreted as sarcoma. Eighty-one cases, that is to say 10 per cent of all tumours classified and reported to the Swedish Cancer Registry as malignant soft tissue tumours during the 6-year period studied (1958–1963) were reclassified as pseudosarcomatous lesions of the soft tissues. Forty-seven cases were classified as pseudosarcomatous proliferative lesions of the soft tissues with or without bone formation 38 cases of nodular fasciitis 1 of proliferative fasciitis and 8 of proliferative myositis. In 3 of these cases there were mixed forms of proliferative fasciitis and proliferative myositis with areas compatible with the diagnosis of nodular fasciitis evident in all cases. Twenty-two cases of atypical fibroxanthomas of the skin were next in frequency followed by 7 ancient neurilemmomas, 2 spindle cell lipomas, 1 pseudomalignant osseous tumour of the soft tissues, 1 pigmented villonodular synovitis and 1 juvenile xanthogranuloma. An attempt is made to explain the reasons for these erroneous diagnoses of sarcoma and it is stressed that for these lesions the conventional histological criteria for malignancy are not valid. The awareness and knowledge of the existence of these particular entities are therefore considered mandatory for an accurate diagnosis.

Key words: Soft tissue tumour; pseudosarcomatous lesion.

Ingvar Dahl, Department of Pathology, Central Hospital, Fack, S-462 01 Vänersborg, Sweden.

Received 29 77   Accepted 29 77

There are several publications in the medical literature describing tumours or tumour-like lesions of the soft tissues having a benign clinical course but often clinically and histologically misinterpreted as sarcoma and thus leading to unnecessary surgical treatment or irradiation or both. Such lesions are nodular fasciitis (*Konwaler et al* 1955, *Allen* 1972, *Dahl et al* 1972) proliferative myositis (*Kern* 1960, *Enzinger & Dulcey* 1967) proliferative fasciitis (*Chung & Enzinger* 1975) myositis ossificans including pseudomalignant osseous tumour of the soft tissues (*Fine & Stout* 1956, *Angervall et al.* 1969) atypical fibroxanthoma of the skin (*Helwig* 1963, *Fretzin & Helwig* 1973, *Dahl* 1976) pigmented villonodular synovitis (*Jaffe et al* 1941, *Moberger et al.* 1968) juvenile xanthogranuloma (*Helwig & Hackney* 1954, *Enzinger* 1965) spindle cell lipoma (*Enzinger & Harvey* 1975, *Angervall et al.* 1976) and ancient neurilemmoma (*Ackerman & Taylor* 1951, Dahl 1977)

This paper presents the various forms of pseudosarcomatous lesions of the soft tissues in a series of 770 cases of malignant soft tissue tumours reported to the Swedish Cancer Registry during a 6-year period (1958–1963) An attempt is made to explain the reasons for these erroneous diagnoses.

MATERIAL AND METHODS

The clinical records paraffin blocks and routinely stained microscopic slides from 770 patients registered at the Swedish Cancer Registry during a 6-year period (1958–1963) with tumours reported as malignant soft tissue tumours located in the skin (code nr 191) the soft tissues and muscle including the retroperitoneal area (code nr 197) and peripheral nervous system (code nr 193.3) were collected The material was re-examined and after excluding malignant tumours (41 cases) such as malignant melanomas and malignant lymphomas as well as various benign tumours (16 cases) which had wrongly been registered as malignant soft tissue tumours there remained 713 cases, 119 of which were retroperitoneally located. Eighty-one of the 713 cases were classified as pseudosarcomatous lesions of the soft tissues and comprise the material for this study

Sections of tissue routinely stained with haematoxylin and eosin or the haematoxylin-van Gieson method or both were available for review in all cases. Sections of paraffin-embedded tissue were specially stained as reported previously (*Dahl et al.* 1972 *Dahl* 1976 *Angervall et al.* 1976 *Dahl & Angervall* 1977 *Dahl* 1977)

TABLE 1 *Pseudosarcomatous Lesions of the Soft Tissues Reported as Sarcoma during a 6-Year Period (1958–1963)*

Form of pseudosarcomatous lesion	No of cases
Pseudosarcomatous proliferative lesion of the soft tissues (nodular fasciitis proliferative fasciitis proliferative myositis and mixed forms)	47
Pseudomalignant osseou tumor of the soft tissues	1
Atypical fibroxanthoma of the skin	22
Pigmented villonodular synovitis	1
Juvenile xanthogranuloma	1
Spindle cell lipoma	2
Ancient neurilemmoma	7
Total	81

RESULTS

The various forms of pseudosarcomatous lesions of the soft tissues of the eighty-one tumours primarily diagnosed as sarcoma are shown in Table 1 The series has been partly reported in earlier papers (*Dahl et al* 1972 *Dahl* 1976 *Angervall et al* 1976, *Dahl & Angervall* 1977 *Dahl* 1977) The clinical findings, the gross and microscopic appearances of the present cases are in accordance with those reported in these papers. Representative areas of the various forms of pseudosarcomatous lesions are shown in Figs 4 to 19

Pseudosarcomatous Proliferative Lesions of the Soft Tissues with or without Bone Formation

Forty-seven cases were classified as pseudosarcomatous proliferative lesions of the soft tissues with or without bone formation (*Dahl & Angervall* 1977) The clinical findings and the microscopic appearances were compatible with the diagnosis of nodular fasciitis in 38 cases proliferative fasciitis in one case and proliferative myositis in 8 cases However in 3 cases there was a mixture of proliferative

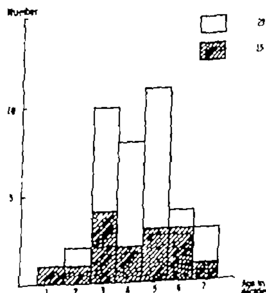


Fig 1 Pseudosarcomatous lesions of the soft tissues The sex and age distribution of 38 cases classified as nodular fasciitis

fasciitis-like and proliferative myositis-like areas within the same lesion and furthermore, areas typical of nodular fasciitis were evident in all cases. Bone formation was evident in one case with osteoid tissue and bone trabeculae distributed intramuscularly in a manner resembling that of proliferative myositis.

The sex and age distribution of the patients is shown in Fig. 1 and Table 6. The youngest patient was 6 years old and the oldest 69 years. The median age was 42 years. The median age of the 9 patients with

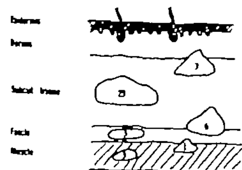


Fig. 2. Pseudosarcomatous lesions of the soft tissues. The anatomical site of 39* cases classified as nodular fasciitis.

* One patient had two lesions.



Fig. 3. Pseudosarcomatous lesions of the soft tissues. The sex and age distribution of 22 cases classified as atypical fibroxanthoma.

TABLE 2. *Pseudosarcomatous Lesions of the Soft Tissues. The Anatomical Location of 39* Cases Classified as Nodular Fasciitis*

Anatomical location		No of cases
Head and neck		4
Upper extremity		22
Upper arm (shoulder)	4	
Forearm	16	
Hand	2	
Chest		4
Abdomen		1
Back		3
Lower extremity		5
Thigh (hip)	4	
Leg	1	
Foot		
Total		39

* One patient had two lesions.

TABLE 3. *Pseudosarcomatous Lesions of the Soft Tissues. Primary Diagnoses of 39* Cases of Nodular Fasciitis*

Primary diagnoses	No of cases
Fibrosarcoma	20
Fibromyxosarcoma	6
Neurofibrosarcoma	4
Synovial sarcoma	2
Fibroliposarcoma	1
Liposarcoma	1
Sarcoma, unspecified	5
Total	39*

* One patient had two lesions.

lesions classified as proliferative fasciitis and proliferative myositis was 59 years compared with 36.5 years for the 38 patients with lesions recorded as nodular fasciitis. Three patients were 15 years old or less, all with lesions classified as nodular fasciitis.

The anatomical location and site of the tumours are shown in Tables 2 and 6 and Fig. 2.

The primary diagnoses of the 47 cases of pseudosarcomatous proliferative lesions of the soft tissues are shown in Tables 3 and 6.

The treatment and follow up of the 9 patients with lesions classified as proliferative fasciitis and proliferative myositis are shown in Table 6

All the 38 patients with lesions classified as nodular fasciitis were treated by local surgical excision of the tumour Because of the initial diagnosis of malignancy wide re excision of the scar area was performed in 27 patients, and more than one re-excision in 4 of them. A skin graft was necessary in order to close the wound in 5 patients and regional lymph node dissection was performed in another patient Three patients received radiotherapy and 1 other received chemotherapy Eight patients were examined at frequent intervals for 5 years or more Follow up information was available in 36 of the 38 patients with the follow up period ranging from 3 to 18.5 years, with a median of 15 years. Five patients died all of intercurrent disease an autopsy was performed in 3 of these patients. Thirty-one patients are alive and well without signs of recurrences or metastases. In 29 of these patients, the follow up period is more than 12 years.

Atypical Fibroxanthoma of the Skin

Twenty two cases in this series were classified as atypical fibroxanthoma of the skin

TABLE 4 *Pseudosarcomatous Lesions of the Soft Tissues The Anatomical Location of 22 Cases Classified as Atypical Fibroxanthoma*

Anatomical location		No of cases
Head and neck		5
Upper extremity		8
Upper arm (shoulder)	6	
Forearm	1	
Hand	1	
Chest		2
Abdomen		1
Back		3
Lower extremity		3
Thigh (hip)		
Leg	2	
Foot	1	
Total		22

Fig 4 Pseudosarcomatous proliferative lesion of the soft tissues. Low-power view of a subcutaneously situated lesion extending partly nodular partly diffusely from fascial and septal planes almost symmetrically into the adjacent fat tissue Haematoxylin van Gieson × 6

Fig 5 Area compatible with a diagnosis of nodular fasciitis. Extravasated erythrocytes with radiating capillaries mixtured with thin spindle shaped fibroblasts and inflammatory cells. Haematoxylin-van Gieson. × 40

Fig 6 Area compatible with a diagnosis of nodular fasciitis. Haphazardly arranged thin, spindle shaped and stellate-like fibroblasts in a matrix rich in mucosubstances. Haematoxylin-van Gieson × 100.

Fig 7 Area compatible with a diagnosis of nodular fasciitis. Cellular area with proliferating s-formed or wavy fibroblasts separating small clefts or slits and more plump fibroblasts arranged focally in a suggestion of whorls. Haematoxylin-van Gieson. × 100

The sex and age distribution of these patients is shown in Fig 3 The median age was 38 years, the range being 15–81 years.

The anatomical location of the tumours is shown in Table 4 The median age of the 5 patients with tumours on the head and neck was 73 years compared to a median age of 35 years for patients with tumours on the trunk and the extremities.

The primary diagnoses of the 22 cases of atypical fibroxanthoma of the skin are shown in Table 5

All patients were treated by local excision of the tumour Because of the initial diagnosis

TABLE 5 *Pseudosarcomatous Lesions of the Soft Tissues. Primary Diagnoses of 22 Cases of Atypical Fibroxanthoma of the Skin*

Primary diagnoses	No of cases
Fibrosarcoma	7
Dermatofibrosarcoma protuberans	8
Neurofibrosarcoma	1
Myosarcoma	1
Leiomyosarcoma	2
Sarcoma, unspecified	3
Total	22



4

5

6

The treatment and follow up of the 9 patients with lesions classified as *proliferative fasciitis* and proliferative myositis are shown in Table 6

All the 38 patients with lesions classified as nodular fasciitis were treated by local surgical excision of the tumour Because of the initial diagnosis of malignancy wide re excision of the scar area was performed in 27 patients, and more than one re-excision in 4 of them A skin graft was necessary in order to close the wound in 5 patients and regional lymph node dissection was performed in another patient Three patients received radiotherapy and 1 other received chemotherapy Eight patients were examined at frequent intervals for 5 years or more. Follow up information was available in 36 of the 38 patients with the follow up period ranging from 3 to 18 5 years with a median of 15 years. Five patients died all of intercurrent disease an autopsy was performed in 3 of these patients. Thirty-one patients are alive and well without signs of recurrences or metastases. In 29 of these patients, the follow up period is more than 12 years.

Atypical Fibroxanthoma of the Skin

Twenty two cases in this series were classified as atypical fibroxanthoma of the skin

TABLE 4 *Pseudosarcomatous Lesions of the Soft Tissues. The Anatomical Location of 22 Cases Classified as Atypical Fibroxanthoma*

Anatomical location		No of cases
Head and neck		5
Upper extremity		8
Upper arm (shoulder)	6	
Forearm	1	
Hand	1	
Chest		2
Abdomen		1
Back		3
Lower extremity		3
Thigh (hip)		
Leg	2	
Foot	1	
Total		22

Fig 4 Pseudosarcomatous proliferative lesion of the soft tissues. Low-power view of a subcutaneously situated lesion extending partly nodular partly diffusely from fascial and septal planes almost symmetrically into the adjacent fat tissue Haematoxylin-van Gieson × 6

Fig 5 Area compatible with a diagnosis of nodular fasciitis. Extravasated erythrocytes with radiating capillaries mixtured with thin *spindle shaped* fibroblasts and inflammatory cells. Haematoxylin van Gieson. × 40

Fig 6 Area compatible with a diagnosis of nodular fasciitis. Haphazardly arranged thin, spindle shaped and stellate-like fibroblasts in a matrix rich in mucosubstances. Haematoxylin-van Gieson. × 100

Fig 7 Area compatible with a diagnosis of nodular fasciitis. Cellular area with proliferating s-formed or wavy fibroblasts separating small clefts or slits and more plump fibroblasts arranged focally in a suggestion of whorls. Haematoxylin-van Gieson. × 100

The sex and age distribution of these patients is shown in Fig 3 The median age was 38 years the range being 15–81 years.

The anatomical location of the tumours is shown in Table 4 The median age of the 5 patients with tumours on the head and neck was 73 years compared to a median age of 35 years for patients with tumours on the trunk and the extremities.

The primary diagnoses of the 22 cases of atypical fibroxanthoma of the skin are shown in Table 5

All patients were treated by local excision of the tumour Because of the initial diagnosis

TABLE 5 *Pseudosarcomatous Lesions of the Soft Tissues Primary Diagnoses of 22 Cases of Atypical Fibroxanthoma of the Skin*

Primary diagnoses	No of cases
Fibrosarcoma	7
Dermatofibrosarcoma protuberans	8
Neurofibrosarcoma	1
Myosarcoma	1
Leiomyosarcoma	2
Sarcoma, unspecified	3
Total	22

Duration of tumour symptoms	Primary diagnoses	Treatment	Duration of follow-up (years)	Comments
1 week	Rhabdomyosarcoma	Excision	15	Alive and well
2 weeks	Neurofibrosarcoma	Wide-excision	8.5 (dead)	Autopsy no tumour
1 week	Fibromyxosarcoma	Excision + Re-excision	0.8 (dead)	Autopsy no tumour
1 week	Myosarcoma	Excision	15	Alive and well
2 weeks	Fibromyxosarcoma	Excision + Re-excision	12.5	Alive and well
3 days	Sarcoma, unspecified	Excision	16	Alive and well
2 weeks	Fibrosarcoma	Biopsy + Wide-excision	13.5	Alive and well
1 week	Rhabdomyosarcoma	Excision + Re-excision	15	Alive and well
1 week	Fibrosarcoma	Excision + Re-excision	17	Alive and well
2 months	Osteogenic sarcoma	Excision + Re-excision. Wide-excision	17	Alive and well
2 months	Synovial sarcoma	Biopsy + Amputation	Not known	Not possible to trace
4 months	Neurofibrosarcoma	Excision + Re-excision	17	Alive and well
1 year	Liposarcoma	Excision + Re-excision	12	Alive and well
8 months	Liposarcoma	Excision	12	Alive and well
12 years	Neurofibrosarcoma	Excision	6	Alive and well
Not known	Neurosarcoma	Excision	15	Alive and well
4 years	Malignant schwannoma	Excision + Re-excision	10.5	Alive and well
2 years	Malignant schwannoma	Excision	14	Alive and well
—	Sarcoma, unspecified	—	— (dead)	Diagnosed at autopsy
Not known	Sarcoma, unspecified	Excision	13 (dead)	Autopsy no tumour
5 years	Neurosarcoma	Excision + Radiation	17	Alive and well

The follow up period is 12 years or more in all these patients.

One lesion in this series was classified as *pigmented villonodular synovitis* 1 as *juvenile xanthogranuloma*, 2 as *spindle cell lipomas* 1 as *pseudomalignant osseous tumour of the soft tissues* and 7 as *ancient neurilemmomas*. The sex and age of these patients as well as the anatomical location and site, size in widest diameter duration of tumour symptoms, primary diagnoses, treatment and duration of follow-up are shown in Table 6.

TABLE 6 *Clinical Findings in 21 Patients with Tumour*

Patient code nr	Sex	Age (years)	Anatomical location	Anatomical site	Size widest d. (cm)
Pseudosarcomatous proliferative lesions of the soft tissues					
547	M	40	Upper arm (brachial m.)	Striated muscle	3.5
653	M	61	Upper arm (deltoid m.)	Striated muscle	7
671	M	63	Back (latissimus dorsi m.)	Striated muscle and subcut. tissue	2
650	M	43	Chest (pectoralis major m.)	Striated muscle	6
388	M	50	Back (latissimus dorsi m.)	Striated muscle	3
618	M	59	Chest (pectoralis major m.)	Striated muscle	5
390	F	61	Thigh (quadriceps m.)	Striated muscle and subcut. tissue	6
147	M	69	Chest (pectoralis major m.)	Subcut. tissue and striated muscle	5
771	M	58	Back (latissimus dorsi m.)	Striated muscle	2
Pseudomalignant osseous tumour of the soft tissues					
1100	F	43	Thigh	Deep subcut. tissue	–
Pigmented villonodular synovitis					
387	M	21	Knee	Deep subcut. tissue and joint capsule	10
Juvenile xanthogranuloma					
344	F	0.5	Forehead	Skin and subcut. tissue	1
Spindle cell lipoma					
625	M	63	Posterior neck	Subcut. tissue	2
1101	M	51	Shoulder	Subcut. tissue	5
Ancient neurilemmoma					
159	F	64	Neck	—	6
377	F	59	Thigh	—	5
360	F	60	Back	—	4
698	F	48	Leg	—	1
187	M	64	Retroperitoneal area	—	13
577	M	55	Retroperitoneal area	—	20
683	M	32	Retroperitoneal area	—	10

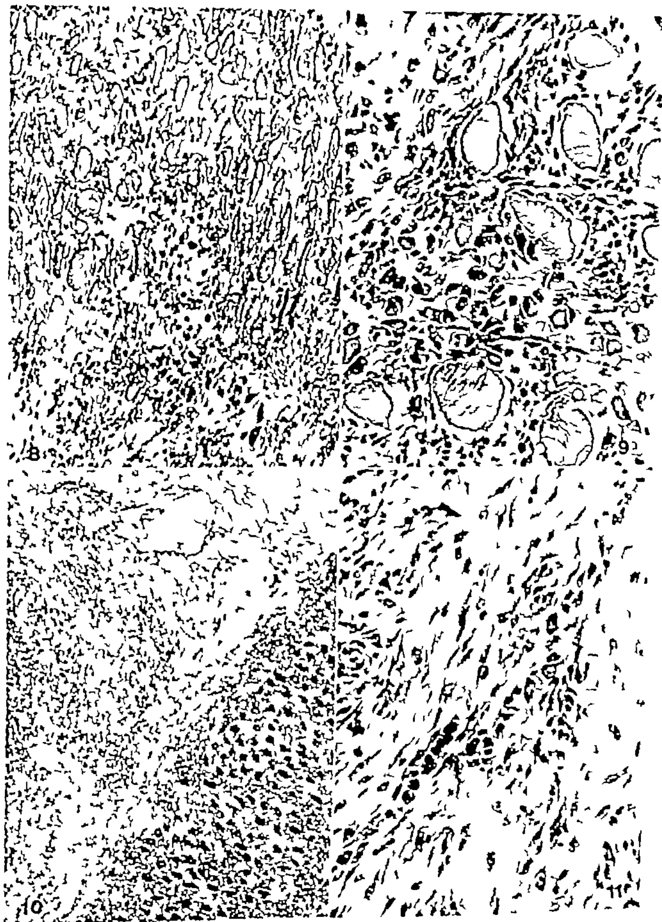
of sarcoma wide re-excision of the skin and adjacent tissue was performed in 11 patients. In one of them a skin graft was necessary to close the wound. Amputation of the whole external ear was performed in one patient. Regional lymph node excision was performed in 2 patients. One patient received radiotherapy after local excision of the tumour.

Follow up information was available in 20 patients, the follow-up period ranging from 2 to 16 years with a median of 13 years. Six patients died all of intercurrent disease, the remaining 14 patients are alive and well without signs of recurrences or metastases.

Duration of tumour symptoms	Primary diagnoses	Treatment	Duration of follow-up (years)	Comments
1 week	Rhabdomyosarcoma	Excision	15	Alive and well
2 weeks	Neurofibrosarcoma	Wide-excision	8.5 (dead)	Autopsy no tumour
week	Fibromyxosarcoma	Excision + Re-excision	0.8 (dead)	Autopsy no tumour
week	Myosarcoma	Excision	15	Alive and well
weeks	Fibromyxosarcoma	Excision + Re-excision	12.5	Alive and well
days	Sarcoma, unspecified	Excision	16	Alive and well
weeks	Fibrosarcoma	Biopsy + Wide-excision	13.5	Alive and well
week	Rhabdomyosarcoma	Excision + Re-excision	15	Alive and well
week	Fibrosarcoma	Excision + Re-excision	17	Alive and well
1 months	Osteogenic sarcoma	Excision + Re-excision Wide-excision	17	Alive and well
2 months	Synovial sarcoma	Biopsy + Amputation	Not known	Not possible to trace
4 months	Neurofibrosarcoma	Excision + Re-excision	17	Alive and well
1 year	Liposarcoma	Excision + Re-excision	12	Alive and well
8 months	Liposarcoma	Excision	12	Alive and well
12 years	Neurofibrosarcoma	Excision	6	Alive and well
Not known	Neurosarcoma	Excision	15	Alive and well
4 years	Malignant schwannoma	Excision + Re-excision	10.5	Alive and well
2 years	Malignant schwannoma	Excision	14	Alive and well
—	Sarcoma, unspecified	—	— (dead)	Diagnosed at autopsy
Not known	Sarcoma, unspecified	Excision	13 (dead)	Autopsy no tumour
5 years	Neurosarcoma	Excision + Radiation	17	Alive and well

The follow-up period is 12 years or more in all these patients.

One lesion in this series was classified as *pigmented villonodular synovitis* 1 as *juvenile xanthogranuloma* 2 as *spindle cell lipomas* 1 as *pseudomalignant osseous tumour of the soft tissues* and 7 as *ancient neurilemmomas*. The sex and age of these patients as well as the anatomical location and site, size in widest diameter duration of tumour symptoms, primary diagnoses, treatment and duration of follow-up are shown in Table 6


8
9
10
11

Figs 8 and 9. Areas compatible with a diagnosis of proliferative myositis. Proliferation of predominantly large mono- and binucleated, ganglion-cell like cells separating bundles and fibres of striated muscle. The cells are focally arranged in small clusters or groups. Haematoxylin and eosin. × 100 and × 250

Figs. 10 and 11. Areas compatible with a diagnosis of proliferative fasciitis. Proliferation of haphazardly arranged large mono- and binucleated cells in a matrix rich in mucosubstances, single mitoses are seen. Note the tendency to cyst-formation and the involvement of the adjacent striated muscle suggestive of proliferative myositis (Fig. 10). Haematoxylin and eosin. × 40 and × 250

DISCUSSION

All lesions in the present series were originally diagnosed histologically as various forms of malignant soft tissue tumours. It is clear that the conventional histological criteria for malignancy are not valid for these lesions. Therefore awareness and knowledge of the existence of these particular entities are mandatory for a correct diagnosis.

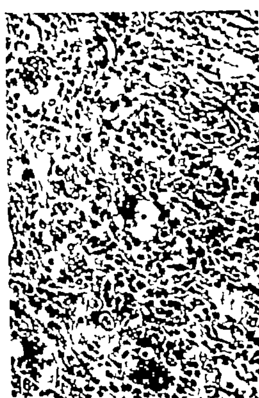
Ten per cent of all tumours classified and reported as malignant soft tissue tumours to the Swedish Cancer Registry during the 6-year period studied were pseudosarcomatous lesions of the soft tissues. If one excludes retroperitoneal sarcomas and pseudosarcomas (3 cases of ancient neurilemmoma) and wrongly registered cases, the percentage rises to 13. It is very probable that the misinterpretation of pseudosarcomatous lesions of the soft tissues as sarcoma occurs to a much lesser extent nowadays than during the period 1958–1963, i.e. the time when the original diagnoses of the lesions in the present series



Fig. 12. Pseudomalignant osseous tumour of the soft tissues. Zoning-phenomenon with central cellular area and peripherally arranged bone trabeculae. Haematoxylin-van Gieson. × 40.

Fig. 13. Pseudomalignant osseous tumour of the soft tissues. Central cellular area with proliferating spindle shaped cells. The nuclei are polymorphous and hyperchromatic. Haematoxylin-van Gieson. × 250.


8
9
10
11




18

19

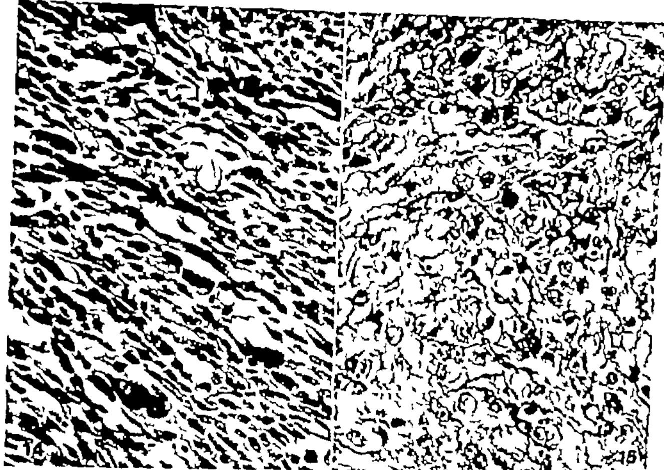


Fig 14 Atypical fibroxanthoma of the skin. Fascicular pattern with proliferating spindle shaped fibroblast-like cells arranged in parallel The nuclei are polymorphous, showing mitotic figures. Haematoxylin-van Gieson × 400

Fig 15 Atypical fibroxanthoma of the skin Haphazardly arranged histiocyte-like cells. The nuclei are large, moderately polymorphous. Haematoxylin-van Gieson. × 400

were made However pseudosarcomatous lesions of the soft tissues commonly require consultation both in the United States (*Enzinger* personal communication) and in Sweden, indicating a need for further knowledge

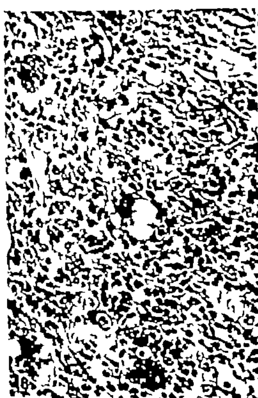
Pseudosarcomatous proliferative lesions of the soft tissues (*Dahl & Angervall* 1977) such as nodular fasciitis, proliferative fasciitis proliferative myositis and mixed forms, were the commonest lesions in the series. These lesion fulfil conventional microscopic criteria for malignancy such as high cellularity cellular and nuclear polymorphism, high frequency of mitoses and an infiltrative growth pattern We feel that the structure and the appearance of the lesion in the light microscope at low magnification are often

Fig 16 Pigmented villonodular synovitis. Mixture of multinucleated giant cells, histiocytic cells, foam cells and inflammatory cells. Haematoxylin and eosin. × 250

Fig 17 Juvenile xanthogranuloma. Mixture of proliferating histiocytes, inflammatory cells and giant cells (*Touton giant cells*) Haematoxylin and eosin × 250

Fig 18 Spindle cell lipoma. *Proliferating spindle shaped cells*, haphazardly distributed bundles of collagen and fat cells. Haematoxylin and eosin. × 250

Fig 19 Ancient neurilemmoma Moderately cellular Antoni type A tissue with single large hyperchromatic nuclei and a thick hyalinized vessel. Haematoxylin-van Gieson. × 250






18


19

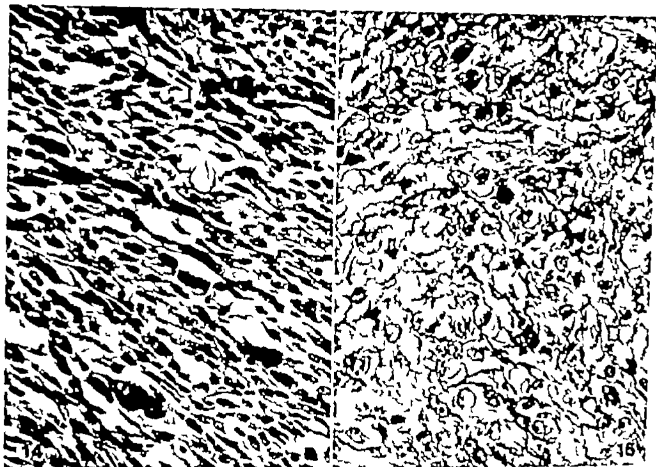


Fig 14 Atypical fibroxanthoma of the skin Fascicular pattern with proliferating spindle shaped fibroblast like cells arranged in parallel The nuclei are polymorphous, showing mitotic figures. Haematoxylin van Gieson. × 400

Fig 15 Atypical fibroxanthoma of the skin Haphazardly arranged histiocyte-like cells. The nuclei are large moderately polymorphous. Haematoxylin-van Gieson. × 400

were made. However pseudosarcomatous lesions of the soft tissues commonly require consultation both in the United States (*Enzinger* personal communication) and in Sweden indicating a need for further knowledge

Pseudosarcomatous proliferative lesions of the soft tissues (*Dahl & Angervall* 1977) such as nodular fasciitis, proliferative fasciitis, proliferative myositis and mixed forms were the commonest lesions in the series. These lesion fulfil conventional microscopic criteria for malignancy such as high cellularity cellular and nuclear polymorphism high frequency of mitoses and an infiltrative growth pattern We feel that the structure and the appearance of the lesion in the light microscope at low magnification are often

Fig 16 Pigmented villonodular synovitis. Mixture of multinucleated giant cells, histiocytic cells, foam cells and inflammatory cells. Haematoxylin and eosin. × 250

Fig 17 Juvenile xanthogranuloma. Mixture of proliferating histiocytes, inflammatory cells and giant cells (Touton giant cells) Haematoxylin and eosin. × 250

Fig 18 Spindle cell lipoma. Proliferating spindle shaped cells, haphazardly distributed bundles of collagen and fat cells. Haematoxylin and eosin. × 250

Fig 19 Ancient neurilemmoma Moderately cellular Antoni type A tissue with single large hyperchromatic nuclei and a thick hyalinized vessel Haematoxylin-van Gieson. × 250

loma can be based on the characteristic mixture of histiocytes, multinucleated foam cells (Touton giant cells) and inflammatory cells (*Enzinger et al* 1969) which was evident in this case.

The diagnosis of sarcoma in the 7 cases of ancient neurilemmomas and the 2 cases of spindle cell lipomas in the series was obviously based on cellularity severe nuclear polymorphism and hyperchromasia. Similar nuclear changes have been described in other benign tumours such as myxoid polyps of the vagina (*Norris & Taylor* 1966) and antrochoanal-nasal polyps-polyposis (*Smith et al* 1974 *Compagno et al.* 1976) which have been confused with sarcoma. The nuclear changes, not combined with mitotic activity are thought to be regressive in nature.

The follow-up information available confirms that the clinical course in all patients with pseudosarcomatous lesions of the soft tissues in the present study was benign. Recurrence may occur but only atypical fibroxanthoma of the skin is known to be capable of metastasizing and then only in exceptional cases (*Latter* 1964 *Abulafia et al* 1968, *Caffier & Sorger* 1973 *Fretzin & Helwig* 1973 *Jacmovich & Abulafia* 1973 *Jacobs et al* 1975 *Dahl* 1976) It is therefore questionable whether or not atypical fibroxanthoma should be included among the pseudosarcomatous lesions of the soft tissues. However in a review of some 300 cases of atypical fibroxanthoma of the skin in the literature, together with an own series of 57 cases, there were only 5 cases of metastasizing atypical fibroxanthoma of the skin (*Dahl* 1976) Further case reports (*Abulafia et al.* 1968, *Jacmovich & Abulafia* 1973 *Larrauri et al.* 1974 *Ferrando et al* 1975) have revealed another ? tentative cases of metastasizing atypical fibroxanthoma of the skin (*Abulafia et al* 1968, *Jacmovich & Abulafia* 1973) It is interesting in this connection that in 4 cases the metastases were limited to regional lymph nodes (*Caffier & Sorger* 1973 *Jacmovich & Abulafia* 1973 *Jacobs et al* 1975 *Dahl* 1976)

In patients with atypical fibroxanthoma of the skin we think it is impossible to predict the clinical course from histological parameters such as cell type cellularity cellular and nuclear atypia and mitotic activity Because the probability of an atypical fibroxanthoma of the skin proving itself malignant by metastasis is so low we advise the surgeon to perform a local excision including a margin of uninvolved tissue with follow-up of the patient. For all other forms of pseudosarcomatous lesions of the soft tissues, simple excision of the lesion for histological classification is considered the treatment of choice.

Supported by a research grant from the Swedish *Cancer Society* 530-K73-02X.

REFERENCES

Abulafia J Grinspan D & Casald A M.. Fibroxanthoma atipico. Arch. argent Derm. *18* 71–89 1968

Ackerman L. V Extra-osseous localized non-neoplastic bone and cartilage formation (so-called myositis ossificans) J Bone Jt Surg. *40 A* 279 298 1958.

Ackerman L. V & Taylor F H.. Neurogenous tumors within the thorax. A clinicopathological evaluation of forty-eight cases Cancer (Philad.) *4* 669–691 1951

Allen P W Nodular fasciitis. Pathology *4* 9–26 1972.

Angervall, L., Dahl I., Kindblom L.-G & Säve-Söderbergh J Spindle cell lipoma. Acta path. microbiol. scand. Sect A, *84* 477–487 1976

Angervall L., Stener B. Stener I & Ahrén C. Pseudomalignant osseous tumour of soft tissue. A clinical, radiological and pathological study of five cases J Bone Jt Surg *51 B* 654–663 1969

Caffier P & Sorger K Das maligne Histiocytom der Haut. Zbl. allg Path. *117* 472–477 1973

Chung E. B. & Enzinger F M Proliferative fasciitis. Cancer (Philad.) *36* 1450–1458, 1975

Compagno J Hyams V J & Lepore M L. Nasal polyposis with stromal atypia. Review and follow-up study of 14 cases Arch. Path. Lab Med *100* 224–226 1976.

Dahl I.: Atypical fibroxanthoma of the skin. A clinico-pathological study of 57 cases Acta path. microbiol. scand. Sect. A *84* 183–197 1976

Dahl I Ancient neurilemmoma (schwannoma) Acta path. microbiol scand. Sect. A, *85* 812–818, 1977

conclusive in distinguishing the lesions from sarcoma (*Dahl & Angervall* 1977) The cell type and structural pattern vary both within and between the lesions and it is important to recognize all forms of pseudosarcomatous proliferative lesions of the soft tissues in order to avoid an erroneous diagnosis of sarcoma To arrive at an accurate diagnosis it should be borne in mind that relatively rapid growth small size and superficial location are repeatedly found in pseudosarcomatous proliferative lesions of the soft tissues. Furthermore, interlacing bundles of anaplastic tumour cells arranged in parallel, which are a common feature of sarcomas of the soft tissues are not observed in pseudosarcomatous proliferative lesions of the soft tissues

The second commonest lesion in the series was atypical fibroxanthoma of the skin originally described in actinically damaged skin of the head and neck in elderly patients (*Helwig* 1963 *Kempson & McGavran* 1964 *Kroe & Pitcock* 1969) This lesion has also been referred to as sarcoma like tumours of the skin following irradiation (*Rachmaninoff et al* 1961), pseudosarcomatous dermatofibroma (*Levan et al* 1963) pseudosarcomatous reticulohistiocytoma (*Gordon* 1964) and pseudosarcoma of the skin (*Finlay-Jones et al* 1971) Atypical fibroxanthoma of the skin occurs at all ages anywhere on the body in non actinically damaged skin areas and in areas which have not been subjected to irradiation (*Fretzin & Helwig* 1973 *Dahl* 1976) This lesion is considered to be closely related to ordinary fibroxanthoma of the skin but shows a greater degree of cellular polymorphism increased number of mono- or multinucleated bizarre cells or both and mitotic figures, some of which are atypical (*Enzinger et al* 1969) Such features may easily lead to the diagnosis of sarcoma (*Dahl* 1976) Some lesions in the series should perhaps be classified as ordinary fibroxanthomas of the skin instead of atypical fibroxanthomas These lesions, however have been included in the group of atypical fibroxanthomas of the skin because they were diffusely growing, cellular with cellular and nuclear polymorphism and mitotic activity the latter finding being rare in ordinary fibroxanthomas of the skin (*Niemi* 1970)

One case of pseudomalignant osseous tumour of the soft tissues (*Fine & Stout* 1956) was originally interpreted as osteogenic sarcoma. There are several reports in the literature pointing out the risk of misinterpreting pseudomalignant osseous tumours as osteogenic sarcomas because of the cellularity and mitotic activity (*Ackerman* 1958 *Jeffreys & Stiles* 1966 *Angervall et al* 1969 *Spjut et al.* 1971 *Lagier & Cox* 1975) In order to arrive at an accurate diagnosis in these bone-forming lesions the demonstration of the maturation changes-zone phenomenon, evident in the present case as well as the lack of anaplasia of the proliferating cells, is mandatory

Pigmented villonodular synovitis has obviously because of its cellularity nuclear polymorphism and indistinct delineation, been misinterpreted as sarcoma (*Moberger et al* 1968) In a review of 143 cases (*Moberger et al* 1968) found 12 cases (8 4 per cent) of pigmented villonodular synovitis previously wrongly classified as synovial sarcoma. The low number only one case of pigmented villonodular synovitis in our series, is probably due to the fact that cases of pigmented villonodular synovitis interpreted as sarcomas might have been reported as sarcoma of bone or extremities to the Swedish Cancer Registry (code nrs 196 and 199.5) and therefore not been included in this study

One case of juvenile xanthogranuloma in a 5 months-old girl was originally diagnosed as a polymorphous fibrosarcomatous tumour probably neurofibrosarcoma Juvenile xanthogranuloma (*Helwig & Hackney* 1954) has been included by *Enzinger* (1965) together with nodular fasciitis and proliferative myositis, as a pseudosarcomatous lesion of the soft tissues The sarcoma diagnosis in the present case was obviously based on spontaneous ulceration of a relatively large lesion extending deeply and diffusely into the subcutaneous tissue and exhibiting high cellularity and mitoses. A diagnosis of juvenile xanthogranu-

ben can be based on the characteristic mixture of histocytes, multinucleated foam cells (Touton giant cells) and inflammatory cells (Enzinger et al. 1969) which was evident in this case.

The diagnosis of sarcoma in the 7 cases of ancient neurilemmomas and the 2 cases of spindle cell lipomas in the series was obviously based on cellularity severe nuclear polymorphism and hyperchromasia. Similar nuclear changes have been described in other benign tumours such as myxoid polyps of the vagina (Norris & Taylor 1966) and antrochoanal-nasal polyps-polyposis (Smith et al 1974, Compagno et al 1976) which have been confused with sarcoma. The nuclear changes, not combined with mitotic activity are thought to be regressive in nature

The follow up information available confirms that the clinical course in all patients with pseudosarcomatous lesions of the soft tissues in the present study was benign. Recurrence may occur but only atypical fibroxanthoma of the skin is known to be capable of metastasizing and then only in exceptional cases (Ladies 1964 Abulafia et al 1968, Caffier & Sorger 1973 Fretzin & Helwig 1973 Jamovich & Abulafia 1973 Jacobs et al. 1975 Dahl 1976) It is therefore questionable whether or not atypical fibroxanthoma should be included among the pseudosarcomatous lesions of the soft tissues. However in a review of some 300 cases of atypical fibroxanthoma of the skin in the literature together with an own series of 57 cases, there were only 5 cases of metastasizing atypical fibroxanthoma of the skin (Dahl 1976) Further case reports (Abulafia et al 1968, Jamovich & Abulafia 1973 Larraurí et al 1974 Ferrando et al 1975) have revealed another 2 tentative cases of metastasizing atypical fibroxanthoma of the skin (Abulafia et al 1968, Jamovich & Abulafia 1973) It is interesting in this connection that in 4 cases the metastases were limited to regional lymph nodes (Caffier & Sorger 1973, Jamovich & Abulafia 1973 Jacobs et al. 1975 Dahl 1976)

In patients with atypical fibroxanthoma of the skin, we think it is impossible to predict the clinical course from histological parameters such as cell type cellularity cellular and nuclear atypia and mitotic activity Because the probability of an atypical fibroxanthoma of the skin proving itself malignant by metastasis is so low we advise the surgeon to perform a local excision including a margin of uninvolved tissue with follow up of the patient. For all other forms of pseudosarcomatous lesions of the soft tissues, simple excision of the lesion for histological classification is considered the treatment of choice.

Supported by research grant from the *Swedish Cancer Society* 530-K73-02X.

REFERENCES

Abulafia J Grinspan D & Casala A 31 Fibroxanthoma atip co. Arch. argent. Derm. *18* 71–89 1968

Ackerman L. V Extra-osseous localized non-neoplastic bone and cartilage formation (so-called myositis ossificans) J Bone Jt Surg. *40 A* 279–298, 1958

Ackerman L. V & Taylor F H Neurogenous tumors within the thorax. A clinicopathological evaluation of forty-eight cases. Cancer (Phılad.) *4* 669–691 1951

Allen, P W Nodular fasciitis. Pathology *4* 9–26 1972.

Angervall, L., Dahl I Kindblom L.-G & Säve-Söderbergh J Spindle cell lipoma. Acta path. microbiol. scand. Sect. A, *84* 477–487 1976.

Angervall L Stener B Stener I & Ahrén C Pseudomalignant osseous tumour of soft tissue A clinical radiological and pathological study of five cases. J Bone Jt Surg. *51 B* 654–663 1969

Caffier P & Sorger K. Das maligne Histiocytom der Haut. Zbl allg Path. *117* 472–477 1973

Chung E. B. & Enzinger F M. Proliferative fasciitis Cancer (Philad.) *36* 1450–1458, 1975.

Compagno J Hyams V J & Lepore M L. Nasal polyposis with stromal atypia. Review and follow-up study of 14 cases. Arch. Path. Lab. Med *100* 224 226 1976.

Dahl I Atypical fibroxanthoma of the skin. A clinico-pathological study of 57 cases. Acta path. microbiol. scand, Sect. A, *84* 183–197 1976.

Dahl I Ancient neurilemmoma (schwannoma) Acta path microbiol scand Sect. A, *85* 812–818 1977

Dahl I & Angervall L Pseudosarcomatous proliferative lesions of soft tissue with or without bone formation. Acta path. microbiol scand Sect. A *85* 577–589 1977

Dahl I Angervall L Magnusson S & Stener B Classical and cystic nodular fasciitis. Pathol. Eur *7* 211–221 1972

Enzinger F M Personal communication

Enzinger F M Recent trends in soft tissue pathology In Tumors of bone and soft tissue Year book medical publishers Inc. Chicago 315–332 1965

Enzinger F M & Dulcey F Proliferative myositis. Report of thirty three cases. Cancer (Philad.) *20* 2213–2223 1967

Enzinger F M & Harvey D A Spindle cell lipoma. Cancer (Philad.) *36* 1852–1859 1975

Enzinger F M Lattes R & Torloni H Histological typing of soft tissue tumours. International histological classification of tumours. No. 3 Geneva. WHO 1969

Ferrando J Mieras C & Pinol Aguadé J Estudio citológico y ultraestructural del fibroxantoma atípico. Med Cut. I L A. *3* 37–46 1975

Fine G & Stout A P Osteogenic sarcoma of the extraskeletal soft tissues. Cancer (Philad.) *9* 1027–1043 1956

Finlay-Jones L R Nicoll P & Ten Seldam R E J Pseudosarcoma of the skin. Pathology *3* 215–222 1971

Fretzin D F & Helwig E B Atypical fibroxanthoma of the skin. A clinicopathologic study of 140 cases. Cancer (Philad.) *31* 1541–1552 1973

Gordon H W Pseudosarcomatous reticulohistiocytoma. A report of four cases. Arch. Derm. *90* 319–325 1964

Helwig E B Atypical fibroxanthoma. In Tumor seminar Proceedings of the 18th annual tumor seminar of San Antonio Society of Pathologists, 1961 Tex St J Med *59* 664–667 1963

Helwig E B & Hackney V C Juvenile xanthogranuloma (*Nevoxantho-endothelioma*) Amer J Path. *30* 625–626 1954

Jacobs D S Edwards W D & Ye R C Metastatic atypical fibroxanthoma of skin. Cancer (Philad.) *35* 457–463 1975

Jaimovich L & Abulafia J Fibroxantoma atípico con metástasis ganglionares. Med Cutánea *7* 139–143 1973

Jaffe H L Lichtenstein L & Sutro C J Pigmented villonodular synovitis bursitis and tenosynovitis Arch Path. *31* 731–765 1941

Jeffreys T E & Stiles P J Pseudomalignant osseous tumour of soft tissue. J Bone Jt Surg *48 B* 488–492 1966

Kempson R L & McGavran M H Atypical fibroxanthomas of the skin. Cancer (Philad.) *17* 1463–1471 1964

Kern W H Proliferative myositis a pseudosarcomatous reaction to injury A report of seven cases. Arch. Path *69* 97–104 1960

Konwaler B E Keasbey L & Kaplan L Subcutaneous pseudosarcomatous fibromatosis (fasciitis) Report of 8 cases. Amer J clin Path. *25* 241–252 1955

Kroe D J & Pitcock J A Atypical fibroxanthoma of the skin. Report of ten cases. Amer J clin Path *51* 487–492 1969

Lagier R & Cox J N Pseudomalignant myositis ossificans. A pathological study of eight cases. Hum. Pathol 6 653–665 1975

Larrauri J Patrón M López Barea F, Calvo M & Contreras F Tumores histiocitarios. Revision de 158 casos. Patologia (Madrid) *7* 75–84 1974

Lattes R Malignant fibroxanthoma of thigh with metastases to inguinal lymph nodes and to viscera. In Tumor seminar Proceedings of the 19th annual tumor seminar of San Antonio Society of Pathologists 1962 Tex. St. J Med. *60* 420–446 1964

Levan N E Hirsch P & Kwong, M Q. Pseudosarcomatous dermatofibroma. Arch. Derm. *88* 908–912, 1963

Moberger G Nilsonne U & Friberg, S Jr Synovial sarcoma. Histologic features and prognosis. Acta orthop. scand Suppl. No. 111 1968.

Niemi K M The benign fibrohistiocytic tumours of the skin Acta derm. venereol (Stockh.) *50* Suppl. 63 1970

Norris H J & Taylor H B. Polyps of the vagina. A benign *lesion resembling sarcoma* botryoides. Cancer (Philad.) *19* 227–232, 1966.

Rachmaninoff N M Donald J R & Cook J C Sarcoma like tumors of the skin following irradiation. Amer J clin. Path. *36* 427–437 1961

Smith C J Echevarria R. & McLelland C A Pseudosarcomatous changes in antrochoanal polyps. Arch. Otolaryng *99* 228–230 1974

Spjut H J Dorfman H D Fechner R E & Ackerman L V Tumors of bone and cartilage. Second series. Fascicle 6 AFIP Washington D C., 1971

Acta path. microbiol. scand. Sect. A, 85: 931–941 1977

FOCAL PREGNANCY-LIKE CHANGES IN THE BREAST

HENRIK W. KIÆR and JOHAN A. ANDERSEN

Department of Pathology, Svendborg Hospital, Svendborg, and
Department of Pathology, Esbjerg Central Hospital, Esbjerg, Denmark

Kiær H. W. & Andersen, J. A. Focal Pregnancy-like Changes in the Breast. Acta path. microbiol. scand. Sect. A, 85: 931–941, 1977.

The aetiology of focal, pregnancy-like mammary changes in non-pregnant and non-lactating women is discussed on the basis of the literature and a material of 31 patients. Such changes were found in one or more glandular lobules in 3 per cent of the breast tissue specimens received in our departments. As a rule, this finding was made in women who had been pregnant and who had been or were on oestrogenic or on contraceptive medication. They occurred in fertile, menopausal, as well as in post-menopausal women. Often they were seen many years after the pregnancy and/or intake of hormones. They were observed also in women who had never been pregnant or on hormone medication, and even in men on oestrogen therapy. It is likely, therefore, that focal pregnancy-like changes in non-pregnant and non-lactating women indicate a selective susceptibility of the mammary glandular tissue to oestrogen. Accordingly, we interpret the change as a normal histological variant.

Key words: breast; focal pregnancy-like changes; selective susceptibility to oestrogen.

Henrik W. Kiær, Department of Pathology, Svendborg Hospital, DK-5700 Svendborg, Denmark.

Received 8.i.77. Accepted 8.i.77.

Focal, secretory, pregnancy-like changes in the breast have been found occasionally in benign as well as in malignant diseases of the breast in women who have not been pregnant at the time of biopsy (3, 7, 9, 10, 12, 18, 20, 24, 28).

Focal pregnancy-like changes (f. p. c.) are taken to mean epithelial changes whose morphology cannot be distinguished in the light microscope from the more diffuse epithelial changes observed in the breast during pregnancy or lactation. In isolated lobules, which may be hypertrophic, there is a simple to stratified epithelium which may consist of cells varying in size with ample pale vacuolated cytoplasm and a nucleus varying in site from basal to luminal. In places there may be appearances suggesting an Arias-Stella reaction. In other areas there is a simple hob-nail epithelium whose nuclei are often pyknotic, varying in size and in site from basal to luminal. There is no transition to apocrine epithelium. The affected acini, which may be a few and up to all those present in the lobule, show a varying degree of ectasia.

The object of the present paper is to discuss, on the basis of the literature and of the present material, the following aetiological

Dahl I & Angervall L Pseudosarcomatous proliferative lesions of soft tissue with or without bone formation Acta path microbiol. scand. Sect. A, *85* 577–589 1977

Dahl I Angervall L Magnusson S & Stener B Classical and cystic nodular fasciitis. Pathol Eur *7* 211–221 1972.

Enzinger F M Personal communication

Enzinger F M Recent trends in soft tissue pathology In Tumors of bone and soft tissue. Year book medical publishers Inc. Chicago 315–332 1965

Enzinger F M & Dulcey F Proliferative myositis. Report of thirty three cases. Cancer (Philad.) *20* 2213–2223 1967

Enzinger F M & Harvey D A Spindle cell lipoma. Cancer (Philad.) *36* 1852–1859 1975

Enzinger F M Lattes R & Torloni H Histological typing of soft tissue tumours. International histological classification of tumours. No 3 Geneva WHO 1969

Ferrando J Mieras C & Pinol Aguadé J Estudio citológico y ultraestructural del fibroxantoma atípico Med. Cut I L.A. *3* 37–46 1975

Fine G & Stout A P Osteogenic sarcoma of the extraskeletal soft tissues. Cancer (Philad.) *9* 1027–1043 1956

Finlay-Jones L R Nicoll P & Ten Seldam R E J Pseudosarcoma of the skin. Pathology *3* 215–222 1971

Fretzin D F & Helwig E B Atypical fibroxanthoma of the skin. A clinicopathologic study of 140 cases. Cancer (Philad.) *31* 1541–1552 1973

Gordon H W Pseudosarcomatous reticulohistiocytoma. A report of four cases. Arch. Derm. *90* 319–325 1964

Helwig E B Atypical fibroxanthoma. In Tumor seminar Proceedings of the 18th annual tumor seminar of San Antonio Society of Pathologists, 1961 Tex. St J Med 59 664–667 1963

Helwig E B & Hackney V C Juvenile xanthogranuloma (Nevoxantho-endothelioma) Amer J Path *30* 625–626 1954

Jacobs D S Edwards W D & Ye R C Metastatic atypical fibroxanthoma of skin. Cancer (Philad.) *35* 457–463 1975

Jaimovich L & Abulafia J Fibroxantoma atípico con metástasis ganglionares. Med Cutánea. *7* 139–143 1973

Jaffe H L Lichtenstein L & Sutro C J Pigmented villonodular synovitis, bursitis and tenosynovitis Arch Path *31* 731–765 1941

Jeffreys T E & Stiles P J Pseudomalignant osseous tumour of soft tissue J Bone Jt Surg *48 B* 488–492, 1966

Kempson R L & McGavran M H Atypical fibroxanthomas of the skin Cancer (Philad.) *17* 1463–1471 1964

Kern W H Proliferative myositis a pseudosarcomatous reaction to injury A report of seven cases Arch. Path. *69* 97–104 1960

Konwaler B E Keasbey L & Kaplan L Subcutaneous pseudosarcomatous fibromatosis (fasciitis) Report of 8 cases. Amer J clin. Path. *25* 241–252 1955

Kroe D J & Pitcock J A Atypical fibroxanthoma of the skin. Report of ten cases. Amer J clin Path. *51* 487–492 1969

Lagier R & Cox J N Pseudomalignant myositis ossificans. A pathological study of eight cases. Hum. Pathol. 6 653–665 1975

Larrauri J Patrón M López Barea F Calvo M & Contreras F Tumores histiocitarios. Revision de 158 casos Patología (Madrid) *7* 75–84 1974

Lattes R Malignant fibroxanthoma of thigh with metastases to inguinal lymph nodes and to viscera. In Tumor seminar Proceedings of the 19th annual tumor seminar of San Antonio Society of Pathologists, 1962 Tex. St. J Med. *60* 420–446 1964

Levan N E Hirsch P & Kwong M Q Pseudosarcomatous dermatofibroma. Arch. Derm. *88* 908–912 1963

Moberger G Nilsonne U & Friberg S Jr Synovial sarcoma. Histologic features and prognosis. Acta orthop scand Suppl. No 111 1968.

Niemi K M The benign fibrohistiocytic tumours of the skin Acta derm.-venerol. (Stockh.) *50* Suppl. 63 1970

Norris H J & Taylor H B Polyps of the vagina. A benign lesion resembling sarcoma botryoides. Cancer (Philad.) *19* 227–232 1966

Rachmaninoff N McDonald J R & Cook J C Sarcoma like tumors of the skin following irradiation. Amer J clin Path. *36* 427–437 1961

Smith C J Echevarria R & McLelland C A Pseudosarcomatous changes in antrochoanal polyps. Arch. Otolaryng *99* 228–230 1974

Spjut H J Dorfman H D Fechner R E & Ackerman L V Tumors of bone and cartilage. Second series. Fascicle 6 AFIP Washington D C., 1971



Fig 2 Same section as in Fig 1 Numerous hob-nail cells in ectatic acini. E en transition to normal epithelium in the marginal area of the lobule H-E, × 125

The patients may be divided into the following groups

(A) Women who had been pregnant, once or several times and who had previously received or were receiving oestrogenic or contraceptive pills. This group comprises 12 patients (Cases 1 2, 4 11 12, 13 15 20 22 26 27 and 31 in Table 1)

(B) Women who had been pregnant, once or several times, but who had never been treated with oestrogenic or contraceptive pills This applied to 16 patients (Cases 3 5 6 7 9 10 17 18, 19 21 23 24 25 28, 29 and 30 in Table 1)

(C) Women who had never been pregnant, who had previously been on oestrogenic or contraceptive medication, but were receiving no hormone therapy at the time of biopsy This applied to two patients (Cases 8 and 14 in Table 1)

(D) Case 16 who had never been pregnant and had never had hormone therapy

The hormone therapy received by the fertile women was in all cases oral contraceptives (gestagenic/oestrogenic pills) while the menopausal and post-menopausal women had received either pure oestrogen medication or contraceptive pills because of menopausal complaints. None of the patients had sought medical advice for abnormal vaginal bleeding during the hormone therapy

One patient (Case 9) had been aware of the lump in the breast since delivery one year previously while in the others there was no relationship to a previous pregnancy The duration of symptoms and/or signs of the possible pathological lesion ranged from 1 week to 1 year (L p c are presumed to



Fig 3 Lobule with varying degrees of acinar ectasia. Epithelium in most sites stratified, pale with pyknotic nuclei. Case 3 H E, × 50

possibilities of f p c. in non pregnant women

(1) Can f p c. be explained as changes persisting from a previous pregnancy? (20 21 22, 24)
(2) Can f p c be of exogenous hormonal origin? (3 6 16 17)
(3) Can f p c. be due to a "selective susceptibility" meaning Is the glandular epithelium in the breast of some women more than usually susceptible to oestrogen-oestrogen/gestagen? (9 10 28)

MATERIAL AND METHODS

The material from the Svendborg Hospital comprises all breast biopsies/tumours and all mastectomy specimens from the period 1st November 1975 to 1st March 1977 a total of 578 specimens. From each specimen an average of 6 sections were cut from different areas. Each section was stained by haematoxylin-eosin and van Gieson F p c. were found in 16 cases (Cases 1–16 Table 1)

The material from the Esbjerg Central Hospital comprises all breast biopsies/tumours and mastectomy specimens from the period 1st January 1976 to 31st December 1976 a total of 507 specimens from which an average of 8 sections were cut. F p c. were found in 15 cases (Cases 17–31 Table 1)



Fig 1 Lobule with many ectatic acini, in most sites lined with hob-nail cells. Normal acini in the marginal areas. Also an ectatic duct. Case 5 H E × 50.

RESULTS

During the named periods there was in both materials a frequency of 3 *per cent f p c* Of the patients 19 were of the fertile age, 4 were menopausal and 8 post menopausal The reasons for consulting a doctor had been 23 had felt a lump in one breast, 7 had noticed tenderness of the breast or had had discharge from the nipple and 1 was suffering from cancerophobia

The patients were treated by removal of the tumour or biopsy if no tumour was palpable Eight patients had mastectomy because of carcinoma or precancerous epithelial changes and one (Case 30) underwent mastectomy because of localized lymph node metastases in the axilla. A primary malignant breast tumour could not be demonstrated by tissue specimen radiography and embedding of the entire glandular tissue from the breast

Microscopic examination disclosed, with varying frequency Fibroadenomatosis, fibrosis, liponecrosis, mastitis, duct ectasia fibroadenoma, lobular carcinoma *in situ* intraductal carcinoma, and carcinoma (cf Table 1) Cases 11 and 14 besides had benign glandular hyperplasia but otherwise no unusual changes for their age F p c. were found in from 1–12 isolated foci, depending to some extent upon the size of the tissue specimen, but never with focal tumour formation. In two cases the f p c. were localized in fibroadenomas.

All affected acini were slightly to moderately ectatic (Figs 1–4)

Relation t any Previous Pregnancies and Possible Previous/Present Hormone Therapy

Interval from discont. of hormone ther to b opsy	Discharge from the nipple	Menopause	Microscopic diagnosis
?	+	—	Fibroadenomatosis. Mastitis.
	—	—	Breast tissue with fibrosis.
	—	—	Fibroadenoma.
ca. 20 years	—	6 months	Breast tissue with fibrosis and duct ectasia.
	—	—	Breast tissue with fibrosis.
	—	—	Fibroadenoma.
	—	—	*Fibroadenomatosis.*
6 months	—	—	Fibroadenoma.
	—	—	*Fibroadenomatosis.*
	—	—	Fibroadenomatosis.
1 month	+	—	Breast tissue with glandular hyperplasia.
2 weeks	—	4 years	Fibroadenomatosis (precancrous type) Lobular carcinoma in situ.
	—	—	Liponecrosis.
5 years	—	+	Periductal mastitis. Breast tissue with glandular hyperplasia.
3 years	—	+	Infiltrating duct carcinoma. Fibroadenomatosis.
	—	+	Fibroadenomatosis (precancerous type) Ductectasia.
	+	—	Fibroadenomatosis.
	—	—	Mastitis.
	—	—	Fibroadenoma.
7 years	—	—	Fibroadenomatosis.
	—	—	Fibroadenomatosis.
7 years	—	—	Fibroadenoma
	—	4 years	Infiltrating lobular carcinoma. Fibroadenomatosis.
	+	—	Fibroadenomatosis.
	—	—	Intraductal carcinoma. Fibroadenomatosis.
2 years	—	Hysterectomy 1963	Fibroadenomatosis. Ductectasia.
	—	—	Infiltrating duct carcinoma. Fibroadenomatosis.
	+	Hysterectomy 1960	Intraductal carcinoma. Ductectasia.
	—	—	I traductal carcinoma.
	—	—	Carcinoma of axillary lymph node. F broadenoma. Ductectasia.

TABLE 1 *31 Patients with Focal Pregnancy-like Changes in the Breast and*

Case No.	Age	No of pregnancies including abortions	No of deliveries	Interval from last pregn./deliv to biopsy	Previous hormone therapy	Hormone therapy at time of biopsy
1	42	3	2	16 years	Sequllarum®	?
2	31	4	0	4½ years	Neovulen® for 2 years	Neovulen®
3	39	2	2	14 years	—	—
4	52	3	3	13 years	+	—
5	39	3	2	12 years	—	—
6	36	5	5	21 months	—	—
7	26	2	2	6 years	—	—
8	23	0	0		Contraceptive pills for 7 years	—
9	26	2	2	1 year	—	—
10	26	2	2	3 years	—	—
11	38	1	0	14 years	Ovanon® for 3 months	—
12	68	1	1	36 years	Metrulen® for 4 years	—
13	34	5	4	10 years	Gestovex® for 7 years	Gestovex®
14	50	0	0		*Cyclovul® for 5 months*	—
15	54	1	1	20 years	Ovestin® total 14 mg	—
16	44	0	0		—	—
17	38	1	0	19 years	—	—
18	30	2	2	1 year	—	—
19	28	3	3	7 years	—	—
20	44	4	2	10 years	Contraceptive pills for 6 months	—
21	52	8	4	15 years	—	—
22	26	1	1	1 year	Contraceptive pills for 1 year	—
23	56	4	3	18 years	—	—
24	49	1	0	22 years	—	—
25	48	1	0	15 years	—	—
26	58	5	2	33 years	Oestrogeninj for 5 years	—
27	39	2	2	6 months	Neolyndiol®	Neolyndiol®
28	59	3	2	33 years	—	—
29	49	3	2	2 months (abortion)	—	—
30	43	4	4	11 years	—	—
31	41	4	4	14 years	Neogentrol® for several years	Neogentrol®

rhoea (11 15 16 19 23 26) fibroadenomatous (1 5 8, 25) tumours (3 6 7 12, 13 14 23 29) and various forms of epithelial proliferation in the breast (5 8 9 12 13 14 17 24 26 28)

Oestrogenic hormones have been used for therapeutic purposes for almost 50 years (2, 16) and the oral contraceptive era was initiated almost 20 years ago (7) It is natural, therefore that many workers have tried to find a correlation between hormone medication and various benign and malignant changes of the breast.

Re question 1 Pregnancy like changes in non-pregnant women have in some cases been explained as being "residual lactation acini" In his material of 27 patients, *Moran* (1935) found that normally f p c. may persist in fibroadenomas up to 15 months after



Fig 6 Same section as in Fig. 5 Superiorly f p c. with a pale, vacuolated epithelium and dark nuclei. H-E, × 125

phase. After she had had an ill-defined lump in the left breast and a retracted nipple for 2 weeks, mastectomy was carried out in December 1976 because of a serious clinical suspicion of cancer Microscopic examination showed severe periductal mastitis and adenomatous glandular hyperplasia (Figs 5 6, 7) without atypical findings except for f p. c Owing to this finding and to the adenomatous hyperplasia of the endometrium and exclusion of exogenous hormonal action, two tests for serum oestriol were done both showed levels within the normal range

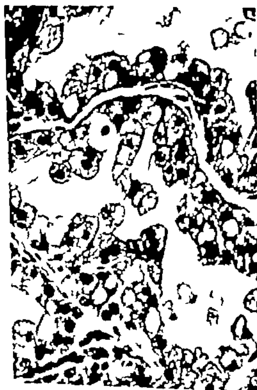


Fig 7 Same section as in Fig 5 In many sites the frequently ample pale cytoplasm is delicately vacuolated. The nuclei are dark and of varying localization in the cells. H E, × 310

DISCUSSION

Much has been written about a possible relationship between hormone therapy (pure oestrogen or contraceptive pills (gestagen/oestrogen) and the occurrence of galactor

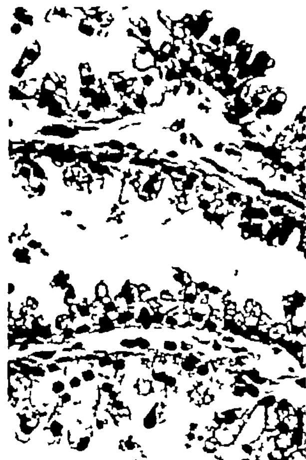


Fig 4 Same section as in Fig 3 Stratified pale epithelium with varying localization of the nuclei H E × 125

cause no symptoms) Five patients had had discharge from the nipple but no other clinical signs of a pituitary tumour

Re Group A In these patients the interval from the last pregnancy/delivery to the time of breast biopsy was from 6 months to 36 years Four were receiving hormones at the time of the biopsy (last pregnancy from 6 months to 20 years previously) In the others 2 weeks to 20 years had elapsed from the discontinuation of hormone therapy to biopsy and from 1 to 36 years from the last pregnancy to biopsy (Table 1)

There is particular reason to emphasize Case 4 (last pregnancy 13 years and last hormone therapy 20 years previously) Case 15 (20 years and 3 years respectively) Case 20 (10 years and 7 years respectively) and Case 26 (33 years and 2 years respectively)

Re Group B In patients without previous or present hormone therapy the interval from the last pregnancy/delivery to biopsy was from less than 2 months (abortion) to 33 years (Table 1)

Re Group C Case 8 had been taking contraceptive pills, with a few breaks, since the age of 16 years, the last course discontinued 6 months prior to the biopsy Case 14 had been treated in 1967 for 5 months with contraceptive pills (Cyclovul®) for metrorrhagia and had at no other time received hormone preparations. In June 1967 she had vaginal bleeding curettage and the microscopic finding was a polypous endometrium in the proliferative phase. In June 1976 again vaginal bleeding curettage and microscopic findings polypous endometrium and adenomatous hyperplasia Control curettage in October 1976 showed a normal proliferative



Fig 5 Benign glandular hyperplasia with hypertrophic lobules. Superiorly ectatic acini with a simple to stratified pale epithelium Case 14 H E × 50



Fig 8 Acini filled with pale uniform cell with regular round, dark nuclei, resembling lobular carcinoma in *si* Case 6. H E, × 125

from a period prior to the oral contraception era, but of course this does not rule out that some of the patients may have received pure oestrogen therapy In 10 women aged 20-55 years on oestrogen therapy *Foote & Stewart* (1945) found a very wide individual variation in response in the form of apocrine metaplasia and epithelial proliferations, but no common characteristics for the entire group In one patient aged 42 years with bilateral breast cancer they found widespread f p. c., in places with transition into apocrine epithelium. In this case there was no information concerning previous pregnancies.

In the present series f p c. were found in 25 women who were not on hormone therapy at the time of biopsy The interval from the discontinuation of the hormone therapy to the biopsy ranged from 2 weeks to 20 years. Two of the patients had never been preg

of biopsy and all had previously been pregnant, the interval between the last pregnancy and biopsy ranging from 6 months to 20 years In some cases we cannot rule out a relationship between contraceptive pills and f p c or a combined effect of contraceptive pills and a fairly recent pregnancy such as in Case 27 who had delivered 6 months before the biopsy Incidentally the breast tissue of this patient did not suggest pregnancy changes

Re question 3 Is the glandular epithelium in the breast of some women more than usually susceptible to oestrogen—gestagen/oestrogen In their large post-mortem series of "normal" breast, *Frantz et al.* (1951) found f p. c in two nulligravidae. No attempt was made to elucidate a possible relationship to oestrogen therapy because of insufficient data. However the material is



Fig 9 Case 6 Another area showing the same changes H E, × 125

lactation has been discontinued. *LeGal* (1961) reported that involution can be de layed or even missed in a lactating adenoma but in his own material f p c. are mentioned only in fibroadenomas in pregnant women and 4 days post partum *McFarland's* (1922) mention of "residual lactation acini" can only be regarded with much reserve, as many of his illustrations claimed to support this the ory show changes typical of fibroadeno-matosis—a condition which he incidentally says does not exist. Moreover it is doubtful whether all his patients with residual lac tation acini had ever been pregnant. In an autopsy study of 800 women *Sandison* (1962) found persisting secretory changes in 30 aged 21–75 years It is not stated how many of these women had been pregnant how long an interval there was between a possible last pregnancy and autopsy or whether any of the patients had received oestrogenic hormones.

Frantz et al (1951) in 225 post mortem examinations of "normal breast found f p c. in 7 patients 4 of whom were in the age group 40 to 50 years Five of these patients had been pregnant from 3 to 48 years be fore they came to autopsy The authors talked of the changes as being persisting secretory cells, and they suspected "some hormonal imbalance and delay of involu tion" but two of their patients had never been pregnant.

In the present material the f p c. may possibly be explained as "residual lactation acini" in those patients who had completed their last pregnancy/lactation within a year of the biopsy but 3 of the patients had never been pregnant Besides it seems to us rather unlikely that pregnancy changes can persist for up to 36 years (*Frantz et al* (1951) 48 years in one case)

Re question 2 That f p c might in some cases be of exogenous hormonal origin has been claimed by int al *Brown* (1970) His patient had secretory changes in a fibro-adenoma but had completed a pregnancy only 5 months before removal of the breast tumour *Haagensen (1971)* has reported on a 71 year-o'd woman whose mammary tissue resembled that of a pregnant woman after 15 mg stilboestrol daily for 3 months, and he mentioned the fact that estrogen makes the breast epithelium grow" In 4 out of 54 women with fibroadenomas and simultaneous intake of contraceptive pills, *Fechner* (1970) found glandular proliferation in the fibro-adenomas and, in two of the patients, also f p c in the surrounding breast tissue He stressed that no other quantitative or qualita-tive differences were found in the fibro-adenomas or in the remaining breast tissue, between the patients and a control group without contraceptive medication. Referring to *Sandison* (1962) Fechner stated that hor mones (contraceptive pills) could be assumed to be the cause of f p c. only in nulliparae but that possibly contraceptive pills gave rise to lobular and acinar hyperplasia. In the opinion of *Goldenberg (1968)* contraceptive pills create a pseudopregnant condition. *Huseby & Thomas* (1954) found f p c in 10 out of 66 post menopausal women on oestrogen therapy for breast cancer One of these patients was a 72 year-o'd nulligravida.

In 1975 *Fechner* reported f p c in a 26-year-old nulligravida

Schwartz & Wilens (1963) observed acinar differentiation in gynaecomastia in 8 out of 28 men on oestrogen therapy for cancer of the prostate and 2 of these 8 exhibited f p c The degree of acinar differentiation and f p c did not correlate with the duration of oestrogen therapy

All patients from the literature in whom benign epithelial changes, including f p c., have been related to oestrogen therapy/con-traceptive pills have been on hormone the-rapy at the time of the biopsy but the dose and the duration of treatment have varied There have been fertile as well as post menopausal women but data concerning past pregnancies have been scarce Therefore it has not been possible to assess a combined effect, if any of pregnancy and exogenous administration of hormones

Within the present material 4 patients were on contraceptive medication at the time

2 Arthes, F G Sartwell P E & Lewison E. F The pill, estrogens, and the breast. Cancer 28 1391–1394 1971
3 Bron J M Histological modification of fibroadenoma of the breast associated with oral hormonal contraceptives. Med. J Aust. 1 276–277 1970
4 Fechner R. E. The surgical pathology of the reproductive system and breast during oral contraceptive therapy In Sommers, S C. (Ed.) Genital & mammary pathology decennial1966-1975 Appleton-Century-Crofts, New York 1975 pp. 114–125
5 Fechner R. E.: Fibrocystic disease in women receiving oral contraceptive hormones. Cancer 25 1332–1339 1970.
6 F hner R E. Breast cancer during oral contraceptive therapy Cancer 26 1204 1211 1970
7 Fechner R E. Fibroadenomas in patients receiving oral contraceptives, Amer J Clin. Path. 53 857–864 1970.
8 Fechner R. E. Benign breast disease in women on estrogen therapy Cancer 29 273–279 1972
9 Foote F W & Stewart F W. Comparative studies of cancerous versus noncancerous breasts. Ann. Surg 121 6–79 1945
10. Frantz V K Pickren J W Melcher G W & Auchincloss H Incidence of chronic cystic disease in so-called "normal breasts Cancer 4 762 783 1951
11 Friedman S & Goldfien, A. Amenorrhea and galactorrhea following oral contraceptive therapy J A. M. A 210 1888–1891 1969
12 Goldenberg, V E Wiegenstein L & Mottet N K Florid breast fibroadenomas in patients taking hormonal oral contraceptives. Am. J Clin Path. 49 52–59 1968.
13 Goldenberg V E Mottet N K & Wolff M Atypical features in breast carcinomas in patients on oral contraceptives. Am. J Clin. Path 50 635 1968.
14 Gould V E Wolff M & Mottet N K Morphologic features of mammary carcinomas in women taking hormonal contraceptives. Am J Clin. Path. 57 139–145 1972.
15 Gregg W J Galactorrhea after contraceptive hormones. New England J Med. 274 1432, 1966.
16 Haagensen C D Diseases of the breast. 2nd ed. W B Saunders company Philadelphia London-Toronto 1971 pp. 63–64 + 75
17 Huseby R. A & Thomas L. B. Histological and histochemical alterations in the normal breast tissues of patients with advanced breast cancer being treated with estrogenic hormones. Cancer 7 54–74 1954
18. I ey V S., Manion W C & Taylor H B.: Vascular lesions in women taking oral contraceptives. Arch. Path. 89 1–8, 1970
19 Kuzma, J F.: The breast. In: Anderson, W A. D (Ed.) Pathology 6th ed. vol. 2. C. V Mosby Company St. Louis 1971 p 1579
20 Le Gal Y Adenomas of the breast: relationship of adenofibromas to pregnancy and lactation. Amer Surg. 27 14 22, 1961
21 McF rland J. Residual lactation acini in the female breast. Arch. Surg. 5 1–64 1922.
22 Moran C S F bro-adenoma of the breast during pregnancy and lactation. Arch. Surg. 31: 688–708, 1935
23 Rosen S W & Gahres E. E.: Nonpuerperal galactorrhea and the contraceptive pill Obstet. Gynec. 29 730–731 1967
24 Sandison A T An autopsy study of the adult human breast. Nat. Cancer Inst. Monogr no. 8 1962, pp 1–145
25 Sartw ll, P E. Arthes, F G & Tonascia, J A.: Epidemiology of benign breast lesions lack of association with oral contraceptive use. New Engl. J Med. 288: 551–554 1973
26. S hackner S H Galactorrhea subsequent to contraceptive hormones. New Engl. J Med. 275 1138, 1966
27 Schwartz I S & Wilens S L The formation of acinar tissue in gynecomastia. Am. J Path. 43 797–807 1963
28. Taylor H B. Oral contraceptives and pathologic changes in the breast. Cancer 28 1388–1390, 1971
29 Vessey M P Doll, R. & Sutton, P M.: Oral contraceptives and breast neoplasia: a retrospective study Brit. Med. J 3 719–724 1972.



Fig 10 Case 6 The same changes showing in periorly transition into f p c. H E × 125

nant and one of these latter two had not received hormone therapy during the past 9 years Besides, one patient had never been pregnant and had never received hormone therapy

These results, plus the fact that significant differences have not been demonstrated in the epithelial changes between oestrogen treated women and matched controls (9 28) support the selective susceptibility hypothesis of *Foote & Stewart* (1945) which is also supported by *Taylor* (1971) F p c in 3 per cent of the present material corresponds to the findings of others *Frantz et al* (1951) 3 1 per cent and *Sandison* (1962) 3 7 per cent.

As a, perhaps rare diagnostic error it is worth mentioning lobular carcinoma *in situ* In Case 6 the first sections of the breast biopsy showed focal areas which might suggest a lobular carcinoma *in situ* but when deeper sections were cut from the block this appearance proved to be due to tangential sectioning of f p c (Figs. 8–10)

Owing to insufficient data, it has not been possible to evaluate a relation, if any to the menstrual cycle

CONCLUSION

Focal pregnancy like changes in the breast were found in non pregnant and non lactating fertile women in menopausal and in post menopausal women. For some time *post partum* (unknown for how long) these changes may presumably be interpreted as "residual lactation acini" but it seems unlikely that they can persist for up to 48 years In many cases pregnancy cannot be the explanation as f p c were found in women who had never been pregnant and in a few cases in men on oestrogen therapy for cancer of the prostate Thus oestrogen therapy may in some cases give rise to f p c. but the effect is unpredictable the extent of the changes extremely variable and there is no relationship to the dose of hormones or to the duration of the treatment. An effect persisting for up to 9 years after the discontinuation of hormone therapy appears unlikely A possible combined effect of pregnancy-conditioned changes and exogenous hormone induced changes up to 13 and 20 years after the last pregnancy and last hormone therapy respectively seems more speculative than reasonable.

In our opinion f p c in non-pregnant. non lactating women are presumably of oestrogenic aetiology but often rather a sign of selective susceptibility than of a given quantitative endogenous and/or exogenous hormonal action Accordingly we interpret the changes as a normal non pathological variation in the histology of the female breast

REFERENCES

1 *Ariel I M* Enovid therapy (norethynodrel with mestranol) for fibrocystic disease Am J Obstet, Gynecol *117* 453–457 1973

(desoxycorticosteroneacetate, Percorten ® micro-crystalline, Ciba-Geigy) were injected subcutaneously once week. The mice were examined on day 21 after commencement of the DOCA/salt treatment. The further treatment was the same for all groups.

Under l ght ether anaesthesia, a catheter was placed in the left carotid artery and connected to Tybjaerg-Hansen capacitance pressure transducer (Simonsen & Weel, Copenhagen) and a G-14 graphic recorder (Danbridge Copenhagen) The blood pressure was subsequently recorded for one hour before the further treatment, in order to obtain "basal" conditions after the anaesthes a. The anaesthesia generally decreased the blood pressure for bout 5 minutes after termination of ether inhalation After this time the mice were conscious, and the blood pressure had reached a stable level, wh ch as rule remained unchanged during the rest of the observ tion time Mice in which bleeding occurred were discharged. After one hour of recording, the mice received 100 µl 5 per cent glucose intraperitoneally and only if no change in blood pressure was observed, this injection was followed 10 min tes later by an intraperitoneal injection of the SQ 20 881 inhibitor (1.33 mg/ml 5 per cent glucose) After injection of the inhibitor the blood pressure recording was continued for one hour Only decreases in blood pressure which commenced immediately and persisted for more than 10 minutes after the injection of the inhibitor are reported. Generally the depressor effect of the inhibitor lasted for the rest of the observation period (one hour) but a slow and slight increase from the depressed blood pressure level was occasionally observed after 20–30 minutes delay During the whole experiment the animals were allowed to move freely in a small box, except when held by the neck for the injections. For comparison of experimental results the student t test w used. The 5 per cent level w used a indicat.ve for gnificance of differences.

Result Discussion and Conclusion

The mean arterial blood pressure wa signif-cantly levated above normal in the Goldblatt one kidney mice the Loomis athymic nude- and normal haired mice nd in the DOCA/salt hyper tens mice before the treatment with the SQ 20 881 *converting enzyme inhibitor compared* with the mean alue observed in the untouched control mice before the treatment ($p < 0.001$ *for all groups*) *The SQ 20 881 inhibitor caused a signif* icant drop in blood pressure in all the consc ous hypertens.ve animals, independent of the ethiology *of hypertension (Table 1 Fig 1) and independent* of the presenc of the thymus. A significant de crease in blood pressure was furthermore observed *in the group of normotens. e mice although the*

TABLE 1 *Effect of SQ 20 881 th M an A t rial Blood Pressu e*

Group of mice	Mean arterial blood pressure ± one SD mm Hg		Δ Blood pressure mm Hg ± SD
	Before SQ 20.881	After SQ 20.881	
Control (n = 20)	1[illegible]0 ± 12 (range 100–140)	113 ± 13 (range 90–140)	$p < 0.01$
Goldblatt one-kidney hypertens (n = 13)	173 ± 14 (range 150–200) $p < 0.001$	145 ± 26 (range 90–190) $p < 0.01$	$p < 0.001$
Loomis hypertens (= 20)	159 ± 10 (range 145–180) $p < 0.001$	125 ± 17 (range 90–160) $p < 0.01$	$p < 0.001$
DOCA/salt hypertens (= 10)	158 ± 8 (*range 145–170*) $p < 0.001$	134 ± 22 (range 100–170) $p < 0.005$	$p < 0.005$

Table 1 show that injection of the SQ 20 881 con erting enzyme inh.bitor was followed by a significant decrease in blood pressure (paired data was used) in all groups of m ce Significant differences in ar terial blood pressure was observed between the hypertens groups of mice and the normotens. e con-*trol group of m ce,* before as well as after injection of the inhibitor

Number of mice

Included are 10 mice carrying the mutant alleles (nu/nu)

BRIEF REPORT

EFFECTS OF THE NONAPEPTIDE SQ 20 881 ON THE BLOOD PRESSURE OF CONSCIOUS NORMOTENSIVE AND CHRONIC HYPERTENSIVE MICE

Ulrik Gerner Svendsen

The University Institute for Experimental Medicine Copenhagen and Department of Clinical Physiology Herlev University Hospital Herlev Denmark

Svendsen, U G Effects of the nonapeptide SQ 20.881 on the blood pressure of conscious normotensive and chronic hypertensive mice Acta path. microbiol scand. Sect. A 85 942-944 1977

Prevention of conversion of angiotensin I to angiotensin II by means of a converting enzyme inhibitor the nonapeptide SQ 20 881 in chronic hypertensive mice was followed by a drop in blood pressure in all mice independent of the ethiology of hypertension In conscious normotensive mice was observed a significant decrease in blood pressure, which however was less than that observed in the hypertensive mice

Key words Renal hypertension converting enzyme inhibitor NMRI mice

Ulrik Gerner Svendsen, The Department of Clinical Physiology Herlev University Hospital, Herlev Ringvej DK 2730 Herlev Denmark.

Received 21.x.77 Accepted 21.x.77

Prevention of conversion of angiotensin I to angiotensin II by means of inhibitors of converting enzyme has been used to elucidate the role of the renin-angiotensin system in the maintenance of the normal and the hypertensive blood pressure levels in experimental animals. Different results have been obtained in different models of experimental hypertension different states of sodium balance and in different animal species (4 8) The present studies were undertaken to determine the effect of a converting enzyme inhibitor the nonapeptide SQ 20.881 on the blood pressure in conscious normotensive mice as well as in mice with three different forms of chronic experimental hypertension.

Material and Methods

Animals Outbred SPF NMRI mice (Gl Bomholtgaard Ltd Ry Denmark) 20-25 g were fed mouse pellets and drank tap water ad libitum. Equal numbers of males and females were used, the sex being of no importance *for the results*. Included were 10 mice carrying the mutant *alleles* (nu/nu) For literature on nude mice, see (9) These mice are congenital athymic and *therefore* unable to perform thymus-dependent immune reactions. *Blockade of the renin system* was obtained by intraperitoneal injection of 2 mg/kg of an angiotensin I converting enzyme inhibitor the synthetic nonapeptide > Glu Trp-Pro-Arg Pro-Gln Ile-Pro-Pro designated SQ 20 881 (Squibb Corp Princeton) The mice were divided into groups *Group A (Controls)* 40 untouched mice. *Group B (Goldblatt one-kidney hypertensive)* 15 unilaterally nephrectomized mice with a Goldblatt silver clip (internal diameter 0 12 mm) on their remaining renal artery The kidney was placed subcutaneously The mice were examined about day 30 after the operation *Group C (Loomis hypertensive)* 20 unilaterally nephrectomized mice (10 haired and 10 nude) with the remaining kidney partly infarcted by ligation of the anterior branch of the renal artery The kidney was placed subcutaneously The mice were examined about day 30 after the operation. *Group D (DOCA and salt hypertensive)* 10 unilaterally nephrectomized mice received 1 per cent saline as drinking water and 6 mg DOCA

ACTA
PATHOLOGICA
ET MICROBIOLOGICA
SCANDINAVICA

INDEX

VOL. 85 A

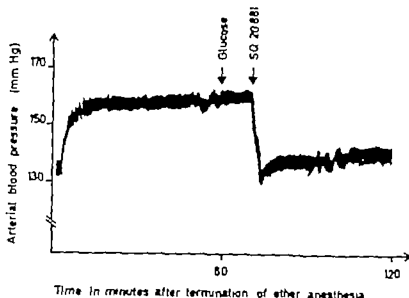


Fig 1 Effect of SQ 20.881 on arterial blood pressure in a conscious mouse with hypertension due to partly infarction of the kidney and contralateral nephrectomy One hour after termination of ether anaesthesia an intraperitoneal injection of glucose was performed followed 10 minutes later by the same volume of the SQ 20 881 converting enzyme inhibitor intraperitoneally An immediate and persistent fall in blood pressure is observed.

decrease was less than that observed in the hypertensive mice. SQ 20.881 did not restore the blood pressure to normotensive levels (Table 1) as also observed by others in hypertensive rats treated with converting enzyme inhibitors (7) The observed transient blood pressure reduction, lasting for 60 minutes or more with its initial effect beginning within the first 2 minutes after the injection, confirms the findings obtained by others using converting enzyme inhibitors either as a single intravenous or as a subcutaneous injection (5) It has been observed previously in anaesthetized rats that a converting enzyme inhibitor (6) as well as the competitive angiotensin-II antagonist saralasin, depresses the mean systemic arterial pressure both in normo- and hypertensive animals, while the blood pressure remains unaffected in normotensive conscious rats (2) This latter observation contrasts with the present finding in conscious normotensive mice. The reason for this difference in response is obscure but several explanations are possible. Thus the data suggest that the renin angiotensin system plays a role for the maintenance of the normal blood pressure in conscious mice which is not the case in other species such as the rat or that the dose of *SQ 20.881* (which was similar to or less than the dose used by others in rats (1 6) and mice (3)) was too large causing a pharmacological cardio-vascular effect although such an effect of larger doses has not been observed in rats (6) finally it is not impossible that the short lasting ether anaesthesia one hour previously had caused an elevat on of the plasma renin concentration which might have persisted at the time of the experiment However the present data in conscious mice agree with those obtained in other species n demonstrating the depressing effect on the blood pressure by converting enzyme inhibitors in hypertensive animals they also show that this effect is seen even under conditions in which the plasma renin concentration is suppressed (DOCA/salt hypertention)

The author is grateful to Miss *Lisbeth Olsen* for her valuable technical assistance. The inhibitor was kindly supplied by Dr *F Giarusso* The Squibb Institute and the Percorten® by Ciba-Geigy Copenhagen This work was supported by grants from the *Danish Medical Research Council* and *Ingeniør Søren Alfred Andersen s Foundation*

References 1 *Bing J* Acta path microbiol. scand Sect. A, *81* 376-378 1973 —2 *Bing J* & *Nielsen K* Acta path. microbiol. scand Sect A, *81* 254-262, 1973 —3 *Bing J* & *Poulsen K* Acta path. microbiol. scand Sect A, *83* 733 736 1975 —4 *Davies J O Freeman R H Johnson J A* & *Spielman W S* Circulation Research, *34* 279-285 1974 —5 *Engel S L Schaeffer T R Gold B* & *Rubin B* Proc. Soc Exp. biol med. *140* 240-244 1972 —6. *Engel S L Schaeffer T R Waugh M H* & *Rubin B* Proc. Soc Exp biol. med. *143* 483-487 1973 —7 *Leyke H F* J Lab. Clin. Med *82* 406 411 1973 —8 *Muller E. D Samuels A J Haber E* & *Barger A C* Science *177* 1108-1109 1972 —9 *Rygaard J* & *Poulsen C O* (eds) Proceedings of the First International Workshop on Nude Mice Gustav Fisher Verlag Stuttgart, 1974 —10 *Wilson C Ledingham J M* & *Floyer M A* In The Kidney Morphology Biochemistry Physiology Eds. *Rouiller C* & *Muller A F* Vol. IV Academic Press, New York & London, 1971

ACTA PATHOLOGICA ET MICROBIOLOGICA SCANDINAVICA

Section A PATHOLOGY

VOL. 85 A. FASC. 1-6 1977

MUNKSGAARD COPENHAGEN

INDEX

VOL. 85 A. FASC. 1–6 1977

Published by the
Scandinavian Societies for Microbiology and Pathology



Distributed by Munksgaard
International Booksellers and Publishers, Ltd.
35 Norre Søgade, DK 1370 Copenhagen K, Denmark

[illegible]

SUPPLEMENTS

Supplement 257 — *Jørgensen, Mogens Jørgen* The Ductal Plate Malformation. Pp. 88. 1977 (Section A)

Supplement 258 — *Boettcher B., Hjort T., Rümke Ph., Shulman S. and Vyazov O. E.* Auto- and Iso-Antibodies to Antigens of the Human Reproductive System. I Results of an International Comparative Study of Antibodies to Spermatozoa and other Antigens Detected in Sera from Infertile Patients Deposited in the WHO Reference Bank for Reproductive Immunology Pp. 69 1977 (Section C)

Supplement 259 — *Mårdh Per-Anders and Rune Grubb* Applications of Gas and High-pressure Liquid Chromatography in Microbiology A Swedish Society for Microbiology Symposium. Pp. 70 1977 (Section B)

Supplement 260 — *Berge Thorbjörn and Lundberg, Sven* (with clinical comments by *Haeger An[illegible]t and Hällén Jan*) Cancer in Malmö 1958–1969 An autopsy study Pp 235 1977 (Section A)

Supplement 261 — *Clemmesen Johannes* Statistical Studies in the Aetiology of Malignant Neoplasms. V Trends and Risks. Denmark 1943–77 Pp. 286 1977 (Section A)

Supplement 262 — *Høiby Niels* Pseudomonas Aeruginosa Infection in Cystic Fibrosis. Diagnostic and Prognostic Significance of Pseudomonas aeruginosa Precipitins Determined by Means of Crossed Immunoelectrophoresis. A Survey Pp 96. 1977 (Section C)

Supplement 263 — *Nilsson Olov* Studies on the Ultrastructure of the Human Parathyroid Glands in Various Pathological Conditions. Pp. 88 1977 (Section A)

ADVICE TO AUTHORS

Usually only articles submitted by Scandinavian authors will be accepted, but the Editorial Board may invite contributions from authors outside Scandinavia.

Submission of a manuscript for publication in this Journal will be held to imply that the work is original, that it has not been published elsewhere, and that, if accepted, it will not be published in any other journal, without the Editor's written permission. Contributions should usually be in English, but papers in French or German can also be accepted (with English summaries)

The Editorial Board takes no responsibility for contents of or views implied or expressed by the authors or advertisements.

Manuscripts should be submitted to the national editor in their final form as top pages, not carbon copies, in doublespaced type-script in English, French, or German. All written matter illustrations, and references should be submitted at the same time.

Authors must note and adopt the ACTA's customary arrangement and style; failure to do so may lead to delay in publication. Instructions to authors are available on request to the Editors.

Ordinary articles should generally not exceed 5 printed pages and not more than 5 pages of illustrative material. They must contain a summary in English not exceeding 250 words. *Brief reports* for immediate publication must not exceed 1½–2 printed pages. Such reports will be published as soon as possible after receipt. Manuscripts will be reviewed by appropriate experts. Since manuscripts will not be insured against loss or damage, contributors are expected to retain duplicate copies of all material submitted for publication. Only illustrations of reasonable technical standards will be accepted. If the limit of 5 pages is exceeded and, if corrections in the proof are particularly numerous or the tabular and illustrative material unusually excessive and/or expensive, authors will be requested to contribute to the cost of publication. Reference to literature should conform to the standards of *World Medical Periodicals* or *World List of Scientific Periodicals*. In general, reviews of a topic unsupported by original observations will not be accepted.

The official abbreviation: Acta path. microbiol. scand. Sect. *A B* or *C*

Supplements: The publication of supplements will be governed by special rules which can be obtained from the Editors.

CONTENTS

Continued from page 4 of cover

ACTA PATHOLOGICA ET MICROBIOLOGICA SCANDINAVICA
Section A Pathology

CONTENTS

Vol. 85 A. Fasc. 6. 1977

Continued on page 3 of cover

VALD. PEDERSENS BOGTRYKKERI A-S
COPENHAGEN

